MATERIALS AND STRUCTURES

MATERIALS AND STRUCTURES

By E. H. SALMON, D.Sc., M.Inst.C.E.

Vol. I

The Elasticity and Strength of Materials

With 396 Illustrations and many Exercises

'Dr. Salmon's text-book is entitled to a high place in this section of engineers' aid books. Part I is devoted to a clear discussion of elementary principles, illustrated by well-chosen examples. Part II is a really excellent and comprehensive résumé of the properties of materials and the methods of testing. A notable and excellent feature is the comprehensive references to original sources which are appended to each chapter. These make the work of special value to the practitioner.'—*Engineering.*

'As a work of reference it would be difficult to over-estimate its value and importance, and it should have a place in the working library of everyone concerned with the problems, theoretical and practical, of engineering materials.'—*Engineering News-Record.*

'He treats the standard lines of work with great clearness, and develops all essential matter with that degree of detail which is desirable if a book is to be of real value to students. . . . Adequate reference is a strong feature and, in conjunction with wide range and excellence of treatment, should render the work of distinct service to advanced students and technical engineers.'—*Nature.*

'A comprehensive and up-to-date text-book. It is more than an introduction to the subject and also forms an admirable foundation from which to build up a sound knowledge of civil engineering.'—*Structural Engineer.*

'Dr. Salmon's book forms a notable addition to engineering literature. It is comprehensive and thorough, covering the usual ground, and containing in addition chapters on the mathematical theory of elasticity and on metallography. Numerous examples are provided for the ordinary student, while the references at the ends of the chapters will enable the advanced student to see the subject as a living one, and will guide him to its extensive and growing literature.'—*Science Progress.*

'It contains a wealth of material and reference, which will make an appeal to a very much wider circle than that represented by Examination candidates.'—*Shipbuilder and Marine Engine-Builder.*

'The lay-out of the subject matter, the completeness and conciseness of the information given, and the excellent references to a great part of the most modern research work in this field, make it a very worthy addition to the desk of any engineer.'—*Bulletin of the British Non-Ferrous Research Association.*

MATERIALS AND STRUCTURES

A TEXT-BOOK FOR ENGINEERING STUDENTS

BY

E. H. SALMON

D.Sc. (ENG.), LONDON, M.INST.C.E.

VOL. II.

THE THEORY AND DESIGN OF STRUCTURES

WITH 516 ILLUSTRATIONS
AND MANY EXERCISES

PREFACE

THIS volume deals with the Theory of Structures and its application to Practical Design. It is intended for the use of students taking their University Degrees in Engineering, for those entering for the Membership Examinations of the Engineering Institutions, and also for the use of those engaged in the practical design of Engineering Structures. It has, therefore, been planned on a comprehensive basis. As far as space has permitted, reference has been made to the more important results of modern research ; a section on Electric Arc-Welding will be found in Chapter VIII. The book also contains much data which should be of service to the practising Engineer. It is intended to help bridge the gap between abstract theory and its practical application. With this end in view, the text has been illustrated not only with worked examples, but with practical designs, carried out step by step, so that they may easily be followed. Care has been taken that these designs, with their details of construction, while satisfying the theoretical requirements, are such that the practical man will approve.

A word of explanation is desirable with regard to Chapters V and VI. The author has often found that the student associates the principle of least work and its variations with a maximum output of cerebral strain-energy—a state of affairs largely due, he believes, to the forbidding systems of notation frequently adopted. In Chapter V an attempt has been made to render this part of the subject more palatable to the majority. More than one line of approach leads up to the general theory, and if the student finds that he arrives finally at the same point, he is nevertheless advised to render himself familiar with them all, for different problems call for different methods of treatment.

In Chapter VI two systems of notation are used. Where a problem is treated graphically or semi-graphically, the standard conventions used throughout the book (see §§ 30 and 51, Vol. I) are adhered to, namely that + bending tends to make the beam convex upward. In tabular calculations, and secondary stress considerations, a clockwise moment is called positive. To distinguish between

the two conventions, the first is designated by a single suffix M_A, the second by a double suffix M_{ab}.

A Classified Bibliography will be found at the end of each chapter. As in Vol. I, no attempt has been made to be exhaustive, but rather to indicate from whence further information may be obtained. A selected series of examples is also given, with answers; and suggestions for practical designs to be worked out.

The examples have been taken, in part, from the questions set for the B.Sc. (Eng.) examinations, London, and the author would like to record his best thanks to the University of London for permitting this.

With the kind permission of the British Standards Institution, reference has been made in the text to the following British Standard Specifications :—

B.S.S. No. 12—1931/32 : Portland Cement ;

B.S.S. No. 153—1923/33 : Girder Bridges, Parts 3, 4, and 5 ;
Appendix 1—1925/30 : Tables of Unit Loadings for Railways and Highways ;

B.S.S. No. 538—1934 : Metal Arc-Welding as applied to Steel Structures ;

official copies of which can be obtained from the British Standards Institution, 28 Victoria Street, London, S.W. 1, price 2s. 2d. net per copy, post free.

The author's grateful thanks are due to Messrs. Dorman Long & Co., Ltd., for permitting the reproduction in the Appendix of certain pages of their Handbook, giving the properties of the rolled steel sections, and also to the British Standards Institution for their kind consent.

An attempt has been made to give due credit to the many authors to whose work reference has been made in the text, particularly in respect to modern research.

E. H. SALMON.

November, 1937.

CONTENTS

CONTENTS

MATERIALS AND STRUCTURES

VOL. II.—THE THEORY AND DESIGN OF STRUCTURES

CHAPTER I

THE FORCES IN FRAMED STRUCTURES

1. **Co-planar Forces—Preliminary.**—The methods employed for the graphical determination of the forces in plane framework are based on the following propositions, proved in books on statics.

Parallelogram of Forces.—If two forces in the same plane, acting at the point O, (i) Fig. 1, be represented in magnitude and direction by the lines OF_1, OF_2, then their *resultant*, that is to say the single force producing effects equivalent to those produced by the two, is represented in magnitude and direction by the line OR, which is the diagonal of the parallelogram OF_1RF_2. The *sense* of the resultant OR, in this case, will be away from O, as shown by the arrow head. A force RO, equal in magnitude to OR, but of opposite sense, that is to say acting towards O, would exactly balance the two given forces and neutralise their effects. Such a force is called the *equilibrant* of the two forces. The convention that ' a force OR ' means a force acting from O to R, and ' a force RO ' means a force acting from R to O, should be observed.

Triangle of Forces.—It is not necessary to draw the complete parallelogram, for the triangle OF_1R, (ii) Fig. 1, gives all the information which can be obtained from the parallelo-
gram in (i). In this triangle $F_1R =$
OF_2. As the arrow heads are ar-
ranged in (ii), OR represents the
resultant. If the direction of the
arrow head on OR were reversed,
RO would be the equilibrant, and
the three forces would be in equili-

Fig. 1.

brium. In this case the arrows would follow each other round the triangle. It follows that three co-planar forces in equilibrium, acting at a point, may be represented in magnitude and direction by the
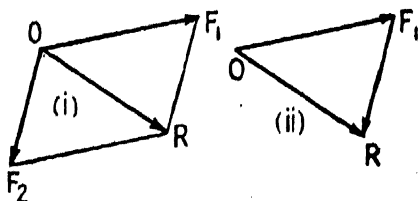
sides of a triangle drawn parallel to the forces, and of which the lengths represent the magnitudes of the forces to scale. The arrow heads representing the sense of the forces will all indicate the same direction round the triangle. Such a triangle
is called the *triangle of forces* for the point.

Polygon of Forces.—By extension, if any number of co-planar forces in equilibrium act at a point, (i) Fig. 2, their resultant or their equilibrant can be determined, in magnitude and direction, by drawing a polygon, (ii), of which the sides are respectively parallel to the forces, and in length represent the magnitude of these forces to scale. The closing line [*ea*, (ii) Fig. 2] is the equilibrant of the given forces ; or, if its sense be reversed, [*ae*, (ii) Fig. 2], it represents their resultant. Even if the forces do not meet

Fig. 2.

in a point, (i) Fig. 3, the magnitude and direction of their resultant, or of their equilibrant, can be found by the polygon of forces, (ii) Fig. 3. Its *position*, relative to the given forces, must be obtained by other means, such as the funicular or link polygon (i) Fig. 3, (see below).

Bow's Notation.—It will be observed that in Figs. 2 and 3, instead of lettering the forces, the spaces between them have been lettered. Thus the force F_1, Fig. 2, is called the force AB, and is represented in the polygon of forces by the line *ab*. This device is commonly known as *Bow's notation*, though it appears to have been due originally to Henrici.

The Funicular or Link Polygon.— As shown above, the magnitude and direction, but not the position, of the resultant of a number of forces acting on a body can be determined by means of the polygon of forces. To obtain the position of the resultant, the *funicular* or *link polygon* may be employed. Let *abcde*, Fig. 3, be the force polygon. Take a pole O,

Fig. 3.

and draw the pencil of rays O*a*, O*b*, O*c*, etc. In the space A, draw a line 1.2 parallel to O*a*; in the space B, a line 2.3 parallel to O*b*; in the space C, a line 3.4 parallel to O*c*; and so on. Suppose that
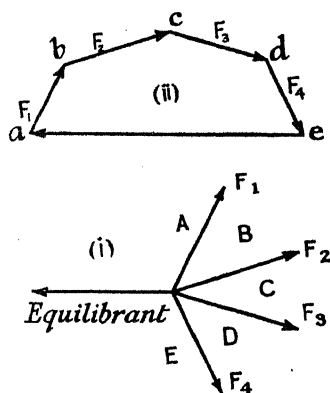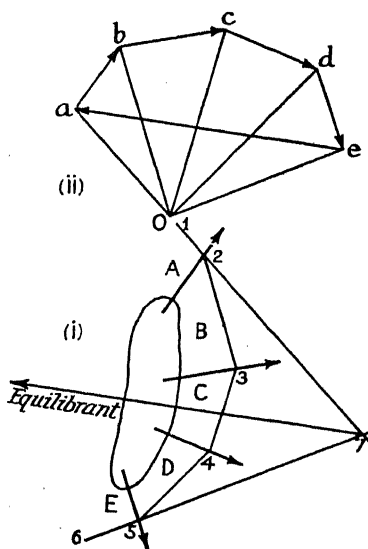
the line 1.2, in the space A, produced if necessary, meet the line 5.6 in the space E, produced if necessary, in the point 7. Then 7 is a point on the line of action of the force *ea*, that is to say on the line of action of the equilibrant or of the resultant, which is thereby determined in position. If the forces are all parallel, the polygon of forces becomes a straight line, *ae*, Fig. 4, of which the length is the magnitude of the resultant. The funicular polygon, 1.2.3.4.5.6, takes the form shown in the figure, and as before, the point 7 fixes the position of the resultant or equilibrant.
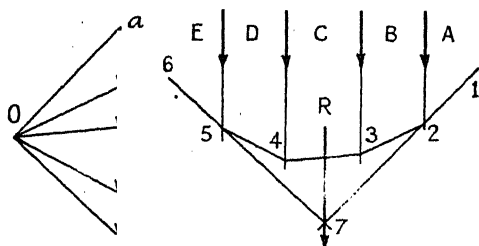
FIG. 4.

2. **Reciprocal Figures.**—Let ABC, (i) Fig. 5, be a triangle, and D any point therein. Join DA, DB, and DC. Bisect all the lines in this figure, and draw lines at right angles to them passing through the points of bisection. Then the three lines at right angles to the sides of the triangle
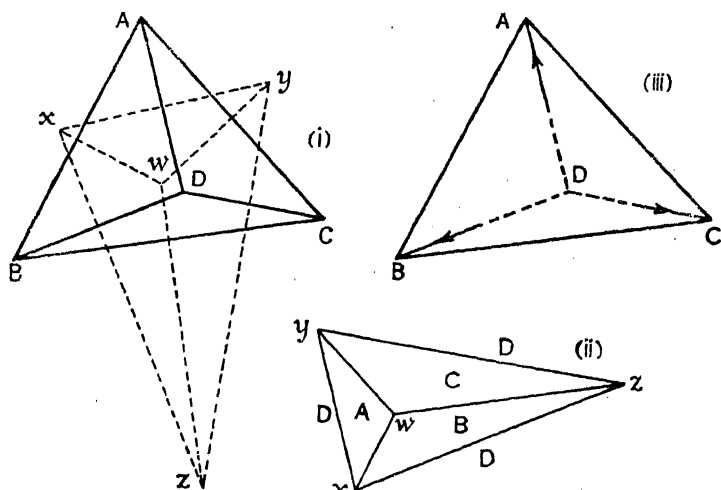
FIG. 5.

ADB will meet in the point x, which is the centre of the circle circumscribing the triangle ADB, and similarly for the other triangles ADC, BDC. Further, the lines *xw, yw*, and *zw* will all meet at the point *w*. If the figure *wxyz*, so formed, be compared with the original figure DABC, it will be found that any three lines in one figure forming a triangle are at right angles to three lines in the other figure which meet in a point. Such figures are said to be *reciprocal*. The dotted figure *wxyz* of (i) Fig. 5 can also be obtained by drawing lines parallel to the

lines of DABC as shown in (ii) Fig. 5. The triangles of (ii) are lettered to correspond with the nodes of (i).

Suppose now that ABC,*(iii) Fig. 5, be a triangular frame subjected to three applied forces DA, DB, and DC, which forces are in equilibrium. These forces may then be represented, in magnitude and direction, by the sides of a triangle. If xy, (ii) Fig. 5, drawn parallel to DA, represent the force DA to scale, then yz, parallel to DC, will represent the force DC, and zx the force DB ; the triangle xyz will, in fact, be the triangle of forces for the three applied forces DA, DB, DC, acting on the frame.

Consider next the point A. There are three forces acting at this point, the applied force DA, and the tensions in the bars AB and AC. Since the point A is at rest, these three forces must be in equilibrium, and can be represented by the sides of a triangle. If the line xy, (ii) Fig. 5, parallel to DA, represent the applied force, the lines wx and yw will represent the forces in the bars AB and AC respectively ; and similarly for the other node points B and C. Hence the lines xy, yz, zx in (ii) represent to scale the external forces in (iii), and the lines wx, wy, wz represent to scale the corresponding internal forces in the bars.

Given therefore a triangular framework acted on by external forces in its own plane, the forces in the bars forming the framework can be determined by drawing a reciprocal figure as defined above. By extension, it is possible to draw a reciprocal figure representing the forces in the members of any plane framework under the action of co-planar forces acting at the nodes, provided that certain conditions set forth below are satisfied. Such a reciprocal figure is called a *stress diagram*, the term ' stress ' in this connection denoting the *total* internal force in a member. As in (ii) above, every such diagram will consist of (*a*) a polygon representing the external forces applied to the framework, and (*b*) lines representing the internal forces in the bars of the framework resulting from the action of the applied forces.

3. Stress Diagrams for Plane Frames.—In order that a complete stress diagram for a plane framework may be drawn the following conditions must be fulfilled :

(1) The framework must be composed of just sufficient bars to divide it into triangles, no more, no less, and the bars must be so arranged that, starting with a triangle as a nucleus, the framework may be built up by the addition of two bars at a time to form a fresh triangle. In such a frame the number of bars will be equal to twice the number of nodes minus three. Frames with less than the requisite number of bars are called *incomplete or imperfect frames*, § 251 ; frames with more than the requisite number of bars are called *redundant frames*, § 71. In neither of these cases can a complete reciprocal figure forming a stress diagram be drawn.

(2) The conditions at the points of support must be statically determinate. No forces or moments must exist which cannot be determined from statical considerations.

* The similarity between the figures ABCD in (i) and (iii) should be observed.

(3) Where three or more bars meet, their central axes must intersect in the same point. The joints are supposed to be frictionless, and to be incapable of resisting a bending moment.

(4) The external or applied forces, together with any external reactions they produce, must be in equilibrium ; and they must be applied at the nodes of the framework. In drawing the polygon of external forces for the stress diagram, these forces must be taken in order (cyclically) round the framework. If the external forces are not applied at the panel points, the loads which they produce at the nodes must first be determined. (i) Fig. 6 shows the method of finding the concentrated loads at the panel points equivalent to a uniform load. For the particular case each load W will evidently be one quarter the total uniform load, and the loads at the end panel points will be W/2.
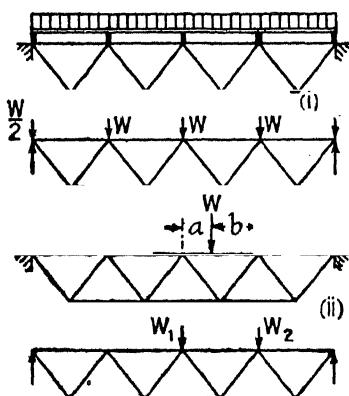
FIG. 6.

In (ii) Fig. 6 the equivalent loads W_1 and W_2 at the panel points can be found by taking moments, $W_1 = Wb/(a+b)$; $W_2 = Wa/(a+b)$.*

Method of Procedure.—As an example of the method of drawing a stress diagram, the case of the plane frame shown in Fig. 7, loaded with two loads W_1 and W_2, will be considered.

First find the reactions R_1 and R_2. In a case like this, where all the loads and also the reactions themselves are vertical, the reactions should be found by the principle of the lever, by taking moments about one of the points of support. If the loads or reactions are not vertical, the methods of § 4 should be used. Having found the reactions, choose a force scale and draw the polygon for the external forces. In this case it is a straight line, ac, (ii) Fig. 7 ; $ab = W_2$, $bc = W_1$, $cd = R_1$ and $da = R_2$. Since the external forces must be in equilibrium, this polygon must be closed, i.e. it must start and finish at a. Remember that the
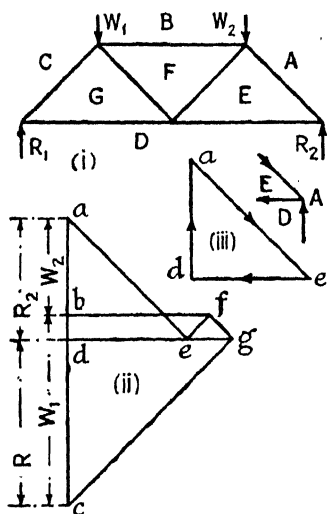
FIG. 7.

* These panel point loads are only approximations. Strictly speaking the continuity, if any, at the panel points should be taken into account. The stress due to local bending must be combined with the direct stress to find the maximum stress in the top flange.

forces must be taken cyclically, that is, in order round the frame. Draw next *ae* parallel to AE, and *de* parallel to DE. Their intersection fixes the point *e*. The triangle *dae* is the triangle of forces for the point of application of R_2. Now the three forces which act at this point must be in equilibrium, and therefore the arrow heads, indicating the sense of these forces, will follow each other round the triangle. This, for clearness, has been shown separately at (iii). It is evident that the force in DE acts away from the joint under consideration, which signifies that the force in DE is a tension. The force in AE acts towards the joint, which signifies that the force in AE is a compression. Having determined the point *e*, (ii) Fig. 7, draw *ef* parallel to EF and *bf* parallel to BF, meeting at *f*. Then *fg* parallel to FG, and *dg* parallel to DG, will fix the point *g*. If the drawing be accurate, a line through *g*, parallel to GC, should pass through *c*. If this last or closing line does not complete the figure, the work is incorrect or inaccurate. The magnitude of the forces in the members can be found by scaling or calculating the length of the lines of the stress diagram. Their sense can be determined by examining the triangle (or polygon) of forces for each joint in turn, as was done above for the triangle *dae*. If the force in the bar act away from the joint under consideration, the force in
the bar is tensile, if towards the joint, the force in the bar is compressive. A consideration as to the probable way in which the structure will deform is often of service as a rough check on the accuracy of this determination.

4. **Stress Diagrams for Plane Frames. The General Case.**—(a) Given a plane frame STUV, Fig. 8, and applied forces W_1, W_2 . . ., to draw the stress diagram, having given the direction, and point of application S, of one reaction (R_1), and only the point of application U of the second (R_2). First find the resultant R of the given forces W_1, W_2 Its magni-
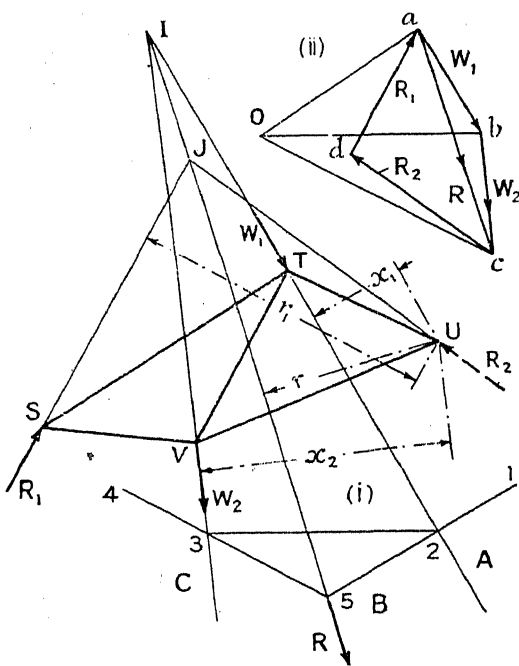

FIG. 8.

tude and direction can be obtained from a force polygon *abc*, (ii), R = *ac*. If there be only two applied forces, W_1 and W_2, the resultant I.5 will pass through their point of intersection I. If there be more than two,

or if the point of intersection be inaccessible, then the position of R may be found by drawing the link polygon 1.2.3.4.5, using the pole O in (ii). In any case I.5 will be parallel to ac. Thus the resultant of the applied forces is completely determined. It is evident that this resultant will be the equilibrant of the two reactions R_1 and R_2. Of these reactions, the points of application S and U are known, and also the direction of one (R_1). Since R, R_1, and R_2 are in equilibrium, their lines of application must meet in a point. Produce the known line of application of R_1 to meet the resultant R in J. Join JU, then JU is the line of application of R_2. Knowing the directions of R_1 and R_2, their magnitudes and sense can be obtained from the force polygon. The line cd, parallel to JU, gives the magnitude of R_2; and da, parallel to SJ, gives the magnitude of R_1. Since the three forces R, R_1 and R_2 are in equilibrium, the arrows in the triangle acd will follow each other round. In this manner the two unknown reactions may be determined. If R_1 does not intersect R in some accessible point, it is necessary to take moments. Take moments about U, the point of application of the reaction R_2, of which the magnitude and direction are both unknown. The moment of R_2 is then zero. (This is often a very useful device when dealing with unknown forces, for otherwise the moment of the unknown force would likewise be unknown.) If r_1 be the perpendicular distance of the reaction R_1 from U, and r be the distance of the resultant R from U, $R_1r_1 = Rr$; from which the magnitude of R_1 can be found. Knowing the magnitude and direction of R_1, the line da in the force polygon, (ii), can be drawn, and hence cd or R_2 is known, both in direction and magnitude. Alternatively, the moment Rr can be obtained by finding $\Sigma(W_1x_1 + W_2x_2 + \ldots)$, i.e. the sum of the moments of all the applied forces about U. Then $R_1r_1 = \Sigma(W_1x + {}_1W_2x_2 + \ldots)$.

Having found R_1 and R_2, *start afresh* with a new force polygon, about which everything is now known. Take the forces in cyclic order, and complete the stress diagram in the usual way, Fig. 9. For clearness, the
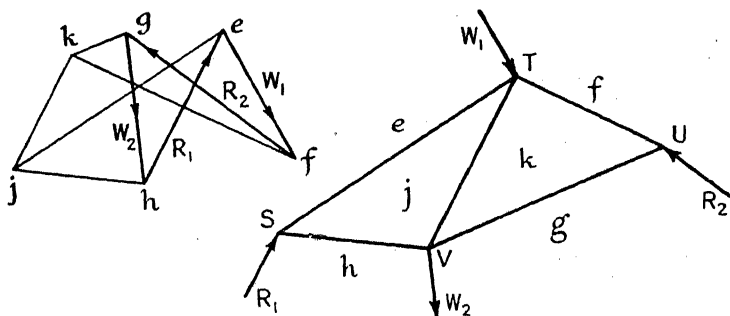
FIG. 9.

force scale is made slightly larger in Fig. 9 than in Fig. 8. The above methods will enable cases such as a roof truss with one end resting on rollers and the other end bolted down to be dealt with, see § 209.

(b) Given a plane frame, and applied forces in equilibrium, to draw the stress diagram if there be three of these forces whose points of application and directions are given, but whose magnitudes are unknown.

Let Fig. 10 represent the frame, and R the resultant of those applied forces which are completely known. R is found by the methods of Case (a). Take moments about I, the intersection of R_2 and R_3, any two of the unknown forces. Then the moments of R_2 and of R_3 about this point will be zero. If r_1 be the distance of R_1, the third unknown force, from I, and r the distance of the resultant R from I, then $R_1 r_1 = Rr$. · This equation determines the magnitude and sense of R_1. The magnitude and sense of R_2 and R_3 can be found by drawing a polygon of the external forces. All the forces acting on the frame are then known and the stress diagram can be drawn in the usual way.
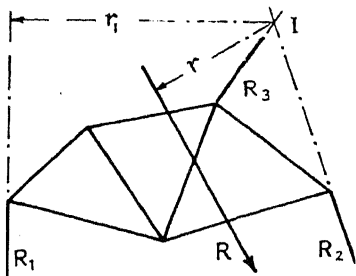
FIG. 10.

(c) In a case like that shown in Fig. 11, it is possible to solve the
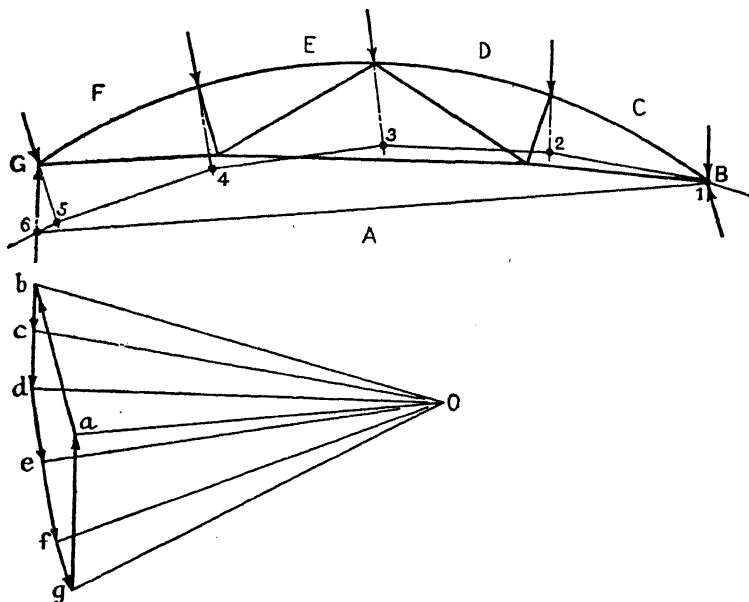
FIG. 11.

problem of Case (a) directly, by means of an application of the funicular polygon. The figure represents a roof truss, acted on by known loads. Of the reactions, GA is vertical, AB is unknown, except that its point of application is B   Draw bg, the load line for the given loads. Take a

pole O, join O*b*, O*c*, O*d*, etc. Draw the funicular polygon 1.2.3.4.5.6, *starting at* B *the point of application of the unknown reaction* AB. 1.2 is parallel to O*c* ; 2.3 is parallel to O*d* ; and so on. This funicular polygon cuts the vertical reaction GA in 6. Since it passes through B it cuts the reaction AB in 1. Hence 6.1 is the closing line of the polygon. Draw O*a* in the force polygon, parallel to 6.1. The vertical line *ga* represents the reaction GA, and the line *ab* represents the reaction AB, in magnitude and direction. Thus all the forces acting on the truss are known, and the stress diagram can be completed.

5. **Hints on Drawing Stress Diagrams.**—It is of service, before starting to draw the stress diagram, to make a rough sketch showing approximately its shape. This is often of assistance in planning the lay-out on the drawing paper, and may save the annoyance of finding out, halfway through, that part of the stress diagram is coming off the paper.

The diagram representing the shape of the frame should be set out to the largest scale which the paper will admit. In many cases a long line in the stress diagram has to be drawn parallel to a short line in the frame diagram, and a small error in the slope of the latter will make a very large error in the stress diagram. In important work, when the lines in the stress diagram are very long, it is desirable to calculate the slope of the member and to set out the line in the stress diagram to the calculated slope. This is particularly necessary in the case of a girder with a curved flange when the radius of curvature is large and there are many panels. A little ingenuity, whereby the geometry of the figure is utilised to obtain the exact slope, will make all the difference to the accuracy of the diagram. If the work is correctly done, the last line should close the figure.

An adjustable set square is of much service for drawing lines in one figure parallel to those in another.

Special Devices.—Special devices are sometimes necessary in order to complete the stress diagram. For example, in a roof truss of the type shown in (i) Fig. 12, the construction breaks down when the point B is
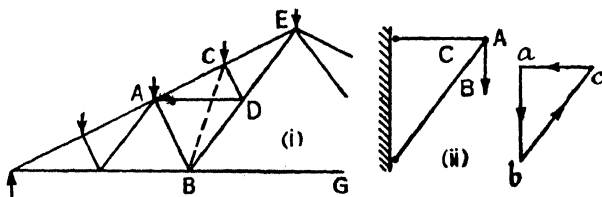
FIG. 12.

reached. This difficulty can be overcome by a device due to Professor Barr. Replace bars AD and DC by a single bar BC ; the stress diagram can now be carried on. Having determined, by means of the interpolated bar, the forces in CE and BG, that bar may be removed, and AD and DC reinserted, when the complete diagram can be drawn. An alternative method is to calculate the force in the bar BG by the method of sections,

§ 8.   Knowing this force the diagram can be completed.   The geometrical symmetry of the stress diagram itself, see Fig. 13, is often a help.

In many cases the outline of the frame itself may be used as its own stress diagram.   A simple instance is shown at (ii) Fig. 12.   The stress diagram (i.e. the triangle of forces for the point A) is a triangle of the same shape as the frame itself.   The lengths of the sides of the frame are
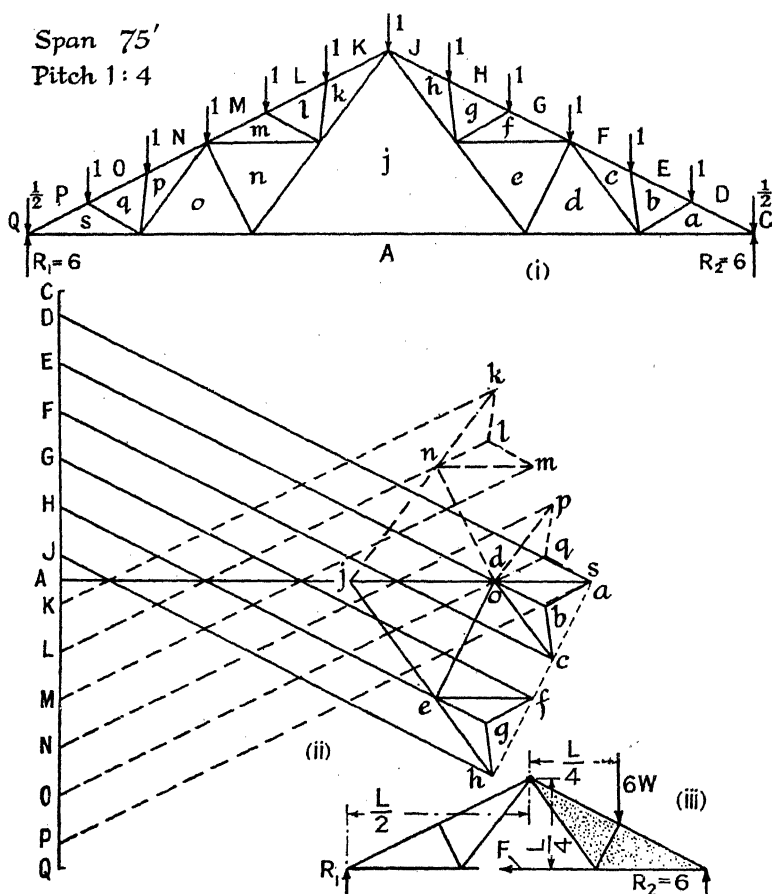
FIG. 13.

known, and these are evidently proportional to the forces in the bars, which may be found by means of a slide rule.

One of the quickest and most accurate methods of determining the forces in a plane framework is to draw the stress diagram and then to calculate the length of the lines of which it is formed.   In many cases the shape of the diagram facilitates this method.

As a check on the graphical process it is well to calculate the force in some of the main members of the frame, even while the stress diagram

is being drawn.   For this purpose the method of sections, § 8, should be used.   In important frames the forces in all the bars should be checked by that method.

6. Roof Truss.—The stress diagrams for the roof truss of an open shed are given in Figs. 13 and 14.   This truss is designed in § 212.   It is 75 feet in span, and is supported on columns.   Fig. 13 is the stress diagram for the dead loads, i.e. for the weight of the roof and of any snow upon it.   Since all the panels of the rafters are of equal length, it is convenient to draw the diagram on the assumption that the loads at
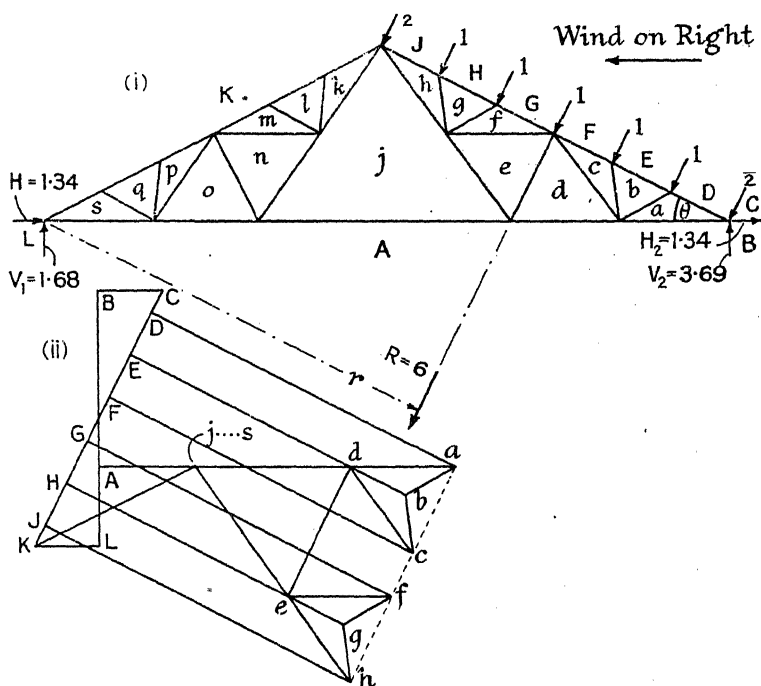
FIG. 14.

the panel points are of unit magnitude.   Those at the two ends will each be ½ unit.   All the loads will be vertical.   Each reaction is vertical, and since there are twelve panels its magnitude will be six units.   Starting from the right-hand end, the stress diagram, (ii), presents no difficulty until the point d is reached, when, in order to continue, the force in the bar Aj must be calculated by the method of sections, § 8.   Cutting Aj, and taking moments about the apex, (iii) Fig. 13,

$$R_2 \times \frac{L}{2} - 6W \times \frac{L}{4} - F \times \frac{L}{4} = 0$$

where F is the force in Aj.   W = 1 unit, $R_2 = 6$ units, hence F = 6 units. The point j in the stress diagram (ii) is thus determined, and the diagram

FORCES IN MEMBERS OF A ROOF TRUSS. FIGS. 13 AND 14

Bar No.	Lettered.	Unit Load Forces.			Actual Forces.			
		Dead.	Wind on Right.	Wind on Left.	Dead.	Wind on Right.	Wind on Left.	Maximum.
1	Da	− 12·30	− 7·25	− 3·76	− 7·01	− 3·48	− 1·81	− 10·49
2	Eb	− 11·26	− 6·57	− 3·76	− 6·42	− 3·15	− 1·81	− 9·57
3	Fc	− 11·40	− 7·25	− 3·76	− 6·50	− 3·48	− 1·81	− 9·98
4	Gf	− 10·96	− 7·25	− 3·76	− 6·25	− 3·48	− 1·81	− 9·73
5	Hg	− 9·91	− 6·57	− 3·76	− 5·64	− 3·15	− 1·81	− 8·79
6	Jh	− 10·06	− 7·25	− 3·76	− 5·74	− 3·48	− 1·81	− 9·22
7	Aa	+ 11·00	+ 7·61	+ 2·02	+ 6·27	+ 3·65	+ 0·97	+ 9·92
8	Ad	+ 9·00	+ 5·37	+ 2·02	+ 5·13	+ 2·58	+ 0·97	+ 7·71
9	je	+ 3·00	+ 3·35	...	+ 1·71	+ 1·61	...	+ 3·32
10	jh	+ 5·00	+ 5·59	...	+ 2·85	+ 2·68	...	+ 5·53
11	ab	− 1·07	− 1·21	...	− 0·61	− 0·58	...	− 1·19
12	bc	− 1·07	− 1·21	...	− 0·61	− 0·58	...	− 1·19
13	cd	+ 2·00	+ 2·24	...	+ 1·14	+ 1·08	...	+ 2·22
14	de	− 2·68	− 3·00	...	− 1·53	− 1·44	...	− 2·97
15	ef	+ 2·00	+ 2·24	...	+ 1·14	+ 1·08	...	+ 2·22
16	fg	− 1·07	− 1·21	...	− 0·61	− 0·58	...	− 1·19
17	gh	− 1·07	− 1·21	...	− 0·61	− 0·58	...	− 1·19
18	Aj	+ 6·0	+ 2·02	+ 2·02	+ 3·42	+ 0·97	+ 0·97	+ 4·39
117	lk	− 1·07	...	− 1·21	− 0·61	...	− 0·58	− 1·19
116	ml	− 1·07	...	− 1·21	− 0·61	...	− 0·58	− 1·19
115	nm	+ 2·00	...	+ 2·24	+ 1·14	...	+ 1·08	+ 2·22
114	on	− 2·68	...	− 3·00	− 1·53	...	− 1·44	− 2·97
113	po	+ 2·00	...	+ 2·24	+ 1·14	...	+ 1·08	+ 2·22
112	qp	− 1·07	...	− 1·21	− 0·61	...	− 0·58	− 1·19
111	sq	− 1·07	...	− 1·21	− 0·61	...	− 0·58	− 1·19
110	jk	+ 5·00	...	+ 5·59	+ 2·85	...	+ 2·68	+ 5·53
109	jn	+ 3·00	...	+ 3·35	+ 1·71	...	+ 1·61	+ 3·32
108	Ao	+ 9·00	+ 2·02	+ 5·37	+ 5·13	+ 0·97	+ 2·58	+ 7·71
107	As	+ 11·00	+ 2·02	+ 7·61	+ 6·27	+ 0·97	+ 3·65	+ 9·92
106	Kk	− 10·06	− 3·76	− 7·25	− 5·74	− 1·81	− 3·48	− 9·22
105	Ll	− 9·91	− 3·76	− 6·57	− 5·64	− 1·81	− 3·15	− 8·79
104	Mm	− 10·96	− 3·76	− 7·25	− 6·25	− 1·81	− 3·48	− 9·73
103	Np	− 11·40	− 3·76	− 7·25	− 6·50	− 1·81	− 3·48	− 9·98
102	Oq	− 11·26	− 3·76	− 6·57	− 6·42	− 1·81	− 3·15	− 9·57
101	Ps	− 12·30	− 3·76	− 7·25	− 7·01	− 1·81	− 3·48	− 10·49

may be completed. It should be noted that all the points a, c, f, h, lie on a straight line.

The forces in the members can be scaled from the diagram, using the

load scale, or may be calculated by trigonometrical methods. They
are tabulated in col. 3 of the preceding table. Tensions are called +,
compressions − . The actual dead load at a panel point, see ¶ 4,
§ 212, is 0·57 ton. Hence the actual forces due to the dead load
are obtained by multiplying the figures in col. 3 by 0·57; they are
tabulated in col. 6. In symmetrical frames, symmetrically loaded,
as in the present case, only one half the stress diagram need be
drawn. The method of numbering the bars in the Table should be
noted ; the force in bar No. 101 will be the same as that in bar No. 1,
and so on.

The stress diagram for the wind on the right is given in Fig. 14.
Since the roof covers an open shed, there will be no forces on the side
opposite to that from which the wind blows, see § 50. The method
of finding the reactions is set forth in § 209, (v) and (vi), Fig. 328.
With unit loads at the panel points the resultant wind load R is 6 units ;
the leverage r can be calculated or scaled, and is 46·1 ft. Hence
$V_2 = Rr/L = 6 \times 46 \cdot 1 \div 75 = 3 \cdot 69$ units. $\theta = 26° 34'$. $V_1 + V_2 =$
$R \cos \theta = 5 \cdot 37$ units, and $V_1 = 1 \cdot 68$ units. The horizontal reactions
$H_1 = H_2 = \frac{1}{2}R \sin \theta = 1 \cdot 34$ units. These are represented in the force
polygon, (ii) Fig. 14, by KL and BC ; and LA and AB represent V_1 and
V_2 respectively. KLABCK is the polygon of external forces, and the
stress diagram can be drawn in the usual way, use being made of the
method of sections to find the force in bar Aj. The forces in the bars due
to the wind on the right, with unit load at each panel point, are given
in col. 4 of the Table. The actual wind load at a panel point is 0·48 ton,
¶ 5, § 212, hence the actual forces due to the wind on the right are obtained
by multiplying the figures in col. 4 by 0·48 ; these forces are tabulated
in col. 7.

In this particular case, since the method of supporting the ends of
the truss is exactly the same on both sides, the stress diagram for the
wind on the left will be of exactly the same shape as that for the wind
on the right, but reversed. The forces in the bars for the wind on the
left, col. 5, can therefore be written down from those in col. 4, noticing
that in col. 5 the force in bar No. 1 is equal to that in bar No. 101, col. 4,
and so on. The actual forces for the wind on the left, col. 8, follow from
col. 5 as before.

Had the method of support at the two sides been different, as in (i)
and (iii) Fig. 328, for example, separate stress diagrams for the wind on
the right and for the wind on the left would have been required, and a
separate determination of the forces in col. 5 necessary.

The maximum force in any bar is the force in col. 6 plus that in col. 7,
or the force in col. 6 plus that in col. 8, i.e. (dead + wind on right) or
(dead + wind on left) whichever be the greater. These maximum
stresses are tabulated in col. 9, and are used to find the dimensions of
the members, § 212. No impact factor need be used for wind loads.
Should the wind reverse the stress in a bar, it must be designed to act
both as a tie and a strut.

7. Separation of Frames.—It has been pointed out that when more bars exist in a frame than are necessary to divide it into triangles, the stress diagram cannot be drawn by the methods just considered, see § 3. (i) Fig. 15, which represents part of a *lattice girder* in which the diagonals are doubled, is such a frame. One diagonal in each bay is redundant. (ii) and (iii) Fig. 15 are frames (N girders) without redundant members, for which stress diagrams can be drawn. If the girder of (ii) be superposed on that of (iii), the girder of (i) is obtained. The

FIG. 15.

forces in the bars of a lattice girder such as (i) can therefore be found by dividing it into two component girders, as shown at (ii) and (iii), and finding the forces in these. When a bar exists in both component girders, the actual force in it will be the algebraic sum of the two component forces.
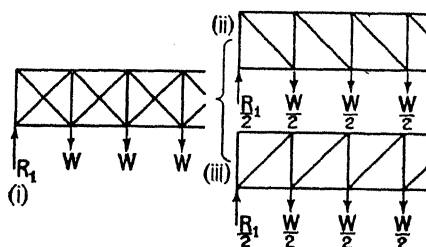
In (i) Fig 16 two N girders of the type shown in (ii) Fig. 15 are superposed one on the other, but the second is shifted half a panel along relatively to the first. This necessitates an extra half panel at each

FIG. 16.

end of the girder as shown at (iii). The combination, (i) Fig. 16, is called a *Linville Truss*.
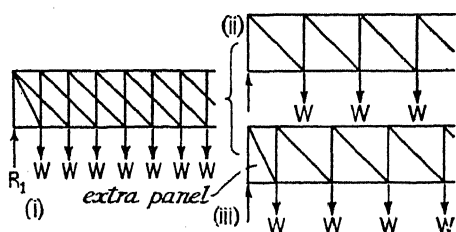
A *double Warren girder*, (i) Fig. 17, splits up into two single Warren girders, (ii) and (iii). In this case the angle which the diagonals make with the horizontal is usually 45°, instead of 60° as in the normal Warren girder, Fig. 275.

A *Bollmann truss*, (i) Fig. 18, can be split up into three component frames (ii), (iii) and (iv) ; and a *Fink truss*, (i) Fig. 19, also can be dissected into three component frames. In this form of truss, frame (iv) has to carry

FIG. 17.

the reactions at the centre of the span from frames (ii) and (iii), as well as its own share of the load.
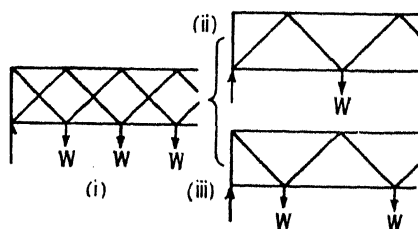
It should be pointed out that this method of treating frames with redundant bars is only an approximation, though it is often sufficiently

accurate for practical purposes. More exact methods of treatment will be found in Chapter V.
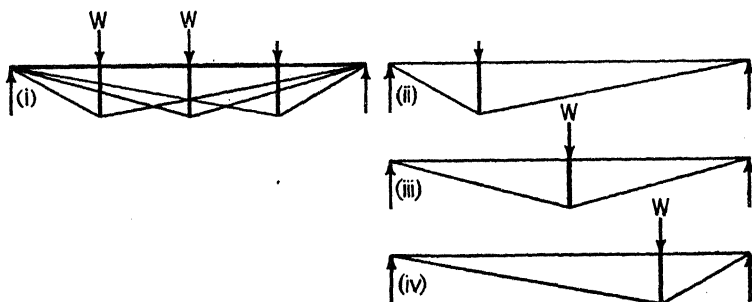
FIG. 18.
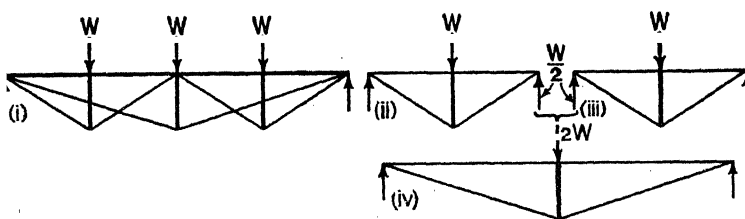
FIG. 19.
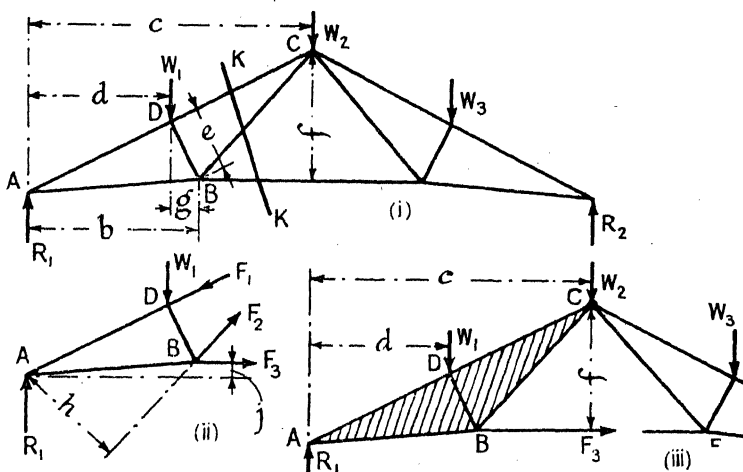
FIG. 20.

8. Method of Sections.—Let (i) Fig. 20 represent a plane, framed structure, and suppose it cut by a section KK. Consider that portion of the frame to the left of KK, (ii) Fig. 20. In place of the three bars which are cut, introduce three forces F_1, F_2, and F_3, of the same

magnitude and acting in the same direction as the stresses in the cut bars. Then the portion of the frame shown in (ii) will be in equilibrium under the forces acting upon it, just as when it formed part of the whole framework. This condition enables the unknown forces F_1, F_2, and F_3 to be determined, and these unknown forces are the forces in the cut bars. By successive applications of the method, the forces in all the bars of the frame can be found. To determine F_1, F_2, and F_3, three methods are usually available :

(a) by taking moments ;
(b) by equating components ;
(c) graphically, by the polygon of forces.

In the case under consideration it will be most convenient to take moments. To find F_1, take moments about B, the point of intersection of F_2 and F_3, the other two unknown forces. Their moment about B is zero, and the fact that their magnitude is at present unknown is immaterial. Assume F_1 to act towards A, and call clockwise moments positive. Then, see (i),

$$R_1 b - W_1 g - F_1 e = 0 \; ; \; \text{and} \; F_1 = \frac{R_1 b - W_1 g}{e}.$$

If the numerical value of this fraction comes out negative, it signifies that the direction assumed for F_1 is incorrect, and that the force acts in the reverse direction to that assumed. The sign of the fraction is not an indication that the force is essentially tensile or compressive. Similarly, to find F_3, take moments about C, the point of intersection of F_1 and F_2. If F_3 act away from A,

$$R_1 c - W_1 (c - d) - F_3 f = 0 \; ; \; \text{and} \; F_3 = \frac{R_1 c - W_1 (c - d)}{f}.$$

All the forces except F_2 are now known. Moments can therefore be taken about any convenient point, say A, in order to determine F_2. Then, see (ii),

$$R_1 \times 0 + W_1 d + F_3 j + F_1 \times 0 - F_2 h = 0$$

from which F_2 can be found.

In many cases it is not necessary to cut more than one bar. Suppose, for example, it be desired to find the force in BE, (iii) Fig. 20. Cut this bar and replace it by the force F_3. The tendency of F_3 is to rotate the shaded portion of the truss about the point C. The moment about C of the forces acting on this shaded portion must evidently be zero, hence

$$R_1 c - W_1 (c - d) = F_3 f \; ; \; \text{and} \; F_3 = \frac{R_1 c - W_1 (c - d)}{f}$$

which determines the magnitude of F_3. This application of the method is very useful in checking the accuracy of a stress diagram.

The weakness of the method of sections is that it is often more laborious accurately to discover the lever arms of the forces than to draw a stress diagram ; and if the lever arms be merely scaled from a diagram of the frame, this method of determining the forces in the bars is not necessarily more accurate than the stress diagram.

In a case like Fig. 21, where the majority of the members of a frame are either horizontal or vertical, and the loads also are vertical, the
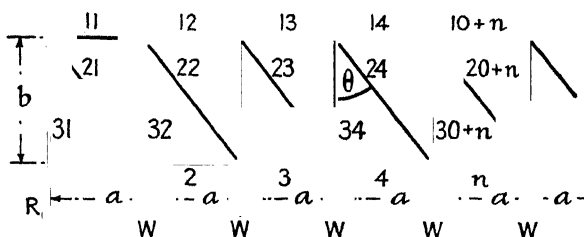
FIG. 21.

method of sections leads to very simple means of determining the forces in the bars. The method of numbering the bars should be observed.

Forces in Flanges.—Cut bar No. 4 ; the frame tends to swing about joint 13.14. Take moments about this joint,

$$F_4 \cdot b = R_1 \times 3a - W(a + 2a) \;;$$

and, generally,

$$F_n \cdot b = R_1(n-1)a - W\{a + 2a + 3a + \; . \; . \; + (n-2)a\}$$
$$= R_1(n-1)a - Wa\{1 + 2 + 3 + \; . \; . \; + (n-2)\}$$

whence, $\quad F_n = \dfrac{(n-1)a}{b} \left\{ R_1 - W\dfrac{n-2}{2} \right\} \;;$

by giving successive values 1, 2, 3, etc. to n, this formula will give the force in each member of the lower flange.

Cut bar No. 13 ; the frame will tend to swing about joint 3.4. Take moments about this joint,

$$F_{13} \cdot b = R_1 \times 3a - W(a + 2a)$$

and, generally,

$$F_{(10 + n)} b = R_1 \cdot na - Wa\{1 + 2 + 3 + \; . \; . \; + (n-1)\}$$

whence, $\quad F_{(10 + n)} = \dfrac{na}{b} \left\{ R_1 - W\dfrac{n-1}{2} \right\} \;;$

by giving successive values 1, 2, 3, etc., to n, this formula will give the forces in the bars forming the upper flange.

Forces in Verticals.—Cut the frame by a diagonal section KK, as shown in Fig. 22. Then the algebraic sum of the vertical forces on the part cut off must be zero ; hence,

$$R_1 - 3W - F_{34} = 0, \quad F_{34} = R_1 - 3W,$$

and, generally,

$$F_{(30 + n)} = R_1 - (n - 1)W.$$
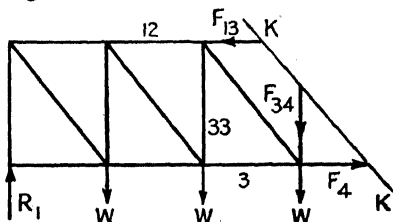
This is an application of method (*b*), p. 16, of applying the method of sections, namely by equating the components in any one direction of all the forces acting on the portion

FIG. 22.

of the frame cut off by the section. By equating horizontal components, it follows that $F_{13} = F_4$ in magnitude, Fig. 22.

Forces in the Diagonals.—The force in bar No. 34 is evidently the vertical component of the force in bar No. 24, Fig. 21, since no external vertical force acts at joint 13.14. Therefore $F_{34} = F_{24} \cos \theta$, and, generally,

$$F_{(20+n)} = F_{(30+n)} \sec \theta = \{R_1 - (n-1)W\} \sec \theta = \{R_1 - (n-1)W\} \frac{\sqrt{a^2 + b^2}}{b}.$$

Where, as in cases like the above, the type of frame lends itself to such treatment, the forces in the bars may be found very quickly by this method.

Equating Components.—The method of equating components used in the above simple example can be extended to find the forces in the bars of any statically determinate plane framework. Let OF, (i) Fig. 23, represent a force F acting at the point O, and making angles θ and ϕ with the two co-ordinate axes Ox and Oy. Then its components parallel to the axes of x and y are $F \cos \theta$ and $F \cos \phi$ respectively. If there be several forces acting at O, the sum of their components, acting parallel to these axes, will be $\Sigma F \cos \theta$ and $\Sigma F \cos \phi$; due account must be taken of sign. Thus components acting in the directions Ox and Oy may be considered as positive, and those acting in the reverse directions as negative. But the sum of the components in any one direction of all these forces must be equal to the component, acting in the same direction, of the resultant of the forces. If R be this resultant, and θ_R and ϕ_R be the angles which it makes with Ox and Oy respectively, then its components parallel to these axes are $R \cos \theta_R$, and $R \cos \phi_R$; and $R \cos \theta_R = \Sigma F \cos \theta$; $R \cos \phi_R = \Sigma F \cos \phi$. But

FIG. 23.

$$R^2 = (R \cos \theta_R)^2 + (R \cos \phi_R)^2 = (\Sigma F \cos \theta)^2 + (\Sigma F \cos \phi)^2$$

from which R can be determined, and hence θ_R and ϕ_R.

At any panel point of a plane frame, let R be the resultant of the external forces acting there, and suppose that not more than two bars meet at the panel point, the forces in which it is desired to determine. Then R will be the equilibrant of these two forces F_1 and F_2, (ii) Fig. 23, and since the panel point is in equilibrium, the sum of the components in any one direction of all the forces acting there must be zero. Hence, resolving parallel to Ox and Oy,

$$F_1 \cos \theta_1 + F_2 \cos \theta_2 + R \cos \theta_R = 0$$
$$F_1 \cos \phi_1 + F_2 \cos \phi_2 + R \cos \phi_R = 0 ;$$

from these equations F_1 and F_2, the unknown forces in the bars, can be found. The correct signs must be given to the terms $R \cos \theta_R$ and
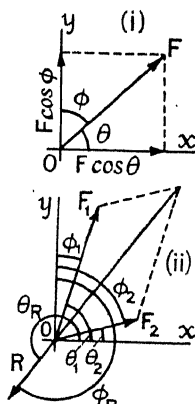
$R \cos \phi_R$ and also to $\cos \theta_1$, $\cos \phi_1$ . . ., when a $+$ sign for F_1 or F_2 will indicate a force acting away from the joint O and therefore a tension, and conversely for a $-$ sign. Note that $+\theta$ is always measured in an anticlockwise direction from Ox, and $+\phi$ in a clockwise direction from Oy. If, in addition to F_1 and F_2, there be other internal forces acting in bars meeting at O, which forces are known, the equations become

$$F_1 \cos \theta_1 + F_2 \cos \theta_2 + \Sigma \, F_k \cos \theta_k + R \cos \theta_R = 0$$
$$F_1 \cos \phi_1 + F_2 \cos \phi_2 + \Sigma \, F_k \cos \phi_k + R \cos \phi_R = 0,$$

where $F_k \cos \theta_k$ and $F_k \cos \phi_k$ represent the components of the known internal forces. Again F_1 and F_2 can be found. This process, applied to every joint in turn of a statically determinate plane frame, will determine the forces in all the bars.

9. Space Frames. Non-Coplanar Forces.—If the bars in a framework do not all lie in one plane, the frame is called a *space frame* in contradistinction to a *plane frame*. The methods of finding the forces in the bars of a space frame are essentially the same as those employed in the case of a plane frame, though the application is rather more complicated.

Space Polygon of Forces. — Given a number of forces acting at a point, but not necessarily all in the same plane, their resultant or equilibrant can be found by drawing a space polygon of forces, of which the sides are respectively parallel to the forces, and in length represent the magnitude of these forces to scale. The closing line is the equilibrant of the given forces ; or, if its direction be reversed, it represents their resultant. Thus if F_1, F_2, and F_3, (i) Fig. 24, be three forces acting at a point O, represented in magnitude and direction by the sides of the figure OABC drawn parallel to the forces, (ii) Fig. 24, the force F_4, represented in magnitude and direction by the closing line CO, is the equilibrant of F_1, F_2, and F_3. Conversely, a force OC, acting in the opposite direction to CO, will be the resultant of F_1, F_2, and F_3. An application of this theorem involves drawing the plan and elevation of the space polygon of forces, see (iii) and (iv) Fig. 27. The sides of the plan and elevation of this polygon will be respectively parallel to the plan and elevation of the forces, and the closing line, in plan and elevation, will represent the plan and elevation of the equilibrant or resultant, as the case may be. A word of caution is necessary : in order to scale the length of a line, its *true length* must be found by the well-known geometrical construction. Only when this is done can the magnitude of the force which it represents be determined.

Equating Components.—As in the case of co-planar forces, the resultant
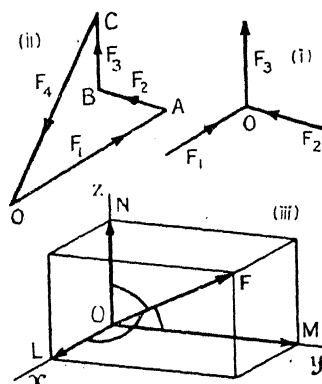
FIG. 24.

of a number of forces acting at a point, but not all lying in the same plane, can be found by determining the components, parallel to the co-ordinate axes, of all the forces. The algebraic sum of all the components parallel to any one axis will be equal to the component of the resultant parallel to that axis. Let OF, (iii) Fig. 24, represent a force F acting at the point O, and let l, m, and n be the direction cosines of the force. That is to say, l is the cosine of the angle xOF, m is the cosine of the angle yOF, and n the cosine of the angle zOF, where Ox, Oy, and Oz are the directions of three co-ordinate axes. Then the component of the force F in the direction of the x axis is Fl; and if there be several forces acting at the point, the sum total of their components in the direction Ox is ΣFl, which is equal to R . l_R, where R is the magnitude of the resultant and l_R its direction cosine. Thus R . $l_R = \Sigma$Fl; and similarly, R . $m_R = \Sigma$Fm; and R . $n_R = \Sigma$Fn. Due account must be taken of the sign of each of the forces. Knowing its three components, the magnitude of R is easily determined, for

$$R^2(l_R{}^2 + m_R{}^2 + n_R{}^2) = (\Sigma Fl)^2 + (\Sigma Fm)^2 + (\Sigma Fn)^2 ;$$
and $$l_R{}^2 + m_R{}^2 + n_R{}^2 = 1.$$
Hence, $$R^2 = (\Sigma Fl)^2 + (\Sigma Fm)^2 + (\Sigma Fn)^2.$$

Having found R, the values of l_R, m_R, and n_R follow at once ($l_R = \Sigma Fl/R$ and so on), and R is completely determined.

10. Forces in the Members of Space Frames.—Given a space frame acted on by a series of external forces, it is possible, by means of the above propositions and their converses, to find the forces in all the members, provided,

(1) that the framework be composed of just sufficient bars to form tetrahedrons, no more, no less, and that it be so arranged that, starting with a tetrahedron (6 bars, four joints) as a nucleus, it might be built up by the addition of three bars at a time to form a fresh tetrahedron. In such a framework the number of bars will be equal to three times the number of joints minus six ;

(2) that where three or more bars meet, their central axes must intersect in the same point, and that the joints are frictionless, and incapable of resisting a bending moment ;

(3) that the external or applied forces, together with the external reactions which they produce, are in equilibrium, and that they are applied at joints of the framework.

Graphical Methods.—Suppose that a number of external forces act at a joint A, (i) Fig. 25, which is the point of intersection of the three bars Nos. 1, 2 and 3, and that it is required to find the forces F_1, F_2 and F_3 in these bars. Find the resultant R, of the external forces, by either of the methods given in § 9. Let AI be the line of intersection of the plane containing R and bar No. 1 with the plane containing bars Nos. 2 and 3 ; and, neglecting for a moment the forces in bars Nos. 2 and 3, suppose that a force $F_{2.3}$ acts along AI, such that the forces R, F_1, and $F_{2.3}$ are in equilibrium. Since they lie in one plane they can be represented in

magnitude and direction by the sides of a triangle, (ii) Fig. 25. The magnitudes of F_1 and $F_{2.3}$ are thus determined. But the forces R, F_1, F_2, and F_3 are in equilibrium ; therefore $F_{2.3}$ must be the resultant of F_2 and F_3. A second triangle of forces, (iii), drawn in the plane containing F_2 and F_3 will determine these two forces. Applications of this method
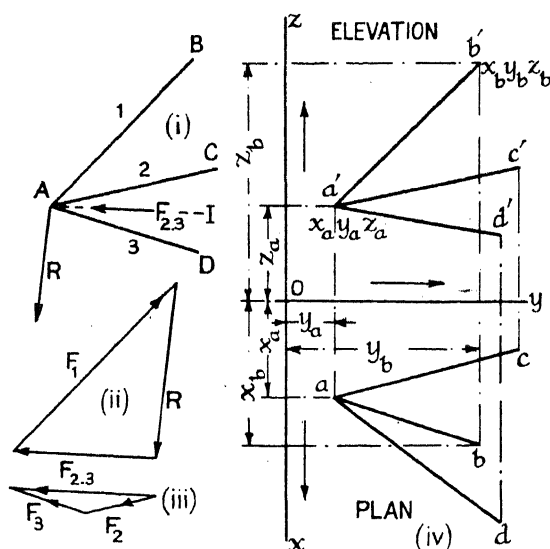
FIG. 25.

will be found in § 11. By thus treating each node of a space frame in turn, the forces in all the bars can be found.

Alternatively, a complete stress diagram (drawn in plan and elevation) may be constructed, but the work is usually complicated.

Equating Components.—Since the sum of the components in any one direction of all the forces acting at A, Fig. 25, must be zero, by resolving parallel to Ox, Oy, and Oz,

$$\left.\begin{array}{l} F_1 l_1 + F_2 l_2 + F_3 l_3 + R.l_R = 0 \\ F_1 m_1 + F_2 m_2 + F_3 m_3 + R.m_R = 0 \\ F_1 n_1 + F_2 n_2 + F_3 n_3 + R.n_R = 0 \end{array}\right\} \qquad . \qquad . \quad (1)$$

where l_R, m_R and n_R are the direction cosines of R, the resultant of the external forces at A, and $l_1 m_1 n_1$, $l_2 m_2 n_2$, $l_3 m_3 n_3$ are the direction cosines of the bars. In these equations everything is known except F_1, F_2, and F_3, the forces in the bars, and there are three equations to determine the three unknowns, which can be found in the usual way. The values are given by the determinants :

$$\frac{F_1}{\begin{vmatrix} l_2 & l_3 & l_R \\ m_2 & m_3 & m_R \\ n_2 & n_3 & n_R \end{vmatrix}} = \frac{-F_2}{\begin{vmatrix} l_1 & l_3 & l_R \\ m_1 & m_3 & m_R \\ n_1 & n_3 & n_R \end{vmatrix}} = \frac{F_3}{\begin{vmatrix} l_1 & l_2 & l_R \\ m_1 & m_2 & m_R \\ n_1 & n_2 & n_R \end{vmatrix}} = \frac{R}{\begin{vmatrix} l_1 & l_2 & l_3 \\ m_1 & m_2 & m_3 \\ n_1 & n_2 & n_3 \end{vmatrix}} \qquad (2)$$

If, in addition to F_1, F_2, and F_3, there be other internal forces acting in bars meeting at A, which forces are known, eq. (1) becomes

$$
\begin{aligned}
F_1 l_1 + F_2 l_2 + F_3 l_3 + \Sigma F_k l_k + R.l_R &= 0 \\
F_1 m_1 + F_2 m_2 + F_3 m_3 + \Sigma F_k m_k + R.m_R &= 0 \\
F_1 n_1 + F_2 n_2 + F_3 n_3 + \Sigma F_k n_k + R.n_R &= 0
\end{aligned}
\quad . \quad (3)
$$

where $F_k l_k$, $F_k m_k$, $F_k n_k$, represent the components of the known internal forces. From these equations F_1, F_2, and F_3 can be found as before. If the correct signs be given to $R.l_R$, $R.m_R$ and $R.n_R$, and also to the direction cosines ($+$ directions for the angles are indicated in (iii) Fig. 24) a $+$ sign for F_1, F_2 or F_3 will indicate a force acting away from the joint A and therefore a tension, and conversely for a $-$ sign. Provided that there be not more than three unknown forces at a node, these can always be determined, and by applying the process to each joint in turn, the force in every member of a space frame may be found.

Tension Coefficients.—A useful method of determining the forces in the bars of space frames has been suggested by Professor Southwell.[23] Let the magnitude of the force F in a bar be expressed in the form $F = \tau L$, where L is the length of the bar and τ is called the *tension coefficient* for the bar. If in eq. (1), $R.l_R = X$, $R.m_R = Y$, $R.n_R = Z$, be the components of the resultant external force R, measured parallel to the three co-ordinate axes, eq. (1) may be written,

$$
\begin{aligned}
\tau_1 L_1 l_1 + \tau_2 L_2 l_2 + \tau_3 L_3 l_3 + X &= 0 \\
\tau_1 L_1 m_1 + \tau_2 L_2 m_2 + \tau_3 L_3 m_3 + Y &= 0 \\
\tau_1 L_1 n_1 + \tau_2 L_2 n_2 + \tau_3 L_3 n_3 + Z &= 0
\end{aligned}
\quad . \quad (4)
$$

Now $L_1 l_1$ is the projection of the bar AB (bar No. 1) on to the x axis, i.e. $(x_b - x_a)$, (iv) Fig. 25; $L_1 m_1$ the corresponding projection on to the y axis $= (y_b - y_a)$ and so on. Hence eq. (4) can be written

$$
\begin{aligned}
\tau_1(x_b - x_a) + \tau_2(x_c - x_a) + \tau_3(x_d - x_a) + X &= 0 \\
\tau_1(y_b - y_a) + \tau_2(y_c - y_a) + \tau_3(y_d - y_a) + Y &= 0 \\
\tau_1(z_b - z_a) + \tau_2(z_c - z_a) + \tau_3(z_d - z_a) + Z &= 0
\end{aligned}
\quad (5)
$$

in which equations the lengths $(x_b - x_a)$ . . . $(z_d - z_a)$ can be measured directly off the plan and elevation of the frame—a great advantage. Solving eq. (5) for τ_1, τ_2 and τ_3, the unknown forces in the bars are at once obtained by multiplying by the lengths of the bars ; $F_1 = \tau_1 L_1$, . . . In an ordinary space frame, three equations such as eq. (5) are written down for every node. These equations, treated as simultaneous, furnish values of τ, and hence of F, for every bar. The conventions as to sign are the same as for eq. (1). A worked example will be found in § 11.

11. Sheer Legs and Tripods.—Consider the forces in a pair of sheer legs, (i) Fig. 26. The two legs or sheer poles AC, AD, are connected together at the point A, and supported at C and D in such a manner that they can swing about the line CD as an axis. The point A is supported by a back stay AB, which can be lengthened or shortened in order to vary the overhang GE, (ii). Alternatively, to effect the same purpose, the

point B may be moved in and out by means of a screw. Sheer legs are used for lifting heavy weights, which are slung from the point A. The forces in the members can be found as follows : The load W and the back stay lie in one plane, which intersects the plane of the legs in the line GA. Let $F_{2.3}$ be the force which, acting along GA, would maintain the load W and the force in the back stay in equilibrium. Then $F_{2.3}$ must be the resultant of the forces in the legs. The magnitude of F_1, the force in the back stay, and of $F_{2.3}$, can be obtained by drawing the triangle of forces (iv) ; $F_{2.3}$ can afterwards be resolved along the two
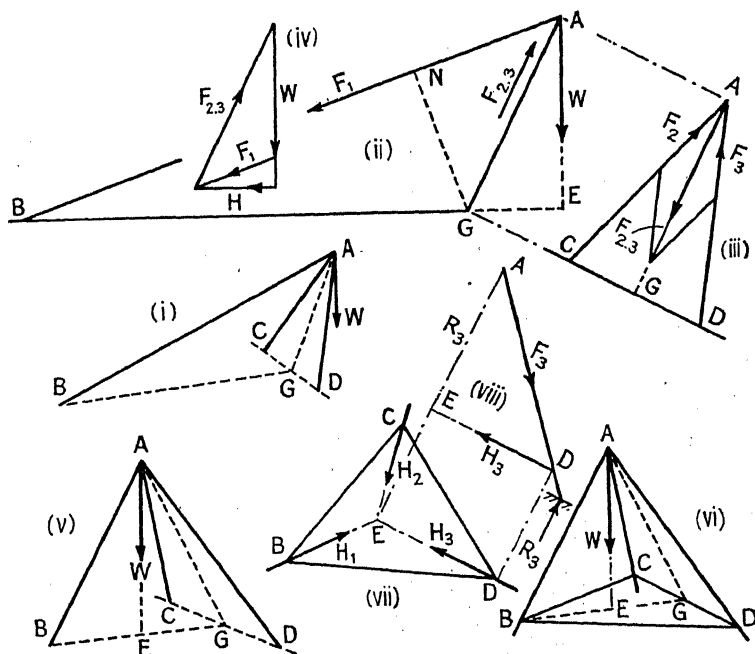
FIG. 26.

legs, as shown at (iii), and the forces F_2 and F_3 determined. It will be noted that, in order to get the true length of the legs AC and AD, the end elevation (iii) must be projected at right angles to GA, otherwise the result will be incorrect. F_1 is a tension, F_2 and F_3 compressions. The magnitude of F_1 might be found by taking moments about G, (ii), $W \times EG = F_1 \times NG$; or, $F_1 = W (EG/NG)$. The horizontal pull H on the screw at B is the horizontal component of F_1,

$$H = F_1 \cdot \frac{EB}{AB} = W \cdot \frac{EG}{NG} \cdot \frac{EB}{AB} = W \cdot \frac{EG \cdot EB}{AE \cdot BG} \cdot$$

The forces in the members of a tripod, (v) Fig. 26, can be found in exactly the same way as those in a pair of sheer legs ; the fact that the bars AC, AD slope inwards instead of outwards makes no difference to the method ; (v) is lettered to correspond with (i). If the feet of the

tripod are tied together by the bars BD, DC, CB, (vi) Fig. 26, find the forces in the bars AB, AC, AD, as before. Then, at the point B, the force in the leg (AB) can be resolved into a vertical and a horizontal component, and similarly at C and D. The vertical components will be equal to the reactions R_1, R_2, R_3, from the ground, the horizontal components H_1, H_2, H_3 must be carried by the triangular frame BCD as shown at (vii), for which the stress diagram can easily be drawn. To obtain these vertical and horizontal components, views must be drawn
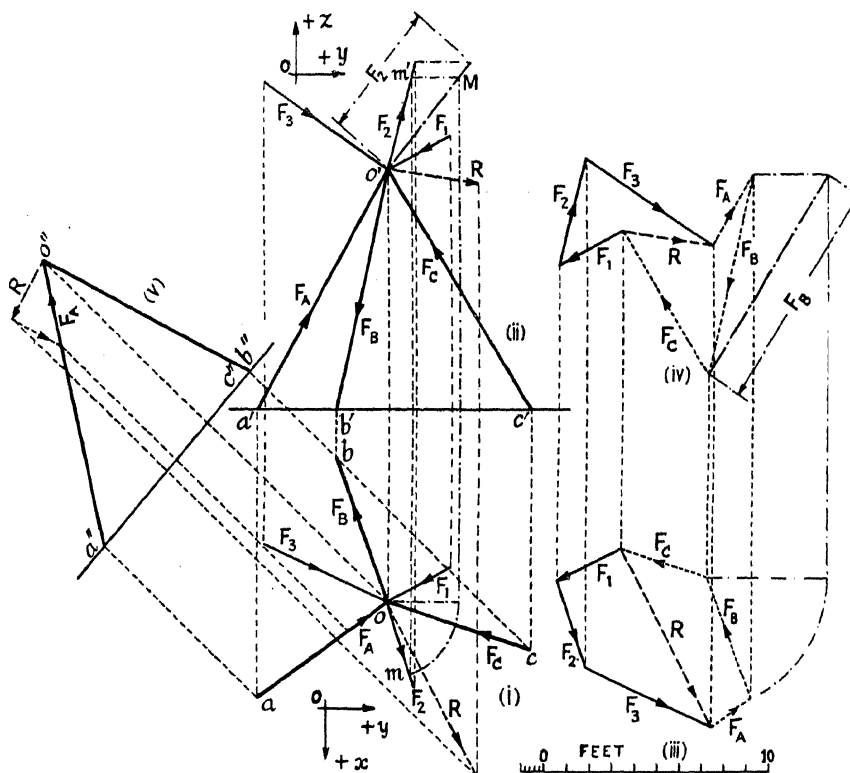
Fig. 27.

showing the true shape of each of the triangles AEB, AEC, AED, as at (viii), where AED, and the resolution of F_3 into H_3 and R_3, are shown.

Graphical Treatment.—Fig. 27 gives the complete geometrical construction for finding the forces in three bars of a space framework which intersect at a point O, due to a number of forces acting at the point. (i) and (ii) are the plan and elevation of the bars, and of the forces acting at O ; (iii) and (iv) are the plan and elevation of the force polygon from which the resultant R is derived ; (v) is an elevation on a plane perpendicular to the plane OBC. Let m, m' be the plan and elevation of any point M in the line of action of the force F_2 ; find the true length of OM by the usual

geometrical construction, shown with dot and dash lines in (i) and (ii). Mark off along $o'M$ in (ii) the magnitude of F_2 to the force scale, and project back to find the plan and elevation of the length thus determined, which plan and elevation represent, both in magnitude and direction, the force F_2. Treat the other forces F_1 and F_3 in a similar way. The plan and elevation of the force polygon in (iii) and (iv) can be set out by drawing lines parallel, and equal in length to the plan and elevation of the forces in (i) and (ii). The closing lines represent the plan and elevation of R, their resultant, which can now be shown in (i) and (ii). To resolve this resultant along the three directions AO, BO, and CO, draw an elevation (v), taken at right angles to the plane BOC, and show the resultant R in this elevation. Then whatever be the forces in BO and CO, their resultant will act along the line $b''o''$ in (v), and by drawing the elevation of the triangle of forces for the point O in (v), the elevation of F_A, the force in AO is determined, and its plan can be obtained by projecting downward to (i).

The resultant R will be the equilibrant of the forces F_A, F_B and F_C, in the bars AO, BO, and CO ; the plan of one of these F_A is known, hence the plan of the other two can be obtained by completing the stress diagram for the point O in plan, as shown in (iii), taking the forces in cyclic order. The elevation of the stress diagram can be found by projecting upward to (iv), and drawing lines parallel to the elevation of the bars in (ii). The plan and elevation of the forces in the three bars meeting at O are thus determined, and the magnitude of these forces can be found by determining the true length of the lines. An example, that for F_B, is given in (iii) and (iv). The above process might be repeated for every node point of a statically determinate space frame ; or, in simple cases, a complete stress diagram can be drawn for the whole frame, in a manner analogous to that for a plane frame.

Application of Tension Coefficients.—The above problem may be solved very simply by means of tension coefficients, § 10. Resolving the external forces parallel to the three co-ordinate axes :

Components parallel to	Ox	Oy	Oz
Of F_1	$+ 0 \cdot 70$	$- 1 \cdot 40$	$- 0 \cdot 70$
F_2	$+ 1 \cdot 80$	$+ 0 \cdot 60$	$+ 2 \cdot 20$
F_3	$+ 1 \cdot 20$	$+ 2 \cdot 80$	$- 1 \cdot 80$
Total (tons) . .	$X = + 3 \cdot 70$	$Y = + 2 \cdot 00$	$Z = - 0 \cdot 30$

Scaled from the plan and elevation, Fig. 27 :

$x_a - x_0 = + 4 \cdot 0$ $x_b - x_0 = - 6 \cdot 0$ $x_c - x_0 = + 2 \cdot 0$
$y_a - y_0 = - 6 \cdot 0$ $y_b - y_0 = - 2 \cdot 4$ $y_c - y_0 = + 6 \cdot 4$
$z_a - z_0 = 10 \cdot 0$ $z_b - z_0 = - 10 \cdot 0$ $z_c - z_0 = - 10 \cdot 0$

feet

Substitute in eq. (5), § 10 :

$$+ 4{\cdot}0\,\tau_1 - 6{\cdot}0\,\tau_2 + 2{\cdot}0\,\tau_3 + 3{\cdot}7 = 0$$
$$- 6{\cdot}0\,\tau_1 - 2{\cdot}4\,\tau_2 + 6{\cdot}4\,\tau_3 + 2{\cdot}0 = 0$$
$$- 10{\cdot}0\,\tau_1 - 10{\cdot}0\,\tau_2 - 10{\cdot}0\,\tau_3 - 0{\cdot}3 = 0.$$

Solve as simultaneous, $\tau_1 = -0{\cdot}1504$; $\tau_2 = +0{\cdot}4174$; $\tau_3 = -0{\cdot}2970$; this must be done accurately.

Lengths of members :

$$OA = L_1 = \sqrt{(x_a - x_0)^2 + (y_a - y_0)^2 + (z_a - z_0)^2}$$
$$= \sqrt{(4{\cdot}0)^2 + (-6{\cdot}0)^2 + (-10{\cdot}0)^2} = 12{\cdot}33 \text{ ft.}$$
$$OB = L_2 = \sqrt{(-6{\cdot}0)^2 + (-2{\cdot}4)^2 + (-10{\cdot}0)^2} = 11{\cdot}91$$
$$OC \quad L_3 = \sqrt{(2{\cdot}0)^2 + (6{\cdot}4)^2 + (-10{\cdot}0)^2} = 12{\cdot}04.$$

Then the force in $OA = \tau_1 L_1 = -0{\cdot}1504 \times 12{\cdot}33 = -1{\cdot}85$ tons

$$OB = \tau_2 L_2 = +0{\cdot}4174 \times 11{\cdot}91 = +4{\cdot}97$$
$$OC = \tau_3 L_3 = -0{\cdot}2970 \times 12{\cdot}04 = -3{\cdot}58$$

The corresponding values, scaled from the original of Fig. 27, were $F_A = -1{\cdot}84$, $F_B = +4{\cdot}94$, $F_C = -3{\cdot}62$ tons.

DEFLECTION OF FRAMEWORK

12. **Deflection of Framework. Graphical Methods.**—The deflection of framed structures may be determined by an application of the principle of work, §§ 69 and 70, or by one of the following graphical processes.

Given a bar of length l and area a, stressed by a force F, the stress in the bar will be F/a, and the strain $\delta l/l$, where δl is the alteration in length due to F. Since the stress $= E \times$ strain, $\dfrac{F}{a} = E\,\dfrac{\delta l}{l}$, and $\delta l = \dfrac{Fl}{Ea}$. The ratio l/a will be denoted by λ ; and $\delta l = \dfrac{F}{E}\lambda$. Consider a simple frame such as ABC, Fig. 28, attached to rigid supports at A and B and carrying a vertical load W at C. If l_1 be the length of the bar AC, a_1 its area, and F_1 the force it sustains due to W, the alteration in length of AC will be $\delta l_1 = \dfrac{F_1 l_1}{Ea_1} = \dfrac{F_1}{E}\lambda_1$. Since the force in AC will be a tension, F_1 will be considered as positive, δl_1 will be an elongation, i.e. a positive addition to the length of the bar. Owing to this elongation C will move to C′, where CC′ represents the alteration in length to a larger scale. The point C is capable of another movement, for the bar AC can swing about the point A as centre, when C will describe an arc struck from that centre. The actual movement, which will be determined by the other bars of the frame, will be very small, and the arc may be represented in Fig. 28 by the line C′C₁ at right angles to CC′. Consider next the bar BC. The force in this will be a compression $-F_2$, and the contraction in length is $\delta l_2 = -F_2\lambda_2/E$. This is represented in Fig. 28 by the distance CC″. But the bar BC is capable of swinging about the point B, and C will

describe an arc about B as centre, represented by the line $C''C_1$. It follows that the final position of C will lie on the line $C'C_1$ and also on the line $C''C_1$, that is to say, its real position must be their intersection C_1. The path of C, therefore, will be from C to C_1. Its vertical displacement is $\Delta_V = CC_2$ and its horizontal displacement is $\Delta_H = C_1C_2$. The method is due to Williot[25].

Example.—Fig. 28 has been drawn accurately to scale for the frame shown in Fig. 105. For the bar AC, $l_1 = 80$ in., $a_1 = 1 \cdot 6$ sq. in., $\lambda_1 = 50$, $F_1 = 8$ tons, and $\delta l_1 = 0 \cdot 0308$ in. For the bar BC, $l_2 = 70$ in., $a_2 = 2 \cdot 5$ sq. in., $\lambda_2 = 28$, $F_2 = -7$ tons, and $\delta l_2 = -0 \cdot 0151$ in. From the diagram $\Delta_V = 0 \cdot 035$ in., $\Delta_H = 0 \cdot 008$ in. (Compare the calculated values given in the example § 70.) $E = 13,000$ tons/sq. in.
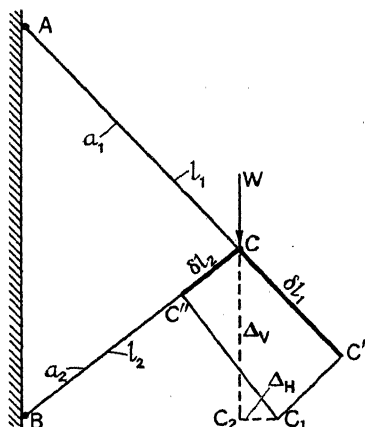
FIG. 28.

The method can be applied to more complicated cases, subject to the conditions that the structure is a perfect frame, and that the forces and alterations in length in all the bars can be found. It is necessary that the position in the distorted frame of one end of a bar be known before that of the other end can be determined.

Suppose it be required to find the displacements of the points C and D of the frame shown in (i) Fig. 29 when a load W is applied at D. A is a fixed point, B is only capable of vertical motion. Find first the forces in all the bars and the corresponding alterations in length. Start the displacement diagram, (ii) Fig. 29, at a pole O, which represents any fixed point on the frame. Since A is a fixed point it will be represented in (ii) by a coincident with the pole. The bar AB will lengthen an amount $ab = \delta l_3$, plotted downward from a, since

FIG. 29.

B moves in that direction. As B is only capable of movement in a vertical direction, b represents the final position, and Ob the total movement of B. Consider next the bar AC. The extension of AC is $\delta l_1 = ac'$, drawn parallel to AC and downward from A, since C will move in that direction. C is also capable of moving about A as centre, which movement is represented

by $c'c$ at right angles to ac'. Similarly, bc'', drawn parallel to BC, represents δl_2, the contraction in length of BC, and is plotted in a direction corresponding with the movement of C towards B. The line $c''c$ at right angles to bc'' represents the motion of C about B as centre. Hence c is the final position, and Oc the total movement of C. In like manner, ad' represents the extension of AD, and $d'd$ the motion of D about A;
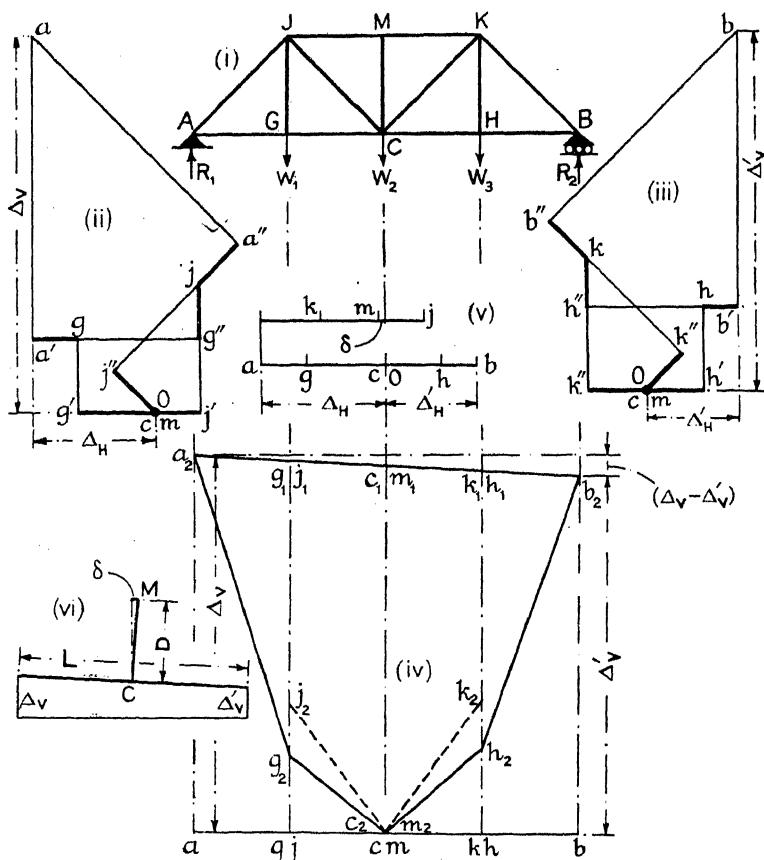
Fig. 30.

cd'' represents the contraction of DC, and $d''d$ the motion of D about C. Therefore d is the final position of D, and Od is its actual movement. Δ_V and Δ_H, respectively, are the vertical and horizontal components of that movement. (ii) Fig. 29 is called the *displacement* or *Williot diagram* for the frame.

Fig. 30 is an application of the method to a bridge truss, unsymmetrically loaded. To find the displacements of the different node points of the truss, assume that C is a fixed point and CM a fixed direction. Find

the displacements of the node points as if each half of the truss were a cantilever projecting from CM, exactly as in the previous case. The diagram for the left-hand cantilever is shown at (ii), and for the right-hand cantilever at (iii). In this instance, since there is no stress in CM, both c and m will coincide with the pole O. Then Og, Oj, Oa, Oh, Ok, and Ob represent the displacements of the points G, J, A, H, K, and B relative to the line CM. But under the conditions shown in Fig. 30, A is a fixed point and AB always remains a horizontal line. In order to obtain the displacements relative to AB, transfer the vertical components of all the displacements to a base line ab, (iv), which represents to scale the bottom flange. Thus $aa_2 = \Delta_V$; $bb_2 = \Delta_V'$; $gg_2 = g'g$ in (ii) is the vertical displacement of G, and so on. Join $a_2 g_2 c_2 h_2 b_2$, and also $a_2 b_2$. Then $a_2 b_2$ represents the real datum line AB, and $g_1 g_2$, $c_1 c_2$, $h_1 h_2$, are the vertical displacements of the node points G, C, H, below this line. Similarly, if jj_2 and kk_2 be the vertical displacements of J and K relative to the pole O, then $j_1 j_2$, $m_1 m_2$, and $k_1 k_2$ are the vertical displacements of the points J, M and K below their original position. To obtain the horizontal displacements of the node points relative to the fixed point A, plot on a base line aOb, (v), the horizontal displacements relative to the pole O, taken from (ii) and (iii); $Oa = \Delta_H$; $Ob = \Delta_H'$; and c coincides with O; Og in (v) $= Og'$ in (ii); Oh in (v) $= Oh'$ in (iii) and so on. Then, in this diagram, ca is the relative movement of A to C. But A is a fixed point and C moves, therefore ac is the movement of C relative to A, and similarly for the other points G, H, and B; ab is the horizontal movement of B. To find the displacements of J and K relative to A, consideration must be given to the fact that the conditions are unsymmetrical, and that Δ_V is not equal to Δ_V', so that the line $a_2 b_2$ in (iv) is not parallel to AB. In other words, if CM retained the vertical position assumed when drawing the displacement diagram, B would have to deflect downward a distance $(\Delta_V - \Delta_V')$. Since this cannot happen, it is necessary to impose on the truss as a whole an anticlockwise rotation about A, to bring b_2 back to the horizontal. The effect of this is to move M a distance δ to the left, such that $\delta = (\Delta_V - \Delta_V')D/L$, see (vi) Fig. 30. The real position of m will then be as shown in (v), displaced a distance δ from the centre line. Plot from the point m, along the upper line in (v), the horizontal displacements mk, mj, of K and J, from (ii) and (iii). Then the distances of k, m, and j, from the vertical through the fixed point a, give the true horizontal displacements of K, M, and J.

The vertical and horizontal displacements of every point on the truss are now known.

Mohr's Method.—An elegant solution of the above problem, due to Mohr,[31] is given in Fig. 31, in which use is made of the Instantaneous Centre theory. If the truss in (i) Fig. 31 be in motion as a rigid body, every node point will move about an instantaneous centre I, and the relative displacement of each point will be proportional to its distance from I. Further, if a pole o be taken, (ii), and a pencil of rays be plotted, representing to scale the displacements of the node points in (i), such
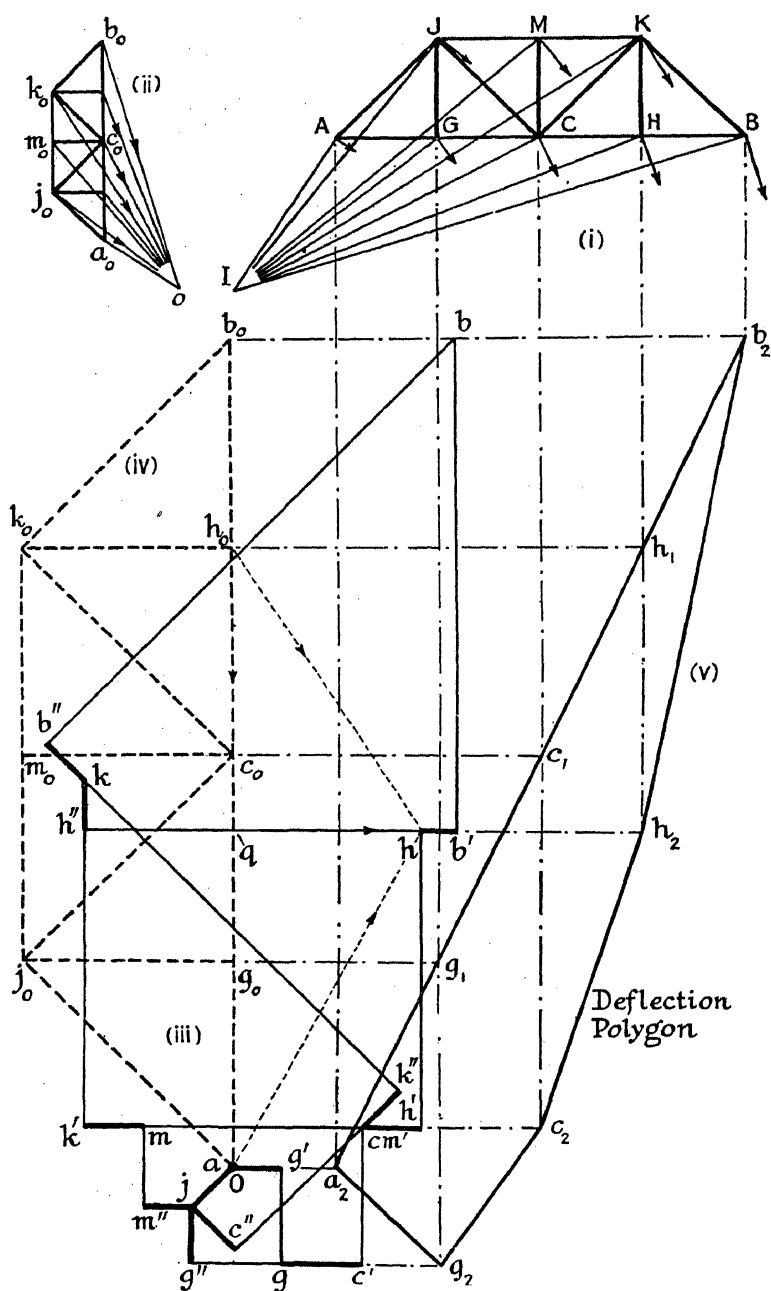
FIG. 31.

that a_0o represents the displacement of A, m_0o the displacement of M, b_0o the displacement of B, and so on, then the outer ends of these rays will coincide with the node points of an outline of the truss, drawn to a different scale and turned through a right angle, as shown at (ii) Fig. 31. This will be evident from the similarity of the two figures (i) and (ii). It will also be evident that every line in (ii) is perpendicular to the corresponding line in (i). Thus a_0o is perpendicular to AI, k_0o to KI, m_0c_0 to MC, a_0b_0 to AB, and so on. Hence, if any line in (ii) can be determined, say a_0b_0, the whole figure can be drawn. The application of the above will be seen in what follows.

Suppose it be desired to find the displacements of the node points of the truss in question when supported and loaded as shown in (i) Fig. 30. Treat A as a fixed point and AJ as a fixed direction, and using the pole O, (iii), draw the Williot displacement diagram for the truss. With these assumed conditions, the new position of the point B will be represented by b, and Ob_0 is the apparent vertical upward displacement of B. But in the actual conditions, (i) Fig. 30, the vertical displacement of B must be zero. Hence the truss as a whole must be given a clockwise rotation about the fixed point A, which becomes the instantaneous centre, to bring B back to the horizontal. Set out on Ob_0 as a base an outline of the truss, shown in broken lines at (iv). From the theory given above [compare (i) and (ii)] it follows that b_0O represents the vertical displacement of B due to the rotation about A which brings B back to the horizontal, and c_0O, g_0O, k_0O, and so on, represent the corresponding displacements of the other node points due to the same rotation ; the coincident points a, O represent the pole o in (ii).

Consider any node point H. It will have a displacement Oh due to the deformation of the truss, plus a displacement h_0O due to the rotation about A. The resultant of these two displacements is h_0h, and this resultant displacement is the actual displacement of H relative to the fixed point A. It can be resolved into two component displacements h_0q downward, and qh to the right. The same reasoning is true for every node point, and it follows that the line joining a node point in the broken line figure (iv), to the corresponding node point in the Williot displacement diagram (iii), gives the true displacement of the node in question, in both magnitude and direction, relative to the fixed point A. Thus b_0b is the horizontal displacement of B, m_0m is the displacement of M, and so on.

The deflection polygon (v) for the lower flange is obtained by direct projection from (i), (iii), and (iv) ; $h_1h_2 = h_0q$ represents the vertical displacement of H, and so on. It will be found that h_1h_2 in (v) Fig. 31 is exactly equal to h_1h_2 in (iv) Fig. 30 ; and qh in (iii) Fig. 31 is exactly equal to ah in (v) Fig. 30, and similarly for the other node points.

Except in the case of composite frames it is convenient to leave E out of account until the end of the calculation, in order to avoid decimal places. Assume in the first place that E = unity, so that $\delta l = F\lambda$, and proceed as before to find the displacements. The results thus obtained must be divided by the real value of E, to get the true magnitudes of the

displacements.   An example worked in this way will be found in § 118, Fig. 188.

13. Temperature Effects.—The Williot diagram can be used to find the displacements due to alterations in temperature.   The extension of a bar of length l, due to a rise in temperature $t°$, is atl, where a is the coefficient of expansion per degree.   If the temperature fall, t is negative, and the alteration in length is a contraction, $- atl$.   These alterations in length due to temperature enter into the construction of the Williot displacement diagram in exactly the same way as those due to stress. In a bar subjected to a force $+ F$ and a temperature alteration $+ t°$, the total alteration in length is

$$\delta l = \frac{Fl}{Ea} + atl \qquad . \qquad . \qquad . \qquad . \qquad (1)$$

It is worth noticing that this equation may be written

$$\delta l \quad \frac{fl}{E} + \frac{(atE)l}{E} \qquad (2)$$

so that the expression atE may be regarded as a stress intensity $= 0·15$ tons/sq. in. per degree C. in mild steel.

(In the two following articles some knowledge of the contents of Chapters V and VI is presumed.)

14. Deflection Polygons. 'Elastic Weight' Method. —This method of finding the deflection polygon of a braced girder is due to Mohr.[24]   It is analogous to that of § 54, p. 95, Vol. I, for beams.   Given a plane frame, (i) Fig. 32, loaded in any manner, to find the deflection polygon for the flanges.   Suppose, for the moment, that the shaded portions of the frame, (ii), are rigid ; then the deflection of the point m will be entirely due to the alteration in length of the bar pq.   To find the vertical displacement of m, apply a unit vertical load there.   From Mohr's work equation, eq. (8), § 81,
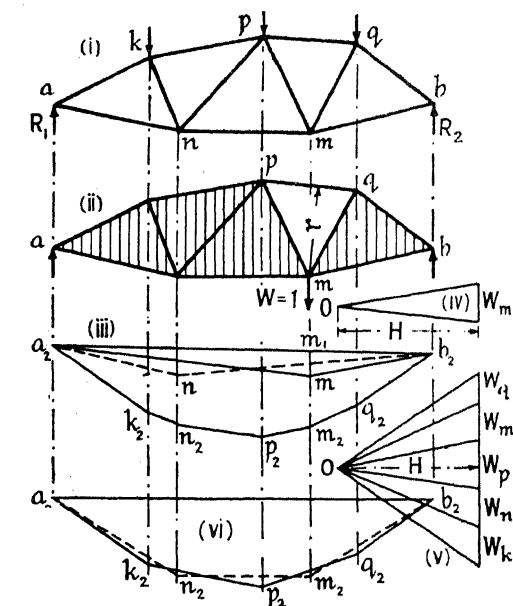
FIG. 32.

$$1 \times y_m = F' . \delta l \qquad (1)$$

where $y_m = m_1 m$ in (iii) is the vertical deflection of m, F' the force in the

bar pq due to the unit load, and δl the alteration in length of pq due to the actual loads on the frame. The deflection curve for the partially rigid frame of (ii) will be $a_2 m b_2$, (iii) Fig. 32. But this diagram might have been obtained by applying a load Wm of a certain magnitude at m, and drawing a bending moment diagram for this load, using the force polygon (iv), in which case the ordinate $m_1 m = ym$ represents the moment at the point m due to a force Wm applied there. But this moment is equal to $Fm \times r$, where Fm is the force in the bar pq due to Wm; hence,

$$ym = Fm \times r \qquad . \qquad . \qquad . \qquad . \quad (2)$$

If a load $W = 1$, applied at m, produce a force F' in the bar pq, and a load Wm produce a force Fm in that bar; then,

$$F' : Fm = 1 : Wm\,; \quad \text{and } Fm = Wm F'$$

From eq. (1) $ym = F' \cdot \delta l$; therefore, from eq. (2),

$$ym = Fm \times r = Wm F' r = F' \cdot \delta l\,;$$

whence,
$$Wm = \frac{\delta l}{\bar{\bar{r}}} \tag{3}$$

If then a load $Wm = \delta l/r$ be applied to the frame in (ii) at the point m, and the moment diagram $a_2 m b_2$ be found in the usual way, using the force polygon (iv), this diagram will be the deflection polygon for the frame. The load Wm is called an 'elastic load.' If F be the actual force and f the actual stress in the bar pq, l and a the length and area of that bar,

$$\delta l = \frac{Fl}{Ea} = \frac{1}{E} \cdot fl\,; \quad \text{and from eq. (3), } Wm = \frac{1}{E} \cdot \frac{fl}{r}.$$

It is convenient to call the value of E unity, and to take its real value into account at the end of the calculation, when

$$Wm = fl/r \qquad . \qquad . \qquad . \qquad . \qquad . \quad (4)$$

Knowing then the actual stress f in the bar and the dimensions of the frame, the elastic load can be found and the moment diagram $a_2 m b_2$, (iii), for the semi-rigid frame (ii) can be drawn.

Scales.—Suppose that the length scale be 1 inch $= a_1$ inches of span, and the load scale be 1 inch $= a_2$ units of elastic load. Then if ym'' be the deflection measured from (iii) in inches, and H'' be the polar distance measured from (iv) in inches, the actual deflection, allowing for the value of E, is

$$ym = \frac{1}{E} \cdot ym'' H'' \times a_1 a_2 \text{ inches } . \qquad . \qquad . \quad (5)$$

Similarly, assuming the rest of the frame to be rigid, and considering the bar kp; if a load $Wn = \delta l/r = fl/Er$, be applied at the point n (δl, r, f, and l have reference to the bar kp), the moment diagram $a_2 n b_2$ in (iii) will give the deflection produced by the alteration in length of kp. If this process be repeated for every panel point, top and bottom, and the ordinates at any one panel point of all the diagrams so obtained be added together, the total deflection of this panel point due to the alteration in length of all the bars in both flanges will be obtained. It is simplest to

set off the elastic loads $W_m, W_n, \ldots = fl/r$ on a load line (v), and to draw the funicular polygon as shown in (iii). The deflection polygon for the top flange is obtained by joining the points $a_2 k_2 p_2 q_2 b_2$; that for the bottom flange is obtained by joining $a_2 n_2 m_2 b_2$, (vi). The argument given above as to scales applies equally well to the complete funicular polygon; the total deflection at any panel point can be obtained from the scaled dimension in (iii) by using eq. (5).

Signs.—The sign of the stress in the bar must be taken into account
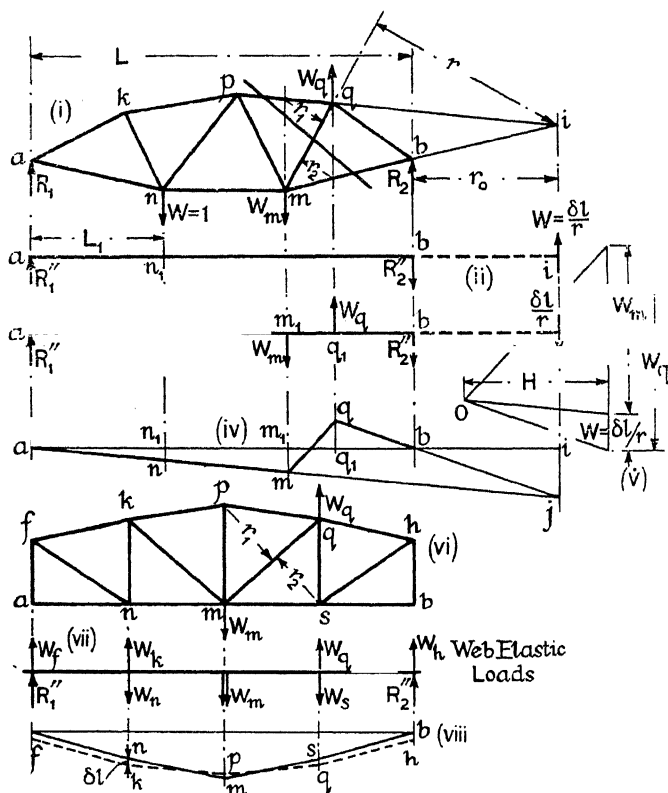
FIG. 33.

in eq. (4). If the stress in pq be compressive and negative, the bar will shorten, y_m will be a downward and positive deflection, and W_m must be a downward load. If the stress in nm be tensile and positive, the bar will lengthen; y_p will be a downward and positive deflection, and W_p must be a downward load. A negative value for f in the upper flange, or a positive value for f in the lower flange, implies therefore a downward load, and vice versa.

Effect of Web Members.—The deflection produced by the extensions and contractions of the web members, which is not taken into account in the above analysis, can also be found by applying a system of 'elastic

loads ' to the panel points, and drawing the deflection polygon for these loads exactly as in (vi) Fig. 32. In (i) Fig. 33, cut the bars pq, qm, and mb by a section as shown, and produce pq and mb to meet in i. Take moments about i ; the moments of the forces in pq and mb are then zero, and the effect of the force in qm can be studied separately. Let the perpendicular distance from i to qm be r.

If $y_n = n_1 n$, (iv), be the vertical deflection of any point n due to the extension δl produced in qm by the actual loads on the girder, from Mohr's work equation, eq. (8), § 81,

$$1 \times y_n = F' \cdot \delta l \quad . \qquad . \qquad . \qquad . \qquad (6)$$

where, as in the case of the flanges, F' is the force in qm due to a unit vertical load applied at n. If R_1' and R_2' be the reactions at a and b (both upward) due to this unit load, $R_2' = L_1/L$; and, taking moments about i, $\quad F'r = R_2' r_0$, whence $\quad F' = r_0 L_1 / rL$, and

$$1 \times y_n = \frac{\delta l}{r} \cdot \frac{r_0 L_1}{L} \qquad (7)$$

By analogy with the analysis for the flanges, if an elastic load $\delta l/r$ be applied at i, the centre of moments for the bar qm under consideration, the moment at the point n due to this load will represent the deflection y_n. Since i lies outside the girder, in order to conform to the conventions as to signs used in (iii) Fig. 32, the elastic load at i must act upwards, when the reaction at a will also act upwards, and the upward moment at n will represent the downward deflection y_n. This may be proved as follows : Let R_1'' and R_2'' (ii) be the reactions at a and b due to the elastic load $\delta l/r$ acting upwards at i. Then $R_1'' = \dfrac{\delta l}{r} \cdot \dfrac{r_0}{L}$; and the

upward moment at $n = R_1'' L_1 = \dfrac{\delta l}{r} \cdot \dfrac{r_0 L_1}{L}$, which from eq. (7) is equal to y_n. But the member qm is a tie, and if the deformation of the panel $pqbm$ be considered, it will be seen that due to the extension of qm the point m will move downwards and the point q upwards.*

To obtain, therefore, a complete deflection polygon corresponding to the extension of qm, two elastic loads must be applied to the girder, W_m downwards at m, and W_q upwards at q, (i and iii). The magnitude of these must be such that they produce the same moment at n as does $\delta l/r$ applied at i, in other words, the values of R_1'' and R_2'' must be the same in both cases, or

$$R_1'' + R_2'' = \frac{\delta l}{r} = W_m + W_q$$

and the sum of the moments of W_m and W_q about any point must equal that of $\delta l/r$. Taking moments about q_1, (iii),

$$\frac{\delta l}{r} \times q_1 i = W_m \times m_1 q_1 ; \text{ and } W_m = \frac{\delta l}{r} \cdot \frac{q_1 i}{m_1 q_1} \qquad \frac{\delta l}{E} \qquad \frac{1}{E} \qquad \frac{fl}{} \qquad (8)$$

* This can be verified by a direct application of Mohr's work equation (eq. 6), by applying a downward load $W = 1$ first at m, for which the value of F' in qm will be positive ; and secondly at q, for which the value of F' will be negative, or opposed to that of δl, showing that the deflection at q will be negative, i.e. upwards.

for $q_1 i / m_1 q_1 = r/r_1$, and $\delta l = fl/\mathrm{E}$. Taking moments about m_1, (iii),

$$\frac{\delta l}{r} \times m_1 i = \mathrm{W}_q \times m_1 q_1 ; \text{ and } \mathrm{W}_q = \frac{\delta l}{r} \cdot \frac{m_1}{m_1 q_1} = \frac{\delta l}{r_2} = \frac{1}{r_2} \cdot \frac{fl}{\mathrm{E}} \quad . \quad (9)$$

for $m_1 i_1 / m_1 q_1 = r/r_2$; r_1 and r_2 are indicated in (i). If, therefore, two elastic loads, $\mathrm{W}_m = fl/r_1$ downwards, and $\mathrm{W}_q = fl/r_2$ upwards, be applied at m and q respectively, the corresponding moment diagram $amqb$, (iv), drawn by means of (v), will be the deflection polygon for the extension of bar qm. The value of E must be taken into account at the end of the calculation. If similar elastic loads for each web member be determined, the total elastic load at each panel point is obtained by addition, and from these a complete web deflection polygon may be drawn. Alternatively, the web elastic loads may be added to the flange elastic loads, and a combined deflection polygon constructed. The treatment as to scales is as set forth for the flange polygon. Mohr's rule for the direction of the web elastic loads is : when the stresses in the flange and the web member are like in sign, the elastic load at their intersection acts downwards ($+$), and upwards ($-$) when they are unlike. In a girder with vertical web members, (vi), it is best to ignore the deformation of the verticals when calculating the web elastic loads, and to construct a diagram, $anmsb$, (viii), showing the deflection polygon for the lower panel points. If these panel points be lowered (or raised) an amount δl, equal to the alteration in length of the verticals, the deflection polygon $fkpqh$ for the upper panel points is obtained.

Worked Example.—To draw the deflection polygon for the upper and lower flanges of the braced girder shown in (i) Fig. 34, when loaded with 12 tons at the point m. Considering first the effect of the deformation of the flanges, the calculations are set forth in tabular form below, the units being tons and inches. The values for the length and area of each bar are given in cols. 2 and 3 of the table ; the radius r is 60 inches, and since the flanges are parallel, this is constant. The force F in each bar is found from a stress diagram in the usual way and tabulated in col. 5.

Bar No.	l	a	r	F	f	Elastic Load. fl/r
1	120	3·66	60	$+ \ 4$	$+ 1·10$	$+ 2·20 \ (k)$
2	120	3·66	60	$+ 12$	$+ 3·28$	$+ 6·56 \ (p)$
3	120	3·66	60	$+ \ 8$	$+ 2·19$	$+ 4·38 \ (q)$
4	120	4·98	60	$- \ 8$	$- 1·61$	$+ 3·22 \ (n)$
5	120	4·98	60	$- 16$	$- 3·21$	$+ 6·42 \ (m)$

Units : tons, inches.

The stress f is found by dividing F by a ; and the magnitude of the elastic load $= fl/r$ is obtained from cols. 6, 2, and 4. Since all the forces in the

upper flange are compressive, and all in the lower flange are tensile, all the elastic loads are positive (downward loads).

The elastic loads on the frame are then as shown in (ii).   The elastic
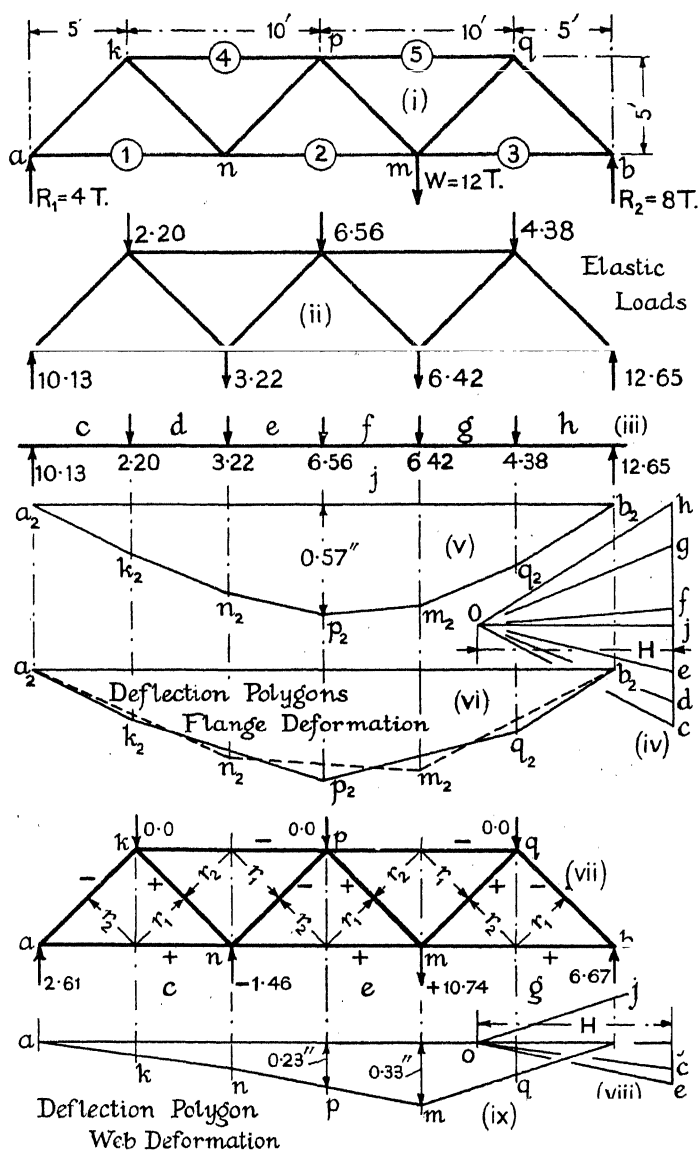
FIG. 34.

load due to the deformation of bar No. 1 acts at k, that due to the deformation of bar No. 4 acts at n, and so on.   The reactions are found in the usual way.   Taking the loads in order on the beam as shown in (iii), the

force polygon (iv) is set out, whence the funicular polygon (v), representing the deflection polygon for flange deformation, is obtained. The deflection polygon for the upper flange is obtained by joining $k_2 p_2 q_2$ in (v), and that for the lower flange by joining $a_2 n_2 m_2 b_2$, see (vi). In Fig. 34 the length scale is $1'' = 120$ inches, hence $a_1 = 120$; (iv) has been set out to a scale $1'' = 20$ units of elastic load, hence $a_2 = 20$; the polar distance $H'' = 1$ inch. The maximum ordinate of the funicular polygon occurs at p and scales $0 \cdot 57''$ in (v). Therefore, from eq. (5), the deflection at p is,

$$y_p = \tfrac{1}{E} \cdot y_p \times H'' \times a \cdot a_2 \quad \tfrac{1}{13000} \times 0 \cdot 57 \times 1 \times 120 \times 20 = 0 \cdot 105 \, \text{inch},$$

which determines the scale of the diagram.

To obtain the deflection polygon for the web members, find in a similar way the elastic loads for each end of each web member from eqs. (8) and (9), as set forth in the following table. The radii r_1 and r_2 are indicated

*Bar No.	l	a	r_1.	r_2	F	f	Elastic Loads.	
							fl/r_1	fl/r_2
6	84·8	3·66	42·4	42·4	− 5·66	− 1·55	— (a)	+ 3·10 (k)
7	84·8	3·66	42·4	42·4	+ 5·66	+ 1·55	− 3·10 (k)	+ 3·10 (n)
8	84·8	2·48	42·4	42·4	− 5·66	− 2·28	− 4·56 (n)	+ 4·56 (p)
9	84·8	2·48	42·4	42·4	+ 5·66	+ 2·28	− 4·56 (p)	+ 4·56 (m)
10	84·8	3·66	42·4	42·4	+ 11·31	+ 3·09	+ 6·18 (m)	− 6·18 (q)
11	84·8	3·66	42·4	42·4	− 11·31	− 3·09	+ 6·18 (q)	— (b)

Units : tons, inches.

in (vii). The force in bar No. 7* is $+$, that in bar No. 4 is $-$, hence the elastic load at k for bar No. 7 is $-$, or upward. The force in bar No. 1 is $+$, and since that in bar No. 7 is $+$, the elastic load at n for bar No. 7 is $+$, or downward, and so on. The elastic loads at a and b do not affect the deflection, and may be ignored. The total elastic load at k is $+ 3 \cdot 10$ from bar No. 6 and $- 3 \cdot 10$ from bar No. 7, or zero. The total elastic load at n is $+ 3 \cdot 10$ from bar No. 7 and $- 4 \cdot 56$ from bar No. 8, or $- 1 \cdot 46$. The complete system of web elastic loads is shown at (vii), from which the force polygon (viii) and the deflection polygon (ix) are set out. The ordinates at p and m, scaled in inches, are given. The same scales as before have been used, hence the actual web deflection at p is

$$y_p = \tfrac{1}{E} \cdot y_p'' \times H'' \times a_1 a_2 = \tfrac{1}{13000} \times 0 \cdot 23 \times 1 \times 120 \times 20 = 0 \cdot 042 \, \text{inch},$$

and similarly $y_m = 0 \cdot 061$ inch.

To obtain the complete deflection polygon for the girder the ordinates of (ix) must be added to those of (v) ; alternatively, the elastic loads of (ii) may be combined with those of (vii), and a complete deflection polygon constructed. These combined elastic loads will be found to be identical with those of (v) Fig. 37, thus establishing the identity of the two methods.

* See Fig. 36.

15. Deflection Polygons. Kinematic Chain Method.—Suppose $jkmn$, (i) Fig. 35, to be a series of bars forming part of a plane framework ; $jkmn$ might, for example, be the upper flange of a braced girder, or the lower flange of an arch. Such a series of bars, separately considered, is sometimes called a *kinematic chain*, or a *bar chain*. Let the ordinates of the points k, m, n, measured from a base line Ox, be y_{m-1}, y_m, y_{m+1}. As in other deflection problems, distances measured to the right and downward will be considered as positive. Let θ be the inclination of any bar to Ox, considered as positive when the bar slopes downward from left to right. Suppose that (ii) be the deflection polygon for the chain
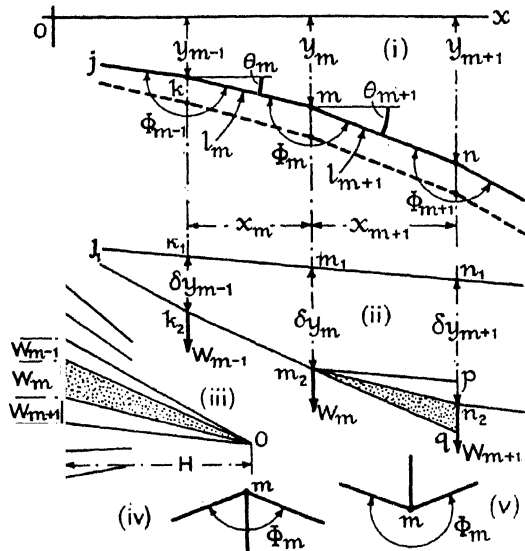
FIG. 35.

under consideration, $j_1 n_1$ being the closing line, and $m_1 m_2 = \delta y_m$ the deflection of the point m. This diagram is obtained from the elastic weights W_m, using the force polygon (iii) as in § 14.

Consider panel mn ; produce $k_2 m_2$ in (ii) to q, and draw $m_2 p$ parallel to $m_1 n_1$; then from the geometry of the figure,

$$pq = (\delta y_m - \delta y_{m-1})x_{m+1}/x_m ; \quad pn_2 = (\delta y_{m+1} - \delta y_m) ;$$

hence, $n_2 q$ $\quad pq - pn_2 = (\delta y_m - \delta y_{m-1})\dfrac{x_{m+1}}{x_m} - (\delta y_{m+1} - \delta y_m).$

But the shaded triangles in (ii) and (iii) are similar. Therefore,

$$\frac{n_2 q}{x_{m+1}} = \frac{W_m}{H} ; \text{ and}$$

$$W_m = H\left\{\frac{\delta y_m - \delta y_{m-1}}{x_m} - \frac{\delta y_{m+1} - \delta y_m}{x_{m+1}}\right\} \qquad . \quad .. \quad (1)$$

From (i) Fig. 35, $km = l_m$, and $x_m = l_m \cos \theta_m$; also,

$$y_m - y_{m-1} = l_m \sin \theta_m ;$$

from which, by differentiation,

$$\delta y_m - \delta y_{m-1} = l_m \cos \theta_m . \delta\theta_m + \delta l_m . \sin \theta_m$$

and, dividing through by $l_m \cos \theta_m = x_m$,

$$\frac{\delta y_m - \delta y_{m-1}}{x_m} \quad \delta\theta_m + \frac{\delta l_m}{l_m} . \tan \theta_m$$

similarly, $\quad \dfrac{\delta y_{m+1} - \delta y_n}{x_{m+1}} = \delta\theta_l \quad + \dfrac{\delta l_{m+1}}{l_{m+1}} \tan \theta_{m+1}$

Substituting in eq. (1),

$$W_n = H\left[\{\delta\theta_m - \delta\theta_{m+1}\} + \left\{\frac{\delta l_m}{l_m} \tan \theta_m - \frac{\delta l_{m+1}}{l_{m+1}} \tan \theta_{m+1}\right\} \right]$$

But $\delta l_m / l_m$ is the strain in the bar km and is equal to f_m/E, where f_m is the stress in the bar km.   Hence,

$$W_m = H\left[\{\delta\theta_m - \delta\theta_{m+1}\} + \frac{1}{\mathrm{E}} \{f_m \tan \theta_m - f_{m+1} \tan \theta_{m+1}\} \right] \quad (2)$$

Further, from (i), if the angle $kmn = \Phi_m$,

$$\Phi_m + \theta_{m+1} - \theta_m = 180° ; \text{ and, } \delta\Phi_m = \delta\theta_m - \delta\theta_{m+1} ;$$

and from eq. (2), assuming a value $H = $ unity,

$$W_m = \left[\delta\Phi_, + \frac{1}{\mathrm{E}} \{f_m \tan \theta_m - f_{m+1} \tan \theta_{m+1}\} \right] \quad (3)$$

an equation giving the elastic loads W_m in terms of the stresses in the bars and the angles of the chain.   The correct sign must be given to the stresses, to the angles, and to the tangents.   The magnitude of $\delta\Phi_m$ must be determined by finding the increases (or decreases) in the angles of all the triangles which compose the frame from the changes in the lengths of the bars ; these can be found from § 116.   Then, for any panel point, $\delta\Phi_m = $ the sum of the changes in all the angles meeting at the point, i.e.

$$\delta\Phi_m = \pm \Sigma\delta A \quad . \quad . \quad . \quad . \quad (4)$$

where δA represents the change in any one angle.   When the bars of the frame are on the same side of the chain as the angle Φ, (iv), the $+$ sign in eq. (4) is to be used ; when they are on the reverse side, (v), the $-$ sign is to be used.   Thus the $+$ sign is taken for the upper flange of a braced girder, and the $-$ sign for the lower.   This sign is to be given to the summation Σ, irrespective of the sign of the components δA.   A positive value for W_m implies a downward load.

For a chain of horizontal bars $\theta = 0$, and

$$W_m = \delta\Phi_m = \pm \Sigma\delta A \quad . \quad . \quad . \quad . \quad (5)$$

When a bar is parallel to the direction of the displacements, $\theta = 90°$, and eq. (3) cannot be used.   It is then best to omit the particular bar from the chain, and to allow separately for the displacement which it

produces. This displacement is evidently equal to the alteration in length of the bar.

Worked Example.—In this example, Fig. 36, the above method is applied to the frame of the worked example of § 14, Fig. 34. The initial stages of the procedure follow the same course as in § 14, except that all the bars are now included, and the radii r are not required. The results
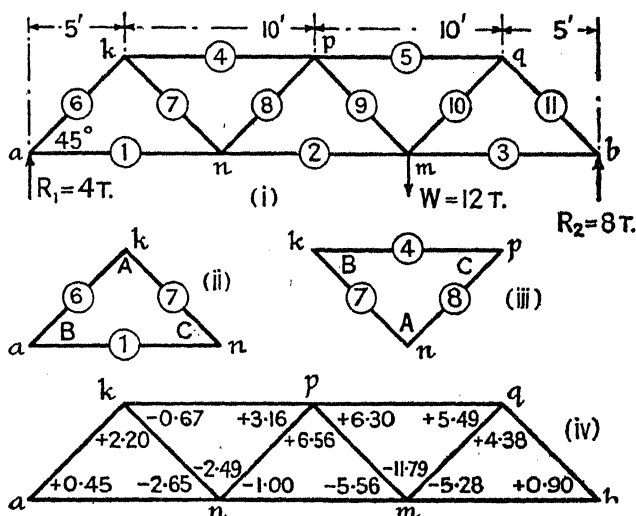
FIG. 36.

are embodied in the table below. The angle θ and tan θ for each bar are also given, from which the values of f tan θ are calculated. θ is the angle which a bar makes with the horizontal, (i) Fig. 35, and a downward slope from left to right is positive.

Bar No.	l	a	F	f	$\theta°$	tan θ	f tan θ
1	120	3·66	+ 4·0	+ 1·10	0	0	0
2	120	3·66	+ 12·0	+ 3·28	0	0	0
3	120	3·66	+ 8·0	+ 2·19	0	0	0
4	120	4·98	− 8·0	− 1·61	0	0	0
5	120	4·98	− 16·0	− 3·21	0	0	0
6	84·8	3·66	− 5·66	− 1·55	− 45	− 1	+ 1·55
7	84·8	3·66	+ 5·66	+ 1·55	+ 45	+ 1	+ 1·55
8	84·8	2·48	− 5·66	− 2·28	− 45	− 1	+ 2·28
9	84·8	2·48	+ 5·66	+ 2·28	+ 45	+ 1	+ 2·28
10	84·8	3·66	+ 11·31	+ 3·09	− 45	− 1	− 3·09
11	84·8	3·66	− 11·31	− 3·09	+ 45	+ 1	− 3·09

Units : tons, inches.

To obtain the values of $\delta\Phi$, the values of δA must be calculated by means of eq. (2), § 116. Consider the triangle akn, (ii) Fig. 36, relettered

ABC to agree with § 116.   From eq. (2), § 116, assuming for the moment that E = unity,

$$\delta A = \frac{1}{E}\{(f_a - f_c)\cot B \qquad + (f_a - f_b)\cot C \qquad \}$$
$$= \{(f_1 - f_6)\cot 45° \qquad + (f_1 - f_7)\cot 45° \qquad \}$$
$$= \{(+1\cdot10 + 1\cdot55) \times 1 + (+1\cdot10 - 1\cdot55) \times 1\} = +2\cdot20$$

$$\delta B = \frac{1}{E}\{(f_b - f_a)\cot C \qquad + (f_b - f_c)\cot A \qquad$$
$$= \{(f_7 - f_1)\cot 45° \qquad + (f_7 - f_6)\cot 90° \qquad \}$$
$$= \{(+1\cdot55 - 1\cdot10) \times 1 + (+1\cdot55 + 1\cdot55) \times 0\} = +0\cdot45$$

$$\delta C = \frac{1}{E}\{(f_c - f_b)\cot A \qquad + (f_c - f_a)\cot B \qquad \}$$
$$= \{(f_6 - f_7)\cot 90° \qquad + (f_6 - f_1)\cot 45° \qquad \}$$
$$= \{(-1\cdot55 - 1\cdot55) \times 0 + (-1\cdot55 - 1\cdot10) \times 1\} = -2\cdot65$$
$$\overline{\Sigma = \qquad 0\cdot00}$$

Observe that $\delta A + \delta B + \delta C = 0$, so that eq. (3), § 116, is satisfied, as must always be the case.

Again, consider the triangle knp, relettered ABC, (iii).   From eq. (2), § 116, if E = 1,

$$\delta A = \{(f_a - f_c)\cot B \qquad + (f_a - f_b)\cot C \qquad \}$$
$$\{(f_4 - f_7)\cot 45° \qquad + (f_4 - f_8)\cot 45° \qquad \}$$
$$\{(-1\cdot61 - 1\cdot55) \times 1 + (-1\cdot61 + 2\cdot28) \times 1\} = -2\cdot49$$

$$\delta B = \{(f_b - f_a)\cot C \qquad + (f_b - f_c)\cot A \qquad \}$$
$$\{(f_8 - f_4)\cot 45° \qquad + (f_8 - f_7)\cot 90° \qquad \}$$
$$\{(-2\cdot28 + 1\cdot61) \times 1 \quad (-2\cdot28 - 1\cdot55) \times 0\} = -0\cdot67$$

$$\delta C = \{(f_c - f_b)\cot A \qquad + (f_c - f_a)\cot B \qquad \}$$
$$\{(f_7 - f_8)\cot 90° \qquad + (f_7 - f_4)\cot 45° \qquad \}$$
$$\{(1\cdot55 + 2\cdot28) \times 0 \qquad + (1\cdot55 + 1\cdot61) \times 1 \qquad \} = +3\cdot16$$
$$\overline{\Sigma = \qquad 0\cdot00}$$

Every triangle in the frame must be similarly treated ; the results are given in (iv) Fig. 36.

Any chain of bars in the frame may be taken as the kinematic chain. Consider first the bottom flange, (viii), Fig. 37 ; for this $\theta = 0$ everywhere, and eq. (5) can be used for the elastic loads, $W_m = -\Sigma\delta A$; the negative sign is taken since it is the lower flange.   From (iv) Fig. 36,

$$W_a = -(+0\cdot45) = -0\cdot45$$
$$W_n = -(-2\cdot65 - 2\cdot49 - 1\cdot0) = +6\cdot14$$
$$W_m = -(-5\cdot56 - 11\cdot79 - 5\cdot28) = +22\cdot63$$
$$W_b = -(+0\cdot90) = -0\cdot90$$

W_a and W_b merely increase the elastic reactions without affecting the funicular polygon, and need not be further regarded.   The elastic loads and reactions are then as shown at (viii), from which the funicular polygon (x), representing the deflection curve, has been set out.   The length

scale is $1'' = 120$ inches, hence $\alpha_1 = 120$; the load scale is $1'' = 20$ units of elastic load, hence $\alpha_2 = 20$; the polar distance $H'' = 1$ inch.* The

Fig. 37.

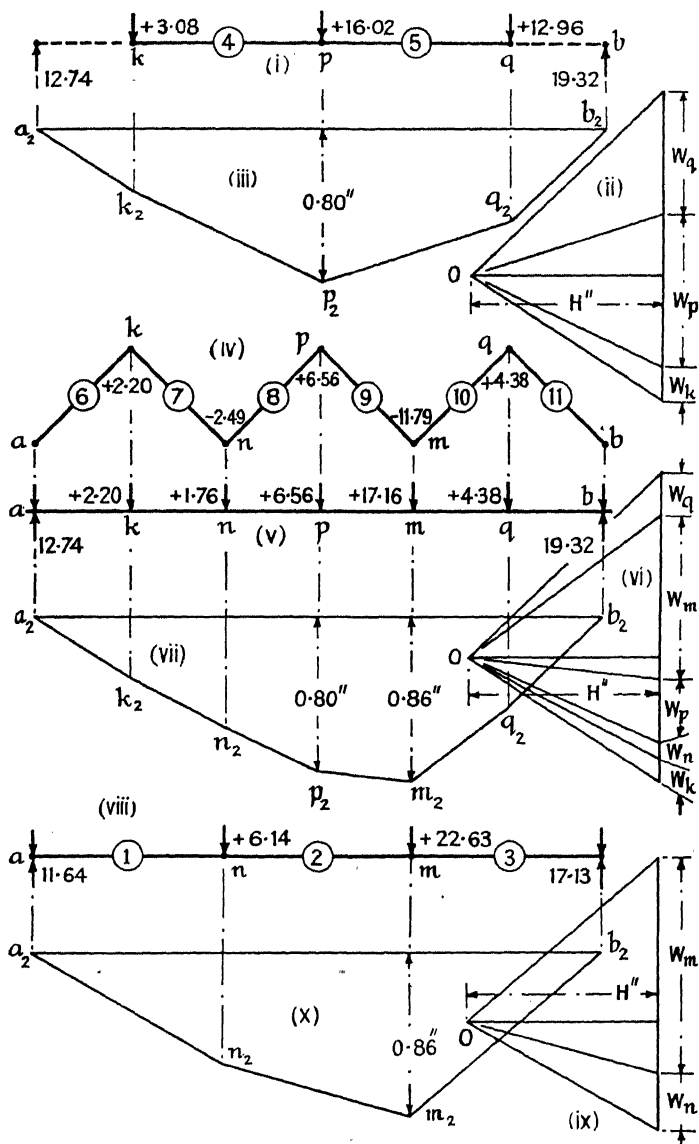* It is to be observed that in setting out the funicular polygon it will seldom be convenient to make $H = 1$ unit of elastic load, as assumed in deducing eq. (3). This is immaterial, since from eq. (2) the loads themselves are proportional to H. A trial with two different polar distances will demonstrate this. As shown above, the scale of the force polygon must be taken into account in the usual way.

maximum ordinate of the funicular polygon occurs at m, and scales $0.86''$. Hence, allowing for E, the deflection at m is

$$y_m = \frac{1}{\mathrm{E}} \cdot y_m'' \times \mathrm{H}'' \times a_1 a_2 = \frac{1}{13000} \times 0.86 \times 1 \times 120 \times 20 = 0.158 \text{ inch,}$$

which gives the scale of the diagram.

Next, consider the top flange; to get the total deflection of each point the flange must be prolonged by means of two bars shown in broken lines in (i) Fig. 37. The values of δA for the triangles thus formed are found in the usual way; the forces in the added bars are zero. Then the values of the elastic loads are given by eq. (5), the $+$ sign being taken,

$$\mathrm{W}_m = +\Sigma\delta A$$

From this equation, $\mathrm{W}_k = +3.08$; $\mathrm{W}_p = +16.02$; $\mathrm{W}_q = +12.96$; these elastic loads and the corresponding reactions are set out in (i) Fig. 37, (iii) is the corresponding funicular polygon. The scales are as before $a_1 = 120$; $a_2 = 20$; $\mathrm{H}'' = 1$ inch; the maximum ordinate y_p scales $0.80''$; hence,

$$y_p = \frac{1}{\mathrm{E}} \cdot y_p'' \times \mathrm{H}'' \times a_1 a_2 = \frac{1}{13000} \times 0.80 \times 1 \times 120 \times 20 = 0.148 \text{ inch.}$$

The two deflection polygons found above might have been obtained by considering the chain of diagonals shown in (iv). This is only possible when there are no vertical bars. The elastic loads are found from eqs. (3) and (4),

$$\mathrm{W}_m = \left[\pm \Sigma\delta A + \frac{1}{\mathrm{E}} \{ f_m \tan\theta_m - f_{m+1} \tan\theta_{m+1} \} \right] \tag{6}$$

The values of δA are reproduced from Fig. 36, the $+$ sign is taken for the upper panel points, and the $-$ sign for the lower. The values for $f_m \tan\theta_m$ are given in the table p. 41 with their correct sign. Take $\mathrm{E} = \text{unity}$. W_a and W_b need not be considered.

$$\mathrm{W}_k = [+\Sigma\delta A + \{(f\tan\theta)_6 - (f\tan\theta)_7\}]$$
$$= +2.20 + \{1.55 - 1.55\} = +2.20.$$
$$\mathrm{W}_n = [-\Sigma\delta A + \{(f\tan\theta)_7 - (f\tan\theta)_8\}]$$
$$= +2.49 + \{1.55 - 2.28\} = +1.76.$$
$$\mathrm{W}_p = +6.56 + 2.28 - 2.28 = +6.56.$$
$$\mathrm{W}_m = -(-11.79) + 2.28 - (-3.09) = +17.16.$$
$$\mathrm{W}_q = +4.38 + (-3.09) + 3.09 = +4.38.$$

The elastic loads and reactions are then as shown in (v), from which the funicular polygon (vii) has been set out to the same scales as before, $a_1 = 120$; $a_2 = 20$; $\mathrm{H}'' = 1$ inch. The deflection curve for the upper flange is got by joining the points $a_2 k_2 p_2 q_2 b_2$; that for the lower flange by joining the points $a_2 n_2 m_2 b_2$. The ordinate y_m scales $0.86''$, hence the deflection at m is

$$y_m = \frac{1}{\mathrm{E}} \cdot y_m'' \times \mathrm{H}'' \times a_1 a_2 = \frac{1}{13000} \times 0.86 \times 1 \times 120 \times 20 = 0.158 \text{ inch.}$$

The ordinate y_p scales $0\cdot80''$, hence

$$y_p = \frac{1}{13000} \times 0\cdot80 \times 1 \times 120 \times 20 = 0\cdot148 \text{ inch.}$$

These values agree exactly with those obtained from the deflection polygons (iii) and (x).

If the values for the deflections found by the elastic weight method, § 14, be compared with those found by the kinematic chain method, § 15, they will be found to be identical.

The effect of differences in temperature on the values of δA can be taken into account by using eq. (1), § 13, otherwise the procedure follows the normal course.

Had the frame of Fig. 36 been supported at b and m, as shown in (i) Fig. 38, and cantilevered out to a, the deflection of a could be found by an exactly similar process, excepting that, since all the external loads are reversed in direction, the elastic loads will all be negative. In the example shown in (i) Fig. 38 the magnitudes of the loads are the same as in Fig. 36. The deflection polygon $a_2n_2m_2b_2$, (x) Fig. 37, turned upside down, will therefore be the deflection polygon for the frame in Fig. 38, but the base line must pass through b_2 and m_2 since the deflection at these points is zero. Hence a_1a_2 represents the vertical deflection of the point a. The scale of the deflection curve is determined exactly as before.
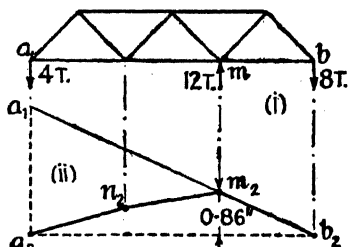
Fig. 38.

BIBLIOGRAPHY
Stresses in Plane Framework

1. RANKINE. Equilibrium of Impressed Forces in a Polygonal Frame. *Manual of Applied Mechanics.* London, 1st ed., 1858.
2. RITTER. *Elementare Theorie und Berechnung eiserner Dach- und Brücken-Konstructionen.* Hannover, 1863.
3. —— *Anwendung der Graphischen Statik.* Zürich, 1888–90.
4. CLERK-MAXWELL. On Reciprocal Figures and Diagrams of Forces. *Phil. Mag.* Apr. 1864, p. 250.
5. —— On the Application of the Theory of Reciprocal Polar Figures to the Construction of Diagrams of Forces. *The Engr.* Nov. 8, 1867, p. 402.
6. FLEEMING JENKINS. On the Practical Application of Reciprocal Figures to the Calculation of Strains on Framework. *Trans. Roy. Soc. Edin.,* vol. xxv, 1869, p. 441.
7. CULMANN. *Die Graphische Statik.* Zürich, 1st ed., 1866 : 2nd ed., 1875.
8. CREMONA. *Le figure reciproche nella Statica Grafica.* Milano, 1872 : trans. HUDSON BEARE, Oxford, 1890.
9. LÉVY. *La Statique Graphique.* Paris, 1874.
10. STEINER. *Die Graphische Zusammensetzung der Kräfte.* Wien, 1876.

11. CHALMERS. *Graphical Determination of Forces in Engineering Structures.* London, 1881.
12. MÜLLER-BRESLAU. *Die Graphische Statik der Baukonstruktionen.* Leipzig, 5th ed., 1912, Bd. I.
13. FÖPPL. *Vorlesungen über technische Mechanik, Bd. II. Graphische Statik,* Leipzig, 7th ed., 1926.
14. MERRIMAN AND JACOBY. *A Text Book on Roofs and Bridges. Pt. II. Graphic Statics.* New York, 5th ed., 1932.
15. JOHNSON, BRYAN and TURNEAURE. *The Theory and Practice of Modern Framed Structures.* Vol. i, *Stresses in Simple Structures.* New York, 10th ed., 1931.

Space Frames

16. RANKINE. Principle of the Equilibrium of Polyhedral Frames. *Phil. Mag.,* Feb. 1864, p. 92.
17. MAYOR. *Statique graphique des systèmes de l'espace,* 1910.
18. —— *Introduction à la statique graphique des systèmes de l'espace.* Lausanne, 1926.
19. V. MISES. Graphische Statik räumlicher Systeme. *Zeit. f. Math. u. Physik,* 1916 : see also KRUPPA, *Zeit. ang. Math. Mech.,* 1924, p. 146.
20. PRAGER. Beitrag zur Kinematik des Raumfachwerkes. *Zeit. ang. Math. Mech.,* 1926, p. 341.
21. FEDERHOFER. *Graphische Kinematik und Kinetostatik des starren räumlichen Systems.* Wien, 1928 ; also *Zeit. ang. Math. Mech.,* 1927, p. 290 ; 1929, p. 312 ; also SOTOFF, 1928, p. 393.
22. BEYER. Neue Wege zur zeichnerischen Behandlung der räumlichen Mechanik. *Zeit. ang. Math. Mech.,* 1933, p. 17 ; see also 1930, p. 618 ; 1931, p. 252.
23. SOUTHWELL. Primary Stress-Determination in Space-Frames. *Engg.* Feb. 6, 1920, p. 165 ; see also Ref. No. 28, Chapter VII, Bib.

Deflection of Framed Structures

24. MOHR. Beitrag zur Theorie des Fachwerks. *Zeit. d. Arch.- u. Ing.-Ver. z. Hannover,* 1875, p. 17.
25. WILLIOT. - Notions pratiques sur la statique graphique. *Ann. Génie civil,* vol. vi, 1877, p. 601 ; for an extension of the method to space frames, see HÜBNER, *Der Zivilingenieur,* 1893, p. 377.
26. KROHN. Der Satz von der Gegenseitigkeit der Verschiebungen etc. *Zeit. d. Arch.- u. Ing.-Ver. z. Hannover,* 1884, p. 269.
27. MÜLLER-BRESLAU. Beitrag zur Theorie des Fachwerks. *Zeit. d. Arch.- u. Ing.-Ver. z. Hannover,* 1885, p. 417.
28. STEWART. Stresses and Deflections in Braced Girders. *Proc. Inst. C.E.,* vol. cix, 1892, p. 269.

Kinematic Theory of Framed Structures

29. GRÜBLER. Beitrag zur Theorie des ebenen einfachen Fachwerks. *Rigasche Industrie-Zeitung,* 1887 ; also *Der Zivilingenieur,* 1883.
30. MÜLLER-BRESLAU. Beitrag zur Theorie des ebenen Fachwerks. *Schweiz. Bauzeit.,* 1887, May, p. 121 ; Nov., p. 129.
31. MOHR. Ueber Geschwindigkeitspläne und Beschleunigungspläne kinematischer Ketten. *Der Zivilingenieur,* 1887.
32. LAND. Kinematische Theorie der statisch bestimmten Träger. *Zeit. d. oest. Ing.- u. Arch.-Ver.* Jg. xl, 1888, pp. 11 and 62.

QUESTIONS ON CHAPTER I

In the following examples, unless otherwise directed, draw the stress diagram, measure and tabulate the forces in the members of the frame, indicating in all cases which are ties (+) and which are struts (−). See Fig. 39 for the outline of the frames.

1. Simple truss, loaded with 10 tons at the centre.
Ans. Forces : AC = − 10 ; AD = + 11·18 ; CD = − 10 tons.

2. Braced cantilever, built into a wall at A and B, carrying a load of 10 tons at C. The members of the top chord are equal and each is the base of an isosceles triangle. (U.L.)
Ans. Forces : BE = − 32·73 ; AD = + 30·63 ; AE = + 3·42 tons.

3. Roof truss, 30 ft. span, loaded as shown.
Ans. Forces : AF = FD = + 3·0 ; AE = 3·35 ; EC = − 2·24 ; EF = 0 : ED = + 2·24 ; CD = + 1·0 tons.

4. Roof truss, 36 ft. span, trusses 8 ft. apart. AD = DC = CE = EB and AF = FG = GC. Find the forces in the bars due to the weight of the roof which is 16 lb./sq. ft. of area covered. (U.L.)
Ans. Forces : AF = − 1·91 ; FG = − 1·53 ; GC = − 1·56 ; AD = + 1·64 ; DE = + 0·93 ; DC = + 0·76 ; GD = FD = − 0·35 ton.

5. Roof truss, subjected to wind loads shown in the figure. Assume that the end A is fixed, and B is supported on a pier which permits movement in a horizontal direction. (U.L.)
Ans. Forces : AG = − 13·7 : GH = − 11·4 ; HC = − 8·9 ; CB = − 12·3 ; AD = DE = + 19·3 ; EF = + 15·3 ; FB = + 10·7 ; CF = + 5·4 ; HF = − 7·1 ; HE = + 2·3 ; GE = − 4·6 tons ; rest zero.

6. Wall crane, upper bearing at A, footstep bearing at B. Load 3 tons. Chain passes over pulley at C.
Ans. Forces : AB = AC = + 4·6 ; BD = DC = − 8·2 ; AD = − 6·5 tons.

7. Foundry crane, upper bearing at A, footstep bearing at B. Load 10 tons at E. Find the stresses in all the members, and draw the bending moment and shearing force diagrams for AB and CE.
Ans. CD = + 16·7 ; FD = − 26 ; CF = + 10 tons ; $S_A = S_B = 13\frac{1}{4}$ tons ; M_F = 320 in.-tons ; S_D = 10 tons ; M_D = 1200 in.-tons.

8. Forces of 10, 9, and 12 lb. act on the rod AB as shown. The rod is kept in equilibrium by two forces, one acting at A, the other at B in the direction CB. Find the magnitude and direction of the force at A, and the magnitude of the force at B. (U.L. Dimensions added.)
Ans. R_A = 11·99 lb. at 72° 36′ with horizontal ; R_B = 14·97 lb.

9. The part of a pin jointed frame shown in the figure is loaded with a vertical dead load of 10,000 lb., and a normal wind pressure of 15,000 lb., both uniformly distributed along AB. Find the supporting forces P, Q, and R, and the forces in the bars which meet at C, indicating the struts and ties. (U.L.)
Ans. P = 12,310 ; Q = 1200 (reversed) ; R = 14,290 ; AC = + 20,100 ; CD = CE = − 9710 ; CB = + 18,980 lb.

10. The principals of a workshop roof, which are 15 ft. apart, are shown in the figure ; AF = FG = GC. A normal wind pressure of 30 lb. per sq. ft. acts on AC. Determine the forces in all the members of the roof, stating the assumptions made in determining them. (U.L.)
Ans. Forces : AF = − 3·93 ; AD = + 4·29 ; DC = + 3·05 ; DE = + 1·31 ; FD = − 1·45 tons. Reactions assumed parallel to loads.
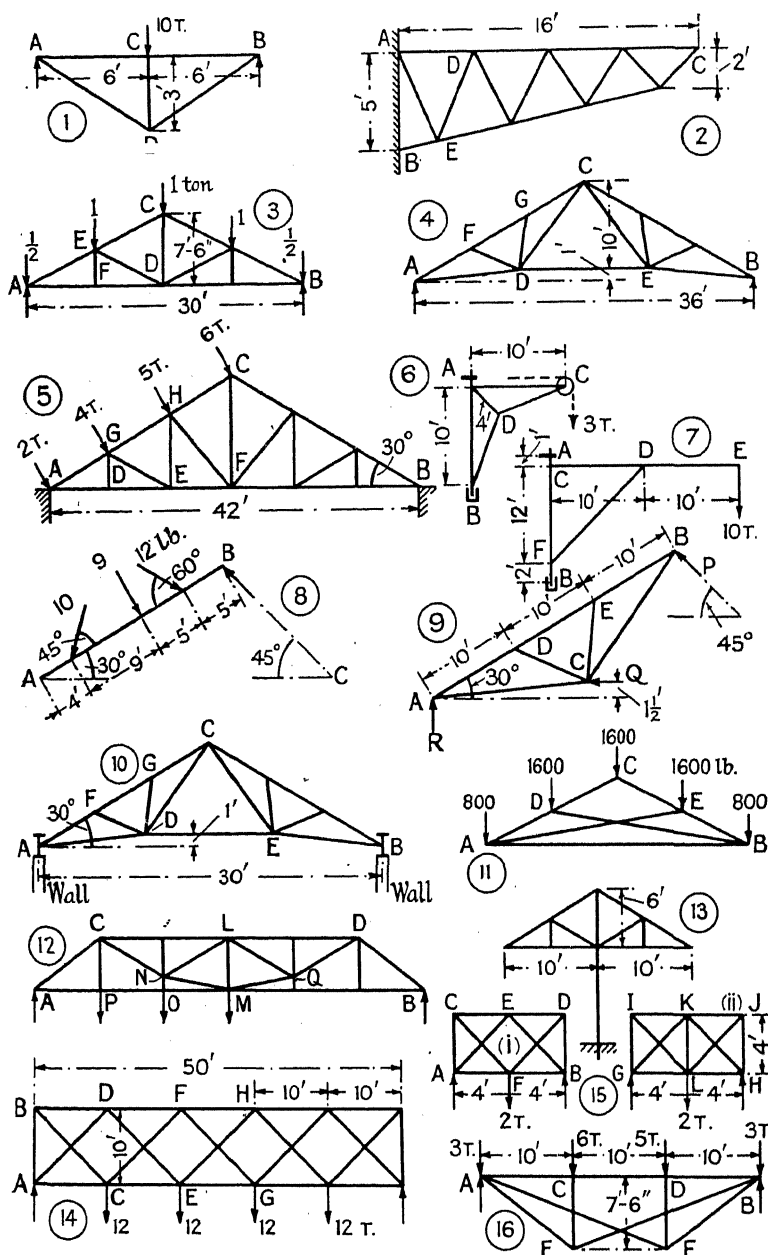
Fig. 39.

11. The figure shows the outline of a roof truss, span 28 ft., height 7 ft. Find graphically the stress in each member.   (U.L.)

Ans.   Forces: AB = + 5760 ;   AD = − 4120 ;   DC = − 1780 ;   AE = BD = − 2120 lb.

12. The span of the frame shown in the figure is 57 ft., LM = 7 ft., NO = 1·8 ft. There are loads of 2 tons at P, 4 tons at O, and 2 tons at M. Find the stresses in the members. (U.L.)

Ans. Forces: A to M = + 7·23; M to B = + 3·64; C to L = − 13·33; L to D = − 8·51; AC = − 8·98; CN = + 6·95; NM = + 3·75; BD = − 4·51; DQ = + 5·55; QM = + 7·38 tons.

13. The double cantilever roof shown in the figure has a span of 20 ft. and a rise of 6 ft. Total dead load 7500 lb. Total normal wind pressure 4500 lb. Find the forces in the members (*a*) due to the dead load, and (*b*) due to the wind pressure when acting on the left-hand side of the roof. (U.L.)

Ans. Forces: Rafter, (*a*) + 1820, + 3640; (*b*) + 1880, + 3070; Horizontal, (*a*) − 1560, (*b*) − 2190; verticals, (*a*) 0, − 5630; (*b*) 0, − 2550; diagonal, (*a*) − 1820; (*b*) − 2550 lb.

14. The double warren girder is supported at the ends and loaded as shown. Find the forces in the members. State the assumptions made. (U.L.).

Ans. See § 7; Forces: AB = − 14·4; AC = + 9·6; CE = + 26·4; EG = + 33·6; BD = − 14·4; DF = − 33·6; FH = − 38·4; AD = − 13·6; BC = + 20·4; DE = + 13·6; CF = − 3·4; EH = FG = + 3·4 tons.

15. The two frames, (i) and (ii), are alike in all respects excepting that (ii) has a vertical bar at the middle. Find the forces in all the members of both frames. State clearly any assumptions made, and justify them. (U.L.)

Ans. Forces: (i) AC = BD = − 1·0; CF = FD = + 1·41; CD = − 1·0; (ii) GI = HJ = − 0·5; IL = LJ = + 0·71; GK = KH = − 0·71; IK = KJ = − 0·5; GL = LH = + 0·5 tons.

16. Find graphically the stresses in all the members of the Bollman truss shown. (U.L.)

Ans. Forces: AB = − 9·8; AE = + 6·7; EB = + 5·7; AF = + 4·7; FB = + 5·6; CE = − 6; DF = − 5 tons.

17. In the frame shown in Fig. 40, AB = BC = CD = DE = 15 ft.: F bisects AB and G bisects DE. BA and DE are continuous. The weight per foot run on AB, BC, CD and DE is 200 lb., and there is a normal wind pressure of 300 lb. per ft. run on CD and 450 lb. per ft. run on DE. The reaction at A is vertical. Estimate the direct stresses in the members, all the joints being pins. Name the struts and ties. Find also the maximum bending moment in DE. (U.L.)

Ans. Reactions V_A = 9486; V_B = 9787; H_B = 8095 lb. Forces in FD = + 10,810, BG = + 21,060 lb. and so on; B.M. at G = 47,520 ft. lb.

18. The trestle shown in Fig. 40 has a top pull of 14 tons exerted upon it in the direction shown. Draw a diagram of the stresses in the members. The diagonal bracing may be assumed to be only capable of withstanding tensile forces. (U.L.)

Ans. Use the methods of § 7.

19. The N girder shown, with six panels each 10 ft. long by 12 ft. high, carries a load of 5 tons at each of the lower panel points. Find by the method of sections the stresses in all the members.

Ans. Forces: AD = 0; DF = + 10·42; FH = + 16·67; CE = − 10·42; EG = − 16·67; GJ = − 18·8; CD = + 16·26; EF = + 9·76; GH = + 3·25; AC = − 12·5; DE = − 7·5; FG = − 2·5; HJ = 0 tons.

20. Each top joint in the truss shown carries a load W. The top boom is divided into equal segments, and the length of the horizontal tie rod is one-half the span. Determine the ratio of depth to span so that the tension

in all the tie-rods shall be the same, and verify your results by drawing a stress diagram.   (U.L.)

Ans. $\sqrt{11/20}$.

21. Show that for a Bollman truss, if n be the number of equal panels, d the depth, l the span, and w the intensity of the uniform load, the horizontal stress in the top member is $\dfrac{wl^2}{6n^2d}\,(n^2 - 1)$.   (U.L)
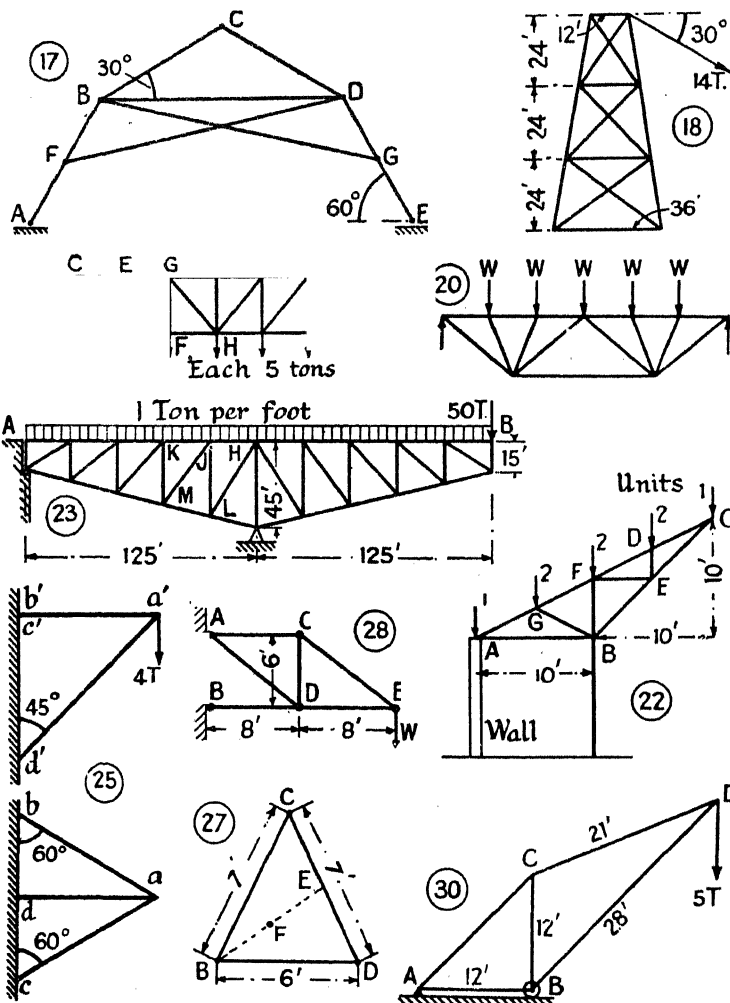

Fig. 40.

22. Find by the method of sections the stresses in the roof truss shown, and draw also the stress diagram.

Ans. $V_A = 0$, $V_B = 8$:. Forces : CF = GA = $+2\cdot24$; FG = $+4\cdot47$; CE = $-2\cdot83$;   EB = $-5\cdot66$;   DE = -2 ;   EF = $+2$;   FB = -3 ; GB = $-2\cdot24$; AB = -2.

THE FORCES IN FRAMED STRUCTURES

23. The figure represents one arm of a cantilever bridge. For the purpose of calculation the load on this frame may be taken as 1 ton per ft. run uniformly spread, together with a concentrated load from the suspended span of 50 tons, acting at B. Find the forces in the four members of the frame meeting in the point J. (I.C.E.)

Ans. Forces : KJ = + 198·9 ; JH = + 256·4 ; JM = + 95·2 ; JL = − 100·9 tons.

24. A lattice girder, 160 ft. span, is made in 10 panels of 16 ft. each. It weighs 40 tons, and the weight per ft. run may be considered as uniform. To float it into position it is placed on a pontoon, with supports under the panel point 32 ft. from each end. Draw the shearing force and bending moment diagrams for the weight of the girder, and give the maximum shearing force in any panel, and the maximum bending moment anywhere. If the flanges are parallel, and 20 ft. apart centre to centre, and the web bracing is of the N type, find the maximum force anywhere in a flange, and also in any web diagonal. (I.C.E.)

Ans. Max. S.F. = 10 tons ; max. B.M. = 160 ft. tons ; max. force in a flange = 80 tons ; max. force in diagonal = 12·8 tons.

25. The figure shows the plan and elevation of a triangulated framework projecting from a wall and carrying a vertical load of 4 tons at its apex. Find the forces in all the bars forming the frame, specifying whether they be tensile or compressive. (I.C.E.)

Ans. Forces : *ab* = + 2·31 ; *ac* = + 2·31 ; *ad* = − 5·66 tons.

26. The legs of a pair of sheer legs are each 45 ft. long, and the feet are spread 25 ft. on the ground. The guy rope is attached to the ground 64 ft.
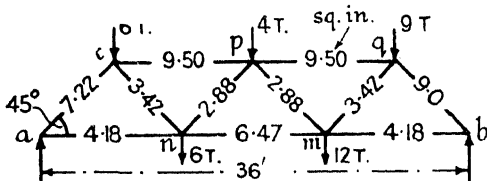
FIG. 41.

from the middle point of the line joining the two feet. A load of 30 tons is suspended from the legs. Find the thrust in each leg and the pull in the guy rope when the legs are 10 ft. out of the perpendicular. (U.L.)

Ans. 18·6 : 9·5 tons.

27. The feet of a tripod resting on smooth ground are tied by horizontal bars forming a triangle BCD, see the figure. E is the mid point of CD, F the mid point of BE. The apex A is 7 ft. above F. Find the stresses in all the bars when 1 ton is suspended at A.

Ans. Forces : AB = − 1220 ; AC = − 700 ; AD = − 660 ; BD = + 250 ; BC = + 290 ; CD = + 140 lb.

28. A cantilever frame of the dimensions shown carries at the point E a load W of magnitude such that it produces a stress in all the ties of 7 tons/sq. in., and in all the struts of 5 tons/sq. in. Determine, preferably by a graphical method, the vertical deflection of the point E. Take Young's modulus = 13,000 tons/sq. in. (I.C.E.)

Ans. 0·46 inch.

29. Find the vertical deflection of the point A of the crane structure shown in Q. No. 2, Chapter V, by means of a Williot diagram.

Ans. 0·079 inch.

30. Find the vertical deflection of the point D when the crane is carrying a load of 5 tons. The mean stress in all the tension members is 5 tons/sq. in. and in all the compression members is 4 tons/sq. in. (Fig. 40).

Ans. 0·70 inch.

31. Find by means of a Williot-Mohr diagram the deflection polygons for the girder shown in Fig. 41. The numbers on the figure represent the areas of the bars.

Ans. Deflections at $k = 0\cdot138$: $p = 0\cdot296$: $q = 0\cdot154$: $m = 0\cdot272$: $n = 0\cdot244$ inch.

32. Solve Q. No. 31 by an application of the kinematic chain method, §15.

33. Suppose the braced frame shown in Fig. 36 to be fixed in position at a, and free to move longitudinally at b. It is loaded at b with a horizontal load of 10 tons, acting in the direction from a to b. Using (i) the elastic weight method, § 14, and (ii) the kinematic chain method, § 15, find the vertical deflection of the lower flange.

Ans. 0·05 inch.

CHAPTER II

TRAVELLING LOADS

16. Maximum Shearing-Force and Maximum Bending-Moment Diagrams.—Let AB, Fig. 42, be a beam, supported at each end, across which the load W travels from left to right. When the load reaches K, the bending-moment diagram will be the triangle $a'k'b'$, (iii) Fig. 42, and when the load reaches J, the bending-moment diagram will be the triangle $a'j'b'$. If similar bending-moment diagrams be constructed for a sufficient number of positions of the moving load, a curve such as $a'k'j'b'$ can be drawn, enveloping them all. The ordinate of this curve, at any section of the beam, will represent the maximum bending moment which will occur there. This curve is called the *maximum bending-moment diagram*. Similarly, the *maximum shearing-force diagram* is a curve, (ii) Fig. 42, enveloping all the shearing-force diagrams. Such curves may be regarded as true bending-moment and shearing-force diagrams, and may be used for the purposes of design.
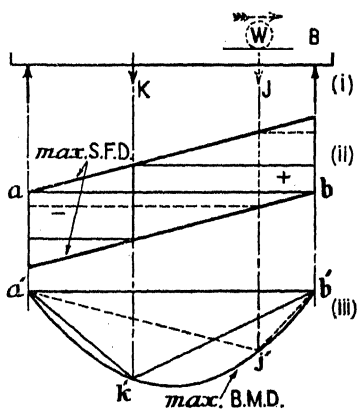
FIG. 42.

In certain cases it is not necessary actually to draw all the shearing-force and bending-moment diagrams, in order to determine the maximum shearing-force and maximum bending-moment diagrams, for these curves can be plotted from their equations, which can be found from the given conditions. The method of attack is as follows : For any section of the beam, find the *position* of the moving load which makes, say the shearing force at that section, a maximum. Put the load in this position, and find an expression for the magnitude of the shearing force at the section. This expression will be the equation to the maximum shearing-force diagram. A similar procedure will determine the equation to the maximum bending-moment diagram. Particular cases are considered in the Articles which follow.

17. Case (1). Single Concentrated Travelling Load.—Let AB, (i) Fig. 43, be a beam of span L, supported at each end, across which travels, from left to right, a single concentrated load W. To draw the maximum

shearing-force diagram, consider any section K, distant x from A, and in the first instance suppose the load to be at a distance z to the left of K. Find the reactions : $R_1L = W(L - x + z)$; and $R_2L = W(x - z)$. The shearing force at K, under these conditions, is $S_K = R_2 = W(x - z)/L$. This is positive, and increases as z diminishes, reaching a maximum when $z = 0$, i.e. when the load arrives at K. Put the load at K $(z = 0)$, then $R_2 = Wx/L$. Hence the maximum positive shearing force at the section K is,

$$\text{max. positive } S_K = \frac{W}{L} \qquad (1)$$

and occurs in front of the load, when the load arrives at K. Eq. (1) is the equation to the straight line af, (ii) Fig. 43, of which the maximum ordinate $bf = W$; and the maximum positive shearing force at K is represented by the ordinate kp.

When W passes to the right of K, a change in the shearing force at that section occurs. It becomes $S_K = R_2 - W = - R_1$, and is negative. But the value of R_1 decreases as the load travels on, and consequently the negative shearing force at K also decreases. It follows that the negative shearing force at K is also a maximum when the load is at K. With the load in this position, $R_1 = W(L - x)/L$. Hence the negative maximum shearing force at the section K is,

Fig. 43.

$$\text{max. negative } S_K = \frac{W}{L}(L - x) \qquad (2)$$

and occurs at the back of the load, when the load is at K. Eq. (2) is the equation to the straight line bg, of which the maximum ordinate $ag = - W$, and the maximum negative shear at K is represented by the ordinate kq.

It should be evident from the above that the maximum shear at K is either kp or kq, not their sum pq.

Consider next the maximum bending moment at K. With the load in the position shown in Fig. 43, the bending moment at K is negative, and equal to $M_K = - R_2(L - x) = \frac{W}{L}(L - x)(x - z)$ which increases as z diminishes, reaching a maximum when $z = 0$, that is when W is at K. If the load pass K, the bending moment at K will be $M_K = - R_1x$. As the load travels on, R_1 diminishes, and therefore M_K diminishes. It follows that the maximum bending moment at K occurs when the load is there, and its magnitude is,

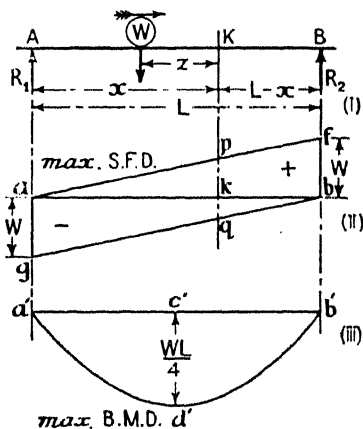$$\text{max. } M_K = \frac{W}{L}(L - x).x \qquad (3)$$

This is the equation to the maximum bending-moment diagram, which is the parabola $a'd'b'$ passing through a' and b', with its vertex at d', (iii) Fig. 43. The maximum ordinate $c'd' = -WL/4$, which is the bending moment at the centre of the beam when the load reaches that point.

Equivalent Uniform Load.—Since the maximum bending-moment diagram is a parabola with its vertex at d', it is evident that an equal bending moment would be produced at every section if the beam were loaded with a suitable uniform load. Such a load is called the *equivalent uniform load*. If its magnitude be w' per unit of length, the maximum ordinate of the bending-moment diagram at the centre of the span would be $-w'L^2/8$. Hence, for equality of bending moments everywhere,

$$\frac{w'L^2}{8} \cdot \frac{WL}{4}, \text{ and } w' = \frac{2W}{L} \qquad (4)$$

18. Case (2). Uniform Travelling Load, longer than the Span.—Let AB, Fig. 44, be a beam of span L, supported at each end, across which travels, from left to right, a uniform load w per unit of length, longer than the span. Consider the shearing force at any section K, distant x from A, when the front of the load has advanced to D, (i) Fig. 44, distant z from A. The shearing force S_K at K, with the load in this position, will be positive and equal to R_2 in magnitude. This reaction, R_2, can be found by taking moments about A. The load on the beam will be wz, and therefore, $R_2L = wz^2/2$. Hence $S_K = R_2 = +wz^2/2L$. This increases in magnitude as z increases, and attains a maximum when the front of the load reaches K, i.e. when $z = x$, max. $S_K = +wx^2/2L$.

FIG. 44.

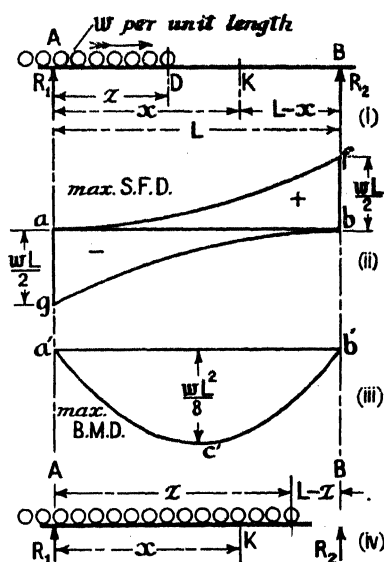When the front of the load passes K, a change occurs; and, for the position shown at (iv), Fig. 44,

$$S_K = R_2 - w(z - x) = \frac{wz^2}{2L} - w(z - x)$$

$$= wx + \frac{w}{2L}(-2Lz + z^2) = wx + \frac{w}{2L}\{(L - z)^2 - L^2\}$$

S_K evidently increases as $\{(L - z)^2 - L^2\}$ increases ; that is to say, as $(L - z)$ increases and z diminishes. Therefore the maximum shearing

force for the load position shown at (iv), Fig. 44, also occurs when $z = x$, i.e. when the front of the load is at K. It follows that

$$\text{max. } S_K = + \frac{wx^2}{2L} \qquad \cdot \qquad \cdot \qquad \cdot \qquad (1)$$

This is the equation to the parabola af, (ii) Fig. 43, with its vertex at a; the maximum ordinate $bf = wL/2$, and abf is the positive maximum shearing-force diagram. It will be evident, on consideration, that the maximum negative shearing-force diagram bag will be an exactly similar diagram to abf, but turned end for end. The maximum negative shearing force at any section such as K occurs when the back of the load is at K, and is then equal to R_1. The magnitude of the maximum ordinate ag is $- wL/2$.

The maximum bending moment at every section of the beam will occur when the travelling load completely covers the beam. This follows from the principle of superposi-tion, § 36, Vol. I, for the addi-tion of a load anywhere on a beam increases the bending moment everywhere. The maximum bending-moment diagram, therefore, is the parabola $a'c'b'$, (iii) Fig. 44, of which the maximum ordinate is $- wL^2/8$.

It is evident, in this case, that the magnitude of the equi-valent uniform load w' is equal to that of the travelling load w per unit of length.

19. Case (3). Uniform Travelling Load, shorter than the Span.—Let AB, Fig. 45, be a beam of span L, supported at each end, across which travels from left to right a uniform load w per unit of length, shorter than the span. Let l be the length of the travelling load, the total weight of which will

FIG. 45.

be wl. Consider the shearing force at any section K, distant x from A, when the front of the load has advanced to D, (i) Fig. 45, distant z from A. The shearing force S_K at K, with the load in the position shown, will be positive and equal to R_2 in magnitude. This reaction, R_2, can be found by taking moments about A, $R_2 L \quad wl \left(z - \frac{l}{2}\right)$. Hence,

$$= R_2 = \frac{wl}{L} \quad - \frac{l}{2}\right).$$ This increases as z increases, and attains a
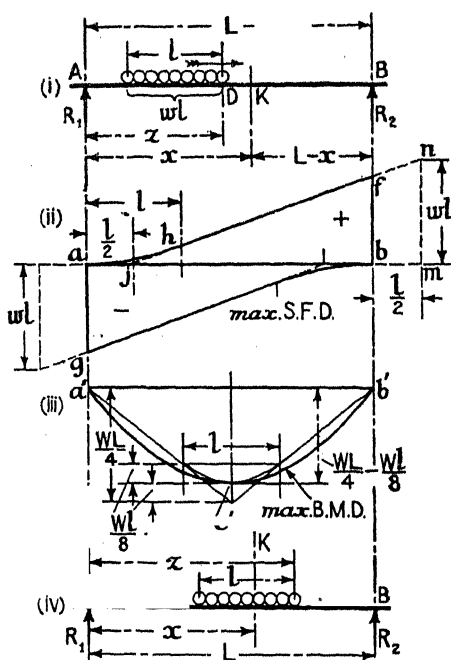
maximum when the front of the load reaches K, i.e. when $z = x$, max. $S_K = + \dfrac{wl}{L}\left(x - \dfrac{l}{2}\right)$. When the front of the load passes K, a change occurs. For the position shown at (iv), Fig. 45,

$$S_K = R_2 - w(z - x) = \frac{wl}{L}\left(z - \frac{l}{2}\right) - w(z - x)$$

$$= w\left(x - \frac{l^2}{2L}\right) - \frac{wz}{L}(L - l)$$

Since $L > l$, $(L - l)$ is positive, and the positive value of S_K decreases as z increases. Hence the positive maximum shearing force at K, for this condition of affairs, also occurs when the front of the load is at K. It follows that

$$\text{max. } S_K = + \frac{wl}{L}\left(x - \frac{l}{2}\right) \quad . \quad . \quad . \quad (1)$$

This is the equation to the straight line jfn, (ii) Fig. 45, of which the ordinate is zero at j ($x = l/2$), and equal to wl at m ($x = L + l/2$). Only the portion hf is of consequence, for until the whole of the load is on the beam, that is, until $x > l$, the above equations will not apply. For values of x less than l, the positive maximum shearing-force diagram will be the parabola ah, tangent to the straight line jf at h, and identical with the positive maximum shearing-force diagram, (ii) Fig. 44, for a load of equal intensity, longer than the span. The complete positive maximum shearing-force diagram, therefore, is the figure ahf. The maximum positive shearing force occurs at B, when the front of the load reaches that point, and is represented by the ordinate $bf = +\ ^{wl}\left(L - \dfrac{l}{2}\right)$.

The negative maximum shearing-force diagram bag will be an exactly similar diagram to abf, but turned end for end. The maximum negative shearing force at any section will occur when the back of the load reaches that section, and is then equal to R_1. The maximum ordinate $ag = -\dfrac{wl}{L}\left(L - \dfrac{l}{2}\right)$.

Consider next the bending moment at K. When the load is in the position shown at (i) Fig. 45, with the front of the load to the left of K, the bending moment at K is $- R_2(L - x)$. R_2 increases as the load advances, and therefore the bending moment at K increases. When the entire load has passed K, the bending moment there will be $- R_1x$. R_1 diminishes as the load travels on, and hence the bending moment at K diminishes. It follows that the maximum bending moment at K must occur after the front of the load has passed K, and before the back of the load has left K ; that is to say, in some such position as is shown at (iv) Fig. 45. The bending moment at K for this load position is,

$$M_K = - R_2(L - x) + \frac{w}{2}(z - x)^2, \text{ where } R_2 \quad \frac{wl}{L}\left(z - \frac{l}{2}\right).$$

Hence, $\qquad M_K = - \dfrac{wl}{L} \left(z - \dfrac{l}{2} \right) (L - x) + \dfrac{w}{2} (z - x)^2.$

To obtain the value of z for which this becomes a maximum, differentiate with regard to z and equate to zero,

$$\frac{dM_K}{dz} = - \frac{wl}{L} (L - x) + w (z - x) = 0 ;$$

or, $\qquad \dfrac{L - x}{L} = \dfrac{z - x}{l}$

and it follows that the maximum bending moment at any section K occurs when the ordinate at that section divides the span and the load in the same ratio. Put the load in this position. The value of z is $z = \dfrac{l}{L} (L - x) + x$, and $z - x = \dfrac{l}{L} (L - x)$. Hence the maximum bending moment at K is,-

$$\begin{aligned} \text{max. } M_K &= - \frac{wl}{L} \left\{ \frac{l(L - x)}{L} + x - \frac{l}{2} \right\} (L - x) + \frac{w}{2} \left\{ \frac{l}{L} (L - x) \right\}^2 \\ &= - \frac{wl}{L} (L - x) \left\{ \frac{l (L - x)}{L} + x - \frac{l}{2} - \frac{l}{2L} (L - x) \right\} \\ &= - \frac{wlx}{L} (L - x) \left(1 - \frac{l}{2L} \right) \qquad . \qquad . \qquad . \qquad . \qquad . \qquad (2) \end{aligned}$$

This is the equation to a parabola passing through a' and b', (iii) Fig. 45, with its maximum ordinate at c', where $x = L/2$. Inserting this value in the above equation

$$\text{max. } M_C = - \left\{ \frac{wlL}{4} - \frac{wl^2}{8} \right\} = - \left\{ \frac{WL}{4} - \frac{Wl}{8} \right\} \qquad . \qquad . \qquad . \qquad (3)$$

if $wl = W$.

If the equivalent uniform load be w' per unit of length,

$$\text{max. } M_C = - \frac{w'L^2}{8} = - \left\{ \frac{WL}{4} - \frac{Wl}{8} \right\} ;$$

whence, $\qquad w' = \dfrac{2W}{L} \left\{ 1 - \dfrac{l}{2L} \right\} \qquad . \qquad . \qquad . \qquad . \qquad (4)$

20. Case (4). Two Concentrated Travelling Loads at a Fixed Distance Apart.—Let AB, Fig. 46, be a beam of span L, supported at each end, across which travel, from left to right, two concentrated loads W_1 and W_2, at a fixed distance l apart. To draw the maximum shearing-force diagram. When the travelling load first enters the span, only one load W_1 will come on the beam. The positive maximum shearing-force diagram for this condition of affairs will be the straight line ah, (ii) Fig. 46, part of the triangle aeb, of which the maximum ordinate $be = W_1$ exactly as in Case (1) for the single concentrated travelling load. When W_1 has passed the point H, distant l from A, both loads will be on the beam, and the conditions will be altered. Consider the shearing force at any section K, distant x from A. While both loads are to the left of

K, the shearing force S_K, at K, will be positive and equal to R_2. This will increase as the load travels on, until W_1 arrives at K. When W_1
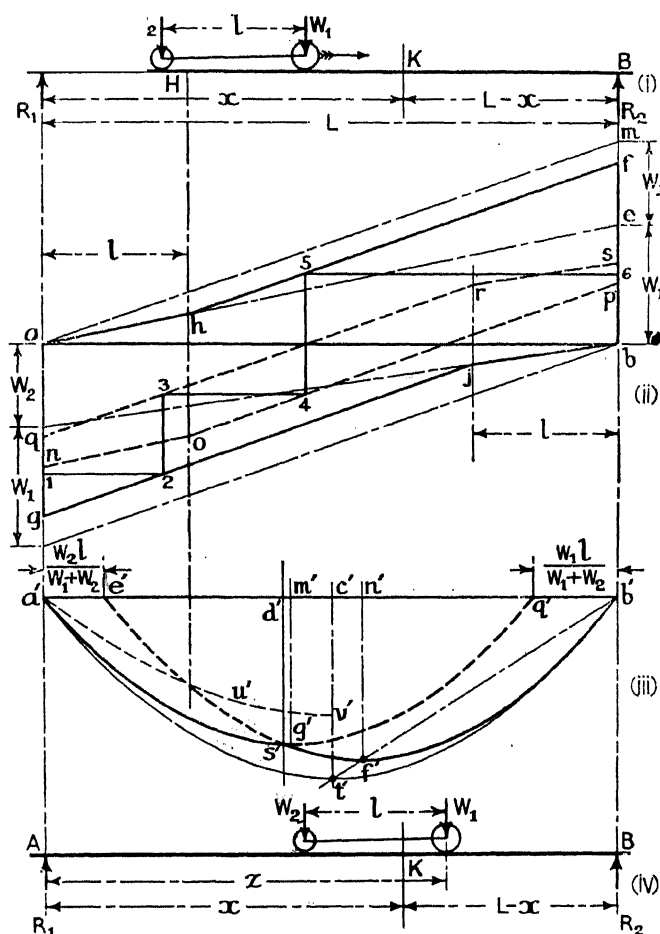
FIG. 46.

passes K there will be a sudden reduction in the positive shearing force at K, which will become $S_K = + (R_2 - W_1)$. This value of S_K also increases as the load advances, until W_2 arrives at K. When W_2 passes K there will be a second reduction in the shearing force at K, which will then have the value $S_K = + (R_2 - W_1 - W_2) = - R_1$, thus becoming negative and equal to the reaction R_1. It follows that the maximum positive shearing force at any section K must occur, either when W_1 is at that section, or when W_2 is there. When W_1 is at K,

$$R_2 L = W_1 x + W_2 (x - l) = (W_1 + W_2) x - W_2 l, \quad \text{and,}$$

$$\text{ax. } S_K \quad R_2 = \left[(W_1 + W_2) \frac{x}{L} - W_2 \frac{l}{L} \right] = S_K \quad (1)$$

When W_2 is at K, $R_2L = W_1 (x + l) + W_2 x = (W_1 + W_2)x + W_1 l$,
and,

$$\text{max. } S_K = R_2 - W_1 = + \left[(W_1 + W_2)\frac{x}{L} - W_1 \frac{L - l}{L} \right] = S_K'' \quad . \quad (2)$$

The graphs of eqs. (1) and (2) are shown in (ii) Fig. 46.   Eq. (1) represents the straight line hf.   Its slope is $(W_1 + W_2)/L$, and therefore it is parallel to am.   When $x = l$, $S_K' = + W_1 l/L$, which is the height of the ordinate of the straight line ae at h.   Hence the graph of eq. (1) passes through h. At $x = L$, the maximum ordinate $bf = + \left[W_1 + W_2 \frac{L - l}{L} \right]$.   The broken line ahf, therefore, is the positive maximum shearing-force diagram for sections immediately in front of W_1.   The maximum shearing force immediately behind W_1 is $[S_K' - W_1]$.   This is represented by the dotted line nop drawn parallel to ahf, and at a distance W_1 below it.   This shearing force may be positive or negative, depending on the position of the load.

Turning next to eq. (2), which represents the maximum shearing force immediately in front of W_2, this is the equation to the straight line qr, with a slope $(W_1 + W_2)/L$, and parallel to hf.   When $x = 0$, the ordinate $aq = - W_1 \frac{(L - l)}{L}$.   When the load W_1 passes B there is a change, for only W_2 will remain on the beam.   This load will then have reached the ordinate through r, distant l from B.   As in Case (1), the maximum shearing force in front of W_2 under these conditions will be the straight line rs, slope W_2/L, of which the maximum ordinate $bs = W_2$.   The dotted line qrs, therefore, is the maximum shearing-force diagram for the front of W_2.   For some positions of the load this shearing force is positive, for others it is negative.   The maximum shearing force immediately behind W_2 is equal to $[S_K'' - W_2]$.   It occurs when W_2 is at the section K, is always negative, and equal to R_1.   This is represented in the diagram by the line gjb, parallel to qrs, and at a distance W_2 below it.   The maximum ordinate $ag = - (aq + W_2) = - \left[W_1 \frac{L - l}{L} + W_2 \right]$.

The complete maximum shearing-force diagram consists, therefore, of the four lines ahf, nop, qrs, gjb ; and, in the case considered, $ahfb$ is the positive maximum shearing-force diagram, and $agjb$ the negative maximum diagram.   It does not follow that the maximum positive shearing force will always be represented by ahf, nor the maximum negative shearing force by gjb ; for in certain cases the point r may lie outside hf, and the point o outside gj.   The relation of the four lines to the actual shearing-force diagram for the particular position of the load shown in (i) Fig. 46 is indicated by the stepped figure 1.2.3.4.5.6.

Consider next the bending moment M_K at K.   When the load is in the position shown at (i) Fig. 46, with W_1 to the left of K, the bending moment at K is $- R_2(L - x)$. R_2 increases as the loads advance, and therefore M_K increases.   When both loads, W_1 and W_2, have passed K, the bending

moment there will be $- R_1 x$. R_1 diminishes as the loads advance, and therefore the bending moment at K diminishes. It follows that the maximum bending moment at K must occur after W_1 has reached K, and before W_2 has left K. Examine an intermediate position as shown at (iv) Fig. 46, when W_1 is distant z from A. For this position,

$$M_K = - [R_2(L - x) - W_1(z - x)], \quad R_2 L = W_1 z + W_2(z - l),$$

and hence

$$M_K = - \left[\{ W_1 z + W_2 (z - l) \} \frac{L - x}{L} - W_1(z - x) \right] \quad . \quad . \quad (3)$$

$$= - \left[W_1 x - W_2 l \frac{L - x}{L} + z \left\{ (W_1 + W_2) \frac{L - x}{L} - W_1 \right\} \right] \quad (4)$$

Consider the coefficient of z in eq. (4). By giving certain values to x this coefficient can be made either positive or negative. If it be positive, the value of M_K will be greater the greater the value of z. But since it has been shown that max. M_K must occur before W_2 has left K, it follows that if this coefficient be positive, the maximum bending moment at K will occur when W_2 is at K. If the coefficient of z be negative, the value of M_K is greater the less the value of z, and since the maximum bending moment at K occurs after W_1 has reached K, it follows that max. M_K occurs when W_1 is at K. For certain values of x, therefore, which make the coefficient of z positive, max. M_K occurs when W_2 is at K. For other values of x, which make the coefficient negative, max. M_K occurs when W_1 is at K. At the limiting position, between each set of values for x, this coefficient will be zero, i.e.,

$$(W_1 + W_2) \frac{L}{ } - W_1 = 0 \; ;$$

from which, $\quad x = \dfrac{W_2}{W_1 + W_2} L, \quad$ and $\quad (L - x) \dfrac{W_1}{W_1 + W_2} L,$

or

$$\frac{x}{L - x} = \frac{W_2}{W_1} \quad (5)$$

If then, a point d' be taken in the line $a'b'$, (iii) Fig. 46, such that $a'd' : d'b' = W_2 : W_1$, for all values of x lying between a' and d' the bending moment at any section will be a maximum when W_2 arrives at that section, and for all values of x lying between d' and b' the bending moment at any section will reach a maximum when W_1 is at the section. The length $a'd'$ is called the field of W_2, and $d'b'$ the field of W_1. In the field of W_2 the bending moment is a maximum under W_2, and in the field of W_1 the bending moment is a maximum under W_1.

For the field of W_1, max. M_K occurs when $z = x$, (W_1 at K). Insert this value in eq. (3), then

$$\text{max. } M_K = - \left[\{ W_1 x + W_2 (x - l) \} \frac{L - x}{L} \right]$$

$$= - \left[\frac{L - x}{L} \{ (W_1 + W_2) x - W_2 l \} \right] \quad . \quad (6)$$

This is the equation to the parabola $e'f'b'$, (iii) Fig. 46. When $x = L$, max. $M_K = 0$; when $x = \dfrac{W_2 l}{W_1 + W_2}$, max. $M_K = 0$. Hence the parabola passes through the points b' and e', where $a'e' = \dfrac{W_2 l}{W_1 + W_2}$. The maximum ordinate $n'f'$ occurs when

$$x = \tfrac{1}{2}\left\{ L + \frac{W_2 l}{W_1 + W_2} \right\}, \text{ or } L - x = \tfrac{1}{2}\left\{ L - \frac{W_2 l}{W_1 + W_2} \right\};$$

and, from eq. (6),

$$n'f' = -\left[\frac{W_1 + W_2}{4L}\left\{ L - \frac{W_2 l}{W_1 + W_2} \right\}^2 \right] . \qquad (7)$$

For the field of W_2, max. M_K occurs when $z = x + l$, (W_2 at K). Inserting this value in eq. (3),

$$\text{max. } M_K = -\left[\{W_1 (x + l) + W_2 x\} \frac{L - x}{L} - W_1 l \right]$$

$$= -\left[\{W_1 + W_2) x + W_1 l\} \frac{L - x}{L} - W_1 l \right]$$

$$= -\left[\frac{x}{L} \{(W_1 + W_2)(L - x) - W_1 l\} \right] . \qquad (8)$$

This is the equation to the parabola $a'g'q'$; max. M_K is zero when $x = 0$, and also when $x = \left\{ L - \dfrac{W_1 l}{W_1 + W_2} \right\}$. Hence the parabola passes through a' and q', where $a'q' = \left\{ L - \dfrac{W_1 l}{W_1 + W_2} \right\}$. The maximum ordinate $m'g'$ occurs when $x = \tfrac{1}{2}\left\{ L - \dfrac{W_1 l}{W_1 + W_2} \right\}$, and is,

$$m'g' = -\left[\frac{W_1 + W_2}{4L}\left\{ L - \frac{W_1 l}{W_1 + W_2} \right\}^2 \right] . \qquad (9)$$

The two parabolas cross on the line $d's'$ which divides the field of W_1 from the field of W_2. The complete maximum bending-moment diagram is $a's'f'b'$.

To obtain the equivalent uniform load it is necessary to determine the smallest parabola which will envelop this diagram. The required parabola will have a common tangent to the larger of the two parabolas forming the maximum bending-moment diagram. Its maximum ordinate $c't'$ is obtained by the geometrical construction shown in (iii) Fig. 46, from which it follows that,

$$c't' = n'f' \frac{b'c'}{b'n'} = -\left[\frac{W_1 + W_2}{4L}\left\{ L - \frac{W_2 l}{W_1 + W_2} \right\}^2 \right] \frac{L}{L - \dfrac{W_2 l}{W_1 + W_2}}$$

$$= -\left[\frac{W_1 + W_2}{4}\left\{ L - \frac{W_2 l}{W_1 + W_2} \right\} \right];$$

but if w' be the equivalent uniform load per unit of length, $c't' = -\dfrac{w'L^2}{8}$, hence

$$w' = \frac{2(W_1 + W_2)}{L^2}\left\{L - \frac{W_2 l}{W_1 + W_2}\right\} \qquad . \qquad . \quad (10)$$

In certain cases it is possible that the maximum bending moment may occur under the greater load when that load alone is on the beam. The maximum bending-moment diagram under W_1, when that load only is on the beam, will be a parabola such as $a'u'v'$, (iii) Fig. 46, obtained as in Case (1), § 17. If $W_1 > W_2$, and $l > \dfrac{W_2}{W_1 + W_2}$ L, this parabola will lie outside $a's'g'$, and thus form part of the complete maximum bending-moment diagram. The enveloping parabola representing the equivalent uniform load must in this case enclose the parabola $a'u'v'$.

21. Case (5). A Series of Concentrated Travelling Loads at Fixed Distances Apart.—When the number of concentrated loads exceeds

(i) Ɔ F E D C

(v) A ————————— B

On the Drawing Paper   On the Tracing Paper.
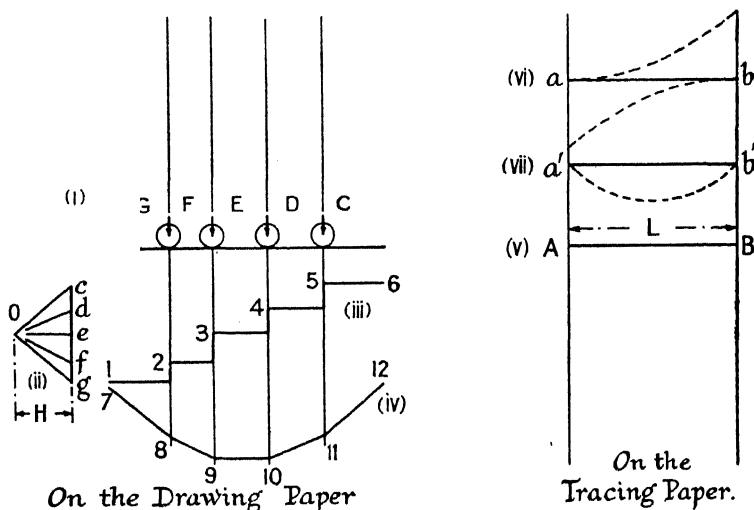
FIG. 47.

two, it is better to adopt graphical means in order to obtain the maximum shearing-force and bending-moment diagrams. The simplest procedure is what is known as the *tracing paper method*. This is an extension of the graphical process of § 33, Vol. I.

Given a span AB, length L, across which travels, from left to right, a series of concentrated loads at fixed distances apart, to draw the maximum shearing-force and bending-moment diagrams. On a sheet of drawing paper, set out the lines of action, CDEFG, (i) Fig. 47, of the series of travelling loads, and suppose them resting on a beam of unlimited span. These lines of action should be extended above and below the beam as

shown. Set off the magnitudes of the loads on the load line *cdefg*, and with any pole O, complete the force polygon (ii). Draw next the stepped figure 1.2.3.4.5.6, part of the shearing force diagram, shown at (iii). Draw also the link polygon 7.8.9.10.11.12, forming part of the bending-moment diagram, shown at (iv). These figures cannot be completed yet,
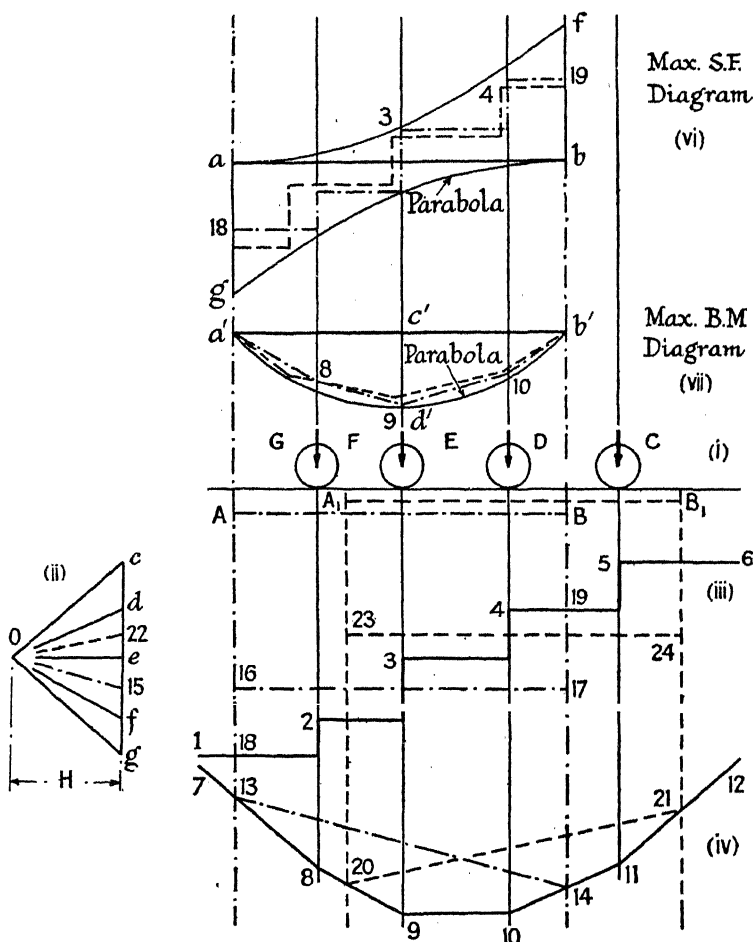
FIG. 48.

for the position of the closing line is unknown. Nothing else should be drawn on the drawing paper.

On a sheet of tracing paper, draw to the length scale used on the drawing paper, a horizontal line AB, (v) Fig. 47, to represent the actual span L, and erect perpendiculars A*a*, B*b*, at the ends of the span. These lines should be prolonged upward and downward as shown. Draw also the

horizontal lines ab and $a'b'$ (vi and vii). No other lines should, at present, be drawn on the tracing paper. The lines ab and $a'b'$ are to form the base lines for the maximum shearing-force and bending-moment diagrams, which will appear later as shown by the dotted lines.

Superpose the tracing paper on the drawing paper so that the combined appearance is as shown in Fig. 48 ; AB, at (i), represents the span. The perpendiculars at the end of the span will cut the link polygon at 13.14. Draw the line 13.14 on the tracing paper, this will be the closing line of the bending-moment diagram for this position of the loads relative to the span AB. In the force polygon draw 0.15 parallel to 13.14. Project across, and draw 16.17 the closing line of the shear-force diagram. No other lines should be drawn on the tracing paper below AB. Then 16.18.3.19.17 is the shearing force diagram for the span AB with the loads in this particular position. Transfer this diagram to the base line ab, (vi). It will appear as the stepped figure a.18.3.19.b in (vi), drawn on the tracing paper. The prolongation of the lines of action of the loads will be found of convenience in this operation. Next transfer the bending-moment diagram 13.8.9.10.14 to the base line $a'b'$, (vii), where it will appear as a'.8.9.10.b', drawn on the tracing paper. The tracing paper can now be shifted until the span occupies another position A_1B_1, when the process is repeated ; 20.21 is the new closing line of the bending-moment diagram, 0.22 the line parallel thereto in the force polygon, and 23.24 the closing line of the shear-force diagram. These new diagrams are now transferred to their respective base lines in (vi) and (vii) as before, which, being on the tracing paper, will move along with the span. To avoid a confusion of lines, this movement has not been shown in Fig. 48.

If the operation be repeated a sufficient number of times, a series of shearing-force and bending-moment diagrams, for many positions of the moving load, will be obtained on the base lines ab and $a'b'$ respectively. It remains to draw enveloping curves, § 16, which curves will be the maximum shearing-force and maximum bending-moment diagrams. It will be seen that in effect the load remains stationary and the span moves, which does not affect the results obtained.

It is usual, though not necessary, to draw parabolas for the enveloping curves, in which case the magnitude of the equivalent uniform load is easily determined. Suppose that bf be the maximum ordinate of the enveloping parabolas abf, abg, (vi) Fig. 48, representing the maximum shearing-force diagrams. If w be the equivalent uniform load per unit of length, which, travelling across the beam, would produce the same maximum shearing force at every cross section, $bf = wL/2$ (see § 18),

and $w = \dfrac{2}{L} (bf)$. bf is measured to the load scale.

If $c'd'$ be the maximum ordinate of the parabola $a'd'b'$, (vii) Fig. 48, representing the maximum bending-moment diagram, the maximum bending-moment at the centre is max. $M_C = c'd' \times H$, where $c'd'$ is measured to the distance scale, and H is the polar distance measured to the load scale. If w' be the equivalent uniform load per unit of length

which would produce the same maximum bending moment at every cross section, max. $M_C = w'L^2/8$; or $w' = \dfrac{8}{L^2}$ (max. M_C) $= \dfrac{8H}{L^2}$ $(c'd')$.

It will usually be found that the value of w' differs from that of w, in which case w should be used for the purpose of designing those portions of the beam which carry the shearing force, and w' for those portions which carry the bending moment.

22. Standard Loadings.—For the purpose of bridge design, certain conventional loadings have been standardised. (i) Fig. 49 shows Cooper's E-72 loading used for main line railway bridges in America. Each unit
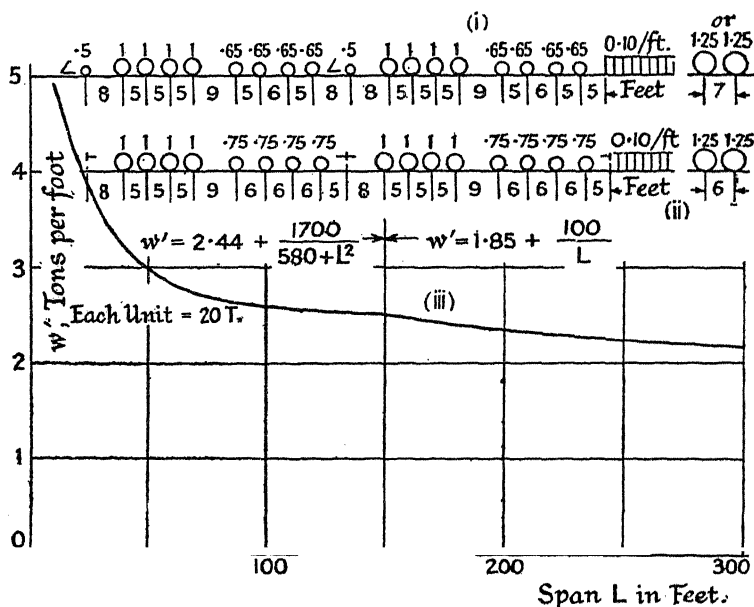
FIG. 49.

of loading represents 72,000 lb. (ii) shows the British Standard loading for main line railway bridges, each unit of loading representing 20 tons.

Values of w', the equivalent uniform load for bending moment at the centre of the span, corresponding to this loading, may be obtained from the curve (iii),

$$L < 150, \quad w' = 2\cdot44 + 1700/(580 + L^2) \text{ tons per foot} \qquad (1)$$
$$L > 150, \quad w' = 1\cdot85 + 100/L \text{ tons per foot} \qquad . \qquad (2)$$

The equivalent uniform loads for bending, given by this curve, are sufficiently accurate for approximate calculation in the case of railway bridges of span greater than 17 ft. For exact values, including values of the maximum shear both at the centre and ends of the span, see Appendix No. 1 [10] to British Standard Specification, No. 153, Parts 3, 4 and 5, 1930.

When designing short spans, cross girders, and rail bearers, the maximum axle loads, shown to the right in (i) and (ii) Fig. 49, must be taken into account.

The equivalent uniform loads given by eqs. (1) and (2) do not take into account the dynamic effects of the moving load, commonly referred to as *impact*. To make allowance for this, an *impact factor i* may be used, see § 61. If the value of w' from eqs. (1) and (2) be multiplied by $(1 + i)$, and the equivalent uniform load thus obtained be treated as a static load on the bridge, the stresses computed therefrom may be taken as equivalent to those produced by the travelling load when crossing the bridge.

Alternatively, the British Bridge Stress Committee (Ref. No. 16, Chap. IV) have published tables of equivalent uniform loads, based on their experiments, and intended for the purpose of design, in which the dynamic effects of the moving load are included.

23. Standard Loading for Highway Bridges.—Particulars of the latest (1931) Ministry of Transport loading for highway bridges are given in Fig. 50. The following explanations accompany the curve.

The uniformly distributed load applicable to the 'loaded length' of the bridge or member in question is selected from the curve or table.

The 'loaded length' is the length of member loaded in order to produce the most severe stresses. In a freely supported span the 'loaded length' would thus be (a) for bending moment; the full span. (b) for shear at the support; the full span. (c) for shear at intermediate points; from this point to the farther support.

In arches and continuous spans the 'loaded length' can be taken from the influence line curves.

. The live load to be used consists of two items : (1) The uniformly distributed load which varies with the loaded length, and which represents the ordinary axle loads of the M.T. standard train, perfectly distributed. (2) An invariable knife edge load of 2,700 lb. per foot of width applied at the section where it will, when combined with the uniformly distributed load, be most effective, i.e. in a freely supported span : (a) for bending moment at midspan ; at midspan point. (b) for shear at the support ; at the support. (c) for shear at any section ; at the section.

This knife edge load represents the excess in the M.T. standard train of the heavy axle over the other axles, this excess being undistributed (except laterally as already assumed).

In spans of less than 10 ft. (i.e. less than the axle spacing) the concentration serves to counteract the over-dispersion of the distributed load.

In slabs the knife edge load of 2,700 lb. per ft. of width is taken as acting parallel to the supporting members, irrespective of the direction in which the slab spans.

In longitudinal girders, stringers, etc., this concentrated loading is taken as acting transversely to them (i.e. parallel with their supports).

. In transverse beams the concentrated loading is taken as acting in line with them (i.e. 2,700 lb. per ft. run of beam).

STANDARD LOAD FOR HIGHWAY BRIDGES
EQUIVALENT LOADING CURVE

TABULATED VALUES

Span	lb/□	Span	lb/□
100	208	1,200	100
150	192	1,300	97
200	180	1,400	94
250	170	1,500	90
300	163	1,600	88
350	156	1,700	85
400	150	1,800	82
450	145	1,900	79
500	140	2,000	77
600	132	2,100	76
700	125	2,200	74
800	119	2,300	73
900	114	2,400	72
1,000	108	2,500	70
1,100	104		

MINISTRY OF TRANSPORT
ROADS DEPARTMENT
SEPTEMBER 1931

Constant at -70#/□'

Distribution Steel in Slabs

The approximate amounts of steel parallel to the supports, as % of main reinforcement.

Span	%	Span	%
4'	40	8'	55
5'	45	10'	60
6'	50	Max. 0.5"/ft.	

Uniformly Distributed Load Lbs per Sq. ft.

Loaded Length in Feet.

TABULATED VALUES.

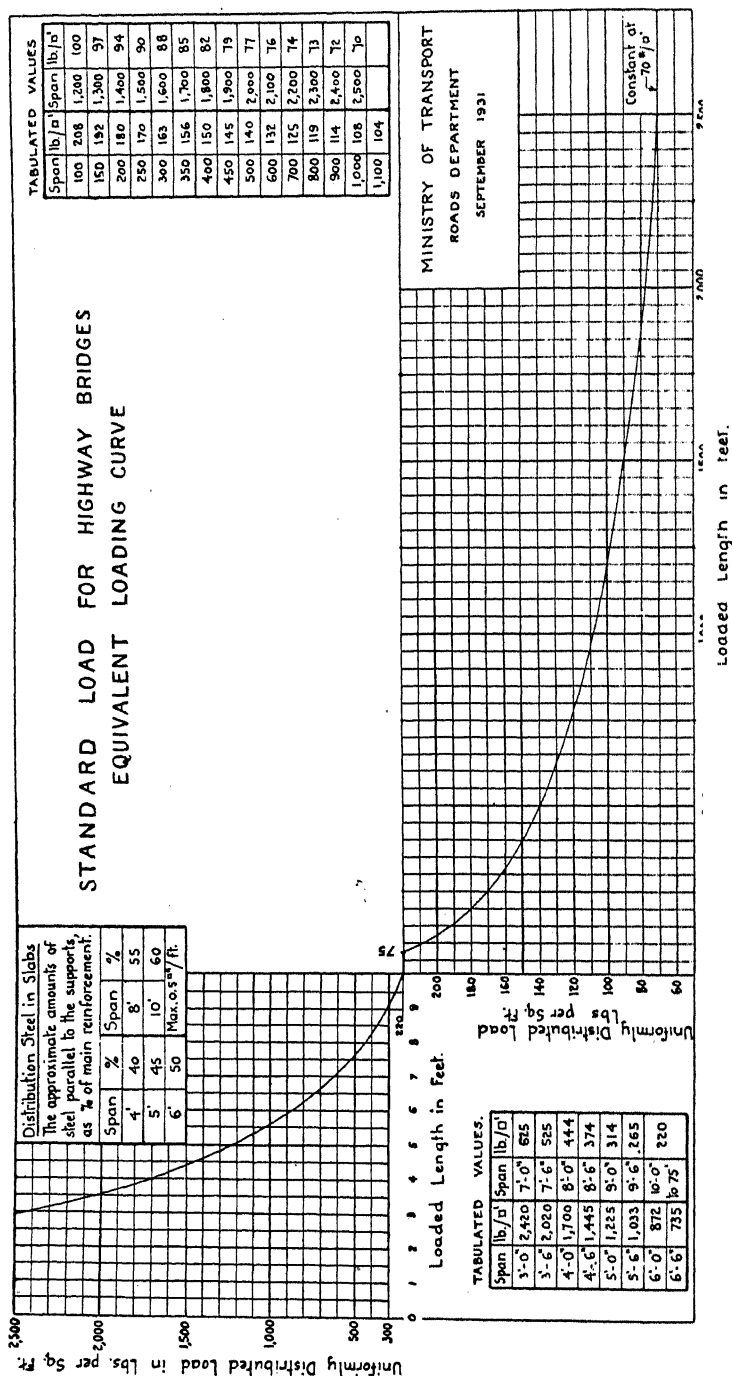| Span	lb/□	Span	lb/□
3'-0"	2,420	7'-0"	625
3'-6"	2,020	7'-6"	525
4'-0"	1,700	8'-0"	444
4'-6"	1,445	8'-6"	374
5'-0"	1,225	9'-0"	314
5'-6"	1,033	9'-6"	265
6'-0"	872	10'-0"	220
6'-6"	735	10'75"	

Uniformly Distributed Load in Lbs. per Sq. Ft.

FIG. 50.

Reproduced by permission of the Controller of H.M. Stationery Office from the Ministry of Transport Memorandum No. 483 on the Lay-out and Construction of Roads, 1937, Appendix 1 (b).

If longitudinal or transverse members are spaced more closely than at 5 ft. centres, the live load allocated to them shall be that calculated on a 5 ft. wide strip. With wider spacing this strip will be equal to the girder spacing.

In all cases, irrespective of span length, one knife edge load of 2700 lb. per foot of width is taken as acting in conjunction with the uniform distributed load appropriate to the span or ' loaded length.'

The loading, which is the minimum recognised by the Ministry, includes the effect of impact, which need not be considered separately. On spans exceeding 75 ft. a reduction has been made in the intensity of the loading, as compared with the standard train, to allow partly for the lower average weight of vehicles in the larger group, and partly for the lessening effect of impact on the longer spans. For spans below 10 ft. the equivalent loading makes allowance for bending moments in both directions, of which only the main bending moment need be calculated. For a discussion of the derivation of the loading, reference may be made to *Reinforced Concrete Bridge Design*, Chettoe and Adams, London, 1933.

24. Position of Load for which the Bending Moment is a Maximum at any Section.—It is sometimes convenient to determine the position of the travelling load for which the bending moment at any section is a maximum. Let $AB = L$ be the span, Fig. 51, K any section distant x from A. Let the sum of all the loads on $AK = \Sigma W'$ and of those on $KB = \Sigma W''$. A load is considered to be still on AK unless it has actually passed K. Suppose the distance of
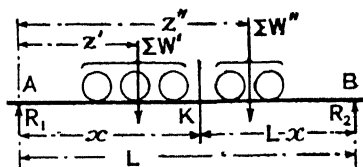
FIG. 51.

the centre of gravity of the loads on AK to be z' from A, and of those on KB to be z'' from A. Then $R_2 L = (\Sigma W') z' + (\Sigma W'') z''$; and the bending moment at K is $M_K = - R_2(L - x) + (\Sigma W'')(z'' - x)$.

Inserting the value of R_2,

$$M = - \quad \{(\Sigma W') z' + (\Sigma W'') z''\} + (\Sigma W'')(z'' - x)$$

Let the loads move a small distance δz to the right, increasing M_K to $M_K + \delta M_K$. Then,

$$M_K + \delta M_K = - \frac{L - x}{} \{(\Sigma W')(z' + \delta z) + (\Sigma W'')(z'' + \delta z)\} + (\Sigma W'')(z'' + \delta z - x)$$

and

$$\delta M_K = - \frac{L - x}{L} \{(\Sigma W') \delta z + (\Sigma W'') \delta z\} + (\Sigma W'') \delta z$$

or

$$\frac{dM_K}{dz} \quad \frac{L - x}{L} \{\Sigma W' + \Sigma W''\} + \Sigma W'' \qquad . \quad (1)$$

Since the bending moment at K is negative, if $\dfrac{dM_K}{dz}$ be negative, the

bending moment has increased and will go on increasing until a load passes K. If, as a load passes K, $\dfrac{dM_K}{dz}$ changes from negative to positive a maximum has occurred, the condition for which is $\dfrac{dM_K}{dz} = 0$, or

$$\frac{\Sigma W' + \Sigma W''}{L} = \frac{\Sigma W''}{L - x} \qquad . \qquad . \qquad . \qquad (2)$$

But $(\Sigma W' + \Sigma W'')/L$ is the average load per unit of length on the whole span, and $(\Sigma W'')/(L - x)$ is the average load per unit of length on the part span KB. Hence, for the bending moment at any section of a beam to reach a maximum, a load must be passing the section, and the average load per unit of length on each part into which the span is divided by the section must be equal to the average load per unit of length on the whole span.

It remains to discover the effect of a load entering or leaving the span. Eq. (1) may be written,

$$\frac{dM_K}{dz} = -\frac{L - x}{L}(\Sigma W') + \left(1 - \frac{L - x}{L}\right)(\Sigma W'')$$

$$= -\frac{1}{L}\{(L - x)(\Sigma W') - x(\Sigma W'')\}$$

If a load enter the span before a load passes K, the value $\Sigma W'$ will be increased; and, from the above expression, the negative value of $\dfrac{dM_K}{dz}$ will be increased. If a load leave the span, the $\Sigma W''$ will be decreased, and again the negative value of $\dfrac{dM_K}{dz}$ will be increased. It is obvious that a load entering or leaving the span cannot make $\dfrac{dM_K}{dz}$ change from negative to positive, and therefore cannot produce a maximum.

In practical cases, with a system of concentrated loads, the numerical averages will not be exactly equal, but the load position which most nearly fulfils the ascertained condition will produce the maximum bending moment at K.

The above propositions are also true if the load be distributed, wholly or in part.

25. Position of Load for which the Bending Moment is a Maximum under a Particular Load.—Suppose it be desired to find the position of the travelling load when the bending moment is a maximum under a particular load such as J, Fig. 52. Let AB = L be the span, and ΣW be

Fig. 52.

the sum of all the loads upon it. Suppose, when the bending moment under load J is a maximum, that load J is at a distance x from A. Let $\Sigma W'$ be the sum of all the loads to the left of J. Further, let the centre
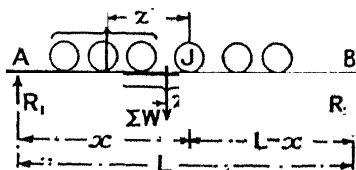
of gravity of all the loads ΣW be z from J, and that of the loads $\Sigma W'$ be z' from J. Then $R_1 L = (\Sigma W)(L - x + z)$, and the bending moment under J is, $M_J = -R_1 x + (\Sigma W') z' = -\dfrac{\Sigma W}{L}(L - x + z)x + (\Sigma W') z'$.

Differentiate with respect to x, z and z' being constant,

$$\frac{dM_J}{dx} = -\frac{\Sigma W}{L} \cdot (L - x + z) + \frac{\Sigma W}{L} \cdot x.$$

The bending moment under J is a maximum when dM_J/dx is zero, i.e. when $x = L - x + z$, or when the particular load, and the centre of gravity of the *whole* load on the beam, are equidistant from the ends of the span, and consequently from the centre of the span.

By finding the maximum bending moment under each load in turn, this proposition can be used to find the maximum bending moment anywhere on a beam, due to a system of concentrated rolling loads.

INFLUENCE LINES

26. Influence Lines.—In the preceding articles, curves have been determined giving the maximum shearing force and maximum bending moment, due to a travelling load, at *every* section of a beam, irrespective of the position of the moving load which produces them. These curves were called maximum shearing-force and maximum bending-moment diagrams. A shearing force or bending moment *influence line* may be defined as a curve giving the shearing force or bending moment at *one particular* section of the beam, for every position of the travelling load. For example, (iii) Fig. 53 is the bending moment influence line for the section K, in the beam AB, when the single concentrated load W travels across the beam. The ordinate $c'd'$ of the influence line represents the bending moment at K when the load is at any position C. The position of the load for which the bending moment at K is a maximum is evident from inspection, and the magnitude of that moment can be easily calculated. The influence-line is therefore a simple means of indicating the effect of travelling loads. Influence lines can be drawn not only for shearing forces and bending moments, but for reactions, stresses in particular members, deflections, and, in fact, for all functions which vary with the position of the moving load.

It is customary to draw influence lines showing the effect of a load of unit magnitude passing over the beam or other structure, from which influence lines the effect of more complicated load systems can be deduced. Shearing-force and bending-moment influence lines for a plain beam, supported at each end, will first be considered.

27. Case (1). Single Concentrated Travelling Load.—Let W, Fig. 53, be a single concentrated load of magnitude unity, travelling across the span AB from left to right. To draw the influence lines for shear and bending moment for any section K of the beam. Let AB = L, and consider any particular section K, distant x from A. Suppose the load

to have reached C, distant z from A. For this position, $R_1 = W \dfrac{L - z}{L}$;

and $R_2 = W \dfrac{z}{L}$. Then S_K, the shearing force at K for this load position,

is equal to $R_2 = Wz/L$ and is positive. Since the magnitude of the

load is unity, $S_K = R_2 = + \dfrac{z}{L}$. On the base line ab, (ii) Fig. 53, draw

the diagram abf, such that bf is unity. Then the ordinate under the

load $cd = bf \cdot \dfrac{ac}{ab} = \dfrac{z}{L}$. That is to say, this ordinate represents to scale

the shearing force at K when the load is at C. This state of affairs will
hold good until W passes to the right of K. The shearing force at K
then becomes negative, and equal to

$R_1 = - W(L - z)/L$; or, since W
is unity, $S_K = - (L - z)/L$. If the
triangle bae be drawn, such that
$ae =$ unity, its ordinate at any section
distant z from A will be $- (L - z)/L$
$= S_K$. This applies while the load is
to the right of K.

A   (i)   B

(ii)   S.F. Influence Line

(iii)   B.M. Influence Line

FIG. 53.

The diagram aj_1kj_2b, thus de-
termined, is called the *shearing force
influence line* for the point K, and
is such that, when unit load is at
any point C, the ordinate cd of the
diagram represents in sign and magni-
tude the shearing force at K. The
scale of the ordinate is evidently the
scale to which $bf = ae =$ unit load.
It is obvious that the shearing force
at K reaches its maximum value
as W arrives at K, i.e. when $z = x$.
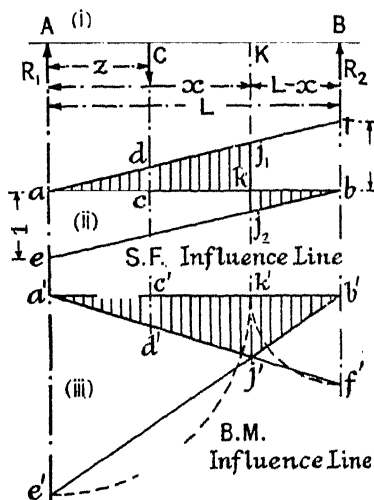
Positive maximum $S_K = \dfrac{x}{L} = kj_1$; negative maximum $S_K = - \dfrac{L - x}{L}$

$= kj_2$. It follows that the maximum shearing force at any section of
the beam occurs when the load arrives at that section.

If W have any value other than unity, the magnitude of the shearing
force, found from the influence line, must be multiplied by the magnitude
of W. In this case it is better to regard the ordinates cd as numerals,
which, multiplied by the magnitude of W in tons, give the shearing
force in tons.

Consider next the bending moment at K when the load is at C. M_K,
for this position, is negative and equal to $- R_2 (L - x) = -Wz (L - x)/L$.

Since the magnitude of W is unity, $M_K = - \dfrac{z}{L} (L - x)$. On the base line

$a'b'$, draw the diagram $a'e'f'b'$, (iii) Fig. 53, such that $a'e' = a'k'$, and
$b'f' = b'k'$. Then $a'f'$ and $b'e'$ will meet at j' in the line $k'j'$. The ordinate

$c'd' = b'f' \cdot \dfrac{z}{L}$ But $b'f' = -b'k' = -(L - x)$, and $c'd' = -\dfrac{z}{L} \cdot (L - x)$

$= M_K$. Hence the ordinate $c'd'$, immediately under the load, represents to scale the bending moment at K when the load is at C. This will be true for every position of the load between A and K. When the load passes to the right of K, the bending moment at K is $M_K = -R_1 x$

$= -\dfrac{W(L - z)}{L} x$; or, since the magnitude of W is unity, $M_K = -\dfrac{L - z}{L} x$.

But $a'e' = -x$; and any ordinate of the line $b'e$ distant z from A,

will equal $-\dfrac{L - z}{L} x = M_K$. Therefore the ordinate of the line $b'e'$,

immediately under the load, will represent to scale the bending moment at K while the load is to the right of K.

The diagram $a'j'b'$, thus determined, is called the *bending moment influence line* for the point K, and is such that, when unit load is at any point C, the ordinate $c'd'$ of the diagram represents to scale the bending moment at K. It is evident that $k'j'$ is the maximum ordinate of the diagram, and therefore the maximum bending moment at K occurs when

the load arrives there, i.e. when $z = x$; max. $M_K = -\dfrac{(L - x) x}{L}$.

Scale.—Since $a'e'$ was made equal to $a'k'$, and $b'f'$ equal to $b'k'$, it follows that the ordinate of the influence line ·must be measured to the

scale to which $a'b' = L$. If this scale be $1'' = a_1$ inches, and $W = 1$ ton, then $M_K = a_1 \times (c'd'$ measured in inches) inch-tons. If W have a value other than unity, the magnitude of the bending moment found from the ordinate of the influence line must be multiplied by the magnitude of W.

It is evident from the above that the maximum bending moment at any section of the beam occurs when the load is at that section.

28. Case (2). A Series of Concentrated Travelling Loads at Fixed Distances Apart.—Suppose that there are several concentrated

Fig. 54.

loads of magnitude W_1, W_2, W_3 at fixed distances apart, travelling across the span AB from A to B (Fig. 54). To find the maximum shearing force and bending moment at any section K by means of influence lines. Let AB $= L$. For the section K, draw the influence lines for shearing
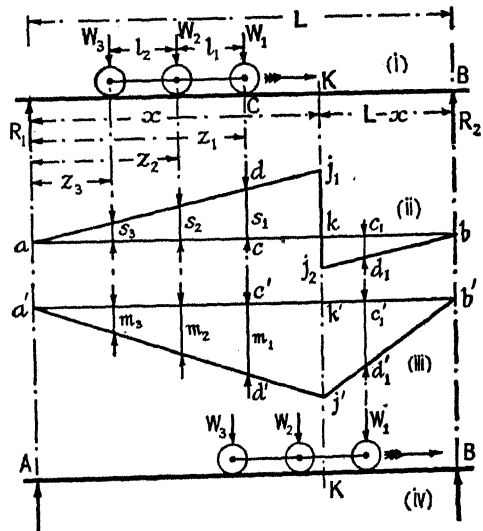
force and bending moment, (ii) and (iii) respectively, as in Case (1). Consider the shearing force at K for any load position such as that shown at (i), where the distances of W_1, W_2, W_3, from A are z_1, z_2, z_3 respectively. From the analysis given in Case (1) it follows that the shearing force at K, due to W_1, will be $W_1 \times cd$, where cd is the ordinate of the shear influence line immediately under W_1. Let $cd = s_1$ (s_1 must not be confused with the shear per unit of depth of § 174). Then the shearing force at K, due to W_1 at C, is $W_1 s_1$. For the load position shown, this is positive in sign. Similarly, the shearing force at K, due to W_2, is $W_2 s_2$, where s_2 is the ordinate of the shear influence line immediately below W_2; and likewise, the shearing force at K, due to W_3, is $W_3 s_3$. The total shearing force at K for this load position is, therefore, $S_K = W_1 s_1 + W_2 s_2 + W_3 s_3 = \Sigma(Ws)$. Due account is to be taken of the sign of the ordinates [for the load position shown at (iv), s_1, represented by $c_1 d_1$, would be negative]. It follows, therefore, that the shearing force at any section K is equal to the algebraic sum of the products obtained by multiplying the magnitude of each load by the ordinate of the shear influence line immediately below it.

Returning to load position (i), it will be evident that, as the load moves on, the ordinates s_1, s_2, s_3, and therefore the positive shearing force at K, will increase, and go on increasing until W_1 reaches K. Let S_K' be the positive shearing force at K when W_1 is there. When W_1 just passes K there will be a sudden drop in the shearing force to a value $S_K' - W_1$; and s_1 will become negative. As the load moves on, this diminished shearing force will increase (for both s_2 and s_3 will increase, and s_1 which is negative will diminish), and go on increasing until W_2 arrives at K. The increase in the shearing force from the moment W_1 leaves K until W_2 arrives there can be found as follows : All the loads have moved a distance l_1, the slope of aj_1 and bj_2 is $+ 1/L$, hence the *positive* increase in each ordinate s is l_1/L. The increase in the shearing force, consequently,

is $W_1 \dfrac{l_1}{L} + W_2 \dfrac{l_1}{L} + W_3 \dfrac{l_1}{L}$ $(\Sigma W) \dfrac{l_1}{L}$; and S_K, when W_2 arrives at K, is

$S_K'' = S_K' - W_1 + (\Sigma W) \dfrac{l_1}{L}$. If S_K'' be less than S_K', the shearing force when W_1 is at K,

$$S_K' - W_1 + (\Sigma W) \dfrac{l_1}{L} < S_K' ; \quad \text{or } \Sigma W < \dfrac{W_1 L}{l_1}.$$

In the same way it can be shown that S_K''', the shearing force at K when W_3 is there, is less than S_K'' when W_2 is there, if $\Sigma W < \dfrac{W_2 L}{l_2}$. It follows that the positive shearing force at K will be a maximum when the first load is at K, unless $\Sigma W > \dfrac{W_1 L}{l_1}$; in the latter alternative it will be a maximum when the second load is at K, unless $\Sigma W > \dfrac{W_2 L}{l_2}$, and so on. By similar reasoning it can be shown that the negative shearing force at

K is a maximum when the last load W_n is at K, unless $\Sigma W > \dfrac{W_n L}{l_{n-1}}$; in the latter alternative it will reach a maximum when the last load but one is at K, unless $\Sigma W > \dfrac{W_{n-1} L}{l_{n-2}}$, and so on.

These criteria must be applied to each load in turn. It sometimes happens that there is apparently more than one maximum value for the shearing force at K, in which case the magnitude of each apparent maximum value must be calculated to determine which is the greatest.

The maximum positive shearing force on the span will usually occur at or very near the end of the span, when the first or second of the heaviest loads of a series is just leaving; and the maximum negative shearing force will occur at or near the other end, when the last or last but one heavy load has just entered the span.

Consider next the bending moment at K for the load position (i). If $c'd' = m_1$ be the ordinate of the bending moment influence line below the load W_1, (iii), the bending moment at K due to W_1 will be $W_1 m_1$. Similarly, if m_2 and m_3 be the ordinates of the bending moment influence line below W_2 and W_3 respectively, the bending moment at K due to W_2 and W_3 will be $W_2 m_2$ and $W_3 m_3$. Therefore the total bending moment at K, for this load position, will be $W_1 m_1 + W_2 m_2 + W_3 m_3 = \Sigma(Wm)$. In this instance, all the values of m are negative. It follows that the bending moment at any section K is equal to the algebraic sum of the products obtained by multiplying the magnitude of each load by the ordinate of the bending moment influence line immediately below it. If the ordinates are measured to the length scale and expressed in inches, and the loads in tons, the bending moment will be in inch-tons.

The result obtained above is evidently true for all positions of the moving load. Suppose that the loads are in the position shown at (iv), and that they move on a short distance δz. Every ordinate m will become $m + \delta m$, and $M_K = \Sigma(Wm)$ will become $M_K + \delta M_K = \Sigma\{W(m + \delta m)\} = \Sigma(Wm) + \Sigma(W. \delta m)$; hence $\delta M_K = \Sigma(W. \delta m)$. Dividing through by δz, and proceeding to a limit, $\dfrac{dM_K}{dz} = \Sigma\left(W. \dfrac{dm}{dz}\right)$ Now $\dfrac{dm}{dz}$ is the slope of the lines $a'j'$ and $b'j'$, (iii) Fig. 54. The slope of $a'j'$ is $\dfrac{dm'}{dz} = -\dfrac{L-x}{L}$, see (iii) Fig. 53 ; and the slope of $b'j' = \dfrac{dm''}{dz} = +\dfrac{x}{L}$. Let $\Sigma W'$ be the sum of all the loads on AK, and $\Sigma W''$ the sum of all the loads on BK. Then,

$$\frac{dM_K}{dz} = (\Sigma W')\frac{dm'}{dz} + (\Sigma W'')\frac{dm''}{dz} = -(\Sigma W')\frac{L-x}{L} + (\Sigma W'')\frac{x}{L}.$$

The bending moment M_K is negative ; if, therefore, $\dfrac{dM_K}{dz}$ be negative, M_K has increased and will go on increasing until a load passes K. If, when this happens, $\dfrac{dM_K}{dz}$ becomes positive, a maximum has occurred, the

condition for which is $\dfrac{dM_K}{dz} = 0$, or $\Sigma W'. (L - x) = \Sigma W''. x$; whence $\dfrac{\Sigma W'}{x} - \dfrac{\Sigma W''}{L - x} = \dfrac{\Sigma W}{L}$; compare eq. (2) § 24. It follows that the bending moment at K is a maximum when a load is there, and when, at the same time, the average load per unit of length on the two sections into which K divides the span is the same, and equal to the average load per unit of length for the whole span. A load is still considered to be on AK unless it has actually passed K. In practical cases the numerical averages will not be exactly equal, but the load position which most nearly fulfils this condition will produce the maximum bending moment at K. This proposition was proved in a different way in § 24.

Worked Example.—As a simple example of the method of using influence lines, the case shown in Fig. 55 will be considered.

$$W_1 = 2 \text{ tons, } W_2 = 10 \text{ tons,}$$
$$W_3 = 5 \text{ tons.}$$

Calculated in the ordinary way the shearing forces and bending moments at K are,

FIG. 55.

When W_1 is at K, $S_K = + 7 \cdot 0$ tons; $M_K = - 700$ inch-tons.

$$W_2 \qquad\qquad\quad + 8 \cdot 4 \qquad\qquad = - 920$$
$$W_3 \qquad\qquad\quad - 2 \cdot 33 \qquad\qquad = - 467$$

Using the influence lines of Fig. 55 to find these shearing forces and bending moments :

When W_1 is at K,

$$W_1 s_1 = \ 2 \text{ tons} \times + 0 \cdot 667 = + 1 \cdot 33 \text{ tons.}$$
$$W_2 s_2 = 10 \quad ,, \quad \times + 0 \cdot 467 = + 4 \cdot 67 \quad ,,$$
$$W_3 s_3 = \ 5 \quad ,, \quad \times + 0 \cdot 20 \ = + 1 \cdot 00 \quad ,,$$
$$S_K = + 7 \cdot 00 \quad ,,$$

When W_2 is at K,

$$W_1 s_1 = \ 2 \text{ tons} \times - 0 \cdot 133 = - 0 \cdot 27 \text{ tons.}$$
$$\ _2 = 10 \quad ,, \quad \times + 0 \cdot 667 = + 6 \cdot 67 \quad ,,$$
$$W_3 s_3 = \ 5 \qquad \times + 0 \cdot 40 \ = + 2 \cdot 00 \quad ,,$$
$$S_K = + 8 \cdot 40 \quad ,,$$

When W_3 is at K (W_1 is off the span),

$$W_1 s_1 = \ 2 \text{ tons} \times \quad 0 \cdot 00 \ = \quad 0 \cdot 00 \text{ tons.}$$
$$W_2 s_2 = 10 \quad ,, \quad \times - 0 \cdot 067 = - 0 \cdot 67 \quad ,,$$
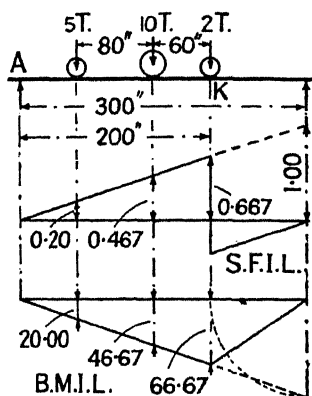$$\ \cdot 5 \quad ,, \quad \times - 0 \cdot 333 = - 1 \cdot 66 \quad ,,$$
$$S_K = - 2 \cdot 33 \quad ,,$$

Note that the negative ordinate for s_3 has been taken, giving the maximum value for $- S_K$.

When W_1 is at K,

$W_1 m_1 = 2$ tons $\times - 66 \cdot 67$ in. $= - 133 \cdot 3$ inch-tons.
$W_2 m_2 = 10$,, $\times - 46 \cdot 67$,, $= - 466 \cdot 7$,, ,,
$W_3 m_3 = 5$,, $\times - 20 \cdot 00$,, $= - 100 \cdot 0$,, ,,

$$M_K = - 700 \cdot 0 \text{ ,, ,,}$$

When W_2 is at K,

$W_1 m_1 = 2$ tons $\times - 26 \cdot 67$ in. $= - 53 \cdot 3$ inch-tons.
$W_2 m_2 = 10$,, $\times - 66 \cdot 67$,, $= - 666 \cdot 7$,, ,,
$W_3 m_3 = 5$ $40 \cdot 0$ $= - 200 \cdot 0$

$$M_K = - 920 \cdot 0 \text{ ,, ,,}$$

When W_3 is at K, and W_1 off the span,

$W_1 m_1 = 2$ tons $\times$ $0 \cdot 00$ in. $= -$ $0 \cdot 0$ inch-tons.
$W_2 m_2 = 10$,, $\times - 13 \cdot 33$,, $= - 133 \cdot 3$,, ,,
$W_3 m_3 = 5$,, $\times - 66 \cdot 67$,, $= - 333 \cdot 3$,, ,,

$$M_K = - 466 \cdot 6$$

To verify the above figures, the influence lines should be set out to a large scale, and the ordinates scaled (or they may be calculated).

Applying the criteria for the maximum values of the shearing force : When W_1 is at K, $\Sigma W = 17$; $W_1 L/l_1 = 2 \times 300 \div 60 = 10$; so that ΣW is greater than $W_1 L/l_1$ and the maximum shearing force does not occur when the first load is at K. When W_2 is at K, $\Sigma W = 17$; $W_2 L/l_2 = 10 \times 300 \div 80 = 37 \cdot 5$; the latter is greater than ΣW and a maximum will occur with W_2 at K. There cannot be a positive maximum with W_3 at K, and it follows that max. $+ S_K$ occurs when W_2 is at K, as proved by the values already calculated. Considering the negative shearing force at K when W_3 is there, $\Sigma W = 15$; $W_3 L/l_{n-1} = 5 \times 300 \div 80 = 18 \cdot 75$, which is greater than ΣW, and therefore, max. $- S_K$ occurs when the last load is there. The value is found above.

Applying the criteria for the maximum bending moment, the average load per unit of length on the whole span AB, when all three loads are on the span, is $17 \div 300 = 0 \cdot 057$ ton/in. When W_1 has just reached K, the average load per unit of length on AK is $17 \div 200 = 0 \cdot 085$ ton/in. and on KB is $0 \cdot 00$. With W_2 at K, the average load per unit of length on AK is $15 \div 200 = 0 \cdot 075$, and on KB is $2 \div 200 = 0 \cdot 02$ ton/in. When W_3 is at K, the average load per unit of length on AB is $15 \div 300 = 0 \cdot 05$, on AK is $0 \cdot 0$, and on BK is $15 \div 100 = 0 \cdot 15$ ton/in. Evidently the position which most nearly makes $(\Sigma W_1)/x = (\Sigma W'')/(L - x) = (\Sigma W)/L$ is when W_2 is at K, and the calculations above show this to be the case.

29. Case (3). Uniformly Distributed Load Shorter than the Span.— Suppose that a uniformly distributed load, w per unit of length, shorter than the span, travels across the span AB, (i), Fig. 56, from

A to B. To find the maximum shearing force and bending moment at any section K by means of influence lines. Let AB $= L$, and let l be the length of the travelling load. Draw the influence lines for shearing force and bending moment for the section K, as in Case (1). Consider the shearing force at K for any position of the moving load such as that shown in (i). Let cd, (ii), be an elementary strip of the shear influence line, δl wide, and lying within the length l; $cd = s$. Then the load over the strip cd is $w \cdot \delta l$; and, from the analysis for Case (1), the shearing force at K due to this load is $w \cdot \delta l \times cd = ws \cdot \delta l$. Hence the total shearing force at K, due to the whole of the moving load, is $S_K = w \int_0^l s.dl$.

But $\int_0^l s.dl$ is the area gh, i.e. the area of the shear influence line immediately

below the moving load. It follows that the shearing force at any section K, due to a uniformly distributed load, is equal to the area immediately below the load of the shear influence line for the section considered, multiplied by w the magnitude of the load per unit of length. If the length scale be 1 inch $= a_1$ inches, and the ordinate scale be a_2 inches $=$ unity, then the shearing force at K is
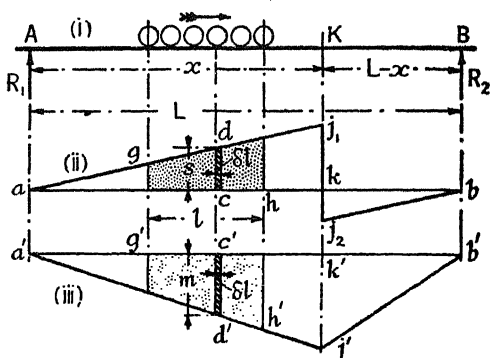
FIG. 56.

$$w \cdot \frac{a_1}{a_2} \text{ (area } gh \text{ measured in square inches)} \Big\} \text{ tons };$$

w being measured in tons per inch of length.

It is evident that the area gh increases as the load moves from A toward B, until the front of the load reaches K. When the front of the load passes K, part of the area under the load becomes negative, and the magnitude of that area is reduced. Hence the maximum positive value of the area, and therefore the maximum positive shearing force at K, occurs when the front of the load arrives at K. Similarly the maximum negative value of the area, and therefore the maximum negative shearing force at K, occurs when the back of the load is at K. These maximum values, calculated from the area gh, are

$$\text{max.} + S_K = \frac{wl}{2} \left\{ \frac{x}{L} + \frac{x-l}{L} \right\} = \frac{wl}{L} \left\{ x \right.$$

$$\text{max.} - S_K = -\frac{wl}{2} \left\{ \frac{L-x}{L} + \frac{L-l}{L} \right\} \qquad -\frac{wl}{L} \left\{ L - x - \frac{l}{2} \right\}$$

It is simpler, however, having found the load positions producing the maximum $+$ and $-$ shearing forces, to place the load in these positions and calculate the values of S_K directly.

In exactly the same manner it may be shown that the bending moment at K, when the moving load is in the position shown in (i) Fig. 56, is

$M_K = w \int_0^l m \cdot dl$; where m is any ordinate such as $c'd'$ of the bending

moment influence line, (iii). Hence it follows that the bending moment at any section K, due to a uniformly distributed load, is equal to the area immediately below the load of the bending moment influence line for the section considered, multiplied by w the magnitude of the load per unit of length.

As pointed out in Case (1), the ordinate of the bending moment influence line is measured to the length scale, 1 inch $= a_1$ inches. Hence one square inch of the diagram represents $a_1{}^2$ in.^{2}; and the bending moment at K will be $\{wa_1{}^2$ (area $g'h'$ in square inches)$\}$ inch-tons, if, as before, w be measured in tons per inch of length.

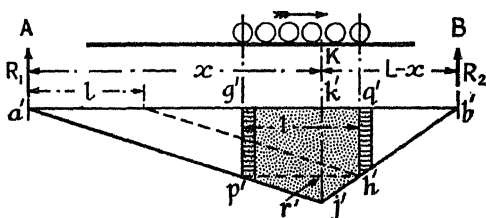It will be evident that, as the load moves from A toward B, the area $g'h'$ will

Fig. 57.

increase, until the position shown in Fig. 57 is reached, when the ordinate $g'p'$ is equal to the ordinate $q'h'$. In this position the area under the load is a maximum, for it is obvious (Fig. 57) that if the load move forward a short distance, the area subtracted is greater than the area added. This is equally true if the load move backward from the position indicated. It follows that the maximum bending moment at K occurs when $g'p' = q'h'$. But if $g'p' = q'h'$, then $p'h'$ is a horizontal line, and by similar triangles, $\dfrac{p'r'}{a'k'} = \dfrac{h'r'}{b'k'}$; or $\dfrac{a'k'}{b'k'} = \dfrac{p'r'}{h'r'}$; that is to say, the span and load are divided in the same ratio (see § 19). Having found the position of the moving load producing the maximum bending moment at K, the magnitude of this moment can easily be found.

A simple geometrical construction for making $g'p'$ equal $g'h'$ is indicated in Fig. 57.

30. Case (4). **Uniformly Distributed Load Longer than the Span.—** Suppose that a uniformly distributed load, w per unit of length, longer than the span, travels across the span AB, Fig. 58, from A to B. To find the maximum shearing force and bending moment at any section K by means of influence lines. Let AB $=$ L. Draw the shearing force and bending moment influence lines for the section K as in Case (1). From the analysis given in Case (3), it follows that when the front of the load has reached any point C, the shearing force at K is equal to the area adc of the shearing force influence line, (ii), immediately beneath the moving

load, multiplied by w. Hence the positive shearing force at K is a maximum when the front of the moving load reaches K, and is equal to the area aj_1k multiplied by w. Similarly the maximum negative shearing force at K occurs when the back of the moving load is at K, and is equal to the area kj_2b multiplied by w. Scales as in Case (3).

The bending moment at K, when the front of the load has reached C, is equal to the area $a'd'c'$ of the bending moment influence line beneath the moving load, (iii) Fig. 58, multiplied by w. Hence it follows that the bending moment at K is a maximum when the whole of the beam is covered, and is equal to the area $a'j'b'$ multiplied by w. Scales as in Case (3).
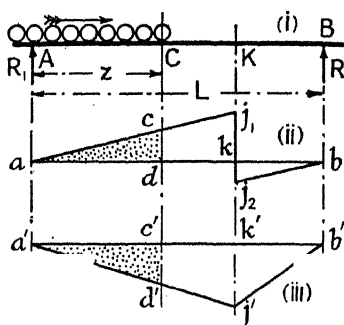
FIG. 58.

31. Use of Influence Lines.—As has been seen, an influence line can be used not only to determine the position of the load when the maximum shearing force or maximum bending moment occurs at the section K, but also to find the values of these maxima. In simple cases it is nevertheless often more convenient to use the influence line merely to determine the position of the load when the maxima occur, and, having placed the load in this position, to calculate the maximum values by one of the ordinary methods. For this purpose a rough sketch of the influence line will often suffice, and no questions arise as to scales.

32. Reaction Influence Lines.—Influence lines can be drawn for the reactions at the ends of a beam. The ordinate under the load W = unity, as it travels across the beam, gives the reaction at the end of the beam. The shape of these influence lines is the same for all beams merely supported at the ends, whether solid, panelled, or braced. This remark applies equally to Figs. 59 and 60.
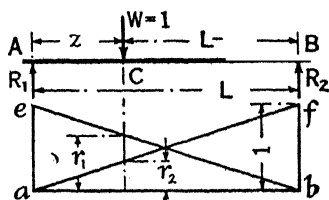
FIG. 59.

Let AB, Fig. 59, be a beam, span L, supported at A and B, and suppose that a load W = unity travels across it from A to B. When the load is at any position C, distant z from A, the reactions at A and B are

$$R_1 = W\frac{L-z}{L} = \frac{L-z}{L}; \quad R_2 = W\frac{z}{L} = \frac{z}{L}; \quad \text{since } W = 1.$$

On a base line ab, set up $ae = bf$ = unity, join af and be, then abe and baf are the reaction influence lines. From the geometry of the figure, the ordinates under the load are

$$r_1 = \frac{L-z}{L} = R_1; \qquad \frac{z}{L} = R_2$$

Therefore the ordinates under the load represent the magnitudes of the reactions, and for any arrangement of concentrated loads

$$R_1 = \Sigma W r_1 ; \qquad R_2 = \Sigma W r_2$$

A second type of reaction influence line, due to Winkler, is shown in (ii) Fig. 60, and is called the *summation influence line* for the reaction R_2. The loads W_1, W_2, W_3 . . . are set up in order, to the load scale, on the reaction line bf, and the points $bcdef$ are joined to a. The loads are next placed in reverse order on the line ab, with the leading load W_1 at a. The summation influence line, $a.1.2.3.4$. is obtained by drawing $a.1$ parallel to ac (coincident) ; 1.2 parallel to ad ; 2.3 parallel to ae ;
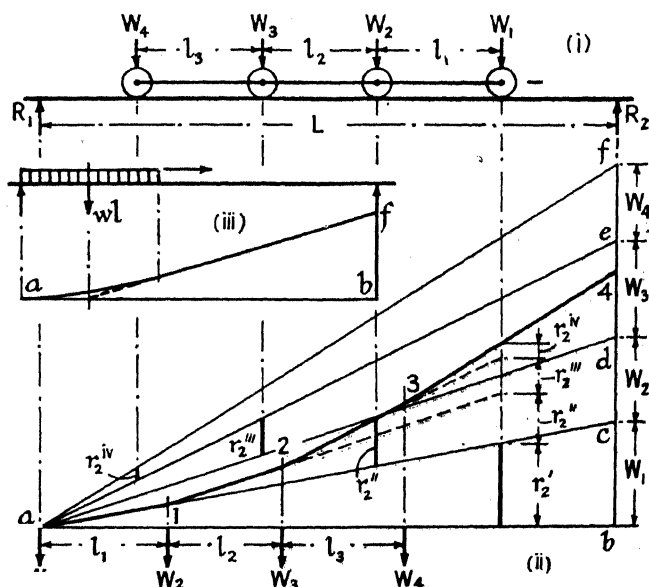
FIG. 60.

and so on. The analogy with the shearing force diagram of Fig. 46 will be evident. The ordinate of the summation influence line under the leading load will give the magnitude of R_2 for the load position indicated.

If Fig. 59 be compared with Fig. 60, it will be seen that acb is the R_2 reaction influence line for the load W_1. Similarly, if ac be regarded as the base line, adc is the R_2 reaction influence line for the load W_2, and so on. Then, for the load position shown in the figure, the reaction R_2 can be found by adding the ordinates under the loads indicated by thick lines,

$$R_2 = r_2' + r_2'' + r_2''' + r_2^{iv}$$

which sum, as shown by the dotted lines, is evidently equal to the ordinate of the summation influence line under the leading load. The reaction R_2 reaches a maximum when W_1 arrived at B, but the diagram

ceases to apply when W_1 passes off the beam. A new summation influence line with W_2 as the leading load can be constructed on the same framework, ac now being the base line.

A diagram similar to (ii) Fig. 60, but reversed, will give the reaction R_1.

For a uniform load, w per unit of length, longer than the span, the line $a.4$ becomes a parabola, the maximum ordinate at B is $wL/2$. The summation influence line for a uniform load shorter than the span is shown in (iii) Fig. 60, the maximum ordinate $bf = \dfrac{wl}{L}(L - \dfrac{l}{2})$, cf. Fig. 45.

33. Influence Lines for Panelled Girders.—Hitherto it has been assumed that the travelling load rolls on the beam itself ; or, if the beam is one of the main girders of a bridge, that the bridge floor or deck transmits the load directly to it, (i) Fig. 291. The theory holds equally for bridges with trough flooring spanning from main girder to main girder, (ii) Fig. 310. In bridges where the loads are transmitted to the main girders by means of cross girders, (ii) Fig. 301, the shape of the influence line is modified. This applies to all panelled floors, whether the main girders be of the plate or lattice type. The influence lines for a plate girder carrying a cross girder floor are found as follows :

Let W, Fig. 61, be a single concentrated load of magnitude unity, travelling across the span AB from A to B, the load being transmitted to the girder AB by means of cross girders, (i). To draw the influence lines for shearing force and bending moment for any section K of the girder AB. Let AB $= L$, and consider the shearing force at the point K lying in the panel K_1K_2 and distant x from A ; $AK_1 = x_1$, $AK_2 = x_2$, $K_1K_2 = L_1$. It will be evident from the figure that no force due to the travelling load can come on the girder AB between K_1 and K_2, and it follows that the shearing force on the girder between these two points must be uniform. Hence the shearing force at K is equal to that at K_1, and it will be sufficient to find the shearing force at the latter point. Suppose the load to have reached C, any position to the left of K_1, distant z from A. For this load position, $R_1 = W\dfrac{L-z}{L}$ and $R_2 = W\dfrac{z}{L}$.

The shearing force at K_1, and therefore at K, is then $S_K = R_2 = Wz/L$ and is positive. Since the magnitude of the load W is unity, $S_K = +z/L$. This expression is exactly the same as in Case (1), § 27, and the influence line aj_1k_1, (ii) Fig. 61, is of exactly the same shape as (ii) Fig. 53, $(bf =$ unity). The ordinate cd represents to scale the shearing force in the panel K_1K_2 when the load is at C, and the maximum ordinate $k_1j_1 = bf \cdot \dfrac{x_1}{L} = \dfrac{x_1}{L}$. When the load passes to the right of K_1, a change occurs.

The load condition while W remains between K_1 and K_2 is shown at (v), Fig. 61. The shearing force at K_1 (and therefore at K) will be $R_2 - P_2$, where P_2 is the downward load transmitted to the main girder by the cross girder at K_2. The magnitude of R_2 is Wz/L as before ; P_2 is found by considering the end reactions of the beam which spans from the cross

girder at K_1 to that at K_2, $P_2 . L_1 = W(z - x_1)$. Hence the shearing force at K_1 or K is,

$$S_K = R_2 - P_2 = W \frac{z}{L} - \frac{W}{L_1}(z - x_1) = \left\{ \frac{z}{L} - \frac{z - x_1}{L_1} \right\}$$

since $W =$ unity. This is the equation to a straight line.

When $z = x_1$, $S_K = + x_1/L = k_1 j_1$ in (ii) ;

when $z = x_2$, $S_K = \left\{ \frac{x_2}{L} - \frac{x_2 - x_1}{L_1} \right\} = \left\{ \frac{x_2}{L} - 1 \right\} = - \frac{L - x_2}{L}$

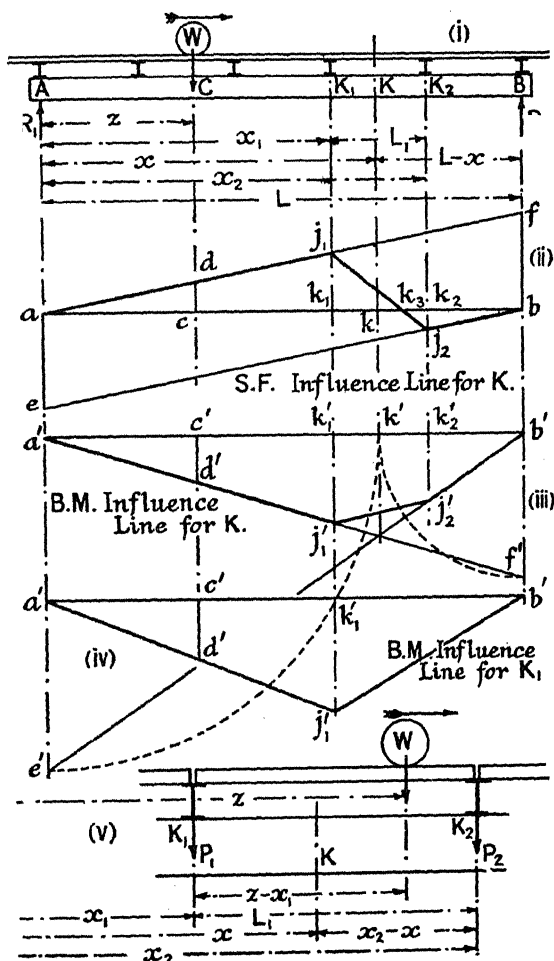Fɪɢ. 61.

becoming negative, and represented in (ii) by $k_2 j_2$. Hence $j_1 j_2$ is the shear influence line for the point K while the load is between K_1 and K_2. When the load passes to the right of K_2 the shearing force at K is negative,

and equal to $- R_1 = - W \dfrac{L - z}{L} = - \dfrac{L - z}{L}$, since W is unity. As in Case (I), § 27, this is represented by the line be (ae = unity), of which any ordinate distant z from a is $- (L - z)/L$. For the point k_2, where $z = x_2$, the ordinate is $- (L - x_2)/L = k_2 j_2$; hence the point j_2 lies on be, and the line bj_2 is the shearing force influence line for load positions to the right of K_2. The complete shearing force influence line, therefore, is the figure $aj_1 j_2 b$, which has exactly the same properties as that of Case (1), § 27. It is evident that the maximum positive shearing force at K (i.e. in the panel $K_1 K_2$) occurs when the load W is at K_1; and the maximum negative shearing force in the panel occurs when the load W is at K_2. When the load is over k_3, the shearing force in the panel is zero.

Consider next the bending moment at K. While the load is at any point C, to the left of K_1, this moment is

$$M_K = - R_2 (L - x) \qquad \cdot W \frac{z}{L} (L - x) = - \frac{z}{L} (L - x),$$

since W = unity, exactly as in Case (1), § 27. This, as before, is represented by the line $a'j_1'$ in (iii), part of the line $a'f'$, where $b'f' = k'b' = (L - x)$. The maximum ordinate $k_1'j_1' = - x_1(L - x)/L$. When the load passes to the right of K_1, the condition of affairs is represented in (v). The bending moment at K is $M_K = - \{R_2(L - x) - P_2(x_2 - x)\}$. Inserting the values of R_2 and P_2 found above, and putting W = unity,

$$M_E \quad - \left\{ W \frac{z}{L} (L - x) - W \frac{z - x_1}{L_1} (x_2 - x) \right.$$

$$- \left\{ \frac{z}{L} (L - x) - \frac{z - x_1}{L_1} (x_2 - x) \right.$$

which is a straight line.

When $z = x_1$, $M_K = - \left\{ \dfrac{x_1}{L} (L - x) \right\} = k_1'j_1'$;

when $z = x_2$, $M_K = - \left\{ \dfrac{x_2}{L} (L \cdot x) - \dfrac{x_2 - x_1}{L_1} (x_2 - x) \right.$

$$= - \left\{ \frac{x_2}{L} (L - x) - (x_2 - x) \right\} = - \left. \frac{x}{L} (L - x_2) \right\},$$

represented in (iii) Fig. 61 by $k_2'j_2'$. Then $j_1'j_2'$ is the influence line while the load is between K_1 and K_2. When the load passes to the right of K_2, $M_K = - R_1 x$. But $R_1 = W \dfrac{L - z}{L}$; or, since W is unity,

$M_K = - \dfrac{L - z}{L} x$. As in Case (1), § 27, this is represented by the line $b'e'$, such that $a'e' = x$. The ordinate at k_2', where $z = x_2$, is $M_K = - \dfrac{x}{L} (L - x_2) = k_2'j_2'$. Hence j_2' lies on the line $b'e'$, and $b'j_2'$ represents the influence line while the load is to the right of K_2. The complete

bending moment influence line, therefore, is the figure $a'j_1'j_2'b'$, of which the ordinate $c'd'$ anywhere represents the bending moment at K when the load is at C. The maximum bending moment at K occurs either when the load is at K_1 or K_2, depending on whether $k'j_1'$ or $k_2'j_2'$ be the greater.

The bending moment influence line thus determined is correct for any point K on the girder, *not a panel point*. The influence line for a panel point, such as K_1, is shown at (iv) Fig. 61, and is exactly the same as that for Case (1), § 27. The fact that the load travels on a floor supported by cross girders makes no difference to the bending moment at a panel point. It is evident that when W is to the left of K_1, the bending moment at K_1 is $- R_2 (L - x_1)$, and when W is to the right of K_1, the bending moment at K_1 is $- R_1 x_1$. These expressions are identical with those of Case (1), § 27, for the values of R_1 and R_2 are independent of the manner in which the load is transmitted to the main girders. Hence the bending moment influence lines in the two cases are identical. (iv) Fig. 61 can be regarded as a particular case of (iii) Fig. 61 in which j_1' and j_2' are coincident.

Having determined the influence lines for shearing force and bending moment, the maximum values of these functions for the section under consideration can be obtained exactly as in Cases (1) to (4) §§ 27 to 30. The following cases are numbered to correspond; the treatment as regards scales is identical.

Case (1). Single Concentrated Travelling Load.—The shearing force and bending moment at K and K_1, when the load is at C, are obtained by multiplying the ordinates s and m directly under the load by the magnitude of the load, exactly as in Case (1), § 27. The maximum value of these ordinates is evident on inspection, and therefore the maximum value of the shearing force and bending moment, and the position of the load at which they occur, are determined.

Case (2). A Series of Concentrated Travelling Loads at Fixed Distances Apart.—The shearing force and bending moment at K or K_1, for any load position, are given by the formulae $S_K = \Sigma(Ws)$ and $M_K = \Sigma(Wm)$, exactly as in Case (2), § 28, the symbols having the same significance. The positions of the load when these functions reach their maximum value can be obtained as follows :

If the loads advance a short distance δz, suppose the ordinates s to increase to $s + \delta s$. $S_K = \Sigma(Ws)$ becomes $S_K + \delta S_K = \Sigma\{W(s + \delta s)\}$. Then $\delta S_K = \Sigma(W . \delta s)$, and in the limit, $\dfrac{d}{dz} S_K = \Sigma\left(W . \dfrac{ds}{dz}\right)$. But $\dfrac{ds}{dz}$ is the slope of the lines aj_1, j_1j_2, and j_2b, (ii) Fig. 61. The slope of aj_1 and j_2b is $+ 1/L$; that of j_1j_2 is $- (L - L_1)/LL_1$.

Let $\Sigma W'$, $\Sigma W''$, and $\Sigma W'''$ be the sum of the loads on AK_1, K_1K_2, and K_2B, respectively ; a load is considered to remain on AK_1 unless it has actually passed K_1, and so on for the other sections. Then,

$$\frac{d}{dz} S_K = \frac{\Sigma W'}{L} - (\Sigma W'') \frac{L - L_1}{LL_1} + \frac{\Sigma W'''}{L}.$$

If S_K be positive, and $\frac{d}{dz} S_K$ be positive, S_K has increased and will go on increasing until a load passes either K_1 or K_2. If, when this happens, $\frac{d}{dz} S_K$ becomes negative, a maximum has occurred, the condition for which is $\frac{d}{dz} S_K = 0$; or, $\frac{\Sigma W' + \Sigma W'''}{L - L_1} = \frac{\Sigma W''}{L_1} = \frac{\Sigma W}{L}$. The shearing force is a maximum, therefore, when a load is at K_1 or K_2, and when at the same time the average load per unit of length on the panel $K_1 K_2$ and that on the rest of the span is the same, and equal to the average load per unit of length on the whole span. This relation is similar to that for the maximum bending moment in § 28. The rule holds for both positive and negative maximum shearing forces, but the positive maximum usually occurs when the front of the load is near K, and the negative maximum when the back of the load is near K. In dealing with the maximum negative shearing force, a modification to the method of estimating $\Sigma W'$, $\Sigma W''$, and $\Sigma W'''$ should be noticed. It should be assumed that a load at K_1 has left AK_1, and that a load at K_2 has left $K_1 K_2$. If the rear of the load is assumed to reach K_2 by a backward movement of the load, it will be seen that this is equivalent to the method of estimation previously given.

In a similar way, for the maximum bending moment,

$$\frac{d}{dz} M_K = \Sigma \left(W \cdot \frac{dm}{dz} \right) = (\Sigma W') \frac{dm'}{dz} + (\Sigma W'') \frac{dm''}{dz} + (\Sigma W''') \frac{dm'''}{dz}$$

where $\frac{dm'}{dz}$, $\frac{dm''}{dz}$, and $\frac{dm'''}{dz}$, are the slopes of the lines $a'j_1'$, $j_1'j_2'$, and $j_2'b'$, (iii) Fig. 61, respectively. The bending moment at K is negative; if $\frac{d}{dz} M_K$ be negative, M_K has increased and will go on increasing until a load passes either K_1 or K_2. If, when this happens, $\frac{d}{dz} M_K$ becomes positive, a maximum has occurred. Hence, for the bending moment to be a maximum at K, a load must be passing K_1 or K_2, and the value of $\frac{d}{dz} M_K$ must change sign as a result.

The bending moment influence line for K_1 (or K_2), (iv) Fig. 61, is of the same shape as that for a non-panelled beam, (iii) Fig. 54. Therefore the condition for the maximum bending moment is the same as in § 28, i.e. that a load must be passing the point in question, and that at the same time the average load per unit of length on the two sections into which the point divides the span must be the same, and equal to the average load per unit of length for the whole span.

Case (3). *Uniformly Distributed Load Shorter than the Span.—* Exactly as in § 29 it may be shown that, for any position of the moving load, the shearing force and bending moment at K are respectively equal

to the area of the shearing force and bending moment influence lines immediately below the load, multiplied by w the magnitude of the load per unit of length. The treatment of the scales is identical. The method of determining the position of the load for maximum positive and negative shearing forces, and for maximum bending moment, is exactly similar ·to that used to find the position of the load for maximum bending moment in § 29, and the reasoning is the same. In each case, as proved in that article, the area of the influence line below the load is a maximum when the ordinates of the influence line at the ends of the load are equal. The application of the graphi-
cal construction pre-
viously given is shown in Fig. 62.

    Case (4). *Uniformly Distributed Load Longer than the Span.*—As in § 30 the shearing force and bending moment at K, for any position of the moving load, are respectively equal to the area of the shearing force and bending moment influ-

FIG. 62.

ence lines immediately below the load, multiplied by w the magnitude of the load per unit of length. The maximum positive shearing force at K occurs when the front of the load reaches k_3, (ii) Fig. 61, and the maximum negative shearing force at K occurs when the back of the load is at k_3. The bending moment at K, K_1, or K_2, is a maximum when the beam is fully covered.
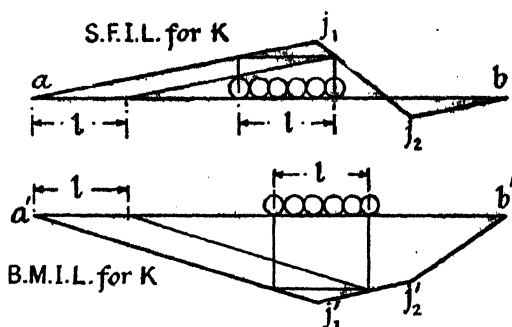
    34. Influence Lines for Braced Girders with Parallel Flanges.—In Fig. 63 a number of braced girders with parallel flanges are shown. In each of these the load is transmitted to the main girders by cross girders attached at the panel points. Consideration will show that the effect of the cross girders on the shearing force and bending moment in all these girders will be exactly the same as in the panelled plate girder shown at (i) of the same figure. Even if the load actually rolls on one of the flanges of a braced girder (not a desirable arrangement as a rule), the panel of the flange carrying the load must act as a girder spanning from panel point to panel point, and transfer the load to the panel points at its ends. The shearing force and bending moment produced by the travelling load at any corresponding section K of any one of these girders will therefore be the same, and the influence lines determined in the preceding article for the plate girder (i) will apply to all.

    Consider first the shearing force in the panel K_1K_2. The influence line for shear aj_1j_2b is shown at (v). The shearing force in the panel, for any kind of travelling load, in any position, can be found from this by the methods previously given. Suppose that its magnitude be S_K.

Since the flanges are parallel, the whole of this shearing force must be carried by the diagonal $K_1 Q_2$. If the force in this bar be F_3, and the
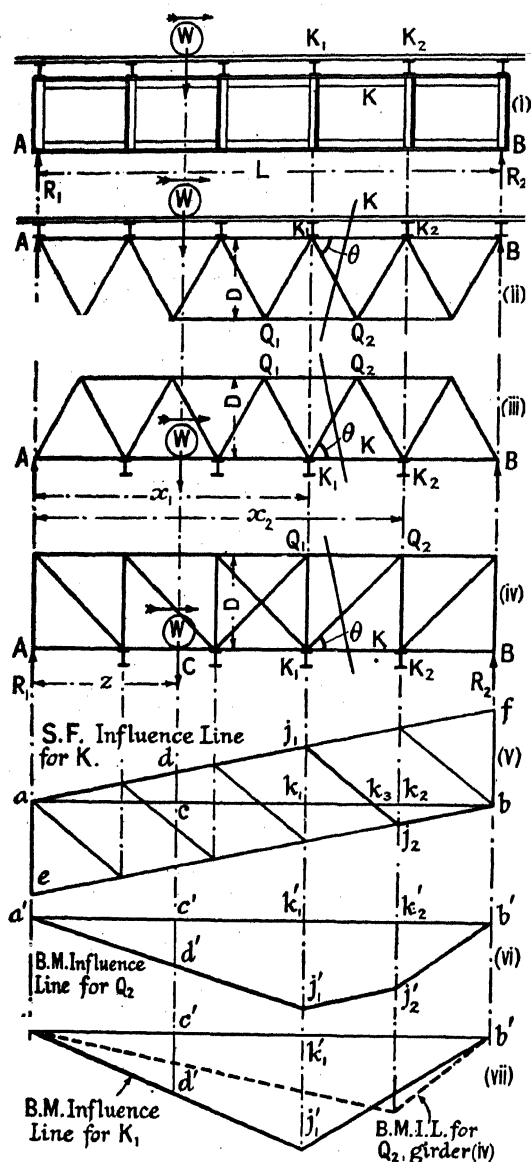
FIG. 63.

angle which it makes with the flanges be θ, the vertical component of the force in the bar, $F_3 \sin \theta$, must equal the shearing force in the panel. Hence $S_K = F_3 \sin \theta$; or $F_3 = S_K \operatorname{cosec} \theta$. The maximum value of

S_K can be found from the influence line, and hence the maximum value of F_3. In the N girder shown at (iv) Fig. 63, if F_4 be the force in Q_2K_2, $F_4 = F_3 \sin \theta = S_K$. The force in this bar is thus determined. As an application of the method, suppose that a single load W tons crosses the girder. When it arrives at C, distant z from A, the shear force S_K is $W \times cd$, where cd is the ordinate of the influence line under C;

$cd = + z/L$, $S_K = + Wz/L$ tons, and $F_3 = + \dfrac{Wz}{L}$ cosec θ tons, which

in this case is a tension; $F_4 = + Wz/L$ tons, a compressive force. The maximum positive value of S_K occurs when the load reaches K_1, the corresponding ordinate being $k_1 j_1$; $k_1 j_1 = + x_1/L$, max. $+ S_K =$

$+ Wx_1/L$ tons, max. $+ F_3 = + \dfrac{Wx_1}{L}$ cosec θ tons; max. $+ F_4 = + \dfrac{Wx_1}{L}$

tons. When the load reaches K_2 the shearing force has changed in sign and is represented by the ordinate $k_2 j_2$, a negative maximum; $k_2 j_2 =$

$-(L - x_2)/L$. Hence, max. $- S_K = - W \dfrac{L - x_2}{L}$ tons, max. $- F_3$

$- W \dfrac{L - x_2}{L}$ cosec θ tons; max. $- F_4 = - W \dfrac{L - x_2}{L}$ tons. The

negative signs indicate that the stress in the bar is reversed in sign.

If a uniform load cross the girder, the maximum positive shearing force in the panel K_1K_2 will occur when the front of the load is over k_3, and the maximum negative shearing force when the back of the load is over k_3, § 33. The thin lines in (v) Fig. 63 represent the position of the line $j_1 j_2$ for all the other panels of the girder. The position of the travelling load producing maximum shearing forces in every panel is thus determined by the one diagram.

Consider next the bending moment in the panel K_1K_2 of girders (ii) and (iii). The influence line $a' j_1' j_2' b'$ for the point Q_2 is shown at (vi). This is identical with (iii) Fig. 61, and is set out in the same way. The bending moment at Q_2, for any kind of travelling load, in any position, can be found from this diagram by the methods previously given; let its magnitude be M_{Q2}. Then if F_1 be the force in the flange member K_1K_2, by the method of sections, § 8, $M_{Q2} = F_1 D$, where D is the depth of the

girder; hence $F_1 = \dfrac{M_{Q2}}{D}$ The maximum value of M_{Q2} can be found

from the influence line as in previous cases, and hence the maximum value of F_1. Since the influence line lies entirely to one side of the base line $a'b'$, the force F_1 cannot reverse in sign.

In the case of girder (iv), Q_2 lies in the same vertical as K_2, and the influence line for Q_2 is of the same type as (iv) Fig. 61 [see the broken lines in (vii) Fig. 63], the method of finding F_1, the force in K_1K_2, being otherwise the same.

It will be observed that, in order to find F_1, the method of sections has been used. The necessary section cuts the bars K_1K_2, K_1Q_2, and Q_1Q_2, Fig. 63; and in order to find the force in K_1K_2, moments were
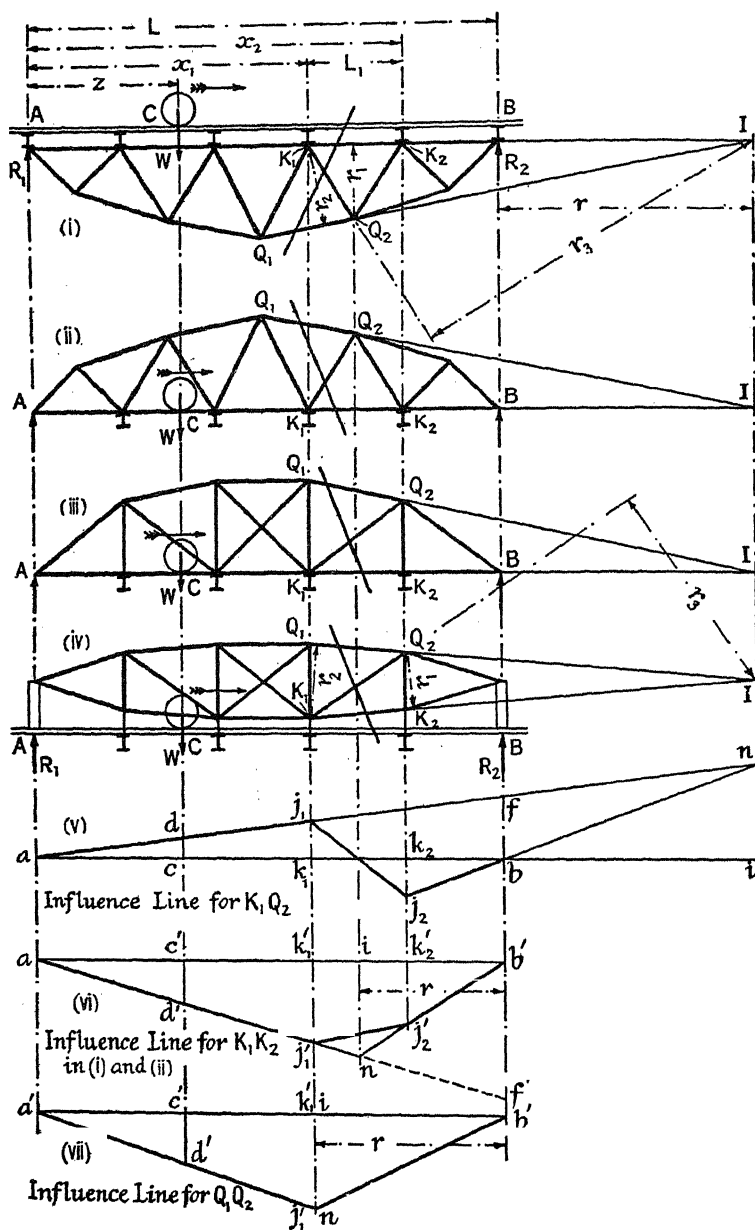
FIG. 64.

taken about Q_2, the point of intersection of the other two cut bars. It was necessary, therefore, to find the bending moment at Q_2, and the influence line for this point was drawn. Similarly, if the force in Q_1Q_2

be required, it is necessary to take moments about K_1, the intersection of K_1K_2 and K_1Q_2. The influence line for K_1 is shown in full lines at (vii). It is similar to (iv) Fig. 61, and set out in a similar manner. Having drawn the influence line, the bending moment M_{K1} at K_1 is known for any position of the travelling load. If F_2 be the force in Q_1Q_2,

$M_{K1} = F_2 D$, and $F_2 = \dfrac{M_{K1}}{D}$. The maximum value of M_{K1} can be found

from the influence line as in previous cases, and hence the maximum value of F_2. Like F_1, F_2 cannot reverse in sign.

35. Influence Lines for Braced Girders with Curved Flanges.—Fig. 64 represents a number of braced girders with curved flanges, in which, as in Fig. 63, the load is transmitted to the main girders by means of cross girders. Since the flanges are not parallel, the curved flange will carry part of the shearing force, and instead of influence lines for shearing force and bending moment, it will be necessary to draw influence lines representing the variation in the force in each particular member of the frame. This is conveniently done by an application of the method of sections. Suppose a load W, of magnitude unity, travelling across the span from A to B, to have reached a point C to the left of K_1 and distant z from A. For this position the reactions are, $R_1 = W(L - z)/L$, and $R_2 = Wz/L$, where AB $= L$. Consider first the bar K_1Q_2 in the panel $K_1Q_1Q_2K_2$. Take a section cutting the bars K_1K_2, K_1Q_2, and Q_1Q_2. To find the force in K_1Q_2, take moments about I, the point of intersection of the other two bars produced ; call clockwise movements positive. Let F_1 be the force in K_1K_2, F_2 that in Q_1Q_2, and F_3 that in K_1Q_2. These three forces, together with R_2, are the only forces acting to the right of the section, and of these, the moments of F_1 and F_2 about I are zero. Then $R_2 r = F_3 r_3$, where r and r_3 are the perpendicular distances of R_2 and F_3, respectively, from I. Hence, inserting the value of R_2, $F_3 =$

$R_2 \cdot \dfrac{r}{r_3} = W\dfrac{z}{L} \cdot \dfrac{r}{r_3}$; and, since W $=$ unity, $F_3 = \dfrac{z}{L} \cdot \dfrac{r}{r_3}$. This is the equation

to the straight line af, (v) Fig. 64, where $bf = \dfrac{r}{r_3}$, $(z = L)$. The part

aj_1, to the left of K_1, will be the influence line representing the variation in F_3 for different positions of the travelling load between A and K_1. It is of the same shape as the shearing force influence line, (ii) Fig. 61, for panelled girders, § 33, except that bf, instead of being unity, is equal to r/r_3. The force in K_1Q_2, for any position of W to the left of K_1, will be represented by the ordinate under the load of this influence line. Thus cd represents the value of F_3 when the load is at C. When the load

arrives at K_1, the value of F_3 is represented by k_1j_1 $\dfrac{x_1}{L} \cdot \dfrac{r}{r_3}$, obtained by

putting $z = x_1$ in the expression for F_3. If the line af be produced to

meet the vertical through I $(z = L + r)$, $in = \dfrac{L + r}{L}$

When the load passes to the right of K_1, a change occurs. While the load remains between K_1 and K_2, the state of affairs will be similar to

that shown in (v) Fig. 61 ; and, in addition to R_2, the downward load P_2, transmitted to the main girder by the cross girder at K_2, must be taken into account in finding the moments about I. As in § 33, $P_2 = W \dfrac{z - x_1}{L_1}$ the symbols having the same significance as before. The equation of moments about I is now, $R_2 r - P_2(L - x_2 + r) = F_3 r_3$. Substituting for R_2 and P_2, $W \dfrac{zr}{L} - \dfrac{W}{L_1} (z - x_1)(L - x_2 + r) = F_3 r_3$; or, since $W =$ unity,

$F_3 = \dfrac{z}{L} \cdot \dfrac{r}{r_3} - \dfrac{(z - x_1)(L - x_2 + r)}{L_1 r_3}$. This is the equation to a straight line.

When $z = x_1$, $F_3 = \dfrac{x_1}{L} \cdot \dfrac{r}{r_3} = k_1 j_1$. When $z = x_2$, since $(x_2 - x_1) = L_1$,

$F_3 = \dfrac{x_2}{L} \dfrac{r}{r_3} - \dfrac{L - x_2 + r}{r_3} = - \dfrac{(L + r)(L - x_2)}{L r_3}$ becoming negative, and represented by $k_2 j_2$. The straight line $j_1 j_2$, (v) Fig. 64, is therefore the influence line for F_3 while W is between K_1 and K_2.

When the load passes to the right of K_2, the moment about I becomes $F_3 r_3 = R_2 r - W(L - z + r)$, for now W itself is to the right of the section and its moment has to be taken into account. Inserting the value of R_2, and putting W equal to unity, $F_3 r_3 = W \dfrac{zr}{L} - W(L - z + r) = \dfrac{zr}{L} - (L - z + r)$, and $F_3 = \dfrac{z}{L} \cdot \dfrac{r}{r_3} - \dfrac{L - z + r}{r_3}$ This is the equation to the straight line $j_2 b$, for when $z = x_2$, F_3 $\dfrac{x_2}{L} \cdot \dfrac{r}{r_3} - \dfrac{L - x_2 + r}{r_3} = k_2 j_2$, and when $z = L$, $F_3 = 0$. If $z = L + r$, the ordinate of the line $j_2 b$ is $\dfrac{L + r}{L} \cdot \dfrac{r}{r_3} = in$; hence the line $j_2 b$ passes through the point n. The complete influence line for the force F_3 in the bar $K_1 Q$ is, therefore, $a j_1 j_2 b$. It is easily constructed by making $bf = r/r_3$, and joining af, which being produced cuts the vertical through I in n. Join nb and produce to j_2. The influence line $a j_1 j_2 b$ is thus determined. The shear influence line, (v) Fig. 63, is evidently a particular case of this diagram, for if the two flanges were parallel, I would lie at infinity, and therefore afn and $j_2 bn$ of (v) Fig. 64 would be parallel, as shown in (v) Fig. 63. The latter diagram is a shearing force influence line, whilst the former gives the actual force F_3 ; the scales are therefore different.

An exactly similar construction gives the influence lines for the flange members $K_1 K_2$ and $Q_1 Q_2$. To find the influence line for F_1, the force in $K_1 K_2$, moments must be taken about Q_2 the point of intersection of the other two bars cut by the section. If, exactly as before, moments be taken about this point of intersection, identical equations for the three branches of the influence line will be obtained, except that, since the point of intersection is now to the left of B, the moment of R_2 about this point is anti-clockwise, and therefore negative, hence r must be considered as negative. Also, the perpendicular distance r_1 of $K_1 K_2$ from

Q_2, the point of intersection, must be substituted for r_3. If therefore, in the equations obtained for each branch of the influence line for F_3, r be made negative and r_1 substituted for r_3, these equations will represent the three branches of influence line for F_1, as shown at (vi) Fig. 64. The construction for the influence line is exactly similar. Make $in = -\dfrac{L-r}{r} \cdot \dfrac{r}{r_1}$ in the vertical through the point of intersection Q_2. Join na' and nb'. Then $a'j_1'j_2'b'$ will be the influence line for the force F_1 in the bar K_1K_2. When, as in (iii) and (iv), Fig. 64, Q_2 and K_2 lie in the same vertical line, j_1', j_2', and n all coincide, and the influence line for K_1K_2 becomes a triangle similar to (vii), but with its vertex in the vertical K_2k_2'.

For the bar Q_1Q_2 the construction is exactly similar. Moments are taken about the point K_1 ; r is negative and equal to $b'k_1'$; the point n lies in the vertical through K_1, and in is equal to $-\dfrac{L-r}{L} \dfrac{r}{r_2}$, where r_2 is the perpendicular distance of Q_1Q_2 from K_1. Join $a'n$ and nb', (vii) Fig. 64. Then $a'j_1'b'$ is the influence line for the force F_2 in Q_1Q_2. (vi) and (vii) Fig. 64 should be compared with (vi) and (vii) Fig. 63. It is evident that the forces in K_1K_2 and Q_1Q_2 cannot reverse ; this applies to all the upper and lower flange members.

Setting out the Influence Lines.—It will be observed that in all cases

$$in \quad : \frac{IA \times IB}{AB} \times \frac{1}{r_m}$$

where IA and IB are the horizontal distances of the intersection point from the ends of the span AB, and r_m is the perpendicular distance of the intersection point from the member. This is a convenient mnemonic for in.

It is further to be observed, in an influence line giving the force in a bar of a plane framework, that the intercept of the influence line on the line of action of a reaction represents the force produced in the bar by that reaction, if the magnitude of the latter be unity.

Thus in (i) Fig. 64, if the girder be conceived as a cantilever fixed in position and direction at A, and loaded at B with a unit reaction $R_2 = 1$, the force F_3 in K_1Q_2, found by taking moments about I ($F_3r_3 = R_2r$), is $F_3 = r/r_3$. But $r/r_3 = bf$ in (v) Fig. 64 (see above), and bf is the intercept of the influence line for F_3 on the line of action of R_2. This proposition really follows from the definition of the influence line, for as cd represents the force F_3 when unit load is at C, so (for the cantilever) bf represents the force F_3 when unit load is just arriving at B. Similarly, the force in K_1K_2 due to $R_2 = 1$ is represented by $b'f'$ in (vi).

Knowing the intercept bf, the influence line is easily set out.

It is convenient, therefore, in order to draw influence lines for every member of a plane framework, to assume it fixed in position and direction at one end, apply a unit reaction at the other, and find by means of a stress diagram or otherwise the force in each bar due to this reaction.

These forces, set up to scale, will give the intercept bf for every influence line.

Use of the Influence Lines. Maximum Values.—The application of the influence lines of Fig. 64, giving the forces in particular bars, is exactly similar to that of influence lines for shear and bending moment. If, under a load of magnitude W, the ordinate of the influence line be u, then the force in the bar due to W is $F = Wu$. If the load be uniformly distributed, the area of the influence line immediately beneath the load gives the force in the bar. The criteria for the maximum area beneath the load, given in § 33, can be used to find the maximum force in the bar. In the case of a train of concentrated loads, the force in the bar for any load position is $F = \Sigma Wu$. Similar conditions hold for the maximum values as in § 33. If, while the loads advance a short distance δz, the ordinates increase to $u + \delta u$, then $F + \delta F = \Sigma\{W.(u + \delta u)\}$, and in the limit, $\dfrac{d}{dz} F : \Sigma \left(W . \dfrac{du}{dz}\right)$, where du/dz is the slope of the influence line. In a three branch influence line, such as (vi), Fig. 64, see Fig. 65,

$$\frac{d}{dz}F = \Sigma\left(W . \frac{du}{dz}\right) = (\Sigma W')\frac{du'}{dz} + (\Sigma W'')\frac{du''}{dz} + (\Sigma W''')\frac{uu}{dz}$$

where du'/dz, du''/dz, and du'''/dz are the slopes of the lines $a'j_1'$, $j_1'j_2'$, $j_2'b'$ respectively, and $\Sigma W'$, $\Sigma W''$, $\Sigma W'''$ are the sum of the loads on AK_1, K_1K_2, and K_2B.

A load is considered to remain on AK_1 unless it has actually passed K_1, and so on. If F be positive, and dF/dz be positive, F has increased due to the increase in z and will go on increasing
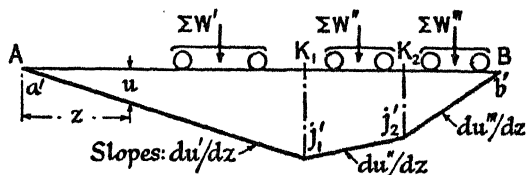
FIG. 65.

until a load passes either K_1 or K_2. If when this happens, dF/dz becomes negative, a maximum has occurred, the condition for which is $dF/dz = 0$. For a maximum value of F to occur, therefore, a load must be passing K_1 or K_2, and the value of dF/dz must change sign as a result. The above theory holds for the influence lines for F_1, F_2 and F_3. In the case of influence lines of the type shown in (vii), Fig. 64, only loads passing K_1 need be considered. In the case of F_3, (v) Fig. 64, when finding the negative maximum value, it should be assumed that a load at K_1 has left AK_1, and that a load at K_2 has left K_1K_2, cf. the parallel case of negative shear in § 33.

Scales.—It will be evident that the ordinates of the influence lines of Fig. 64 are ratios. Thus $bf = r/r_3$; $in = \dfrac{L + r}{r_3}$, and so on. If the diagram be set up to a scale 1 inch = a units, an ordinate u, measured in inches, represents $u'' \times a$ units ; and if this ordinate occur under a load

of magnitude W tons, the force in the bar due to W is $Wu'' \times a$ tons. If the length scale be 1 inch $= a_1$ inches, 1 square inch of the diagram under a distributed load of w tons per inch of length represents a force in the bar of waa_1 tons. The sign of the force in a web member depends on the arrangement of the bars in the frame.

INFLUENCE LINES FOR DIRECTION-FIXED AND CONTINUOUS BEAMS

36. Influence Lines for Direction-fixed Beams.—Let AB, Fig. 66, be a beam of uniform cross-section, $EI =$ constant, direction-fixed at A and merely supported at B. To find the influence lines for the reactions, shearing force, and bending moment. Remove the travelling load and the support at B, and draw the deflection curve, akb, (ii), for a downward load $W =$ unity placed at B. This curve is the deflection influence line for the point B of the cantilever AB. For, from Maxwell's reciprocal deflection theorem, § 84, the deflection y_C of the cantilever at C, due to unit load at B, is equal to y_B the deflection at B due to unit load at C. In the notation of § 85, $y_{cb} = y_{bc}$. That is to say, the ordinate y under the load $W = 1$ placed at C, gives the deflection of the beam at B. From eq. (2), § (52), Vol. I, the equation to this curve is
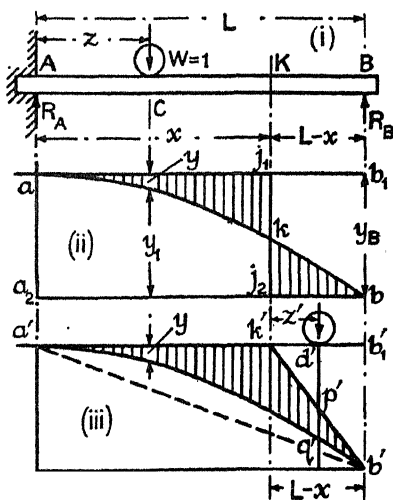
FIG. 66.

$$y = \frac{1}{EI}\left[\frac{Lz^2}{2} - \frac{}{6}\right] \qquad (1)$$

where z is the distance of the load from A.

Using the properties of the influence line, the deflection of the cantilever at B due to the travelling load $W = 1$ at C is Wy. Remove this load and apply the upward reaction R_B at B. R_B is the upward reaction on the *beam* at B when W is at C. The upward deflection of the cantilever at B produced by this force is $- R_B y_B$, where $y_B = b_1 b$. But in the actual beam, if both ends remain at the same level, the deflection at B must be zero. Hence, when both W and R_B act together on the beam, the upward and downward deflections at B must exactly neutralise, and $Wy - R_B y_B = 0$, or since $W = 1$,

$$R_B = \frac{y}{y_B} \qquad . \qquad . \qquad . \qquad . \qquad . \qquad (2)$$

But y_B is constant; hence y, the ordinate under the load, represents to some scale the reaction R_B, and the curve akb on the base line ab_1 is the

influence line for the reaction R_B. Since both y and y_B are measured to the same scale, the actual scale is immaterial, and it is convenient to make $y_B = b_1b$ represent unit load. Further, $R_A + R_B = W$; hence,

$$R_A = W - R_B = 1 - \frac{y}{y_B} = \frac{y_B - y}{y_B} = \frac{y_1}{y_B}, \text{ since } W = 1 \text{ and } R_B = y/y_B.$$

But y_1 is the ordinate under the load of the curve akb measured from the base line a_2b, and it represents to the same scale as before the reaction R_A; this curve is therefore the reaction influence line for R_A.

The shearing force influence line for any point K can be found as follows : When the load is to the left of K, the shearing force at K is equal to $+ R_B = y/y_B$, and the ordinate under the load between the curve and aj_1 represents the shearing force at K. When the load is to the right of K, the shearing force at K is $(W - R_B)$, and the ordinate between the curve and the base line j_2b represents the shearing force. Hence the shaded figure in (ii) is the shearing force influence diagram for K. The shearing force is measured to the scale to which b_1b represents unit load.

The bending moment influence line may be obtained as follows : When W is to the left of K as shown in (i), the bending moment at K is

$$M_K = - R_B(L - x) = - \frac{y}{y_B}(L - x) = - y\frac{L - x}{y_B} \qquad . \quad (3)$$

But $(L - x)/y_B$ is constant. If then the curve ab in (ii) be repeated in (iii), the ordinate y under the load, measured downward from $a'k'$, represents to some scale the bending moment at K. When W passes to a distance z' to the right of K

$$M_K = - R_B(L - x) + Wz' = - \frac{y}{y_B}(L - x) + z' = - \frac{L - x}{y_B}\left\{y - y_B\frac{z'}{L - x}\right\} \quad (4)$$

since $W = 1$. Join $k'b'$, and draw the vertical $d'p'q'$. Then $d'q' = y$, and $d'p' = y_Bz'/(L - x)$. Hence,

$$M_K = - \frac{L - x}{y_B}\{d'q' - d'p'\} = - \frac{L - x}{y_B}\{p'q'\} \quad . \quad . \quad (5)$$

and the ordinate $p'q'$ represents the bending moment M_K, when the load is to the right of K, to the same scale that y represents M_K when the load is to the left of K. Therefore the shaded figure in (iii) is the bending moment influence diagram for the point K; $a'k'b'$ is the base line from which the ordinates under the load are measured downward to the curve.

If y and $p'q'$ be measured in tons to the scale to which y_B represents 1 ton, and $(L - x)$ be expressed in inches, the product will represent the bending moment at K for a unit load in inch-tons.

The influence line for the support moment M_A at A is obtained by moving K to A and joining $b'a'$, as indicated by the broken line. The ordinate under the load between the curve and this line, measured to the scale to which y_B represents 1 ton, multiplied by L in inches, gives M_A in inch-tons.

If the support B sink to a distance Δ below that at A, eq. (2) will be modified, $Wy - R_B y_B = \Delta$, and for unit load

$$R_B = (y - \Delta)/y_B \quad . \quad (6)$$

The base line ab_1 of (ii) must then be lowered a distance Δ/y_B. That this line crosses the curve shows that, when $W = 1$ gets sufficiently near A, the cantilever will cease to bear on the support B, or must be held down by a negative reaction represented by the ordinate between the curve and the line. The rest of the analysis for this case follows a parallel course.

Influence Lines for Beams Direction-fixed at both Ends.—The influence lines for a uniform beam (EI = const.), direction-fixed at both ends, can be obtained in an analogous fashion to the above. Let (i), Fig. 67, represent the beam, across which a load $W =$ unity travels from left to right. The bending-moment diagram for one load position D is shown in (ii). On p. 148, Vol. I, it is shown that $R_B = Wn^2(3 - 2n)$; where, with the present symbols ($l_1 = z$), $n = z/L$. Hence, if $W = 1$,

$$R_B = n^2(3 - 2n)$$

$$\circ \quad = \frac{z^2}{L^3}(3L - 2z) \quad . \quad (7)$$

In a manner analogous to (ii) Fig. 66, plot from this equation the curve akb, (iii) Fig. 67 ; $b_1 b = 1$ ton. Then as in Fig. 66, the ordinate under the load, between the curve and the base line $ab_1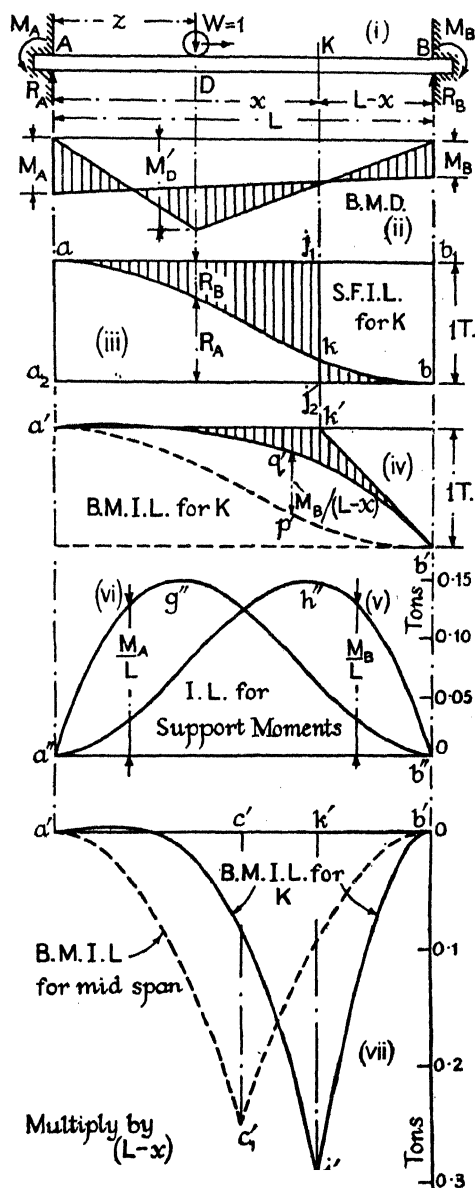$, will represent the reaction R_B ; and the corresponding ordinate between the base line $a_2 b$ and the curve will represent the reaction R_A. The curve is therefore the

FIG. 67.

reaction influence line for the beam. Similarly, the shaded figure is the shearing force influence line for the point K, cf. (ii) Fig. 66.

The bending moment influence line for the point K can be set out as follows : While W is to the left of K (considering the right-hand moments and forces),

$$M_K = M_B - R_B (L - x) = \left\{ \frac{M_B}{L - x} - R_B \right\} (L - x) \quad . \quad (8)$$

When W moves to a distance z' to the right of K

$$M_K = M_B - R_B(L - x) + Wz' = \left[\frac{M_B}{L - x} - \left\{ R_B - \frac{z'}{L - x} \right\} \right] (L - x) \quad (9)$$

since $W = 1$. If eqs. (8) and (9) be compared with eqs. (3) and (4), it will be seen that they are similar in form except that the factor M_B occurs in eqs. (8) and (9). Set out therefore a diagram (iv) similar to (iii) Fig. 66. Reproduce the curve akb from (iii) Fig. 66, shown dotted in (iv) ; join k' to b', to take account of the factor $z'/(L - x)$ exactly as in (iii) Fig. 66. The diagram thus constructed is the influence line for the negative bending moment at K. This must be combined with the diagram for M_B, the positive bending moment. From p. 148, Vol. I, $M_B = WLn^2 (1 - n)$, and since $W = 1$ and $n = z/L$,

$$\frac{M_B}{L} = n^2 (1 - n) = z^2 (L - z)/L^3 \quad . \quad . \quad (10)$$

This equation is plotted in (v) [max. ord. $= 4/27$ when $n = 2/3$] to 10 times the scale of (iv), where the curve $a''h''b''$ represents the value of M_B/L for every position of the moving load ; it is the influence line for M_B. The ordinate of this curve under the load, measured in tons, multiplied by L in inches, gives the value of M_B in inch-tons. The influence line for M_A is exactly similar but reversed, (vi). Increase the ordinates of (v) in the ratio $L/(L - x)$, thus obtaining $M_B/(L - x)$, and plot them upward from the curve $a'p'b'$ in (iv) as indicated. The resulting diagram will then represent eqs. (8) and (9), and is the bending moment influence line for the point K. The scale of (iv) is too small for practical use, and this influence line has been replotted to 10 times the scale in (vii). For accurate work, the difference in the calculated ordinates of $a'k'b'$ and $a'q'b'$ should be plotted in (vii). The ordinate under the load of (vii) measured in tons, multiplied by $(L - x)$ measured in inches [see eqs. (8) and (9)], gives the bending moment at K in inch-tons. Thus in (vii), if $L = 160$ in., $(L - x) = 48$ in., and the maximum ordinate $k'j' = 0.294$ ton ; max. $M_K = 14.1$ inch-tons, when $W = 1$, which can easily be checked. The influence line for the mid point of the span, obtained in exactly the same way, is shown dotted in (vii) ; each curve is a parabola, maximum ordinate $= c'c'_1 = 0.25$ ton. For this point $(L - x) = L/2$, so that max. $M_C = \frac{1}{4} \times \frac{L}{2} = \frac{L}{8}$ as it should.

37. Influence Lines for Continuous Beams.—Let ABC, (i) Fig. 68, be a continuous beam, not necessarily of uniform cross section, supported

at A, B, and C. Suppose that a concentrated load W = unity cross the beam from left to right. To find the influence lines for the reactions, shearing force, and bending moment, remove the support B and place the unit load at B. Draw the deflection curve abc, (ii) Fig. 68, for this load condition.

Reaction Influence Lines.—From § 40, the curve abc is the deflection influence line for the point B on the beam AC, and for any position D of the unit load W, the deflection produced at B is Wy, where $y = d_1d$ is the ordinate of the curve under the load. If W be removed from the beam, and an upward load R_B (the reaction acting on the continuous beam) be applied at B, the deflection produced by this load will be $-R_B y_B$, where $y_B = b_1b$ is the ordinate of the curve at B. If both loads W and R_B act together on the beam, the total deflection at B will be $Wy - R_B y_B$. In the case of the continuous beam ABC, if all three supports remain at the same level, the deflection at B will be zero, and $Wy - R_B y_B = 0$; or, since $W = 1$, $R_B = y/y_B$, and the ordinate of the curve abc under the load, divided by y_B, gives the reaction R_B. But y_B is constant; hence, to some scale, $R_B = y$. In other

FIG. 68.

words, abc is the reaction influence line for R_B. Since y and y_B are measured to the same scale, the scale of the diagram is immaterial.

The influence lines for R_A and R_C can be obtained from the same curve. Place the load $W = 1$ at any position D distant z from A. Take moments about A,

$$R_C (L_1 + L_2) + R_B L_1 \quad Wz \; ;$$

whence $$R_C = \frac{1}{L_1 + L_2} \{Wz - R_B L_1\} = \frac{1}{L_1 + L_2} \left\{ z - \frac{y}{y_B} L_1 \right\}$$

$$\therefore \frac{L_1}{y_B (L_1 + L_2)} \left\{ \frac{y_B z}{L_1} - y \right\} \; ; \text{ since } W = 1, \text{ and } R_B = y/y_B.$$
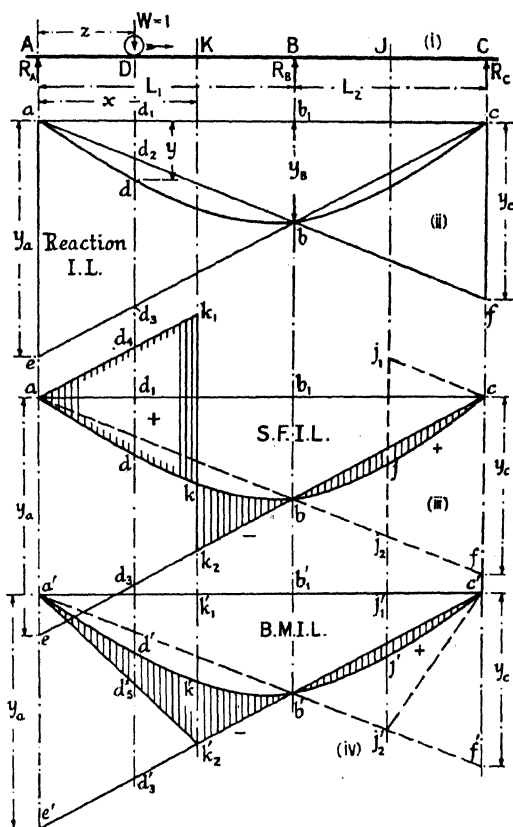
In (ii) Fig. 68, draw abf and cbe ; let $ae = y_a$ and $cf = y_c$. Then $y_c = cf = y_B \dfrac{L_1 + L_2}{L_1}$ and $d_1 d_2 = y_B \dfrac{z}{L_1}$; hence, $R_C = \dfrac{1}{y_c}\{d_1 d_2 - d_1 d\} = -\dfrac{1}{y_c} d_2 d$, and the ordinates between the curve $adbc$ and the base line abf, divided by y_c, give the reaction R_C. When the curve falls below the base line, R_C is negative, that is to say, it acts downward.

Similarly, the ordinates between the curve and the base line ebc, divided by y_a, give the reaction R_A. Thus for the load position shown in (i), $R_A = + d_3 d / y_a$. As before, the scale of the diagram is immaterial, since both y_a and $d_3 d$ are measured to the same scale.

Shear Influence Line.—When W is in the position shown in (i) Fig. 68, the shearing force at any section K is

$$S_K = - R_A + W = W - \frac{d_3 d}{y_a} = \frac{1}{y_a} \{y_a - d_3 d\}$$

since $W = 1$. In (iii) the curve and base lines from (ii) have been repeated. Draw ak_1 parallel to eb. Then, considering the ordinate under the load, $d_3 d_4 = y_a$, and $dd_4 = y_a - d_3 d$. Hence, $S_K = dd_4 / y_a$; and the ordinate under the load between the curve $adbc$ and the line ak_1, divided by y_a, represents the shearing force at K. When W passes K, the shearing force at K is equal to $- R_A$, represented by the ordinate between the same curve and the line $k_2 c$ divided by y_a, see (ii). The shaded figure in (iii) is therefore the shearing force influence line for the point K. Ordinates measured above the curve imply positive shear, those measured below imply negative shear. As in the case of the reactions, the scale of the diagram is immaterial, since both the ordinate dd_4 and the value of y_a are measured to the same scale. The broken lines to the right of the figure represent the corresponding shearing force influence line for a point J in the span BC.

Bending Moment Influence Line.—When W is to the left of K, as shown in (i), the bending moment at K is

$$M_K = - R_A x + W(x - z) = - \frac{d_3 d}{y_a} x + W(x - z)$$

$$= - \frac{x}{y_a}\left\{d_3 d - y_a \frac{x - z}{x}\right\} ; \text{ since } R_A = \frac{d_3 d}{y_a}, \text{ and } W = 1.$$

In (iv), the curve and base lines from (ii) have been repeated. Join $a' k_2'$. Then, considering the ordinate under the load, $d_3' d_5' = y_a \dfrac{x - z}{x}$ and $d' d_5' = d_3' d' - d_3' d_5'$, whence, $M_K = - \dfrac{x}{y_a}(d' d_5')$.

For the point K, x is constant and y_a is constant ; hence the ordinate under the load between the curve $a'd'b'c'$ and the line $a'k_2'$ represents to some scale the bending moment at K. When W passes K, the bending moment $M_K = - R_A x$, represented by the ordinate between the curve and the line $k_2' c'$ multiplied by x/y_a as before. Therefore the shaded figure is the bending moment influence line for the point K. Ordinates

measured below the curve imply a negative bending moment, ordinates measured above the curve imply a positive bending moment.

The vertical scale of the diagram is immaterial, since y_a and $d'd_5'$ are both measured to the same scale, but the correct value must be given to x. If the loads are expressed in tons and x is in inches, the bending moment will be in inch-tons. The broken lines to the right of the figure represent the corresponding bending moment influence line for a point J in the span BC.

38. Influence Lines for Lattice Braced Continuous Girders.—The method of treatment for a girder on three supports, Fig. 69, is similar to that used in § 37 for solid beams. Take away the intermediate support and apply a unit load there. Find the deflection polygon abc, (ii) Fig. 69, for the loaded flange by means of a Williot diagram or otherwise, §§ 12, 14, 15, or 70. Draw abf, cbe. Then, exactly as in § 37, if $d_1d_2dd_3$ be the ordinate under a load $W = 1$ at any point D, see Fig. 68,

$$R_B = \frac{y}{y_B} \; ; \quad R_A = \frac{d_3d}{y_a} ; \quad R_C = -\frac{d_2d}{y_c} \qquad (1)$$

the scale of the diagram is immaterial; (ii) Fig. 69 is therefore the reaction influence line for the girder.

To obtain the influence line for the web member K_1Q_2, consider the effect of the unit travelling load and the central reaction separately. Repeat in (iii) the polygon abc and the line cbe from (ii), producing the latter to cut the vertical through I, the intersection point of Q_1Q_2 and K_1K_2, in n. Join na and produce it to cut the vertical through Q_1K_1 in k_1; join k_1k_2. Evidently ak_1k_2c is the influence line for the bar K_1Q_2 (cf. Fig. 64) when the support B is removed, and the ordinate under the load represents the force in K_1Q_2 in these conditions. The force in K_1Q_2 due to R_B will vary as the magnitude of R_B, that is to say will vary as the ordinate y, under the load, of the curve abc [eq. (1)]. Hence the curve abc to some scale is the influence line for the force in K_1Q_2 due to R_B. But when W is at B, the total force in the bar due to both W and R_B must be zero, and the diagram has been so drawn that the difference between the ordinates of the two curves at B is zero. Therefore both curves are to the same scale, and the difference between their ordinates under the load represents the actual force in K_1Q_2; i.e. the figure is the influence line for the bar K_1Q_2. To find the scale, remove the reaction R_A and find the force F_a in K_1Q_2 due to a unit reaction applied at A. This will be represented in the diagram by the ordinate $ae = y_a$, § 35. If then a force of 1 unit produce a force F_a in K_1Q_2, represented by y_a, the actual force in the bar will be

$$\text{Force in } K_1Q_2 \quad \begin{Bmatrix} \text{Ordinate of influence} \\ \text{line under the load} \end{Bmatrix} \times \frac{F_a}{y_a} \qquad (2)$$

The influence lines for the web members where the flanges are parallel are indicated to the left of the diagram. Both the magnitude and the sign of F_a will be different in different bars. Ordinates above the curve

abc are to be considered as positive, i.e. they represent a tension in a bar such as K_1Q_2.

The influence line for the flange member KK_1 is set out in (iv) ; the curve *abc* and the line *cbe* are reproduced from (ii) as before. The triangle $a'k_2'c'$ represents the influence line for the bar when the support
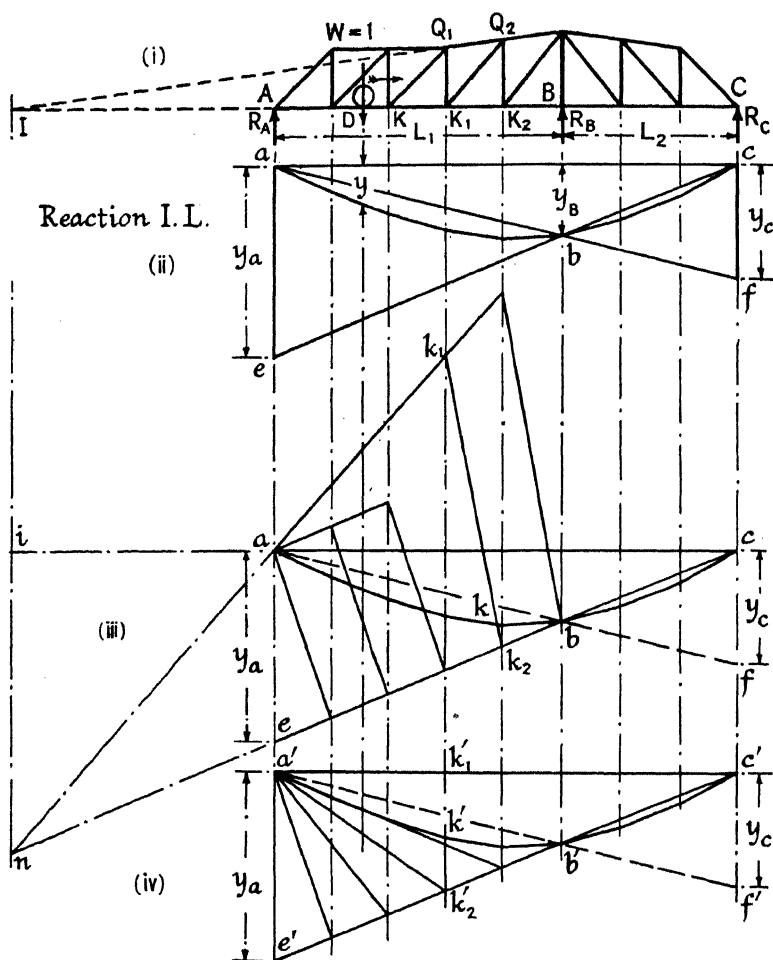
Fɪɢ. 69.

B is removed ; the curve $a'b'c'$ is the influence line for the force in KK_1 due to R_B. Since the force in KK_1 is zero when W is at B, the line $c'b'e'$ has been drawn to pass through b', and consequently the scales of the diagrams are the same. If Fa be the force in KK_1 due to $R_A = 1$,

$$\text{Force in } KK_1 = \left\{ \begin{array}{l} \text{Ordinate of influence} \\ \text{line under the load} \end{array} \right\} \times \frac{Fa}{y_a} \qquad (3)$$

Ordinates measured downward from the curve represent a negative bending moment producing a tension in the lower flange members.

The forces in the bars of span L_2 can be found in a similar way, but for this purpose the line $a'b'f'$ must be used, and the scale of the diagram determined by multiplying the ordinates by F_c/y_c, where F_c is the force in a bar due to a unit reaction at C.

39. Use of Characteristic Points.[29]—The bending moment influence lines for a uniform beam, continuous over two spans, can be found by the construction shown in (i) Fig. 70. This is a combination of the constructions shown in (iv) Fig. 130, Vol. I, and (ii) Fig. 128, Vol. I. For any
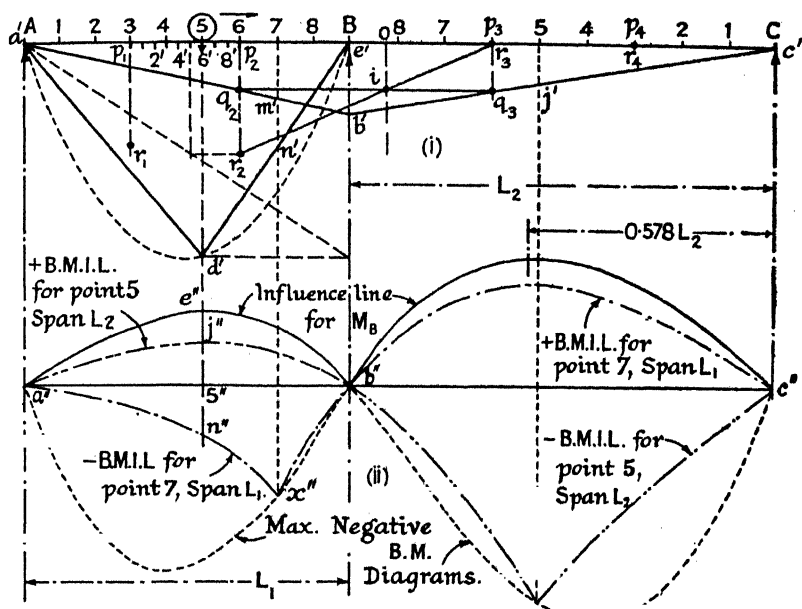
FIG. 70.

one position of the load $W = $ unity, the negative bending moment diagram is the triangle $a'd'e'$. The locus of d' is the parabola shown : maximum ordinate $WL_1/4 = L_1/4$. Divide the span L_1 into say nine equal parts, $a'.1.2.3. \ldots e'$; and also the distance p_1p_2 into nine equal parts $p_1.1'.2'.3'. \ldots p_2$. When the load is at any point 5, the dotted construction determines the characteristic point r_2; r_3 coincides with p_3. Join r_2r_3, and find the intersection point i. The intersection points for every position of the moving load lie on the vertical oi. Since q_2iq_3 is a horizontal line, the base line $a'b'c'$ can be drawn in. In (ii) Fig. 70, on the ordinate under the load, make $5''e''$ equal to $b'e'$; e'' is a point on the M_B influence line (M_B is the support moment at B). Similarly, $5''n'' = m'n'$, plotted downward on the same vertical, gives a point n'' on the negative bending moment influence line for the point 7 in the

span L_1; and $5''j'' = 5j'$ gives a point on the positive bending moment influence line for the point 5 in the span L_2. The same construction can be applied to every point in both spans; the resulting diagrams are shown in the figure. For the unit load, the maximum positive bending moment occurs when the load is $0 \cdot 578$ of the span from the supported ends. The maximum negative bending moment at any point occurs when the load is over that point. The locus of x'' gives the maximum negative bending moment diagrams for the spans. It may be shown * that the equation to the line $a''e''b''$ is

$$M_B = b'e' = \frac{n(1 - n^2)L_1{}^2}{2(L_1 + L_2)}$$

and to the line $a''x''b''$ is

$$M = - n(1 - n)L_1 \left\{ 1 - \frac{n(1 + n)L_1}{2(L_1 + L_2)} \right\}$$

where nL_1 is the abscissae of the points measured from A. To plot similar curves for the span BC, interchange L_2 for L_1, when the abscissae become nL_2, measured from C.

If the ends A and C of the beam be direction-fixed instead of merely supported, the construction of (ii) Fig. 128, Vol. I, must be replaced by that of (iv) in the same figure. That is to say, the line q_2q_3, passing through i, must be drawn parallel to r_1r_4 and not horizontally; r_1 can be found by the construction used to find r_2. The base line will pass through r_1 and r_4.

General Case. — The solution when the beam is continuous over many spans and when I varies in

FIG. 71.

each is shown in Fig. 71. The positions of the $p_1, p_2 \ldots p_n$ points are found as set forth in § 79, Vol. I. These are determined once
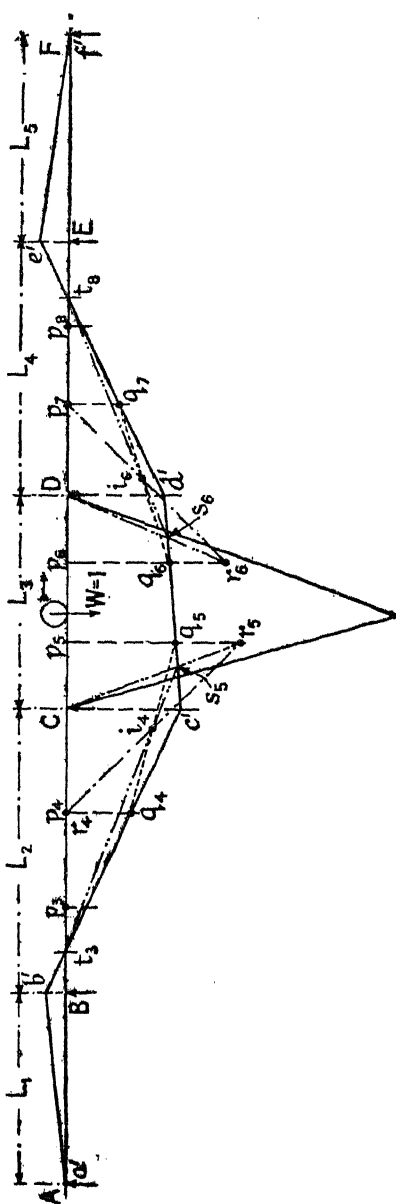
* *Characteristic Points.* Salmon. *Select. Eng. Pap. I.C.E.*, No. 46, 1927, p. 33.

for all for the different spans, and do not alter with the position of the moving load. Suppose that a load $W = $ unity be travelling across span L_3. Determine the points t_3 and t_8 by the Ostenfeld construction, Fig. 127, Vol. I ; the conditions at the ends of the beam must be known, it does not matter what they are. The characteristic points r_5, r_6 are found by the construction used in Fig. 134, Vol. I ; r_4 and r_7 coincide with p_4 and p_7. Find the intersection points i_4 and i_6 and hence the points s_5 and s_6 by the construction shown in Fig. 71. The s points lie on the base line, which can be drawn in. It will pass through t_3 and t_8. The positive and negative bending-moment influence lines for different points on the beam can be plotted exactly as in Fig. 70.

If the girder is uniform from end to end, the p points divide the span into thirds, otherwise the construction is the same.

40. Influence Lines for Elastic Displacements.—Mohr [23] pointed out that the deflection curve for a unit load, placed at a particular point on a beam, is the *deflection influence line* for that point.

Let AB, Fig. 72, be the beam, and suppose that $a_2c_2k_2b_2$ be the deflection curve for a load $W = $ unity placed at K. Then $a_2c_2k_2b_2$ is the influence line giving the deflection of the beam at K. This follows from Maxwell's law of reciprocal deflections, §84, which states that the deflection at a point K, produced by a unit load applied at C, is equal to the deflection produced at C by the same load applied at K. In the present instance y_C, the ordinate of the
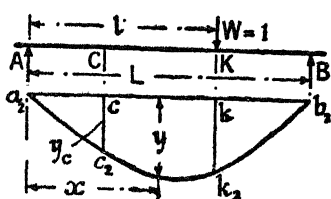
FIG. 72.

deflection curve at C, is the deflection produced at C by unit load at K, and it is equal to the deflection produced at K when a unit load acts at C. In other words, the ordinate under the load of the curve $a_2c_2k_2b_2$ represents the deflection at K, hence $a_2c_2k_2b_2$ is the deflection influence line for the point K. If there be a number of moving loads, the deflection at K, $y_K = \Sigma\, Wy$, where y is the ordinate of the influence line under a load W, exactly as in the case of shearing force and bending moment influence lines.

The theory is equally true for the deflection of braced girders, and for displacements generally, provided that all the loads be parallel.

For a uniform beam, $EI = $ constant, the equation to the curve $a_2c_2k_2$ [see eq. (25), §52, Vol. I ; $W = $ unity] is

$$y \quad \frac{L - l}{6EI} \{l\,(2L - l)\,x - x^3\}$$

and to the curve k_2b_2 is

$$y = \frac{l}{6EI} \cdot \frac{1}{L} \{x^3 - 3Lx^2 + 2L^2x + l^2x - Ll^2\}$$

The curve $a_2k_2b_2$ is of frequent occurrence in influence lines, and the

following graphical method of setting it out may be used. In Fig. 73 let $AK = nL$; calculate

$$KK_2 = \frac{n^2(1-n)^2L^3}{3EI} = \frac{n(1-n)L^3}{6EI} \cdot 2n(1-n)$$

$$KK_3 = \frac{n(1-n)^2(1+n)L^2}{6EI} = \frac{n(1-n)L^3}{6EI} \cdot (1-n^2)$$

$$KK_4 = \frac{n^2(1-n)(2-n)L^3}{6EI} = \frac{n(1-n)L^3}{6EI} \cdot n(2-n)$$

and set them up as ordinates under the load. Join AK_2, BK_2, BK_3, AK_4. Let 1.6 be any ordinate of the curve. Draw 2.3, parallel to AK_4 ;
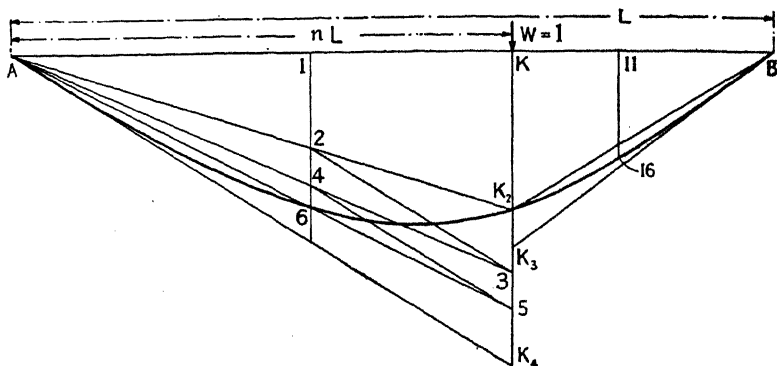
FIG. 73.

join A.3, cutting 1.6 in 4. Draw 4.5 parallel to AK_4 ; join A.5 cutting 1.6 in 6 ; then 6 is a point on the curve. Similarly, by drawing lines parallel to BK_3 and joining to B, the point 16 on the ordinate 11.16 is determined. It is unnecessary and confusing actually to draw all the construction lines ; the points 3, 4, 5, and 6 can be marked with a pencil.

If EI be not constant, the deflection curve for unit load at K must be found by the methods of § 54, Vol. I. For braced girders, use the methods of §§ 12, 14, 15, Chapter I, or of § 70 Chapter V in order to find the displacement curve.

Worked Example.—To find the deflection of the panel point m of the braced girder shown
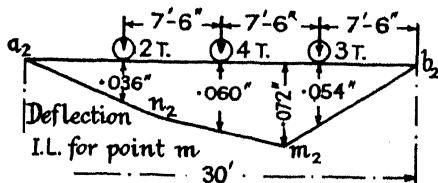
FIG. 74.

in Fig. 36 when the load system shown in Fig. 74, travelling across the girder, reaches the position indicated. The deflection polygon for the bottom flange of this girder, when loaded with 12 tons at the point m, is given in Fig. 37. The corresponding deflection polygon of the girder, when loaded with 1 ton at the same point, is obtained by dividing the ordinates of Fig. 37 by 12. It is shown in Fig. 74 ; the

maximum ordinate being $0 \cdot 86 \div 12 = 0 \cdot 072$ inch. This deflection polygon is the deflection influence line for m. The ordinates y under the loads are indicated in Fig. 74 and the calculation for the deflection is as follows :

$$W_1 y_1 = 2 \text{ T.} \times 0 \cdot 036 \text{ in.} = 0 \cdot 072 \text{ inch.}$$
$$W_2 y_2 = 4 \text{ T.} \times 0 \cdot 060 \text{ in.} = 0 \cdot 240$$
$$W_3 y_3 = 3 \text{ T.} \times 0 \cdot 054 \text{ in.} = 0 \cdot 162$$

Deflection at $m = y_m = 0 \cdot 474$ inch.

BIBLIOGRAPHY

Max. B.M. and S.F. Diagrams. Equivalent Uniform Loads.

1. CULMANN. *Die Graphische Statik.* Zürich, 1866.
2. PEGRAM. Specifications for Strength of Iron Bridges. *Trans. Amer. Soc. C.E.*, 1886, vol. xv, p. 474 ; see also MONCRIEFF, *Proc. Inst. C.E.*, vol. cxli, 1899–1900, p. 94.
3. ALEXANDER. *Analytical Theory of Bending Moments Produced by Travelling Load Systems.* Tracts 8vo, vol. 313, Library, Inst. C.E. ; see also *Proc. Inst. C.E.*, vol. cxli, 1899–1900, p. 91.
4. FARR. Moving Loads on Railway Underbridges. *Proc. Inst. C.E.*, vol. cxli, 1899–1900, p. 2 ; see also vol. ccii, 1915–16, p. 368.
5. ROSS. The Assimilation of Railway Practice in Respect of Loads on Bridges up to 200 Ft. Span. *Proc. Inst. C.E.*, Supp. to vol. cliv, p. 20. (Eng. Conf. 1903).
6. GRAHAM. Axle-Loads on Railway Bridges. *Proc. Inst. C.E.*, vol. clviii, 1903–4, p. 323.
7. LILLY. Moving Loads on Railway Underbridges. *Proc. Inst. C.E.*, vol. clviii, 1903–4, p. 380.
8. BAMFORD. Moving Loads on Railway Underbridges. *Engg.*, Sept. 7, 1906, p. 307.
9. CAPPER. Maximum Bending-Moment and Shearing-Force Diagrams for Moving Loads. *Engg.*, Mar. 1, 1935, p. 219 ; see also pp. 345, 396.
10. B.S.I. Tables of Unit Loadings for Railways and Highways. B.S.S. No. 153, Appendix I, 1925–30.
11. MINISTRY OF TRANSPORT. Roads Dept. Standard Loading for Highway Bridges, 1931.
12. A.R.E.A. General Specifications for Steel Railway Bridges, 1935.

Influence Lines.

13. WINKLER. Vortrag über die Berechnung von Bogenbrücken. *Mitt. d. Arch.- u. Ing.-Ver. f. Böhmen*, 1868.
14. —— *Theorie der Brücken.* Wien, 1873 : 3rd ed., 1886.
15. MOHR. Beitrag zur Theorie der Holz- und Eisen-Constructionen. *Zeit. d. Arch.- u. Ing.-Ver. z. Hannover*, 1868, p. 19.
16. —— Beitrag zur Theorie des Fachwerks. *Zeit. d. Arch.- u. Ing.-Ver. z. Hannover*, 1874, p. 509 : 1875, p. 17 : also *Technische Mechanik*, Berlin, 3rd ed., 1928.
17. FRÄNKEL. Ueber die ungünstigste Einstellung eines Systems von Einzellasten auf Fachwerkträgern mit Hilfe von Influenzkurven. *Der Civilingenieur*, 1876, pp. 218, 441.
18. MÜLLER-BRESLAU. *Die Graphische Statik der Baukonstruktionen.* Leipzig, 5th ed., 1912, Bd. I, p. 134.

19. SWAIN. On the Calculation of the Stresses in Bridges for Actual Concentrated Loads. *Trans. Amer. Soc. C.E.*, vol. xvii, 1887, p. 21.
20. LEA. The Determination of the Stresses in Lattice-Girders when Subjected to Concentrated Travelling Loads. *Proc. Inst. C.E.*, vol. clxi, 1904–5, p. 261.
21. MOLITOR. *Kinetic Theory of Engineering Structures.* New York, 1911. Chaps. iv, v, viii–x.
22. MÜLLER. Ueber Einflusslinien und Einflussdiagramme (Differential Coefs. of Influence Lines). *Zeit. ang. Math. Mech.*, 1932, p. 36 ; see also NEMÉNYI, 1930, p. 383 ; and *Eng. Ab. I.C.E.*, 1932, No. 52 : 68.

Influence Lines for Continuous Girders.

23. MOHR. Ref. No. 16 (1875).
24. LÉVY. *La Statique Graphique*, iie partie, Paris, 1874.
25. MÜLLER-BRESLAU. Einflusslinien für kontinuerliche Träger mit drei Stützpunkten. *Zeit. d. Arch.- u. Ing.-Ver. z. Hannover*, 1884, p. 278 ; see also *Graphische Statik*, Bd. II, Abt. i, § 14 *et seq.*
26. LEA. Influence-Diagrams for Continuous Girders. *Proc. Inst. C.E.*, vol. clxxxv, 1910–11, p. 277.
27. MOLITOR. Ref. No. 21, Chaps. ix and x.
28. MAGNEL. Influence Lines for Continuous Beams. *Engg.*, Feb. 15, 1918, p. 163.
29. SALMON. Characteristic Points. *Select. Eng. Pap. I.C.E.*, No. 46, 1927.
30. BLACKADDER. A Direct Method for the Construction of Influence Lines for Continuous Girders. *Select. Eng. Pap. I.C.E.*, No. 119, 1931.

QUESTIONS ON CHAPTER II

1. A single concentrated load of 5 tons rolls across a beam of 40 ft. span ; (a) Plot on a common base line the shearing-force diagrams for load positions at intervals of 5 ft. from one end of the beam to the other. Show that the enveloping curves are straight lines. (b) Plot on a common base line the bending moment diagrams for the same load positions. Show that the enveloping curve is a parabola. What is the equivalent uniformly distributed load ?

Ans. 0·25 ton per foot.

2. Two connected loads of 6 tons and 10 tons, spaced 12 ft. apart, roll along a girder which is freely supported on a span AB of 30 ft. Draw curves of maximum bending moment and maximum shearing force, and show the positions of the loads for maximum bending moment. (U.L.)

Ans. See § 20 ; max. S.F. = 13·6 tons at A ; max. B.M. = 86·7 ft.-tons, under the 10-ton load, 12 ft. 9 in. from A.

3. A rolling load, length $\frac{1}{4}$L, intensity w per ft. run, traverses a girder of span L. Find for a point K distant $\frac{1}{4}$L from the left-hand support, (a) the maximum positive and negative shear forces, and (b) the maximum bending moment. Indicate the positions of the load when these occur. (U.L.)

Ans. Max. $+ S_K = 5wl/96$; front of load at K. Max. $- S_K = 13wl/96$; back of load at K: Max. $M_K = - 7wl^2/144$; back of load $l/12$ from K.

4. A braced girder of 160 ft. span has to carry a uniformly distributed load of 1 ton per foot run, and a uniformly distributed rolling load of $2\frac{1}{4}$ tons per foot run. Over what length of the girder will it be necessary to put counter bracing ? (U.L.)

Ans. The middle 48·6 ft.

5. A locomotive and tender, with loads as shown in Fig. 75, pass over a bridge of 60 ft. span. Draw by the tracing paper method the maximum

shearing-force and bending-moment diagrams, and determine the equivalent uniform loads, (i) for shear, (ii) for bending moment. (U.L.)

Ans. Follow the method of § 21.

6. In Q. No. 2, show that the bending moment under the 10-ton load is a maximum when that load, and the centre of gravity of the two loads, are equidistant from the centre of the beam.

7. Four loads of 11, 16, 19, and 14 tons respectively, connected together at 10-ft. intervals, centre to centre, roll along a girder of 50 ft. span. Find the position of the loads when the maximum bending moment is produced and the value and position of that moment. (U.L.)

Ans. Max. B.M. occurs when the 14-ton load is 13 ft. from the end of the beam ; 494·8 ft.-tons ; under the 19-ton load.

8. A locomotive, with wheel loads as shown in Fig. 75, passes over a plate girder bridge of 60 ft. span, from left to right. Determine the maximum
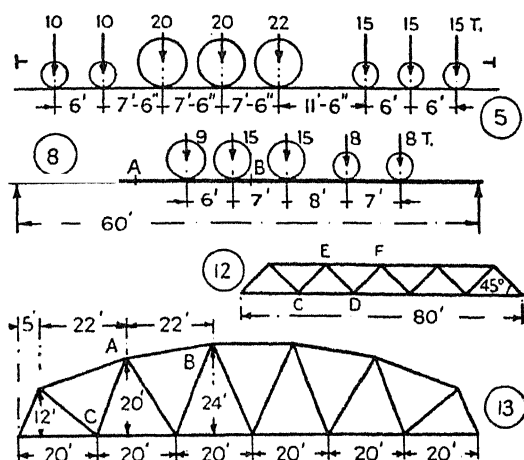
FIG. 75.

bending moment produced at the points A and B distant 15 ft. and 30 ft. respectively from the left-hand reaction.

Ans. Max. B.M. at A = 478 ft.-tons ; at B = 622 ft.-tons.

9. A rolling load of 4 tons travels across a beam AB of 40 ft. span. Draw a diagram such that the ordinate at any point C represents the bending moment at a point D 10 ft. from A when the load is at C. Dimension the maximum ordinate. Hence show that if two 4-ton loads, coupled together 8 ft. apart, cross the beam, the maximum bending moment at D occurs when one of the loads is at D. Show on the diagram the position of the two loads when this maximum occurs. (I.C.E.)

Ans. Max. ordinate = 30 ft.-tons.

10. What is an influence line ? The main girders of a through bridge of 120 ft. span are warren girders, the lower flanges of which are divided into 6 panels of 20 ft. each. A uniform travelling load of 2 tons per foot run, longer than the span, crosses the bridge. Draw a simple diagram which determines the position of the load when the shearing force is a maximum in any panel. Hence determine the maximum shearing force in the 4th panel from the end of the bridge at which the train enters. (I.C.E.)

Ans. See (v) Fig. 63 ; 18 tons per girder.

11. Solve Q. No. 3 by means of influence lines.

12. A bridge has two main girders as shown in Fig. 75. A uniform live load of 2 tons per foot (longer than the span) crosses the bridge from right to left. Find the maximum forces in the members CD, EF, and CE of one girder. (U.L.)

Ans. Forces; CD = + 80; EF = − 96; CE = + 25·45 or − 5·66 tons.

13. Draw to scale diagrams showing the variations of the forces in AB and AC, Fig. 75, as a load of 1 ton travels along the girder. Show how these diagrams may be used to find the maximum forces in AB and AC for a uniform travelling load of 2 tons per foot run longer than the span, and find these maximum forces. (U.L.)

Ans. Forces: AB = − 72·7; AC = + 8·54; − 18·26 tons; if load carried by two main girders.

14. A rolling load of 2 tons carried on two axles 6 ft. centre to centre, crosses a floor supported by longitudinal beams carried on cross girders 10 ft. centre to centre, Fig. 76. Assuming that the longitudinal beams are merely supported where they connect on to the cross girders, find the maximum load which comes on a cross girder as the load rolls along the floor.

Ans. 1·4 tons.

15. A locomotive with axle loads as shown in Fig. 76 passes over a single line bridge of 60 ft. span. Determine the maximum shearing force at the end and at the centre of the span. (U.L.)

Ans. 46·8; 18·3 tons.

16. Solve Q. No. 8 by the aid of an influence diagram. (U.L.).

17. In Q. No. 5 determine the maximum bending moment at the centre of the span, and the maximum

FIG. 76.

shearing force at the ends, by means of influence lines. Compare these results with those obtained in Q. No. 5.

Ans. Max. B.M. = 1031·3 ft.-tons. Max. S.F. = 74·6 tons.

18. The figure represents the outline of one leaf of a small swing foot-bridge, pivoted at A and B and standing out cantilever fashion. A load of 1 ton rolls along the frame from A to H. Find the maximum forces which occur in the four bars meeting in the point C due to this moving load, and state whether they are tensile or compressive. (I.C.E.)

Ans. Max. forces: CD = + 3·33; CE = + 1·22; CG = + 3·64; CF = − 1·0 tons.

19. If the beam in Q. No. 2 were fixed in direction at each end, find the maximum bending moment which occurs at the central cross section as the specified load rolls across the beam.

Ans. 38·4 ft.-tons.

20. Find the maximum deflection of the point *m* in Fig. 41 when the given load system, Fig. 76, travels across the beam from left to right.

Ans. 0·163 inch, when the leading load is at *m*. (Find the deflection polygon for the girder with a unit vertical load at *m*. This is the deflection influence line.)
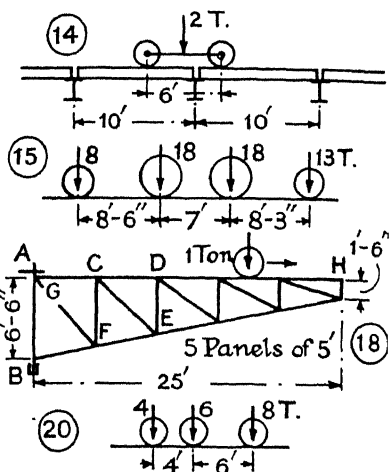
CHAPTER III

WIND PRESSURE

41. Its Importance.—The pressure of wind on a large exposed structure such as a long-span bridge, or a very tall building, may be one of the chief straining actions to which it is subjected. In small, low, and shielded structures the effect of wind pressure may be relatively unimportant, but in ordinary design it is usually necessary to take it into account.

42. Wind Velocity and Pressure.—Many observations have been made of the velocity and pressure of the wind. The velocity is usually measured by means of an anemometer of the revolving cup type. For measuring the pressure, a *Dines tube*, which is an adaptation of the Pitot tube, is commonly used. This is often calibrated to read the velocity, but the instrument measures the pressure. In addition, estimates of the force due to wind pressure can be obtained from vehicles overturned during a storm.

To correlate such observations, it is necessary to know the relation between pressure and velocity. From a number of experiments [16] it has been found that $P = 0 \cdot 0032 V^2$, where P is the pressure in lb./sq. ft. on a flat square surface normal to the direction of the wind, and V is the velocity of the wind in miles per hour. [10] This constant varies with the barometric height and moisture content of the air.

Forth Bridge Records.—A number of records of wind pressure, over a long series of years, were made at the Forth Bridge. Owing to the type of gauge used there is good reason to think that the readings were much too high, but the results are of interest as showing the variation in wind pressure likely on such a structure.

Pressure in lb./sq. ft.	Gauge No.				
	1	2	3	4	5
Maximum	55	50	65	20	55
Average	28	23	50	13	30
Minimum	20	15	18	10	20
Height of gauge above high water (ft.) . . .	214	163	378	50	214

The records [15] of the wind gauges erected on the bridge itself, during fifteen of the most violent storms which occurred between January 1901 and February 1906, are given in the preceding Table.

The position of the gauges is shown in Fig. 77. These gauges were pressure plate revolving gauges, each having an area of $1\frac{1}{2}$ square feet.

When a large 300 sq. ft. gauge recorded 19 lb./sq. ft., a gauge of $1\frac{1}{2}$ sq. ft., at its centre, recorded 28·5 lb./sq. ft., and a $1\frac{1}{2}$ sq. ft. gauge at the right-hand top corner recorded 22 lb./sq. ft. When on another occasion the large gauge recorded 18 lb./sq. ft., the small centre gauge recorded $23\frac{1}{2}$ lb./sq. ft., and the small corner gauge 22 lb./sq. ft.

From a study [19] of the records taken at different meteorological stations, it appears probable that in the British Isles, even in the most violent storms, the mean wind velocity seldom exceeds 75 miles per hour (18 lb./sq. ft.), with occasional gusts which may reach, but seldom exceed, 100 m.p.h. (32 lb./sq. ft.). In India, during cyclones, the corresponding figures are 90 m.p.h. (26 lb./sq. ft.), and 120 m.p.h. (46 lb./sq. ft.), respectively. Velocities of over 200 m.p.h. have been recorded at Mount Washington, U.S.A. Such velocities are very exceptional.

43. Wind Structure.—It is evident from the Forth Bridge observations that the wind pressure increases with increase in height (compare gauges 3 and 4). The following figures are taken from a Weather Report of the Meteorological Office :

Height in metres	$\frac{1}{2}$	1	2	3	4
Relative Wind Velocity	0·50	0·59	0·73	0·80	0·85

	5	10	15	20	25	30
	0·89	1·00	1·07	1·13	1·17	1·20

For heights up to 30 m., formulae of the type $V = kH^n$ have been proposed to represent the variation in velocity, where n ranges from $\frac{1}{5}$ to $\frac{1}{4}$. Curves representing the variations in wind velocity up to a height of 500 m. have been given by Dines in the Fourth Report on Wind Structure to the Advisory Committee on Aeronautics, and by others.

Lateral Variation.—A second point brought out by the Forth Bridge observations is that the average pressure per square foot on a large area is much less than that on a small area. Thus the pressure recorded
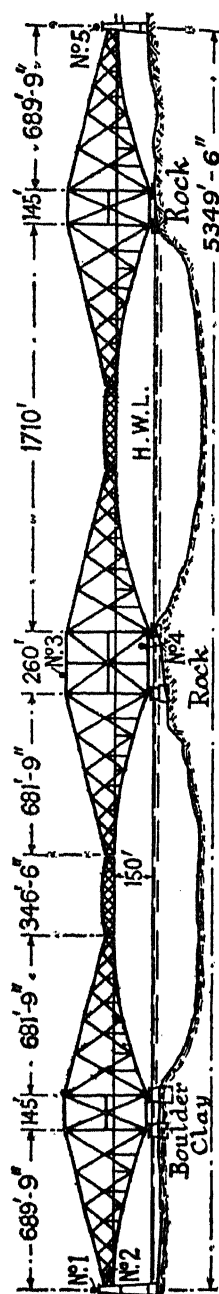
areas, one at the centre and one at the top corner of the large gauge, is much greater than the average pressure over the whole large gauge. It appears from Stanton's experiments,[10] however, that, in a steady wind, size has little effect, i.e. the dimensional effect is small. The explanation is to be sought in the lateral variation in velocity which occurs in all actual winds. Dines * has recorded that simultaneous readings of velocity instruments of the same type, placed as close together as 11 ft., were in the ratio of 3 to 5, and that the velocity recorded by one instrument was increasing at a moment when that recorded by the other was decreasing. Such want of uniformity would affect a small surface more than a large one. It is evident that a gust of limited extension, which would produce a heavy pressure on a small area, would not much affect the average pressure on a large area. It is common, therefore, to assume a greater mean pressure on small structures than on large. On the other hand, observations made at the Tower Bridge † appear to show that, for spans up to 250 feet, lateral variations in wind velocity are not considerable. It also appears probable that such variations decrease with increasing height.

According to Dr. Simpson, if V be the greatest mean velocity of the wind in miles per hour,

Maximum velocity in gusts $= 1 \cdot 3V + 1 \cdot 5$

Minimum velocity in gusts $= 0 \cdot 65V - 1 \cdot 0$

These formulae apply to Great Britain. Remfry [19] takes as the factor for lateral variation in wind pressure, $V^2/(1 \cdot 3V + 1 \cdot 5)^2$.

44. Dynamic Action of Gusts.—The question arises as to whether wind pressure should be treated as a live or as a dead load. Very little information is available as to the time rate of increase of wind velocity. Cases are on record when the velocity rose from zero to 33 miles per hour in one minute, from 9 to 62 miles per hour in about two minutes, and from 6 to 45 miles per hour in five minutes. Considered as live loads these rates of increase are very slow, and the dynamic increment due to them must be very small. It appears quite unwarrantable, therefore, to treat the wind pressure as a suddenly applied load, or to apply an impact factor to the wind load.

Synchronous vibrations may, however, be set up in tall structures such as chimneys, see Omori, and Pagon, Ref. No. 42, Bib., and the effect may be serious.

45. The Coefficient C.—The pressure of the wind, as determined by the formula $P = 0 \cdot 0032V^2$, is the mean intensity of resultant pressure on a square flat plate placed normally to the direction of the wind. It is convenient to express the mean intensity of resultant pressure on any other shape of plate, or on a body placed in the wind stream, in the form $P = 0 \cdot 0032CV^2$, where C is a coefficient to be determined experimentally, and equal to unity in the case of the square flat plate placed normally to the wind.

* *Quar. Jour. Roy. Meteor. Soc.*, 1894, vol. xx, p. 183.
† *Proc. Inst. C.E.*, vol. ccxvi, 1922–3, p. 36.

I

In what follows, unless otherwise indicated, by the term *pressure* is to be understood an intensity of pressure, usually expressed in lb./sq. ft. The mean resultant pressure on a plate or body is the total force on the plate or body due to the wind, divided by the face area of the plate, or divided by the projected area of the body, measured normal to the direction of the wind.

46. Wind Pressure on a Flat Plate Normal to the Wind.—Fig. 78 illustrates the distribution of pressure on a square flat plate placed normally to a uniform current of air.[9] The section shown is taken across a diameter at right angles to a side. It will be seen that there is a positive pressure on the windward side, and a negative pressure or suction on the leeward side. The resultant pressure is the added effect of these. The positive pressure reaches a maximum at the centre of the plate, and is equal to $p = \frac{1}{2}\rho v^2$ lb./sq. ft., where ρ denotes the weight per cubic ft. of the air in lb. $\div g$ in ft./sec.^{2}, and v is its velocity in ft./sec. This maximum is the same for all shapes of plates. The negative pressure is practically uniform except near the edges. The ratio of the in-tensities of positive and negative pres-sures at the centre of the plate varies

FIG. 78.

with its shape. In the square plate this ratio is $1 : 0\cdot57$; in a circular plate it is $1 : 0\cdot48$; and in a rectangular plate $(l : b = 25)$ it is $1 : 0\cdot69$. It follows that the mean resultant pressure, and hence the value of C, is different for different shapes of plates.

	C.
Square plate	1·0
Circular plate	1·0
Rectangular plate * $l : b = 15$	1·2
30	1·4
60	1·6

47. Effect of Shape.—The shape of an object exposed to the wind has considerable effect on the magnitude of the force exerted by the wind upon it. Thus the force on a cylinder is only about one half, and that on a sphere only about one-third of the force on a flat plate placed normal to the wind, and of equal projected area. The values of the coefficient C giving the relative pressures will be found in the Table [7] below. In all cases the pressure $P = 0\cdot0032CV^2$ is that on the projected area normal to the wind.

	C.		C.
Square flat plate	1·0	Cylindrical tower	0·52†
Cube, or square tower, one face normal to wind	0·90	Octagonal tower	0·60
Cube, or square tower, diagonal normal to wind	0·63	Sphere . .	0·36†

* According to Flachsbart's experiments [29] the effect of l/b (the aspect ratio) is only appreciable for values above 10.

† These values are affected by turbulence, roughness of surface, etc., and vary with the Reynolds' number.

For a prism of square cross section (face normal to wind) Dr. Nøkkentved (*Proc. Amer. Soc. C.E.*, September 1936), gives

Ratio of height to side =	2·3	3·0	5·0
C :	05	1·30	1·50	1·91

For a lattice girder 29 ft. long by 3 ft. 7½ in. deep, with a double system of lattice bracing, C = 1·26 (Stanton [10]). Melbourne University experiments [7] give C = 1·45 for a lattice girder of an ordinary type. More recently, Flachsbart [29] has carried out a series of experiments on model braced girders of different types, and concludes that the maximum wind force F_W on a girder occurs when the wind is normal to the girder, and is

$$F_W = pa\mathrm{K}_d = \tfrac{1}{2}\rho v^2 a\mathrm{K}_d = \tfrac{1}{2}\rho v^2 \phi\mathrm{A}\mathrm{K}_d \qquad . \qquad . \quad (1)$$

where K_d = a coefficient (the drag coefficient).
p = max. theoretical wind pressure on the girder = $\tfrac{1}{2}\rho v^2$ (see above) (lb./sq. ft.).
v = the velocity of the wind (ft./sec.).
ρ = the density of the air (wt. per cub. ft./g).
a = the sum of the projected area of all the bars (sq. ft.).
A = the area of the contour of the girder (sq. ft.).
ϕ = a/A, a fullness factor.

Usually $\phi \gtreqless 0\cdot25$, when K_d is approximately constant and equal to 1·6 ; when $\phi < 0\cdot25$, K_d varies with ϕ, but approximates to 1·8. The type of framework, type of bar profile, and shape of contour make no practical difference to the value of F_W (the difference is less than 10 per cent.).

Since the value of K_d for a square plate = 1·27, it follows from the above, if $P = 0\cdot0032V^2$, that when $\phi \gtreqless 0\cdot25$, C = 1·26 ; when $\phi < 0\cdot25$, C = 1·42.

Distance Apart in Diameters.

Fɪɢ. 79.

48. Shielding.—If two similar plates be placed one behind the other in a current of air, it is found that the windward plate shields the leeward plate to an extent depending on their distance apart. The results of some experiments on pairs of parallel circular plates by Stanton,[9] are given in the following table :

Distance apart in Diameters .	0	1	1½	2	3	4
Value of C for the pair . .	1·0	0·83	0·74	0·89	1·44	1·73

and are plotted in Fig. 79. The interesting fact appears that when the plates are 1½ diameters apart, the total pressure on the two plates is only about ¾ of that on a single plate, and in these circumstances, the pressure on the leeward plate is found to act in the opposite direction to that on the windward plate. These experiments were made using circular discs ;
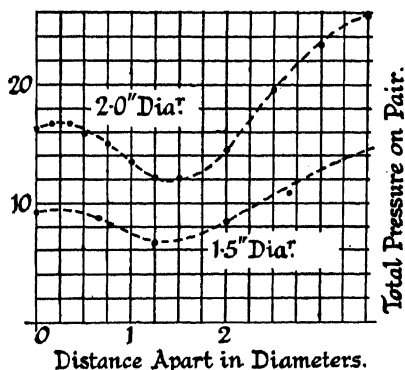
it was found that the shielding effect was considerably less in the case of long rectangular bars. In the case of parallel plates, without holes, at moderate distances apart, the air in the region between the plates was at a uniform pressure. This suggested that the resultant pressure on a short cylinder would be nearly the same as that on two plates of the same dimensions as its ends, which proved to be the case.

Lattice Girders.—The shielding effect in the case of similar, similarly situated, models of lattice girders was found to be independent of the scale ; but in two lattice models of the same type, but with different widths of bars, when the models were the same number of times the width of the bars apart, the shielding effect was greater for the wider bars.

The total pressure on *two lattice girders*, each of depth D, placed a distance D apart, was $1 \cdot 29$ times that on one. If these girders were connected by a roadway, top or bottom, this figure was reduced to $1 \cdot 15$; or to $1 \cdot 25$ when the distance apart was 2D ; so that if $C = 1 \cdot 26$ for the single girder, $C = 1 \cdot 26 \times 1 \cdot 25 = 1 \cdot 58$ for the pair. If the angle of incidence of the wind was not normal, there was a slight increase in the pressure, which amounted to approximately 5% when the angle of incidence was 75°.

In the above experiments the openings were approximately 50 per cent. of the total area.

In the case of model single web lattice girders tested in pairs (no floor), Sir Benjamin Baker obtained the following results :

Distance apart in terms of depth	.	.	.	.	1	2	3	4
Ratio of pressure on pair to that on single girder	.		1·2	1·5	1·7	1·8

The addition of one or more extra girders, placed between the outer girders, made little difference to the total wind load (about 4% for 3 to 4 diameters apart). For the single girder $C = 1 \cdot 15$.

In continuation of the work summarised in § 47, Flachsbart and Winter [29] made a series of experiments on model braced girders in pairs, the more important results of which are as follows : The influence of the leeward girder on the windward girder is small even at small distances apart. The shielding influence of the windward girder is considerable. The wind velocity and pressure close behind a lattice girder takes a wave formation with minima values behind the bars, and maxima values behind the open panels. This formation equalises slowly with increasing distance, and the shielding effect is still perceptible at relatively large distances apart. The efficacy of the shielding depends primarily on the fullness factor ϕ, § 47 ; the relative distance apart of the girders ; and congruency (i.e. whether the bars of the girders lie exactly one behind the other), this is chiefly important at small distances apart. The effect of type of girder is small.

The experimental results for congruent girders are plotted in (i) Fig. 80 ; where, if F_w, eq. (1), § 47, is the wind force on the windward girder, ψF_w is the wind force on the leeward girder, and $(1 + \psi) F_w$ that on the pair. The values of ψ for $\phi = 0 \cdot 6$ to $1 \cdot 0$ are shown by dotted

lines, because they depend to some extent on the aspect ratio l/b of the individual members of the frame. For values of ϕ between $0\cdot1$ and $0\cdot6$, it is sufficiently accurate to use $\psi = 1\cdot15\ [1\cdot0 - 1\cdot45\ (B/D)^{\frac{1}{4}}]$; B denotes the distance apart of the girders, and D their depth. Obliquity of the wind direction had little effect on the value of F_w, but increased the value of ψ slightly, the maximum effect occurring at an obliquity of $25°$. In all the experiments the girders were unconnected by a roadway, which would slightly reduce the total wind load on the pair (see *supra*). (ii) Fig. 80 gives approximately the relation between ψ and ϕ for a pair of girders placed $B = D$ apart, but shifted relatively half a bay, under normal wind loading.

Plate Girders.—For these $\phi = 1$, (i) Fig. 80, but the value of ψ depends to some extent on the aspect ratio L/D, and on the presence of a roadway. [According to Melbourne University experiments,[7] for a plate girder bridge with a roadway top or bottom, if $B = D$, $C = 1\cdot0$; if $B = 2D$, $C = 1\cdot20$.]

Tall Masts.—From experiments on model sections of square lattice braced masts, it appears that, under normal wind pressure, the forces on planes parallel to the wind are negligible, and the mast may be treated as two parallel girders, using the formulae given above. When the wind acts diagonally, the total wind force may be increased by 20 per cent. (or even more), depending on the type of framework. For maximum effect the wind force may be taken as acting at $45°$, though the angle of obliquity for a maximum was in some cases about $25° - 30°$.

FIG. 80.

From tests on a $\frac{1}{30}$th scale model, Katzmary and Seitz * found that, under diagonal wind pressure, the maximum wind force on a tall mast was $1\cdot5$ times the normal wind force F_w on one face; and equivalent to forces equal to F_w acting simultaneously on two perpendicular faces.

49. Wind Pressure on Inclined Surfaces.—Fig. 81 shows the distribution of pressure on flat plates inclined at angles of $30°$ and $45°$, respectively, to the direction of the wind.[9] It will be observed that these distributions differ considerably from the distribution of pressure on a plate normal to the wind, particularly as regards the negative pressure on the back of the plate due to eddies.

A number of formulae have been proposed to express the relation
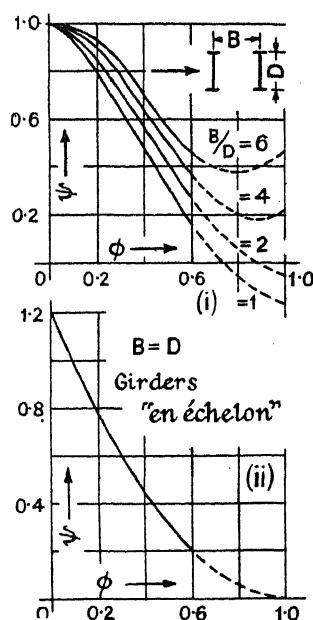
* *Der Bauingenieur*, 1934, p. 218.

between p, the resultant normal pressure on a plate inclined at $\theta°$ to the direction of the wind, and P, the pressure on a plate normal to the wind.
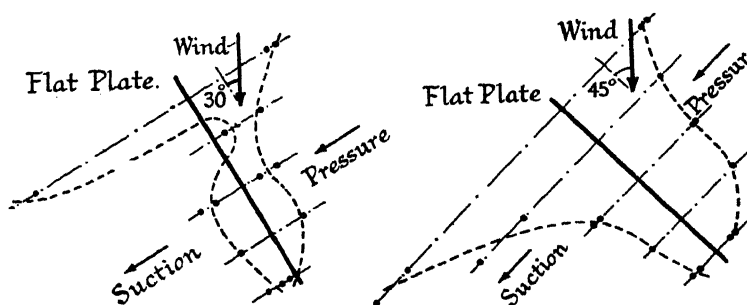
Let $p = \text{KP}$, where p and P are both expressed in lb. per sq. ft. of the *face* area of the plate. Then according to the formula derived by

Duchemin's Formula

$$\frac{p}{P} = \frac{2 \sin \theta}{1 + \sin^2 \theta}$$
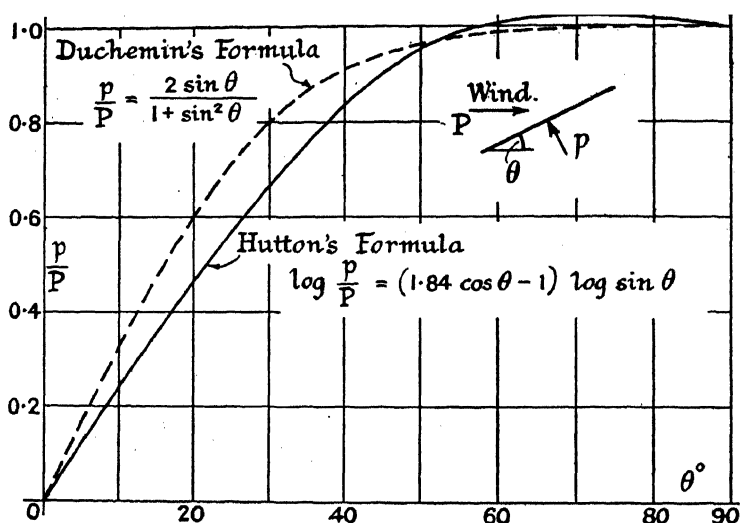
Hutton's Formula

$$\log \frac{p}{P} = (1 \cdot 84 \cos \theta - 1) \log \sin \theta$$

Hutton [1] from his experiments with a whirling machine, made in 1786–7, see Fig. 82 * :

$$\log \text{K} = \log (p/\text{P}) = (1 \cdot 84 \cos \theta - 1) \log \sin \theta \quad . \quad . \quad (1)$$

By Duchemin's formula, [2]

$$\text{K} = \frac{p}{\text{P}} = \frac{2 \sin \theta}{1 + \sin^2 \theta} \quad . \quad . \quad (2)$$

* $p/\text{P} = \theta°/45$ approx: max. $= 1$.

while Rayleigh [3] deduced theoretically that

$$K = \frac{p}{\text{?}} = \frac{(4 + \pi)\sin\theta}{4 + \pi\sin\theta} \tag{3}$$

This latter formula gives the positive pressure on the front of the plate, not the resultant pressure. Stanton found that, in the case of a rectangular plate, the value of K depends on whether the longitudinal or transverse axis be inclined to the wind. It will be seen that, according to Hutton's formula, the resultant pressure on a plate inclined at from about 60° to 90° to the wind is more than that on a normal plate, Fig. 82. This is an experimental fact ; the increased pressure is the effect of eddies, which increase the negative pressure on the back of the plate.

The most commonly occurring case of wind acting on an inclined surface is that of an ordinary roof. As will be seen in the next article, however, the effects of wind on a sloping roof surface are very different from those on an inclined flat plate placed in the wind stream.

50. **Wind Pressure on Roofs and Chimneys.**—Many experiments have been made to determine the distribution of wind pressure on roofs. Fig. 83 shows the distribution of external pressure on three closed-in buildings with ∧ roofs, as determined at the N.P.L.[9] The roof angles in the three cases were 45°, 30°, and 60°, and the pressures were measured for three different wind velocities, 10·0, 13·6 and 16·8 m.p.h. It will be noticed, that, due to eddies, there is a negative pressure or suction on the leeward side of the building, first observed by Irminger,[8] of the same order of magnitude as the normal pressure on the windward side ; and that in the case of the 30° roof, (ii) Fig. 83, the positive pressure on the windward slope is small. These observations have been confirmed and extended by other experiments. In addition, there is the internal pressure (i.e. the pressure inside the building) to be taken into account, see *infra*. This subtracts from the external pressure. In a closed-in building the internal pressure is found to be negative ; that is to say, it increases the resultant pressure on a surface which carries a positive external pressure, and diminishes the resultant negative pressure on a surface which carries an external suction. In the case of a building with open windows and doors, or in an open shed, the resultant pressures on the sloping surfaces may differ considerably from those on a closed-in building.
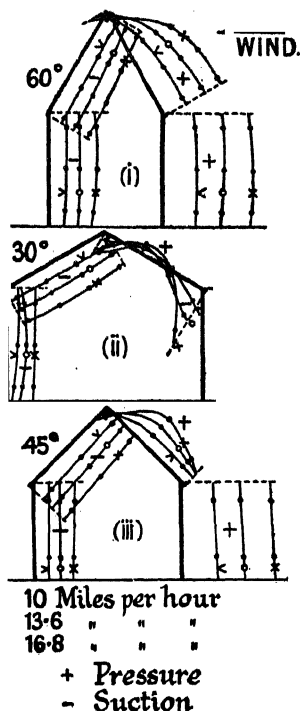

WIND.

60° (i)

30° (ii)

45° (iii)

10 Miles per hour
13·6 „ „ „
16·8 „ „ „

+ Pressure
- Suction

FIG. 83.

According to the N.P.L. experiments,[10] in the case of a building provided with windows and doors, the worst effects produced by the wind occur when the windows and doors on the windward side are all open, and those on the leeward side shut. In these circumstances the values found for the coefficient K were as follows :

Angle of roof	30°	45°	60°
Windward slope, $K =$	+ 0·47	+ 0·88	+ 1·06
Leeward slope, $K =$	− 0·69	not determined	− 1·00

As in the case of the flat plate inclined to the wind, the pressure on the 60° slope is greater than that on the normal plate.

In the case of the open shed roof, contrary to what might perhaps have been expected, the difference in pressure on the leeward side was so small as to be negligible. It would appear that the wind blowing under the roof, i.e. through the building, produces a suction which, practically speaking, balances the exterior suction due to eddies from the windward slope. In this case the values of K were :

Angle of roof	30°	45°	60°
Windward slope, $K =$	+ 0·47	+ 0·88	+ 1·06
Leeward slope, $K =$		negligible	

For the purposes of design, the following interpolated values may be used :

Ratio rise to span	$\frac{1}{5}$	$\frac{1}{4}$	$\frac{1}{3}$	$\frac{1}{2}$
K, windward slope	+ 0·3	+ 0·4	+ 0·6	+0·9
K, leeward slope :—				
(i) Ordinary buildings	− 0·5	− 0·6	− 0·75	− 0·9
(ii) Open shed		negligible.		

+ pressure.   − suction.

In all the above cases, KP is the *total* pressure on the slope, i.e. the difference between the external and internal pressures.

Collating all the published experimental work on the subject, the American Committee on Wind Bracing in Steel Buildings [40] (Fifth Progress Report) propose the following as the maximum likely values for K_e, where $K_e P$ is the external pressure on the roof.

Windward slope :—

$\theta = 20°$ or less	20°–30°	30°	30°–60°	> 60°
$K_e = - 0·7$	$(0·07\theta − 2·1)$	0	$(0·03\theta − 0·9)$	0·9

Leeward slope :—
$K_e = - 0·6$ for all values of θ.

To obtain the value of K, the coefficient K_i for the internal pressure must be taken into account ; $K = K_e − K_i$.

Internal Pressure.—The value of the coefficient K_i has been variously estimated, depending chiefly on the arrangement of the window openings. Irminger and Nøkkentved [24] point out that an airtight building cannot exist in practice, and cite a case in which an impervious covering was stripped from the roof in the first storm. Relief holes were thereafter

fitted, which completely cured the trouble. For a 'leaky' building, they find that if the leaks are uniformly distributed throughout the building, K_i does not vary with the wind velocity or the area of the leaks, but is affected by the shape of the building, i.e. by the distribution of external pressure. For such cases they suggest the values $K_i = -0.25$ to -0.35 ; K_i is always negative.

The maximum positive internal pressure is produced when all the windows and doors are open on the windward side, and closed on the leeward side ; and the maximum negative internal pressure, when the conditions are reversed. The Australian experiments [25] suggest a range for $K_i = +0.8$ to -0.5.

Curved Roofs.—Fig. 84 shows the average of a number of readings, under various conditions as to height of walls, open and closed ends and sides, of the external pressure on a building with a semicircular roof, made at Perdue University. The wind is blowing from left to right.

The American Committee (l.c.) suggest the following procedure for curved roofs : a representative circular arc is described, passing through the two eaves and the ridge, and subtending at its centre an angle ϕ. The ratio of the height of the arc to the span of the roof is called r. The arc is divided into three parts (cf. Fig. 84) subtending at its centre the angles α, β and γ respectively. The angle α, starting at the windward eave, is $\alpha = (r/4 + 0.125)\,\phi$; $\gamma = \phi/4$.

FIG. 84.

For segment α :	$r =$ less than 0.2	0.2 to 0.35*	*0.25 and over
Roof on elevated supports. K_e :	-0.9	$-(2.1 - 6r)$	$+(2.8r - 0.7)$
Arc starts from ground level. $K_e =$			$+1.4r$

For segment β : Any type of support $K_e = -(r + 0.7)$
For segment γ : Any type of support $K_e = -0.5$.
Flat Roof. $K_e = -0.7$ all over.

These are the maximum likely values of K_e ; to obtain K the value of K_i must be subtracted ; $K = K_e - K_i$.

Knowing the value of K, and of P for a given wind velocity, the roof should be designed to carry the pressure $p = KP$, see §§ 6, 212, 209.

For the distribution of pressure on the surface of an *airship shed*, see *Arrol's Bridge and Structural Engineers' Handbook*, 1st ed., London, 1920, p. 180 *et seq.*
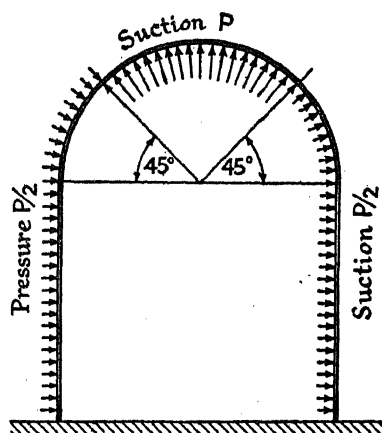
* Thus in the original.

Circular Chimney.—Fig. 85 shows the distribution of wind pressure on a 12·6-in. diameter model, 5 ft. long, of a *circular chimney*, as determined by Dryden and Hill.[43] The wind speed was 80 ft./sec. ($\log_{10} vD/\nu = 5\cdot7$; vD/ν is Reynolds' number). Section (i) was taken 0·5 in. (0·05D), and (ii) about 17 ins. (1·4D) from the top end. In these
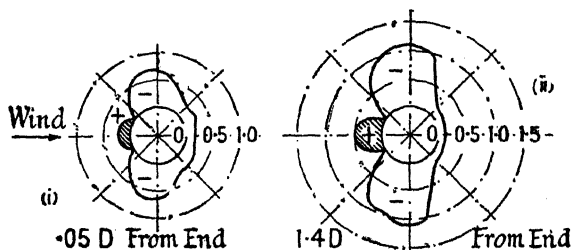

FIG. 85.

diagrams, pressures p, normal to the surface, are indicated by polar co-ordinates. The shaded areas represent positive pressure, non-shaded areas negative pressure. The pressures are expressed in the non-dimensional unit $p/\rho v^2$, the scale being indicated by the concentric circles ; v = velocity in ft./sec., ρ = the density of the air in lb. per cub. ft. $\div g = 0\cdot00237$. As may be seen from Fig. 85, the general shape of the pressure distribution was very similar from one end of the chimney to the other. The pressure on the chimney in pounds per sq. ft. of projected area may be expressed by the formula $P = \rho v^2 K_d$, where K_d is a non-dimensional drag coefficient varying with the aspect ratio L/D and the Reynolds' number ; provisionally fixed at 0·4. The great magnitude of the negative lateral pressure in (ii) Fig. 85, should be noted.

51. Effect of Position and Neighbouring Buildings.—As in the case of a flat plate, the angle of incidence of the wind makes very considerable
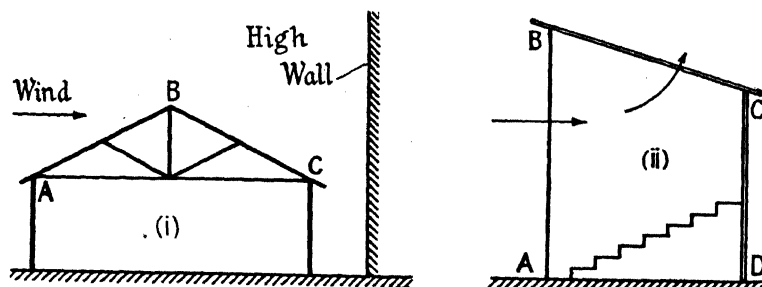

FIG. 86.

difference to the distribution of pressure on a building.[24]   Also the presence of neighbouring buildings may completely modify the effects of the wind. The information given in § 50 has been obtained from experiments on single models and only applies to isolated buildings. In a case such as (i) Fig. 86, where an open shed stands close to a higher building, there

may be considerable 'uplift' on the leeward side BC,* as also in a grandstand with an open front (ii), and the coefficients in § 50 would be quite inapplicable to such cases.

Experimental studies [27, 28] to obtain some exact information regarding the effect of adjacent buildings have been undertaken both in America and at the N.P.L. From such experiments it may be possible to lay down some general rules for guidance in design, but the problem is complicated by so many different considerations that it is unlikely that definite wind pressure values in particular circumstances can ever be obtained without special experiments.

52. Wind Pressure on Structures and Buildings. Practical Assumptions.—From the figures given in §§ 42 and 43, it would appear that in Great Britain it is sufficient on isolated structures up to 30 ft. high to assume a horizontal wind pressure of 20 lb./sq. ft. in unexposed areas, which might be increased to 25 lb./sq. ft. for structures up to 100 ft. high. Projections should be designed to resist 30 lb./sq. ft. In very exposed areas a pressure of 30 lb./sq. ft. should meet all requirements. It is customary to permit a 25 per cent. increase in the allowable stresses when the stresses due to wind are combined with the dead and live load stresses.

Buildings.—According to the L.C.C. Code of Practice, 1932, for buildings in the London area a wind pressure of 15 lb./sq. ft. should be assumed on the upper two-thirds of the vertical projection of the surface of such buildings, with an additional pressure of 10 lb./sq. ft. on all projections above the general roof level. On the sea coast, and in other very exposed positions, these pressures should be increased by 10 lb./sq. ft. A 33⅓ per cent. increase in the allowable stresses is permitted when the wind stresses are combined with the other stresses in the structure. If the height of a building is less than twice its average width, wind pressure may, in general, be neglected, provided that the building is adequately stiffened by floors and walls.

According to the Standard Specification of the American Institute of Steel Construction for structural steel for buildings, the wind pressure should depend on the conditions of exposure. If the steel frame during erection be designed to carry a wind pressure of not less than 20 lb./sq.ft., and the finished structure a wind pressure of not less than 15 lb./sq. ft., acting on the vertical projection of the exposed surfaces, when the wind stresses are combined with those due to the other loads, the permissible working stresses may be increased by 33⅓ per cent. (20,000 + 6600 = 26,600 lb./sq. in. in direct tension and compression, 1936).

For a discussion of wind pressure on buildings and methods of resisting it, see *Wind Stresses in Buildings*, R. Fleming, New York, 1930.

Bridges.—It has been customary to specify that a bridge carrying a railway should be designed to resist a horizontal wind load of 50 lb./sq. ft. on the unloaded structure, or 30 lb./sq. ft. on the bridge when carrying a train. In the case of a road bridge the latter figure is reduced to

* See some remarks in Beck's *Structural Steelwork*, London, 1920, p. 239.

20 lb./sq. ft. These figures have been very generally adopted by engineers for many years, and are embodied in the British Standard Specification, but for bridges intended for use in this country, 50 lb./sq. ft. appears to be an excessive allowance, see § 42. As the result of a study of the available data, Remfry[19] suggests that, for bridges in this country, a wind pressure on unloaded spans up to 1000 ft. in length of $40 - 0 \cdot 016L$ lb./sq. ft. should be assumed; and on similar loaded spans, of $35 - 0 \cdot 013L$ lb./sq. ft. (L = span in feet.) For Indian bridges an increase of about 40 per cent. is recommended.

When the stress due to wind is combined with the stresses due to the dead load, the live load plus impact, and the centrifugal and longitudinal forces, it is permissible to increase the allowed stress by 25 per cent., since it is unlikely that all these loads will produce their maximum effects simultaneously.

The General Specifications for Steel Railway Bridges, 1935, of the American Railway Engineering Association require that, for fixed spans less than 400 ft. in length, a moving wind load of 30 lb./sq. ft. shall be allowed for, acting on 1½ times the face area of the floor system, plus the vertical projection of all trusses, but not less than 200 lb. per lineal foot, acting at the loaded flange, and 150 lb. per lineal foot at the unloaded flange. The wind load on the train, which is supposed to act simultaneously with the above, is to be taken as a moving load of 300 lb. per lineal foot on one track, applied 8 ft. above the base of the rail. Alternatively, the unloaded bridge must carry a wind pressure of 50 lb./ sq. ft. An increase of 25 per cent. ($18,000 + 4500 = 22,500$ lb./sq. in. in direct tension) in the allowable stresses is permitted when the wind load stress is combined with that due to the dead load + live load + impact + centrifugal force + longitudinal forces.

If the bridge is not required to conform to the British Standard Specification, it would appear that the wind pressures suggested by Remfry and given above might be provisionally adopted as best representing the information available; except that most engineers would consider that it is not necessary to assume more than 30 lb./sq. ft. on a loaded span in normal circumstances in Great Britain.

Wind pressure on a bridge has three main effects :
(i) It tends to overturn bodily the bridge (with or without the train).
(ii) The wind pressure on the bridge proper forms a lateral load on the structure. That on the train forms a lateral rolling load on the structure.
(iii) The wind pressure on the train will increase the pressure on the leeward rail, and therefore increase the vertical load on the leeward girder of the bridge.

The factor of safety against overturning should not be less than $1 \cdot 5$ under the worst conditions likely to occur. As an example of the method of calculation, consider the deck bridge shown diagrammatically in Fig. 87.

Let W_1 be the weight of the bridge proper, F_1 the total wind pressure on it; let W_2 be the weight of the train and F_2 the wind pressure on it when it covers the bridge. Then the overturning moment is $F_1 r_1 + F_2 r_2$, and the righting moment is $(W_1 + W_2)B/2$. The factor of safety is

$$\eta = \frac{(W_1 + W_2)B/2}{F_1 r_1 + F_2 r_2} > 1 \cdot 5$$

or, considering the empty bridge,

$$\eta = \frac{W_1 B/2}{F_1 r_1} > 1 \cdot 5$$

Both these conditions must be satisfied.

In calculating the exposed area of the structure itself, the area of all double surfaces must be taken into account according to the principles discussed in § 48. A worked example will be found in § 196. The wind load on the bridge must be assumed to act at the centre of area of the exposed surfaces. For the purpose of calculation the area of a railway train can be taken at 10 sq. ft. per lineal foot, and the pressure may be assumed to act at a point 7 ft. 6 in. above the top of the rail. The vehicles should be supposed empty, and of the lightest type likely to cross the bridge.

Fig. 87.

The lateral wind load on the bridge must be carried to the abutments by horizontal wind girders provided in the plane of the upper and/or lower flanges for the purpose, see § 191. The flanges of the main girders are arranged to form the flanges of the wind girders, and lateral bracing is provided to form the webs. The wind pressure on the train is evidently a lateral rolling load on the bridge, and the wind girder in the plane of the loaded flanges must be designed to carry this rolling load. Suitable portal and sway bracing is also necessary to prevent distortion, § 191.

The tendency to concentrate load on the leeward rails and girder is one of the most important effects of the wind pressure on a bridge, though it is sometimes neglected in design. It will be apparent from Fig. 87, if r_2' be the height of the point of application of F_2 above the rails, that the effect of the moment of the wind load $F_2 r_2'$ will be to increase the load on the leeward rail and decrease it on the windward rail by an amount $R_1'' = R_2''$, such that $R_2'' G = F_2 r_2'$. Hence, due to wind, the load on the leeward rail is increased from $W_2/2$ to $W_2/2 + F_2 r_2'/G$. In a similar way the load on the leeward girder is increased by an amount R_2', Fig. 87,
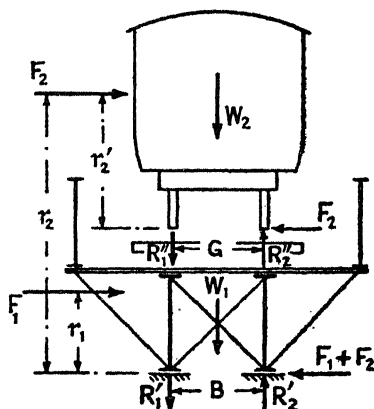
such that $R_2'B = F_1r_1 + F_2r_2$, and the total load on the leeward girder is increased from $(W_1 + W_2)/2$ to

$$\left(\frac{W_1 + W_2}{2}\right) + \frac{(F_1r_1 + F_2r_2)}{B}$$

In certain cases these increases may produce the largest part of the increase in stress due to wind.

BIBLIOGRAPHY

Experiments on Wind Pressure.

HUTTON. *Math. and Phil. Tracts*, vol. iii, London, 1812.

DUCHEMIN. *Mémorial de l'Artillerie*, t. v, Paris, 1842, p. 275.

RAYLEIGH. *Scientific Papers*, vol. i, Cambridge, 1902, p. 291.

DINES. On Wind Pressure upon an Inclined Surface. *Proc. Roy. Soc.*, A, vol. xlviii, 1890, p. 233.

WESTHOFEN. The Forth Bridge. *Engg.*, Feb. 28, 1890, p. 221.

LANGLEY. Experiments in Aerodynamics. *Smithsonian Contributions to Knowledge*, 801. Washington, 1891.

KERNOT. Wind Pressure. *Rpt. Aust. Assoc. Adv. Sci.*, vol. v, 1893, p. 573 ; vol. vi, 1895, p. 741 ; *Proc. Inst. C.E.*, vol. clxxi, 1907–8, p. 218.

IRMINGER. Experiments on Wind Pressure. *Ingeniøren*, 1894, p. 101 : see *Proc. Inst. C.E.*, vol. cxviii, 1893–4, p. 468 : also *Engg.*, Dec. 27, 1895, p. 787 : and NIELSEN, *Engg.*, Oct. 9, 1903, p. 508.

9. STANTON. On the Resistance of Plane Surfaces in a Uniform Current of Air. *Proc. Inst. C.E.*, vol. clvi, 1903–4, p. 78.

10. —— Experiments on Wind-Pressure. *Proc. Inst. C.E.*, vol. clxxi, 1907–8, p. 175.

11. —— The Air-Resistance of Plates. *Engg.*, May 8, 1908, p. 605.

12. —— Report on the Measurement of the Pressure of the Wind on Structures. *Proc. Inst. C.E.*, vol. 219, 1924–5, p. 125.

13. EIFFEL. *Recherches expérimentales sur la résistance de l'air*. Paris, 1907.

14. —— *Nouvelles recherches sur la résistance de l'air et l'aviation*. Paris, 2nd ed., 1920.

15. HUNTER. The Structural Design of Engineering Factories. *Trans. Jun. Inst. Engrs.*, vol. xvii, 1906–7, p. 197 : (Later Forth Bridge exps.).

16. JOHNS. Air-Resistance to Plane Surfaces. *Engg.*, Mar. 10, 1911, p. 299. (Values for the const. 0·0032.)

17. BOARDMAN. Wind Pressure against Inclined Roofs. *Jour. West. Soc. Eng.*, vol. xvii, 1912, p. 331.

18. SMITH, A. Wind Pressure on Buildings. *Jour. West. Soc. Eng.*, vol. xvii, 1912, p. 986 : vol. xix, 1914, p. 369.

19. REMFRY. Wind-Pressures, and Stresses caused by the Wind on Bridges. *Proc. Inst. C.E.*, vol. ccxvi, 1922–3, p. 3. See also WIDDOP, *Proc. N.Z. Soc. C.E.*, vol. viii, 1922, p. 86.

20. TOMLINSON. Modern Ideas on Wind Force and Roof Truss Design, *Trans. Inst. Engrs. Aust.*, vol. v, 1924, p. 3. (Approx. Formulae.)

21. DRYDEN AND HILL. Wind Pressures on Structures. *U.S. Bur. Stnds.*, Sci. Paper No. 523, 1926 : see *Engg.*, Aug. 27, 1926, p. 268.

22. —— Wind Pressure on a Model of a Mill Building., *U.S. Bur. Stnds.*, Res. Pap., No. 301, 1931 : *B. of S. Jour. Res.*, vol. x, Apl. 1933.

23. GÖTTINGEN EXPS. *Jahrbuch Deu. Gesellschaft f. Bauingenieurwesen.*, 1927, p. 87 : 1928, p. 160.

24. IRMINGER AND NØKKENTVED. Wind Pressure on Buildings. Exp. Research, 1st Ser., *Ingeniorvidenskabelige Skrifter*, A, No. 23, 1930 : 2nd Ser., A, No. 42, 1936.

25. RICHARDSON AND MILLER. Pressure of an Air Stream on Model Buildings, *Jour. Inst. Engs. Aust.*, vol. iv, 1932, p. 277.

26. SYLVESTER. An Investigation of Pressure and Vacua produced on Structures by Wind. *Rensselœr Poly. Inst.*, New York, Eng. and Sci. Ser. No. 31 ; see *Engg.*, July 1, 1932, p. 4.

27. BAILEY. Wind Pressure on Buildings. *Selec. Eng. Pap. I.C.E.*, No. 139, 1933.

28. HARRIS. Influence of Neighboring Structures on the Wind Pressure on Tall Buildings. *U.S. Bur. Stnds. Jour. Research*, Jan. 1934, Pap. No. 637 ; see *Engg.*, June 29, 1934, p. 735.

29. FLACHSBART U. WINTER. Modellversuche über die Belastung von Gitterfachwerken durch Windkräfte, (i) Einzelne ebene Gitterträger. *Die Bautechnic*, 12 (*Stahlbau*, 7) 1934, p. 65 : (ii) Räumliche Gitterfachwerke, *Die Bautechnic*, 13 (*Stahlbau*, 8) 1935, p. 57 ; see also *Eng. News-Rcd.*, Oct. 11, 1934, p. 456.

Wind Pressure on Tall Buildings.

30. JONSON. The Theory of Frameworks with Rectangular Panels and its Application to Buildings which have to Resist Wind. *Trans. Amer. Soc. C.E.*, vol. lv, 1905, p. 413.

31. WILSON. Wind Bracing with Knee Braces or Gusset Plates. *Eng. Record*, Sept. 5, 1908, p. 272.

32. SMITH, A. Wind Stresses in the Frames of Office Buildings. *Jour. West. Soc. Eng.*, vol. xx, 1915, p. 341.

33. WILSON AND MANEY. Wind Stresses in the Steel Frames of Office Buildings. *Univ. Illinois : Eng. Exp. Stn.*, Bull. No. 80, 1915.

34. FLEMING. Wind Stresses in Many-Storied Buildings. *Engg.*, May 25, 1928, p. 625.

35. —— *Wind Stresses in Buildings*, New York, 1930.

36. ROSS AND MORRIS. The Design of Tall Building Frames to Resist Wind. *Proc. Amer. Soc. C.E.*, May 1928, p. 1395 ; also Bull. No. 48, *Eng. Exp. Stn. Ohio State Univ.*, 1929.

37. SPURR. *Wing Bracing.* New York, 1930 : see also LARGE, CARPENTER AND MORRIS, Bull. No. 93, *Eng. Exp. Stn. Ohio State Univ.*, 1936.

38. SUTHERLAND AND BOWMAN. *An Introduction to Structural Theory and Design.* New York, 1930.

39. GREGOR. *Der praktische Stahlhochbau*, Berlin, 1931, Bd. II, Teil 2.

40. AMER. SOC. C.E. Committee on Wind Bracing in Steel Buildings. Progress Rpts. I, Jan. 1931, II, *Proc.* Feb. 1932 ; III, *Proc.* Dec. 1933 ; V, *Proc.* Mar. 1936 (Rounded and Sloping Roofs).

41. GOLDBERG. Wind Stresses by Slope-Deflection and Converging Approximations. *Trans. Amer. Soc. C.E.*, vol. 99, 1934, p. 962.

Wind Pressure on Tall Chimneys.

42. (OMORI). Wind Pressure on Tall Chimneys. *Engg.*, Sept. 27, 1918, p. 334 (vibrations) ; see also PAGON, *Eng. News-Rcd.*, July 12, 1934, p. 41.

43. DRYDEN AND HILL. Wind Pressure on Circular Cylinders and Chimneys. Res. Pap. No. 221. *U.S. Bur. Stnds. Jour. Res.*, vol. v, Sept. 1930, p. 653 ; see also *Engg.*, May 1, 1931, p. 565. For similar tests on a Model of a Gas-holder see BAUMHAUER, *Eng. Ab. I.C.E.*, 1920, No. 4 : 25.

44. FLEMING. Wind Pressure on Chimneys. *Engg.*, Aug. 3, 1934, p. 123.

QUESTIONS ON CHAPTER III

1. Discuss the effect of wind pressure on structures, and state what assumptions you would make as to wind pressure on : (a) a double track lattice-girder railway bridge 50 ft. deep, and 350 ft. span ; (b) a large open shed 600 ft. long, 100 ft. high, and 150 ft. span. (U.L.)

2. Calculate by Hutton's formula, or by another formula commonly used, the normal pressure per square foot on a plate sloping at an angle of 25° to the horizontal, if the wind is blowing at 50 miles per hour. State briefly the results of some recent experiments on the distribution and intensity of the pressure of wind on roofs. (U.L.)

Ans. 4·5 lb./sq. ft. (Hutton) ; 5·7 lb./sq. ft. (Duchemin).

3. Find the bending moment at the foot of a cylindrical chimney 18 ft. in diameter, 200 ft. high, on the assumption that the intensity of the wind pressure varies as the square root of the height above the ground. At a height of 100 ft. it is 24 lb./sq. ft. on a flat surface. The coefficient of wind resistance for a cylinder is 0·6. (U.L.)

Ans. 586,400 ft.-lb.

4. A chimney 120 ft. high, 12 ft. square at the base and 9 ft. square at the top, is subjected to a wind pressure of 30 lb/sq. ft. Find the maximum wind load on the chimney, and the point at which it acts.

Ans. 34,000 lb. (diagonally 99 per cent. of this) : 57·14 ft. up.

5. The area of a lattice girder is made up as follows : Bottom flange 200 sq. ft., top flange 160 sq. ft., verticals 150 sq. ft., diagonals 230 sq. ft. Take the value of C, § 47, as 1·3, and find the total wind load on the girder under a wind pressure of 30 lb./sq. ft.

Ans. 12·9 tons.

6. Two such girders (Q. No. 5), placed 0·85D apart, connected together by a plate deck, form a bridge. The side area of the floor system proper is 430 sq. ft. What is the total wind load on the empty bridge ?

Ans. Assume the pressure on the pair is 1·1 times that on a single girder, § 48 ; total wind load = 12·9 × 1·1 + 5·8 = 20·0 tons.

CHAPTER IV

WORKING STRESSES—IMPACT

53. Working Stresses. Suitable Values.—The choice of suitable working stresses for given conditions, involving as it does the real relationship between the calculated stresses and the material properties, is not a simple problem ; many difficult considerations come into question.

54. Calculated Stresses. Their Conventional Character.—In the first place it must be remembered that anything like a true determination of the stresses in a structure from the nature of the case, is, practically speaking, impossible. All ordinary theory assumes that the structure is perfectly elastic, and that it is initially unstrained. It assumes that the joints (usually riveted) are frictionless pins ; or, if an attempt be made to allow for secondary stresses, that the joints are perfectly rigid. Indeterminate stresses occur of which no account whatsoever is taken in ordinary calculations. Now a perfectly elastic structure is a mathematical abstraction. Nearly every member of a structure has to be straightened cold, which means that the yield point is exceeded in many places, and that initial stresses are set up in every member. The shop processes, punching, drilling, riveting, welding, all induce initial stresses, often of considerable magnitude. Any thoughtful person who has watched a braced structure being drifted up tight, and then riveted up, must come away with very qualified views as to the possibility of determining accurately the real stresses in structures from theoretical considerations. The joints are never frictionless pins, which means that deformation stresses, § 114, often of considerable magnitude, will be induced in the structure. These, in certain cases, may be calculated, on the assumption that the joints are rigid, which riveted joints never are. Even in the simplest of members the stresses are of a complex nature, as a glance at Fig. 320, Vol. I, which represents the stress distribution in a tension specimen, will show.

In most instances it is not possible accurately to define even the load conditions, and in many cases the stresses are found from conventional loadings on conventional assumptions. Thus the bending stresses on a ship in a seaway are estimated by assuming the ship to be poised on a wave of conventional length and height. At sea the ship will meet with waves of all lengths and heights, and it is unlikely that she will ever be poised on one, as is assumed. The floor and wind loads assumed to act on a tall building are merely conventions, as are the methods employed in finding the stresses. The ordinary methods of calculating the primary stresses in a bridge are likewise quite conventional.

55. The Quality of the Material. Conventional Tests.—If the factors which represent the quality of the material be carefully considered, it will be found that they, too, are of a conventional nature. The quality factor most easily and most frequently determined is the ultimate tensile strength of the material, and engineers quite rightly insist that the material must be perfectly satisfactory in this important particular. Yet the load intensity implied by the expression ' ultimate tensile strength ' has no physical existence. It is determined by measuring the area before the experiment, and the maximum load three-quarters the way through, when the area is considerably reduced, and dividing the one by the other. It is a conventional ' stress ' implying a certain quality of material.*

Nor can the proportional limit or the yield point be regarded as definite standards of quality. The proportional limit is one of the most variable of all the properties of materials. Its position depends very largely on the previous history of the material. Overstraining in one direction may reduce it to nearly zero in the other, § 241, Vol. I, and it is not uncommon to find perfectly satisfactory material in which the proportional limit is very low. It is probable that the primitive proportional limit is exceeded at times during the life of every structure, at least in places, without in the least endangering the existence of the structure.

The yield point, too, depends on the previous history of the material, and by overstraining and recovery it can be raised up to the maximum load point, § 241, Vol. I. Not only so, but the upper yield point has been shown to vary in position with the shape of the specimen and other test conditions, § 216, Vol. I. The position of the yield point in material which has been subjected to shop processes, cold straightening and the like, is very variable.

The following figures are taken from the Progress Report of the

Average Stress in 1000 lb./sq. in.			
	Highest.	Lowest.	
Tension.			
Proportional limit	39·7 *	25·1 †	* 8″ × 32 lb. I-Beam.
Yield point	41·8 *	31·7 †	† 10″ × 20 lb. Channel
Ultimate strength	64·2 *	52·2 †	†† 10″ × 15 lb. Channel.
Compression.			‡ 10″ × ⅜″. Plate.
Proportional limit	37·6 ‡	22·5 ††	
Yield point	40·9 *	30·9 †	

* Most test figures are equally conventional. Thus, in the rotating bar fatigue test, the ' fatigue limit ' is a calculated bending stress on the original area, whereas the mischief is being done by an intense stress concentration at the bottom of a crack. The ball hardness test is also quite conventional. It is singular that the conventional test figures from both these experiments bear a constant ratio to the equally conventional ultimate tensile strength. Again, one of the early objections taken to the notched bar test was to its conventional character.

Special Committee on Steel Column Research of the American Society of Civil Engineers (*Proc.*, Feb. 1929, p. 412) and give the results of tests on 204 tension specimens and 182 compression specimens. They well illustrate the variable nature of the material properties in commercial rolled steel members [see also p. 359].

56. Overstraining and Recovery.—The mutability of the proportional limit and the accompanying loss of elasticity in ordinary steel, referred to above, would be a serious matter were it not for the wonderful property of materials called recovery after overstrain which, as Muir proved, § 243, Vol. I, takes place not only when the load which overstresses the member has been removed, but also while the load is still acting on the bar ; it is not too much to say that without this property, steel structures, as at present constructed, could not exist. When a structure, for example a bridge, is first erected, the material everywhere will be in a state of initial stress set up during manufacture. As it deflects under its own weight, and still more when the test load is applied, these stresses will be augmented by both the primary and secondary stresses which occur. It is very probable that the proportional limit in many of the members will be low, and will at once be exceeded. Locally, where stress concentrations occur, it is more than likely that the yield point will be overstepped. If passing the proportional limit and yield point meant immediate failure of the member, the structure would at once collapse. Fortunately, due to the ductility of the material, the effect of such high stress concentrations is mitigated. The metal yields slightly and allows the stress to redistribute itself.* Temporarily, the material which has thus yielded has lost its elasticity, but it becomes strain-hardened, and in time recovers its elasticity ; the yield point rises to at least the point to which the overloaded material was stressed, see § 241, Vol. I. In riveted structures there is no doubt that the secondary stresses are relieved also by the ' give ' of the riveted joints.

The material thus overstrained has lost some of its ductility, so that the process of overstraining and recovery cannot be repeated an indefinite number of times ; but having once been overstrained and reached a state of comparative ease, further applications of loads of the same magnitude as before would not produce stresses above the yield point, raised as the latter would be by the previous overstressing.

57. The Factor of Safety.—The method commonly adopted of overcoming the difficulties which the choice of a suitable working stress involve is to assume a sufficiently large factor of safety. Questions then arise as to what is intended to be covered by the factor of safety, and to what material property the ratio in question should rightly be applied.

The factor of safety must cover :

(i) Defects in the material.
(ii) Initial stresses due to cold straightening, punching, riveting, and shop processes generally. Cooling stresses in castings.

* For a study by Haigh of the effect of ductility in mollifying the high stress concentration at the edges of a hole, see § 67 at end.

(iii) Faulty workmanship.

(iv) Erection stresses.

(v) Deformation and other secondary and indeterminate stresses.

(vi) Stresses due to secondary flexure, buckling, particularly in compression members.

(vii) Stresses due to temperature variations not otherwise allowed for.

(viii) Loss of area due to corrosion.

(i) Mild steel is now so reliable that defective material is exceptional ; in cast iron and timber flaws are always to be feared. Welded material is sometimes faulty.

(ii) High initial stresses may be set up during the severe treatment which the material gets during the shop processes. Sir Benjamin Baker suggests* that due to cold rolling, the real stress in a plate girder flange may be twice the nominal stress. Attention has repeatedly been called to the effect of cold straightening in bringing about the early collapse of struts.† The effects of cooling stresses in castings are well known.

(iii) Even with the most accurate and careful workmanship it is hardly possible to ensure that the lengths of members are absolutely exact, or that the rivet holes are in perfect alignment. When the workmanship is not first-class the errors may be considerable. Large initial stresses may be the result. An error of 1/100th inch in the length of a tie bar 10 feet long would result in an initial stress of over 1 ton/sq. in. when the member is forced into place, unless relief occurs by the distortion and stressing of some other part. Not only so, but due to poor bearing, and eccentricity of loading resulting from faulty workmanship, the stresses produced by the applied loads may be much increased. It is not unknown in old bridge trusses, where the tension members are formed of two parallel flat bars, to find one bar carrying all the load, the other being slightly buckled !

(iv) Severe stresses may be induced in a structure during erection resulting from inaccurate setting out of columns, inadequate temporary supports, settlement of foundations and similar causes.

(v) Deformation stresses may be due to stiff joints in framed structures § 114, the bending produced by the cross-girder loading in a bridge, § 112, and other similar causes. Theoretically, these stresses may, in particular cases, reach high magnitudes. In the case investigated in ¶ 9, § 118, the deformation stress was 75 per cent. of the primary stress, and other estimations have been made in which the deformation stresses in the webs of bridge trusses are of this order.‡ There is no doubt that these high theoretical values are much reduced by the give of the riveted joints, and redistribution due to plastic yield (see also §§ 56 and 67), for in properly designed frames, no serious effect due to secondary stress

* *Proc. Inst. C.E.*, vol. cxli, p. 83.

† Howard, *Proc. Amer. Soc. Test. Mat.*, vol. viii, 1908, p. 336.

‡ Grimm, *Secondary Stresses in Bridge Trusses.* New York, 1908.

appears to occur in practice.* Lurching, § 62, may set up torsional strains in a bridge, which, with other not easily calculated stresses, must be covered by the factor of safety.

.(vi) Secondary flexure, the buckling of plates between the rivets, the buckling of outstanding plates, web buckling, and similar effects, considerably increase the stresses in compression members. Rusting between two plates in contact forces the plates apart and results in local stresses of a like nature.

(vii) In statically indeterminate structures of any considerable magnitude an estimation of the stresses due to changes in temperature is usually made, but in many structures no provision is made for expansion, and the material must carry the temperature stresses. A commonly occurring example is the ordinary steel frame building, in which expansion in the floor beams can only occur by bending, and so stressing, the columns. Expansion joints in bridges are often unsatisfactory, in which case the structure has to carry the temperature stresses. A 12° F. variation in temperature would produce a stress of 1 ton/sq. in. if the member is prevented from expanding.

(viii) Steel structures in exposed positions are subject to continual rusting, in spite of their protective coating of paint. There is therefore a progressive loss of area and increase in stress in the structure due to corrosion. In special cases the thickness of the material theoretically necessary is increased on this account.

An exact determination of the stresses enumerated above is not possible. To make provision for their occurrence a sufficiently high factor of safety must be used. The value assumed should depend on the accuracy with which the true primary stresses can be determined, and to what extent the secondary effects are allowed for directly. It does not follow that in given circumstances the same factor of safety would be applicable to different materials. Attempts are sometimes made to estimate the probable magnitudes of all the stresses in a member, including those which occur under the heads (i) to (viii) above ; and it is argued that if the maximum stress intensity, thus determined, does not exceed the proportional limit of the material, the structure will be safe. From what has gone before it will be evident that, at best, the proceeding is the comparison of a questionable estimate of the maximum stress with a variable material property for a standard. Nor is the matter greatly improved if the primitive yield point be substituted for the primitive proportional limit ; the yield point is also a variable material property. Fortunately, it can only be raised, not lowered, by overstrain, but it is not a fixed standard of comparison ; nor, in the case of repetition of stress, does it bear a definite relationship to the limiting range of stress. Also the question arises as to whether the upper or lower yield point, § 216, Vol. I, is the true criterion, and what it is to be

---

* In large modern bridges, initial distortion of the main girders is sometimes resorted to in order to minimise distortion stresses when under load, see *Jour. Inst. C.E.*, Feb. 1937, p. 91.

in the case of hard steels and non-ferrous metals which exhibit no yield point, Figs. 260, 262, Vol. I. The true criterion in the case of combined stresses is still a disputed point, Chap. XVI, Vol. I.

58. Working Stresses. What should Determine them ?—What then is the real basis which should determine the working stress in a material ? The answer is *successful practice.*

The real criterion on which working stresses are based is something like the following : Experience has shown that if, in ordinary structures, a mild steel with an ultimate tensile strength of from 28 to 33 tons/sq. in. and an elongation of not less than 20 per cent. in 8 inches be used, and the

Material.	Units : tons/sq. in.			Working Stress.					
	Ultimate Strength.	Yield Point.	Minimum Elongation, %.	Direct Tension, net area.	Direct Compression gross area.	Direct Shear, Web Plates.	In Rivets. Shear Stress.	In Rivets. Bearing Pressure.	
Structural mild steel B.S. No. 15, 'A' steel	28–33	14–18	20 in 8″	8 *9	6·8 *7·65	5·0 *5·5			
Structural rivet steel B.S. No. 15, 'A' steel	25–30		25 in 8 diars.				6 *6	12 *15	
Admiralty 'D' steel (high elastic limit) 0·33% C; 1·1 — 1·4% Mn	37–43	(17)†	17 in 8″	10·5	9·0	6·5			B
Structural nickel steel 0·3% C; 3% Ni	38–44	22–25	20 in 8″	12·0	10·2	7·5			B
Nickel rivet steel .	31–35	20 min.	25				8	16	B
Silicon steel ‡ 0·38% C.; 0·2% Si; 0·9% Mn	35–42	20–22	715 Ult.	10·5	9·0	6·5			B
Chromador steel 0·22% C; 0·9% Cr; 0·8% Mn; 0·3% Cu .	37–43	§ 22–26	17 in 8″	‖11·5 12·5	9·8 10·6	7·0 7·5			A B
Chromador rivet steel . .	30–36						‖7·5 8	15 16	A B
Cast iron ; breaking load 28 cwt. on 36-in. span, deflection ⅓ in. .				2·5	10·0				

* B.S. No. 153, 1933, for Girder Bridges.
† Minimum proportional limit.
‡ As used for Sydney Harbour Bridge.
§ Minimum = 23 tons/sq. in. on material ½-inch in thickness.
‖ Makers suggest a 50% increase in stresses allowed for mild steel.
A = Ordinary structural work.   B = First-class bridge work.

stresses (so-called) in the members be determined by certain simple well-known methods and rules, provided that the areas and sizes be so proportioned that these stresses do not exceed certain limits (e.g. 8 tons/sq. in. in simple uniform tension), the structure will be satisfactory in practice.

The question then arises as to what should be the standard of reference in altered circumstances, or for new or different materials. In altered circumstances the engineer has to rely on his judgment supplemented by special tests. The true standard of reference for a new material should depend on the predominating stress conditions under which it will work. Where constant reversal of stress occurs, the fatigue limit will be the determining factor. In other cases the ultimate tensile strength should decide. In ductile materials not likely to fail by fatigue, either the ultimate tensile strength or the lower yield point may be used. Professor Haigh, who has made a special study of this question, considers that the latter may be used with confidence. Comparing the new Chromador steel with a ductile mild steel,* he shows that their properties are very similar, and that the ultimate strength, lower yield point, and endurance limits of the two steels all bear the same ratio 1·45–1·5 to 1, which may be regarded as the ratio of their strengths; but the mild steel has the greater elongation.

In work-hardened material, where the yield point is artificially raised in a higher ratio than the ultimate tensile strength, implying a reduced capacity for further strain hardening, the ratio of the working stresses should not be raised in direct proportion to the yield points.

59. Normal Working Stresses.—In normal circumstances, the working stresses given in the Table on p. 134 are commonly adopted. ·

Steel castings should comply with B.S.S. No. 30 for Steel Castings for Marine Purposes, Grade B ; stresses should not exceed those specified for structural mild steel.

For working stresses in *welds* see § 145 ; in *masonry* see .§ 356 ; in *concrete* see § 374 ; and in *reinforced-concrete* see § 309.

IMPACT

60. Impact in Bridges.—It has long been recognised that some allowance must be made for the ' liveness ' of a load travelling over a bridge. One of the earliest methods of making such allowance was to double the live load and add it to the dead load, treating the sum as a static load on the bridge or member. This is equivalent to regarding the live load as a suddenly applied load, and leads to an unnecessarily large area for the members, for in no ordinary bridge is the load thus applied.

Efforts to introduce a more exact procedure have followed two lines of thought. In the first, an attempt was made to allow for the variation in the stress in the members as the train travelled across by a *range of stress* formula, based on Wöhler's or other repetition of stress formulae.

* *Engineering*, December 28, 1934, p. 698.

In the second, the effects of the liveness of the load is expressed as an addition to the live load ; this addition is referred to as the effect of *impact*.

A full discussion on the subject of range of stress formulae will be found in Fidler.[31]. The work of Stone,[32] who originated a well-known formula of this type, may also be consulted. From the considerations set forth in § 66, it may be concluded that, provided impact be properly taken into account, with the working stresses adopted in modern bridge-work, no question of fatigue will arise.

61. Impact Formulae.—The method of providing for impact in bridges, commonly adopted, is to use an impact formula. This expresses the fractional increment, called the *impact factor*, by which the live load stress must be increased in order to take account of the 'liveness' of the load. The original of such formulae is the *Pencoyd formula*

$$i = \frac{300}{300 + L} \quad . \quad . \quad . \quad . \quad . \quad (1)$$

where $i =$ the impact factor,

and $L =$ the length in feet of that portion of the span covered by the train when the maximum stress due to the travelling load occurs in the member under consideration.

In the case of cross girders, L is usually taken as twice their distance apart ; in the case of rail bearers L is taken as their effective span. Eq. (1) is plotted in Fig. 93.

The Pencoyd formula has been replaced by a number of modifications based on stress or deflection measurements on actual bridges. The method of determination is as follows :

The stress f_{av} in a particular member is measured by means of a recording extensometer while a train is just crawling over the bridge. The
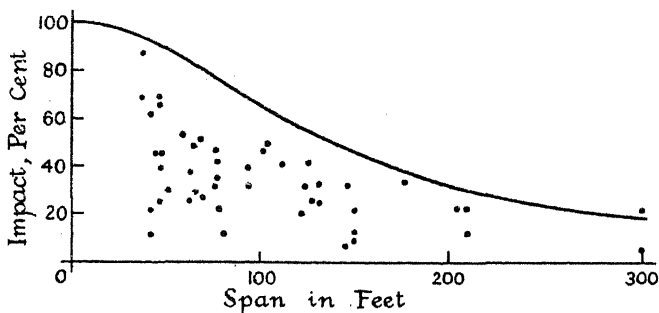

FIG. 88.

train is then run over the bridge at speed, and the maximum stress, f_{max}, is similarly recorded, (i) Fig. 96. The ratio $(f_{max} - f_{av})/f_{av}$ is the fractional increment in stress due to impact, i.e. the impact factor. In other experiments the impact factor is calculated from deflectometer readings obtained from similar experiments.

The experiments are repeated for a number of bridges of differing

spans, and at different speeds. The results are plotted as shown in Fig. 88. The enveloping curve represents the maximum increment in stress likely as the result of impact. This figure embodies the results of some deflection experiments reported by a special Committee of the American Railway Engineering Association in 1910.[6] Many other experiments were made, including a large number made with extensometers. Professor Turneaure has suggested the following formula to represent the collected results :

$$i = \frac{30,000}{30,000 + L^2} \qquad \cdot \qquad \cdot \qquad \cdot \qquad \cdot \quad (2)$$

the symbols having the same significance as in eq. (1). This formula has been replaced in the 1935 A.R.E.A. Standard Specification for Railway Bridges by the following :

$$\begin{array}{l} L < 100 \text{ ft.} \quad i = 1 - 0 \cdot 006\ L + 1/S\ ;\quad \text{max.} = 1.\} \\ L > 100 \text{ ft.} \quad i = 0 \cdot 1 + 18/(L - 40) + 1/S. \end{array} \quad (2A)$$

where L = span in ft. of main girders, cross girders, and rail bearers.

S = spacing in ft. of main girders and rail bearers, and span of cross girders. 1/S is the allowance for lurching.

Much work has been done, and many experiments have been made, by the Indian Railway Bridge Engineers to determine a suitable allowance for impact. Their 1925 [14] Report gives the following expression

$$i = \frac{65}{45 + L} \qquad \cdot \qquad \cdot \qquad \cdot \qquad \cdot \quad (3)$$

for the impact factor to be used for the purposes of design.

The Ministry of Transport formula,[9] which has been adopted as the British Standard for Girder Bridges (No. 153, Pt. 3, 1933), is as follows :

$$i = \frac{120}{90 + \dfrac{n+1}{2}\ L} \qquad \cdot \qquad \cdot \qquad \cdot \quad (4)$$

with a maximum of $1 \cdot 15$; n = the number of tracks.

For comparison, eqs. (1), (2), (3), and (4), have been plotted in Fig. 93.

In all the above formulae, i is the impact factor for steam locomotives, and except in eq. (2A), L is the loaded length as in the Pencoyd formula.

62. The Causes of Impact.—The factors causing impact stresses in railway bridges are enumerated by the American Committee (A.R.E.A.) [6] as follows : (1) Unbalanced forces from the locomotive driving wheels ; (2) rough and uneven track ; (3) flat or irregular wheels ; (4) eccentric wheels ; (5) rapidity of application of load ; (6) deflection of cross girders and rail bearers, giving rise to variations in the action of the vertical load ; to which should be added, (7) lurching of the locomotive, causing periodical shifting of the weight from one wheel to another. Of all these factors, the action of the unbalanced driving wheels was shown conclusively by the tests to be the most influential in causing impact ;

at least 80 per cent. of the increase in stress or deflection was found to be due to this cause. When properly balanced compound and electric locomotives were used, the impact was found to be small. In most tests, ordinary heavy two-cylinder locomotives were employed ; the crawl speed was 8–10 m.p.h., the maximum speeds ranged from 60–70 m.p.h. The experiments were made on plate girder bridges ranging from 25 to 100 feet span, and on braced girder bridges ranging from 60 to 500 feet span. For spans above 75 feet, the impact stresses increased with the speed up to a certain limit and then diminished. In spans of 250 to 300 feet in length, the maximum impact occurred at speeds of 25 to 30 m.p.h., speeds of 50 to 60 m.p.h. giving much lower results. It was shown that the maximum impact occurred when the revolutions per second of the driving wheels coincided closely with the natural rate of vibration of the loaded structure. There is, therefore, a critical speed for every bridge, which depends on its flexibility, the dead and live loads, and the diameter of the driving wheels of the locomotive. In short spans the critical speed is so high that it was not reached in the experiments ; in long spans it is, in many cases, below the ordinary running speeds. Experiments with deflectometers showed that the deflection of the bridge could be divided into two parts : a general deflection which was, practically speaking, unaffected, whatever the speed ; and oscillations about this general deflection curve due to the periodic forces from the locomotive driving wheels. These observations have been both confirmed and extended by the work of the British Bridge Stress Committee [16] and the Indian Bridge Standards Committee.[14]

Except in short spans, the major cause of impact, therefore, is the *hammer-blow,** that is to say, the unbalanced vertical force from the locomotive balance weights. This up-and-down force is periodic—pulsating—and should its period happen to synchronise with the natural period of vibration of the partly loaded bridge, large deflections and stresses are likely to be set up due to resonance. The number of pulses per second of the periodic force is evidently equal to the revs. per sec. of the locomotive driving wheels ; which, with a diameter of 6 ft. 6 in., at a speed of 70 m.p.h., make almost exactly 5 revs. per sec.

The approximate natural period of vibration of a bridge, loaded or unloaded, can be found by the methods of §§ 155–157, Vol. I. For the unloaded bridge, eq. (9), § 157, Vol. I can be used

$$\tau = \frac{1}{n} = \frac{2L^2}{\pi} \bigg/ \sqrt{\frac{w}{EIg}}$$

where w is the weight of the bridge per unit of length (work in inches and tons, and take g in inches per sec. per sec.). The natural frequency of the bridge in any condition can be found experimentally by setting up oscillations therein, and observing the frequency at which resonance occurs.

---

* Mr. Wragge (*Proc. Inst. C.E.*, vol. cxli, 1899–1900, p. 100) reports the case of a runaway locomotive down a long incline, which broke the rails in a number of places. The distance apart of the breakages corresponded exactly with the circumference of the driving wheels ; these carried heavy balance weights.

The apparatus used to incite the oscillations consists of two eccentrically loaded disks, so mounted that their speeds of rotation, sense of rotation, and eccentricity of loading are separately adjustable. These disks are driven by an electric motor, and the whole apparatus is carried on a trolley, which can be clamped down. Periodic forces of known magnitude, direction, and frequency can thus be applied to the bridge. The behaviour of the structure under these forces can be ascertained by observing the deflections or the stresses produced. Unless resonance occurs, the deflections remain small, but during the resonance range the amplitude of oscillation attains high values. The natural frequency can most easily be found from observations on the energy supplied to the motor.[20] The oscillation-energy in a vibrating system increases as the square of the amplitude, and if the square of the amplitude be plotted on a frequency base line, the curve would rise very rapidly in the resonance range. It therefore follows that a curve representing the energy output of the motor would rise very rapidly when resonance occurs, and as will be seen in Fig. 89, which represents actual readings on a bridge of 71 m. (233 ft.) span, this is found to be the case. Wattmeter readings of the motor input serve therefore to determine the natural frequency.
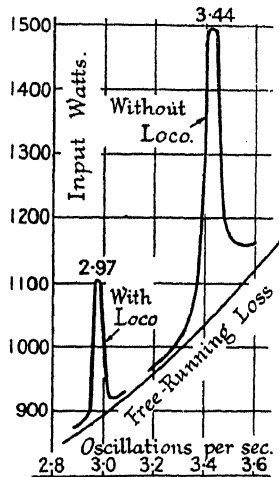

Fig. 89.

The natural frequency of unloaded bridges ranges from a mean of about 9 vibrations per second for a span of 50 feet to a mean of about $2\frac{1}{2}$ vibrations per second for a span of 300 feet. The natural frequency of loaded or partly loaded bridges is, of course, smaller.

In short spans, L < 40 feet, the frequency of the pulsating force (which may be taken as 6 revs. per sec. as a maximum) is too low for synchronism to occur. The effect of the hammer blow is of the nature of a push, and it can almost be regarded as a static load. Fig. 90 is a

Fig. 90.

typical graph showing the deflection of the centre of the girder as the locomotive passes. At each blow the girder deflects an amount proportional to the load, and then recovers. There is practically speaking no oscillation. In long spans, at the highest speeds, the frequency of the pulsating load is too high for synchronism to occur. There may be resonance at lower speeds, but the hammer blow is then smaller, for its intensity varies as the square of the speed. At spans between 100 and

200 feet, synchronism will occur at high speeds. Fig. 91 shows a typical graph of the deflection at the centre of the girder as the locomotive crosses the span at the critical speed. The deflection begins when the leading axle enters the bridge, and continues until the last axle has left it, so that the base line represents a length equal to the span plus the total wheel base. The oscillations gradually increase as the locomotive travels across, reach a maximum, and then die away, but the bridge is left oscillating after the locomotive has gone. It was shown in § 163, Vol. I, that the effect of a periodic force, synchronising with the natural frequency of a spring, would be to produce an indefinitely large amplitude of vibration, were it not for damping effects. That this does not occur in a bridge, and consequently bring about its destruction, is due partly to the energy wasted in friction at the bearings of the bridge and in the springs of the locomotive, and that transmitted to the ground through the abutments ; and partly to the changing natural frequency of the bridge as the train travels across, so that the period of synchronisation is short. So effective
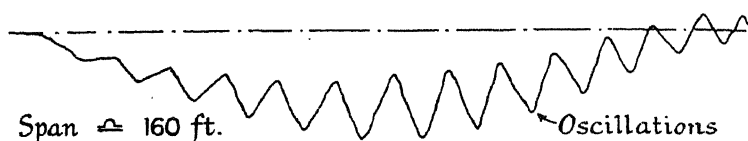

Span ≃ 160 ft.   Oscillations

FIG. 91.

is the damping, that at the critical speeds the amplitude of vibration is found to be proportional to the force producing it.

An interesting point which the British Bridge Stress Committee discovered is that, in bridges of from 130 to 150 feet span, not only were large oscillations set up at speeds corresponding with the natural frequency of the loaded bridge, but oscillations of even greater amplitude occurred at speeds well above the critical speed. Professor Inglis showed that this effect was due to the action of the spring gear of the locomotive. In spans of from 200 to 300 feet, the engines oscillate as one with the mass of the bridge. In shorter spans, and at certain speeds, the springs of some locomotives come into play to such an extent that only the wheels and the non-spring-borne parts of the locomotive oscillate with the bridge, the spring-borne parts moving in a path of their own. This has the effect of raising the natural frequency of the loaded bridge above that for the bridge and engine oscillating as one and, in consequence, synchronism occurs at much higher speeds.

63. **Impact Allowances.**—For the purpose of estimating the effect of hammer blow, Professor Inglis [25] has given the following formulae. Let

L = the span of the bridge in feet.

N = revs. per sec., and D = the diameter in feet of the driving wheels.

v = the velocity of the locomotive = πDN.

P = hammer blow in tons.

y_c = the central deflection of the bridge in feet due to a *static* load P applied there.

y_d = the dynamic increase in the above deflection in feet, when the locomotive is passing the centre of the bridge.

W_b = the total weight of the bridge in tons.

W_u = the part of the weight of the locomotive which is unsprung.

W_s = the part of the weight of the locomotive which is spring-borne.

$W_l = W_u + W_s$ = the total weight of the locomotive (excluding the tender).

n_0 = the natural frequency of oscillation of the unloaded bridge.

n_b = the damping coefficient of the bridge (experimental value).

$n = v/2L = \pi DN/2L$.

w_d = the combined equivalent uniform load, tons/ft., expressing the effect of the hammer blow.

Long Bridges.—L > 200 feet.

Maximum state of oscillation developed when $N = n_0\sqrt{\dfrac{W_b}{W_b + 2W_l}}$;

the static deflection is then $y_C = Pg/2\pi^2 W_b n_0^2$

in which circumstances $y_d = \frac{1}{2}y_C \dfrac{Nn_b'}{n^2 + (n_b')^2}$ ft.

where $n_b' = n_b W_b/(W_b + 2W_l)$

Bending moment at the centre resulting from the inertia of the bridge $= \frac{1}{8}W_b LN^2 y_d$ ft.-tons.

Equivalent uniformly distributed load $= W_b N^2 y_d$ tons.

Concentrated load at the centre of the bridge due to the vertical acceleration of the locomotive $= 4\pi^2 N^2 W_l y_d/g$ tons.

Equivalent uniformly distributed load $= \pi^2 W_l N^2 y_d/4$.

Total combined uniformly distributed load representing the effect of the

hammer blow $= w_d L = (W_b + \dfrac{\pi^2}{4}W_l)N^2 y_d$ tons.

Example.—Span L = 270 ft. ; W_b = 450 t. ; n_0 = 3 ; n_b = 0·12 ; W_l = 100 t. ; v = 15N ; P = 0·5N².

For maximum oscillation N=$3\sqrt{450/650}$=2·50 ; P = 0·5N²=3·13 t. $n = 15 \times 2\cdot5 \div 2 \times 270 = 0\cdot069$; $n_b' = 0\cdot12 \times 450 \div 650 = 0\cdot083$; $y_C = 3\cdot13 \times 32\cdot2 \div (2\pi^2 \times 450 \times 3^2) = 0\cdot00126$; $y_d = \frac{1}{2} \times 0\cdot00126 \times 2\cdot50 \times 0\cdot083 \div (0\cdot069^2 + 0\cdot083^2) = 0\cdot0112$ ft.

Hence, $w_d L = (450 + \dfrac{\pi^2}{4} \times 100)2\cdot5^2 \times 0\cdot0112 = 48\cdot8$ tons.

If two similar locomotives, in tandem, are on the bridge together, and the hammer blows are in phase and l feet apart, the above equations are modified as follows :

$$N = n_0 \sqrt{\dfrac{W_b}{W_b + 4W_l \cos^2(\pi l/2L)}} \qquad n_b' = \dfrac{n_b W_b}{W_b + 4W_l \cos^2(\pi l/2L)}$$

y_C is now the central deflection due to the combined action of the two hammer blows P, statically applied at a distance $l/2$ each side of the centre, the same expression for y_d holds, and

$$w_d L = \left(W_b + W_l \pi^2 \frac{L - l}{2L} \cos \frac{\pi l}{2L} \right) N^2 y_d \text{ tons.}$$

Medium Span Bridges.—$100 < L < 200$. If N_2 be the r.p.s. when the maximum state of oscillation occurs, $N_2{}^2$ is the larger root of the equation

$$N^4 - N^2 n_1{}^2(1 + n_s{}^2/n_2{}^2) + n_1{}^2 n_0{}^2 = 0$$

and
$$y_d = y_C \frac{n_0{}^2}{2N_2 n_b} \left[1 - \frac{4F_s}{\pi P} \frac{N_2{}^2}{N_2{}^2 - n_s{}^2} \right] \text{ feet.}$$

The total combined uniformly distributed load representing the effect of the hammer blow $= w_d L = W_b N_2{}^2 y_d$ tons.

In these equations :

$n_1{}^2 = n_0{}^2 W_b/(W_b + 2W_u)$; $n_2{}^2 = n_0{}^2 W_b/(W_b + 2W_l)$

n_s = the frequency of oscillation of the locomotive on its springs (taken in an example = 3).

F_s = the frictional resistance of the springs (mean value taken = 8 tons).

n_b is taken as $0 \cdot 36$ for a 150 ft. span.

If two similar locomotives are in tandem on the bridge together, and the hammer blows are in phase and distant l_1 from the two ends of the bridge, the same formulae apply, but $n_1{}^2$ and $n_2{}^2$ are replaced by $n_1{}^2 = n_0{}^2 W_b/[W_b + 4W_u \sin^2(\pi l_1/L)]$; $n_2{}^2 = n_0{}^2 W_b/[W_b + 4W_l \sin^2 (\pi l_1/L)]$
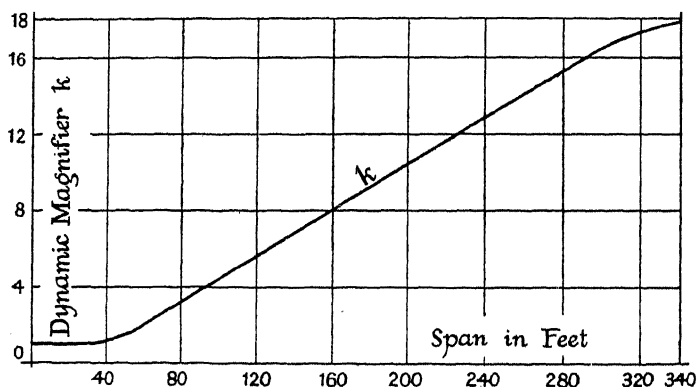

FIG. 92.

and y_C is found for two hammer blows P, statically applied at a distance $(L/2 - l_1)$ from each side of the centre.

For spans of from 50 to 100 ft., take $N_2 = 6$ in all the above, and apply the static load P at the centre of the span.

The Bridge Stress Committee give experimental values, Fig. 92, for a 'dynamic magnifier' k such that $y_C + y_d = k y_C$, from which y_d can be found, and hence w_d as above. The values obtained thus considerably

exceed the theoretical values. Further information is required regarding the values of n_b and F_s. The Committee take three typical loadings, A, B and C, as representative of normal British practice. Loading A applies to three- and four-cylinder locomotives (weight = 20 B.S.I. units), in which, owing to the method of balancing, the hammer blow is relatively small, and may be taken as $0 \cdot 2N^2$. Loading B applies to two-cylinder locomotives (weight = 16 B.S.I. units), in which the hammer blow is considerable, viz. $0 \cdot 5N^2$. Loading C, in which the hammer blow reaches $0 \cdot 6N^2$, may be regarded as exceptional. The allowance for *lurching* is estimated at $N/24$ths the live load per rail, so that the corresponding equivalent uniformly distributed load is $N/24$ths the uniformly distributed live load. Rail joints and unevenness in the tracks produce effects equivalent to a static point load of $N^2/6$ tons, or to an equivalent uniformly distributed load of $N^2/3$ tons. In the case of the example given above, therefore, the *total uniformly distributed* load would be, since $N = 2 \cdot 5$ r.p.s.,

Weight of the Bridge	= 450 tons.
Live load ' B ' (16 B.S.I. units for 270-ft. span) = 16 × 30 =	480 ,,
Hammer blow effect as calculated	= 49 ,,
Lurching = $2 \cdot 5/24$ths of 480 tons	= 50 ,,
Rail joints = $2 \cdot 5^2/3$	= 2 ,,
Total for this particular case . .	= 1031 ,,

Short Spans.—L < 40 ft. The Indian Bridge Standards Committee (see Gelson [27]) have made special investigations regarding the necessary impact allowances in short span bridges, L < 40 ft., and find that, for such spans, lurching is the most important factor. For a X.C. class ' Pacific ' locomotive with a total hammer blow $P = 0 \cdot 526N^2$ tons, they give as the impact factor under one coupled wheel $V/100$, where V is the speed in m.p.h. ; this includes the effect of both lurch and hammer blow. The maximum rail joint effect under one driving wheel ($\frac{3}{4}$ inch gap, 2 ft. timber spacing) is $1 \cdot 6$ tons at 10 m.p.h., $3 \cdot 8$ tons at 30 m.p.h., and 5 tons at 50 m.p.h. and above ; i.e. at 60 m.p.h. a total impact effect of $(0 \cdot 6W + 5)$ tons per driving wheel ; $W =$ the wheel load. The combined impact factor is shown by the line JJ, Fig. 93.

The magnitude of rail joint and of lurching effects depends on the standard of track maintenance. Rail joints should be avoided in spans under 60 ft., and placed where possible near the ends of bridges.

64. Approximate Values.—The Bridge Stress Committee express their results in the form of tables of equivalent uniformly distributed loads based on the standard B.S.I. loadings. If from the tabulated figures for loading A at 6 r.p.s. (bending moment) the equivalent impact factor be calculated, the dotted curves (i) and (ii), Fig. 93, are obtained, (i) applies to single track and (ii) to double track bridges.[17] These curves take account of hammer blow and rail joint effect ; lurching ($i = N/24$) is to be added thereto. The equivalent uniform loads,

including impact, for loadings A and B are found to be, practically speaking, equal. If, therefore, the bridge be designed to carry loading A it will carry loading B, but it must be understood that the impact factor
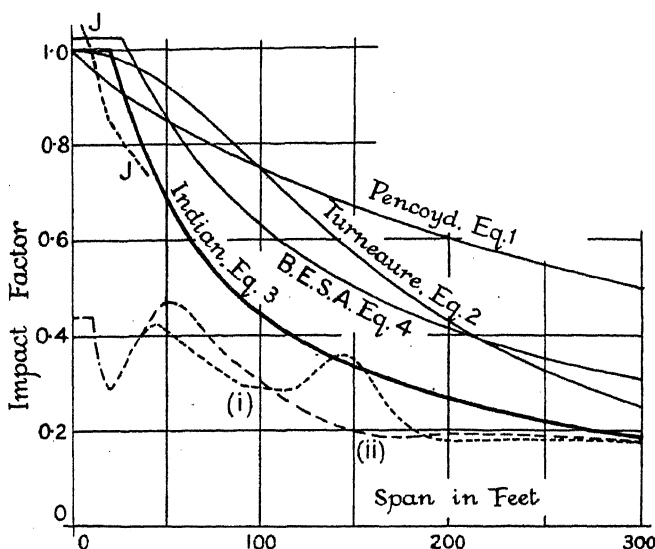

Fig. 93.

is different in the two cases, for the hammer blow is not proportional to the weight of the locomotive, but is greater in the lighter engine.

Web Members.—The percentage increase in shearing force necessary to allow for impact in web members suggested by the British Com-
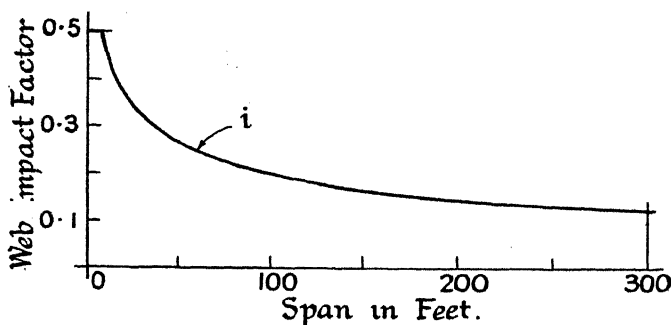

Fig. 94.

mittee is considerably lower than has been hitherto adopted. The web impact factor (for hammer blow and rail joint effects) given in Fig. 94, $i = 2 \cdot 4/(2 + \sqrt{L})$, represents approximately the proposed allowance (see the Report for exact figures). The impact factor in this curve is intended

to apply to all web members, though it would appear that the effect of impact is greatest at the $\frac{3}{4}$ points of the span. There appears to be no justification for the 'loaded length' procedure commonly adopted with the 'Pencoyd' type formulae, but the value of i should be increased by N/24 to allow for lurching;

$$\text{total } i = \text{N}/24 + 2\cdot4/(2 + \sqrt{\text{L}}) \qquad . \qquad . \qquad . \quad (1)$$

The suggested load increments for *rail bearers* (including the effect of lurching), can be expressed with fair accuracy by the formula

$$i = 2\cdot1/(\tfrac{1}{2} + \sqrt[3]{\text{L}}), \text{ max.} = 0\cdot8 \qquad . \qquad . \qquad . \quad (2)$$

and those for *cross girders* by

$$i = 5/(6 + \text{L}), \text{ max.} = 0\cdot46 \qquad . \qquad . \qquad . \quad (3)$$

The Committee consider that no allowance for lurching is necessary in the case of cross girders. In both formulae L denotes the pitch of the cross girders, and they apply for a range of 0 to 30 ft. These values have reference to loading A at a speed of 6 r.p.s.

On Fig. 93 is plotted the Indian Covering Formula, eq. (3), § 61, and it will be seen that, in the present state of knowledge, it represents a practical working compromise for long and short spans, cf. eq. (2A), § 61. It may be used for ordinary design, and it is suggested, for both flange and web members, see § 196.

65. **Impact in Road Bridges.**—In their loading requirements for road bridges, § 23, the Ministry of Transport include for an impact factor of 50 per cent. The B.S.S. for Girder Bridges calls for an impact factor of $\frac{2}{3}$ that given by eq. 4, § 61; max. $0\cdot7$. The American Committee on Impact on Highway Bridges [22] suggest an impact allowance of 25 per cent. in floor beams, suspenders, and trusses of less than 40 ft. span; for longer spans they propose as an impact coefficient $i = 50/(\text{L} + 160)$; L = span in ft.

Impact in road bridges is caused by wheels passing over obstacles; either by shock when the obstacle is struck, or when the wheels drop back on to the roadway. The higher the percentage of unsprung weight, the greater is the ratio of blow to static load. The greater the speed, the greater is the blow. On floors, the percentage impact increment decreases as the load increases.

66. **Repetition of Stress in Bridges. Fatigue.**—The question next arises as to whether it is necessary to make allowance for the effect of the repetition of stress which occurs in a bridge, in addition to the allowance for impact. Both the American and British Committees who investigated the impact problem conclude that it is unnecessary. Another school of thought holds that the effect of repetition of stress must be the same in a bridge as in a machine, and argues that when failures occur they are usually due to fatigue, quoting some remarks of Sir Benjamin Baker in support of this view.

It is worth while considering the question from first principles. (i) Fig. 95 shows the outline of the N bridge of § 196 ; (ii) gives the influence lines for web members Nos. 24 and 25, and (iii) that for flange member No. 5. Suppose that a uniformly distributed load, twice as long as the span, cross the bridge; the consequent variation in the force, and therefore in the stress, in bar No. 5 is shown in (i) Fig. 96. The rectangle AD represents the stress in the bar due to the dead load. The variation in stress due to the travelling load can be obtained from the influence line, (iii) Fig. 95. When the front of the load has reached d', the ordinate at
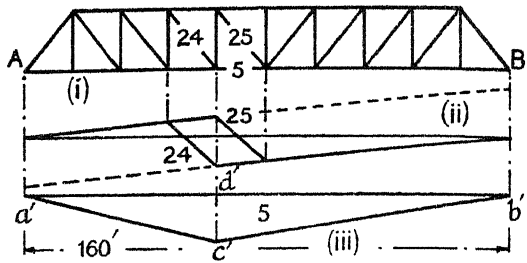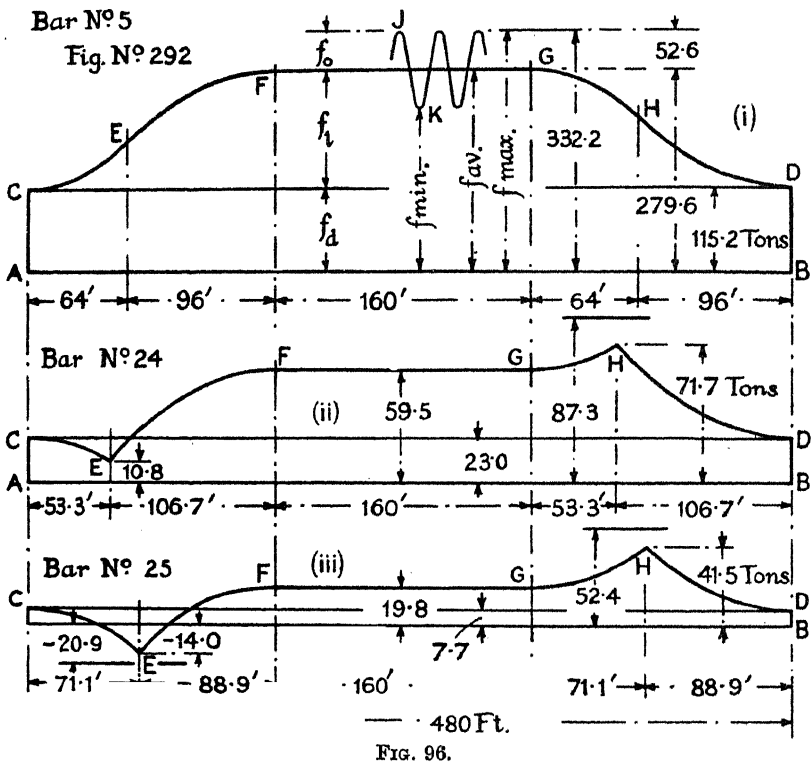

FIG. 95.

FIG. 96.

E, (i) Fig. 96, which represents the stress, will be proportional to the area $a'd'c'$. When the front of the load has reached b', the ordinate at F will be proportional to the area $a'c'b'$, (iii) Fig. 95. The span is now

completely covered and will remain so during the next 160 feet of travel, the corresponding stress in the bar remaining constant. As the load rolls off the span, the area under the load gradually diminishes as indicated by GHD. The figure CFGD will represent, therefore, the variation in the stress in the bar due to the travelling load during the passage of the 320-foot train. Assuming the train to be headed by one or more locomotives, the stresses set up by the hammer blow must be superposed on the curve CFGD. These will reach their maximum in the range FG (cf. Fig. 91), and are represented in Fig. 96 by the wave outline.

The average stress in the bar (f_{av}) during the passage of the train will rise, therefore, from AC at the beginning, to a maximum between F and G, and then die away to BD = AC at the end. This is a relatively slow variation. The maximum and minimum stresses, f_{max} and f_{min}, are represented by the crest and trough of the wave line. Reproducing these values on the repetition of stress diagram (cf. Fig. 347, Vol. I) for a 28-ton mild steel, Fig. 97, it will be seen that the average stress during
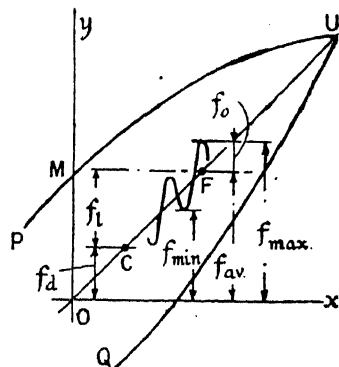
FIG. 97.

the passage of the train travels up the line OU from C to F and down again; with superimposed oscillations as represented diagrammatically in the figure. So far as is known, no repetition of stress experiments in which the average stress of the cycle is varied during the experiment have been made, but assuming that no injurious effects from fatigue will arise, provided that the stress does not overstep the limiting range of stress represented by the lines PU, QU, it may be shown that in bridges designed by the ordinary conventional methods there is no necessity to make special allowance for fatigue. This conclusion can conveniently be established by means of a Haigh diagram, Fig. 98.
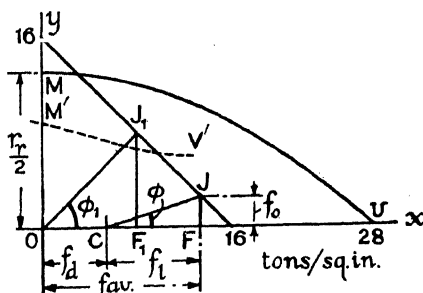
In this diagram the average stress OF of a cycle is plotted

FIG. 98.

along the x axis, and the semi-range of stress FJ as an ordinate. Then J represents the maximum stress of a cycle. The limiting range of stress in the case of mild steel appears as a Gerber parabola MU (§ 286, Vol. I), in which OU represents the ultimate strength = 28 tons/sq. in., and OM = $r_r/2$ = 13 tons/sq. in. is the semi-range of stress for reversals of stress (0 $\pm$ $r_r/2$). Every point on a line 16.16 at 45° represents the

maximum stress in a cycle for which $f_{max} = f_{av} + r/2 = 16$ tons/sq. in., and so on.

Suppose that the permissible working stress in the conventional calculations is limited to 8 tons /sq. in.,* and as a safe estimate, assume that the indeterminate and secondary stresses enumerated in § 57 have the effect of doubling all the calculated stresses †, so that in reality $f_{max.} = 16$ tons/sq. in. Along Ox, in Fig. 98, mark off $OC + CF = f_d + f_l$ to represent the dead and live load stresses, and $FJ = f_0$ vertically to represent the stress due to the oscillations. Then, $f_{max} = f_d + f_l + f_0 = 16$ tons/sq. in. is represented by the point J. But $f_{max} = f_d + f_l(1 + i)$, where i is the impact factor; therefore $f_{max} = f_d + f_l + f_0 = f_d + f_l(1 + i)$, and $i = f_0/f_l = \tan \phi$; see (i) Fig. 96.

For the purpose of setting out this diagram the forces have been taken from the stress sheet, § 196, and doubled for the reason explained. It is evident that the point J lies so far below the line MU representing the limiting range of stress, that no question of fatigue can in this case arise. M'V' in the same diagram represents the results of fatigue experiments by Haigh [41] on mild steel specimens ($f_{ult} = 26·6$ tons/sq. in.) pierced with a small hole as a stress raiser, see § 67. The point J lies well below this line, showing that no fatigue will occur even at stress concentrations. As the worst case which might arise, suppose that in a very short span the dead load is negligible compared with the live load, that $\tan \phi$ has the maximum value $\tan \phi_1 = 1$, Fig. 93, and $f_{max.} = 16$ tons/sq. in. The point J_1, Fig. 98, plotted as before, will represent these extreme conditions. J_1 still lies well inside MU, but just outside M'V', suggesting that if the effects of fatigue ever became serious in a bridge, it would be at a stress concentration in a short main girder or rail bearer. In such members oscillations do not occur, § 62, and failure by repetition of stress is unlikely.

The curve representing the variation in f_{av} for web member No. 24 is shown in (ii) Fig. 96. On this should be superposed the stress variation due to hammer blow. Except that the variation in the average stress is rather more complex than in the case of the flange, it is clear that the arguments which apply to the flange member will also apply to the web member. (iii) Fig. 96 shows the stress variation in bar No. 25 in which the stress actually reverses, so that at one moment during the passage of the train the point E lies below the origin. It does not appear that this fact affects the conclusions reached, particularly as both the average and hammer-blow stresses will be small. Also there appears to be no necessity or justification for the increase in the area of the member to allow for ' reversal ' called for in certain specifications.

67. Effect of Holes and Yield.—In establishing the above theory, use

* In the B.S.S. for Girder Bridges, 1933, the permissible working stress in tension has been increased to 9 tons/sq. in., but the same arguments hold if f_{max}. does not exceed 16 tons/sq. in.

† It is taken for granted that the maximum wind pressure is unlikely to occur at the same moment in which the other stresses all reach their maximum, see § 52.

has been made of the ordinary Gerber Parabola for mild steel. This curve is obtained from experiments on plain specimens in which great care is taken to avoid stress concentrations. Every riveted bridge member is pierced with holes, and theoretically the stress at the edge of a hole rises to three times the average stress in the member, Fig. 325, Vol. I. It becomes necessary, therefore, to investigate as to what is the effect of the holes in bridge members subjected to repetition of stress.

Some experiments by Wilson and Haigh [34] are illustrated in Fig. 99. The material was a soft mild steel; ultimate strength $= 22\frac{1}{2}$ tons/sq. in., yield point 13 tons/sq. in., elongation $22\frac{1}{2}$ per cent. in 3 inches. The specimens were all $1\frac{1}{2}$ inches wide and $\frac{1}{16}$th inch thick, shaped as shown in the figure. Specimens (iii) to (vii) were scale models of a $9 \times \frac{3}{8}$ in. tie bar, with $\frac{15}{16}$ in. holes. The holes were drilled. The results of repetition of stress experiments in a Haigh machine were as follows :
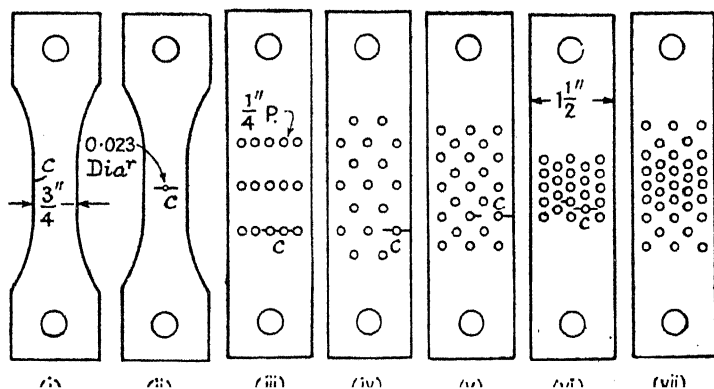
Range of stress
tons/sq. in.

(i) Solid bar	$6\frac{1}{2} \pm 6$ $7\frac{1}{2} \pm 6$	Unbroken at N = 2,852,000. Yielded slowly ($f_y = 13$ tons/sq. in.).
(ii) Similar bar to (i) with a small hole to produce a 3 : 1 stress concentration.	$6 \pm 5\frac{1}{2}$ $6\frac{1}{2} \pm 6$	Unbroken at N = 2,786,000. Fractured at N = 998,000.
(iii) Model tie bar with rows of holes at a spacing equivalent to a 3" pitch.	6 ± 5 $8 \pm 5\frac{1}{2}$	Unbroken at N = 2,578,000. Fractured at N = 908,000 (slight elongation).
(iv) With zig-zag riveting . .	7 ± 5	Fractured at N = 534,000.
(v) Ditto at closer pitch . .	7 ± 5	Fractured at N = 456,000.

N = number of reversals. In specimens (iii), (iv) and (v) the stress is calculated on the minimum net area of the bar normal to the pull.

Taking the safe range of stress in the material as $6\frac{1}{2} \pm 6$ tons/sq. in., ($f_{max} = 12\frac{1}{2}$ tons/sq. in.), it will be seen that in such soft steel the effect

of the holes is not large. It will further be observed that in all the specimens with holes, the crack c which leads to fracture starts at the edge of a hole, and is normal to the line of the pull, which suggests that the crack was started by the stress concentration at the edge of the hole. This is true even in (vi) with the close pitch of holes, showing that the arrangement of holes longitudinally has little effect on the fatigue strength of the member. Specimen (vii) was unbroken.

Experiments by Haigh and Beale [36] on specimens similar to (ii), but made of cold rolled high tensile strip, showed that in hard steel the stress concentration does reduce the fatigue limits, but the specimen behaved as if the stress in the plate were increased 2·15 times, instead of to three times its nominal amount as theory predicts. Varying the diameter of the hole from 0·0365 to 0·200 inch made little difference.

Some further experiments on this subject were made by Haigh and Robertson [40] on a 0·16 C rolled mild steel in the normalised condition. This steel had a high manganese content (0·75 per cent.). Its properties were: ultimate strength 30·2 ; upper yield point 22·0 ; lower yield point 18·75, tons/sq. in ; elongation 26·8 per cent. in 13½ diameters. The limiting range of stress of this material, for reversals, was 0 ± 14 tons/sq. in., and when $f_{av} = 3·3$, was $3·3 \pm 14·6$ tons sq. in. When a 0·0312 in. diameter hole was drilled in the 0·50 in. cylindrical mid-part of the test piece, the limiting ranges of stress were $0 \pm 7·5$ and $6·0 \pm 6·5$ tons/sq. in., or approximately one-half of those for unpierced test pieces. Professor Haigh concludes also from these experiments that in the pierced test pieces, while $f_{av} < 6$ tons/sq. in., the limiting range of stress is nearly independent of the magnitude of the average stress.

It appears, therefore, that while in a very soft mild steel the limiting range of stress is very little reduced by stress concentrations due to holes, in hard steel or medium mild steels it will be halved in value.

The Effect of Plastic Flow at the Yield Point.—Suppose that in a repetition of stress experiment on a mild steel, the maximum stress of the cycle be gradually increased. When f_{max} exceeds the upper yield point, Lüders' lines break out and spread over the surface of the specimen, which begins to lengthen as in an ordinary tension test, showing that plastic flow is taking place. Considerable cyclic permanent set appears, but as Bairstow showed (§ 289, Vol. I, p. 556), provided that the range of stress remain within certain limits, this cyclic permanent set gradually dies out and the specimen regains its elasticity due to strain-hardening, but is permanently elongated. Haigh [40] found that if a specimen in which plastic flow has just started be immediately subjected to further cycles of stress, the limiting range of stress is reduced ; but if a period of rest occur between the first production of plastic flow and the subsequent repetitions of stress, the limiting range is not much affected.

It has been seen that local yield may be of great service in relieving stress concentrations in structures, and the experimental work cited above confirms the practical experience that no deleterious effects due

to fatigue are likely to arise as a result of such local yield. This conclusion is subject, however, to certain limitations. In the Haigh [37] diagram shown in (i) Fig. 100, MU represents the fatigue limit and YY the yield point. Provided that the real stress in the material,
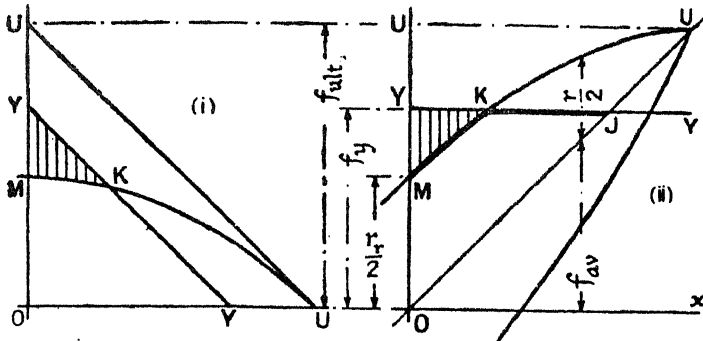

FIG. 100.

as represented by a point such as P, Fig. 101, lies within the area OMKY, no question either of fatigue or plastic yield can arise. In the ordinary repetition of stress diagram, (ii) Fig. 100, which is lettered to correspond with (i), the real maximum stress must lie below the line MKJ. If the maximum stress fall within the shaded area, Professor Haigh points out, that fatigue failure will precede yield, and no benefit from the latter is to be expected.

The following explanation of the effect of ductility in mitigating the evils of high stress concentration at the edge of a hole is due to Haigh.[37]   In the Haigh diagram, Fig. 101, let Y_1Y_1 and M_1U_1 represent the yield point and fatigue limit in a very hard alloy steel, $f_T = 60$ tons/sq. in., and suppose that a nominal stress cycle 10 ± 5 tons/sq. in. be applied to a specimen of this steel pierced by a small hole. The point P represents the nominal maximum
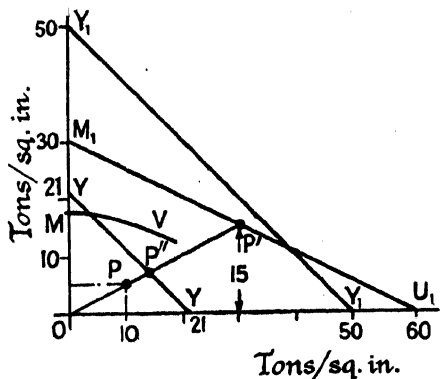

FIG. 101.

stress of the cycle, but the effect of the hole will be to cause a theoretical stress concentration at the edges of the hole of three times this nominal value, and the theoretical maximum stress is, therefore, 45 tons/sq. in., represented in the diagram by the point P′. This point lies on the fatigue limit M_1U_1, which in these conditions would be reached before the yield point $Y_1Y_1 = 50$ tons/sq. in.   A crack would form at the edge of the hole, and the material would fail by fatigue.

Next suppose that a similar pierced specimen of mild steel, $f_T = 30$ tons/ sq. in., be tested. YY represents the yield point, and the parabola MV represents the fatigue limit. If a gradually increasing stress cycle be applied, in which as before the ratio $f_{av}/r = 2$, when the nominal stress cycle reaches $4\frac{2}{3} \pm 2\frac{1}{3}$ tons/sq. in., the real maximum stress at the edges of the hole will reach 21 tons/sq. in., represented by P'' on the yield point line, the metal at the edges of the hole will flow, and the stress will redistribute itself. When the stress cycle 10 ± 5 tons/sq. in. is reached, the stress at the edge of the hole will still be 21 tons/sq. in., not 45 tons/sq. in. as in the hard steel. P'' falls well below the fatigue limit line MV, and it follows that this ductile steel is better able to resist such stress cycles than the hard alloy steel of double its ultimate strength. Such considerations should be reflected in the factor of safety.

BIBILIOGRAPHY

Impact.

1. STOKES. Discussión of a Differential Equation Relating to the Breaking of Railway Bridges. *Trans. Camb. Phil. Soc.*, vol. viii, 1849, p. 707.
2. MELAN. Ueber die dynamische Wirkung bewegter Lasten auf Brücken. *Zeit. d. oest. Ing.- u. Arch. Ver.* Jg. xlv, 1893, p. 293 ; see trans. *Gov. India Tech. Pap.*, No. 45.
3. CHATLEY. The Dynamic Increment of a Single Rolling Load on a Supported Beam. *Rpt. Brit. Assoc.* 1914 ; see *Engg.*, Sep. 11, 1914, p. 327.
4. ROBINSON. Vibration of Bridges. *Trans. Amer. Soc. C.E.*, vol. xvi, 1887, p. 42.
5. TURNEAURE. Some Experiments on Bridges under Moving Train-Loads. *Trans. Amer. Soc. C.E.*, vol. xli, 1899, p. 410.
6. AMER. RY. ENG. ASSOC. Reports of Committee XV (Iron and Steel Structures). *Proc.*, vol. xii, Pt. 3, 1911, p. 26 : vol. xvii, 1916, p. 116.
7. ANDERSON. On Impact Coefficients for Railway Girders. *Proc. Inst. C.E.*, vol. cc, 1914–15, p. 178 : vol. cci, 1915–16, p. 301.
8. FEREDAY-PALMER. Stress Recorder. *Engg.*, Jan. 30, 1920, p. 138 ; see also *Proc. Inst. C.E.*, vol. 228, p. 86.
9. MINISTRY OF TRANSPORT. Tests on Railway Bridges in Respect of Impact Effects. London, 1921.
10. TIMOSHENKO. On the Forced Vibrations of Bridges. *Phil. Mag.*, May 1922, p. 1018.
11. INGLIS. Theory of Transverse Oscillations in Girders, and its Relation to Live-Load and Impact Allowances. *Proc. Inst. C.E.*, vol. ccxviii, 1923–4, p. 225.
12. —— Oscillations in a Bridge Caused by the Passage of a Locomotive. *Proc. Roy. Soc.*, A, vol. cxviii, 1928, p. 60.
13. HOWLAND. Transverse Oscillations in Girders. *Select. Eng. Pap. I.C.E.*, No. 23, 1924.
14. INDIAN RAILWAY BOARD. Report of Bridge Sub-Committee on Impact. *Tech. Pap.* No. 247, 1925 ; see COLAM, *Proc. Inst. C.E.*, vol. 228, p. 127 ; and *Eng. Ab. I.C.E.*, 1929, No. 40 : 82. *Tech. Pap.* Nos. 187, 194,

198, 199, 211, 224, 225, 228, Indian Ry. Bd., 1917–21, may also be consulted.

15. INDIAN BRIDGE STANDARDS COMMITTEE. 7th Rpt., 1929; 10th Rpt., 1931; 12th Rpt., 1933, Lurching.

16. BRIDGE STRESS COMMITTEE. Report of, London, 1928; see *Engg.*, Feb. 1, 1929, pp. 143, 187.

17. GRIBBLE. Impact in Railway Bridges with Particular Reference to the Report of the Bridge Stress Committee. *Proc. Inst. C.E.*, vol. 228, 1928–29, p. 46.

18. EWING. The Vibrations of Railway Bridges. *Jour. Roy. Soc. Arts*, May 3, 1929, p. 624.

19. HORT. Stossbeanspruchungen und Schwingungen der Hauptträger statisch bestimmter Eisenbahnbrücken. *Bautechnik*, 6, 1928, p. 37.

20. BERNHARD U. SPÄTH. Rein dynamische Verfahren zur Untersuchung der Beanspruchungen von Bauwerken. *Bautechnik*, 7 (*Der Stahlbau*, 2), 1929, p. 61 ; see also *Eng. Ab. I.C.E.*, 1929, No. 40 : 83.

21. BERNHARD. Dauerversuche an genieteten und geschweissten Brücken. *Zeit. Ver. deu. Ing.*, Nov. 23, 1929, p. 1675.

22. AMERICAN SOC. C.E. Final Report of the Special Committee on Impact in Highway Bridges. *Proc. Amer. Soc. C.E.*, vol. lv, 1929, p. 728 ; see *Eng. Ab. I.C.E.*, 1929, No. 40 : 81.

23. HYDE AND LINTERN. The Vibrations of Roads and Structures. *Proc. Inst. C.E.*, vol. 227, 1928–29, p. 187 ; also AUGHTIE, BATSON AND BROWN. Impact of Wheels on Roads. *Proc. Inst. C.E.*, vol. 237, 1933–34, p. 27.

24. INTER. RAILWAY CONFERENCE, MADRID. Static and Dynamic Stresses in Bridges·; see *Engg.*, June 13, 1930, p. 755.

25. INGLIS. Impact in Railway Bridges. *Proc. Inst. C.E.*, vol. 234, 1931–32, p. 358.

26. —— *A Mathematical Treatise on Vibrations in Railway Bridges.* Camb., 1934.

27. GELSON. Moving-Load Stresses in Short-Span Railway Bridges. *Proc. Inst. C.E.*, vol. 237, 1933–34, p. 314.

Repetition of Stress : Fatigue.

28. LAUNHARDT ; WEYRAUCH. Ref. No. 72, Chap. XVIII, Vol. I.

29. GERBER. Ref. No. 73, Chap. XVIII, Vol. I.

30. GOODMAN. Ref. No. 74, Chap. XVIII, Vol. I.

31. FIDLER. *A Practical Treatise on Bridge Construction.* London, 3rd ed., 1901, chap. xiii, p. 248.

32. STONE. The Determination of the Safe Working Stress for Railway Bridges of Wrought Iron and Steel. *Trans. Amer. Soc. C.E.*, vol. xli, 1899, p. 467.

33. GRAHAM. Impact and Fatigue in Railway Bridges. *The Engr.*, Nov. 14, 1902, p. 465; Jan. 2, 1903, p. 3.

34. WILSON AND HAIGH. The Influence of Rivet Holes on the Strength and Endurance of Steel Structures. *Rpt. Brit. Assoc.*, 1922 ; see *Engg.*, Sep. 8, 1922, p. 309.

35. —— Stresses in Bridges. *Rpt. Brit. Assoc.*, 1923 ; see *Engg.*, Sep. 28, 1923, p. 411, 446.

36. HAIGH and BEALE. The Influence of Circular Holes on the Fatigue Strength of Hard Steel Plates. *Rpt. Brit. Assoc.*, 1924 ; see *Engg.*, Aug. 29, 1924, p. 286.

37. HAIGH. The Relative Safety of Mild and High-Tensile Alloy Steels under Alternating and Pulsating Stresses. *Proc. Inst. Auto. Eng.*, vol. xxiv, 1929–30, p. 320 ; see *Engg.*, Feb. 14, 1930, p. 231.

154 MATERIALS AND STRUCTURES

38. HAIGH. Brittle Fracture in Metals. *Engg.*, Nov. 28, 1930, p. 685.
39. HAIGH and THORNE. Rupture by Fatigue. *Proc. 3rd Int. Cong. App. Mech.* Stockholm, 1930, p. 300.
40. HAIGH and ROBERTSON. Plastic Strain in Relation to Fatigue in Mild Steel. *Rpt. Brit. Assoc.*, 1931 ; see *Engg.*, Sep. 18, 1931, p. 389.
41. HAIGH. Fatigue in Structural Steel. *Engg.*, Dec. 28, 1934, p. 698 (Mild Steel and Chromador Steel).
42. LEA. Repeated Stresses on Structural Elements. *Jour. Inst. C.E.*, Nov. 1936, p. 93.
43. GARLEPP. Zulässige Spannungen und Dauerfestigkeit im Kran- und Verladebrückenbau. *Maschinenbau.* Bd. 10, 1931, p. 86 : see *Eng. Ab. I.C.E.*, 48 : 222.

CHAPTER V

THE APPLICATION OF THE STRAIN-ENERGY THEORY TO FRAMED STRUCTURES

68. Work done in Deforming a Framed Structure.—It will be assumed that all the members of the frame are simple ties or struts, that the cross section of each member is uniform from end to end, and that the whole of the work done is expended in straining these members. Tensions will be considered as positive forces, compressions as negative forces. Then, if F be the force in any one bar due to the deformation of the frame, l the length of the bar, and a its area, the alteration in length due to F will be $\delta l = Fl/Ea$; the work done by F will be $\tfrac{1}{2}F.\delta l = F^2 l/2Ea$, and if U be the total internal work stored up in the whole structure

$$U = \frac{1}{2E} \Sigma F^2 \frac{l}{a} \qquad . \qquad . \qquad . \qquad . \quad (1)$$

Now l/a is a constant for any one bar, which, if the dimensions be known, can be calculated ; let $l/a = \lambda$. Except in the rare cases where E is different in different bars of the structure, it is more convenient from an arithmetical point of view not to introduce the numerical value of E until the final stage of the calculation.

Eq. (1) can then be written

$$U = \frac{1}{2E} \Sigma F^2 \lambda \ . \qquad . \qquad . \qquad . \qquad . \quad (2)$$

The summation must include all the bars forming the structure. It is best to make the calculation in tabular form thus :

Bar No.	Length l.	Area a.	$\lambda = \dfrac{l}{a}$.	Force in bar F.	$F^2\lambda$.
1	l_1	a_1	λ_1	F_1	$F_1{}^2\lambda_1$
2	l_2	a_2	λ_2	F_2	$F_2{}^2\lambda_2$
3	l_3	a_3	λ_3	F_3	$F_3{}^2\lambda_3$
$\vdots$	$\vdots$	$\vdots$	$\vdots$	$\vdots$	$\vdots$
n	l_n	a_n	λ_n	F_n	$F_n{}^2\lambda_n$
					$\Sigma F^2\lambda$

The addition of the final column is $\Sigma F^2 \lambda$, and $U = \frac{1}{2E} \Sigma F^2 \lambda$. In making this table the length and area of each bar must be known, λ can then be found. The values of F are determined from a stress diagram or other appropriate process. It is usually convenient to use *inches* and *tons* as units.

69. Deflection of Framed Structures.—The principle of work may be used to determine the deflection of a framed structure. In a simple frame, like that shown in Fig. 102, the vertical deflection of the point C can be found by equating the external work done by the load to the internal work stored in the structure. It will be assumed that the wall to which the frame is attached is sensibly rigid, that is to say, that A and B are fixed points. Then if y be the vertical deflection of C, external work done by the load is $\frac{W}{2}y$, since the load increases gradually
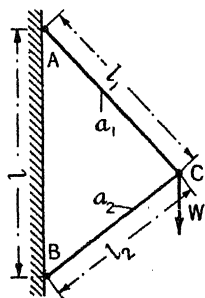
FIG. 102.

from zero to the value W. If l_1 and l_2, a_1 and a_2 be the lengths and areas of the bars AC and BC respectively, and F_1 and F_2 the forces therein, then from eq. (1) of the preceding Article, the internal work is

$$U = \frac{1}{2E} \Sigma F^2 \frac{l}{a} = \frac{1}{2E} \left\{ F_1^2 \frac{l_1}{a_1} + F_2^2 \frac{l_2}{a_2} \right\}$$

Now the triangle ABC, Fig. 102, will represent the triangle of forces for the point C. Hence

$$F_1 = W \cdot \frac{AC}{AB} = W \frac{l_1}{l}; \qquad F_2 = -W \cdot \frac{BC}{AB} = -W \frac{l_2}{l};$$

and,
$$U = \frac{W^2}{2E} \left\{ \frac{l_1^2}{l^2} \cdot \frac{l_1}{a_1} + \frac{l_2^2}{l^2} \cdot \frac{l_2}{a_2} \right\} = \frac{W^2}{2El^2} \left\{ \frac{l_1^3}{a_1} + \frac{l_2^3}{a_2} \right\} . \qquad . \qquad . \qquad (1)$$

But the internal work U must equal the external work $\frac{1}{2}Wy$;

therefore,
$$y = \frac{2U}{W} = \frac{W}{El^2} \left\{ \frac{l_1^3}{a_1} + \frac{l_2^3}{a_2} \right\} \qquad . \qquad . \qquad . \qquad (2)$$

70. Determination of the Displacements of the Node Points in Framed Structures.—Given a framed structure in equilibrium under a system of loads, as in Fig. 103, to find the displacement of the point of application of any load along the line of action of that load. This is the general theorem of which the above is a particular case. Let ABCD, (i) Fig. 103, be the frame under the action of a system of loads W_1, W_2, $W_3 \cdots$ As a result of the application of these loads the frame will deform slightly, and each of the points A, B, C and D will move a small distance from its original position. The movement of A, the point of application of W_1, can be resolved into two components, one at right angles to, and the other along the line of action of, W_1. Call the latter component Δ_1. Then Δ_1

is the displacement of A along the line of action of W_1, and therefore the distance moved by that force. Hence the work done by W_1 is $\frac{1}{2}W_1\Delta_1$. No work is done by W_1 in consequence of the second component at right angles to the line of action. If the movement of A along the line of action be in an opposite direction to the sense of the force W_1, then Δ_1 is negative, and the external work done by W_1 would be negative.

In a similar way, if Δ_2 be the displacement of B along the line of action of W_2, and Δ_3 the displacement of C along the line of action of W_3, the external work done by all the applied loads is

$$\tfrac{1}{2}(W_1\Delta_1 + W_2\Delta_2 + W_3\Delta_3 + \ldots)$$

FIG. 103.

which must be equal to U the internal work stored in the structure

$$U = \tfrac{1}{2}(W_1\Delta_1 + W_2\Delta_2 + W_3\Delta_3 + \ldots) \qquad . \qquad . \quad (1)$$

Suppose that one of the forces, say W_1, be increased to $(W_1 + \delta W_1)$, the structure remaining in equilibrium ; and that, in consequence, Δ_1 becomes $(\Delta_1 + \delta\Delta_1)$, Δ_2 becomes $(\Delta_2 + \delta\Delta_2)$, Δ_3 becomes $(\Delta_3 + \delta\Delta_3)$ and so on. Then, neglecting the second order of small quantities, the increase in work done will be, see (ii) Fig. 103,

$$\delta U = \left\{ W_1 + \frac{\delta W_1}{} \right\} \delta\Delta_1 + W_2 . \delta\Delta_2 + W_3 . \delta\Delta_3 + \ldots$$

and dividing through by δW_1,

$$\frac{\delta U}{\delta W_1} - W_1 \frac{\delta\Delta_1}{\delta W_1} + \frac{\delta\Delta_1}{2} + W_2 \frac{\delta\Delta_2}{\delta W_1} + W_3 \frac{\delta\Delta_3}{\delta W_1} +$$

In the limit, when δW_1 is very small,

$$\frac{\partial U}{\partial W_1} = W_1 \frac{\partial\Delta_1}{\partial W_1} + W_2 \frac{\partial\Delta_2}{\partial W_1} + W_3 \frac{\partial\Delta_3}{\partial W_1} + \qquad (2)$$

the symbols of partial differentiation indicate that δU is the result of a variation in W_1 alone. Differentiate eq. (1) with respect to W_1,

$$\frac{\partial U}{\partial W_1} = \frac{1}{2} \left\{ \Delta_1 + W_1 \frac{\partial\Delta_1}{\partial W_1} + W_2 \frac{\partial\Delta_2}{\partial W_1} + W_3 \frac{\partial\Delta_3}{\partial W_1} + \right. \qquad (3)$$

Multiply eq. (3) by two, and subtract eq. (2), then, $\Delta_1 \cdot \dfrac{\partial U}{\partial W_1}$. In a

similar manner it may be shown that $\Delta_2 = \dfrac{\partial U}{\partial W_2}$; $\Delta_3 = \dfrac{\partial U}{\partial W_3}$; and generally,

$$\Delta = \frac{\partial U}{\partial W} \qquad . \qquad . \qquad . \qquad . \qquad . \quad (4)$$

That is to say, the displacement of the point of application of any load, along the line of action of that load, is equal to the partial differential
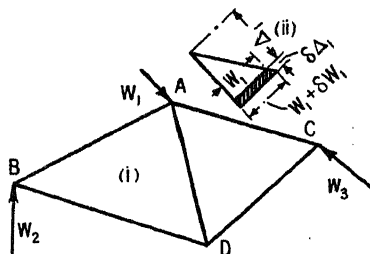
coefficient of the expression for the internal work, with respect to the load in question.

Particular Case.—This theorem may be applied to the example of Fig. 102, in order to find Δ the displacement of C along the line of action of W, i.e. vertically downwards. The calculation is as follows : The

internal work due to W is given by eq. (1), § 69, $U = \dfrac{W^2}{2El^2}\left\{\dfrac{l_1{}^3}{a_1} + \dfrac{l_2{}^3}{a_2}\right\}$

Differentiating this expression with regard to W, $\Delta = \dfrac{\partial U}{\partial W} = \dfrac{W}{El^2}\left\{\dfrac{l_1{}^3}{1} + \dfrac{l_2{}^3}{a_2}\right\}$

which is the value obtained for y in eq. (2), § 69.

If the load in such an example have a definite numerical value, it is necessary, in order to differentiate, to call its value W. The numerical value is afterwards inserted in the differential coefficient in order to obtain the numerical value of Δ.

By means of eq. (4) the displacement in any direction of any node point of a framed structure can be readily determined. Suppose, for example, it be desired to find the displacement of the point G, Fig. 104, in a vertical direction. Apply an extra load W' at G, acting vertically downward, and find U the total internal work due to all the
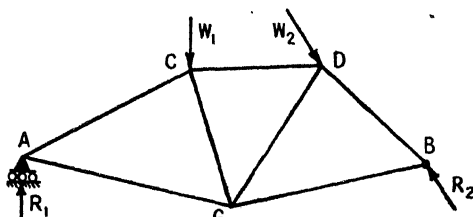

FIG. 104.

forces acting on the structure inclusive of W'. To do this it will first be necessary to find the extra reactions produced by W', as otherwise the forces in the bars due to W' cannot, in general, be obtained. The directions and magnitudes of these extra reactions will depend on the manner in which the frame is supported, and are found in the usual way. Then Δ, the displacement of G along the line of action of W', i.e. in a vertical direction, from eq. (4) is $\Delta = \dfrac{\partial U}{\partial W'}$. This displacement includes the effect of W'. But the equation holds for all values of W', and therefore when W' = 0. If W' be put equal to zero in the expression for Δ, the displacement of the point in question due to the action of the applied loads by themselves will be obtained.

In symbolic form,

$$\Delta = \left(\frac{\partial U}{\partial W'}\right)_{W' = 0} \qquad (5)$$

which is the displacement required.

The value of U is determined by the methods of § 68. It will include terms containing W' (see example below) as well as those due to the actual loads. It is then only necessary to differentiate the expression so obtained with respect to W', and to put W' = 0 in the differential

coefficient, in order to obtain the required displacement Δ. It is to be understood that if Δ comes out negative, the displacement will be in an opposite direction to that assumed for the force W'. The load W' is called a *virtual load*.

Example.—Given a plane frame ABC, of the dimensions shown in Fig. 105, to find the horizontal displacement of C due to a vertical load of 10 tons applied at that point. The calculation for U should be made in tabular form, after the manner of § 68, as set forth below.

Bar No.	l	a	λ	F_W	F'	F	$F^2\lambda$
	in.	sq. in.		tons.			
1	80	1·6	50	$+8$	$+0\cdot61\,W'$	$8+0\cdot61\,W'$	$50\,(8+0\cdot61\,W')^2$
2	70	2·5	28	-7	$+0\cdot72\,W'$	$-7+0\cdot72\,W'$	$28\,(-7+0\cdot72\,W')^2$
							$\Sigma\,F^2\lambda$

In the second and third columns of the table the lengths and areas of the members are entered, from which the values of λ are calculated. In column 5 the magnitudes of F_W the force in each member due to the actual load ($W = 10$ tons) are tabulated. These are obtained from the triangle of forces for the point C which is represented by the triangle ABC. Since it is required to find the horizontal displacement of C, a virtual horizontal load W' will be applied at that point, acting away from AB. The triangle of forces for this load is the triangle bca, (ii), and the forces in the members calculated therefrom are entered in the sixth column under the head F'. The total force F in each member when W' is acting is $F_W + F'$; and the addition of the final column gives $\Sigma\,F^2\lambda$, whence $U = \dfrac{1}{2E}\,\Sigma\,F^2\lambda$.
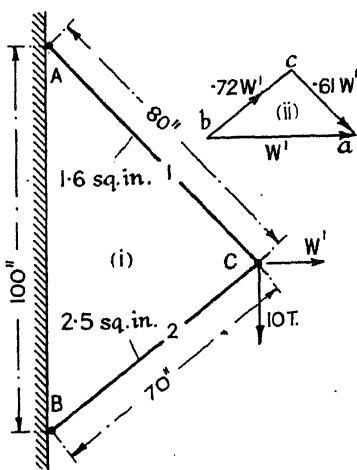

Fig. 105.

$$U = \frac{1}{2E}\,[50(8+0\cdot61W')^2 + 28(-7+0\cdot72W')^2]$$

$$= \frac{1}{2E}\,[4572 + 205\cdot8W' + 33\cdot1(W')^2]$$

from which $\qquad \dfrac{\partial U}{\partial W'} = \dfrac{1}{2E}\,[205\cdot8 + 66\cdot2W'].$

Putting $W' = 0$ in this expression, the horizontal displacement of C in the direction of W' is $\Delta = \left(\dfrac{\partial U}{\partial W'}\right)_{W'=0} = 0 \cdot 0079$ inch, if $E = 13,000$ tons/sq. in.

The above method can be simplified as follows : It is evident from the table that the magnitude of F, the total force in each bar, is always made up of two parts, F_W the force due to the actual loads, and F' the force due to the virtual load W'. Of these parts, F_W is constant with respect to W', and F' appears in the form cW', where c is a coefficient independent of W' and merely depending on the shape of the frame. Thus for bar No. 1 of the preceding example, $F_W = 8$, $c = 0 \cdot 61$, $F' = 0 \cdot 61W'$, and $F = (8 + 0 \cdot 61W')$. Hence, for any one of the bars composing the frame, the value of $F^2\lambda$ is $(F_W + cW')^2\lambda$, and the total internal work is $U = \dfrac{1}{2E} \Sigma (F_W + cW')^2\lambda$. Differentiating this with respect

to W', $\dfrac{\partial U}{\partial W'} = \dfrac{1}{2E} \Sigma 2(F_W + cW') \, c\lambda.$

Then, putting $W' = 0$, $\Delta = \left(\dfrac{\partial U}{\partial W'}\right)_{W'=0} = \dfrac{1}{E} \Sigma F_W c\lambda,$

see eq. (5). It is evident that the value of Δ is independent of the value of W', for none of the factors on the right-hand side depend on the value of W'. Now $c = F'/W'$ (see above) ; give to W' the value unity, then $c = F'$, where F' is now the magnitude of the force in a bar due to the application of a virtual load W' of magnitude unity. Then the above equation, which is true whatever be the value of W', becomes

$$\Delta = \frac{1}{E} \Sigma F_W F'\lambda \quad . \quad \quad . \quad \quad . \quad \quad . \quad (6)$$

(compare eq. (6), § 144, Vol. I, for the deflection of a beam due to bending). Hence, to determine Δ, the displacement in any direction of any node point on a frame, apply a virtual load $W' = $ unity to the point in question, acting in the direction of the required displacement. Find F_W the force due to the actual loads, and F' the force due to the unit virtual load, in all the bars ; the magnitude of Δ is then obtained from eq. (6). If F_W or F' be a tensile force, it is to be given a plus sign, if compressive, a minus sign. If the value of Δ come out positive, it implies that the displacement is in the same direction (sense) as the virtual load ; if it come out negative, the displacement is in the reverse direction. It is best to use a tabular method of calculation as shown below.

Example.—To find the horizontal displacement of C in the previous example, Fig. 105, by this modified method. W' the horizontal virtual load is now unity. The tabular calculation becomes—

Bar No.	l	a	λ	F_W	F'	$F_W F'\lambda$
1	in. 80	sq. in. 1·6	50	tons. + 8	tons. + 0·61	+ 244
2	70	2·5	28	− 7	+ 0·72	− 141·1
						$\Sigma = + 102·9$

and Δ (hoz.) $= \frac{1}{E} \Sigma F_W F'\lambda \quad \frac{102·9}{13000} \quad 0\cdot0079$ inch, as before.

Similarly, to obtain the vertical displacement of C, a virtual load $W' =$ unity should be applied at C acting vertically downward, in addition to the load of 10 tons already acting there. It will evidently produce forces in the bars of the same sign, but of one-tenth the magnitude, of those due to the actual load. The tabular calculation becomes—

Bar No.	l	a	λ	F_W	F'	$F_W F'\lambda$
1	in. 80	sq. in. 1·6	·50	tons. + 8	tons. + 0·8	+ 320
2	70	2·5	28	− 7	− 0·7	+ 137·2
						$\Sigma = + 457·2$

and Δ (vert.) $= \frac{1}{E} \Sigma F_W F'\lambda = \frac{457·2}{13000} = 0\cdot035$ inch.

From these calculations it is evident that since Δ is positive in each case, C moves $0\cdot0079$ inch horizontally away from AB, and $0\cdot035$ inch vertically downward. By combining these two displacements the actual movement of C is determined. (Compare the Example § 12.)

The vertical displacement of C might have been obtained directly from eq. (4), using the equation $U = \frac{1}{2E} \Sigma F^2\lambda$ in order to find the internal work, as was done in the first particular case of this article. The calculation is—

Bar No.	l	a	λ	F	$F^2\lambda$
1	in. 80	sq. in. 1·6	50	+ 0·8 W	+ 32 W²
2	70	2·5	28	− 0·7 W	+ 13·7 W²
					$\Sigma F^2\lambda = + 45·7\ W^2$

$$U = \frac{1}{2E} \Sigma F^2\lambda = \frac{1}{2E} (45\cdot7\ W^2)\ ; \quad \Delta = \frac{\partial U}{\partial W} = \frac{45\cdot7 W}{E}$$

Putting $E = 13,000$ tons/sq. in., and $W = 10$ tons, $\Delta = 0\cdot035$ inch, as before.

In all cases in which a virtual load is applied to a structure, corresponding virtual reactions will, of necessity, be called into play, in order to maintain the equilibrium ; for the structure must be in equilibrium both before and after the application of the virtual load. Usually the structure will rest on fixed supports, at which the virtual reactions will act, and their magnitude can be found by the ordinary means. In the case of a structure thus supported, the displacements determined by the methods of this article will be displacements relative to the fixed supports. Thus, in the case of (i) Fig. 106, the virtual reactions at A and B due to W' can be found by taking moments, and the vertical displacement of C is the deflection of that point below the line AB. In general, it is necessary to know these reactions in order to determine the forces in the bars due to the virtual load, and hence to obtain the internal work. In a few
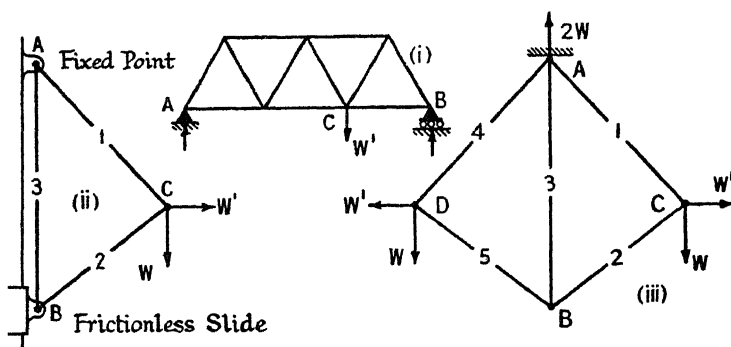
Fig. 106.

simple cases, for example Fig. 105, it is possible to determine the forces in the bars without direct reference to the reactions. If, however, the frame of Fig. 105 be modified by the introduction of a third bar AB, as shown at (ii) Fig. 106, so arranged that B is capable of vertical movement, and a virtual load W' be applied at C in order to find the horizontal displacement of that point, it will be found necessary to take the horizontal virtual reactions at A and B into account in order to determine the forces in the bars.

Suppose that two such frames be united back to back, as shown at (iii) Fig. 106, and that the complete frame is suspended from a fixed point A. So far as the applied loads W, W, are concerned, the frame is in equilibrium ; but if a virtual load W' be applied at C, in order to find the horizontal displacement of that point, it must be balanced by a second force W' at D, in order to maintain the equilibrium, and the question then arises as to the effect of this second force on the theorems established above. It is evident that the displacement of C away from AB will be the same in both (ii) and (iii) Fig. 106, and further, that the displacement

of D away from AB will likewise be of the same magnitude. [It may be imagined that bar No. 3 of (iii) is a duplicate member consisting of two bars each of the same area as bar No. 3 of (ii).] But from eq. (5), the horizontal displacement of C in (ii) is

$$\Delta = \left(\frac{\partial U}{\partial W'}\right)_{W' = 0} = \frac{\partial}{\partial W'}\left\{U_1 + U_2 + U_3\right\}_{W' = 0} \qquad . \qquad . \quad (7)$$

where U_1, U_2, and U_3 represent the internal work stored up in bars No. 1, 2, and 3 respectively. Applying this same equation to (iii)

$$\Delta = \left(\frac{\partial U}{\partial W'}\right)_{W' = 0} \quad \frac{\partial}{\partial W'}\left\{U_1 + U_2 + U_3 + U_3 + U_4 + U_5\right\}_{W' = 0} \quad (8)$$

which, since bar No. 3 is a duplicate bar appearing in both the identical frames of which (iii) is the combination, is exactly double the displacement given by eq. (7). In other words, eq. (8) gives the horizontal movement of C plus that of D in the opposite direction; that is to say, the displacement of C relative to D. If D were a fixed point, and A were capable of movement horizontally, eq. (8) would give the actual displacement of C. This is an important consideration, and applies to any displacement found by the application of a virtual load. Such a displacement is the movement of the point in question relative to the point (or points) at which the virtual reaction (or reactions) acts.

REDUNDANT FRAMES

71. Redundant Frames.—It was pointed out in § 3 that one of the necessary conditions for the statical determination of the stresses in a framed structure is that the frame must consist of sufficient members to divide it into triangles, no more, no less. If there be more than the number of bars necessary for complete triangulation, some of the bars are redundant, and the frame is called a *redundant frame*. The ordinary statical means of determining the stresses being inadequate in such cases, a redundant frame is sometimes referred to as a *statically indeterminate structure*, see § 87.

72. Stresses in Redundant Frames.— The principle of work is a convenient method of determining the forces in the bars of a redundant frame. Suppose

FIG. 107.

that an extra member CD, (i) Fig. 107, be introduced into the frame shown in Fig. 105. This member is not necessary for equilibrium, and is therefore redundant. Consider the force F_3 in this bar, and suppose it to be a tension. So far as the bars AC, CB are
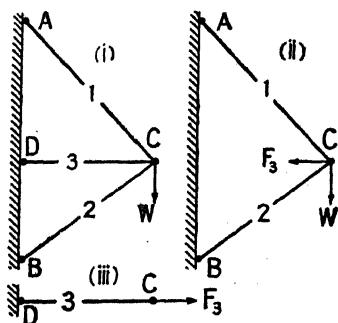
concerned, the force F_3 in CD has the effect of a horizontal pull at C, (ii) Fig. 107 ; so far as the bar CD itself is concerned, F_3 is a longitudinal tension, (iii) Fig. 107 ; (ii) and (iii) represent, therefore, the component parts of the redundant frame shown at (i). From (ii) it will be clear that F, the actual force in a bar such as AC of the frame, will be made up of two parts, F_W the force due to W, determined in the usual way after removal of the redundant member, and F_R the force due to the load F_3 which replaces the redundant member, i.e. $F = F_W + F_R$. In the case of the redundant member itself, (iii) Fig. 107, the only force in it is F_3.

Owing to the action of F_3, internal work will be stored up in the bars AC and BC of (ii), and in the bar CD of (iii). The internal work due to F_3 in any one of the bars will be $\frac{1}{2}F_R \cdot \delta l$, where F_R is the force in the bar due to F_3, and δl is the total alteration in length of the bar. Hence the total internal work stored up in the frame due to F_3 is $U_R = \frac{1}{2}\Sigma F_R \cdot \delta l$, the summation embracing all the members of the frame, including the redundant member. Now δl, the total alteration in length of any bar, is made up of two parts, that due to F_W and that due to F_R. In symbols,

$$\delta l = \frac{Fl}{Ea} = (F_W + F_R)\frac{l}{Ea} = \frac{1}{E}(F_W + F_R)\lambda, \text{ whence}$$

$$U_R = \frac{1}{2E}\Sigma(F_W + F_R)F_R\lambda \qquad . \qquad . \qquad . \quad (1)$$

This internal work is entirely due to F_3, an internal force, and not to the action of any external force on the frame. But unless some external force does work on the frame, no internal work can be stored up in it, and it follows that U_R must be zero. Hence, if E be constant,

$$\Sigma(F_W + F_R)F_R\lambda = 0 \quad . \qquad . \qquad . \qquad . \quad (2)$$

In other words, the total internal work done by the force in a redundant member on all the members of the frame, including itself, is zero.

This principle, embodied in eq. (2), enables the force in the redundant member to be calculated. It is best to adopt a tabular method of procedure as in the example below. Tensile forces are considered as positive, compressive forces negative.

Example.—Suppose that a horizontal member CD, in Fig. 107, be introduced into the frame shown in Fig. 105. Its length is 55·6 in., its area 1·39 sq. in. To find the force in this member due to a vertical load of 10 tons applied at C. The calculation is given in the Table, p. 165. The triangle of forces for F_3 is similar to (ii) Fig. 105 ; but, assuming F_3 to be a tension, the signs will be reversed.

From eq. (2), $\Sigma(F_W + F_R) F_R\lambda = 0$, hence $- 102·9 F_3 + 73·1 F_3^2 = 0$, see the Table, or $F_3 = 1·41$ tons, which is the force in the redundant member CD. Since the result comes out positive it follows that F_3 is a tension, as was assumed.

The force F_W in CD, bar No. 3, is quite correctly given as zero in

column 5 of the Table, for the bar has been removed from the frame. The total force in CD is $F_W + F_R = 0 + F_3 = F_3$, as given in column 7, which must be the case.

Bar No.	l	a	λ	F_W	F_R	$(F_W + F_R)$	$(F_W + F_R) F_R \lambda$
1	in. 80	sq. in. 1·6	50	tons. $+ 8$	$- 0·61F_3$	$+ 8 - 0·61F_3$	$-50 (8 - 0·61F_3) \times 0·61 F_3$
2	70	2·5	28	$- 7$	$- 0·72F_3$	$- 7 - 0·72F_3$	$-28(-7-0·72F_3) \times 0·72F_3$
3	55·6	1·39	40	0	$+ F_3$	$+ F_3$	$+ 40 F_3{}^2$

$$\Sigma (F_W + F_R) F_R \lambda = - 102·9 F_3 + 73·1 F_3{}^2$$

It will be observed that, by the addition of the redundant member, the force in bar No. 1 has been reduced from 8 tons to $8 - 0·61 \times 1·41 = 7·14$ tons, but the force in bar No. 2 has been increased from $- 7$ to $- 7 - 0·72 \times 1·41 = - 8·02$ tons, so that had bar No. 2 been designed to carry 7 tons only, it would be overstrained by the addition of the redundant member.

The method may be summarised as follows : Remove the redundant member from the frame, and find the values of F_W the force in each of the remaining bars due to the actual loads $W_1\ W_2\ \ldots$ Remove the loads $W_1\ W_2 \ldots$ replace the redundant member by the force F_r which it carries, and find the values of F_R the force in every bar, including the redundant member, due to F_r. Then the force in the redundant member is given by the equation $\Sigma(F_W + F_R)F_R\lambda = 0$, due account being taken of the signs of the forces. The theorem holds equally well for a frame of any type. In a case like that shown in Fig. 108, the redundant bar CD is replaced by the two forces F_rF_r, each equal to the force in CD. The frame will remain in equilibrium, and the reactions will not be affected. The total internal work done by the two internal forces F_r must be zero, and eq. (2) will therefore be applicable. In finding the value of F_R for the various bars, both forces F_r must be taken into account, but in some cases it may be convenient to treat them separately.

Fig. 108.

Now the value of F_R for any bar can be written in the form $F_R = cF_r$ (compare § 70), where c is a coefficient depending on the shape of the frame. The coefficient c is the value of F_R when F_r, the force in the
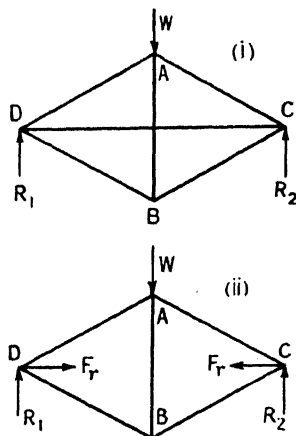
redundant member, is made equal to unity; let this value of F_R be called F', so that $c = F'$. Then eq. (2) becomes,

$$\Sigma(F_W + cF_r)cF_r\lambda = \Sigma(F_W + F_rF')F_rF'\lambda = 0$$

or, dividing each term by F_r,

$$\Sigma F_W F'\lambda + F_r\Sigma(F')^2\lambda = 0$$

from which	$F_r = -$	. (3)

an expression giving the force in the redundant member. In each case the summation includes every bar in the frame, but as pointed out above, the value of F_W for the redundant bar is zero. This formula leads to what is probably the simplest method of determining the force in a redundant member. Remove the redundant member and find the force F_W in all the remaining bars due to the actual load or loads. F_W for the redundant member is zero. Next, replace the redundant member by unit loads [for example, the two forces F_r in (ii) Fig. 108 will be put equal to unity], remove the applied loads and find F' the force in each remaining bar due to these unit loads. The value of F' for the redundant member is' unity. Both F_W and F' are now known for every bar of the frame, and eq. (3) can be solved, giving the value of F_r. As before, tensions are positive, compressions negative. A positive. answer indicates that the force in the redundant member acts on the frame in the same direction as the unit loads, a negative answer that the assumed direction should be reversed. The actual force in any bar is $F = F_W + F_rF'$.

The application of this method to the worked example on p. 164 is as follows :

Bar No.	l	a	λ	F_W	F'	$F_W F'\lambda$	$(F')^2\lambda$
	in.	sq. in.		tons.			
1	80	1·6	50	+ 8	− 0·61	− 244·0	+ 18·6
2	70	2·5	28	− 7	− 0·72	+ 141·1	+ 14·5
3	55·6	1·39	40	0	+ 1·0	0	+ 40·0
						$\Sigma = -102·9$	$+ 73·1$

From eq. (3), $F_3 = - \dfrac{102·9}{73·1}$ 1·41 tons.

73. Frames with more than one Redundant Member.—Suppose that a second redundant member CG, (i), Fig. 109, be added to the frame shown in Fig. 107. The frame will then dissect into three parts, (ii) (iii) and (iv) Fig. 109 ; (ii) shows the forces acting on the non-redundant bars, the redundant bars in (i) being replaced by the forces F_3 and F_4 which they carry ; (iii) and (iv) show the forces on the redundant bars.

Then, as before, the internal work done by the internal force F_3 on all the bars of the frame which remain after removal of the redundant members, but including that done on bar No. 3, is zero. Likewise, the internal work done by the internal force F_4 on all the bars which remain, but including that done on bar No. 4, is zero. The internal work stored in any bar due to F_3 is $\frac{1}{2}F_{R3} \cdot \delta l$, where F_{R3} is the force in that bar due to F_3, and δl is the total elongation of the bar. This elongation is in part due to F_W, the force in the bar due to the actual loads, in part due to F_{R3}, and in part due to F_{R4}, the force in the bar due to F_4. In symbols,
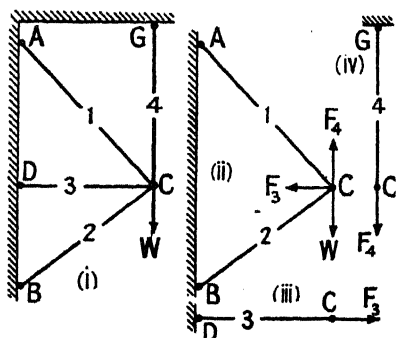
Fig. 109.

$\delta l = \dfrac{1}{E}(F_W + F_{R3} + F_{R4})\lambda$; and therefore the total work stored in all

the bars of the frame, due to F_3, is $U_{R3} = \dfrac{1}{2E}\Sigma(F_W + F_{R3} + F_{R4})F_{R3}\lambda$,

which is zero. Hence, if E be constant,

$$\Sigma(F_W + F_{R3} + F_{R4})F_{R3}\lambda = 0 \quad . \quad . \quad (1)$$

By exactly similar reasoning it follows that the internal work stored in any bar due to F_4 is $\frac{1}{2}F_{R4}\delta l$; and, therefore, that the total work stored in the frame due to F_4 is $U_{R4} = \dfrac{1}{2E}\Sigma(F_W + F_{R3} + F_{R4})F_{R4}\lambda$;

consequently, $\quad \Sigma(F_W + F_{R3} + F_{R4})F_{R4}\lambda = 0 \quad\quad (2)$

From eqs. (1) and (2), solved in tabular fashion as in the previous article, the values of F_3 and F_4 can be obtained. It is more convenient to adopt the artifice of replacing the redundant members by unit forces. As before, $F_{R3} = cF_3$, where c is a coefficient for the bar depending on the shape of the frame. If F' be the value of F_{R3} when F_3 is made equal to unity, $c = F'$, and $F_{R3} = F_3F'$. Similarly, $F_{R4} = F_4F''$, where F'' is the value of F_{R4} when F_4 is made equal to unity. Inserting these values in eqs. (1) and (2),

$$\Sigma(F_W + F_3F' + F_4F'')F_3F'\lambda = 0,$$
and $\quad\quad \Sigma(F_W + F_3F' + F_4F'')F_4F''\lambda = 0,$

from which $\quad \Sigma F_W F'\lambda + F_3\Sigma(F')^2\lambda + F_4\Sigma F'F''\lambda = 0 \quad . \quad . \quad (3)$

$$\Sigma F_W F''\lambda + F_3\Sigma F'F''\lambda + F_4\Sigma(F'')^2\lambda = 0 \quad . \quad . \quad (4)$$

The solution of these two equations will give the values of F_3 and F_4, the unknown forces in the redundant members.

Example.—Given a frame of the type shown in Fig. 109, of the dimensions given in the following Table, and loaded with a vertical load of 10 tons at C, to find the stresses in the redundant members, bars Nos. 3

and 4. This is exactly the same frame as in the previous example, with the addition of the member CG. Tensions are +, compressions — .

Bar No.	l	a	λ	F_W	F'	F''	$F_W F'\lambda$	$F_W F''\lambda$	$F'F''\lambda$	$(F')^2\lambda$	$(F'')^2\lambda$
	in.	sq. in.		tons.	tons.	tons.					
1	80	1·6	50	+ 8	− 0·61	− 0·8	− 244·0	− 320·0	+ 24·4	+ 18·6	+ 32·0
2	70	2·5	28	− 7	− 0·72	+ 0·7	+ 141·1	− 137·2	− 14·1	+ 14·5	+ 13·7
3	55·6	1·39	40	0	+ 1	0	—	—	—	+ 40·0	—
4	57·5	1·15	50	0	0	1	—	—	—	—	+ 50·0

$$\Sigma = -102\cdot9 - 457\cdot2 + 10\cdot3 + 73\cdot1 + 95\cdot7$$

In this Table the values of F_W, the force in the bars remaining after removal of the redundant members, due to the load of 10 tons, are the same as in the previous example. The values of F', the force in the bars due to a unit load replacing the redundant bar No. 3, are identical with those of F_R, column 6 of the Table on p. 165, if $F_3 = 1$. The values of F'', the force in the bars due to a unit load replacing the redundant bar No. 4, are evidently one-tenth the values of F_W, and of reversed sign. It is to be observed that F_W for each of the redundant bars is zero, and also that F'' for bar No. 3, and F' for bar No. 4 are likewise zero. Inserting the numerical values of the summations in eqs. (3) and (4),

$$- 102\cdot9 + 73\cdot1F_3 + 10\cdot3F_4 = 0$$
$$- 457\cdot2 + 10\cdot3F_3 + 95\cdot7F_4 = 0$$

from which $F_3 = 0\cdot75$ ton, and $F_4 = 4\cdot70$ tons. Since both answers come out positive, the assumed directions for the unit loads were correct, and both F_3 and F_4 are tensions.

Knowing F_3 and F_4, the forces in all the bars of the frame can at once be determined. For example, the actual force in bar No. 1 is $F_W + F_3F'$ $+ F_4F'' = 8 - 0\cdot75 \times 0\cdot61 - 4\cdot7 \times 0\cdot8 = 3\cdot78$ tons ; and in bar No. 2 is $- 7 - 0\cdot75 \times 0\cdot72 + 4\cdot7 \times 0\cdot7 = - 4\cdot25$ tons.

Note.—In general, two unit forces ($F_r = 1$) must be applied to replace each redundant bar; see Fig. 108.

74. Redundant Frames. General Case.—The method of the preceding article will apply whatever be the number of redundant bars in the frame. If in a framework of n bars, the pth, qth, and rth be redundant, it may be shown, exactly as in § 73, that

$$\left.\begin{array}{l} \Sigma(F_W + F_{Rp} + F_{Rq} + F_{Rr})F_{Rp}\lambda = 0 \\ \Sigma(F_W + F_{Rp} + F_{Rq} + F_{Rr})F_{Rq}\lambda = 0 \\ \Sigma(F_W + F_{Rp} + F_{Rq} + F_{Rr})F_{Rr}\lambda = 0 \end{array}\right\} \qquad . \quad (1)$$

[compare eq. (1), § 73], which equations, solved as simultaneous, will give the values of F_p, F_q, and F_r, the forces in the redundant bars. If there be m redundant bars in the frame, m equations of the above type will be

obtained, from which the m unknown forces can be determined. If, as in the previous article, $F_{Rp} = F_p F'$; $F_{Rq} = F_q F''$; and $F_{Rr} = F_r F'''$, eq. (1) becomes,

$$\left.\begin{array}{l} \Sigma(F_W + F_p F' + F_q F'' + F_r F''')F'\lambda = 0 \\ \Sigma(F_W + F_p F' + F_q F'' + F_r F''')F''\lambda = 0 \\ \Sigma(F_W + F_p F' + F_q F'' + F_r F''')F'''\lambda = 0 \end{array}\right\} \qquad . \quad . \quad (2)$$

and

$$\left.\begin{array}{l} \Sigma F_W F'\lambda + F_p \Sigma F' F'\lambda + F_q \Sigma F'' F'\lambda + F_r \Sigma F''' F'\lambda = 0 \\ \Sigma F_W F''\lambda + F_p \Sigma F' F''\lambda + F_q \Sigma F'' F''\lambda + F_r \Sigma F''' F''\lambda = 0 \\ \Sigma F_W F'''\lambda + F_p \Sigma F' F'''\lambda + F_q \Sigma F'' F'''\lambda + F_r \Sigma F''' F'''\lambda = 0 \end{array}\right\} \quad . \quad (3)$$

from which the law of formation is evident, and corresponding equations can be at once written down for any number of redundant bars. The summations embrace all members of the frame.

To find the forces in the redundant members, remove all these members from the frame, and find the force F_W in all the bars remaining due to the actual loads. F_W for each redundant bar is zero. Next, remove the actual loads and replace one of the redundant members by two loads of unit magnitude, acting one at each point of attachment of the redundant bar. Find the force F' in all the remaining bars due to these unit loads. F' for this particular redundant bar is unity, for all the others zero. Next, remove these unit loads and replace a second of the redundant bars by two other loads of unit magnitude. Find the force F'' in all the remaining bars due to these loads ; F'' for the second redundant bar is unity, for all the others zero. Repeat this process for every redundant bar. The value of F_W, F', F'', F''', . . . for every bar in the structure is now known. Effect the summations implied in eq. (3) by a tabular calculation. If there be m redundant bars, there will be $\frac{1}{2}(m)(m + 3)$ summations necessary, from which the magnitudes of the forces in the redundant members can be obtained by inserting the numerical additions in eq. (3). Tensions should be called $+$, compressions $-$. For convenience in calculation, the forces in all redundant members should be assumed to be tensions and called positive. If the roots of eq. (3) come out positive, it implies that this assumption is correct ; if negative, that the force is, in fact, a compression.

For a worked example, see § 76.

75. Principle of Least Work.—It follows from the principle of conservation of energy that the work stored up in an elastic system in equilibrium, due to the action of external forces, must always be a minimum. This is called the *principle of least work,* and it is true whatever may be the character of the strains produced. By its aid the forces in the members of a redundant frame can be determined.

For a framed structure, the principle of least work may be deduced from § 70 thus : Let (i), Fig. 110, be a frame containing a redundant member CD. Replace the redundant member by the two forces $F_r F_r$, each equal to the force in that member, which will be assumed

tensile, (ii) Fig. 110. The equilibrium of the frame will not be affected by this. Then from eq. (4), § 70, the displacement of the point C relative to the point D is $\Delta = \dfrac{\partial U}{\partial W} = \dfrac{\partial U}{\partial F_r}$, where U is the total internal work stored in the system shown at (ii), and W, in the present case the force F_r, is the force applied at C in the direction CD. Each of the points C and D will be displaced by an amount $\Delta/2$.

But if the force in CD is a tensile force, the deformation of the frame must have increased the length CD; that is to say, both C and D have moved away from AB to positions such as C' and D', (ii) Fig. 110. The movement of C and D is therefore in an opposite direction to the sense of the forces F_r, and the sign of Δ is negative. Let δl_r be the actual increase in length of the bar CD, of which the original length was l_r.

FIG. 110.

Then $\delta l_r = -\Delta = -\dfrac{\partial U}{\partial F_r}$. But if a_r be the area of CD, the alteration of length due to a force F_r is,

$$\delta l_r = \frac{F_r l_r}{E a_r} = \frac{1}{E} F_r \lambda_r = -\frac{\partial U}{\partial F_r}$$

and therefore, $\qquad \dfrac{\partial U}{\partial F_r} + \dfrac{1}{E} F_r \lambda_r = 0$ . . . (1)

Now the total work stored in the whole structure is $U_T = U + \dfrac{1}{2E} F_r^2 \lambda_r$, where U is the internal work stored in the essential bars of the frame shown at (ii), Fig. 110, and $\dfrac{1}{2E} F_r^2 \lambda_r$ is the internal work stored in the redundant member. But the first differential coefficient of this expression with respect to F_r is $\dfrac{\partial U_T}{\partial F_r} = \dfrac{\partial U}{\partial F_r} + \dfrac{1}{E} F_r \lambda_r$, which, by eq. (1), is equal to zero ; it is possible to show also that $\partial^2 U_T / \partial F_r^2$ is positive, whence it follows that the magnitude of F_r is such that the total work done is a minimum.

Now $U_T = \dfrac{1}{2E} \Sigma F^2 \lambda$, see eq. (2), § 68, the summation including the
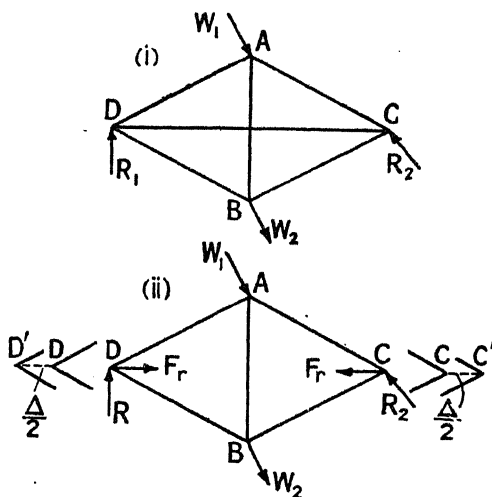
redundant member. Since, for a minimum,

$$\frac{\partial U_T}{\partial F_r} = 0 \ ; \ \ \frac{\partial}{\partial F_r} \ \frac{1}{2E} \ \Sigma F^2 \lambda \Big\} \ : 0,$$

and

$$\frac{\partial}{\partial F_r} \Sigma F^2 \lambda = \frac{\partial}{\partial F_r} \Sigma (F_W + F_R)^2 \lambda = 0 \qquad . \ (2)$$

for $F = F_W + F_R$, § 72. From this equation the unknown force F_r can be determined.

In like manner, if there be more than one redundant bar, and each be replaced in the frame by forces equal to the force which it carries, the first partial differential coefficient of the expression for the total internal work stored in the frame with respect to the force in each of the redundant members will be zero, and the second will be positive, therefore the total work done must be a minimum. If, in a frame, the pth, qth, and rth bars be redundant, three equations similar to eq. (1) will be obtained.

$$\frac{\partial U}{\partial F_p} + \frac{1}{E} \ F_p \lambda_p = 0 = \frac{\partial U_T}{\partial F_p} \Big\backslash$$

$$\frac{\partial U}{\partial F_q} + \frac{1}{E} \ F_q \lambda_q = 0 \qquad \frac{\partial U_T}{\partial F_q} \qquad (3)$$

$$\frac{\partial U}{\partial F_r} + \frac{1}{E} \ F_r \lambda_r \quad \ 0 = \frac{\partial U_T}{\partial F_r} \Big/$$

from which the three forces F_p, F_q, and F_r can be obtained, and so on, however many redundant bars there may be. .

Putting in the value $U_T = \frac{1}{2E} \ \Sigma F^2 \lambda$, eq. (3) becomes,

$$\frac{\partial U_T}{\partial F_p} - \frac{\partial}{\partial F_p} \left\{ \frac{1}{2E} \ \Sigma F^2 \lambda \right\} = 0 = \frac{\partial}{\partial F_p} \ \Sigma F^2 \lambda$$

and so on. Hence, since $F = F_W + F_{Rp} + F_{Rq} + F_{Rr}$,

$$\frac{\partial}{\partial F_p} \Sigma F^2 \lambda = \frac{\partial}{\partial F_p} \ \Sigma (F_W + F_{Rp} + F_{Rq} + F_{Rr})^2 \lambda = 0$$

$$\frac{\partial}{\partial F_q} \Sigma F^2 \lambda = \frac{\partial}{\partial F_q} \ \Sigma (F_W + F_{Rp} + F_{Rq} + F_{Rr})^2 \lambda = 0 \qquad (4)$$

$$\frac{\partial}{\partial F_r} \Sigma F^2 \lambda = \frac{\partial}{\partial F_r} \ \Sigma (F_W + F_{Rp} + F_{Rq} + F_{Rr})^2 \lambda = 0$$

These equations, solved as simultaneous, give the values of F_p, F_q, and F_r.

Example.—The following is an application of the above theory to the example of Fig. 109. F_3 and F_4, the unknown forces in the redundant members, will be supposed tensile, as before. The calculation for the total work done is given in the following Table (see § 73). F_{R3} is the force in a bar due to F_3, and F_{R4} that due to F_4. Tensions are positive, compressions negative.

Bar No.	l	a	λ	F_W	F_{R3}	F_{R4}	$(F_W + F_{R3} + F_{R4})$	$(F_W + F_{R3} + F_{R4})^2\lambda$
	in.	sq. in.		tons.	tons.	tons.		
1	80	1·6	50	$+ 8$	$-0·61F_3$	$- 0·8F_4$	$(+ 8 - 0·61F_3 \\ - 0·8F_4)$	$50(+ 8 - 0·61F_3 \\ - 0·8F_4)^2$
2	70	2·5	28	$- 7$	$- 0·72F_3$	$+ 0·7F_4$	$(- 7 - 0·72F_3 \\ + 0·7F_4)$	$28(- 7 - 0·72F_3 \\ + 0·7F_4)^2$
3	55·6	1·39	40	0	$+ F_3$	0	$+ F_3$	$+ 40F_3{}^2$
4	57·5	1·15	50	0	0	$+ F_4$	$+ F_4$	$+ 50F_4{}^2$

Then U_T, the total internal work stored in the frame, is

$$\frac{1}{2E} \Sigma(F_W + F_{R3} + F_{R4})^2\lambda = \frac{1}{2E} \text{ (addition of the last column).}$$

The magnitude of F_3 and F_4 must be such that U_T is a minimum, i.e. $\dfrac{\partial U_T}{\partial F_3}$ and $\dfrac{\partial U_T}{\partial F_4}$ must both equal zero [see eq. (3)]. It is convenient to differentiate the last column line by line, and then add the results, thus :

$$\frac{\partial U_T}{\partial F_3} = 100(8 - 0·61F_3 - 0·8F_4)(- 0·61)$$
$$+ 56(- 7 - 0·72F_3 + 0·7F_4)(- 0·72) + 80F_3 = 0$$

$$\frac{\partial U_T}{\partial F_4} = 100(8 - 0·61F_3 - 0·8F_4)(- 0·8)$$
$$+ 56(- 7 - 0·72F_3 + 0·7F_4)(+ 0·7) + 100F_4 = 0$$

whence,

$$- 102·9 + 73·1F_3 + 10·3F_4 = 0 ; \quad - 457·2 + 10·3F_3 + 95·7F_4 = 0$$

Solving these equations as simultaneous,

$$F_3 = + 0·75 \text{ ton, } F_4 = + 4·70 \text{ tons, as before.}$$

It will be seen that the above process is, in effect, a solution of eq. (4). For a further worked example of the method, see § 76.

It may be shown that the equations of § 74 for any redundant frame follow from the principle of least work thus : Suppose that the pth, qth, and rth bars of the frame be redundant ; and, as before, let F_p, F_q, and F_r be the forces in these redundant bars. Replace each redundant member by two forces, each equal to the force in the replaced bar. Then the force in any member due to F_p will be $c'F_p$; due to F_q will be $c''F_q$; and due to F_r will be $c'''F_r$; where c', c'', and c''', are coefficients depending on the shape of the frame. Hence U_T, the total internal work, will be given by an expression of the form

$$U_T = \frac{1}{2E} \Sigma(F_W + c'F_p + c''F_q + c'''F_r)^2\lambda$$

the summation including all the bars of the frame (compare § 72, and the Table above). But from eq. (3), $\dfrac{\partial U_T}{\partial F_p} = \dfrac{\partial U_T}{\partial F_q} = \dfrac{\partial U_T}{\partial F_r} = 0,$

whence, $\dfrac{\partial U_T}{\partial F_p} = 0 = \Sigma(F_W + c'F_p + c''F_q + c'''F_r)c'\lambda$

$\dfrac{\partial U_T}{\partial F_q} = 0 = \Sigma(F_W + c'F_p + c''F_q + c'''F_r)c''\lambda$

$\dfrac{\partial U_T}{\partial F_r} = 0 = \Sigma(F_W + c'F_p + c''F_q + c'''F_r)c'''\lambda$

Since the force in any bar due to F_p is $c'F_p$, it follows that c' will be equal to F', the force in the bar due to F_p, if F_p = unity. Similarly $c'' = F''$, and $c''' = F'''$. The above equation becomes, therefore,

$$\begin{rcases} \Sigma(F_W + F_pF' + F_qF'' + F_rF''')F'\lambda = 0 \\ \Sigma(F_W + F_pF' + F_qF'' + F_rF''')F''\lambda = 0 \\ \Sigma(F_W + F_pF' + F_qF'' + F_rF''')F'''\lambda = 0 \end{rcases} \quad (5)$$

This equation is identical with eq. (2) of § 74, and it follows that the other equations and methods of that article are deducible from the principle of least work.

76. Redundant Frame. Worked Example.—As a practical example of the above theory, consider the unsymmetrically loaded plane frame shown at (i) Fig. 111. To find the areas of cross section of the members,
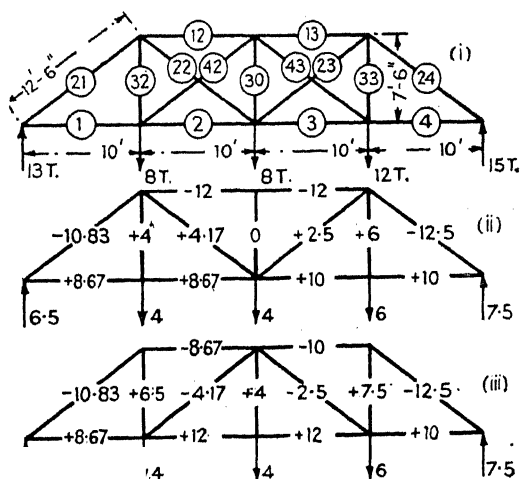
Fig. 111.

it must be divided into its component frames (ii) and (iii). The forces in all the bars can then be found in the usual way, and are given in the Table on p. 174; the combined bar forces for the complete frame are given in column 4.

The necessary areas of cross section can now be found, and are given in column (3) of the second Table. Knowing the values of l and a, the values of λ can be calculated; these are tabulated on p. 175. The gross area of the members should be inserted in column (3), both for ties and struts.

Bar No.	Forces in Bars.		
	Frame (ii).	Frame (iii).	Total.
1	+ 8·67	+ 8·67	+ 17·33
2	+ 8·67	+ 12·0	+ 20·67
3	+ 10·0	+ 12·0	+ 22·0
4	+ 10·0	+ 10·0	+ 20·0
12	− 12·0	− 8·67	− 20·67
13	− 12·0	− 10·0	− 22·0
21	− 10·83	− 10·83	− 21·67
22	+ 4·17	—	+ 4·17
23	+ 2·5	—	+ 2·5
24	− 12·5	− 12·5	− 25·0
42	—	− 4·17	− 4·17
43	—	− 2·5	− 2·5
30	0·0	+ 4·0	+ 4·0
32	+ 4·0	+ 6·5	+ 10·5
33	+ 6·0	+ 7·5	+ 13·5

The calculations for the stresses in a redundant frame depend essentially on the alteration in length of the bars. In most ties, the rivet holes only occur at the ends of the member, and it is the gross area which determines the alteration in length δl. In ties composed of sections riveted together throughout their length, the area lost by rivet holes would increase the total extension from panel point to panel point, but it is usual to neglect this increase in ordinary calculations. Any effect which the attachments at the ends of the bars may have is also neglected.

The next step is to remove the two redundant members No. 42 and No. 43 from (i) Fig. 111, and to calculate the values of F_W from the given loads (i), Fig. 112. *Note*: F_W must not be

Fig. 112.

taken from the combined forces in col. 4 of the first Table ; in this case the values of F_W are double the figures given in col. (2) of that Table. The values of F' and F'' are found by replacing the redundant members, one at a time, by two forces of unit magnitude, supposed tensile, as shown at (ii) and (iii), Fig. 112, and calculating the forces in the remaining bars. In the present instance, as shown in the figure, only one panel is affected, the forces in the remaining bars being zero. The values of F_W,

Bar No.	l	a	λ	F_W	F'	F''	$F_W F'\lambda$	$F_W F''\lambda$	$F' F''\lambda$	$(F')^2\lambda$	$(F'')^2\lambda$	Actual Force F	From Col. 4, Tab. 1
	in.	sq. in.		tons.	tons.	tons.						tons.	tons.
1	120	4.34	27.7	+17.33	0	0						+17.33	+17.33
2	120	4.34	27.7	+17.33	−0.8	−0.8	−384.1			+17.7	+17.7	+18.63	+20.67
3	120	4.34	27.7	+20.0	0	0		−443.2				+19.59	+22.0
4	120	4.34	27.7	+20.0	0	0						+20.0	+20.0
12	120	7.22	16.6	−24.0	−0.8	0	+318.7			+10.6		−22.7	−20.67
13	120	7.22	16.6	−24.0	0	−0.8		+318.7			+10.6	−24.41	−22.0
21	150	7.22	20.8	−21.67	0	0						−21.67	−21.67
22	150	2.17	69.2	+8.33	+1.0	0	+576.7			+69.2		+6.70	+4.17
23	150	2.17	69.2	+5.0	0	+1.0		+346.0			+69.2	+5.51	+2.5
24	150	7.22	20.8	−25.0	0	0						−25.0	−25.0
42	150	2.17	69.2	—	+1.0	0				+69.2		−1.63	−4.17
43	150	2.17	69.2	—	0	+1.0					+69.2	+0.51	−2.5
30	90	2.17	41.4	0	−0.6	−0.6			+14.9	+14.9	+14.9	+0.67	+4.0
32	90	2.17	41.4	+8.0	−0.6	0	−198.7			+14.9		+8.98	+10.5
33	90	2.17	41.4	+12.0	0	−0.6		−298.1			+14.9	+11.69	+13.5
							+312.6	−76.6	+14.9	+196.5	+196.5		

$$\Sigma = +312.6 - 76.6 + 14.9 + 196.5$$

F′, and F″ are carried to the second Table, and the calculation follows the course set forth in § 73. If F_{42} and F_{43} be the actual forces in the two redundant bars, since there are only two redundant members, eqs. (3) and (4), § 73, reduce to,

$$\Sigma F_W F'\lambda + F_{42}\, \Sigma(F')^2\lambda + F_{43}\, \Sigma F'F''\lambda = 0$$
$$\Sigma F_W F'\lambda + F_{42}\, \Sigma F'F''\lambda + F_{43}\, \Sigma(F'')^2\lambda = 0$$

Inserting numbers from the Table,

$$312 \cdot 6 + 196 \cdot 5F_{42} + \quad 14 \cdot 9F_{43} = 0$$
$$- 76 \cdot 6 + \quad 14 \cdot 9F_{42} + 196 \cdot 5F_{43} = 0$$

from which, $F_{42} = -1 \cdot 63$ tons, and $F_{43} = +0 \cdot 51$ ton. The actual force F in every bar may now be calculated. In any bar

$$F = F_W + F_{42}F' + F_{43}F'',$$

§ 73. Thus in bar No. 2,

$$F_2 = +17 \cdot 33 + (-1 \cdot 63)(-0 \cdot 8) + 0 \cdot 51 \times 0 = +18 \cdot 63 \text{ tons,}$$

and so on for the others. These values are tabulated in the last column but one of the second Table, and for comparison the approximate values from the first Table are given in the final column.

As an alternative treatment of the problem, the method of least work, § 75, will next be applied. The calculation is given in the third Table, which is self explanatory. The first five columns have been taken from the preceding Tables; cols. 8 and 9 are obtained from col. 7 by differentiating line by line. Let $F_{42} = F_p$, and $F_{43} = F_q$; then from eq. (4), § 75, and by addition from the last two columns of the Table,

$$\frac{\partial}{\partial F_p}\, \Sigma F^2\lambda = +625 \cdot 2 + 393 \cdot 0F_p + 29 \cdot 8F_q = 0$$

$$\frac{\partial}{\partial F_q}\, \Sigma F^2\lambda = -153 \cdot 2 + 29 \cdot 8F_p + 393 \cdot 0F_q = 0$$

These equations are evidently the same as those previously obtained, except that the coefficients are doubled. The values of $F_{42} = F_p$, and F_{43} F_p, are therefore the same as before, as are also the values of F obtained from col. 6 of the third Table.

77. Displacements of Redundant Frames. —Having found the forces in the redundant bars, and thence the actual forces in the remaining bars, the displacement (Williot) diagram, § 12, can then be drawn in the usual way for the frame without the redundant bars, which diagram gives the displacements of all the node points in the frame. Alternatively, the methods of § 15 or § 70 may be applied.

$$\Delta_u = 0 \cdot 0023 = \delta l_3$$

Fig. 113.

As a simple instance, consider the example of § 73. From the data there given, $F_1 = 3 \cdot 78$ tons, $\lambda_1 = 50$, and hence $\delta l_1 = 0 \cdot 0145$ inch ;
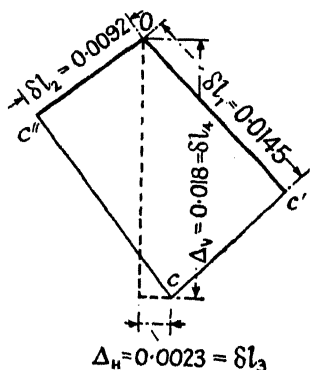
Bar No.	λ	F_W	F_{Rp}	F_{Rq}	$F = F_W + F_{Rp} + F_{Rq}$	$F^2\lambda$	$\dfrac{\partial}{\partial F_p}\,\Sigma F^2\lambda$	$\dfrac{\partial}{\partial F_q}\,\Sigma F^2\lambda$
		tons.	tons.	tons.	tons.			
1	27.7	$+17.33$	0	0	$+17.33$	27.7×17.33^2	0	0
2	27.7	$+17.33$	$-0.8\,F_p$	0	$+17.33 - 0.8\,F_p$	$27.7(17.33 - 0.8\,F_p)^2$	$27.7 \times 2(17.33 - 0.8\,F_p)(-0.8)$	0
3	27.7	$+20.0$	0	$-0.8\,F_q$	$+20.0 - 0.8\,F_q$	$27.7(20.0 - 0.8\,F_q)^2$	0	$27.7 \times 2(20.0 - 0.8\,F_q)(-0.8)$
4	27.7	$+20.0$	0	0	$+20$	27.7×20^2	0	0
12	16.6	-24.0	$-0.8\,F_p$	0	$-24.0 - 0.8\,F_p$	$16.6(-24.0 - 0.8\,F_p)^2$	$16.6 \times 2(-24 - 0.8\,F_p)(-0.8)$	0
13	16.6	-24.0	0	$-0.8\,F_q$	$-24.0 - 0.8\,F_q$	$16.6(-24.0 - 0.8\,F_q)^2$	0	$16.6 \times 2(-24 - 0.8\,F_q)(-0.8)$
21	20.8	-21.67	0	0	-21.67	$20.8(-21.67)^2$	0	0
22	69.2	$+8.33$	$+F_p$	0	$+8.33 + F_p$	$69.2(8.33 + F_p)^2$	$69.2 \times 2(8.33 + F_p)$	0
23	69.2	$+5.0$	0	$+F_q$	$+5.0 + F_q$	$69.2(5.0 + F_q)^2$	0	$69.2 \times 2(5.0 + F_q)$
24	20.8	-25.0	0	0	-25.0	$20.8(-25.0)^2$	0	0
42	69.2	$-$	$+F_p$	0	$+F_p$	$69.2\,F_p^2$	$69.2 \times 2\,F_p$	0
43	69.2	$-$	0	$+F_q$	$+F_q$	$69.2\,F_q^2$	0	$69.2 \times 2\,F_q$
30	41.4	0	$-0.6\,F_p$	$-0.6\,F_q$	$-0.6\,F_p - 0.6\,F_q$	$41.4(-0.6\,F_p - 0.6\,F_q)^2$	$41.4 \times 2(-0.6\,F_p - 0.6\,F_q)(-0.6)$	$41.4 \times 2(-0.6\,F_p - 0.6\,F_q)(-0.6)$
32	41.4	$+8.0$	$-0.6\,F_p$	0	$+8.0 - 0.6\,F_p$	$41.4(8.0 - 0.6\,F_p)^2$	$4.14 \times 2(8.0 - 0.6\,F_p)(-0.6)$	0
33	41.4	$+12.0$	0	$-0.6\,F_q$	$+12.0 - 0.6\,F_q$	$41.4(12.0 - 0.6\,F_q)^2$	0	$41.4 \times 2(12.0 - 0.6\,F_q)(-0.6)$

$F_2 = 4\cdot25$ tons, $\lambda_2 = 28$, and hence $\delta l_2 = 0\cdot0092$ inch. The displacement diagram for the point C is shown to scale in Fig. 113, from which $\Delta_V = 0\cdot018$ inch, and $\Delta_H = 0\cdot0023$ inch. As a check on the accuracy of the working, it will be observed that Δ_V must be the alteration in length of bar No. 4, i.e. δl_4, and Δ_H the alteration in length of bar No. 3, i.e. δl_3. But

$$F_4 = \frac{E \times \delta l_4}{\lambda_4} = \frac{13000 \times 0\cdot018}{50} = 4\cdot7 \text{ tons.}$$

$$F_3 = \frac{E \times \delta l_3}{\lambda_3} = \frac{13000 \times 0\cdot0023}{40} = 0\cdot75 \text{ ton}$$

as given in § 73, which verifies the values of Δ_V and of Δ_H. It will be noted that the displacement diagram indicates an extension of both bars, implying that both forces are tensile.

LEAST WORK—GENERAL THEORY

78. General Expression of Least Work.—The principle of least work is equally true whatever may be the character of the strains set up in the statically indeterminate structure. The total internal work stored up, due to whatever agency, must be a minimum. If an indeterminate force, bending moment, or shearing force act on the structure, the magnitude of that force, moment, or shearing force must be such that the total internal work, including the effect of the unknown force or moment, is a minimum. If then an expression be found for the total internal work stored up in the structure, the first differential coefficient of this expression with respect to the unknown force or moment must be zero. This is true for each of the unknowns separately considered, however many there be. By equating each differential coefficient to zero, a sufficient

FIG. 114.

number of equations is obtained to determine all the unknown forces or. moments.

The general expression for the total strain energy in a member of length l, (i) Fig. 114, subjected to a direct force F, a shearing force S, a bending moment Mb, and a twisting moment Mt has been shown to be [see eq. (5), § 148, Vol. I],

$$U = \frac{1}{2E}\int_0^l \frac{F^2}{a} \cdot dx + \frac{1}{2G}\int_0^l \frac{\zeta S^2}{a} \cdot dx + \frac{1}{2E}\int_0^l \frac{Mb^2}{I} \cdot dx + \frac{1}{2}\int_0^l \frac{Mt^2}{\Phi} \cdot dx \quad (1)$$

a is the area, I the moment of inertia, ζ a coefficient depending on the distribution of shear stress over the cross section, and Φ the torsional rigidity of the cross section.

To make this expression applicable to structures generally, it is necessary to modify it slightly. In order to include the case of a curved beam, δx will be changed to δl, an elementary length of the centre line,
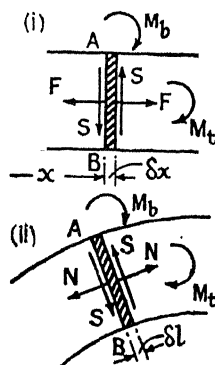
(ii) Fig. 114. Also, in the case of a curved beam, the symbol F for the normal force on the cross section will be replaced by N, to distinguish it from the longitudinal force in a bar which might form part of the same system. Using F to denote such a longitudinal force, and assuming the area of the bar to be constant as in an ordinary braced frame, the first integral becomes for a tie bar or a strut

$$\frac{1}{2E}\int_0^l \frac{F^2}{a} \cdot dx = \Sigma \frac{F^2 l}{2Ea}$$

the sign Σ indicating that all such bars in the frame under consideration are to be included. Again, in order that the equation may apply to composite frames, § 245, the symbols E and G will be retained within the integral. Then eq. (1) becomes

$$U = \Sigma \frac{F^2 l}{2Ea} + \int_0^l \frac{N^2}{2Ea} \cdot dl + \int_0^l \frac{\zeta S^2}{2Ga} \cdot dl + \int_0^l \frac{M_b^2}{2EI} \cdot dl + \int_0^l \frac{M_t^2}{2\Phi} \cdot dl \quad (2)$$

It is to be understood that only such terms as are applicable are to be included in any particular case, and that if more than one member of the structure is subjected to bending and/or torsion, a summation sign Σ is to be prefixed to the appropriate term.

If then there be at some place in the structure a force F_0 on a bar ; a direct force N_0 ; a shearing force S_0 ; a bending moment M_{b_0} ; and/or a twisting moment M_{t_0} ; each an indeterminate magnitude, it follows from the principle of least work that the magnitude of each of these unknowns must be such that the internal work U is a minimum with respect to each unknown separately considered, i.e. that

$$\frac{\partial U}{\partial F_0} = \frac{\partial U}{\partial N_0} = \frac{\partial U}{\partial S_0} = \frac{\partial U}{\partial M_{b_0}} = \frac{\partial U}{\partial M_{t_0}} = 0 \qquad . \qquad . \quad (3)$$

Instead of finding U by effecting the integrations in eq. (2) and then differentiating, it is often convenient first to differentiate eq. (2) and afterwards to integrate, see § 79 following.

The wider application of the above equations will be found in § 91, et seq.

79. Applications of the Principle of Least Work. —Consider the case of a rigid rectangular frame subjected to tensile forces WW as shown in Fig. 115. This frame is statically indeterminate. Bending moments will be set up in all the bars of the frame, the magnitudes of which may be found by means of the principle of least work. Due to the symmetry of the conditions, the stresses on the cross section at A will be equivalent to a longitudinal tension W/2 and a bending moment M_0; the shearing force at this section will be zero. The internal work stored up in the frame can be obtained from eq. (1), § 78 ; to simplify the analysis, the work stored up due to the longitudinal tensions, and shearing forces, will
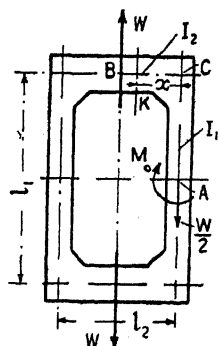
Fig. 115.

be neglected in comparison with that due to the bending moments. Then, for the quadrant AB, using the third term of eq. (1),

$$U_{AB} = \frac{1}{2E}\int_0^l \frac{M_b^2}{I} \cdot dx = \frac{1}{2EI_1}\int_A^C M_0^2 \cdot dx + \frac{1}{2EI_2} M_K^2 \cdot dx$$

where $M_K = M_0 + Wx/2$ is the bending moment at any point K in CB, distant x from C; hence,

$$U_{AB} = \frac{1}{2EI_1}\int_0^{l_1/2} M_0 \; dx + \frac{1}{2EI_2}\int_0^{l_2/2}\left(M_0 + \frac{Wx}{2}\right) dx$$

or for the whole frame,

$$U = 4\left[\frac{1}{2EI_1} \cdot \frac{M_0^2 l_1}{2} + \frac{1}{2EI_2}\left\{\frac{M_0^2 l_2}{2} + \frac{M_0 W l_2^2}{2} + \frac{}{96}\right\}\right]$$

The statically indeterminate magnitude in this equation is M_0, and from eq. (3), § 78,

$$\frac{\partial U}{\partial M_0} = 0 = 4\left[\frac{M_0 l_1}{2EI_1} + \frac{1}{2EI_2}\left\{M_0 l_2 + \frac{W l_2}{}\right\}\right]$$

whence,

$$M_0 = -\frac{W I_1 l_2^2}{8(I_1 l_2 + I_2 l_1)}$$

The negative sign implies that M_0 acts in the opposite direction to that shown in Fig. 115. Knowing M_0 the bending moment and stress everywhere in the frame can be found.

An investigation of the stresses in the transverse framing of a ship calls for an application of the principle of least work. Fig. 116 represents half such a transverse frame. Assume that it is cut through at A, and let N_0, S_0, and M_0 denote the direct force, the shearing force, and the bending moment, respectively, acting on the cut section, all at present unknown. Then, knowing the external water pressure, and the internal and deck loads WW acting on the frame, the corresponding values of N, S, and M, at any section K,

FIG. 116.

can be calculated in terms of N_0, S_0, and M_0. The total internal work stored up in the frame can be calculated from the second, third, and fourth terms of eq. (2), § 78,
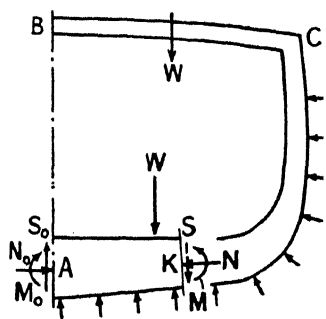
$$U = \frac{1}{2E}\int_A^B \frac{N^2}{a} \cdot dl + \frac{1}{2G}\int \frac{\zeta S^2}{} \cdot dl + \frac{1}{2E}\int_A^B \frac{M_b^2}{I} \cdot dl$$

integration being taken right round the frame from A to B; or, if the conditions be asymmetrical, right round the complete frame. In this problem there are three statically indeterminate magnitudes, N_0, S_0, and M_0, so that the value of U must be a minimum with regard to each

[eq. (3), § 78] ; or $\dfrac{\partial U}{\partial N_0} = \dfrac{\partial U}{\partial S_0} = \dfrac{\partial U}{\partial M_0} = 0$. These three equations serve to determine the three unknowns and hence the stresses everywhere in the frame.

It is convenient in practical cases to write these expressions thus :

$$\frac{\partial U}{\partial N_0} = \frac{1}{E}\int_A^B \frac{N}{a} \cdot \frac{\partial N}{\partial N_i}\, dl + \frac{1}{G}\int_A^B \frac{\zeta S}{a} \cdot \frac{\partial S}{\partial N_i} + \frac{1}{E}\int_A^B \frac{M_b}{I}\, \frac{\partial M_b}{\partial N_0}\, dl = 0$$

$$\frac{\partial U}{\partial S_0} = \frac{1}{E}\int_A^B \frac{N}{a} \cdot \frac{\partial N}{\partial S_0}\, dl + \frac{1}{G}\int_A^B \frac{\zeta S}{a} \cdot \frac{\partial S}{\partial S_0}\, dl + \frac{1}{E}\int_A^B \frac{M_b}{I}\, \frac{\partial M_b}{\partial S_0}\, dl = 0$$

$$\frac{\partial U}{\partial M_0} = \frac{1}{E}\int_A^B \frac{N}{a} \cdot \frac{\partial N}{\partial M_0}\, dl + \frac{1}{G}\int_A^B \frac{\zeta S}{a} \cdot \frac{\partial S}{\partial M_0}\, dl + \frac{1}{E}\int \frac{M_b}{I}\, \frac{\partial M_b}{\partial M_0}\, dl = 0$$

that is, to differentiate first, and integrate afterwards.

For practical examples see Biles, *The Design and Construction of Ships*, Vol. I, Chap. xxvi.

As a simple example of this class of problem, consider the semicircular ring DAC shown in Fig. 117, of uniform cross section a, and mean radius R, the ends CD of which are tied together by a rod of area a_r. The ring rests on a support at A, and is loaded with vertical loads WW at C and D. It is required to find the pull P in the rod CD, and hence the stresses in the ring. The structure is statically indeterminate, and in this case, it will be convenient to take P as the statically indetermin- ate magnitude. Suppose that at A the thrust in the ring is N_0, the shearing force S_0, and the bending moment M_0, the corresponding values at any section K, making an angle θ with AB, being, N, S, and M. Consider the equilibrium of the portion AK of the ring.
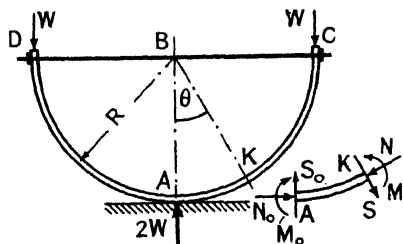
FIG. 117.

Equating vertical components, $S_0 = N \sin \theta + S \cos \theta$

Equating horizontal components, $N_0 = N \cos \theta - S \sin \theta$

Taking moments about A, $M_0 \quad M - S(R \sin \theta) - NR(1 - \cos \theta)$.

From the conditions of the problem, $N_0 \quad P$; $S_0 = W$; and $M_0 = PR - WR = (P - W)R$; whence,

$W = N \sin \theta + S \cos \theta$; $\quad P = N \cos \theta - S \sin \theta$;

$N = W \sin \theta + P \cos \theta$; $\quad S = W \cos \theta - P \sin \theta$;

$(P - W)R = M - SR \sin \theta - NR (1 - \cos \theta)$

and, $\qquad M = R\{P \cos \theta - W (1 - \sin \theta)\}$

From the first term of eq. (1), § 78, and the second, third and fourth terms of eq. (2). § 78, the internal work stored in half the structure is

$$U = \frac{1}{2E}\int_B^C \frac{P^2}{a_r} \cdot dx + \frac{1}{2E}\int_A^C \frac{N^2}{a} \cdot dl + \frac{1}{2G}\int_A^C \frac{\zeta S^2}{a} \cdot dl \quad \frac{1}{2E}\int_A^C \frac{M^2}{I} \cdot dl$$

where $dl = \text{R} \cdot d\theta$ is an element of length of the arc AC. Putting in the known values,

$$U = \frac{\text{P}^2}{2\text{E}a_r}\int_0^{\text{R}} dx + \frac{\text{R}}{2\text{E}a}\int_0^{\pi/2}(\text{W} \sin\theta + \text{P} \cos\theta)^2 \, d\theta$$

$$+ \frac{\text{R}\zeta}{2\text{G}a}\int_0^{\pi/2}(\text{W} \cos\theta - \text{P} \sin\theta)^2 \, d\theta + \frac{\text{R}^3}{2\text{EI}}\int_0^{\pi/2}\{\text{P} \cos\theta - \text{W}(1 - \sin\theta)^2\}d\theta$$

$$= \frac{\text{P}^2\text{R}}{2\text{E}a_r} + \frac{\text{R}}{2\text{E}a}\left\{\frac{\pi}{4}(\text{W}^2 + \text{P}^2) + \text{WP}\right\} + \frac{\text{R}\zeta}{2\text{G}a}\left\{\frac{\pi}{4}(\text{W}^2 + \text{P}^2) - \text{WP}\right\}$$

$$+ \frac{\text{R}^3}{2\text{EI}}\left\{\frac{\pi}{4}\text{P}^2 - \text{WP} + \left(\frac{3\pi}{4} - 2\right)\text{W}^2\right\}$$

In this equation P is the statically indeterminate magnitude, and for U to be a minimum,

$$\frac{\partial U}{\partial \text{P}} = 0 = \frac{\text{PR}}{\text{E}a_r} + \frac{\text{R}}{2\text{E}a}\left\{\frac{\pi}{2}\text{P} + \text{W}\right\} + \frac{\text{R}\zeta}{2\text{G}a}\left\{\frac{\pi}{2}\text{P} - \text{W}\right\} + \frac{\text{R}^3}{2\text{EI}}\left\{\frac{\pi}{2}\text{P} - \text{W}\right\}$$

whence,

$$\text{P} = \text{W}\frac{\dfrac{\text{R}^2}{2\text{EI}} + \dfrac{\zeta}{2\text{G}a} - \dfrac{1}{2\text{E}a}}{\dfrac{\pi\text{R}^2}{4\text{EI}} + \dfrac{\pi\zeta}{4\text{G}a} + \dfrac{\pi}{4\text{E}a} + \dfrac{1}{\text{E}a_r}}$$

If the work done by the direct and shearing forces be neglected, $\text{P} = 2\text{W}/\pi$.

This result could have been obtained rather more easily by the device of differentiating first and integrating afterwards. Thus, from the first expression for U, p. 181,

$$\frac{\partial U}{\partial \text{P}} = \frac{1}{\text{E}a_r}\int_0^{\text{R}} \text{P} \cdot dx + \frac{\text{R}}{\text{E}a}\int_0^{\pi/2}\text{N} \cdot \frac{\partial \text{N}}{\partial \text{P}} \, d\theta$$

$$+ \frac{\text{R}\zeta}{\text{G}a}\int_0^{\pi/2}\text{S} \cdot \frac{\partial \text{S}}{\partial \text{P}} \, d\theta + \frac{\text{R}}{\text{EI}}\int_0^{\pi/2}\text{M} \cdot \frac{\partial \text{M}}{\partial \text{P}} \, d\theta = 0$$

Inserting the known values for N, S, M, $\dfrac{\partial \text{N}}{\partial \text{P}}$, $\dfrac{\partial \text{S}}{\partial \text{P}}$, and $\dfrac{\partial \text{M}}{\partial \text{P}}$,

$$\frac{\text{PR}}{\text{E}a_r} + \frac{\text{R}}{\text{E}a}\int_0^{\pi/2}(\text{W} \sin\theta + \text{P} \cos\theta) \cos\theta \cdot d\theta - \frac{\text{R}\zeta}{\text{G}a}\int_0^{\pi/2}(\text{W} \cos\theta - \text{P} \sin\theta) \sin\theta \cdot d\theta$$

$$+ \frac{\text{R}}{\text{EI}}\int_0^{\pi/2}\text{R}^2\{\text{P} \cos\theta - \text{W}(1 - \sin\theta)\} \cos\theta \cdot d\theta = 0$$

Multiplying out and collecting terms,

$$\frac{\text{P}}{\text{E}a_r} + \frac{\text{P}\zeta}{2\text{G}a}\int_0^{\pi/2}(1 - \cos 2\theta) \, d\theta + \frac{\text{P}}{2}\left\{\frac{1}{\text{E}a} + \frac{\text{R}^2}{\text{EI}}\right\}\int_0^{\pi/2}(1 + \cos 2\theta) \, d\theta$$

$$+ \frac{\text{W}}{2}\left\{\frac{1}{\text{E}a} - \frac{\zeta}{\text{G}a} + \frac{\text{R}^2}{\text{EI}}\right\}\int_0^{\pi/2}\sin 2\theta \cdot d\theta - \frac{\text{WR}^2}{\text{EI}}\int_0^{\pi/2}\cos\theta \cdot d\theta = 0$$

whence, as before,

$$P\left\{\frac{\pi R^2}{4EI} + \frac{\pi\zeta}{4Ga} + \frac{\pi}{4Ea} + \frac{1}{Ea_\eta}\right\} = W\left\{\frac{R^2}{2EI} + \frac{\zeta}{2Ga} - \frac{1}{2Ea}\right\}$$

The above frame may be regarded as an inverted, semicircular, tied arch, loaded with a single load 2W at the crown.

VIRTUAL WORK

80. More General Theory. Virtual Work.—The following is a more general treatment of the application of the work theory to framed structures. It includes the effect of temperature alterations, and of movements of the abutments (reaction displacements). Using the principle of virtual work, it leads to the theorems of Maxwell, Betti, and Mohr.

Let F = the force in a bar of a braced structure due to any cause whatsoever.

a = the area of the bar.

l = the length of the bar.

λ = the ratio l/a.

t = the alteration in temperature.

α = the coefficient of expansion per degree.

The positive alteration in length (extension) of the bar due to a force + F (tension), and an increase in temperature + $t°$, is

$$\delta l = \frac{Fl}{Ea} + \alpha t l \qquad (1)$$

In Fig. 118, let AB be the bar, and suppose that, as the result of the deformation of the structure, AB move to A'B'. Let the coordinates of A be x_a, y_a; of B be x_b, y_b; of A' be $(x_a + \delta x_a)$, $(y_a + \delta y_a)$; and of B' be $(x_b + \delta x_b)$, $(y_b + \delta y_b)$. Then the lengths AB and A'B' are, respectively
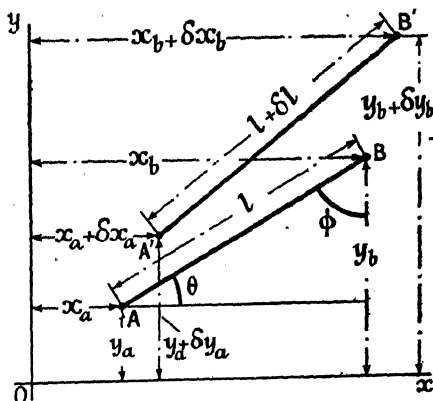
FIG. 118.

$$l^2 = (x_b - x_a)^2 + (y_b - y_a)^2$$

$$(l + \delta l)^2 = \{(x_b + \delta x_b) - (x_a + \delta x_a)\}^2 + \{(y_b + \delta y_b) - (y_a + \delta y_a)\}^2$$

Multiply out the latter equation, and neglect the second order of small quantities, since the displacements are very small. Then,

$$l^2 + 2l \cdot \delta l = (x_b - x_a)^2 + 2(x_b - x_a)(\delta x_b - \delta x_a)$$
$$+ (y_b - y_a)^2 + 2(y_b - y_a)(\delta y_b - \delta y_a).$$

Subtract from this the expression for l^2, and divide all through by $2l$,

$$\delta l = (\delta x_b - \delta x_a)\cos\theta + (\delta y_b - \delta y_a)\cos\phi \qquad . \qquad . \quad (2)$$

where $\cos\theta = (x_b - x_a)/l$; $\cos\phi = (y_b - y_a)/l$.

From eq. (1),

$$\delta l = (\delta x_b - \delta x_a) \cos \theta + (\delta y_b - \delta y_a) \cos \phi = \frac{Fl}{Ea} + atl \quad . \quad (3)$$

By a similar analysis it may be shown that in a space frame, if the coordinates of A and B are respectively x_a, y_a, z_a ; x_b, y_b, z_b,

$$\delta l = (\delta x_b - \delta x_a) \cos \theta + (\delta y_b - \delta y_a) \cos \phi + (\delta z_b - \delta z_a) \cos \psi$$

$$\frac{Fl}{Ea} + atl \quad . \quad (4)$$

where $\cos \psi = (z_b - z_a)/l$.

Eqs. (3) and (4) give δl, the alteration in length of the bar, in terms of the displacements, parallel to the axes of coordinates, δx_a, δy_a, δz_a ; δx_b, δy_b, δz_b, of its ends.

Equilibrium of a Panel Point.—In a structure in equilibrium, all the forces acting at any one panel point must be in equilibrium. If at a panel point, $W_1 W_2 W_3 \ldots$ be the external loads, and $F_1 F_2 F_3 \ldots$ be the forces in the bars, then resolving parallel to the coordinate axes,

$$\begin{aligned} \Sigma W_x + \Sigma F \cos \theta &= 0 \\ \Sigma W_y + \Sigma F \cos \phi &= 0 \\ \Sigma W_z + \Sigma F \cos \psi &= 0 \end{aligned} \quad . \quad . \quad . \quad . \quad (5)$$

The symbol ΣW_x denotes the sum of the components parallel to the axis of x of all the external loads ; the $\Sigma F \cos \theta$ denotes the sum of the corresponding components of the forces in the bars ; and similarly for the other equations. In a plane frame the third equation disappears.

Virtual Work.—In a structure in equilibrium, suppose that a number of forces FF . . . act at any panel point. These forces may be external and/or internal forces. Each will have a component $F \cos \zeta$ parallel to any arbitrary axis of reference, where ζ is the angle which the force makes with that axis. For equilibrium, the resultant force in any direction must be zero, hence

$$\Sigma(F \cos \zeta) = 0 \quad . \quad . \quad (6)$$

where the summation includes all the forces and loads acting at the panel point. Suppose that, without destroying the equilibrium, the panel point be given a small arbitrary displacement Δ in the direction of the axis of reference. Then the work done by any one force is $(F \cos \zeta)\Delta$,* and the total work done by all the forces acting at the panel point is

$$\Sigma(F \cos \zeta)\Delta = \Delta \times \Sigma(F \cos \zeta) = 0 . \quad . \quad . \quad (7)$$

since, from eq. (6), $\Sigma(F \cos \zeta) = 0$.

But the expression $(F . \cos \zeta)\Delta$ may be written $F(\Delta . \cos \zeta)$, and $(\Delta . \cos \zeta)$ is the projection of the displacement Δ on to the direction of the force F, which for any particular force F_p may be denoted by Δ_p, hence

$$\Sigma(F \cos \zeta)\Delta = \Sigma F_p \Delta_p = 0 \quad . \quad . \quad . \quad (8)$$

* Not $\frac{1}{2}(F \cos \zeta)\Delta$, for the force F remains constant during the displacement Δ, see (ii) Fig. 103.

This is called the *law of virtual work*. It implies that in a structure in equilibrium, the total work done by all the forces acting at a panel point resulting from a small arbitrary displacement Δ of that point is zero. This is true for any panel point in the structure and therefore for every panel point, and thus for the whole structure. It is to be observed that the displacement Δ is quite arbitrary, and is in no way dependent on the magnitude and directions of the forces FF. Δ might be due to a real set of loads acting on the structure, and the forces FF be due to a virtual load system, also in equilibrium. It will be convenient to denote the forces FF by italic capitals, as has been done in eq. (8), to indicate that these forces and the displacement Δ are quite independent one of the other.

If the displacement Δ be made in a time δt, the velocity of the panel point is $\dfrac{d}{dt}(\Delta p)$, and eq. (8) becomes

$$\Sigma\, F.\frac{d}{dt}\,(\Delta p) = 0 \qquad . \qquad . \qquad . \qquad . \qquad (9)$$

which is called the *law of virtual velocities*.

81. Mohr's Work Equations.[4]—Suppose that certain arbitrarily chosen loads WW be applied to a statically determinate structure, so as to form with the corresponding reactions a system in equilibrium. These
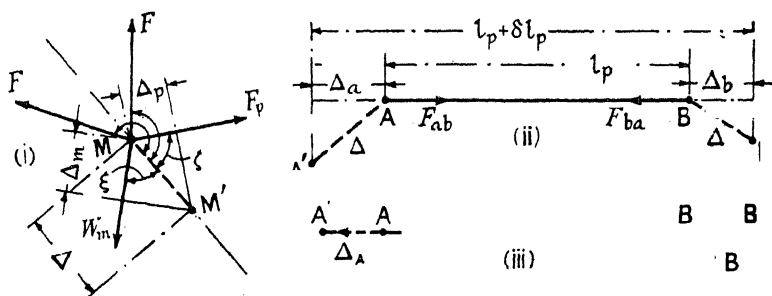
FIG. 119.

loads, combined with any temperature changes, will produce forces FF in the members of the structure. Next suppose that all the panel points of the structure be subjected to certain very small arbitrary displacements $\Delta\Delta$; these displacements, for example, might be due to a second load system applied to the structure. The magnitude and direction of the displacement of each panel point will, in general, be different.

Consider any panel point, (i), Fig. 119, and take the direction of the displacement Δ as the axis of reference. Suppose the external force W_m, which acts at the panel point, to make an angle ξ with the axis of reference, and the forces FF to make angles $\zeta\,\zeta$ with the same direction. Then, from the law of virtual work, eq. (8), § 80,

$$(W_m \cos \xi)\Delta + \Sigma(F \cos \zeta)\Delta = 0 \qquad . \qquad . \qquad . \qquad (1)$$

This expression gives the virtual work done at any panel point. It may be written

$$W_m \Delta_m + \Sigma F_p \Delta_p = 0 \qquad . \qquad . \qquad . \quad (2)$$

where Δ_m denotes the projection of Δ on to the external load W_m, and Δ_p the projection of Δ on to any particular force F_p. Eq. (2) holds for every panel point; hence the total virtual work for the whole structure is

$$\Sigma W_m \Delta_m + \Sigma F_p \Delta_p = 0 \qquad . \qquad . \qquad . \quad (3)$$

These summations include every external load, including the reactions, and every member in the structure.

Consider AB, the pth bar of the frame, (ii), Fig. 119. Let the projections on to this bar of the displacements $\Delta\Delta$ at A and B be Δ_a and Δ_b. As shown in (ii), both Δ_a and Δ_b are extensions. Hence, at A, the force in the bar, F_{ab}, is a tension and acts away from the panel point. Similarly at B, the force F_{ba} acts away from the panel point. Both F_{ab} and F_{ba}, therefore, act in opposite directions to their respective displacements and the work which they do is negative. This is always true of internal forces. It may be noticed, in passing, that if an external load be applied to the bar, the displacement which it produces is in the same direction as the load, and the work done is always positive, (iii), Fig. 119 ; if, however, the projection of the displacement at a panel point on to an external load acting there be opposite in sense to that load, the work done by that external force will be negative.

Returning to (ii) Fig. 119, the work done by the two forces F_{ab} and F_{ba} will be $- (F_{ab}\Delta_a + F_{ba}\Delta_b)$. But $F_{ab} = F_{ba} = F_p$, the tension in the bar, and $(\Delta_a + \Delta_b) = \delta l_p$ the alteration in length of the bar. Hence the work done is $- F_p \cdot \delta l_p$. The same reasoning applies to every bar in the frame, and therefore the factor $\Sigma F_p \Delta_p$ in eq. (3), which represents the total internal virtual work, may be replaced by $- \Sigma(F_p \cdot \delta l_p)$, and eq. (3) becomes

$$\Sigma W_m \Delta_m - \Sigma(F_p \cdot \delta l_p) = 0 \; ; \; \text{or,} \; \Sigma W_m \Delta_m = \Sigma(F_p \cdot \delta l_p) \qquad . \quad (4)$$

Given, therefore, a framework in equilibrium under a load system, which framework is subjected to very small arbitrary displacements, the external virtual work done by the external loads is equal to the internal virtual work resulting from the deformation of the frame ; and since the total virtual work done is zero [see eq. (8), § 80], each component, external and internal, is likewise zero.

$$\Sigma W_m \Delta_m = \Sigma(F_p \cdot \delta l_p) = 0 \qquad . \qquad . \qquad . \quad (5)$$

The term $\Sigma W_m \Delta_m$ includes the reactions, see eq. (3). If, therefore, the reactions RR suffer small displacements $\Delta_r \Delta_r$ in their own directions, due to movements of the abutments or other causes, eq. (4) may be written

$$\Sigma W_m \Delta_m + \Sigma R \Delta_r - \Sigma(F_p \cdot \delta l_p) = 0 \qquad . \qquad . \qquad . \quad (6)$$

where $\Sigma W_m \Delta_m$ now includes only the applied forces. This is the general form of the virtual work equation for a framed structure. It must be remembered that Δ_m, Δ_r, and δl_p are all displacements brought about

by the same cause, which cause is independent of the loads and forces W_m, R, and F_p.

The theory is equally true if W, R, and F, represent the actual loads and reactions producing the displacements Δ, in which case eq. (6) may be written,

$$\Sigma W_m \Delta_m + \Sigma R \Delta_r = \Sigma(F_p \cdot \delta l_p) = \Sigma\left(\frac{F_p{}^2 l}{Ea} + F_p atl\right) \quad . \quad (7)$$

In eq. (6), suppose all the arbitrary loads W to be removed except one, the magnitude of which is unity, then

$$1 \times \Delta_m + \Sigma R \Delta_r - \Sigma(F_p \cdot \delta l_p) = 0$$

and $\qquad \Delta_m = \Sigma(F_p' \cdot \delta l_p) - \Sigma R' \Delta_r \, . \qquad . \qquad . \qquad . \quad (8)$

in which equation F' and R' denote the forces in the bars and the reactions due to the unit load.

From this equation the displacement Δ_m of any panel point, in any direction, due to an actual load system WW, can be found by applying a unit force at the panel point in the required direction, and effecting the summations implied in eq. (8). In this case δl_p will denote the alteration in length of the bars due to the load system WW combined with that due to alterations in temperature, if any. In the particular case where the temperature remains constant, and Δ_r is zero at each support, $\delta l_p = F_W l_p / E a_p = F_W \lambda_p / E$, where, as in § 70, F_W is the actual force in the pth bar. Eq. (8) then becomes

$$\Delta_m = \frac{1}{E} \Sigma F_W F_p' \lambda \qquad . \qquad . \qquad . \qquad . \quad (9)$$

[see eq. (6), § 70.]

Eqs. (6) and (8) are known as Mohr's work equations.

82. Relative Displacement.—The *relative displacement* between any two panel points M and N, Fig. 120, of a framed structure in equilibrium under a system of applied loads WW can be obtained from Mohr's second work equation, eq. (8), § 81, as follows : Apply two unit loads $W_m =$ unity acting in opposite directions along the line MN. Then if Δ_m be the relative displacement of M to N, from eq. (8), § 81,
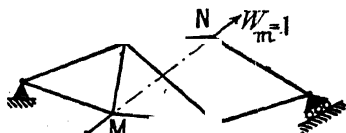
FIG. 120.

$$\Delta_m = \Sigma F' \cdot \delta l - \Sigma R' \Delta_r \qquad . \qquad . \qquad . \qquad . \quad (1)$$

In this equation δl denotes the alteration in length of a bar due to the actual load system WW, temperature changes, and reaction displacements Δ_r if the latter affect the value of δl ; F' denotes the force in a bar, and R' a reaction due to the unit loads.

From eq. (1), § 80, $\qquad \delta l = \dfrac{F_W l}{Ea} + atl = \dfrac{F_W \lambda}{E} + atl$

where F_W denotes the actual force in the bar due to the applied loads WW, and the reaction displacements. Then from eq. (1),

$$\Delta_m = \Sigma F'(F_W \lambda/E + \alpha t l) - \Sigma R' \Delta_r \qquad . \qquad . \qquad . \quad (2)$$

If the value of Δ_m comes out negative, it implies that the displacement is in the opposite direction to that assumed for the forces $W_m = 1$.

83. Self-Stressed Frames.—Let (i), Fig. 121, represent part of a re-dundant frame in which the redundant member has been made too short by an amount Δ. By heating the bar or otherwise it could be got into place and attached. When it cooled it would shorten and stress the frame. Such a frame is called a *self-stressed frame*. If the resulting stress in the re-dundant bar be F_r, the corresponding alteration in length of the bar will be $\delta l_r = F_r \lambda_r / E$. Owing to the action of the forces $F_r F_r$ on the frame, (ii) Fig. 121, the points M and N will come together a distance Δ_m ; and the amount by which the redundant bar lengthens, plus the amount by which M and N come together, must equal Δ,
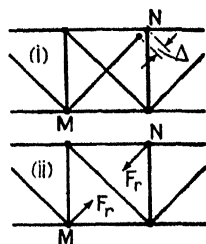
$$\Delta = \delta l_r + \Delta_m \qquad . \qquad . \qquad . \qquad . \qquad . \quad (1)$$

FIG. 121.

Δ_m can be found from eq. (2), § 82. The applied loads are $F_r F_r$, and using the symbol F_R for the force F_W which they produce in a bar, $\Delta_m = \Sigma F' F_R \lambda/E$; F' denotes the force in a bar due to the unit loads $W_m W_m$ applied along the line MN ; the other terms in the equation vanish. Then, from eq. (1),

$$\Delta = F_r \lambda_r / E + \Sigma F' F_R \lambda/E$$

But if F' is the force in a bar due to unit loads acting along MN, F_R the force in the bar due to the loads $F_r F_r$ which act along the same line must be

$$F_R = F_r F'$$

Hence,

$$E\Delta = F_r \lambda_r + F_r \Sigma(F')^2 \lambda$$

and,

$$F_r = \frac{E\Delta}{\lambda_r + \Sigma(F')^2 \lambda} \cdot \qquad \qquad . \quad (2)$$

In this equation $\Sigma(F')^2 \lambda$ does not include the redundant bar itself. Knowing F_r, the initial stresses $F_R = F_r F'$ in all the bars can be found directly.

Worked Example.—Suppose that the bar CD of Fig. 107 is made 1/100 inch too short, and forced into place. Find the initial forces in the bars of the frame. Remove the bar CD and apply a unit load acting from C towards D. The forces F' produced in the remaining bars by this load are $F_1' = -0 \cdot 61$, $F_2' = -0 \cdot 72$, see the Table, p. 166. The values of λ for the bars are 50 and 28 ; hence,

$$\Sigma(F')^2 \lambda = (-0 \cdot 61)^2 \times 50 + (-0 \cdot 72)^2 \times 28 = 33 \cdot 1$$

λ_r for the redundant bar $CD = 40$, and $\Delta = + 0 \cdot 01$ inch, Δ is $+$ since the redundant bar is short. Then, from eq. (2),

$$F_r = \frac{13000 \times 0 \cdot 01}{40 + 33 \cdot 1} = + 1 \cdot 78 \text{ tons.}$$

which is the initial force in the redundant bar, and is tensile. The initial force in bar No. $1 = F_R = F_r F_1' = 1 \cdot 78 \times (- 0 \cdot 61) = - 1 \cdot 09$ tons ; and in bar No. $2 = F_R = F_r F_2' = 1 \cdot 78 \times (- 0 \cdot 72) = - 1 \cdot 28$ tons ; both compressive.

Note.—Even if the redundant bar is too long, still apply the forces $F_r = 1$ in the direction shown in Fig. 121, but call Δ negative, for the force in the redundant bar will be compressive. Any bar in a panel containing superfluous bars can be regarded as a redundant bar.

If the force F' in the redundant bar be called $+ 1$, as in the Table on p. 166, the term $(F')^2 \lambda$ for this bar $= \lambda_r$, and eq. (2) may be written,

$$F_r = \frac{E\Delta}{\Sigma(F')^2 \lambda} \qquad . \qquad . \qquad . \qquad . \qquad . \quad (3)$$

where the summation now includes the redundant bar. The denominator is obtained at once from the sum of the last column $\Sigma(F')^2 \lambda$ in the Table, and such a tabular solution is by far the best method of treatment.

84. Reciprocal Displacements. Maxwell's and Betti's Theorems.— Suppose that a load $W_m = $ unity be applied at the point M of the frame AB, Fig. 118, in the direction indicated, and that it produces forces F_m, and extensions $F_m l / Ea = F_m \lambda / E$ in the different bars of the framework. To find the displacement of the point N in the direction indicated in Fig. 122, due to W_m, apply a unit load W_n at N acting

FIG. 122.

in that direction, and suppose that this load produces forces F_n in the bars. Then, from eq. (6), § 70, the displacement of N, due to W_m applied at M, is
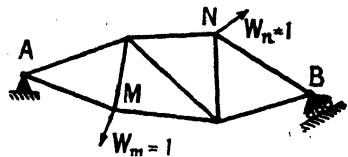
$$\Delta_{nm} \quad \frac{1}{E} \Sigma F_m F_n \lambda \qquad (1)$$

since in this case $F_m = F_W$ and $F_n = F'$.

Again, suppose that a load $W_n = $ unity be applied at the point N of the same frame AB in the direction indicated in Fig. 122, and that it is required to find the displacement of the point M in the direction indicated in the figure. The force W_n will produce forces F_n and extensions $F_n \lambda / E$ in the different bars of the frame. Apply a unit load W_m at M, acting in the given direction, and suppose that this load produces forces F_m in the bars of the frame. Then, from eq. (6), § 70, the displacement Δ_{mn} of M, due to W_n acting at N, will be

$$\Delta_{mn} = \frac{1}{E} \Sigma F_n F_m \lambda \qquad (2)$$

since in this case $F_n = F_W$ and $F_m = F'$.

Now it will be obvious, since both loads are of unit magnitude and both are applied to the same frame and in the same directions, that the forces F_m and F_n in the bars of the frame will be the same in both equations (1) and (2). Hence,

$$\Delta_{nm} = \frac{1}{E} \Sigma F_m F_n \lambda = \frac{1}{E} \Sigma F_n F_m \lambda = \Delta_{mn}$$

and, $\Delta_{mn} = \Delta_{nm}$.   .   .   .   (3)

which is Maxwell's law of reciprocal displacements.[3]

Stated in words, the displacement of any point N in a particular direction, due to a unit load applied at a point M in a second direction, is equal to the displacement of M in the second direction, due to unit load applied at N in the first direction.

The law is equally true if Δ_{nm} represent the *relative displacement* between any two points NN_1, due to unit loads applied at another pair of points MM_1 along the line joining them ; and if Δ_{mn} represent the relative displacement between any two points MM_1, due to unit loads applied at another pair of points NN_1 along the line joining the latter. This follows from § 82 by a similar proof.

Maxwell's theorem can be proved by a direct application of the principle of work as follows : Apply a load $W_m =$ unity to the point M of the frame AB in Fig. 122 in the direction shown, and suppose that it produces displacements Δ_{mm} and Δ_{nm} at the points M and N respectively in the directions indicated in the figure. Then the work done by W_m in producing these displacements will be $\frac{1}{2}W_m \Delta_{mm}$. Next apply the load $W_n =$ unity at N in the direction shown, producing further displacements Δ_{mn} and Δ_{nn} at the points M and N in the said directions. Then W_m will do a further amount of work $W_m \Delta_{mn}$, and W_n an amount of work $\frac{1}{2}W_n \Delta_{nn}$. The total amount of work done by the two loads is, therefore,

$$U = \tfrac{1}{2}W_m \Delta_{mm} + W_m \Delta_{mn} + \tfrac{1}{2}W_n \Delta_{nn} \ . \quad . \quad . \ (4)$$

Again, to the same frame, apply a load $W_n =$ unity to the point N in the direction shown, producing displacements Δ_{mn} and Δ_{nn} at the points M and N respectively in the directions indicated. The work done by W_n will be $\frac{1}{2}W_n \Delta_{nn}$. Next apply the load $W_m =$ unity at M, producing displacements Δ_{mm} and Δ_{nm} at M and N in the given directions. Then the work done by W_m will be $\frac{1}{2}W_m \Delta_{mm}$, and W_n will do a further amount of work $W_n \Delta_{nm}$. The total amount of work done by both loads is, therefore,

$$U = \tfrac{1}{2}W_n \Delta_{nn} + \tfrac{1}{2}W_m \Delta_{mm} + W_n \Delta_{nm} \ . \quad . \quad . \ (5)$$

But the total amount of work done by applying the two loads to the frame must be the same, irrespective of the order in which they are applied. Hence, from eqs. (4) and (5),

$$U = \tfrac{1}{2}W_m \Delta_{mm} + W_m \Delta_{mn} + \tfrac{1}{2}W_n \Delta_{nn} = \tfrac{1}{2}W_n \Delta_{nn} + \tfrac{1}{2}W_m \Delta_{mm} + W_n \Delta_{nm}$$

or, $W_m \Delta_{mn} = W_n \Delta_{nm}$;   whence $\Delta_{mn} = \Delta_{nm}$,

since $W_m = W_n = 1$, which proves Maxwell's law.

Angular Displacements.—Maxwell's law of reciprocal displacements is equally true for angular displacements. Suppose that loads WW be applied to the frame shown in Fig. 123 at right angles to the line MM_1, forming a couple of unit magnitude.
This will produce an angular displacement θ_{mm} of the line MM_1, and an angular displacement θ_{nm} of the line NN_1. The work done will be $\frac{1}{2}M_m\theta_{mm}$, where M_m = unity is the magnitude of the applied couple. Next suppose that a couple M_n of unit magnitude be applied to the line
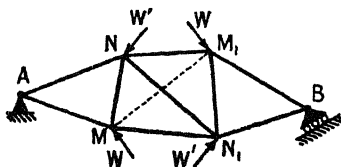
FIG. 123.

NN_1. This will produce a further angular displacement of the line MM_1 of θ_{mn}, and an angular displacement of the line NN_1 of θ_{nn}. The work done by M_n will be $\frac{1}{2}M_n\theta_{nn}$; and, in addition, the couple M_m will do a further amount of work $M_m\theta_{mn}$. Hence the total amount of work done by both couples is

$$U = \tfrac{1}{2}M_m\theta_{mm} + M_m\theta_{mn} + \tfrac{1}{2}M_n\theta_{nn} \quad . \quad . \quad . \quad (6)$$

Again, by applying the couples in the reverse order, it can be shown, as before, that the total work done is

$$U = \tfrac{1}{2}M_n\theta_{nn} + \tfrac{1}{2}M_m\theta_{mm} + M_n\theta_{nm} \quad . \quad . \quad . \quad (7)$$

Since the total work done by the two couples must be the same, irrespective of the order in which they are applied, from eqs. (6) and (7), since $M_m = M_n =$ unity,

$$\theta_{mn} = \theta_{nm} \quad . \quad . \quad . \quad . \quad . \quad (8)$$

which is Maxwell's law for angular displacements.

Betti's Law.[3]—Maxwell's theorem is a particular case of a more general theorem due to Betti.

Suppose that a framework is in equilibrium under two systems of loading W_m . . . and W_n . . . simultaneously applied in given directions. Remove all the loads, and then reapply the group W_m . . .; this will produce displacements Δ_{mm} . . . of the points of application of the group of loads W_m . . ., and displacements Δ_{nm} . . . of the points of application of the group W_n . . ., all in the given directions. Then, as in the preceding case, the work done by the loads W_m . . . will be $\frac{1}{2}\Sigma W_m\Delta_{mm}$. Next, reapply the load group W_n . . ., which will produce displacements of the points of application of the load group W_m . . . of Δ_{mn} . . ., and of the points of application of the load group W_n . . . of Δ_{nn} . . . The work done due to the application of the load group W_n . . . will be $\Sigma W_m\Delta_{mn} + \frac{1}{2}\Sigma W_n\Delta_{nn}$; and the total work done by the two load systems will be

$$U = \tfrac{1}{2} \Sigma W_m\Delta_{mm} + \Sigma W_m\Delta_{mn} + \tfrac{1}{2} \Sigma W_n\Delta_n \quad . \quad . \quad (9)$$

Again, remove all the loads and reapply the load group W_n . . . separately. This will produce displacements of the points of application of the load group W_m . . . of Δ_{mn} . . ., and of the load group W_n . . .

of Δ_{nn} . . ., all in the given directions. The work done by the load group W_n . . . will be $\frac{1}{2}\Sigma W_n \Delta_{nn}$. Next, reapply the load group W_m . . ., which will produce displacements of the points of application of the load group W_m . . . of Δ_{mm} . . ., and of the load group W_n . . . of Δ_{nm} . . . The resulting work done will be $\frac{1}{2}\Sigma W_m \Delta_{mm} + \Sigma W_n \Delta_{nm}$. Hence the total work done by the application of the two load groups will be

$$U = \tfrac{1}{2}\Sigma W_n \Delta_{nn} + \tfrac{1}{2}\Sigma W_m \Delta_{mm} + \Sigma W_n \Delta_{nm} \qquad . \qquad . \ (10)$$

But the total amount of work done by applying the two load systems to the same frame must be the same, irrespective of the order in which the loads are applied. Hence, from eqs. (9) and (10),

$$U = \tfrac{1}{2}\Sigma W_m \Delta_{mm} + \Sigma W_m \Delta_{mn} + \tfrac{1}{2}\Sigma W_n \Delta_{nn}$$

$$= \tfrac{1}{2}\Sigma W_n \Delta_{nn} + \tfrac{1}{2}\Sigma W_m \Delta_{mm} + \Sigma W_n \Sigma_{nm}$$

and, $\qquad\qquad \Sigma W_m \Delta_{mn} = \Sigma W_n \Delta_{nm} \qquad . \qquad . \qquad . \ (11)$

which is Betti's law, a generalised form of Maxwell's law of reciprocal displacements. If each load group consist of a single force $W_m = W_n$ = unity, eq. (11) becomes $\Delta_{mn} = \Delta_{nm}$, which is Maxwell's law.

It will be evident from the nature of the proof that both Maxwell's and Betti's laws also hold for redundant frames and solid bodies. Betti's law holds equally well for angular as for linear displacements.

85. Maxwell's Law. Simple Examples.—The application of Maxwell's law to some simple examples will next be considered :

FIG. 124.

(a) Let AB, (i) Fig. 124, be a cantilever of uniform cross section, $EI = \text{const.}$, loaded with a load $W = \text{unity}$ at B. The equation to the deflection curve, eq. (2), § 52, Vol. I, is

$$y = \frac{W}{EI}\left\{ \frac{Lx^2}{2} - \frac{x^3}{6} \right\}$$

origin being taken at A. Hence the deflection at C, distant l from A, if $W = 1$, is

$$y_{cb} \quad \frac{1}{EI}\left\{ \frac{Ll^2}{2} - \frac{l^3}{6} \right\} = \frac{l^2}{2EI}\left\{ L - \frac{l}{3} \right\}$$

Now suppose the load removed from B and placed at C. Then, according to Maxwell's law, the deflection y_{bc} at B, with unit load at C, is equal to the deflection y_{cb} at C, with unit load at B. Hence

$$y_{bc} = y_{cb} = \frac{l^2}{2EI}\left\{ L - \frac{l}{3} \right\}$$

which, as proved in eq. (9), § 55, Vol. I, is the case.

(b) In (ii), Fig. 124, let AB be a beam, $EI = \text{const.}$, supported at A and B, and loaded with a load $W = \text{unity}$ at D distant l_2 from A. The
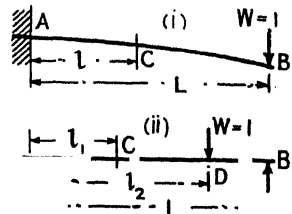
equation to the deflection curve between A and D, see eq. (25), § 52, Vol. I, is

$$y = \frac{W}{6EI} \cdot \frac{L - l_2}{L} \{l_2(2L - l_2)x - x^3\}$$

origin being taken at A. Hence the deflection at C, distant l_1 from A, if W = 1, is

$$y_{cd} = \frac{L - l_2}{6EIL} \{l_2 l_1(2L - l_2) - l_1^3\} = \frac{(L - l_2)l_1}{6EIL} \{l_2(2L - l_2) - l_1^2\}$$

Now suppose the load removed from D and placed at C, distant l_1 from A. The equation to the deflection curve between C and B, is

$$y = \frac{W}{6EI} \cdot \frac{l_1}{L} \{x^3 - 3Lx^2 + 2L^2x + l_1^2x + Ll_1^2\}$$

origin being taken at A, loc. cit. Hence the deflection at D, distant l_2 from A, if W = 1, is

$$y_{dc} = \frac{l_1}{6EIL} \{l_2^3 - 3Ll_2^2 + 2L^2l_2 - l_1^2l_2 - Ll_1^2\}$$

It is easy to show that $y_{cd} = y_{dc}$, proving Maxwell's law for the particular case.

86. **Application to Statically Indeterminate Structures.**—In certain cases of external indeterminateness, § 88, Maxwell's law is of great help in constructing the influence lines. As a simple example, consider the case of a two-hinged arch, Fig. 125. Suppose the pin at A be removed and a vertical force W = unity be applied at the point Q, (i). This will produce a horizontal displacement Δ_{aq} of the point A. Next suppose the vertical force be removed, and a horizontal force of unit magnitude acting in the direction B to A be applied at A, (ii). This will produce a vertical displacement Δ_{qa} at Q, and a horizontal displacement Δ_{aa} at A. Then by Maxwell's law, $\Delta_{aq} = \Delta_{qa}$. If now the unit vertical force at Q be again applied, and the unit horizontal force be replaced by one of magnitude H, acting from A to B, such that the point A is pushed back an amount Δ_{aq} to its original position, (iii), it is evident that H will be the actual horizontal force on the pin when the arch is carrying the unit vertical load ; that is to say, H is the horizontal thrust of the arch. But if a unit force at A produce a displacement Δ_{aa}, and

FIG. 125.

H produce a displacement Δ_{aq}, $\dfrac{H}{1} = \dfrac{\Delta_{aq}}{\Delta_{aa}} = \dfrac{qa}{\Delta_{aa}}$

and

$$H = \frac{1}{\Delta_{aa}} \cdot \Delta_{qa} \qquad (1)$$

Now Δ_{aa} depends only on the unit load at A, and is a constant for the arch. Therefore H $\propto$ as Δ_{qa}, the vertical deflection at Q due to the unit load at A. If, therefore, a displacement diagram be drawn, showing the value of Δ_{qa} (due to a unit horizontal load at A) everywhere, (iv) Fig. 125, the ordinate of this diagram under the unit load W will represent to some scale the value of H, and the diagram is the influence line for H. The values of Δ_{qa} for the unit horizontal load at A can be found by the methods of §§ 12, 15 or 94. The value of Δ_{aa} must be similarly calculated.

Eq. (1) may be written in the form

$$X \cdot \Delta_{aa} = 1 \cdot \Delta_{qa} \qquad . \qquad . \qquad . \qquad . \quad (2)$$

where X ($=$ H) is the statically indeterminate magnitude ; Δ_{aa} is the displacement of its point of application due to a unit load acting in the opposite direction ; and Δ_{qa} the displacement of any other point on the structure due to the same unit load.

It will be noticed that the statically indeterminate magnitude always acts in the opposite direction (sense) to the unit force at its point of application which produces displacements of the same sign as W.

The application of the above theory to direction-fixed and continuous girders is given in §§ 36–38, and to a two-hinged braced arch in § 94. The theory may be extended to include the case of redundant frames and cases of multiple redundancy [Molitor,[16] p. 127 ; Müller-Breslau,[10] p. 128].

STATICALLY INDETERMINATE STRUCTURES

87. Conditions of Indeterminateness.—(i) Fig. 126 represents an ordinary N girder merely supported at each end. It is statically determinate ; the reactions can be found by taking moments about each end in succession ; the forces in the bars can be found by drawing a stress diagram or by the method of sections. Suppose that, for the purpose of strengthening the girder or otherwise, a central prop or support is introduced as shown in (ii). It is now no longer possible to find the reactions by taking moments (i.e. by the principle of the lever), and until they are known the forces in the bars cannot be found. The structure is now statically indeterminate. Next, suppose that, instead of the central prop, extra bars are introduced into the girder as shown in (iii). The structure has now become a redundant frame, and although the reactions can be found by taking moments, the forces in the bars cannot be found from a stress diagram or by the method of sections. The frame shown in (iii) is also an indeterminate structure.

It is apparent, therefore, that there are two possible conditions of indeterminateness : (i) external, (ii) internal. The latter condition,
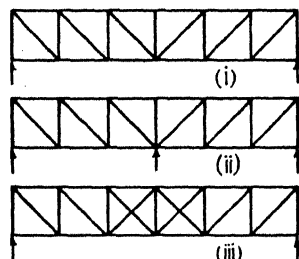
brought about by the introduction of redundant members into the frame, has already been discussed in § 71 *et seq.* ; the former condition will be considered in the next article.

From the above simple cases two tests for statical indeterminateness may be distinguished : (i) if all the reactions cannot be found by statical means (the loads not necessarily being vertical) the structure is externally indeterminate ; (ii) if, knowing the reactions, the forces in all the members cannot be found by drawing a stress diagram, or by the method of sections, the structure is internally indeterminate. A third test may be included : if stresses are set up in the structure due to alterations in temperature, the structure is statically indeterminate either externally, internally, or both.

It should be added that while test (ii) shows that the structure is statically indeterminate, it does not follow that it is a redundant frame ; it might be an imperfect frame (§ 3).
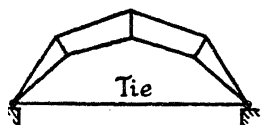
FIG. 127.

Tests (ii) and (iii) prove that structures such as the arched rib tied together at its feet, the *tied arch,* Fig. 127, are internally statically indeterminate, for the stresses in neither the arch nor the tie can be found by statical means, and both stresses are affected by temperature. This is typical of many structures where members subjected to bending are combined with other members subjected to direct stress ; see for example Figs. 117, 373, and 386. If, in Fig. 127, the tie be removed, and the feet be anchored down to rigid abutments, the arch would then be externally indeterminate instead of internally.

88. External Conditions of Indeterminateness.—If a beam be supported on rollers at each end, as shown in (i) Fig. 128, the external conditions are statically determinate. In this case there are only two external restraints, the two vertical reactions. A beam thus merely supported is free to move horizontally. Such motion would usually be undesirable, but the beam may be anchored down at one end as shown at (ii) without making it indeterminate, for the reactions may still be found by statical methods, and since the girder is free to expand at one end, alterations in temperature will not set up stresses in the girder.
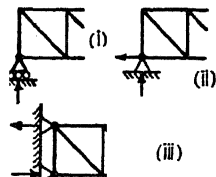
FIG. 128.

There are now three restraints, the two vertical reactions and possibly the horizontal reaction preventing motion, but the beam is still statically determinate. If, however, hinges as in (ii) be put at both ends, the reactions cannot be found by statical methods ; alterations in the overall length due to temperature alterations are prevented, and temperature stresses will be set up ; the girder is externally statically indeterminate. There are four restraints, the vertical and horizontal reactions at both ends.

It is evident, therefore, that when there are only three restraints the structure is externally statically determinate; when there are more than three such restraints the structure is externally indeterminate. When there are four restraints, i.e. one more than three, the conditions are spoken of as simply or singly indeterminate; when there are more indeterminate restraints than one, i.e. more than four restraints in all, the conditions are said to be multiply indeterminate. The direction-fixed beam shown in (iii) Fig. 128 is an example of multiple indeterminateness. There are three restraints at each end, the one vertical and two horizontal reactions.

89. **Solution of Statically Indeterminate Problems.**—The stresses in a statically indeterminate structure must be found from a consideration of its elastic properties. Thus in a beam, direction-fixed at each end (see Chapter VI, Vol. I), an expression is found for the slope of the beam at its ends, which, being equated to zero, gives the magnitude of the end-fixing moments. These known, the stresses everywhere can be determined. In a two-hinged arch (§ 220) the horizontal motion of the pins is calculated. If the abutments are rigid, this motion is zero, a condition which determines the horizontal thrust of the arch and hence the stresses in the arch.

In general, use is made of strain-energy considerations, either an application of the principle of work (§ 74), the principle of least work (§ 78), or the principle of virtual work (§ 80), all of which lead to the same fundamental equations (§ 91).

The general method of treatment is this : Reduce the statically indeterminate structure to a statically determinate structure by removing one or more restraints in the case of external indeterminateness, or by removing one or more redundant bars in the case of internal indeterminateness. The framework which remains is called the *principal statically determinate system.* Find by separate computations the forces in the members of the principal system due to (*a*) the applied loads, and (*b*) each of the at present unknown forces XX which replace the restraints and/or the redundant bars which have been removed. From the sets of forces thus obtained, the unknown forces XX can be found by means of the equations of § 91. Knowing the forces XX, the actual forces in all the members of the indeterminate frame can be found.

The application, in the case of simple and multiple redundancy in a plane framework, has been given in §§ 72 and 74. In § 72, F_r, the force in the redundant bar, is the unknown X, F_W denotes the forces in the bars of the principal system due to the applied loads, and F' those due to $X = F_r = $ unity ; X is made equal to unity for convenience. Then from eq. (3), § 72,

$$X = F_r = -\frac{\Sigma F_W F' \lambda}{\Sigma (F')^2 \lambda} \quad . \quad . \quad . \quad . \quad (1)$$

and the actual force in any bar of the redundant frame is

$$F = F_W + F_r F' \quad . \quad . \quad . \quad . \quad (2)$$

In the case of multiple redundancy (see § 74), sufficient bars must be removed to render the principal system statically determinate; and by applying the same process in turn for each bar removed, sufficient equations are obtained to find the stresses in them all.

90. **Choice of the Principal Statically Determinate System.**—The right choice of the principal system has much to do with the accuracy and simplicity of the calculations. In some cases the best procedure is evident. For example, a two-hinged arch should be transformed into a girder supported at each end by replacing the pins by vertical and horizontal forces. The horizontal force H is taken as X, the statically indeterminate unknown. In the case of a suspension bridge with a stiffening girder without joints, the calculation is much simplified by taking the force in the lowest link of the chain as the statically indeterminate unknown. The stiffening girder then becomes the principal system, and when the said link is removed, the forces F_W due to the applied loads in both chain and suspension rods all become zero, see § 238. In the case of a plate web system, one of the reactions may be used as the unknown; or, again, the bending moment at a particular point, say over a support, may be more suitable.

As a general rule, the simplest possible principal system should be chosen, having regard to the calculation of the stresses. It should differ as little as possible from the statically indeterminate structure, particularly as regards the magnitude of the deformations. When possible, it is usually best to choose the *beam* which most nearly corresponds. As an example of the possibilities in the choice of a principal system, consider the case of a direction-fixed arch, (i) Fig. 129. One of four principal systems may be used. One of the simplest is the corresponding beam, (ii) (cf. § 222). The arch may also be transformed into a cantilever (iii), or divided in the middle and considered as two cantilevers (iv) (cf. Fig. 348). A three-hinged arch, (v), may be used as the principal system, but although closest in character to the direction-fixed arch, the stresses therein are more difficult to determine, and the influence lines more difficult to set out, than those for the simple beam, (ii). The relative magnitude of the deflections in these structures stands in the order (i), (v), (ii), (iv), (iii); but the simplicity of the beam and cantilever makes them the more desirable choice. The method of treatment is the same for them all.
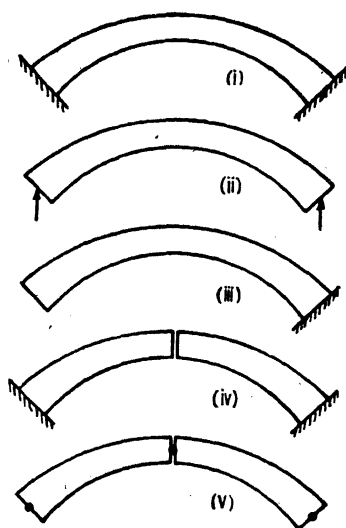
FIG. 129.

91. General Equation for Statically Indeterminate Structures.—The general equation for the total strain energy in a structure is

$$U = \Sigma \frac{F^2 l}{2Ea} + \int_0^l \frac{N^2}{2Ea} \cdot dl + \int_0^l \frac{\zeta S^2}{2Ga} \cdot dl + \int_0^l \frac{Mb^2}{2EI} \cdot dl + \int_0^l \frac{Mt^2}{2\Phi} \cdot dl$$
$$+ \Sigma F a t l + \Sigma R \Delta_r \qquad . \qquad . \qquad . \qquad . \quad (1)$$

see eq. (2), § 78, where the symbols are defined. The two last terms for temperature stresses and reaction displacements, §§ 80 and 81, have been added for completeness, but these effects are best treated separately (see § 93), and these terms will be omitted in what follows.

Framed Structure.—For a structure entirely composed of bars subjected only to longitudinal forces, all the terms of eq. (1) but the first will vanish.

$$U = \Sigma \frac{F^2 l}{2Ea} \tag{2}$$

Suppose the structure to be indeterminate, and that it can be made determinate by the removal of a single restraint or redundant bar. Then, if XX be the forces replacing the restraint or redundant member ; F_W the force due to the applied loads in any member of the principal system ; and F′ the force due to X = 1 in that member ; the actual force in the same member of the indeterminate frame under the applied loads will be

$$F = F_W + XF' \qquad . \qquad . \qquad . \qquad . \qquad . \quad (3)$$

[cf. § 72 ; $F_r = X$]. Differentiate eq. (2) with respect to X. By the principle of least work the first differential coefficient must be zero, § 75, and,

$$\frac{\partial U}{\partial X} = \Sigma \frac{Fl}{Ea} \cdot \frac{\partial F}{\partial X} = 0.$$

But from eq. (3), $\partial F/\partial X = F'$; hence,

$$\Sigma \frac{Fl}{Ea} \cdot \frac{\partial F}{\partial X} = \Sigma \frac{FF'l}{Ea} = \Sigma \frac{F_W F'l}{Ea} + X \Sigma \frac{(F')^2 l}{Ea} = 0$$

and

$$X = - \frac{\Sigma \frac{F_W F'l}{Ea}}{\Sigma \frac{(F')^2 l}{Ea}} \qquad . \quad (4)$$

[cf. eq. (3), § 72]. The summations include all the bars of a structure, but in a redundant bar $F_W = 0$.

Plate Web System.—In a plate web system, for example an arched rib subjected to a normal force, a shearing force, and a bending moment, the second, third, and fourth terms of eq. (1) are retained :

$$U = \int_0^l \frac{N^2}{2Ea} \cdot dl + \int_0^l \frac{\zeta S^2}{2Ga} \cdot dl + \int_0^l \frac{M^2}{2EI} \cdot dl \qquad . \qquad . \quad (5)$$

Let X be the statically indeterminate unknown which replaces a restraint or redundancy, and denote by N′, S′, and M′ the normal force, shearing force, and bending moment respectively due to the action of X = 1

acting alone on the principal system. Then, if N_W, S_W, and M_W be the corresponding values due to the applied loads, the normal force on any section of the indeterminate structure will be

$$N = N_W + XN' \tag{6}$$

the shearing force will be

$$S = S_W + XS' \tag{7}$$

and the bending moment will be

$$M = M_W + XM' \tag{8}$$

Differentiate eq. (5) with respect to X; as before the first differential coefficient must equal zero,

$$\frac{\partial U}{\partial X} = \int_0^l \frac{N}{Ea} \cdot \frac{\partial N}{\partial X} \, dl + \int_0^l \frac{\zeta S}{2Ga} \cdot \frac{\partial S}{\partial X} \, dl + \int_0^l \frac{M}{EI} \cdot \frac{\partial M}{\partial X} \, dl = 0$$

and from eqs. (6), (7), and (8), $\quad \dfrac{\partial N}{\partial X} = N'$; $\quad \dfrac{\partial S}{\partial X} = S'$; $\quad \dfrac{\partial M}{\partial X} = M'$,

hence,

$$\int_0^l \frac{NN'}{Ea} \cdot dl + \int_0^l \frac{\zeta SS'}{Ga} \cdot dl + \int \frac{MM'}{EI} \cdot dl = 0 \tag{9}$$

Introduce the values of N, S, and M, from eqs. (6), (7), and (8); as before, each term splits into two of the type

$$\int_0^l \frac{N_W N'}{Ea} \, dl + X \int_0^l \frac{(N')^2}{Ea} \, dl \; ;$$

whence,

$$X = -\frac{\displaystyle\int_0^l \frac{N_W N'}{Ea} \cdot dl + \int_0^l \frac{\zeta S_W S'}{Ga} \cdot dl + \int_0^l \frac{M_W M'}{EI} \cdot dl}{\displaystyle\int_0^l \frac{(N')^2}{Ea} \cdot dl + \int_0^l \frac{\zeta (S')^2}{Ga} \cdot dl + \int_0^l \frac{(M')^2}{EI} \cdot dl} \tag{10}$$

Having determined X, the actual values of the normal and shearing forces and of the bending moments can be found from eqs. (6), (7), and (8).

In most cases the deformation and strain energy due to shear are relatively small, and the S terms may be neglected. When the direct stress is also relatively small, or non-existent, the N terms may also be neglected, and

$$X = \frac{\displaystyle\int_0^l \frac{M_W M'}{EI} \cdot dl}{\displaystyle\int_0^l \frac{(M')^2}{EI} \cdot dl} \qquad . \qquad . \qquad . \qquad . \tag{11}$$

In cases like the tied arch of Fig. 127, where both beams and tie bars (or struts) occur in the same structure, eq. (4) must be combined with eq. (10) in order to find the value of X.

$$X = -\frac{\displaystyle\Sigma \frac{F_W F' l}{Ea} + \int_0^l \frac{N_W N'}{Ea} \, dl + \int_0^l \frac{\zeta S_W S'}{Ga} \, dl + \int_0^l \frac{M_W M'}{EI} \, dl}{\displaystyle\Sigma \frac{(F')^2 l}{Ea} + \int_0^l \frac{(N')^2}{Ea} \, dl + \int_0^l \frac{\zeta (S')^2}{Ga} \, dl + \int_0^l \frac{(M')^2}{EI} \, dl} \qquad . \tag{12}$$

For many purposes this equation may be simplified by omitting the N and S terms as was done in eq. (11).

Applications of these formulae will be found in §§ 94, 238, 245, 248, etc.

92. Multiple Indeterminateness.—If there be more than four external restraints or more than one redundant bar, sufficient restraints or redundant bars must be removed from the structure to make it statically determinate. If X_1, X_2 . . . be the corresponding statically indeterminate unknowns, U must be differentiated with respect to each. In this way sufficient equations are obtained to determine all the unknowns. Thus, for a framed structure with two redundant bars, eq. (3) § 91 becomes

$$F = F_W + X_1F' + X_2F'' \qquad . \qquad . \qquad . \qquad . \qquad . \qquad (1)$$

F' is the force in a bar of the principal system due to $X_1 = 1$; F'' that due to $X_2 = 1$. Then, from eq. (2), § 91,

$$\frac{\partial U}{\partial X_1} = \Sigma \frac{Fl}{Ea} \cdot \frac{\partial F}{\partial X_1} = 0 \; ; \; \frac{\partial U}{\partial X_2} = \Sigma \frac{Fl}{Ea} \cdot \frac{\partial F}{\partial X_2} = 0$$

From eq. (1), $\dfrac{\partial F}{\partial X_1} = F'$; $\dfrac{\partial F}{\partial X_2} = F''$; and

$$\Sigma \frac{(F_W + X_1F' + X_2F'')l}{Ea} \cdot F' = 0 \; ; \; \Sigma \frac{(F_W + X_1F' + X_2F'')l}{Ea} \cdot F'' = 0$$

or
$$\Sigma \frac{F_WF'l}{Ea} + X_1 \Sigma \frac{(F')^2l}{Ea} + X_2 \Sigma \frac{F'F''l}{Ea}$$

$$\Sigma \frac{F_WF''l}{Ea} + X_1 \Sigma \frac{F'F''l}{Ea} + X_2 \Sigma \frac{(F'')^2l}{Ea} = 0 \left.\right| \qquad (2)$$

[cf. eqs. (3) and (4), § 73].

These equations, solved as simultaneous, will give the values of X_1, X_2 . . . The equations for N, S, and M can be treated in an exactly similar way. It is possible in certain cases, by suitably choosing the conditions, to make to vanish all terms such as $X_1\Sigma(F'F''l/Ea)$ which contain products of F' and F''. The equations then reduce to a series of the same type as in a singly indeterminate system, each with a single unknown.

93. Temperature Stresses and Reaction Displacements.—The alteration in length of a bar of length l, when temperature alterations are taken into account, is $\delta l = Fl/Ea + atl$, eq. (1), § 80. Hence the internal work in a framed structure composed of bars is $\frac{1}{2}\Sigma F^2l/Ea + \Sigma Fatl$. If there be reaction displacements Δ_r, this work will be increased by an amount $\Sigma R\Delta_r$. The total internal work is, therefore,

$$U = \tfrac{1}{2}\Sigma\frac{F^2l}{Ea} + \Sigma Fatl + \Sigma R\Delta_r \qquad . \qquad (1)$$

Suppose that a reaction be taken as the statically indeterminate unknown X, so that $R = X$, and $\Delta_r = \Delta_x$; then as in eq. (3), § 91,

$$F = F_W + XF' ; \qquad \partial F / \partial X = F' \qquad (2)$$

and

$$\frac{\partial U}{\partial X} = \Sigma \frac{Fl}{Ea} \cdot \frac{\partial F}{\partial X} + \Sigma atl \frac{\partial F}{\partial X} + \Delta_x$$

(the other reactions disappear during differentiation) ; then as in eq. (4), § 91,

$$X = - \frac{\Sigma \dfrac{F_W F' l}{Ea} + \Sigma F' atl + \Delta_x}{} \qquad (3)$$

The parts of X due to temperature and reaction displacements are evidently

$$X_t = - \frac{\Sigma F' atl}{\dfrac{(F')^2 l}{Ea}} ; \quad X_r = - \frac{\Delta_x}{\Sigma \dfrac{(F')^2 l}{Ea}} \qquad . \qquad . \qquad . \quad (4)$$

so that these effects can be studied separately, as usually is desirable. If the reaction displacements be zero, X_t in the temperature equation may represent any statically indeterminate unknown, chosen for convenience.

The summations include all the bars in the structure ; increase in temperature is considered positive ; a displacement in the same sense as its reaction is considered positive.

Temperature and reaction stresses can only occur in cases of external indeterminateness unless, in any indeterminate structure, the temperature is different in different bars. If the structure rest on elastic supports these must be treated as part of the elastic system ; the reaction displacement equations will not apply.

94. **Design of Two-Hinged Braced Arch. Outline Programme.**—As an example of the application of the general formulae, the method of design for a large two-hinged braced arch will be very briefly set forth. The outline of the arch is shown in (i) Fig. 130. The system is singly statically indeterminate. Take for the statically indeterminate unknown $X = H$, the horizontal thrust of the arch. In the first instance, consider only the bending moments on the arch.* Then from eq. (11), § 91,

$$X = \frac{\displaystyle\int_0^l \frac{M_W M'}{EI} \, dl}{\displaystyle\int_l \frac{(M')^2}{EI}} \qquad \frac{\displaystyle\int_0^l M_W M' \frac{I_0}{I} \, dl}{\displaystyle\int_0^l (M')^2 \frac{I_0}{I} \, dl}$$

* To conform with the symbols used in the general strain-energy equations, M' in this article signifies the bending moment due to the unit load, and must be distinguished from M' in Chapter XIII.

Here $E =$ const. and disappears ; I_0 is the moment of inertia at the crown. Assume that $I \propto d^m$, where d is the depth of the frame, and m a
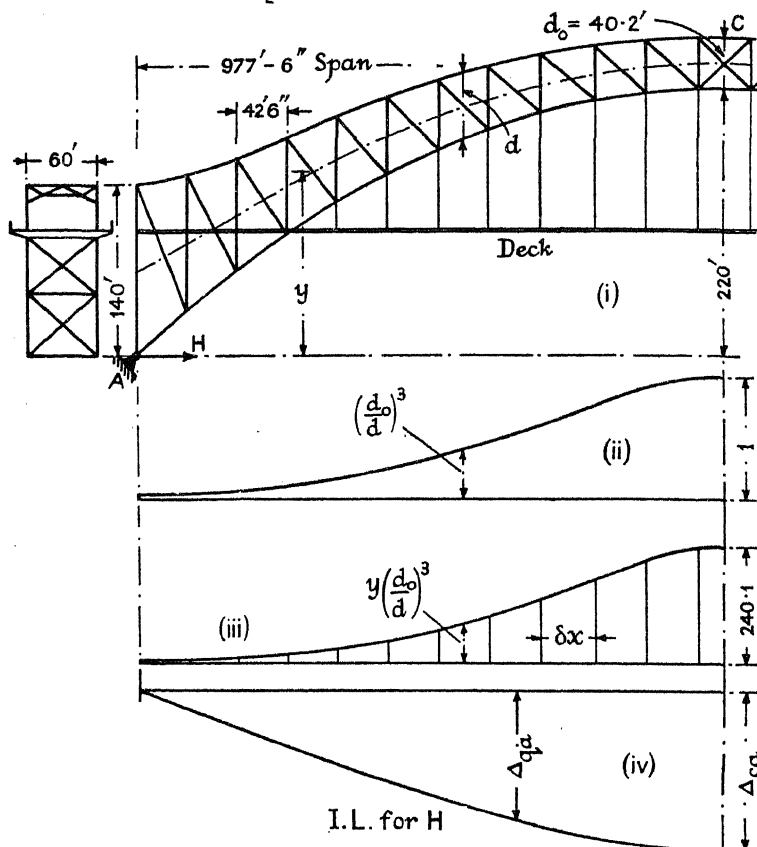
FIG. 130.—Hell Gate Arch.

constant ranging from $2\frac{1}{2}$ to 3 in braced arches ; $m = 3$ for the Hell Gate arch, Fig. 130 [Krivoshein [28]] ; then $I_0/I = (d_0/d)^m$.

In such long-span arches, *for the preliminary calculations*, it is sufficiently accurate to take $\delta l = \delta x =$ const. $=$ the panel length, Fig. 131 ; also when $X = 1$, $M' = 1 \times y$, hence

$$X = -\frac{\Sigma M_W y \left(\dfrac{d_0}{d}\right)^m}{\Sigma y^2 \left(\dfrac{d_0}{d}\right)}$$

The depths d_0 and d can be obtained from the outline, and X found by tabular calculation (compare § 220 and the Table, p. 491).
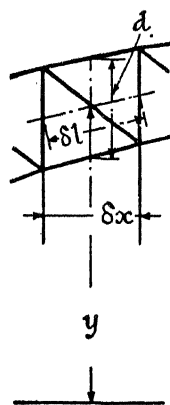
FIG. 131.

Ordinate.	y	d	$\left(\dfrac{d_0}{d}\right)^m$	M_W	$y\left(\dfrac{d_0}{d}\right)^m$	$M_W\, y\left(\dfrac{d_0}{d}\right)^m$	$y^2\left(\dfrac{d_0}{d}\right)^m$
0							
1							
2							
3							
⋮							
n							

The value of H for a particular load system producing M_W is given at once from the summations of the last two columns.

For the purpose of design it is necessary to determine the influence line for H ; to do this the theory of § 86 will be used ; $H = \Delta_{qa}/\Delta_{aa}$, eq. (1), § 86. Assuming that $\delta l = \delta x$, the vertical deflection of the arch anywhere, Δ_{qa}, Fig. 132, due to a unit horizontal load acting at A, can be found from eq. (3), § 53, Vol. I, which becomes
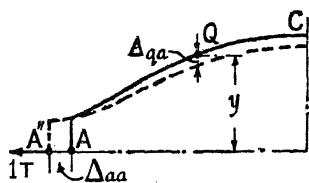
FIG. 132.

$$\Delta_{qa} \quad \iint \frac{M}{EI} \, . \, dx \, . \, dx.$$

The horizontal displacement Δ_{aa} is given by eq. (10), § 91, Vol. I ; which, if $\delta l = \delta x$, becomes

$$\Delta_{aa} = \int_0^L \frac{M}{EI}\, y \, . \, dx$$

In both these expressions M, the bending moment at any section of the arch due to a unit horizontal load at A, is $M = 1 \times y$. Hence,

$$H = \frac{\Delta_{qa}}{\Delta_{aa}}\ \frac{\iint \dfrac{M}{EI} \, . \, dx \, . \, dx}{\int_c^L \dfrac{M}{EI}\, y \, . \, dx}\ \frac{\iint y\left(\dfrac{d_0}{d}\right)^m dx \, . \, dx}{\int_0^L y^2\left(\dfrac{d_0}{d}\right)^? dx}$$

E is constant and cancels out ; $1/I$ is represented by $(d_0/d)^m$ as before. To find the curve for the deflection Δ_{qa}, plot a diagram representing $y(d_0/d)^m$ everywhere, (iii) Fig. 130 (instead of M/EI as in § 54, Vol. I), and using this as a " load curve " find the " bending moment diagram " (iv), which will be the required deflection curve. Use the ordinate $y(d_0/d)^m$ of each division δx, (iii) Fig. 130, as the " load," not the area $y(d_0/d)^m \times \delta x$, when the integral in the denominator becomes $\Sigma y^2(d_0/d)^m$, the length δx cancelling out top and bottom. This summation is given in the Table above. Then from § 86, the deflection curve (iv) Fig. 130 is the

influence line for H, but the ordinates must be divided by $\Sigma y^2(d_0/d)^m$ to get numerical values.

From the influence line, the value of H for any load condition can be found, and hence all the forces in the bars and the necessary areas. The latter can then be used for a more accurate determination of H and of the forces in the members. The effect of temperature variations and reaction displacements must also be examined.

For the application of the above theory to a number of long-span bridges, Krivoshein [28] may be consulted.

BIBLIOGRAPHY
Strain-Energy Methods.

1. MÉNABRÉA. Nouveau principe sur la distribution des tensions dans les systèmes élastiques. *Comptes Rendus*, xlvi, 1858, p. 1056.
2. COTTERILL. On an Extension of the Dynamical Principle of Least Action. *Phil. Mag.*, Apl. 1865, pp. 299, 380, 430.
3. MAXWELL. On the Calculation of the Equilibrium and Stiffness of Frames. *Phil. Mag.*, Apl. 1864, p. 294 (Reciprocal Displacements); see also BETTI, *Il nuovo Cimento*, ser. 2, tt. 7 and 8, 1872; and RAYLEIGH, *Proc. Lond. Math. Soc.*, vol. iv, 1873: *Phil. Mag.*, Dec. 1874, p. 452, and Mar. 1875, p. 183: *Scientific Papers*, vol. i, Cambridge, 1902, p. 179.
4. MOHR. Beitrag zur Theorie des Fachwerks. *Zeit. d. Arch.- u. Ing.-Ver. z. Hannover*, 1874, p. 509; also in same Zeitschrift 1874, p. 223; 1875, p. 17; 1881, p. 243; also *Technische Mechanik*. Berlin, 3rd ed., 1928.
5. CASTIGLIANO. Nuova teoria intorno all' equilibro dei sistemi elastici. *Trans. Acad. Sci. Turin*, vol. x, 1875, p. 380.
6. —— *Théorie de l'équilibre des systèmes élastiques et ses applications.* Torino, 1879; trans. by ANDREWS, *Elastic Stresses in Structures.* London, 1919.
7. FRÄNKEL. Das Prinzip der kleinsten Arbeit, etc. *Zeit. d. Arch.- u. Ing.-Ver. z. Hannover*, 1882, p. 63.
8. SWAIN. On the Application of the Principle of Virtual Velocities to the Determination of the Deflections and Stresses of Frames. *Jour. Frank. Inst.*, Feb. 1883, p. 102, et seq.
9. MÜLLER-BRESLAU, Der Satz von der Abgeleiteten der ideelen Form-änderungs-Arbeit. *Zeit. d. Arch.- u. Ing.-Ver. z. Hannover*, 1884, p. 211.
10. —— *Die Graphische Statik der Baukonstruktionen*, Bd. II, Abt. i, Stuttgart, 5th ed., 1922.
11. AM ENDE. On the Calculation of Frameworks with Superfluous Parts. *The Engr.*, Feb. 1, 1895, p. 89; also Mar. 13, 1885; Nov. 19, 1886; May 18, 1888; Nov. 9, 1890; Sept. 21, 1894.
12. MARTIN. *Statically Indeterminate Structures and the Principle of Least Work.* London, 1895.
13. MÜLLER. Zur Berechnung mehrfach statisch unbestimmter Tragwerke. *Zen. d. Bauverwaltung*, 1907, p. 23.
14. PIRLET. Die Berechnung statisch unbestimmter Systeme. *Der Eisenbau*, 1910, p. 331; 1914, p. 51.
15. CHURCH. *The Mechanics of Internal Work.* New York, 1910.
16. MOLITOR. *Kinetic Theory of Engineering Structures.* New York, 1911.
17. LANDER AND COTTON. An Application of the Graphical Method of Deflections to Statically Indeterminate Frames. *Proc. Inst. C.E.*, vol. cxcvii, 1913–14, p. 298.

18. BENDIXSEN. *Die Methode der Alpha-Gleichungen, etc.* Berlin, 1914; see also OSTENFELD, *Der Eisenbau*, 1921, p. 275; *Eng. Ab. I.C.E.*, 1922, No. 11 : 108.
19. OSTENFELD. *Die Deformations-methode.* Berlin, 1926.
20. FARREN. The Calculation of Stresses in a Redundant Structure by the Method of Comparison of Deflections. *Rpts. and Mem. Ad. Com. for Aero.*, No. 769, 1921.
21. PIPPARD. On a Method for the Direct Design of Framed Structures having Redundant Bracing. *Rpts. and Mem. Ad. Com. for Aero.*, No. 793, 1922.
22. —— *Strain Energy Methods of Stress Analysis.* London, 1929.
23. LEA. Statically Indeterminate and Non-Articulated Structures. *Engg.*, Mar. 17, 1922, p. 313: also *Phil. Mag.*, vol. xv, May 1933 (Maxwell Theorem).
24. LARARD. Reciprocal Load-Deflection Relationships for Structures. *Engg.*, Sept. 7, 1923, p. 287.
25. SOUTHWELL. On Castigliano's Theorem of Least Work. *Phil. Mag.*, Jan. 1923, p. 193.
26. LAMB. The Principle of Virtual Velocities and its Application to the Theory of Elastic Structures. *Select. Eng. Pap. I.C.E.*, No. 10, 1923.
27. PARCEL AND MANEY. *An Elementary Treatise on Statically Indeterminate Stresses.* New York, 2nd ed., 1936.
28. KRIVOSHEIN. *Simplified Calculation of Statically Indeterminate Bridges.* Prague, 1930.
29. VAN DEN BROEK. *Elastic Energy Theory*, New York, 1931.
30. EBNER. Zur Berechnung statisch unbestimmter Raumfachwerke (Zellwerke). *Bautechnic* 10 (*Der Stahlbau*, 5), 1932, p. 1: see also *Eng. Ab. I.C.E.*, 1932, No. 51 : 69.

QUESTIONS ON CHAPTER V

(*Unless otherwise instructed, take* E = 13,000 *tons/sq. in.*)

1. Find (a) by the principle of work, and (b) from eq. (4), § 70, the vertical deflection of the point C of the triangular frame shown in Fig. 133. It is constructed of 3 × 3 × ⅜ in. angles (area 2·1 sq. in.); W = 2 tons.
Ans. 0·027 in.

2. Find the displacement of the point A of the crane shown in Fig. 133 when loaded with 5 tons. Area of jib = 9 sq. in.; area of tie 3 sq. in.; E = 30,000,000 lb./sq. in. (U.L.)
Ans. 0·104 in. hoz.; 0·079 in. vert.

3. Find the horizontal movement of the point C of the frame shown in Fig. 133 due to a vertical load of 10 tons applied at the point A. BA = AC = CD = BD = 6 ft. 8 in. long, area = 3·75 sq. in.; AD = 4 ft. long, area = 2·11 sq. in.
Ans. 0·0028 in.

4. Find by means of eq. (6), § 70, the vertical deflection of the point p of the girder shown in (i) Fig. 34, § 14, loaded as shown, (a) taking all the members of the girder into account, (b) neglecting the deformation of the web members.
Ans. (a) 0·148 in.; (b) 0·105 in., cf. Figs. 37 and 34.

5. If the girder of Q. No. 4 be inclined at 30°, Fig. 133, and supported on rollers at its lower end, find (a) the vertical displacement of the point m when unit load is applied there, and (b) the horizontal displacement of the rollers.
Ans. (a) 10·3 × 10⁻³ in.; (b) 5·04 × 10⁻³ in.

6. In Q. No. 5, suppose the unit load to be applied horizontally at b instead of at m, and find the vertical displacement of m.

Ans. $5 \cdot 04 \times 10^{-3}$ in., proving Maxwell's law for the particular case, see § 84.

7. The outline shown in Fig. 133 represents a swing-bridge supported on its roller path at A and B. Find the forces in the bars of the central panel when loaded as indicated. Assume that the reactions are vertical. Areas : AB = CD = 92 ; AC = BD = 58 ; AD = CB = 22 sq. in.

Ans. Forces : AB = $-$ 366 ; CD = $+$ 404 ; AC = BD = $-$ 132 ; AD = CB = $-$ 35 tons.

8. Find the forces in all the bars of the redundant frame loaded as shown in Fig. 133.

Ans. Forces : AF = $+$ 2·41 ; FB = $+$ 2·44 ; CE = $-$ 3·30 ; ED = $-$ 3·27; EF = $+$ 4·24 ; DB = $-$ 2·46 ; AE = $-$ 3·40 ; CF = $+$ 4·68 ; FD = $+$ 4·09 ; EB = $-$ 3·05, tons.

9. State the principle of Least Work. A lattice girder of the Warren type, loaded as shown, Fig. 134, has four equal bays in the lower boom. The girder is supported at the ends and in the centre. All the members have the same area and the same length. Find the reactions and the force in the top flange above the central support. (U.L.)

Ans. Reactions : 3·95, 12·11, 3·95 tons ; $+$ 2·44 tons.

10. A wall crane ABC, Fig. 134, loaded as shown, has free pin joints at B and C, and a stiff riveted joint at A ; AB may be treated as rigid. Find the forces in the bars and the bending moment at A. (U.L. modified.)

FIG. 133.

Ans. Forces : BC = $+$ 3·68 ; AB = $-$ 3·25 tons M_A 84 inch-tons.

11. Three parallel rectangular beams of the same material, each 3 in. wide and 9 in. deep, are pitched 10 ft. apart with their ends resting on two parallel stone walls 20 ft. apart, the tops of the two walls being in the same horizontal plane. A fourth beam of the same material, width and depth, supporting a uniformly distributed load of total magnitude W, rests centrally across the three beams. Find in terms of W the pressures exerted by the ends of the beams on the walls. (U.L.)

Ans. Outer Reactions 11W/80 ; Inner Reactions 18W/80.

12. A rolled steel beam 10 in. deep, max. I $=$ 166 in.^{4}, is used as a beam of 20 ft. span. It carries a load of 10 tons uniformly distributed. The centre of the beam, before the load is put on, just rests in a saddle carried by two ¾-in. diameter bolts, 3 ft. long, Fig. 134. At the upper ends the bolts are connected to a rigid support, and the two ends of the beam rest on
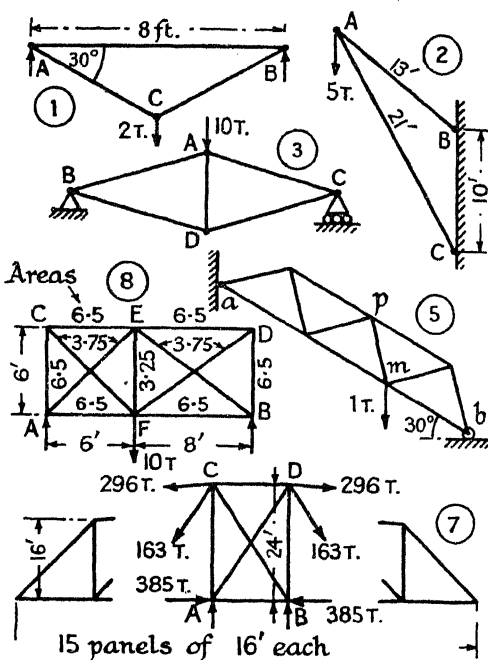
rigid supports. Determine (a) the force in the bolts; (b) the maximum deflection of the beam; (c) draw the bending moment diagram for the beam. (U.L.)

Ans. (a) 6·11 tons in the two; (b) 0·019 in. (Questions of this type can be most easily solved by equating the stretch of the bolts to the deflection of the beam, each expressed in terms of P the pull in the bolts.)

13. A davit, 2 in. diameter, consists of a vertical part 4 ft. high and a curved part at its upper end forming a quadrant of a circle 4 ft. radius. A load suspended from the end of the curved part produces a stress in the material due to bending of 8000 lb./sq. in. Calculate the vertical displacement of the weight, taking bending moments only into account. $E = 30 \times 10^6$. (U.L.)

Ans. 1·1 in.

14. Fig. 135 represents part of a trough floor carrying an axle load. If the span of the troughs is 12 ft., the spacing of the rails 5 ft. centres; the I of a complete trough 436 in.[4]; that of a rail 31 in.[4]; and the load is spread over 5 troughs, show that a unit axle load will be distributed as indicated in the figure. [Cf. Martin,[12] p. 63.]

Fig. 134.

15. Find by means of a Williot-Mohr diagram, § 12, the deflection polygon for the girder of Fig. 41 when a vertical load of 1 ton is placed at m. Hence find from Maxwell's theorem the vertical deflection of m when the girder is loaded as shown in Fig. 41.

Ans. 0·272 in.
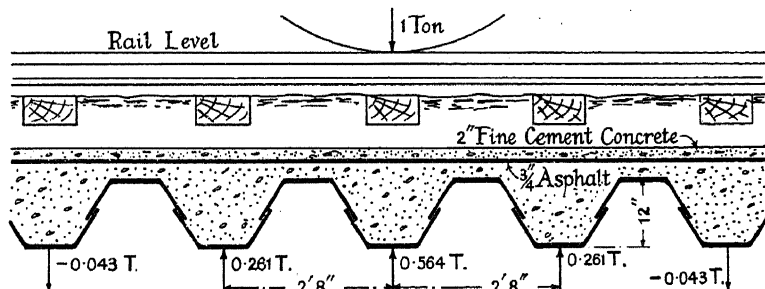
Fig. 135.

16. AB is a uniform beam supported at B and direction-fixed at A. Using Maxwell's theorem, draw the influence line for the reaction R_2 as a load W = 1 travels across the beam from A to B.

Ans. The I.L. for R_2 is the deflection curve of the beam when loaded with unit load at B, R_2 being removed. Cf. § 36.
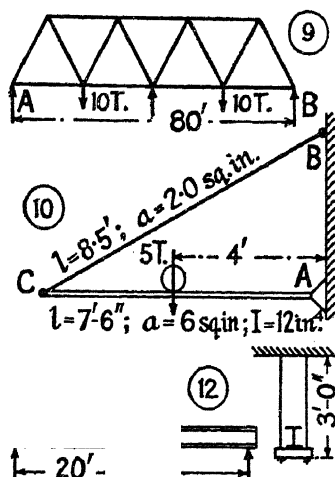
CHAPTER VI

BRACKET LOADS ON STANCHIONS

95. Bracket Loads on Stanchions.—Stanchions are often subjected to bending moments at points intermediate between their ends; one of the commonest cases is that shown in Fig. 136, where the stanchion carries a bracket supporting the rails for a travelling crane. In many instances these applied bending moments are so large that the additional bending moment due to the effect of the longitudinal load can be neglected in comparison therewith. In such cases, so far as bending moments are concerned, the member may be treated as a beam in a vertical position, and the shearing-force and bending-moment diagrams are easy to obtain. The real difficulty of the problem is that the end conditions met with in practice cannot be defined with precision, and a more or less probable assumption must be made as to the degree of constraint which will exist.

96. Bending-Moment and Shearing-Force Diagrams.—*Case* (1). Let AB, (i) Fig. 137, be a stanchion of length L, fixed in position but not in direction at A and B, and acted on by a moment of magnitude M at the point D distant l from A. This moment will call into play two equal reactions R_1 and R_2 at A and B, of which the magnitude can be found by taking moments about B ; $R_1 L = M$, or $R_1 = R_2 = M/L$. The direction of R_1 and R_2 will be as shown in the figure. The shearing force will be positive and uniform from end to end of the stanchion, (ii), its magnitude is equal to $R_1 = + M/L$. Due to the reaction R_1, the bending moment will increase uniformly from zero at A to $+ R_1 l$ at D. This is shown by the line $a'g'$ in (iii), where $d'g' = + R_1 l = + Ml/L$. Due to the reaction R_2, the bending moment will increase uniformly from zero at B to $- R_2(L - l)$ at D. This is shown by the line $b'h'$, and $d'h' = - R_2(L - l)$
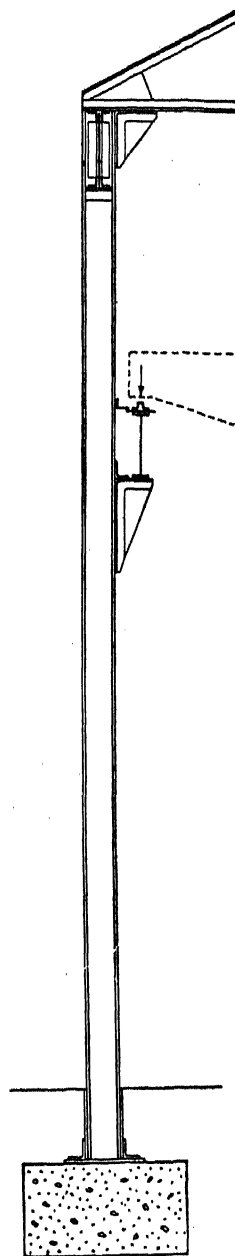
FIG. 136.

$= - M(L - l)/L$. The bending moment changes in sign (i.e. is zero) at D, and there is a point of inflexion in the deflection curve there, (iv), but $d'g' + d'h' = g'h' = M$. Knowing the bending moment everywhere, the deflection and stresses can be found in the usual way. It does not follow that the deflection is zero at D.
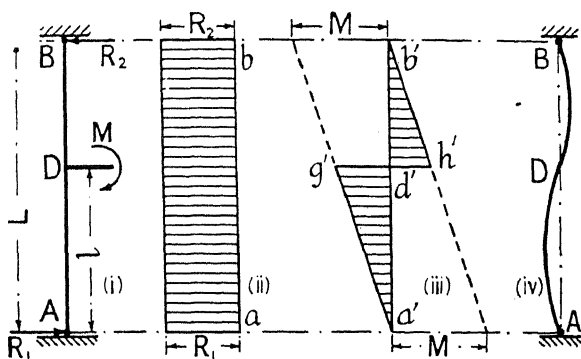
FIG. 137.

Case (2). *Position- and Direction-fixed Ends.*—If the ends be fixed in direction as well as in position, (i) Fig. 138, the member may be regarded as a direction-fixed beam, and the simplest way of dealing with the
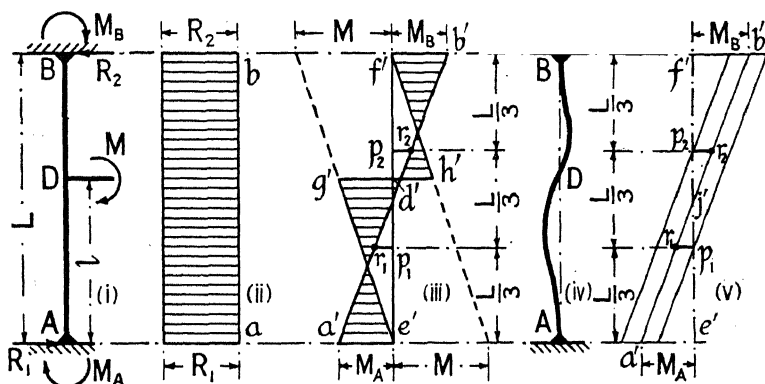
FIG. 138.

problem is by the Characteristic Point method.* Let $e'g'h'f'$ in (iii) be the bending-moment diagram, assuming that the ends are merely position-fixed (Case 1). Then if r_1 and r_2 be the characteristic points (see § 71, Vol. I), by definition, if EI be constant,

* For an alternative method see § 97.

$$p_1 r_1 = \frac{2}{L^2} \{\text{Moment of the area of the Bending-Moment diagram about } f'\}$$

$$= \frac{2}{L^2} \left\{ (d'g') \frac{l}{2} \times \left(L - l + \frac{l}{3} \right) + (d'h') \frac{L - l}{2} \times \frac{2}{3} (L - l) \right\}$$

$$d'g' = + \frac{Ml}{L} ; \quad d'h' = - \frac{M(L - l)}{L} ; \text{ and}$$

$$p_1 r_1 = \frac{2M}{L^3} \left\{ \frac{l^2}{2} \left(L - \frac{2l}{3} \right) - \frac{(L - l)^3}{3} \right\} = \frac{M}{3L^2} \{L^2 - 3(L - l)^2\} . \qquad . \quad (1)$$

Similarly,

$$p_2 r_2 = \frac{2}{L^2} \{\text{Moment of the area of the Bending-Moment diagram about } e'\}$$

$$= \frac{2}{L^2} \left\{ (d'g') \frac{l}{2} \times \frac{2l}{3} + (d'h') \frac{L - l}{2} \times \left(l + \frac{L - l}{3} \right) \right\}$$

$$= \frac{M}{3L^3} \{2l^3 - (L - l)^2 (L + 2l)\} = - \frac{M}{3L^2} \{L^2 - 3l^2\} . \qquad . \quad (2)$$

As shown in (iii), Fig. 138, the values of $p_1 r_1$ and $p_2 r_2$ are plotted from the line $e' f'$ at points $L/3$ from the ends of the span, due regard being paid to sign. Since the beam is direction-fixed at each end, the base line $a' b'$ will pass through both characteristic points, and the bending-moment diagram, (iii), can be completed. The ordinate $a' e'$ represents the direction-fixing moment M_A and is negative ; $b' f'$ represents the direction-fixing moment M_B and is positive. The shaded area is the complete bending-moment diagram.

Consider the double triangle $a' e' f' b'$ in (iii), which is isolated, for clearness, in (v). Draw through p_1 and p_2 lines parallel to $a' b'$. Then, from the geometry of the figure, since p_1 and p_2 divide the span into equal parts, $M_A + (p_2 r_2) = 2(p_1 r_1 + p_2 r_2)$; $M_B + (p_1 r_1) = 2(p_1 r_1 + p_2 r_2)$; or, $M_A = 2(p_1 r_1) + (p_2 r_2)$; $M_B = (p_1 r_1) + 2(p_2 r_2)$.

In these expressions the signs of the magnitudes involved have been ignored for the moment. Inserting the values of $p_1 r_1$ and $p_2 r_2$ from eqs. (1) and (2), and neglecting the sign of $p_2 r_2$,

$$M_A = \frac{2M}{3L^2} \{L^2 - 3(L - l)^2\} + \frac{M}{3L^2} \{L^2 - 3l^2\} = \frac{M}{L^2} \{- L^2 + 4Ll - 3l^2\}$$

This is the numerical value of M_A, which is a negative bending moment. Giving to it its correct sign,

$$M_A = - \frac{M}{L^2} \{- L^2 + 4Ll - 3l^2\} = \frac{M}{L^2} \{L^2 - 4Ll + 3l^2\} = \frac{M}{L^2} \{L - l\} \{L - 3l\} \quad (3)$$

Similarly, $M_B = \frac{M}{3L^2} \{L^2 - 3(L - l)^2\} + \frac{2M}{3L^2} \{L^2 - 3l^2\}$; or since M_B is a positive bending moment,

$$M_B = \frac{Ml}{L^2} \{2L - 3l\} \qquad . \qquad . \qquad . \qquad . \quad (4)$$

Particular Cases.—If $l = L/2$; $d'g' = -d'/h' = M/2$; $p_1r_1 = -p_2r_2$
$= M/12$; $-M_A = +M_B = M/4$.

If $l = nL$; $d'g' = +nM$; $d'h' = -M(1-n)$; $p_1r_1 = M\{(\frac{1}{3}-(1-n)^2\}$;
$p_2r_2 = -M\{\frac{1}{3} - n^2\}$; $M_A = M(1-n)(1-3n)$; $M_B = M\{n(2-3n)\}$.

Fig. 139 shows the variation in p_1r_1 and p_2r_2 for different values of n.

From the form of the above equations it is evident that the signs of M_A and M_B will depend on the value of n.

Having determined the direction-fixing moments, the reactions R_1 and R_2 can be found, and the shearing-force diagram plotted. Take moments about B, $R_1L = M - M_A + M_B$ [since M_A is a negative moment, this implies that the numerical values of all three moments add, as indicated in (i) Fig. 138] or, from eqs. (3) and (4),

$$R_1L = M - \frac{M}{L^2}\{L^2 - 4Ll + 3l^2\}$$
$$+ \frac{Ml}{L^2}\{2L - 3l\}$$

FIG. 139.

and, $\qquad R_1 = R_2 = \frac{6Ml}{L^3}\{L - l\} = \frac{6M}{L}\{n(1 - n)\}$ . . . . (5)

if $l = nL$. The shearing-force diagram is a rectangle, (ii), of height $R_1 = R_2$.
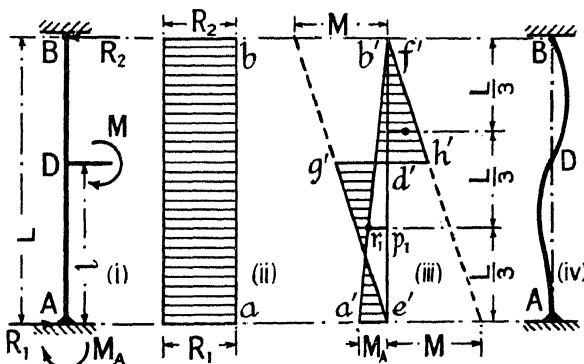
FIG. 140.

Case (3). *Position-fixed at each End, Direction-fixed at Lower End.*— If the stanchion be fixed in position but not in direction at the top end, Fig. 140, the bending moment there will be zero. If it be fixed both in

position and direction at the lower end, the base line will pass through the characteristic point r_1. Draw the bending-moment diagram $e'g'h'f'$, (iii), on the assumption that the ends are merely position-fixed (Case 1), set up the characteristic points r_1 and r_2 as before; the heights p_1r_1 and p_2r_2 are given by eqs. (1) and (2). Then the base line $a'b'$ will pass through f' and r_1 as shown in (iii), $a'e'$ represents the negative direction-fixing moment M_A, and the shaded area is the complete bending-moment diagram. From the geometry of the figure, $a'e' = \frac{3}{2}\,p_1r_1$; or, from eq. (1),

$$M_A = -\frac{M}{2L^2}\{L^2 - 3(L - l)^2\} = -\frac{3M}{2}\left\{\frac{1}{3} - (1 - n)^2\right\} \qquad (6)$$

if $l = n\mathrm{L}$. To find the reactions, take moments about B ;

$$R_1 L = M - M_A = M + \frac{M}{2L^2}\{L^2 - 3(L - l)^2\}\ ;$$

whence, $\qquad R_1 = R_2 = \frac{3Ml}{2L^3}\{2L - l\} = \frac{3M}{2L}\{n(2 - n)\} \qquad . \quad (7)$

if $l = n\mathrm{L}$. The shearing-force diagram is a rectangle, (ii), of height $R_1 = R_2$.

Case (4). *The Continuous Stanchion.*—The characteristic point method of treatment is very convenient if the stanchion be continuous past a floor or other lateral support, as in Fig. 141, which represents the bending-moment diagram for a stanchion, position-fixed at the top end, position- and direction-fixed at the lower end, and continuous over the support B. The point B is assumed to remain fixed in position. Suppose that the moment of inertia of AB is I_1 and of BC is I_2. Make $e'f' = L_1$, and $f'c' = L_2I_1/I_2$. [It is to be understood that the vertical length scale of the span BC is altered in the ratio $I_1 : I_2$, see § 78, Vol. I.] Set up the characteristic points r_1 and r_2 for the span AB, as in Case 2 ; the character-
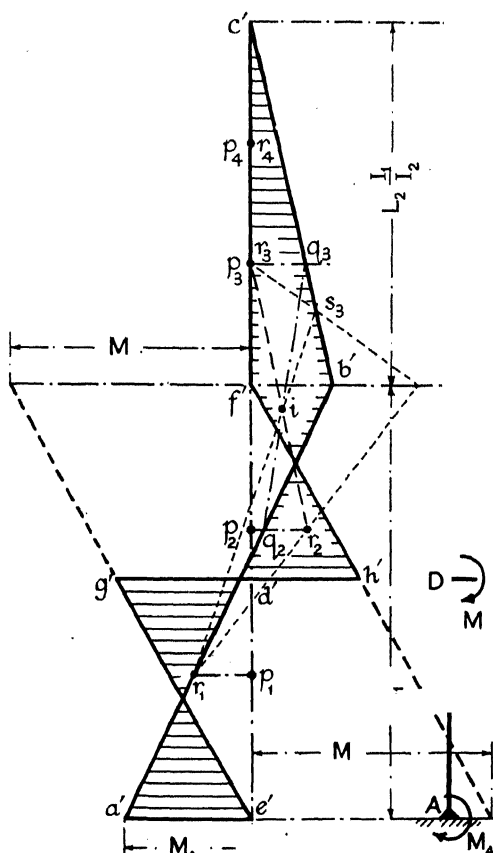
FIG. 141.

istic points for the unloaded span BC will be r_3 and r_4. Then, since the stanchion is position-fixed only at C, the bending moment there will be zero, and the base line will pass through c'. Since the stanchion is position- and direction-fixed at A, the base line will pass through the characteristic point r_1. The base line, therefore, is $a'b'c'$, which can be easily obtained by the methods of § 73, Vol. I ; the modified Ostenfeld construction to determine s_3 should be noted. The verification of the work is that q_2q_3 passes through the intersection point i. The shaded figure is the complete bending-moment diagram, $a'e'$ represents the negative bending moment at A, and $b'f'$ the positive bending moment at B. Having determined these support moments, the reactions at A, B, and C, can be found in the usual way, and the shearing-force diagram can then be plotted.

97. Deflection Curves.—The support moments and deflection in any of the above cases may be found by the methods of § 55, Vol. I, or by direct integration. Consider the general case shown in Fig. 142. Let the span AB = L, and suppose that a bending moment M acts on the stanchion at D, distant l from A. Support moments M_A and M_B also act on the stanchion at A and B respectively. These may be of any magnitude and sign, but are shown for convenience as positive moments.

If the stanchion were merely position-fixed at A and B, the bending moment due to the applied moment M, at any point K lying between A and D and distant x from A, would be $M' = + Mx/L$. Due to the support moments,

FIG. 142.

there will be a bending moment at K of magnitude

$$M'' = M_A + \frac{M_B - M_A}{L}x \quad \text{(cf. § 57, Vol. I).}$$ The total bending moment at K is, therefore,

$$M' + M'' \quad \frac{Mx}{L} + M_A + \frac{M_B - M_A}{L}x = M_A + \beta x,$$

where $\beta = \dfrac{M + M_B - M_A}{L}$. Hence, if y be the deflection at K,

$$EI \cdot \frac{d^2y}{dx^2} = M_A + \beta x$$

$$EI \cdot \frac{dy}{dx} = M_A x + \tfrac{1}{2}\beta x^2 + C_1 \qquad\qquad (1)$$

$$EI \cdot y = \tfrac{1}{2}M_A x^2 + \tfrac{1}{6}\beta x^3 + C_1 x + C_2 \qquad . \qquad . \qquad (2)$$

If the end A is fixed in position, $y = 0$ when $x = 0$, and $C_2 = 0$.

Consider next the bending moment at any point K', coordinates x and y as before, lying between D and B. If the ends of the stanchion were merely position-fixed, the bending moment at K', due to the applied
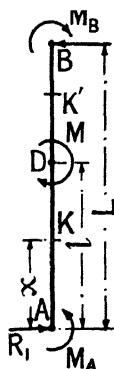
moment M, would be $M' = -M(L - x)/L$.   Due to the support moments,

$M'' = M_A + \dfrac{M_B - M_A}{L} x$, as before.

The total bending moment at K' is, therefore,

$$M' + M'' = -\frac{M(L - x)}{L} + M_A + \frac{M_B - M_A}{L}x = (M_A - M) + \beta x.$$

Hence, $EI \cdot \dfrac{d^2y}{dx^2} = (M_A - M) + \beta x$

$$EI \cdot \frac{dy}{dx} = (M_A - M)x + \tfrac{1}{2}\beta x^2 + C_3 \qquad . \qquad . \qquad . \qquad . \quad (3)$$

$$EI \cdot y = \tfrac{1}{2}(M_A - M)x^2 + \tfrac{1}{6}\beta x^3 + C_3 x + C_4 \qquad . \qquad . \qquad . \quad (4)$$

If the end B be fixed in position, $y = 0$ when $x = L$, and

$$0 = \tfrac{1}{2}(M_A - M)L^2 + \tfrac{1}{6}\beta L^3 + C_3 L + C_4$$

or, $EI \cdot y = -\tfrac{1}{2}(M_A - M)(L^2 - x^2) - \tfrac{1}{6}\beta(L^3 - x^3) - C_3(L - x)$. (5)

At D, where $x = l$, $EI \cdot \dfrac{dy}{dx}$ from eqs. (1) and (3), and $EI \cdot y$ from

eqs. (2) and (5) must be the same.   It is assumed that A and B are position-fixed, and therefore that $C_2 = 0$.

$$\left(EI \cdot \frac{dy}{dx} \right)_{x = l} = M_A l + \tfrac{1}{2}\beta l^2 + C_1 = (M_A - M)l + \tfrac{1}{2}\beta l^2 + C_3$$

whence, $C_1 = Ml + C_3$;   or, $C_3 - C_1 = Ml$.   .   .   . (6)

$(EI \cdot y)_{x = l} = \tfrac{1}{2}M_A l^2 + \tfrac{1}{6}\beta l^3 + C_1 l = -\tfrac{1}{2}(M_A - M)(L^2 - l^2) - \tfrac{1}{6}\beta(L^3 - l^3) - C_3(L - l)$

or, $\tfrac{1}{2}(M_A - M)L^2 + \tfrac{1}{2}Ml^2 + \tfrac{1}{6}\beta L^3 - (C_3 - C_1)l = -C_3 L$;   whence, from

eq. (6), $C_3 = -\tfrac{1}{2}(M_A - M)L - \tfrac{1}{6}\beta L^2 + \tfrac{1}{2}\dfrac{Ml^2}{L}$

and $C_1 = -\tfrac{1}{2}(M_A - M)L - \tfrac{1}{6}\beta L^2 + \tfrac{1}{2}\dfrac{Ml^2}{L} - Ml$.   . (7)

Substituting for β,

$$\left. \begin{array}{l} C_1 = \dfrac{L}{6}\{2M - 2M_A - M_B\} - \dfrac{Ml}{2L}\{2L - l\} \\[3mm] C_3 = \dfrac{L}{6}\{2M - 2M_A - M_B\} + \dfrac{Ml^2}{2L} \end{array} \right\} \qquad . \qquad . \qquad . \quad (8)$$

Particular Cases.   *Case* (1).   *Position-Fixed Ends.*—$M_A = M_B = 0$;

$\beta = M/L$; $C_1 = \dfrac{ML}{3} - \dfrac{Ml}{2L}\{2L - l\}$; $C_3 = \dfrac{ML}{3} + \dfrac{Ml^2}{2L}$.   Insert these values

in eqs. (1) and (3), (2) and (5).

From A to D, if $l = nL$,

$$\frac{dy}{dx} = \frac{M}{6EIL}\{2L^2 - 6Ll + 3l^2 + 3x^2\} = \frac{M}{6EIL}\{L^2(2 - 6n + 3n^2) + 3x^2\}$$

$$y = \frac{M}{6EIL}\{(2L^2 - 6Ll + 3l^2)x + x^3\} = \frac{M}{6EIL}\{L^2(2 - 6n + 3n^2)x + x^3\}$$

At D, where $x = l$, $y = \dfrac{Ml}{3EIL}(L - l)(L - 2l) = \dfrac{Ml^2}{3EI}n(1 - n)(1 - 2n)$

From D to B,

$$\frac{dy}{dx} = \frac{M}{6EIL}\{2L^2 + 3l^2 - 6Lx + 3x^2\} = \frac{M}{6EIL}\{L^2(2 + 3n^2) - 6Lx + 3x^2\}$$

$$y = \frac{M}{6EIL}\{2Lx - x^2 - 3l^2\}\{L - x\} = \frac{M}{6EIL}\{2Lx - x^2 - 3n^2L^2\}\{L - x\}$$

From these equations the slope and deflection everywhere can be obtained.

Case (2). *Position- and Direction-fixed Ends.*—If the stanchion be direction-fixed at A and B, $dy/dx = 0$ when $x = 0$, and when $x = L$. From eq. (1), $C_1 = 0$; and from eq. (3), $C_3 = - (M_A - M)L - \tfrac{1}{2}\beta L^2$. Hence from eq. (8),

$$C_1 = \frac{L}{6}\{2M - 2M_A - M_B\} - \frac{Ml}{2L}\{2L - l\} = 0,$$

whence $\qquad 2M_A + M_B = \dfrac{M}{L^2}\{2L^2 - 6Ll + 3l^2\}$;

further, $\quad C_3 = \dfrac{L}{6}\{2M - 2M_A - M_B\} + \dfrac{Ml^2}{2L} = - (M_A - M)L - \tfrac{1}{2}\beta l^2$;

whence, inserting the value of β, $\quad M_A + 2M_B = \dfrac{M}{L^2}\{L^2 - 3l^2\}$;

and therefore, $\quad M_A = \dfrac{M}{L^2}\{L^2 - 4Ll + 3l^2\}$; $\quad M_B = \dfrac{Ml}{L^2}\{2L - 3l\}$

[compare eqs. (3) and (4), § 96]. $\beta = \dfrac{M + M_B - M_A}{L} = \dfrac{6Ml}{L^3}(L - l)$.

Insert these values in eqs. (1) and (3), (2) and (5). From A to D, if $l = nL$,

$$\frac{dy}{dx} = \frac{M}{EIL^3}\{L(L - 3l)x + 3lx^2\}(L - l) = \frac{M}{EIL}\{(1 - 3n)Lx + 3nx^2\}\{1 - n\}$$

$$y = \frac{M}{2EIL^3}\{L(L - 3l)x^2 + 2lx^3\}(L - l) = \frac{M}{2EIL}\{(1 - 3n)Lx^2 + 2nx^3\}\{1 - n\}$$

At D, where $x = l$,

$$y = \frac{Ml^2}{2EIL^3}\{L - 2l\}(L - l)^2 = \frac{ML^2}{2EI} \cdot n^2(1 - n)^2(1 - 2n)$$

From D to B, since from eq. (6), $C_3 = Ml$,

$$\frac{dy}{dx} = \frac{M}{EIL^3}\{L^3l - (4L - 3l)Llx + 3(L - l)lx^2\}$$

$$\qquad - \frac{Mn}{EIL}\{L^2 - (4 - 3n)Lx + 3(1 - n)x^2\}$$

$$y = \frac{Ml}{2EIL^3}\{(2L - l)Lx - 2(L - l)x^2 - L^2l\}(L - x)$$

$$\qquad = \frac{Mn}{2EIL}\{(2 - n)Lx - 2(1 - n)x^2 - nL^2\}(L - x)$$

Case (3).   *Position-fixed at each End, Direction-fixed at Lower End.*— Since the stanchion is position-fixed, merely, at B; $M_B = 0$. Since it is direction-fixed at A, $dy/dx = 0$ when $x = 0$, and from eq. (1), $C_1 = 0$; hence, from eq. (6), $C_3 = Ml$. From eq. (8),

$$C_1 = \frac{L}{6}\{2M - 2M_A\} - \frac{Ml}{2L}\{2L - l\} = 0\ ;$$

whence, $M_A = -\frac{M}{2L^2}\{L^2 - 3(L - l)^2\}.$

$\beta = \dfrac{M + M_B - M_A}{L} = \dfrac{3Ml}{2L^3}\{2L - l\}.$ Insert these values in eqs. (1) and (3), (2) and (5),

From A to D, if $l = nL$,

$$\frac{dy}{dx} = \frac{M}{4EIL^3}[2\{3(L - l)^2 - L^2\}Lx + 3(2L - l)lx^2]$$

$$= \frac{M}{4EIL}[2\{3(1 - n)^2 - 1\}Lx + 3n(2 - n)x^2]$$

$$y = \frac{M}{4EIL^3}[\{3(L - l)^2 - L^2\}Lx^2 + (2L - l)lx^3]$$

$$= \frac{M}{4EIL}[\{3(1 - n)^2 - 1\}Lx^2 + n(2 - n)x^3]$$

At D, where $x = l$,

$$y = \frac{Ml^2}{4EIL^3}\{(2L - l)^2 - 2L^2\}(L - l)$$

$$= \frac{ML^2}{4EI}n^2(1 - n)\{2 - 4n + n^2\}$$

From D to B,

$$\frac{dy}{dx} = \frac{Ml}{4EIL^2}\{4L^3 - 3(2L - l)(2Lx - x^2)\}$$

$$= \frac{Mn}{4EI}\{4L^2 - 3(2 - n)(2Lx - x^2)\}$$

$$y = \frac{Ml}{4EIL^3}\{(2L - l)(2Lx - x^2) - 2L^2l\}(L - x)$$

$$= \frac{Mn}{4EIL}\{(2 - n)(2Lx - x^2) - 2nL^2\}(L - x)$$

Case (5).   *Position- and Direction-fixed at* A, *quite Free at* B.—At A where $x = 0$, $y = 0$ and $dy/dx = 0$. Hence, from eq. (1), $C_1 = 0$, and from eq. (2), $C_2 = 0$. Since the stanchion is quite free at B, $M_B = 0$, and for equilibrium, $M_A = M$; therefore $\beta = 0$. Eq. (1) becomes, $\dfrac{dy}{dx} = \dfrac{Mx}{EI}$; which gives the slope between A and D. At D, where $x = l$, $\dfrac{dy}{dx} = \dfrac{Ml}{EI}$. From eq. (2), giving the deflection between A and D, $y = \dfrac{Mx^2}{2EI}$;

which becomes $y = \dfrac{Ml^2}{2EI}$ at D. From eq. (3), $EI \cdot \dfrac{dy}{dx} = C_3$, hence C_3/EI is the slope from D to B, and therefore at D. But the slope at D is Ml/EI. Hence $C_3 = Ml$. From eq. (4), $EI \cdot y = C_3 x + C_4 = Mlx + C_4$. At D, where $x = l$, $y = \dfrac{Ml^2}{2EI}$; therefore $C_4 = -\dfrac{Ml^2}{2}$, and $y = \dfrac{Ml}{2EI}\{2x - l\}$; which gives the deflection between D and B.

98. Bracket Loads. A Closer Approximation.—In the preceding articles it has been assumed that the applied moment acts at a point. In many practical cases the moment is applied through the medium of a bracket, (i) Fig. 143. If the depth of the bracket be small compared
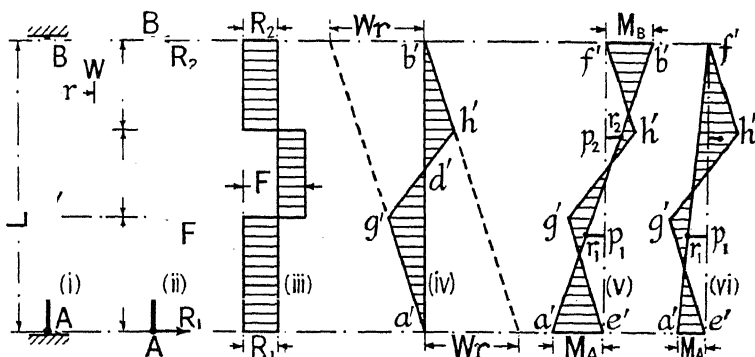
FIG. 143.

with the height of the stanchion, no serious error is introduced by assuming that the moment is applied at the centre of the depth of the bracket. If the depth of the bracket be considerable, a somewhat closer approximation may be obtained by replacing the applied moment by two forces FF, such that the moment $Fl_2 = M = Wr$, where W is the applied load and r its distance from the centre line of the stanchion. The shearing-force and bending-moment diagrams can be obtained in a manner similar to that used in the previous cases. They are given in Fig. 143; (iii) and (iv) are the shearing-force and bending-moment diagrams for a stanchion position-fixed at each end. The magnitude of R_1 and R_2 is $M/L = Wr/L$, whence the shearing-force diagram can be drawn. The bending-moment diagram is similar to (iii) Fig. 137, except that $g'h'$ is a sloping line instead of being horizontal.

(v) is the bending-moment diagram for a stanchion position- and direction-fixed at both ends. The figure $e'g'h'f'$ is similar to (iv); the direction-fixing moment at A is,

$$M_A = a'e' = \frac{Wr}{L^2}\{l_3^2 - 2l_1l_3 - l_1l_2\};$$

and the direction-fixing moment at B is,

$$M_B = b'f' = \frac{Wr}{L^2}\{2l_1l_3 + l_2l_3 - l_1^2\},$$

hence the bending-moment diagram (v) can be completed. The reactions are,

$$R_1 = R_2 = \frac{Wr}{L^3}\{3l_1l_2 + 6l_1l_3 + 3l_2l_3 + l_2^2\},$$

from which the shearing-force diagram can be set out. It is similar to (iii).

(vi) is the bending-moment diagram for a stanchion position-fixed at both ends, direction-fixed at the lower end only. The figure $e'g'h'f'$ is set out as before; the direction-fixing moment at A is,

$$M_A = a'e' = -\frac{Wr}{2L^2}\{l_1^2 + 2l_1l_2 + 2l_1l_3 - l_2l_3 - 2l_3^2\};$$

$M_B = 0.$ The reactions are,

$$R_1 = R_2 = \frac{Wr}{2L^3}\{3l_1^2 + 6l_1l_2 + 6l_1l_3 + 3l_2l_3 + 2l_2^2\};$$

the shearing force diagram is similar to (iii).

The characteristic points for the bending-moment diagram (iv) are,

$$p_1r_1 = \frac{Wr}{3L^2}\{l_1^2 + 2l_1l_2 + 2l_1l_3 - l_2l_3 - 2l_3^2\}$$

$$p_2r_2 = \frac{Wr}{3L^2}\{2l_1^2 + l_1l_2 - 2l_1l_3 - 2l_2l_3 - l_3^2\}$$

These may be used in the case of direction-fixed and continuous stanchions. The expressions as they stand give the correct sign to p_1r_1 and p_2r_2.

PORTAL BRACING

99. Portal Bracing.—If a rectangular frame ACDB, (i) Fig. 144, with pin joints, be subjected to a sideways force F, it is necessary for the stability of the frame to introduce stiffening, such for example as the diagonal AD, to prevent lateral deformation. If the frame form the portal or entrance to a bridge, or is part of a building such that a passageway is required through it, it is not possible to introduce the diagonal AD, and some form of *portal bracing* must be used. The simplest type of portal bracing is shown at (ii) Fig. 144. The diagonal reappears as the bar GD, and CDHG forms a rigid panel. If, then, the columns AC and BD be made sufficiently strong to carry the bending moments which

FIG. 144.

will be set up in them, the frame will resist the sideways force F. It will be assumed in the first instance that all the joints are pin joints, and incapable of carrying a bending moment. Suppose that the force F act at C ; there will be an overturning moment Fh on the frame. This will call into play vertical reactions R_1 and R_2 at A and B respectively. R_1 will be a downward force, and R_2 an upward force. They will be equal in magnitude, and form a couple R_1b, equal to the overturning moment Fh. Then $R_1b = Fh$; and $R_1 = R_2 = Fh/b$. In addition to the vertical reactions at A and B, horizontal reactions F_1 and F_2 respectively will act at these points, such that $F_1 + F_2 = F$. Under the action of the force F, the columns will deflect and the panel CDHG will move to the right. If the panel were absolutely rigid, it follows that the movement of G to the right of A would be equal to the movement of H to the right of B. If, further, the column AC be of the same length
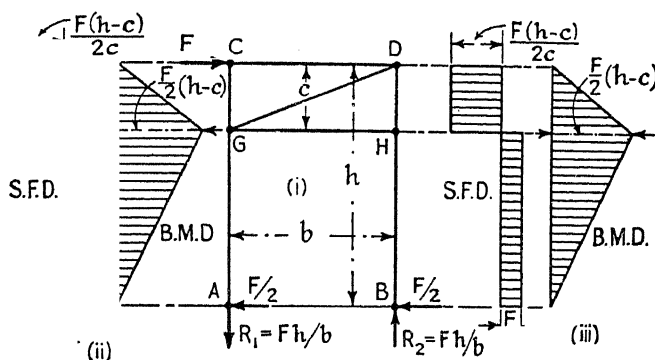
FIG. 145.

and cross section as the column BD, it follows that the force F_1 would equal the force F_2, for GA and HB may be regarded as two cantilevers projecting from G and H respectively, and each deflected an equal amount by the forces F_1 and F_2. Strictly speaking, the elastic deformation of the panel CDHG should be taken into account, but to do this considerably complicates the analysis. It will be assumed for present purposes that $F_1 = F_2 = F/2$. Having determined the reactions, the forces in the members can be found by the method of sections, § 8. Cut the bar GH and replace it by F_{GH}, the force in the bar. Take moments about D of the forces acting on BD. Then $F_2h = F_{GH}.c$, $F_{GH} = \dfrac{F_2h}{c} = \dfrac{Fh}{2c}$, and is compressive. Next cut the bar CD and replace it by F_{CD}, the force in the bar. Take moments about G of the forces acting on AC. Then $F_1(h - c) + Fc = F_{CD}.c$, and

$$F_{CD} = F + F_1 \left\{ \frac{h - c}{c} \right\} = F + \quad h - c \quad \frac{F(h + c}{2}$$

This also is a compressive force. If F_{GD} be the force in the diagonal GD, its vertical component, $F_{GD} \sin \theta = R_2$. Hence, $F_{GD} = R_2 \operatorname{cosec} \theta$ $= \dfrac{Fh}{bc} \sqrt{b^2 + c^2}$; a tensile force.

The bending-moment and shearing-force diagrams for the two columns are shown in (ii) and (iii) Fig. 145. The shearing force in AG and BH is $F/2$; that in GC is $F - F_{CD} = F(h - c)/2c$; and that in HD is $F_{GH} - F/2 = F(h - c)/2c$ also. The maximum bending moment occurs at G and H and is $F(h - c)/2$. In addition, there is a longitudinal force Fh/b in AG and BD. The longitudinal force in CG is zero. The members AG and BD must be designed to carry both the longitudinal force and the bending moment.

If the force F may act either to the right or to the left of the frame, it is usual to cross-brace the panel, (i) Fig. 146.

FIG. 146.

This is the case when F is a load due to wind pressure. If the cross-bracing be constructed of flat bars, which are incapable of withstanding compression, only the diagonal in tension need be taken into account when finding the forces in the members, see (ii) and (iii) Fig. 146. If both diagonals are capable of resisting tension and compression, the method of superposition, § 7, must be applied, and the frame split up into two component frames, each carrying one half of the force F, (ii) and (iii) Fig. 147. Having found the forces in the members of each simple frame, they must be combined in the usual way in order to find the forces in the compound frame.

Should the force F act at some point other than

FIG. 147.

C, or if the length and moment of inertia of the columns AC and BD be not the same, the above simple expressions will no longer hold. The more general case is treated in § 104.

100. Portals with Direction-fixed Bases.—Suppose the column bases to be rigidly attached to foundations of such a nature that the columns may be considered as direction-fixed at A and B, Fig. 148. As before, it will be assumed that AC and BD are of equal length, and that the moment of inertia of these members is the same. The force F at C will bend the columns to the shape shown at (ii). There will evidently be a reversal of the curvature in the lengths AG and BH, and points of inflexion such as K, (ii) Fig. 148, will exist, where the bending moment is zero. If these points of inflexion can be determined, the methods of
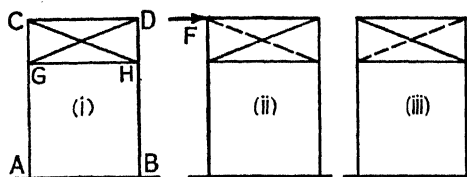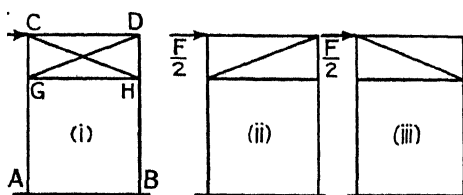
the preceding article can ·be applied, for that portion of the frame above the points of inflexion J and K, Fig. 149, is in exactly the same condition as is the frame shown in Fig. 144. The reactions R_1, R_2, F_1, and F_2, may be assumed to act at J and K respectively, instead of at A and B. Consider the right-hand column BHD, Fig. 148. If the panel CDHG
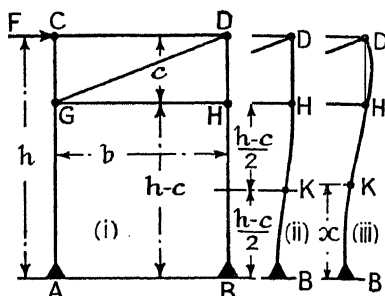
FIG. 148.
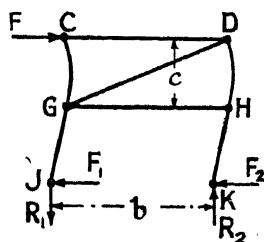
FIG. 149.

were perfectly rigid, so that the member DH always remained parallel to itself as shown at (ii) and did not deflect, it is evident that the curve BKH would be symmetrical about its centre point, and the point of inflexion K would lie half-way between B and H. Actually, if D and H are pin joints, the member will bend as indicated at (iii), and K will no longer bisect BH. Nevertheless, as will be seen, its true position is very close to the mid-point, so that for practical purposes it may be assumed to coincide therewith.

Consider the flexure of the column BD. To bend it into the form shown at (iii) Fig. 148, which is reproduced at (i) Fig. 150, forces F_D at D and F_H at H must act upon it. These forces are for the moment unknown, but if the panel CDHG retain its shape, their combined action must bend the column in such a way that the points D and H will still lie in a
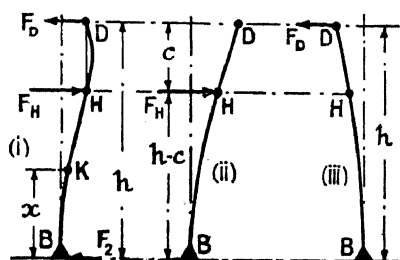
FIG. 150.

vertical straight line after the deformation of the column, (i) Fig. 150. That is to say, the deflection of D and the deflection of H, each to the right of B, must be equal in magnitude. The deflections produced by the two forces F_D and F_H can best be examined by isolating their effects, as shown at (ii) and (iii) Fig. 150. In each figure the column can be regarded as a cantilever, fixed at its lower end and loaded with a single load. From eq. (9), § 55, Vol. I, the deflection at D due to F_H, (ii), is

$$y_D = \frac{F_H}{EI} \cdot \frac{(h-c)^2}{2} \left| h - \frac{h-c}{3} \right\} \quad \frac{F_H(h-c)^2}{6EI} \{2h + c\}$$

and the deflection at H due to F_H is $y_H = \dfrac{F_H(h - c)^3}{3EI}$. The deflection at

D due to F_D, (iii), is $y_D = \dfrac{F_D h^3}{3EI}$; and the deflection at H due to F_D

is $y_H = \dfrac{F_D}{EI}\left\{\dfrac{h \cdot (h - c)^2}{2} - \dfrac{(h - c)^3}{6}\right\}$, see eq. (2), § 52, Vol. I. Hence

the total deflection at D, when both forces act together, is

$$y_D = \frac{F_H(h - c)^2}{6EI}\{2h + c\} - \frac{F_D \cdot h^3}{3EI} \qquad . \qquad . \quad (1)$$

and the total deflection at H, when both forces act together, is

$$y_H = \frac{F_H(h - c)^3}{3EI} - \frac{F_D}{6EI}(h - c)^2(2h + c) \qquad . \qquad . \quad (2)$$

But if D and H lie in the same vertical straight line after distortion of the column, y_D from eq. (1) must be equal to y_H from eq. (2). Equating these values, it follows that

$$\frac{F_H}{F_D} = \frac{3h^2 - c^2}{3(h - c)^2} \qquad . \qquad . \qquad . \qquad . \quad (3)$$

At K, the point of inflexion, the bending moment must be zero. The bending moment at K is $F_H(h - c - x) - F_D(h - x)$, where $BK = x$. If this bending moment be zero,

$$\frac{F_H}{F_D} = \frac{h - x}{h - c - x} = \frac{3h^2 - c^2}{3(h - c)^2} \quad \text{[from eq. (3)]}$$

whence, $\qquad\qquad x = \dfrac{h - c}{2} \cdot \dfrac{3h - c}{3h - 2c} \qquad . \qquad . \qquad . \quad (4)$

This equation determines the point of inflexion K. In practical cases, K will be found to lie very near the mid-point of BH. Thus if $c = h/3$, $x = 1 \cdot 143\,(h - c)/2$. In view of the approximate nature of the assumptions made regarding portal bracings, for all practical purposes K may be taken as lying midway between B and H. The error thus introduced is on the side of safety, and allows for a small imperfection in the direction-fixing.

All the analyses given in this Chapter for portal bracings of this type, and loaded with a force F at C, may therefore be applied equally well to portals with pin joints at the feet A and B, or to portals with direction-fixed feet. In the latter case the reactions must be assumed to act at the points of inflexion J and K, Fig. 149, which can be regarded as virtual feet. For practical purposes these points of inflexion can be regarded as lying midway between the points A and G, and B and H, respectively.

It must be remembered that the values of R_1 and R_2, for portals with direction-fixed feet, must be determined by taking moments about J and K. Thus in Fig. 149, $F \times DK = R_1 \times JK$. From Fig. 148, $DK = h - x$, and $JK = AB = b$. Therefore, $R_1 = R_2 = F \cdot \dfrac{h - x}{h}$.

If $x = (h - c)/2$, $R_1 = R_2 = F \cdot \dfrac{h + c}{2b}$, not $F. h/b$ as in the case where A and B are pin joints. The fixing moments at the feet of the columns are $M_1 = F_1 x$ at A, and $M_2 = F_2 x$ at B. If $F_1 = F_2 = F/2$, and $x = (h-c)/2$,
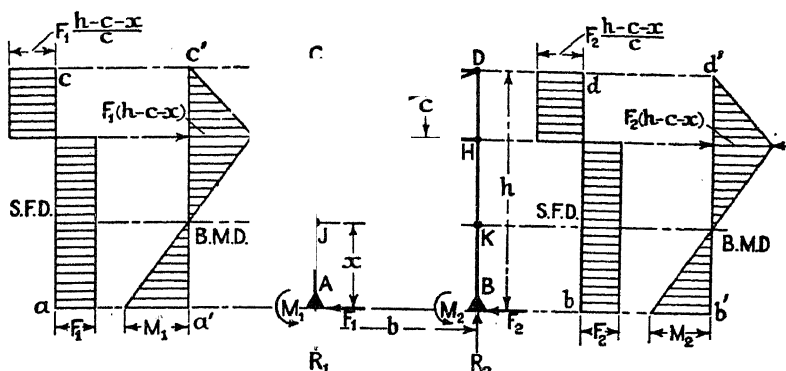
FIG. 151.

then $M_1 = M_2 = F(h - c)/4$. The bending-moment and shearing-force diagrams are shown in Fig. 151.

101. Braced Portals.—Having determined the reactions at the feet of the portals, the stresses in the members can be found by the method
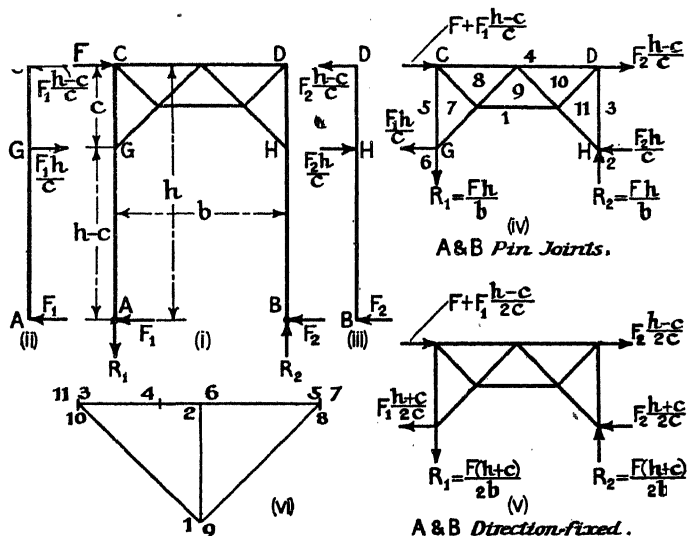
FIG. 152.

of sections, as in § 99. Alternatively, a stress diagram can be drawn ; (vi) Fig. 152 is a typical example. To draw this diagram, the equivalent forces acting at the joints must be determined. It is evident that the

pressure on the framework at the point H, (i) Fig. 152, due to the force F_2, will be much enhanced owing to the leverage at which the force F_2 acts. The two members AGC and BHD can be regarded as levers, acted on by the forces and reactions shown at (ii) and (iii). Consider BD, (iii) ; to balance F_2 at B, a force $F_2(h - c)/c$ at D is required. Hence the reaction at H is $F_2 h/c$. Similarly, the force at C is $F_1(h - c)/c$, and at G is $F_1 h/c$. If, therefore, the portal bracing proper be isolated, the equivalent forces acting on it will be as shown at (iv). A little consideration will show that the forces acting on the framework will be opposite in direction to the reactions on the levers shown at (ii) and (iii). To the force at C must be added the applied load F which also acts there. The
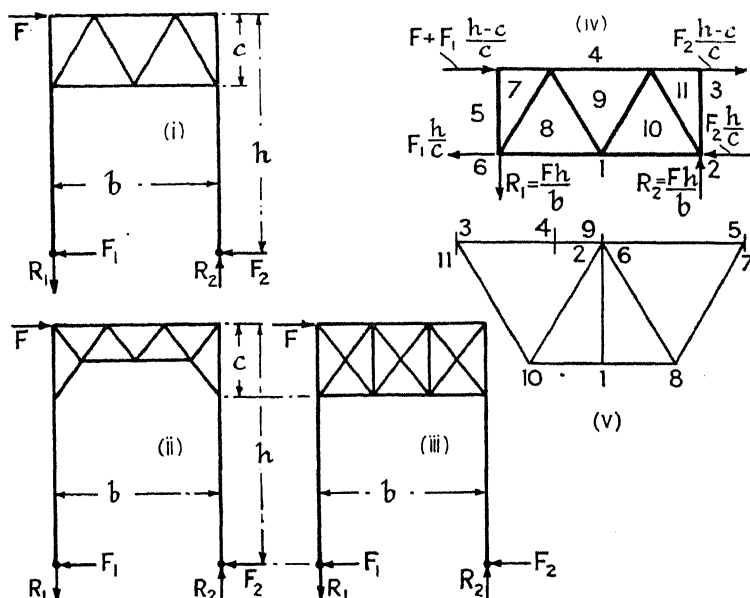
FIG. 153.

stress diagram for (iv) is shown at (vi). For the conditions indicated $R_1 = R_2 = Fh/b$. If $F_1 = F_2 = F/2$, the force at C is $F + F(h - c)2c$; that at D is $F(h - c)/2c$, and those at G and H are $Fh/2c$.

Direction-fixed Bases.—If the portal be direction-fixed at A and B, the forces F_1 and F_2 may be taken as acting at J and K, the points of inflexion (see Fig. 149). If these points bisect the members AG and BH, so that $GJ = HK = (h - c)/2$, then the magnitudes of the forces will be as shown at (v). It is evident that in order to obtain the values shown in (v) from those given in (iv), all that is necessary is to substitute $(h - c)/2$ for $(h - c)$ everywhere ; or, what is equivalent, to substitute $(h + c)/2$ for h. This applies also to the values of R_1 and R_2.

Some other types of portal bracings are shown in Fig. 153 ; and the stress diagram for type (i), when A and B are pin joints and a lateral

force F acts at C, is given at (v). The equivalent forces on the bracing, (iv), are the same as those in (iv) Fig. 152. In cases like (iii) Fig. 153, the bracing must be divided up into two component frames each carrying one-half the load, and the stresses thus found properly compounded, in order to obtain the forces in the actual members.

102. **Portal with Knee Braces.**—In this form of portal, Fig. 154, the member CD must have a girder cross-section, suitably arranged to
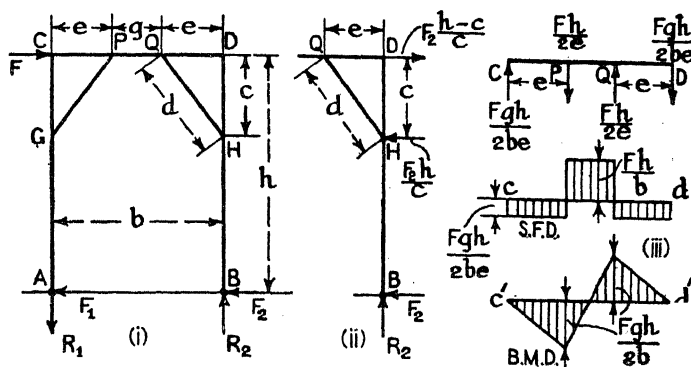
FIG. 154.

carry the bending moments set up. As in previous cases, the equivalent load at the panel point H, due to the force F_2, will be $F_2 h/c$, (ii) Fig. 154. The triangle QDH will represent the triangle of forces for the point H, hence the compressive force in the diagonal HQ is $F_2 . hd/ce$, and its vertical component is $F_2 h/e$. The tensile force in the bar DH is evidently $(F_2 h/e - R_2)$. If $F_1 = F_2 = F/2$ as before, and $R_1 = R_2 = Fh/b$,

then the force in the diagonal is $F . \dfrac{hd}{2ce}$, and its vertical component is $\dfrac{Fh}{2e}$.

The force in the bar DH is

$$Fh\left(\frac{1}{2e} - \frac{1}{b}\right) = Fh . \frac{b - 2e}{2be} = F . \frac{gh}{2be}.$$

The vertical forces on the girder CD, and the corresponding shearing-force and bending-moment diagrams, are shown at (iii) Fig. 154. The shearing-force and bending-moment diagrams for the bars AC and BD are as shown in Fig. 145. The longitudinal force in the bar DQ is $F . \dfrac{h - c}{2c}$

(tensile) ; that in PQ is $F . \dfrac{h - c}{2c} - F . \dfrac{h}{2c} = -\dfrac{F}{2}$, and is compressive ;

that in CP is $-\dfrac{F}{2} - F . \dfrac{h}{2c} - F . \dfrac{h + c}{2c}$, compressive. The member CD must be designed to carry these longitudinal loads in addition to the bending moment and shearing force. The force in GP is equal in

Q

magnitude to that in HQ, but is tensile ; and that in CG is equal to that in DH, but is compressive. The forces in AG and HB $= \pm Fh/b$.

103. Plate Girder Portal.—The panel CH is sometimes made in the form of a stiff plate girder, Fig. 155. If the cross-section of this girder
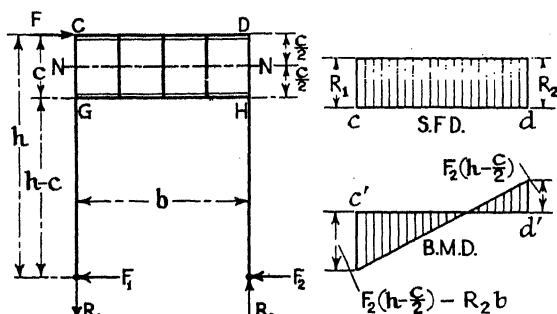
FIG. 155.

be symmetrical, the neutral axis NN will lie at a distance $c/2$ from CD. The shearing-force and bending-moment diagrams for the girder CH are then as shown in Fig. 155. At DH the shearing force is equal to R_2, and at CG equal to R_1. The bending moment at DH is $F_2\left(h - \dfrac{c}{2}\right)$, and at CG is $F_2\left(h - \dfrac{c}{2}\right) - R_2b$. If $F_1 = F_2 = F/2$, and $R_1 = R_2 = Fh/b$, the bending moment at DH is $\dfrac{F}{2}\left(h - \dfrac{c}{2}\right)$, and at CG is $-\dfrac{F}{2}\left(h + \dfrac{c}{2}\right)$.

104. Portals Carrying Lateral Loads. More General Cases.—Let (i) Fig. 156 represent a portal, acted on by a force F at C, and a uniformly
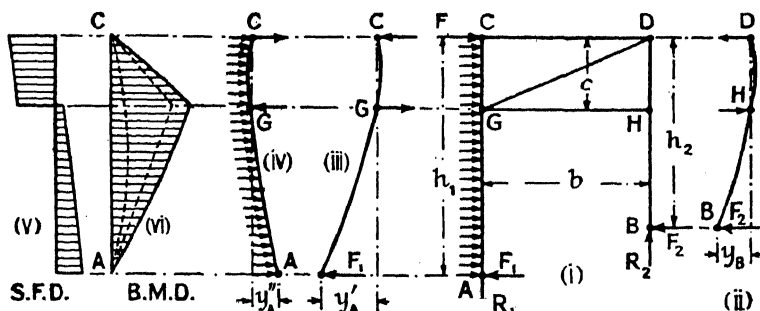
FIG. 156.

distributed load w per unit of length on the column AC. It will be assumed that all the joints are pin joints, including those at A and B. Suppose the columns AC and BD to be of different heights h_1 and h_2, and that their respective moments of inertia be I_1 and I_2. Let the

vertical reactions at A and B be R_1 and R_2, and the horizontal reactions F_1 and F_2, respectively. Then, since the external forces must be in equilibrium,

$$R_1 = R_2 \; ; \; F + wh_1 = F_1 + F_2 \qquad . \qquad . \qquad . \qquad . \quad (1)$$

and, taking moments about A,

$$Fh_1 + \frac{wh_1{}^2}{2} - F_2(h_1 - h_2) - R_2 b = 0 \quad . \qquad . \qquad . \quad (2)$$

Suppose that the panel CDHG remain rigid in shape, and consider the column BD, (ii) Fig. 156. From eq. (11), § 55, Vol. I, the deflection of B from the straight line DH will be $y_B = \dfrac{F_2 h_2 (h_2 - c)^2}{3EI_2}$. To find the deflection of A from the straight line CG, it is convenient to divide the forces acting on AC into two groups as shown at (iii) and (iv). From the equation used above, the deflection of A due to the force F_1, (iii), will be, $y_A' = \dfrac{F_1 h_1 (h_1 - c)^2}{3EI_1}$. From eq. (10), § 55, Vol. I, the deflection of A due to the uniform load, (iv), will be $y_A'' = \dfrac{wh_1(h_1 - c)}{24EI_1}\{3h_1{}^2 - 5h_1 c + c^2\}$. The actual deflection of A will be the difference between y_A' and y_A''.

$$y_A = y_A' - y_A'' = \frac{F_1 h_1 (h_1 - c)^2}{3EI_1} - \frac{wh_1 (h_1 - c)}{24EI_1}\{3h_1{}^2 - 5h_1 c + c^2\}$$

$$= \frac{h_1(h_1 - c)}{3EI_1}\left[F_1(h_1 - c) - \frac{w}{8}\{3h_1{}^2 - 5h_1 c + c^2\} \right]$$

But since the panel CDHG remains rigid, the deflection of the two points A and B, found as above, must be the same, for it is the actual movement of the portal ; in other words, $y_A = y_B$, whence

$$\frac{h_1(h_1 - c)}{3EI_1}\left[F_1(h_1 - c) - \frac{w}{8}\{3h_1{}^2 - 5h_1 c + c^2\} \right] = \frac{F_2 h_2 (h_2 - c)^2}{3EI_2}$$

From eq. (1), $F_2 = F + wh_1 - F_1$; hence

$$F_1\left\{ 1 + \frac{I_2}{I_1} \cdot \frac{h_1(h_1 - c)^2}{h_2(h_2 - c)^2} \right\}$$

$$= F + wh_1 + \frac{w}{8} \cdot \frac{I_2}{I_1} \frac{h_1(h_1 - c)}{h_2(h_2 - c)^2}(3h_1{}^2 - 5h_1 c + c^2) \qquad . \quad (3)$$

From eq. (3) the value of F_1 can be found, F_2 is obtained from eq. (1), and R_1 and R_2 from eq. (2). All the external forces on the frame are thus discovered, and the stresses in all the members can be found as in previous cases. The shearing-force and bending-moment diagrams for the column AC are as shown at (v) and (vi), those for BD are similar to (iii) Fig. 145.

Particular Cases.—If $w = 0$, from eq. (3),

$$F_1 = \left\{ \frac{I_1 h_2 (h_2 - c)^2}{I_1 h_2 (h_2 - c)^2 + I_2 h_1 (h_1 - c)^2} \right\} F \; ;$$

and from eq. (1),

$$F_2 = \left\{ \frac{I_2 h_1 (h_1 - c)^2}{I_1 h_2 (h_2 - c)^2 + I_2 h_1 (h_1 - c)^2} \right\} F.$$

If $h_1 = h_2 = h$, and $I_1 = I_2$, from eq. (3)

$$2F_1 = F + wh + \frac{w}{8(h - c)} \{3h^2 - 5hc + c^2\},$$

and

$$F_1 = \frac{F}{2} + \frac{w}{16} \left\{ \frac{11h^2 - 13hc + c^2}{h - c} \right\} ;$$

hence from eq. (1)

$$F_2 = \frac{F}{2} + \frac{w}{16} \frac{(5h^2 - 3hc - c^2)}{h - c}$$

Direction-fixed Feet.—If the feet A and B of the portal be direction-fixed, it may be assumed as a rough approximation that the points of inflexion J and K occur midway between A and G and B and H (see § 100 and Fig. 148); which points may be regarded as the feet of the portal, and the above equations may be applied. This assumption ignores the fact that the lateral deflection of the parts JA and KB of the columns will not, in general, be equal. A more correct solution may be obtained as follows: From eqs. (6) and (3), § 52, Vol. I, and eq. (9), § 55, Vol. I, considering (i) Fig. 157,

FIG. 157.

$$y_C = \frac{wh_1^4}{8EI_1} - \frac{(F_3 - F)h_1^3}{3EI_1} + \frac{F_4(h_1 - c)}{6EI_1}(2h_1 + c) \quad (4)$$

Using eq. (5), § 52, Vol. I,

$$y_G = \frac{w(h_1 - c)^2(3h_1^2 + 2h_1 c + c^2)}{24EI_1} - \frac{F_3 - F}{6EI_1}(h_1 - c)^2(2h_1 + c) + \frac{F_4(h_1 - c)^3}{3EI_1} \quad (5)$$

Considering (ii) Fig. 157,

$$y_D = - \frac{F_5 h_2^3}{3EI_2} + \frac{F_6(h_2 - c)^2}{6EI_2}(2h_2 + c) \quad (6)$$

$$y_H = - \frac{F_5}{6EI_2}(h_2 - c)^2(2h_2 + c) + \frac{F_6(h_2 - c)^3}{3EI_2} \quad (7)$$
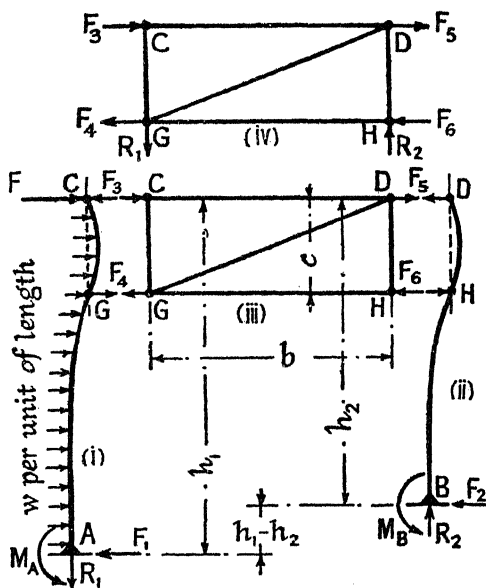
If, as assumed in § 100, the rectangle CDHG remain rigid in shape, $y_C = y_G = y_D = y_H = \Delta$, the sideways deflection of the portal.

Equate y_C to y_G,

$$F_4 = \frac{4(F_3 - F)(3h_1{}^2 - c^2) - w(4h_1{}^3 - c^3)}{12(h_1 - c)^2} \tag{8}$$

Equate y_D to y_H,

$$F_6 = F_5 \frac{3h_2{}^2}{3(h_2 - c)^2} \quad . \quad . \quad . \tag{9}$$

Equate y_C to y_D, and use eqs. (8) and (9),

$$F_5 = (F_3 - F)\frac{I_2}{I_1}\frac{(3h_1 + c)(h_1 - c)}{(3h_2 + c)(h_2 - c)} + \frac{w}{4c}\frac{I_2}{I_1}\frac{(h_1{}^3 - 3h_1{}^2c - 3h_1c^2 - c^3)(h_1 - c)}{(3h_2 + c)(h_2 - c)} \tag{10}$$

Also from (iii) Fig. 154,

$$F_3 - F_4 + F_5 - F_6 = 0 \ . \quad . \quad . \quad . \tag{11}$$

From the four equations (8), (9), (10), and (11), the four unknowns F_3, F_4, F_5, and F_6 can be found. It is simplest to substitute numbers before solving. From (i) and (ii) Fig. 157,

$$M_A = \frac{wh_1{}^2}{2} - (F_3 - F)h_1 + F_4(h_1 - c) \quad . \quad . \tag{12}$$

$$M_B = -F_5h_2 + F_6(h_2 - c) \quad . \quad . \quad . \tag{13}$$

$$F_1 = wh_1 + F - F_3 + F_4 ; \quad F_2 = -F_5 + F_6 \quad . \tag{14}$$

Taking moments of the external forces about A,

$$R_1 = R_2 = \frac{1}{b}\left\{\frac{wh_1{}^2}{2} + Fh_1 - F_2(h_1 - h_2) - (M_A + M_B)\right\} \quad . \tag{15}$$

Knowing $F_3 \ldots F_6$, and the reactions R_1, R_2, the forces in the bars of the framework CDHG can be found, (iv) Fig. 157 ; the bending-moment and shearing-force diagrams for the columns AC and BD can also be set out.

Worked Example.—In the portal shown in Fig. 157 let $h_1 = h_2$ = 25 ft., $c = 7$ ft. 6 in., $b = 17$ ft. 6 in., and $I_1 = I_2$. Let $F = 20$ tons, and $wh_1 = 10$ tons. To find the values of F_3, F_4, F_5 and F_6 ; F_1, F_2 ; R_1 and R_2.

From eq. (8), $588F_4 = 1164F_3 - 27{,}253$;

from eq. (9), $49F_6 = 97F_5$;

from eq. (10), $396F_5 = 396\ F_3 - 8{,}117$;

from eq. (11), $F_3 - F_4 + F_5 - F_6 = 0$.

Eliminate F_4, F_5, and F_6 from the last equation,

$F_3 = 39{,}060 \div 1152 = 33 \cdot 9$ tons ; $F_4 = 12{,}207 \div 588 = 20 \cdot 76$ tons ;
$F_5 = 33 \cdot 9 - 8{,}117 \div 396 = 13 \cdot 41$ tons ; $F_6 = 97 \times 13 \cdot 41 \div 49$
$$= 26 \cdot 55 \text{ tons.}$$

From eq. (14),

$F_1 = 10 + 20 - 33 \cdot 9 + 20 \cdot 76 = 16 \cdot 86$ tons ; $F_2 = -13 \cdot 41 + 26 \cdot 55$
$$= 13 \cdot 14 \text{ tons.}$$

From eqs. (12) and (13),

$M_A = 10 \times 25/2 - 13 \cdot 9 \times 25 + 20 \cdot 76 \times 17\frac{1}{2} = 140 \cdot 8$ ft.-tons.

$M_B = -13 \cdot 41 \times 25 + 26 \cdot 55 \times 17\frac{1}{2} = 129 \cdot 38$ ft.-tons.

From eq. (15),

$R_1 = R_2 = \dfrac{1}{17 \cdot 5}\{10 \times 25/2 + 20 \times 25 - (140 \cdot 8 + 129 \cdot 38)\} = 20 \cdot 28$ tons.

FRAMEWORK WITH STIFF JOINTS

SLOPE-DEFLECTION METHODS

105. Stiff Framework.—There are many practical structures which depend for stability entirely on the stiffness of their joints : a common case is that of the ordinary bicycle; and Vierendeel has shown that it is possible, and even economical, to construct open-web girders of large span with no diagonals, the safety of the frame depending solely on the stiffness of its joints (§ 249).

It is usual, in calculating the stresses in such frames, to assume that the joints are perfectly rigid, and to neglect the deformations due to the longitudinal loads in the members. The results obtained are approximate only, and are not applicable unless the joints in the framework possess considerable rigidity. Some typical examples are given below.

Method of Attack.—One of the simplest methods of treating a stiff framework is to apply the theorems given in § 55, Vol. I. It was there shown that if AB, (i) Fig. 158, be a uniform beam subjected to a bending moment M_A at A, and M_B at B, (ii) Fig. 158, the deflection of the beam at the point A, below the tangent at B, is equal to $\dfrac{1}{EI} \times$ (moment of the area of the bending moment diagram about A). That is to say,
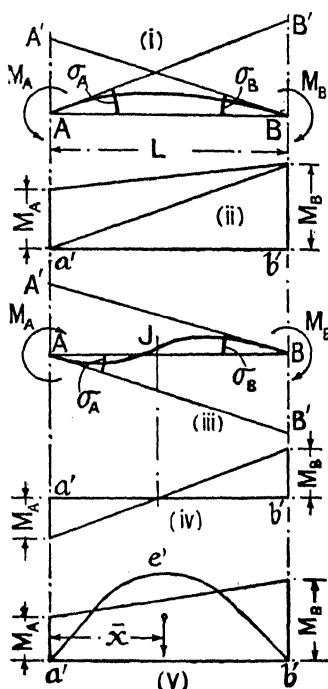
FIG. 158.

$$A'A = \frac{1}{EI}\left\{M_A L \times \frac{L}{3} + \frac{M_B L}{2} \times \frac{2L}{3}\right\} = \frac{L^2}{6EI}\{M_A + 2M_B\} \qquad (1)$$

and similarly, $\qquad\qquad B'B = \dfrac{L^2}{6EI}\{2M_A + M_B\} \qquad\qquad . \quad (2)$

Then σ_A, the slope of the beam at A, is

$$\sigma_A = - \frac{B\dot{B}}{AB} = - \frac{L}{6EI}\{2M_A + M_B\} \qquad . \qquad . \quad (3)$$

and σ_B, the slope at B, is

$$\sigma_B = + \frac{A'A}{AB} = + \frac{L}{6EI}\{M_A + 2M_B\} \qquad . \qquad . \quad (4)$$

As indicated, σ_A must be regarded as a negative slope, to agree with the convention regarding signs, Fig. 80, Vol. I, viz. that a distance measured to the right is positive, and a downward deflection is positive. From eqs. (3) and (4),

$$M_A = - \frac{2EI}{L}(2\sigma_A + \sigma_B); \quad M_B = + \frac{2EI}{L}(\sigma_A + 2\sigma_B) \qquad . \quad (5)$$

These equations can also be obtained from first principles thus:

At a distance x from A the bending moment is $\left\{ M_A + \dfrac{M_B - M_A}{L}x \right\}$.
Hence,

$$EI \cdot \frac{d^2y}{dx^2} = M_A + \frac{M_B - M_A}{L}x$$

$$EI \cdot \frac{dy}{dx} = M_A \cdot x + \frac{M_B - M_A}{L} \cdot \frac{x^2}{2} + EI \cdot \sigma_A$$

$$EI \cdot y = M_A \cdot \frac{x^2}{2} + \frac{M_B - M_A}{L} \cdot \frac{x^3}{6} + EI \cdot \sigma_A x$$

when $x = L$, $y = 0$, hence $\sigma_A = - \dfrac{L}{6EI}\{2M_A + M_B\}$

when $x = L$, $\dfrac{dy}{dx} = \sigma_B$, hence $\sigma_B = + \dfrac{L}{6EI}\{M_A + 2M_B\}$.

The above results are equally true when, as in (iii) and (iv) Fig. 158, M_A is negative and M_B positive. There is then a point of inflexion at J. The particular case when σ_A is zero, i.e. when the beam is direction-fixed at A, is important. From eq. (3), if $\sigma_A = 0$,

$$M_A = - \frac{M_B}{2} \qquad . \qquad . \qquad . \qquad . \qquad . \quad (6)$$

i.e. M_A is one-half the magnitude of M_B and opposite in sign. The point of inflexion then lies at a distance $L/3$ from A. If $M_A = 0$, i.e. if the beam be merely supported at A,

$$A'A \quad \frac{M_B L^2}{3EI}; \quad B'B = \frac{M_B L^2}{6EI}; \quad \sigma_A = - \frac{M_B L}{6EI}; \quad \sigma_B = + \frac{M_B L}{3EI} \qquad (7)$$

If, in addition to the moments M_A and M_B, external loads act on the beam between A and B producing bending moments represented by the

diagram $a'e'b'$, (v) Fig. 158, of which the area is a and the centre of area lies at a distance $\bar{x}$ from A ; then, using the same theorems as before,

$$A'A = \frac{L^2}{6EI}\{M_A + 2M_B\} + \frac{a\bar{x}}{EI} \; ; \; B'B = \frac{L^2}{6EI}\{2M_A + M_B\} + \frac{a(L-\bar{x})}{EI} , \quad (8)$$

$$\left.\begin{array}{l} \sigma_A = - \left[\dfrac{L}{6EI}\{2M_A + M_B\} + \dfrac{a(L - \bar{x})}{EIL}\right] \\[2ex] \sigma_B = + \left[\dfrac{L}{6EI}\{M_A + 2M_B\} + \dfrac{a\bar{x}}{EIL}\right] \end{array}\right\} \quad (9) \text{ and } (10)$$

If the nature of the load be such that the bending moment produced is everywhere negative, i.e. opposite in sign to M_A and M_B in (i), the area a must be given a negative sign.

The above formulae hold while the supports A and B remain at the same level. Suppose that, as shown at (i) Fig. 159, the support B sink to a point Δ below A. Let W, acting at a distance z from A, be the resultant downward load on AB; let M_A and M_B be the support moments at A and B respectively. Taking moments about B,

$$M_A + W(L - z) = R_1L + M_B$$

whence,

$$R_1 = \frac{1}{L}\{(M_A - M_B) + W(L - z)\} \quad . \quad (11)$$

Similarly, taking moments about A,

$$R_2 = \frac{1}{L}\{(M_B - M_A) + Wz\} \quad . \quad (12)$$

FIG. 159.

The deflection of the beam at A, below the tangent at B, is

$$A'A = \frac{1}{EI}\left\{\begin{array}{l}\text{moment of the area of the bending-}\\ \text{moment diagram about A}\end{array}\right. \quad (13)$$

Conceive the beam as a cantilever projecting from B, carrying the load W, and acted on at A by an upward load R_1 and a bending moment M_A. Let $a'b'd'c'$, (ii) Fig. 159, be the bending-moment diagram for the downward load on AB ; area $= a_1$; distance of centre of area from $A = \bar{x}_1$; moment of area about $A = a_1\bar{x}_1$. The bending-moment diagram for the load R_1 is the triangle $a_1'b_1'd_1'$, (iii), where $b_1'd_1' = - R_1L$. The area of this triangle is $- R_1L^2/2$; distance of centre of area from $A = 2L/3$; moment of area about $A = - \dfrac{R_1L^2}{2} \wedge \dfrac{2L}{3} = - R_1L^3/3$.

The bending-moment diagram for the moment M_A is the rectangle $a''d''$, (iv) Fig. 156 ; area M_AL ; distance of centre area from $A = L/2$; moment of area about $A = M_AL \times L/2 = M_AL^2/2$. Then, from eq. (13),

$$A'A = \frac{1}{EI}\left\{a_1\bar{x}_1 - \frac{R_1L^3}{3} + \frac{M_AL^2}{2}\right\}$$
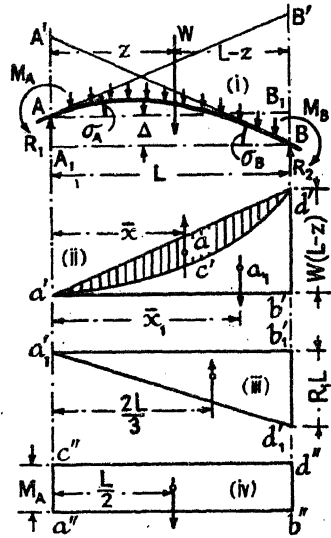
Inserting the value of R_1 from eq. (11),

$$A'A = \frac{1}{EI}\left[a_1\bar{x}_1 - \frac{L^2}{3}\{(M_A - M_B) + W(L - z)\} + \frac{M_A L^2}{2}\right]$$

$$= \frac{1}{EI}\left[\frac{L^2}{6}\{M_A + 2M_B\} - \qquad (L - z) - a_1\bar{x}_1\right] \qquad (14)$$

But $\dfrac{WL^2}{3}(L - z) = \left\{W(L - z)\dfrac{L}{2}\right\}\dfrac{2L}{3}$, which is the moment of the area of the triangle $a'b'd'$ in (ii) about A, for $b'd' = W(L - z)$. Hence $\left\{\dfrac{WL^2}{3}(L - z) - a_1\bar{x}_1\right\}$ is the difference between the moment of the area of the triangle $a'b'd'$ and the moment of the area $a'b'd'c'$, both about A. In other words, it is the moment of the shaded area $a'd'$ in (ii) about A. But this shaded area is the bending-moment diagram for the downward load on AB, considering AB as a beam merely supported at the ends. Denoting this shaded area by $- a$, and the distance of its centre of area from A by $\bar{x}$, eq. (14) becomes

$$A'A = \frac{L^2}{6EI}\{M_A + 2M_B\} + \frac{a\bar{x}}{EI} \qquad . (15)$$

identical with $A'A$ in eq. (8).

Similarly, it may be shown that

$$B'B = \frac{L^2}{6EI}\{2M_A + M_B\} + \frac{a(L - \bar{x})}{EI} \qquad . (16)$$

In eqs. (15) and (16) the area a, if due to a downward load, is to be regarded as essentially negative.

From Fig. 159, $B'B = B'B_1 + B_1B = \sigma_A L + \Delta$; and,

$$\sigma_A = (B'B - \Delta)/L = -\left[\frac{L}{6EI}\{2M_A + M_B\} + \frac{a(L - \bar{x})}{EIL} - \frac{\Delta}{L}\right] \qquad . (17)$$

The negative sign denotes that σ_A is an upward slope from left to right.

Also, $\qquad A'A = A'A_1 - AA_1 = \sigma_B L - \Delta$

$$\sigma_B = +\left[\frac{L}{6EI}\{M_A + 2M_B\} + \frac{a\bar{x}}{EIL} + \frac{\Delta}{L}\right] . \qquad . (18)$$

If $\Delta = 0$, eqs. (17) and (18) reduce to eqs. (9) and (10). If, also, $a = 0$, they reduce to eqs. (3) and (4).

Signs.—Unless otherwise specified, the conventions as to signs, used in Vol. I, will be followed here. A moment tending to make the beam convex upward will be regarded as positive, (i) Fig. 160. Distances measured to

FIG. 160.

the right, and downward deflections, will also be regarded as positive. Thus, in (ii) Fig. 160, CD_1 is a positive direction, and D_1D' is
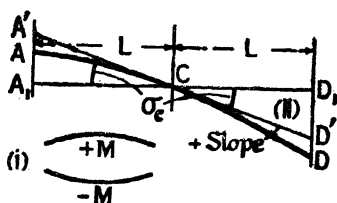
positive. CA_1 is a negative direction and A_1A' is negative. Hence, $\sigma_C = \dfrac{D_1D'}{CD_1} = \dfrac{A_1A'}{CA_1}$ is a positive slope ; $D_1D' = +\sigma_CL$; $A_1A' = -\sigma_CL$. $D'D$ and $A'A$ are both deflections below the tangent at C and therefore positive :

$$D_1D = D_1D' + D'D = + \sigma_CL + D'D . \qquad . \qquad . (19)$$
$$A_1A = A_1A' + A'A = - \sigma_CL + A'A . \qquad . \qquad . (20)$$

These equations hold equally well for the case shown in Fig. 161,
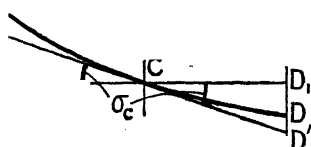
FIG. 161.   FIG. 162.
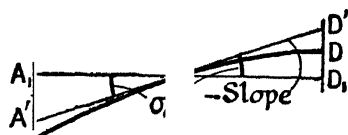
where σ_C is a positive slope as in Fig. 160, but $D'D$ and $A'A$ are deflections above the tangent, and therefore negative.

In Fig. 162, CD_1 is positive ; D_1D' is upward and therefore negative ; CA_1 is negative ; A_1A' is downward and positive. Hence,

$$\sigma_C = \frac{D_1D'}{CD_1} = \frac{A_1A'}{CA_1} \text{ is a negative slope ; and therefore,}$$

$$D_1D' = + \sigma_CL ; \quad A_1A' = - \sigma_CL.$$

$D'D$ and $A'A$ are both deflections below the tangent and therefore positive ; hence,

$$D_1D = D_1D' + D'D = + \sigma_CL + D'D ;$$
$$A_1A = A_1A' + A'A = - \sigma_CL + A'A ;$$

equations identical with eqs. (19) and (20).

In Fig. 163, the slope σ_C is negative as in Fig. 162, but $D'D$ and $A'A$ are deflections above the tangent and therefore negative ; eqs. (19) and (20) hold as before.

Particular Cases.—Suppose that in (ii) Fig. 160, or in Fig. 163, A and A_1 coincide, so that $A_1A = 0$, and eq. (20) becomes $0 = A_1A' + A'A = - \sigma_CL + A'A$. Then

FIG. 163.

$$A_1A' = - A'A ; \text{ and } \sigma_CL \quad A_1A' = A'A \qquad . \qquad . (21)$$

Similarly, if in Fig. 161 or in Fig. 162, D and D_1 coincide, $D_1D = 0$ and eq. (19) becomes $0 = D_1D' + D'D = + \sigma_CL + D'D$. Then

$$D_1D' = - D'D ; \text{ and } \sigma_CL = + D_1D' \quad D'D \qquad . (22)$$

Slope-Deflection Equations.—If the values of M_A and M_B be found from eqs. (17) and (18),

$$M_A = - \left[\frac{2EI}{L} \left\{ 2\sigma_A + \sigma_B - \frac{3\Delta}{L} \right\} + \frac{2a}{L} \left\{ 2 - \frac{3\bar{x}}{L} \right\} \right] \quad . \quad . \quad (23)$$

$$M_B = + \left[\frac{2EI}{L} \left\{ \sigma_A + 2\sigma_B - \frac{3\Delta}{L} \right\} - \frac{2a}{L} \left\{ \frac{3\bar{x}}{L} - 1 \right\} \right] \quad . \quad . \quad (24)$$

These expressions are known as the slope-deflection equations, given here in their general form. The last term in each will be recognised as the values of M_1 and M_2 in eq. (4), § 60, Vol. I, since σ_A, σ_B and Δ are there all zero. When the bending moment due to the external loads acting on the member is negative, a is to be given a minus sign.

In certain cases, particularly where the framework consists of the combination of a large number of vertical and horizontal members, it is more convenient to adopt the following conventions as to signs :

A clockwise external *bending moment* is called positive.

A clockwise *change of slope* in an end tangent is called positive.

A *deflection* measured away from the base line in the same direction as a positive slope is called positive.

If these conventions be applied to Fig. 159, it will be seen that M_A must be regarded as a negative moment and its sign changed throughout, otherwise the analysis still holds, hence eqs. (23) and (24) become

$$M_{ab} = \frac{2EI}{L} \left\{ 2\sigma_A + \sigma_B - \frac{3\Delta}{L} \right\} + \frac{2a}{L} \left\{ 2 - \frac{3\bar{x}}{L} \right\} \quad . \quad . \quad . \quad (25)$$

$$M_{ba} = \frac{2EI}{L} \left\{ \sigma_A + 2\sigma_B - \frac{3\Delta}{L} \right\} - \frac{2a}{L} \left\{ \frac{3\bar{x}}{L} - 1 \right\} \quad . \quad . \quad . \quad (26)$$

where $M_{ab} = - M_A$ and $M_{ba} = M_B$. The first suffix denotes the node point, the second determines the particular member.

These equations must be applied in turn to each member of the framework. A number of equations is thus obtained, and these, treated as simultaneous, give the values of the unknown support moments. When the number of members is large, these values must be determined to many significant figures, otherwise incorrect results are obtained. Applications will be found in §§ 109 and 113.

Note.—Whenever this second series of conventions is employed, double suffixes will be used to designate the moments. When a single capital letter suffix is used, it denotes that the ordinary conventions as to sign, Fig. 80, Vol. I, are implied.

106. Stiff Portal Carrying a Vertical Load. Hinged Feet.—As a simple example of the application of the theorems of the preceding article to a stiff framework, consider the portal ACDB shown in Fig. 164, with stiff joints at C and D and hinged feet A and B. Suppose the top member CD to be symmetrically loaded with a vertical load as shown. It will be assumed that the two columns AC and BD are of equal length and

have the same moment of inertia I_1, and that the moment of inertia of CD is I_2. Under this loading the frame will distort into the shape shown dotted in (i) ; for since the joints at C and D are rigid, the members CA and DB will tend to spread outwards as CD deflects. This will be resisted by the hinged joints A and B, and horizontal reactions F_1 and F_2, of equal magnitude, will be called into play. The vertical reactions R_1 and R_2 will be unaffected by the rigidity of the joints at C and D.

For the purpose of analysing the conditions thus set up, it is convenient to open out the frame as shown at (ii) Fig. 164, by rotating each of the legs CA and DB through a right angle. Since the angles at C and D
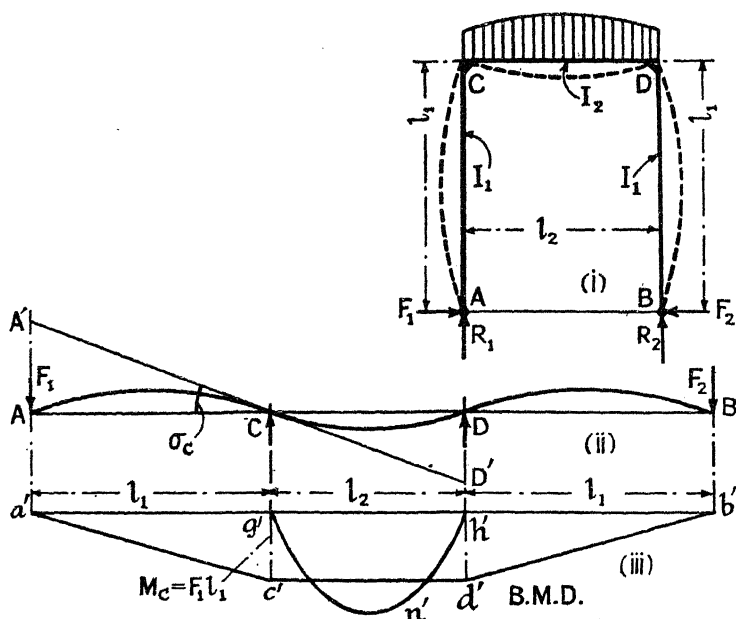
FIG. 164.

are right angles, both before and after distortion, the four points ACDB will open out into the straight line AB in (ii), and the deflection curve in (ii) will be a continuous curve. It is then evident that ACDB is a continuous girder ; and the bending-moment diagram will be as shown at (iii), $g'n'h'$ being the negative diagram due to the applied load, and $a'c'd'b'$ the positive diagram due to the horizontal reactions F_1 and F_2 ; $a'c'd'b'$ is the base line. Since the feet A and B are hinged, the bending moment at these points will be zero ; at C the bending moment is $M_C = F_1 l_1 = F_2 l_1 = M_D$. The magnitude of F_1, and hence the bending moment everywhere, can be found by the methods of § 105.

Let $A'CD'$, (ii), represent the slope over the support C. Then $A'A$ is the deflection of the beam at A, below the tangent at C, and is equal to the moment of the area of the bending-moment diagram $a'c'g'$ about a' ;

from eq. (7), § 105, $A'A = \dfrac{M_C l_1^2}{3EI_1}$, and hence the slope of the tangent at

C is $\sigma_C = \dfrac{A'A}{AC} = \dfrac{M_C l_1}{3EI_1} = \dfrac{F_1 l_1^2}{3EI_1}$, since $M_C = F_1 l_1$. This span, AC, is an example of the Particular Case given on p. 234, and the value of σ_C used above follows from eq. (21), § 105. Again, considering span CD, σ_C is also equal to $- D'D/CD$, see eq. (22). $D'D$ is the deflection of the beam at D above the tangent at C, and is therefore negative ; hence σ_C is a positive slope, as shown. From eq. (8), § 105,

$$D'D = \left\{ \dfrac{l_2^2}{6EI_2} \, (2M_C + M_D) + \dfrac{a l_2}{2EI_2} \right\} = \dfrac{3F_1 l_1 l_2^2}{6EI_2} + \dfrac{a l_2}{2EI_2} = \dfrac{l_2}{2EI_2} \{F_1 l_1 l_2 + a\}.$$

where $- a$ is the area of the negative bending-moment diagram $g'n'h'$, $\bar{x} = l_2/2$, and $M_C = M_D = F_1 l_1$. The slope of the tangent at C is, therefore,

$\sigma_C = - \dfrac{D'D}{CD} = - \dfrac{1}{2EI_2} \{F_1 l_1 l_2 + a\}$. Equating this to the value of σ_C

previously obtained, $\sigma_C = \dfrac{F_1 l_1^2}{3EI_1} = - \dfrac{1}{2EI_2} \{F_1 l_1 l_2 + a\}$; from which

$F_1 = - \dfrac{a}{l_1 l_2 \left\{ 1 + \frac{2}{3} \dfrac{I_2 l_1}{I_1 l_2} \right\}}$. Knowing the value of F_1, the bending-moment

diagram can be drawn, and the stresses due to bending in all the members can be determined. These must be combined with the stresses due to the longitudinal loads R_1 and R_2 in the members AC and BD, and with those due to the longitudinal load $F_1 = F_2$ in CD.

Particular Cases.—If the load on CD be a uniform load of w per unit of length, the negative bending-moment diagram is a parabola, maximum ordinate $- \frac{1}{8}w l_2^2$, and area $a = - \frac{1}{12}w l_2^3$. In this case,

$$F_1 = \dfrac{w l_2^2}{12 l_1 \left\{ 1 + \frac{2}{3} \dfrac{I_2 l_1}{I_1 l_2} \right\}} \; ; \quad R_1 = R_2 = \dfrac{w l_2}{2}.$$

For a single concentrated load W at the centre of CD, the bending-moment diagram is a triangle, maximum ordinate $- \frac{1}{4}W l_2$, and area $- \frac{1}{8}W l_2^2$; whence,

$$F_1 = \dfrac{W l_2}{8 l_1 \left\{ 1 + \frac{2}{3} \dfrac{I_2 l_1}{I_1 l_2} \right\}} ; \quad R_1 = R_2 = \dfrac{W}{2}.$$

The bending-moment diagram (iii) could very conveniently have been obtained by the method of characteristic points, and the value of F_1 obtained from M_C (see § 108).

107. Stiff Portal Carrying a Vertical Load. Direction-fixed Feet.—If the feet A and B of the portal of the previous article be direction-fixed instead of hinged, (i) Fig. 165, the deflection curve will take the shape shown in (i) and (ii) Fig. 165, and the slope at A and B will be zero. The bending-moment diagram is shown at (iii) ; there will be a negative

bending moment $M_A = M_B$ at A and B respectively, and the bending moment at C is

$$M_C = M_A + F_1 l_1 = M_B + F_2 l_1 = M_D \qquad . \qquad . \quad (1)$$

Since the slope at A is zero, it follows from eq. (6), § 105, that $M_A = -\frac{1}{2}M_C$, and that the point of inflexion in AC is $\frac{1}{3}l_1$ from A. From eqs. (21) and (4), § 105, the slope σ_C is

$$\sigma_C = \frac{A'A}{AC} = \frac{l_1}{6EI_1}\{M_A + 2M_C\} = \frac{M_C l_1}{4EI_1} ; \quad \text{since } M_A = -\frac{1}{2}M_C. \quad \text{If}$$

now the span CD be considered, from eqs. (22) and (9), § 105, the slope σ_C is

$$\sigma_C = -\frac{D'D}{CD} = -\left\{ \frac{l_2}{6EI_2}(2M_C + M_D) + \frac{al_2}{2EI_2 l_2} \right\} = -\frac{1}{2EI_2}\{M_C l_2 + a\}$$
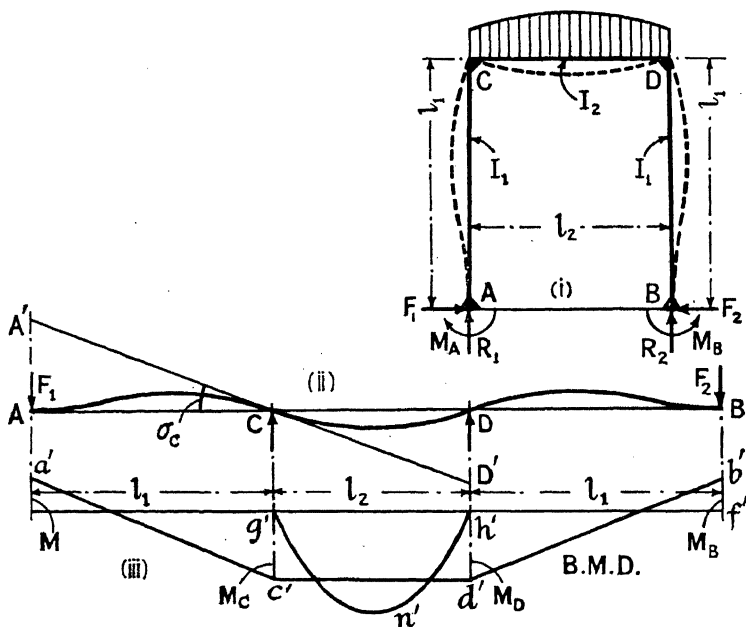
FIG. 165.

where $-a$ is the area of the negative bending-moment diagram $g'n'h'$, and $M_C = M_D$. Equating the two expressions for σ_C,

$$\sigma_C = \frac{M_C l_1}{4EI_1} = -\frac{1}{2EI_2}\{M_C l_2 + a\} ;$$

whence,

$$M_C = -\frac{}{l_2\left\{1 + \frac{1}{2}\dfrac{I_2 l_1}{I_1 l_2}\right\}} \quad M_D ; \text{ and } M_A \quad \frac{}{2l_2\left\{1 + \frac{1}{2}\dfrac{I_2 l_1}{I_1 l_2}\right\}} \quad M_B \quad . \quad (2)$$

From eq. (1), $M_C = M_A + F_1 l_1 = -\dfrac{M_C}{2} + F_1 l_1$; whence,

$$F_1 = \frac{3M_C}{2l_1} = - \frac{3a}{2l_1 l_2 \left\{1 + \frac{1}{2}\dfrac{I_2 l_1}{I_1 l_2}\right\}} \tag{3}$$

Particular Cases.—If the load on CD be a uniform load of w per unit of length, the area of the negative bending-moment diagram is $-\frac{1}{12}wl_2{}^3$, and

$$M_C = M_D = \frac{wl_2{}^2}{12\left\{1 + \frac{1}{2}\dfrac{I_2 l_1}{I_1 l_1}\right\}} \; ; \; M_A = M_B = - \frac{wl_2{}^2}{24\left\{1 + \frac{1}{2}\dfrac{I_2 l_1}{I_1 l_1}\right\}}$$

$$F_1 = F_2 = \frac{wl_2{}^2}{8l_1\left\{1 + \frac{1}{2}\dfrac{I_2 l_1}{I_1 l_2}\right\}} \; ; \; R_1 = R_2 = \frac{wl_2}{2}.$$

For a single concentrated load W at the centre of CD, $a = -\frac{1}{8}Wl_2{}^2$, and,

$$M_C = M_D = \frac{Wl_2}{8\left\{1 + \frac{1}{2}\dfrac{I_2 l_1}{I_1 l_1}\right\}} \quad M_A = M_B = - \frac{Wl_2}{16\left\{1 + \frac{1}{2}\dfrac{I_2 l_1}{I_1 l_2}\right\}}.$$

$$F_1 = F_2 = \frac{3Wl_2}{16l_1\left\{1 + \frac{1}{4}\dfrac{I_2 l_1}{I_1 l_2}\right\}} \; , \; R_1 = R_2 = \frac{W}{2}.$$

108. Stiff Portals. Application of Characteristic Points.—When, as in the two preceding sections, the portal and the load system are both symmetrical about a vertical centre line, the method of characteristic points furnishes a neat solution. Consider three contiguous spans of a continuous beam, AC, CD, DB, (i) Fig. 166, of which CD alone is loaded. Both the beam and the load system are symmetrical about the centre of CD. If the value of I for the spans AC and DB is different from that for span CD, the length scale for AC and DB must be adjusted as explained in § 78, Vol. I.* In the first instance, suppose that the beam is merely supported at A and B. Since the spans AC and DB are unloaded, the characteristic point r_2 will coincide with p_2, and r_5 will coincide with p_5, (ii). Then, if $a'c'd'b'$ is the base line, and $M_C = M_D$ are the support moments at C and D ; from the geometry of the figure

$$p_3 r_3 = c'g' + r_3 q_3 = c'g' + r_2 q_2 \cdot \frac{l_1}{l_2} = c'g' + \tfrac{2}{3}c'g' \cdot \frac{l_1}{l_2}$$

Hence,

$$M_C = c'g' = \frac{3l_2}{2l_1 + 3l_2} p_3 r_3 = M_D$$

where $p_3 r_3$ is the height of the characteristic point for the span CD. To determine $M_C = M_D$, all that is necessary is to draw a horizontal line

* If the span CD be plotted to a scale $1'' = a$ inches of span, AC and DB must be plotted to a scale $1'' = aI_1/I_2$ inches of span.

r_4jk, making $jk = l_1/3$ (k lies on the vertical through p_5), join k to O, the centre point of $g'h'$, cutting $h'j$ in d'; then $a'c'd'b'$ is the required base line, and $M_C = M_D = c'g' = d'h'$. If the ends A and B of the beam are fixed in direction, (iii), the same construction holds, but $jk = l_1/4$; also the base line $a'c'd'b'$ passes through the characteristic points r_1, r_6,
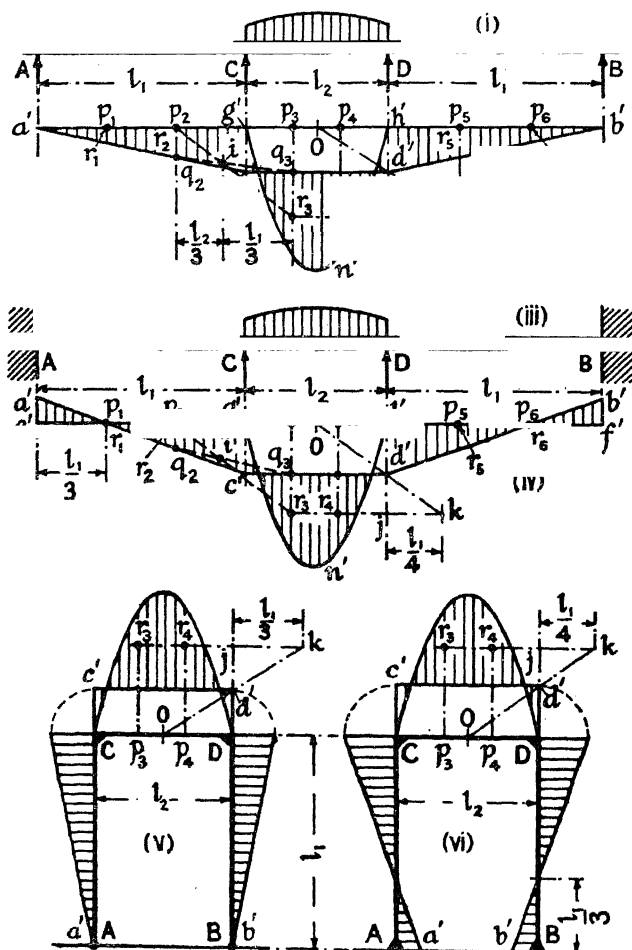
FIG. 166.

next to the fixed ends, as shown in (iv) Fig. 166. It is not correct, on the ground that r_1 and r_6 are points of inflexion, to treat p_1g' and p_6h' as spans merely supported at p_1 and p_6, because the deflection at p_1 and p_6 is not zero.

The application to stiff portals is shown in (v) and (vi) Fig. 166. In (v), the feet A and B of the portal are hinged, and when opened out the system is represented by (i). In (vi) the feet are fixed in direction,

and when opened out the system is represented by (iii). Provided that the portals and the loading thereon are symmetrically arranged, this is the quickest method of dealing with such cases.

If it be preferred to set out AC, CD, and DB, all to the same scale, make $jk = l_1 I_2/3 I_1$ and $l_1 I_2/4 I_1$ in (v) and (vi) respectively.

109. Stiff Portal carrying a Vertical Load. More General Case.— If the load on CD be unsymmetrical, or if the legs AC and BD be of unequal length or of unequal stiffness, the above theory will not apply. In any of these circumstances, the slope over the support C will be different
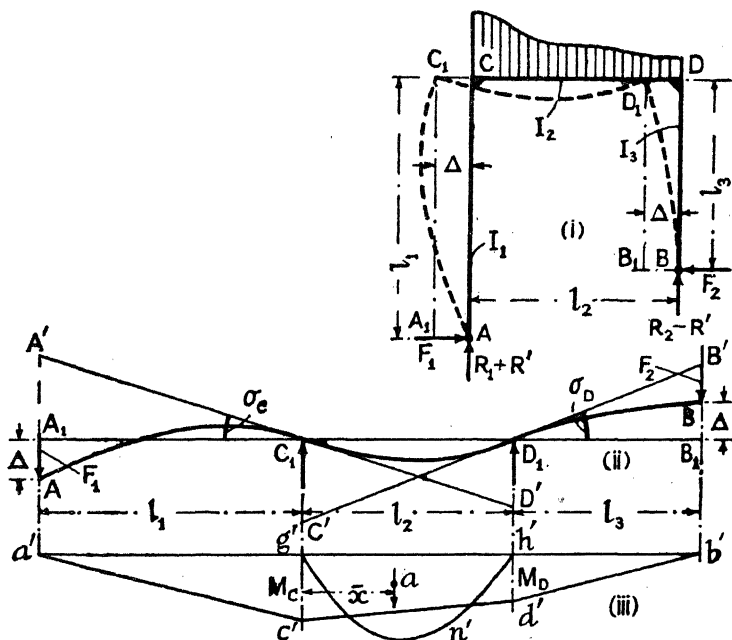
FIG. 167.

from the slope over the support D ; and, in order to attain a position of equilibrium, the portal must deflect sideways as shown in Fig. 167. Otherwise the horizontal force F_1 would be different from the force F_2, which cannot be the case unless an external horizontal force is applied to the frame. The behaviour of a simple model will make this point clear.

Case (1).—In the first instance, suppose the feet A and B of the portal to be hinged. The distorted shape of the frame is shown dotted at (i) Fig. 167. If the frame be opened out, so that the verticals through C_1 and D_1 come into line with $C_1 D_1$, the deflection curve $AC_1 D_1 B$, (ii) Fig. 167, is obtained ; (iii) is the corresponding bending-moment diagram. The difference between these diagrams and (ii) and (iii) of Fig. 164 will be evident. Let the lengths of AC, CD, and DB, (i) Fig. 167, be l_1, l_2, and l_3 ; and their respective moments of inertia be I_1, I_2, and I_3. From the general conditions of equilibrium the following relations hold :

$F_1 = F_2$; $R_1 + R_2 = W$, the total vertical load. These vertical reactions are increased and diminished by an amount R', found by taking moments about the foot B, $F_1(l_1 - l_3) = R'l_2$; so that the total vertical reactions at A and B are $(R_1 + R')$ and $(R_2 - R')$ respectively. The bending moment at C is

$$M_C = F_1 l_1, \text{ and at D is } M_D = F_2 l_3 = F_1 l_3 \qquad . \qquad . \quad (1)$$

Consider the span $A_1 C_1$, (ii) Fig. 167. From eq. (20), § 105,

$$A_1 A = A_1 A' + A'A = - \sigma_C l_1 + A'A$$

But $A_1 A = \Delta$, the sideways deflection of the portal; and from eq. (7), § 105, $A'A$, the deflection of the beam at A below the tangent at C_1, is $M_C l_1{}^2/3EI_1$; hence,

$$\Delta = - \sigma_C l_1 + \frac{M_C l_1{}^2}{3EI_1} \qquad . \qquad . \qquad . \qquad . \quad (2)$$

From eq. (22), § 105, considering the span $C_1 D_1$, $\sigma_C = - D'D_1/l_2$. $D'D_1$ is the deflection of the beam at D_1 above the tangent at C_1, which from eq. (8), § 105, is

$$D'D_1 = \frac{l_2{}^2}{6EI} (2M_C + M_D) + \frac{a(l_2 - \bar{x})}{EI_2}$$

where $- a$ is the area of the negative bending-moment diagram $g'n'h'$, and $\bar{x}$ is the distance of its centre of area from g'. Then

$$\sigma_C = - \frac{D'D_1}{l_2} = - \left\{ \frac{l_2}{6EI_2} (2M_C + M_D) + \frac{a(l_2 - \bar{x})}{EI_2 l_2} \right\} \qquad (3)$$

From eqs. (2), (3), and (1),

$$\Delta = l_1 \frac{l}{6EI_2} (2M_C + M_D) + \frac{a(l_2 - \bar{x})}{EI_2 l_2} \right\} + \frac{M_C l_1{}^2}{3EI_1}$$
$$- \frac{F_1 l_1{}^3}{3EI_1} + \frac{F_1 l_1 l_2}{6EI_2} (2l_1 + l_3) + \frac{a(l_2 - \bar{x})l_1}{EI_2 l_2} \qquad (4)$$

Next consider the span $D_1 B_1$. From eq. (19), § 105,

$$B_1 B = B_1 B' + B'B = + \sigma_D l_3 + B'B.$$

Here, $B_1 B = - \Delta$, measured upward; and from eq. (7), § 105, $B'B$, the deflection of the beam at B below the tangent at D_1, is $M_D l_3{}^2/3EI_3$. Hence,

$$- \Delta = \sigma_D l_3 + M_D l_3{}^2/3EI_3 \qquad . \qquad . \qquad . \quad (5)$$

Again, considering the span $C_1 D_1$, from eq. (21), § 105, $\sigma_D = C'C_1/l_2$, where $C'C_1$ is the deflection of the beam at C_1 above the tangent at D_1; hence, using eq. (10), § 105,

$$\sigma_D = \frac{C'C_1}{l_2} = \left\{ \frac{l_2}{6EI_2} (M_C + 2M_D) + \frac{a\bar{x}}{EI_2 l_2} \right\} \qquad (6)$$

From eqs. (5), (6), and (1),

$$\Delta = - l_3 \frac{l_2}{6EI_2} (M_C + 2M_D) + \frac{a\bar{x}}{EI_2 l_2} \right\} - \frac{M_D l_3{}^2}{3EI_3}$$
$$= - \frac{F_1 l_3{}^3}{3EI_3} \frac{F_1 l_2 l_3}{6EI_2} (l_1 + 2l_3) - \frac{a\bar{x} l_3}{EI_2 l_2} \qquad (7)$$

From eqs. (4) and (7),

$$F_1 = \frac{3a\{l_1 l_2 - \bar{x}(l_1 - l_3)\}I_1 I_3}{l_2\{I_2 I_3 l_1{}^3 + I_1 I_3 l_2(l_1{}^2 + l_1 l_3 + l_3{}^2) + I_1 I_2 l_3{}^3\}} \qquad (8)$$

Knowing F_1, the bending moments everywhere, the longitudinal forces in the members, and the stresses everywhere can be found. The value of Δ is obtained from eq. (4) or eq. (7).

In cases where the vertical legs are of the same length and cross-section, $l_1 = l_3$ and $I_1 = I_3$; eq. (8) then becomes

$$F_1 = - \frac{}{l_1 l_2 \; 1 + \tfrac{2}{3} \dfrac{I_2 l_1}{I_1 l_2}}$$

the same expression as was obtained in § 106 for a symmetrical load. Putting this value in eq. (4) for Δ,

$$\Delta = - \frac{al_1}{EI_2} \cdot \frac{2\bar{x} - l_2}{2l_2} = - \frac{al_1}{EI_2}\left\{ \frac{\bar{x}}{l_2} - \tfrac{1}{2} \right\}$$

which is evidently zero for a symmetrical load, when $\bar{x} = \tfrac{1}{2}l_2$. It is to be remembered that, for a downward load on CD, a is a negative area.

Slope-Deflection Method.—The above results can also be obtained from the *slope-deflection equations* (23) and (24), § 105. Consider span AC, (ii) Fig. 167; the foot A is hinged, therefore $M_A = 0$. The span is unloaded, therefore $a = 0$; taking origin at A and comparing the span with AB, Fig. 159, it is evident that Δ is an upward deflection and therefore negative. Inserting these values in eqs. (23) and (24), § 105,

$$0 = -\left[\frac{2EI_1}{l_1}\left\{ 2\sigma_A + \sigma_C + \frac{3\Delta}{l_1} \right\} \right]; \quad M_C = +\left[\frac{2EI_1}{l_1}\left\{ \sigma_A + 2\sigma_C + \frac{3\Delta}{l_1} \right\} \right].$$

Treating the loaded span CD in a similar way, C and D remaining at the same level, and $\Delta = 0$,

$$M_C = -\left[\frac{2EI_2}{l}\{2\sigma_C + \sigma_D\} + \frac{2a}{l_2}\left\{ 2 - \frac{3\bar{x}}{l_2} \right\} \right]$$

$$M_D = +\left[\frac{2EI_2}{l_2}\{\sigma_C + 2\sigma_D\} - \frac{2a}{l_2}\left\{ \frac{3\bar{x}}{l_2} - 1 \right\} \right]$$

Similarly, for the unloaded span DB, where Δ is again upward and negative,

$$M_I = -\left[\frac{2EI_3}{l_3}\left\{ 2\sigma_D + \sigma_B + \frac{3\Delta}{l_3} \right\} \right]; \quad 0 = +\left[\frac{2EI_3}{l_3}\left\{ \sigma_D + 2\sigma_B + \frac{3\Delta}{l_3} \right\} \right]$$

From the first pair of equations,

$$\Delta = -\sigma_C l_1 + \frac{M_C l_1{}^2}{3EI_1} \qquad . \qquad . \qquad . \qquad . \quad (2)$$

From the second pair of equations,

$$\sigma_C = -\left\{ \frac{l_2}{6EI_2}(2M_C + M_D) + \frac{a(l_2 - \bar{x})}{EI_2 l_2} \right\} \qquad . \qquad . \quad (3)$$

$$\sigma_D = +\left\{ \frac{l_2}{6EI_2}(M_C + 2M_D) + \frac{a\bar{x}}{EI_2 l_2} \right\} \qquad . \qquad . \quad (6)$$

From the third pair of equations,

$$\Delta = - \sigma_D l_3 - \frac{M_D l_3{}^2}{3EI_3} \tag{5}$$

as previously obtained. The solution follows as before.

It is evident from the above that had the value of Δ been assumed positive, the values of the moments and slopes would not have been affected.

Case (2).—If the feet of the portal are direction-fixed at A and B, Fig. 168, the deflection curve when opened out will be as shown at (ii)
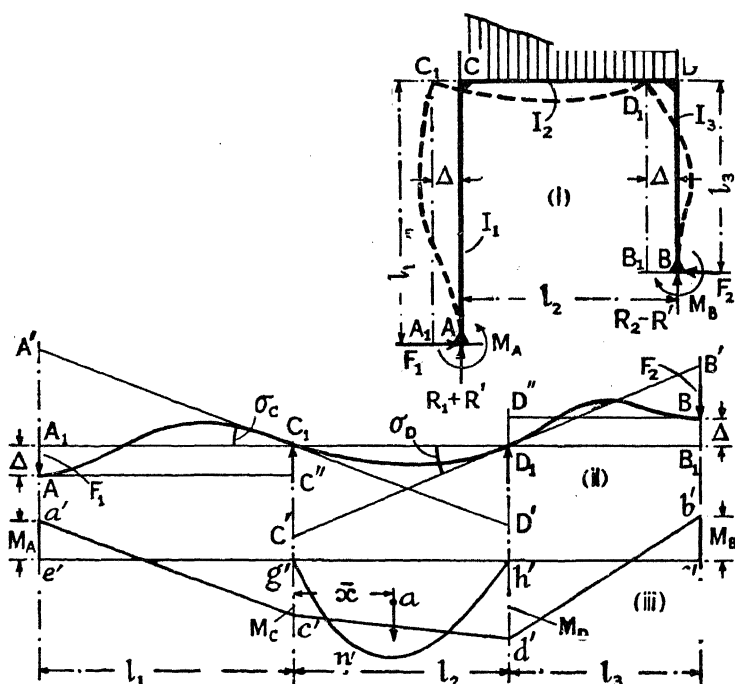
FIG. 168.

Fig. 168; the corresponding bending-moment diagram is shown at (iii), where M_A and M_B appear as negative bending moments to agree with the deflection curve (ii). Actually, their sign will depend on the arrangement of the frame and its load. In the working which follows, therefore, the sign of M_A and M_B will be taken as positive, as shown in (i) Fig. 168. If, from the resulting expressions, their magnitude is found to be negative, the deflection curve and bending-moment diagram will be as shown in (ii) and (iii) Fig. 168, otherwise these figures must be corrected to suit.

As in the previous case, $F_1 = F_2$; and $R_1 + R_2 = W$, the total load. Taking moments about B, $F_1(l_1 - l_3) + M_A - M_B = R'l_2$, where the total vertical reactions at A and B are $(R_1 + R')$ and $(R_2 - R')$ respectively.

From (ii), $C''C_1$, the deflection of the beam at C_1 above the tangent at A, is $- \Delta$; from eq. (2), § 105,

$$C''C_1 = \frac{l_1^2}{6EI_1}(2M_A + M_C) = - \Delta \qquad (9)$$

From eq. (20), § 105, considering the span A_1C_1, $A_1A = - \sigma_C l_1 + A'A$, where $A_1A = \Delta$, and, from eq. (1), § 105, $A'A = \frac{l_1^2}{6EI_1}(M_A + 2M_C)$. Hence,

$$\Delta = - \sigma_C l_1 + \frac{l_1^2}{6EI_1}(M_A + 2M_C) \qquad . (10)$$

Considering the span C_1D_1, as in Case 1, eq. (3),

$$\sigma_C = - \frac{D'D_1}{l_2} \qquad \frac{l_2}{|6EI}(2M_C + M_D) + \frac{a(l_2 - \bar{x})}{EI_2 l_2} \qquad . (11)$$

where $- a$ is the area of the negative bending-moment diagram $g'n'h'$, and $\bar{x}$ is the distance of its centre of area from g'. Inserting the value of σ_C from eq. (11) in eq. (10),

$$\Delta = l_1 \left\{ \frac{l_2}{6EI_2}(2M_C + M_D) + \frac{a(l_2 - \bar{x})}{EI_2 l_2} \right\} + \frac{l_1^2}{6EI_1}(M_A + 2M_C) \quad . (12)$$

From eq. (19), § 105, considering span D_1B_1, $B_1B = \sigma_D l_3 + B'B$; where $B_1B = - \Delta$, and from eq. (2), § 105, $B'B = \frac{l_3^2}{6EI_3}(2M_D + M_B)$; hence,

$$- \Delta = \sigma_D l_3 + \frac{l_3^2}{6EI_3}(2M_D + M_B) \qquad . . . (13)$$

Again, considering the span C_1D_1, as in Case 1, eq. (6),

$$\sigma_D \qquad \frac{C'C_1}{l_2} = \frac{l_2}{|6EI_2}(M_C + 2M_D) + \frac{a\bar{x}}{EI_2 l_2}$$

Inserting this value in eq. (13),

$$\Delta = - l_3 \left\{ \frac{l_2}{6EI_2}(M_C + 2M_D) + \frac{a\bar{x}}{EI_2 l_2} \right\} - \frac{l_3^2}{6EI_3}(2M_D + M_B) \quad . (14)$$

From eq. (1), § 105, $D''D_1$, the deflection of the beam at D_1 below the tangent at B is

$$D''D_1 = \frac{l_3^2}{6EI_3}(M_D + 2M_B) = \Delta \qquad . (15)$$

Neglecting any bending moment produced by the vertical reactions R_1 and R_2 in AC and BD, resulting from the deflection Δ,
$M_C = F_1 l_1 + M_A$; $M_D = F_2 l_3 + M_B = F_1 l_3 + M_B$,

$$F_1 = F_2 = \frac{M_C - M_A}{l_1} = \frac{M_D - M_B}{l_3} \qquad . . . (16)$$

Collecting equations (9), (12), (14), (15) and (16),

$$\Delta = - \frac{l_1^2}{6EI_1}(2M_A + M_C) \qquad \qquad \qquad \qquad (9)$$

$$\frac{l_1^2}{6EI_1}(M_A + 2M_C) + l_1 \left\{ \frac{l_2}{6EI_2}(2M_C + M_D) + \frac{a(l_2 - \bar{x})}{EI_2 l_2} \right\} \qquad (12)$$

$$- l_3 \left\{ \frac{l_2}{6EI_2}(M_C + 2M_D) + \frac{a\bar{x}}{EI_2 l_2} \right\} - \frac{l_3^2}{6EI_3}(2M_D + M_B) \qquad (14)$$

$$= \frac{l_3}{6EI_3}(M_D + 2M_B) \qquad \qquad \qquad \qquad (15)$$

$$\frac{M_C - M_A}{l_1} = \frac{M_D - M_B}{l_3} \qquad \qquad \qquad \qquad (16)$$

From these five equations the five unknowns M_A, M_B, M_C, M_D, and Δ can be found ; F_1 follows from eq. (16)

$$R' = \{F_1(l_1 - l_3) + M_A - M_B\}/l_2 \qquad \qquad (17)$$

whence the total reactions at A and B can be found.

Particular Case.—Let $l_3 = l_1$, $I_3 = I_1$, then

$$\frac{6E\Delta}{l_1} = - \frac{l_1}{I_1}(2M_A + M_C) \qquad \qquad \qquad (9A)$$

$$= \frac{l_1}{I_1}(M_A + 2M_C) + \left\{ \frac{l_2}{I_2}(2M_C + M_D) + \frac{6a(l_2 - \bar{x})}{I_2 l_2} \right\} \qquad (12A)$$

$$= - \left\{ \frac{l_2}{I_2}(M_C + 2M_D) + \frac{6a\bar{x}}{I_2 l_2} \right\} - \frac{l_1}{I_1}(2M_D + M_B) \qquad (14A)$$

$$\frac{l_1}{I_1}(M_D + 2M_B) \qquad \qquad \qquad \qquad (15A)$$

$$M_C - M_A = M_D - M_B ; \quad R' = (M_A - M_B)/l_2$$
$$(16A \text{ and } 17A)$$

Equate (9A) to (15A) and use (16A),
$$2M_D + M_B = - 3M_A ;$$
$$M_B = - \frac{M_A + 2M_C}{3}, \quad M_D = \frac{M_C - 4M_A}{3}$$

Equate (12A) to (14A) and eliminate M_B and M_D,
$$(M_A - M_C)(2I_1 l_2 + I_2 l_1) = 3aI_1 \qquad (18)$$

Equate (9A) to (14A) and eliminate M_B and M_D,
$$M_A(8I_1 l_2 + 15I_2 l_1) - M_C(5I_1 l_2 - 3I_2 l_1)$$
$$- 18aI_1 \bar{x}/l_2 = 0 \qquad (19)$$

From eqs. (18) and (19) M_A and M_C can be found, and hence all the other unknowns.

In Fig. 169, $I_2 = 2I_1$; $a = - 36$ ft.²/tons ; $\bar{x} = 8$ ft. ; from eqs. (18) and (19),

FIG. 169.

$$7(M_A - M_C) = - 9 ; \quad 48M_A + 3M_C = - 16 ; \quad M_A = - 0·389 ;$$
$$M_B = - 0·467 ; \quad M_C = + 0·896 ; \quad M_D = + 0·818 \text{ ft./tons.}$$
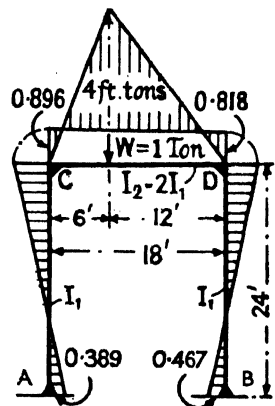
110. Stiff Portal carrying a Single Lateral Load.—*Case* (1). *Hinged Feet.*—Let ACDB, (i) Fig. 170, be a stiff portal subjected to a lateral load F at C. The joints at C and D are rigid, and the feet A and B are hinged. Let the lengths of the three members forming the portal be l_1, l_2, and l_3, and their moments of inertia I_1, I_2, and I_3, respectively. For equilibrium, horizontal forces F_1 and F_2, and vertical forces R_1 and
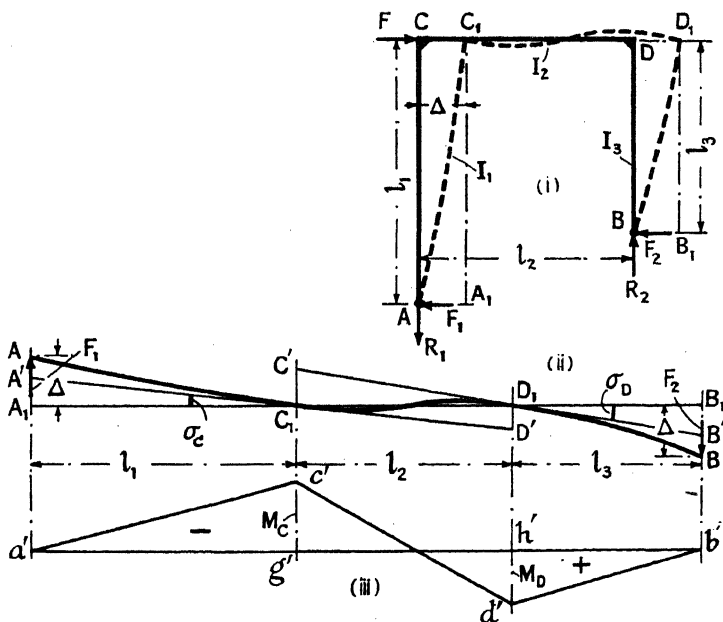
FIG. 170.

R_2, will be called into play at A and B, as shown in (i), such that $F_1 + F_2 = F$, and $R_1 = R_2$. Then, taking moments about A and B,

$$R_2 l_2 = Fl_1 - F_2(l_1 - l_3)$$
$$R_1 l_2 = Fl_3 + F_1(l_1 - l_3) \; ;$$

and
$$R_1 = R_2 = \frac{1}{l_2}\{Fl_3 + F_1(l_1 - l_3)\} = \frac{1}{l_2}\{F_1 l_1 + F_2 l_3\} \; . \qquad . \quad (1)$$

Owing to this arrangement of forces, the frame will distort as shown by the dotted lines in (i), moving to the right a distance Δ. Since the joints at C and D are rigid, they will remain at right angles after distortion, and if the frame be opened cut as shown at (ii), the deflection curves of the three members will form a continuous curve. The corresponding bending-moment diagram is shown at (iii). Let the bending moment at C be M_C, and that at D be M_D. Consider the span A_1C_1, (ii). From eq. (20), § 105,

$$A_1A = A_1A' + A'A = -\sigma_C l_1 + A'A$$

But $A_1A = -\Delta$ (an upward displacement), for AA_1 is the sideways deflection Δ of the portal. From eq. (7), § 105, $A'A$, the deflection of the beam at A above the tangent at C_1, is $M_C l_1^2/3EI_1$; hence,

$$-\Delta = -\sigma_C l_1 + M_C l_1^2/3EI_1 \qquad \cdot \qquad \cdot \qquad \cdot \qquad (2)$$

From eq. (22), § 105, considering the span C_1D_1, $\sigma_C = -D'D_1/l_2$. $D'D_1$ is the deflection of the beam at D_1, above the tangent at C_1, which from eq. (2), § 105, is

$$D'D_1 = \frac{l_2^2}{6EI_2}(2M_C + M_D) ; \text{ whence } \sigma_C = -\frac{l_2}{6EI_2}(2M_C + M_D) \qquad (3)$$

From eqs. (2) and (3),

$$\Delta = -\frac{l_1 l_2}{6EI_2}(2M_C + M_D) - \frac{M_C l_1^2}{3EI_1} \qquad \cdot \qquad \cdot \qquad \cdot \qquad (4)$$

Next consider the span D_1B_1. From eq. (19), § 105,

$$B_1B = B_1B' + B'B = + \sigma_D l_3 + B'B.$$

Here $B_1B = +\Delta$ (a downward displacement) ; and from eq. (7), § 105, $B'B$, the deflection of the beam at B below the tangent at D_1, is $M_D l_3^2/3EI_3$; hence

$$\Delta = \sigma_D l_3 + M_D l_3^2/3EI_3 \qquad \cdot \qquad \cdot \qquad \cdot \qquad (5)$$

Again, considering the span C_1D_1, $\sigma_D = C'C_1/l_2$, where $C'C_1$ is the deflection of the beam at C_1 below the tangent at D_1. From eq. (1), § 105, $C'C_1 = \frac{l_2^2}{6EI_2}(M_C + 2M_D)$; hence, $\sigma_D = \frac{l_2}{6EI_2}(M_C + 2M_D)$. Inserting this value in eq. (5), and equating the resulting value of Δ to that given in eq. (4),

$$\Delta = \frac{l_2 l_3}{6EI_2}(M_C + 2M_D) + \frac{M_D l_3^2}{3EI_3} = -\frac{l_1 l_2}{6EI}(2M_C + M_D) - \frac{M_C l_1^2}{3EI_1} \qquad (6)$$

whence,

$$M_C\left\{\frac{2l_1^2}{I_1} + \frac{l_2}{I_1}(2l_1 + l_3)\right\} + M_D\left\{\frac{l_2}{I_2}(l_1 + 2l_3) + \frac{2l_3^2}{I_3}\right\} = 0 \qquad \cdot \qquad (7)$$

But, neglecting any bending moment produced in AC and BD by the vertical reactions R_1 and R_2, resulting from the deflection Δ, $M_C = -F_1 l_1$; $M_D = F_2 l_3$; hence

$$F_1 + F_2 = -\frac{M_C}{l_1} + \frac{M_D}{l_3} = F ; \text{ or, } M_C l_3 - M_D l_1 + F l_1 l_3 = 0 \quad \cdot \quad (8)$$

By solving eqs. (7) and (8) as simultaneous, the unknown bending moments M_C and M_D can be found, and hence F_1, F_2, R_1, R_2, and Δ.

Particular Case.—If $l_1 = l_3$, and $I_1 = I_3$, so that the frame is symmetrical, eq. (7) becomes $M_C + M_D = 0$, and $M_C = -M_D$. From eq. (8), $M_D = -M_C = F l_1/2$; $F_1 = F_2 = F/2$; $R_1 = R_2 = F l_1/l_2$; and, from eq. (6), $\Delta = \frac{F l_1^2}{6E}\left\{\frac{l_1}{I_1} + \frac{l_2}{2I_2}\right\}$.

Case (2).   *Direction-fixed Feet.*—The analysis in the case of a portal with direction-fixed feet, Fig. 171, is of a similar character.   As before, $F_1 + F_2 = F$; $R_1 = R_2$.   Taking moments about A and B,

$$R_2 l_2 = F l_1 - F_2(l_1 - l_3) - (M_A - M_B)$$
$$R_1 l_2 = F l_3 + F_1(l_1 - l_3) - (M_A - M_B) ;$$

whence $$R_1 = R_2 = \frac{1}{l_2}\{F l_3 + F_1(l_1 - l_3) - (M_A - M_B)\}$$

$$= \frac{1}{l_2}\{F_1 l_1 + F_2 l_3 - (M_A - M_B)\} \tag{9}$$
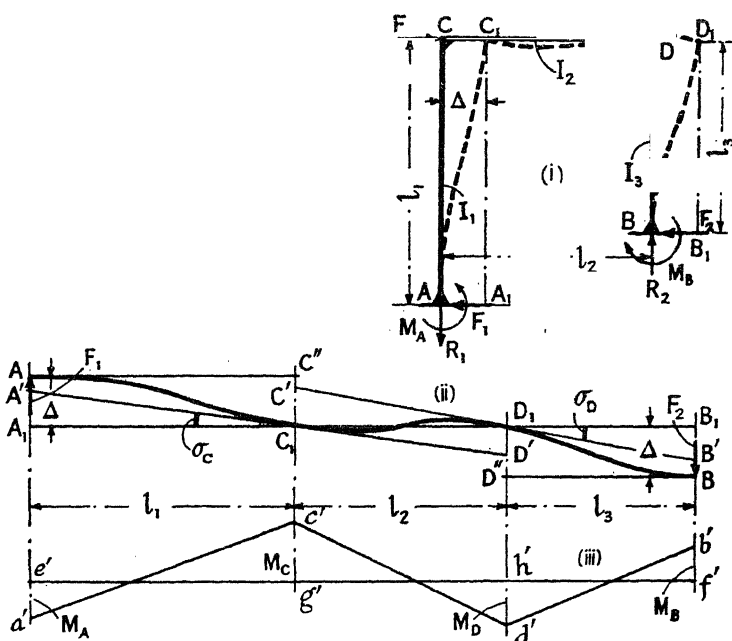
Fig. 171.

As in § 109, and as shown in (i) Fig. 171, both M_A and M_B have at present been taken as positive.   Their real sign will be given by the equations deduced.

The distorted shape of the frame is indicated in (i) and (ii) ; (iii) is the corresponding bending-moment diagram ; M_C and M_D denote the bending moments at C and D respectively.

From (ii), $C''C_1$, the deflection of the beam at C_1 below the tangent at A, is equal to Δ the deflection of the frame to the right ; hence from eq. (2), § 105,

$$C''C_1 = \frac{l_1^2}{6EI_1}(2M_A + M_C) = \Delta \tag{10}$$

From eq. (20), § 105, considering the span A_1C_1, $A_1A = -\sigma_c l_1 + A'A$,

where $A_1A = -\Delta$ (an upward displacement); and, from eq. (1), § 105,
$A'A = \dfrac{l_1{}^2}{6EI_1}(M_A + 2M_C)$, hence

$$- \Delta = - \sigma_C l_1 + \frac{l_1{}^2}{6EI_1}(M_A + 2M_C) \tag{11}$$

From eqs. (22) and (2), § 105, considering the span C_1D_1,

$$\sigma_C = - \frac{D'D_1}{} \qquad \frac{l_2}{6EI} \cdot (2M_C + M_D) \tag{12}$$

Inserting this value in eq. (11),

$$\Delta = - \frac{l_1{}^2}{6EI_1}(M_A + 2M_C) - \frac{l_1 l_2}{6EI_2}(2M_C + M_D) \tag{13}$$

From eq. (19), § 105, considering the span D_1B_1, $B_1B = \sigma_D l_3 + B'B$;
where $B_1B = \Delta$, and $B'B = \dfrac{l_3{}^2}{6EI_3}(2M_D + M_B)$; hence

$$\Delta = \sigma_D l_3 + \frac{l_3}{6EI_3}(2M_D + M_B) \qquad . \qquad . \qquad . \tag{14}$$

Again, from eqs. (21) and (1), § 105, considering the span C_1D_1,

$$\sigma_D = \frac{C'C_1}{l_2} = \frac{l_2}{6EI_2}(M_C + 2M_D)$$

Inserting this value in eq. (14),

$$\Delta = \frac{}{6EI_2}(M_C + 2M_D) + \frac{l_3{}^2}{6EI_3}(2M_D + M_B) \qquad . \tag{15}$$

From (ii), $D''D_1$, the deflection of the beam at D_1 above the tangent at B, is equal to $-\Delta$ (an upward displacement), hence from eq. (1), § 105,

$$D''D_1 = \frac{l_3{}^2}{6EI_3}(M_D + 2M_B) = -\Delta \qquad . \tag{16}$$

Neglecting any bending moment produced by the vertical reactions R_1 and R_2 in AC and BD, resulting from the deflection Δ,

$$M_C = M_A - F_1 l_1; \qquad M_D = F_2 l_3 + M_B \qquad . \qquad . \tag{17}$$

Hence, $\qquad F_1 + F_2 \quad F = \dfrac{M_A - M_C}{l_1} + \dfrac{M_D - M_B}{l_3} \qquad . \qquad . \tag{18}$

Collecting results,

$$\Delta = \frac{l_1{}^2}{6EI_1}(2M_A + M_C) \qquad . \qquad . \qquad . \qquad . \qquad . \tag{10}$$

$$= - \frac{l_1{}^2}{6EI_1}(M_A + 2M_C) - \frac{l_1 l_2}{6EI_2}(2M_C + M_D) \qquad . \qquad . \tag{13}$$

$$= \frac{l_2 l_3}{6EI_2}(M_C + 2M_D) + \frac{l_3{}^2}{6EI_3}(2M_D + M_B) \qquad . \qquad . \tag{15}$$

$$= - \frac{l_2{}^3}{6EI_3}(M_D + 2M_B) \qquad . \qquad . \qquad . \qquad . \qquad . \tag{16}$$

$$F \quad \frac{M_A - M_C}{l} + \frac{M_D - M_B}{l} \qquad . \qquad . \qquad . \qquad . \tag{18}$$

These five equations will give the five unknowns M_A, M_B, M_C, M_D, and Δ ; R_1 and R_2 follow from eq. (9), and F_1 and F_2 from eq. (17).

Particular Case.—If $l_1 = l_3$, and $I_1 = I_3$, so that the frame is symmetrical, $M_A = - M_B$; $M_C = - M_D$; $F_1 = F_2 = F/2$.

From the collected equations,

$$M_A = - M_B = \frac{Fl_1}{2}\left(\frac{I_1 l_2 + 3I_2 l_1}{I_1 l_2 + 6I_2 l_1}\right) \qquad \qquad . \quad (19)$$

$$- M_C = M_D = \frac{Fl_1}{2}\left(\frac{3I_2 l_1}{I_1 l_2 + 6I_2 l_1}\right) \qquad . \qquad . \qquad . \quad (20)$$

$$\Delta = \frac{Fl_1{}^3}{12EI_1}\left(\frac{2I_1 l_2 + 3I_2 l_1}{I_1 l_2 + 6I_2 l_1}\right) \qquad . \qquad . \qquad . \quad (21)$$

and from eq. (9),

$$R_1 = R_2 = \frac{3FI_2 l_1{}^2}{l_2(I_1 l_2 + 6I_2 l_1)} \qquad . \qquad . \qquad . \qquad . \quad (22)$$

111. Stiff Portal carrying any Lateral Load.—*Case* (1). *Hinged Feet.*— As in § 110, Fig. 170, let ACDB, Fig. 172, be the portal ; suppose that the
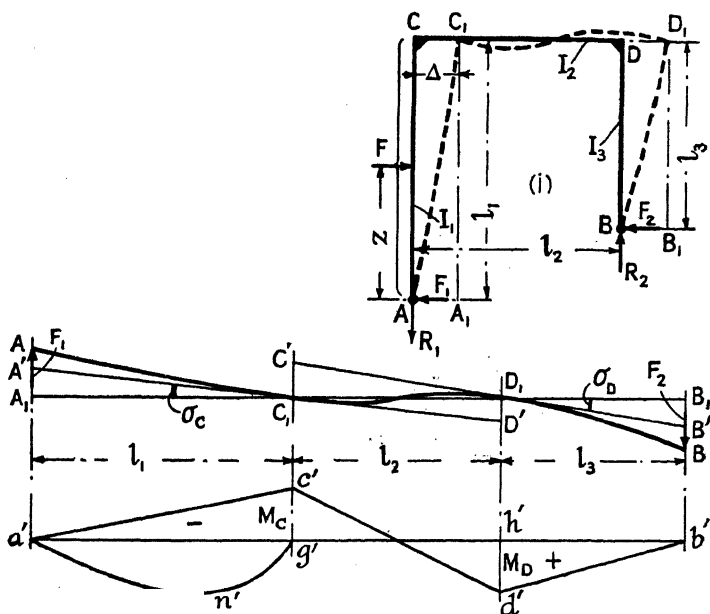
FIG. 172.

lateral load be distributed in any way over the leg AC such that F is its resultant, acting at a distance z from A. The joints at C and D are rigid, but the feet A and B are hinged. Let the lengths of the three members forming the portal be l_1, l_2 and l_3, and their moments of inertia be I_1, I_2, and I_3, respectively. For equilibrium, horizontal forces F_1

and F_2, and vertical forces R_1 and R_2, will be called into play at A and B, such that $F_1 + F_2 = F$, and $R_1 = R_2$. The analysis for this case follows very similar lines to that of Case 1, § 110, and the equations have been numbered to correspond. Taking moments about A,

$$R_2 l_2 = Fz - F_2(l_1 - l_3) \; ;$$

whence, $\qquad R_1 = R_2 = \dfrac{1}{l_2}\{(F_1 + F_2)z - F_2(l_1 - l_3)\}$

$$= \frac{1}{l}\{F_1 z + F_2(z - l_1 + l_3)\} \qquad . \qquad (1)$$

The distorted shape of the frame is indicated in (ii) Fig. 172 ; and the bending-moment diagram in (iii). These are very similar to the corresponding diagrams in Fig. 170, but there will be a negative bending-moment diagram $a'n'g'$, due to the load on the member AC, to be taken into account.

Consider the span $A_1 C_1$, (ii) Fig. 172. From eq. (20), § 105, $A_1 A = A_1 A' + A'A = -\sigma_C l_1 + A'A$; as in § 110, $A_1 A = -\Delta$, and from eq. (15), § 105, $A'A = \dfrac{M_C l_1{}^2}{3EI_1} \cdot \dfrac{a\bar{x}}{EI_1}$; where $-a$ denotes the area of the negative bending-moment diagram $a'n'g'$, and $\bar{x}$ is the distance of its centre of area from A. Hence,

$$-\Delta = -\sigma_C l_1 + \frac{M_C l_1{}^2}{3EI_1} + \frac{a\bar{x}}{EI_1} \qquad . \qquad . \qquad (2)$$

From eqs. (22) and (2), § 105, considering the span $C_1 D_1$,

$$\sigma_C = -\frac{D'D_1}{l_2} - \frac{l_2}{6EI} (2M_C + M_D) \qquad (3)$$

From eqs. (2) and (3),

$$\Delta = \frac{l_1 l_2}{6EI_2}(2M_C + M_D) - \frac{M_C l_1{}^2}{3EI_1} - \frac{a\bar{x}}{EI_1} \qquad (4)$$

In like manner, from eq. (19), § 105, considering span $D_1 B_1$, $B_1 B = B_1 B' + B'B = +\sigma_D l_3 + B'B$; where $B_1 B = +\Delta$, and from eq. (7), § 105, $B'B = M_D l_3{}^2/3EI$; hence

$$\Delta = \sigma_D l_3 + M_D l_3{}^2/3EI_3 \; . \qquad . \qquad . \qquad . \qquad (5)$$

Considering span $C_1 D_1$, from eq. (1), § 105, $\sigma_D = \dfrac{l_2}{6EI_2}(M_C + 2M_D)$; hence, from eqs. (5) and (4),

$$\Delta = \frac{l_2 l_3}{6EI_2}(M_C + 2M_D) + \frac{M_D l_3{}^2}{3EI_3} = -\frac{l_1 l_2}{6EI_2}(2M_C + M_D) - \frac{M_C l_1{}^2}{3EI_1} - \frac{a\bar{x}}{EI_1} \; . \quad (6)$$

whence,

$$M_C\left\{\frac{2l_1{}^2}{I_1} + \frac{l_2}{I_2}(2l_1 + l_3)\right\} + M_D\left\{\frac{l_2}{I_2}(l_1 + 2l_3) + \frac{2l_3{}^2}{I_3}\right\} = -\frac{6a\bar{x}}{I_1} \qquad . \qquad (7)$$

Neglecting any bending moment produced in AC and BD by the vertical reactions R_1 and R_2, resulting from the deflection Δ,

$$M_C = -F_1 l_1 + F(l_1 - z) \; ; \qquad M_D = F_2 l_3 \; ;$$

hence, $M_C = - F_1 l_1 + (F_1 + F_2)l_1 - Fz = F_2 l_1 - Fz = \dfrac{M_D l_1}{l_3} - Fz$

or, $\qquad M_C l_3 - M_D l_1 + F l_3 z = 0$ . . . . . (8)

If eqs. (7) and (8) be solved as simultaneous, the unknown bending moments M_C and M_D and the reactions can be found.

Particular Cases.—(a) If the load F be concentrated at C, $z = l_1$, $a = 0$, and the equations reduce to eqs. (7) and (8) of § 110.

(b) If the load F be uniformly spread over the member AC, $z = l_1/2$, the bending moment diagram is a parabola of which the maximum ordinate is $- Fl_1/8$, $a = - \frac{2}{3} \times l_1 \times Fl_1/8 = - Fl_1^2/12$, $\bar{x} = l_1/2$, and $a\bar{x} = - \frac{1}{12}Fl_1^2 \times l_1/2 = - \frac{1}{24} Fl_1^3$. If this value be substituted in eq. (7), eqs. (7) and (8) can be solved as simultaneous.

(c) If the load condition be as in Particular Case (b), and $l_1 = l_3$, $I_1 = I_3$, so that the frame is symmetrical, Fig. 173, $z = l_1/2$, $a = - \frac{1}{12}Fl_1^2$, $\bar{x} = l_1/2$, and $a\bar{x} = - \frac{1}{24}Fl_1^3$.
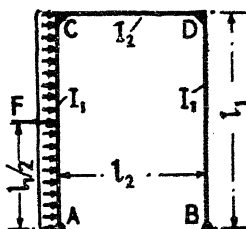
FIG. 173.

Eqs. (7) and (8) become

$$(M_C + M_D)\dfrac{3I_1 l_2 + 2I_2 l_1}{T} = \dfrac{Fl_1^2}{A}$$

$$(M_C - M_D) = - \dfrac{Fl_1}{2} \; ;$$

whence,

$$M_C = \dfrac{3Fl_1}{8} \cdot \dfrac{2I_1 l_2 + I_2 l_1}{3I_1 l_2 + 2I_2 l_1} \qquad . \qquad . \qquad . \qquad . \quad (9)$$

$$M_D = \dfrac{Fl_1}{8} \cdot \dfrac{6I_1 l_2 + 5I_2 l_1}{3I_1 l_2 + 2I_2 l_1} \qquad . \qquad . \qquad . \quad (10)$$

From eq. (6),

$$\dfrac{Fl_1^2}{48EI_1 I_2} \cdot (2I_1 l_2 + 5I_2 l_1) \qquad . \qquad . \qquad . \quad (11)$$

$$F_2 \qquad \dfrac{M_D}{l_1} = \dfrac{F}{8} \cdot \dfrac{6I_1 l_2 + 5I_2 l_1}{3I_1 l_2 + 2I_2 l_1} \qquad . \qquad . \qquad . \quad (12)$$

$$F_1 = F - F_2 = \dfrac{F}{8} \cdot \dfrac{18I_1 l_2 + 11I_2 l_1}{3I_1 l_2 + 2I_2 l_1} \qquad . \qquad . \quad (13)$$

Taking moments about B,

$$R_1 = R_2 = \dfrac{Fl_1}{2l_2} \qquad . \qquad . \qquad . \qquad . \qquad . \quad (14)$$

Case (2). *Direction-fixed Feet.*—The corresponding analysis for a laterally loaded portal with direction-fixed feet, Fig. 174, is as follows : If F be the resultant of the external forces which act on the member AC, $F_1 + F_2 = F$, and $R_1 = R_2$. Taking moments about A and B, and

assuming for the present, as shown in (i) Fig. 174, that M_A and M_B are both positive,

$$R_2 l_2 = Fz - F_2(l_1 - l_3) - (M_A - M_B)$$
$$R_1 l_2 = F(z - l_1 + l_3) + F_1(l_1 - l_3) - (M_A - M_B) \qquad . \qquad . (15)$$

$$R_1 = R_2 = \frac{1}{l_2} \{F_1 z + F_2(z - l_1 + l_3) - (M_A - M_B)\} \quad . \qquad . (16)$$

The distorted shape of the frame is shown at (ii) Fig. 174; (iii) is the
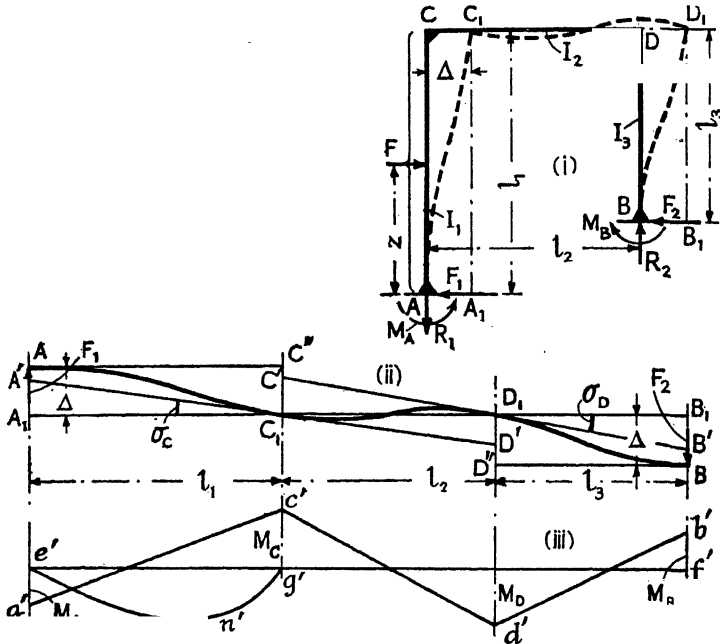
FIG. 174.

bending-moment diagram. From eq. (16), § 105, considering the span $A_1 C_1$,

$$C''C_1 = \frac{l_1^2}{6EI_1} (2M_A + M_C) + \frac{a(L - \bar{x})}{EI_1} \qquad . (17)$$

where $- a$ denotes the area of the negative bending-moment diagram $e'n'g'$, (ii) Fig. 174, and $\bar{x}$ is the distance of its centre of area from A'.

From eq. (20), § 105, considering the span $A_1 C_1$, $A_1 A = - \sigma_C l_1 + A'A$, where $A_1 A = - \Delta$; from eq. (15), § 105,

$$A'A = \frac{l_1^2}{6EI_1}(M_A + 2M_C) + \frac{a\bar{x}}{EI_1},$$

and from span $C_1 D_1$, $\sigma_C = - \frac{l_2}{6EI_2} (2M_C + M_D)$; eq. (12), §110. Hence,

$$\Delta = - \frac{l_1^2}{6EI_1} (M_A + 2M_C) - \frac{l_1 l_2}{6EI_2}(2M_C + M_D) - \frac{a\bar{x}}{EI_1} \qquad . (18)$$

Similarly, as in § 110, $B_1B = \sigma_D l_3 + B'B = \Delta$; where

$$B'B = \frac{l_3{}^2}{6EI_3}(2M_D + M_B),$$

and from span C_1D_1, $\sigma_D = \dfrac{l_2}{6EI_2}(M_C + 2M_D)$. Hence,

$$\Delta = \frac{l_2 l_3}{6EI_2}(M_C + 2M_D) + \frac{l_3{}^2}{6EI_3}(2M_D + M_B) \qquad (19)$$

Also, from (ii),

$$D''D_1 = \frac{l_3{}^2}{6EI_3}(M_D + 2M_B) \qquad (20)$$

Neglecting any bending moment produced by the vertical reactions R_1 and R_2 in AC and BD, resulting from the deflection Δ,

$$M_C = M_A - F_1 l_1 + F(l_1 - z) \; ; \quad M_D = F_2 l_3 + M_B \qquad (21) \text{ and } (22)$$

$$(M_A - M_C)l_3 + (M_D - M_B)l_1 - Fl_3 z = 0 \qquad (23)$$

Collecting results :

$$\wedge - \frac{l_1{}^2}{6EI_1}(2M_A + M_C) + \frac{a(L - \bar{x})}{EI_1} \qquad . \qquad . \qquad . \qquad (17)$$

$$- - \frac{l_1{}^2}{6EI_1}(M_A + 2M_C) - \frac{l_1 l_2}{6EI_2}(2M_C + M_D) - \frac{a\bar{x}}{EI_1} \qquad (18)$$

$$= \frac{l_2 l_3}{6EI_2}(M_C + 2M_D) + \frac{l_3{}^2}{6EI_3}(2M_D + M_B) \qquad (19)$$

$$= - \frac{l_3{}^2}{6EI_3}(M_D + 2M_B) \qquad . \qquad . \qquad . \qquad (20)$$

$$(M_A - M_C)l_3 + (M_D - M_B)l_1 - Fl_3 z = 0 \qquad . \qquad . \qquad (23)$$

The above five equations will give the five unknowns M_A, M_B, M_C, M_D, and Δ ; F_1 and F_2 can be obtained from eq. (22) ; R_1 and R_2 from eq. (16).

Particular Cases.—(d) If the load F be concentrated at C, $z = l_1$, $a = 0$, and the equations reduce to eqs. (10), (13), (15), (16), and (18) of § 110.

(e) If the load F be uniformly spread over the member AC, $z = l_1/2$, $a = - \frac{1}{12}Fl_1{}^2$, $\bar{x} = l_1/2$, and $a\bar{x} = - \frac{1}{24}Fl_1{}^3$ [cf. Particular Case (b) above].

(f) If $l_1 = l_3$, $I_1 = I_3$, so that the frame is symmetrical, and the load be uniformly spread over the member AC ; using the values given in Particular Case (e), the five equations become :

$$\Delta = \frac{l_1{}^2}{6EI_1}(2M_A + M_C) - \frac{Fl_1{}^3}{24EI_1} \qquad . \qquad . \qquad . \qquad . \qquad . (24)$$

$$- \Delta = \frac{l_1{}^2}{6EI_1}(M_A + 2M_C) + \frac{l_1 l_2}{6EI_2}(2M_C + M_D) - \frac{Fl_1{}^3}{24EI_1} \qquad . (25)$$

$$\frac{l_1 l_2}{6EI_2}(M_C + 2M_D) + \frac{l_1{}^2}{6EI_1}(2M_D + M_B) \qquad . (26)$$

$$\Delta = \frac{l_1^2}{6EI_1}(M_D + 2M_B) \tag{27}$$

$$M_A = M_B + M_C - M_D + \frac{Fl_1}{2} \tag{28}$$

Eliminate M_A from eqs. (24) and (25) by means of eq. (28). Add eqs. (24) and (25), and eqs. (26) and (27) ; subtract the latter sum from the former ; a value for $(M_C - M_D)$ is thus obtained. Add eqs. (25) and (26), and eqs. (24) and (27) ; from twice the former sum subtract the latter sum ; a value for $(M_C + M_D)$ is thus obtained. M_C and M_D can now be found ; M_B follows from the addition of eqs. (26) and (27), and M_A from eq. (28) ; Δ can be obtained from eq. (27), F_1 and F_2 from eq. (22), and R_1 and R_2 from eq. (16). The values are as follows :

$$M_A = \frac{Fl_1}{24} \cdot \frac{15I_1^2 l_2^2 + 73I_1 I_2 l_1 l_2 + 30I_2^2 l_1^2}{(2I_1 l_2 + I_2 l_1)(I_1 l_2 + 6I_2 l_1)} \tag{29}$$

$$M_B = -\frac{Fl_1}{24} \cdot \frac{9I_1^2 l_2^2 + 35I_1 I_2 l_1 l_2 + 18I_2^2 l_1^2}{(2I_1 l_2 + I_2 l_1)(I_1 l_2 + 6I_2 l_1)} \tag{30}$$

$$M_C = -\frac{Fl_1^2 I_2}{24} \cdot \frac{23I_1 l_2 + 6I_2 l_1}{(2I_1 l_2 + I_2 l_1)(I_1 l_2 + 6I_2 l_1)} \tag{31}$$

$$M_D = \frac{Fl_1^2 I_2}{24} \cdot \frac{25I_1 l_2 + 18I_2 l_1}{(2I_1 l_2 + I_2 l_1)(I_1 l_2 + 6I_2 l_1)} \tag{32}$$

$$\Delta = \frac{Fl_1^3}{16EI_1} \cdot \frac{I_1 l_2 + 2I_2 l_1}{I_1 l_2 + 6I_2 l_1} \tag{33}$$

$$F_1 = \frac{F}{2} \cdot \frac{13I_1 l_2 + 6I_2 l_1}{2I_1 l_2 + I_2 l_1} \qquad F_2 = \frac{F}{2} \cdot \frac{3I_1 l_2 + 2I_2 l_1}{2I_1 l_2 + I_2 l_1} \tag{34}$$

$$R_1 = R_2 = \frac{Fl_1^2 I_2}{l_2(I_1 l_2 + 6I_2 l_1)} \tag{35}$$

It will be observed that M_A and M_D are positive moments, and M_B and M_C negative moments [see (iii) Fig. 174].

112. Lateral Framing of a Bridge.—The bending moments induced in the lateral framing of a bridge due to cross-girder loading may be simply obtained by means of Characteristic Points. It will be assumed that the frame ACDB, (i) Fig. 175, is continuous, and that all the joints are stiff. The area of the bending-moment diagram for the cross-girder, (ii), is $Wl_3(l_2 - l_3)$. Hence the heights of the characteristic points for this span (see § 75, Vol. I) are

FIG. 175.

$$p_1 r_1 = p_2 r_2 = \frac{2}{l_2^2}\left\{ \begin{matrix} \text{moment of the area of the bend-} \\ \text{ing-moment diagram about } a' \end{matrix} \right\}$$

$$= \frac{2}{l_2^2} \cdot \frac{Wl_3 l_2}{2}(l_2 - l_3) = W\frac{l_3(l_2 - l_3)}{l_2} \tag{1}$$
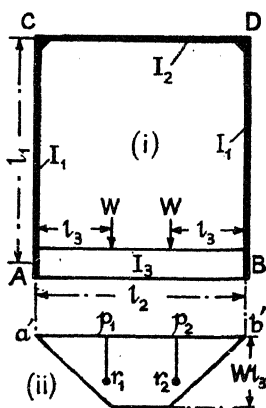
In Fig. 176, set out the spans AB $= l_2$, BD $= l_1$, CD $= l_2$ as shown, and erect the characteristic points p_1r_1 and p_2r_2, just found, for the span AB ; those for the spans BD and DC will lie on the datum line AC, since these spans are unloaded. Find the intersection points i_3 and i_4. Since the moments of inertia of the three spans are I_3, I_1, I_2, respectively,

$$\frac{p_2k_3}{p_3k_3} = \frac{r_2i_3}{r_3i_3} = \frac{I_3l_1}{I_1l_2}; \text{ and } \frac{p_4i_4}{p_5i_4} = \frac{r_4i_4}{r_5i_4} = \frac{I_1l_2}{I_2l_1}$$

See § 78, Vol. I, at end.

Suppose that $a'b'd'c'$, Fig. 176, be the required base line. Since both frame and loading are symmetrical about the centre line, it follows that the bending moment at A is equal to that at B, and the bending moment
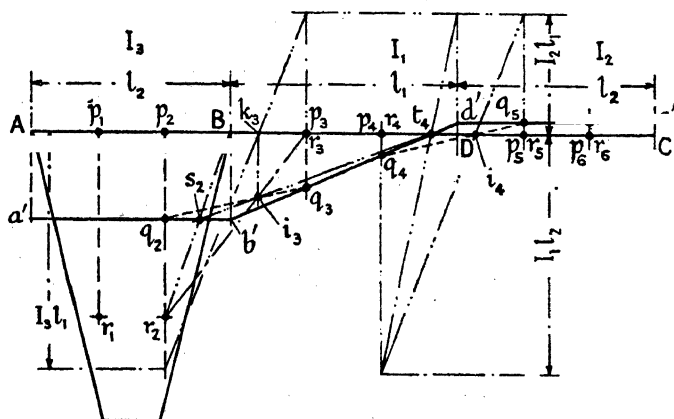
FIG. 176.

at C is equal to that at D. In Fig. 176, $a'A = b'B$ and $d'D = c'C$. Further, from the theory of characteristic points, q_2q_3 must pass through i_3, and q_4q_5 must pass through i_4. Then by similar triangles,

$$\frac{t_4p_4}{t_4D} = \frac{p_4q_4}{Dd'} = \frac{p_4q_4}{p_5q_5} = \frac{p_4i_4}{p_5i_4} = \frac{I_1l_2}{I_2l_1}$$

This relation fixes t_4, which can be obtained by the construction indicated in Fig. 176. A definite point t_4 on the base line is now known. Join r_2B, draw t_4i_3 and produce it to cut r_2B in s_2 (cf. Fig. 71) ; s_2 is a point on the base line $a'b'$ which can be drawn in (a horizontal line) ; draw $b't_4d'$ and $d'c'$; then $a'b'd'c'$ is the complete base line, and the bending moment everywhere is determined.

This construction can be used for a double track railway bridge if both tracks are equally loaded ; the characteristic points are found from the area of the cross-girder bending-moment diagram as indicated above. It breaks down if the conditions are unsymmetrical.

113. Networks. Moment Distribution.—(i) Fig. 179 illustrates a typical network of beams and columns such as might form part of the skeleton

of a steel-framed building. As normally constructed, with bolted or riveted cleats, the joints between the beams and columns, although possessing considerable stiffness, cannot be considered as rigid (§§ 378 and 378A). Usually the beams are treated as isolated spans. When for the purpose of resisting wind pressure, or due to the nature of the construction, stiff joints are introduced, an exact and complete solution is possible, but becomes very laborious if there are a large number of bays. The problem may be solved by slope-deflection methods, § 105 (see for example Wilson and Maney [1] and Wilson, Richart and Weiss [2]), or the Moment Distribution method of Hardy Cross [19] may be applied. In certain cases, the tabular procedures of Takabeya [15] and Unold [25] possess advantages, and Bateman [26] has adapted strain-energy methods to give a practicable solution. Model analysis, § 380, has also been pressed into service. Usually, however, in practical cases, simplifying assumptions are made as to the points of inflection and load distribution ; for a discussion of such practical methods Fleming's book, *Wind Stresses in Buildings* (New York, 1930), may be consulted ; see also Bib., Chapter III, Ref. No. 30–41.

For frames with semi-stiff joints, see Baker.[24]

Moment Distribution.—The method of moment distribution for treating stiff framework, mentioned above, is a procedure in which, by successive arithmetical approximation, the node-point moments in a network can be found with sufficient accuracy for practical purposes. For a frame in which the node points are all fixed in position, and the I of each member is constant throughout its length, the theory is as follows : Imagine that all the node points in the framework are prevented from rotating. Each member will then be direction-fixed at its ends, and the end fixing moments of the loaded spans can be calculated in the usual way ; the end moments of the unloaded spans will be zero. Next suppose that one of the node points is released, the others remaining direction-fixed. The bending moments at the node point at the moment of release will, generally speaking, be unbalanced ; that is to say, if clockwise moments be called positive and anti-clockwise negative, the algebraic sum of the moments at the node point will show a resultant moment in one direction or the other. This resultant moment will bend all the members which meet at the node point through the same angle ; they will share the moment in proportion to their *stiffness*, which may be defined as the bending moment necessary to produce unit rotation of the end of a member, i.e. as M''/σ, where M'' is the end bending moment acting on the member and σ the angular change which it produces. But from eq. (7), § 105, M''/σ is proportional to I/L ; therefore the unbalanced bending moment at the node must be distributed, i.e. apportioned, among the members which meet there in proportion to the different values of I/L. But it follows from eq. (6), § 105, that in a uniform beam, merely supported at one end and direction-fixed at the other, if a bending moment M'' be applied at the supported end of the beam, it will induce a fixing moment $M''/2$ at the other. If, therefore, a bending moment M''

is distributed to one end of a member, a bending moment $M''/2$ must be distributed to the other; this step is termed the *carry-over*. The following procedure, therefore, is to be applied in turn to every node point:
(a) From the algebraic sum of the direction-fixing moments there, the unbalanced moment must be found. (b) This moment must be distributed among the members meeting at the node in proportion to the values of I/L. (c) A moment equal to one-half the value of the distributed moment must be carried over to the other end of the member. Due to the carry-over, there will again be unbalanced moments at the node points, and steps (a), (b) and (c) must be repeated several times until the want of balance is negligible. The method is best illustrated by an example:

Let CDE, (i) Fig. 177, represent a continuous beam merely supported at C, direction-fixed at E, and loaded as indicated. The value of I/L for span CD is $300/288 = 1 \cdot 042$ and for span DE is $600/384 = 1 \cdot 563$,
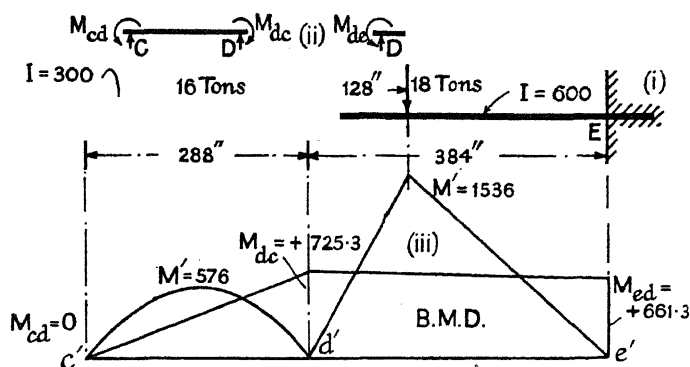
FIG. 177.

the ratio being $2 : 3$. Make a table, p. 260, with a column for the moment at the end of each member, and a column at each node point for the unbalanced moment (U.M.). The symbol M_{cd} denotes the external moment at node C acting on the member CD, (ii) Fig. 177. Clockwise moments are $+$, anti-clockwise $-$. It is convenient to indicate the ratios I/L for the different members. Calculate the direction-fixing moments at the end of each span and enter them in the top line. For the uniform load, the direction-fixing moments are $WL/12$, and for a concentrated load, $M'l_2/L$ and $M'l_1/L$, where $M' = Wl_1l_2/L$ is the bending moment under the load when the ends of the span are freely supported (see p. 148, Vol. I).

Step (a).—Calculate the unbalanced moment at each node point, i.e. the algebraic sum of all the D-F moments there, enter it in the column marked U.M.

Step (b).—Distribute this moment among the members meeting at the node point. At C there is only one member CD, merely supported at C, so that this must carry the whole unbalanced moment 384 inch-tons.

MATERIALS AND STRUCTURES

At D, the U.M. = 640 ; CD and DE meet there, and this moment must be divided between them in the ratio 2 : 3 (see p. 259), i.e. DC carries 256 and DE carries 384. At E the member is direction-fixed, so that this node is not released and there is no U.M. Enter the distributed moments in their appropriate column, *changing the sign.**

Units : tons, inches, inch-tons.

Node Point.	C (supported).		D (continuous).			E (direction-fixed).	
	M_{cd}	U.M.	M_{dc}	M_{de}	U.M.	M_{ed}	U.M.
Ratio I/L	2		2	3		3	
D-F moment	− 384	− 384	+ 384	− 1024	− 640	+ 512	0
Distribution (b)	+ 384		+ 256	+ 384		0	
Carry-over (c)	+ 128	+ 128	+ 192	0	+ 192	+ 192	0
(b)	− 128		− 76·8	−115·2		0	
(c)	− 38·9	− 38·9	− 64	0	− 64	− 57·6	0
(b)	+ 38·9		+ 25·6	+ 38·4		0	
(c)	+ 12·8	+ 12·8	+ 19·4	0	+ 19·4	+ 19·2	0
(b)	− 12·8		− 7·8	− 11·6		0	
(c)	− 3·9	− 3·9	− 6·4	0	− 6·4	− 5·8	0
(b)	+ 3·9		+ 2·6	+ 3·8		0	
(c)	+ 1·3	+ 1·3	+ 2·0	0	+ 2·0	+ 1·9	0
(b)	− 1·3		− 0·8	− 1·2		0	
(c)	− 0·4	− 0·4	− 0·6	0	− 0·6	− 0·6	0
(b)	+ 0·4		+ 0·3	+ 0·3		0	
Totals . .	0·0		+ 725·5	− 725·5		+ 661·1	
Exact . .	0		+ 725·3	− 725·3		+ 661·3	

Step (c).—Carry over a moment of half the magnitude of the distributed moment to the other end of the beam. The first distributed moment M_{cd} is + 384, so that + 192 is added to M_{dc} and so on. On examination it will be seen that the sum of the node point moments in the first two lines in the Table exactly balance, but the moments carried over are out of balance. There is an unbalanced moment of + 128 at C, and of + 192 at D. Hence steps (b) and (c) must be repeated again and again until the want of balance becomes negligible ; the algebraic sums of columns M_{cd}, M_{dc}, M_{de} and M_{ed} then give the bending moments at the nodes. It will be seen that the values obtained are very nearly exact. This method may be applied to networks ; see a worked example below.

It may also be extended to apply to cases such as that shown in (i) Fig. 178, in which the node points are not fixed in position. Suppose first that the ends of all the members are held fixed in direction. Each vertical will then take the shape shown in (ii). Equating the + and

---

* In order that the algebraic sum of the moments in each column may give the resulting moment. Thus at D, M_{de} = − 1024 loses − 384 and becomes − 1024 + 384 = − 640.

– moments on CH, $M_{ch} + M_{hc} = -F_3L_3$, and since from symmetry $M_{ch} = M_{hc}$, $M_{ch} = M_{hc} = -F_3L_3/2$, while the ends remain fixed in direction. From § 63, Vol. I, the deflection of C relative to H is

$$\Delta = \frac{M_{ch}L_3{}^2}{6EI_3} - \frac{F_3L_3{}^3}{12EI_3} \quad \text{and} \quad F_3 = \frac{cI_3}{L_3{}^3}, \text{ where } c = 12E\Delta. \text{ Since } \Delta \text{ must}$$

be the same for all verticals, c is a constant, and

$$F = F_1 + F_2 + F_3 = c \left\{ \frac{I_1}{L_1{}^3} + \frac{I_2}{L_2{}^3} + \frac{I_3}{L_3{}^3} \right\} \; ; \text{ whence, } F_1 = \frac{FI_1}{L_1{}^3} \div \Sigma \frac{I}{L^3} \; ;$$

$$M_{ad} = M_{da} = -\frac{F_1L_1}{2} - -\frac{FI_1}{2L_1{}^2} \div \Sigma \frac{I}{L^3} \; ; \; M_{bg} = M_{gb} = -\frac{FI_2}{2L_2{}^2} \div \Sigma \frac{I}{L^3} \; ;$$

and $M_{ch} = M_{hc} = -\dfrac{FI_3}{2L_3{}^2} \div \Sigma \dfrac{I}{L^3}$. If $L_1 = L_2 = L_3$, $M_{ad} = -\dfrac{FI_1L}{2\Sigma I}$, and

so on. In the direction-fixed condition, if there are no vertical loads, all the moments in the horizontal DGH are zero. From these equations and the data given in the figure, the D-F moments can be calculated and entered in the Table, p. 262 ; the distribution as far as the first step (c)
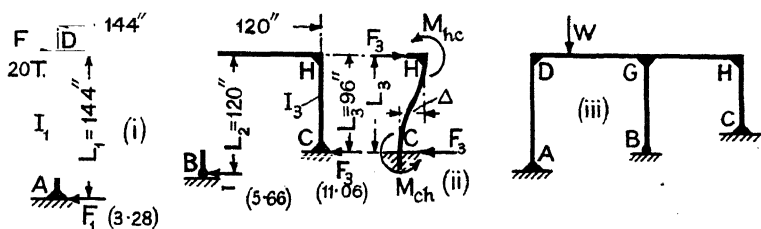
FIG. 178.

follows as before. At this point a modification is necessary. For equilibrium, the sum of the moments top and bottom of all the verticals must be zero (see for example Fig. 169). As the result of steps (b) and (c) certain moments have been distributed to the verticals, of which the sum will not be zero. Add these moments for each vertical and enter the sum $(b) + (c)$ in the U.M. column in step (c) (the figure should be enclosed in brackets). Thus for vertical AD the sum is $0 + 59 \cdot 1 = (+ 59 \cdot 1)$ at the bottom and $0 + 118 \cdot 1 = (+ 118 \cdot 1)$ at the top. For the bottom of BG the sum is $+ 339 \cdot 6 + 60 \cdot 0 = (+ 399 \cdot 6)$, and at the top $+ 119 \cdot 9 + 169 \cdot 8 = (+ 289 \cdot 7)$, and so on. Add all the moments in brackets ; their sum is $+ 1308 \cdot 9$. Divide this moment between the verticals in proportion to the values of I/L^2, changing the sign (see the equation for $M_{ad} = M_{da}$ above, which moments are proportional to $I_1/L_1{}^2$). For this purpose the values of I/L^2 for the ends of each vertical are given at the head of the table. The moments thus distributed are entered in step (d). The sum of the ratios I/L^2 (top and bottom) is $37 \cdot 52$, and $4/37 \cdot 52$ of $-1308 \cdot 9 = -139 \cdot 6$ is distributed to the top and bottom of AD, and so on. The U.M. moment for step (c) is next calculated as before, to which is added the moment just distributed to the vertical. Thus at D, $0 + 49 \cdot 9 - 139 \cdot 6 = -89 \cdot 7$; at A (D-F), U.M. $= 0$.

Node Point.	A (D-F)		D (continuous)			B (hinged)		G (continuous)				C (D-F)		H (continuous)		
	M_{ad}	U.M.	M_{da}	M_{dg}	U.M.	M_{bg}	U.M.	M_{gd}	M_{gb}	M_{gh}	U.M.	M_{ch}	U.M.	M_{hg}	M_{hc}	U.M.
Ratio I/L.	4·0		4·0	4·0		4·8		4·0	4·8	4·8		6·0		4·8	6·0	
Ratio I/L².	4·0		4·0			5·76			5·76			9·0			9·0	
D.-F. Moment.	− 286·2	0	− 286·2	0	− 236·2	− 339·6	− 339·6	0	− 339·6	0	− 339·4	− 530·8	0	0	− 530·8	− 530·8
(b)	0		+ 118·1	+ 118·1	(+ 118·1)	+ 339·6	(+ 339·6)	+ 99·8	+ 119·9	+ 119·9	(+ 289·7)	0		+ 235·9	+ 294·9	(+ 294·9)
(c)	+ 50·1	(+ 50·1)	0	+ 49·9	− 89·7	+ 60·0	− 140·9	+ 50·1	+ 169·8	+ 118·0	+ 140·0	+ 147·5	(+ 147·5)	+ 60·0	− 313·9	− 253·9
(d)	− 139·6	0	− 139·6	+ 44·9		− 200·9		− 43·0	− 200·9	+ 51·5		− 313·9	0	+ 112·8	+ 141·1	
(b)	+ 22·4	(+ 22·4)	+ 44·9	+ 21·5	(+ 44·9)	+ 140·9	(+ 115·2)	+ 22·4	− 51·5	+ 56·4	(+ 18·9)	+ 70·5	(+ 70·5)	− 25·7	0	(+ 141·1)
(c)	− 44·0	0	− 44·0	+ 32·7	65·5	+ 25·7	89·1	− 25·2	+ 70·4	− 30·3	85·8	− 99·1	0	+ 55·5	− 99·1	− 124·8
(d)	+ 16·4	(+ 16·4)	+ 32·7	+ 12·6		+ 63·4		+ 16·4	− 63·4	+ 27·8		+ 34·7	(+ 34·7)	+ 15·2	+ 69·8	
(b)	− 25·7	0	0		(+ 32·7)	− 89·1	(+ 73·9)		− 30·8		(+ 14·3)	− 57·9	0	− 57·9	0	(+ 69·8)
(c)			− 25·7		38·3	+ 15·2	52·2		+ 44·6		51·8				− 57·9	73·1
(d)						− 37·0			− 37·0							

The sum is entered in the U.M. column, step (d), and distributed in the usual way, step (b), the whole process recurring. When the true moments have been found by adding up the columns of the Table, the values of F_1, F_2, F_3, and Δ can be calculated by considering the equilibrium of the verticals.

The above process may be extended to treat cases such as (iii) Fig. 178, where the loading is vertical but unsymmetrically applied, and/or the frame is unsymmetrical. Assume that the frame is prevented from deflecting sideways, i.e. that the node points are fixed in position, and find all the node-point moments, either by moment distribution, characteristic points or otherwise. It will be found that the sum of the moments thus obtained, top and bottom of the verticals, $M_{ad} + M_{da} + M_{bg} + M_{gb} + \ldots = \Sigma M_v$ is not zero. Divide the ΣM_v between the verticals in proportion to the values of I/L^2, changing the sign as above, enter them in the top line of a table, and find the moments at all nodes by moment distribution as on p. 262. Add these algebraically to the position-fixed moments at the nodes, to obtain the true moments in the frame.

Use of Characteristic Points.—If the node points be fixed in position, the method of characteristic points may be applied to networks.*

Consider ZA, (ii) Fig. 179, any one of the unloaded spans attached to the loaded span at A. From eq. (4), § 105, if σ_A be the slope of this span at A,

$$\sigma_A = \frac{L'}{6EI'} \left(M_Z' + 2M_A' \right),$$

a single dash denoting that all the symbols have reference to span ZA. Let $M_Z' = k'M_A'$; where k' is a coefficient depending on the end conditions at Z. Then,

$$\sigma_A = \frac{L'M_A'}{6EI'} (k' + 2) \qquad . \qquad . \qquad . \qquad . \quad (1)$$

The normal shape of the bending-moment diagram for span ZA will be as shown in (iii) Fig. 179. There will be a point of inflexion at t'; hence M_Z', and therefore k', will be negative. (In cases where the beam is cantilevered over the support Z, M_Z' and k' will be positive.) Let the distance $Zt' = v'$; then $k' = -v'/(L' - v')$. If the span ZA is merely supported at Z, $v' = 0$ and $k' = 0$; if the span is fixed in direction at Z, $z'a'$ will pass through the characteristic point r_3, $v' = L'/3$, and $k' = -\frac{1}{2}$. If the span ZA is continuous with another span ZY, length L'', the point t' must be fixed by the Ostenfeld construction shown, (v), but for this purpose, to allow for different values of I, the span L'' must be adjusted in length as explained in § 78, Vol. I; the adjusted length is $L'' \times I'/I''$. In (iii) Fig. 179, assuming that the span YZ is merely supported at Y, it may be shown from the geometry of the figure that

$$v' \quad \frac{(L')^2}{2L'' + 3L'}, \text{ and } k' = -\frac{v'}{L' - v'} = -\frac{L'}{2(L' + L'')} \qquad (2)$$

* See Salmon's 'Characteristic Points,' *Select. Pap. I.C.E.*, No. 46, 1927, p. 18.

a simple formula from which k' is at once determined. L'' is here the adjusted length. If the end conditions at Y are otherwise than merely supported, the point t'' for the span YZ must first be determined, and the distance $t''Z$ substituted for L'' in eq. (2). Thus, if the span is fixed in direction at Y, $t''Z = \frac{2}{3}L''$. If the beam is continuous with a further span XY, t'' must be obtained by the Ostenfeld construction, using adjusted lengths of span, or a previous application of eq. (2) may be made. For many practical problems the girder may be taken as merely supported at Y, whatever may be its true condition. It may be shown (l.c.)
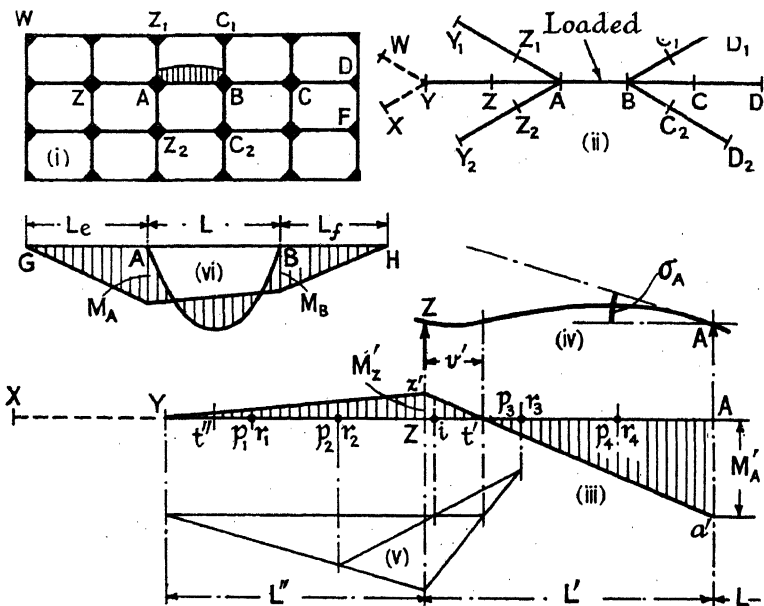
FIG. 179.

that the difference in effect on the loaded span is negligible, whether Y be merely supported or fixed in direction.

From eq. (1), $$M_A' = \frac{6EI'\sigma_A}{(k'+2)L'} \qquad . \qquad (3)$$

If there be a number of spans all rigidly attached to A, so that at support A each bends through the angle σ_A, (iv), it follows that M_A, the total support moment for the loaded span AB, is the sum of all such moments as M_A' in all the unloaded spans attached at A,

$$M_A = \Sigma M_A' = \Sigma \{6EI'\sigma_A/(k'+2)L'\} \qquad (4)$$

Suppose now that the network to the left of A is replaced by a single unloaded span AG, of length L_e, merely supported at G, (vi) Fig. 179,

and with a moment of inertia I_e so chosen that it exactly reproduces the effect of the complete network it replaces, M_A and σ_A remaining as before. Then, as in eq. (3), since $k_e = 0$, G being merely supported,

$$M_A' - \frac{6EI_e\sigma_A}{(k_e + 2)L_e} - \frac{3EI_e\sigma_A}{L_e} = M_A \qquad . \qquad . \qquad . \quad (5)$$

Equating the values of M_A from eqs. (4) and (5),

$$M_A = \Sigma \left\{ \frac{6EI'\sigma_A}{(k' + 2)L'} \right\} \frac{3EI_e\sigma_A}{L_e} \quad \text{and} \frac{I_e}{L_e} = 2\Sigma \left\{ \frac{I'}{(k' + 2)L'} \right\} \quad (6)$$

From eq. (2) the value of k' for each attached unloaded span can be found, and hence I_e/L_e can be calculated. From the considerations of § 78, Vol. I, it is immaterial what value is given to I_e provided that the ratio I_e/L_e is correct. Make $I_e = I$, the moment of inertia of the loaded span. Then the span AG is given by

$$L_e = \frac{I}{2\Sigma \left\{ I'/(k' + 2)L' \right\}} \qquad . \qquad . \qquad . \qquad . \quad (7)$$

In an exactly similar way the equivalent span $BH = L_f$, replacing the network to the right of B, can be found. The complete bending-moment diagram can then be drawn, and the values of M_A and M_B obtained. The bending moment M_A' at the end of any one of the unloaded spans is given by

$$\frac{M_A'}{M_A} = \frac{I'/(k' + 2)L'}{\Sigma\{I'/(k' + 2)L'\}} = \frac{2I'L_e}{(k' + 2)IL'} . \qquad . \qquad . \quad (8)$$

and similarly for M_B'. Knowing the values of M_A' and M_B' the bending-moment diagrams for the complete network can be set out.

It may be shown from the geometry of the bending-moment diagram for spans GA, AB, BH, that

$$M_A = - M_{ab} = \frac{3L\{L(2h_1 - h_2) + 2L_fh_1\}}{4(L + L_e)(L + L_f) - L^2}$$

and

$$= + M_{ba} = \frac{3L\{L(2h_2 - h_1) + 2L_eh_2\}}{4(L + L_e)(L + L_f) - L^2}$$

. . (9)

where $h_1 = p_1r_1$ and $h_2 = p_2r_2$ are the heights of the characteristic points for the span AB, and L_e, L, and L_f are the lengths of spans GA, AB, and BH, respectively. Each loaded span must be separately considered and the results combined.

Worked Example.—As an example of the methods of solution for a simple network, the case illustrated in Fig. 180 will be treated (i) by slope-deflection methods, (ii) by the method of moment distribution, and (iii) by the use of characteristic points.

From eqs. (25) and (26), § 105, the slope-deflection equations are

$$M_{ab} = \frac{2EI}{L} \left\{ 2\sigma_A + \sigma_B - \frac{3\Delta}{L} \right\} + \frac{2a}{L} \left\{ 2 - \frac{3\bar{x}}{L} \right\} \quad . \qquad . \quad (25)$$

$$M_{ba} = \frac{2EI}{L} \left\{ \sigma_A + 2\sigma_B - \frac{3\Delta}{L} \right\} - \frac{2\bar{a}}{L} \left\{ \frac{3\bar{x}}{L} - 1 \right\} \qquad (26)$$

In this case the node points are fixed in position and $\Delta = 0$. For span CD, $WL/8 = 576$, $WL/12 = 384$; for span DE, M' under the load $= 18 \times 128 \times 256 \div 384 = 1536$; $M_A'' = 1536 \times 256 \div 384 = 1024$; $M_B'' = 1536 \times 128 \div 384 = 512$; units :—inches, tons. If, in eqs. (25) and (26), σ_A, σ_B and Δ are all put equal to zero, the span must be direction-fixed at its ends, and

$$M_{ab} = \frac{2a}{L}\left\{2 - \frac{3\bar{x}}{L}\right\}; \quad M_{ba} = -\frac{2a}{L}\left\{\frac{3\bar{x}}{L} - \right.$$

are the direction-fixing moments M_A'' and M_B'' at the ends of the span,
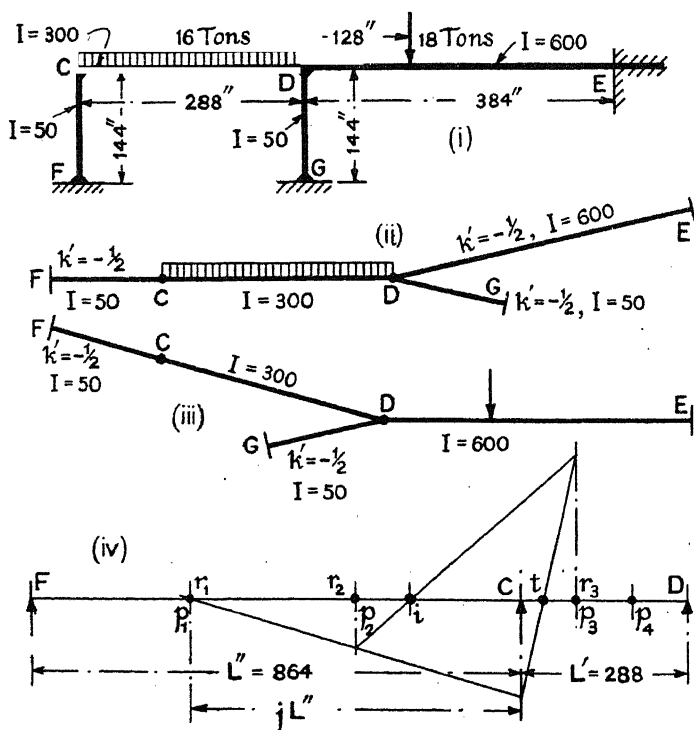
FIG. 180.

i.e, ± 384 in span CD and -1024 and $+512$ in span DE, which determines the values of the terms containing $\bar{x}$. Apply eqs. (25) and (26) to each span of the frame in turn :

Span FC, direction-fixed at F, $\sigma_F = 0$; $I/L = 50/144$; unloaded, $a = 0$.

$$M_{fc} = \frac{2 \times 50E}{144}\{0 + \sigma_C\}; \quad M_{cf} = \frac{2 \times 50E}{144}\{0 + 2\sigma_C\} \qquad . \ (10)$$

hence $M_{cf} = 2M_{fc}$.

Span CD, $I/L = 300/288$; $M_C'' = - M_D'' = - 384$,

$$M_{cd} = \frac{2 \times 300E}{288} \{2\sigma_C + \sigma_D\} - 384$$

$$M_{dc} = \frac{2 \times 300E}{288} \{\sigma_C + 2\sigma_D\} + 384 \qquad . \quad (11)$$

Span GD, direction-fixed at G, $\sigma_G = 0$; $I/L = 50/144$; unloaded, $a = 0$.

$$M_{gd} = \frac{2 \times 50E}{144} \{0 + \sigma_D\}; \quad M_{dg} = \frac{2 + 50E}{144} \{0 + 2\sigma_D\} \qquad . \quad (12)$$

hence $M_{dg} = 2M_{gd}$.

Span DE, direction-fixed at E, $\sigma_E = 0$; $I/L = 600/384$; $M_D'' = -1024$; $M_E'' = + 512$.

$$M_{de} = \frac{2 \times 600E}{384} \{2\sigma_D + 0\} - 1024 \Bigg]$$

$$M_{ed} = \frac{2 \times 600E}{384} \{\sigma_D + 0\} + 512 \Bigg\} \qquad . \quad . \quad . \quad (13)$$

Further, since the algebraic sum of the moments at any node point must be zero,

$$M_{cf} + M_{cd} = 0 \; ; \; M_{dc} + M_{dg} + M_{de} = 0 \qquad . \quad . \quad (14)$$

From eqs. (12), (13) and (14),

$$\sigma_D = - \frac{144}{200E} M_{dg} = \frac{384}{2400E} \Big\{ M_{de} + 1024 \Big\} \; ; \text{and } M_{dg} = M_{dc} + M_{de} \quad . \quad (15)$$

whence $\qquad\qquad 9M_{dc} + 11M_{de} + 2048 = 0 \qquad . \quad . \quad . \quad (16)$

From eqs. (10), (14), (15) and (11),

$$\sigma_C \quad \frac{144}{200E} M_{cf} = - \frac{144}{200E} M_{cd} \qquad\qquad (17)$$

$$M_{cd} + 384 = \frac{600E}{288} \left\{ -\frac{288}{200E} M_{cd} + \frac{384}{2400E} (M_{de} + 1024) \right\}$$

whence $\qquad\qquad 12M_{cd} - M_{de} + 128 = 0 \qquad . \quad . \quad . \quad (18)$

From eqs. (11), (17) and (15),

$$M_{dc} - 384 = \frac{600E}{288} \left\{ - \frac{144}{200E} M_{cd} + \frac{384}{1200E}(M_{de} + 1024) \right\}$$

whence $\qquad\qquad 6M_{dc} + 9M_{cd} - 4M_{de} - 6400 = 0 \qquad\qquad (19)$

Solving eqs. (16), (18), and (19) as simultaneous,

$$\left. \begin{array}{l} 9M_{dc} + 11M_{de} + 2048 = 0 \\ 12M_{cd} - M_{de} + 128 = 0 \\ 6M_{dc} + 9M_{cd} - 4M_{de} - 6400 = 0 \end{array} \right\}$$

$$M_{cd} = - 72 \cdot 6 \; ; \; M_{dc} = + 680 \cdot 3 \; ; \; M_{de} = - 742 \cdot 8$$

whence from eqs. (13), (14), (10), $2M_{ed} = M_{de} + 2048$, and $M_{ed} = 652 \cdot 6$; $M_{cf} = - M_{cd} = + 72 \cdot 6$; $M_{fc} = \frac{1}{2}M_{cf} = + 36 \cdot 3$; $M_{dg} = - M_{dc} - M_{de} = + 62 \cdot 5$; and $M_{gd} = \frac{1}{2}M_{dg} = + 31 \cdot 3$. Knowing the node-point moments, the bending-moment diagrams for each member can be set out.

The tabular calculation for the moment distribution method is given on p. 269. The direction-fixing moments M_A'' M_B'' for the spans CD and DE have already been calculated and are given in the top line. The values of I/L for the different spans are as follows : FC and GD $= 50/144 = 0 \cdot 347$; CD $= 300/288 = 1 \cdot 042$; DE $= 600/384 = 1 \cdot 563$; ratios $2 : 6 : 9$. The process is exactly similar to that on p. 260.

The two methods evidently agree very closely.

Treating the same problem by the method of characteristic points, it is first assumed that only span CD is loaded. To the left of C, (ii) Fig. 180, the only span is FC, for which $k' = - \frac{1}{2}$, since F is direction-fixed, and from eq. (7),

$$L_e = \frac{I}{2\Sigma\{I'/(k' + 2)L'\}} = \frac{300}{(2 \times 50) \div (1 \cdot 5 \times 144)} = 648$$

To the right of D, (ii) Fig. 180, spans DG and DE are direction-fixed at G and E respectively, therefore $k' = - \frac{1}{2}$ for each, and from eq. (7),

$$L_f = \frac{300}{2\left\{\dfrac{50}{1 \cdot 5 \times 144} + \dfrac{600}{1 \cdot 5 \times 384}\right\}} = 117 \cdot 8$$

For the loaded span CD, $L = 288$, and the heights of the characteristic points are $p_1 r_1 = h_1 = p_2 r_2 = h_2 = WL/12 = 384$. Then from eq. (9),

$$- M_{cd} = 121 \cdot 0 ; \qquad M_{dc} = 366 \cdot 0$$

These values can be checked graphically in the usual way.

$M_{cf} = - M_{cd} = + 121 \cdot 0$; $\quad M_{fc} = \frac{1}{2}M_{cf} = + 60 \cdot 5$. From eq. (8),

$$M_{de} = - M_{dc} \frac{2I'L_f}{(k' + 2)IL'} = - \frac{366 \times 2 \times 600 \times 117 \cdot 8}{1 \cdot 5 \times 300 \times 384} = - 299 \cdot 5.$$

$M_{dg} = - M_{dc} - M_{de} = - 366 \cdot 0 + 299 \cdot 5 = - 66 \cdot 5$; since E and G are direction-fixed, $M_{ed} = \frac{1}{2}M_{de} = - 149 \cdot 8$; $M_{gd} = \frac{1}{2}M_{dg} = - 33 \cdot 2$.

Next assume that only span DE is loaded. The network to the left of D is shown in (iii) Fig. 180. The I of CD is 300, and that of FC is 50, hence the adjusted length of the latter, altered in this ratio, is $144 \times 300/50 = 864$. Since F is direction-fixed, the support moment line passes through the adjacent characteristic point, and the Ostenfeld construction, (iv) Fig. 180, starts at $p_1 = r_1$. From this construction * $Ct = 38 \cdot 4$,

---

* If preferred, Ct can be calculated from the expression $\dfrac{(L')^2}{3(L' + L'') - L''/j}$; L'' is the adjusted length.

Units : tons, inches, inch-tons.

Node Point	F (D-F)		C (continuous)			G (D-F)		D (continuous)				E (D-F)	
	M_{fc}	U.M.	M_{cf}	M_{cd}	U.M.	M_{gd}	U.M.	M_{dg}	M_{dc}	M_{de}	U.M.	M_{ed}	U.M.
Ratio I/L	2		2	6		2		2	6	9		9	
D-F Moment	0	0	0	− 384	− 384	0	0	0	+ 384	− 1024	− 640	+ 512	0
Step (b)	0	0	+ 96	+ 288		0	0	+ 75·3	+ 225·9	+ 338·8		+ 169·4	0
(c)	+ 48	0	0	+ 113	+ 113	+ 37·7	0	0	+ 144·0	0	+ 144	0	0
(b)	− 14·1	0	− 28·2	− 84·8		− 8·5	0	− 17·0	− 50·8	− 76·2		− 38·1	0
(c)	0	0	0	− 25·4	− 25·4	0	0	0	− 42·4	0	− 42·4	0	0
(b)	+ 3·2	0	+ 6·4	+ 19·0		+ 2·5	0	+ 5·0	+ 14·9	+ 22·4		+ 11·2	0
(c)	0	0	0	+ 7·5	+ 7·5	0	0	0	+ 9·5	0	+ 9·5	0	0
(b)	− 0·9	0	− 1·9	− 5·6		− 0·6	0	− 1·1	− 3·4	+ 5·0		+ 2·5	0
(c)	0	0	0	− 1·7	− 1·7	0	0	0	+ 2·8	0	− 2·8	0	0
(b)	+ 0·2	0	+ 0·4	+ 1·3		+ 0·2	0	+ 0·3	− 1·0	+ 1·5		+ 0·8	0
(c)	0	0	0	+ 0·5	+ 0·5	0	0	0	+ 0·7	0	+ 0·7	0	0
(b)			− 0·1	− 0·4				− 0·1	− 0·2	0·4			
Totals	+ 36·4		+ 72·6	− 72·6		+ 31·3		+ 62·4	+ 680·4	− 742·9		+ 652·8	
Slope-Deflection	+ 36·3		+ 72·6	− 72·6		+ 31·3		+ 62·5	+ 680·3	− 742·8		+ 652·6	

$Dt = 249 \cdot 6$, and for the span CD, $k' = -38 \cdot 4/249 \cdot 6 = -0 \cdot 154$, whence $(k' + 2) = 1 \cdot 846$. For the span GD, $k' = -\frac{1}{2}$, since G is direction-fixed. Hence from eq. (7)

$$L_e = \frac{I}{2\Sigma\{I'/(k' + 2)L'\}} = \frac{600}{2\left\{\dfrac{300}{1 \cdot 846 \times 288} + \dfrac{50}{1 \cdot 5 \times 144}\right\}} = 377 \cdot 0$$

On the right-hand side there is no network and the beam is direction-fixed at E. Hence the equivalent span L_f is zero (only true when the end is direction-fixed). The heights of the characteristic points for the span DE are $p_1 r_1 = h_1 = 853 \cdot 3$ and $p_2 r_2 = h_2 = 682 \cdot 7$, easily found from the direction-fixing moments 1024 and 512 previously given, or calculated direct. Using these values in eq. (9),

$$M_{de} = -443 \cdot 5 \; ; \qquad M_{ed} = 802 \cdot 3$$

These results may be checked graphically. From eq. (8),

$$M_{dc} = -M_{de}\frac{2I'L_e}{(k' + 2)IL'} = 443 \cdot 5 \frac{2 \times 300 \times 377}{1 \cdot 846 \times 600 \times 288} = +314 \cdot 5 \; ;$$

$M_{cd} = -k'M_{dc} = 0 \cdot 154 \times 314 \cdot 5 = +48 \cdot 4$; $M_{dg} = -M_{de} - M_{dc} = 443 \cdot 5$ $-314 \cdot 5 = +129 \cdot 0$; $M_{gd} = \frac{1}{2}M_{dg} = +64 \cdot 5$; $M_{cf} = -M_{cd} = -48 \cdot 4$; $M_{fc} = \frac{1}{2}M_{cf} = -24 \cdot 2$.

Adding the moments for the two load conditions,

$M_{fc} = +60 \cdot 5 - 24 \cdot 2 = +36 \cdot 3$; $M_{cf} = +121 \cdot 0 - 48 \cdot 4 = +72 \cdot 6$
$M_{cd} = -121 \cdot 0 + 48 \cdot 4 = -72 \cdot 6$; $M_{dc} = +366 \cdot 0 + 314 \cdot 5 = +680 \cdot 5$
$M_{gd} = -33 \cdot 2 + 64 \cdot 5 = +31 \cdot 3$; $M_{dg} = -66 \cdot 5 + 129 \cdot 0 = +62 \cdot 5$
$M_{de} = -299 \cdot 5 - 433 \cdot 5 = -743 \cdot 0$; $M_{ed} = -149 \cdot 8 + 802 \cdot 3 = +652 \cdot 5$

These values agree closely with those found by the other methods.

SECONDARY STRESSES IN FRAMED STRUCTURES

114. Secondary and Deformation Stresses. Effect of Stiff Joints.— The conditions, § 3, necessary to enable the forces in the members to be determined by statical considerations are fulfilled in very few frames in practice. The joints usually possess a considerable degree of stiffness, which stiffness, when the frame deforms, sets up bending moments in all the members, producing *deformation stresses*. The centre lines of the members frequently do not meet in a common point at a node, whence result other secondary bending moments and stresses. The horizontal members are stressed by their own weight, and no member can be made perfectly straight. The stresses which occur owing to these and other like causes are called *secondary stresses*, and they increase or decrease, depending on their sign, the *primary stresses* produced by the longitudinal loads in the members.

It is possible to estimate the magnitude of the secondary stresses by making certain simplifying assumptions, but the problem is complicated by the fact that the joints are not perfectly rigid and the degree of

stiffness is difficult to determine. Also the difficulties are increased by the interaction between the primary longitudinal forces and the effects of the secondary bending moments, which may increase any original curvature in the member, an important consideration in the struts. An exact treatment is necessarily very involved, and is usually not attempted. Experience has shown that in small frames the secondary stresses may be neglected. When it is desired to take the deformation stresses into account, it is common to assume that the joints are perfectly rigid.

115. **Calculation of Deformation Stresses.**—For the purpose of computing the deformation stresses in a braced frame, it will be assumed (i) that the joints are perfectly stiff, (ii) that the effect of the longitudinal load on the deflected member may be neglected.

Suppose that A and B be two node points in a framework of which the joints are frictionless hinges, and that the centre line of the member AB coincides with the straight line joining A to B. Should the frame distort, A will move to A', B to B', the centre line of the member will still coincide with the straight line joining the two node points, the member making the small angular movement necessary.

In a frame in which the joints are rigid, this angular movement would, in part, be prevented, due to the stiffness of the adjacent members. It follows that when the frame distorts, each member must bend, taking one or other of the shapes shown in (i) or (iii) Fig. 181. If the tangents to the ends of the curved centre line A'B'
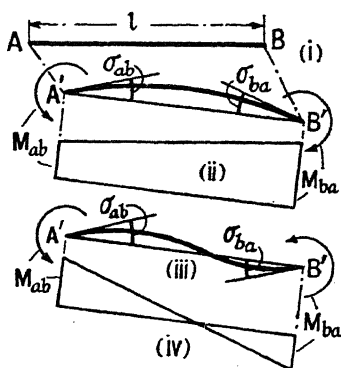
Fig. 181.

angles σ_{ab} and σ_{ba} with the straight line joining A' to B', the bending moments acting at A' and B' are given by eq. (5), § 105,

$$M_{ab} = -\frac{2EI}{l}(2\sigma_{ab} + \sigma_{ba}) \; ; \quad M_{ba} \quad + \frac{2EI}{l}(\sigma_{ab} + 2\sigma_{ba}).$$

M_{ab} and M_{ba} are to be regarded as moments external to AB, imposed on that member by the rest of the framework, analogous to the direction-fixing moments in a direction-fixed beam. The notation adopted should be observed. The first suffix denotes the node point, the second determines the particular bar. It will be convenient, when considering these moments, to adopt the convention that clockwise moments are positive and anti-clockwise moments negative, irrespective of the manner in which they deflect the member. M_{ab} in Fig. 181 must then be regarded as a negative moment, and given a negative sign, when the minus sign will disappear from eq. (5) above mentioned, which will become

$$M_{ab} = \frac{2EI}{l}(2\sigma_{ab} + \sigma_{ba}) \; ; \quad M_{ba} = \frac{2EI}{l}(\sigma_{ab} + 2\sigma_{ba}) \qquad . \quad (1)$$

The angles σ_{ab} and σ_{ba} must be found from the deformations produced in the framework. They can be calculated either from the elongations of the bars, or from the displacements of the node points. Both methods are given below. As in the case of the moments, it will be assumed that $+ \sigma$ is an angular displacement in a clockwise direction, measured from the straight line joining the displaced node points A'B'.

116. Calculation of Deformation Stresses from the Elongations.— As a preliminary to this method, it is necessary to determine the alterations in the angles of a triangle due to alterations in the lengths of its sides. It is convenient for this purpose to use the ordinary trigonometrical symbols. Let ABC, (i) Fig. 182, be the triangle, a, b, and c its
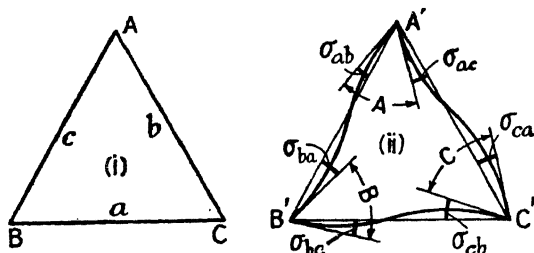
FIG. 182.

sides, A, B, and C, the opposite angles. Suppose that, due to some cause or other, the sides lengthen to $a + \delta a$, $b + \delta b$, $c + \delta c$; and that consequentially the angles alter to $A + \delta A$, $B + \delta B$, and $C + \delta C$. From a well-known trigonometrical theorem,

$$\cos A = \frac{b^2 + c^2 - a^2}{2bc}$$

Differentiate with regard to A, treating a, b, and c as functions of A, for the magnitude of δA will depend on the alteration in the length of each side,

$$- 2\delta A . \sin A = \frac{\delta b}{c} - \frac{b . \delta c}{c^2} + \frac{\delta c}{b} - \frac{c . \delta b}{b^2} - \frac{2a . \delta a}{bc} + a^2 \left\{ \frac{\delta c}{bc^2} + \frac{\delta b}{cb^2} \right\}$$

$$\delta A = - \frac{1}{2 \sin A} \left\{ \frac{(a^2 + b^2 - c^2}{bc} . \frac{\delta b}{b} + \frac{a^2 + c^2 - b^2}{bc} . \frac{\delta c}{c} - \frac{2a . \delta a}{bc} \right\}$$

Using the relations : $\dfrac{a}{\sin A} = \dfrac{b}{\sin B} = \dfrac{c}{\sin C}$; $a = b \cos C + c \cos B$;

$$\delta A \quad \left\{ - \frac{\delta b}{b} \cot C - \frac{\delta c}{c} \cot B + \frac{\delta a (b \cos C + c \cos B)}{bc \sin A} \right\}$$

$$= \left\{ \frac{\delta a}{a} - \frac{\delta c}{c} \right\} \cot B + \left\{ \frac{\delta a}{a} - \frac{\delta b}{b} \right\} \cot C \qquad . \qquad . \qquad . \quad (1)$$

δA, thus determined, is the alteration in the angle A due to the alterations in the lengths of the sides. Since δa is the alteration in length of

the side a, $\delta a / a$ is the strain in the bar $BC = f_a / E$, where f_a is the stress in this bar, and so on for the others. Therefore,

$$\delta A = \frac{1}{E}\{(f_a - f_c)\ \cot\ B + (f_a - f_b)\ \cot\ C\}$$

Similar expressions can be obtained for the alterations in the other angles, hence

$$\delta A = \frac{1}{E}\{(f_a - f_c)\ \cot\ B + (f_a - f_b)\ \cot\ C\}$$

$$\delta B = \frac{1}{E}\{(f_b - f_a)\ \cot\ C + (f_b - f_c)\ \cot\ A\} \qquad (2)$$

$$\delta C = \frac{1}{E}\{(f_c - f_b)\ \cot\ A + (f_c - f_a)\ \cot\ B\}$$

Since the three angles of the triangle must equal two right angles, it follows that

$$\delta A + \delta B + \delta C = 0 \qquad . \qquad . \qquad . \qquad . \quad (3)$$

From these formulae the alteration in the angles of any triangle in a framework can be calculated from the alterations in the lengths of its

Temperature Changes.—If a bar of length l be subjected to an increase in temperature $t°$ in addition to a stress f, the alteration in length is

$$\delta l = \frac{fl}{E} + atl \qquad \text{and} \qquad \frac{\delta l}{l} = \frac{1}{E}(f + atE) \ ;$$

a is the coefficient of linear expansion per degree. Thus, for the bar BC, if t_a be the increase in temperature, $\dfrac{\delta a}{a} = \dfrac{1}{E}(f_a + at_aE)$, and so on for the other bars of the triangle. Eq. (2) will then become

$$\delta A = \frac{1}{E}[\{(f_a + at_aE) - (f_c + at_cE)\}\cot\ B$$
$$+ \{(f_a + at_aE) - (f_b + at_bE)\}\cot\ C] \qquad . \qquad . \qquad . \quad (4)$$

and similarly for the other members of the equation.

It will be evident that if t be the same for all the bars, δA, δB, and δC will be unaltered by the change in temperature.

Deformation Angles.—Let A'B'C', (ii) Fig. 182, represent the position of the three nodes of the triangle ABC after the deformation has taken place. If the joints at A, B, and C were frictionless pins, the bars of the frame would be represented by the straight lines joining the points A', B', and C', and the included angles would change to A', B', and C'. If, as now assumed, the joints are perfectly stiff, the angles A, B, and C must remain constant, and the bars must bend, as indicated in the figure. For the purpose of this analysis it will be supposed that the angle σ is positive at each node, as shown in (ii) Fig. 182, i.e. that σ, measured from the straight line joining the displaced node points, is an angular displacement in a clockwise direction. If the value of σ is found by calculation to be negative, it implies that the angular displacement is anti-clockwise.

Consider the angle at A'. Since the connection between the bars is perfectly rigid, the angle between the tangents to the bent centre lines at A' must remain constant, and equal to the angle A, as indicated in (ii). It follows that the angle $A' = A + \sigma_{ac} - \sigma_{ab}$; or $A' - A = \delta A = \sigma_{ac} - \sigma_{ab}$, and similarly for the other angles. Therefore,

$$\delta A = \sigma_{ac} - \sigma_{ab} ; \quad \delta B = \sigma_{ba} - \sigma_{bc} ; \quad \delta C = \sigma_{cb} - \sigma_{ca} \quad . \quad . \quad (5)$$

and from eq. (3),

$$\sigma_{ac} - \sigma_{ab} + \sigma_{ba} - \sigma_{bc} + \sigma_{cb} - \sigma_{ca} = \delta A + \delta B + \delta C \quad (6)$$

If M_{ab} be the bending moment acting on the member AB at A, resulting from the angular distortion σ_{ab}; and that at B, due to σ_{ba}, be M_{ba}; from eq. (1), § 115,

$$M_{ab} = \frac{2EI_{ab}}{l_{ab}}(2\sigma_{ab} + \sigma_{ba}) ; \quad M_{ba} = \frac{2EI_{ab}}{l_{ab}}(\sigma_{ab} + 2\sigma_{ba}) \quad (7)$$

from which,

$$\sigma_{ab} = \frac{l_{ab}}{6EI_{ab}}(2M_{ab} - M_{ba}) ; \quad \sigma_{ba} = \frac{l_{ab}}{6EI_{ab}}(2M_{ba} - M_{ab}) \quad (8)$$

Further, however many bars meet at a node point such as A,

$$\Sigma\delta A = \Sigma\sigma \quad . \quad . \quad . \quad (9)$$

Due consideration must be given to signs. Thus in Fig. 183,

$$\delta(BAC) + \delta(DAC)$$
$$= (\sigma_{ac} - \sigma_{ab}) + (\sigma_{ad} - \sigma_{ac})$$

and so on.

Unless an applied bending moment act at the node, the sum of all the bending moments acting on the members meeting at the node must be zero :

$$\Sigma M_{ab} = 0 \quad . \quad . \quad (10)$$

FIG. 183.

The above equations, applied successively to every triangle or node in the frame, suffice to determine all the unknown bending moments M_{ab} . . .

Worked Example.—As a simple application of the above theory, the deformation stresses which would be induced in the frame shown in Figs. 28 and 184, § 12, were it constructed with stiff joints, will be determined. From § 12, AB = 100 in.; AC = 80 in.; BC = 70 in.; $Cc' = 0.0308$ in.; $Cc'' = 0.0151$ in. Suppose that $I_{ac} = 0.8$ in.[4]; $I_{bc} = 2.8$ in.[4]; then the values of $2EI/l$ are as follows :

for the bar AC, $2EI/l = 2E \times 0.8/80 = 0.02E$
for the bar BC, $= 2E \times 2.8/70 = 0.08E$

From the trigonometry of the figure,

$$\cot A = 1.035 ; \quad \cot B = 0.764 ; \quad \cot C = 0.118.$$
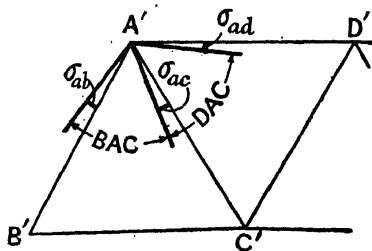
In eq. (1),

$$\frac{\delta a}{a} = \cdot\ \frac{0 \cdot 0151}{70} - 0 \cdot 000216\ ;\ \frac{\delta b}{b} \cdot \frac{0 \cdot 0308}{80}\qquad 0 \cdot 000385\ ;\ \frac{\delta c}{c}\quad 0\ ;$$

whence, $\delta A = - 0 \cdot 000236$; $\delta B = + 0 \cdot 000469$; $\delta C = 0 \cdot 000233$; so that eq. (3) is satisfied.

From eq. (5),

$$\delta A = \sigma_{ac} - \sigma_{ab} = - 0 \cdot 000236$$
$$\delta B = \sigma_{ba} - \sigma_{bc} = + 0 \cdot 000469$$
$$\delta C = \sigma_{cb} - \sigma_{ca} = - 0 \cdot 000233$$

Since AB is a rigid wall, $\sigma_{ab} = \sigma_{ba} = 0$, and $\sigma_{ac} = - 0 \cdot 000236$; $\sigma_{bc} = - 0 \cdot 000469$. From eq. (7),

$$M_{cb} = \frac{2EI_{bc}}{l_{bc}}(\sigma_{bc} + 2\sigma_{cb})\ ;$$

$$M_{ca} = \frac{2EI_{ac}}{l_{ac}}(\sigma_{ac} + 2\sigma_{ca})\ ;\ \text{whence,}$$

$$\frac{M_{cb}}{0 \cdot 08E} - \frac{M_{ca}}{0 \cdot 02E}$$
$$= \sigma_{bc} - \sigma_{ac} + 2(\sigma_{cb} - \sigma_{ca})\ ;$$

from eq. (10), $M_{ca} + M_{cb} = 0$.

Putting in the known values of σ_{ac}, σ_{bc}, and $(\sigma_{cb} - \sigma_{ca})$,

$$M_{cb} = - 0 \cdot 145 \text{ in.-tons}\ ;$$
$$M_{ca} = + 0 \cdot 145 \text{ in.-tons}\ ;$$

if $E = 13,000$ tons per sq. in.

From eq. (7), see above,

$$\sigma_{ca} = \tfrac{1}{2}\left\{\frac{M_{ca} \cdot l_{ca}}{2E \cdot I_{ca}} - \sigma_{ac}\right\} = +0 \cdot 000398\ ;$$

FIG. 184.

and $\qquad M_{ac} = 0 \cdot 02E(2\sigma_{ac} + \sigma_{ca}) = - 0 \cdot 019$ in.-tons.

$$\sigma_{cb} = \tfrac{1}{2}\left\{\frac{M_{cb} \cdot l_{cb}}{2E \cdot I_{cb}} - \sigma_{bc}\right\} = + 0 \cdot 000165$$

and $\qquad M_{bc} = 0 \cdot 08E(2\sigma_{bc} + \sigma_{cb}) = - 0 \cdot 803$ in.-tons.

The values of the secondary bending moments are therefore,

$$M_{ac} = - 0 \cdot 019\ ;\ M_{ca} = + 0 \cdot 145$$
$$M_{bc} = - 0 \cdot 803\ ;\ M_{cb} = - 0 \cdot 145 \text{ in.-tons.}$$

The corresponding stresses can be found from the section moduli of the cross-section, and combined with the longitudinal stress in the usual way (cf. ¶ 9, § 118).

117. Calculation of Deformation Stresses from the Displacements.— In the case of triangulated framework, such as ordinary lattice girders, the deformation stresses are most conveniently found from the displacements of the node points by a method due to Mohr.[36, 37] Let AB, (i) Fig. 185, be the original position of a member of such a frame, and A'B' its shape and position when the frame has distorted. The movements
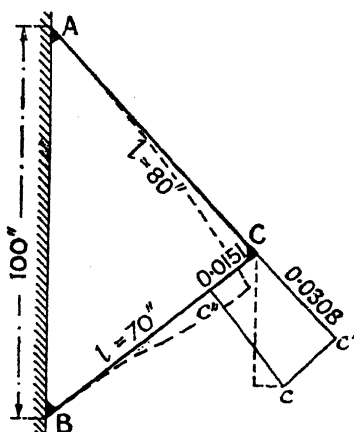
AA' and BB' are the displacements resulting from the distortion of the frame, and can be found by the methods of Chapter I, § 12 *et seq*. The curvature is due to the stiffness of the joints. As before, let the angle between the straight line A'B' and the tangents at the ends of the bar be σ_{ab} and σ_{ba}; let the corresponding bending moments acting on the member be M_{ab} and M_{ba}. The relations between these angles and bending moments are given by eq. (1), § 115,

$$M_{ab} = \frac{2EI}{l}(2\sigma_{ab} + \sigma_{ba}) \; ; \quad M_{ba} = \frac{2EI}{l}(\sigma_{ab} + 2\sigma_{ba}) \qquad . \quad (1)$$

A clockwise bending moment is considered as positive.

In moving from AB to A'B' the member rotates through an angle ψ, which will be considered positive if it take place in a clockwise direction. Let the angles between the original position AB and the tangents to the curve at the ends of the member be ϕ_A and ϕ_B respectively, as shown in (i) and (ii). Like ψ, the angle ϕ will be considered positive when it represents a rotation in the clockwise direction. All these angles will be very small, and it is unnecessary to distinguish between the angle and its tangent. Then
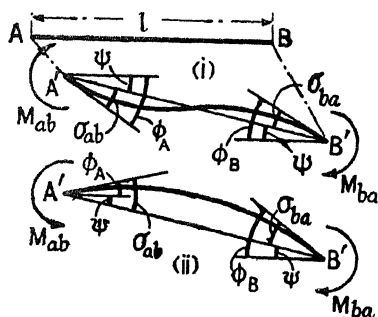
FIG. 185.

$$\phi_A = \psi + \sigma_{ab} \; ; \qquad \phi_B = \psi + \sigma_{ba} \qquad . \qquad (2)$$

These equations hold equally well in cases like that of A', (ii) Fig. 186, where both ϕ_A and σ_{ab} are negative, ψ being positive. From eqs. (1) and (2),

$$M_{ab} = \frac{2EI}{l}\{2(\phi_A - \psi) + (\phi_B - \psi)\} = \frac{2EI}{l}\{2\phi_A + \phi_B - 3\psi\} \quad . \quad (3)$$

$$M_{ba} = \frac{2EI}{l}\{(\phi_A - \psi) + 2(\phi_B - \psi)\} = \frac{2EI}{l}\{\phi_A + 2\phi_B - 3\psi\} \quad . \quad (4)$$

Let (i) Fig. 186 be part of a triangulated frame. The secondary bending moments at any panel point such as D will be as shown at (iii) (some will be negative); and since this point remains in equilibrium under these moments, it follows that
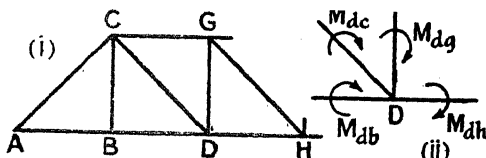
FIG. 186.*

$$\Sigma M = M_{dh} + M_{dg} + M_{dc} + M_{db} = 0 \qquad (5)$$

* In (ii) Fig. 186 the moments shown are external to the member (cf. Fig. 181 and the accompanying remarks on notation). Thus the moment M_{db} acts at D and tends to make DB convex upward.

As before, an external clockwise moment is considered positive. For each member of the frame, equations like (3) and (4) can be written down, and for each panel point an equation like (5). If, as assumed, the joints be perfectly rigid, the value of ϕ is the same for the ends of all members meeting at any one panel point. The value of ψ is different for each member, but it can readily be found from a Williot diagram (see the worked example, p. 279) ; or, having determined the displacements of all the panel points by the methods of § 12, the values of ψ can be calculated as follows :

Let δx_a and δy_a be the horizontal and vertical displacements of the point A, and δx_b, δy_b the corresponding displacements of the point B, (i) Fig. 187. In (ii) draw AB″ parallel and equal to A′B′. Then the angle BAB″ is the angle ψ, and if the small extension of the member be neglected, $\psi = \text{BB″}/l$. From the geometry of the figure, BB″ is made up of two parts such that

$$\text{BB″} = (\delta y_b - \delta y_a)\cos\theta + (\delta x_b - \delta x_a)\sin\theta,$$

where θ is the angle which AB makes with the horizontal. Hence,

FIG. 187.

$$\psi = \frac{(\delta y_b - \delta y_a)\cos\theta + (\delta x_b - \delta x_a)\sin\theta}{l} \tag{6}$$
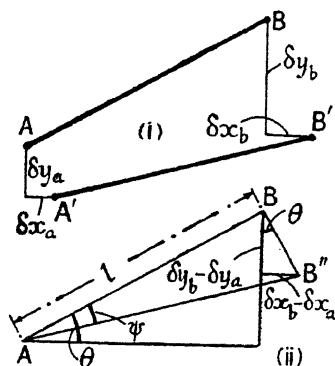
If θ be very small, $\psi = (\delta y_b - \delta y_a)/l$. If the correct signs be given to δy and δx [all shown positive in (i) Fig. 187], eq. (6) determines automatically the correct sign for ψ.

As will be seen later, eqs. (3), (4) and (5) suffice to determine the values of ϕ, and hence the unknown bending moments.

Worked Example.—The deformation stresses in the frame of Figs. 28 and 184, and § 12, supposing it made with stiff joints, will be determined by the above method as an example, and also as a check on the results obtained on p. 275.

The displacements of the point C are given in Fig. 184. The rotation $c'c$ about the point A scales $0 \cdot 0188$ inch, and the rotation $c''c$ about B scales $0 \cdot 0328$ inch. The values of ψ are, therefore,

Bar AC, $\qquad \psi_1 = + \dfrac{0 \cdot 0188}{80} = + 0 \cdot 000235$

Bar BC, $\qquad \psi_2 = + \dfrac{0 \cdot 0328}{70} = + 0 \cdot 000469$

These values are positive because in each case the rotations are clockwise. As on p. 274,

$$\text{for the bar AC,} \quad 2\text{EI}/l = 0 \cdot 02\text{E}$$
$$\text{for the bar BC,} \quad 2\text{EI}/l = 0 \cdot 08\text{E}$$

Eqs. (3) and (4), for each member, become

$$M_{ac} = 0 \cdot 02E \ (2\phi_A + \phi_C - 3\psi_1)$$
$$M_{ca} = 0 \cdot 02E \ (\phi_A + 2\phi_C - 3\psi_1)$$
$$M_{bc} = 0 \cdot 08E \ (2\phi_B + \phi_C - 3\psi_2)$$
$$M_{cb} = 0 \cdot 08E \ (\phi_B + 2\phi_C - 3\psi_2)$$

and for the point C, from eq. (5), $M_{ca} + M_{cb} = 0$.

Assuming as before, that AB is rigid, and that the connections at A and B are perfectly stiff, $\phi_A = \phi_B = 0$. Hence,

$$M_{ca} + M_{cb} = 0 \cdot 02E \ (2\phi_C - 3\psi_1) + 0 \cdot 08E \ (2\phi_C - 3\psi_2) = 0$$
$$10\phi_C = 3\psi_1 + 12\psi_2; \quad \text{and } \phi_C = + \ 0 \cdot 000633.$$

Taking $E = 13{,}000$ tons per sq. in., and substituting in the above equations,

$$M_{ac} = - \ 0 \cdot 019 \ ; \quad M_{ca} = + \ 0 \cdot 146$$
$$M_{bc} = - \ 0 \cdot 805 \ ; \quad M_{cb} = - \ 0 \cdot 146 \quad \text{in.-tons.}$$

These figures agree, practically speaking, with those found by the previous method. The difference is due to small errors in scaling the values of $c'c$ and $c''c$. In this particular case the numerical values of ψ_1 and ψ_2 should be respectively equal to δA and δB of § 116. If these values ($\psi_1 = \delta A = 0 \cdot 000236$; $\psi_2 = \delta B = 0 \cdot 000469$) be used, almost identical values are obtained for the moments. The displacement method is quicker.

A positive sign indicates a clockwise moment, and the frame will bend as indicated in Fig. 184. It is worth while noticing that whereas M_{cb} is negative, σ_{cb} is positive, § 116.

118. Deformation Stresses in Braced Girder. Worked Example.— To find the deformation stresses in a braced girder, the method of procedure is as follows : Set out in tabular form, as in the worked example following, the values of ψ and $2EI/l$ for each bar. Write down eqs. (3) and (4), § 117, for each bar, introducing the values of ψ and $2EI/l$. If there be n panel points there will be $4n - 6$ such equations, giving the values of M in terms of ϕ. Write down eq. (5), § 117, for each panel point, and substitute therein the values of M obtained from eqs. (3) and (4) ; n equations will thus be obtained containing ϕ as the only unknown. From these equations the n values of ϕ can be found. Substituting in eqs. (3) and (4), § 117, the values of $M_{ab} \ldots$ are obtained. Knowing the values of $M_{ab} \ldots$ the maximum stress in any member can be found in the usual way.

*Worked Example.—*To find the deformation stresses in the braced girder shown in Fig. 188. The dimensions are given in the figure ; the girder carries a load of 50 tons at its centre point.

1. Find the forces in all the bars in the usual way, and tabulate them (see col. 5 of the Table on p. 279).

2. Draw the Williot diagram, (ii) Fig. 188, for the frame. In this case, since the frame and the load are symmetrical about the centre, take D as a fixed point and DG as a fixed direction. It is only necessary

to draw the diagram for one-half of the girder. The displacements are dimensioned in (ii). Take E as unity for this purpose.

In general the Williot diagram for the whole truss must be drawn, but it is not necessary, for the present purpose, to make the angular correction given in § 12, because a movement of the truss as a whole cannot affect the deformation stresses.

3. From the rotations in the Williot diagram, find the angles ψ for every bar. Tabulate the values; col. 8 of the Table. As an example, consider the bar CD and take D as a fixed point. The angular motion of CD about D is given by the rotation $c''c$ in the diagram. Hence $\psi_{cd} = c''c/l_{cd}$. The motion of C, from c'' to c, is clockwise with respect to D, therefore ψ_{cd} is positive. In this way the value and sign of ψ for every bar can be found. It is best to tabulate ψl ($c''c$ for bar CD) and calculate the value of ψ therefrom. Start with the fixed point of the Williot diagram and follow the course thereof.

4. Assuming the value of E to be unity, find the value of $2EI/l$ for each member. Hence find the values of $\psi . 2EI/l$, and tabulate them; cols. 9 and 10 of the Table.

5. Write out equations (3) and (4), § 117, for every bar of the girder. Since in this case the conditions are symmetrical, only one-half of the girder need be considered.
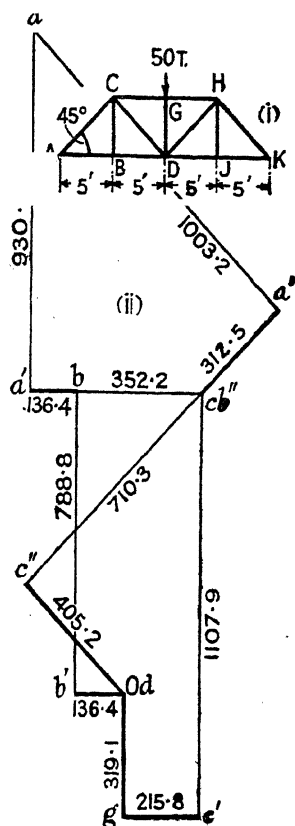
FIG. 188.

Bar.	Length l in.	Gross Area. a sq. in.	Moment of Inertia I in.^{4}	Force in Bar. F tons.	$\delta l = \dfrac{Fl}{Ea}$ in.	ψl	ψ	$\dfrac{2EI}{l}$	$\dfrac{2\psi EI}{l}$
AB	60	11·0	95·3	+ 25	+ 136·4	+ 930·4	+ 15·51	3·18	+ 49·32
BD	60	11·0	95·3	+ 25	+ 136·4	+ 788·8	+ 13·15	3·18	+ 41·82
CG	60	13·9	200·7	− 50	− 215·8	+ 1107·9	+ 18·47	6·69	+ 123·56
AC	84·85	9·6	20·7	− 35·36	− 312·5	+ 1003·2	+ 11·83	0·49	+ 5·80
CD	84·85	7·4	44·3	+ 35·36	+ 405·2	+ 710·3	+ 8·37	1·04	+ 8·70
CB	60	5·8	7·6	0	0	+ 352·2	+ 5·87	0·25	+ 1·47
GD	60	9·4	16·3	− 50	− 319·1	0	0	0·54	0

E = unity.

Bar.

AB. $M_{ab} = \dfrac{2EI}{l}\{2\phi_A + \phi_B - 3\psi\}$ $M_{ba} = \dfrac{2EI}{l}\{\phi_A + 2\phi_B - 3\psi\}$

$M_{ab} = 6.36\phi_A + 3.18\phi_B - 147.96$

$M_{ba} = 3.18\phi_A + 6.36\phi_B - 147.96$

BD. $M_{bd} = 6.36\phi_B + 3.18\phi_D - 125.46$

$M_{db} = 3.18\phi_B + 6.36\phi_D - 125.46$

CG. $M_{cg} = 13.38\phi_C + 6. \qquad - 370.68$

$M_{gc} = 6.69\phi_C + 13.38\phi_G - 370.68$

AC. $M_{ac} = 0.98\phi_A + 0.49\phi_C - 17.40$

$M_{ca} = 0.49\phi_A + 0.98\phi_C - 17.40$

CD. $M_{cd} = 2.08\phi_C + 1.04\phi_D - 26.10$

$M_{dc} = 1.04\phi_C + 2.08\phi_D - 26.10$

CB. $M_{cb} = 0.50\phi_C + 0.25\phi_B - 4.41$

$M_{bc} = 0.25\phi_C + 0.50\phi_B - 4.41$

GD. $M_{gd} = 1.08\phi_G + 0.54\phi_D - 0$

$M_{dg} = 0.54\phi_G + 1.08\phi_D - 0$

In this particular case it is evident from the symmetry of the conditions that there is no angular motion of the panel points D and G. Therefore, $\phi_D = \phi_G = 0$; and $M_{dg} = M_{gd} = 0$.

6. Write out equation (5), § 117, $\Sigma M = 0$, for each panel point.

Panel Point.

A. $M_{ac} + M_{ab} = 0$
B. $M_{ba} + M_{bc} + M_{bd} = 0$
C. $M_{ca} + M_{cb} + M_{cd} + M_{cg} = 0$
D. $M_{db} + M_{dc} + M_{dg} + M_{dh} + M_{dj} = 0$
G. $M_{gc} + M_{gd} + M_{gh} = 0$.

From symmetry, in the last two equations, $M_{gd} = 0$; $M_{gc} = - M_{gh}$; $M_{dg} = 0$; $M_{dc} = - M_{dh}$; $M_{db} = - M_{dj}$. There remain three equations to determine the three unknowns ϕ_A, ϕ_B, and ϕ_C. Introducing the values of M_{ab} ... from ¶ 5, above,

A. $7.34\phi_A + 3.18\phi_B + 0.49\phi_C = 165.36$
B. $3.18\phi_A + 13.22\phi_B + 0.25\phi_C = 277.83$
C. $0.49\phi_A + 0.25\phi_B + 16.94\phi_C = 418.59$

It is possible to solve these simultaneous equations directly, but when there are many bars in the frame, the work is laborious. It is better to use a method of successive approximation suggested by Mohr. If the three equations be examined, it will be seen that in the first the coefficient of ϕ_A is the largest; in the second that of ϕ_B; and in the third that of ϕ_C.

As a first approximation therefore, assume that

$\phi_A = \phi_B = \phi_C = \phi_A'$ in the first equation,
$\phi_A = \phi_B = \phi_C = \phi_B'$ in the second equation,
$\phi_A = \phi_B = \phi_C = \phi_C'$ in the third equation,

whence, $\phi_A' = + 15 \cdot 02$; $\phi_B' = + 16 \cdot 69$; $\phi_C' = + 23 \cdot 68$.
Now write the equations in the form :

$$\phi_A'' \left\{ 7 \cdot 34 + 3 \cdot 18 \frac{\phi_B'}{\phi_A'} + 0 \cdot 49 \frac{\phi_C'}{\phi_A'} \right\} = 165 \cdot 36$$

$$_B'' \left\{ 3 \cdot 18 \frac{\phi_A'}{\phi_B'} + 13 \cdot 22 + 0 \cdot 25 \frac{\phi_C'}{\phi_B'} \right\} = 277 \cdot 83$$

$$\phi_C'' \left\{ 0 \cdot 49 \frac{\phi_A'}{\phi_C'} + 0 \cdot 25 \frac{\phi_B'}{\phi_C'} + 16 \cdot 94 \right\} = 418 \cdot 59$$

Insert the values of ϕ_A', ϕ_B', and ϕ_C'; whence

$$\phi_A'' = + 14 \cdot 21; \quad \phi_B'' = + 16 \cdot 91; \quad \phi_C'' = + 24 \cdot 02.$$

From a third similar approximation, using the values ϕ'' instead of ϕ',

$$\phi_A''' = + 13 \cdot 84; \quad \phi_B''' = + 17 \cdot 10; \quad \phi_C''' = + 24 \cdot 04.$$

Collecting the results :

	1st Approx.	2nd Approx.	3rd Approx.	Exact Solution.
$\phi_A =$	$+ 15 \cdot 02$	$+ 14 \cdot 21$	$+ 13 \cdot 84$	$+ 13 \cdot 41$
$\phi_B =$	$+ 16 \cdot 69$	$+ 16 \cdot 91$	$+ 17 \cdot 10$	$+ 17 \cdot 34$
$\phi_C =$	$+ 23 \cdot 68$	$+ 24 \cdot 02$	$+ 24 \cdot 04$	$+ 24 \cdot 07$

As will be seen, the third approximation is sufficiently accurate for most practical purposes, the maximum error being about 3 per cent.

7. Knowing the values of ϕ, calculate the magnitudes of $M_{ab} \ldots$ from the equations given in ¶ 5. (In finding the values given below the exact values of ϕ have been used.)

$M_{ab} = - 7 \cdot 53$; $M_{bd} = - 15 \cdot 18$; $M_{cg} = - 48 \cdot 62$;
$M_{ba} = + 4 \cdot 96$; $M_{db} = - 70 \cdot 32$; $M_{gc} = - 209 \cdot 65$;
$M_{ac} = + 7 \cdot 53$; $M_{cd} = + 23 \cdot 97$; $M_{cb} = + 11 \cdot 96$; $M_{gd} = 0$;
$M_{ca} = + 12 \cdot 76$; $M_{dc} = - 1 \cdot 07$; $M_{bc} = + 10 \cdot 28$; $M_{dg} = 0$.

The above values are in inch-tons. Checking the moments at each panel point by means of equation (5), § 117, $\Sigma M_{ab} = 0$,

Panel
Point.

A. $M_{ab} + M_{ac} = - 7 \cdot 53 + 7 \cdot 53 = 0 \cdot 00$,
B. $M_{ba} + M_{bc} + M_{bd} = + 4 \cdot 96 + 10 \cdot 28 - 15 \cdot 18 = + 0 \cdot 06$,
C. $M_{ca} + M_{cb} + M_{cd} + M_{cg} = + 12 \cdot 76 + 11 \cdot 96 + 23 \cdot 97 - 48 \cdot 62$
$$= + 0 \cdot 07,$$

the error is within $0 \cdot 1$ inch-ton. The moments at D and G must perforce satisfy equation (5), owing to the symmetry of the frame.

The values for $M_{ab} \ldots$ are shown on (i) Fig. 189.

8. Although not essential for the calculation of the secondary stresses it is of interest to compute the values of σ. From equation (2), § 117,

$$\sigma_{ab} = \phi_A - \psi_{ab} = + 13\cdot41 - 15\cdot51 = -2\cdot10$$
$$\sigma_{ba} = \phi_B - \psi_{ab} = + 17\cdot34 - 15\cdot51 = +1\cdot83$$
$$\sigma_{bd} = \phi_B - \psi_{bd} = + 17\cdot34 - 13\cdot15 = +4\cdot19$$
$$\sigma_{db} = \phi_D - \psi_{bd} = \quad\; 0 - 13\cdot15 = -13\cdot15$$

and so on. These values are shown on (ii) Fig. 189, together with the values of ψ and ϕ.

FIG. 189.*

9. As a typical example of the method of calculating the deformation stresses in the members, consider the case of the top flange GC, (i) Fig. 190. The bending moment at G is $M_{gc} = -209\cdot25$, and at C is $-48\cdot62$ inch-tons, both anti-clockwise moments, (ii). The bending-moment diagram is shown at (iii). The maximum bending moment at G is carried by a deep gusset, and the maximum stress will occur at the point H, where the bending moment is found to be $155\cdot84$ inch-tons. If it be assumed that the cross-section at H is equivalent to the normal

---

* The moments shown in (i) Fig. 189 are moments external to the member, acting at the panel points and imposed on the member by the rest of the frame (cf. Fig. 181 and the accompanying text).

cross-section of the flange, $I = 200 \cdot 7$ in.[4] (see the Table). The neutral axis lies at a distance $4 \cdot 10$ in. below the top of the member which is $10 \cdot 32$ in. deep, so that $v_1 = + 4 \cdot 10$, and $v_2 = - 6 \cdot 22$ in. The area of the member is $13 \cdot 9$ sq. in., and the compressive force in it is 50 tons, so that the direct compressive stress is $50 \div 13 \cdot 9 = 3 \cdot 60$ tons/sq. in.
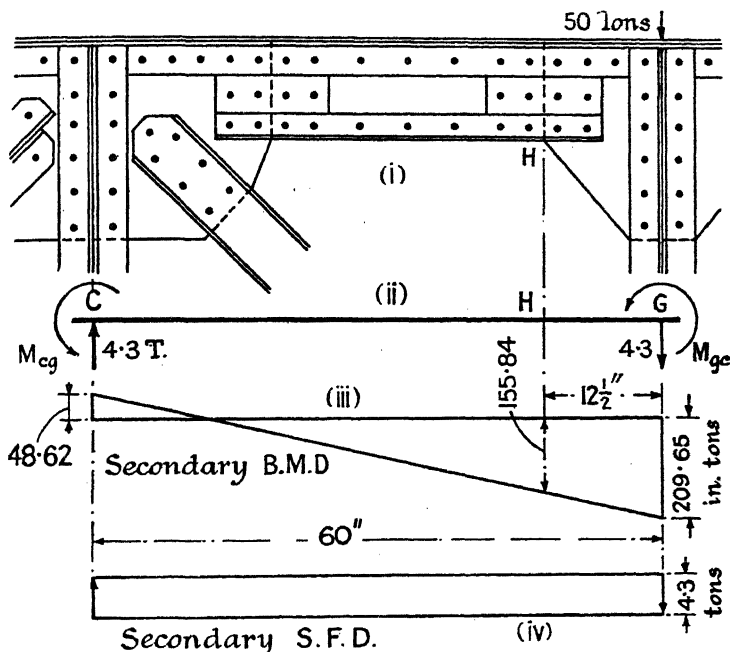
FIG. 190.

The bending moment, $155 \cdot 84$ inch-tons, will produce a compressive stress in the extreme top fibres of

$$f = \frac{Mv_1}{I} = \frac{155 \cdot 84 \times 4 \cdot 1}{200 \cdot 7} = 3 \cdot 18 \text{ tons/sq. in.}$$

and a tensile stress in the lowest fibres of

$$f = \frac{Mv_2}{I} = \frac{155 \cdot 84 \times 6 \cdot 22}{200 \cdot 7} = 4 \cdot 83 \text{ tons/sq. in.}$$

The maximum stress at the top of the flange is, therefore, $3 \cdot 60 + 3 \cdot 18 = 6 \cdot 78$ tons/sq. in. (compressive), and at the bottom is $3 \cdot 60 - 4 \cdot 83 = 1 \cdot 23$ tons/sq. in. (tensile). Thus the stresses on the cross-section at H are :

maximum stress $= 6 \cdot 78$ tons/sq. in. (compressive)
mean stress $\quad = 3 \cdot 60$ tons/sq. in. (compressive)
minimum stress $= 1 \cdot 23$ tons/sq. in. (tensile).

The deformation stresses in every member can be found in a similar way, and combined with direct stress.

It will be seen that, according to this calculation, the stress in the top flange is almost doubled by the deformation stress. In practice this large augmentation of the stress will be mitigated, to some extent, by two effects which have been neglected. Due to the bending moments M_{gc} and M_{cg} there will be a shearing force in GC. The shearing-force diagram is shown in (iv), and the magnitude of the constant shearing force is evidently $(209 \cdot 65 + 48 \cdot 62) \div 60 = 4 \cdot 3$ tons. This means that $4 \cdot 3$ tons will be transferred along GC by the shearing force in that member, and an equal amount will be similarly transferred along the corresponding member to the right. The total load of 50 tons stressing the members of the frame will thus be reduced by no less than $8 \cdot 6$ tons due to this shear, with a corresponding reduction in the direct forces in the members, which forces will be still further reduced owing to the shear in the other members of the frame. The actual reduction will, in reality, not be so large as would thus appear, because, with reduced forces in the members, the secondary bending moments will also be reduced, but both primary and secondary stresses will be less than the calculation suggests.

The riveted joints in a braced frame are not stiff joints as has been assumed, but possess considerable elasticity, which again will reduce the calculated stresses. To take exact account of these effects would be difficult, but it is possible to make allowance for them in the calculation. For an example, reference may be made to the work of Wyss (*Beitrag zur Spannungsuntersuchung an knotenblechen eiserner Fachwerke*. Heft 262, Forschungsarbeiten V.D.I. Berlin, 1923), who also determines the stresses experimentally. The above girder has been made to correspond approximately with the experiments of Wyss, and it is of interest to observe that, at the section H in the member GC, the measured force was $46 \cdot 17$ tons instead of 50 tons ; and the measured shearing force was $3 \cdot 05$ tons instead of $4 \cdot 3$ tons. Instead of a theoretical mean compressive stress of $0 \cdot 514$ t/cm^2, the measured stress at the top of the flange was $0 \cdot 90$ t/cm^2 (compressive), and at the bottom was $0 \cdot 119$ t/cm^2 (tensile). The metric sections used do not correspond exactly with those assumed in the worked example above, and at H the area was $15 \cdot 06$ sq. in. Increasing the above stresses proportionately to the respective areas, and converting them to British units, the

maximum stress $= 6 \cdot 30$ tons/sq. in. (compressive)
mean stress $= 3 \cdot 60$ tons/sq. in. (compressive)
minimum stress $= 0 \cdot 84$ ton/sq. in. (tensile).

These stresses may be compared with those computed in the worked example.

10. The values of the deformation angles given in (ii) Fig. 189 can be checked by the method of § 116. As a typical example, consider the triangle GDC, (i) Fig. 191, relettered ABC in (ii) to suit the equations of § 116. The stresses in the members, found from the Table, p. 279, are as shown. Taking E $=$ unity, and substituting in equation (2), § 116,

$$\delta A = \frac{1}{E}\{(f_a - f_c) \cot B + (f_a - f_b) \cot C\}$$
$$= \{(+\ 4\cdot78 + 5\cdot32)1 + (+\ 4\cdot78 + 3\cdot60)1\} \quad = +\ 18\cdot48$$

$$\delta B = \frac{1}{E}\{(f_b - f_a) \cot C + (f_b - f_c) \cot A\}$$
$$= \{(-\ 3\cdot60 - 4\cdot78)1 + (-\ 3\cdot60 + 5\cdot32)0\} \quad = -\ 8\cdot38$$

$$\delta C = \frac{1}{E}\{(f_c - f_b) \cot A + (f_c - f_a) \cot B\}$$
$$= \{(-\ 5\cdot32 + 3\cdot60)0 + (-\ 5\cdot32 - 4\cdot78)1\} \quad = -\ 10\cdot10$$
$$\text{Sum} = \quad \overline{0\cdot00}$$

See eq. (3), § 116.

The results for all the triangles of the frame, thus determined, are shown in (i), Fig. 191. Comparing (ii), Fig. 189, with (i), Fig. 191, in the
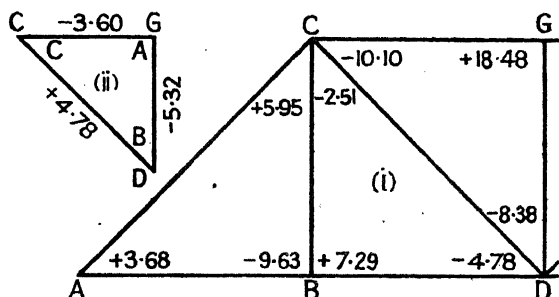
FIG. 191.

light of equation (5), § 116, the maximum difference in the angles will be found to be $0\cdot01$. Thus from (ii), Fig. 191, considering the point C,

$$\sigma_{cg} - \sigma_{cd} = +\ 5\cdot60 - 15\cdot70 = -\ 10\cdot10 \quad \text{v.} -\ 10\cdot10 = \delta(\text{GCD})$$
$$\sigma_{cd} - \sigma_{cb} = +\ 15\cdot70 - 18\cdot20 = -\ 2\cdot50 \quad \text{v.} -\ 2\cdot51 = \delta(\text{DCB})$$
$$\sigma_{cb} - \sigma_{ca} = +\ 18\cdot20 - 12\cdot24 = +\ 5\cdot96 \quad \text{v.} +\ 5\cdot95 = \delta(\text{BCA})$$

and so on.

119. Secondary Stresses. Experimental Determinations.—The results of five years' study by the Swiss Commission [43] on secondary stresses in 14 bridges, statically loaded, may be briefly summarised as follows : Only direct stress measurements give reliable information regarding secondary stresses, angular displacements are misleading. The measured secondary stresses agree closely with the calculated values. Secondary stresses occur in all members about both principal axes of the cross-section. The yield of the gussets and riveted connections has an important influence, which can only be taken into account approximately. Stiffness at the panel points always acts in a favourable sense, distributing the moments and diminishing the stresses. If, owing to

secondary stresses, the proportional limit is exceeded in the extreme fibres of the bar, these stresses do not continue to increase proportionally to the primary stresses. Except in the case of S-bending, reduction in the assumed crippling length of struts as the result of stiff joints is not justified. A stiff continuous bridge floor has an important effect in diminishing the effect of impact, and in reducing the deflection, and consequently the secondary stresses. In an ordinary lattice girder bridge, with deep main girders, when the axes of the members intersect at a point, and the slenderness ratio of the bars in the plane of the main girders ranges from 40 to 60, the secondary stresses attain values ranging from 15 to 20 % of the permitted primary stresses. Except in rare cases the secondary stresses are always increased when the axes do not meet in a point.

Secondary stresses need not be considered in any member in which the ratio of width to length, measured parallel to the plane of distortion, is less than 1 : 10 (A.R.E.A. 1935 Spec.).

BIBLIOGRAPHY

Slope-Deflection Methods. Rigid Framework.

1. WILSON and MANEY. Wind Stresses in the Steel Frames of Office Buildings. *Univ. Illinois Eng. Exp. Stn.*, Bull. No. 80, 1915.
2. WILSON, RICHART and WEISS. Analysis of Statically Indeterminate Structures by the Slope-Deflection Method. *Univ. Illinois Eng. Exp. Stn.*, Bull. No. 108, 1918.
3. ENGESSER. Die Berechnung der Stockwerkrahmen. *Der Eisenbau*, 1920, p. 81.
4. STRASSNER. *Berechnung statisch unbestimmter Systeme.* Bd. II, Berlin, 1921.
5. —— *Neuere Methoden zur Statik der Rahmentragwerke.* Bd. I, Berlin, 3rd ed., 1925.
6. SUTER. *Die Methode der Festpunkte.* Berlin, 2nd ed., 1932.
7. BORDIER. Étude de la continuité dans un réseau rectangulaire des poutres et de piliers. *Le Génie civil*, t. lxxxiv, 1924, p. 248.
8. BLEICH. *Die Berechnung statisch unbestimmter Tragwerke nach der Methode des Viermomentensatzes.* Berlin, 2nd ed., 1925.
9. GEHLER. *Der Rahmen.* Berlin, 1925.
10. LÖSER. Berechnung von Stockwerkrahmen für senkrechte Lasten. *Der Bauingenieur*, 1925, p. 615.
11. WORCH. Studien zur Berechnung und Konstruktion mehrstieliger Stockwerkrahmen. *Der Bauingenieur*, 1925, p. 679.
12. KLEINLOGEL. *Mehrstielige Rahmen.* Berlin, 2nd ed., 1927.
13. —— *Rahmenformeln.* Berlin, 6th ed., 1929.
14. MISÉ. Elastic Distortions of Rigidly Connected Frames. *Mem. Coll. Eng. Kyushu Imp. Univ.*, Japan, vol. iv, 1927, p. 275.
15. TAKABEYA. Analysis of Rectangular Building Frames by the Mechanical Tabulation Method. *Mem. Fac. Eng. Hokkaido Imp. Univ.*, Japan, vol. i, 1927, p. 155 ; 1928, p. 219.
16. HOOL and KINNE. *Stresses in Framed Structures.* New York, 1923.
17. ABELES. Die Durchbeigung statisch unbestimmter Rahmen-Tragwerke. *Beton u. Eisen*, Oct. 5, 1929, p. 346.
18. REIGER. *Berechnung statisch unbestimmter Systeme.* Bd. I, *Einfache Rahmenträger.* Leipzig, 1929.

19. CROSS. The Method of Distribution of Fixed-End Moments. *Jour. Amer. Conc. Inst.*, Dec. 1929, p. 669.

20. —— Analysis of Continuous Frames by Distributing Fixed-End Moments. *Trans. Amer. Soc. C.E.*, vol. 96, 1932, p. 1.

21. LARGE and MORRIS. Moment-Distribution Method of Structural Analysis Extended to Lateral Loads and Members of Variable Section. Bull. No. 66, *Eng. Exp. Stn. Ohio State Univ.*, 1931.

22. STINEMANN. Moment and Shear Diagrams for Continuous Beams and Rigid Building Frames. *Jour. Amer. Conc. Inst.*, 1930, p. 211.

23. ELWITZ. *Der Zweistielige Stockwerkrahmen.* Düsseldorf, 1932.

24. BAKER. See Ref. No. 32, Chap. XX, Bib.

25. UNOLD. *Die praktische Berechnung der Stahlskelettrahmen.* Berlin, 1933.

26. BATEMAN. The Stability of Tall Building Frames. *Select. Eng. Pap. I.C.E.*, No. 167, 1934.

27. GOLDBERG. Wind Stresses by Slope-Deflection and Converging Approximations. *Trans. Amer. Soc. C.E.*, vol. 99, 1934, p. 962.

27A. SOUTHWELL. Stress-Calculation in Frameworks by the Method of Systematic Relaxation of Constraints. *Proc. Roy. Soc.* (A), vol. 151, 1935, p. 56 ; vol. 153, 1936, p. 41 ; also RICHARDS, *Jour. Inst. C.E.*, Feb. 1937, p. 196.

Secondary Stresses.

28. ENGESSER. Ueber die Durchbiegung von Fachwerkträgen und die hierbei auftretenden zusätzlichen Spannungen. *Zeit. f. Baukunde*, 1879.

29. —— Die Zusatzkräfte und Nebenspannungen eiserner Fachwerkbrücken. Berlin, 1892.

30. AISIMONT. Haupt-Spannung und Secundär-Spannung. *Zeit.f. Baukunde*, 1880, p. 27.

31. MANDERLA. Die Berchnung der Sekundärspannungen welche im einfachen Fachwerk infolge starrer Knotenverbindungen auftreten. *Allgemeine Bauzeitung* (Foerster's), Wien, 1880, p. 34.

32. WINKLER. Vorträge über Brückenbau. Theorie der Brücken. Heft II, Wien, 1881, p. 248.

33. MÜLLER-BRESLAU. Zur Theorie der Biegungsspannungen in Fachwerkträgern. *Allegemeine Bauzeitung*, 1885, p. 85; also *Zeit. d. Arch- u. Ing. Ver. z. Hannover*, 1886, p. 399.

34. LANSBERG. Ebene Fachwerksysteme mit festen Knotenpunkten, etc. Centralblatt d. Bauverwaltung, 1885, p. 165.

35. —— Beitrag zur Theorie des Fachwerks. *Zeit. d. Arch.- u. Ing. Ver. z. Hannover*, 1885, p. 361 ; 1886, p. 195.

36. MOHR. Die Berechnung der Fachwerke mit starren Knotenverbindungen. *Der Zivilingenieur*, 1892, p. 577 ; 1893, p. 67.

37. —— Die Berechnung der Nebenspannung in Fachwerken mit Steifen Knotenverbindungen. *Der Eisenbau*, 1912, p. 181 ; also 1910, pp. 2 and 93.

38. HIROI. *Statically Indeterminate Stresses in Frames Commonly Used for Bridges.* New York, 1905.

39. GRIMM. *Secondary Stresses in Bridge Trusses.* New York, 1908.

40. MOLITOR. Ref. No. 16, Chap. V, Bib. ; chap. xiii, p. 226.

41. PIRLET. Einflusslinien der Spannungen in Fachwerken mit Starren Knotenpunktsverbindungen. *Der Eisenbau*, 1912, pp. 202, 245.

42. V. ABO. Secondary Stresses in Bridges. *Trans. Amer. Soc. C.E.*, vol. lxxxix, 1926, p. 1.

43. ROŠ. Rpt. of Technische Kommission des Verbandes Schweizerischer Brücken-und Eisenhochbaufabriken ; see *Schweiz. Bauzeit*, Bd. 80, 1922, p. 168 ; Bd. 81, 1923, p. 44 ; also *Eng. News.-Rcd.*, vol. 87, p. 982.

QUESTIONS ON CHAPTER VI

1. Fig. 192 shows a column fixed at one end and pin-jointed at the other. A load $W = 1$ ton is attached to a bracket 2 ft. long, measured from the centre of the column. Draw the diagram of bending moment produced on the column. (I.C.E.)

Ans. $M_A = 8$; $M_B = 0$; $M_D = 13\frac{1}{3}$ in.-tons.

2. Suppose that the stanchion ABC shown in Fig. 141 is of uniform cross section from top to bottom, that the lower end is direction-fixed, and the upper end position-fixed. $AB = 20$ ft., $BC = 12$ ft., $AD = 14$ ft. It carries a load of 10 tons on the bracket at D, which load acts at a distance 18 in. from the centre line of the column. Draw the bending-moment diagram for the column and find the maximum bending moment anywhere on the column.

FIG. 192.

Ans. $M_A = 4 \cdot 68$; $M_B = 1 \cdot 69$; $M_C = 0$; $M_D = 7 \cdot 93$ ft.-tons. (max.).

3. In the braced portal shown in (i) Fig. 153, $h = 25$ ft., $b = 17$ ft. 6 in., $c = 7$ ft. 6 in. If $F = 2$ tons, find the forces in all the members and the maximum shearing force and bending moment in the legs.

Ans. Forces in girder : top flange $- 4\frac{1}{3}$, $- 1$, $+ 2\frac{1}{3}$ t. ; bottom flange $\pm 1\frac{3}{4}$ t. ; diagonals $\pm 3 \cdot 32$ t. ; verticals zero. Forces in legs $\pm 2 \cdot 86$ t. ; max. B.M. $= 210$ in.-tons ; max. S.F. $= 2\frac{1}{3}$ t.

4. If in Q. No. 3 the feet of the portal are fixed in direction, find the forces in all the members and the maximum shearing force and bending moment in the legs.

Ans. Forces in girder : top flange $- 3\frac{1}{6}$, -1, $+ 1\frac{1}{6}$ t. ; bottom flange $\pm 1 \cdot 08$ t. ; diagonals $\pm 2 \cdot 16$ t. ; verticals zero. Forces in legs $\pm 1 \cdot 86$ t. ; max. B.M. $= 105$ in.-tons ; max. S.F. $= 1\frac{1}{6}$ t.

5. In the knee-braced portal shown in Fig. 154, $h = 25$ ft., $b = 17$ ft. 6 in., $c = 7$ ft. 6 in., $e = 6$ ft. If $F = 2$ tons, draw the bending-moment and shearing-force diagrams for AC, CD, and DB, and find the longitudinal forces in all the members.

Ans. In AC and BD, max. B.M. $= 210$ in.-tons, max. S.F. $= 2\frac{1}{3}$ t. ; in CD, max. B.M. $= 94 \cdot 3$ in.-tons, max. S.F. $= 2 \cdot 86$ t. ; forces in AG and BH $= \pm 2 \cdot 86$ t. ; in GC and DH $= \mp 1 \cdot 31$ t. ; in CP, PQ, QD $= - 4\frac{1}{3}$, $- 1$, and $+ 2\frac{1}{3}$ t. ; in GP and HQ $= \pm 5 \cdot 34$ t.

6. Find the sideways deflection Δ of the portal in the worked example of § 104. Take $I_1 = I_2 = 3000$ in.^{4}, and $E = 13,000$ tons/sq. in.

Ans. $0 \cdot 35$ in.

7. Draw the bending-moment and shearing-force diagrams for the columns of the worked example of §104. Find the positions of the points of inflexion.

Ans. AJ $= 9 \cdot 4$, BK $= 9 \cdot 85$ ft.

8. On the assumption that the points of inflexion occur half-way between A and G, B and H, in Fig. 157 ; find the values of F_1 to F_6. Compare these values with the correct values given in §104.

Ans. $F_1 = 17 \cdot 43$, $F_2 = 12 \cdot 57$, $F_3 = 35 \cdot 71$, $F_4 = 23 \cdot 14$, $F_5 = 14 \cdot 66$, $F_6 = 27 \cdot 23$ tons.

9. Suppose that the portal shown in Fig. 169 be loaded with a single load of 1 ton at the centre of span CD, find by the method of Characteristic Points the bending moments at A, B, C, and D, (a) if the feet A and B are hinged ; (b) if they are direction-fixed.

Ans. (a) $M_A = M_B = 0$; $M_C = M_D = + 0 \cdot 81$ ft.-tons ; (b) $M_A = M_B = - 0 \cdot 482$; $M_C = M_D = + 0 \cdot 964$ ft.-tons.

10. If in the portal of Fig. 169, $I_1 = 300$ in.^{4}, $E = 13,000$ tons/sq. in.,
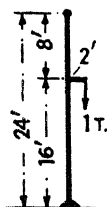
find the sideways deflection Δ when the portal is loaded as indicated in that figure. Find also the vertical reactions at A and B.

Ans. $\Delta = 0·005$ in. ; $R_A = 0·671$ $R_B = 0·329$ ton.

11. Assuming that, by fitting a diagonal or otherwise, the points A, B, C, and D, of the portal in Fig. 169 are constrained to remain fixed in position, find by the method of Characteristic Points, and of Moment-Distribution, the values of M_A, M_B, M_C and M_D.   Hence find the percentage error which would be introduced by neglecting the sideways deflection Δ of the portal in Fig. 169.

Ans. $M_A = -0·495$; $M_B = -0·362$; $M_C = +0·991$; $M_D = +0·724$ ft.-ton ; errors $+27$ %, $-22\frac{1}{2}$ %, $+10\frac{1}{2}$ %, $-11\frac{1}{2}$ %.

12. Using the values found in Q. No. 11, verify by Moment-Distribution the values given in Fig. 169 when sideways deflection is permitted.

CHAPTER VII

ELASTIC STABILITY PROBLEMS

120. Buckling of Flat Plates under Edge Thrusts.—Let OABC, (i) Fig. 193, be a thin flat rectangular plate compressed along the edges OC, AB by a thrust p_1 per unit of length, and along the edges OA, CB by a thrust p_2 per unit of length. It is required to find the conditions under which the plate will buckle. Suppose, as indicated in the figure, that it has buckled upwards slightly. Take origin at O, let OA be the
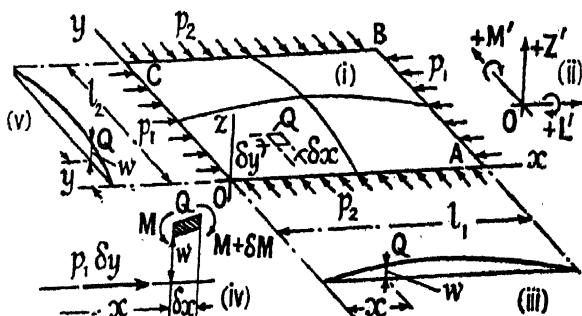
FIG. 193.

axis of x, OC be the axis of y, and consider an element of plate at Q $(x \cdot y)$. Let the upward deflection of the plate at Q be w. Then [see eq. (11), § 186, Vol. I], the equation representing the equilibrium of the plate is

$$\nabla^4 w = \left\{ \frac{\partial^4 w}{\partial x^4} + \frac{\partial^4 w}{\partial y^4} + 2 \frac{\partial^4 w}{\partial x^2 \cdot \partial y^2} \right\} = \frac{1}{D} \left\{ Z' - \frac{\partial L'}{\partial y} + \frac{\partial M'}{\partial x} \right\} \qquad (1)$$

where Z' is the resultant normal external force, and L' and M' are the resultant external moments acting on the element. $+ L'$ and $+ M'$ are clockwise moments looking away from the origin [see (ii) Fig. 193]; Z', L', and M' are all expressed per unit of area of the element. From eq. (6), § 186, Vol. I, the flexural rigidity of the plate

$$D = \tfrac{2}{3} E h^3 \frac{m^2}{m^2 - 1} = \frac{E t^3}{12} \cdot \frac{m^2}{m^2 - 1}$$

where $t = 2h$ is the thickness of the plate, and $1/m$ is Poisson's ratio ; m may be taken as $10/3$. In the present case there is no external force normal to the plate, and $Z' = 0$.

Let the bending moment due to p_1 on the element at Q, (iii) and (iv) Fig. 193, at any section x, be M ; and at $(x + \delta x)$ be $(M + \delta M)$. Then

$(M + \delta M) - M = \delta M$ is the resultant external bending acting on the element at Q which causes the bending moment M_{xx}' to change to $(M_{xx}' + \delta M_{xx}')$ in the length δx (see Fig. 245, Vol. I) ; and M', the corresponding external bending moment per unit of area of the element, is

$$M' = \frac{\delta M}{\delta x . \delta y} \; ; \; \text{but } \delta M : \; \frac{\partial M}{\partial x} . \delta x \; ; \; \text{therefore } M' = \frac{1}{\delta y} . \frac{\partial M}{\partial x}$$

The force acting on the width δy is $p_1 . \delta y$. At the section distant x from the axis of y it acts at a leverage w, hence $M = - p_1 w . \delta y$. This is an anti-clockwise moment about the axis of y and therefore negative. Hence,

$$\frac{\partial M}{\partial x} = - p_1 . \delta y \frac{\partial w}{\partial x} \; ; \; M' = \frac{1}{\delta y} . \frac{\partial M}{\partial x} = - p_1 \frac{\partial w}{\partial x} \; ;$$

and

$$\frac{\partial M'}{\partial x} = - p_1 \frac{\partial^2 w}{\partial x^2}$$

Similarly, the external moment L' acting on the element is

$$L' = \frac{\delta L}{\delta x . \delta y} = \frac{1}{\delta x} . \frac{\partial L}{\partial y}$$

where the moment $L = p_2 w . \delta x$. This is a clockwise moment about the axis of x and therefore positive ; see (ii). Then

$$\frac{\partial L}{\partial y} = p_2 . \delta x \frac{\partial w}{\partial y} \; ; \; L' = \frac{1}{\delta x} . \frac{\partial L}{\partial y} \; : p_2 \frac{\partial w}{\partial y}$$

and

$$\frac{\partial L'}{\partial y} = p_2 \frac{\partial^2 w}{\partial y^2}$$

Substituting these values in eq. (1),

$$\frac{\partial^4 w}{\partial x^4} + \frac{\partial^4 w}{\partial y^4} + 2 \frac{\partial^4 w}{\partial x^2 . \partial y^2} = - \frac{1}{D} \left\{ p_1 \frac{\partial^2 w}{\partial x^2} + p_2 \frac{\partial^2 w}{\partial y^2} \right\} \tag{2}$$

[It is worth noticing the analogy between this equation and the differential equation for the equilibrium of an ideal long column. From eq. (1), § 99, Vol. I,

$$\frac{d^2 y}{dx^2} = - a^2 y = - \frac{W}{EI} y \; ; \; \text{whence,} \; \frac{d^4 y}{dx^4} = - \frac{W}{EI} . \frac{d^2 y}{dx^2}$$

In this case y, not w, denotes the deflection. Observe that in both cases, due to the curve being concave towards the axis of x, the curvature is negative, which accounts for the minus sign.]

Boundary Conditions.—Suppose that the edges of the plate are freely supported and remain in the plane of the origin. Then $w = 0$ when $x = 0$ and $x = l_1$; also when $y = 0$ and $y = l_2$. Further, there can be no bending moment at the edges. From eqs. (7) and (8), § 186, Vol. I, the bending moments at any sections $x = x$ and $y = y$ are

$$M_{xx}' = - D \left\{ \frac{\partial^2 w}{\partial x^2} + \frac{1}{m} . \frac{\partial^2 w}{\partial y^2} \right\} \; ; \; M_{yy}' = - D \left\{ \frac{\partial^2 w}{\partial y^2} . \frac{1}{m} \frac{\partial^2 w}{\partial x^2} \right\}$$

Hence it follows that

$$\left\{\frac{\partial^2 w}{\partial x^2} + \frac{1}{m}\frac{\partial^2 w}{\partial y^2}\right\} = 0 \quad \text{when } x = 0 \text{ and when } x = l_1$$

$$\left\{\frac{\partial^2 w}{\partial y^2} + \frac{1}{m}\frac{\partial^2 w}{\partial x^2}\right\} = 0 \quad \text{when } y = 0 \text{ and when } y = l, \tag{3}$$

$$w = 0 \qquad \text{when } x = 0, \ x = l_1, \ y = 0, \text{ and } y = l_1$$

It will be found by differentiation that all members of eq. (3) are satisfied by

$$w = A \sin \frac{r_1 \pi x}{l_1} \sin \frac{r_2 \pi y}{l_2} \tag{4}$$

where r_1 and r_2 are integers, and A is a constant. This expression will also satisfy eq. (2) if

$$\frac{r_1^4 \pi^4}{l_1^4} + \frac{r_2^4 \pi^4}{l_2^4} + 2\frac{r_1^2 \pi^2}{l_1^2}\frac{r_2^2 \pi^2}{l_2^2} = \frac{1}{D}\left\{p_1 \frac{r_1^2 \pi^2}{l_1^2} + p_2 \frac{r_2^2 \pi^2}{l_2^2}\right\}$$

or

$$\left\{\frac{r_1}{l_1^2} + \frac{r_2}{l_2^2}\right\} = \frac{1}{\pi^2 D}\left\{p_1 \frac{-}{l_1^2} + p_2 \frac{-}{l_2^2}\right\} \tag{5}$$

The minimum values of p_1 and p_2 which will cause the plate to buckle will correspond to the values $r_1 = r_2 = 1$, when the plate will bend as shown in (i) Fig. 193, each axis being a semi-sine wave. Then

$$\left\{\frac{1}{l_1^2} + \frac{1}{l_2^2}\right\}^2 = \frac{1}{\pi^2 D}\left\{\frac{p_1}{l_1^2} + \frac{p_2}{l_2^2}\right\}$$

and

$$\frac{p_1}{l_1^2} + \frac{p_2}{l_2^2} = \frac{\pi^2 E t^3}{12}\frac{m^2}{m^2 + 1}\left\{\frac{1}{l_1^2} + \frac{1}{l_2^2}\right\} \tag{6}$$

this equation determines the critical values of p_1 and p_2. If $p_2 = 0$,

$$p_1 = \frac{\pi^2 E t^3 l_1^2}{12}\frac{m^2}{m^2 - 1}\left\{\frac{1}{l_1} + \frac{1}{l_2^2}\right\}^2 \tag{7}$$

Bryan's formula.[1] If l_1/l_2 is large, the plate buckles into squares

$(l_1 = l_2)$, and

$$p_1 = \frac{\pi^2 E t^3}{3 l_2^2}\frac{m^2}{m^2 - 1} \qquad . \qquad . \qquad . \tag{8}$$

121. Buckling of Flat Plates. Strain-Energy Methods.—Solutions to many problems involving the buckling of flat plates can be obtained by strain-energy methods. An expression for the internal work stored up in a slightly deflected plate can be obtained from the equations of § 186, Vol. I. It is shown in that article that the stress components on an element $\delta x . \delta y$ of the plate, Fig. 244, Vol. I, are equivalent to stress couples (per unit of length) M_{xx}' and M_{xy}' acting about axes parallel to Oy, and stress couples M_{yy}' and M_{xy}' acting about axes parallel to Ox. As in § 143, Vol. I, the work done by a stress couple is $\delta U = \frac{1}{2}M . \delta\sigma$, where $\delta\sigma$ is the change of slope in the length of the element. From eq. (7), § 186, Vol. I,

$$M_{xx}' = -D\left\{\frac{\partial^2 w}{\partial x^2} + \frac{1}{m} . \frac{\partial^2 w}{\partial y^2}\right\},$$

and the stress couple acting on the element of width δy is

$$M_{xx}' \, \delta y = - D\left\{\frac{\partial^2 w}{\partial x^2} + \frac{1}{m} \cdot \frac{\partial^2 w}{\partial y^2}\right\}\delta y$$

From Fig. 246, Vol. I, and the descriptive text, $\sigma_x = - \partial w/\partial x$, where $+ w$ is the deflection of the plate in the z direction, hence

$$\delta\sigma_x = \frac{\partial \sigma_x}{\partial x} \cdot \delta x = - \frac{\partial^2 w}{\partial x^2} \cdot \delta x,$$

and $\qquad \delta U = \tfrac{1}{2}M_{xx}'\delta y \cdot \delta\sigma_x = \left[\frac{D}{2}\left\{\frac{\partial^2 w}{\partial x^2} + \frac{1}{m} \cdot \frac{\partial^2 w}{\partial y^2}\right\}\frac{\partial^2 w}{\partial x^2}\right]\delta x \, \delta y$

Similarly, for M_{yy}', using eq. (8) (l.c.),

$$\delta U = \left[\frac{D}{2}\left\{\frac{\partial^2 w}{\partial y^2} + \frac{1}{m}\frac{\partial^2 w}{\partial x^2}\right\}\frac{\partial^2 w}{\partial y^2}\right]\delta x \, \delta y$$

From eq. (9) (l.c.), $M_{xy}' = - D\left\{\dfrac{m-1}{m}\right\}\dfrac{\partial^2 w}{\partial x \cdot \partial y}$

and the stress couple acting on the width δy about an axis parallel to Ox is $M_{xy}'\delta y$. The change of slope in the length AD, Fig. 245, Vol. I, is $\delta\sigma_y$, where $\sigma_y = - \partial w/\partial y$.

Therefore, $\delta\sigma_y = \dfrac{\partial\sigma_y}{\partial x} \cdot \delta x = -- \dfrac{\partial^2 w}{\partial x \cdot \partial y} \cdot \delta x$

and $\qquad \delta U = \tfrac{1}{2}M_{xy}'\delta y \cdot \delta\sigma_y = \left[\frac{D}{2}\left\{\frac{m-1}{m}\right\}\left\{\frac{\partial^2 w}{\partial x \cdot \partial y}\right\}^2\right]\delta x \, \delta y$

Similarly, for the stress couple $M_{xy}'\delta x$ acting about an axis parallel to Oy,

$$\delta U = \left[\frac{D}{2}\left\{\frac{m-1}{m}\right\}\left\{\frac{\partial^2 w}{\partial x \cdot \partial y}\right\}^2\right]\delta x \, \delta y$$

Hence the total strain energy stored in the element is

$$\delta U = \frac{D}{2}\left[\left\{\frac{\partial^2 w}{\partial x^2} + \frac{1}{m} \cdot \frac{\partial^2 w}{\partial y^2}\right\}\frac{\partial^2 w}{\partial x^2} + \left\{\frac{\partial^2 w}{\partial y^2} + \frac{1}{m} \cdot \frac{\partial^2 w}{\partial x^2}\right\}\frac{\partial^2 w}{\partial y^2}\right.$$
$$\left. + 2 \cdot \frac{m-1}{m}\left\{\frac{\partial^2 w}{\partial x \cdot \partial y}\right\}^2\right]\delta x \, \delta y$$

and for the whole plate,

$$U = \frac{D}{2}\iint\left[\left\{\frac{\partial^2 w}{\partial x^2}\right\}^2 + \left\{\frac{\partial^2 w}{\partial y^2}\right\}^2 + \frac{2}{m}\left\{\frac{\partial^2 w}{\partial x^2} \cdot \frac{\partial^2 w}{\partial y^2}\right\} + \frac{2(m-1)}{m}\left\{\frac{\partial^2 w}{\partial x \cdot \partial y}\right\}^2\right]dx \, dy$$

which may be written

$$U = \frac{D}{2}\iint\left[\left\{\frac{\partial^2 w}{\partial x^2}\right\}^2 + 2\frac{\partial^2 w}{\partial x^2} \cdot \frac{\partial^2 w}{\partial y^2} + \left\{\frac{\partial^2 w}{\partial y^2}\right\}^2 + \frac{2}{m}\left\{\frac{\partial^2 w}{\partial x^2} \cdot \frac{\partial^2 w}{\partial y^2}\right\}\right.$$
$$\left. - 2\frac{\partial^2 w}{\partial x^2} \cdot \frac{\partial^2 w}{\partial y^2} + \frac{2(m-1)}{m}\left\{\frac{\partial^2 w}{\partial x \cdot \partial y}\right\}^2\right]dx \, dy$$

$$U = \frac{D}{2}\iint\left[\{\nabla^2 w\}^2 - 2\frac{m-1}{m}\left\{\frac{\partial^2 w}{\partial x^2} \cdot \frac{\partial^2 w}{\partial y^2} - \left(\frac{\partial^2 w}{\partial x \cdot \partial y}\right)^2\right\}\right]dx \, dy \qquad (1)$$

This expression gives the total strain energy stored in the plate, due to the stress couples, in terms of the deflection w. In problems on the buckling of thin plates, the strain energy due to the stress resultants $X_{x'}, Y_{y'} \ldots$, § 186, Vol. I, may be neglected in comparison with that due to the stress couples, just as in Euler's formula for long slender columns the direct compression is neglected. The integration is to be taken over the whole area of the plate.

Particular Case.—Applying the above analysis to the case discussed in § 120 ; from eq. (4), § 120, if $r_1 = r_2 = 1$,

$$w \quad A \sin \frac{\pi x}{l_1} \sin \frac{\pi y}{l_2}$$

$$\frac{\partial^2 w}{\partial x^2} \quad -\frac{\pi^2 A}{l_1^2} \sin \frac{\pi x}{l_1} \sin \frac{\pi y}{l} \cdot \quad \frac{\partial^2 w}{\partial y^2} = -\frac{\pi^2 A}{l_2^2} \sin \frac{\pi x}{l_1} \sin \frac{\pi y}{}$$

$$\frac{\partial^2 w}{\partial x \cdot \partial y} \quad \frac{\pi^2 A}{l_1 l_2} \cos \frac{\pi x}{l_1} \cos \frac{\pi y}{l_2}$$

Then,

$$(\nabla^2 w) \quad \frac{\partial^2 w}{\partial x^2} + \frac{\partial^2 w}{\partial y^2} \quad -\pi^2 A \left\{ \frac{1}{l_1^2} + \frac{1}{l_2^2} \right\} \sin \frac{\pi x}{l_1} \sin \frac{\pi y}{l_2}$$

$$\int_0^{l_1} \int_0^{l_2} (\nabla^2 w)^2 \, dx \, dy \quad \pi^4 A^2 \left\{ \frac{1}{l_1^2} + \frac{1}{l_2^2} \right\} \frac{l_1 l_2}{4} \tag{2}$$

and

$$-\left(\frac{\partial^2 w}{\partial x \cdot \partial y} \right)^2 \right\} dx \, dy = 0 \qquad . \qquad . \tag{3}$$

Hence,

$$U = \frac{D}{2} \left[\pi^4 A^2 \left\{ \frac{1}{l_1^2} + \frac{1}{l_2^2} \right\}^2 \frac{l_1 l_2}{4} \right] \qquad . \qquad . \qquad . \tag{4}$$

This is the internal strain energy. The external work done will be due to the external couples L acting about the x axis, and M about the y axis. As in the case of the stress couples, the work done is $\delta U = \frac{1}{2} M \cdot \delta \sigma$, where $\delta \sigma$ is the angle through which the couple rotates. At the point Q, (iii) Fig. 193, $M = -p_1 w \cdot \delta y$, and $\sigma \quad + \frac{\partial w}{\partial x}$ hence $\delta \sigma = \frac{\partial^2 w}{\partial x^2} \cdot \delta x$, and the work done on the element by M is

$$\delta U = -\frac{1}{2} p_1 w \cdot \frac{\partial^2 w}{\partial x^2} \, \delta x \, \delta y$$

[*Note :* As in the case of struts, where $M = -EI \cdot d^2 y/dx^2 = -EI \cdot d\sigma/dx$, if M is assumed positive, $d\sigma/dx$ must be negative, and vice versa.]

Similarly, the work done by couple $L = p_2 w \cdot \delta y$ is

$$\delta U = -\frac{1}{2} p_2 w \cdot \frac{\partial^2 w}{\partial y^2} \, \delta x \, \delta y$$

and the total external work is

$$U_e = -\frac{1}{2} \int_0^{l_1} \int_0^{l_2} \left\{ p_1 w \frac{\partial^2 w}{\partial x^2} + \frac{\partial^2 w}{\partial y^2} \right\} dx \, dy \tag{5}$$

Integrate each term by parts,* thus

$$\int_0^{l_1} p_1 w \frac{\partial^2 w}{\partial x^2}\, dx = \left[p_1 w \cdot \frac{\partial w}{\partial x} \right]_0^{l_1} - \int_0^{l_1} p_1 \left(\frac{\partial w}{\partial x} \right)^2 dx$$

since w is zero when $x = 0$ and when $x = l_1$, the first term on the right-hand side vanishes, and $\displaystyle\int_0^{l_1} p_1 w \frac{\partial^2 w}{\partial x^2}\, dx = - \int_0^{l_1} p_1 \left(\frac{\partial w}{\partial x} \right)^2 dx$

Similarly, $\displaystyle\int_0^{l_2} p_2 w \frac{\partial^2 w}{\partial y^2}\, dy = - \int_0^{l_2} p_2 \left(\frac{\partial w}{\partial y} \right)^2 dy,$

and $\qquad U_e = \tfrac{1}{2} \displaystyle\int_0^{l_1} \int_0^{l_2} \left\{ p_1 \left(\frac{\partial w}{\partial x} \right)^2 + p_2 \left(\frac{\partial w}{\partial y} \right)^2 \right\} dx\, dy$ . . (6)

Since $w = A \sin \dfrac{\pi x}{l_1} \sin \dfrac{\pi y}{l_2}$,

$$\frac{\partial w}{\partial x} = \frac{\pi A}{l_1} \cos \frac{\pi x}{l_1} \sin \frac{\pi y}{l_2}\,; \quad \frac{\partial w}{\partial y} = \frac{\pi A}{l_2} \sin \frac{\pi x}{l_1} \cos \frac{\pi y}{l_2}$$

and $U_e = \pi^2 A^2 \left\{ \dfrac{p_1}{l_1^2} + \dfrac{p_2}{l_2^2} \right\} \dfrac{l_1 l_2}{4}$ . . (7)

Equating the internal and external work, eqs. (4) and (7),

$$\frac{D}{2} \left[\pi^4 A^2 \left\{ \frac{1}{l_1^2} + \frac{1}{l_2^2} \right\}^2 \frac{l_1 l_2}{4} \right] = \pi^2 A^2 \left\{ \frac{p_1}{l_1^2} + \frac{p_2}{l_2^2} \right\} \frac{l_1 l_2}{4}$$

whence, $\qquad \dfrac{1}{\pi^2 D} \left\{ \dfrac{p_1}{l_1^2} + \dfrac{p_2}{l_2^2} \right\} = \left\{ \dfrac{1}{l_1^2} + \dfrac{1}{l_2^2} \right\}^2$. (8)

Cf. eqs. (5) and (6), § 120.

It will be noted that the integral

$$\int_0^{l_2} \int_0^{l_1} \left\{ \frac{\partial^2 w}{\partial x^2} \cdot \frac{\partial^2 w}{\partial y^2} - \left(\frac{\partial^2 w}{\partial x \cdot \partial y} \right)^2 \right\} dx\, dy$$

from eq. (1) vanishes ; see eq. (3). It may be proved that this is true for all slightly bent rectangular plates whose edges lie in a plane ($w = 0$) and are freely supported ($M = 0$ everywhere on the boundary). It is also true for a similar plate with clamped edges ; see the following example.

· **122. Rectangular Plate with Clamped Edges subjected to Edge Thrusts.**—Let ABCD, Fig. 194, be a thin flat rectangular plate subjected to compressive forces p_1 per unit of length along the edges AB, CD, and to compressive forces p_2

FIG. 194.

per unit of length along the edges AD and BC. In this case the edges are fixed in direction. It is required to find the conditions under which
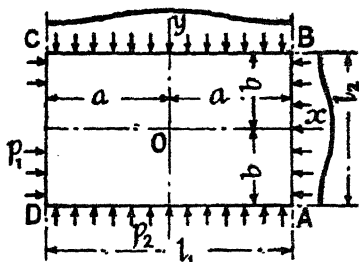
* If $u = w$, $du = \dfrac{\partial w}{\partial x} \cdot dx$; if $dv = \dfrac{\partial^2 w}{\partial x^2} \cdot dx$, $v = \dfrac{\partial w}{\partial x}$.

the plate will buckle. Suppose, as indicated in the figure, that it has buckled upwards slightly. Take origin at O, the centre of the plate. By analogy with § 120, suppose that the curvature is sinusoidal, and let

$$w \quad \lambda\left(1 + \cos\frac{\pi x}{a}\right)\left(1 + \cos\frac{\pi y}{b}\right) \qquad . \qquad . \quad (1)$$

It will be found that this equation will satisfy all the boundary conditions, viz, that $w = 0$ and $dw/dx = 0$ where $x = \pm a$; and that $w = 0$ and $dw/dy = 0$ where $y = \pm b$. From eq. (1),

$$\frac{\partial w}{\partial x} = -A\frac{\pi}{a}\sin\frac{\pi x}{a}\left(1 + \cos\frac{\pi y}{b}\right) ; \quad \frac{\partial w}{\partial y} = -A\frac{\pi}{b}\sin\frac{\pi y}{b}\left(1 + \cos\frac{\pi x}{a}\right)$$

$$\frac{\partial^2 w}{\partial x^2} \quad -A\frac{\pi^2}{a^2}\cos\frac{\pi x}{a}\left(1 + \cos\frac{\pi y}{b}\right) ; \quad \frac{\partial^2 w}{\partial y^2} = -A\frac{\pi^2}{b^2}\cos\frac{\pi y}{b}\left(1 + \cos\frac{\pi x}{a}\right)$$

$$\frac{\partial^2 w}{\partial x \cdot \partial y} \quad + A\frac{\pi^2}{ab}\sin\frac{\pi x}{a}\sin\frac{\pi y}{b}$$

$$\nabla^2 w = \left(\frac{\partial^2 w}{\partial x^2} + \right.$$

$$= -\pi^2 A\left\{\frac{1}{a^2}\cos\frac{\pi x}{a}\left(1 + \cos\frac{\pi y}{b}\right) + \frac{1}{b^2}\cos\frac{\pi y}{b}\left(1 + \cos\frac{\pi x}{a}\right)\right\}$$

The internal strain energy can be found from eq. (1), § 121,

$$U = \frac{D}{2}\int\int\left[\left\{\nabla^2 w\right\}^2 - 2\frac{m-1}{m}\left\{\frac{\partial^2 w}{\partial x^2}\cdot\frac{\partial^2 w}{\partial y^2} - \left(\frac{\partial^2 w}{\partial x \cdot \partial y}\right)^2\right\}\right]dx\,dy$$

the integration being taken over the whole area of the plate. Considering the second term of the integral separately, for the four quarters of the plate,

$$4\int_0^a\int_0^b\left\{\frac{\partial^2 w}{\partial x^2}\cdot\frac{\partial^2 w}{\partial y^2} - \left(\frac{\partial^2 w}{\partial x \cdot \partial y}\right)\right\}$$

$$= 4\frac{\pi^4 A^2}{a^2 b^2}\int_0^a\int_0^b\left\{\cos\frac{\pi x}{a}\cos\frac{\pi y}{b}\left(1 + \cos\frac{\pi x}{a}\right)\left(1 + \cos\frac{\pi y}{b}\right)\right.$$

$$\left. - \sin^2\frac{\pi x}{a}\sin^2\frac{\pi y}{b}\right\}dx\,dy$$

$$= 0.$$

This is true of any slightly bent plate when the edges are direction-fixed, for, as proved in treatises on Analytical Solid Geometry,

$$\int\int\left\{\frac{\partial^2 w}{\partial x^2}\cdot\frac{\partial^2 w}{\partial y^2} - \left(\frac{\partial^2 w}{\partial x \cdot \partial y}\right)^2\right\}dx\,dy = \int\int\frac{dx \cdot dy}{R_1 R_2} = 0$$

where R_1, R_2 are the principal radii of curvature of the curved middle surface at the point xy, and the integration is taken over the whole area of the closed surface ; the normals all round the boundary remaining parallel and normal.

The internal strain energy for the four quarters of the plate is, therefore,

$$
\begin{aligned}
U &= \frac{4D}{2} \int_0^a \int_0^b (\nabla^2 w)^2 \, dx \, dy \\
&= 2\pi^4 D A^2 \int_0^a \int_0^b \left\{ \frac{1}{a^2} \cos \frac{\pi x}{a} \left(1 + \cos \frac{\pi y}{b} \right) + \frac{1}{b^2} \cos \frac{\pi y}{b} \left(1 + \cos \frac{\pi x}{a} \right) \right\}^2 dx \, dy \\
&= \frac{\pi^4 D A^2 ab}{2} \left\{ \frac{3}{a^4} + \frac{3}{b^4} + \frac{2}{a^2 b^2} \right\} \tag{2}
\end{aligned}
$$

The external work done can be obtained from eq. (6), § 121, which will hold equally well for the clamped plate. Adjusting the limits to include the four quarters of the latter,

$$
\begin{aligned}
U_e &= \frac{4}{2} \int_0^a \int_0^b \left\{ p_1 \left(\frac{\partial w}{\partial x} \right)^2 + p_2 \left(\frac{\partial w}{\partial y} \right)^2 \right\} dx \, dy \\
&= 2\pi^2 A^2 \int_0^a \int_0^b \left\{ \frac{p_1}{a^2} \sin^2 \frac{\pi x}{a} \left(1 + \cos \frac{\pi y}{b} \right)^2 + \frac{p_2}{b^2} \sin^2 \frac{\pi y}{b} \left(1 + \cos \frac{\pi x}{a} \right)^2 \right\} dx \, dy \\
&= \frac{3\pi^2 A^2 ab}{2} \left\{ \frac{p_1}{a^2} + \frac{p_2}{b^2} \right\} \tag{3}
\end{aligned}
$$

Equating the internal and external work, eqs. (2) and (3),

$$
\frac{\pi^4 D A^2 ab}{2} \left\{ \frac{3}{a^4} + \frac{3}{b^4} + \frac{2}{a} \right\} \quad \frac{3\pi^2 A^2 ab}{} \left\{ \frac{p_1}{a^2} + \frac{p_2}{b^2} \right.
$$

and

$$
\frac{p_1}{a^2} + \frac{p_2}{b^2} \right\} = \frac{\pi^2 D}{3} \left\{ \frac{3}{a^4} + \frac{3}{b^4} + \frac{2}{a^2 b^2} \right\} \tag{4}
$$

Let $2a = l_1$, and $2b = l_2$, as in Fig. 193; also $D = \dfrac{Et^3}{12} \cdot \dfrac{m^-}{m^2 - 1}$; see § 120, where t is the thickness of the plate. Then

$$
\left\{ \frac{p_1}{l_1^2} + \frac{p_2}{l_2^2} \right\} = \frac{m^2}{m^2 - 1} \cdot \frac{\pi^2 E t^3}{9} \left\{ \frac{3}{l_1^4} + \frac{3}{l_2^4} + \frac{2}{l_1^2 l_2^2} \right\} \tag{5}
$$

which gives the critical values of the loads p_1 and p_2 which would cause the plate to buckle. If $p_2 = 0$, and l_2 is very great compared with l_1,

$$
p_1 = \frac{m^2}{m^2 - 1} \cdot \frac{\pi^2 E t^3}{3 l_1^2} \tag{6}
$$

which gives the side-crippling thrust on a long thin plate stiffened along its edges.

The above is a classic problem and the solution given is only an approximation.

123. Slender Cantilever.—A simple experiment with a thin flat strip, placed on edge and used as a cantilever, will demonstrate that the free end may refuse to remain in the plane of bending, but will deflect sideways, twisting the strip as it goes, until a position of equilibrium is reached, or complete failure occurs. The effect is due to want of elastic stability,

and may occur in any cantilever or beam in which the lateral and torsional stiffness are relatively small. (i) Fig. 195 shows a slender **I** beam thus deflected by a terminal load W which is applied at the neutral axis. Let $I_z = y^2 \cdot da$ and $I_y = z^2 \cdot da$ be the maximum and minimum moments of inertia of the cross-section, and Φ its torsional rigidity. Take origin at O, and let Ox, Oy, Oz, as shown in the figure, be the co-ordinate axes ; OKB is the bent centre line of the cantilever. Consider the stresses on the cross-section at K, the co-ordinates of which point are x, y, and z, and suppose that the angle of twist there is θ. If L denote the length of the cantilever, the bending moment at K is $M = W(L - x)$, with components about the two principal axes of the cross-section at K of $M \cos \theta$ and
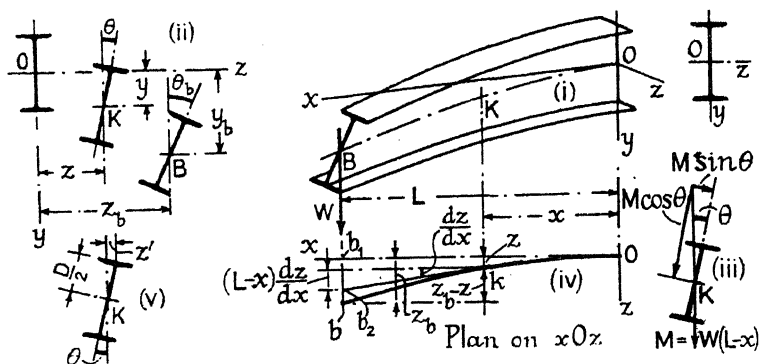
FIG. 195.

$M \sin \theta$, (iii) ; which, since θ is very small, may be written $W(L - x)$, and $W(L - x)\theta$. Then the differential equations giving the shape of the bent centre line are

$$\frac{d^2y}{dx^2} = \frac{M}{EI} = \frac{W(L - x)}{EI_z} \qquad . \qquad . \qquad (1)$$

$$\frac{d^2z}{dx^2} = \frac{W(L - x)}{EI_y}\theta \qquad (2)$$

In addition to these bending moments there will be a twisting moment M_t at K, which can be found from the plan, (iv). Okb is the bent central axis ; kb_2, tangent thereto, is a prolongation of the axis of the beam at K. The twisting moment, see (iv), is

$$W \cdot bb_1 = W\left\{(z_b - z) - (L - x)\frac{dz}{dx}\right\} = M_t$$

This moment will be resisted partly by the torsional stiffness of the cross-section, and partly by the lateral stiffness of the flanges. In moving through an angle θ, a torsional resistance moment $(\Phi \cdot d\theta/dx)$ will be called into play [see eq. (1), § 130, Vol. I] ; also the flanges will be deflected a distance z' from their normal position [see (v), Fig. 195]. If I′ be the

moment of inertia of a flange about the axis Oy, the shearing force in the flange corresponding to this deflection will be

$$S' = - EI' \cdot \frac{d^3 z'}{dx^3} = - \frac{EI'D}{2} \cdot \frac{d^3 \theta}{dx^3}$$

for $z' = \theta \times D/2$. There will be similar shearing forces in both top and bottom flanges acting in opposite directions, and the two will produce a torsional resistance moment of

$$S' \times D = - \frac{EI'D^2}{2} \frac{d^3 \theta}{dx^3}$$

The total twisting moment M_t must equal the sum of the two torsional resistance moments, whence

$$M_t = W \left\{ (z_b - z) - (L - x) \frac{dz}{dx} \right\} \quad \Phi \frac{d\theta}{dx} - \frac{EI'D^2}{2} \cdot \frac{d^3\theta}{dx^3} \quad . \quad (3)$$

Differentiate with regard to x, and substitute the value of $d^2 z / dx^2$ from eq. (2),

$$\frac{EI'D^2}{2} \cdot \frac{d^4\theta}{dx^4} - \Phi \frac{d^2\theta}{dx^2} - \frac{W^2(L - x)^2 \theta}{EI_y} = 0 \tag{4}$$

which gives the condition for elastic stability.

Particular Cases.—If the cross-section of the cantilever be a thin deep rectangle, so that I' is zero, eq. (4) reduces to

$$\frac{d^2\theta}{dx^2} + a^2(L - x)^2 \theta = 0 ; \text{ where } a^2 = \frac{W^2}{\Phi EI_y}$$

This equation can be solved in terms of Bessel functions. The solution is

$$\theta = \sqrt{L - x} \left[A \cdot J_{\frac{1}{4}} \left\{ \frac{a}{2} (L - x)^2 \right\} + B \cdot J_{-\frac{1}{4}} \left\{ \frac{a}{2} (L - x)^2 \right\} \right] \quad . \quad (5)$$

where A and B are constants of integration. When $x = L$, $z = z_b$; therefore, from eq. (3), since $I' = 0$, $d\theta/dx = 0$, and $A = 0$. When $x = 0$, $\theta = 0$, hence,

$$J_{-\frac{1}{4}} \left\{ \frac{aL^2}{2} \right\} = 0 ; \quad \frac{aL^2}{2} = 2, \text{ very nearly ;}$$

$$\sqrt{\frac{W^2}{\Phi EI_y}} = \frac{4}{L^2} ; \text{ and } W = \frac{4\sqrt{\Phi EI}}{L^2} \tag{6}$$

which gives the critical value of the load which produces instability. For a thin deep rectangle, $D \times t$, the value of Φ is $\frac{1}{3}Dt^3 G$ approx., and $I_y = \frac{1}{12}Dt^3$. Inserting these values in eq. (6),

$$W = \frac{2}{3} \frac{Dt^3 \sqrt{EG}}{L^2} \tag{7}$$

In the case of a thin deep rectangular beam, span L, carrying a central load W, if the ends are prevented from twisting, then each half of the beam may be regarded as a cantilever similarly situated to that in Fig. 195,

but of length $L/2$ and carrying a load $W/2$ at its end. From eqs. (6) and (7) the critical load is given approximately by

$$W = \frac{16\sqrt{\Phi EI_y}}{L^2} = \frac{8}{3}\frac{Dt^3\sqrt{EG}}{L^2} \qquad . \qquad . \qquad . \quad (8)$$

It will be observed that eq. (4) may be written

$$\frac{EI'D^2}{2} \cdot \frac{d^4\theta}{dx^4} - \Phi\frac{d^2\theta}{dx^2} \cdot \frac{M^2\theta}{EI_y} = 0 \qquad (9)$$

and it may be shown that this equation holds generally. In the case of a deep rectangular cantilever, length L, carrying a uniform load of w per unit of length, $M = w(L - x)^2/2$, and

$$\Phi\frac{d^2\theta}{dx^2} + \frac{w^2(L-x)^4}{4EI_y}\theta = 0$$

of which the solution, in terms of Bessel functions, is

$$\theta = \sqrt{L-x}\left[A \cdot J_{\frac{1}{6}}\left\{\frac{a}{3}(L-x)^3\right\} + B \cdot J_{-\frac{1}{6}}\left\{\frac{a}{3}(L-x)^3\right\}\right] \quad . \quad (10)$$

where $a^2 = w^2/4\Phi EI_y$. As in eq. (5), when $x = L$, $d\theta/dx = 0$, and $A = 0$; when $x = 0$, $\theta = 0$ and

$$J_{-\frac{1}{6}}\left\{\frac{a}{3}(L-x^3)\right\} = 0 \; ; \;\; \text{whence} \;\; \frac{aL^3}{3} = 2\cdot15 \; ;$$

$$\sqrt{\frac{w^2}{4\Phi EI_y}} = \frac{6\cdot45}{L^3} \; ; \; \text{and} \; w = \frac{12\cdot9\sqrt{\Phi EI_y}}{L^3} \qquad (11)$$

If the sides of the rectangle are $D \times t$

$$w = \frac{2\cdot15Dt^3\sqrt{EG}}{L^3} \qquad (12)$$

In certain simple cases of slender I beams, eq. (9) can be solved directly. Suppose the cantilever of Fig. 195 to carry a terminal couple M; then eq. (9) becomes

$$\frac{d^4\theta}{dx^4} - \beta\frac{d^2\theta}{dx^2} - \gamma M^2\theta = 0 \qquad . \qquad . \qquad . \qquad . \quad (13)$$

where $\beta = 2\Phi/EI'D^2$; and $\gamma = 2/E^2I'I_yD^2$. The solution $\theta = \theta_b(1 - \cos \pi x/2L)$ will satisfy the end conditions; $\theta = 0$ when $x = 0$; $\theta = \theta_b$ when $x = L$. Differentiate eq. (13) with respect to x,

$$\frac{d^5\theta}{dx^5} - \beta\frac{d^3\theta}{dx^3} - \gamma M^2\frac{d\theta}{dx} = 0 \; ;$$

from which $\quad \dfrac{\pi^5\theta_b}{32L^5}\sin\dfrac{\pi x}{2L} + \beta\dfrac{\pi^3\theta_b}{8L^3}\sin\dfrac{\pi x}{2L} - \gamma M^2\dfrac{\pi\theta_b}{2L}\sin\dfrac{\pi x}{2L} = 0$

whence, $\quad M^2 = \dfrac{1}{\gamma}\left[\dfrac{\pi^4}{16L^4} + \beta\dfrac{\pi^2}{4L^2}\right]$

$$= \frac{\pi^2 EI_y\Phi}{4L^2}\left[\frac{\pi^2 EI'D^2}{8\Phi L^2} + 1\right] \qquad . \quad (14)$$

This gives the critical value for M at which the cantilever will buckle sideways.

Timoshenko,[5] using strain-energy methods, has solved the problem for a number of different conditions. A few of his results are given below :

(a) For a cantilever, length L, carrying a terminal load W, the critical value of the load is given by

$$W = (k \sqrt{EI_y \Phi})/L^2 \; ; \text{ where if}$$

βL^2	0·1	1·0	2·0	4·0	8·0	12·0	24·0	40·0
k	44·3	15·7	12·2	9·76	8·03	7·20	6·19	5·64

(b) Beam, span L, supported at each end, carrying a single central load W ; the critical value for W is $W = (k \sqrt{EI_y \Phi})/L^2$; where if

$\beta L^2 =$	0·4	4·0	8·0	16	32	64	96	160	∞
$k' =$	86·4	31·9	25·6	21·8	19·6	18·3	17·9	17·5	17·0
$k'' =$	268	88·8	65·5	50·2	40·2	34·1	31·8	30·0	

If the ends of the beam are restrained from rotating about a vertical axis, use k'' instead of k'. In both cases the load is supposed to be applied at the neutral axis.

(c) Beam, span L, supported at each end, and carrying a uniformly distributed load w per unit of length, the ends being free to rotate about vertical axis ; the critical value of w is $w = (k \sqrt{EI_y \Phi})L^3$; where if

$\beta L^2 =$	0·4	4·0	8·0	16	32	64	96	160	∞
$k_1/8 =$	17·9	6·63	5·32	4·54	4·08	3·81	3·73	3·65	3·54
$k_2/8 =$	11·6	4·54	3·80	3·43	3·28	3·22	3·25	3·27	3·54
$k_3/8 =$	27·7	9·77	7·43	6·01	5·09	4·50	4·30	4·08	3·54

Use k_1 when load is applied along neutral axis ; k_2 when load is applied to top flange ; k_3 when load is applied to bottom flange.

If the ends of the beam are restrained from rotating about a vertical axis, k_1 becomes k_1'', where if

$\beta L^2 =$	0·4	4	8	16	32		128	200	400
$k_1'' =$	488	160·8	119·2	91·2	73·04	58·00	55·84	53·44	51·20

If the beam be subjected to an axial thrust W' in addition to the lateral load, the critical values for the latter should be multiplied by $\sqrt{(1 - W'L^2/\pi^2 EI_y)}$ when the ends are free to rotate about a vertical axis ; or by $\sqrt{(1 - W'L^2/4\pi^2 EI_y)}$ when the ends are restrained from thus rotating.

For a number of additional results see Case, *Strength of Materials*, (London, 1925), pp. 383–4.

ELASTIC VIBRATIONS OF FRAMED STRUCTURES

124. **Elastic Vibrations of Open Web Girders.**—Rayleigh's device, § 155, Vol. I, in which it is assumed that the elastic displacement y_0 of a beam is everywhere proportional to the deflection Y produced by the static effect of the load thereon, can be used with success to find

the periodic time of vibration of an open web girder, if it be assumed that the proposition holds for every panel point of the girder separately and simultaneously.

Let it be assumed that all the panel points are vibrating with the same frequency, and that they all pass their mid-points together. Then, as in § 155, Vol. I, if U be the total energy in the system at any moment, $U = U' + U''$, where U' is the strain energy and U'' the kinetic energy in the system. At the mid-position the strain energy $U' = 0$, and

$$U'' = \frac{1}{2g} \Sigma W v_0^2,$$ where W is the weight at any panel point, and v_0 is

its velocity in a vertical direction. Since, in a framed structure, the displacement of a panel point will not in general be vertical, both x and y components of the motion should be taken into account, but in a girder the x component is always relatively small and can be neglected. The vertical component of the retarding force acting on a weight W will vary from zero at the mid-position to a maximum F in the extreme position, and the work which it does in bringing the weight to rest is $\frac{1}{2}F y_0$, where y_0 is the maximum vertical displacement. But this retarding force is the elastic resistance to motion of the beam, and therefore $\frac{1}{2}F y_0$ is the corresponding strain energy stored in the beam when in the extreme position; that is to say, $U' = \Sigma \frac{1}{2}F y_0$. In this position the weights are at rest, and $U'' = 0$. Then, if the total energy in the system remain

constant, $U = U' + U'' = 0 + \dfrac{1}{2g} \Sigma W v_0^2 = \frac{1}{2}F y_0 + 0$; and

$$\frac{1}{g} \Sigma W v_0^2 = \Sigma F y_0 \qquad (1)$$

Suppose that the equation of motion is

$$y = y_0 \sin (at + \beta) ; \quad v = \frac{dy}{dt} = a y_0 \cos (at + \beta)$$

then, since the maximum value of $\cos (at + \beta) = 1$, $v_0 = a y_0$. Using Rayleigh's device, let $y_0 = qY$; and in consequence, $F = qW$; where Y is the actual static deflection at the weight W; then eq. (1) becomes

$$\frac{a^2}{g} \Sigma W y_0^2 = \Sigma F y_0 ; \quad \text{whence,} \quad \frac{a^2}{g} \Sigma WY^2 = \Sigma WY$$

and the periodic time τ is given by

$$\tau^2 = \frac{4\pi^2}{a^2} = \frac{4\pi^2}{g} \cdot \frac{\Sigma WY^2}{\Sigma WY} \qquad . \qquad (2)$$

identical with eq. (9), § 155, Vol. I. In many cases it is simplest to find the values of Y for the complete load system by means of a Williot diagram, or by one of the other methods given in Chapter I. Howland [20] suggests the following alternative. If M and N be any two loaded panel points of the frame, and a unit load at M produce a vertical deflection y_{nm} at N, a load W_m at M will produce a deflection $W_m y_{nm}$ at N. Therefore the

value of Y at N is $\Sigma\, W_m\, y_{nm}$, where the summation includes all the loaded panel points. Hence eq. (2) may be written

$$\tau^2 = \frac{4\pi^2}{g} \cdot \frac{\Sigma\, W_n(\Sigma\, W_m\, y_{nm})^2}{\Sigma\, W_n(\Sigma\, W_m\, y_{nm})} \qquad \cdot \quad \cdot \qquad (3)$$

Howland's paper may be consulted for more exact methods of treatment, including an analysis taking the inertia of the frame into account.

125. Lateral Vibrations in Columns.—The equation for the equilibrium of a rotating shaft under the action both of centrifugal force and an end thrust T is

$$EI\frac{d^4y}{dx^4} = \frac{wa^2}{g}y - T\frac{d^2y}{dx^2} \qquad \cdot \quad \cdot \quad \cdot \quad \cdot \quad (1)$$

see § 164, Vol. I, at end. In this equation the term wa^2y/g represents the lateral force due to centrifugal action. The corresponding equation for lateral vibrations in a column will be exactly similar, except that the term representing the steady, outwardly acting, centrifugal force will be replaced by $-\dfrac{w}{g} \cdot \dfrac{d^2y}{dt^2}$, the accelerating force produced by the vibrations, which always acts toward the centre of the column and therefore is negative. The symbol w denotes the weight of the column per unit of length. Then eq. (1) becomes

$$EI\frac{d^4y}{dx^4} = -\frac{w}{g} \cdot \frac{d^2y}{dt^2} - T\frac{d^2y}{dx^2} \cdot \qquad \cdot \quad \cdot \quad \cdot \quad (2)$$

The equation of motion is $y = y_0 \sin (at + \beta)$, and $\dfrac{d^2y}{dt^2} = -a^2y$, whence eq. (2) becomes

$$EI\frac{d^4y}{dx^4} - \frac{wa^2}{g}y + T\frac{d^2y}{dx^2} = 0 \qquad \cdot \quad \cdot \quad \cdot \quad (3)$$

As in eq. (1) the solution is (ibid.),

$$y = A \sin \gamma_1 x + B \cos \gamma_1 x + C \sinh \gamma_2 x + D \cosh \gamma_2 x \quad \cdot \quad \cdot \quad (4)$$

where

$$\left.\begin{aligned} \gamma_1^2 &= \frac{T}{2EI} + \sqrt{\left(\frac{T}{2EI}\right)^2 + \frac{wa^2}{gEI}} \\ \gamma_2^2 &= -\frac{T}{2EI} + \sqrt{\left(\frac{T}{2EI}\right)^2 + \frac{wa^2}{gEI}} \end{aligned}\right\} \qquad \cdot \quad \cdot \quad (5)$$

If the ends are merely position-fixed, $y = 0$ and $\dfrac{d^2y}{dx^2} = 0$ when $x = 0$ and $x = L$, whence $(\gamma_1^2 + \gamma_2^2)A \sin \gamma_1 L = 0$; $\sin \gamma_1 L = 0$; and $\gamma_1 L = r\pi$. Putting $r = 1$,

$$\gamma_1^2 = \frac{\pi^2}{L^2} = \frac{T}{2EI} + \sqrt{\left(\frac{T}{2EI}\right)^2 + \frac{wa^2}{gEI}} \qquad \cdot \quad \cdot \quad (6)$$

The fundamental periodic time $\tau = 2\pi/\alpha$ is, therefore,

$$\tau = \frac{2\pi}{\alpha} = \left\{ \frac{4w\mathrm{L}^4}{g\mathrm{EI}} \div \left(\pi^2 - \frac{\mathrm{TL}^2}{\mathrm{EI}} \right) \right\}^{\frac{1}{2}} \tag{7}$$

Solutions for the cases in which the ends are perfectly, or imperfectly, direction-fixed will be found in Bateman.[24]

TORSION IN THIN-WALLED PRISMS AND FRAMED STRUCTURES

126. Torsion in Thin Cylindrical Shells.—The effect of torsion on a cylindrical shell of any shape of cross-section, in which the wall thickness is small compared with the dimensions of the cross-section, may be found as follows (see Batho [27]) :

Let Fig. 196 represent an elementary length of the shell cut off by two parallel planes δl apart. The shell is subjected to a twisting moment M_t acting about an axis parallel to a generatrix. Let δc be an element of length of the circumference, and consider the equilibrium of the rectangular element $\delta l . \delta c$, indicated in Fig. 196. Suppose FF to be the shearing forces tangential

FIG. 196.

to the boundary acting on the sides δc, and SS the longitudinal shearing forces acting on the sides δl. Then, for equilibrium, $S . \delta c = F . \delta l$, or

$$\frac{F}{\delta c} = \frac{S}{\delta l}$$

If O be any point in the plane of the cross-section JK, and r the perpendicular distance of the force F from O, the moment of F about O is Fr. The sum of the moments about O of all such forces as F on every element right round the circumference is evidently the twisting moment M_t on the cross-section,

$$M_t = \Sigma \, \mathrm{F}r = \frac{S}{\delta l} \Sigma \, r . \delta c.$$

But $r . \delta c$ is twice the area of the shaded triangle in the figure, hence $\Sigma \, r.\delta c$, taken right round the boundary, is twice the area A of the cross-section, and

$$M_t = \frac{\widetilde{S}}{\delta l} . 2\mathrm{A} \; ; \; \text{or}, \quad \frac{S}{\delta l} : s = \frac{M_t}{2\mathrm{A}} \tag{1}$$

where s is the shearing force per unit of length on any generatrix of the shell. The shear stress,

$$f_s = \frac{s}{t} = \frac{M_t}{2\mathrm{A}t} = \frac{M_t}{Z_t} \qquad . \qquad . \qquad . \qquad . \tag{2}$$
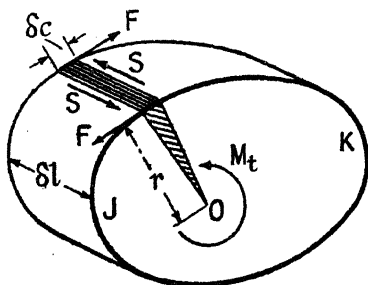
where $Z_t = 2At$ is the torsional section modulus; t is not necessarily constant, but the maximum shear stress occurs where t is a minimum. The shear stress f_s must be equal to the shear stress on δc at right angles to δl. The latter stress is evidently

$$\frac{F}{t \cdot \delta c} = \frac{S}{t \cdot \delta l} = \frac{M_t}{2At}$$

Since M_t and A are constant for every cross-section, it follows from eq. (1) that s is constant everywhere. If, in addition, t be constant, f_s is also constant. Further, since O is any point in the plane of the cross-section JK, the stresses are independent of the position of the axis of the twisting moment; see § 132, Vol. I.

The angle of twist $\delta\theta$ in the length δl can be found from the principle of work. The work done by the twisting moment in moving through the angle $\delta\theta$ is $\frac{1}{2}M_t \cdot \delta\theta$. The shear strain energy stored in the element $\delta l \cdot \delta c$ is

$$U = \frac{f_s^2}{2G} \text{ (vol. of the element)} = \frac{1}{2G}\left(\frac{M_t}{2At}\right)^2 t \cdot \delta l \cdot \delta c.$$

Then,

$$\tfrac{1}{2}M_t \cdot \delta\theta = \Sigma\frac{1}{2G}\left(\frac{M_t}{2At}\right)^2 t \cdot \delta l \cdot \delta c$$

the summation being taken right round the boundary; and therefore

$$\delta\theta = \frac{M_t \cdot \delta l}{4GA^2}\Sigma\frac{\delta c}{t} = \frac{M_t c}{4GA^2 t} \cdot \delta l \qquad . \qquad . \qquad . \quad (3)$$

if c be the total length of the circumference and t be constant. Hence the angle of twist θ in a length l of the shell is

$$\theta = \frac{M_t c l}{4GA^2 t} = \frac{M_t l}{\Phi} \qquad . \qquad . \qquad . \quad (4)$$

where $\Phi = \dfrac{4GA^2 t}{c}$ is the torsional rigidity of the shell.

Applying the above theory to a thin rectangular section B × D, wall thicknesses t and t_1, of which t is the smaller, (i) Fig. 197, $A = B \times D$; $c = 2(B + D)$; $Z_t = 2At = 2BDt$. From eq. (1),
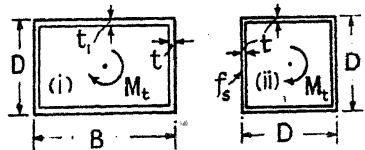
FIG. 197.

$$s = \frac{M_t}{2BD} \qquad . \qquad . \qquad . \qquad . \quad (5)$$

From eq. (2), f_s in the side B = $M_t/2BDt_1$; and,

$$\max. f_s = \frac{M_t}{2BDt} \qquad . \qquad . \qquad . \qquad . \quad (6)$$

From eq. (3),

$$\delta\theta = \frac{M_t \cdot \delta l}{4GA^2}\Sigma\frac{\delta c}{t} = \frac{M_t \cdot \delta l}{4GB^2D^2}\left\{\frac{2B}{t_1} + \frac{2D}{t}\right\};$$

whence $\qquad\qquad \theta = M_t l \; \dfrac{Bt + Dt_1}{2GB^2D^2tt_1} \quad \dfrac{M_t l}{\Phi}$. (7)

where $\Phi = \dfrac{2GB^2D^2tt_1}{Bt + Dt_1}$; see § 132, Vol. I.

For a square cross-section of side D and constant thickness t, (ii) Fig. 197,

$$ s = \frac{M_t}{2D^2} \,; \; f_s = \frac{M_t}{2D^2 t} \,; \; \Phi = GD^3t \qquad . \; (8) $$

If it be assumed that f_s is constant, this stress can be found from first principles thus : Total shearing force in one side $= Dtf_s$; moment about central axis $= Dtf_s \times D/2$; hence,

$$ M_t = 4Dtf_s \times D/2 = 2D^2tf_s $$

and $\qquad\qquad\qquad f_s = M_t/2D^2t.$

In a riveted tube, the shearing force due to M_t on a longitudinal or a transverse seam of rivets will be s per unit of length, and the rivets must be designed to carry this. Föppl found by experiment that the value of Φ in riveted cross-sections was considerably reduced owing to the give of the rivets ; see § 132, Vol. I.

127. Application to Framed Structures.—The theory may be applied to framed structures.[27] Let Fig. 198 represent a framed structure
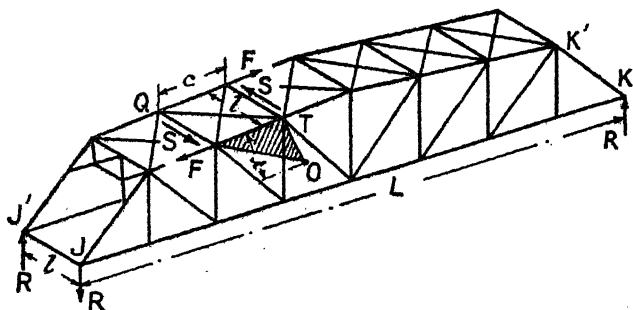
FIG. 198.

composed of two similar plane frames JK, J'K' connected together by lateral bracing. These frames may be the girders of a bridge or an arch, their outline being immaterial. Suppose that due to settlement or otherwise, up and down reactions RR are called into play at JJ'KK', as shown in the figure, such that the structure is subjected to a twisting moment $R \times l$. Considering a panel QT in the upper lateral bracing, let SS be the lateral shearing forces, due to the twisting moment, acting on the panel (cf. Fig. 196), and let FF be the longitudinal forces acting at the panel points which balance them. Then for equilibrium,

$$ S \times c = F \times l $$

where c is the length of the longitudinal member. Since there are no external forces acting on the lateral bracing, it is evident that the magnitude of S must be the same in each panel; S is therefore constant from end to end of the girder.

Let O be any point in the plane JTK, and r the perpendicular distance of F from O. Then the moment of F about O is Fr. The sum of the moments of the forces FF, at all the panel points of both top and bottom flanges of the framework JK, must evidently be equal to the twisting moment R $\times$ L produced by the two external forces RR acting at J and K in the same plane, i.e.

$$RL = \Sigma\, Fr = \Sigma \frac{Sc}{l} r = \frac{S}{l} \Sigma\, cr.$$

But cr is twice the area of the shaded triangle in Fig. 198. Hence, twice the sum of areas of all such triangles, formed by joining the ends of each bar in both flanges to O, represents Σcr. The sum of the areas of all these triangles is equal to the total area A of the frame JK, hence

$$RL = \frac{2SA}{l} \quad \text{or } S = \frac{RLl}{2A} \tag{1}$$

It will be evident that, had a panel of the bottom lateral system been considered, the same value for S would have been obtained; it follows that S is constant and has the same value in each flange.

If the moment Rl = M$_t'$ about an axis parallel to the plane JK be regarded as the twisting moment on the structure,

$$S = \frac{M_t'L}{2A} \tag{2}$$

Knowing S, the forces in all the bars of the lateral bracing can be found, and also those in the main girders due to the forces acting at the panel points. The stress diagram giving the forces in the members of the girder JK of Fig. 198 is shown in Fig. 199, R being taken as unity.
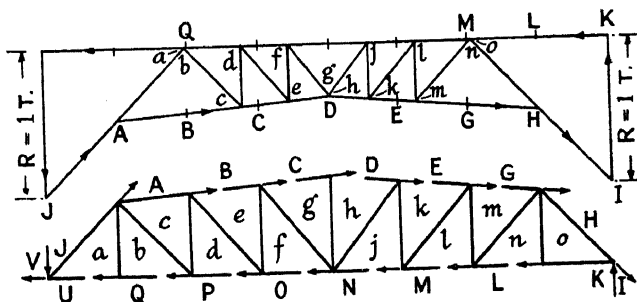
FIG. 199.

BIBLIOGRAPHY

Theories of Elastic Stability.

See Refs. Nos. 24 to 28. Bib., Chap. XIII, Vol. I.

Buckling of Flat Plates Subjected to Edge Thrusts.

1. BRYAN. On the Stability of Elastic Systems. *Proc. Camb. Phil. Soc.*, vol. vi, 1886–89, p. 199 ; also *Proc. Lond. Math. Soc.*, vol. xxii, 1891, p. 54.
2. REISSNER. Ueber die Knicksicherheit ebener Bleche. *Zentralblatt d. Bauerverwaltung*, 1909, p. 93.
3. TIMOSHENKO. Stabilität versteifter Platten. *Der Eisenbau.* Bd. xii, 1921, p. 147 ; see also Ref. No. 5.
4. PRESCOTT. *Applied Elasticity.* London, 1924, p. 479.

Buckling of Flat Plates Subjected to Shear Forces.

5. TIMOSHENKO. Sur la stabilité des systèmes élastiques. *Ann. d. Ponts et Chaussées.* Part. tech., 9ᵉ série, t. xvii, 1913, p. 386 ; also REISSNER, Ref. No. 2.
6. SOUTHWELL AND SKAN. On the Stability under Shearing Forces of a Flat Elastic Strip. *Proc. Roy. Soc.* A, vol. cv, 1924, p. 582.
7. WAGNER. Ebene Blechwandträger mit sehr dunnen Stegblech *Zeit. f. Flugtechnik u. Motorluftschiffahrt.* Bd. xx, 1929, p. 200 *et seq.* ; see also TIMOSHENKO, *Proc. 3rd Int. Cong. App. Mech.*, vol. iii, Stockholm, 1930, p. 12.
8. BERGMANN U. REISSNER. Ueber die Knickung von Wellblechstreifen bei Schubbeanspruchung. *Zeit. f. Flug. u. Motorluftschiffahrt.* Bd. xx, 1929, p. 475 ; Bd. xxi, 1930, p. 306 ; Bd. xxiii, 1932, p. 6 ; also SCHMIEDEN, *ibid.*, Bd. xxi, 1930, p. 61.
9. BERGMANN. Ueber Schubknickung von Isotropen und Anisotropen Platten. *Proc. 3rd Int. Cong. App. Mech.*, vol. iii, Stockholm, 1930, p. 82.
10. SEYDEL. Ueber das Ausbeulen eines Orthotropen Plattenstreifens bei Schubbeanspruchung. *Proc. 3rd Int. Cong. App. Mech.*, vol. iii, Stockholm, 1930, p. 89 ; also *Luftfahrtforschung*, Bd. viii, 1930, p. 71.

Lateral Stability of Deep Beams.

11. PRANDTL. *Kipperscheinungen.* Nuremberg, 1899.
12. MICHELL. Elastic Stability of Long Beams under Transverse Forces. *Phil. Mag.*, Sept. 1899, p. 298.
13. TIMOSHENKO. See Ref. No. 5 above, t. xvi, p. 75 ; also, Beams Without Lateral Support. *Trans. Amer. Soc. Civ. Eng.*, vol. lxxxvii, 1924, p. 1247.
14. —— Problems Concerning Elastic Stability in Structures. *Proc. Amer. Soc. Civ. Eng.*, Apl. 1929, p. 855.
15. PRESCOTT. The Buckling of Deep Beams. *Phil. Mag.*, Oct. 1918, p. 297, and Feb. 1920, p. 194 ; also *Applied Elasticity*, 1924, p. 499.
16. FEDERHOFER. Berechnung der Kipplasten gerader Stäbe mit veränderlicher Höhe. *Proc. 3rd Int. Cong. App. Mech.*, vol. iii, Stockholm, 1930, p. 66. For beams with curved axes and constant cross section, see *Der Eisenbau*, 1921, Heft 11 ; *Die Bautechnik*, 1924, p. 306.
    For the stability of plane framework with or without stiff joints, see v. MISES U. RATZERSDORFER. *Zeit. ang. Math. Mech.*, 1925, p. 218 ; 1926, p. 181. For the stability of Compression Flanges in Girders, see Bib., Chap. X, Refs. Nos. 17 to 22.

Elastic Vibrations in Framed Structures.

17. ENGESSER. Ueber die Schwingungsdauer eiserner Brücken. *Zeit. d. oest. Ing.- u. Arch. Ver.* Jg. xliv, 1892, p. 386 ; see also STEINER, *ibid.*, p. 113.
18. REISSNER. Zur Dynamik des Fachwerks. *Zeit.- f. Bauwesen.* Bd. xlix, 1899, p. 477 ; Bd. liii, 1903, p. 135.
19. POHLHAUSEN. Berechnung der Eigenschwingungen statisch-bestimmter Fachwerke. *Zeit. ang. Math. Mech.*, 1921, p. 28.
20. HOWLAND. The Vibration of Frames. *Select. Eng. Pap. I.C.E.*, No. 47, 1927.
21. PRAGER. Berechnung der Eigenschwingungen von Rahmenfundamenten. *Der Bauingenieur.* Bd. 8, 1927, p. 129, also p. 923; see also *Zeit. tech. Phys.* Bd. 10, 1929, p. 275.
22. KOHNO. The Theory of Vibrations of Rectangular Frames. *Jour. Inst. Jap. Arch.*, 1927, p. 1363.
23. TIMOSHENKO. *Vibration Problems in Engineering.* New York, 1928.
24. BATEMAN. The Transverse Vibrations of a Simple Strut. *Select. Eng. Pap. I.C.E.* No. 101, 1930.
25. BAN. Ueber die Knicklast und die Eigenschwingungszahl eines längs-belasteten Stabes. *Mem. Col. Eng. Kyoto Imp. Univ.*, vol. vi, Oct. 1931, p. 275.
For Pulsations, see Chap. IV, Bib., Refs. Nos. 10–13.
For Anti-Vibration Devices for Buildings, see *Zeit. Ver. deu. Ing.*, May 2, 1931, p. 544.

Torsion in Thin-Walled Prisms and Framed Structures.

26. BREDT. Kritische Bemerkungen zur Drehungselasticität. *Zeit. Ver. deu. Ing.*, July 11, 1896, p. 785 (Hollow Sections, p. 815).
27. BATHO. Torsional Stresses in Framed Structures and Thin-Walled Prisms. *Rpt. Brit. Assoc.*, 1915 ; see *Engg.* Oct. 15, 1915, p. 392. Also ROY, *Proc. 3rd Int. Cong. App. Mech.*, vol. ii, Stockholm, 1930, p. 39 ; and LEDUC, *ibid.*, p. 52.
28. SOUTHWELL. On the Determination of the Stresses in Braced Frameworks (includes the effects of torsion and shear). *Rpts. and Mem. Ad. Com. for Aero.*, No. 737, 1921 ; Nos. 790, 791, 819, 1922.

CHAPTER VIII

MANUFACTURE OF STRUCTURAL STEELWORK

128. Structural Material.—Ordinary steel structures are built up of plates and sections of mild steel (ult. tensile str. = 28 to 33 tons/sq. in.) rolled to definite sizes and shapes.

Plates.—These can be obtained in all sizes up to the following maximum sizes : length 40 ft., width 108 in., thickness $1\frac{1}{2}$ in., but the

Plate

Flat 12″×½″

4″×4″   6″×3½″   10″×3½″   6″×6″   5″×4″

Angles   Bulb Angle   Tees.
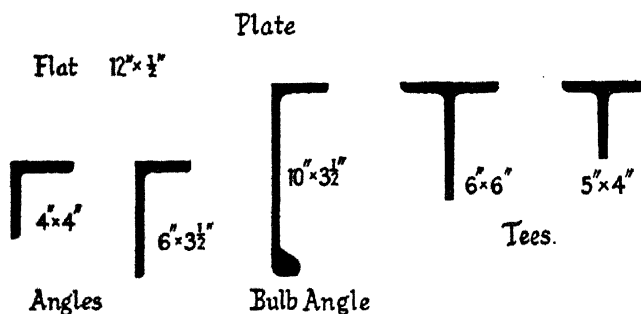
FIG. 200.

dimensions, area, and weight of any particular plate are subject to certain limitations, and extreme sizes are charged extra (see § 140). Such plates must be sheared to the exact size required. Plates rolled in a *universal mill* can be rolled to a definite width (usually not exceeding 45 in.) and have square edges ; edge planing after shearing to width is then unnecessary.

Flats.—These are narrow plates with square edges rolled to a definite width and thickness. They can be obtained in widths ranging from 2 to 20 in. and in thicknesses ranging from $\frac{1}{4}$ to 1 inch.

The more common rolled sections are illustrated in Figs. 200 and 201.

Equal Angles.—These can be obtained in sizes ranging from $1\frac{1}{4}$ × $1\frac{1}{4}$ × $\frac{3}{16}$ to 9 × 9 × $\frac{13}{16}$ in., and in lengths up to 60 ft. When the sum of the width and depth of the angle is less than 6 inches or greater than 12 inches, extras are charged ; also when the thickness is less than $\frac{3}{8}$ inch.

Unequal Angles.—These range in size from 2 × $1\frac{1}{2}$ × $\frac{3}{16}$ to 10 × 4 × $\frac{13}{16}$ in. They can be obtained up to 60 ft. in length, and are subject to similar limits and extra charges for extreme sizes and thicknesses as the equal angles.

Bulb Angles.—These are chiefly used for shipbuilding work. They range in size from $4 \times 2\frac{1}{2} \times 6 \cdot 29$ lb./ft. to $15 \times 4 \times 45 \cdot 40$ lb./ft., and can be obtained up to 60 ft. in length. When the sum of the width and depth of the angle is less than 9 inches or greater than $12\frac{1}{2}$ inches, extras are charged ; also when the thickness is less than $\frac{3}{8}$ inch.

Tees.—These range in size from $1\frac{1}{2} \times 1\frac{1}{2} \times \frac{1}{4}$ to $6 \times 6 \times \frac{3}{8}$ in. They can be obtained up to 60 ft. in length. When the added width and depth of the tee is less than 6 inches or greater than 12 inches, extras are charged ; also when the thickness is less than $\frac{3}{8}$ inch.

Channels.—These range in size from $3 \times 1\frac{1}{2} \times 4 \cdot 6$ lb./ft. to $17 \times 4 \times 51 \cdot 28$ lb./ft., and can be obtained up to 60 ft. in length. Extreme sizes are subject to extra charge.

Zeds.—These may be obtained ranging in size from $3 \times 3 \times 2\frac{1}{2}$ to $12 \times 3\frac{1}{2} \times 3\frac{1}{2}$ in., of different thicknesses, and up to 40 ft. in length without extra charge for length. Extreme sizes are charged extra.
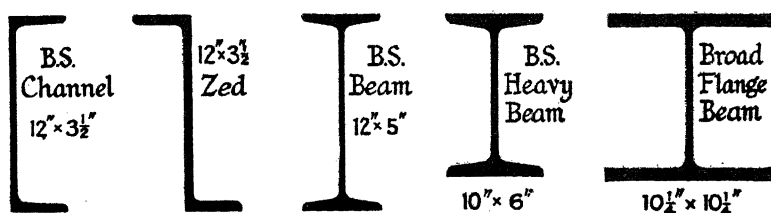
FIG. 201.

Beams.—In 1924 the British Standards Institution standardised two series of beam sections. The first series (girder sections) referred to as NBSB range in size from $3 \times 1\frac{1}{2} \times 4$ lb./ft. to $24 \times 7\frac{1}{2} \times 95$ lb./ft. The second series (heavy beams and pillars) referred to as NBSHB range from $4 \times 3 \times 10$ lb./ft. to $18 \times 8 \times 80$ lb./ft. In B.S. No. 4, 1932, the two series are merged into one, and additional sections have been added. Beams are obtainable up to 50 ft. in length without extra charge. Extreme sizes are charged extra.

Broad Flange Beams ranging in size from $4 \times 4 \times 13\frac{1}{4}$ lb./ft. to $40 \times 12 \times 234$ lb./ft. can be obtained. These sizes are approximate only, the actual dimensions are in metric units. Broad flange beams are rolled in a *Grey Mill,* and by this process it is possible to obtain a wider flange than in ordinary rolls ; which, in some cases, is an advantage.

Tables of the properties of the normal rolled sections are given in the Appendix. These are reproduced from the Handbook of Messrs. Dorman Long & Co., Ltd., by their kind permission.

129. In the Girder Shop.—It is now proposed to follow the course of a steel structure, such as a girder bridge, through the shops. This description is in no sense intended as a treatise on the practical manufacture of structural steelwork, but is intended to give to the student who is unfamiliar with the different shop processes, ideas as to the methods

employed. The practical art of structural steel construction can only be learned in the shops.

130. Drawing Office Work.—It will be assumed that the order has been secured for the construction of a girder bridge, and that a specification and detailed plans have been supplied. *Working lists of material* are first made, showing the size and shape of every piece of material and its position in the job. For the bridge in question there would be separate lists for the main girders, cross girders, rail bearers, flooring, and so on. From these lists the orders for the material are written out. In ordering plates from the mills, ¼ inch is added to the length and width of each plate, so that there is a margin of ⅛ inch all round for planing off. Sectional material (flats, angles, channels, etc.) may be ordered to the net length, but a margin of 1 inch is often added. If there are many short lengths of the same section, a long bar is ordered from which they may be cut. An extra ¼ inch is added to the length for each cut.

Meanwhile shop drawings are got out, detailing each separate part, and showing the position of every rivet hole. Practical operations can now be commenced.

131. The Template Shop.—The first step is to set out a main girder full size on the floor of the template shop. This is done with chalk and line, steel tapes, etc. Wooden templates of the exact size of each finished steel part are then made, the dimensions for which are taken from the full size set out. Some typical examples are shown in Fig. 202. (i) is the template for a girder flange ; (ii) that for a web ; (iii) shows the method of constructing a template for the flange angles. A template for a corner gusset is shown at (iv) ; and (v) shows how the template for a tension member of an open web girder would be made. Templates for small gussets, such as those for a roof truss, might be made of sheet zinc, sometimes even of cardboard or brown paper. In simple roof trusses, where the angles between the members can be easily ascertained, the shape of the gussets is sometimes set out directly on the templates, thus dispensing with the full size set out.

As will be seen from Fig. 202, all the necessary rivet holes are drilled
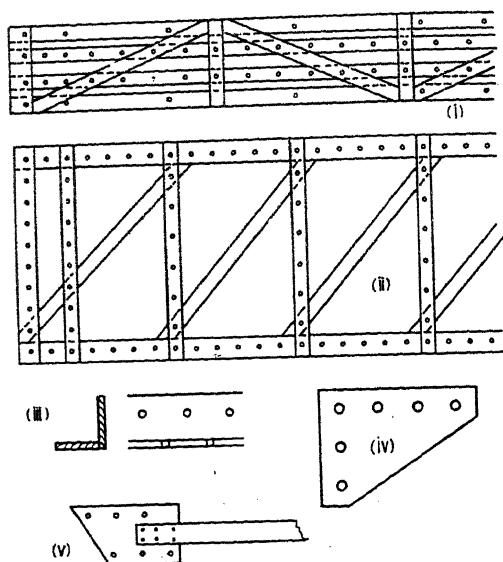
FIG. 202.

in the templates, exactly in the positions where they are to be placed in the job.   The finished templates will thus show the shape and size of each piece of material, and the position of each rivet hole therein.   These sizes and positions will correspond with the full size set out, and if the actual plates and sections be cut and holed to these templates, they should be of the correct sizes to build the structure.

In marking off a long row of holes in a template, the template maker squares across from a long steel scale fixed to his bench.   If the rivets have been arranged on a regular pitch of even inches, 3 in., 4 in. or 6 in., it is easy to do this ; if the pitches are odd and uneven, a great deal of time is wasted and mistakes are likely to occur.

It will also be readily understood that great economy will be effected if as many parts as possible be made of the same size, so that only one template need be made for them all.

132. The Material. Sorting and Straightening.—In the meantime the material will be arriving from the mills.   It is first sorted and laid out in proper order, so as to be readily available when required.   The next step is to straighten it.   Material direct from the rolling mills is seldom
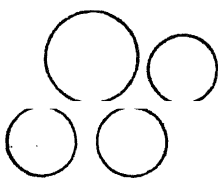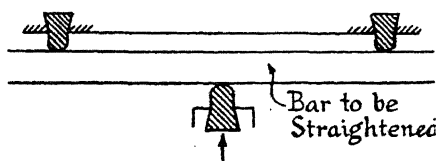
FIG. 203.   FIG. 204.

or never straight, the plates are slightly buckled and the sectional material slightly curved.   The plates are straightened by passing them through rolls as indicated in Fig. 203.   These rolls may have three or more rollers. Thin plates are straightened by hammering on a heavy surface plate. Sectional material is straightened by bending in a bending machine, illustrated diagrammatically in Fig. 204.   For heavy sections the machine is power operated, either hydraulically or by means of gear.   Light sections may be straightened on a hand-operated machine, or by hammering.

133. Planing and Cutting to Length.—The edges of the plates are now planed down to size in an edge-planing machine.   The plate or plates are clamped down to the bed of the machine and the tool moves, reversing at the end of its travel and cutting both ways.   The sectional material is cut to length, either in a cold saw or cropped in a shearing machine.   Large sections are cut in a circular saw ; small sections in a power hack-saw.   Angles and flats may be cropped ; gussets, etc., are sheared to size.

134. Marking Off.—The plates are next carried to the marking-off tables, the templates are clamped to them, and the holes marked with a

centre punch of the type shown in Fig. 205. This punch should be a good fit in the holes in the template. The centre of every hole is thus accurately transferred to the plate. In some yards a short length of tube dipped in whiting is afterwards passed through the hole in the template, leaving a white circle on the plate, which indicates more clearly the position of the hole. Instructions to the puncher or driller are usually painted on the plates at this juncture.

If the plate has to be cut to a special shape, as indicated by the shape of the template [for example a corner gusset, (iv) Fig. 202], this shape is also marked off on the plate. It should be remembered that there is no easy way of making a curve in a girder shop. If a curved edge is required, it is marked off from the template, and, if convex outward, sheared as closely as possible in a shearing machine. The edge is afterwards trimmed to shape by means of a pneumatic chisel. When convenient, as in the web of a plate girder, this may be done after the flange angles have been riveted to the plate; the angles then form a guide for the chisel. If the curve be concave, the only way of producing it is to go round the curve with a punch, and afterwards trim the rags off with a chisel.* It is not difficult to understand why girders with curved flanges cost more per ton than those with straight parallel flanges.

In some yards the wood templates are dispensed with as far as possible, and the marking off is done on the plates themselves, or from one part to another, the rivet holes being centre-punched as before. There is considerable difference of opinion as to which system leads to the more accurate work. In the highest class of modern bridgework, steel templates and jigs, sometimes with bushed holes, are used.

135. Punching, Reaming, and Drilling.—The next step is to make the rivet holes. There are three methods of doing this : (a) punching, (b) punching and reaming, (c) drilling from the solid. Punching is the oldest and quickest method of holing the plates. The modern punch is of the type shown in (i) Fig. 206. It carries a small nipple at its centre which is intended to enter the hole left by the centre punch. The rivet hole should then be correctly centred. In good punched work the holes should come together so well that a mandril $\frac{1}{16}$ in. less in diameter than
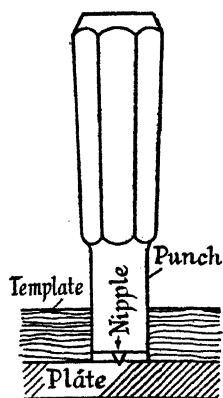
FIG. 205.
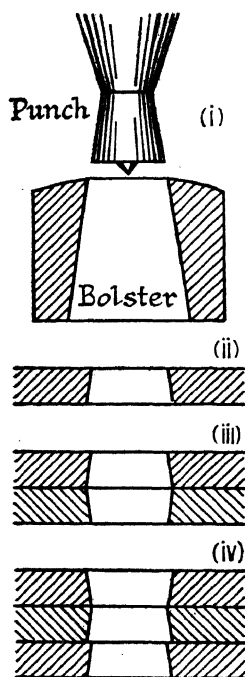
FIG. 206.

* Flame cutting with an oxy-acetylene blowpipe is a modern alternative.

the rivet holes will pass easily through them.   The normal rivet is $\frac{1}{16}$ in. less in diameter than the hole it is to fill, and it should then pass freely into the holes.   If not, the hole should be reamed out true, and a larger rivet used.   Owing to the necessary clearance in the bolster, the punched hole is always slightly tapered, (ii) Fig. 206, and the plates should be punched from the sides which are to be in contact, otherwise the state of things shown at (iii) will exist, and it is open to question whether the rivet will fill the hole.   The two top plates are correctly placed in (iv), but if a third plate is added as shown, it is impossible to avoid an irregular hole. Another disadvantage of punching is the lengthening of the member which takes place along a row of punched holes.   This may be quite appreciable unless the punch is kept sharp, and the clearance in the bolster is made as small as possible.   If the row of holes in the bar is not symmetrically placed, curvature is the result, which necessitates re-straightening.   In wide stiff plates the lengthening of the punched edges tends to crinkle the margins of the plates.   All this helps to destroy the accuracy of the work.

These objections to punching have led to its prohibition in first-class work, though an enormous amount of successful structural steelwork, even of the largest type, has been constructed with punched holes.   Until recent years the usual alternative was to punch the holes $\frac{1}{4}$ in. less in diameter than the finished dimension, and afterwards to ream them out to size.   The work was assembled as far as possible, service-bolted together, and the drill or reamer put through the holes with the plates in position.   The process ensures true parallel holes, and, in addition, any material injured by punching is removed.   Troubles due to lengthening are not entirely overcome, but most of the objections to punching are obviated.   For the purpose of reaming, a series of radial drilling machines are used, the work is assembled on trolleys and then run under the drills. In structures too large to be handled in one piece, such for example as large open-web girders, the separate parts would be assembled, and all the holes reamed at the radials except those for connecting the different parts together, which would be reamed *in situ* after the work as a whole is assembled.

With the advent of modern high-speed tool steels, this process has been very largely superseded by drilling from the solid, thus eliminating the initial punching altogether.   As far as possible the plates are assembled in batches, the top plate only being centre-punched, and the drill passed right through the batch.   For example, the several thicknesses of a girder flange would be assembled, clamped together, and drilled as one piece.   In tank work, where many plates are alike, the top plate of one batch may be used as a template for the purpose of drilling the next batch.   The accuracy of the process is evident, and when care is taken in the design to make many plates alike, both as to size and arrangement of rivet holes, the method is very economical.   There is one drawback : after drilling, the plates in the batch should be taken apart and the fraze or burr left by the drills removed, otherwise the rivets cannot draw the plates up together tightly, and rusting between them will be the inevitable

result. To do this is not only an extra expense, but in a case like the girder flange with many plates, when once the plates have been separated it is never possible to get them back absolutely in the same place, so that to some extent the accuracy of the process is sacrificed. Nevertheless, drilling from the solid is by far the best method of making the rivet holes, and is gradually eliminating the other methods.

136. The Smithy.—The plates and sectional material are now ready for erection, with the exception of those parts which have to be worked hot. These are made in the smithy. The commonest of these parts are the kneed and joggled stiffeners used in plate girders (Fig. 262). There are two methods of constructing such members ; they may be hand forged (Fig. 207 will suggest the smith's method of forging a kneed stiffener), or if there are many alike, they may be more quickly and easily produced in a hydraulic press by means of suitable dies. Bent gussets and plates are also made in the smithy, and such parts as require welding in the forge, though such welding should be avoided as far as possible in structural
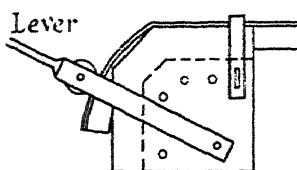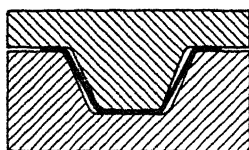
FIG. 207.   FIG. 208.

work. Trough sections for bridge floors form part of the smith's work. These are pressed between blocks in heavy hydraulic presses as indicated in Fig. 208. With the exception of stiffeners for plate girders, all parts which have been made hot should afterwards be properly annealed. Heating the steel injures the microstructure, annealing is necessary to restore it to a proper condition. For this reason, as far as possible, all bends should be made cold.

All smith's work should be sound and clean ; if the metal has been burnt, the part should be rejected.

137. Erection.—The next step is the assembling and erection. The various parts are brought together in position, drifted up tight, and service-bolted together. Drifts are either taper pins 6 to 8 in. long with about $\frac{1}{4}$-in. taper in their length, or cylindrical pins turned down a little at each end so that they may easily be driven in and out either way. Their function is to bring the work up together tightly before the service bolts are put in. It will easily be understood that by flogging a taper pin into the rivet holes with sufficient force, much damage may be done to the plates, and the use of drifts to enlarge unfair holes is rightly prohibited.

Where two surfaces come together permanently, they should first be cleaned and given a coat of hot linseed oil. Much rusting between the plates is obviated by this precaution.

After everything is properly adjusted and bolted up tight, any necessary reaming, and odd holes needing countersinking, are attended to, and the work is then ready for riveting.

138. Riveting.—If the work is not too large for transport in one piece, it will now be completely riveted up. This is the ideal state of affairs, for ' shop ' riveting is always better than ' field ' riveting. Very often, owing to its size, the structure has to be sent away in parts. Only such riveting can then be done as is consistent with the proposed methods of transport and re-erection. Occasionally the structure has to be shipped ' piece small,' i.e. all in separate pieces, when the whole of the riveting has to be done after re-erection.

There are several methods in use for closing the rivets : hydraulic, pressure pneumatic, percussive pneumatic, and hand riveting. The last-mentioned was the earliest process, and if the rivets do not exceed $\frac{7}{8}$-in. diameter, given skilful men, excellent work may be turned out. Since the shank of the rivet has to be ' upset ' through the whole of its length in order to fill the hole, the rivet should be brought to a welding heat from end to end, with a white-hot point. When it cools it will contract and draw the plates tightly together.

Except in positions where a machine riveter cannot be employed, hand riveting has now been superseded by machine riveting ; although, if a large number of countersunk rivets have to be closed, some still prefer hand riveting. With pressure riveting, either hydraulic or pneumatic, an enormous force is used to close the rivet. This force may range from 20 to 60 tons or more, depending on the size of the rivet. Such forces are sufficient to expand the rivet and fill the hole, even if the rivet be fairly cool. Not only so, but with such great pressures, the plates are forced together irrespective of the contraction of the rivet. This contraction is a source of danger with pressure riveting, for if the plates are already hard up before the rivet contracts, when the contraction occurs something has to give, and that something is the rivet. Large initial strains in the rivet may be the result, and it is no uncommon thing for the heads to fly off. With pressure riveting, therefore, a fairly cool shank and a hot point are desirable. Given these conditions, the best work of all is that done by pressure riveters. There is not much to choose between hydraulic and pressure pneumatic riveting, but for certain practical reasons the latter appears to be gaining ground at the expense of the former.

Pneumatic percussion riveting partakes more of the character of hand riveting, except that the blows are delivered by means of a pneumatic hammer. It is a very much quicker process. As in hand riveting, a hot shank and a white-hot point are necessary, otherwise the holes will not be properly filled, and the plates will not be drawn together as they should be ; the pneumatic hammer delivers blows and does not operate by pressure. Properly done, such riveting should be superior to hand riveting.

Whichever system be used, the rivets should completely fill their

holes; the heads should be well formed, and concentric with the shanks. Loose rivets, or rivets with cracked, burnt or badly formed heads, should be cut out and replaced.

139. Finishing Off. Painting.—The work has now reached its final stages. After any necessary finishing touches have been given, and the final inspection has been made, assuming that any specified tests of the complete structure have been satisfactory, the work is ready for painting. It is first scraped and cleaned to remove any rust and then given the required number of coats of paint.

If, by general agreement, structural material were given a coat of boiled oil immediately it comes from the rolls, and before it gets cold, the work of cleaning and painting would be simplified and much subsequent rusting and repainting avoided.

If the work is to be re-erected, erection marks are now painted on all the members so that they can be easily reassembled on arrival at their destination. The structure is now ready for despatch. Unless it is to go as a whole it must be dismantled, and suitable protection provided for parts which may be injured during transit. The smaller pieces will be packed in cases.

140. Practical Points affecting the Design.—It will be evident from the foregoing that the cost of manufacture will be very greatly affected by the details of design. Emphasis has already been laid on the necessity for simple straight line designs, with regular rivet pitches, and with as many parts as possible made to the same template, but there are other points which considerably affect the cost of the work and the time of delivery. One of the most important of these is the size of the rolled sections which are chosen. Rolling mills work to a programme which is settled a week or so in advance and is determined by the orders in hand. If very common everyday sections are chosen, one or more of the mills are sure to be rolling them, and they can be quickly and easily obtained. If unusual sections are called for, even though they can be found in the British Standard list, it means waiting until sufficient orders accumulate to warrant putting in the rolls, and the more out-of-the-way the section, the longer the wait. Unless a large quantity of an unusual section (say from 20 to 50 tons) be required, such a section should not be specified. The cheapest and commonest of all sections are plates and angles for general work, and rolled beam sections for steel-framed buildings. All sizes and thicknesses of plates can be readily obtained up to the maximum dimensions rolled. The more common sizes of rolled sections other than beams are indicated in the following list:

Equal Angles.	Unequal Angles.	Tees.	Channels.	Flats.
4 × 4	4 × 3	6 × 3	6 × 3	3″, 4″
3 × 3	5 × 3	4 × 3	8 × 3½	5″, 6″
3½ × 3½	6 × 3½	5 × 3	9 × 3	8″, 9″
2½ × 2½	3 × 2		10 × 3½	10″, 12
6 × 6	6 × 3		12 × 3½	
4½ × 4½	6 × 4		15 × 4	

Tees and **I** beams are rolled to definite shapes which cannot be altered. Channels are also rolled to definite shapes, but the thickness of the web can be slightly increased by moving the rolls further apart if the quantity required justify the alteration. Plates, angles, and flats should be ordered in thicknesses of $\frac{1}{8}$ths of an inch, i.e. $\frac{3}{8}$, $\frac{1}{2}$, $\frac{5}{8}$ inch, etc., but if the quantity required warrant the difference, $\frac{1}{16}$ths may be introduced. The width of flats should be given in even inches.

As to length, it is generally not advisable to go to the maximum lengths the makers can roll. An extra price is charged for such extreme lengths ; difficulties regarding transport and handling in the shops occur, which usually more than counterbalance the saving of a joint. In ordinary work the following lengths should not be much exceeded : Angles 40–45 ft., tees 30–40 ft., channels and **I** beams 30–35 ft., plates and flats 35 ft. Extras are also charged for extremely wide plates, and there is a maximum area which may not be exceeded for a given thickness. Makers' handbooks should be consulted for these details, but in ordinary structures it is usually not advisable to exceed 6 ft. in the width of a plate.

In any structure, the fewest number of different sections consistent with good design should be used, and it is usually more economical to use the same section for different members, even though it be slightly too heavy for some, rather than introduce a small quantity of a new section.

ELECTRIC ARC-WELDING

141. Electric Arc-Welding.—The art of fusion welding as a means of making joints in structural work has been greatly developed in recent years. Both gas (oxy-acetylene) welding and electric arc-welding are used, but the latter has been much more extensively applied. It opens up a new range of possibilities in the manufacture of structural steelwork. In suitable circumstances, with proper electrodes and skilled labour, joints can be made equal in strength to that of the solid bar which they connect. Among its advantages may be instanced : (i) saving in weight of steel, probably in ordinary structures of the order of 10–15 per cent. ; (ii) economy in cost ; (iii) convenience in construction ; (iv) no loss of area caused by holes in tension members ; (v) reduction in the size of gussets and other connections ; (vi) reduction of noise during construction.

On the other hand, there are certain disadvantages yet to be overcome in connection with the process : (i) Good arc-welding depends, more perhaps than in any other practical operation, on the skill and care of the operator, and so far, except for visual inspection (much is revealed to the trained eye), no simple and practical field test for soundness has been devised. (ii) Resulting from the process of welding, severe internal stresses may be set up in the vicinity of the weld, and considerable distortion of the parts may take place. (iii) The ductility of welded joints is often considerably less than that of the parts which they connect. (iv) Welded joints are very rigid joints—this is sometimes an advantage,

often a disadvantage, but always to be taken into account in design. (v) The fatigue strength of welded joints is low, in some cases only one-half that of the steel. Much can be done by proper design and by practical manipulation to minimise some of the above objections.

Electric arc-welding is of great utility in connection with the strengthening of existing structures.

142. Method of Operation.—It is not proposed here to discuss the technique of welding, but merely to outline the process. The essential feature in electric arc-welding is to deposit a bead or fillet of weld metal between the parts to be joined in such a way that the edges of those parts are melted, and the bead is fused into both. It is not a mere soldering process. The fusion is effected by means of an electric arc. The parts to be joined form one electrode, the other is a steel rod or wire which melts during the operation and forms the deposited metal. Direct current is commonly used, at pressures up to 80 volts on open circuit, and for large work a current up to 300 amps. is required. Alternating current is also employed. The welding rod, called *the electrode*, may be of bare wire, but preferably is provided with a coating whose chief function it is to melt and form a flux to protect the molten metal from oxidization. The size of the electrode and the amperage is varied to suit the size of the work. Large fillets are built up by the addition of a number of *runs*, see Fig. 211 ; the surface of one run must be thoroughly cleaned of all oxide and slag before the next is applied. The work generally, before and during welding, must be kept clean, and the mill scale, etc., removed by means of a wire brush.

Common Faults.—The chief faults to be avoided in welding are : (i) *Incomplete Fusion.* The deposited weld metal must be thoroughly fused with the parent metal along all surfaces. (ii) *Lack of Penetration.* The weld metal must penetrate right into the roots of the joint. (iii) *Slag Inclusions.* As far as possible the weld must be free from non-metallic inclusions, blow-holes, etc. (iv) *Undercutting and Overlap.* The weld must possess a convex contour, and the parent metal must not be undercut (melted away along the edges of the weld). The weld metal should not overlap the parent metal along the edges without being properly fused thereto.

143. Types of Weld.—The different types of weld and their names are shown in Figs. 209 and 210. *Single and double* V *Butt Welds* are illustrated at (i) Fig. 209. The angle of the V should not be less than 70°, and the edge of the plate should not be sharp but left square for about $\frac{1}{16}$ in. The gap between the plates may be $\frac{1}{16}$ in. for plates $\frac{3}{8}$ in. thick and under, and $\frac{1}{8}$ in. for thicker plates. When one plate only is bevelled, the angle is made 45° and the gap $\frac{1}{8}$ in. Plates under $\frac{1}{8}$ in. thick need no V. The wide extremity of the weld is *reinforced,* i.e. made convex, so that the area is 10 per cent. greater than that of the plate. In single V butts, unless the two plates rest on a third, to which they are to be attached, the underside of the V should be reinforced by a run of weld metal to ensure that the fusion penetrates right to the bottom of the V.

Butt welds are largely used for pipes, ship plates, tanks, and similar constructions.

Fillet welds are shown at (ii), (iii) and (iv). These are usually made triangular in shape (45°), reinforced on the outer surface, see Fig. 212 ; (iii) is called a *longitudinal* or *shear fillet*; and (iv) a *transverse* or *tension*

Single V Butt Weld. (i) Double V Butt Weld
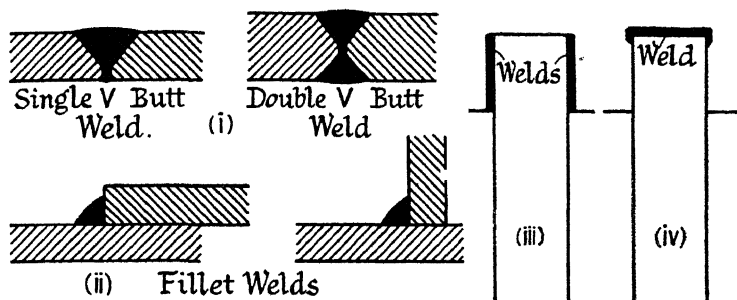
(ii) Fillet Welds

FIG. 209.

fillet, which should be returned at its ends as indicated. Shear fillets are commonly used for structural constructions. Long fillet welds may be continuous when required for strength or watertightness, but intermittent welds, in which the parts are welded together in short lengths with gaps between, are often sufficient for strength. Very short intermittent welds, called tack welds, may be used as temporary attachments for the parts to be connected, and afterwards be incorporated with the continuous joint. This proceeding diminishes contraction stresses. Some examples of *slot welds* are given in Fig. 210. A rectangular slot is formed in the member to be connected of width b_1 not less than its thickness t. The weld is made inside the slot ; its depth t_1 should not be less than one-half the width b_1. Such welds are used for the connection of heavy structural members; the weld is placed in shear.

144. Admiralty Practice.—As typical of good British practice, the following is abstracted from *Notes on Welding Practice in British Warships* communicated to the *Welding Symposium*, London,[31] 1935, by the Director of Naval Construction.

FIG. 210.

Fillet Welds.—The overlap for plates is $3t$ up to and including 10 lb. plating (10 lb./sq. ft.), $4t$ for heavier plating ; $\frac{1}{8}$-in. and $\frac{3}{16}$-in. fillets are made with one run of 10-gauge electrodes ; $\frac{1}{4}$-in. fillets with 1 run of 8 gauge. Larger fillets are made with a first run of 10 gauge to ensure good penetration in the corner, and subsequent runs of 8 gauge. For a $\frac{3}{4}$-in. fillet, nine runs are used. The manner in which $\frac{1}{4}$-in. and $\frac{1}{2}$-in.
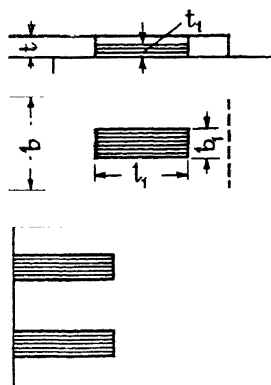
fillets are built up is shown in Fig. 211. In Admiralty practice the leg in shear is made 25 per cent. longer than that in tension. Such welds exhibit an ultimate strength which exceeds 26 tons/sq. in. on the theoretic throat area.

Butt Welds.—A 60° V weld is used. The plate is left $\frac{1}{16}$-in. square at the bottom. For plates up to and including 10 lb., a $\frac{1}{16}$-in. gap is used ; $\frac{3}{32}$ in. from 10 to 15 lb., and $\frac{1}{8}$ in. for plates over 15 lb. The first run at the bottom of the V is made with a 10-gauge electrode, and
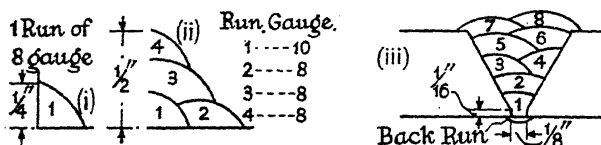
FIG. 211.

successive runs of specified length with 8 gauge, until the joint is reinforced 10 per cent. To ensure complete penetration at the bottom, it is important to make a back run and to arrange the design so that this may be done. For plates $\frac{3}{8}$ in. thick a 10-gauge electrode is used, and an 8 gauge for thicker plates. A typical example is shown in (iii) Fig. 211. For all the more important work, high quality, heavily-coated electrodes are used. Direct current is employed, with the electrode on the positive pole.

145. Strength of Welds.—In a fillet weld the dimension a is given as the size of the weld, Fig. 212. The minimum width b is called the *throat* of the weld, and the breaking load, divided by the area of the plane containing b, is called the ultimate strength of the weld. In making this calculation, the extra width due to the reinforcement is neglected. The same convention is used for both shear and tension welds. In a butt weld, the width of the weld in the plane of the minimum width (less the reinforcement) is called the *throat*, and the breaking load divided by this area is called the ultimate strength of the weld.
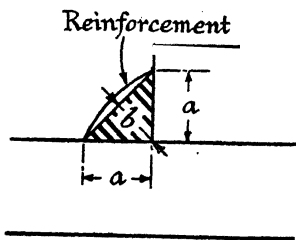
FIG. 212.

The ultimate strength of welds, as determined by experiment, varies considerably with the test conditions. Probably the most extensive series of tests are those carried out by the American Welding Society.[10] In these tests, bare wire electrodes were used, the ultimate strength of the deposited metal averaging about 50,000 lb./sq. in., which may be taken as the ultimate strength of butt welds. The ultimate strength of fillet welds in shear averages about 40,000 lb./sq. in., and in tension 45,000 lb./sq. in.

According to Freeman's experiments,[22] using coated electrodes (Quasi-arc), on specimens welded on the flat under shop conditions, with

slightly reinforced fillets, Fig. 212, when $a < \frac{1}{2}$ in., the ultimate strength of longitudinal shear fillets, (iii) Fig. 209, is $12 \cdot 8\,a$ tons per inch of length, and of transverse tension fillets with returned ends, (iv) Fig. 209, is $21 \cdot 3\,a$ tons per inch of length, or 20 per cent. less if the ends are not returned.

Working Stresses.—The 1930 American Building Code for Fusion Welding permits the following stresses on the throat area : shear 11,300 ; tension 13,000 ; compression 15,000 lb./sq. in. Fillet welds placed transversely to the direction of the stress are to be considered as in shear, so that the safe load on both types, (iii) and (iv), Fig. 209, of fillet welds is $8000a$ lb. per inch of length, where a is in inches. These values apply to joints made with bare wire electrodes.

With electrodes possessing the specified mechanical properties, the British Standard permits a working stress in butt welds in tension or shear of 85 per cent. of the permissible stress in the parent metal, or for butt welds in compression of 100 per cent. of such stress. For fillet welds in shear, the permitted stress is 5 tons/sq. in., or $3 \cdot 56\,a$ tons per inch of length ; and for fillet welds in tension, the permitted stress is 6 tons/sq. in., or $4 \cdot 24\,a$ tons per inch of length. The safe load on slot welds of the proportions prescribed above, Fig. 210, is $5b_1$ tons per inch of length.

In these formulae the length to be used is the length of weld of full cross section, exclusive of any craters at the ends, unless the latter are properly filled up. All the above values are for quiescent loads.

Mechanical Tests.—The British Standard requires from test specimens of deposited weld metal a minimum *ultimate tensile strength* of 28 tons/ sq. in., a minimum *elongation* of 20 per cent. in $3 \cdot 54$ diameters, and an Izod *impact value* of 30 ft.-lb. *Butt welds* in tension must exhibit an ultimate strength of 28 tons/sq. in., and stand a 90° *cold bend test* round a diameter of 4 times the thickness. The ultimate strength of *fillet welds* must be 27 tons/sq. in. in tension, and 18 tons/sq. in. in shear. For details of the tests and method of constructing the specimens, the British Standard for Metal Arc Welding should be consulted.

Non-destructive Tests.—While it is true that the characteristics of a bad weld, faulty manipulation, etc., can be recognised by an experienced eye, particularly if the inspector be present while the welding is in progress, the need for a non-destructive test of the finished work, whereby imperfect fusion, lack of penetration, inclusions, blow-holes, and other hidden faults would be made manifest, has often been felt. Of the methods proposed, only X-ray examination appears to have reached the practical stage, and this particularly for butt welds in pressure vessels, when the material is not too thick. The measurement of magnetic reluctance, or of the drop in electric potential, across the weld has been tried ; positions where the magnetic or electric resistance is abnormally high indicating faulty welding. Alternatively, in the Sperry test, an observation of current deflection by magnetic means is used as an indication. None of these methods has yet passed the experimental stage, and like the X-ray test are not very suitable for the examination of fillet welds. Listening

through a medical stethoscope while the joint is being tapped has been tried in America.

146. Fatigue in Welds.—Experiment has shown that the fatigue strength of welded joints is low compared with that of the parent metal. In some rotating bar tests on fillet welds made with bare wire electrodes, Petersen and Jennings [35] found that the limiting range of stress of the welded joint was approximately one-half that of the steel. More recent experiments made at the N.P.L.,[37] on a 20 million reversal basis, exhibit a limiting range of stress in rotating bar test-specimens, of deposited weld metal, of about two-thirds that of mild steel of the same tensile strength ; and in the case of fillet and butt welds, subject to direct stress fatigue tests, not much over one-half. For these welds, high-class covered electrodes were used ; with bare wire electrodes even lower results were obtained.

These low values are due to the presence of blow-holes and slag inclusions in the weld metal, which act as 'stress raisers,' and to stress concentrations in the welded joints. It was found in the N.P.L. experiments and others that fatigue fractures in the weld metal always commence at blow-holes or inclusions, whilst those in joints commence at areas of marked stress concentration at the roots of the fillets. Uneven distribution of stress along a fillet weld is of great importance in joints subjected to repeated loading.

Direct stress fatigue tests on a 5 million cycle (minimum) basis, by Haigh,[36] using specimens turned to $\frac{1}{2}$-inch diameter from 1-inch mild steel plates with V butt welds, showed a limiting range of stress between $0 \pm 5\frac{1}{4}$ and 0 ± 6 tons/sq. in. The welds were of good quality, but deliberately made to contain small flaws due to cavities or slag inclusions, such as are always liable to be present in practice. In a solid mild steel specimen of 28/30 ton steel, yield point about 16 tons/sq. in., the corresponding limiting range of stress would be about $0 \pm 11\frac{1}{4}$ to 0 ± 12 tons/sq. in. ; but Professor Haigh points out that a small hole drilled right through the centre of the solid specimen as a 'stress raiser' would diminish these figures to about $0 \pm 8\frac{1}{2}$ to 0 ± 9 tons/sq. in., whereas a similar 'stress raiser' through the weld did not affect the strength, for the crack started elsewhere at a slag inclusion.

Similar tests in which the mean stress was not zero gave the following limiting ranges of stress :

$$+ 10 \pm 4; \quad + 6 \pm 4 \cdot 5; \quad 0 \pm 6; \quad - 3 \pm 7; \quad - 5 \pm 8.$$

In another series of tests, made on specimens in which the skin was not removed by turning, slightly better results were obtained, showing that surface irregularities do not further weaken the joint. In a further series of tests on double V butt welds, in which the fusion between the parent metal and the weld metal was not good, and in which the weld metal had not fused at the bottom of the V's, the limiting range of stress was only 0 ± 3 to $0 \pm 3\frac{1}{2}$ tons/sq. in. reckoned on the gross section of the plate.

In a series of fatigue tests made by the V.D.I. Berlin,[38] the specimens consisted of a welded member 6 to 8 ft. long forming the central panel in the tension flange of an experimental bridge girder of about 50 ft. span. The stress repetitions were effected by means of an oscillator, § 62; the frequency was regulated to avoid resonance. The experiments were made on a 2 million cycle basis. A number of different types of joint were tested, both electrically and oxy-acetylene welded, and three different qualities of steel were used.

It was found that the shape of the joint has much greater influence than any other factor. The fatigue strength was approximately the same for all three kinds of steel, and unless the constant stress is high, high tensile steel has no great advantage. The number of cycles to fracture was about the same for bare wire electrodes as for the covered electrodes used. Static tensile strength is of less importance than good ductility. For side (shear) fillet welds, a minimum elongation of 15 per cent. in the weld metal is essential. Butt welds resist fatigue better than fillet welds, and continuous welds better than intermittent welds. The endurance limit of plain butt welds was $5 \cdot 7 \pm 5 \cdot 7$ tons/sq. in., which was increased to $7 \cdot 6 \pm 7 \cdot 6$ by machining the surface of the welds. They should be thoroughly welded at the root. The endurance limit depends on the shape of the member itself as well as on that of the joint. Stress concentrations and abrupt changes in section must be avoided. Smooth curves between the parent metal and the weld should be used. Concave welds are better for end fillets than convex welds.

147. Contraction Stresses. Distortion. Effect of Rigidity.—As the welding proceeds, not only is the weld metal deposited in a molten state, but the temperature of the parts being joined is also raised to the melting point, and the metal in the immediate vicinity expands considerably. As the weld cools, the weld metal and the other heated parts contract. This contraction is resisted by the cooler parts of the structure and initial stresses are set up. Serious stress concentrations may be the result, particularly at the ends of joints and at the roots of fillets. It is quite possible also that the thermal disturbance may result in the release or redistribution of existing internal stresses in the parts, caused by rolling or subsequent cold work.

The effect of the stress concentrations is shown in the early failure of welded joints under repeated stress (see *supra*); and even under a dead load the parent metal may give way at a low stress, as did many of the plates in Freeman's experiments,[22] which, though of normal 28/33 ton mild steel, *tore* across at about 20 tons/sq. in. with little sign of ductility.

In thin constructions, contraction stresses and the release of internal stresses result in distortion of the parts.

These effects may be mitigated by careful design and proper manipulation during welding. Whenever possible, freedom to move should be permitted to at least one of the parts to be joined. This is essential in the case of butt welds. A tie bar should not be butt welded at each end between two rigid flanges; fillet welds should be used. The stiffer parts

of a structure should be welded first, and the less rigid members attached later, otherwise distortion occurs in the latter. It is possible to avoid distortion by giving initial set or curvature to one or other of the parts, e.g. in a stiffener to be attached to a bulkhead in a ship ; the edges of thin plates are sometimes kept stretched while the welding proceeds. ' Step-back ' welding should be adopted for long continuous runs. In this the operator welds a short length AB, then stops and starts again at C behind A and welds from C to A, and so proceeds. As far as possible the work should be so arranged that the tensile and compressive stresses set up tend to balance one another. Pressure vessels are annealed or otherwise heat treated to eliminate initial stress.

Two factors alleviate the effects of initial stress. Each subsequent run partially anneals those previously deposited, and so reduces the contraction stresses ; and, further, there is little doubt that under dead loading, plastic yield and strain hardening—which take place when, due to stress concentrations the yield point is exceeded locally—are the salvation of the situation, and every improvement in the ductility of welded joints is of the greatest importance.

Rigidity.—Welded joints are rigid joints. The percentage elongation in bars with welded joints is frequently small. Experiment [16] has shown that secondary stresses in frameworks are higher with welded than with riveted joints. There are many cases in which it is customary to neglect any rigidity which a riveted joint may possess, where in welded construction such neglect might be serious. This rigidity must always be borne in mind in design.

148. Combined Welded and Riveted Joints.—Owing to the much greater rigidity of welded joints compared with riveted joints, a partly welded partly riveted joint is not a very satisfactory one, for the weld carries the major portion of the load. Such combinations, however, are frequently used in strengthening existing bridges and structures, in which cases the objection is not so important, for the rivets will be carrying the stress due to the dead load of the structure before the welding takes place, and the weld comes in to carry the major portion of the live load stress. Professor Kayser [24] has made several experimental studies of combined welded and riveted joints, and concludes that the ultimate strength of the combination is that of the welds plus two-thirds of that of the rivets. Short longitudinal fillets should be employed where possible, and not transverse fillets, which prevent deformation in the direction of the load.

149. Typical Welded Constructions. Method of Calculation.—
Minimum Size of Weld.—For thicknesses of $\frac{1}{4}$ in. and over, the minimum size of weld should be $a = \frac{1}{4} + \frac{1}{3}(t - \frac{1}{4})$, and in length $1\frac{1}{2}$ in., where t is the thickness of the member being attached. Size of welds : $\frac{1}{4}, \frac{5}{16}, \frac{3}{8}, \frac{1}{2}, \frac{5}{8}, \frac{3}{4}, \frac{7}{8}, 1$ inch.

Allowance for Crater.—In the equations given below, l is the length of the weld of full cross-section exclusive of any crater (unless the latter be filled in) or of any portion tapering, or not up to size.

Ties and Struts.—In a member in direct tension or compression, connected by fillet welds in shear, if both member and welds are symmetrically placed with respect to the axis of load, (i) Fig. 213,

$$F = 2ls \; ; \; \text{and} \; l = F/2s \quad . \quad . \quad . \quad . \quad (1)$$

where F is the force in the member in tons, l is the length of each weld in inches, and s is the safe shear force per inch of length = $3 \cdot 56\,a$ tons/in. for a dead load. The length l should not be less than $\frac{3}{4}$ the breadth of the member. If the weld is carried round the top end of the member, (ii) Fig. 213, and the conditions are symmetrical,

$$F = 2ls + Bs_t \; ; \; \text{and} \; l = (F - Bs_t)/2s \quad . \quad . \quad . \quad (2)$$

where B is the breadth of the member, and s_t the safe load on the weld per inch of breadth = $4 \cdot 24\,a$ tons/in. for a dead load.

If the conditions are unsymmetrical, as for example in (iii), where an angle is attached to a gusset, it is necessary so to design the joint that the effect of eccentricity is reduced to a minimum, and the weld must be made longer on the side nearest the centre of area of the angle. For the conditions shown in (iii), $F = s(l_1 + l_2)$; $l_1 + l_2 = F/s$. Taking moments,

$$sl_1 \times B = Fv_1 \; ; \; l_1 = Fv_1/Bs \; ; \; l_2 = F(B - v_1)/Bs \quad (3)$$

In cases where the length for attachment is perforce short, a combination of fillet and slot welds may be used, (iv) Fig. 213. The area of the slot weld in shear is b_1l_1 ($t_1 > b_1/2$, Fig. 210) and the safe load on it is $5b_1l_1$ tons. The welds must be so arranged that the resultant force carried by them acts along the axis of the angle. Where the member consists of a single bar attached to one side of a gusset plate, Fish [26] recommends a 50 % increase in the theoretical strength of the welds to take account of the eccentricity of loading perpendicular to the plane of the gusset plate (cf. § 151). When it is not possible to return the weld at the end, as is done in (i) and (iii) Fig. 213, $\frac{1}{2}$ in. should be allowed for the end crater.

No deduction for loss of area is customary in tension members attached by welds.

Plate Girders.—Welded plate girders are formed of one or more flange plates top and bottom welded directly to the web plate. No flange angles are required. For convenience in welding, each flange plate is made slightly narrower than the one inside it. It is customary to use one or two thick plates, rather than a number of thin ones, to save welding. The welds connecting the flange plates are usually made intermittent, but a continuous weld is carried round the ends of an added flange plate and for a short distance at each side along the girder. It is better, but not essential, to make the welds connecting the web to the flanges continuous. In intermittent welding, the distance between the welds should not exceed $16t$ in tension members, nor $12t$ in compression members, where t is the thickness of the thinner plate. The welds should be arranged as shown at (ix) Fig. 213. The web stiffeners are formed of flat bars on each side of the web, of thickness not less than $\frac{1}{12}$th their
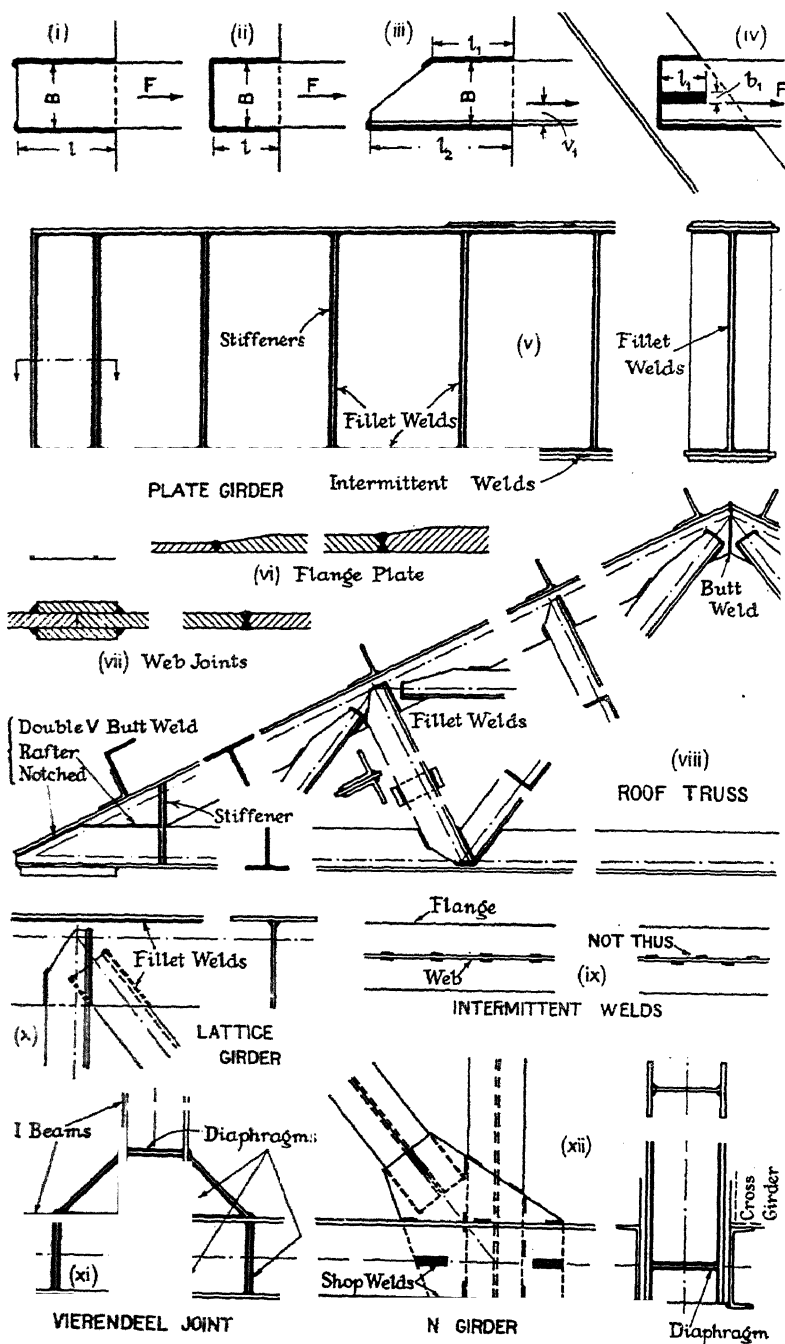
FIG. 213.

breadth. These are welded to the web and to the flanges top and bottom. It is better to make these welds continuous. The end stiffeners are similarly arranged. Joints in the flange plates are made with outside covers as in a riveted girder; but it is becoming common, instead of using a number of flange plates, to use a single plate of varying thickness, butt welded where the changes occur (vi). Web joints may be made with double covers as in a riveted girder, fillet welded to the web, or may be butt welded (vii). The area of the flange plates, web thickness, and spacing of the stiffeners are all determined exactly as in the case of a riveted girder (§ 172 *et seq*.), except that the gross area is taken for both tension and compression flanges. The design follows a similar course and the same stresses may be used. The unsupported length of the web plate may be taken as the distance between the two flanges, or the pitch of the web stiffeners, whichever be the lesser. The values of s_1 and s_2 are calculated as in §§ 175-6, and the size of the welds must be chosen to resist these shearing forces per inch of length. When the welds are made continuous, they are usually more than sufficiently strong. In flange joints with an outside cover, the cover is made slightly narrower than the outside flange plate, and of an area at least equal to that of the cut plate. The welding must be sufficiently strong to transfer the total load from the cut plate to the cover and back again, and if through plates intervene, the welding connecting them must likewise carry this load in the vicinity of the joint [see (iv) Fig. 257]. In web joints with double cover plates, fillet welded to the web, the fillet welds must be sufficiently strong to carry the shearing force at the joint. The worth of the web to resist bending is the worth of these fillet welds.

Roof Truss.—(viii) Fig. 213 shows a welded roof truss. The construction generally is of the usual type, but the joints are made without gussets; the members are welded one- to another by means of fillet welds. The rafters are either T bars, or double angles welded together at intervals; the other members of the truss are of angle section. Field joints (for shipment) may be bolted, or the joints may be made by welding at the site before the truss is lifted into place. The design follows the lines of § 212. Care must be taken that the axes of all the members meeting at a node intersect in a common point, so that the welds shall not be eccentrically loaded, and the procedure given above for the design of the welds for ties and struts must be followed.

Braced Frames.—The construction of light braced frames (x) is similar to that adopted for roof trusses. A detail suitable for a heavier open web girder is given in (xii). A joint suitable for a Vierendeel girder is shown in (xi).

Steel Frame Buildings.—Some details of welded constructions, and connections between beams and columns, in steel-framed buildings, are given in Fig. 214. In the case of a beam directly attached by double fillet welds to a support whose capacity to resist a moment is small (i), the weld may be designed to resist merely the vertical reaction R in direct shear, when R = 2ls. The effective value of a in such cases (iv)
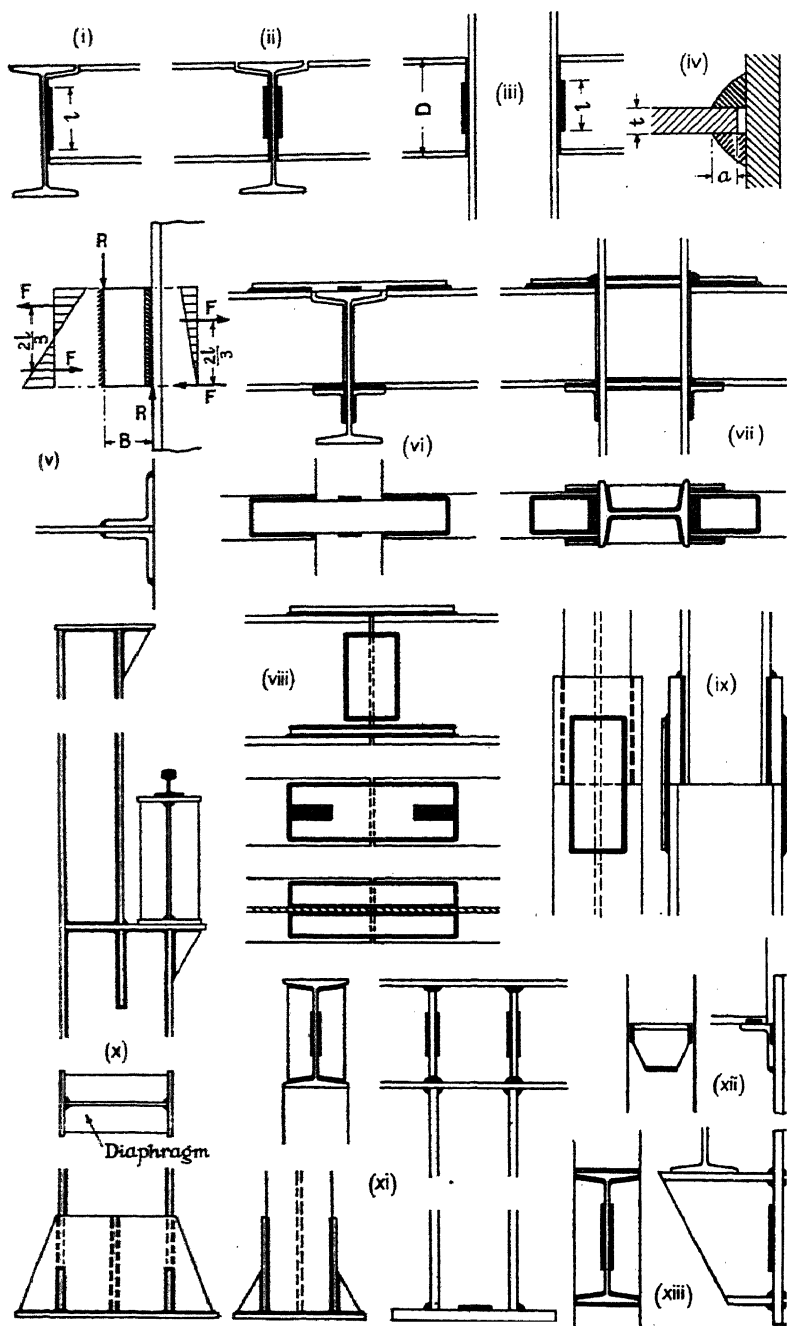
FIG. 214.

should be observed. Where, as in (ii) and (iii), the beams tend to act as if continuous, Mr. Fish* recommends the proportions for the weld $l < 2D/3$; $a > 4t/5$; where t is the thickness of the web of the I beam. The intention is that the web should deform before the weld. In this case the above method can be used, and R $= 2ls$. A connection made with two angle cleats (v) will transmit little fixing moment, but the welds are subject to a local bending moment R × B due to eccentricity. In one weld, at the outstanding toe of a cleat, $F = 3RB/4l$; and the horizontal shear per inch $= 3RB/l^2$. The vertical shear per inch $= R/2l$. Combining these,

$$\text{Safe R} = ls \div \sqrt{(3B/l)^2 + \tfrac{1}{4}} \qquad . \qquad . \qquad . \quad (4)$$

The connections shown in (vi) and (vii) are designed to carry the fixing moment at the support, and (viii) represents a joint between two lengths of beam intended to resist the bending moment. In these details the flange connections must transmit the actual force in the flanges, and in (viii) and (xiii) the web connection must be designed to carry the total shearing force. A joint between two column lengths is shown in (ix), which also indicates how a change in section may be made. If the stress be wholly compressive and the ends are machined perfectly square, the covers used need only be sufficient in size to preserve the alignment. If the joint be subjected in addition to a bending moment of some magnitude, the cover plates and the welds must be designed to resist it. Column details are shown in (x) and (xi). That in (xi) is built up from flat plates and welded. Welded brackets are illustrated at (xii) and (xiii).

BIBLIOGRAPHY

Constructional Steelwork

1. FARNSWORTH. *Constructional Steelwork.* London, 1905.
2. ATKIN. *Constructional Steelwork.* London, 1924.
3. —— *The Erection of Engineering Structures and Plant.* London.
4. STEWART. *The Practical Design of Simple Steel Structures.* Vol. i, *Shop Practice.* London, 1929.
5. SCHAPER. *Grundlagen des Stahlbaues.* 6th ed., Berlin, 1933.

Electric Arc-Welding.

6. ELECTRIC WELDING. London. THE WELDER. London.
7. B.S. SPECIFICATION. *Metal Arc-Welding as Applied to Steel Structures.* No. 538—1934.
8. AMER. WELDING SOC. *Code for Fusion Welding and Gas-Cutting, etc. Part A, Structural Steel,* 1930 (revised 1935).
9. AMERICAN WELDING SOC. Journal. New York.
10. —— Report on Tests of 1395 Specimens by the Structural Steel Welding Committee, 1931.
11. LOBO. Strength of Butt Welds. *Jour. Amer. Weld. Soc.,* Apl. 1929.
12. VOGEL. Design of Joints for Welded Structures. *Jour. Amer. Weld. Soc.,* Apl. 1929 ; also *Gen. Elec. Rev.,* vol. xxxii, 1929, p. 332 (tests).
13. SMITH, J. H. Stress-Strain Characteristics of Welded Joints. *Jour. Amer. Weld. Soc.,* Sep. 1929.

* See Fish, *Arc-Welded Steel Frame Structures,* New York, 1933, where the strengths of many different forms of welded connections are examined in detail.

14. DUSTIN. Le calcul des joints soudés en charpente métallique. *Le Génie Civil*, t. xciv, 1929, p. 330.

15. ZEIT. VER. DEU. ING. Electric Welding Number, Dec. 7, 1929; also Nov. 15, 1930, Schweisstechnik.

16. GEHLER. Versuche mit geschweissten Fachwerkträgern. *Zeit. Ver. deu. Ing.* Dec. 7, 1929, p. 1747; see *Eng. Ab. I.C.E.*, 1930, No. 44 : 90.

17. LINCOLN PRIZE PAPERS. *Arc Welding. Amer. Soc. Mech. Engs.* (republished, New York, 1929).

18. JENNINGS AND JAKKULA. Strength Investigations on Welded Beam Connections. *Jour. Amer. Weld. Soc.* Apl. 1930.

19. EDWARDS, WHITTEMORE AND STANG. Strength of Welded Shelf Angle Connections. *U.S. Bur. Stnds. Jour. Res.*, vol. v, 1930, p. 781; see also LYSE AND SCHREINER, 1934.

20. MACKAY AND BAIN. Distribution of Stress in Parallel Welding Fillets. *Can. Jour. Res.*, 1930, p. 260 : HOVGAARD, *Zeit. ang. Math. Mech.*, 1931, p. 341.

21. VOGEL. Shear Tests for Welds. *Jour. Amer. Weld. Soc.* Oct. 1930.

22. FREEMAN. The Strength of Arc-Welded Joints. *Proc. Inst. C.E.*, vol. 231, 1930–1, p. 283.

23. JENNINGS. The Effect of Welding Procedure on Shrinkage Strains in Butt-Welded Joints. *Jour. Amer. Weld. Soc.* Apl. 1931; see also LOTTMANN, *Zeit. Ver. deu. Ing.*, Sept. 20, 1930, p. 1340; see p. 1560.

24. KAYSER. Versuche über das Zusammenwirken von Neitverbindung und Schweissnaht. *Der Stahlbau.* Jg. 3, 1930, p. 145; Jg. 4, 1931, 121; Jg. 5, 1932, p. 145; Jg. 7, 1934, p. 113; see *Eng. Ab. I.C.E.*, 1931, No. 49 : 84; 1933, No. 55 : 86–7, No. 61 : 78.

25. WELDING SYMPOSIUM. Amer. Soc. Test. Mat., 1931.

26. FISH. *Arc-Welded Steel Frame Structures.* New York, 1933.

27. SECOND LINCOLN PRIZE PAPERS. *Designing for Arc-Welding.* Cleveland, Ohio, 1933. *Procedure Handbook of Arc-Welding Design and Practice*, 4th. ed., Ohio, 1936.

28. BARDTKE. *Technique of Modern Welding.* (Trans., KENNEY.) London, 1933.

29. BIERETT U. GRÜNING. Spannungszustand und Festigkeit von Stirnkehlnahtverbindungen. *Der Stahlbau.* Jg. 6, 1933, p. 169.

30. HAIGH. Constructional Tests on Mild Steel Rolled Sections with Electrically-Welded Joints. *Trans. I.N.A.*, vols. lxxv, lxxvi, lxxvii, 1933–4–5.

31. WELDING SYMPOSIUM. *Iron and Steel Inst.* London, 1935; see *Engg.* May 24, 1935, p. 551 et seq.

32. SCHREINER. The Behaviour of Fillet Welds subjected to Bending Stress. *Journ. Amer. Weld. Soc.* vol. 14, No. 9, Sup. p. 1, 1935.

33. GROVER. Tests to Failure of Arc-Welded Bridge Girders. *Eng. News-Rcd.*, vol. 115, p. 392, 1935.

Fatigue Tests on Welds.

34. BERNHARD. Dauer Versuche an geneiteten und geschweissten Brücken. *Zeit. Ver. deu. Ing.*, Nov. 23, 1929, p. 1675; also SPÄTH, July 6, 1929, p. 963.

35. PETERSEN AND JENNINGS. Fatigue Tests on Fillet Welds. *Proc. Amer. Soc. Test. Mat.*, vol. xxx, Pt. II, 1930, p. 384; also PETERSEN, Large Specimens, *Proc.* 1929; and JENNINGS, *Jour. Amer. Weld. Soc.* Sep. 1930.

36. HAIGH. Fatigue Strength of Butt Welds. *The Welder*, May 1935, p. 548.

37. HANKINS. Fatigue Tests and Non-destructive Tests on Welds. *The Welder*, May 1935, p. 548.

38. VER. DEU. ING. Dauerfestigkeitsversuche mit Schweissverbindungen. Berlin, 1935; see BONDY, *Electric Welding*, Dec. 1935, p. 55.

CHAPTER IX

THE DESIGN OF TENSION AND COMPRESSION MEMBERS

150. Tension Members.—Having given the force F and the safe working stress f_t in a tie bar, the net area required is $a = \text{F} \div f_t$. As will be seen from the following articles, however, there are a number of points concerning the design of tension members which need consideration apart from a determination of their area.

151. Types of Tension Members.—Fig. 215 shows some typical cross-sections used for tie bars in structures. The *round bar* (i), although
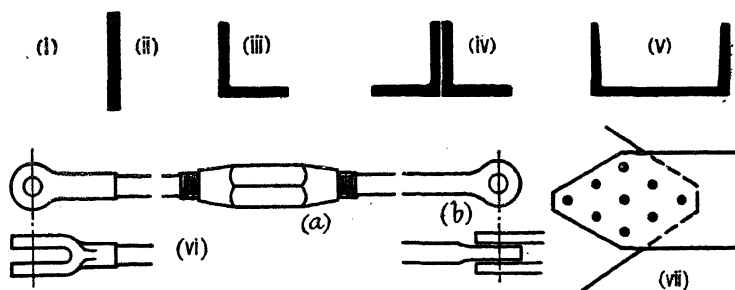
FIG. 215.

perhaps the theoretically perfect form of tie, is not much used in modern structures on account of the difficulty in making suitable attachments and joints. The common practice is to fork the ends of the bar, (vi), and attach it by means of a pin. In large ties this means an expensive and difficult piece of smith's work, which, in addition, is not always reliable. The same objections apply to welded joints in a bar. The structural designer should bear in mind the old maxims : ' Keep out of the smith's shop,' ' Beware of the fire.' For the above reasons, round tie bars have dropped out of use, except where the diameter is small, say not much greater than 1-in. diameter, when the forked ends may be drop-forged and electrically welded on to the bar. A turnbuckle (vi, *a*) is usually provided in the length of the bar, not to adjust the tension therein, but to adjust its length. It is difficult to weld two forked ends on to a rod so that the centres of the pins may be an exact distance apart. The ends of the rod are sometimes flattened and forged into an eye (vi, *b*), which is attached by a pin.

Flat bars, (ii) Fig. 215, are used as tie bars. They may range in size from $2\frac{1}{2}$ or 3 in. wide and $\frac{5}{16}$ or $\frac{3}{8}$ in. thick in a roof truss, to say 12 or 18 in. wide and 1 in. or more in thickness in a lattice girder. They are attached by means of riveted joints, and the rivets are so arranged that only the area of one rivet hole is lost, (vii), (see also § 154). In bridge girders such ties would be placed in pairs, one on each side of a gusset plate, (v) Fig. 225 ; the rivets are then in double shear. The use of flat bar ties in large girders, however, is no longer customary.

Stiff Ties.—The modern practice is to make a tie of such a section that it can resist accidental compressive and bending stresses. In a riveted framework there may be considerable bending in the ties due to secondary stresses (§ 114). A light tie is made of angle section, (iii) Fig. 215 ; or two angles back to back (iv) ; a channel section attached by its web (v) may be used. The angle sections would be attached as shown at (i), (ii), or (iia) Fig. 216, and it is usual to specify that only one-half of the
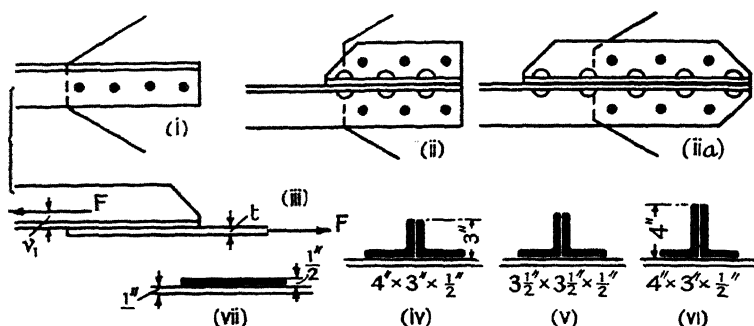
FIG. 216.

area of the outstanding flange should be counted in as forming part of the area of the tie. This is intended as an approximate allowance for the unequal distribution of stress in the member. It will be evident from (iii) Fig. 216, that the angle is an eccentrically loaded tie, the eccentricity e_2 being $(v_1 + t/2)$, where v_1 is the distance of the centre of area from the back of the angle, and t the thickness of the gusset plate. It was shown in § 120, Vol. I, that the maximum stress in an eccentrically loaded tie occurs at the ends and is

$$f_t = \frac{F}{a}\left\{1 + \frac{e_2 v_1}{\kappa^2}\right\} ; \text{ or in this case, } f_t = \frac{F}{a}\left\{1 + \frac{v_1(v_1 + t/2)}{\kappa^2}\right\}$$

As a particular example, consider a $3 \times 3 \times \frac{3}{8}$ in. angle, attached to a $\frac{3}{4}$-in. gusset plate by four $\frac{13}{16}$-in. rivets, and subjected to a load of 10 tons, (iii) Fig. 216. The net area of the angle is $2\cdot11$ sq. in. less one rivet hole $\frac{13}{16} \times \frac{3}{8} = 1\cdot80$ sq. in. ; so that, neglecting the eccentricity, the stress would be $10 \div 1\cdot8 = 5\cdot56$ tons/sq. in. If only one-half the area of the outstanding flange be counted in, after deducting the area of one rivet hole in the other flange, the net area is $1\cdot31$ sq. in. and the corre-

sponding stress is $10 \div 1 \cdot 31 = 7 \cdot 63$ tons/sq. in. Using the formula for eccentric loading, and finding the stress on the gross area of the angle, $v_1 = 0 \cdot 88$; $e_2 = v_1 + t/2 = 0 \cdot 88 + 0 \cdot 19 = 1 \cdot 07$; $\kappa^2 = 0 \cdot 81$; and

$$ft = \frac{F}{a}\left\{1 + \frac{v_1(v_1 + t/2)}{\kappa^2}\right\} = \frac{10}{2 \cdot 11}\left\{1 + \frac{0 \cdot 88 \times 1 \cdot 07}{0 \cdot 81}\right\} = 10 \cdot 3 \text{ tons/sq. in.}$$

All the dimensions are in inches. This is the stress on the gross area. In the way of a rivet hole the stress would be increased to approximately

$$10 \cdot 3 \times \frac{3}{3 - \frac{13}{16}} = 14 \cdot 2 \text{ tons/sq. in.}$$

If it be assumed that the line of action of the load is fixed by the centroid of the *net* area of the angle, $v_1 = 0 \cdot 99$, $e_2 = v_1 + t/2 = 0 \cdot 99 + 0 \cdot 19 = 1 \cdot 18$, $\kappa^2 = 0 \cdot 85$, $a = 1 \cdot 8$, and

$$ft = \frac{10}{1 \cdot 8}\left\{1 + \frac{1 \cdot 18 \times 0 \cdot 99}{0 \cdot 85}\right\} \qquad 13 \cdot 2 \text{ tons/sq. in.}$$

That these high stresses really occur in practice is very unlikely, for the type of construction (the angle attached by its back) is very common and shows no signs of weakness. They appear, however, to afford justification for the custom of neglecting one-half of the area of the outstanding flange. It is evident that the stiffness of the end attachments must, partially at least, direction-fix the ends of the tie, and the stress due to bending is much reduced.

From the point of view of eccentric loading, the detail shown in (ii) Fig. 216 is no better than that shown in (i), and there appears to be no justification for counting in more area in the one case than in the other. The additional cleat shown at (ii) is useful in situations in which it is difficult to get sufficient rivets in the main angle ; (iia), in which the cleat is lengthened, is a better detail than (ii).

As to the best form of section to use for a tie attached by its back to a gusset plate, it is instructive to compare the maximum stress produced in the three sections shown at (iv), (v), and (vi), Fig. 216, all of the same sectional area, but of different vertical dimensions. The figures for the gross sections are :

	(iv)	(v)	(vi)
e_2	$1 \cdot 07$	$1 \cdot 30$	$1 \cdot 57$
v_1	$0 \cdot 82$	$1 \cdot 05$	$1 \cdot 32$
κ^2	$0 \cdot 73$	$1 \cdot 10$	$1 \cdot 53$
$\left(1 + \dfrac{e_2 v_1}{\kappa^2}\right)$	$2 \cdot 20$	$2 \cdot 24$	$2 \cdot 35$

The maximum stress $ft = \dfrac{F}{a}\left\{1 + \dfrac{e_2 v_1}{\kappa^2}\right\}$ is therefore not very different in the three cases, but is least in the shallowest section, in which it is $2 \cdot 2$ times the mean stress, F/a.

This calculation suggests that a flat bar (vii) would most nearly approach the ideal conditions. For the particular case indicated, $v_1 = 0 \cdot 25$; $e_2 = 0 \cdot 5$; $\kappa^2 = \frac{1}{48}$; and $(1 + e_2 v_1/\kappa^2) = 7$! That is to say,

the maximum stress is seven times the mean. There is no doubt that the stiffness of the end connections is usually sufficient to direction-fix the ends of a flat bar tie, which possesses little resistance to bending, for
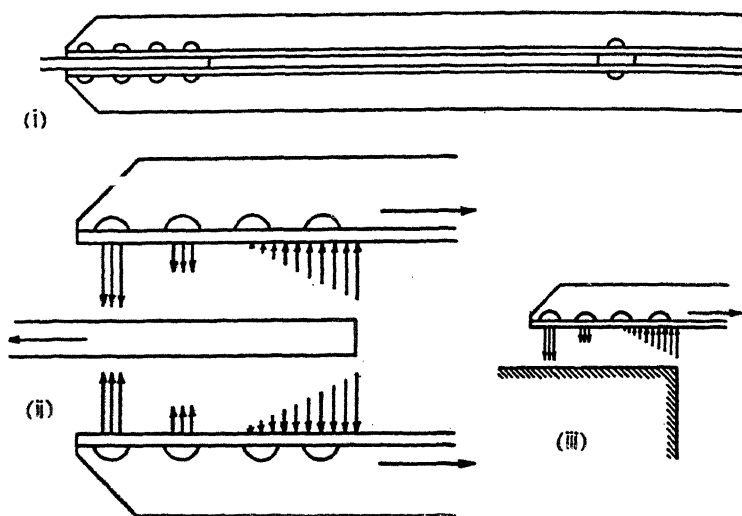
FIG. 217.

the successful employment of many such ties proves that the excessive stress indicated in this calculation does not occur.

If similar angles be placed one on each side of a gusset plate as shown in (i) Fig. 217, the total net area of each angle may be counted in as forming part of the tie; for although, if each bar were separately considered, it would appear to be eccentrically loaded, the eccentricity moment is neutralized by the moment of the forces called into play between the angles and the gusset plate. These forces are represented in (ii) Fig. 217; the eccentricity moment will be completely nullified unless the implied tension in the rivets exceed the initial tension set up due to the rivets cooling. It will be evident that if the gusset plate were infinitely stiff, a similar set of reaction forces would be called into play in the case in

FIG. 218.

which there is one angle instead of two, (iii) Fig. 217, and again the effect of the eccentricity would be nullified. In practice, no connection possesses infinite rigidity, but as suggested above, the stiffness of the end connections undoubtedly reduces the stresses due to eccentricity of loading.

Experimental Results.—A number of the above theoretical deductions have been confirmed by experiment. Professor Batho,[3] experimenting
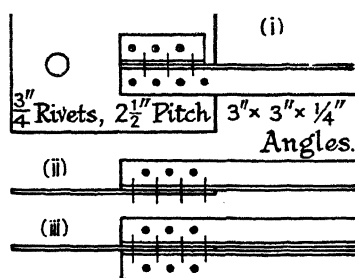
on specimens of the type indicated in Fig. 218, both with and without additional cleats, found that, with single angles attached by their backs [as in (ii) Fig. 218] to gusset plates 3 in. wide, the ratio of maximum to mean stress in the angle ranged from 2·3 to 2·8. By increasing the width of the gusset plate to 14 in., this ratio was reduced in certain cases by 35 %, showing that the effect of stiffness of the gusset in its own plane is considerable.

Adding an additional cleat (i) had little or no effect on the maximum stress produced, (i) Fig. 219. A tie formed of double angles, one on each side of the gusset plate, (iii) Fig. 218, acted as a concentrically loaded specimen, and the stress was very much more nearly uniform, (ii) Fig. 219. Again, the effect of an additional cleat on the maximum stress was negligible. (i) Fig. 219 shows the measured distribution of strain over the central cross-section of a single angle attached by its back to a gusset 3 in. wide; and (ii) shows the corresponding distribution in the case of the double angles with a gusset plate in between, the mean stress being the same in the two cases. The linear distribution of strain should be observed. It will also be noticed that the stress in the single angle reverses.

Large Ties.—(i) to (iii) Fig. 220 shows a type of tension member commonly used in large bridges. The four angles are connected together by batten plates or lattice bracing. The attachment to the gusset

FIG. 219.

plates is shown at (i), and the full net area of the angles may be counted in. The batten plates or lattice bars may be placed between the angles (ii),

FIG. 220.

which leaves a narrow space difficult to paint properly ; or the two angles may be riveted together with tack rivets and a double system of secondary bracing proyided (iii). The latter is the better construction but is more

expensive. For very heavy ties two channels may be used, attached by their backs to the gussets, with the outstanding flanges connected by batten plates or lattice bracing, Fig. 221.

FIG. 221.

152. The Net Area of a Tension Member.—Let Fig. 222 represent a tension member in which the rivets in the inner rows are staggered with respect to those in the outer rows. Considering the cross-section ABHEG, it is evident that there is a reduction in area due to three rivet holes, but if the rivets in the inner rows are sufficiently close to those in the outer rows, fracture might take place along the line ABCHDEG; in other words, the loss of area would be greater than that due to three rivet holes. Experiments by Moberley [1] appear to show that in such a member the likelihood to fracture along the diagonal line BCHDE and along BHE will be equal, provided that the area along BCHDE is 4/3 that along BE; that is to say,

when $2(p' - d) = \frac{4}{3}(c - d)$

or $p' = (2c + d)/3$ . . (1)

FIG. 222.

d denotes the diameter of the rivet hole. As the outcome of his investigation of this subject, Young [7] gives rules which lead to the following : For equal resistance along either BCHDE or BHE,

$k = 3c/5$; or, $p' = 0 \cdot 78c$. (2)

When k is less than this, the number of rivet diameters to be subtracted from the width c is

$$n = 2 \cdot 5 (1 - k/c) \; ; \; \text{max.} = 2, \text{min.} = 1 \quad . \quad . \quad (3)$$

When $c = 3d$ (minimum value), Young's value for k giving equal resistance along the two lines agrees well with Moberley's, but gets relatively larger as c/d increases.

From the results of his experiments, Loudon [9] concludes that the stress concentration at the edges of the holes is the important factor, and that failure may be expected to begin in the edge distance AB or EG. He finds that as k/c increases from 0 to $0 \cdot 3$ there is little increase in the strength of the member ; the strength then increases until $k/c = 0 \cdot 8$, above which value the increase in strength is small. He suggests that the number of rivet diameters which should be deducted from the width c is $(2 \cdot 6 - 2k/c)$, max. $= 2$.

Alternatively, if the old Board of Trade rule for similar joints in boiler plates be applied,

$$k = \tfrac{1}{10} \sqrt{(11c + 4d)\,(c + 4d)} \quad . \quad . \quad . \quad (4)$$

This rule has been used with success for many years. It leads to

$$p' = (3c + 2d)/5 \quad . \quad . \quad . \quad . \quad (5)$$

for equality of resistance, which is less than either Moberley's or Young's value for p'. The corresponding number of rivet diameters to be subtracted from the width c is

$$n = 2 - \frac{100k^2}{(11c + 4d)\,(c + 4d)} ; \; \text{min.} = 1 \quad . \quad . \quad (6)$$

The new boiler rule is $k = (c + 2d)/3$, not very different from eq. (4).

A commonly occurring case in girder flanges is that shown in Fig. 223, to which the above equations will not directly apply. If, in view of Loudon's remarks, this arrangement be regarded as equivalent to Fig. 222 with the rivet at H omitted, from eq. (3) the number of rivet diameters to be subtracted from the width $2c = 2c_1 + c_2$ is

$$m = 2n - 1 = 5\,(1 - k/c) - 1 = 4 - 5k/2c_1$$

$$\left(0 \cdot 8 - \frac{k}{2c_1}\right) ; \; \text{max.} = 3, \text{min.} = 1 \; . \; (7)$$

or a maximum of 4 from the overall width shown in Fig. 223. For equality of resistance,

$$k = 6c_1/5 ; \text{ and } p' = 1 \cdot 56c_1 \quad . \quad (8)$$

FIG. 223.

Similarly, from eq. (6),

$$m = 2n - 1 = 3 - \frac{50k^2}{(11c_1 + 2d)\,(c_1 + 2d)} \quad \text{min.} : \quad (9)$$

For equality of resistance,

$$k = \tfrac{1}{5} \sqrt{(11c_1 + 2d)\,(c_1 + 2d)} ; \text{ and } p' = \frac{2(3c_1 + d)}{} \quad (10)$$

According to German experiments,[4] for equality of resistance, the area along ABCDEG should be $1 \cdot 25$ times that along AG.

In no case should p' be less than $3d$.

153. Eye Bars.—In suspension bridges and other structures where it is essential to reduce the weight of the structure itself to a minimum, *eye bars* of flat bar section with enlarged ends are used for the tension members. The usual forms of these are shown in Fig. 224 ; (i) and (ii) give the proportions formerly used for hammered eye bars, (iii) those for the hydraulically forged eye bars common in American practice. The proportions of these eye bars are intended to be such that the bar
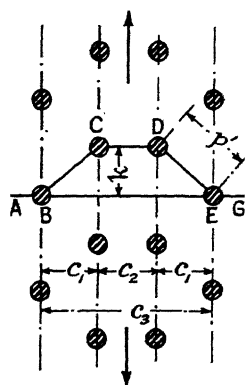
is equally strong in all directions. A typical pin connection is shown at (iv). In calculating the diameter of the pin, it is necessary to examine (a) the bearing pressure between the eye bars and the pin, (b) the shear stress, and (c) the bending stresses in the pin. To determine the latter, the pin is regarded as a beam loaded with the tensions in the bars which it connects, (v) and (vii). By judiciously arranging the bars the bending stresses may be reduced to a minimum.
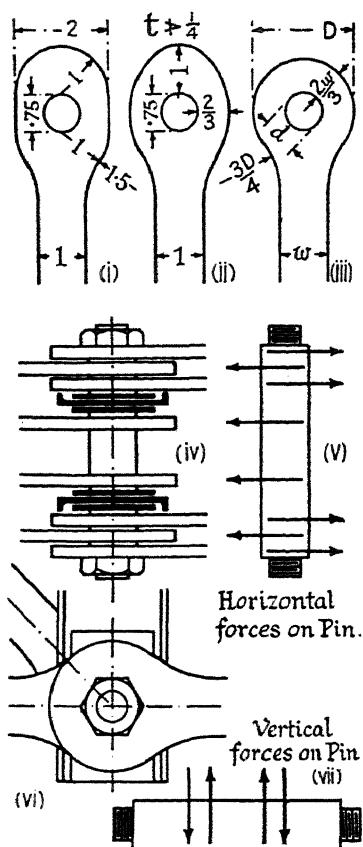
FIG. 224.
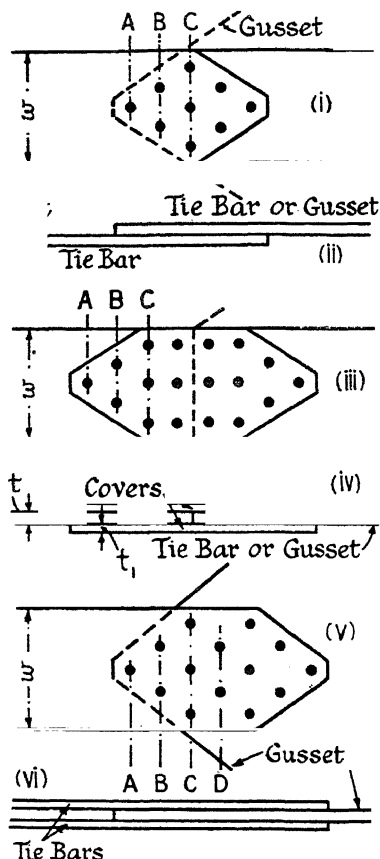
FIG. 225.

154. Joints in Flat Tension Members.—The various types of riveted joint used for flat tension members are illustrated in Fig. 225 ; (i) and (ii) show a lap joint, (iii) and (iv) a butt joint. These joints may be used to connect two parts of the bar, or to attach the member to the gusset plates at its ends, as indicated by the dotted lines in (i) and (iii). Wherever possible a tie bar should be made in one piece.

The conventional calculation for the lap joint (i) and (ii) is as follows : Suppose that f_t be the safe tensile stress in the material, w the width of

the bar, t its thickness, and d the diameter of the rivet hole. Then, at section A, where the bar is weakened by one rivet hole, the resistance to tearing is $F_t = (w - d)tf_t$. Suppose that there are n rivets in the joint. These are in single shear, and if f_s be the safe shear stress in the rivets, the resistance to shearing is $F_s = n \times \dfrac{\pi}{4} d^2 f_s$. If the joint is to be equally strong in shear as in tension, $F_s = F_t$; and

$$n \times \frac{\pi}{4} d^2 f_s = (w - d)tf_t \; ; \; \text{or} \; n = \frac{(w - d)tf_t}{\dfrac{\pi}{4} d^2 f_s}$$

This equation gives the required number of rivets. It does not follow that the joint is weakest either at section A or in shear ; it might fail by tearing at B and shearing one rivet at A, or by tearing at C and shearing the rivets at A and B. The resistance to tearing at B and shearing at A is $F_s' = (w - 2d)tf_t + \dfrac{\pi}{4} d^2 f_s$; the resistance to tearing at C and shear-ing at A and B is $F_s'' = (w - 3d)tf_t + \dfrac{3\pi}{4} d^2 f_s$. The true strength of the joint is the least of the four calculated resistances, which must be equal to the actual force in the member. The tensile resistance of the uncut bar is $F = wtf_t$. The minimum efficiency of the joint is obtained by dividing the least resistance of the joint by the resistance of the uncut bar.

The strength of a joint in which the rivets are in double shear, (iii) and (iv), (v) and (vi), Fig. 225, can be investigated in a similar way. Suppose that the two tie bars in (v) are each 12 in. × ⅝ in., the gusset plate ¾ in. thick, and the rivet holes $\frac{15}{16}$ in. diameter. Take $f_s = \frac{3}{4} f_t$; $f_b = 2f_s$, and design the joint. The resistance of the two bars to tearing at section A, (v), is $F_t = 2(12 - \frac{15}{16}) \times \frac{5}{8} f_t = 13 \cdot 82 f_t$. The resistance to shear of one rivet in double shear is $2 \times \dfrac{\pi}{4} \times (\frac{15}{16})^2 f_s = 1 \cdot 38 f_s$; the bearing resistance of one rivet in a ¾-in. plate is $\frac{3}{4} \times \frac{15}{16} \times f_b = \frac{3}{4} \times \frac{15}{16} \times 2 f_s = 1 \cdot 40 f_s$. The rivet is weakest in shear and bearing need not be further considered. If there be n rivets in the joint, the total resistance to shear is

$$F_s = n \times 1 \cdot 38 f_s = n \times 1 \cdot 38 \times \tfrac{3}{4} f_t = 1 \cdot 03 n f_t.$$

Equating the resistance to shearing to the resistance to tearing, $F_s = F_t = 1 \cdot 03 n f_t = 13 \cdot 82 f_t$, whence $n = 14$. A suitable arrangement of rivets is shown at (vi) Fig. 225. The resistance to shear of this joint is $F_s = 14 \times 1 \cdot 38 f_s = 14 \times 1 \cdot 38 \times \frac{3}{4} f_t = 14 \cdot 49 f_t$. The resistance to tear-ing at B and shearing at A is

$$F_s' = 2(12 - 2 \times \tfrac{15}{16}) \times \tfrac{5}{8} f_t + 1 \cdot 38 \times \tfrac{3}{4} f_t = 13 \cdot 68 f_t.$$

The resistance to tearing at C and shearing at A and B is

$$F_s'' = 2(12 - 3 \times \tfrac{15}{16}) \times \tfrac{5}{8} f_t + 3 \times 1 \cdot 38 \times \tfrac{3}{4} f_t = 14 \cdot 58 f_t.$$

The resistance at section D is obviously greater than that at C. The minimum resistance is that to tearing at B and shearing at A, i.e. $13 \cdot 68 f_t$. The resistance to tearing of the two solid plates is $2 \times 12 \times \frac{5}{8} \times f_t = 15 f_t$, hence the efficiency of the joint is $13 \cdot 68 f_t \div 15 f_t = 0 \cdot 91$, or the strength of the joint is 91 % of that of the solid bars.

For the results of experimental work on riveted joints see §§ 375, 376.

DESIGN OF COLUMNS

155. Types and Classification.—The majority of columns found in ordinary engineering practice may be roughly grouped into three classes : (i) simple *solid columns* of which the struts in roof principals may be regarded as typical ; (ii) *bridge compression members*, usually built-up columns, some of the largest size ; (iii) *stanchions in buildings*, usually combinations of I beams or channels with flange plates. There is a certain amount of overlapping between the groups ; for example, solid round stanchions are used in buildings, and bridge compression members may be simple solid sections or built up of rolled beams and flange plates, but the division is convenient and sufficiently accurate.

Aeroplane struts form a class by themselves, and will not be discussed here.
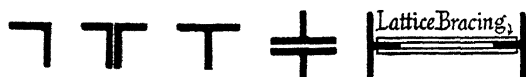
FIG. 226.

Solid Columns.—Fig. 226 shows the sections commonly used for solid columns. These consist of angles and tees, either singly or in combination. The form in which two tees are placed wide apart, and connected together by lattice bracing, is relatively so stiff about the axis perpendicular to the plane of the lattice bracing, that it may be regarded as two solid sections bending about an axis parallel to the lattice bracing.
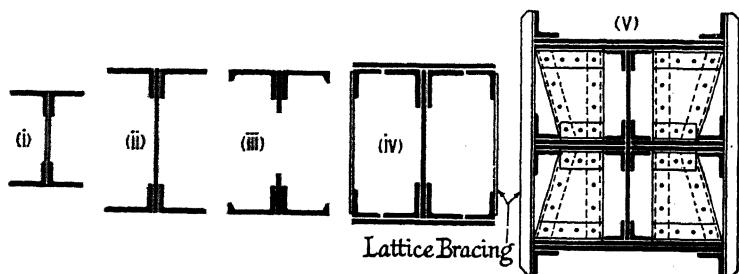
FIG. 227.

Bridge Compression Members.—Figs. 227 and 228 show two different classes of bridge compression members. Those in Fig. 227 all have a central web to carry the shear force. In (i), suitable for light struts, it is of lattice construction, in the others it is a flat plate. The figure

illustrates the modification in type which takes place as the magnitude of the load increases, and a larger flange area becomes necessary ; (v) shows a design suitable for a very large bridge. In (iv) and (v) the outstanding flanges should be connected by secondary bracing, either batten plates or lattice bracing, to prevent them from buckling.

Fig. 228 shows another class of bridge compression member in which

(i)   (ii)   (iii)

(iv)
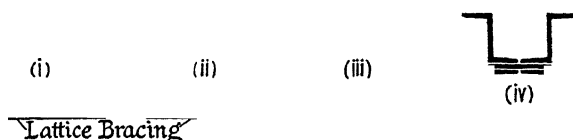
Lattice Bracing

FIG. 228.

the flanges are of channel section ; these are connected together by two lines of lattice bracing. In (iii) the lattice bracing has been replaced by plates, (iv) may be regarded as an analogous construction built up from zed bars. It is probable that, considered merely as a column, (i) is the most economical of all practical types (Salmon's *Columns*, p. 184), but the compression members in a bridge have to resist other straining actions besides those due to the longitudinal load ; in particular, they have to carry secondary bending moments from the cross girders, which
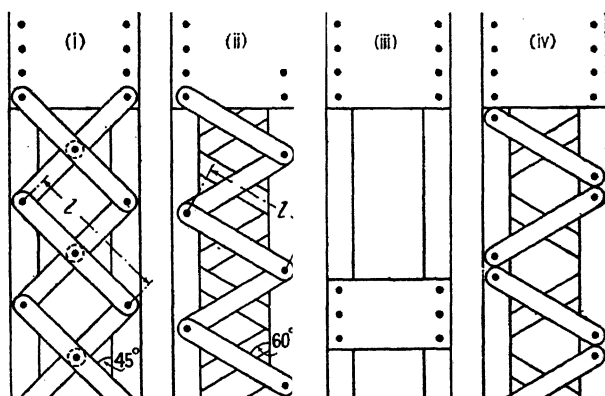
FIG. 229.

are usually attached to the vertical columns. Members with a central web of the type shown in Fig. 227 are more suitable for resisting such strains than those of Fig. 228, and are more convenient for the attachment of the cross girders (see Fig. 309). Modern practice tends, therefore, to the adoption of the types shown in Fig. 227.

The common types of lattice bracing are shown in Fig. 229. When the lattice bracing is double, (i), the angle of the lattice should be 45° ; when single, (ii), the angle should be 60°. Batten plates are shown at (iii). Each of these types makes an efficient bracing if properly designed ;

FIG. 230.

Holding Down Bolt
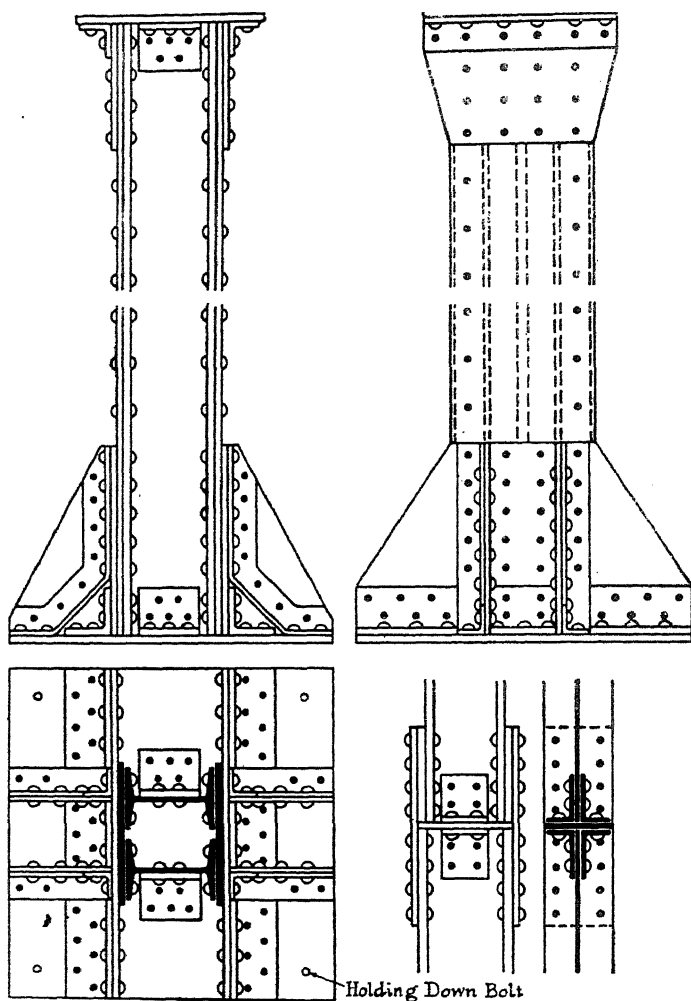
FIG. 231.

(i) is most suitable for heavy columns, (iii) for lighter ones.   Lattice bracing with independent ends, (iv), is not so efficient a·· the other types, and should only be used for members of small importance.

The minimum width for lattice bars is 2 in. for $\frac{5}{8}$ in. rivets, $2\frac{1}{4}$ in.

for $\frac{3}{4}$ in. rivets, and $2\frac{1}{2}$ in. for $\frac{7}{8}$ in. rivets. When arranged as shown in (ii) Fig. 229, the minimum thickness is $l/40$, or with doubled bars riveted together at their intersections, (i) Fig. 229, the minimum thickness is $l/60$. The minimum thickness of batten plates should not be less than $\frac{1}{50}$th the distance between the rivet lines; and except in unimportant positions, not less than 3 rivets should be used to connect them to each flange. The pitch of the lattice bracing should be determined from secondary flexure considerations, § 160. The methods of attachment used for bridge compression members are given in Chapter XI.

Stanchions in Buildings.—The common types of cross section used for stanchions in buildings are shown in Fig. 230. Where space is limited, the circular cross section (i) may be adopted. If made of cast iron, the column is usually of hollow cylindrical form, (ii). For heavy stanchions, combinations of beams and flange plates are used, (iii), (iv) and (v). The sections shown at (iii) and (iv) Fig. 228, are also employed. Typical caps and bases are shown in Figs. 231 to 233.

Fig. 232 shows a slab base for a stanchion. The end of the member is machined all over after riveting, and bolted to the slab. Such a construction may conveniently replace the top tier of beams in a grillage (Fig. 466). According to the L.C.C. Code of Practice (1932), assuming the pressure beneath the slab to be uniformly distributed,

the minimum thickness $t = \sqrt{\dfrac{W(B - b)}{12D}}$ or

$\sqrt{\dfrac{W(D - d)}{12B}}$, whichever be the less.
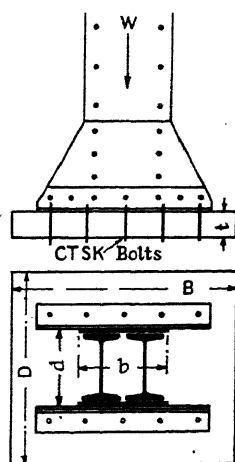
FIG. 232.

Fig. 231 shows how a change of section may be made just above a floor; Fig. 233 shows how a joint may be made between floors. Only when it is impossible to make the stanchion in one piece owing to its length, or to the position in which it is to be erected, are such joints permitted. The abutting surfaces both at the ends and at joints should be machined absolutely square so that the surfaces butt all over.

A number of details of the connections between floor beams and stanchions are given in Figs. 251 and 252.

156. The Practical Column.—The mathematical theory of the strength of columns and its underlying conceptions have been discussed in Chapter VIII, Vol. I, in which chapter will also be found a short résumé of the experimental work, together with some of the better known empirical formulae for columns. Unfortunately, most of this theoretical and experimental work has very little direct bearing on the column as found in a structure.

The ordinary practical column is a short sturdy member, more or less rigidly connected to the adjacent members at each of its ends, and sharing the general deformation of the structure. It is initially curved, but this curvature may be greatly modified by the secondary bending moments at its ends. It is not a homogeneous member; often it is built up of separate parts, and it is the strength of these parts which determines the strength of the whole. Local secondary flexure may be the determining cause
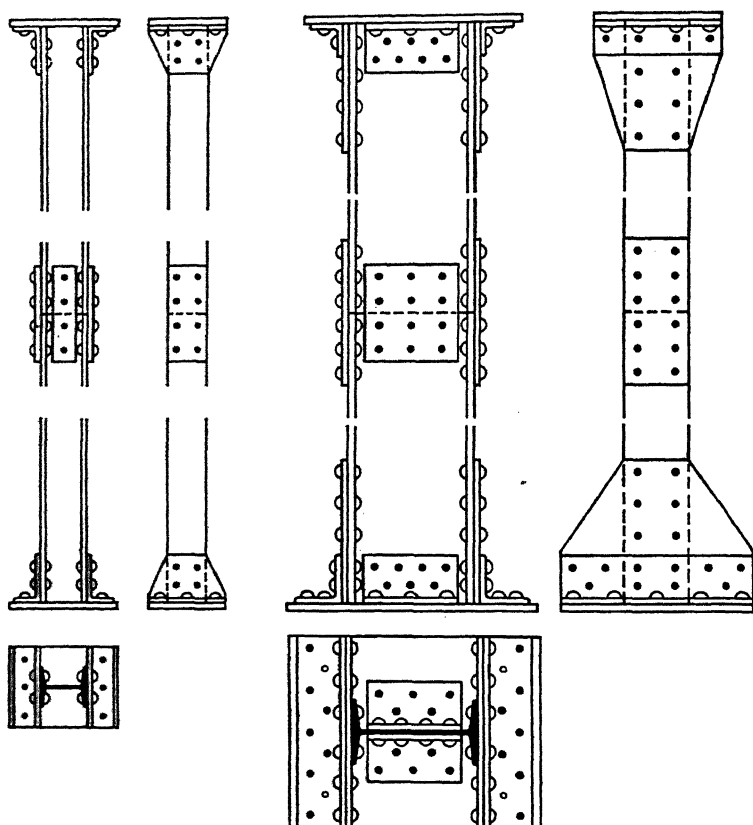
Fig. 233.

of failure. The adequacy or otherwise of the secondary bracing, lattice bars, batten plates, etc., may have an important effect on the strength of the column.

It is evident that a formula based on experiments on small solid columns will not take these factors into account, and it becomes necessary to consider their influence on design.

157. The End Conditions.—The practical end conditions are quite different from either the ordinary mathematical conceptions or the usual experimental conditions. In the ordinary mathematical theory either

perfect freedom in direction or perfect fixity in direction is assumed, and in most experimental work attempts have been made to approximate to these ideal conditions. It follows that the results obtained are not directly applicable to the practical case. The practical column is not free in direction, for its angular movement is severely restrained by the stiffness of the parts to which it is attached ; it is not fixed in direction, for it shares the angular deformation of the panel points at its ends ; it may bend in a single bow, in many cases the curvature is S-shaped, (ii) Fig. 189. From the calculations of the deformation stresses in a number of bridge trusses, it would appear that most of the struts proper, i.e. the vertical members, take an S shape, so that the maximum stress occurs at their ends. In many cases the top flange bends into a single bow, but the member should not be regarded as free in direction at its ends. It is an initially curved column, resisting the secondary bending moments due to the deformation of the frame in addition to the longitudinal load, its own weight forming a lateral load on the member. The ends are constrained to take definite inclinations owing to their connections to the rest of the structure.

The problem may be treated analytically on the following lines, but the resulting equations are not simple. Let it be assumed that the deformation bending moments M_{ab}, M_{ba}, at the ends of a column AB have been calculated on the usual assumptions, § 115, namely that the members were originally straight, and that they are rigidly attached at their ends to the rest of the structure, but neglecting any effect which the longitudinal loads may have on the deformation moments. From these moments, the inclinations σ_{ab}, σ_{ba}, at A and B can be found, ¶ 8, § 118. These angles are determined, not by the behaviour of the particular member AB alone, but by the shape and stiffness of the frame as a whole ; on the assumptions made, they are definite and fixed for a particular load condition. The longitudinal load acting on the curved compression members will tend to increase the angles σ ; its effect on the curved tension members will be to decrease these angles. Usually both tension and compression members connect on to the same gussets, and the two effects will tend to neutralise one another. The ' give ' in the riveted joints will tend to lessen both effects. If then it may be assumed that the values of σ, as calculated from the deformations, are substantially the values of σ for the column in the truss, the equation to the bent centre line of the column can be found, and hence the stresses in the member.

The simpler case of an originally straight member, subjected to

FIG. 234.

applied bending moments M' at its ends, which moments are of the same magnitude and sign, Fig. 234, the ends of the column being held fixed at the inclination produced by these moments, is treated in the author's *Columns*, Variation 5, p. 59. It is there shown that until the longitudinal
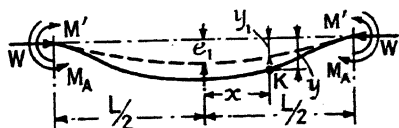
load exceeds $P = \pi^2 EI/L^2$, the maximum compressive stress will occur at the centre of the column, and is (eq. 149),

$$f_c = \frac{W}{a}\left[1 + \frac{8e_1v_1}{\kappa^2}\frac{1}{a^2(L^2 + 4e^2_1)}\left\{\frac{aL}{2}\operatorname{cosec}\frac{aL}{2}\right\}\right]$$

$$= \frac{W}{a}\left[1 + \frac{M'}{W}\cdot\frac{v_1}{\kappa^2}\left\{\frac{\pi}{2}\sqrt{\frac{W}{P}}\operatorname{cosec}\frac{\pi}{2}\sqrt{\frac{W}{P}}\right\}\right] \quad . \quad (1)$$

for

$$M' = \frac{8e_1 EI}{L^2 + 4e_1}; \quad a^2 \simeq \frac{W}{EI}; \quad \text{and} \quad \frac{aL}{2} = \frac{\pi}{2}\sqrt{\frac{W}{P}} \ (l.c.).$$

Until the load attains the value $W = P = P_2/4$, $(P_2 = 4\pi^2 EI/L^2)$, the column will bend into a single bow. When $W > P_2/4$, the reversed curvature commonly associated with direction-fixed ends will occur (cf. Fig. 235).

The Special Committee on Steel Column Research of the American Society of Civil Engineers [14] (p. 1221), who reach the same equation, write it in the form

$$W = \frac{f_c a}{1 + j\cdot\frac{\pi}{2}\sqrt{\frac{W}{P}}\operatorname{cosec}\sqrt{\frac{W}{P}}} \quad . \quad . \quad (2)$$

where $j = \left\{\frac{M'v_1}{a\kappa^2} : \frac{W}{a}\right\}$; i.e. the ratio of the maximum fibre stress due to the deformation bending moments to the load per square inch on the column. Assuming the value $j = 0\cdot25$, and putting $f_c = f_y = 36{,}000$ lb./sq. in. at the failure point, the Committee find that the formula gives almost identical values to the ordinary secant formula, eq. (8), § 106, Vol. I, if in that equation $e_2v_1/\kappa^2 = 0\cdot25$, and P be replaced by $P_2 = 4\pi^2 EI/L^2$. Hence they conclude that 'the strength of a column in a truss under the conditions assumed is not much less than that of a pivoted-end column of one-half the length.'

Ross,* assuming the column, no matter what the end conditions may be, to be an originally straight, eccentrically loaded, hinged-end member, calculates the values of M'/W from a number of published secondary stress determinations. He suggests the general value $e_2 = M'/W + L/500$ as an equivalent eccentricity for practical columns. The final term is included to take account of imperfections in the conditions.

The objection to the above methods of proceeding is that, in determining the deformation bending moments, or what is equivalent, the angular deformation of the panel points, any effect which the longitudinal load on the column has on these angular movements is neglected. Further, the deformation stresses are calculated on the assumption of perfect rigidity of the joints. Allowance is sometimes made for the stiffness of the gussets, but any relief from the 'give' of the riveted joints or other mitigating circumstances is ignored. Experiments suggest that in a bridge truss these effects tend to neutralize one another, for the cal-

---

* *Trans. I.E. Aust.*, vol. viii, 1927, p. 3.

culated and observed values show a fair measure of agreement, § 119 ; but the rigidity of the joints commonly used in steel-framed buildings certainly falls far short of that presumed in ordinary deformation stress calculations.

Further, in order to apply such methods, it is necessary first of all to calculate the deformation stresses in the frame, and in order to effect this, cross-sections for the columns must be assumed. These must afterwards be modified to suit the more exact procedure, and a recalculation made if necessary. In view of the lengthy computation involved in secondary stress determinations, this is impracticable in ordinary structural design.

What is wanted is experimental evidence as to the degree of imperfection common in practical direction-fixed ends,* what angular deformation is probable, and what shape the deflection curve is likely to take. Such information can only be obtained from observations on actual structures, which observations should clear up the uncertainties mentioned above. Knowing the probable slope of the ends of the column, or an equivalent indication of the real end conditions, it will not be difficult to design the member.

Meanwhile it is fortunate that the ratio L/κ in practical columns is, and should be, kept small. The bending moment resulting from the effect of the curvature is then small, and the corresponding bending stress is small relative to the direct stress. Errors in the assumptions made regarding the end conditions are thus not vitally important.

Where, due to the attachment of beams, external bending moments are applied to columns (e.g. cross girders in bridges ; steel-frame building construction), severe bending stresses may be set up therein. In such cases the column is acting as part of a continuous girder system, and should be so designed.

158. The Value of 'q' in Practical Columns.—In the absence of accurate information regarding the end conditions, referred to above, the method usually employed to take into account the direction-fixing, partial or otherwise, is to assume a probable value for q ; qL is the free length of the column, and in initially straight columns is equal to λ, the semi-wave length of the deflection curve (see §§ 103 and 118, Vol. I). It must be understood that this method is at best a rough approximation which leaves out of account important factors, and may be misleading. In the first place it should be observed that the values of q, as determined for initially straight columns under ideal conditions, do not apply to the practical column, which is always initially curved. It will be evident

* In 1913 [*London University Thesis on 'Columns*,' republished 1921 (see p. 271)] the present writer remarked that ' the most pressing point for future research on the subject of columns is undoubtedly the question of the degree of imperfection common in practical direction-fixed ends. . . . A complete answer to this question is difficult, but at present the designer has *no real data whatsoever regarding practical end conditions*.' He goes on to suggest that, from a determination of the actual deflection curve of columns forming part of a framed structure, a new development of the column theory may grow, with secondary stress considerations as an underlying basis. The question is one of *probability* as to the end conditions likely in everyday practice, and on such a point too much evidence cannot be obtained (see § 158A).

that the value of q, for an initially straight column, and that for an initially curved column, both with position-fixed ends, Figs. 164 and 170, Vol. I, will be the same. Yet the behaviour of the columns will be quite different. Again, Fig. 235 represents the initial and final deflection curves of an initially curved column, direction-fixed at its ends. The equation to the curve [see eq. (9), § 108, Vol. I] is

$$y = \frac{4e_1}{aL \sin aL/2} \left\{ \cos ax - \cos \frac{aL}{2} \right\} \quad \text{where } \frac{aL}{2} = \pi \sqrt{\frac{W}{P_2}} \qquad (1)$$

The dotted line represents the initial deflection ; the full lines represent the shape of the column when $W = 0 \cdot 25 P_2$ and when $W = 0 \cdot 81 P_2$ respectively. The position of the points of no bending moment are also shown. It will be seen that up to one-quarter Euler's crippling load for a direction-fixed column, i.e. for all working loads, the deflection curve is a single loop ; and q falls slowly from $0 \cdot 58$ to
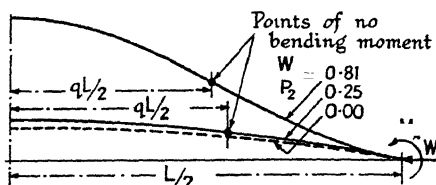
FIG. 235.

$0 \cdot 56$ as W increases from 0 to $P_2/4$. Only when W exceeds $P_2/4$ does the familiar reversed curvature associated with direction-fixed ends appear, and not until $W = P_2$ does $q = \frac{1}{2}$, as in originally straight columns. To obtain the points of inflexion,[*] and hence the semi-wave length λ, put $d^2y/dx^2 = 0$ in eq. (1), when $\cos ax = 0$, $ax = \pi/2$,

$$= \frac{L}{4} \sqrt{\frac{P_2}{W}} = \frac{\lambda}{2} ; \text{ and } \lambda = \frac{L}{2} \sqrt{\frac{P_2}{W}} \qquad (2)$$

The semi-wave length is evidently a function of W ; if $W = P_2/4$, $x = L/2$, $\lambda = L$, and the point of inflexion coincides with the point of application of the load, as is evident from the figure ; when $W = P_2$, $\lambda = L/2$, as in the ideal straight column. It is evident that the equation $qL = \lambda$ does not hold for initially curved columns, and the values of q for ideal columns are not applicable to practical columns. If, however, the correct value is determined for q, i.e. for the distance between the points of no bending moment, the maximum compressive stress at the centre of the column is given by

$$f_c = \frac{W}{a} \left[1 + q^2 \frac{e_1 v_1}{\kappa^2} \cdot \frac{8P_1}{\pi^2 W} \left\{ \sec \frac{\pi}{2} \sqrt{\frac{W}{P_1}} - 1 \right\} \right] \qquad (3)$$

where $P_1 = \pi^2 E I/(qL)^2$, and e_1 is the initial deflection in the whole length of the column (see *Columns*, eq. 204, p. 73). Under working conditions, if $\frac{W}{P_1} < \frac{1}{5}$, this equation may be replaced by

$$f_c = \frac{W}{a} \left[1 + q^2 \frac{e_1 v_1}{\kappa^2} \left\{ 1 + 1 \cdot 25 \frac{W}{P_1} \right\} \right] \qquad (4)$$

[*] Not the points of no bending moment (see § 86, Vol. I).

a simple equation giving the maximum stress under working conditions in an imperfectly direction-fixed column. The equation assumes, in effect, that the direction-fixing is sufficiently imperfect that the maximum stress occurs at the centre of the column.

Evidence as to the value of q in practical cases is very meagre. For columns with initial curvature, if the direction-fixing be perfect, the theoretical value of q varies from $0 \cdot 58$ to $0 \cdot 56$ as W/P_2 varies from 0 to $\frac{1}{4}$. For position-fixed ends, $q = 1$. Practical end conditions probably lie about midway between these limits, $q = 0 \cdot 78$. For members attached by large gussets to stiff adjacent members, for example, the web compression members in ordinary bridge girders, q may be taken as $0 \cdot 7$. The compression flange would not be so well fixed as this, and q may be taken as from $0 \cdot 78$ to $1 \cdot 0$, depending on the relative stiffness of the web members. Calling perfect direction-fixing 4, and perfect freedom in direction 1, from observations on a bridge truss, Kayser [35] estimates that the degree of direction-fixing in a diagonal web strut may be taken as $2 \cdot 42$.

For members attached by small gussets to adjacent members not stiffer than themselves, for example, ordinary struts in roof trusses, take $q = 1$. As an example of approach to perfect direction-fixing, the following case may be cited. Two rows of angle struts, 48 in all, each leg attached by gussets, Fig. 236, and standing on a flat slab base,

FIG. 236.

were accidentally over-loaded and buckled. They all behaved as direction-fixed members, bending in a direction corresponding to the least radius of gyration, and the failure load approximated very closely to that of a perfectly direction-fixed member.
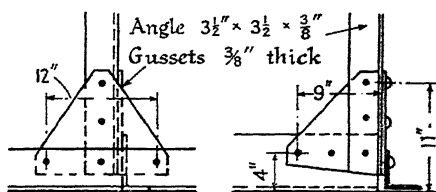
Stanchions in Steel-framed Buildings.—The value of q for stanchions in buildings is difficult to estimate. A column, standing on a wide base which rests on hard material, and rigidly attached at its upper end to the members of a stiff floor system past which it is continuous, might be regarded as imperfectly direction-fixed at each end, $q = 0 \cdot 7$. In ordinary cases, for single storey buildings, and for the top and bottom storeys of other buildings, it is safer to take the value $q = 1$ for the stanchions. Where a stanchion is continuous past a floor at both ends, and rigidly attached at each end to deep and stiff floor beams, it may be considered as imperfectly direction-fixed at both ends. A value $q = 0 \cdot 7$ may be taken in this case also. These assumptions may be completely altered by the imposed bending moments from the beams.

Stanchions in buildings are commonly regarded as 'eccentrically loaded,' which may be approximately true when the floor beams rest on a plain shelf angle. When side and top cleats are employed (Figs. 251 and 252) the connections will transmit a bending moment, and the whole construction becomes a network of continuous spans, with weak places

where the beams join the columns. The ordinary methods of calculating the eccentricity have no real applicability. There is great need of experimental determination of the degree of direction-fixing to guide the designer (see § 378A). The conventional methods of design make no pretence at an accurate determination of the bending moments and stresses. They will be found in all the manufacturers' Pocket Books, and will not be repeated here.

159. **Magnitude of the Imperfections** (see § 111, Vol. I).—In solid columns with position-fixed ends assume an initial deflection

$$e_1 = \frac{L}{750} + \frac{D}{40}, \text{ plus an eccentricity } e_2 = \frac{L}{1000} + \frac{D}{40};$$

add $L/160$ to e_2 in the case of built-up columns. In all direction-fixed

columns assume an initial deflection of $e_1 = \frac{L}{750} + \frac{D}{40}$. D is the depth of

the cross-section in the plane of bending. Use a working stress in compression 15 % less than in tension, to allow for reductions in the strength of the material (*l.c.*).

160. **Secondary Flexure. The Built-up Column.**—The majority of large, practical columns are built up girder fashion, and consist of two
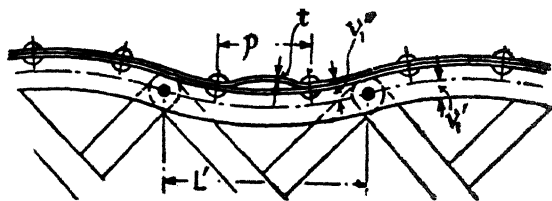
FIG. 237.

flanges connected by a web or webs, Figs. 227 and 228. Experiment has shown that well-designed members, thus constructed, usually fail due to the flange buckling between the panel points, or due to the flange plates on the concave side of the column buckling between the rivets, Fig. 237. It is evident that the stresses caused by primary and secondary flexure will add, so that if secondary flexure is possible in a column, the maximum stress will be increased thereby. It is probably that secondary flexure plays a much more important role in determining the strength of compression members than is usually recognised. All thin material in compression exhibits wave formation, and even short lengths of channel and other sections fail by local buckling. The secondary flexure of outstanding flanges and plates much reduces the strength of such parts. Experiments by Talbot and Moore [11] on a specimen of thin material showed extreme fibre stresses 40 to 50 % in excess of the average stress. These extreme fibre stresses varied in a very irregular way, sometimes occurring on one side of the channel which formed the flange of the column, and at a nearby cross-section on the other side. These channels showed

evidence of considerable local flexure, to which these irregularities appear to be due. The authors conclude that local want of straightness may be much more important than curvature of the centre line or than eccentricity of loading. In some heavier wrought iron specimens the effect of local curvature was not so pronounced. Howard and Buchanan,[12] from some experiments on large size columns of normal construction, conclude that in such columns an ultimate strength coincident with the yield point in the individual parts should be attained, whilst from the ease with which local buckling then takes place, no higher resistance will be realised or should be expected.

Many analyses have been given for columns taking secondary flexure into account. The following approximate treatment for a column with flanges of equal area $a/2$ leads to a simple expression for practical use. Let AA, Fig. 238, represent the central cross section of a lattice-braced column, and suppose that the deflection at this section, measured from the load line, is y_0. The forces F' and F'' in the two flanges, obtained by taking moments about any convenient point, are

$$F' = W\left(\frac{1}{2} + \frac{y_0}{h}\right) \; ; \; F'' = W\left(\frac{1}{2} - \frac{y_0}{h}\right) \quad . \quad (1)$$

where W is the load on the column, and h is the distance between the centres of area of the two flanges. If the value of y_0 were known, the force F' on the elementary flange column of length L', (ii), would be known, and the latter could be designed to carry this load. Con-

FIG. 238.

sider the flexure of the column as a whole, and suppose that at the moment of failure its condition may be represented by the Johnson parabolic formula, eq. (9), § 116, Vol. I,

$$f_r = f_y - c_2\left(\frac{qL}{\kappa}\right)^2$$

where f_y is the yield point stress, and $c_2 = f_y^2/4\pi^2 E$. From the fundamental stress equation for a column, $f_a = f_c - f_b$. If, at the failure point, $f_a = f_r$, the load per square inch; f_c, the maximum stress $= f_y$; then the stress due to bending

$$f_b = c_2\left(\frac{qL}{\kappa}\right)^2 = \frac{Wy_0}{Z} = \frac{2Wy_0}{ah}$$

where Wy_0 is the bending moment on the cross section, and $Z = ah/2$ is the section modulus. This supposes f_b to be the stress due to bending at the centre of area of the flange proper. Then

$$y_0 = \frac{c_2 ah}{2W}\left(\frac{qL}{\kappa}\right)^2$$
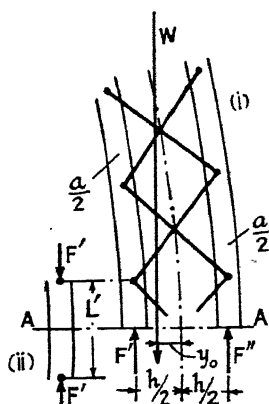
and, from eq. (1),

$$F' = W \left\{ \frac{1}{2} + \frac{c_2 a}{2W} \left(\frac{qL}{\kappa} \right)^2 \right\} \quad \frac{W}{2} + \frac{c_2 a}{2} \left(\frac{qL}{\kappa} \right)^2 \tag{2}$$

This equation gives the load on an elementary flange column, (ii) Fig. 238. Considering the latter separately, and applying the Johnson parabolic formula to it,

$$\frac{F'}{a/2} = fy - c_2 \left(\frac{q'L'}{\kappa'} \right)^2$$

where q', L' and κ' all have reference to the elementary flange column. From eq. (2),

$$\frac{2}{a} \left\{ \frac{W}{2} + \frac{c_2 a}{2} \left(\frac{qL}{\kappa} \right)^2 \right\} = fy - c_2 \left(\frac{q'L'}{\kappa'} \right)^2$$

whence,

$$\frac{W}{a} = fy - c_2 \left\{ \left(\frac{qL}{\kappa} \right)^2 + \left(\frac{q'L'}{\kappa'} \right)^2 \right\} \tag{3}$$

The Johnson parabolic formula holds therefore for the built-up column, if $(qL/\kappa)^2$ be replaced by $\{(qL/\kappa)^2 + (q'L'/\kappa')^2\}$.[*] In ordinary circumstances q' may be taken as unity for the elementary flange column. W in eq (3) is the ultimate strength of the column, and a suitable factor of safety must be applied.

The above analysis is admittedly approximate. A rational treatment of the problem will be found in Chapter II of the author's *Columns*. Using the same symbols as in eq. (3), § 158, it may be shown that (*l.c.*)

$$F' = \frac{W}{h} \left[q^2 \frac{8P_1 e_1}{\pi^2 W} \left\{ \sec \frac{\pi}{2} \sqrt{\frac{W}{P_1}} - 1 \right\} + \frac{h}{2} \right] . \tag{4}$$

or, if $W/P_1 < 1/5$, i.e. under working conditions,

$$F' = \frac{W}{h} \left[q^2 e_1 \left(1 + 1 \cdot 25 \frac{W}{P_1} \right) + \frac{h}{2} \right] \tag{5}$$

From this value of F', the maximum stress f_c in the column may be found. Treating the elementary column as position-fixed at its ends, if the eccentricity of loading be e_2' and the initial curvature e_1'

$$f_c = \frac{F'}{a/2} \left[1 + \left\{ 1 + \frac{3F'}{2P} \right\} \frac{v_1'}{(\kappa')^2} (e_1' + e_2') \right] . \tag{6}$$

eq. (8), § 107, Vol. I. Here v_1', κ', e_1', e_2', all have reference to the elementary flange column, and $F'/P < \frac{1}{5}$, where $P = \pi^2 EI'/(L')^2$. The equation gives the maximum stress under working conditions. For such a column take $e_1' = L'/375$, $e_2' = L'/500$, or in round figures, $e_1' + e_2' = L'/200$.

Tertiary Flexure.—In the case of tertiary flexure, Fig. 237, where the flange plate cripples between the rivets, the stress f_c, found from eq. (6), should be multiplied by $(1 + p/80t)$ [*Columns*, p. 108] to get the true

---

[*] An equivalent expression was obtained from another analysis by Engesser, *Zentralblatt der Bauverwaltung*, Berlin, 1909, p. 136.

maximum stress in the flange plate. This value only holds when $t^2/p^2 \geqq 3 \cdot 7 f_c / E$. Also it should be observed that tertiary flexure can only occur when the flange plate lies on the concave side of the elementary flange column, in which case v_1' becomes v_1'' (see Fig. 237). These formulae enable the stress in a built-up column subjected to secondary and tertiary flexure to be calculated.

Integral Action.—In America this question has been considered from a different view-point, and experiments have been made to determine proportions for the column which will result in *integral action*. If these proportions be adopted in the design, it is assumed that the effect of secondary flexure in the column will be unimportant. From their study of existing data, the American Committee on Steel Column Research [17] find that no failures primarily due to buckling occurred when the local L/κ was less than 25 (' The tests studied were, however, too limited in number to be at all conclusive ') ; and that a ratio of rivet pitch to thickness of 20 is sufficiently low to develop the full strength of the column.

The U.S. Bureau of Standards experiments [30] indicate that the safe ratio of plate width to thickness for structural steel is about 40, provided that the width w is measured between the rivet lines, and that the plates are well restrained at the edges. From eq. (8), § 120, the maximum edge thrust per square inch which the plate will stand without buckling is

$$f = \frac{\pi^2 E t^2}{3 w^2} \cdot \frac{m^2}{m^2 - 1} \quad \cdot \quad \cdot \quad \cdot \quad \cdot \quad (7)$$

Putting $f =$ the proportional limit stress (37,700 lb./sq. in.), and taking $m = 10/3$, $w/t = 53$, at which ratio the plate should be equally inclined to buckle or pass the proportional limit. It is necessary, however, to allow for initial buckles and irregularities of the plate, and the experiments indicate 40 as a safe limit. If $t > \frac{5}{8}$ in., and the edges are not well stiffened, the overall width should be taken instead of the width between the rivet lines.

According to Roark (1913), an outstanding plate, perfectly direction-fixed along one edge and free at the other, will buckle when the unit load exceeds

$$f = 0 \cdot 6 E (t/B)^2 \quad \cdot \quad \cdot \quad \cdot \quad \cdot \quad (8)$$

where B is the breadth of the outstanding flange.

The Committee conclude that such plates will carry the proportional limit stress of 30,000 lb./sq. in. without buckling, provided that the ratio of outstanding width to thickness does not exceed 20.

Tests on large bridge members indicate great difficulty in securing integral action of the several ribs of a large member by means of lattice-bars only. Longitudinal diaphragms or cover-plates should be used [see (v) Fig. 227].

161. The Effect of Elastic Breakdown at the Yield Point.—The consequences which follow the sudden ' give ' at the yield point are discussed in § 112, Vol. I. Many experimenters have called attention to the effect of yield in bringing about the failure of a column. Marshall's

experiments (1887) showed that, when $L/\kappa < 100$, with either flat or hinged ends, failure occurred when the load per square inch reached the yield point. For comparison, the plotted results of some tests made at Watertown Arsenal (1908–9) on Rolled I-Beams are given in Fig. 239.

Actually, as the discussion on Buchanan's experiments (1907), and on Tetmajer's experiments (Jensen, 1908), showed, failure occurs when the stress in the extreme fibre reaches the yield point.

In large and built-up specimens it is the *local effect* of yielding which is the dangerous factor. Howard (1908 and 1911) remarks that it is axiomatic that the ultimate strength of iron and steel columns of the usual proportions is limited to the yield point of the material, and that it is the minimum value of the yield point as found in the component parts which determines the ultimate resistance of columns. Hence variations of 25 % and over in the yield point, as found in the plates and angles, would overshadow those considerations which find expression in empirical formulae for columns which take no account of such variations. This conclusion has been confirmed by the later experiments on built-up columns, and the American Column Research Committees concur that in all columns showing integral action, failure occurs when the maximum stress in the material exceeds the compressive yield point (except in those cases where L/κ is so large that buckling takes place earlier) ; and further, that the compressive yield point may be taken as substantially equal to the tensile yield point.

Experiments made in 1936 by the U.S. Bureau of Standards [14] on large, relatively short, built-up specimens of carbon-manganese steel, show that the ratio of yield strength of the column to that of the material was about 0·95 ; and confirm that Bryan's formula, eq. (7), § 160, gives the buckling strength of the web plate.

The above conclusions are drawn from observations on columns in a testing machine, and it is important to distinguish between the behaviour of such columns and those in a truss. In the testing machine, as pointed out in § 112, Vol. I, when the extreme fibres pass the yield point, the line of resistance moves away from the centre-line, virtually increasing the initial curvature, which results in increasing deflection and increased stress. The process is cumulative, for the load can follow up the increasing deflection, and rapid failure results. In a truss, the action of the longitudinal load is only one of the agencies straining the column. A large part of the maximum stress therein will be due to deformation bending moments ; and, particularly when S-bending occurs, the maximum stress will occur at the ends of the column. Exceeding the yield point locally will probably relieve the conditions instead of making them worse. Not only so, but instead of the load following up
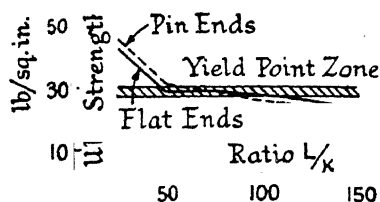
Fig. 239.

its advantage, the ' give ' in the member will bring about a redistribution of the load over the frame, giving time and opportunity for elastic recovery to play its part.

These remarks do not apply to isolated columns, nor to other cases where the load is free to follow up the increasing deflection. The danger of sudden collapse due to the local buckling (secondary flexure) of an elementary flange column, or other local part, must not be overlooked.

162. **Experiments on Large Columns.**—From the considerations of the two preceding articles, it is to be expected that the ultimate strength of large columns will fall short of that of small solid specimens, and this is found experimentally to be the case. From the collected results of a large number of column tests on large specimens of all lengths which showed integral action, .the American Committee [16] conclude that a Johnson parabola, beginning at the yield point for $L/\kappa = 0$ and tangent to the Euler curve, fairly represents the experimental results for all grades of structural steel, including structural nickel steel. In its generalised form the equation to the parabola is, § 116, Vol. I,

$$f_r = f_y - \frac{f_y^2}{4\pi^2 E}\left(\frac{qL}{\kappa}\right)^2 \qquad (1)$$

For flat-ended specimens the Committee give $q = 0\cdot56$, and for a structural steel in which f_y ranges from 34,000 to 38,000 lb./sq. in., eq. (1) becomes

$$f_r = 36{,}000 - 0\cdot36\ (L/\kappa)^2 \qquad . \qquad . \qquad . \qquad (2)$$

For specimens with pin ends the Committee find that $q = 0\cdot78$.

163. **Practical Empirical Formulae.**—Adopting the parabolic formula as the most convenient empirical expression, and writing it in the form $f_a = c_1 - c_2 \left(\dfrac{qL}{\kappa}\right)^2$, the constants may be so chosen that f_a represents the safe working load per square inch on the member. The parabola will then be tangent to the Euler curve, Fig. 240, $f_p = \dfrac{\pi^2 E}{\eta(qL/\kappa)^2}$, where η is the factor of safety against buckling. It follows that $\eta = 4\pi^2 E c_2/c_1^2$, and the validity limit of Euler's formula is $qL/\kappa = \sqrt{c_1/2c_2}$. Limiting the working stress in direct compression to $6\cdot8$ tons/sq. in. and taking $\eta = 3$ as the minimum factor of safety for Euler's formula, $c_1 = 6\cdot8$, $c_2 = 1/3700$ and

$$f_a = 6\cdot8 - \frac{1}{3700}\left(\frac{qL}{\kappa}\right)\text{tons/sq. in.} \qquad . \qquad . \qquad (1)$$

This equation may be used to obtain the safe load per square inch on a column intended to be concentrically loaded, such as a bridge compression member. As will be seen from Fig. 240, it agrees closely with the straight line column formula for pin ends given in the British Standard for Girder Bridges, 1923. It makes no allowance for secondary

The 1935 A.R.E.A. Specification for Steel Railway Bridges gives the following parabolic formulae for columns ($L/\kappa < 140$), ·

For pin ends, $f_a = 15{,}000 - \tfrac{1}{3}\,(L/\kappa)^2$.   .   (2)

For riveted ends, $f_a = 15{,}000 - \tfrac{1}{4}\,(L/\kappa)^2$.   .   (3)

Units: lb./sq. in.

In the British Standard for Girder Bridges (B.S. No. 153, 1933), the maximum working stress in compression is raised from 6·8 to 7·65 tons/sq. in., when the column formulae become

For pin ends, $f_a = 9(1 - 0\cdot0054\,L/\kappa)$.   .   .   (4)

For riveted ends, $f_a = 9(1 - 0\cdot0038\,L/\kappa)$.   .   .   (5)

max. $f_a = 7\cdot65$.   Units: tons/sq. in.

For small solid struts, the ordinary Johnson parabolic formula, eq. (3), § 164, may be used, with a factor of safety $\eta = 3$ for concentrically
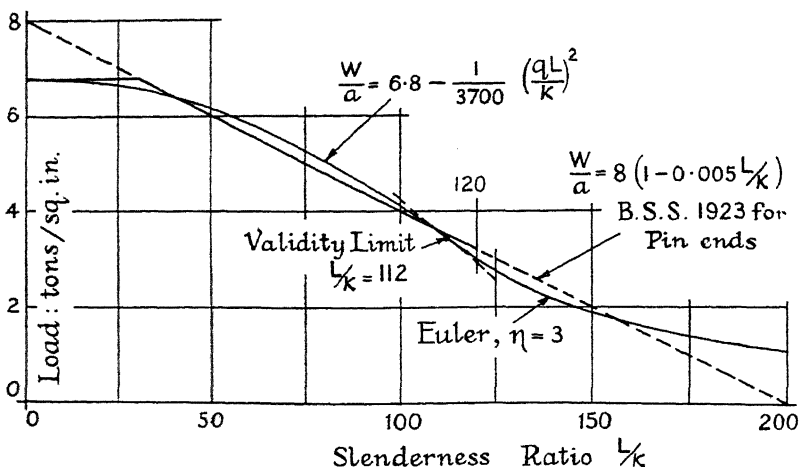
FIG. 240.

loaded members, and $\eta = 4$ for members attached by their backs as in a roof truss, Fig. 243, to allow for the eccentric attachment (see § 167).

In the L.C.C. Code of Practice (1932) for Steel Buildings, the Perry formula for struts is adopted:

$$\eta f_a = \tfrac{1}{2}\left[f_y + \frac{P}{a}\left\{1 + \frac{e_1 v_1}{\kappa^2}\right\}\right] - \tfrac{1}{2}\sqrt{\left[f_y + \frac{P}{a}\left\{1 + \frac{e_1 v_1}{\kappa^2}\right\}\right]^2 - 4\frac{P}{a}f_y} \quad (6)$$

[cf. eq. (10), § 105, Vol. I].   Here a is the area in sq. in.; f_a the safe load, tons/sq. in.; $P = \pi^2 EI/(qL)^2$.   The following are the values (due to Professor Robertson) for the constants: Factor of safety $\eta = 2\cdot36$;

yield stress,[*] $f_y = 18$ tons/sq. in. ; $e_1 = 0 \cdot 003 \, qL/\kappa$; $E = 13{,}000$ tons/sq. in. ; max. $f_a = 7 \cdot 2$ tons/sq. in.

All the above formulae apply to mild steel columns. For alloy steels the A.R.E.A. rules are (L/κ < 130),

Silicon Steel. ($f_y = 45{,}000$ lb./sq. in. min.)

$$\text{For pin ends,} \quad f_a = 20{,}000 - 0 \cdot 61 \, (L/\kappa)^2 \quad . \quad . \quad (7)$$

$$\text{For riveted ends,} \quad f_a = 20{,}000 - 0 \cdot 46 \, (L/\kappa)^2 \quad . \quad . \quad (8)$$

Nickel Steel. ($f_y = 50{,}000$ lb./sq. in. min.)

$$\text{For pin ends,} \quad f_a = 22{,}500 - 0 \cdot 76 \, (L/\kappa)^2 \quad . \quad . \quad (9)$$

$$\text{For riveted ends,} \quad f_a = 22{,}500 - 0 \cdot 57 \, (L/\kappa)^2 \quad . \quad . \quad (10)$$

Units : lb./sq. in.

164. Asimont's Device.[36]—This device obviates the trial and error method of finding the area of a column. It is particularly suited for use with a parabolic formula of the type

$$\frac{W}{a} = c_1 - c_2 \left(\frac{qL}{\kappa} \right)^2$$

in which W denotes the load and a the area of the column. Let $a = g\kappa^2$, where g is a constant depending on the shape of the cross section. Then

$$(qL/\kappa)^2 = \frac{g}{a}(qL)^2, \quad \text{and} \quad \frac{W}{a} = c_1 \left\{ 1 - \frac{c_2}{c_1} \cdot \frac{g}{a}(qL)^2 \right\}$$

whence,

$$a = \frac{W}{c_1} + \frac{c_2}{c_1} g(qL)^2 \quad . \quad . \quad . \quad . \quad (1)$$

[*] The test values for mild steel published by the *British Steel Structures Research Committee*, 1st Report, 1931, again illustrate the variation in the yield point exhibited by ordinary structural steel (cf. the Table, p. 130), as do those by F. R. Freeman, *Proc. Inst. C.E.*, vol. 231, p. 283. The variation with thickness in Freeman's results should be noted.

Units : tons/sq. in.	Max.	Mean.	Min.
Tensile Yield Point. (Research Committee.)			
Works tests on 11 flat specimens . . .	22·3	18·5	15·8
Laboratory tests on 12 flat specimens . .	19·0	15·8	13·55
Laboratory tests on 12 small cylindrical specimens	21·0	15·2	13·0
Compressive Yield Point. (Research Committee.)			
Laboratory test on 12 small cylindrical specimens	16·7	15·4	14·0

Tensile Yield Point. (Freeman's Tests.) Table V.

Average of Series 14 and 15 ; 29 tests in all . . . } Thickness . $\frac{1}{8}$ $\frac{3}{16}$ $\frac{1}{4}$ $\frac{3}{8}$ $\frac{1}{2}$ inch.
Yield Point 18·1 15·4 15·9 15·1 14·3 tons/sq. in.

an equation which gives the area of the column in terms of known quantities. Eq. (1), § 163, becomes

$$a = \frac{1}{6 \cdot 8}\left\{ W + \frac{g(qL)^2}{3700} \right\} \text{ sq. in.} \qquad \cdot \qquad \cdot \qquad \cdot \qquad (2)$$

where W is in tons. The ordinary Johnson parabola for mild steel specimens, eq. (9), § 116, Vol. I,

$$f_r = 40,000 - \tfrac{4}{5}(qL/\kappa)^2 \qquad \cdot \qquad \cdot \qquad \cdot \qquad \cdot \qquad (3)$$

becomes

$$a = \frac{1}{40,000}\left\{ \eta W + \frac{4g(qL)^2}{3} \right\} \text{ sq. in.} \qquad \cdot \qquad \cdot \qquad (4)$$

where η is the factor of safety and W is in lb.

The value of g is best obtained from a cross section exactly similar to the one it is proposed to use. Knowing I_{min}, $g = a/\kappa^2 = a^2/I_{min}$. Values of g are given below:

	Cross Section.						g
Circle	.	.	.	.	.	.	4π
Hollow Circle, mean diameter D, thickness t	.	.	.	.	$25t/D$
Square	.	.	.	.	.	.	12
Rectangle B × D, B > D	.	.	.	.	.	$12B/D$
*Equal Angles, D × D × t	.	.	.	.	.	$50t/D$ approx.
*Equal Tees, D × D × t	.	.	.	.	.	$45t/D$ approx.
8″ × 6″ × 35 lb. B.S.B.	.	.	.	.	.	5·43
14″ × 8″ × 70 lb. B.S.B.	.	.	.	.	.	6·36
11″ × 11″ × 76 lb. Broad Flange Beam	.	.	.	2·82

The smaller the value of g, the more efficient the cross section as a strut.

Having found the necessary value for a, and chosen the cross section, the safe load for the member must be verified by the column formula, because g is sensitive to small changes in shape of cross section.

165. Shearing Force in Columns.—From eq. (4), § 119, Vol. I, the shearing force in a column with direction-fixed ends and an initial deflection e_1, is

$$S = \frac{4We_1}{L}\left(\operatorname{cosec} \frac{aL}{2} \right) \sin ax \qquad (1)$$

and

$$\frac{dS}{dx} = \frac{4We_1}{L}\left(a \operatorname{cosec} \frac{aL}{2} \right) \cos ax$$

S is a maximum when $\cos ax = 0$, or $ax = \pi/2$. But

$$a = \frac{2\pi}{L}\sqrt{\frac{W}{P_2}}; \quad P_2 = \frac{4\pi^2 EI}{L^2}$$

(§ 108, Vol. I); therefore S is a maximum when $x = \frac{L}{4}\sqrt{\frac{P_2}{W}}$. When $W = P_2/4$, $x = L/2$, and the maximum shearing force $S = 4We_1/L$ occurs at the ends of the column. This holds for all values of W less than $P_2/4$, for x cannot be greater than $L/2$. If $W/P_2 > \tfrac{1}{4}$, there will

* It is best to calculate the values from similar cross sections.

be a point of inflexion in the half length of the column, and the maximum shear will occur there. Putting $ax = \pi/2$ in eq. (1),

$$\text{max. } S = \frac{4We_1}{}\cosec \pi \sqrt{\frac{W}{P_2}} \qquad (2)$$

The curve in Fig. 241 represents the ratio (max.S/W) plotted on a base line representing W/P_2, taking the value of e_1 as $L/750$ for initial curvature plus an equal amount for variation in the modulus of elasticity. On the same diagram the values of (max.S/W), as determined in the American Railway Engineering Association experiments [13] on columns with flat ends, have been plotted. These values were calculated from strain-gauge measurements on lattice bars, and owing to the tendency to flexure in these thin
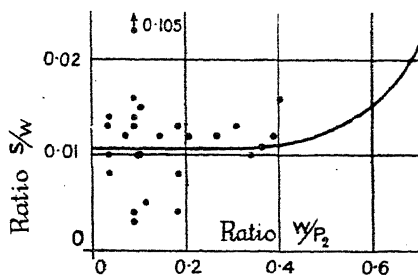
FIG. 241.

bars, are probably an over- rather than an under-estimate. The figure confirms that the shearing force in concentrically loaded columns, due to the longitudinal load, is small. Such members have also to resist the shearing force resulting from the deformation stresses (see Fig. 190), and in the case of S-bending, if L/κ be small, the shearing force may be greater than when the column bends into a single loop. Jensen (1908) showed that in an originally straight column with position-fixed ends, if the eccentricity e_2 lie on opposite sides of the central axis at the two ends, thus producing S-shaped bending, the maximum shearing force occurs in the middle of the column and is given by

$$\text{max. } S = \frac{2e_2W}{L}\left\{\frac{\pi}{2}\sqrt{\frac{W}{P}}\cosec \frac{\pi}{2}\sqrt{\frac{W}{P}}\right. \qquad (3)$$

where $P = \pi^2 EI/L^2$. This is considerably greater than if the eccentricity at the two ends lie on the same side of the column.

For these reasons it is necessary to design the column for a greater shearing force than is suggested by eq. (2), and it is usual to specify that a shearing force equal to $2\frac{1}{2}\%$ of the longitudinal load, assumed to be uniform from one end of the column to the other, be provided for.

If the column have a plate web, e.g. (ii) Fig. 227, or (iv) Fig. 230, the methods of § 175 may be used to find the requisite pitch of the rivets connecting the web plate to the flange. It frequently occurs that the theoretical pitch is so large that practical considerations become the determining factor. In the case of a lattice-braced column, the shearing force must be resolved along the diagonal bars. Two experimental studies have been made on the strength of lattice bars. According to the experiments of Talbot and Moore,[11] the ultimate strength of lattice bars attached by $\frac{1}{2}$-in. bolts was

$$f_r = 21{,}400 - 45\, l/\kappa = 21{,}400 - 156\, l/t \quad \text{lb./sq. in.} \qquad (4)$$

and according to the experiments of the American Column Research Committee,[17] on lattice bars attached by $\frac{3}{4}$-in. bolts,

$$f_r = 25,000 - 42 \, l/\kappa = 25,000 - 146 \, l/t \quad \text{lb./sq. in.} \qquad . \quad (5)$$

Eqs. (4) and (5) give the ultimate strength; $l =$ the length and t the thickness of the bars.

For a worked example of a lattice-braced column, see § 167.

166. Batten-Plate Columns.—In this type of column, Fig. 242, the lattice bracing is replaced by batten plates as shown, spaced according to the shearing force. Emperger[21] made a number of experiments on flat-ended columns with various kinds of web bracing, and found that if the batten plates be suitably arranged, it was possible to make a batten-plate column equally as strong as a similar lattice-braced column. He concluded that each batten plate should be attached to the flanges by at least two rivets on each side, and that L/κ for the flange, considered as a column bending between the panel points, should not exceed one-half that of the column as a whole. Emperger's conclusion regarding the efficiency of properly arranged batten plates has been confirmed by later experiments, but the American Column Research Committee found that, under oblique loading producing a 5 % shear, the superior rigidity of the solid and lattice-braced columns over the batten-plate columns was marked. When the shearing force is large, the batten plates may need to be placed so close together that this type of column would possess no advantage, but under concentric loads, when the shearing force is small, the economy of the batten-plate column is evident. It is also far easier to paint.

Elaborate theories for the strength of batten-plate columns, taking into account the distortion of the webs,

Fig. 242.

have been given by Müller-Breslau,[19] Engesser,[22] and others. The following approximate treatment appears to give good results. Find the necessary cross section for the flanges, taking into account the secondary flexure of the elementary flange columns, § 160 ; for these, $q' = 1$. Take S as equal to $2\frac{1}{2}$ % of W. Then from Fig. 242, if F_s be the longitudinal force on the rivet group on one side of the batten plate, taking moments about B,

$$S'L' = F_s \times h \, ; \text{ and } F_s = \frac{S'L'}{h} \qquad . \qquad . \qquad . \quad (1)$$

where S' is the shearing force carried by one line of batten plates. Normally there will be batten plates back and front of the column, and S' = S/2. From Fig. 242, taking moments about the centre point of the batten plate,

$$F_s \times h = 2M = S'L' \, ; \text{ and } M = S'L'/2 \qquad . \qquad . \quad (2)$$

M is the bending moment on one group of rivets. Each rivet group must carry therefore a longitudinal force F_s', a bending moment M, and
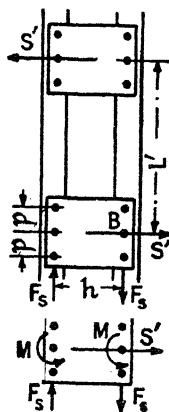
a transverse force $S'/2$; and must be designed accordingly. The batten plate itself must carry a bending moment M.

167. Worked Examples.—An angle strut, 8 ft. long, is attached by one leg to stiff gussets at each end, (i) Fig. 243, and loaded with 10 tons. Find the necessary size of angle. Use the Johnson parabolic formula and a factor of safety of 4.

The member may be assumed to be imperfectly direction-fixed at each end, and a value $q = 0.78$ may be used ; hence $qL = 0.78 \times 96 = 75$ inches. For an angle of medium size the value of $g = 6$. Applying eq. (4), § 164,

$$a = \frac{1}{40,000}\left\{\eta W + \frac{4g(qL)^2}{3}\right\}$$

$$\frac{1}{40,000}\left\{4 \times 10 \times 2240 + \frac{4 \times 6 \times 75^2}{3}\right\} \quad 3.37 \text{ sq. in.}$$

The nearest angle section is a $4 \times 4 \times \frac{1}{2}$, area 3.75 sq. in., min. $\kappa = 0.78$, so that $g = 3.75 \div 0.78^2 = 6.2$. The ratio $qL/\kappa = 75 \div 0.78 = 97$. Checking the section by the Johnson formula,

$$\text{safe } W = \frac{a}{\eta}\left\{40,000 - \frac{4}{3}\left(\frac{qL}{\kappa}\right)^2\right\} \div 2240$$

$$\frac{3.75}{4}\left\{40,000 - \frac{4}{3} \times 97^2\right\} \div 2240 \quad 11.5 \text{ tons.}$$

Using the Rankine-Gordon formula, eq. (3), § 116, Vol. I, R 35·6 tons and $\eta = 3.56$.

A question arises in connection with the above problem. The angle section is attached by its back to the gusset, as shown in Fig. 243. Is it, or is it not, eccentrically loaded; if so, what is the eccentricity ? At first sight it would appear that the load acts at a positive eccentricity equal to the distance e_2 between the centre of the gusset and the centre of area of the cross section of the angle. As in the parallel case of the tie, § 151, if the gusset and the connection thereto were perfectly stiff, the ends of the column would be perfectly fixed in direction, and the column would not be eccentrically loaded. The condition of perfect direction-fixing implies that a fixing moment acts at the end of the column. This may be regarded as set up by the load acting at a negative eccentricity e_2', (ii) Fig. 243 [compare (iii) Fig. 167, Vol. I], and it must overcome any bending moment due to an apparent positive eccentricity, for obviously the load cannot have both a positive and a negative eccentricity at the same time. The effect of the apparent positive eccentricity e_2 is that the fixing moment must be greater, and the gusset must be stiffer, than if the load were concentrically applied ;
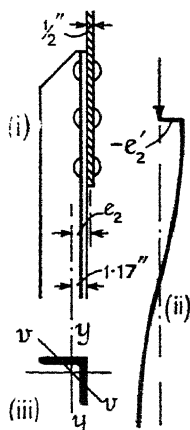
FIG. 243.

but if the direction-fixing be perfect, the strength of the column proper is not affected.

In practical cases the direction-fixing is imperfect, and the designer has to make the best estimate he can as to the degree of imperfection. A liberal estimate of the value of q, which increases as the stiffness of the gusset decreases, is desirable in such cases. The value $q = 0 \cdot 78$ used above implies a state midway between perfect direction-fixing and complete freedom in direction without eccentricity.

Another point in connection with the above example is worth consideration. In the working above, it has been assumed that the angle bends about the axis vv (iii), i.e. in the direction of the least radius of gyration, whereas the eccentricity e_2, due to the angle being attached by its back, implies bending about the two principal axes at once (non-uniplanar bending, § 84, Vol. I), and the stiffness of the gusset in its own plane helps to fix the ends of the member for bending about both axes. It is of interest to determine what the stress in the angle would be if bending took place entirely about the axis yy (iii), on the assumption that the gusset is perfectly flexible. The eccentricity e_2 would then exercise its full effect on the column itself, and the eccentricity formula, eq. (8), § 106, Vol. I, must be applied. The distance of the centre of area of the $4 \times 4 \times \frac{1}{2}$ in. angle from the back of the flange is $1 \cdot 17$ in. ; if the gusset be $\frac{1}{2}$ in. thick, $e_2 = 1 \cdot 17 + 0 \cdot 25 = 1 \cdot 42$ in. Then, from the equation quoted, the maximum stress at the centre of the angle is

$$f_c = \frac{W}{a} \left\{ 1 + \frac{e_2 v_1}{\kappa^2} \sec \frac{\pi}{2} \sqrt{\frac{W}{P}} \right\}$$

For bending about the axis yy, L = 96 in., I = $5 \cdot 46$ in.^{4}, and Euler's crippling load is

$$P = \frac{\pi^2 EI}{L^2} = \frac{\pi^2 \times 13,000 \times 5 \cdot 46}{} = 76 \text{ tons.}$$

W = 10 tons, a $3 \cdot 75$ sq. in., $e_2 = 1 \cdot 42$ in., $v_1 = 1 \cdot 17$ in., $\kappa^2 = \frac{1}{\cdot}$ $= \frac{5 \cdot 46}{3 \cdot 75}$ $1 \cdot 45$ in.^{2}, and

$$f_c = \frac{10}{3 \cdot 75} \left\{ 1 + \frac{1 \cdot 42 \times 1}{1 \cdot 45} \cdot 17 \sec \left(90^\circ \times \frac{10}{76} \right) \right\} = 6 \cdot 30 \text{ tons/sq. in.}$$

Although not to be regarded as an accurate estimate of the stress in the member, this figure indicates that even if the direction-fixing be negligible, the stress would not exceed an allowable figure. There is no question of crippling, for the factor of safety on Euler's formula is $76 \div 10 = 7 \cdot 6$. Since $W/P < 1/5$ the approximate formula, eq. (8), § 107, Vol. I, might have been used :

$$f_c \quad \frac{W}{a} \left\{ 1 + \left(1 + \frac{3W}{2P} \right) \frac{e_2 v_1}{\kappa^2} \right\}$$

$$\frac{10}{3 \cdot 75} \left\{ 1 + \left(1 + \frac{3 \times 10}{2 \times 76} \right) \frac{1 \cdot 42 \times 1 \cdot 17}{1 \cdot 45} \right\} = 6 \cdot 33 \text{ tons/sq. in.}$$

Bridge Compression Member.—The method of designing bridge compression members of the type shown in Fig. 227 is indicated in ¶ 16, § 196. In the following example a column of the type shown in Fig. 228 will be considered. The length of the member is 25 ft. = 300 in.; it carries a load of 120 tons; the distance between the gusset plates is 17½ in. The column as designed is shown in Fig. 244. Assuming that the average stress in the column will be about 6 tons/sq. in., an area of 20 sq. in. will be required. Try two 15 × 4 × 36·4 lb./ft. B.S.C., area 10·7 sq. in., and consider bending about the axis *xx*, i.e. in the plane of the truss. The *κ* of a single channel, and therefore of the pair about this axis, is 5·71. The column will be attached by strong gussets to stiff flanges, and *q* may be taken as 0·7. Hence, for the column as a whole, $qL/\kappa = 0·7 \times 300 \div 5·71 = 36·8$; and, from eq. (1), § 163, the safe load per square inch is $f = 6·8 - (36·8)^2/3700 = 6·43$ tons/sq. in., and the safe load on the member is 21·4 × 6·43 = 137·6 tons, showing that from this aspect the proposed section is adequate.

The lattice bracing must carry a shearing force of 2½ % of 120 = 3 tons, or 1½ tons per side. As shown in Fig. 244, the centre lines of the rivets will be 13 in. apart. Adopting a single 60° system, the length of each bar will be 15 in., and from the rules given in § 155 the minimum thickness = 15 ÷ 40 = ⅜ in. Assuming that 15/16 rivet holes are used, the minimum width of the bar will be 2½ in. The minimum *κ* of a 2½ × ⅜ in. bar will be 0·108 in.; and *l/κ* for the bar will be 15 ÷ 0·108 = 139. From eq. (5), § 165, the crippling load per sq. in. will be

$$f_r = 25,000 - 42 \times 139 = 19,160 \text{ lb./sq. in.}$$

or, adopting a factor of safety of 4, the bar is worth

$$2½·\times \tfrac{3}{8} \times (19,160 \div 4)/2240 = 2 \text{ tons.}$$

Resolving the actual shearing force of 1½ tons along the bar, the force acting along the bar is 1·73 tons, and the proposed section may be adopted. A 15/16 rivet will easily carry the force of 1·73 tons.

Considering bending about the *yy* axis, the bottom end of the member will be attached to a stiff cross girder, and the top end to some light lateral bracing (cf. Fig. 309). In addition, both ends will be firmly attached to the top and bottom flanges of the truss, but the stiffness of the latter will be their torsional stiffness, which is much less than their flexural stiffness. On the whole, the end conditions are less satisfactory than for bending about the *xx* axis, and a value *q* = 0·8 will be assumed. The value of $\kappa_y = 7·86$ in., and $qL/\kappa = 0·8 \times 300 \div 7·86 = 30·5$. In this direction the secondary flexure of the elementary flange columns must be taken into account. The unsupported length L′ of these columns is 15 in.; *κ′* of the channel for bending about *y′y′* axis is 1·12; *q′* must
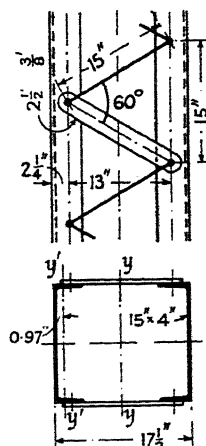
FIG. 244.

be taken as unity, therefore $q'L'/\kappa' = 1 \times 15 \div 1\cdot12 = 13\cdot4$, within the value 25 for integral action, § 160. To allow for secondary flexure, the term $(qL/\kappa)^2$ in the parabolic formula must be replaced by $\{(qL/\kappa)^2 + (q'L'/\kappa')^2\}$ [see eq. (3), § 160], whence eq. (1), § 163, becomes

$$f_a = 6\cdot8 - \frac{1}{3700}\left\{\left(\frac{qL}{\kappa}\right)^2 + \left(\frac{q'L'}{\kappa'}\right)^2\right\} = 6\cdot8 - \frac{(30\cdot5)^2 + (13\cdot4)^2}{3700}$$

$$= 6\cdot5 \text{ tons/sq. in.}$$

or practically the same as for the xx axis.

The column may be considered as satisfactory.

It will be evident, as Krohn [18] pointed out, that in such cases I_{min} of the column as a whole must be *greater* about yy than about xx, to allow for secondary flexure.

It is of interest to calculate the maximum fibre stresses at the centre of the column using the rational formulae. For bending about xx,

$e_1 = L/750 + D/40 = 300 \div 750 + 15 \div 40 = 0\cdot77$ in. ;

$P_1 = \pi^2 EI/(qL)^2 = 2028$ tons ; $W/P_1 = 0\cdot06$, and from eq. (4), § 158,

$$f_c = \frac{W}{a}\left[1 + q^2\frac{e_1 v_1}{\kappa^2}\left\{1 + 1\cdot25\frac{W}{P_1}\right\}\right]$$

$$\frac{120}{21\cdot4}\left[1 + (0\cdot7)^2\frac{0\cdot77 \times 7\cdot5}{5\cdot71^2}\{1 + 1\cdot25 \times 0\cdot06\}\right] = 6\cdot13 \text{ tons/sq. in.}$$

For bending about yy, $e_1 = 300 \div 750 + 17\cdot5 \div 40 = 0\cdot84$ in. ; $P_1 = 2950$ tons $(qL/\kappa = 30\cdot5)$; $W/P_1 = 0\cdot04$, and from eq. (5), § 160, $[h = 17\cdot5 - 2 \times 0\cdot97 = 15\cdot56$ in., see Fig. 244]

$$F' = \frac{W\cdot}{h}\left[q^2e_1\left\{1 + 1\cdot25\frac{W}{P_1}\right\} + \frac{h}{2}\right]$$

$$= \frac{120}{15\cdot56}\left[(0\cdot8)^2 \times 0\cdot84\{1 + 1\cdot25 \times 0\cdot04\} + \frac{15\cdot56}{2}\right] = 64\cdot4 \text{ tons.}$$

Hence, from eq. (6), § 160,

$$f_c = \frac{F'}{a/2}\left[1 + \left\{1 + \frac{3F'}{2P}\right\}\frac{v_1'}{(\kappa')^2}(e_1' + e_2')\right]$$

$P = 7640$ tons ; $(e_1' + e_2') = L'/200 = 15 \div 200 = 0\cdot075$ in.

$\therefore 4 - 0\cdot97 = 3\cdot03$ in.

$$f_c \quad \frac{64\cdot4}{10\cdot7}\left[1 + \left\{1 + \frac{3 \times 64\cdot4}{2 \times 7640}\right\}\frac{3\cdot03}{(1\cdot12)^2} \times 0\cdot075\right] = 7\cdot13 \text{ tons/sq. in.}$$

If the column bend about both axes at once

max. $f_c = 6\cdot13 + 7\cdot13 - (120 \div 21\cdot4)$ $7\cdot65$ tons/sq. in.

BIBLIOGRAPHY

Tension Members

1. MOBERLEY. Account of some Tests of Riveted Joints for Boiler Work. *Proc. Inst. C.E.*, vol. lxix, p. 337 ; vol. lxxii, p. 226.
2. BATHO. The Distribution of Stress in Certain Tension Members. *Trans. Can. Soc. C.E.*, vol. xxvi, 1912, p. 224.

3. BATHO. The Effect of the End Connections on the Distribution of Stress in Certain Tension Members. *Jour. Frank. Inst.*, Aug. 1915, p. 129.
4. DEUTSCHER STAHLBAU-VERBAND. Berichte des Ausschusses für Versuche im Eisenbau. Ausgabe B, Heft 1, Berlin, 1915; see also RUDELOFF, *Der Bauingenieur*, 1921, p. 450.
5. SCOBEL. The Design of Pin Joints Based on Ultimate Strength. *Trans. I.N.A.*, vol. lix, 1917, p. 92.
6. BEKE. A Study of the Stresses in Eye-Bar Heads. *Eng. News.-Rcd.* Aug. 11, 1921, p. 234; see *Eng. Ab. I.C.E.*, 1922, No. 10 : 87.
7. YOUNG. True Net Sections of Riveted Tension Members. *Univ. Toronto Eng. Res. Bull.* No. 2, p. 233.
8. SONNTAG. See Ref. No. 7. Chap. XX, Bib.
9. LOUDON. *Riveted Tension Members. Univ. Toronto Eng. Res. Bull.* No. 9, 1932, p. 231.

Tests on Large Compression Members

10. WATERTOWN ARSENAL. Reports of the Tests of Metals. 1881–85, Built-up W.I. Cols.; 1909–10–11–13–14, Steel Tubes; Rolled and Built-up Steel Sections (Year of Publication).
11. TALBOT AND MOORE. Tests of Built-up Steel and Wrought-Iron Compression Pieces. *Trans. Amer. Soc. C.E.*, vol. lxv, 1909, p. 202.
12. HOWARD. Some Tests of Large Steel Columns. *Trans. Amer. Soc. C.E.*, vol. lxxiii, 1911, p. 429.
13. AMER. RY. ENG. ASSOC. Column Tests. *Proc.*, vol. xvi, 1915, p. 636; vol. xix, 1918, p. 789.
14. GRIFFITH AND BRAGG. Tests of Large Bridge Columns. Tech. Paper No. 101, *U.S. Bur. Stnds.* 1918; also TUCKERMAN AND STANG, Tech. Paper No. 328, 1926; and STANG, WHITTEMORE AND SWEETMAN, *U.S. Bur. Stnds. Jour. Res.*, vol. 16, 1936, pp. 595, 627.
15. AMER. SOC. C.E. Final Report of Special Committee on Steel Columns and Struts. *Trans.*, vol. lxxxiii, 1919–20, p. 1583.
16. —— Reports of Special Committee on Steel Column Research (1st Prog. Rpt.) *Trans.*, vol. lxxxix, 1926, p. 1485; see *Eng. Ab. I.C.E.*, 1926, No. 29 : 93.
17. (2nd Prog. Rpt.). *Trans.*, vol. xcv, 1931, p. 1152; Final Report. *Trans.*, vol. xcviii, 1933, p. 1403.

The Built-Up Column. Secondary Flexure

18. KROHN. Beitrag zur Untersuchung der Knickfestigkeit gegliederter Stäbe. *Zen. d. Bauver.*, Berlin, Oct. 21, 1908, p. 559; see also ENGESSER, ibid., Mar. 10, 1909, p. 136; SALIGER, *Zeit. d. oest. Ing.- u. Arch. Ver.*, Wien, Jan. 5, 1915, p. 5; GÉRARD, *Rev. Univ. d. Mines*, 1913, p. 178.
19. MÜLLER-BRESLAU. Ueber exzentrische gedrücte gegliederte Stäbe. *Sitzungsberichte d. k. Preuss. Akad. d. Wissenschaften*, Berlin, 1910, p. 166 : also *Der Eisenbau*, 1911, p. 339.
20. SALMON. *Columns*. London, 1921, chap. ii.

Batten-Plate Columns

See Refs. Nos. 17, 18 and 19 above.

21. EMPERGER. Welchen Querband bedarf eine Eisensäule. *Beton u. Eisen*, Feb. 19, 1908, p. 71 *et seq.*
22. ENGESSER. Ueber die Knickfestigkeit von Rahmenstäben. *Zen. d. Bauver.*, Mar. 10, 1909, p. 136; *Der Eisenbau*, 1911, p. 385; also KROHN, Ref. No. 18.

23. PETERMANN. Müller-Breslau's Knickversuche mit Rahmenstäben. *Der Bauingenieur*, 1926, p. 979; also Knickversuche mit Rahmenstäben aus St. 48. *Der Bauingenieur*, 1931, p. 509.
24. FLEMING AND WEISKOPF. Batten-Plate Columns : Their Status and a Design Theory. *Eng. News-Rcd.*, Mar. 11, 1926, p. 412.

Experiments on Shear in Columns

25. WATERTOWN ARSENAL. Reports of the Tests of Metals (Experiments with different types of Lattice Bracing), 1910, p. 829 *et seq.* (Year of Publication).
26. TALBOT AND MOORE. See Ref. No. 11.
27. HOWARD. See Ref. No. 12.
28. AMER. RY. ENG. ASSOC. See Ref. No. 13.
29. AMER. SOC. C.E. Column Research Committee. See Ref. No. 17, pp. 1177–79, 1242 (2nd Prog. Rpt.).

Crippling of Web Plates in Columns

30. JOHNSTON. Compressive Strength of Column Web Plates and Wide Web Columns. Tech. Paper, No. 327, *U.S. Bur. Stnds.* 1926 ; also *Engg.*, Mar. 11, 1927, p. 296 ; Sep. 25, 1925, pp. 378, 778.
31. AMER. SOC. C.E. Column Research Committee. See Ref. No. 17, p. 1237 (2nd Prog. Rpt.).
32. MELAN. Ueber die Stabilität von Stäben welche aus einem mit Rand-winkeln Verstärkten Blech Bestehen. *Proc. 3rd Int. Cong. App. Mech.*, vol. iii, Stockholm, 1930, p. 59.

Experimental Determination of Direction-Fixing

33 FÖPPL, L. Bestimmung der Knicklast eines Stabes aus Schwingungs-versuchen. *Beiträge z. tech. Mech. u. tech. Phys.* 1924.
34. ENGLER. Eine neue Methode zur Untersuchung der Knickfestigkeit und des Einspannungsgrads. *Der Bauingenieur*, 1926, p. 343 ; see *Eng. Ab. I.C.E.*, 1926, No. 29 : 94.
35. KAYSER. Versuchstechnische Bestimmung des Einspannungsgrades der Druckdiagonalen einer Eisenbahnbrücke. *Der Bauingenieur*, 1931, p. 643 ; see *Eng. Ab. I.C.E.*, 1932, No. 50 : 99.

Miscellaneous

36. ASIMONT. Eine Knickungs-Formel. *Zeit. d. Bayer. Arch. u. Ing. Ver.* Bd. viii, Heft 6, 1876–7, p. 119.
37. MISES U. RATZERSDORFER. Die Knicksicherheit von Rahmentragwerken. *Zeit. ang. Math. Mech.* 1926, p. 181.

QUESTIONS ON CHAPTER IX

1. Design and sketch neatly a forked joint to connect two mild steel rods $1\frac{1}{2}$ in. diameter. The safe tensile, shearing and bearing stresses are to be 7, 5 and 9 tons/sq. in. respectively. Take the strength in double shear as $1\frac{3}{4}$ that in single shear. Sketch also a suitable screw connection for tightening a bar of that size. (U.L.)

Ans. Pin $1\frac{3}{4}$ in. diam. ; min. inside width of fork 1 in. ; min. thickness of fork $\frac{1}{2}$ in.

2. A double cover plate butt joint in a tie-bar 15 in. wide, 1 in. thick, has cover plates $\frac{5}{8}$ in. thick and the rivets are 1 in. diameter. In one half of the joint there are five rows of rivets containing 1, 2, 3, 4 and 4 rivets respectively.

The tensile, shearing and bearing stresses allowable are 8, 6 and 12 tons/sq. in. respectively. Find the maximum safe load consistent with these conditions. (U.L. modified.)

Ans. 110 tons ; test all possible methods of failure.

3. Two lengths of a bar 12 in. wide and $\frac{3}{4}$ in. thick are to be connected by a double cover butt-joint. The diameter of the rivet holes is 1 in. Design a suitable joint. Tensile stress 8 tons/sq. in., shear stress 6 tons/sq. in., bearing stress 12 tons/sq. in. (U.L. modified.)

Ans. $1 + 2 + 3 + 2 = 8$ rivets each side ; butt covers $\frac{1}{2}$ in. thick.

4. It is proposed to use as a tie-bar two 4 by 3 by $\frac{3}{8}$ in. angles placed back to back to form a T section. At each end of the tie, this T section is riveted to one side of a $\frac{3}{8}$-in. gusset plate, so that the tie is eccentrically loaded. In order to keep the stress as small as possible, find whether it is better so to construct the T that the 4-in. flanges, or the 3-in. flanges, are riveted to the gusset plate. If the load in the tie be 10 tons, and the reactions act along the middle plane of the gusset plates, find the maximum stress for the better arrangement. The properties of a 4 by 3 angle are : Area $= 2 \cdot 48$ sq. in. ; co-ordinates of the centroid, measured from the back of the angle, $= 1 \cdot 27$, $0 \cdot 77$ in. ; moments of inertia about axes through the centroid and parallel to the flanges $= 3 \cdot 89, 1 \cdot 87$ in. units.

In this question you may neglect the rivet holes. (I.C.E.)

Ans. Better to rivet the 4-in. flanges to the gusset plate. Max. stress $+ 4 \cdot 0$ tons/sq. in.

5. Criticise the connection shown in (i) Fig. 245, and stating the assumptions made, show how you would estimate the stresses in the

FIG. 245.

rivets at AA. Re-design the joint and recalculate the stresses in these rivets. Assume that the rivets are in single shear, and $\frac{3}{4}$ in. in diameter. (U.L. modified.)

Ans. Shear stresses in (i) $4 \cdot 49$; $3 \cdot 38$; $4 \cdot 49$ tons/sq. in. ; in (ii) all $3 \cdot 38$ tons/sq. in.

6. A strut in a braced framework is 11 ft. 6 in. effective length and carries a load of $17 \cdot 0$ tons. The section required is to consist of two angles back to back with a $\frac{3}{8}$-in. space between them. Using the Johnson-parabolic formula, find a suitable cross section. Take $q = 1$ and provide a factor of safety of 3.

Ans. $4 \times 3 \times \frac{3}{8}$ in. double.

7. Design a bridge compression member of the type shown in Fig. 244, and to conform to the conditions there laid down. Its length, centre to centre of the flanges of the main girder, is 30 ft., and the load it carries is 140 tons. The width over the backs of the channels is $18\frac{1}{2}$ in.

Ans. Channel required : B.S.C. $17 \times 4 \times 44 \cdot 34$ lb./ft. ; 60° lattice bracing $2\frac{1}{2} \times \frac{7}{16}$ inch.

8. Design a batten-plate column with channel section flanges, 20 ft. long, to carry a load of 100 tons. Take $q = 0 \cdot 7$. See §166.

Ans. Refer Fig. 242 : Two channels $12 \times 3\frac{1}{2} \times 26 \cdot 37$ lb./ft., 15 in. apart overall ; $L' = 24, h = 11, p = 3$ in. ; three rivets $\frac{13}{16}$-in. holes ; $\frac{5}{16}$-in. batten plates.
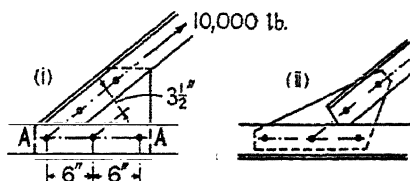
CHAPTER X

THE DESIGN OF BEAMS AND GIRDERS

168. Beam Sections.—It is evident from the expression for the moment of resistance of a beam, § 40, Vol. I, that, for a given depth of cross section, the material is more valuable for the purpose of resisting a bending moment the further it can be placed from the neutral axis. At the same time it is necessary to provide an efficient web connecting the tension and compression flanges, in order to resist the shearing force. These considerations have led to cross sections of the type shown in (i) Fig. 246, called **I** or *beam* sections. For a given area of cross section, such a profile will have a much greater section modulus than a rectangular section of the same depth. For example, a $12 \times 5 \times 30$ lb./ft.
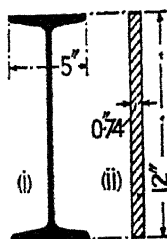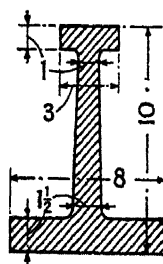
FIG. 246.   FIG. 247.

NBSB, (i) Fig. 246, has an area of $8 \cdot 83$ sq. in., and a section modulus of $34 \cdot 5$ in.³ A rectangle of the same depth and area, (ii), would have a width of $0 \cdot 74$ in., and a section modulus of $17 \cdot 8$ in.³, not much over one-half of that of the **I** section. Not only so, but such a thin rectangle, placed on edge, would make a very unsatisfactory beam, having very little lateral stiffness, whereas the **I** section is far stiffer both vertically and laterally. For these reasons, the great majority of steel beams are made of **I** section. The rolled sections suitable for use as beams are shown in Fig. 201.

In the case of cast-iron beams, the area of the tension flange is made much greater than that of the compression flange, Fig. 247, since cast iron is much weaker in tension than in compression. The neutral axis then falls much closer to the tension than to the compression flange, and consequently the stress in tension is much less than in compression. Many rules have been given for the correct proportions of a cast-iron beam section; the proportions shown in Fig. 247 were suggested by

Professor Goodman. If the tension flange be made too wide and thin, weakness due to unequal cooling results. Except in special cases, cast-iron beams are now seldom used in structural work.

Timber beams are usually made rectangular in cross section. Relatively short timber beams commonly fail by longitudinal shearing, and their strength in this direction should always be examined.

169. Use and Application of Mild Steel Beams.—Mild steel **I** beams are very suitable for the construction of steel-framed buildings,
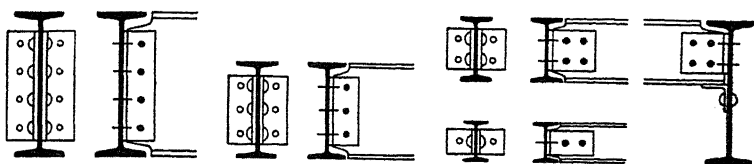
FIG. 248.

and are very extensively used for this purpose. They require little workmanship beyond straightening, cutting to length, and the provision of the necessary attachments. These attachments have been more or less standardised for the different sizes of beams. Typical angle cleats for the connection of beams to beams are shown in Fig. 248 ; fish-plate

Double Covers
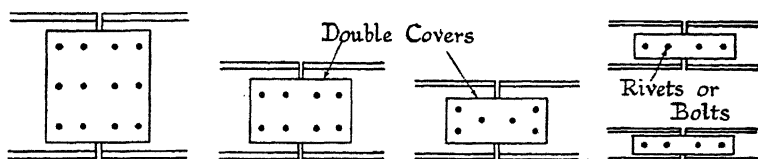
Rivets or Bolts

FIG. 249.

connections in Fig. 249 ; and attachments of beams to stanchions in Figs. 251 and 252. In a design, the load which these connections will safely carry should be properly calculated, and sufficient rivets or bolts should be provided to carry the forces coming upon the connections. Fish-plates of the type shown in Fig. 249 are unsuitable for resisting a bending moment, and where such moments exist, flange covers must be fitted, Fig. 250. When one beam by itself is insufficient to resist a bending moment, more than one may be used, side by side, fitted with cast iron or mild steel separators, (i) Fig. 253. In such arrangements, care must be taken that the load is equally distributed between the beams. Alternatively, the section modulus of an **I** beam may be increased by the addition of flange plates, (ii) Fig. 253. Such combinations are called *compound*

FIG. 250.

Bolts
shown thus

Bevelled
Washer
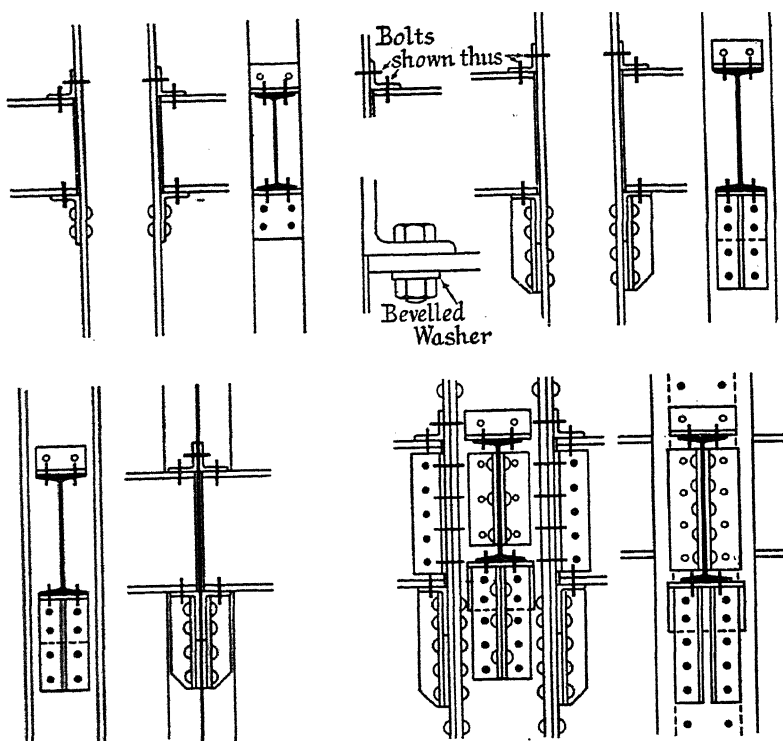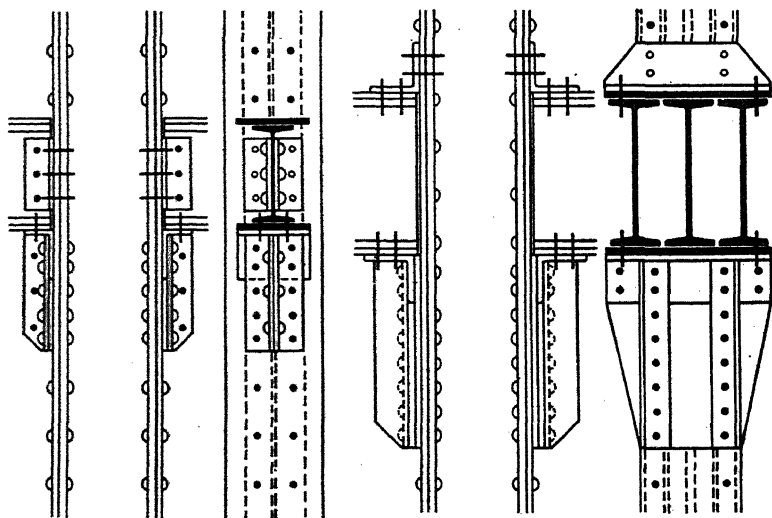
FIG. 251.

FIG. 252.

beams or girders. The length and cross section of the flange plates may be determined by the methods of ¶ 9, § 181. Alternative types of compound girders are shown in (iii) and (iv) Fig. 253.
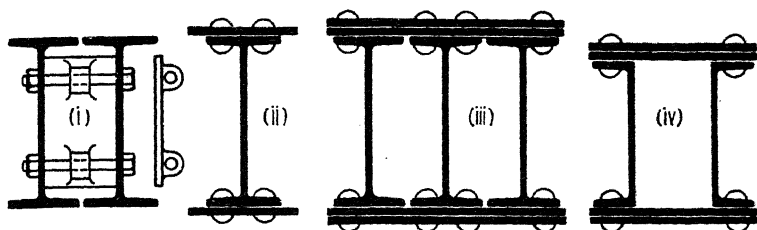
FIG. 253.

Proportions.—The depth of a beam should not be less than $\frac{1}{24}$th the span, and the breadth B should not be less than $\frac{1}{50}$th the unsupported length as defined in § 171. The deflection should not exceed $\frac{1}{360}$th the span, particularly if the beam is to support plastered ceilings or brick walls. If, however, the beam is encased in concrete, e.g. filler floor beams, the L.C.C. Code of Practice permits a depth of $\frac{1}{32}$nd the span.

Working Stresses.—For ordinary dead loads, the permissible stress on the net area of the tension flange and on the gross area of the compression flange should not exceed 8 tons/sq. in. If, however, the ratio l/B exceed 20, the stress in the compression flange should not exceed $f_c = 11 - 0\cdot15\ l/B$, unless the flange is embedded in a concrete floor, when a stress of 8 tons/sq. in. is permissible. The strength of the web should be examined by the methods of § 174, and stiffeners provided if required. The pitch of the longitudinal riveting can be found as in § 175. The safe shear stress on the closed area (L.C.C., nominal area) of shop rivets, and on tight-fitting turned bolts, may be taken as 6 tons/sq. in. ; on field rivets as 5 tons/sq. in., and on black bolts as 4 tons/sq. in., the area of the bolt itself being used. The shearing resistance· of rivets or bolts in double shear may be taken as twice that in single shear, and the safe bearing pressure as twice the safe shear stress.

170. **Plate Girders.**—When the span and/or the loading are too great to permit the employment of rolled steel beams, singly or in combination, *plate girders* are used, Fig. 272. In a riveted plate girder the flanges are built up of plates or flats, and are attached to a web plate by means of flange angles. The web plate is stiffened by a series of vertical stiffeners, Fig. 262. In very large and heavy plate girders, two or more webs may be used. Suitable end bearings must be provided, Fig. 267.

171. **Types and Proportions of Plate Girders.**—The most economical form of plate girder is that with parallel flanges, in which the area of the flanges is everywhere proportioned to the bending moment, Fig. 272. In special cases, plate girders of varying depth are used. (i) Fig. 254 represents what is called a *fish-bellied* girder, in which the bottom flange is curved. This is a common type in large overhead travelling cranes,

and is adopted to save headroom. (ii) is called a *hog-backed* girder, sometimes employed for large-span plate girders on railways. This type is often considered to present a better appearance than that with parallel flanges, but unless the ci cumstances warrant the use of the more expensive
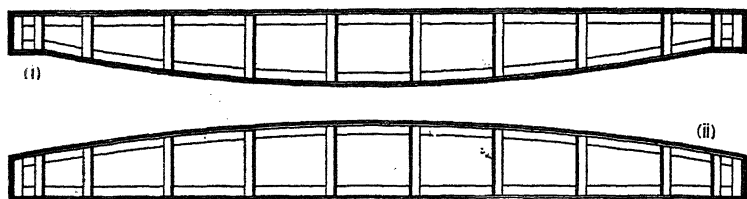
FIG. 254.

curved flange, the plain parallel girder should be adopted. When more than one web is used, the girder is called a *box girder*, Fig. 255. This type should be selected only when it is impossible to carry the shear on one web, or when very wide flanges are a necessity. It must be so arranged that it can be riveted up, and it should be possible afterwards to paint the inside.

Proportions.—In order that the deflection of a plate girder shall not exceed permissible limits, the depth D should not be less than $\frac{1}{20}$th the span L. For economy, the ratio of depth to span should be from $\frac{1}{12}$ to $\frac{1}{10}$. The ratio of breadth B to unsupported length l, as defined below, should not exceed $\frac{1}{40}$. The minimum value of B is determined by the tendency of the compression flange to deflect laterally when the girder is loaded. This flange is really a strut subjected to a longitudinal load increasing from zero at the

FIG. 255.

supports to a maximum near the centre of the span. Mathematical theories have been given for the strength of compression flanges considered as struts, but in ordinary cases it is usually considered sufficient to limit the unsupported length l of the flange.

By the expression 'unsupported length' is to be understood the distance between lateral supports which are sufficiently rigid as substantially to prevent lateral deflection where

FIG. 256.

they occur, so that the flange can only deflect laterally in the manner indicated in Fig. 256. Such lateral support may be provided by transverse members attached to the compression flange, or as in the case of half-through bridges, (iii) Fig. 297, by stiff brackets rigidly
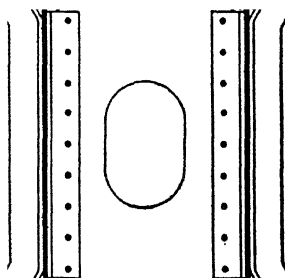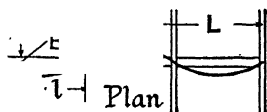
attached to stiff cross girders.* If the ratio l/B, thus defined, does not exceed 20, the full working stress in compression (6·8 tons/sq. in. on the gross section for ordinary dead loads) may be used when designing the flange. If the ratio l/B exceed 20, the stress in compression on the gross area should not exceed

$$f_c = 9·4 - 0·13 l/B \quad . \quad . \quad . \quad . \quad (1)$$

for ordinary dead loads.

172. **Flanges.**—The flanges are constructed of a series of flats or plates, Figs. 258 and 272. Flats and universal plates have the advantage that the edges do not require to be planed. Except in small and unimportant girders, the thickness of a single plate should not be less than $\frac{3}{8}$ in. ; it should not exceed $\frac{3}{4}$ in. Only the innermost flange is carried the full length of the girder ; the usual graphical process for determining the length of the other plates from the bending-moment diagram is shown in Fig. 271. The length of a curtailed plate should be made two or three rivet pitches longer than is theoretically necessary, to facilitate the transference of the stress to that plate.

For economy, in all but very large girders, the cross section of the top and bottom flanges should be made the same. When calculating the requisite area of the tension flange, it is necessary to make a deduction for the area of the rivet holes cut therein; the gross area of the compression flange can be taken as carrying the stress, but the permissible stress will depend on the value of l/B as explained in § 171. A separate calculation and figure, as indicated in Fig. 271, must therefore be made for the compression flange. This calculation may determine the area and arrangement of both flanges, unless the difference be so great as to warrant a different construction in the two flanges, but often the area necessary in the tension flange will suffice for the compression flange.

The method of finding the requisite area is set forth in full in ¶ 9 of the worked example, § 181, to which reference should be made. Usually only the flange plates and the flange angles are assumed to form the flange area, but where suitable covers (see vii, Fig. 261) are provided at the web joints to transmit the stress, certain standard specifications permit $\frac{1}{8}$th of the depth of the web to be counted in as forming part of the flange. Except in large heavy girders, it is usually preferable to increase the flange area rather than introduce the heavy web joints which this necessitates. The remarks in ¶ 13, § 181, regarding the stress distribution in deep flanges require consideration.

Joints.—If the length of a flange plate exceeds about 35 ft. it is, as a rule, better to use two shorter plates connected by a suitable joint. Typical flange plate joints are shown in Figs. 257 and 259. When one flange plate is cut, a single outside cover is provided, (i) Fig. 257. If the joint can be arranged near to the point at which a second flange plate

---

* It is doubtful whether this type of construction really prevents lateral deflection, and the British Standard for Girder Bridges limits the ratio of l/B to 15, and the ratio L/B to 40, where L is the overall length of the flange.

ends, this second flange plate, if of suitable thickness, can be extended to form the cover for the first, (ii) Fig. 257. The length of the extension must be equal to that of the separate cover (not one-half this length) in order to give the load an opportunity to get back on to the cut plate before the second plate is required to help resist the bending moment.
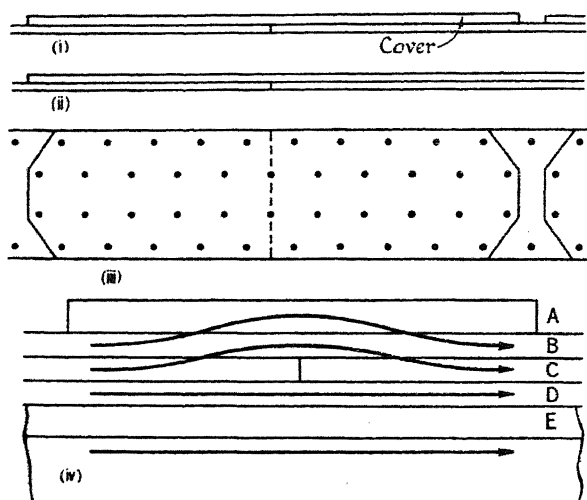
FIG. 257.

It is not necessary that the cover or extended plate be placed in contact with the cut plate, other plates may intervene, as shown in (iv) Fig. 257. Some confusion in thought often occurs as to whether the rivets in a flange joint are in single or double shear. In a case like (iv) Fig. 257, it would appear at first sight that the rivets which pass through the cut plate are in double shear. Consideration will show that this is not so. Since the flange plate C is cut, the load in it has to be transferred through the rivets to the plate B as indicated in the figure by the arrows, and the load normally carried by B is similarly transferred to the cover A. On the opposite side of the joint a reversal of the process takes place. Now a rivet transferring load from C to B is in single shear, and a rivet transferring load from B to the cover A is in single shear. The plate D and the flange

FIG. 258.

angles E have each their own load to carry, and do not affect the question. If it be desired to put the flange rivets in double shear, underneath covers must be added as shown in Fig. 258, in addition to the top covers. It must be clearly understood that neither flange plate B, nor flange plate D, (iv) Fig. 257, can act as a cover to the cut plate C. If any plate be cut, a cover of at least equal area must be added to make up the strength; it is usual to make the cover about $1\frac{1}{8}$ times the thickness of the cut plate.
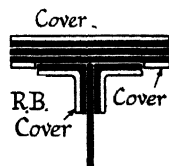
The method of design of flange joints is indicated in the following examples : Suppose that, in a joint of the type shown in (i) Fig. 257, the cut plate is $16 \times \frac{1}{2}$ in., and the diameter of the closed rivet is $\frac{13}{16}$ in. Let the working stress in tension be 8 tons/sq. in., and in shear be $0 \cdot 75$ of $8 = 6 \cdot 0$ tons/sq. in. Then the resistance to tension of the plate, less two $\frac{13}{16}$-in. rivet holes, is $(16 - 2 \times \frac{13}{16}) \times \frac{1}{2} \times 8 = 57 \cdot 5$ tons. A $\frac{13}{16}$-in. rivet in single shear is worth $\frac{\pi}{4} \times (\frac{13}{16})^2 \times 6 = 3 \cdot 1$ tons. Hence $57 \cdot 5 \div 3 \cdot 1 = 19$ rivets are required on each side of the joint. There will be four rows of rivets as shown in plan, (iii) Fig. 257, i.e. four rows of five rivets each side of the joint. The cover should be $1\frac{1}{8} \times \frac{1}{2} = \frac{9}{16}$ in. thick.

Grouped Flange Joints.—When there are a number of flange plates, and all require to be cut, the joints are grouped together as shown in Fig. 259. There is a substantial saving in length of cover by so doing, and the grouped plates are convenient for transport.

As an example of the method of design, suppose that three plates are
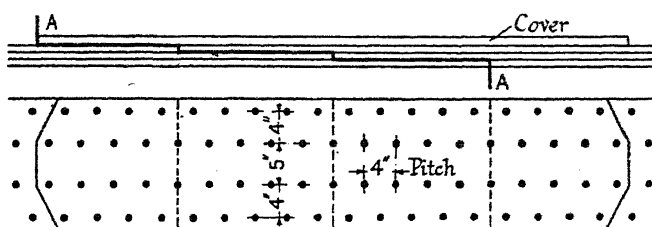
FIG. 259.

cut, Fig. 259, each 16 in. $\times \frac{9}{16}$ in. The diameter of the closed rivet is $\frac{15}{16}$ in. Let the working stress in tension be 8 tons/sq. in., and in shear be 6 tons/sq. in. There will be four rows of rivets in plan, arranged as shown in Fig. 259. From eq. (9), § 152, if the longitudinal pitch be 4 in., $k = 2$, and $c_1 = 4$ in.,

$$m = 3 - \frac{50k^2}{(11c_1 + 2d)(c_1 + 2d)} = 2 \cdot 26$$

and $m + 1 = 3 \cdot 26$ rivet diameters must be subtracted from the flange width. The resistance to tension of the three flange plates is, therefore, $3(16 - 3 \cdot 26 \times \frac{15}{16}) \times \frac{9}{16} \times 8 = 175$ tons. If the joint fail by shear along the line AA, three groups of rivets will be sheared. Suppose that each group contain n rivets, worth $\frac{\pi}{4} \times (\frac{15}{16})^2 \times 6 \cdot 0 = 4 \cdot 1$ tons per rivet. The resistance to shear of the three groups is then $3n \times 4 \cdot 1$ tons, which should be equal to the resistance to tension, or $3n \times 4 \cdot 1 = 175$ tons ; hence $n = 15$, and each group must contain 15 rivets. With a longitudinal pitch of 4 in., two of the rivets must pass through each joint, preferably two on the inner rows, as shown in Fig. 259, and must not be counted in. It is evident from (iv) Fig. 257, which shows how the load is transferred

from plate to plate, that the number of rivets in each group should be the same. The proposed arrangement is therefore equivalent to three groups of 16 rivets worth $3 \times 16 \times 4 \cdot 1 = 197$ tons. The resistance to tension of the three solid plates is $3 \times 16 \times \frac{9}{16} \times 8 = 216$ tons. Hence the shearing efficiency is $197 \div 216 = 0 \cdot 91$, and the tearing efficiency $175 \div 216 = 0 \cdot 81$. From eq. (9), § 152, had the longitudinal pitch been $6\frac{1}{4}$ in., $k = 3 \cdot 25$, only two rivet holes need have been deducted, and the tearing efficiency would have been $0 \cdot 88$.

173. **Flange Angles.**—The flange is united to the web by means of flange angles. These must be of sufficient size to transmit the shearing force from the web to the flange, and to accommodate the rivets which are necessary. If one row only of rivets is required to attach the angles to the web, the vertical leg of the angles need not exceed $3\frac{1}{2}$ to 4 in. in width ; the horizontal leg may be made wider if desired. The flange angles are usually made a little thicker than the web plate ; their area may be counted in as forming part of the flange.

When the length of the flange angles exceeds about 40 ft. it is necessary to make joints in them. These joints are usually grouped as shown in
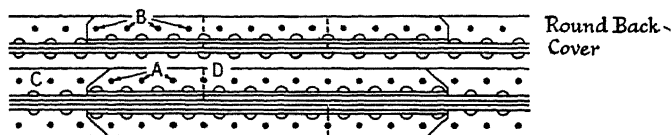
FIG. 260.

Fig. 260. The joints are covered by means of *round back covers* as shown. These consist of angle sections with a rounded edge, usually machined out of a piece of ordinary angle section to fit into the root of the flange angle. The method of design for such joints is as follows :

Suppose that the section of each flange angle be $4 \times 4 \times \frac{1}{2}$ in. (area $= 3 \cdot 75$ sq. in.) and that the diameter of the closed rivet be $\frac{13}{16}$ in. Let the safe tensile stress be 8 tons/sq. in. ; the safe shear stress $\frac{3}{4}$ of 8 $= 6$ tons/sq. in. ; and the safe bearing pressure on the rivets twice the safe shear stress $= 2 \times 6 = 12$ tons/sq. in. Then the net area of one flange angle is $3 \cdot 75$ sq. in. less the area of one rivet hole $= \frac{1}{2} \times \frac{13}{16}$ $= 0 \cdot 41$ sq. in., i.e. $3 \cdot 75 - 0 \cdot 41 = 3 \cdot 34$ sq. in. Its tensile resistance at 8 tons/sq. in. is $3 \cdot 34 \times 8 = 26 \cdot 7$ tons. The joint would fail due to the angle C, Fig. 260, pulling out and shearing the rivets marked A and B in the figure. Of these rivets, those marked A are in single shear, those marked B, since there is a round-back cover on each side of the web, are in double shear. A rivet in single shear is worth $\frac{\pi}{4} \times (\frac{13}{16})^2 \times 6 = 3 \cdot 1$ tons, and a rivet in double shear bearing in the angle $\frac{1}{2}$ in. thick is worth $\frac{1}{2} \times \frac{13}{16} \times 12 = 4 \cdot 8$ tons. Suppose there be n rivets marked A in single shear, and $(n + 1)$ rivets marked B in double shear. Then the total shearing resistance to the angle C being pulled out is $3 \cdot 1n + 4 \cdot 8(n + 1)$

$= 7 \cdot 9n + 4 \cdot 8$ tons. Equating this to the tensile resistance of the angle, i.e. $26 \cdot 7$ tons, $n = 2 \cdot 8$. That is to say, 3 rivets in single shear and 4 rivets in double shear must be provided as shown in Fig. 260. At the point D, where the angle C is cut, it is evident that the load on the joint is carried by one flange angle and two round back covers. Hence the net area of two round back covers must be at least equal to that of one flange angle, or the net area of each cover must be $3 \cdot 34 \div 2 = 1 \cdot 67$ sq. in. For a 4×4 in. angle, a $3\frac{1}{2} \times 3\frac{1}{2}$ in. cover would be used. If this be made $\frac{3}{8}$ in. thick, the net area, after deducting a rivet hole, is $2 \cdot 1$ sq. in., which is ample.

If, instead of grouping the joints, a round back cover be fitted on one flange angle only, its net area must be at least equal to that of the cut flange angle. Such a cover is of necessity rather thick, and the rivets will come fairly close to the inside corner. Care must be taken that it is possible to insert and close up these rivets. In this case, all the rivets through the cover are in single shear.

174. Web.—The web of an ordinary plate girder consists of a single plate attached to the flanges by the flange angles, and stiffened at intervals by web stiffeners. Except for small and unimportant girders, the thickness of a web plate should not be less than $\frac{3}{8}$ in. ; it is better not to exceed $\frac{3}{4}$ in. If a thicker web than $\frac{3}{4}$ in. be required, the advisability of two webs should be considered. Joints in web plates are made with butted joints, usually with double covers, (i) and (ii) Fig. 261. Such joints must be of sufficient strength to carry the shearing force at the joint, but in this country are not often designed to resist a bending moment. A web stiffener may be used to form a cover for a web joint, (iii), and it is sometimes considered good practice to provide a stiffener at each web joint, (vi). The

Fig. 261.

methods of effecting a change in thickness in web plates is shown at (iv) and (v) Fig. 261 ; in large and important girders it may be economic to vary the thickness of the web plate with the varying shearing force, but it is usually more economical to keep one web thickness throughout.

(vi) and (vii) Fig. 261 show the type of web joint which would be
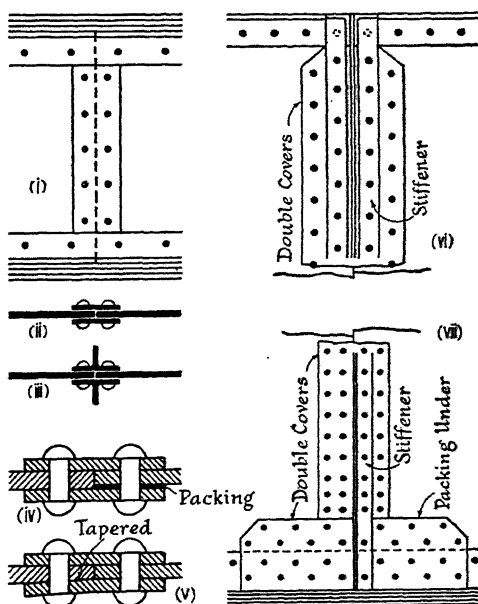
used in large plate girders such as might be employed in railway spans ; (vii) also shows the method adopted for covering the web joint when it is desired to count in part of the web as helping to resist the bending moment. The covers, top and bottom, are extended, and sufficient rivets provided to carry the bending stress in the web.

Web Stiffeners.—Fig. 262 shows the usual types of web stiffeners. For all except very large plate girders these consist of angles, (i), placed, as shown in the figure, on both sides of the web plate. These angles are either joggled at the ends, (ii), to fit over the flange angles so that when riveted up they clamp the web plate ; or flat bar packing may be inserted between the web and the stiffeners as shown at (iii). In ordinary circumstances, the flange of the angle stiffener which is attached to the web need not be more than 3 in. wide, unless the rivets exceed $\frac{7}{8}$ in. in diameter, but the outstanding flange should be made at least as wide as the flange angle itself. It was common, formerly, to use tee bars for web stiffeners, but since this involves odd riveting through the flange angles, an angle
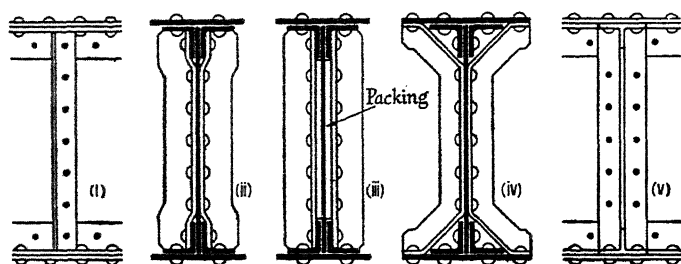
FIG. 262.

stiffener is to be preferred. When the flange plates are wide, kneed stiffeners, (iv) and (v) Fig. 262, are used to give better support to the flange. There is justification for using tee bars in this case, as the rivet pitches through the flange angles are unaffected, and the stiffener can be attached to the flange by two rivets, whereas with an angle stiffener there could be only one. The type of stiffener used in very large single web girders is shown in (ii) Fig. 267 and Fig. 286. In the case of box girders, internal diaphragm plates, Fig. 255, are inserted at intervals to prevent distortion and to help equalise the shearing force between the webs. Handholes or manholes must be cut in these plates to give access to the space enclosed.

The web stiffeners have three separate functions. In the first place they must stiffen the web plate against buckling by the shearing force ; secondly, they must prevent the girder from twisting or racking sideways ; stiffeners of the type shown in (ii) and (iii) Fig. 262 are made to butt tightly between the flange angles with this end in view ; and thirdly, they must distribute any concentrated load which comes on the girder over the depth of the web plate. To satisfy this latter condition, a stiffener must be placed under every concentrated load on the girder ; to prevent

twisting and racking, the pitch of the stiffeners should not exceed 6 ft. or the depth of the girder, whichever be the greater; further, in order to prevent the web plate from buckling, there is a minimum pitch for the stiffeners, which depends on the thickness of the web plate (see the next paragraph). Those stiffeners which come under a concentrated load should be treated as columns and designed by a column formula; they may be taken for this purpose as approximately equivalent to a column equal in length to $\frac{8}{10}$ths the depth of the girder, and with both ends fixed in position but free in direction (position-fixed). When the girder is shallow, all that is necessary is to see that sufficient area is provided in the stiffener angles to carry the concentrated load, and sufficient rivets to transmit it to the web plate.

Thickness of Web Plate.—The thickness of the web plate and the
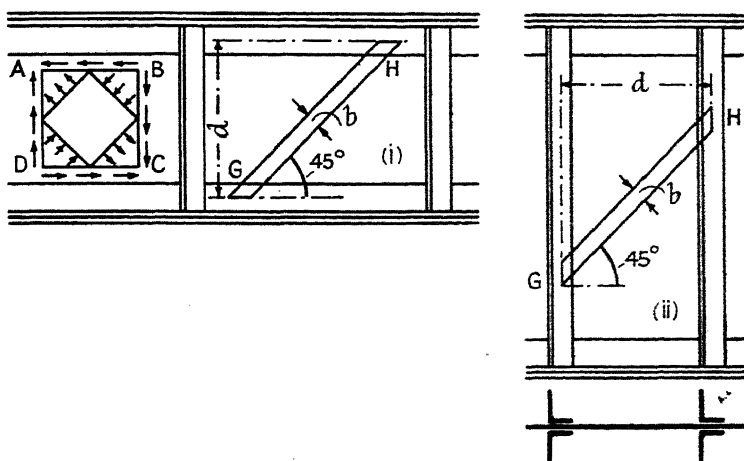
<p style="text-align:center">FIG. 263.</p>

spacing of stiffeners must be such that the web is able to carry the shearing force without buckling or shearing. The following elementary theory is commonly applied to the end bays, where the stress in the web is principally a shear.

It was shown in §§ 15 and 16, Vol. I, that the shear stress on any two vertical planes, such as AD, BC of the web, (i) Fig. 263, must be accompanied by shear stresses of equal intensity on the planes AB, CD at right angles thereto, and that these shear stresses are together equivalent to tensile and compressive stresses of the same intensity as the shear stress, at right angles to one another, but in directions making an angle of 45° with those of the shear stresses. It follows that on any strip of the web such as GH, Fig. 263, making an angle of 45° with the flange, there is a compressive stress of equal intensity to the shear stress. The strength of such a strip to resist compression will determine the resistance of the web. If the strip be considered as a column of breadth b, thickness t

and length $\sqrt{2} \times d$, direction-fixed at both ends, and its strength be determined by a strut formula, a relation is obtained from which the dimensions of the web can be ascertained.

A convenient straight-line formula is

$$s = 5\tfrac{1}{2}t - d/20 \quad \text{tons per inch of depth} \quad . \quad . \quad . \quad (1)$$

where

s = the safe shearing force per inch of depth (tons/in.).

t = the thickness of the web (inches).

d = the distance apart of the stiffeners centre to centre, (ii), or the distance centre to centre of the flange angles, (i), whichever be the lesser (inches).

For the purpose of fixing the thickness of the web, it may be assumed that the shearing force is uniformly spread over the depth thereof [cf. (iii) Fig. 266], when the shear per inch of depth is equal to S, the total shear force at the section, divided by D_1, the depth of the web plate. Then, for the proposed thickness of the web and spacing of stiffeners, the value of s as determined from eq. (1) must be greater than S/D_1.

In order to determine the thickness of the web and the best arrangement of the stiffeners, it is convenient to construct a *shear per inch of depth diagram*, of which the ordinates everywhere represent the values of S/D_1. By a simple graphical process it is then easy to obtain the necessary dimensions of the web. The method is fully explained in the worked example, ¶ 8, § 181.

In no case should the shear stress f_s on the gross area of the web plate exceed 5 tons/sq. in., corresponding to a value $s = 5t$ tons per inch of depth, however closely the stiffeners be placed.

Timoshenko's Theory.[14, 15]—Timoshenko treats the web-plate problem as one of elastic stability. He considers a rectangular panel of the web,
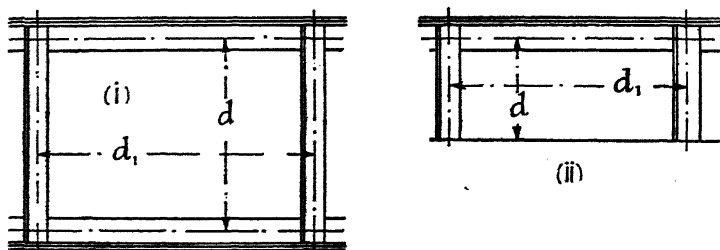
FIG. 264.

supported along all its edges, and subjected to both shear and bending stress, and concludes from his analysis that a small compressive stress superposed on the pure shear stress has little effect on the tendency to buckle due to shear; that the critical conditions for buckling due to pure compression are but slightly affected by the presence of a small

shearing stress ; and that if the web be stable under the shear stress at the ends of the girder, and also under the compressive stress near the centre, in ordinary circumstances it will be stable everywhere.

Assuming, therefore, that at the ends of the girder the panels are subjected to pure shear, if in (i) Fig. 264, d_1 and d are the longer and shorter sides of the rectangular panel into which the web plate is divided by its stiffeners ; t the thickness of the web ; D the flexural rigidity of the plate ; $1/m = 3/10$, Poisson's ratio ; then $D = \dfrac{Et^3}{12} \cdot \dfrac{m^2}{m^2 - 1}$, and if f_s (crit.) be the critical shear stress which would cause the web plate to cripple,

$$f_s \text{ (crit.)} = k\frac{\pi^2}{d^2 t} D = k\frac{\pi^2 E}{12} \cdot \frac{m^2}{m^2 - 1}\left(\frac{t}{d}\right)^2 = 11{,}750\, k\left(\frac{t}{d}\right)^2 \text{ tons/sq. in.} \quad (2)$$

where k is a coefficient given in the following table.

Ratio d_1/d	1·0	1·2	1·4	1·5	1·6	1·8	2·0	2·5	3·0	∝
k	9·42	8·0	7·3	7·1	7·0	6·8	6·6	6·3	6·1	5·35
k_1	1·70	1·47	1·36	1·34	1·33	1·34	1·38	1·41	1·34	—

This formula applies to panels in which the edges are merely supported, and in which the plates were originally mathematically plane. Timoshenko considers that ordinary stiffeners are not sufficiently rigid to justify assuming that the edges of the plate are direction-fixed.

For panels which are relatively very wide, $k = 5 \cdot 35$; putting f_s (crit.) $= 9$ tons/sq. in., the yield point of the material in shear, $d/t = 83 \cdot 6$, which may be regarded as the validity limit of the formula (cf. § 99, Vol. I), for it follows that, when d/t is less than 83, an ' ideal ' web would fail in direct shear, and for values above 83 by buckling. Eq. (2) applies equally to wide or deep panels, but d is always the narrower dimension. If, as in (ii) Fig. 264, the lower edge be unrestrained, replace k by k_1.

Considering the upper half of a central panel subjected to pure compression, Timoshenko finds for the critical stress at which the plate will buckle

$$f_c \text{ (crit.)} = kE\frac{m^2}{m^2 - 1}\left(\frac{t}{d}\right)^2 = 14{,}290k\left(\frac{t}{d}\right)^2 \text{ tons/sq. in.} \quad . \quad (3)$$

Ratio d_1/d	0·4	0·5	0·6	0·67	0·75	0·8	0·9	1·0	1·5	2·0	3·0	∝
k	23·9	21·1	19·8	19·7	19·8	20·1	21·1	21·1	19·8	19·7	19·8	19·7

d is the depth of the panel as shown in (i) Fig. 264 ; the value of f_c (crit.) depends on the wave length of the buckles, and is not much affected

by the spacing of the vertical stiffeners. Horizontal stiffeners are much more effective. Putting $k = 19\cdot7$, and f_c (crit.) $= f_y = 16$ tons/sq.in., $d/t = 132\cdot6$, which is the validity limit for the formula. As both equations (2) and (3) are of the Euler type, the factor of safety should not be less than 3.

175. Riveting.—The usual diameter d of the rivets for different thicknesses of plate t is as follows : thicknesses under $\frac{3}{8}$ in., $d = \frac{5}{8}$ in. ; thicknesses between $\frac{3}{8}$ and $\frac{1}{2}$ in., $d = \frac{3}{4}$ in. ; thicknesses between $\frac{1}{2}$ and $\frac{5}{8}$ in., $d = \frac{7}{8}$ in. ; thicknesses over $\frac{5}{8}$ in., $d = 1$ in. When many thicknesses have to be riveted together, it is common to increase these diameters slightly. The diameter d should not be less than $\frac{1}{4}$ the grip length, i.e. the total thickness through which the rivet passes. The distance of the rivet centre from the edge of the plate should not be less than $1\frac{1}{2}d$, if that edge be planed or rolled; nor less than $1\frac{2}{3}d$, if the edge be sheared. In neither case should the distance of the rivet centre from the edge exceed 8 times the thickness of the thinnest outside plate, otherwise rusting will occur between the plates. The rivet pitch p should not be less than $3d$ nor exceed 16 times the thickness of the thinnest outside plate. In angles with two lines of staggered rivets, the pitch in each line may be twice this limit, but nowhere should the pitch exceed 12 in. As far as possible, simple uniform pitches 3, 4, or 6 in. should be used. The diameters of the rivets themselves are manufactured to eighths of an inch, $\frac{5}{8}$, $\frac{3}{4}$, $\frac{7}{8}$; and the holes should be drilled or punched $\frac{1}{16}$ in. larger, in order that the hot rivet may be inserted.

The safe load on a rivet may be calculated on the area of the closed rivet, the diameter of which may be taken as equal to that of the rivet hole, for the rivet, if properly closed, should fill the hole. The bearing area of such rivets may be taken as the diameter of the hole multiplied by the thickness of the metal through which it passes. In the case of field rivets, the permissible working stresses are to be reduced by 20 per cent. The shearing strength of rivets in double shear may be taken as twice that of similar rivets in single shear. In calculating the net area of parts in tension, if the holes be drilled, or punched and reamed, the diameter of the hole as shown on the drawings should be used. In punched work, the hole should be assumed $\frac{1}{8}$ in. larger than the figured dimension, to allow for the taper and for damage to the metal round the hole during punching. If the holes be countersunk, the diameter may be taken as $\frac{1}{8}$ in. larger than the figured dimension, to allow for the loss in area.

Longitudinal Pitch.—The shear per inch of depth diagram may be utilised to determine the longitudinal pitch of the riveting. The shear stress in any two directions at right angles is of the same intensity, and therefore, as was seen in (i) Fig. 263, the shear on any horizontal plane AB is equal to the shear on the vertical plane AD. Hence the shear force per inch of length at any section on the row of rivets joining the web plate to the flange angles is equal to the shear per inch of depth at that section. This can be shown from first principles thus : Let K_1K_2, Fig. 265,

represent a length l of the girder, so short that the shearing force S on it may be regarded as sensibly constant. Let the bending moment at K_1 be M_1, and at K_2 be M_2. Then, taking moments about K_2, $M_1 + Sl = M_2$; or $M_2 - M_1 = Sl$. Suppose that the force in the flanges corresponding to M_1 be F_1, and to M_2 be F_2; then $M_1 = F_1 D$ and $M_2 = F_2 D$. Hence,

$$F_2 D - F_1 D = Sl, \text{ and } \frac{F_2 - F_1}{l} = \frac{S}{D}. \text{ But } (F_2 - F_1) \text{ is the increase of force}$$

in the flange in a distance l. This increase is brought about by the transfer of horizontal shearing force from the web to the flange angles through the rivets in the flange angles. In other words, $(F_2 - F_1) \div l$ is the shear force per inch of length on the row of rivets connecting the flange angles to the web, and it is equal to $S \div D$, the shear force per inch of depth. For practical purposes D can be taken as equal to D_1, § 174.

For the purpose of determining the thickness of the web, it was sufficiently accurate to assume that the shearing force was uniformly spread over the depth of the web. This is not strictly true, and in the interests of economy, when determining the pitch of the longitudinal riveting, it is worth while taking the true distribution into account. This distribution, for the girder considered in § 181, is shown in (iii) Fig. 266, and it is evident that the ordinates s_1 and s_2, representing the actual shearing force per inch of length on the rivets through the flange angle, are considerably less than S/D_1 the average value. If P_1 be the safe load on a rivet in single shear, p_1 the pitch of rivets connecting the flange plates to the flange angles, and there be n_1 rows through the two angles, the safe shear force per inch of length on the rivets is $n_1 P_1/p_1$, which must be equal to, or greater than, s_1. Similarly, if P_2 be the safe load on a rivet in double shear, p_2 the pitch of the rivets connecting the flange angles to the web, and there be n_2 rows of such rivets, $n_2 P_2/p_2$ must be equal to, or greater than, s_2.
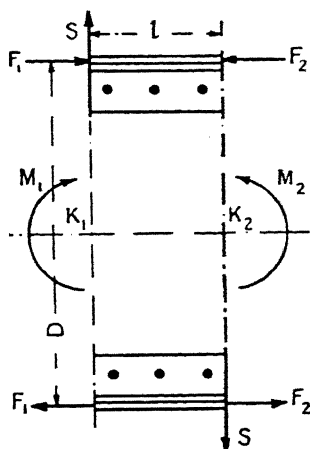
FIG. 265.

Let $s_1 = \lambda_1 \dfrac{S}{D_1}$, and $s_2 = \lambda_2 \dfrac{S}{D_1}$. The values of λ_1 and λ_2 can be found from Fig. 266, or by the theory given in § 81, Vol. I. If a' be the area of the flange plates outside the angles, and v' the distance of the centre of this area from the neutral axis, then $s_1 = Sa'v'/I$ [eq. (4), § 81, Vol. I]. But $s_1 = \lambda_1 S/D_1$, hence,

$$S\frac{a'v'}{I} = \lambda_1 \frac{S}{D_1}; \quad \text{and } \lambda_1 = \frac{D_1}{I} a'v' \tag{5}$$

Similarly, if a'' be the added areas * of the two flange angles, and v'' the distance of their centre of area from the neutral axis,

$$s_2 = \frac{S}{I}(a'v' + a''v'') = \lambda_2\frac{S}{D_1} ; \text{ and } \lambda_2 = \frac{D_1}{I}(a'v' + a''v'') \qquad (6)$$

The gross area may be used in calculating I, a', and a'', but if the rivet holes are subtracted in the calculation for I, they must be subtracted from a' and a''. The value of λ_1 and λ_2 will be different at different points in the length of the girder, depending on the number of flange plates. The full line, (iii) Fig. 266, represents the shear distribution if there be one flange plate, and the thin dotted line in the lower part of the diagram represents
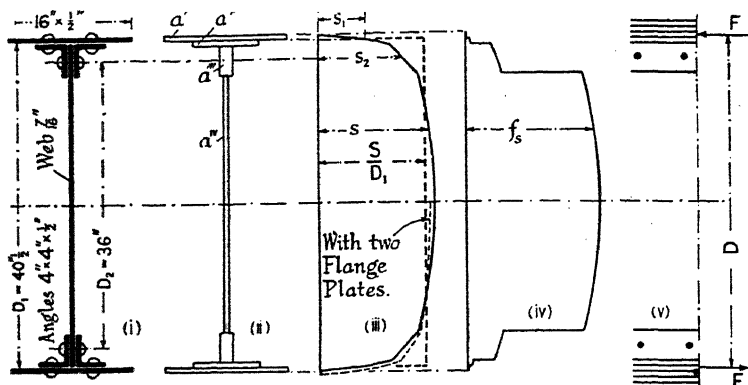
FIG. 266.

the distribution if there be two. For practical purposes it is usually sufficient to calculate λ_2 for the end cross section, where the shear is greatest, and to assume that the value thus obtained applies everywhere. The value of λ_1 is more variable, and the effect of the addition of a flange plate should be examined (see the worked example, § 181).

It follows from the above that

$$\frac{n_1P_1}{p_1} \gtreqqless s_1 \gtreqqless \lambda_1\frac{S}{D_1} ; \text{ and } \frac{n_2P_2}{p_2} \gtreqqless s_2 \gtreqqless \lambda_2\frac{S}{D_1}.$$

Hence,

$$\frac{n_1P_1}{p_1\lambda_1} \gtreqqless \frac{S}{D_1} ; \text{ and } \frac{n_2P_2}{p_2\lambda_2} \gtreqqless \frac{S}{D_1} \qquad (7)$$

from which the values of p_1 and p_2 can be obtained. From eqs. (5), (6), and (7),

$$p_1 \lesseqqgtr \frac{n_1P_1I}{Sa'v'} ; \quad p_2 \lesseqqgtr \frac{n_2P_2I}{S(a'v' + a''v'')} \qquad (8)$$

---

* It will be observed that in calculating the above value of λ_2 the angles have been treated as a complete unit, instead of being divided into two rectangles, as was done in obtaining (iii) Fig. 266. This is not only more correct, it is more convenient. The difference made to λ_2 is not large in the case of a plate girder, but in a Z section composed of two angles riveted together, the effect is more important.

It is convenient to proceed graphically. On the shear per inch of depth diagram, of which the ordinates represent S/D_1, plot horizontal lines representing $\dfrac{n_1 P_1}{p_1 \lambda_1}$ and $\dfrac{n_2 P_2}{p_2 \lambda_2}$ for different values of p_1 and p_2. It is then easy to choose suitable pitches (see ¶ 10, the worked example, § 181).

In many cases it is sufficiently accurate to assume that $\lambda_1 = \lambda_2 = 1$, when

$$\frac{n_1 P_1}{p_1} \gtrless \frac{S}{D_1} ; \text{ and } \frac{n_2 P_2}{p_2} \gtrless \frac{S}{D_1} \qquad . \qquad . \quad (9)$$

This is the common assumption.

176. Distribution of Shearing Force.—The method of determining this is given in § 81, Vol. I. The calculation for the end cross-section of the girder in the worked example, § 181, is as follows :

Part (Fig. 266).		a'	v'	$a'v'$	$a'(v')^2 + I'$
a'	$16 \times \frac{1}{2}$	8	20·5	164	3,360
a''	$8\frac{7}{16} \times \frac{1}{2}$	4·2	20·0	84	1,680
a'''	$3\frac{1}{2} \times 1\frac{7}{16}$	5·0	18·0	90	1,620 + 5
a^{iv}	$16\frac{1}{4} \times \frac{7}{16}$	7·1	8·12	58	470 + 160
Inch units . .		24·3		396	7,295
					2
					$I = 14,590 \text{ in.}^4$

$$S = 47 \cdot 8 \text{ tons, } (\P \ 7, \ § \ 181).$$

$$s = \frac{S}{I} \cdot \Sigma a'v' = \frac{47 \cdot 8}{14,590} \times 164 = 0 \cdot 54$$

$$248 = 0 \cdot 81$$
$$338 = 1 \cdot 11$$
$$396 = 1 \cdot 30 \text{ tons/inch.}$$

The gross areas have been used in the above, and the values of $\Sigma a'v'$ are taken from col. 5 of the table. The mean value of $s = \dfrac{S}{D_1} = \dfrac{47 \cdot 8}{40 \cdot 5} = 1 \cdot 18$ tons/inch. The above values are plotted in (iii) Fig. 266, the straight line representing the mean value of the shear per inch. From the values of s, the shear stress f_s everywhere can be obtained by dividing by the breadth b of the cross section, remembering that where changes in the breadth occur there are two values of b for one value of s [see (iv) Fig. 266]. Thus, where

$s = 0 \cdot 54$	$b = 16$	$= 0 \cdot 034$
	$= 8\frac{7}{16}$	$= 0 \cdot 064$
$= 0 \cdot 81$	$= 8\frac{7}{16}$	$= 0 \cdot 096$
	$= 1\frac{7}{16}$	$= 0 \cdot 56$
$= 1 \cdot 11$	$= 1\frac{7}{16}$	$= 0 \cdot 77$
	$= \frac{7}{16}$	$= 2 \cdot 53$
$= 1 \cdot 30$	$= \frac{7}{16}$	$= 2 \cdot 07$

177. The Ends of the Girder and its Supports.—At the ends of the girder, vertical stiffeners must be provided of sufficient strength to carry the
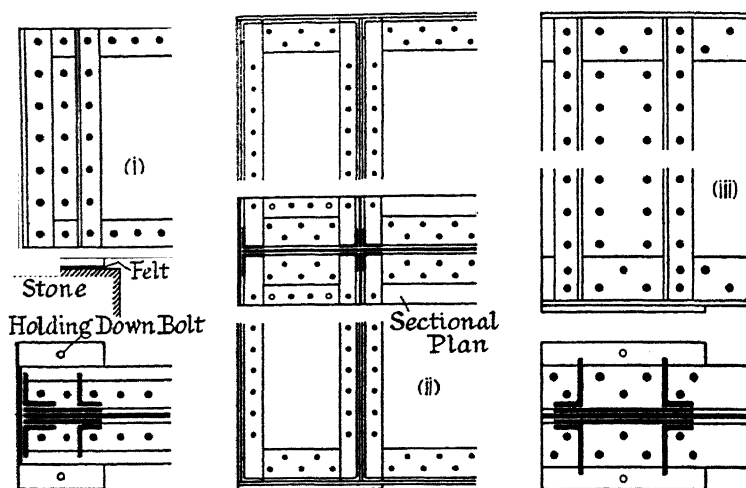
FIG. 267.

end reactions and to spread them over the depth of the web plate, Figs. 267 and 268. The construction shown in (i) Fig. 267 is that common in this country. The ends of the girder are closed with a plate of the same width as the flange plates, and the flange angles are carried round the ends of the girder. An additional stiffener is usually provided to share the reaction ; the area resisting this load is indicated in the plan. (ii) Fig. 267 shows the end stiffening for a large plate girder. (iii) Fig. 267 and Fig. 268 are variants more common in America and Germany, which present some advantages. The stiffening is made symmetrical with regard to the reaction, and no attempt is made to close the ends of the girder. The wide plate shown in (i) Fig. 267, however, helps to prevent lateral deflection of the top flange at the ends of the girder. Whatever construction be used, the area provided must be such that the permissible compressive stress in the material is not exceeded, and sufficient rivets must be provided to transfer the load to the web plate. Where the stiffeners are of considerable length compared with their lateral dimensions, they should be examined as struts, as explained in § 174.
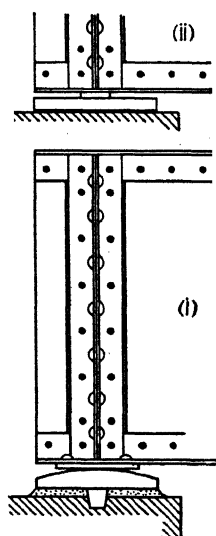
FIG. 268.

If the ends of the girder are carried on walls or brick abutments, *wall* or *bearing plates* are riveted to the underside of the girder at its ends, (i) Fig. 267, as in the case of rolled steel beams. These plates are made of

mild steel and should not be less than $\frac{3}{4}$ in. thick. They rest in turn on bedstones which transmit the pressure to the brickwork. Between the wall plate and the bedstone is placed a thickness of hair felt, in order to bring about a more uniform distribution of pressure ; otherwise, when the girder deflects, there is a tendency to concentrate the reaction on the front edge of the wall plate, which sometimes has the effect of cracking the stone. With the object of spreading the reaction more uniformly over the stone and brickwork, a bolster plate of limited area is sometimes riveted to the underside of the girder, which bolster plate rests on the wall plate, Fig. 272 and (ii) Fig. 268. This also fixes the position of the reactions more definitely. (i) Fig. 268 shows another construction designed with the same objects in view. If the span of girder exceed 50 ft., the ends may be carried on a cast-iron bedplate of the type shown in Fig. 269. One end of the girder is then left free to slide, to allow for
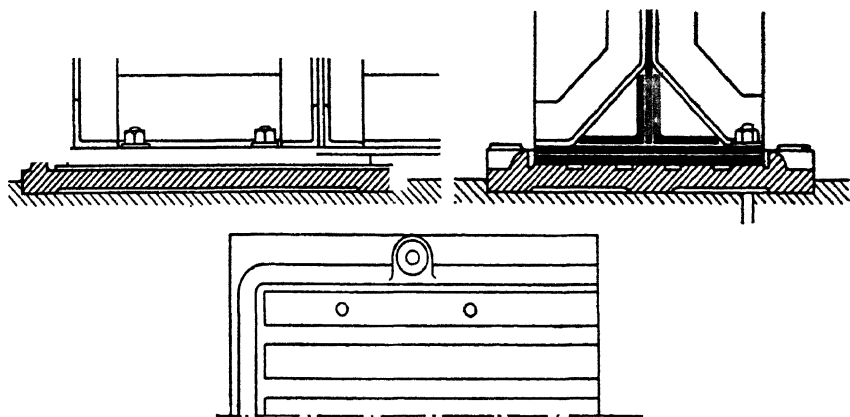
FIG. 269.

alterations in length due to changes in temperature. The ends of very large plate girders may be carried on rocker bearings of the type shown in Fig. 307.

If the ends of the girder be seated on a stanchion, the cap of the latter would be arranged as shown in Figs. 231 and 233.

The safe bearing pressure between the wall plate and the bedstone will fix the size of the wall plate, and the safe bearing pressure between the bedstone and the brickwork will fix the size of the bedstone. When, as in (i) Fig. 267, no special precaution is taken to obtain a uniform pressure distribution, the safe bearing pressure on bedstones and their supports may be taken as : granite 20 ; hard sandstone 16 tons/sq. ft. ; on blue bricks set in 1 : 3 cement mortar as 12 ; on London stocks set in 1 : 3 cement mortar as 6 ; and on ordinary bricks set in 1 : 2 lime mortar as 3 tons/sq. ft. When the end bearings are capable of spreading the load uniformly, these pressures may be increased by 25 %.

178. Deflection and Camber.—The deflection of the girder may be found by the methods and formulae of Chap. V, Vol. I. A close approxi-

mation can be obtained by assuming that the curvature is circular, when the maximum deflection is $y = ML^2/8EI$. M and I are respectively the bending moment and moment of inertia at the centre of the girder, and E may be taken at 9,000–10,000 tons/sq. in. to allow for the give of the riveting. The maximum deflection should not exceed $\frac{1}{400}$th the span. Large and important plate girders are often given an initial camber, so that when deflected under the load they become straight. An old practical rule for the amount of this camber is $\frac{3}{8}$ in. per 10 ft. of span. Small girders should be built straight.

179. Weight of Plate Girders.—The probable weight of a plate girder may be found from Unwin's formula

$$w = \frac{WLr}{Cf - Lr}$$

W = total equivalent *distributed* load in tons on the girder, exclusive of its own weight.

w = weight of girder itself, in tons.

L = actual span in feet.

r = ratio of span to depth.

f = maximum stress in flanges, tons/sq. in.

C = a coefficient ranging from 1,400–1,500 in small plate girders, and from 1,500–1,800 in large plate girders.

For irregular load distributions, W may be taken as the uniform load producing the same maximum bending moment on the girder. In the case of live loads the necessary allowance for impact must be made.

180. Girders with Curved or Sloping Flanges.—If the flanges of the girder be not parallel, the following modifications to the methods of this chapter must be made : Let AB, (i) Fig. 270, be a girder with a curved bottom flange, and suppose that at any section KK the components of the force F in the bottom flange are a horizontal force H and a vertical force V. Then the force in the top flange at the section will be H, and the bending moment at the section will be $M = HD$, where D is the
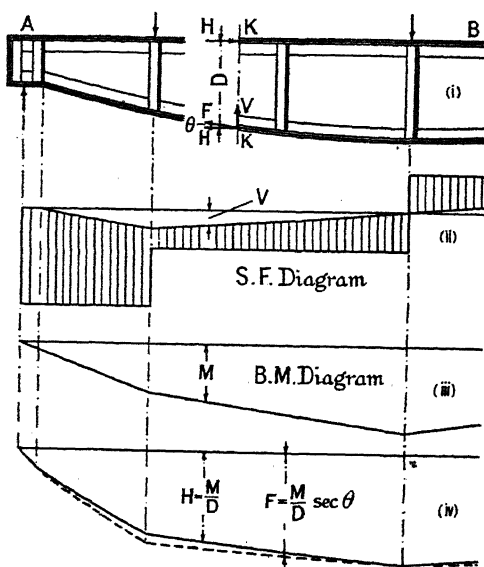
FIG. 270.

distance between the centres of area of the two flanges at the section. Hence $H = M/D$, and $V = H \tan \theta = M \tan \theta / D$, if θ be the angle which

the force in the lower flange makes with the horizontal. This vertical force V, in the case shown, reduces the shearing force at the section. To find the true shearing force on the web of the girder everywhere, draw shearing-force and bending-moment diagrams, (ii) and (iii) Fig. 270, as if the flanges were parallel. From (iii), draw the full line in (iv), of which the ordinates represent $H = M/D$. Then V is obtained by multiplying these ordinates by the appropriate value of tan θ. Plot these values of V downwards from the base line of the shearing-force diagram (ii), so that the ordinates subtract; then the shaded diagram represents the shearing force on the web. This can be transferred to a new base line and used to design the web. The full line in (iv), representing H, may be used to design the upper flange. Since $F = H \sec \theta$, it is necessary to multiply the ordinates of this diagram by sec θ everywhere, in order to obtain a diagram representing the force F in the curved lower flange, which is shown by the dotted line in (iv), and may be used for the design of this flange. The longitudinal riveting in the straight flange may be determined from a shear per inch of depth diagram obtained from the corrected shearing-force diagram, and in which the ordinates represent $s = (S - V)/D$. To determine the longitudinal riveting in the curved flange, a separate diagram must be used in which the ordinates represent $(S - V) \sec \theta /D$.

The above theory applies equally to a hog-backed girder.

181. Plate Girder. Worked Example.—It is required to design a plate girder to carry the system of loads shown in (i) Fig. 271. The clear span is 50 ft., and the ends of the girder are supported on walls. It is an advantage not to make the girder too deep.

1. *Type.*—Parallel flanges ; single web plate ; drilled holes $\frac{13}{16}$-in. diameter for $\frac{3}{4}$-in. rivets ; material, mild steel.

2. *Actual Span.*—The larger end reaction is about 44 tons. Assuming a safe bearing pressure of 16 tons/sq. ft. between the wall plate and the bedstone, Fig. 272, a bearing area of 2·75 sq. ft. is required, say a wall plate 20 in. square. The clear span is 50 ft. If the ends be arranged as shown in Fig. 272, the actual span or distance between the reactions is 52 ft. = 624 in.

3. *Depth and Width.*—The minimum depth of the girder is $\frac{1}{20} \times 624 = 32$ in. For economy a depth of $\frac{1}{12} \times 624 = 52$ in. is required. Since it is advantageous to reduce the depth of the girder, the mean of 42 in. will be taken. This value for D implies a dimension $D_2 = 36$ in. between the rivet centres in the flange angles, which is convenient in that it is a multiple of several even rivet pitches. Assuming that the loads are brought on to the girder by beams running laterally to it, the top flange may be considered as reasonably well supported in this direction ; if B be limited to L/40, $B = \frac{1}{40} \times 624 = 16$ in., a convenient dimension. The ratio l/B, § 171, is $15 \times 12 \div 16 = 11·25 : 1$, and the maximum safe working stress on the gross area of the compression flange may be used.

4. *Working Stresses.*—Safe tensile stress, $f_t = 8$ tons/sq. in. ; max. safe compressive stress on the gross area of the compression flange, $f_c = 6·8$ tons/sq. in. Direct shear on gross area of web plate not to

FORCE IN FLANGES DIAGRAM
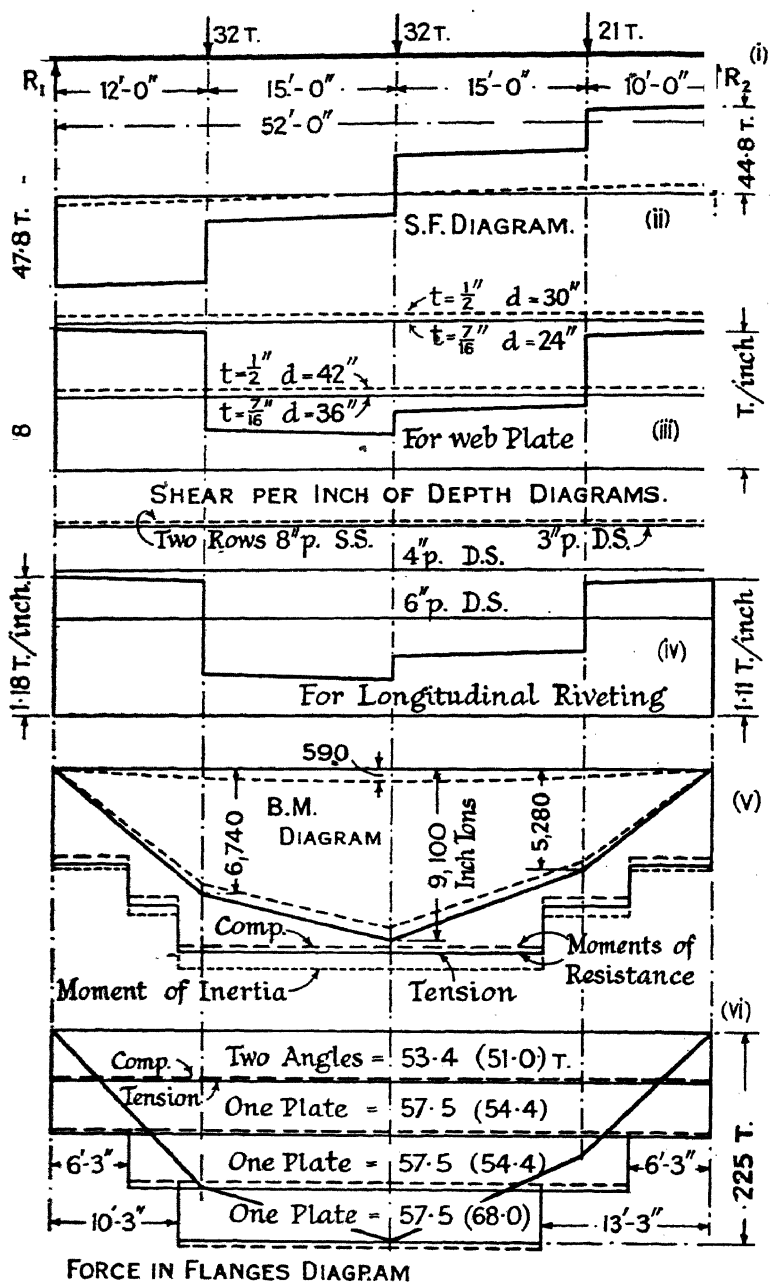
FIG. 271.

exceed 5 tons/sq. in.   Safe shear stress on rivets $f_s = \frac{3}{4}f_t = 6$ tons/sq. in. ; safe bearing pressure $f_b = 2f_s = 12$ tons/sq. in.

5. *Weight of Girder.*—The bending moment at the centre of the girder due to the applied loads is approximately 8,500 in.-tons.   The equivalent uniformly distributed load W, necessary to produce this bending moment, is given by

$$\frac{WL}{8} = 8500 ; \text{ or } W = \frac{8 \times 8500}{624} = \text{say } 110 \text{ tons.}$$

$$r = \frac{L}{D} = \frac{624}{42} = 14\cdot8 ; \text{ L in feet} = 52 ; \text{ C} = 1500 ; f = 8 \text{ tons/sq. in.}$$

Hence, by Unwin's formula, § 179,

$$w = \frac{WLr}{Cf - Lr} = \frac{110 \times 52 \times 14\cdot8}{1500 \times 8 - 52 \times 14\cdot8} = 7\cdot6 \text{ tons,}$$

which will be the weight of the girder.

6. *End Bearings.*—The larger reaction, including the weight of the girder, can now be calculated.   It is $44\cdot0 + 3\cdot8 = 47\cdot8$ tons.   With the wall plate 20 in. square, as proposed, the pressure on the stone is $47\cdot8$ tons $\div 2\cdot78$ sq. ft. $= 17\cdot2$ tons/sq. ft., which is permissible on a hard sandstone.   The proposed arrangement at the end may therefore be adopted, and the exact span taken at 52 ft.

7. *Shearing Force and Bending Moment Diagrams.*—These can now be set out, (ii) and (v) Fig. 271.   The maximum shearing force at the end is $47\cdot8$ tons, and the maximum bending moment under the central 32-ton load is 9,100 in.-tons.   This includes the bending moment due to the weight of the girder itself, which is 590 in.-tons at the centre.

8. *Web Plate and its Stiffening.*—The distance D_2, centre to centre of rivets in the flange angles, has been fixed at 36 in.   Adding the $2\frac{1}{4}$ in. punchings of the 4×4 in. flange angles, top and bottom, Fig. 272, the total depth of the web plate is $D_1 = 36 + 2\frac{1}{4} + 2\frac{1}{4} = 40\frac{1}{2}$ in.   Set out a shear per inch of depth diagram, (iii) Fig. 271, which is obtained by dividing the ordinates of the shearing force diagram everywhere by D_1. For convenience, the lower half of the diagram should be inverted as shown. The maximum ordinates at the two ends will be $47\cdot8 \div 40\frac{1}{2} = 1\cdot18$ tons per inch ; and $44\cdot8 \div 40\frac{1}{2} = 1\cdot11$ tons per inch, respectively.   From eq. (1), § 174, $s = 5\frac{1}{2}t - \frac{1}{20}d$, find the worth of say $\frac{7}{16}$ in. and $\frac{1}{2}$ in. web plates, with stiffeners at various distances d apart.

	$d =$ 24	30	36	42 inches.
If $t = \frac{1}{2}$ in.,	$s = 1\cdot55$	$1\cdot25$	$0\cdot95$	$0\cdot65$
If $t = \frac{7}{16}$ in.,	$s = 1\cdot2$	$0\cdot9$	$0\cdot6$	$0\cdot3$ tons/inch.

Plot these values as horizontal lines on the shear per inch of depth diagram, as shown in (iii) Fig. 271.   From a consideration of the plotted values it is evident that a $\frac{7}{16}$ in. web plate stiffened every 24 in. will carry the shearing force over the end panels, and that the spacing of stiffeners can be increased to 36 in. over the centre panels.   If a $\frac{1}{2}$ in. web plate be used, d can be increased to 30 in. in the end panels, and to 42 in. in the

centre panels. Probably the $\frac{7}{16}$ in. plate is the better alternative, particularly as the requisite pitches work in better with the distance between the loads ; it will therefore be adopted.

9. *Flanges.*—If F be the total force in a flange, (v) Fig. 266, and D the distance between the centres of area of the two flanges, the moment of resistance of the cross-section, on the assumption that the flanges carry the whole of the bending moment, is F × D, which is equal to the bending moment M ; hence F = M/D. To determine the cross-section of the flanges, therefore, set out a diagram, (vi) Fig. 271, representing the force in the flange at every cross-section. This is obtained by dividing the ordinates of the bending-moment diagram everywhere by D. A difficulty arises in that D cannot be determined until the cross-section is known, but for practical purposes D may be taken as equal to D_1, the depth of the girder over the backs of the angles, in this case $40\frac{1}{2}$ in. Since the maximum bending moment is 9,100 in.-tons, the maximum force in the flanges is $9,100 \div 40\frac{1}{2} = 225$ tons. The working stress in tension is 8 tons/sq. in. ; hence the area required is $225 \div 8 = 28 \cdot 2$ sq. in. This can be made up as follows, allowance being made for $\frac{13}{16}$ in. drilled holes suitable for $\frac{3}{4}$ in. rivets :

Two $4 \times 4 \times \frac{1}{2}$ in. flange angles, area of each $3 \cdot 75$ sq. in., less one $\frac{13}{16}$ in. rivet hole, giving a net area of $3 \cdot 34$ sq. in., and each worth, at 8 tons/sq. in., $3 \cdot 34 \times 8 = 26 \cdot 7$ tons. Three $\frac{1}{2}$ in. plates, 16 in. wide (as before decided), each less two $\frac{13}{16}$ in. rivet holes, giving a net area per plate of $(16 - 2 \times \frac{13}{16}) \times \frac{1}{2}$ sq. in., which, at 8 tons/sq. in., will carry $57 \cdot 5$ tons. The total worth of the two angles and three plates is $2 \times 26 \cdot 7 + 3 \times 57 \cdot 5 = 225 \cdot 9$ tons, which is just sufficient. The values of the angles and flange plates are plotted as full lines in (vi) Fig. 271.

The gross area of the compression flange can be used, working at $6 \cdot 8$ tons/sq. in. (see ¶ 4, above). The two angles are worth $2 \times 3 \cdot 75 \times 6 \cdot 8 = 51 \cdot 0$ tons ; each $\frac{1}{2}$ in. flange plate is worth $8 \times 6 \cdot 8 = 54 \cdot 4$ tons ; to make up the requisite section, the outside flange plate must be made $\frac{5}{8}$ in. thick, worth $16 \times \frac{5}{8} \times 6 \cdot 8 = 68 \cdot 0$ tons. The total worth of the two angles and three flange plates is then $227 \cdot 8$ tons. These values, given in brackets, are plotted in (vi) as dotted lines, and as will be seen they determine the necessary length of the flange plates. The angles and one flange plate will be carried the full length of the girder, the other plates are cut short, but made two or three rivet pitches longer than is theoretically necessary.

The cross-section of the girder will then be as shown in Fig. 272. Both flanges will be made alike, except that the thickness of the shortest plate on the compression side will be $\frac{1}{8}$ in. thicker than the corresponding plate on the tension side. This is the most convenient way of providing the necessary area.

10. *Longitudinal Riveting.*—It will be assumed that the rivet holes are drilled $\frac{13}{16}$ in. diameter, that $f_s = 6 \cdot 0$ and $f_b = 12 \cdot 0$ tons/sq. in. The method of determining the pitch of the longitudinal riveting is set forth in § 175. The value of I for the cross-section with a single flange

plate is 14,590 in.[4] (§ 176) ; $D_1 = 40\frac{1}{2}$ in. ; the area of a flange plate is $16 \times \frac{1}{2} = 8$ sq. in. ; $v' = 20\frac{1}{2}$ in., and $a'v' = 8 \times 20\frac{1}{2} = 164$. The area of the two angles is $7 \cdot 5$ sq. in., $v'' = 19 \cdot 1$ in., and $a''v'' = 7\frac{1}{2} \times 19 \cdot 1 = 143$; hence, $a'v' + a''v'' = 164 + 143 = 307$. Then, from eqs. (5) and (6), § 175,

$$\lambda_1 = \frac{D_1}{I} a'v' = \frac{40\frac{1}{2}}{14,590} \times 164 = 0 \cdot 46 ;$$

and $\qquad \lambda_2 = \frac{D_1}{I} (a'v' + a''v'') = \frac{40\frac{1}{2}}{14,590} \times 307 = 0 \cdot 85.$

Dealing first with the riveting in double shear connecting the flange angles to the web plate, the safe load on a $\frac{13}{16}$ in. rivet bearing in a $\frac{7}{16}$ in. web plate is $P_2 = \frac{13}{16} \times \frac{7}{16} \times 12$ tons/sq. in. $= 4 \cdot 26$ tons. There is one row of rivets, therefore $n_2 = 1$, and

$$s_2 = \frac{n_2 P_2}{p_2 \lambda_2} = \frac{1 \times 4 \cdot 26}{p_2 \times 0 \cdot 85} = \frac{5 \cdot 01}{p_2}.$$

If $p_2 = 3''$, $s_2 = 1 \cdot 67$; if $p_2 = 4''$, $s_2 = 1 \cdot 25$; if $p_2 = 6''$, $s_2 = 0 \cdot 83$ tons per inch. Plotting these values as horizontal lines on the shear per inch of depth diagram, (iv) Fig. 271, it is evident that a 6 in. pitch will be ample over the middle bays of the girder, and a 4 in. pitch will be sufficient for the end bays. Considering next the rivets connecting the flange plates to the flange angles, there are two rows of rivets in plan passing through the flange angles, hence $n_1 = 2$. Each row is in single shear, and the worth of one rivet is $P_1 = \frac{\pi}{4} \times \quad)^2 \times 6$ tons/sq. in. $= 3 \cdot 11$ tons. Hence

$$s_1 = \frac{n_1 P_1}{p_1 \lambda_1} = \frac{2 \times 3 \cdot 11}{p_1 \times 0 \cdot 46} = \frac{13 \cdot 52}{p_1}.$$

If $p_1 = 8''$, $s_1 = 1 \cdot 69$ tons per inch. This is also plotted as a horizontal line on (iv) Fig. 271, and it is evident that two rows of 8 in. pitch would be sufficient to carry the shear. This pitch, in addition to being rather long from a practical point of view, will not work in with the 6 in. pitch in double shear, nor with the pitch of the stiffeners. A 6 in. pitch will therefore be adopted. It is desirable to examine the effect on λ_1 and λ_2 of the addition of a flange plate to the cross-section, top and bottom. I then becomes 21,660 in.[4], and

$$\lambda_1 = \frac{40\frac{1}{2} (168 + 164)}{21,660} = 0 \cdot 62 ; \lambda_2 = \frac{40\frac{1}{2} (168 + 164 + 143)}{21,660} = 0 \cdot 89.$$

Thus λ_2 is but slightly altered, λ_1 is increased from $0 \cdot 46$ to $0 \cdot 62$. The value of s_1 for two rows of rivets at 6 in. pitch is then

$$\frac{n_1 P_1}{p_1 \lambda_1} \quad \frac{2 \times 3 \cdot 11}{6 \times 0 \cdot 62} \quad 1 \cdot 67 \text{ tons per inch,}$$

practically the same value as for an 8 in. pitch when $\lambda_1 = 0 \cdot 46$. Evidently a 6 in. pitch in these rows is sufficient.

11. *Joints.*—The inner flange plate will be over 53 ft. long, and should be made in two pieces. The calculation for the joint is given as a worked example in § 172. The middle flange plate is 39′—8½″ long. If possible this should be obtained in one piece, otherwise a grouped joint for the two cut plates should be used. The flange angles are 53′—0½″ long and must be made in two pieces. The calculation for the joint is given in § 173. The joints should be staggered as shown in Fig. 272, and not placed all in the same neighbourhood. The web joint should be placed near the centre of the girder where the shear is small. It is provided with double covers ; the necessary pitch of rivets can be obtained from the shear per inch of depth diagram, exactly as in the case of the longitudinal riveting. In this instance a 4 in. pitch will be employed, though more than sufficient.

12. *Stiffeners at the Ends and under the Loads.*—The maximum shearing force at the ends is 47·8 tons. This has to be distributed over the depth of the girder by the end stiffeners. A rivet in double shear, bearing in a $\frac{7}{16}$ in. plate, is worth 4·26 tons. Hence the minimum number of rivets required is 47·8 ÷ 4·26 = 12. It will be seen from Fig. 272 that there are 16 rivets in the two end verticals, but a margin in strength is desirable, as the load may not be equally divided between the rivets. If the direct compressive stress in the material is not to exceed 6·8 tons/ sq. in., an area of 47·8 ÷ 6·8 = 7·1 sq. in. is required. The added area of the two 4 × 4 × ½ in. vertical angles, together with that of the two 4 × 3 × ⅜ in. end vertical stiffeners, is 12·4 sq. in., without taking the end plate into consideration. There is therefore ample strength.

To spread the applied load of 32 tons down the web plate, 32 ÷ 4·26 = 8 rivets in double shear are required, and a net area of 32 ÷ 6·8 = 4·7 sq. in. A 4 in. pitch is therefore necessary through the stiffeners under the load, and since the area of two stiffener angles is only 4·96 sq. in., they will be reinforced by a plate as shown, which will help to give lateral stiffness to the girder in the vicinity of the applied loads.

13. *Moments of Inertia and Resistance of the Cross-Section.*—The moments of inertia and resistance of each cross-section should now be computed, making due allowance for the rivet holes in the bottom flange.* At the central load the moment of inertia is 28,400 in.⁴ ; the values of v for the extreme fibres are 23·2 in. on the tension side, and 20·4 in. on the compression side ; hence the safe moments of resistance are

$$fZ = fI/v = \frac{28,400}{23\cdot2} \times 8 = 9,790 ; \text{ and } \frac{28,400}{20\cdot4} \times 6\cdot8 = 9,460 \text{ in.-tons in}$$

tension and compression respectively. The diagrams representing the moments of inertia and moments of resistance in both tension and compression have been plotted on the bending-moment diagram, (v) Fig. 271. The moment of resistance diagrams lie everywhere outside the bending-moment diagram, proving that the girder nowhere works at more than 8·0 tons/sq. in. in tension, or than 6·8 tons/sq. in. in compression. In

* For an alternative method of making allowance for rivet holes, see a letter from W. H. Thorpe, *Engineering*, September 22, 1922, p. 363.

plotting these diagrams no account has been taken of the joint in the web plate. The efficiency of this joint is only 30 %, and at a section through the joint, so far as its resistance to bending is concerned, the web should be considered as a plate 32 in. deep, $\frac{7}{16}$ in. thick, and at an efficiency of 0·3. If this be done, I will be reduced by about 2,000 in.⁴, and the moment of resistance in compression by about 660 to 8,800 in.-tons. The web joint has been kept at a considerable distance from the point of maximum bending moment, otherwise it would have been necessary to increase further the thickness of the top plate in order to keep within the allowed stress.

It may appear surprising, having made the flange plates and flange angles sufficiently strong to carry the bending moment everywhere, that the moment of resistance, even counting in part of the web at 30 %, falls below that required. The explanation of the anomaly lies in the fact that the *average* stress over the thick flanges is considerably less than the maximum. Only in the extreme fibres will the maximum permissible stresses be reached, whereas in (vi) Fig. 271, the whole flange areas were assumed to work at 6·8 and 8·0 tons/sq. in. respectively.

14. *Deflection and Camber.*—If it be assumed that M/I is constant from one end of the girder to the other and equal to 9,100 in./tons ÷ 28,400 in.⁴, the maximum deflection will be given by the formula [eq. (15), § 52, Vol. I],

$$y = \frac{ML^2}{8EI} = \frac{9,100 \times 624^2}{8 \times 10,000 \times 28,400} = 1 \cdot 56 \text{ in.}$$

Here E has been taken at 10,000 tons/sq. in. to allow for the ' give ' of the rivets. As will be seen from the shape of the I diagram, this value for y is an over-estimate. As a check, a practical formula given by W. H. Thorpe * may be used. For mild steel plate girders with parallel flanges,

$$y = \frac{L^2}{cD} \cdot f = \frac{52^2}{4,000 \times 3 \cdot 5} \times 6 \cdot 8 = 1 \cdot 32 \text{ in.}$$

where L = span in feet ; c = constant = 4,000 for mild steel girders ; D = depth in feet, = $\frac{43}{12}$ = 3·5 in the present instance ; f = the mean stress in the extreme fibres in tons/sq. in., estimated on the gross section. This in the present case may be taken at 6·8 tons/sq. in., and the value of y is 1·32 in. The maximum permissible deflection is 1/400th the span = 1/400 × 624 = 1·56 in., so that the actual deflection should not exceed the allowed limit. If the girder is built with a camber of ¾ in. per foot, this would equal 52 × ¾ = 2 in.

15. *Setting out the Girder.*—Set out first the centre lines of the flange rivets, and of the web stiffeners. Arrange if possible that the latter come on regular rivet pitches. Put in the rivets ; as simple and uniform an arrangement as the circumstances will permit should be the objective. The rivets passing through one leg of a flange angle should be staggered relative to those through the other leg. When, as in the present case,

* *Engineering*, April 14, 1905, p. 466.
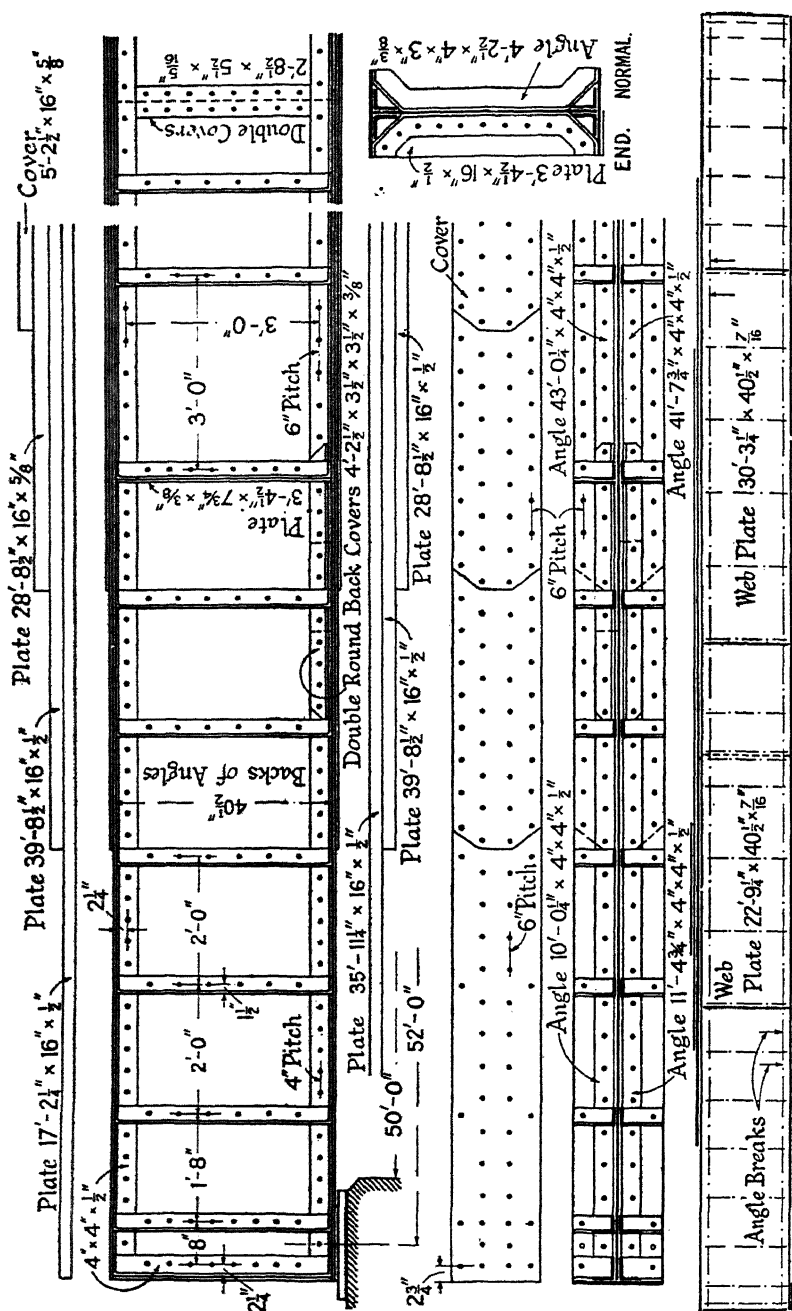
FIG. 272.

52' 0" *Plate Girder.*

Number Required	Length Ft.	Length in.	Breadth or Section Inches.		Unit Weight. lb.	Weight of One. lb.	Weight of Number. lb.	Remarks.
Net sizes.					*Plates*			
2	1	8	20	1½	61·2	170	340	Wall plate.
1	28	8½	16	⅝	25·5	976	976	Flange plate.
2	5	2¼	16	⅝	25·5	177	354	Covers to flange plates.
2	39	8½	16	½	20·4	1,080	2,160	Flange plates.
2	35	11¼	16	½	20·4	978	1,956	
1	28	8½	16	½	20·4	781	781	
2	17	2¼	16	½	20·4	468	936	
2	3	4½	16	½	20·4	92	184	,, ,, Vertical plate at ends.
2	1	1½	16	½	20·4	31	62	Bolster plate.
1	30	3¼	40½	7/16	17·85	1,823	1,823	Web plate.
1	22	9¼	40½	7/16	17·85	1,372	1,372	
							10,944	
					Angles.			
2	43	0¼	4 × 4	½	12·75	549	1,098	Flange angles.
2	41	7¾	4 × 4	½	12·75	531	1,062	
2	11	4¾	4 × 4	½	12·75	145	290	
2	10	0¼	4 × 4	½	12·75	128	256	
* 4	4	2½	4 × 4	½	12·75	54	216	End vertical angles.
4	4	2½	3½ × 3½	⅜	8·45	36	144	Round back covers.
*44	4	2½	4 × 3	⅜	8·45	36	1,584	Vertical stiffeners.
							4,650	
					Flat Bar.			
3		4½	7¾	¾	9·88	33	198	Web stiffeners.
2		8½	5½	5/16	5·84	16	32	Covers to web plates.
							230	

Total weight of plates and bars　.　.　| 15,824 | = 7·06 tons.

Rivets 5%　= 0·35 ,,

Weight of girder　= 7·41 ,,

* An allowance to be made for forging.

there are four rows in plan, the outer rows should be staggered relative to the inner rows. From the drawing it will be seen that, over the whole of the centre portion of the girder, at any one section, only two holes are cut out of a flange plate, and only one out of a flange angle. Near the end of the girder, owing to the change from 6 to 4 in. pitch in the rivets connecting the flange angles to the web, in some cases the rivets in the two legs of the flange angles come close together. There are, however, no joints in the web plate in this neighbourhood, and the strength of the

uncut web will more than compensate for the close proximity of the rivet holes, otherwise it would have been necessary to subtract the area of two rivet holes from each flange angle. Having settled the position of all the rivets, put in the angles and plates, seeing that the lengths are convenient and the joints properly staggered.

16. *Quantities and Weight.*—Finally, the quantities can be taken out, and the weight of the girder calculated. The method of setting out the results is shown in the table on p. 399. It will be seen that the actual weight of the girder as designed comes to 7·41 tons, as compared with the estimate of 7·6 tons. The sizes given in the table are the net sizes given on the drawings. In making up the order for the material, $\frac{1}{4}$ in. is added to the length and width of all the plates (except to the width of flat bars and universal plates), and 1 in. to the length of all angles, to allow for planing and cutting to length.

BIBLIOGRAPHY

Plate Girders

1. LILLY. *The Design of Plate Girders.* London, 1904–1908.
2. LLOYD-JONES. Distribution of Stresses in Plate-Girders. *Proc. Inst. C.E.*, vol. clxviii, 1906–7, p. 189.
3. MOORE. *Design of Plate Girders.* New York, 1913.
4. FLEMING. Plate-Girder Design and Practice. *Eng. News-Rcd.*, vol. 90, 1923, p. 1032 ; see *Eng. Ab. I.C.E.*, 1923, No. 17 : 66.
5. B.S.I. See Ref. No. 22, Chap. XI, Bib.
6. MONTAGNON. The Effect of Adding Flange-Plates to Plate-Web Girders. *Select. Eng. Pap. I.C.E.*, No. 109, 1931.
7. HOVGAARD. A New Theory of the Distribution of Shearing Stresses in Riveted and Welded Connections, etc. *Trans. I.N.A.*, vol. lxxiii, 1931, p. 108.

Stresses in Web Plates

8. WILSON. Specifications for the Strength of Iron Bridges. *Trans. Amer. Soc. C.E.*, vol. xv, 1886, p. 389 ; see also *Eng. News*, Aug. 11, 1898, p. 90 ; Sep. 8, 1898, p. 155.
9. TURNEAURE. Tests of the Stress in Plate-Girder Stiffeners. *Eng. News.* Sep. 23, 1898, p. 186 ; *Jour. West. Soc. Eng.*, vol. xii, 1907, p. 788.
10. GRIBBLE. Plate-Girder Webs. *Engg.* Feb. 21, 1902, pp. 236, 253 ; see also THORPE, *Engg.* Nov. 18, 1904, p. 671.
11. LILLY. Web Stresses in Plate Girders. *Engg.*, Feb. 1, 1907, p. 136. Also Ref. No. 1, *supra.*
12. COKER. An Optical Determination of the Variation of Stress in a Thin Rectangular Plate Subjected to Shear. *Proc. Roy. Soc. A*, vol. 86, 1912, p. 291.
13. MOORE AND WILSON. Strength of Webs of I-Beams and Girders. *Univ. Illinois, Eng. Exp. Stn. Bull.* No. 86, 1916 ; see also Bull. No. 68, 1913.
14. TIMOSHENKO. Ref. No. 5, Chap. VII, p. 386.
15. —— The Stability of the Webs of Plate Girders. *Engg.* Aug. 24, 1934, p. 207 ; see also HOVEY, *Engg.* Dec. 28, 1934, p. 715.
16. INGLIS. Stress Distribution in a Rectangular Plate having Two Opposing Edges Sheared in Opposite Directions. *Proc. Roy. Soc. A*, vol. 103, 1923, p. 598.

See also Refs. Nos. 5 to 10, Chap. VII, Bib.

Crippling of Compression Flanges

17. ENGESSER. See Ref. No. 29, Chap. VI.
18. BLEICH. See Ref. No. 13, Chap. XI.
19. SCHWEDA. Die Bemessung des Endquerrahmens offener Brücken. *Der Bauingenieur*, 1928, p. 535.
20. SCHÄFER. Zur Knicksicherheit offener Brücken. *Der Bauingenieur*, 1928, p. 700.
21. TIMOSHENKO. Elastic Stability in Structures. *Trans. Amer. Soc. C.E.*, vol. 94, 1930, p. 1003.
22. PROCTOR. The Stability of the Compression-Flanges of Through-Bridge Plate-Girders. *Jour. Inst. C.E.* Mar. 1936, p. 322.

Steel-Frame Buildings

23. KETCHUM. *The Design of Steel Mill Buildings.* New York, 5th ed., 1932.
24. —— *Structural Engineers' Handbook.* New York, 3rd ed., 1924.
25. BECK. *Structural Steelwork.* London, 1920.
26. AMERICAN INSTITUTE OF STEEL CONSTRUCTION. *Specification for Buildings*, 1936 ; also *Manual of Steel Construction*, 1930.
27. HOOL AND KINNE. *Steel and Timber Structures.* New York, 1924.
28. VOSS AND VARNEY. An Analysis of the Structural Design of American Buildings. Bk. II, *Steel Construction.* New York, 1927.
29. GREGOR. Der Praktische Stahl-hochbau. Bd. II, Teil 2, Berlin, 1931.
30. BLEICH. *Stahlhochbau.* Bd. I, Ihre Theorie, etc. Berlin, 1933.

Girders Curved in Plan

31. GIBSON and RITCHIE. *A Study of the Circular-Arc Bow Girder.* London, 1914 ; see KNIGHT, *Engg.* Jan. 18, 1918, p. 55. Also UNOLD, *Zeit. Ver. deu. Ing.*, Bd. 64, 1919, p. 852 ; DÜSTERBEHN, *Der Eisenbau*, Bd. 11, 1920, p. 74 ; Bd. 12, 1921, p. 249 ; see *Eng. Ab. I.C.E.*, 1922, No. 11 : 110 ; and YAMADA, *Mem. Coll. Eng.*, Kyushu Imp. Univ., Japan, vol. iii, 1926.

QUESTIONS ON CHAPTER X

1. A beam, intended for use as a bulkhead stiffener in a ship, is formed of two $6 \times 3\frac{1}{2} \times 0.5$ in. angles placed back to back and riveted together so as to form a Z section 9 in. deep overall. The properties of a $6 \times 3\frac{1}{2}$ angle are : area $= 4.50$ sq. in., distance of centroid from shorter flange 2.06 in., I about an axis parallel to the shorter flange and passing through the centroid $= 16.36$ in. units. Find the moment of inertia and section modulus of the compound section about an axis parallel to the $3\frac{1}{2}$-in. flange, and passing through its centroid. Neglect the rivet holes. (I.C.E.)
Ans. 19.18 in.^{3}

2. If f_t be the maximum tensile stress in the lower flange of the cast-iron beam section shown in Fig. 247, and D the overall depth, prove that the moment of resistance is $f_t Z = 0.077 D^3 f_t$; neglect the fillets. (Low's *Applied Mechanics*, p. 112.)

3. A beam, 20 ft. span, supported at each end, is loaded with 12 tons evenly spread over 6 ft. of its length, one end of the load coinciding with the centre of the beam. Draw the shearing force and bending moment diagrams, dimension their maximum ordinates, and the position where the maximum

2 D

bending moment occurs. To economise head room it is proposed to use for this beam two 10 × 6 N.B.S.H.B. No. 6, with cast-iron separators. Comment on this proposal from the point of view of (a) allowable stress, (b) probable deflection. Section modulus of a 10 × 6 beam = 41-in. units. (I.C.E.)

Ans. (a) Stress = 6·8 tons/sq. in., quite permissible; (b) the ratio depth/span = $\frac{1}{24}$, may be permitted, but the deflection might be found excessive for certain purposes.

4. A compound beam of 20 ft. span is formed of two 12 × 5 × 30 lb./ft. N.B.S.B. No. 10 (a = 8·83, I = 206·9 in. units) with a 12 × $\frac{1}{2}$ in. plate added top and bottom. Each plate is connected by one line of rivets through each beam; the rivets are in line across the girder. If the safe stress in compression is not to exceed 6·8, and in tension 8·0 tons/sq. in., find the safe distributed load. Find also the maximum direct shear stress in the webs of the beam, and the necessary pitch of the rivets. What will be the deflection of the girder when carrying this load?

Ans. 30·3 tons; 2·2 tons/sq. in.; 9·6 in., use 6-in. pitches; 0·52 in. (if E = 13,000 tons/sq. in.).

5. Choose a suitable B.S.B. for the beam AB in Fig. 273. Stress 8 tons/ sq. in. Assume that the end A is direction-fixed.

Ans. 12 × 5 × 30 lb./ft. N.B.S.B. No. 10.

6. Make sketches showing approximately the distribution of (a) the normal stress due to bending, (b) the shear stress, over the cross section of a plate girder. Hence justify the practical assumption that the flanges carry the bending moment, and the web the shearing force; also that the shearing force may be regarded as uniformly spread over the depth of the web plate. (I.C.E.)
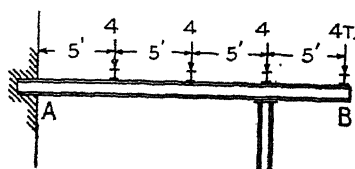
FIG. 273.

7. The span of a plate girder is 40 ft. and it carries four loads of 20 tons each which divide the span into 5 equal panels of 8 ft. Find the maximum bending moment and the necessary cross section at the centre of the girder, assuming that the stress in compression is not to exceed 6·8 and in tension 8·0 tons/sq. in. Take the depth of the girder as $\frac{1}{12}$th the span. Rivets, $\frac{3}{4}$ in. diameter in $\frac{13}{16}$-in. drilled holes.

Ans. M = 5760 in.-tons; D_1 = 40 in.; each flange to consist of two 4 × 4 × $\frac{1}{2}$ in. angles, one 12 × $\frac{1}{2}$ and one 12 × $\frac{5}{8}$ in. flange plate.

8. A plate girder is 26 ft. span and 2 ft. deep. The total shearing force at the ends is 33 tons. Find the pitch of the rivets connecting the angles to the web near the ends. The web is $\frac{1}{2}$ in. thick, and the rivets are $\frac{3}{4}$ in diameter. Take f_s = 6 and f_b = 12 tons/sq. in. (U.L.)

Ans. p = 3·28 in. (say 3 in. pitch). Note: In this example take $\frac{3}{4}$ in. as the diameter of the closed rivet, and λ = 1.

9. The maximum shearing force in the end panel of a plate girder of a through bridge is 230 tons. The web plate is 6 ft. 6 in. deep over the backs of the angles and $\frac{3}{4}$ in. thick; the flange plate, top and bottom is 18 × $\frac{5}{8}$ in., and the flange angles are 6 × 6 × $\frac{3}{4}$ in.; there are two rows of rivets in each leg of each angle. The rivets are $\frac{7}{8}$ in. diameter in $\frac{15}{16}$ in. holes; find the *theoretical* pitches necessary to connect the angles to the web and to the flange plates. Take f_s = 6 tons/sq. in., and f_b = 12 tons/sq. in.

Ans. p_1 = 18·1; p_2 = 7·48 in.

10. The ends of the girder in Q. No. 7 are supported on bed stones. The web is $\frac{1}{2}$ in. thick. Design the ends of the girder, making a dimensioned sketch showing the arrangement and sizes of the stiffeners, and the number

sponding stress is $10 \div 1 \cdot 31 = 7 \cdot 63$ tons/sq. in. Using the formula for eccentric loading, and finding the stress on the gross area of the angle, $v_1 = 0 \cdot 88$; $e_2 = v_1 + t/2 = 0 \cdot 88 + 0 \cdot 19 = 1 \cdot 07$; $\kappa^2 = 0 \cdot 81$; and

$$f_t = \frac{F}{a}\left\{1 + \frac{v_1(v_1 + t/2)}{\kappa^2}\right\} = \frac{10}{2 \cdot 11}\left\{1 + \frac{0 \cdot 88 \times 1 \cdot 07}{0 \cdot 81}\right\} = 10 \cdot 3 \text{ tons/sq. in.}$$

All the dimensions are in inches. This is the stress on the gross area. In the way of a rivet hole the stress would be increased to approximately

$$10 \cdot 3 \times \frac{3}{3 - \frac{13}{16}} = 14 \cdot 2 \text{ tons/sq. in.}$$

If it be assumed that the line of action of the load is fixed by the centroid of the *net* area of the angle, $v_1 = 0 \cdot 99$, $e_2 = v_1 + t/2 = 0 \cdot 99 + 0 \cdot 19 = 1 \cdot 18$, $\kappa^2 = 0 \cdot 85$, $a = 1 \cdot 8$, and

$$f_t = \frac{10}{1 \cdot 8}\left\{1 + \frac{1 \cdot 18 \times 0 \cdot 99}{0 \cdot 85}\right\} \quad 13 \cdot 2 \text{ tons/sq. in.}$$

That these high stresses really occur in practice is very unlikely, for the type of construction (the angle attached by its back) is very common and shows no signs of weakness. They appear, however, to afford justification for the custom of neglecting one-half of the area of the outstanding flange. It is evident that the stiffness of the end attachments must, partially at least, direction-fix the ends of the tie, and the stress due to bending is much reduced.

From the point of view of eccentric loading, the detail shown in (ii) Fig. 216 is no better than that shown in (i), and there appears to be no justification for counting in more area in the one case than in the other. The additional cleat shown at (ii) is useful in situations in which it is difficult to get sufficient rivets in the main angle ; (ii*a*), in which the cleat is lengthened, is a better detail than (ii).

As to the best form of section to use for a tie attached by its back to a gusset plate, it is instructive to compare the maximum stress produced in the three sections shown at (iv), (v), and (vi), Fig. 216, all of the same sectional area, but of different vertical dimensions. The figures for the gross sections are :

	(iv)	(v)	(vi)
e_2	$1 \cdot 07$	$1 \cdot 30$	$1 \cdot 57$
v_1	$0 \cdot 82$	$1 \cdot 05$	$1 \cdot 32$
κ^2	$0 \cdot 73$	$1 \cdot 10$	$1 \cdot 53$
$\left(1 + \frac{e_2 v_1}{\kappa^2}\right)$	$2 \cdot 20$	$2 \cdot 24$	$2 \cdot 35$

The maximum stress $f_t : \dfrac{F}{a}\left\{1 + \dfrac{e_2 v_1}{\kappa^2}\right\}$ is therefore not very different in the three cases, but is least in the shallowest section, in which it is $2 \cdot 2$ times the mean stress, F/a.

This calculation suggests that a flat bar (vii) would most nearly approach the ideal conditions. For the particular case indicated, $v_1 = 0 \cdot 25$; $e_2 = 0 \cdot 5$; $\kappa^2 = \frac{1}{48}$; and $(1 + e_2 v_1/\kappa^2) = 7$! That is to say,

CHAPTER XI

BRIDGE CONSTRUCTION. GIRDER BRIDGES

182. Girder Bridges. Definitions.—The *superstructure* of a girder bridge is composed of (*a*) *main girders* which support the floor system ; (*b*) *the floor system* suitably arranged to carry the traffic ; (*c*) *secondary bracing* resisting lateral and other distorting forces. The *substructure* consists of the *foundations, abutments,* and *intermediate piers,* if any.

If the floor system is placed on top of the main girders, the bridge is called a *deck bridge,* Fig. 87. If the traffic passes between the main girders, the bridge is called a *through bridge,* (ii) Fig. 306. If the bridge carries a railway it is termed a *railway bridge*; if it carries a roadway it is called a *road bridge.* If part of the bridge is made movable, leaving a clear opening to permit the passage of traffic past the bridge, it is called an *opening bridge,* otherwise it is termed a *fixed span.* There are various types of opening bridges, of which the commonest is the *swing bridge,* (i) Fig. 283, in which the movable span turns about a vertical axis. In a *traversing bridge* the movable span is drawn backward on rollers. In a *bascule bridge* the movable span is hinged about a horizontal axis, and lifts up like an ancient drawbridge ; the Tower Bridge, London, is a well-known example. A variation of the bascule type is the *rolling lift bridge,* (ii) Fig. 283, in which the lifting span carries circular segments which roll over suitable paths as the span rises. In a *vertical-lift bridge* the movable span is lifted vertically.

183. Other Types of Bridges.—In place of main girders, the floor system may be supported by : (i) *arches* (Arched Bridges, Chapter XIII) ; (ii) *suspension chains* (Suspension Bridges, Chapter XIV) ; or (iii) by *cantilevers* (Cantilever Bridges, Chapter XIV).

184. Main Girders.—The main girders of a bridge may be either of the *plate* or *braced* type. For spans above 60 to 80 ft. a braced girder should be used, as this type is lighter, and the area exposed to the wind is less. Braced girders cost more per ton than plate girders, and the latter are to be preferred for shorter spans. Such plate girders are similar in general construction to that shown in Fig. 272 ; some details are given in Figs. 267, 286, and 298.

Braced girders are classified according to the arrangement of the web bracing. The simplest type is the N girder, (i) Fig. 274, sometimes called a *Pratt* truss. In this design the shorter (vertical) web members are struts, and the longer ones ties. The vertical members are convenient

for the attachment of cross girders and the overhead sway bracing, § 191 and Fig. 309. The diagonals are not necessarily placed at 45°. The arrangements shown at (i) and (ii) are suitable for through bridges, and (iii) for a deck bridge. In ordinary circumstances (ii), with the inclined end post, may be regarded as the simplest and best type of main girder. The *Howe* truss, a timber construction at one time common in America,
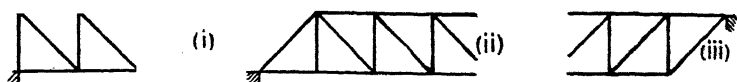
FIG. 274.

is similar in outline to the Pratt truss, except that the diagonals, which are timber struts, slope the other way. The verticals are in tension, and take the form of iron or steel bolts. For a composite truss of timber and steel, this arrangement is rather more convenient to construct than the Pratt truss.

(i) Fig. 275 represents a type called a *Warren* girder. At (i) and (ii) the web diagonals are inclined at 60° ; at (iii) and (iv) they are inclined
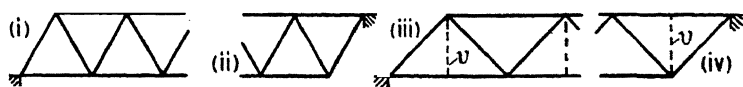
FIG. 275.

at 45°. In the latter case it is usual to insert vertical members vv to reduce the pitch of the cross girders supporting the bridge floor. (i) and (iii) are suitable for through bridges, (ii) and (iv) for deck bridges.

Sometimes a duplicate system of web bracing is used, as shown in Figs. 276 and 277. Type (i), Fig. 276, is obtained by inverting one Warren girder of type (iii), Fig. 275, superposing it on another, and omitting the verticals vv. It is called a *lattice* or *double Warren* girder.
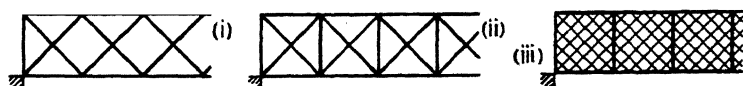
FIG. 276.

(ii) Fig. 276 is the result of treating two N girders of type (i) Fig. 274 in a similar way. Type (ii) differs from type (i) only in the introduction of the verticals, which are intended to equalise the load between the two component frames. In the *Linville* truss, Fig. 277, two N girders are superposed, but one is moved half a bay along relative to the other. An extra member j must be introduced at each end to complete the framework. Two advantages are claimed for the Linville truss : first, it

halves the pitch of the cross girders, thus reducing the span of the rail bearers, § 188 ; secondly, the diagonals give support to the long vertical struts at the point where they cross. Linville trusses are only suitable for very large spans. Types (i) and (ii) are suitable for through bridges, and (iii) for a deck bridge.

Multiple web girders of the types shown in Figs. 276 and 277 are not nowadays regarded with much favour by bridge engineers.

Two lattice girders, (i) Fig. 276, may be superposed, one being moved half a bay along relative to the other, to form a *double lattice* girder ;
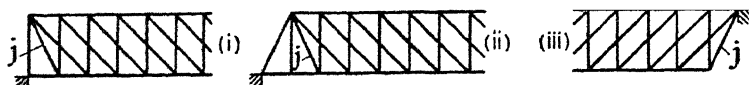
FIG. 277.

and (iii) Fig. 276 may be regarded as a *multiple lattice* girder. This type is common for small light spans. The web is composed of a number of flat bars placed diagonally and riveted together at their points of intersection. The web thus formed is stiffened by vertical stiffeners of the kind used in plate girders, and intended to serve a similar purpose. It is usual to make the area of the diagonal bars such that, at any vertical section, the vertical component of the safe load in all the bars cut by the section is equal to the shearing force at the section. Hence it results that the bars are made of greater area towards the points of support.

FIG. 278.

(i) Fig. 278 shows a *Baltimore* truss. The bracing is of the N type, Fig. 274, but secondary members are introduced to support intermediate cross girders. In (i) the load from these cross girders is carried back to the panel points of the lower flange, in (ii) it is transferred to those of the top flange. The short verticals from which the intermediate cross girders are suspended are called sub-verticals.

FIG. 279.

Girders with Curved Flanges.—(i) and (ii) Fig. 279 represent girders of the N and Linville types with curved upper flanges. The curvature is often introduced with the intention of improving the appearance of the bridge ; in long spans it has other advantages (see *infra*). Such girders

cost more per ton than those with straight parallel flanges, and the extra expense should only be incurred when the circumstances justify the expenditure.

Girders of the type shown at (i) Fig. 280 are called *bowstring* girders, from their similarity to a bow and string. If the load were uniform, and

FIG. 280.

the shape of the curve parabolic, the area of cross-section of the flanges would be constant, and no diagonal bracing would be required in the web. Since, in practice, the load will not be uniform, and the bridge must carry a moving load, these theoretical considerations will not hold, and, as shown in Fig. 280, diagonals must be introduced in the web. The type reduces therefore to a girder with a curved upper flange. Owing to its greater depth where the bending moment is large; the reduction in the shearing force carried by the web members due to the curved flange (see § 180); and to the shortness of the heavy web members near the ends, where the shearing force on the web is large; the bowstring girder is economical in weight. Consequently, it is properly employed in bridges of long span, where the weight of the bridge itself is a most important part of the total load to be carried. The girder may be inverted, when the curved member becomes the tension flange.

(ii) Fig. 280 shows the arrangement used in the famous Saltash bridge of 455 ft. span, sometimes called a *bow and chain* girder. The thrust from the bow is neutralised by the tension in the chain. The roadway is suspended from the girder by means of vertical suspension rods.
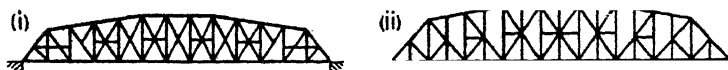
FIG. 281.

Fig. 281 shows two types of long span girders of American design. (i) is the Hawkesbury bridge of 410 ft. span, and (ii) a span of 490 ft. over the Ohio River. Fundamentally, the bracing is of the N type, but secondary members are introduced to halve the effective length of each main member. In (ii), the secondary bracing is arranged to support intermediate cross girders. In both types the depth is reduced toward the supports, and the truss approximates in outline to the bowstring girder. Fig. 282 shows a 160 m. span over the Danube, a type common on the Continent.

FIG. 282.

It is to be clearly understood that the special types of main girder shown in Figs. 277 to 281 are quite unsuitable for ordinary short and

medium span bridges.   Their justification is for long span girder bridges, where it is imperative to reduce the weight of the main girders to a minimum, even at the expense of increased cost of production.

(i) Fig. 283 shows the type of main girder used in a *swing bridge*,
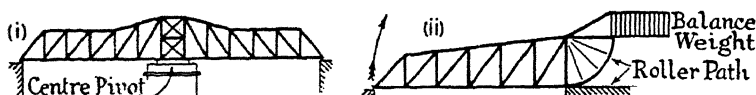
FIG. 283.

and (ii) that for a *rolling lift* bridge.   Web bracing of the type shown in Fig. 282 is commonly used for such bridges.

185. Counterbracing.—Near the centre of the girder the shearing force due to the dead load, represented in Fig. 284 by the line cd, will be small. It results that, over a certain length of the middle of the girder, the positive shearing force due to the travelling load, represented by the line ae, will be greater than the negative shearing force due to the dead load ; and the negative shearing force due to the travelling load, represented by fb, will be greater than the positive shearing force due to the dead load.   As the train passes over the bridge, therefore, the sign of the shear force in this region will be reversed ;

FIG. 284.

and, in consequence, the sign of the forces in the web bracing will also be reversed, the ties becoming struts, and the struts ties.   The length gh, Fig. 284, over which this occurs, can easily be found by inverting the line cd as shown in the figure.   In plotting the lines ae and bf, the live load should be multiplied by $(1 + i)$ where i is the impact factor.
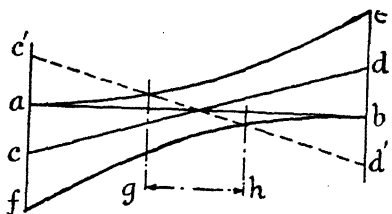
The members in which the stress is reversed must be of such a type that they will act equally well as ties or as struts.   They should be designed first to resist the compressive load, second to resist the tensile load ; in order to allow for the alternations in stress, certain standard specifications require that one-half the smaller gross area thus obtained be added to the larger gross area, in order to obtain the total gross area necessary.

FIG. 285.

When, as in the older bridges, the tension members are of flat bar cross-section, they are incapable of acting as struts, and *counter-braces*, cc Fig. 285, are inserted.   These are tension members, sloping in the opposite direction to the normal ties.   When the stress reverses, the normal tie will give slightly under the compressive load, and the counter-brace will take up the reversed shear.   If the reversed stress be small,
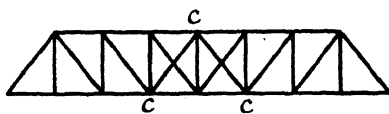
two parallel flat bar ties can be converted into a strut by the introduction of secondary bracing between the ties, in which case counter-braces are unnecessary. In girders with a duplicate system of web bracing of the type shown in Fig. 276, if flat bar ties are used, the second system must carry the reversed shear, otherwise it should be proportioned between the two systems. With the stiff tension members commonly used in modern girders, counter-bracing is unnecessary.

186. Plate Web Main Girders. Details of Construction.—Some typical examples of plate web main girders are shown in Figs. 267, 286,
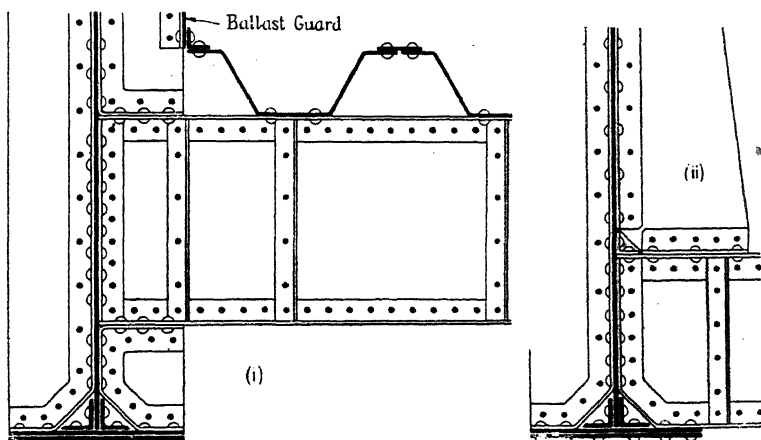
FIG. 286.

and 298. That shown in Fig. 286 is suitable for through or half-through bridges; Fig. 298 represents a deck bridge. The methods and rules of Chap. X may be used for the purpose of designing these girders, but the live load must be multiplied by $(1 + i)$, where i is the impact factor, § 61, in order to obtain the equivalent dead load.

187. Open Web Main Girders. Details of Construction.—*Compression Flange.*—The compression flange of braced girders should
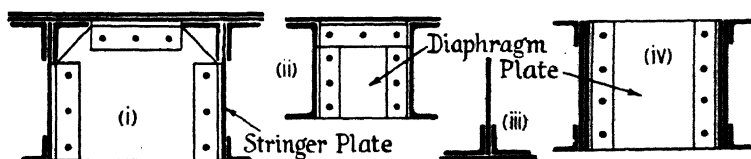
FIG. 287.

be of trough section, made up of plates and angles, or of channels, as shown at (i) and (ii) Fig. 287. The outstanding edge of the stringer plate, (i), should be stiffened by an angle as shown, to prevent it from buckling, and diaphragm plates should be introduced to prevent the section from distorting. Tie plates or lattice bracing are fitted to prevent secondary

flexure, § 160.   In small girders, a tee section, similar to (iii), may be used. The breadth of the flange should not be less than $\frac{1}{40}$th its overall length, unless adequate lateral supports are provided, when the breadth should not be less than $\frac{1}{15}$th the distance between such supports.   In shallow girders these supports may take the form of stiff brackets of the type used in plate girders, Figs. 286 and (iii) 297 ; but where possible, a lateral system of wind bracing is introduced, Fig. 295, which gives effective support to the flange.

Tension Flange.—The tension flange may be similar in form to the compression flange (i), (ii), and (iii), Fig. 287 ; or it may be constructed of plates placed vertically, with stiffening angles, (iv) Fig. 287. This construction has the advantage that water cannot lodge therein ; with trough sections, suitable drainage holes must be provided. The type shown at (iv) enables the cross girders to be slung below the main girders, (i) Fig. 288, and the attachment of the web bracing is slightly more convenient. The gain in height, when the cross girders are slung below the main girders, may enable overhead lateral bracing to be fitted which would otherwise be impracticable.

Design of Flanges.—Having determined the forces in the flanges, the lengths and arrangement of the plates and angles in the tension flange can be obtained from a ' force in the flanges diagram ' similar to (vi) Fig. 271, or by the method of ¶ 12, § 196. The members of the compression flange should be designed as columns imperfectly direction-fixed at their ends ; eq. (1), § 163 may be used. For examples, see ¶ 13, § 196.

Joints in the Flanges.—The joints used in flange plates and angles of open web girders are of a similar type to those used in plate web girders, §§ 172 and 173, and are similarly designed.   Grouped joints are usual to facilitate transport.   The joints in the stringer plates are butt joints with double covers (see Fig. 309).

Riveting in the Flanges.—The riveting in the flanges should be arranged so that the rivet pitches are uniform and an even 3, 4, or 6 inches.   The rules given on p. 384 for maximum pitches should be followed.   As far as possible the rivets should be staggered across the flange, to minimise the loss of area due to rivet holes in the tension flange.

Web Bracing.—Stiff sections are used for the tension members, Figs. 220 and 221.   Such sections are capable of carrying secondary bending moments or accidental compressive forces.   The methods of design discussed in Chap. IX may be followed.   For the web compression members of bridges, I sections are preferred, Fig. 227, with the web of the I placed transversely, Fig. 309. This facilitates the attachment of the cross girders and overhead bracing, and the combination forms a stiff construction capable of resisting lateral deformation and cross girder deflection, § 112.   The methods of Chap. IX can be used for the design of the web compression members.

End Posts.—These have to carry the·end reactions.   They may be made of trough section similar to the compression flange, or may be of H section, (iv) Fig. 227, with stiffened plate edges.   Special consideration

is necessary regarding the attachments of the end cross girders and the end bearings, Fig. 307.

Connection of Web Bracing to Flanges.—If the number of rivets required is small, the web bracing may be connected directly to the stringer plates; otherwise stiff gussets are provided, riveted to the latter, Fig. 308 and (i) Fig. 310, to which gussets the web bracing is attached. Sufficient rivets must be provided in the ends of the bracing to transfer the load to the gussets, and sufficient rivets through the gussets and stringer plates to transfer the load to the flanges. The axes of all the members taking on to a gusset plate should meet in a common point, and the rivets in each member should be symmetrically placed about its centre line. A tension member should not be weakened by more than one rivet hole. As far as possible the regular pitch in the flanges should not be upset. Compromise regarding these conditions is often unavoidable, but every effort should be made to fulfil them.

188. Cross Girders.—The weight of the bridge floor and of the live load coming upon it is transferred to the main girders by *cross girders,*
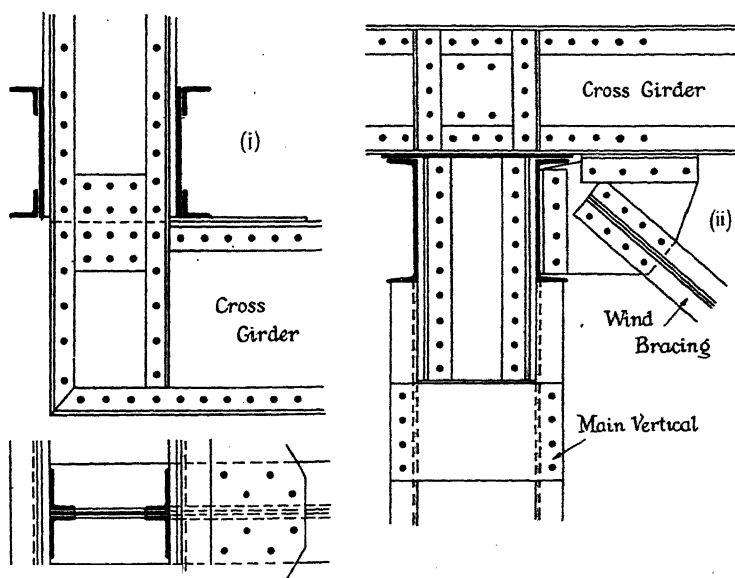
FIG. 288.

which are placed at the panel points of the main girders and transversely to them. Cross girders are normally of the plate-web type; sections composed of four angles and a web plate, with no flange plates, are to be preferred; for small spans, rolled steel beams may be used. Typical examples of cross girders and the methods of attachment to plate-web main girders are shown in Figs. 286 and 293, and to open-web main girders in Figs. 288, 292 and 309. (i) Fig. 288 and Figs. 292 and 309 show the

constructions used for through bridges ; and (ii) Fig. 288 that used for deck spans. In (i) Fig. 288 the cross girder is slung below the main girder and the load transmitted directly to the verticals.

In railway bridges the pitch of the cross girders should not be less than the distance apart of the most heavily loaded axles crossing the bridge, for however closely the cross girders be spaced, each one must be capable of carrying the load due to the most heavily loaded axle. When the available depth of construction is limited, the pitch of the cross girders must be kept small ; in plate girder spans up to about 80 ft., a pitch of cross girders of 7 to 8 ft. may be regarded as a minimum. This may be considerably increased in longer spans, and with open-web main girders the arrangement of the web bracing is usually the deciding factor. With the modern tendency to deep main girders and single N bracing, in spans up to 200 ft., cross girder pitches of 16 to 20 ft. are common, but an excessive pitch means very deep floor longitudinals and is not economical. In very long spans these dimensions may be greatly exceeded, but the weight of the floor is then so much smaller, relatively to the weight of the main girders, that the design of the latter entirely governs the situation.

In ordinary road bridges, the panel length of the main girders and the depth of the cross girders and longitudinals are the determining factors.

The cross girders are usually treated as freely supported beams of span equal to the distance between the centres of the main girders, and are designed by the methods of Chap. X. Actually, their attachment to the verticals of the main girders is usually capable of carrying a considerable bending moment, and the cross girders, main girder verticals, and overhead bracing, act to some extent at least as a stiff frame. The deflection of the cross girder under its load thus sets up bending moments in the main girder verticals (see § 112), and to reduce these moments as much as possible, stiff cross girders are desirable. Their depth should not be less than $\frac{1}{8}$ to $\frac{1}{10}$ their span.

Strictly speaking, the rivet section at the ends of the cross girders should be designed to carry the bending moments at the ends of these girders. If this be not done, an ample rivet section should nevertheless be provided at the ends, for it is at these places that signs of weakness show themselves in practice.

189. Rail Bearers.—In many types of railway bridge floors, the load from the train is carried by longitudinal girders placed directly under the rails and spanning from cross girder to cross girder, Figs. 293 and 309, called *rail bearers*. In small spans, rolled steel beams may be used, and plate girders in longer spans. Sections composed of four angles and a web plate with no flange plates are to be preferred. The rail bearers may be designed by the methods of Chap. X ; their depth should not be less than $\frac{1}{12}$th their span. Strictly speaking, rail bearers form partially continuous girders over the cross girders, and with flat floor plates, Fig. 309, the degree of direction-fixing may be considerable. In the ordinary conventional calculations, however, they are treated as girders freely

supported at each end, with a span equal to the pitch of the cross girders. As in the case of the cross girders, and for similar reasons, an ample rivet section at the ends of the rail bearers is good practice, in default of a proper design taking into account the support moments.

190. Bridge Floors.—These may be divided into two classes, (i) solid floors, (ii) open floors. In the former there is a continuous deck from end to end of the bridge. This has the advantages that it can be made watertight, and is much safer in the case of derailment. Solid floors are used for railway bridges in the neighbourhood of towns, where dripping water is objectionable, and are imperative in the case of road bridges. Open floors are used in railway bridges crossing rivers, and in other situations where there is no objection to the rain dropping through. Direct support is provided for the timbers to which the rails are attached, but there is no continuous deck. Open floors have the great advantage of lightness, and are used in long span bridges where lightness is obligatory; they have the advantage that all the metal work is exposed and rapidly dries after rain; they can also be readily scraped and painted.

Desiderata.—The points to be aimed at in designing a bridge floor are : strength, stiffness, lightness, good drainage, freedom from corrosion, no ungetatable spots.

Solid Floors.—These can be subdivided into (i) plate floors—flat or buckled plates ; (ii) trough flooring ; (iii) jack arches ; (iv) reinforced-concrete floors. These types may take different forms depending on whether the bridge is a railway or a road bridge, and in the former case whether the floor is ' free ' or ' tied.' If the floor is ballasted, and the rails are laid on sleepers unconnected to the structure of the bridge, it is called a *free floor*, and has the advantage that the continuity of the permanent way is preserved. Ballasted floors are heavy and not suitable for long spans, but are advantageous on curves where superelevation is necessary. In long spans, the ballast would be such a large addition to the weight proper of the bridge, that either an open floor is used, or the rails are supported on longitudinal timbers bolted to the structure of the bridge, called *way-beams*. This is spoken of as a *tied floor*, Fig. 293.

Plate Floors.—Fig. 309 shows a typical flat plate floor for a through railway bridge. The floor plating is usually about $\frac{3}{8}$ in. thick, and is attached directly to the tops of the cross girders and rail bearers by $\frac{3}{4}$ in. diameter rivets at 6 in. pitch. Vertical ballast guards are provided at the sides of the deck as shown, thus forming a trough which contains and confines the ballast. The object is to keep the ballast and timber away from the main structure of the bridge, thus minimising corrosion. The trough is made watertight by coatings of asphalt or bitumen sheeting, and a drainage system is provided to lead away the water caught in the trough.

Buckled and cambered plates, (i) and (ii) Fig. 289, are sometimes used instead of flat plates for bridge floors. Buckled plates can be obtained from 3 to 6 ft. square and from $\frac{1}{4}$ to $\frac{1}{2}$ in. thick ; a common thickness in bridge floors is $\frac{5}{16}$ in. They can also be obtained in long

lengths with a series of buckles end to end, (i). Buckled plates should be placed with the concave surface upward, and attached to supports on each side of the square by $\frac{3}{4}$ in. diameter rivets at 6 in. pitch. A drain hole should be provided at the centre of each buckle. The depth of the buckle should not be less than $\frac{1}{20}$th the clear span, nor less than
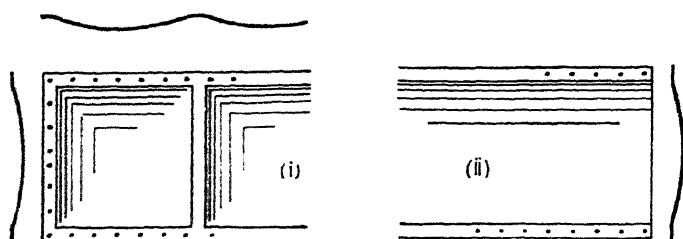
FIG. 289.

2 in. In cambered plates these limits should be increased by 50 %. (i) Fig. 291 shows a deck span with a longitudinal girder under each rail and a buckled plate floor.

Trough Floors.—Steel troughs are frequently used for bridge floors, particularly in road bridges; they form a stiff continuous floor. The troughs may either be rolled to shape (i) Fig. 290, or pressed out of a steel plate, (ii) and (iii). In stock sizes the dimension a may range from 4 to 16 in., and b from 1 to 3 ft. The thickness t ranges from $\frac{5}{16}$ to
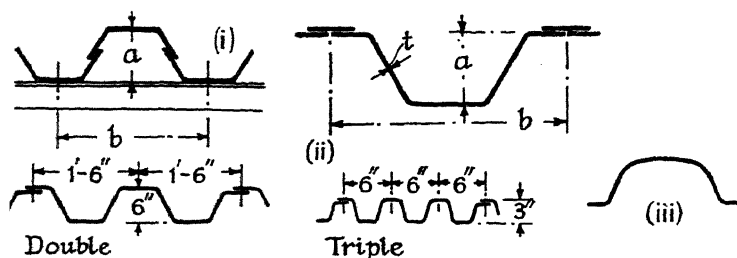
FIG. 290.

$\frac{3}{8}$ in. In the case of the rolled troughing, (i), the thickness of the horizontal part, or flanges of the trough, is increased, thus giving a better disposition of the material. Weights, section moduli, and other particulars of standard troughs will be found in the makers' catalogues.

In railway bridges, if the troughing is made to run longitudinally, no rail bearers are required, Fig. 286; in plate girder spans the troughing may be placed transversely and supported directly by the main girders, when neither cross girders nor rail bearers will be required. This arrangement is also very suitable in small road bridges, (ii) Fig. 310. In very small road bridges the troughing will carry the load from abutment to

abutment, and the main girders can be dispensed with. The application of trough flooring to railway bridges is shown in Figs. 135 and 286.

Trough floors have the disadvantage that it is difficult to make a watertight attachment between the troughs and the main girders, and also to provide efficient drainage. Unless each trough be separately drained, it is best to fill the whole construction with concrete to a level of 2 to 3 in. above the top of the troughs, made watertight by means of a ¾ in. layer of asphalt, which is protected from the picks of the permanent way men by a 2 in. covering of concrete, Fig. 135.

The troughs are designed as beams. When the troughs are placed transversely to the rails, a wheel load may be taken as spread over a 5 ft. width of the troughing * (cf. Q. No. 14, Chap. V). When sleepers 9 ft. long are placed transversely to the troughs, a 10 ft. width of the troughing may be counted in as resisting the bending moment.

Jack Arches.—A type of jack arch floor is shown in (ii) Fig. 291. The arches may run transversely or longitudinally to the bridge. This
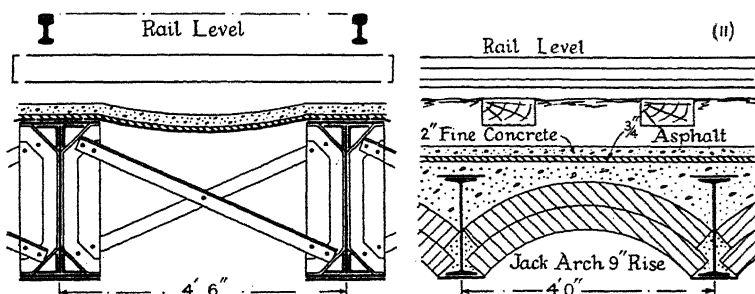
FIG. 291.

construction is heavy, and its use is confined to small bridges where ample construction depth is available, but the cost of upkeep is very small. To prevent water percolating between the arches and the steelwork and setting up corrosion, a waterproofing of asphalt is provided as indicated in Fig. 291.

Reinforced-Concrete Floors.—Reinforced-concrete floors are frequently used for steel bridges of both the railway and roadway types. A typical road bridge example is shown in Fig. 292.

Tied Floors.—Examples of this type of floor are given in Fig. 293. (i) Fig. 293 illustrates a three-girder railway bridge with longitudinal way beams. These are carried in troughs and let in with bitumen to prevent rusting. The timbers are well creosoted and have a long life. All the main steelwork of the bridge is exposed. This type of floor is much lighter and the first cost is much lower than the ballasted floor ; there is far less riveting at the site. The cost of maintenance is higher. As an example of a long span bridge floor, (ii) Fig. 293 shows the troughs and way beams of the reconstructed floor of the Forth Bridge.

* For a calculation of the distribution of load over trough flooring, see Martin, *Statically Indeterminate Structures*, London, 1895, p. 63.

Open Floors.—This type of floor is illustrated in Fig. 294, which is typical of American practice, where open floors are common.
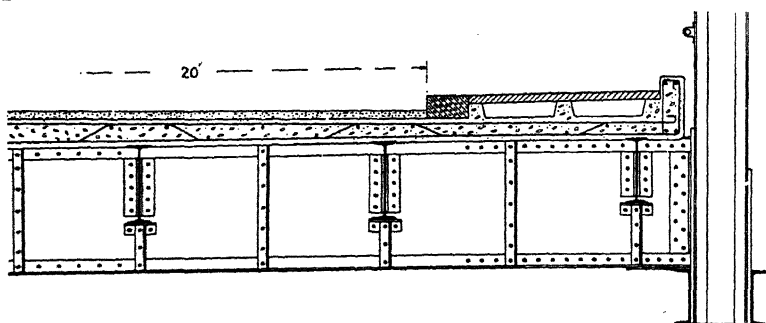
Fig. 292.
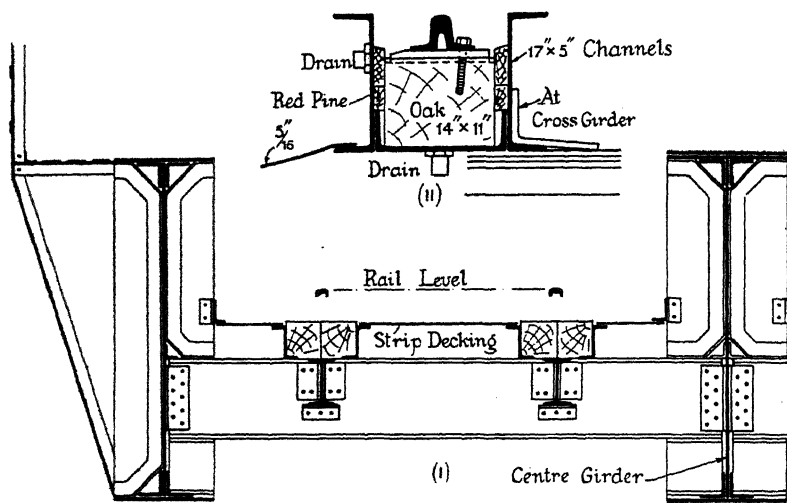
Fig. 293.
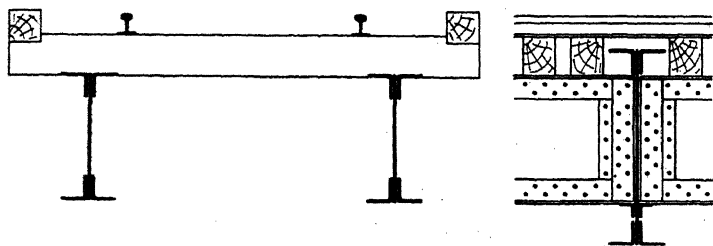
Fig. 294.

For a comparison of the relative weights and costs of ordinary railway bridge floors, see ' Floors for Railway Underbridges,' *The Engineer*, April 16, 1920, p. 391.

191. Wind Bracing in Bridges.—To resist wind pressure and other lateral forces on a bridge, secondary bracing called *wind* or *lateral bracing* is provided. This takes different forms depending on the type of the bridge. In a deep through bridge, the top flanges and bottom flanges are braced together in a horizontal plane, (ii) and (iii) Fig. 295, thus forming two *wind girders*, whose func-

tion it is to transmit the wind load to the abutments. The flanges of the main girders form the flanges of the wind girders, and the stresses due to the vertical loads and those due to the lateral loads must be properly combined. The web of the wind girder is usually cross-braced, as the wind may blow in either direction; the cross girders are sometimes utilised to form the transverse members of the web. When a plate or trough floor exists, this may be arranged to form the web of the wind girder. The cross-bracing of the top and bottom

Fig. 295.

wind girders is similarly arranged, but in the former case the wind load has to be carried down to the abutments by end portals, as indicated in (iii) Fig. 295. The feet, A and B, of these portals are usually assumed to be direction-fixed ; they are designed by the methods of Chap. VI, § 99 *et seq.* When designing the end bearings of the main girders, it should not be overlooked that the wind load will come upon them.
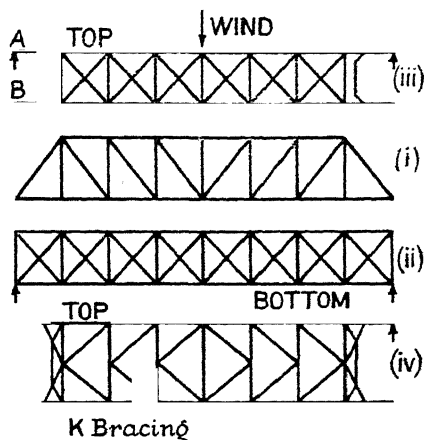
K-bracing.—It has been pointed out that, due to the vertical loading on the bridge, stresses of considerable magnitude may be induced in the web bracing of the wind girder ; for, as indicated in Fig. 296, the web members of the wind girders are altered in length by the shortening of the top flanges and the lengthening of the bottom flanges of the main girders, caused by the vertical load. These secondary stresses are obviated by using a type of web bracing called K-*bracing*, (iv) Fig. 295, to which this

Fig. 296.

objection does not apply. K-bracing also has the advantage in a wide bridge of reducing the length of the diagonal members of the lateral bracing. It may be used for secondary bracing in other positions, and is sometimes adopted for the main web bracing of large girders (cf. Fig. 379), but it would appear that this is not advantageous in spans of less than 350 ft.*
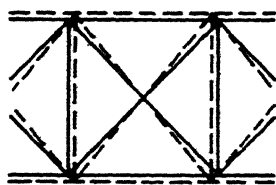
* *Eng. News-Record*, vol. 106, p. 553.

Details of wind girder bracing are given in (i) and (ii) Fig. 297, and 308. The wind pressure on the main girders proper is assumed to be shared between the top and bottom wind girders. That on the train goes via the rails to the wind girder of the loaded flanges, in (ii) Fig. 306 to the

Bottom Flange

Plan looking up

Attachment to
Rail
Bearer

(i)

(iii)

(ii)

(iv)
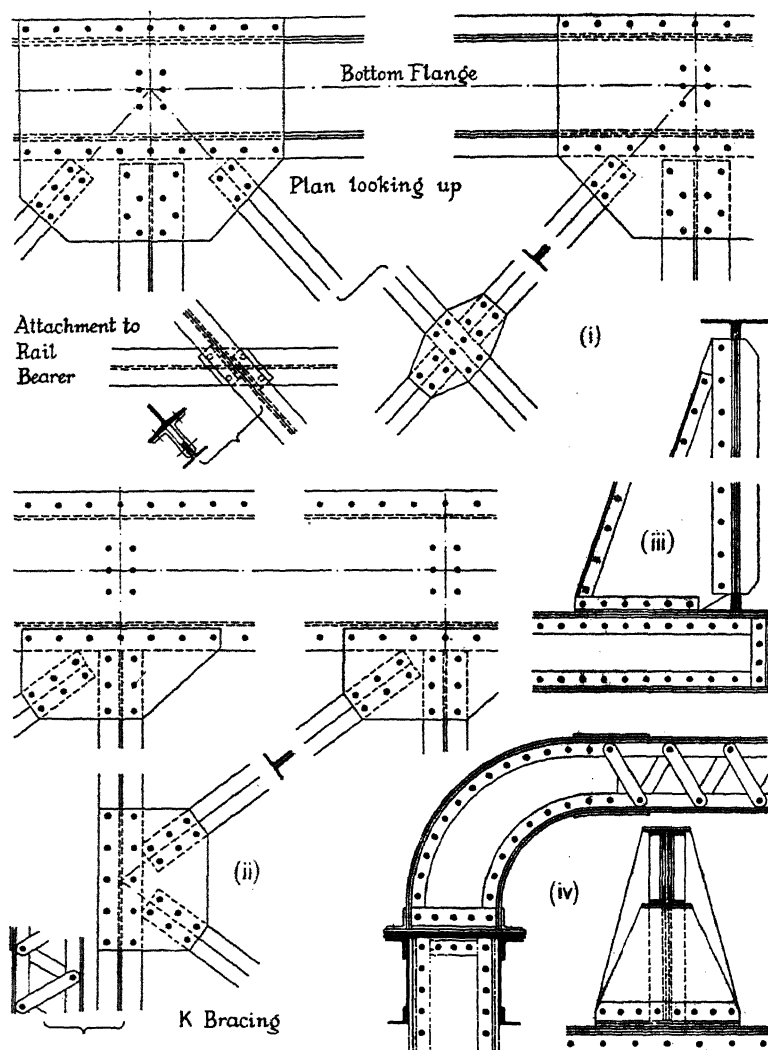
K Bracing

FIG. 297.

lower wind girder, on which it forms a rolling load, § 52, *Bridges,* and the web bracing must be designed accordingly, § 196, ¶ 19.

Portal and Sway Bracing.—The transverse lateral bracing in a through bridge is of two types. That which occurs at the ends of the bridge is

called *portal bracing*. As was seen above, its chief function is to transfer the lateral forces from the overhead wind girder to the abutments. It also serves to stiffen the ends of the bridge. *Sway bracing* is placed at the intermediate verticals. It may range from a simple corner gusset to a construction similar to the end portals. Its function is to stiffen the cross-section of the bridge against lateral distortion and to prevent lateral deflection of the compression flange. Some details of construction of portal and sway bracing will be found in Figs. 307 and 309. Any of the types of portal bracing considered in Chap. VI may be used for bridges if convenient.

Half-through Spans.—In half-through spans it is not possible to put overhead bracing, and the wind girder at the lower flange must carry the whole wind load to the abutments. Transverse stiffness is obtained by fitting large gussets where the cross girders occur, rigidly attached to cross girders and to the web verticals. Examples are shown in (ii) Fig. 286 and (iii) Fig. 297.

Where head room permits, the top flanges are sometimes connected together by curved overhead girders, (iv) Fig. 297. These provide some lateral stiffness and help to equalise the wind loads between the main girders.

Deck Spans.—In a deck bridge, Fig. 298, the lower flanges AB are cross-braced to form the lower wind girder;

FIG. 298.

the floor system is usually arranged to act as the web of the wind girder in the plane of the top flanges CD. The details of construction of the wind girders are similar to those in a through bridge. The main girders are cross-braced in a vertical plane, as shown in Fig. 298, to resist lateral distortion. This bracing occurs in line with the web verticals of the main girders.
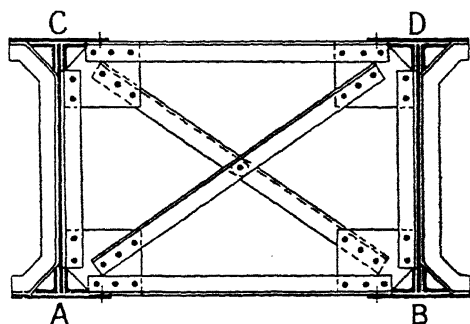
192. End Bearings.—The ends of the main girders of a bridge are supported on bearings. In a small bridge these may be simple sliding bearings similar to Fig. 269. It has been suggested * that such bearings, in that they dissipate energy in sliding friction, have the advantage that they reduce vibration and the effect of impact. In large bridges it is customary to provide bearings capable of angular movement so as to allow for the deflection of the bridge, and to make these bearings at one end in such a way that they will permit the bridge to lengthen or shorten with changes in temperature. A common type of such bearings is shown in Fig. 307. The angular movement is obtained by allowing the part attached to the girder to rotate about a pin ; the longitudinal motion is obtained by mounting the bearing proper on a nest of rollers. These need

* Ref. No. 17, Bib., Chapter IV.

not be completely circular; space is gained by adopting the shape indicated and fitting a parallel motion. The pressure per lineal inch on rollers of mild steel should not exceed $d/4$ tons, where d is the diameter of the rollers in inches; and d should not be less than 4 ins. An example of American practice is given in Fig. 299.

ROCKER BEARING   FIXED BEARING

Holding down Bolts   Drain Hole
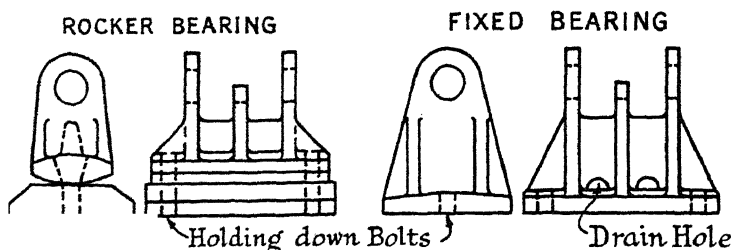
FIG. 299.

Bearings should be placed in an accessible position, as otherwise, with years of inattention, they become unworkable.

193. Loads on Bridges.—*Dead Load.*—The dead load consists of the weight of the bridge itself plus any other permanent load which it has to carry. The weight of the floor system must be estimated as nearly as possible from an existing bridge. Useful information on the weight of steel bridges of many types, including both the main girders and bridge floors, has been given by Thorpe.[28] Weights of different types of bridge floors will be found in *The Engineer*, April 16, 1920, p. 391. The following figures are a rough guide to the weights of complete bridge floors, including rail bearers and cross girders, if any.

Single-Track Railway Bridges.	*lb./sq. ft.*
Flat plate, ballasted floor, Fig. 309 (ballast trough)	125
Flat plate, transverse sleepers, unballasted . .	55
Trough floor, concreted and ballasted, (i) Fig. 286 and Fig. 135	235
Trough floor, unballasted	60
Jack arch floor, on cross girders, (ii) Fig. 291 .	330
Reinforced-concrete floor	230
Longitudinal girders, 30-ft. span, (i) Fig. 291. .	160

The width of the floor has been taken as the distance centre to centre of the main girders. The above figures should be increased by 15–20 % in the case of double-track bridges, and reduced by 5–10 % in three-girder bridges, Fig. 293.

Road Bridges.	*lb./sq. ft.*
Buckled plate, concreted, 2-in. asphalt surface	120
Trough floor, concreted, 3-in. asphalt surface	180
Wood deck, 5 in. thick, hardwood blocks, 9 × 5 × 3 in. . . .	60
Reinforced-concrete floor, Fig. 292	130

The weight of the floor of a bridge will vary considerably with the circumstances (spacing of cross girders and longitudinals, thicknesses, kind of material) and it is preferable to estimate the weight of the flooring

próper independent of the cross girders and longitudinals, and to design the latter as plate girders (see the worked example, § 196). The following figures are useful :

One track of permanent way complete (rails 95 lb. per yard)	168 lb. /lin. ft.
Ditto, tramway track .	100 lb. /lin. ft.
Asphalt or cement concrete	140 lb./cub. ft.
Ballast (gravel) . .	120 lb. /cub. ft.
Ditto, screened broken stone or granite chippings	90 lb./cub. ft.
Macadam . . .	160 lb. /cub. ft.
Tar macadam . .	140 lb. /cub. ft.
Creosoted timber . .	47 lb. /cub. ft.

The weight of the cross girders and longitudinals can be estimated by Unwin's formula, using the constant C of § 179. The same formula can be used to find the weight of the main girders, but if these are of the open web type (ordinary plain girders), the constant C should be increased to 1,800–1,900, and f taken as the stress in the compression flange. When applying Unwin's formula, the live load must be reduced to an equivalent dead load by means of a suitable impact factor (see ¶ 9, § 196).

The weight of the wind and other secondary bracing should be estimated as nearly as possible from a similar existing bridge. In default of any better information it may be taken, in bridges of the type of § 196, as 15 % of the weight of main + cross + longitudinal girders, a very rough estimate.

If the floor is supported on cross girders, the loads on the main girders must be taken as concentrated at the panel points. If the main girders are of the plate type, and the floor system transfers its load direct, e.g. a trough floor with the troughs running transversely, the load on the main girders can be taken as uniformly spread. For girders of less than 200 ft. span the whole load may be supposed to act on the flange which carries the floor. In longer spans the load should be correctly proportioned between the flanges.

Live Load and Impact Allowance.—A public rail or road bridge in this country must be designed to carry the standard loading specified by the Ministry of Transport. For each track of a main line railway bridge this consists of the system of wheel loads shown in (ii) Fig. 49, each unit being taken as 20 tons. A main road bridge must carry the Ministry of Transport Standard Load for Highway Bridges. From Fig. 50, the equivalent loading, including impact, for all spans may be obtained. In the case of railway bridges the specified impact allowance is given by eq. 4, § 61.

When the design is not subject to Official Regulations, but the bridge has to carry a particular class of traffic, the procedure given in the worked example, ¶ 8, § 196, may be followed. Either the equivalent uniform load, corresponding to the given travelling load, may be used to find the stresses in the members of the main girders; or these stresses may be determined directly for the actual axle loads by means of influence lines. In ordinary bridges the two methods lead to very similar results, and for road bridges of over 20 ft. span the first method is all that is necessary. The heaviest axle loads are the most important consideration in the

design of the floor system. Footwalks should be designed to carry a load of 84 lb./sq. ft. without impact.*

Wind Pressure.—The usual stipulations for wind pressure on bridges are discussed in § 52. The method of treatment in design will be evident from the worked example, ¶ 19, § 196.

Longitudinal Forces.—There is evidently a longitudinal force acting at the rail level equal in magnitude to the tractive force which the locomotive exerts on the train, and acting in a direction opposite to the motion. A clearer idea of this effect may be obtained by considering the forces called into play when a man pushes a truck along the track ; with whatever force he pushes the truck forward with his arms, he pushes, or tends to push, the track backward with his feet.

Similarly, if the brakes be applied to the moving train while it is crossing the bridge, there will be a negative accelerating force acting on the train which will have an equal reaction at the rail level, in this case in the direction of motion.

Various empirical rules have been given for the magnitude of these longitudinal forces. Formulae equivalent to the requirements of the British Standard Specification [22] for single-track railway bridges are given in ¶ 20, § 196. The original may be consulted for further details. For a more recent investigation of these effects, and of the action of the track in transmitting the load, see Gelson, *Proc. Inst. C.E.*, vol. 237,

FIG. 300.

1933–34, p. 333 ; and also p. 402 for the relevant Indian Bridge Rules. When the bridge carries two or more tracks, accelerating and braking should be supposed to take place simultaneously on alternate tracks.
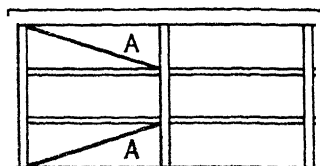
These longitudinal loads must be carried back, via the flanges to which the floor is attached, to the fixed end-bearings. When the bridge has a plate or other continuous floor, this may be arranged to transmit the load either to the flanges or direct to the bearings. In the case of an open floor, diagonal members AA, Fig. 300, should be provided to transmit the load from the rail bearers to the bearings. For the method of allowing for the stress in the flanges when they transmit the load, see ¶ 21, § 196.

Centrifugal Loads.—If the track on a bridge is curved, there will be a lateral load w_c tons per foot due to centrifugal force. If V be the maximum speed of the train in miles per hour, w the weight of the train in tons per foot, and R the radius of the curve in feet, the centrifugal force will be

$$w_c = \frac{w(5280V)^2}{32 \cdot 2 \times 60^4 \times R} = \frac{wV^2}{15R} \text{ tons per foot.}$$

This load must be regarded as a lateral travelling load on the train and bridge, and may be assumed to act at a point 6 ft. above the rail level.

---

* According to Johnson's experiments the weight of a densely packed crowd may reach as much as 181 lb./sq. ft.—*Engg.*, September 21, 1906, p. 375.

It should be treated in a manner similar to the lateral wind load. No allowance for impact is necessary, but it should be assumed that each track on the bridge is loaded.

194. Secondary Stresses.—Except in the portals at the ends of a bridge, which must be designed to carry the wind pressure down to the bearings, it is customary in conventional designs to neglect the effect of secondary and deformation stresses. When the span exceeds 200 ft., the deformation stresses due to vertical and lateral deflection, and also those due to cross-girder deflection, § 112, should be taken into account.

195. Permissible Stresses. Combination of Stresses.—In conventional bridge designs, the calculated primary stresses in the structure for dead plus live load plus impact should not exceed the permitted stresses set forth in the Specification. For the combination of these primary stresses with the stresses due to wind, longitudinal force, centrifugal force, temperature, and deformation, if such exist, a 25 % increase in the said permitted stresses may be made.

NOTE—The following design has been worked through from first principles. The modifications necessary to make it conform to B.S.S. No. 153 are indicated in § 197 following.

196. Worked Example. Open Web Girder Bridge.—*Design for a Single Track Through Railway Bridge,* 160 *ft. span, with ballasted track, to carry a train of locomotives of the type shown in Fig.* 301.

1. *Permissible Stresses.*—In direct tension 8 tons/sq. in. On the gross area of compression members 6·8 tons/sq. in. Direct shear on the gross area of web plates not to exceed 5 tons/sq. in.

On rivets : 6 tons/sq. in. in shear ; 12 tons/sq. in. bearing pressure.

Impact Factor : $i = 65/(45 + L)$ [max. $= 1$].

2. *Type of Main Girders.*—Parallel flanges ; N bracing ; inclined end posts. *Floor* : Flat plate floor, supported by cross girders and rail bearers. *Wind bracing* : Horizontal wind girder top and bottom, portal bracing between each end post, and at each vertical. (ii) Fig. 301 shows the general outline of the bridge.

3. *Actual Span.*—The actual span will be the distance between the centres of the pins of the rocker bearings, viz. 160 ft. This span is to be used in all calculations.

4. *Depth of Main Girders and Arrangement of Panels.*—The depth of the main girders should be from $\frac{1}{10}$ to $\frac{1}{8}$ the span. Adopting the latter figure, the depth of the main girders will be 20 ft. to the centres of the flanges. It will then be possible to obtain the standard head room of 14 ft. 6 in. above the rail level, and at the same time make the overhead bracing of a reasonable depth, Fig. 309. The span of 160 ft. may be divided into 8 panels of 20 ft., or 10 panels of 16 ft. The latter alternative will be adopted as the better arrangement.

5. *Width of the Bridge.*—The standard clear width is 14 ft. 7½ in. To obtain this clearance, the main girders must be placed from 17 to 18 ft. centre to centre. A mean of 17 ft. 6 in. will be adopted.

6. *Bridge Floor—Rail Bearers.*—The cross girders are riveted to the
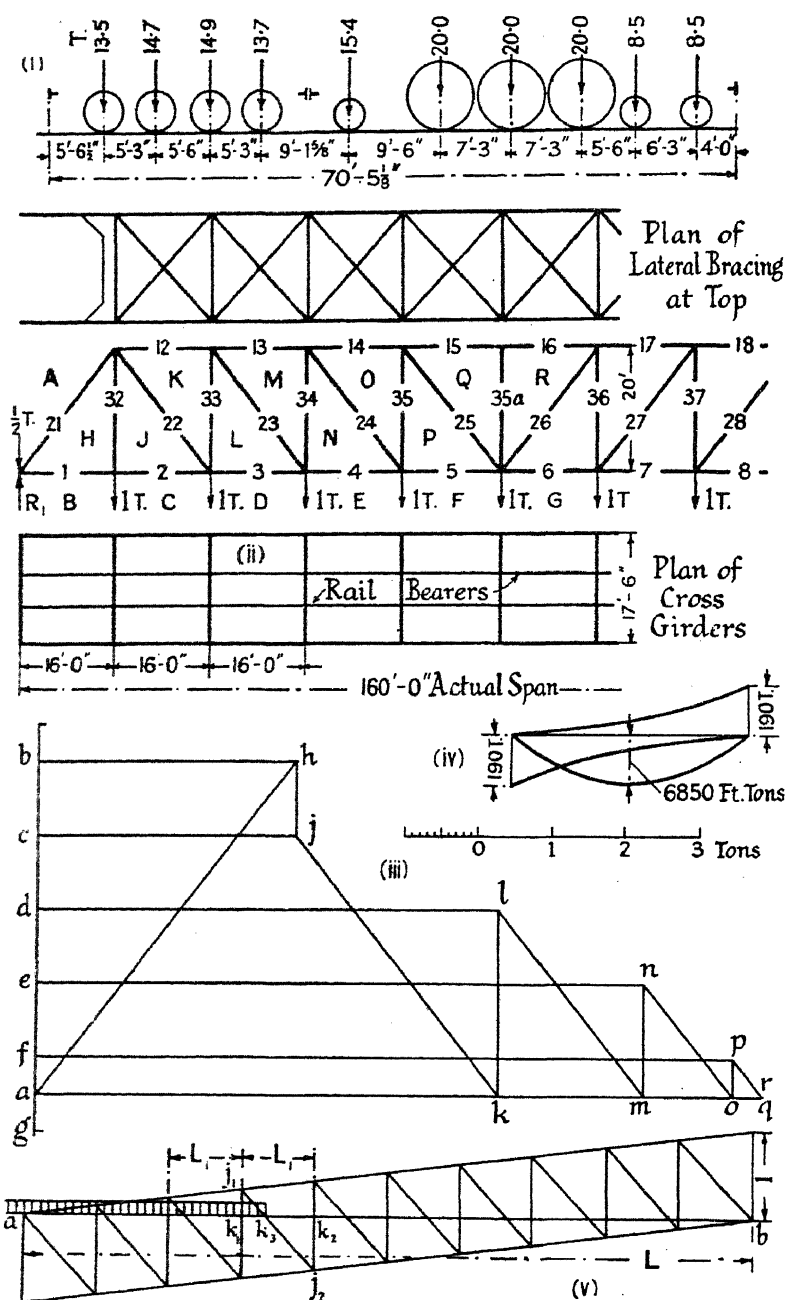
FIG. 301.

verticals of the main girders, so that the span of the rail bearers is 16 ft. From Fig. 309 it will be evident that, in addition to the live load, each rail bearer will support an area of floor $16 \times 4 \cdot 2$ sq. ft. A single track, including rails at 95 lb. per yard, chairs and sleepers, weighs $0 \cdot 075$ ton per lineal foot.

Allowing for a depth of ballast of 9 in., i.e. 4 in. under the sleepers, 2 in. of fine concrete, 1 in. of asphalt, and a $\frac{3}{8}$ in. floor plate, the total weight per sq. ft. of the floor system, other than the girders which support it, can be taken at $0 \cdot 07$ ton/sq. ft.

The dead load carried by a rail bearer is, therefore, $16 \times 4 \cdot 2 \times 0 \cdot 07$ $= 4 \cdot 7$ tons, or adding say $0 \cdot 6$ ton for its own weight $= 5 \cdot 3$ tons. The dead load bending moment is $\dfrac{5 \cdot 3 \times 16 \times 12}{8} = 128$ in.-tons. The maximum shearing-force and bending-moment diagrams for the travelling load, (i) Fig. 301, on a rail bearer can be found by the methods of § 21 or § 28. From the impact formula given, since L = the distance centre to centre of the cross girders = 16 ft., $i = 1$. If, for comparison, i be calculated from eq. (2), § 64, $i = 2 \cdot 1/(\frac{1}{2} + \sqrt[3]{L}) = 0 \cdot 7$. The load on each driving axle is 20 tons, or 10 tons per wheel. Hence the corresponding load on a rail bearer is $10(1 + i) = 20$ tons, and similarly for the other wheel loads. The maximum shearing-force diagram is given in (i) Fig. 302. The maximum bending moment anywhere on the rail bearer will occur at J when two driving wheels and the trailing wheel of the bogie are in the position shown in (ii) Fig. 302. This can be proved by means of § 25. The maximum bending moment due to this load arrangement is 1215 in.-tons; that at J due to the dead load is 126 in.-tons. Hence the rail bearer must withstand a total bending moment of $126 + 1215 = 1341$ in.-tons. The ratio of depth to span should not be less than $\frac{1}{12}$; a minimum depth of 16 in., therefore, is required. A $20 \times 7\frac{1}{2} \times 89$ lb. B.S.B. will be a suitable section, $Z = 167 \cdot 3$ in.^{3}, so that the stress will be $1341 \div 167 \cdot 3 = 8 \cdot 02$ tons/sq. in., which may be permitted. No holes must be cut in the bottom (tension) flange near the centre, for the support of lateral bracing or other reasons.

From the maximum shearing-force diagram, (i) Fig. 302, it will be seen that the maximum shearing force at the ends of the rail bearer is $35 \cdot 46$ tons. The web of the B.S. beam is $0 \cdot 6$ in. thick and $17 \cdot 4$ in. deep; area $= 10 \cdot 44$ sq. in. Hence the mean stress per square inch is $35 \cdot 46$ $\div 10 \cdot 44 = 3 \cdot 40$ tons/sq.in. Applying the formula $s = 5\frac{1}{2}t - d/20$, eq. (1), § 174, the safe shear per inch of depth on this web, without any stiffeners, is $s = 5\frac{1}{2} \times 0 \cdot 6 - 17 \cdot 4/20 = 2 \cdot 43$ tons per inch; and the safe shearing force is $17 \cdot 4 \times 2 \cdot 43 = 42 \cdot 3$ tons. The depth of the web is only 29 times its thickness; and the compression flange of the girder is prevented from deflecting sideways by the floor plating, so that there is little tendency for the beam to distort laterally. In these circumstances no intermediate stiffeners are required.

The rivets to be used in this design are $\frac{7}{8}$ in. diameter in $\frac{15}{16}$-in. holes.

Considering the riveting in the angle cleats at the ends of the rail bearer, those passing through the 0·6 in. web plate are in double shear ; each is worth $\frac{13}{18} \times 0 \cdot 6 \times 12 = 6 \cdot 75$ tons, and $35 \cdot 46 \div 6 \cdot 75 = 6$ are required, 7 are provided. Since the load $35 \cdot 46$ tons comes all from one side of the cross girder, the rivets connecting the cleats to the cross girder must be regarded as being in single shear, each worth $0 \cdot 69 \times 6 = 4 \cdot 14$ tons ; and $35 \cdot 46 \div 4 \cdot 14 = 9$ will be required. These rivets are field rivets, and their number must consequently be increased by 15 %. Five in each cleat
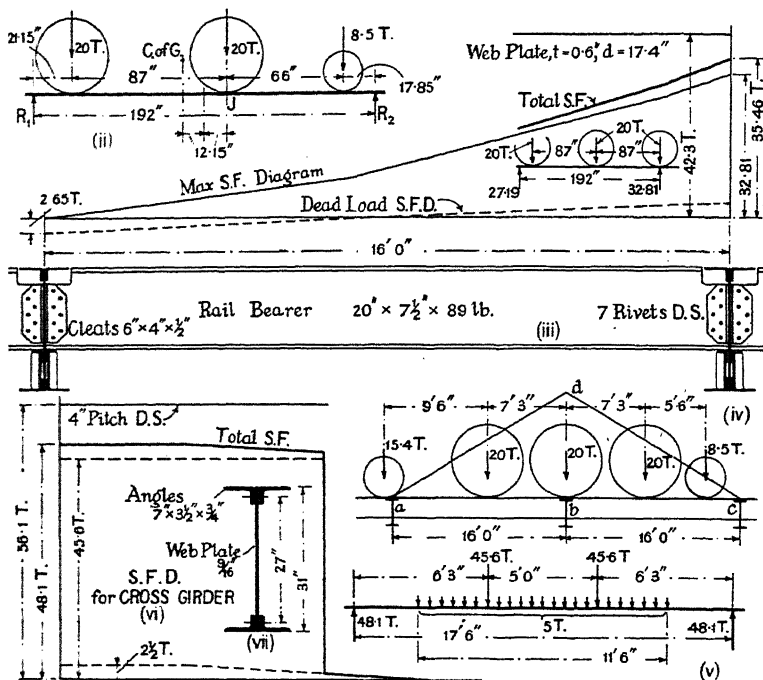
FIG. 302.

and three in the shelf angle will be provided. The rail bearer is shown in (iii) Fig. 302.

7. *Bridge Floor—Cross Girders.*—Each cross girder supports an area of bridge floor $16 \times 11\frac{1}{2}$ sq. ft., weighing $0 \cdot 07$ ton/sq. ft. $= 12 \cdot 9$ tons. To this must be added $2 \times 0 \cdot 6$ tons, the weight of two rail bearers, plus approximately $1\frac{1}{2}$ tons for its own weight, including brackets, etc., a total of $15 \cdot 6$ tons. Of this, $2 \times 5 \cdot 3 = 10 \cdot 6$ tons is conveyed direct by the rail bearers, leaving 5 tons which may be considered, for practical purposes, as uniformly spread. To find the position of the travelling load which produces the maximum load on a cross girder, use may be made of a reaction influence line, (iv) Fig. 302. Consider the cross girder at b ; the reaction from the rail bearer span ab can be obtained from the reaction influence line for the right-hand reaction of span ab, which is the triangle

adb, § 32. Similarly, the reaction from the span *bc* will be given by the triangle *bdc*, which is the reaction influence line for the left-hand reaction of the span *bc*. The triangle *adc*, therefore, is the influence line for the total reaction on the cross girder *b* from the two rail bearers *ab* and *bc* ; and, for any load position, the sum of the ordinates, each multiplied by the magnitude of its load, will give the reaction. By trial, it can be shown that the maximum reaction carried by the cross girder occurs when the loads are in the position shown in (iv) Fig. 302, and that it is 43·6 tons.

If the usual assumption for cross girders be made, that L in the impact formula is twice their distance apart, L = 32 ft. and i = 65 ÷ (45 + 32) = 0·85, which value includes the effect of lurching. Had eq. (3) § 64 been used, i = 5/(6 + L), where L = 16 ft., i = 0·23, a much smaller figure, but in this case no allowance is made for lurching. Using the value 0·85, the equivalent static reaction on the cross girder is 43·6 × 1·85 = 80·6 tons, or per rail bearer = 40·3 tons. The total equivalent dead load on a cross girder is, therefore, 2 × 5·3 + 5 + 2 × 40·3 = 96·2 tons, disposed as shown in (v) Fig. 302. The maximum bending moment occurs at the centre and is 3597 in.-tons ; the shearing-force diagram is shown at (vi) Fig. 302, the maximum shearing force being 48·1 tons. The girder can be designed as a plate girder, Chap. X. The necessary cross-section is shown in (vii) Fig. 302, for which Z_t = 452·6 in.³, and the maximum tensile stress is 3597 ÷ 452·6 = 7·95 tons/sq. in. ; Z_c = 490·1, and the maximum compressive stress is 7·34 tons/sq.in. Since the compression flange is reinforced by the floor plating of the bridge, this stress may be permitted. The web plate is $\frac{9}{16}$ in. thick ; taking d = 27 in., and D_1* = 29½ in., it is worth [eq. (1), § 174] 1·74 × 29½ = 51·3 tons, which is sufficient. The average shear stress is 48·1 ÷ (29½ × $\frac{9}{16}$) = 2·9 tons/sq. in. A $\frac{15}{16}$ in. rivet, bearing in a $\frac{9}{16}$ in. plate, is worth 6·32 tons ; λ_2 = 0·83 [eq. (6), § 175] ; hence the safe shear force ($S_2 = s_2 \times D_1$) on a row of rivets at 4 in. pitch, connecting the flange angles to the web plate, is $\dfrac{6·32}{4 \times 0·83} \times 29½$ = 56·1 tons. A 4 in. pitch will therefore be adequate at the ends of the girder; a 6 in. pitch will be used between the rail bearers where the shear is small [see (vi) Fig. 302].

The maximum shearing force at the ends of the cross girder being 48·1 tons, 48·1 ÷ 6·32 = 8 rivets in double shear will be required to connect the end cleats to the web. A rivet in single shear is worth 0·69 × 6 = 4·14 tons ; and 48·1 ÷ 4·14 = 12 rivets will be required to attach the cross girder to a main girder. These rivets will be field rivets, on which account not less than 14 must be provided. The cross girder is shown in Fig. 309, and the attachment to a main girder in Fig. 308.

A $\frac{3}{8}$ in. flat floor plate, with ballast guards, Fig. 309, will be used to contain the ballast.

* In a cross-section of the above type with no flange plates, D_1 should be taken inside, not outside, the flanges of the angles. In this case D_1 = 31 − 2 × $\frac{3}{4}$ = 29½ inches.

8. *Determination of the Equivalent Rolling Loads.*—The equivalent uniform rolling loads for both shear. and bending should next be determined for a train of locomotives, (i) Fig. 301. The methods of § 21 may be employed. The actual wheel loads should be used for this purpose, without additions for impact. In the present instance, the equivalent uniform rolling load for shear is found to be 380 tons, or 2·38 tons per ft.; the maximum shearing force at the ends of the span due to this load being ± 190 tons, (iv) Fig. 300. The equivalent uniform rolling load for bending is 342·5 tons, or 2·14 tons per ft.; and the maximum bending moment at the centre of the span is 6850 ft.-tons = 82,200 in.-tons. It is worth noticing that the average weight per foot of the locomotive is 148·75 tons ÷ 70·4 ft. = 2·12 tons per ft., a close check on the equivalent uniform rolling load for bending in spans of this length.

9. *Estimation of the Total Dead Load.*—The total dead load on the bridge is found by adding the weights of the floor system, the main girders, and the overhead wind bracing. From ¶ 7 above, the weight of the floor system carried by one cross girder is 15·6 tons, and there are 10 panels. Hence the total weight of the floor system is 156 tons. The weight of the main girders may be estimated as follows : The equivalent rolling load is 342·5 tons, and the impact factor for the main girders (see ¶ 1) is

$$i = \frac{65}{45 + L} = \frac{65}{45 + 160} = 0·32.$$ Hence the equivalent uniform static load is 342·5 × 1·32 = 452 tons. As a first estimate, the weight of the wind and portal bracing may be taken as 15 tons. The total equivalent uniform load carried by the main girders, exclusive of their own weight, is, therefore, 156 + 452 + 15 = 623 tons, or 312 tons per girder. The weight of each main girder may be estimated by Unwin's formula, § 179,

$$w = \frac{WLr}{Cf - Lr} = \frac{312 \times 160 \times 8}{1900 \times 6·8 - 160 \times 8} = 34·3 \text{ tons}$$

where r, the ratio of span to depth, is taken as 8 ; f, the stress in the compression flange = 6·8 tons/sq. in. ; and C for girders of this type may be taken as 1900. The total dead weight of the bridge is, therefore, 156 + 2 × 34·3 + 15 = 240 tons, or 12·0 tons per panel point of each main girder, since the dead load may be taken as uniformly spread.

10. *Estimation and Tabulation of the Forces in the Members.*—The forces in all the members of the main girders, due to the dead load, may now be ascertained. This is most conveniently done by drawing a stress diagram for a main girder, with unit load at each panel point, (iii) Fig. 301, and checking the results obtained by calculation. The forces in all the members, with unit load at the panel points, are transferred to the stress sheet, p. 430 ; the actual forces due to the dead load are obtained by multiplying these figures by the real panel point load, 12·0 tons. The forces due to the live load will be determined from the equivalent rolling loads. The maximum forces in the flanges will occur when the equivalent rolling load covers the whole span. In this case (see ¶ 9), the impact factor is 0·32, and the equivalent uniform static load is 342·5 × 1·32

$= 452$ tons ; or $452 \div 20 = 22 \cdot 6$ tons per panel point. The actual forces in the flange members are obtained by multiplying the forces due to the unit load by $22 \cdot 6$ (see the stress sheet).

The maximum forces in the web members, due to the live load, are found from the equivalent rolling load for shear. The position of this load, when the shear force in each panel is a maximum, can be obtained from an influence line (v) Fig. 301 [compare (v) Fig. 63]. As a particular case, consider panel 4. It was explained in § 34 that the positive shearing force is a maximum in this panel when the front of the load has advanced to k_3, (v) Fig. 301. From the geometry of the figure, $k_1 j_1 = 0 \cdot 3$; $k_2 j_2 = 0 \cdot 6$; hence, $k_1 k_3 = \frac{3}{9} k_1 k_2 = \frac{3}{9} L_1$, and $ak_3 = 3\frac{3}{9} L_1$, where L_1 is the panel length. In a similar way, for the nth panel, $k_1 k_3 = \frac{n-1}{9} L_1$, and

$$ ak_3 = \left\{ (n-1) + \frac{n-1}{9} \right\} L_1 = \frac{10}{9}(n-1)L_1 = \frac{n-1}{9}L, \text{ since there are} $$

10 equal panels. If the load per unit of length be unity, the reaction

$$ R_2 = 1 \times \frac{(ak_3)^2}{2L} = \frac{1}{2L}\left(\frac{n-1}{9}L\right)^2 = \frac{(n-1)^2 L}{162}. \text{ Also [see § 33 and (v)} $$

Fig. 61],

$$ P_2 = 1 \times \frac{(k_1 k_3)^2}{2L_1} = \frac{1}{2L_1}\left(\frac{n-1}{9}L_1\right)^2 = \frac{(n-1)^2 L_1}{162} = \frac{(n-1)^2 L}{10 \times 162} $$

But the shearing force in the nth panel is

$$ S = R_2 - P_2 = \frac{(n-1)^2 L}{162} - \frac{(n-1)^2 L}{10 \times 162} = \frac{(n-1)^2 L}{180}. $$

Since the equivalent rolling load is $2 \cdot 38$ tons per ft. of length, and $L = 160$ ft., $S = 2 \cdot 38(n-1)^2 \frac{160}{180}$; or, per main girder, $S = 1 \cdot 056 (n-1)^2$ tons. It is convenient to make the calculation in the tabular form given on p. 430. In this table the length ak_3 and the shearing force S are found from the above formulae by giving successive values 1, 2, 3, . . . to n. In the present state of knowledge (see § 64) the same impact factor, $0 \cdot 32$, will be used for all the web members as for the flanges ; the procedure commonly adopted with the Pencoyd formula will not be used. From the equivalent shearing force in the panel, the forces in the two web members composing it are at once obtained. It should be noted that the two web members in panel 4 are Nos. 24 and 34, and so on. The force in the vertical is equal to the equivalent shearing force $S(1 + i)$, that in the diagonal is $S(1 + i) \sec \theta$, Fig. 21.

In carrying these forces to the stress sheet, every bar in the web must be included, and care must be taken to give the correct sign to the forces. Thus the shearing force considered above produces compression in the diagonals of panels 2, 3, 4, and 5, and tension in the verticals. When the front of the load has passed the centre of the girder and the slope of the diagonals reverses, the force in the diagonals becomes tensile, and that in the verticals compressive. Verticals Nos. 32 and 39 are exceptions

STRESS IN THE WEB MEMBERS DUE TO THE TRAVELLING LOAD.

Panel n	Length ak₂	Shearing Force S.	Equivalent Shearing Force S (1 + i)*	Force in the Bars. Tons.	
				Diagonals.	Verticals.
	Feet.	Tons.	Tons.		
1	0	0	0	0	—
2	17·8	1·06	1·40	1·8	Special
3	35·6	4·22	5·57	7·2	5·6
4	53·3	9·50	12·54	16·1	12·6
5	71·1	16·90	22·31	28·6	22·3
6	88·9	26·40	34·85	44·7	34·9
7	106·7	38·00	50·16	64·3	50·2
8	124·4	51·74	68·30	87·5	68·3
9	142·2	67·58	89·21	114·3	Special
10	160·0	85·54	112·91	144·6	—

* $i = 0·32$ for all bars.

One Main Girder.   STRESS SHEET.

Bar.		Length (Feet).	Force in Bar (Tons).			
No.	Lettered.		Unit Load.	Dead Load.	Live Load.	Dead + Live Load.
1	BH	16·0	+ 3·6	+ 43·2	+ 81·4	+124·6
2	CJ	16·0	+ 3·6	+ 43·2	+ 81·4	+124·6
3	DL	16·0	+ 6·4	+ 76·8	+144·6	+221·4
4	EN	16·0	+ 8·4	+100·8	+189·8	+290·6
5	FP	16·0	+ 9·6	+115·2	+217·0	+332·2
12	AK	16·0	− 6·4	− 76·8	−144·6	−221·4
13	AM	16·0	− 8·4	−100·8	−189·8	−290·6
14	AO	16·0	− 9·6	−115·2	−217·0	−332·2
15	AQ	16·0	−10·0	−120·0	−226·0	−346·0
21	AH	25·61	− 5·76	− 69·1	+ 0·0	− 69·1	−213·7
22	JK	25·61	+ 4·48	+ 53·8	− 1·8	+ 52·0	+168·1
23	LM	25·61	+ 3·20	+ 38·4	− 7·2	+ 31·2	+125·9
24	NO	25·61	+ 1·92	+ 23·0	− 16·1	+ 6·9	+ 87·3
25	PQ	25·61	+ 0·64	+ 7·7	− 28·6	− 20·9*	+ 52·4*
26		25·61	+ 0·64	+ 7·7	+ 44·7	+ 52·4	
27		25·61	+ 1·92	+ 23·0	+ 64·3	+ 87·3	
28		25·61	+ 3·20	+ 38·4	+ 87·5	+125·9	
29		25·61	+ 4·48	+ 53·8	+114·3	+168·1	
30		25·61	− 5·76	− 69·1	−144·6	−213·7	
32	HJ	20·0	+ 1·0			+ 48·1†
33	KL	20·0	− 2·5	− 30·0	+ 5·6	− 24·4	− 98·3
34	MN	20·0	− 1·5	− 18·0	+ 12·6	− 5·4	− 68·2
35	OP	20·0	− 0·5	− 6·0	+ 22·3	+ 16·3*	− 40·9*
35a	QR	20·0	− 0·0	− 0·0	—	—	
36		20·0	− 0·5	− 6·0	− 34·9	− 40·9	
37		20·0	− 1·5	− 18·0	− 50·2	− 68·2	
38		20·0	− 2·5	− 30·0	− 68·3	− 98·3	
39		20·0	+ 1·0			+ 48·1†

* Stress reverses   † Compression

in that they merely act as hangers for the end but one cross girders, and are therefore always in tension. The correct sign is given to all the forces in the stress sheet.

11. *The Stress Sheet.*—All the forces may now be entered on the stress sheet. For the top and bottom flanges, only one-half the girder need be considered. The forces in all the web members should be included. Cols. 1 and 2 designate the bars. Col. 3 gives their length centre to centre of the panel points. Col. 4 gives the forces due to unit load at the panel points. The forces due to the dead load, Col. 5, are obtained by multiplying the forces in Col. 4 by 12 tons (see ¶ 9). The live load forces in the flanges, Col. 6, are likewise obtained by multiplying the forces in bars Nos. 1–5, and 12–15, given in Col. 4, by 22·6 tons. The remainder of the forces in Col. 6 are entered from the table in ¶ 10. The addition of the dead and live load forces is given in Col. 7, taking account of signs. So far, no consideration has been given to the negative shearing force which occurs at any section when the tail of the train is at that section, § 34; but it is evident that the negative shearing force in panel 4, when the tail of the train is at k_3 in that panel, will be exactly equal to the positive shearing force in the symmetrically placed panel 7, when the front of the train is at k_3 in panel 7, and so on for the other panels. Not only so, but since the diagonals slope in opposite directions on the two sides of the centre, the negative shearing force in panel 4 will produce forces in the web members of that panel of the same sign as the positive shearing force produces in panel 7. The forces due to the dead load in the two panels are also equal and of like sign. If then the total force in bar No. 27 from Col. 7 be entered opposite bar No. 24 in Col. 8, this will give the total force in bar No. 24 when the maximum negative shearing force occurs in panel 4, and similarly for the other web members. Only the forces in the web members for one-half the girder need thus be entered. These members must be capable of carrying the larger of the two forces given in Cols. 7 and 8. In two bars, Nos. 25 and 35, the stress actually reverses, and special treatment is necessary.

12. *Bottom Flange.*—The type of cross-section proposed for the bottom flange at the centre of the bridge is shown in Fig. 303. The worth of the four $4 \times 3\frac{1}{2} \times \frac{1}{2}$ in. angles, less two $\frac{15}{16}$ in. rivet holes in each, at 8 tons/sq. in., is $4(3·5 - 2 \times \frac{1}{2} \times \frac{15}{16}) \times 8 = 82$ tons. The net width of a flange plate is $18 - 4 \times \frac{15}{16} = 14·25$ in. Then,

Angles $4'' \times 3\frac{1}{2}'' \times \frac{1}{2}''$
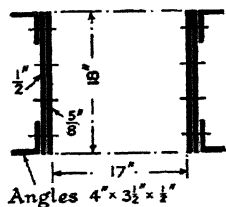
FIG. 303.

Bar No.			1 & 2	3	4	
Force in Bar			124·6	221·4	290·6	332·2 tons.
Worth of 4 angles			82·0	82·0	82·0	82·0 tons.
Worth of Plates	.	.	42·6	139·4	208·6	250·2 tons.
Net Area at 8 tons/sq. in.		.	5·4	17·4	26·1	31·3 sq. in.
Thickness required	.	.	0·38	1·23	1·84	2·20 in.
Use	. . .	.	2 at $\frac{3}{8}$	2 at $\frac{5}{8}$	2 at $\frac{5}{8}$	2 at $\frac{5}{8}$ in.
					+2 at $\frac{1}{4}$	+2 at $\frac{1}{4}$

The two angles and one $\frac{5}{8}$ in. plate must extend from end to end on each side of the flange, and an additional $\frac{1}{2}$ in. plate will be required on each side for bars Nos. 4, 5, 6, and 7.

13. *Top Flange.*—The normal cross-section is shown in Fig. 304. The width, centre to centre of the rivet lines through the top plate, is $22\frac{1}{2}$ in. According to the American rule, § 160, in order to develop the full strength of the plate, the thickness should not be less than $\frac{1}{40}$th of this dimension, say 0·56 in. ; the flange plate has therefore been made $\frac{9}{16}$ in. thick. The particulars of the cross-section are : area 45·2 sq. in., min. I = 1681 in.^{4}, min. $\kappa = 6·09$ in. For practical purposes the centre of area can be taken as 5 in. below the backs of the upper angles. Using eq. (1), § 163,

Angles 4″×4″×$\frac{1}{2}$″

Angles $3\frac{1}{2}$″× $3\frac{1}{2}$″×$\frac{1}{2}$″

$22\frac{1}{2}$″

27″×$\frac{9}{16}$″

17″
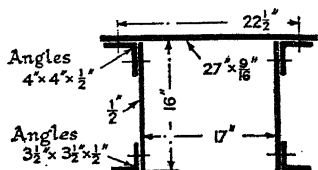
FIG. 304.

$$fa = 6·8 - \frac{1}{3700}\left(\frac{qL}{\kappa}\right)^2$$

$L = 16$ ft. $= 192$ in. ; the member may be taken as imperfectly direction-fixed, $q = 0·78$, $\kappa = 6·09$, whence $qL/\kappa = 0·78 \times 192 \div 6·09$

$= 24·6$, $fa = 6·8 - \dfrac{24·6^2}{3700} = 6·63$ tons/sq. in., and the safe load on the

section is $45·2 \times 6·63 = 299·6$ tons ; this section would be suitable for bars Nos. 12 and 13.

To increase the safe load to 346 tons, either the 4×4 in. angles might be doubled on each side, or a second flange plate, say $\frac{7}{16}$ in. thick, might be added. The first expedient is lighter, but the second allows the gusset plates to take on to the rows of rivets through the 4×4 in. flange angles, and enables a longer attachment for the verticals to be made. If the second alternative be adopted, the area $= 57$ sq. in. ; min. I $= 2002$ in.^{4} ; $\kappa = 5·92$ in. ; and $qL/\kappa = 25·3$. The safe stress, therefore, is again 6·62 tons/sq. in., and the safe load is $57·0 \times 6·62 = 377$ tons. Taking secondary flexure into account, the pitch of the rivets connecting the flange plates is 6 in., κ' for a $\frac{7}{16}$ in. plate bending between the rivets is $t \div \sqrt{12} = 0·126$ in. Since there are many identical elementary spans in line, each may be considered as direction-fixed at the ends, $q' = 0·56$, and $q'L'/\kappa' = 0·56 \times 6 \div 0·126 = 26·7$, hence from eq. (3), § 160, with the constants from eq. (1), § 163,

$$fa = 6·8 - \frac{1}{3700}\left[\left(\frac{qL}{\kappa}\right)^2 + \left(\frac{q'L'}{\kappa'}\right)^2\right]$$

$$= 6·8 - \frac{1}{3700}[25·3^2 + 26·7^2] = 6·43 \text{ tons/sq. in.}$$

and the safe load is $57·0 \times 6·43 = 366$ tons.

The $\frac{7}{16}$ in. plate must extend over panels 14, 15, 16, and 17.

14. *End Posts. Bar No.* 21.—The force in this bar is $- 213\cdot7$ tons, its length is $25\cdot61$ ft. It is proposed to use the same cross-section as that for the top flange, bar No. 12, min. $\kappa = 6\cdot09$ in. Assuming the ends to be imperfectly direction-fixed, $q = 0\cdot78$, $qL/\kappa = 25\cdot61 \times 12 \times 0\cdot78 \div 6\cdot09 = 39\cdot4$; and from eq. (1), § 163,

$$f_a = 6\cdot8 - \frac{1}{3700}\left(\frac{qL}{\kappa}\right)^2 = 6\cdot38 \text{ tons/sq. in.}$$

The area of the member $= 45\cdot2$ sq. in., hence the safe load is $45\cdot2 \times 6\cdot38 = 288$ tons, which is ample. The strength of the member as part of the portal bracing must also be considered. To carry the load of $213\cdot7$ tons, 52 rivets in single shear at $4\cdot14$ tons per rivet are necessary. As will be seen from Fig. 307, 60 rivets have been provided, some in double shear, see ¶ 17.

15. *Tension Members.*—In each case a section consisting of four angles connected by batten plates will be used, (i) Fig. 305. The calculations, given below, include the vertical bar No. 32, which is a tension member. For the consideration of bar No. 25 as a column, see ¶ 16. Tension members, thus constructed, may be regarded as concentrically loaded, and the full net area may be counted in.
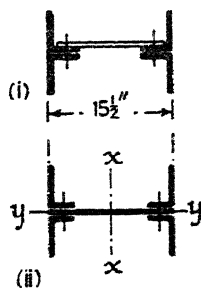
FIG. 305.

Bar No. . . .	22	23	24	25	32
Force in bar, tons . .	$+168\cdot1$	$+125\cdot9$	$+87\cdot3$	$+52\cdot4$	$+48\cdot1$
Net area at 8 tons/sq. in.	$21\cdot1$	$15\cdot8$	$11\cdot0$	$6\cdot6$	$6\cdot1$
Net area per angle .	$5\cdot28$	$3\cdot95$	$2\cdot75$	$1\cdot65$	$1\cdot53$
Rivets required at $4\cdot14$ tons per rivet single shear . . .	41	31	22	13	12
Add 15% for field rivets	47	36	26	15	14
Rivets per angle . .	12	9	7	4	4
Angle section required .	$6\times4\times\frac{3}{4}$	$5\times4\times\frac{5}{8}$	$5\times3\frac{1}{2}\times\frac{1}{2}$	$5\times3\frac{1}{2}\times\frac{1}{2}$	$4\times3\times\frac{1}{2}$

Treating bar No. 22 as a typical example, and subtracting two rivet holes from each angle, the loss of area if the material be $\frac{3}{4}$ in. thick is $2 \times \frac{15}{16} \times \frac{3}{4} = 1\cdot41$ sq. in. The required gross area is therefore $5\cdot28 + 1\cdot41 = 6\cdot69$ sq. in. A suitable section would be a $6 \times 4 \times \frac{3}{4}$ in. angle (area $6\cdot94$ sq. in.), as given.

16. *Compression Members (Verticals).*—The length between the centre lines of the flanges is 20 ft. $= 240$ in. The type of section proposed for the verticals is shown in (ii) Fig. 305. Considering the bending about the yy axis, the members are attached by stiff gussets to the heavy flange members, and q may be taken as $0\cdot7$; $qL = 0\cdot7 \times 240 = 168$ in. The calculations are set out in tabular form on p. 434 ; the safe load per square inch is found from eq. (1), § 163.

2 F

Bar No.	33	34	35	25
Force in bar, tons	− 98·3	− 68·2	− 40·9	− 20·9
Section {Angles	5×3×½	5×3×⅜	5×3×⅜	5×3½×½
proposed {Web	15¼×⅜	15¼×⅜	15¼×⅜	Batten Plates.
Gross area, sq. in.	20·8	17·2	17·2	16·0
Min. κ	2·1	2·0	2·0	2·27
Ratio, qL/κ	80	84	84	109
Safe load, tons/sq. in. . .	5·07	4·89	4·89	3·59
Safe load on member, tons . .	105	84	84	57
Rivets required at 4·14 tons per rivet in single shear	24	17	10	(6)
Add 15% for field rivets . .	28	20	12	—
Rivets per angle	7	5	3	(4)
Shear, 2½% of W, tons . .	2·5	1·7	1·1	0·6

Lighter sections for bars Nos. 34 and 35 could be designed if lattice webs were used, but this entails narrow spaces between the angles which cannot be kept painted. The plate is to be preferred, and the extra weight is not serious. The shearing stresses on plate and rivets are small. Bar No. 25 should be examined for bending about the xx axis ($qL = 0·8 \times 307·3 = 245·9$ in.) as a batten plate column, § 166, taking into account local flexure. It will be found to be much stronger in this direction than about yy.

17. *Rivets in Gussets.*—As typical of the method of calculation, the attachment of bar No. 12 to the end top gusset will be considered, Fig. 307. The load in this member is 221·4 tons, and at 4·14 tons per rivet in single shear, 54 shop or 62 field rivets are required. Apportion these to correspond with the areas of the different parts of the member.

Top plate 27 × ¼ in. .	.	.	.	.	area = 15·2	rivets : 21
Two stringers 16 × ¼ .	.	.	.		16·0	22
Two angles 4 × 4 × ¼ .	.	.	.		7·5	10
Two angles 3¼ × 3¼ × ¼	.	.	.		6·5	
					45·2	62

Approximately ½ × 21 + ⅙ × 22 + ½ × 10 = 20 rivets must be provided in the top row through each 4 × 4 angle. It is impossible to do this, and the rivets must be placed in double shear by introducing short lengths of angle inside the gusset plate; 10 rivets bearing in the ¾ in. gusset plate are then sufficient. Approximately ½ × 9 + ⅙ × 22 = 8 rivets are required through each 3¼ × 3¼ angle.

The horizontal force on the rivets connecting the gussets at the foot of bar No. 35 to the bottom flange, Fig. 308, is the horizontal component of the force in bar No. 24, i.e. 87·3 sin θ = 54·5 tons, and 14 shop rivets are required. The other gussets may be similarly treated.

18. *Joints.*—The girder has been arranged for dispatch in parts and re-erection at the site. The field rivets are shown as open circles, the shop rivets as black circles. Assuming that 43 ft. lengths can be handled,

it will be necessary to make joints in the flanges ; these may conveniently be placed in bars Nos. 2, 4, 7, and 9, towards the centre, in the bottom flange ; and in bars Nos. 13, 16, and 18, towards the centre, in the top flange ; thus breaking joint as far as possible. A typical joint for the bottom flange, bar No. 7, is shown in Fig. 309. It is of the grouped variety and may be designed by the methods of § 172, but should be examined in the light of Fig. 257. Double-butt covers are used for the plates, round-back covers for the angles. The batten plates also are utilised as covers for the latter.

19. *Wind Pressure.*—Adopting the proposals of § 52, the empty bridge will be designed to resist a wind pressure of $40 - 0 \cdot 016L = 37 \cdot 5$ lb./sq. ft. ; it will be sufficient to adopt the usual 30 lb./sq. ft. for the loaded bridge. In order to calculate the area exposed to wind of one main girder, the value of C, § 45, for the members must first be fixed. The two sides of the bottom flange are 1 diameter apart, and from Stanton's experiments with flat plates $C = 0 \cdot 83$. To allow for the ' cup ' effect of the outstanding angles, take $C = 1$. This value may also be assumed for the compression flange, the end posts, and the verticals. The diagonals average about $1\frac{1}{2}$ diameters deep, and $C = 0 \cdot 74$. It will be an error on the safe side, therefore, if C be taken as unity for all the members, in which case the area exposed to wind is :

Bottom flange	.	.	.	.	.	240
Top flange .	.	.	.	.	.	179
End posts .	.	.	.	.	.	72
Verticals	.	.	.	.	.	134
Diagonals .	.	.	.	.	.	165
Gussets	.	.	.	.	.	20

810 sq. ft.

The area of the contour of the girder is about 3,100 sq. ft., so that ϕ, the fullness factor (see § 47), is $810 \div 3100 = 0 \cdot 26$, and according to Flachsbart's experiments, $C = 1 \cdot 26$ for a single girder, agreeing with Stanton's experiments. The main girders are $17 \cdot 5 \div 20 = 0 \cdot 88D$ apart, and are connected by a floor ; C for the pair will be taken as $1 \cdot 5$ (see § 48). The total pressure on one main girder at 37·5 lb./sq. ft. is therefore $1 \cdot 26 \times 37 \cdot 5 \times 810 \div 2240 = 17 \cdot 1$ tons, 7·9 tons acting on the top flange and 9·2 on the bottom flange. The total pressure on the pair is $1 \cdot 5 \times 37 \cdot 5 \times 810 \div 2240 = 20 \cdot 3$ tons ; or on the leeward girder is $20 \cdot 3 - 17 \cdot 1 = 3 \cdot 2$ tons ; 1·5 on the top and 1·7 on the bottom. On the windward girder at 30 lb./sq. ft., the corresponding figures are : top flange 6·3, bottom flange 7·4 tons.

The depth exposed to wind by the ballast trough is $18\frac{1}{2}$ in., which will be doubled to allow for the exposed area on the leeward side, rails, etc. The depth of the rail bearers is 20 in., and since they are 5 ft. apart, take $C = 1\frac{1}{2}$. The exposed area of the floor system is then $160(37 + 1\frac{1}{2} \times 20) \div 12 = 894$ sq. ft., and the wind load at $37\frac{1}{2}$ lb./sq. ft. is 15 tons ; at 30 lb./sq. ft. it is 12 tons.

The area of the train may be taken as 10 sq. ft. per foot of length,

equivalent at 30 lb./sq. ft. to a wind load of 0·134 ton/ft., or 21·4 tons on the completely covered bridge. The exposed areas of the leeward girder in this condition are 251 sq. ft. at the top, and 240 sq. ft. at the bottom. Assuming the same shielding ratio as before, the corresponding wind loads will be 0·9 and 0·8 ton.

The wind loads on the bridge in the two conditions are then as shown in Fig. 306. The maximum wind load on the upper wind girder is,
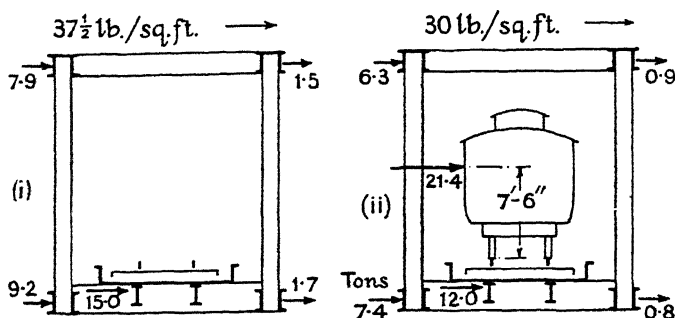
FIG. 306.

therefore, $7·9 + 1·5 = 9·4$ tons; and on the lower wind girder is $7·4 + 12·0 + 0·8 = 20·2$ tons, plus the rolling wind load of $0·134$ ton/ft. The upper wind girder is shown in Fig. 301. There are 8 panels, and the load per panel is $9·4 \div 8 = 1·2$ tons. Dividing this load equally between the double system of bracing, the forces in the diagonals are found to be (tons) :

Panel No. 2—2·9   2·1   1·3   0·5—Panel No. 5.

The end reaction to be carried by the portal is 4·7 tons. The maximum wind force in bar No. 15 is 12·9 tons.

There are 10 panels in the lower wind girder and the load per panel is 2·02 tons. The shearing force in any panel due to the rolling wind load is given by the formula established in ¶ 10,

$$S = \frac{(n-1)^2 L}{180} \times 0·134 = \frac{8}{9} \times 0·134(n-1)^2 \text{ tons.}$$

Dividing the loads equally between the two systems of bracing, the maximum forces in the diagonals are (tons) :

	10	9	8	7	6
Static load	6·16	4·80	3·43	2·06	0·69
Rolling load	6·54	5·17	3·96	2·91	2·02
Total	12·70	9·97	7·39	4·97	2·71

The maximum load in bar No. 5, when the span is fully covered, and the wind load is $20·2 + 21·4$ tons, is 46·9 tons.

In addition, there will be an increase in the force in the flange members due to the concentration of load on the leeward girder, which

will be a maximum when the bridge is fully covered. Taking moments about the plane of the lower wind bracing, which carries the shearing force [see (ii) Fig. 306],

$$
\begin{array}{lll}
7\cdot2 \text{ tons} & \times \ 20\cdot7 \text{ ft.} & = \ 149\cdot1 \\
21\cdot4 & \times \ 11\cdot75 & = \ 251\cdot5 \\
12\cdot0 & \times \ \ 2\cdot5 & = \ \ 30\cdot0 \\
8\cdot2 & \times \ \ 0\cdot75 & = \ \ \ 6\cdot2 \\
\hline
48\cdot8 & & 436\cdot8 \text{ ft.-tons.}
\end{array}
$$

The distance between the main girders is $17\cdot5$ ft. centres; hence the extra downward force on the leeward girder is $436\cdot8 \div 17\cdot5 = 25\cdot0$ tons, or $2\cdot50$ tons per panel. From the stress sheet, the forces in bars No. 15 and No. 5, with unit loads at the panel points, are -10 and $+9\cdot6$ tons respectively. Hence the extra wind forces in these bars are $-2\cdot50 \times 10 = -25\cdot0$, and $+2\cdot50 \times 9\cdot6 = +24\cdot0$ tons.

The forces in the flanges due to wind pressure must be properly combined with the other forces in the flanges (see ¶ 21, below). The diagonal bracing is designed in the usual way to resist the forces calculated above, working at normal stresses.

The portal is designed to carry a load of $4\cdot7$ tons by the methods of § 101, assuming the lower ends to be fixed in direction. Again it will be found that the end posts will carry the wind load without extra stiffening. The upper transverse struts, Fig. 309, must be designed to carry one-half the wind load per bay, viz. $1\cdot0$ ton. This sway bracing, including the corner brackets, should be made as deep as possible to give lateral rigidity to the bridge.

20. *Longitudinal Forces.*—The longitudinal reactions at the rail heads due to acceleration and braking may be assumed to be :

Acceleration : $P = \dfrac{35S}{L+75} - \dfrac{35 \times 190}{160+75} = 28\cdot3$ tons (max. $= 0\cdot26S$).

Braking :

$' = \left\{ \dfrac{21}{L+90} + 0\cdot13 \right\} S = \left\{ \dfrac{21}{250} + 0\cdot13 \right\} \times 190 = 40\cdot7$ tons (max. $= 0\cdot26S$)

where S is the maximum shearing force at the end of the span due to the travelling load [190 tons, (iv) Fig. 292]. The force of $40\cdot7$ tons will be transmitted through the ballast trough to the 11 cross girders and thence to the main girders. There will therefore be a lateral force of $1\cdot85$ tons on each end of a cross girder. The stress produced thereby is small, otherwise a construction similar to Fig. 300 should be used. The forces in the members of a lower flange, due to these cross-girder loads, will increase in equal steps of $1\cdot85$ tons from $\pm 1\cdot85$ tons at the free end of the girder to $\pm 18\cdot5$ tons at the fixed end.

21. *Combined Stresses.*—The stresses due to the dead, live, and wind loads will combine in the top flange; in the bottom flange the combination must include the longitudinal forces. Thus the combination of forces in bar No. 15 is : dead $+$ live $= 346\cdot0$, wind $= 12\cdot9 \div 25\cdot0$,

FIG. 307.

FIG. 308.

PLAN OF FLOOR PLATING

JOINT IN BOTTOM FLANGE

FIG. 309.

total = 383·9 tons, or well within the allowed increase of 25 %, § 195. In bar No. 5 the combination is : dead + live = 332·2, wind = 46·9 + 24·0, longitudinal force = 11·1, total = 414·2 tons. The allowable load on the section, ¶ 12, at 8 tons/sq. in. is 338·5 tons, or plus 25 % = 423·1 tons, so that again the permitted increase is not exceeded. If the other members of the bottom flange be similarly examined, they will be also found to be adequate.

22. *End Bearings.*—From ¶ 9, the total load to be carried by the end bearings is 240 + 380 × 1·32 = 742 tons, or 186 tons per bearing. Allowing 20 tons/sq. ft. on a hard sandstone bedstone, an area of base 39 in. × 37 in. will be provided. The load on the projected area of the rocker pin should not exceed 2 tons/sq. in. to prevent seizing, and that on the rollers should not exceed $0 \cdot 25d$ tons per inch of length (d = diameter of pin in inches). These bearings, one fixed and one sliding, are shown in Fig. 307.

23. *Camber.*—The main girders should be built with a camber, so that the loaded bridge will not sag below the horizontal. To effect this, the length of the top flange members should be increased by $\frac{1}{8}$ in. per 10 ft. of length, = 0·2 in. in the present design.

24. *Materials and Workmanship.*—All materials and workmanship should be of the highest possible class and conform to the British Standard for Girder Bridges (B.S. No. 153, Pts. 1 and 2, 1933).

197. Single Track Railway Bridge, 160 ft. Span. § 196.—Redesign to conform to B.S. No. 153,* Parts 3, 4, and 5, 1933.—*Loading.*—Ministry of Transport 20 unit loading ; see Fig. 49. Total equivalent distributed load = 400 tons ; Maximum shear at the abutments = 220 tons, cf. (iv) Fig. 301 ; Maximum axle loads, two of 25 tons, 6 ft. apart ; Uniformly distributed load on a rail bearer = 70 tons, maximum shear at a support = 42·5 tons ; Maximum reaction on a cross girder = 56·9 tons.

Impact Factor.—Use eq. (4), § 61.

Wind Pressure.—50 lb./sq. ft. on the unloaded bridge ; 30 lb./sq. ft. on the loaded bridge.

Permissible Stresses.—9 tons/sq. in. tension ; 7·65 tons/sq. in. compression ; 5·5 tons/sq. in. web shear ; 6 tons/sq. in. rivet shear ; 15 tons/ sq. in. rivet bearing ; strut formulae, see eqs. (4) and (5), § 163.

Combined Stresses.—The combination of dead, live, including impact, wind, and longitudinal stresses, must not exceed 10·5 tons/sq. in.

The general course of the calculations as given in § 196 should be followed, the loads and stresses should be adjusted as above.

* Students can obtain copies of this and other British Standards through their college or school for 1s.

BIBLIOGRAPHY

Treatises

1. WINKLER. *Theorie der Brücken.* Wien, 3rd ed., 1886.
2. FIDLER. *A Practical Treatise on Bridge Construction.* London, 4th ed., 1924.
3. MERRIMAN AND JACOBY. *A Text-Book on Roofs and Bridges. Pt. III, Bridge Design.* New York, 4th ed., 1907.
4. MEHRTENS. *Eisenbrückenbau.* 3 vols., Leipzig, 1908-20-23.
5. BURR AND FALK. *The Design and Construction of Metallic Bridges.* New York.
6. KETCHUM. *Design of Highway Bridges of Steel, Concrete and Timber.* New York, 1923.
7. KUNZ. *The Design of Steel Bridges.* New York, 1915.
8. SKINNER. *Types and Details of Bridge Construction.* New York, 1904.
9. BIRD. *The Practical Design of Plate Girder Bridges.* London, 1920.
10. WADDELL. *Economics of Bridgework.* New York, 1921.
11. —— *Bridge Engineering.* New York, 1925.
12. LASKUS. *Hölzerne Brücken.* 2nd ed., Berlin, 1922.
13. BLEICH. *Theorie und Berechnung der eisernen Brücken.* Berlin, 1924.
14. MELAN. *Der Brückenbau.* Bd. 3, t. 1, *Eiserne Brücken.* 3rd ed., Leipzig, 1927.
15. —— *Eiserne Balkenbrücken.* Berlin, 1928.
16. SCHAPER. *Stählerne Brücken.* Berlin, 6th ed., 1934.
17. HUNTER. *Bridge and Structural Engineers' Handbook* (Arrol's Practice). London, 2nd ed., 1928.
18. URQUHART AND O'ROURKE. *Design of Steel Structures.* New York, 1930.
19. TAYLOR. *Modern Bridge Construction.* London, 1930.
20. ABRAHAMS. *The Design of Steel Bridges.* London, 1932.
21. SCHAPER. *Grundlagen des Stahlbaues.* Berlin, 6th ed., 1933.
22. B.S.I. British Standard Specification for Girder Bridges. No. 153, London, 1933, Pts. 1–5.
23. A.R.E.A. General Specification for Steel Railway Bridges. American Railway Engineering Association, 1935.

Memoirs

24. DEITZ. Beitrag zum statisch bestimmten gegliederten Balkenträger mit zweifachem Ausfüllsystem (K-bracing). *Zeit. Ver. deu. Ing.*, Mar. 4, 1899, p. 230 ; see also HAESELER, *Süddeutsche Bauz.*, 1898, p. 97.
25. WILSON. The Design of Wind Bracing in Steel Structures (K-Bracing). *Engg.* June 9, 1911, p. 745 ; see also *Eng. News.-Rcd.* Apr. 2, 1931, p. 553 ; and *Eng. Ab. I.C.E.*, 1931, No. 48 : 86.
26. FINDLAY. Note on the Floor System of Girder Bridges. *Proc. Inst. C.E.*, vol. cxli, 1899–90, pp. 17 and 100 ; see also AM ENDE, p. 38, and WANSBROUGH, *Proc. New Zealand Soc. C.E.*, vol. 12, p. 243, and *Eng. Ab. I.C.E.*, 1927, No. 30 : 90.
27. THORPE. *The Anatomy of Bridgework. Engg.* Nov. 18, 1904, p. 670 *et seq.* ; republished, London, 1906.
28. —— *Steel Bridge Weights. Engg.* Oct. 30, 1925, p. 534 ; republished, London, 1926.
29. KEADBY ROLLER LIFT BRIDGE. *Proc. Inst. C.E.*, vol. cciii, 1916–17, p. 33 ; also *Engg.* Nov. 2, 1917, p. 456 *et seq.* (very full details).
30. BRIDGE FLOORS. Floors for Railway Under-bridges. *The Engr.* Apl. 16, 1920, p. 391 (comparative weights and cost).
31. GRIBBLE. Present Day Problems and Tendencies in Railway Bridge Design. *Engg.* Sept. 8, 1922, p. 307.

32. WILSON AND HAIGH. Stresses in Bridges. See Ref. No. 35, Chap. IV.
33. REMFRY. The Interaction in Bridgework of the Deck System on the Main Girders. *Proc. Inst. C.E.*, vol. ccxviii, 1923–4, p. 181.
34. WADDELL. Suitability of the Various Types of Bridges for the Different Conditions Encountered at Crossings. *Jour. West. Soc. of Eng.*, vol. xxxii, 1927, p. 313.
35. —— The Weight of Metal in Steel Trusses. *Proc. Am. Soc. C.E.*, Feb. 1935.
36. FEREDAY. The Science and Art of Bridge Building. *Jour. Inst. Eng. Aust.*, vol. 4, 1932, p. 129 ; see *Engg.* Sept. 2, 1932, p. 276.
37. GELSON. See Ref. No. 27, Chap. IV, Bib.
38. NICHOLS. Pre-Stressing Bridge Girders. *Jour. Inst. C.E.* Feb. 1937, p. 91.
39. WILSON. The Bearing Value of Rollers. *Univ. Illinois Eng. Exp. Stn.* Bull. No. 263, 1934.

QUESTIONS ON CHAPTER XI

1. *Design for Hinged Gangway.* (i) Fig. 310.; 120 ft. span ; heights and clearances as shown in (i). To carry the following alternative loadings : (a) 112 lb./sq. ft. ; (b) moving column of men 200 lb./ft. run ; (c) 4-wheeled trolley, wheel base 6 ft., gauge 4 ft., to carry 2 tons. Wind pressure 20 lb./sq. ft. Use the normal stresses for mild steel, § 59. Design the struts by the Johnson parabolic formula, eq. (3), § 164, factor of safety $= 3$; $qL/\kappa <$ 120 ; if arranged as in Fig. 310, take $q = 0 \cdot 6$ for verticals, $q = 1$ for top flange. As a first approximation take the weight of the gangway as 25 tons.

2. *Design for a Small Road Bridge.* (ii) Fig. 310 ; 25 ft. clear span ; 17 ft. clear between the parapets ; Ministry of Transport loading for road bridges, § 23. Stresses for mild steel as in B.S.S. No. 153, see § 59 ; wind pressure 20 lb./sq. ft. When designing the troughing, consider a strip of roadway 5 ft. wide. In the first instance take the weight of the floor as 120 lb./sq. ft.

3. *Through Railway Bridge.* Redesign the bridge of § 196 to conform to the British Standard Specification No. 153, 1933, using the Ministry of Transport 20 unit loading, see § 197.

4. In § 196, check the maximum forces in some of the members as found from the uniformly distributed load, by using influence lines and the actual axle loads.

5. *Deck Bridge.* Design a double track plate girder deck bridge, 50 ft. span, with 4 main girders, (i) Fig. 291 (*cf.* Fig. 87). Spacing of main girders, 4 ft. 6 in., 6 ft. 7½ in., 4 ft. 6 in. The weight of the floor, including permanent way, may be taken as 190 lb./sq. ft. Equivalent uniform rolling load per track, for bending, 3 tons/ft. ; max. shear at abutments 89 tons, at centre 28½ tons. Impact factor $0 \cdot 7$; wind pressure and stresses as in § 197.

Detail at A

(i)

Portal

Normal

Every 3rd Bay

8' 0"

A

B   C

120 ft. Span

Detail at B

Wind Bracing at Lower Flange

6' 0"   4"

3"

Detail at C

Cross Section

(ii)

3' 6"   10' 0"

2" Asphalt

25' 0"

4 thus

10' 0"
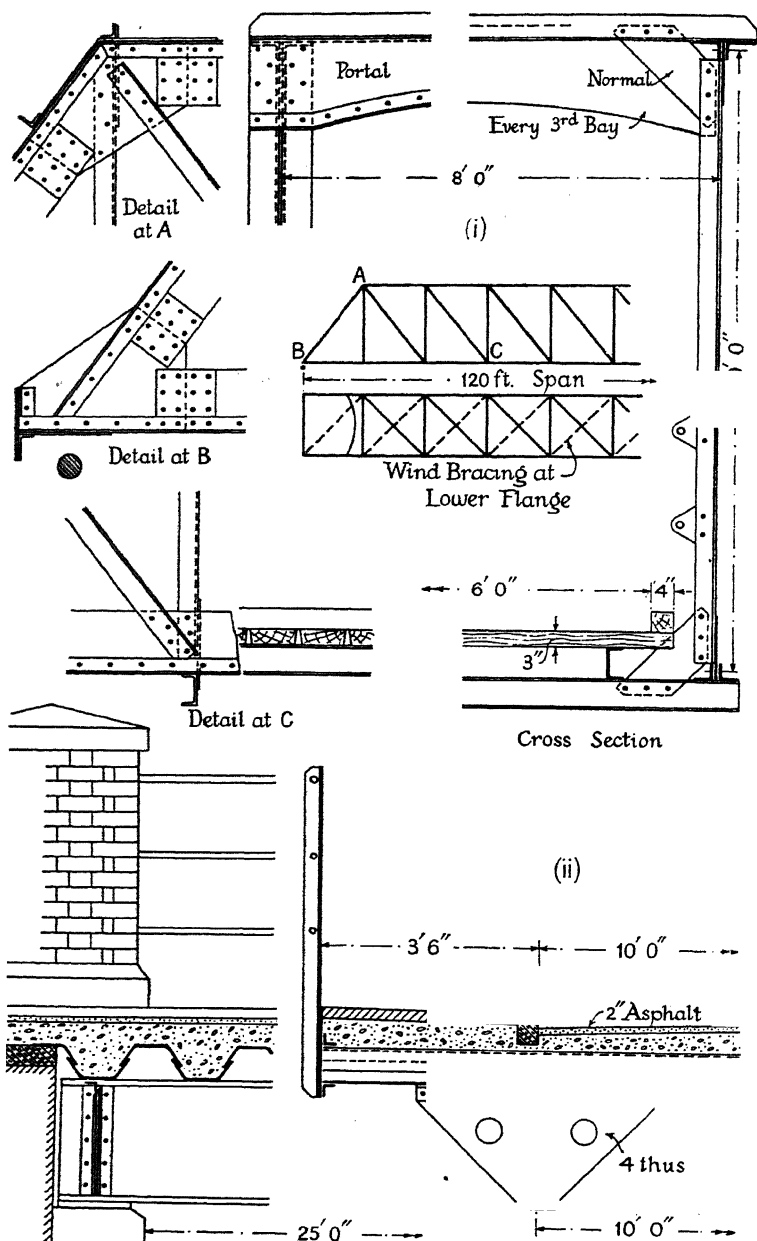
Fig. 310.

CHAPTER XII

THE DESIGN OF ROOFS

198. The Construction of Roofs.—The outer watertight covering of a roof is supported by a system of framework made up of (i) the *principals* or *roof trusses* which span from abutment to abutment and support the whole structure ; (ii) a series of longitudinal beams called *purlins* which rest on the principals and carry the roof over the space between them ; (iii) *secondary rafters, sash bars, boarding,* etc., to which the covering proper is attached, which are supported by the purlins ; (iv) *wind bracing* to prevent the principals from overturning when the wind blows on the
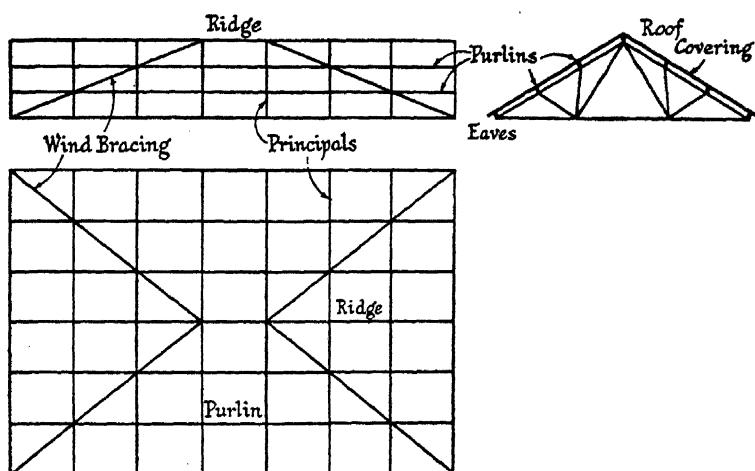
FIG. 311.

ends of the building. *Drainage arrangements* to carry off the rain water, and *means of ventilation,* complete the roof system. Fig. 311 shows a typical roof framework.

The upper longitudinal edge of a roof is called the *ridge,* and the lower longitudinal edges are called the *eaves.*

199. Principals or Roof Trusses.—These consist of frames of the form shown in Figs. 312 to 315. The two members sloping down from the ridge to the eaves are called the *main rafters.* Their lower ends rest on the abutments and are provided with suitable bearing surfaces called *shoes.* These ends are connected together by the *main tie bar* and are thus prevented from spreading. Except in very small roofs, the main rafters are supported at points intermediate between their ends by means

of struts and ties. The point of attachment of every purlin should be thus supported, otherwise the main rafters must be designed to carry the bending moments which will be set up in them.

The commoner types of roof principals may be divided into three classes : (1) King and Queen post principals ; (2) Trussed rafter principals ; and (3) Curved rafter principals.

(1) *King and Queen Post Principals.*—These are illustrated in Fig. 312. The centre vertical, (ii) Fig. 312, is called the *King-post*, and the inter-
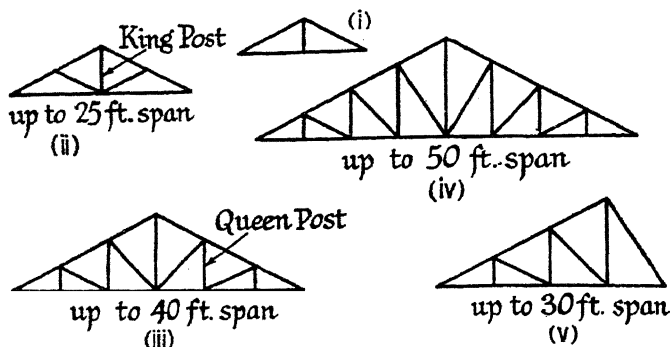
FIG. 312.

mediate verticals, (iii), are called *Queen-posts*. The truss shown at (iv) is sometimes called an *English truss*. If each main rafter be divided into four panels it may be used for spans up to about 50 ft. (v) represents what is called a *saw-tooth* or *workshop* truss of this class. One rafter is given a much greater slope than the other. The covering on the greater slope is of glass and should be given a northern outlook. The interior is thus well lighted without direct sunshine. The covering on the other slope may be of slates or other suitable material. This type of roof has been much used for workshops, weaving sheds, and factories, a series of such trusses being placed side by side, like the teeth of a saw. It is quite common, however, in modern workshops, to make the whole covering of glass.

FIG. 313.

King and Queen post principals are very convenient for *hipped* roofs (roofs with sloping ends), in that the vertical members lend themselves to the attachment of the half-trusses necessary in such cases. They are open to the objection that the longer members are struts and the shorter ones ties. This means a somewhat uneconomical design, and for this reason the second class of principal, called *trussed rafter* principals, Fig. 314, are more commonly used. An attempt to remedy this defect is shown in Fig. 313, in which design the verticals or shorter members are struts ; but if (viii) Fig. 314 be compared with it, it will be seen that the latter, in which the struts are at right angles to the main rafter, is a better design.

(2) *Trussed Rafter Principals.*—In this class of principal the rafter is supported by trusses consisting of secondary struts and ties, one of which trusses is shown isolated at (i) Fig. 314 [compare the trussed beam,

up to 25 f^t span
(ii)

up to 65 f^t span
(v)

up to 40 f^t span
(iii)

up to 80 f^t span
(vi)

up to 50 f^t span
(iv)

up to 30 f^t span
(vii)

up to 40 f^t span
(viii)
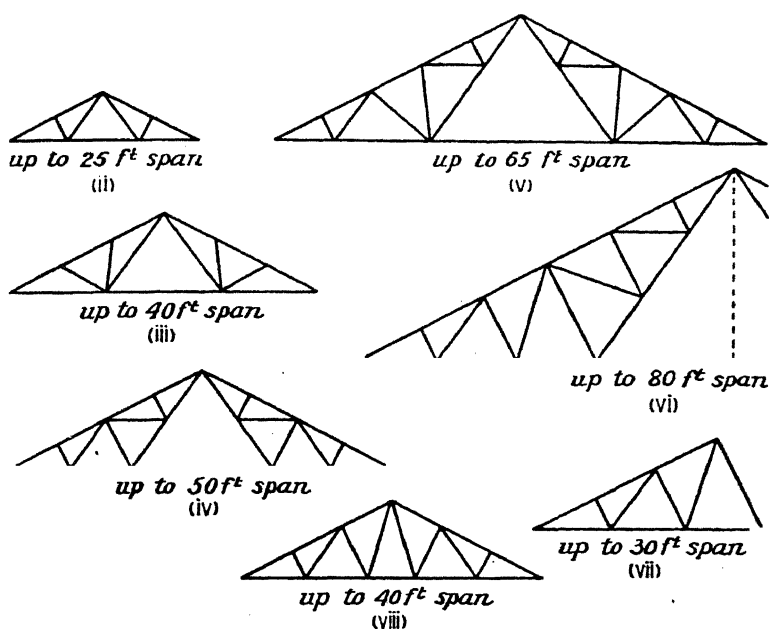
FIG. 314.

(ii) Fig. 19]. These trusses are connected together by the main tie bar. The various forms taken by this class of principal are shown in Fig. 314. In all of them the shorter members are struts, and the longer members ties. This is considered the most economical type of roof principal;

(ii)

(i)
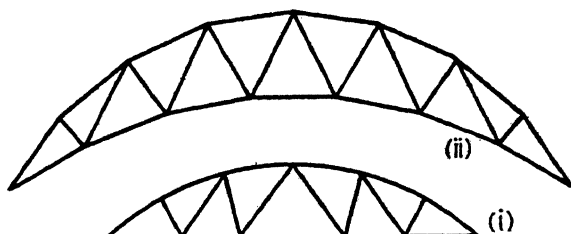
FIG. 315.

Poncelet was probably the originator. The design shown at (iv) is sometimes called a *Fink, French,* or a *Belgian* truss. Occasionally a rod, shown dotted in (vi), depending from the apex, is introduced with the object of supporting the weight of the main tie bar, if this be very long. A saw-tooth or workshop roof of this class is shown at (vii).

(3) *Curved Rafter Principals.*—Two types are illustrated in Fig. 315, (i) for small and (ii) for large roofs. Curved roofs are expensive and should only be used if and when the circumstances require them. They are most suitable for very large spans. Inexpensive roofs for small and unimportant spans are made from curved sheets of corrugated sheeting. These form their own principals ; tie bars are fitted at intervals to prevent the roof from spreading.

200. **Spacing and Proportions of Principals.**—In ordinary roofs the principals are usually plaaced from 10 to 15 ft. apart, the exact spacing depending to some extent on the length of the building and other circumstances. Too wide a spacing involves heavy purlins and is uneconomical. Too narrow a spacing means unnecessary weight and cost in the principals. It should be borne in mind that the difference in weight of principals at 10 ft. spacing, and that of principals at 15 ft. spacing, *per principal*, is usually not very great. Good practice seems to indicate the limits given above for spans of from 25 to 75 ft. For smaller spans a closer spacing may be found economical, and for very large spans the spacing may be increased with advantage. An old rule is from $\frac{1}{8}$ to $\frac{1}{4}$ the span.

Slope of Roof.—The slope of the roof depends on the nature of the covering. For sheet zinc the slope may be as flat as 1 in 10 ; for corrugated sheeting the minimum slope is 1 in 5 ; for slates 1 in 2 ; and for plain tiles 1 in 1. A very common slope for the main rafters of roof principals is 1 in 2, corresponding to an angle with the horizontal of 26° 34'. This is suitable for corrugated sheeting, glass or slates. Tiles require a higher pitch or the rain will penetrate. Where heavy snowfalls are to be expected, a high-pitched roof should be used. The *pitch* is defined as the *rise ÷ span*, so that if the slope be 1 : 2 the pitch is 1 : 4.

Panelling of Main Rafters.—The types of principal suitable for different spans are indicated in Figs. 312 and 314. The figures given are to be regarded as indications rather than as rigid limits. The panels into which the length of the main rafter is divided need not be less than 6 ft., and should not much exceed 7 ft.

Camber of Tie Bar.—The main tie bar is sometimes made with a camber, Fig. 316, which may be about $\frac{1}{40}$th the span. The advantages of a camber are : shorter struts, greater head room, and better appearance. Nevertheless, in modern workshop buildings, the tie bar is usually made straight, as shown in Figs. 319 and 331 ; this is more economical, and the principal so constructed is more rigid and better able to withstand possible reversals of stress.

FIG. 316.

Details of Construction.—Fig. 317 shows the sections commonly used for the members of roof principals, and the usual methods of construction.* A modern roof is nearly always built up entirely of angles, which are connected by rivets and gussets. An angle bar is the cheapest form of rolled section, and the most convenient for attachment. The main

* For welded details see § 149.

rafter is usually of T section, for which a tee bar is sometimes used, but more commonly it is made of two angles, (i) Fig. 317, placed back to back. Such a section forms a good strut, and attachments can readily be made by means of gussets. Single or double angles, as may be required, (ii), are
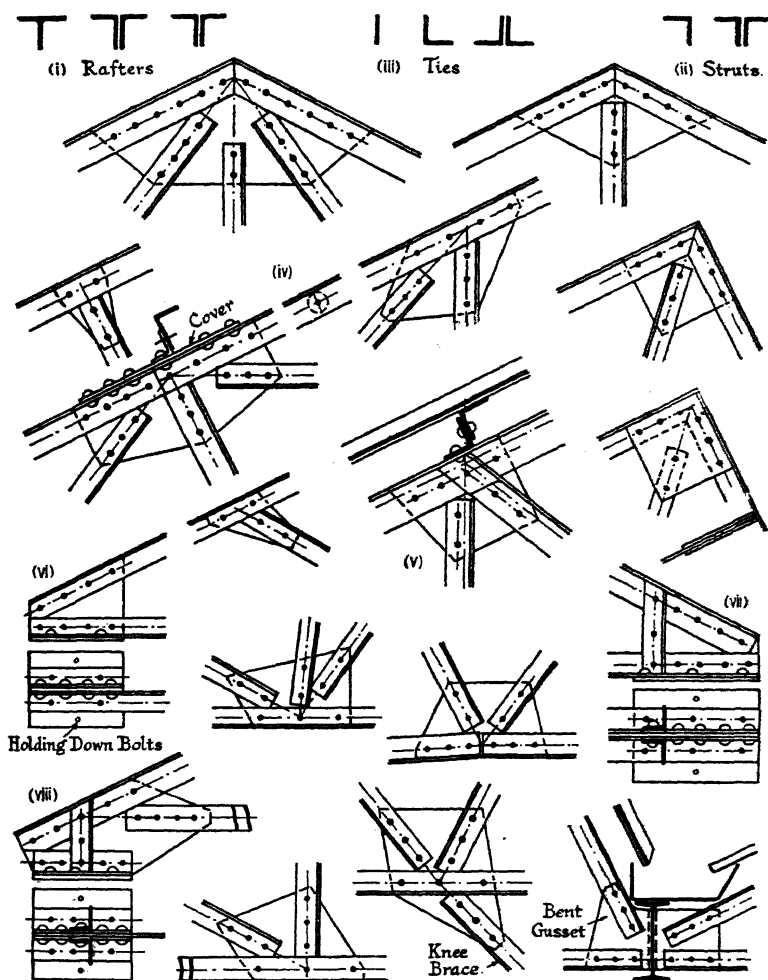
FIG. 317.

used for the struts. The tie bars also should be made of angles, (iii), in order that they may resist compression, should the stress in them be reversed due to any cause. Trusses thus constructed are easy to handle and transport. Flat bars placed on edge are sometimes used for ties, but these will not resist compression. Round bars are not used for ties in roofs of any magnitude. Welds and forked ends, which have to be

2 G

made in the smithy, are both expensive and often unreliable. Only when the diameter of the bars does not much exceed 1 in., so that the ends can be drop-forged, are round bars commercially practicable, and even then they are more expensive than angles. Right-and-left-handed screw couplings are introduced with the object of adjusting the length of members with forged ends, which are difficult to make to an exact dimension. In modern forms of riveted construction, all angles and gussets are drilled to template, and the work is sufficiently accurate without means for adjusting length.

The sections used in ordinary roof principals are small and thin. For the ties and struts, the angles range from $2\frac{1}{2} \times 2\frac{1}{2} \times \frac{1}{4}$ in., which may be regarded as the minimum section, to about $3 \times 3 \times \frac{5}{16}$ in., doubled if necessary. For small roofs, the main rafter would be made of two $2\frac{1}{2} \times 2\frac{1}{2} \times \frac{1}{4}$ in. angles back to back, and for larger spans of two $4 \times 3 \times \frac{3}{8}$ in. angles back to back, with the longer legs vertical. The gusset plates would be $\frac{5}{16}$ in. thick for the smaller spans, and $\frac{3}{8}$ in. thick for the larger. The rivets would be $\frac{5}{8}$ in. diameter for material thicknesses less than $\frac{5}{16}$ in. thick, and for $2\frac{1}{2} \times 2\frac{1}{2}$ in. angles; and $\frac{3}{4}$ in. diameter for material thicknesses over $\frac{5}{16}$ in., and angles wider than $2\frac{1}{2}$ in. Only one size of rivet should be used in a roof, and as few different sections as possible should be employed.

Where roof principals have to be sent away in parts, and riveted up at the site, the number of rivets in the ends of the members to be thus riveted should be increased by 20 % over the number theoretically necessary.

Fig. 317 shows a number of details of the riveted connections. In arranging these joints, care should be taken that the axes of members which meet intersect in a point, so as to reduce secondary stresses to a minimum. This has been done correctly in (v) ; it is more usual to make the rivet centre lines thus intersect, as shown in the other details. All members should be arranged as simple ties or struts, and not subjected to secondary bending moments. The details should be quite plain and simple. If possible, the ends of the members should be cropped square. Occasionally, members are joggled over the main rafter as shown at (v), but although this makes a rigid connection it is more expensive. However small the load in a member, there should be at least two rivets connecting it to the gusset, so that if one prove defective the roof would nevertheless still hold up. Further, the second hole enables a service bolt to be inserted and the principal to be properly bolted together while the rivet is put in. When a member is formed of two angles, the gusset is placed between them. Washers are then required to hold the angles at the correct distance apart, (iv) Fig. 317. These washers should be spaced at distances not exceeding 2 ft. apart. It is an objection to this arrangement that the narrow space between the angles is difficult to paint properly. As far as possible, all gussets should be so shaped that they can be cut from stock sizes of flat bar with the minimum number of cuts. At the same time, the standard distance from the edge of the plate to

the outside rivet centre—say $1\frac{1}{4}$ in. for a $\frac{3}{4}$ in. rivet—should not be greatly exceeded. Fig. 318 shows the method of setting out a gusset.

Shoes.—Cast-iron shoes are no longer used to carry the lower ends of the main rafters, but the principal is so arranged that suitable bearing surfaces are provided ; (vi) and (vii) Fig. 317 show typical arrangements. A sole plate is riveted to the angles forming the main tie bar, on which plate the principal rests. Vertical stiffening angles as shown at (vii) are sometimes fitted to give lateral rigidity. A modification, suitable for cases in which the main tie bar is formed of flats, is shown at (viii). Here the sole plate is attached by two angle cleats. The holding-down bolts pass through the sole plate. If the principal rest on a wall, these bolts would be lewis or rag bolts let into a stone template. If the load per unit area be greater than the stone is able to support, or if the end of the principal be intended to slide, a wall plate is introduced between the sole plate and the stone template. To permit the shoe to slide, and thus allow for expansion and contraction due to changes in temperature, the holes through the sole plate at one end are sometimes slotted. The effectiveness of this device may be doubted. In very large roofs a roller
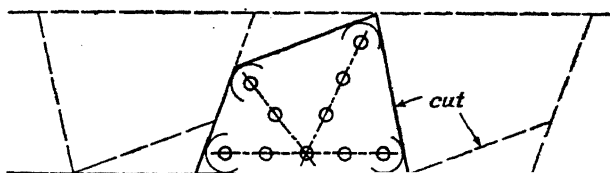
FIG. 318.

bearing is provided under one shoe, similar in design to those used to permit the ends of bridges to expand, Fig. 307.

It will be observed that in (vi) and (vii) Fig. 317 no attempt is made to arrange the intersection of the axes of the main rafter and tie bar vertically over the line of the reaction, as should be theoretically the case ; (viii) is an attempt to effect this. The arrangements shown at (vi) and (vii) are nevertheless the usual ones in practice. In workshop buildings, where the roof is supported on columns, the design shown in Fig. 331 is common. Here the object is to obtain as rigid a connection as possible.

Workshop Buildings.—A typical arrangement of the roof principals, and their supporting columns, in a workshop building is indicated in Fig. 319.

201. Purlins.—The usual types of purlins and the methods used to attach them to the main rafters are illustrated in Fig. 320. The commonest arrangement is an angle section bolted to short angle cleats, which are riveted to the main rafter, (i). For wide spacing of the principals, a light beam section forms a suitable purlin, (ii), or a channel, (iv), may be used. If the roof is to be boarded over, timber purlins are convenient, which are sometimes supported by a continuous angle, (iii).
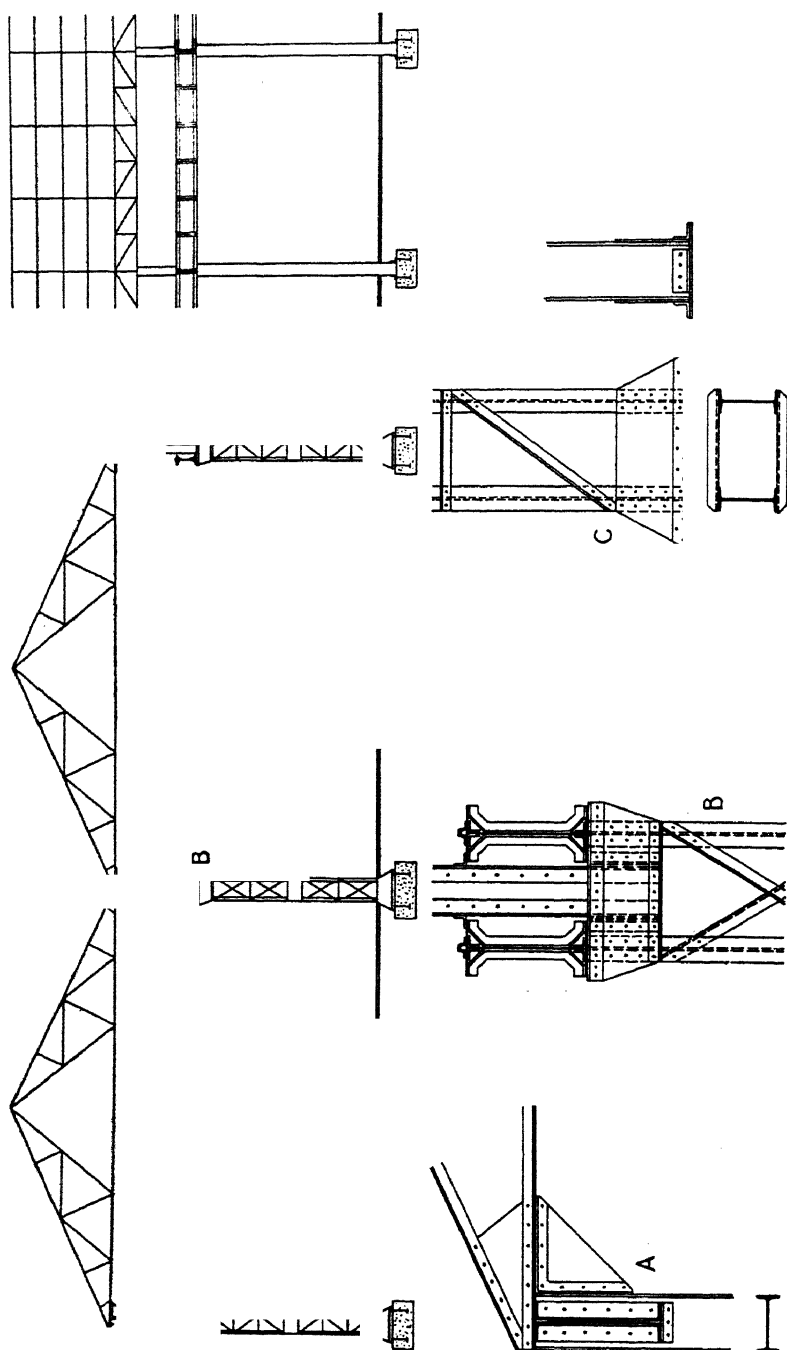
Fig.

Joints in purlins should occur over a main rafter. Some details are shown in (v) and (vi) Fig. 320. The spacing of the purlins depends on (i) the kind of roof covering, (ii) the arrangement of panels of the main rafter. The purlin should be placed immediately over a panel point, in order not to set up bending moments in the main rafter. If, owing to the nature of the covering, as in (ii) Fig. 327, it be unavoidable that purlins come intermediately between the panel points, the rafter should be designed as a laterally loaded strut. This makes a heavy main rafter and is to be avoided if possible. Purlins should be designed as girders spanning
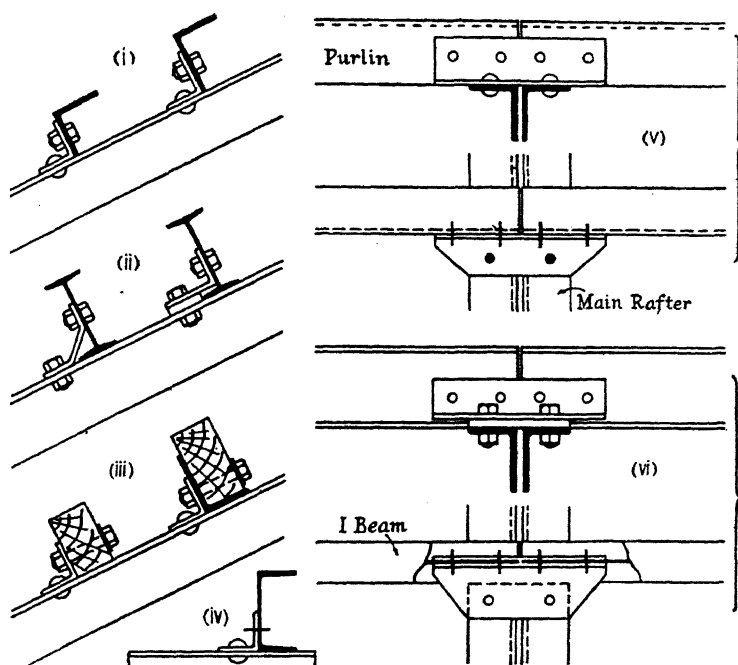
FIG. 320.

between the principals and carrying the loads on the roof. As a rule they are continuous over more than one span and should be treated as continuous girders, though the continuity is poor at places where a joint occurs. It is probably sufficiently accurate for most practical purposes to take the maximum bending moment on the purlins as $WL/10$, intermediate between that for direction-fixed and freely-supported beams. Their depth should not be less than $\frac{1}{40}$ their span.

Since the purlins are usually placed perpendicularly to the rafter, they are evidently subjected to bending in more than one plane, due to the weight of the roof, though in some cases the roof covering offers some support in its own plane. In these circumstances the design can only be a rough approximation.

In cases where the distance between the principals is considerable, purlins are often made in the form of lattice girders. They are then placed intercostally between the principals, and attached to the bracing of the latter.

202. Secondary Rafters, Sash Bars, etc.—Except in very large roofs these bars are of small size, and the scantlings are determined as the result of successful practice. For glass, T bar sashes about $2 \times 1\frac{1}{2} \times \frac{1}{4}$ in. may be used, spaced from 1 ft. 6 in. to 2 ft. 0 in. apart, provided that the spacing of the purlins does not exceed about 6 ft. Boarding to carry slates may be from 1 in. to $1\frac{1}{4}$ in. in thickness, if the pitch of the purlins does not exceed 2 ft. 6 in. to 3 ft. Corrugated iron is attached directly to the purlins and needs no secondary rafters.

203. Wind Bracing.—If the wind act on the ends of the building, it will tend to overturn the principals about the shoes as fulcrums. This

FIG. 321.

tendency is resisted to some extent by the rigidity of the roof as a whole, and by the stiffness of the roof covering. In small and unimportant roofs this resistance appears to be sufficient, but in roofs of any magnitude it is necessary to introduce special wind bracing to prevent such over-turning. Some typical arrangements are shown in Fig. 321, and details of construction in Fig. 322. In (i) Fig. 321, diagonal braces are fitted in the plane of the main rafters, connecting together the two end principals. These braces, with the main rafters and purlins, form a braced girder by

which the longitudinal load is transmitted to the abutments; (ii) and (iii) are modifications of the arrangement. In (iv), the bracing is put in the plane of the main strut AB. Two lattice girders, as shown in section, are thus formed, which prevent the principals from overturning. If the wind bracing is put on top of the main rafter, it should be attached to a gusset placed between the main rafter and the purlin cleat, (ii) Fig. 322. If it is put underneath the main rafter, it may be attached by cleats as shown at (iii). This arrangement is suitable for the bracing shown at (ii) Fig. 321. Details of the wind bracing illustrated in (iv) Fig. 321 are given in (iv) Fig. 322 ; here the purlin forms the top flange of the lattice girder, and a longitudinal angle in the plane of the main tie bars forms the lower flange. ·Sometimes the roof is braced from end to end in the plane of the main tie bars.
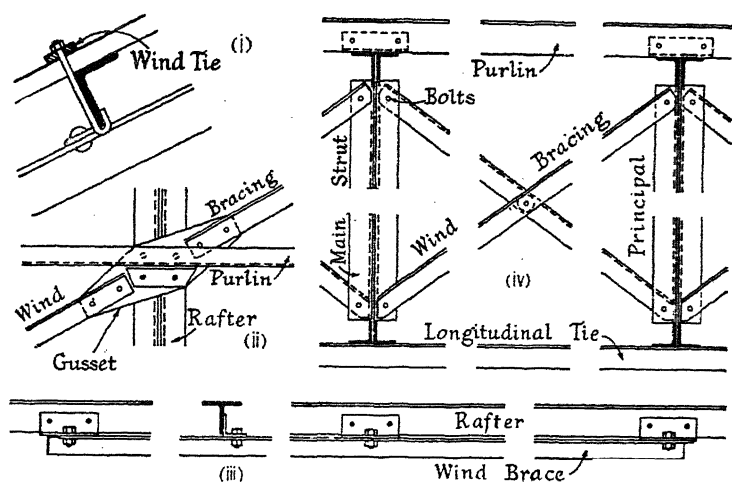
FIG. 322.

The common arrangement of the framework at the ends of a building, when it is to be enclosed by corrugated sheeting, is shown in (v) Fig. 321. The wind pressure is transmitted from the sheeting to the verticals, and thence via the wind bracing in the roof to the walls or side framework. A strong horizontal girder is provided at the level of the eaves, often of the braced type. This transmits a large proportion of the end wind pressure direct to the sides. When the depth of this girder is considerable, the weight of the outstanding flange must be suspended from the roof structure.

204. Ventilators.—Three methods of constructing ventilators for roofs are shown in Fig. 323. (i) is called a hooded ventilator ; in the design shown the hood is formed of a bent steel plate $\frac{1}{8}$ in. thick, but curved galvanised corrugated steel sheeting is often used for the purpose. In (ii) and (iii) louvres are fitted ; these may be fixed as shown, or may be movable. Curved baffles, as illustrated in the figure, should be provided,

to prevent the entrance of driving rain. When the lantern, (ii), is very large and heavy, special bars may be necessary in the truss to support it.
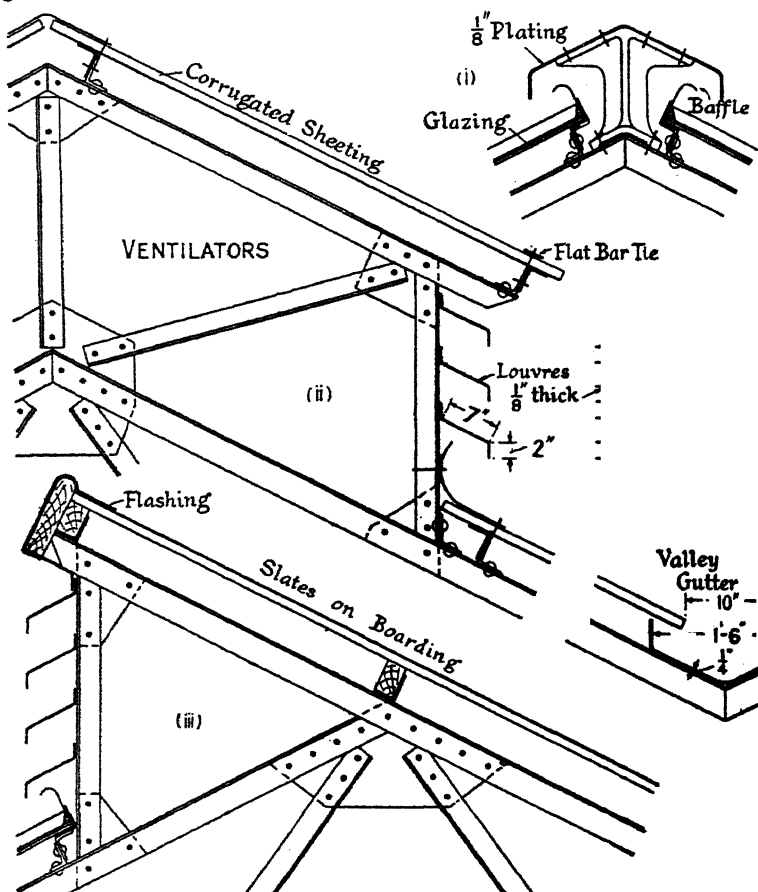
FIG. 323.

205. Very Large Roofs.—For very large roofs, arched principals may be used. Fig. 324 illustrates a type suitable for a large hall. A two-hinged arch, or as in Fig. 324 a three-hinged arch, may be employed. The feet of the principals may be tied together by a horizontal tie as shown, otherwise abutments of sufficient strength to resist the thrust of the arch must be provided, (ii). As an

FIG. 324.

alternative to the arch, the span may be subdivided and combinations of elementary roof trusses made use of. Examples can be seen at large railway termini.
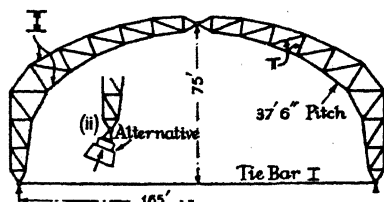
206. Roof Coverings.—The three commonest kinds of roof coverings are glass, corrugated sheeting, and slates.

Glass.—In modern workshop and factory building practice it is quite usual for the whole roof covering to be made of glass. With efficient ventilation, a coat of whitewash in the summer, and steam heating in winter, an equable temperature is secured, with plenty of light and air. The glass is usually rough cast plate glass, in sheets from 6 ft. to 6 ft. 6 in. long, 18 in. to 24 in. in width, and $\frac{1}{4}$ in. in thickness. As previously mentioned, it is laid in **T** bar sashes (about $2 \times 1\frac{1}{2} \times \frac{1}{4}$ in. for a span of 6 ft.), (i) Fig. 325, with putty. The glass sheets should have an overlap of 2 to 3 in. There are many forms of glazing without putty, designed to obviate cost of upkeep, and possible trouble due to the unequal ex-
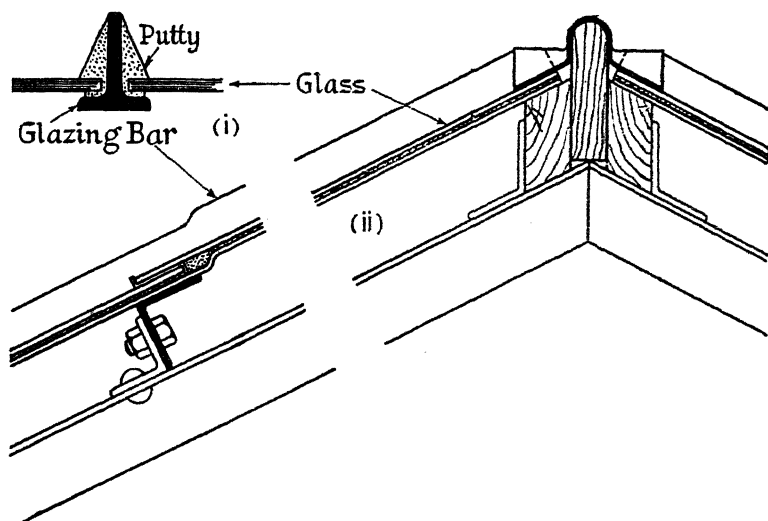
FIG. 325.

pansion of the glass and steel. They are more expensive than putty glazing. (ii) Fig. 325 shows a typical arrangement of glass roof. Combinations of glass with other forms of roof covering are very common, and in saw-tooth roofs the steeper slope is glazed.

Galvanised Corrugated Sheeting is a cheap and light roof covering much used for sheds. It is supplied in sheets up to 12 ft. long, from 2 ft. 0 in. to 2 ft. 6 in. in width, with corrugations at either 6, 5, 4, or 3 in. pitch, and of thickness ranging from 16 to 28 W.G. The depth of the corrugations is one-quarter the pitch. For roofing, the usual pitches are 5 or 3 in.; and, owing to rusting, the thickness should not be less than 18 W.G. The standard widths are either 5 or 6 corrugations at 5 in. pitch, giving sheets 2 ft. 1 in. or 2 ft. 6 in. centres; or 8 or 10 corrugations at 3 in. pitch, giving sheets 2 ft. 0 in. or 2 ft. 6 in. centres. There is an overlap of 1 in. at each side, making the overall width of the sheet 2 in.

more. (i) Fig. 326 shows a typical arrangement of this kind of roof covering. The sheeting is laid directly on angle purlins and secured by hook bolts which are $\frac{5}{16}$ or $\frac{3}{8}$ in. diameter and spaced 15 in. apart, or galvanised straps $\frac{3}{4} \times \frac{1}{8}$ in., secured by screw bolts, (ii) Fig. 326, may be used. The corrugations should run down the roof from ridge to eaves. Where the sheets join, they should be arranged to lap over a purlin, and the width of the overlap should be 6 in., (i). There should be a rivet or a $\frac{1}{4}$ in. screw bolt in each corrugation through the lap, or alternatively the pitch of the hook bolts should be reduced to 5 or 6 in. The joints along the sides of the sheets should be made as shown at (iv) or (v) Fig. 326; (iv) is the common arrangement. The pitch of the rivets or
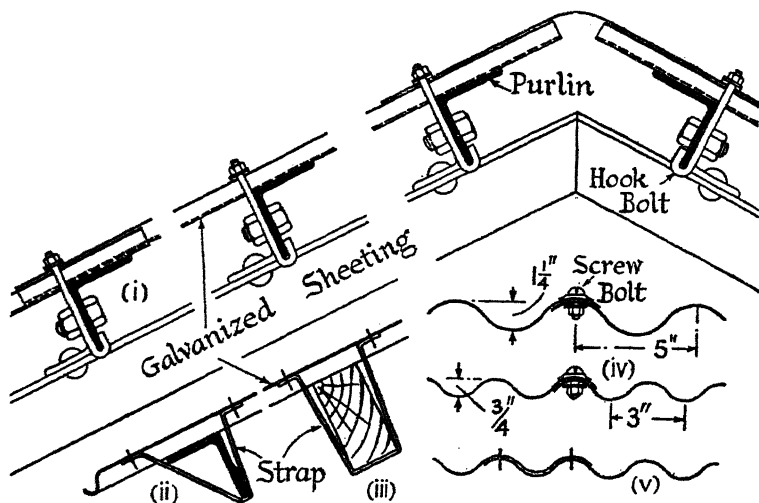
FIG. 326.

screw bolts through these joints should be 12 in. In all cases the holes for the rivets or screw bolts should be made through the ridge of the corrugation, and all bolts should be furnished with curved washers to prevent leakage. To preclude the wind from lifting the sheets, should it get underneath them, the hook bolts should be placed at 9 or 10 in. pitch at the eaves, instead of at the normal pitch of 15 in. Alternatively, a flat bar wind tie as shown at (i) Fig. 322 may be fitted. When wooden purlins are used, the sheeting is usually attached by screws, spaced 10 to 12 in. pitch, and fitted with curved washers. This pitch is decreased to 5 or 6 in. where laps occur. The straps shown at (iii) Fig. 326 are a better means of attachment.

The following rule has been given for the strength of corrugated sheeting. If L denote the span between the supports in feet, t the thickness of metal in inches, d the depth of the corrugations in inches, w the applied load in lb./sq. ft., and η the factor of safety, then

$L = c\sqrt{\dfrac{td}{\eta w}}$. The value of c for wrought-iron sheeting is 316 and for mild steel sheeting is 373. For ordinary roofs the value of η may be taken as 3.

Slates are largely used as a roof covering. They may be laid on boards and nailed in the usual way, (i) Fig. 327, in which case a common size would be 16 × 8 in.

Duchess slates, 24 × 12 in., may be used, attached to angle purlins, (ii) Fig. 327, which are spaced $10\frac{1}{2}$ in. apart, allowing a 3 in. overlap for the slates. If the span between the principals does not exceed 8·feet, purlins $1\frac{1}{2} \times 1\frac{1}{2} \times \frac{1}{4}$ in. can be used, which section should be increased to $2 \times 2 \times \frac{1}{4}$ in. for spans up to 10 feet.
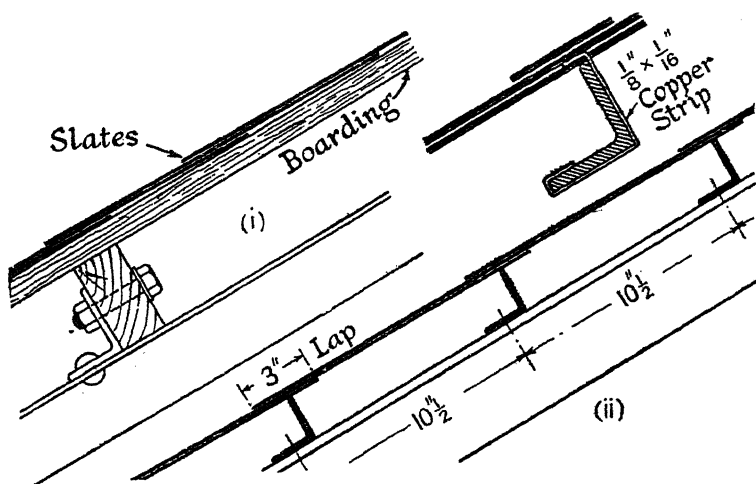
FIG. 327.

Tiles of many varieties are used for roof coverings. They are heavy, and require a high pitch or the rain will get underneath them. They are supported in a similar manner to slates.

Zinc sheets, laid on boarding with wooden rolls, may be used when an exceptionally low-pitched roof is required. This is a very light form of covering.

Asbestos sheeting, plain and corrugated, and asbestos tiles are also used for roof coverings.

207. Weights of Roof Coverings (Approximate) in pounds per square foot of area covered by the roof.

$\frac{1}{4}''$ glass	3·5
Metal sash bars and putty for same	2·5
Corrugated sheeting, including laps and fastenings:—	
5″ corrugations, 16 S.W.G.	5·0
3″ „ 18 S.W.G.	4·0
Slates, including fastenings, 16″ × 8″	6·0
„ „ „ 24″ × 12″	10·0

Felt	. . . .	0·3
Boarding, per inch of thickness	. . . .	3·5
Zinc sheets	. . . .	1·5
Tiles	. . . .	10 to 20
Steel purlins	. . . .	2 to 4
Wood purlins	. . . .	1 to 3
Snow in British Isles	. . . .	5 to 6
Wind	. . . .	see § 52

Typical roofs :—

¼″ glass	. . . .	3·5	Corrugated sheeting, 16 W.G.	5·0
Sash bars, etc.	. . .	2·5	Purlins	2·0
Purlins	. . . .	2·0		—
		—		7·0
		8·0		

Slates, 16″ × 8″	. . .	6·0	Slates, 24″ × 12″ .	. . 10·0
Boarding, 1″ thick	. .	3·5	Purlins, 10¼″ pitch	. . 4·0
Purlins	. . .	3·5		—
		—		14·0
		13·0		

208. Weights of Principals.—The approximate weight of a modern roof principal of the type discussed in § 200 is given by the formula

$$w = \frac{k}{l}\left\{1\cdot8 + \frac{L^2}{1800}\right\} \text{lb./sq. ft.} \qquad . \qquad . \qquad . \quad (1)$$

where w denotes the weight in lb. per square foot of area covered by the roof, l the spacing of the principals, and L the span, both dimensions in feet; k is a coefficient depending on the type of roof covering. For corrugated sheeting $k = 9\cdot5$, for glazed roofs $k = 10$, for slates on boarding $k = 12$. This formula holds for spans ranging from 25 to 80 ft. when the purlins are from 6 to 7 ft. apart, and the spacing of the principals ranges from 10 to 15 ft. A closer pitch of purlins increases the value of w. For principals of the type shown at (v) Fig. 314, in which the main strut is duplicated, add 10 per cent. to the weight given by the formula.

This formula is based on some weights given in Arrol's Handbook,[5] to which reference should be made for details and scantlings of the principals.

209. The Forces in the Members of the Principals.—When finding the forces in the members of the principals, it is convenient to treat the dead loads and the wind loads separately, and afterwards to combine their effects.

Having determined the weight of the roof covering, the weight of the principals, and of the snow, if any, the total dead load per square foot of area covered is known. In large roofs the weight of the wind bracing may be of sufficient importance to be taken into account. The dead load which each principal supports can be found, and hence the load per panel point. The stress diagrams for the dead load present little difficulty. Both loads and reactions are vertical. When the panels are of equal length, it is convenient to assume that the loads are of unit magnitude, and to find the actual forces in the bars by multiplication, see § 6.

The considerations determining the wind pressure on the roof have been set forth in § 50, from which the normal pressure on the roof surfaces can

be found, and hence the wind loads at each panel point. Before the stress diagrams for these loads can be drawn, the reactions at the points of support must be determined. These depend on the method of supporting the roof. In large roofs, in order to allow for expansion due to temperature changes, it is not uncommon so to arrange the supports that one end of the roof, such as A, (i) Fig. 328, is free to slide in a horizontal
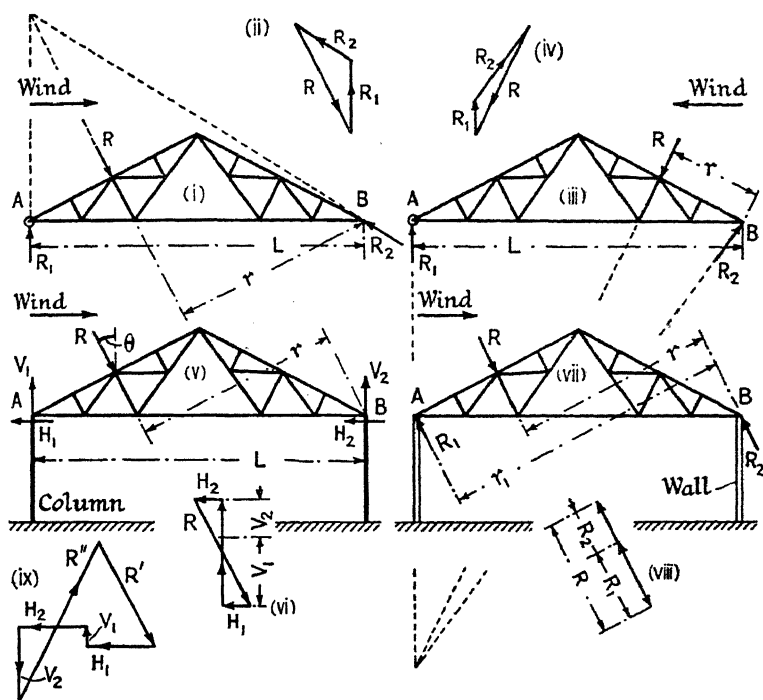
FIG. 328.

direction. The reaction R_1, at the free end, is then usually assumed to be vertical. But the resultant wind load R and the two wind reactions R_1 and R_2 are the only external forces due to wind which act on the roof. They must therefore be in equilibrium, and their lines of action must meet in a point. This condition enables the direction of the second reaction to be found. Two cases arise, (a) when the wind is on the left, (i) Fig. 328, and (b) when the wind is on the right, (iii) Fig. 328. Knowing the magnitude of R, and the direction of the reactions, their magnitude can be obtained by drawing the triangle of forces for the external forces, as shown in (ii) and (iv). Alternatively, if the point of intersection is inaccessible, the magnitude of R_1 can be found by taking moments about B ; thus, $R_1 \times L = R \times r$. Knowing R and R_1, the triangle of external forces can be drawn, which completely determines R_2. When, as in this case, the conditions are different at the two supports, two stress

diagrams must be drawn, one for the wind on the left, the other for the wind on the right.

In many cases the roof is supported on columns, (v) Fig. 328; it is then rigidly attached at each end, Fig. 331. If each column be of the same length and cross-section, it is reasonable to assume that the horizontal deflection due to wind pressure at the upper end of each column will be the same; or in other words, the values of H_1 and H_2, the horizontal reactions at A and B, (v) Fig. 328, will be equal, and $H_1 = H_2 = \frac{1}{2}R \sin \theta$. The sum of the vertical reactions, $V_1 + V_2 = R \cos \theta$. The magnitude of the vertical reaction at A can be found by taking moments about B; $V_1 L = Rr$. The polygon of external forces can now be drawn, (vi) Fig. 328, for all the reactions are known. The worked example, § 212, is a case of this type, and the stress diagram for the wind load is given in Fig. 14.

If the columns are different in length or in cross-section, the deflections Δ at the upper end of each may still be assumed to be equal, but H_1 and H_2 will be different. If H_1 be the horizontal force necessary to produce a horizontal deflection Δ at the top of the column at A, and H_2 the force necessary to produce an equal deflection at the top of the column at B, from eq. (3), § 52, Vol. I,

$$\Delta = \frac{H_1 l_1{}^3}{3EI_1} = \frac{H_2 l_2{}^3}{3EI_2}; \text{ or } \frac{H_1}{H_2} = \frac{I_1 l_2{}^3}{I_2 l_1{}^3}$$

where I and l are the respective moments of inertia and lengths of the columns. Further, $H_1 + H_2 = R \sin \theta$. From these two equations H_1 and H_2 can be found, and hence the polygon of external forces can be drawn as before.

When as in (vii) Fig. 328, the roof is supported on two walls, each of which could sustain the whole horizontal component of the wind pressure without considerable deflection, the problem is indeterminate, but it is usual to assume that the reactions will be parallel to the load as shown in the figure. In this case, taking moments about B, $R_1 r_1 = Rr$. The triangle of external forces becomes the straight line shown at (viii).

If, in any of the above cases, there be a negative wind pressure on the leeward side of the roof, as discussed in § 50, it must be taken into account when finding the reactions. Thus, if (v) Fig. 328 were a closed-in building with windows and doors, the polygon of external forces would take the form shown in (ix). R' is the positive pressure on the windward side, R'' is the negative pressure on the leeward side of the roof.

Having found the reactions, the stress diagrams for the wind loads may be drawn, and the forces in the bars due to wind determined. When the panels are of equal length, it is convenient to do this for unit loads, and afterwards to find the actual forces by multiplication (see § 6).

The forces in the bars due to the dead load, and those due to the wind loads, should be combined in order to find the maximum forces in the bars, as explained in § 6. These maximum forces should be used in the

design of the bars. For the method of procedure and suitable working stresses, see the worked example following, § 212.

210. Roofs with Knee Braces.—Lateral stiffness may be imparted to a roof supported on columns by the introduction of knee braces GU, ST, as indicated in (i) Fig. 329. The forces in the bars of the roof truss due to the vertical loads are unaffected by this, and in considering the effect of the knee braces, only wind pressure or other lateral forces need be treated. The roof truss with its supporting columns becomes, in effect, a braced portal, and the methods of § 101 may be applied.

In the first instance, suppose the structure to be an open shed, and
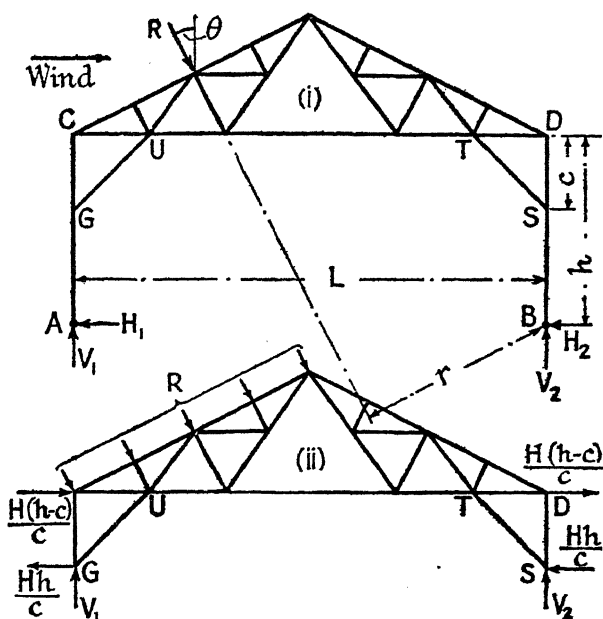
FIG. 329.

that A and B, the feet of the columns, may be regarded as hinged joints; further, that the length and cross-section of each column is the same. Let R, (i) Fig. 329, be the resultant wind pressure on the roof. V_1 and V_2, the vertical components of the reactions, may be found by taking moments about B,

$$V_1 L = Rr \; ; \quad \text{also,} \; V_1 + V_2 = R \cos \theta \; . \qquad . \qquad . \quad (1)$$

In the assumed circumstances, each of the horizontal components H_1 and H_2 of the reactions may be taken as equal to one-half of the horizontal component of the resultant wind pressure R,

$$H_1 = H_2 = H = \tfrac{1}{2} R \sin \theta \; . \qquad . \qquad . \qquad . \quad (2)$$

Apply the method of § 101 to this case, that is to say, regard the member BD as a lever hinged at D; the reaction at S will be Hh/c.

Again, by taking moments about S, the reaction at D will be $H(h - c)/c$, (cf. § 101), and similarly for the member AC. If now, as in (ii) Fig. 329, that part of the structure above GS be isolated, the external forces acting on the roof will be as shown, and the forces due to wind in all the bars can be found in the usual way.

More General Case. Direction-fixed Feet.—In the general case, Fig. 330, the columns may be of unequal length and stiffness. If the building be enclosed there may be, in addition to the wind pressure R' on the windward side of the roof, a suction R'' on the leeward side; also a lateral wind pressure on the windward side of the building and a suction
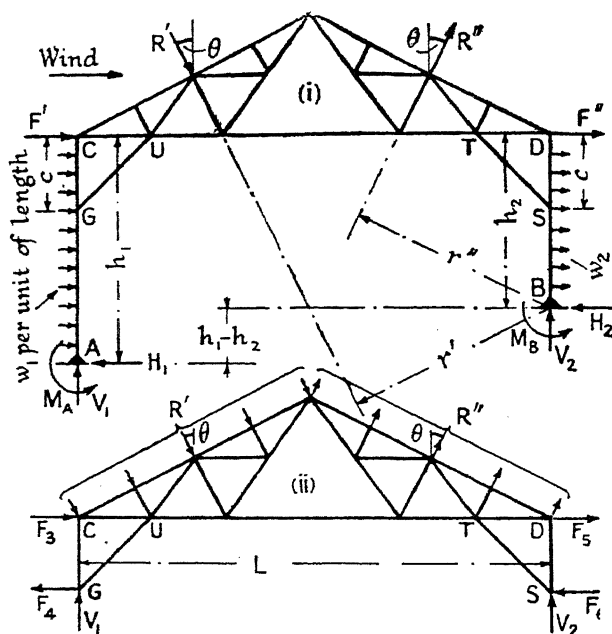
FIG. 330.

on the leeward side, (ii) Fig. 83. The latter are represented in the figure by a uniform pressure and suction w_1 and w_2 per unit of length on the columns AC and BD respectively, together with concentrated loads F' and F'' at C and D. Not only so, but the feet A and B may be fixed in direction or approximate thereto.

The procedure then follows a course similar to that for the portal with direction-fixed feet, § 104. If the frame GCDS, (ii) Fig. 330, be assumed to remain sensibly rigid, the reaction-forces F_3, F_4, F_5, and F_6 between the columns AC, BD and this frame may be found as in § 104; eqs. (4) and (5), § 104, for column AC, will apply to both columns of the roof truss. Thus

$$y_C \quad \frac{w_1 h_1^4}{8EI_1} - \frac{(F_3 - F')h_1^3}{3EI_1} + \frac{F_4(h_1 - c)^2}{6EI_1}(2h_1 + c) \qquad . \quad (3)$$

$$\dot{y}_G = \frac{w_1(h_1 - c)^2(3h_1{}^2 + 2h_1c + c^2)}{24EI_1} - \frac{F_3 - F'}{6EI_1}(h_1 - c)^2(2h_1 + c)$$
$$+ \frac{F_4(h_1 - c)^3}{3EI_1} \qquad . \qquad . \qquad . \quad (4)$$

$$y_D = \frac{w_2h_2{}^4}{8EI_2} - \frac{(F_5 - F'')h_2{}^3}{3EI_2} + \frac{F_6(h_2 - c)^2}{6EI_2}(2h_2 + c) \qquad . \qquad . \quad (5)$$

$$y_S = \frac{w_2(h_2 - c)^2(3h_2{}^2 + 2h_2c + c^2)}{24EI_2} - \frac{F_5 - F''}{6EI_2}(h_2 - c)^2(2h_2 + c)$$
$$+ \frac{F_6(h_2 - c)^3}{3EI_2} \qquad . \qquad . \quad (6)$$

But $y_C = y_G = y_D = y_S = \Delta$.

Put $y_C = y_G$,
$$F_4 = \frac{4(F_3 - F')(3h_1{}^2 - c^2) - w_1(4h_1{}^3 - c^3)}{12(h_1 - c)^2} \qquad . \qquad . \quad (7)$$

Put $y_D = y_S$,
$$F_6 = \frac{4(F_5 - F'')(3h_2{}^2 - c^2) - w_2(4h_2{}^3 - c^3)}{12(h_2 - c)^2} \qquad . \qquad . \quad (8)$$

Put $y_C = y_D$, and use eqs. (7) and (8),

$$(F_5 - F'')\frac{4c(3h_2 + c)(h_2 - c)}{I_2} = (F_3 - F'')\frac{4c(3h_1 + c)(h_1 - c)}{I_1}$$
$$+ \frac{w_1}{I_1}(h_1{}^3 - 3h_1{}^2c - 3h_1c^2 - c^3)(h_1 - c)$$
$$- \frac{w_2}{I_2}(h_2{}^3 - 3h_2{}^2c - 3h_2c^2 - c^3)(h_2 - c) \quad (9)$$

From (ii) Fig. 330,
$$F_3 - F_4 + F_5 - F_6 + (R' + R'') \sin \theta = 0 \qquad . \qquad . \quad (10)$$
$$V_1 + V_2 - (R' - R'') \cos \theta = 0 \qquad . \qquad . \quad (11)$$

Taking moments of the external forces about B, (i) Fig. 330,

$$V_1L + w_1h_1\left(h_2 - \frac{h_1}{2}\right) + \frac{w_2h_2{}^2}{2} + (F' + F'')h_2 - R'r' + R''r''$$
$$- (M_A + M_B) = 0 \qquad . \qquad . \quad (12)$$

From a consideration of the forces acting on the columns,
$$H_1 = w_1h_1 + F' - F_3 + F_4 \; ; \; H_2 = w_2h_2 + F'' - F_5 + F_6 \qquad . \quad (13)$$

$$M_A = \frac{w_1h_1{}^2}{2} - (F_3 - F')h_1 + F_4(h_1 - c) \qquad . \qquad . \qquad . \quad (14)$$

$$M_B = \frac{w_2h_2{}^2}{2} - (F_5 - F'')h_2 + F_6(h_2 - c) \qquad . \qquad . \qquad . \quad (15)$$

The forces F_3, F_4, F_5, and F_6 can be found from eqs. (7–10) by inserting numerical values. From eqs. (11) and (12), V_1 and V_2 can be found, hence the forces in the framework (ii) Fig. 330 can be determined. By the use of eqs. (13), (14), and (15), the shearing-force and bending-moment diagrams for the columns can be set out.

2 H

211. Snow and/or Wind.—Snow and wind may be regarded as occasional loads on a roof, and some difference of opinion exists as to the necessity of allowing for their combination. It is pointed out that snow cannot lodge in severe wind storms, but there is the possibility that the snow may have fallen and consolidated before the wind storm commences. In northern latitudes several feet of snow, frozen hard, may form a serious addition to the loads on the roof. It would appear rational, in this country, if the probable wind loads be calculated as set forth in § 50, to allow also for a moderate snow load, say 5 lb./sq. ft., on all but steep roofs, in addition to the wind load. If the wind loads be estimated in the conventional manner by Duchemin's or Hutton's formula, the snow need only be allowed for as an alternative to the wind.

212. Worked Example.—*Design for a roof principal of the trussed rafter type. The roof covers an open shed in an exposed position.*—The span, centre to centre of the columns, is 75 ft., and the spacing of the principals is 12 ft. 6 in. The covering is of galvanised sheeting 16 W.G. Horizontal wind pressure 30 lb./sq. ft. ; snow 5 lb./sq. ft.

(1) *Safe Stresses.*—In direct tension and compression, $f_t = f_c = 8$ tons/sq. in. In direct shear, $f_s = \frac{3}{4} f_t = 6$ tons/sq. in. Safe bearing pressure in rivet holes, $f_b = 2f_s = 12$ tons/sq. in. Struts to be designed by the Johnson parabolic formula, factor of safety = 3, which is to be increased to 4 when the angle is attached by its back ; qL/κ not to exceed 120.

(2) *Rivets.*—Rivet holes (drilled) $\frac{3}{4}$ in. diameter will be used throughout. The area of the closed rivet will therefore be 0·44 sq. in., and the worth of a rivet in single shear = 0·44 × 6 = 2·64 tons. Assuming that the rivets bear in a $\frac{5}{16}$-in. plate (the thickness of the gussets), the worth of a rivet in a double shear is $\frac{3}{4} \times \frac{5}{16} \times 12 = 2\cdot81$ tons.

(3) *Type of Principal.*—For a span of 75 ft. the type of principal shown in Fig. 331, with a pitch of 1 : 4, will be adopted. The spacing of the purlins will then be about 7 ft., a suitable distance. There will be no camber. All the members of the principal will be of angle section.

(4) *Dead Weight of Roof.*—From the Table in § 207, the dead weight of the specified type of roof covering will be 7 lb./sq. ft., including fastenings and purlins. The weight of the principal itself can be found from eq. (1), § 208. For corrugated sheeting $k = 9\cdot5$, and

$$ w : : \frac{9\cdot5}{12\cdot5} \left(1\cdot8 + \frac{75^2}{1800} \right) = 4 \text{ lb./sq. ft. approx.} $$

The total dead weight per square foot of area covered is, therefore,

Principal	4·0
Covering	7·0
Snow	5·0

16·0 lb./sq. ft.

From Fig. 331 it will be seen that the width of roof (measured horizontally) supported at one panel point is (75 + 1·5) ÷ 12 = 6·38 ft.

Galv. Sheeting 16 W.G.

Angle 3"×3"×¼"

Angle 3"×3"×¼"

Angles 3½"×3×¼"
Double

Cleats 3"×2½"×¼"

5" Corrugations

Corrugated Sheeting 16 W.G.

Angle 5"×3"×5⁄16" Double

Angles 3½"×3×¼"

Angle 3"×3"×¼"

Angles 3"×3"×¼" Double.

19'—1½"

(i)

Pitch 1:4
Spacing of Principals 12'-6"

5⁄16" Washer.

5⁄16" Cover.

All Rivet Holes ¾" Dia.
All Gussets 5⁄16" thick

75'-0" Centres

essed
Gutter.

12"

9"

Wind
Bracing

Purlins

Principals

Longitudinal View Covering Removed.
(ii)

19'-0"

25'-0"

25'-0"

12'-6" 12'-6"

Fig. 331.

Hence the load per panel point is $(6 \cdot 38 \times 12\frac{1}{2} \times 16) \div 2240 = 0 \cdot 57$ ton. This figure has been used in § 6 to calculate the forces in the bars due to the dead load.

(5) *Wind Load on Roof.*—Use will be made in this connection of the results of Stanton's experiments, § 50. As shown in the Table, p. 120, the value of K for the windward side of the roof of an open shed, if the pitch be 1 : 4, is $0 \cdot 4$. Therefore the normal pressure on the windward side of the roof, due to a horizontal wind pressure of 30 lb./sq. ft., is $30 \times 0 \cdot 4 = 12$ lb./sq. ft. The negative pressure on the leeward side is negligible (*l.c.*). The load at a panel point, due to a normal pressure of 12 lb./sq. ft., is that on an area $7 \cdot 13 \times 12\frac{1}{2}$ sq. ft., the pitch of the panel points being $7 \cdot 13$ ft. ; this load is $7 \cdot 13 \times 12\frac{1}{2} \times 12 \div 2240 = 0 \cdot 48$ ton. It will be assumed that the snow has consolidated on the roof before the wind rises, and hence that both snow and wind loads act simultaneously.

(6) *Calculation of Forces in the Members.*—The stress diagrams for the dead and wind loads should now be drawn, and the forces in all the members of the principal should be calculated. These diagrams are given in Figs. 13 and 14, and the method is set forth in § 6. Since the roof is supported on columns, it should be assumed that one-half the horizontal component of the wind pressure is carried by each column, as explained in § 209. The maximum force in each member is given in the Table on p. 12. It is not necessary to treat the wind as a live load (see § 44).

(7) *Calculation of the Scantlings.*—In the present case, the roof itself, and the forces in all the members, are symmetrical about the centre line, and it is only necessary to consider one-half the roof.

Rafter.—Bars Nos. 1–6. The forces in the different panels of this member range from $- 8 \cdot 79$ to $- 10 \cdot 49$ tons ; the same section will be used throughout. Consider first the lowest panel, bar No. 1 ; its length to the centres of the gussets may be taken as 72 in., the force in it is $- 10 \cdot 49$ tons. It is riveted to gussets at each end ; the lower one forms part of the shoe of the truss and possesses considerable rigidity, the other will hardly do more than hold the bar fixed in position. The condition of the member evidently approximates to that of a column position- and direction-fixed at the lower end, and position-fixed at the other. It will probably not be far wrong to take $q = 0 \cdot 8$ (§ 158), so that the length $qL = 0 \cdot 8 \times 72 = 58$ in. Using the Johnson parabolic formula and applying Asimont's device, § 164, the necessary area of the member is given by eq. (4), § 164,

$$ a = \frac{1}{40{,}000} \left\{ \eta W + \frac{4g(qL)^2}{3} \right\} \text{ sq. in.} $$

Double angles, forming a tee section, will be used, for which g ranges from $2 \cdot 6$ to $3 \cdot 30$. Taking a mean value of $3 \cdot 0$, and adopting a factor of safety of 3,

$$ a = \frac{1}{40{,}000} \left\{ 3 \times 10 \cdot 49 \times 2240 + \frac{4 \times 3 \times (58)^2}{3} \right\} = 2 \cdot 10 \text{ sq. in.} $$

Two $3\frac{1}{2} \times 3 \times \frac{1}{4}$ in. angles, back to back, have a total area of $3\cdot12$ sq. in., which is more than sufficient. The minimum κ of this section is $1\cdot09$, so that $\dfrac{qL}{\kappa} = \dfrac{58}{1\cdot09} = 54$. From the Johnson formula, eq. (3), § 164, the crippling load on this section is

$$R = a\left\{40{,}000 - \frac{4}{3}\left(\frac{qL}{\kappa}\right)^2\right\} \div 2240 = \frac{3\cdot12}{2240}\left\{40{,}000 - \frac{4}{3}(54)^2\right\} = 50 \text{ tons};$$

hence the factor of safety $\eta = \dfrac{50}{10\cdot49} = 4\cdot7$. There is therefore ample strength.

Testing the bay immediately above this, bar No. 2, the load is $9\cdot57$ tons. The gussets which hold this bar are only two-hole gussets attached to a light angle, the degree of direction-fixing is small, and it will be safer to take $q = 1$; since $L = 85\frac{1}{2}$ in., the value of qL/κ is $85\frac{1}{2} \div 1\cdot09 = 79$. Applying the Johnson formula, $R = \dfrac{3\cdot12}{2240}\left\{40{,}000 - \dfrac{4}{3}(79)^2\right\} = 44$ tons; and $\eta = 44 \div 9\cdot57 = 4\cdot6$.

Considering next the possibility of bending in a direction at right angles to the plane of the principal, the panel points are held in position by the purlins. The degree of direction-fixing is small, and q should be taken as 1. The value of κ for primary bending in this direction $= 1\cdot29$, and $qL/\kappa = 85\frac{1}{2} \div 1\cdot29 = 67$. Rivets (with $\frac{5}{16}$ in. washers) about 27 in. apart will be used to connect the two angles; $qL/\kappa = 30$ for the single angle; hence qL/κ for the double section $= \sqrt{67^2 + 30^2} = 74$ (see § 160). It will be evident from the preceding calculation that there is ample strength in this direction.

The $\frac{5}{16}$ in. gussets will be placed between the two angles, so that the rivets are in double shear. The worth of a $\frac{3}{4}$ in. rivet in double shear is $2\cdot81$ tons, hence the minimum number of rivets necessary at the lower end of the rafter is $10\cdot49 \div 2\cdot81 = 4$, and at the upper end, bar No. 6, is $9\cdot22 \div 2\cdot81 = 4$.

If possible, these angles should be made in one piece from ridge to eaves, otherwise joints must be made over the central gusset.

(8) *Struts.*—The main strut, bar No. 14, is 128 in. long, panel point to panel point, and the load in it is $- 2\cdot97$ tons. The value $q = 1$ should be taken for this member, so that $qL = 128$. If the value of qL/κ is to be less than 120, the smallest section which can be used is two $3\frac{1}{2} \times 3 \times \frac{1}{4}$ angles back to back, min. $\kappa = 1\cdot09$, $qL/\kappa = 128 \div 1\cdot09 = 118$. The crippling load for this strut, $a = 3\cdot12$ sq. in., using the Johnson formula, is $R = \dfrac{3\cdot12}{2240}\left\{40{,}000 - \dfrac{4}{3}(118)^2\right\} = 29\cdot8$ tons; and $\eta = 29\cdot8 \div 2\cdot97 = 10$. The strength is therefore more than sufficient in both directions. A $3 \times 2\frac{1}{2} \times \frac{1}{4}$ in. double angle would carry the load, but the ratio $qL/\kappa = 138$.

Two rivets in double shear at each end are required.

The size of secondary struts, bars Nos. 11, 12, 16, and 17, is likewise determined by the ratio qL/κ. Their length is 77 in., and the force in them $1 \cdot 19$ tons. The minimum value of κ for a $3 \times 3 \times \frac{1}{4}$ in. angle is $0 \cdot 59$ in. Hence, taking $q = 1$, the value of $qL/\kappa = 77 \div 0 \cdot 59 = 130$. This is over the limit, but the crippling load of the strut, according to the Johnson formula, is $14 \cdot 7$ tons, and the factor of safety is $14 \cdot 7 \div 1 \cdot 19 = 12 \cdot 3$. This is three times as much as is necessary, and the section will be adopted. Two rivets in single shear will be used in each end.

For a study of the stresses in a strut attached by its back (as are the above members), see § 167.

(9) *Diagonal Ties.*—Bars Nos. 9 and 10 (made in one piece). The maximum load occurs in bar No. 10, and is $+ 5 \cdot 53$ tons. At $8 \cdot 0$ tons/ sq. in. the net section required is $5 \cdot 53 \div 8 = 0 \cdot 7$ sq. in. Try a $3 \times 3 \times \frac{1}{4}$ in. angle. The gross area is $1 \cdot 43$ sq. in. Deducting the area of a rivet hole in the vertical flange, $\frac{3}{4} \times \frac{1}{4} = 0 \cdot 19$ sq. in., and one-half the area of the outstanding flange, § 151, $\frac{1}{2} \times 2 \cdot 75 \times \frac{1}{4} = 0 \cdot 35$ sq. in., the net area is $1 \cdot 43 - 0 \cdot 19 - 0 \cdot 35 = 0 \cdot 89$ sq. in., so that the section is worth $0 \cdot 89 \times 8 = 7 \cdot 1$ tons and is sufficiently strong. Three rivets in single shear, each worth $2 \cdot 64$ tons, will be required.

(10) *Main Tie Bar.*—Bars Nos. 7, 8, and 18. The maximum force occurs in bar No. 7 and is $9 \cdot 92$ tons. Two angles, $3 \times 3 \times \frac{1}{4}$ in., back to back, will be used, and, from the preceding calculation, will evidently carry the load. In fact, since these angles are attached one each side of the gussets, they are not eccentrically loaded, and the total net area might be counted in (see § 151). To carry the load of $9 \cdot 92$ tons, $9 \cdot 92 \div 2 \cdot 81 = 4$ rivets in double shear are required in the ends of this member. These rivets share the vertical reaction at the supports, and the arrangement shown in Fig. 331 will be adopted.

The double angle section will be carried right across, but owing to the great length of the bars, joints must be introduced at the panel points where bars Nos. 8 and 18, 108 and 18, meet. The maximum force in bar No. 8 is $7 \cdot 71$ tons, and in No. 18 is $4 \cdot 39$ tons. Four rivets, two in double shear, two in single shear, will easily carry the load. The arrangement of the joint is shown in (i) Fig. 331.

(11) *Secondary Ties.*—Bars Nos. 13 and 15, maximum load $2 \cdot 22$ tons. A $2\frac{1}{2} \times 2\frac{1}{2} \times \frac{1}{4}$ in. angle will easily carry this load, and 2 rivets in single shear are required.

(12) *Choice of Sections.*—Unless there are a large number of principals to be made, all of the same type, it is doubtful whether it is worth while to introduce the new section $2\frac{1}{2} \times 2\frac{1}{2} \times \frac{1}{4}$ in. for the above members. In the present design a $3 \times 3 \times \frac{1}{4}$ in. will be used for bars Nos. 13 and 15, and as both main struts and rafters are $3\frac{1}{2} \times 3 \times \frac{1}{4}$ in., there will only be two sections in the roof. This modification will increase the weight of each principal by 38 lb., but probably will not increase the cost.

(13) *Purlins.*—The area supported by a purlin is $12 \cdot 5 \times 7 \cdot 13$ sq. ft. When carrying its maximum load, it supports a dead weight of 7 lb. for the covering, plus 5 lb. for the snow = 12 lb./sq. ft. of area covered. The

component of this, normal to the sloping surface, is $12 \times (2/\sqrt{5})$ $= 10\cdot8$ lb./sq. ft. Adding to this the normal wind pressure, 12 lb./sq. ft., the total normal pressure is $22\cdot8$ lb./sq. ft., and the normal load on the purlin is $12\cdot5 \times 7\cdot13 \times 22\cdot8 \div 2240 = 0\cdot91$ ton. Taking the maximum bending moment as WL/10 (see § 201),

$$M = \frac{WL}{10} = \frac{0\cdot91 \times 12\cdot5 \times 12}{10} = 13\cdot7 \text{ inch-tons,}$$

and at 8 tons/sq. in. the required section modulus is $Z = 13\cdot7 \div 8$ $= 1\cdot71$ in.³. A $5 \times 3 \times \frac{5}{16}$ in. angle, $Z = 1\cdot83$, is sufficiently strong. The ratio of span to depth is $150 \div 5 = 30/1$, which is permissible in such cases. The above calculation neglects the effect of the component in the plane of the roof covering. There is little doubt that the latter is resisted, partially at least, by the stiffness of the covering in its own plane.

The purlins at the ridge act as part of the longitudinal wind bracing, (ii) Fig. 331, and are stressed as struts. They, however, carry only one-half of the normal pressure on the intermediate purlins.

(14) *Lay-out of Roof.*—The general arrangement of the roof is shown in (ii) Fig. 331. To complete the structure, the columns, their foundations, the girders supporting the intermediate principals, the longitudinal wind bracing, and the covering (if any) down to the eaves at the ends, must be designed. Suitable drainage arrangements must also be planned.

BIBLIOGRAPHY

Roof Construction

1. MERRIMAN AND JACOBY. *A Text Book on Roofs and Bridges.* New York, vol. i, 1926 ; vol. ii, 1932.
2. RICKER. *A Treatise on the Design and Construction of Roofs.* New York, 1912.
3. HOWE. *The Design of Simple Roof-Trusses in Wood and Steel.* New York.
4. HUNTER. The Structural Design of Engineering Factories. *Trans. Jun. Inst. Engrs.,* vol. xvii, 1906–7, p. 197.
5. —— *Bridge and Structural Engineers' Handbook* (Arrol's). London, 2nd ed., 1928.
6. BECK. *Structural Steelwork.* London, 1920.
7. SPENCER. *The Practical Design of Steel-Framed Sheds.* London, 1915.
8. GESTESCHI. *Hölzerne Dachkonstruktionen.* Berlin, 4th ed., 1928.
9. DISCHINGER U. KRAUS. *Dachbauten* (R.C. constr.). Berlin, 1928.
10. GREGOR. *Der Praktische Stahlhochbau,* Bd. I. Berlin, 5th ed., 1930.
11. BLAKE. *Roof Coverings, Their Manufacture and Application.* New York.

Drainage of Roofs

12. FIDLER, H. *Notes on Construction in Mild Steel,* London, 1907, p. 282.
13. KETCHUM. *The Design of Steel Mill Buildings,* New York, 5th ed., 1932, p. 456.

14. BECK. The Drainage of Roofs. *Architect's Journal.* July 23, Aug. 13, Sept. 10, Oct. 1 and 22, 1924.
For Wind Pressure on Roofs, see Bib., Chap. III.
For Tests on Roofs, see Refs. Nos. 24 and 25, Chap. XX.

QUESTIONS ON CHAPTER XII

In the following designs for roof trusses, assume that the horizontal wind pressure is 20 lb./sq. ft., and the weight of snow 5 lb./sq. ft. In closed-in buildings, take account of the negative pressure on the leeward side of the roof. The safe stresses and rivet details given in § 212 may be used.
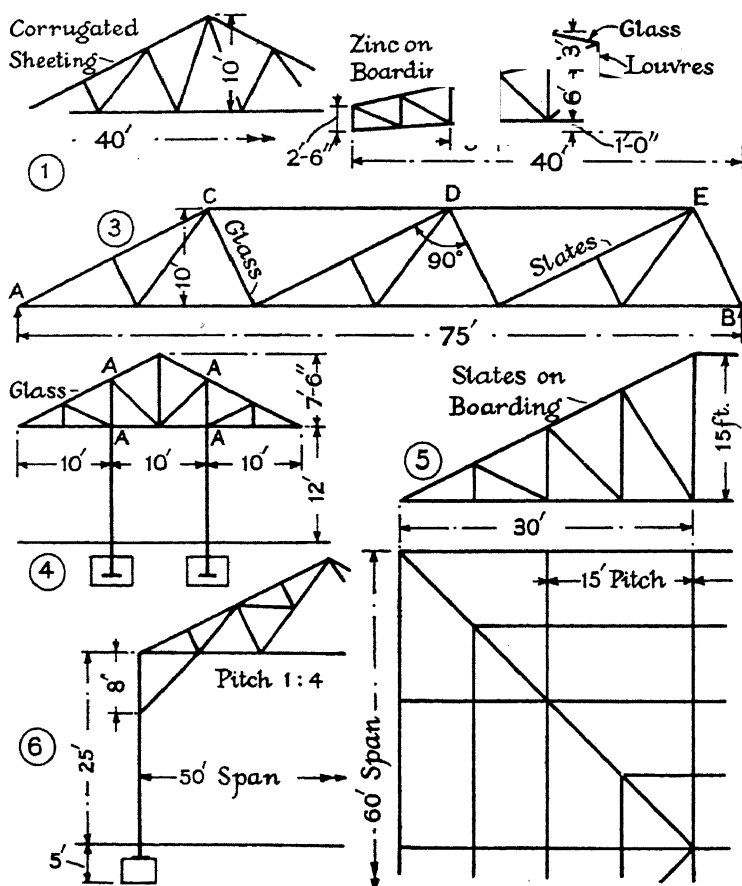
FIG. 332.

1. Roof over an open shed. Principals spaced 10 ft. apart, and carried on columns.

2. Roof over a building. Principals spaced 8 ft. apart and carried on brick walls.

3. Compound roof truss covering a factory building. Principals spaced 10 ft. apart and carried on columns. Neglect any effect which one truss may have in shielding the next from the wind. Hint : Find the forces in the members CD, DE by the method of sections.

4. The sketch represents the roof for an island railway platform. AA are two longitudinal girders running the full length of the roof. The columns are spaced 25 ft. apart longitudinally, and the pitch of the principals is 12 ft. 6 in.

5. Design the hipped end for the roof indicated in the figure.

6. Knee-braced roof truss for a closed-in building. Columns and principals spaced 12 ft. 6 in. apart. The roof is covered with glass. In this case the columns may be taken as hinged about the bottom of the concrete base.

CHAPTER XIII

ARCHES

213. Arches. Definition.—An arch, Fig. 335, may be loosely defined as a curved structure which supports a system of loads by virtue of the end thrusts which sustain it. It follows that the curvature must be convex to the direction of the applied loads. An arch may be, and normally is, subjected to bending moments throughout its length, but it is to be distinguished from a curved beam in that its stability is dependent on these thrusts.

214. The Linear Arch. The Line of Thrust.—If, for a system of vertical loads W_1, W_2, W_3 . . ., Fig. 333, a load line dg and pole O be
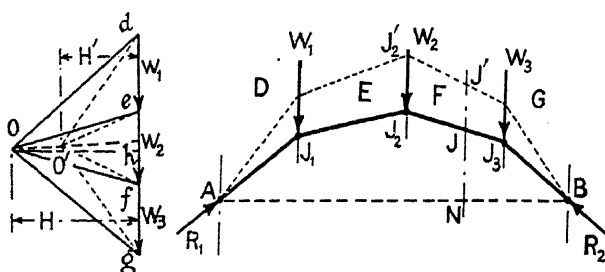
FIG. 333.

taken, and a funicular polygon AJ_2B be drawn, passing through the points AB, this funicular polygon represents the shape which a series of links would assume under the action of the given system of loads. Such a series of links would form an elementary arch which would support this particular load system. It is clear that the arrangement is in equilibrium, for the three forces meeting at the point J_1, viz. the thrusts in the links AJ_1 and J_1J_2 and the vertical load W_1, are represented in direction and magnitude by the sides of the triangle Ode in the force polygon. Similarly, the three forces which meet at the point J_2 are represented by the triangle Oef, and so on for the other points. The funicular polygon represents, therefore, the direction of the thrust at every point in this elementary arch ; and the magnitude of the thrust in each link is given by the lengths of the lines Od, Oe, Of . . . in the force polygon, measured to the force scale. Such a funicular polygon is termed a *linear arch*. Although in equilibrium under the particular load system, such a series of links would evidently be highly unstable, for the slightest variation in the load system would bring about the destruction of the whole arrangement.

For this reason a practical arch must possess rigidity, so that it will retain its shape notwithstanding the inevitable changes in the magnitude and direction of the thrusts which result from variation in the load conditions. For each load condition, however, there will be a funicular polygon corresponding to the linear arch AJ_2B, which will represent the direction of the thrust everywhere in the arch. This is called the *line of thrust*, and when it is known, the bending moment and stresses in the arch at every cross-section can be determined.

215. The Horizontal Thrust of the Arch.—Suppose that AJ_2B, Fig. 333, represents the line of thrust for an arch which is carrying the system of vertical loads W_1, W_2, W_3 . . . At any point J the direction of the line of thrust is J_2J_3. The magnitude of the thrust along J_2J_3 is given by Of in the force polygon, measured to the force scale, and so on. At the ends of the arch the directions of the thrust are given by the lines AJ_1 and BJ_3 respectively, and it is obvious that the reactions R_1 and R_2 at the supports are equal in magnitude to the thrusts in AJ_1 and BJ_3, but reversed in sense. It follows that in an arch the abutments must be capable of carrying not only vertical reactions, but both the vertical and horizontal components of these inclined reactions.

Draw a horizontal line Oh in the force polygon, and let $Oh = H$. The length H, measured to the force scale, is evidently the horizontal component of each of the forces Od, Oe, Of . . . That is to say, the horizontal component of the thrust in the arch is everywhere the same, provided that all the loads be vertical. Further, since H is the horizontal component of the thrusts in both AJ_1 and BJ_3, it is the horizontal component of the inclined reactions, i.e. it is the horizontal force which each abutment must carry. The vertical components of the reactions can be obtained by taking moments of the applied forces about A or B, or from the force polygon, Fig. 333. The magnitude of H must be obtained from the conditions of equilibrium of the arch.

It is clear that, by varying the position of the pole O, an indefinite number of lines of thrust corresponding to the load line dg can be drawn to pass through A and B. Only one of these can be the true line of thrust, and there can only be one value for H. The methods by which this is determined are given later. In the meantime it is useful to find the relations between two lines of thrust for a given load system, each passing through A and B.

From the properties of the funicular polygon, the moment M of all the vertical forces to the left of any section JN, Fig. 333, is given by the ordinate JN, measured to the distance scale, multiplied by H measured to the force scale (see § 33, Vol. I), i.e. $M = H \times JN$. M would evidently be the bending moment at the cross-section in a similarly situated beam. Let $AJ_2'B$, shown dotted, be the polygon corresponding to a new pole O' and a new polar distance H'. Then, as before, the moment M at the same section is $H' \times J'N$. Hence,

$$M = H \times JN = H' \times J'N \; ; \; \text{or} \; \frac{H}{H'} = \frac{J'N}{JN} \qquad (1)$$

That is to say, the ordinates at any section J'JN of two similarly situated funicular polygons vary inversely as the polar distances of the corresponding force polygons.

In certain simple cases the foregoing considerations are sufficient to determine the horizontal thrust of the arch. Let (i) Fig. 334 represent a parabolic arch carrying a uniformly distributed load, w per unit of length. The funicular polygon, or line of thrust, for this load condition, like the bending-moment diagram for a similarly loaded beam, will be a parabola. Hence a parabolic linear arch, theoretically, will support the load. If H be the horizontal thrust of such an arch, and D its rise, at the centre of the funicular polygon the moment
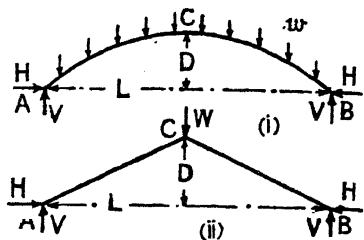
FIG. 334.

$$M = \frac{wL^2}{8} = H \times D \; ; \text{ and } H = \frac{wL^2}{8D} \qquad (2)$$

In a practical parabolic arch, thus loaded, the theoretical linear arch will form the centre line of the arch, and there will be no bending moment anywhere in the arch (cf. § 216). The stress on every cross-section will be a pure normal stress.

The above is true for every parabolic arch passing through A and B, with its vertex at C. The flatter the arch, the greater the horizontal thrust. The end conditions, whether hinged or fixed, do not affect the problem. This case is the converse of the suspension chain considered in § 233.

Similar reasoning applies to the pair of rafters carrying a load W as shown in (ii) Fig. 334. Here the funicular polygon is a triangle corresponding to the bending-moment diagram for a beam carrying a central concentrated load,

$$M = \frac{WL}{4} = H \times D \; ; \text{ and } H = \frac{WL}{4D} \qquad . \qquad . \quad (3)$$

For the technical terms used in connection with arches, see Fig. 479.

216. The Bending-Moment Diagram for an Arch.—Given a system of vertical loads on an arch, to find the bending moment everywhere. Let ACB, (i) Fig. 335, be the centre line of an arch, and suppose that STU be the line of thrust corresponding to the load system. Consider any plane section K_1KK_2 normal to the centre line, and let F, (ii), be the thrust of the arch at this section. The direction of F will be that of the line of thrust at the point where it crosses the section K_1K_2, and its magnitude is given by the line Of, drawn parallel to F, in the force polygon (iii). F is evidently the resultant of all the forces acting on the arch to the right of K_1K_2.

Unless F act through the centre of area K of the cross-section, it will

produce a bending moment at the section of magnitude M, equal to the moment of the force F about K. Draw a vertical through K cutting the line of thrust at J, (ii) Fig. 335. Then F may be resolved into two components acting at J, F sin ϕ in a vertical direction, and F cos ϕ acting horizontally ; ϕ is the angle which F makes with the horizontal. The moment of the vertical component about K is zero, the moment of the horizontal component is F cos ϕ × JK. Hence the moment of F about K, which is equal to the sum of the moments of its two components, is 0 + F cos ϕ × JK, and the bending moment at K is M = F cos ϕ × JK.
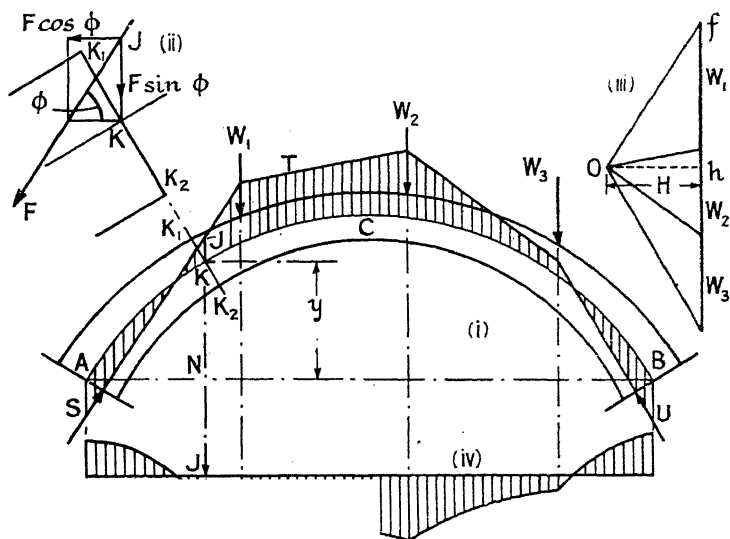
FIG. 335.

Now F cos ϕ = H, the horizontal thrust of the arch, represented by Oh in the force polygon, (iii). If JK = μ, then

$$M = H \times JK = H\mu \qquad (1)$$

That is to say, the bending moment at any cross-section is equal to the horizontal thrust H of the arch multiplied by μ, the vertical distance between the line of thrust and the centre line of the arch at the cross-section. This is known as Eddy's theorem.[12] Since all the loads are vertical, H is constant ; the ordinate μ represents, therefore, to some scale, the bending moment at the cross-section, and the shaded area in (i) Fig. 335 may be regarded as the bending-moment diagram for the arch, with STU as the base line. If preferred, it might be plotted from a straight base line as shown at (iv). If μ be measured to the length scale in inches, and H to the force scale in tons, M = Hμ is in inch-tons.

Signs.—Ordinates measured above the line of thrust are considered as positive and represent a bending moment tending to increase the curva-

ture of the arch. Ordinates measured below the line of thrust represent a negative bending moment tending to decrease the curvature.

From the above theory an important equation can be deduced which applies to all arches. It will be evident from Fig. 335 that eq. (1), $M = H \times JK = H\mu$, may be written $M = H(-JN + KN)$ [in (iv) Fig. 335, μ at section K is negative]. But from the theory of the funicular polygon [cf. eq. (2), § 33, Vol. I], $H(-JN) = M'$, the bending moment at the section K of a similarly loaded beam. If the arch be hinged at the ends, the support moments are zero, and the beam is merely supported at its ends; if, as in Fig. 335, there be support moments represented by SA and UB at the ends of the arch, equal support moments must be applied at the ends of the beam. These must be determined by the methods of § 222. As before, a bending moment tending to make the beam concave upward is considered negative. Further, if the ordinate of the centre line of the arch $KN = y$, the expression for M may be written

$$M = H \times JK = H(-JN + KN) = M' + Hy \quad . \quad . \quad (2)$$

This equation is deduced in a different manner for a three-hinged arch in § 217, eq. (2).

It is evident that if the true line of thrust for the arch can be found, the bending moment everywhere is known, and the stress in the material can be found. There are three cases to consider, (i) a three-hinged arch, (ii) a two-hinged arch, and (iii) an arch in which the ends are fixed in direction.

217. The Three-hinged Arch.—In a three-hinged arch, Fig. 336, a hinge or joint is provided at the springings A and B, and also at the crown C. Neglecting any friction there may be, it is evident that the hinges can transmit no bending moment; i.e. μ at a hinge is zero, and the line of thrust passes through the centre of the hinge. The problem reduces, therefore, to finding a line of thrust for the given system of loads which passes through three given points. A graphical solution is simple,

Fig. 336.

and to make the problem more general it will be assumed that the hinges A, B, and C, (i) Fig. 337, are not symmetrically placed. With a load line dg, and any pole O_1, draw the force polygon (ii) for the given load system. Starting with a line in the space F, parallel to O_1f, *and passing through* C, draw the line of thrust A_1CB_1, cutting the verticals through A and B in A_1 and B_1 respectively. This line of thrust will, in general, not pass through A and B. Join A_1B_1 and draw O_1h in the force polygon parallel to A_1B_1. Through h, draw Oh parallel to AB, and take a new pole O such that $H : H_1 :: CN_1 : CN$; where H and H_1 represent the polar

distances of the poles O and O_1, and CN and CN_1 are the vertical heights of C above the lines AB and A_1B_1 respectively. Then a line of thrust drawn to suit the pole O will pass through A, B, and C.

This is the true line of thrust for the three-hinged arch. The ordinate μ at any section K, Fig. 336, is now known, and the bending moment there is $M = H\mu$; H is measured to the force scale, μ to the length scale.
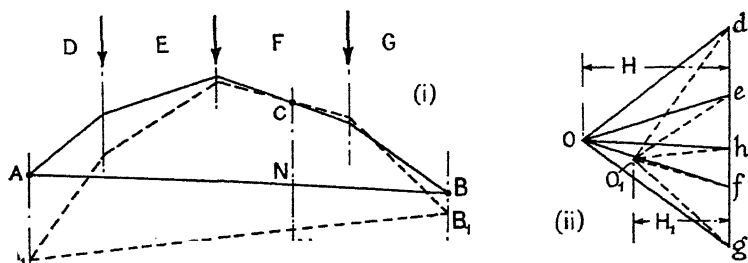
FIG. 337.

Analytical Treatment.—The bending moment at any section of a three-hinged arch carrying vertical loads may be found analytically as follows : Let ACB, Fig. 338, represent the arch, span L, rise D, and let K be any point on the centre line. Since the forces acting on the pin C are in equilibrium, they cannot in any way affect the external forces acting on the structure. Therefore the vertical reactions V_1 and V_2, acting at A and B respectively, can be found by taking moments of the vertical forces about B and A in turn, exactly as in the case of a beam. The
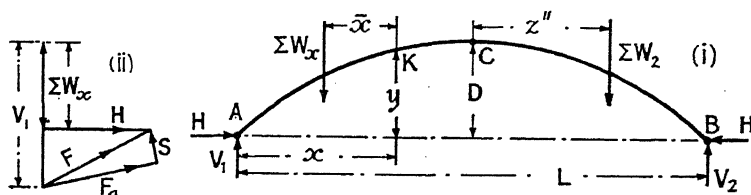
FIG. 338.

horizontal thrust can be found by taking moments about the pin C. Let ΣW_2 be the total load acting on the right-hand side of the arch, and z'' the distance of its centre of gravity from C. Then,

$$(\Sigma W_2)z'' - V_2\frac{L}{2} + HD = 0 \quad \text{or, } H = \frac{V_2L}{2D} - \frac{(\Sigma W_2)z''}{D} \quad (1)$$

which determines the horizontal thrust H.

Consider next the forces acting on the arch to the left of section K. The moment of these forces about K will be the bending moment at K. Let ΣW_x be the total load acting on the arch to the left of K, and $\bar{x}$ the distance of its centre of gravity from K ; then,

$$M_K = - V_1x + (\Sigma W_x)\bar{x} + Hy = M_K' + Hy \quad (2)$$

where $M_K' = - V_1 x + (\Sigma W_x)\bar{x}$. M_K' is the negative bending moment which would occur at a section K distant x from the left-hand reaction of a beam, supported at the ends, and carrying a like vertical load system to the arch. In Fig. 336 M_K' is represented to scale by JN, and KN represents Hy ; the difference $JK = \mu$ represents M_K, the bending moment on the arch. Having found H, the true polar distance is known, and the line of thrust can be drawn.

Alternatively, the magnitude and direction of the thrust at K can be determined as follows : Consider the forces to the left of K. The vertical component of the thrust at K is $(V_1 - \Sigma W_x)$. The horizontal component is H. The resultant F of these two components, (ii) Fig. 338, represents in magnitude and direction the thrust at K. This may be resolved normally and tangentially to the cross-section as shown. The normal component F_a produces a direct stress on the cross-section, the tangential component S produces a shear stress. The bending moment at K can be found from eq. (2) above ; the bending and direct stresses must be properly combined.

218. Three-hinged Spandrel-braced Arch.—In a three-hinged spandrel-braced arch, (i) Fig. 339, it is not necessary to draw the line of
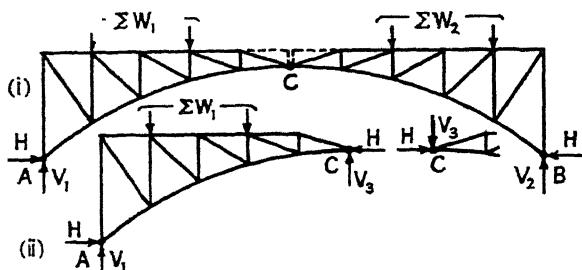
FIG. 339.

thrust. The reactions on all three pins should be determined, and the forces in the bars found by drawing a stress diagram, or otherwise as may be convenient. The reactions V_1, V_2, and H can be obtained by the analytical method of § 217. The reactions at the pin C can be found by considering the equilibrium of one-half the arch, (ii). The horizontal reaction at C is evidently equal to H ; the vertical reaction $V_3 = \Sigma W_1 - V_1$. All the external forces are now known and the stress diagram for each half of the arch can be drawn.

Worked Example.—(i) Fig. 340 represents the outline of a three-hinged spandrel-braced arch. It carries three loads of 10, 20, and 30 tons respectively in the positions shown. Draw the stress diagram for the left-hand side of the arch (I.C.E.). Find the vertical reactions by taking moments about the right-hand end pin. Using the panel length as a unit, $V_1 \times 10 = 30 \times 2 + 20 \times 7 + 10 \times 9$; $V_1 = 29$ tons ; $V_2 = 10 + 20 + 30 - 29 = 31$ tons.

Find H by taking moments about the centre pin ; for the left-hand

side of the arch, (ii), $29 \times 70 - 10 \times 56 - 20 \times 28 = H \times 25$; $H = 36 \cdot 4$ tons. $V_3 = \Sigma W_1 - V_1 = 10 + 20 - 29 = 1$ ton. The external forces on the left-hand side of the arch are then as shown in (ii). They are evidently in equilibrium. The stress diagram can be drawn in the usual way ; it is shown in (iii). To obtain an accurate stress diagram for a structure with a curved flange such as (i) Fig. 340, the outline (ii) must be set out to a large scale.
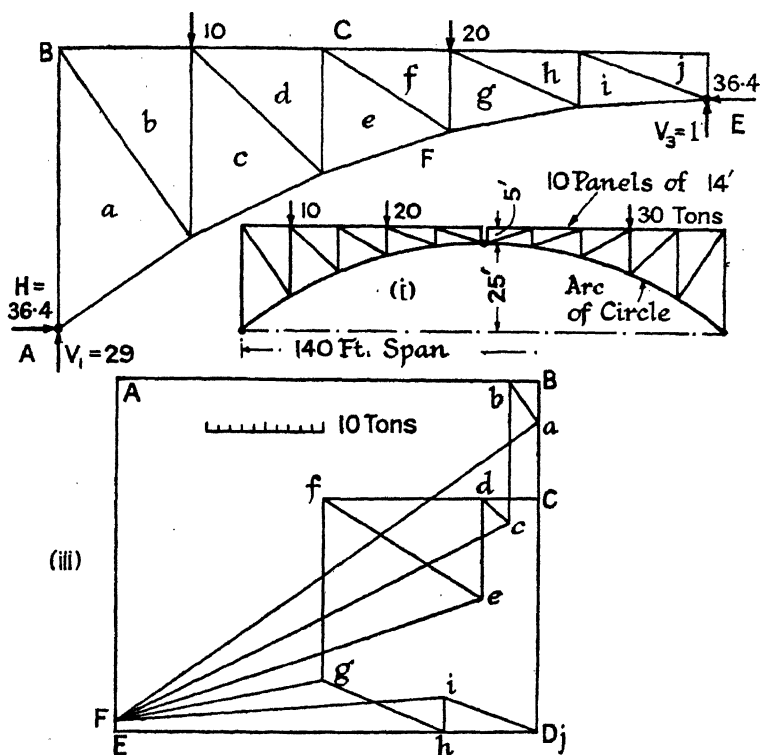
FIG. 340.

219. Unsymmetrical Three-hinged Arch. Any Load System.—The more general problem of an unsymmetrical three-hinged arch, carrying loads which are not vertical, can be solved graphically by the method shown in Fig. 341. Let ACB be the arch, R' the resultant of all the loads on the arch between A and C, and R'' the resultant of all the loads between C and B. First suppose that R' is the only load on the arch. Join BC and produce to cut R' in G_1, join AG_1. Then BG_1 is the line of action of the reaction R_2', and AG_1 that of the reaction R_1'. The magnitudes of these reactions can be found by resolving the resultant R' along G_1B and G_1A as shown at (ii). Next suppose that R'' is the only load on the arch. Join AC and produce to cut R'' in G_2; join BG_2. Then AG_2 is

the line of action of the reaction R_1'', and BG_2 is the line of action of the reaction R_2''. The magnitude of these reactions can be found by resolving R'' along G_2A and G_2B as shown at (iii). When R' and R'' both act on the arch, the magnitude and direction of the total reactions can be found by combining R_1' and R_1'' to find R_1 as at (iv), and by combining R_2' and R_2'' to find R_2 as at (v). The thrust R_3 on the pin at C can be found by combining R_1'' and R_2' as shown at (vi).

The line of thrust can now be set out. In (vii), let pq and qr represent R' and R'' respectively. Then rO and Op, drawn parallel to R_2 and R_1, will represent in magnitude and direction these reactions, and O will be the true pole. Set out $W_1 \ldots W_6$ the components of R' and R'',
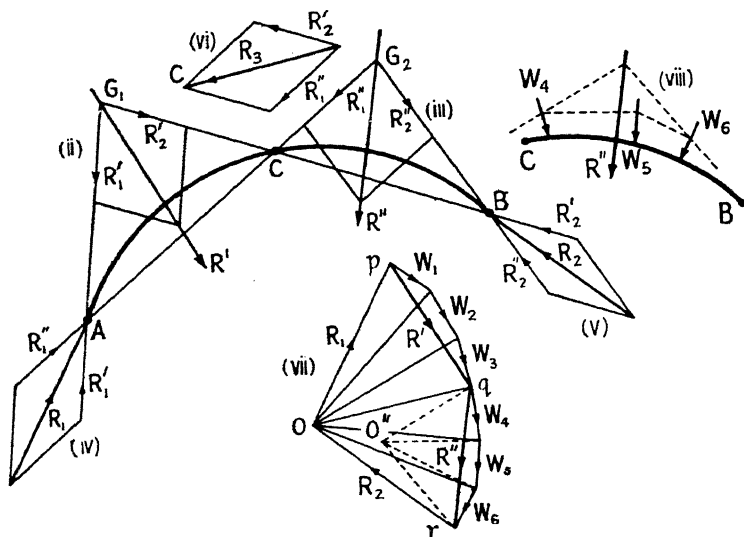
FIG. 341.

join to the pole O, and draw the line of thrust in the usual way. It will pass through the three pins.

For the purpose of finding R' and R'' from the given loads on the arch, subsidiary funicular polygons can be used as shown at (viii). The force polygon for (viii) is shown by the broken lines in (vii), the pole being O''.

When the loads are not vertical, the horizontal thrust of the arch, H, is not constant. H_1, the horizontal thrust at A, is the horizontal component of R_1; H_2, the horizontal thrust at B, is the horizontal component of R_2; and H_3, the horizontal thrust at C, is the horizontal component of R_3. The sum of the horizontal components of all the external forces acting on the arch to the left of C, including H_1, must be equal to the sum of the horizontal components of all the external forces acting on the arch to the right of C, including H_2, and each sum must be equal to H_3 in magnitude. Eddy's theorem, § 216, will still apply : that is to say, the

bending moment at any cross-section of the arch is equal to the horizontal thrust H multiplied by μ, the vertical distance between the line of thrust and the centre line of the arch at the cross-section, $M = H\mu$; but in this case, H is the horizontal component of the thrust on the particular cross-section.

220. Two-hinged Arch.—In a two-hinged arch, Fig. 342, hinges are provided at the springings A and B only.   It follows that the line of thrust must pass through the points A and B.   An indefinite number of lines of thrust can be drawn passing through two points A and B, and in order to determine the true line of thrust, a second condition must be taken into
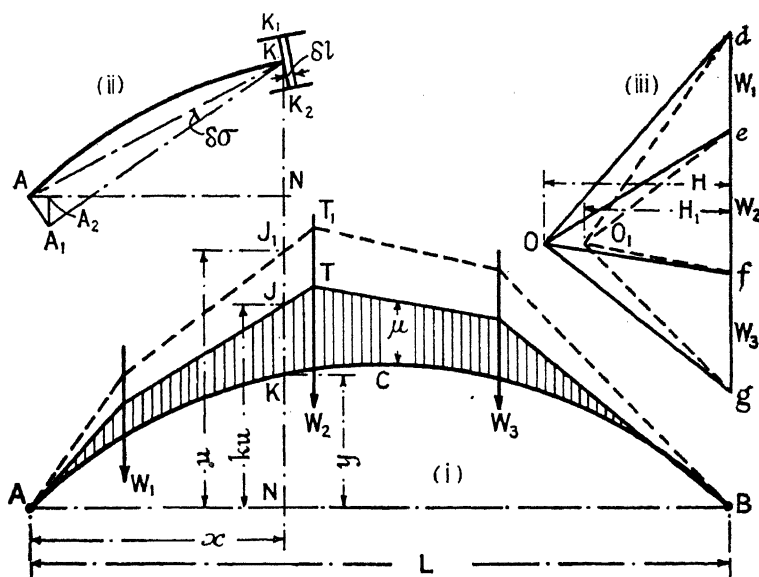
FIG. 342.

account.   This condition is that the distance between the points A and B is assumed to remain constant.

Consider a thin slice of the arch K_1KK_2, (ii) Fig. 342, contained between two normal sections, and δl in thickness.   Suppose that the bending moment which acts on the slice is M, and that it causes a change of slope $\delta\sigma$ in the elementary length δl.   Then from eq. (5), § 91, Vol. I, $\dfrac{M}{EI} = \dfrac{\delta\sigma}{\delta l}$, where I is the moment of inertia of the cross-section at K.   As a consequence of this change of slope, suppose that A would move to A_1 were it free to do so.   It is to be understood that AA_1 is the motion resulting from the deformation of the elementary strip only ; it is the motion which would occur if the arch to the right of the strip were held fixed, and the pin at A removed, the portion of the arch to the left of the strip remaining rigid.   Then the angle AKA_1 is the change of slope $\delta\sigma$,

that is to say, $\delta\sigma = \dfrac{AA_1}{AK} = \dfrac{M}{EI} \cdot \delta l$. Now the horizontal component of the motion AA_1 is AA_2. But, by similar triangles,

$\dfrac{AA_2}{AA_1} = \dfrac{KN}{AK}$; hence, $AA_2 = \dfrac{AA_1}{AK} \cdot KN = y \cdot \delta\sigma = \dfrac{M}{EI}y \cdot \delta l$, if $KN = y$.

AA_2 is the horizontal motion of A due to the deformation of the elementary strip δl. Similarly, every elementary strip from A to B will cause a horizontal movement of A, some a positive motion, some a negative motion. The total horizontal movement of A is the addition of all these motions, which is $\displaystyle\int_A^B \dfrac{M}{EI}y \cdot dl$. But if AB is a fixed length, the horizontal motion of A must be zero. Hence,

$$\int_A^B \dfrac{M}{EI}y \cdot dl = 0 \qquad\qquad . \quad (1)$$

Graphical Procedure.—For the given system of vertical loads on the arch, take any pole O_1, (iii) Fig. 342, polar distance H_1, and draw a line of thrust AT_1B, making it pass through A and B. The construction given in § 217 can be used for this purpose. Let the ordinate J_1N of this line of thrust, measured on the vertical KN, be u. Suppose that ATB be the true line of thrust, at present unknown, which also passes through A and B, and let the ordinate JN of this, measured on the vertical KN, be ku, where k is a constant. If the value of k can be discovered, and a new line of thrust be drawn using a polar distance $H = H_1 \div k$, the ordinates of the new line of thrust will be k times those of the old, eq. (1), § 215; that is to say, H will be the true polar distance and will represent to the force scale the true horizontal thrust of the arch.

Now from § 216, the bending moment at K is

$$M = H \cdot KJ = H(KN - JN) = H(y - ku) \qquad . \qquad . \quad (2)$$

(KJ in Fig. 342 is negative). Insert this value of M in eq. (1),

$$\int_A^B \dfrac{M}{EI}y \cdot dl = \int_A^B \dfrac{H}{EI}(y - ku)y \cdot dl = 0.$$

In this equation H, the horizontal thrust, is constant; E and k are constant; I may or may not vary. The integral can therefore be written,

$$-\dfrac{H}{E}k\int_A^B \dfrac{yu}{I} \cdot dl + \dfrac{H}{E}\int_A^B \dfrac{y^2}{I} \cdot dl = 0 \; ; \; \text{or,} \; k = \dfrac{\displaystyle\int_A^B \dfrac{y^2}{I} \cdot dl}{\displaystyle\int_A^B \dfrac{yu}{I} \cdot dl} \qquad (3)$$

If the values of I, y, and u are such that the integrals can be evaluated, the value of k is thus determined. It is usually necessary to adopt some semi-graphical procedure such as the following : Divide the centre line ACB into a number of equal parts each δl long. Measure the values of

y and u at the centre of each part, and tabulate the corresponding values of y^2/I and yu/I ; add these up.   Then since δl is constant,

$$k = \Sigma_A^B \frac{y^2}{I} \div \Sigma_A^B \frac{yu}{I} \;\; ; \text{ and } H = H_1 \left[\Sigma_A^B \frac{yu}{I} \div \Sigma_A^B \frac{y^2}{I} \right] \quad . \quad . \quad (4)$$

The following tabular arrangement should be used :

Ordinate.	y	u	I	$\dfrac{yu}{I}$	$\dfrac{y^2}{I}$
0	* *	* *	* *	* *	* *
1	* *	* *	* *	* *	* *
2	*· *	* *	* *	* *	* *
...	* *	* *	* *	* *	* *
...	* *	* *	* *	* *	* *
n					
				Σ	Σ

Inserting the summations in eq. (4), the value of H is determined, and the correct line of thrust can be set out.   The ordinate μ at any section between the line of thrust and the centre line, measured to the length scale, multiplied by H measured to the force scale, gives the bending moment at the section.   Alternatively, the bending moment M can be calculated from eq. (2), § 216, $M = M' + Hy$.

Analytical Treatment.—The value of H may also be found as follows : From eq. (2), § 216, $M = M' + Hy$, where M' is the moment about K of all the vertical forces to the left of that point ; i.e. it is equal to the bending moment* at a section K distant x from the left-hand reaction of a beam, span L, supported at the ends and carrying a like vertical load system to the arch.   Then from eq. (1),

$$\int_A^B \frac{M}{EI}y \, . \, dl = \int_A^B \frac{M' + Hy}{EI}y \, . \, dl = \int_A^B \frac{M'}{EI}y \, . \, dl + H\int_A^B \frac{y^2}{EI} \, . \, dl = 0$$

from which
$$H = - \frac{\displaystyle\int_A^B \frac{M'}{I}y \, . \, dl}{\displaystyle\int_A^B \frac{y^2}{I} \, . \, a} \qquad\qquad (5)$$

In finding M', the usual convention is to be observed that a bending moment making the beam concave upward is negative.

In cases where direct integration is impossible, the semi-graphical

* M' in this chapter is to be distinguished from the same symbol used in § 94.

procedure previously used can be adopted, and the centre line divided into equal parts δl, when

$$H = [\Sigma_A^B (- M'y/I) \div \Sigma_A^B y^2/I] \qquad (6)$$

the tabulation taking the form

Ordinate.	y	$- M'$	I	$- M'y/I$	y^2/I

Knowing H, the true line of thrust can be drawn, or the bending moment M everywhere can be calculated from eq. (2), § 216, $M = M' + Hy$.

From the theory of the funicular polygon, $- M' = H_1u$, Fig. 342, $H_1yu/I = - M'y/I$, and eq. (6) follows directly from eq. (4).

Integration Device.—Each integral in eq. (3) contains the factor $\delta l/I$; the semi-graphical integration described above is simplified if the parts into which the centre line ACB is divided are so chosen that $\delta l/I$ is constant for each part. The following graphical method of doing this is due to R. Mayer.* Assuming that the two halves of the arch are symmetrical, on a base line OC, Fig. 343, representing $l/2$ the developed length of the half centre line, plot a curve TU representing the value of $1/I$ for every point in the half arch. Divide this curve into a number of parts by means of the ordinates 0 . . . 5, which need not be equally spaced. Unequal spacing is convenient in that it permits sudden
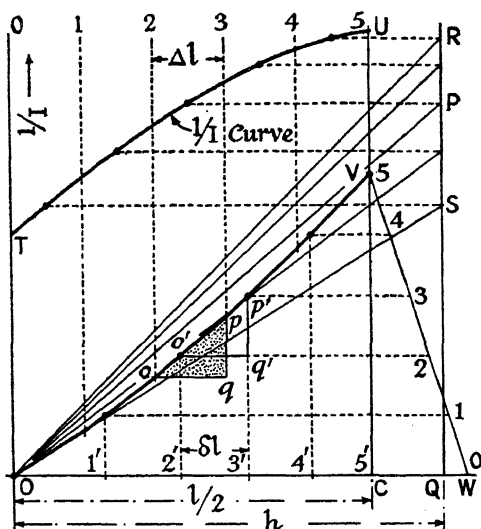
FIG. 343.

variations in $1/I$ to be taken into account more easily (see the worked example, §. 221). Project across from the centre of each element on to a vertical RQ at a convenient distance from O. Using O as pole, and RQ as 'load' line, draw the funicular polygon OV, such that op in the space 2 . 3 is parallel to OP and so on. Then by similar triangles,

$$\frac{pq}{oq} = \frac{PQ}{OQ}; \text{ or, } pq = \frac{PQ}{OQ} \cdot oq = \frac{1}{h}\left(\frac{\Delta l}{I}\right) \qquad . \quad (7)$$

* *Der Bauingenieur*, Bd. 6, 1925, p. 466.

since, for the element 2 . 3, $PQ = 1/I$; $oq = \Delta l$; whilst $OQ = h$. Now CV is the sum of all such elements as pq, hence

$$CV = \frac{1}{h}\Sigma_0^{l/2}\frac{\Delta l}{I} \qquad . \quad . \quad . \quad . \quad (8)$$

Divide the distance CV into n equal parts (in the figure there are five) by means of the sloping line VW, and project across to cut the funicular polygon. Then the triangle $o'p'q'$ corresponds exactly with the triangle opq, and as in eq. (7), $p'q' = \frac{1}{h}\left(\frac{\delta l}{I}\right)$. But $p'q' = 1/n$th of CV and is constant for every segment such as $2' . 3'$. Therefore the segments $0 . 1'$; $1' . 2' \ldots$ represent values of δl for which $\delta l/I$ is constant, and are those required for the integration. For clearness, $l/2$ in the figure has been divided into five parts only; in practical work a closer subdivision is necessary. It will be observed from eq. (7) that

$$pq = \frac{PQ . oq}{OQ} = \text{(area of the } 1/I \text{ curve between the ordinates 2 . 3)} \div h.$$

Hence CV represents the area OTUC, and the curve OV might be set out by repeated use of a planimeter or by means of an integraph.

From eqs. (3), (4) and (6), if $\delta l/I$ be constant, $k = \Sigma_A^B y^2 \div \Sigma_A^B yu$; and

$$H_1[\Sigma_A^B yu \div \Sigma_A^B y^2] \quad [\Sigma_A^B (- M'y) \div \Sigma_A^B y^2] \quad . \qquad (9)$$

To effect the integration therefore, divide the centre line of the arch into parts δl obtained from Fig. 343; measure y and u at the centre of each part; tabulate the values of yu and y^2; add them up; then insert the sums in eq. (9) to find the value of H.

Particular Case. As a first approximation it is sometimes assumed that $I = I_0 \sec \theta$, where I_0 is the moment of inertia at the crown of the arch, and θ is the inclination of the arch to the horizontal at any section. Then $dl \quad dx \times \sec \theta$, and the integrals of eq. (3) become

FIG. 344.

$$\frac{1}{I_0}\int_A^B y^2 . dx; \qquad \frac{1}{I_0}\int_A^B yu . dx$$

whence, from eqs. (4) and (6),

$$H = H_1\left[\int_A^B yu . dx \div \int_A^B y^2 . dx\right] = \left[\int_A^B - M'y . dx \div \int_A^B y^2 . dx\right] \quad (10)$$

As an example of the above method of treatment, consider the case of a *two-hinged parabolic arch* ACB [(i) Fig. 344], span L, rise D, in which
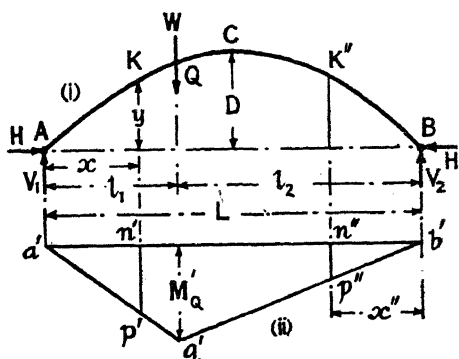
$I = I_0 \sec \theta$, and carrying a single concentrated load W at a point Q distant l_1 from A.   The equation to the parabola is

$$y = \frac{4D}{L^2} x(L - x) \qquad (11)$$

The bending-moment diagram for the load W, were it carried by a beam of span L, would be the triangle $a'q'b'$ [(ii) Fig. 344] of which the maximum ordinate is $M_Q' = - Wl_1l_2/L$, and the ordinate at any section distant x from A is

$$n'p' \qquad M' = - \frac{Wl_1l_2}{L} \times \frac{}{l_1} = - \frac{Wl_2x}{L}.$$

Similarly, working from the other end, the ordinate at any section distant x'' from B is $n''p'' = - Wl_1x''/L$.   Then the integral [eq. (10)],

$$\int_A^B - M'y \,.\, dx = + \int_0^{l_1} \frac{Wl_2x}{L} y \,.\, dx + \int_0^{l_2} \frac{Wl_1x''}{L} y \,.\, dx''.$$

Eq. (11) for y, owing to its symmetrical form, will hold for both these integrals if x be changed to x'' for the second.   Then,

$$\int_0^{l_1} \frac{Wl_2x}{L} y \,.\, dx = \frac{Wl_2}{L} \times \frac{4D}{L^2} \int_0^{l_1} (L - x)x^2 \,.\, dx \; ;$$

and

$$\int_A^B - M'y \,.\, dx = \frac{WDl_1{}^3l_2}{3L^3}[4L - 3l_1] + \frac{WDl_1l_2{}^3}{3L^3}[4L - 3l_2]$$

$$- \frac{WDl_1l_2}{3L^2}[l_1{}^2 + 3l_1l_2 + l_2{}^2] \; ; \text{ for } L = l_1 + l_2$$

The integral [eq. (10)],

$$\int_A^B y^2 \,.\, dx = \frac{16D^2}{L^4} \int_0^L x^2(L - x)^2 \,.\, dx = \frac{8}{15} D^2L.$$

Then, from eq. (10),

$$H = \left[\int_A^B - M'y \,.\, dx \div \int_A^B y^2 \,.\, dx \right] = \frac{5Wl_1l_2}{8L^3D}[l_1{}^2 + 3l_1l_2 + l_2{}^2] \qquad (12)$$

or, in terms of a single variable l_1,

$$H = \frac{5W}{8L^3D} \, l_1(L - l_1)(L^2 + Ll_1 - l_1{}^2) \; . \qquad . \;(13)$$

Knowing the magnitude of H, the bending moment everywhere in the arch can be found.

FIG. 345.

In a two-hinged *circular* or *segmental arch* of uniform cross-section (I = const.) carrying a single concentrated load W, Fig. 345, if R be the radius of the centre line, R and θ current co-ordinates,
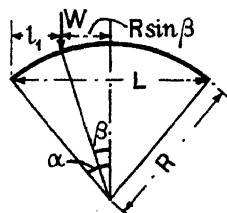
$$y = R(\cos \theta - \cos \alpha) \; ; \quad dl = R \,.\, d\theta.$$

From eq. (5),

$$H = - \int_0^{2a} M'y \cdot dl \div \int_0^{2a} y^2 \cdot dl$$

$$= W \frac{\frac{1}{2}(\sin^2 \alpha - \sin^2 \beta) - \cos \alpha(\alpha \sin \alpha + \cos \alpha - \beta \sin \beta - \cos \beta)}{\alpha - 3 \sin \alpha \cos \alpha + 2\alpha \cos^2 \alpha} \quad (14)$$

For a semicircular arch ($\alpha = 90°$),

$$H = W \cos^2 \beta / \pi = \frac{4W}{\pi L^2} \left\{ l_1(L - l_1) \right\} \quad . \quad . \quad . \quad . \quad (15)$$

221. Two-hinged Arch. Worked Example.—The span of a two-hinged circular arched rib is 180 ft., rise 30 ft., (i) Fig. 346; it carries
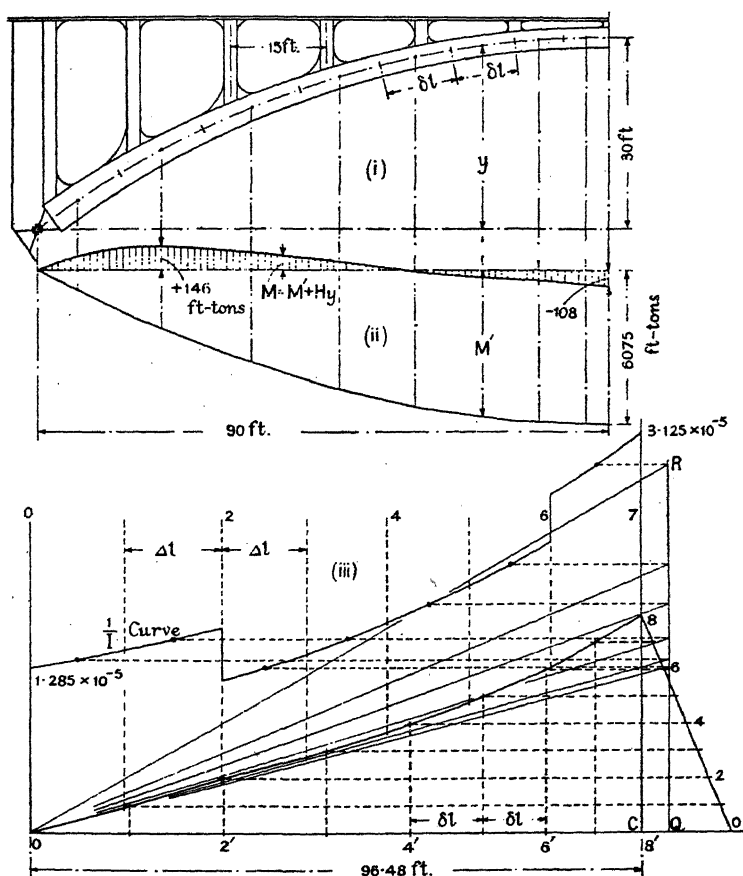
FIG. 346.

a total dead load of $1\frac{1}{2}$ tons per foot (measured horizontally). I at the crown $= 3 \cdot 20 \times 10^4$ in.⁴, I at the springings $= 7 \cdot 78 \times 10^4$ in.⁴ The

variation in $1/I$ is shown in (iii) Fig. 346. Find the horizontal thrust of the arch and the bending moment everywhere.

If R be the radius of the centre line of the arch,

$$(2R - 30)\,30 = 90^2\,; \quad \text{and } R = 150 \text{ ft.}$$

The length of the centre line of the arch from springings to crown is 96·48 ft.

From the given variation in $1/I$, find by the integration device of Fig. 343 the lengths δl for which $\delta l/I$ is constant. The construction is given in (iii) Fig. 346. It will be noted that the Δl ordinates have been chosen to suit the sudden variations in $1/I$. The values of δl are given in column 3 of the Table, the half centre line being divided into 8 parts.

The centre line can now be divided up, (i) Fig. 346, and the value of y at the centre of each δl division scaled or calculated, and entered in column 4 of the Table.

The load is transmitted to the arch by verticals placed 15 ft. apart, so that the load on each is $15 \times 1\frac{1}{2} = 22\frac{1}{2}$ tons. Set out the M′ diagram, (ii) Fig. 346. This may be done graphically or by calculation, treating the loads as if they were carried on a beam of 180 ft. span supported at each end. The value of $-$ M′ for the centre ordinate of each δl division is entered in column 5 of the Table. If y is given in feet, $-$ M′ should be given in ft.-tons. The values of $-$ M′y and y^2 can now be calculated and entered in columns 6 and 7. The summations $\Sigma\,(-\,$M′$y)$ and $\Sigma\,y^2$ are obtained by addition. From eq. (9), § 220,

$$H = \frac{\Sigma\,(-\,M'y)}{\Sigma\,y^2} = \frac{875,610}{4,402 \cdot 6} = 198 \cdot 9 \text{ tons.}$$

As both the arch and the load are symmetrical about the centre of the span, only one-half the arch is included in the above summations. Had the conditions been in any way unsymmetrical, it would have been necessary to include the whole arch.

A rough check on the value of H can be obtained by supposing the arch to be of parabolic outline, when from eq. (2), § 215,

$$H = \frac{wL^2}{8D} = \frac{1\frac{1}{2} \times 180^2}{8 \times 30} = 202 \cdot 5 \text{ tons.}$$

The value of M everywhere is most easily obtained from eq. (2), § 216, M = M′ + Hy. The values of Hy are given in column 8 of the Table, and the algebraic sum of columns 5 and 8 give the values of M, which are entered in column 9. These values are plotted in (ii) Fig. 346; the shaded area represents the dead load bending-moment diagram for the arch.

222. Arch Direction-fixed at each End.—If the arch be fixed in direction at its ends, there will be a bending moment at each abutment, which prevents any angular movement of the end cross-sections, exactly as in the case of a direction-fixed beam. As a consequence, the line of thrust will not pass through the points A and B, but will be displaced vertically by distances μ_1 and μ_2, as shown in (i) Fig. 347, where ACB is

the centre line of the arch and A′T′B′ the true line of thrust. From § 216, the fixing moment at A is $M_1 = H\mu_1$, and at B is $M_2 = H\mu_2$. To

Ordinate.	1/I	δl*	y	— M′	— M′y	y²	Hy	M=M′+Hy
	1/in.⁴	ft.	ft.	ft.-tons.	ft.-tons.	ft.²	ft.-tons.	ft.-tons.
0	1·285×10⁻⁵							
		15·6	4·53	802	3,630	20·5	901	+ 99
1								
		14·6	12·30	2,300	28,290	151·3	2,446	+146
2								
		16·2	18·86	3,635	68,560	355·7	3,751	+116
3								
		13·3	23·75	4,674	111,010	564·1	4,724	+ 50
4								
		11·6	26·81	5,346	143,330	718·8	5,333	— 13
5								
		10·1	28·65	5,732	164,220	820·8	5,698	— 34
6								
		7·7	29·58	5,949	175,970	875·0	5,883	— 66
7								
		7·4	29·94	6,032	180,600	896·4	5,955	— 77
8	3·125×10⁻⁵							

(1/I column note, running vertically: "For variation see (iii) Fig. 346.")

Totals: 875,610   4,402·6

* Giving equal values of δl/I.

$$H \quad \frac{875,610}{4,402\cdot6} = 198\cdot9 \text{ tons.}$$

FIG. 347.

find the line of thrust for a direction-fixed arch, these distances μ_1 and μ_2 must be determined, in addition to the constant k of § 220. There are

thus three unknowns, and three conditions of equilibrium must be taken into account. It will be assumed (*a*) that the horizontal distance between the points A and B remains constant ; (*b*) that the vertical movement of A relative to B is zero ; (*c*) that the ends remain fixed in their original direction, i.e. that the change of slope from A to B is zero (compare § 58, Vol. I). The first two conditions imply that the ends are fixed in position, the third that they are fixed in direction.

As in § 220, consider a thin slice K_1KK_2, (ii) Fig. 347, normal to the centre line at K and δl in thickness. Owing to the deformation of this thin slice, suppose that A would move to A_1 [see (ii)] were it free to do so. Then the angle $AKA_1 = \delta\sigma$, the change of slope in the elementary length δl ; and, as in § 220, $\delta\sigma = \dfrac{AA_1}{AK} = \dfrac{M}{EI} . \delta l$, where M is the bending moment on the slice. The horizontal component of the motion AA_1 is AA_2, where

$$AA_2 = \frac{AA_1}{AK} . KN = y . \delta\sigma = \frac{M}{EI} y . \delta l ;$$

if $KN = y$. But AB is constant, hence the total horizontal movement of A relative to B is zero, and

$$\int_A^B \frac{M}{EI} y . dl = 0 \qquad . \qquad . \qquad . \qquad . \qquad (1)$$

Similarly, the vertical component of the motion AA_1 is A_1A_2, where, by similar triangles, $A_1A_2 = \dfrac{AA_1}{AK} . AN = x . \delta\sigma = \dfrac{M}{EI} x . \delta l$, if $AN = x$. But A and B are fixed points, and the total vertical movement of A relative to B is zero, hence

$$\int_A^B \frac{M}{EI} x . dl = 0 \qquad . \qquad . \qquad . \qquad . \qquad (2)$$

Now the bending moment M on the elementary slice is made up of two parts : M_h, the bending moment which would exist if the ends of the arch were hinged, and M'', due to the fixing moments; so that $M = M_h + M''$ (*cf.* § 57, Vol. I). The value of M'' at A is $H \times \mu_1$, and at B is $H \times \mu_2$. Hence the trapezoid $ABB'A'$, (i) Fig. 347, can be regarded as a fixing-moment diagram. At the section KN, distant x from A, the fixing moment is $H \times NN'$, where NN' is the ordinate of the trapezoid ;

$NN' = \mu_1 + (\mu_2 - \mu_1)x/L$, and therefore, $M'' = H \left\{ \mu_1 + (\mu_2 - \mu_1)\dfrac{x}{L} \right\}$.

To obtain the value of M_h, proceed as in the case of the two-hinged arch. With a pole O_1, (iii) Fig. 347, and a polar distance H_1, draw any line of thrust AT_1B, passing through A and B, of which the ordinate $J_1N = u$. Suppose that ATB would be the true line of thrust on the arch if the fixing moments were zero, and let the ordinate JN of this curve $= ku$. Then, from § 216, $M_h = H \times JK = H(KN - JN) = H(y - ku)$. [KJ in Fig. 347 is negative]. The true bending moment at K is, therefore,

$$M = M_h + M'' = H(y - ku) + H \left\{ \mu_1 + (\mu_2 - \mu_1)\frac{x}{L} \right\} \qquad . \qquad (3)$$

Inserting this value in eq. (1),

$$\int_A^B \frac{M}{EI} y \cdot dl = \int_A^B \frac{H}{EI}\left[(y - ku) + \left\{ \mu_1 + (\mu_2 - \mu_1)\frac{x}{L} \right\} \right] y \cdot dl = 0.$$

Since H, E, and k are constant, this equation may be written

$$\frac{H}{E} \int_A^B \frac{1}{I}\left[(y - ku) + \left\{ \mu_1 + (\mu_2 - \mu_1)\frac{x}{L} \right\} \right] y \cdot dl = 0$$

or, $- k\int_A^B \frac{yu}{I} \cdot dl + \int_A^B \frac{y^2}{I} \cdot dl + \mu_1 \int_A^B \frac{y}{I} \cdot dl + \frac{\mu_2 - \mu_1}{L} \int_A^B \frac{xy}{I} \cdot dl = 0$. (4)

Similarly, from eq. (2),

$$\int_A^B \frac{M}{EI} x \cdot dl = \int_A^B \frac{H}{EI}\left[(y - ku) + \left\{ \mu_1 + (\mu_2 - \mu_1)\frac{x}{L} \right\} \right] x \cdot dl = 0$$

which reduces to

$$- k\int_A^B \frac{xu}{I} \cdot dl + \int_A^B \frac{xy}{I} \cdot dl + \mu_1 \int_A^B \frac{x}{I} \cdot dl + \frac{\mu_2 - \mu_1}{L} \int_A^B \frac{x^2}{I} \cdot dl = 0 \;.\; (5)$$

The third condition of equilibrium is that the change of slope from one end of the centre line of the arch to the other is zero. Now the change of slope in the elementary length δl is $\delta\sigma = \frac{M}{EI} \cdot \delta l$. Hence the total change of slope from A to B is

$$\int_A^B \frac{M}{EI} \cdot dl = 0 \tag{6}$$

Inserting the value of M from eq. (3),

$$\int_A^B \frac{M}{EI} \cdot dl = \int_A^B \frac{H}{EI}\left[(y - ku) + \left\{ \mu_1 + (\mu_2 - \mu_1)\frac{x}{L} \right\} \right] dl = 0$$

which, since H, E, and k are constant, reduces to

$$- k\int_A^B \frac{u}{I} \cdot dl + \int_A^B \frac{y}{I} \cdot dl + \mu_1 \int_A^B \frac{dl}{I} + \frac{\mu_2 - \mu_1}{L} \int_A^B \frac{x}{I} \cdot dl = 0 \quad . \; (7)$$

From the three equations (4), (5), and (7) the three unknowns μ_1, μ_2, and k can be determined, provided that the integrations can be effected. The semi-graphical method used for the two-hinged arch may be adopted. Divide the centre line ACB into a number of equal parts each δl long. Measure the values of x, y, and u at the centre of each part, tabulate the values of all the integrals in eqs. (4), (5), and (7), and make the necessary additions. Since δl is constant, these equations become

$$- k\Sigma_A^B \frac{yu}{I} + \Sigma_A^B \frac{y^2}{I} + \mu_1 \Sigma_A^B \frac{y}{I} + \frac{\mu_2 - \mu_1}{L} \Sigma_A^B \frac{xy}{I} = 0 \quad . \quad . \; (8)$$

$$- k\Sigma_A^B \frac{xu}{I} + \Sigma_A^B \frac{xy}{I} + \mu_1 \Sigma_A^B \frac{x}{I} + \frac{\mu_2 - \mu_1}{L} \Sigma_A^B \frac{x^2}{I} = 0 \quad . \quad . \; (9)$$

$$- k\Sigma_A^B \frac{u}{I} + \Sigma_A^B \frac{y}{I} + \mu_1 \Sigma_A^B \frac{1}{I} + \frac{\mu_2 - \mu_1}{L} \Sigma_A^B \frac{x}{I} = 0 \quad . \quad . \; (10)$$

three simultaneous equations giving the values of μ_1, μ_2, and k. The method of tabulation to be adopted is the following :

Ordinate.	x	y	u	I	$\dfrac{1}{I}$	$\dfrac{x}{I}$	$\dfrac{y}{I}$	$\dfrac{u}{I}$	$\dfrac{x^2}{I}$	$\dfrac{y^2}{I}$	$\dfrac{xy}{I}$	$\dfrac{xu}{I}$	$\dfrac{yu}{I}$
0	* *	* *	* *	* *	* *	* *	* *	* *	* *	* *	* *	* *	* *
1	* *	* *	* *	* *	* *	* *	* *	* *	* *	* *	* *	* *	* *
2	* *	* *	* *	* *	* *	* *	* *	* *	* *	* *	* *	* *	* *
3	* *	* *	* *	* *	* *	* *	* *	* *	* *	* *	* *	* *	* *
...	* *	* *	* *	* *	* *	* *	* *	* *	* *	* *	* *	* *	* *
...	* *	* *	* *	* *	* *	* *	* *	* *	* *	* *	* *	* *	* *
n													

$$\quad\quad A_1 \quad A_2 \quad A_3 \quad A_4 \quad A_5 \quad A_6 \quad A_7 \quad A_8 \quad A_9$$

Denoting the summations by $A_1 \ldots A_9$, and putting $\mu_1 = X$ and $(\mu_2 - \mu_1)/L = Y$, eqs. (8) to (10) become

$$\left.\begin{array}{l} A_3 X + A_7 Y - A_9 k + A_6 = 0 \\ A_2 X + A_5 Y - A_8 k + A_7 = 0 \\ A_1 X + A_2 Y - A_4 k + A_3 = 0 \end{array}\right\} \qquad . \ (11)$$

These equations may be solved as simultaneous in the usual way, or by means of the following determinant :

$$\frac{X}{\begin{vmatrix} A_7 & A_9 & A_6 \\ A_5 & A_8 & A_7 \\ A_9 & A_4 & A_3 \end{vmatrix}} : \frac{-Y}{\begin{vmatrix} A_3 & A_9 & A_6 \\ A_2 & A_8 & A_7 \\ A_1 & A_4 & A_3 \end{vmatrix}} = \frac{-k}{\begin{vmatrix} A_3 & A_7 & A_6 \\ A_2 & A_5 & A_7 \\ A_1 & A_2 & A_3 \end{vmatrix}} = \frac{-1}{\begin{vmatrix} A_3 & A_7 & A_9 \\ A_2 & A_5 & A_8 \\ A_1 & A_2 & A_4 \end{vmatrix}} \qquad . \ (12)$$

Great accuracy is necessary when solving this equation in order to obtain a correct result.

Knowing k, the correct polar distance $H = H_1/k$ can be found, and hence the line of thrust, ATB can be drawn. This is not the true line of thrust, which passes through A_1 and B_1. Since μ_1 and μ_2 have been determined, these points are known. Lower the line of thrust ATB by an amount equal to the ordinate of the trapezoid ABB′A′ at each section (i.e. J becomes J′, where JJ′ = NN′, and so on). Then A′T′B′ is the true line of thrust, and the shaded area is the bending-moment diagram for the arch. At any cross-section, the ordinate μ of this diagram, measured to the length scale, multiplied by H measured to the force scale, is the bending moment M at the section.

If the integration device of § 220 be used so that $\delta l/I = $ const. for each

segment, eqs. (4), (5), and (7) still hold, but I in the denominator of each term must be put equal to unity.

Since $H = H_1/k$, k may be replaced by H_1/H; and since $- M' = H_1 u$, where M' is the 'beam' bending moment (see the *Analytical Treatment*, § 220), eqs. (8), (9), and (10) may be written

$$\frac{1}{H} \Sigma_A^B \frac{M'y}{I} + \Sigma_A^B \frac{y^2}{I} + \mu_1 \Sigma_A^B \frac{y}{I} + \frac{\mu_2 - \mu_1}{L} \Sigma_A^B \frac{xy}{I} = 0 \qquad (13)$$

$$\frac{1}{H} \Sigma_A^B \frac{M'x}{I} + \Sigma_A^B \frac{xy}{I} + \mu_1 \Sigma_A^B \frac{x}{I} + \frac{\mu_2 - \mu_1}{L} \Sigma_A^B \frac{x^2}{I} = 0 \qquad (14)$$

$$\frac{1}{H} \Sigma_A^B \frac{M'}{I} + \Sigma_A^B \frac{y}{I} + \mu_1 \Sigma_A^B \frac{1}{I} + \frac{\mu_2 - \mu_1}{L} \Sigma_A^B \frac{x}{I} = 0 \qquad (15)$$

These equations may also be used if the integration device of § 220, $\delta l/I = $ const., be adopted; but I in the denominator of each term must be put equal to unity.

In finding M', the usual convention is to be observed that a bending moment which makes the beam concave upward is negative.

FIG. 348.

Analytical Method for Influence Lines. Symmetrical Arch.—For the purpose of constructing influence lines, if the arch be symmetrical, it is convenient to take origin at the crown* and consider each half of the arch separately. The co-ordinates x, y of any point K on the arch are as indicated in Fig. 348, not as in Fig. 347. The three unknowns at the crown of the arch are H, the horizontal thrust; V_0, the vertical shearing force; and M_0, the bending moment. From the three conditions of equilibrium set forth on p. 492, these unknowns can be determined. As before, bending moments tending to make the arch convex upward are called positive. Suppose that a single load W is applied at the point G distant z from the origin, and consider the deformation of the left-hand half of the arch. The bending moment at any point K between A and G is

---

* A further simplification of the equations results if origin be taken at the *elastic centre* O_E of the arch. $C_0 O_E = \int_A^c (y/EI)\, dl \div \int_A^c (1/EI)\, dl$. In this equation y is the ordinate to the centre line measured from AB. This procedure involves the preliminary summations indicated in order to find O_E, which minimises its advantages.

$M = W(x - z) - Hy - V_0x + M_0$; and at any point K between G and C is $M = - Hy - V_0x + M_0$. From eq. (1) the horizontal movement of C relative to A is

$$\int_C^A \frac{M}{EI} y \cdot dl = \int_G^A \frac{1}{EI}\{W(x - z) - Hy - V_0x + M_0\}y \cdot dl +$$

$$\int_C^G \frac{1}{EI}\{- Hy - V_0x + M_0\}y \cdot dl$$

$$= \int_G^A \frac{W}{EI}(x - z) y \cdot dl - \int_C^A \frac{1}{EI}\{Hy + V_0x - M_0\}y \cdot dl.$$

Treating the right-hand side of the arch in a similar way, the horizontal movement of C is

$$\int_C^B \frac{1}{EI}\{- Hy + V_0x + M_0\}y \cdot dl.$$

The sum of these two horizontal movements is the increase in span of the arch due to W, and this from Condition (a), the span remaining constant, is zero,

$$\int_G^A \frac{W}{EI}(x - z)y \cdot dl - \int_C^A \frac{1}{EI}\{Hy + V_0x - M_0\}y \cdot dl$$

$$+ \int_C^B \frac{1}{EI}\{- Hy + V_0x + M_0\}y \cdot dl = 0.$$

Since the arch is symmetrical, $AC = CB = l/2$, where l is the length of the centre line. Hence the equation reduces to

$$W\int_G^A \frac{(x - z)y}{I} \cdot dl - 2H\int_0^{\frac{l}{2}} \frac{y^2}{I} \cdot dl + 2M_0\int_0^{\frac{l}{2}} \frac{y}{I} \cdot dl = 0 \qquad . (16)$$

From eq. (2), considering the left-hand side of the arch, the vertical movement of C is

$$\int_C^A \frac{M}{EI} x \cdot dl = \int_G^A \frac{W}{EI}(x - z)x \cdot dl - \int_C^A \frac{1}{EI}\{Hy + V_0x - M_0\}x \cdot dl.$$

Considering the right-hand side of the arch, the vertical movement of C is

$$\int_C^B \frac{1}{EI}\{- Hy + V_0x + M_0\}x \cdot dl.$$

If, from Condition (b), the two supports A and B remain on the same level, these two vertical movements must be equal,

$$\int_G^A \frac{W}{EI}(x - z)x \cdot dl - \int_C^A \frac{1}{EI}\{Hy + V_0x - M_0\}x \cdot dl$$

$$= \int_C^B \frac{1}{EI}\{- Hy + V_0x + M_0\}x \cdot dl$$

or, since the arch is symmetrical,

$$W \int_G^A \frac{(x-z)x}{I} \cdot dl - 2V_0 \int_0^{\frac{l}{2}} \frac{x^2}{I} \cdot dl = 0$$

whence,

$$V_0 = \frac{W \int_G^A \frac{(x-z)x}{I} \cdot dl}{2 \int_0^{\frac{l}{2}} \frac{x^2}{I} \cdot dl} \tag{17}$$

From eq. (6), considering the left-hand side of the arch, the change of slope from C to A is

$$\int_C^A \frac{M}{EI} \cdot dl = \int_G^A \frac{W}{EI}(x-z) \cdot dl - \int_0^A \frac{1}{EI}\{Hy + V_0 x - M_0\} \cdot dl$$

and, considering the left-hand side, the change of slope from C to B is

$$\int_C^1 \frac{1}{EI}\{-Hy + V_0 x + M_0\} \cdot dl.$$

From Condition (c), since both ends of the arch are fixed in direction, the total change of slope from A to B is zero, hence

$$\int_G^A \frac{W}{EI}(x-z) \cdot dl - \int_0^A \frac{1}{EI}\{Hy + V_0 x - M_0\} \cdot dl + \int_C^B \frac{1}{EI}\{-Hy + V_0 x + M_0\} \cdot dl = 0$$

whence, taking account of symmetry,

$$W \int_G^A \frac{(x-z)}{I} \cdot dl - 2H \int_0^{\frac{l}{2}} \frac{y}{I} \cdot dl + 2M_0 \int_0^{\frac{l}{2}} \frac{dl}{I} = 0 . \tag{18}$$

Treating eqs. (16) and (18) as simultaneous,

$$H = \frac{W \int_G^A \frac{(x-z)y}{I} \cdot dl \times \int_0^{\frac{l}{2}} \frac{dl}{I} - W \int_G^A \frac{(x-z)}{I} \cdot dl \times \int_0^{\frac{l}{2}} \frac{y}{I} \cdot dl}{2\left[\int_0^{\frac{l}{2}} \frac{y^2}{I} \cdot dl \times \int_0^{\frac{l}{2}} \frac{dl}{I} - \left\{\int_0^{\frac{l}{2}} \frac{y}{I} \cdot dl\right\}^2\right]} . \tag{19}$$

and

$$M_0 = \frac{W \int_G^A \frac{(x-z)}{I} y \cdot dl \times \int_0^{\frac{l}{2}} \frac{y}{I} \cdot dl - W \int_G^A \frac{(x-z)}{I} \cdot dl \times \int_0^{\frac{l}{2}} \frac{y^2}{I} \cdot dl}{2\left[\int_0^{\frac{l}{2}} \frac{y^2}{I} \cdot dl \times \int_0^{\frac{l}{2}} \frac{dl}{I} - \left\{\int_0^{\frac{l}{2}} \frac{y}{I} \cdot dl\right\}^2\right]} \tag{20}$$

The three unknowns H, V_0, and M_0 can be found from eqs. (19), (17), and (20), and without solving simultaneous equations. If, for the

2 K

purpose of effecting the summations, the length l be divided into equal segments δl as in eqs. (8), (9), and (10),

$$H : \frac{W\Sigma_G^A \frac{(x-z)}{I} y \times \Sigma_C^A \frac{1}{I} - W\Sigma_G^A \frac{(x-z)}{I} \times \Sigma_C^A \frac{y}{I}}{2\left[\Sigma_C^A \frac{y^2}{I} \times \Sigma_C^A \frac{1}{I} - \left\{\Sigma_C^A \frac{y}{I}\right\}^2\right]} \qquad . (21)$$

$$\frac{W\Sigma_.^A \frac{(x-z)x}{I}}{2\Sigma_C^A \frac{x^2}{I}} \qquad . (22)$$

$$M_0 : \frac{W\Sigma_G^A \frac{(x-z)y}{I} \times \Sigma_C^A \frac{y}{I} - W\Sigma_G^A \frac{x-z}{I} \times \Sigma_A^C \frac{y^2}{I}}{2\left[\Sigma_C^A \frac{y^2}{I} \times \Sigma_C^A \frac{1}{I} - \left\{\Sigma_C^A \frac{y}{I}\right\}^2\right]} \qquad . (23)$$

If the integration device of § 220 be used, so that $\delta l/I = $ const. for each segment, eqs. (21), (22), and (23) will hold, but I in the denominator of each term must be put equal to unity.

In *elliptic arches*, or arches of the *basket-handle* type, it is best to use eqs. (19), (17), and (20) with dl altered to δl, for the purpose of effecting the summations, and to take shorter segments δl near the springings where the curvature is great.

Knowing H, V_0 and M_0, the bending moment everywhere in the arch can be calculated from the expressions for M given above.

223. Effect of Direct Thrust.—The above equations neglect the shortening of the arch axis due to the normal thrust F_a, Fig. 338. This is chiefly of importance in flat arches. The contraction in length of the strip $K_1 K_2$, (ii) Fig. 347, due to F_a, will be $F_a . \delta l/Ea$, where a is its area. The horizontal projection of this is $F_a . \delta l \times \cos\theta/Ea$, where θ is the inclination of the arch axis at K; and the total *shortening* of the span, supposing the ends were free to move, would be

$$\cdot \cos\theta . dl = \int_A^B \frac{(H\cos\theta + V\sin\theta)\cos\theta}{Ea} dl \qquad \int_A^B \frac{H}{Ea} . dl . \quad (1)$$

for $F_a = H\cos\theta + V\sin\theta$, eq. (2), § 229, and it is customary to assume for this purpose that $H\cos\theta + V\sin\theta = H\sec\theta$, which is only approximately true even when the inclination of the line of thrust to the arch axis is everywhere small.

Two-hinged Arch.—The expression on p. 485 for the *decrease* * in the span, leading to eq. (5), § 220, if corrected for the effect of direct thrust, should read, therefore,

$$\int_A^B \frac{M'}{EI} y . dl + H \int_A^B \frac{y^2}{EI} . dl + \int_A^B \frac{H}{Ea} . dl = 0$$

* See AA₂ (ii) Fig. 342.

and
$$H = - \frac{\int_A^B \frac{M'}{I} y \cdot dl}{\int_A^B \frac{y^2}{I} \cdot dl + \int_A^B \frac{1}{a} \cdot dl} \tag{2}$$

Direction-fixed Arches.—The expression on p. 496 for the alteration in the span, leading to eq. (16), § 222, if corrected for the effect of direct thrust, should read,

$$\int_G^A \frac{W}{EI}(x - z)y \cdot dl - \int_C^A \frac{1}{EI}\{Hy + V_0 x - M_0\} y \cdot dl$$
$$+ \int_C^B \frac{1}{EI}\{ - Hy + V_0 x + M_0\} y \cdot dl - \int_A^B \frac{H}{Ea} \cdot dl = 0$$

and eq. (16), § 222, becomes

$$W \int_G^A \frac{(x - z)}{I} y \cdot dl - 2H \left[\int_0^{\frac{l}{2}} \frac{y^2}{I} \cdot dl + \int_0^{\frac{l}{2}} \frac{dl}{a} \right] + 2M_0 \int_0^{\frac{l}{2}} \frac{y}{I} \cdot dl = 0 \tag{3}$$

To take account of this effect of the direct thrust, therefore, the term $\int (y^2/I)dl$ must be replaced by $\left[\int (y^2/I)dl + \int (1/a)dl \right]$ in the denominator of eqs. (19) and (20), § 222, and also in the numerator of eq. (20) ; similarly with eqs. (21) and (23), § 222, which become

$$H = \frac{W\Sigma_G^A \frac{(x - z)y}{I} \times \Sigma_C^A \frac{1}{I} - W\Sigma_G^A \frac{x - z}{I} \times \Sigma_C^A \frac{y}{I}}{2\left[\left\{ \Sigma_C^A \frac{y^2}{I} + \Sigma_C^A \frac{1}{a} \right\} \times \Sigma_C^A \frac{1}{I} - \left\{ \Sigma_C^A \frac{y}{I} \right\}^2 \right]} . \tag{4}$$

$$M_0 : \frac{W\Sigma_G^A \frac{(x - z)y}{I} \times \Sigma_C^A \frac{y}{I} - W\Sigma_G^A \frac{x - z}{I} \times \left\{ \Sigma_C^A \frac{y^2}{I} + \Sigma_C^A \frac{1}{a} \right\}}{2\left[\left\{ \Sigma_C^A \frac{y^2}{I} + \Sigma_C^A \frac{1}{a} \right\} \times \Sigma_C^A \frac{1}{I} - \left\{ \Sigma_C^A \frac{y}{I} \right\}^2 \right]} \tag{5}$$

Eq. (22), § 222, for V_0, may be used as it stands.

224. Abutment Displacements.—The above theory can be modified to take into account either horizontal, vertical, or angular displacements of the abutments, by equating the expressions representing the motions of the ends of the span to the said abutment displacements instead of to zero. Care must be taken regarding signs. See also § 93.

225. Temperature Stresses in Arches.—If the coefficient of linear expansion of the arch be a, and an increase in temperature $t°$ occur, every dimension of the arch would increase by at times its original length were it free to do so. Thus the span L of the arch would become $L(1 + at)$ in length. This increase in length is prevented by the rigidity
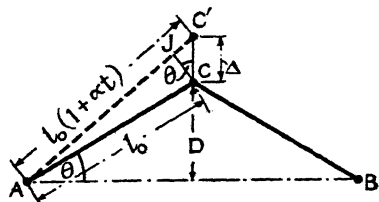
of the abutments, with the result that, in two-hinged and direction-fixed arches, temperature stresses and bending moments are set up which need to be taken into account. In a three-hinged arch an increase in temperature merely causes the crown of the arch to rise an amount Δ, which can be calculated. The distance l_0 from pin to pin, Fig. 349, becomes $l_0(1 + at)$, and $JC' = l_0at$. From the geometry of the figure,

$$\sin \theta = \frac{JC'}{C'C} = \frac{l_0at}{\Delta} = \frac{D}{l_0}\;;\; \text{and } \Delta = \frac{l_0{}^2at}{D}\frac{L^2 + 4D^2}{4D}\;at \qquad (1)$$

This movement relieves the arch of stresses primarily due to temperature.

Two-hinged Arch.—The attempt of a two-hinged arch to increase in span when the temperature rises is prevented by the abutments, which means that the horizontal thrust H is increased by an amount Ht. This extra force prevents the expansion. It produces at any section K, Fig. 342, a bending moment $M = Ht \times y$, where y is the ordinate at K. It was proved in § 220 that a bending moment M, acting on an elementary length δl of the arch, produces an alteration in length in the span AB of $(M/EI)y \cdot dl$, which, summed from end to end of the arch, implies a total alteration in length of span of

$$\int_A^B \frac{M}{EI}\,y \cdot dl = \int_A^B \frac{Ht}{EI}\,y^2 \cdot dl.$$

This is the negative alteration in length produced by Ht, and it must be equal in magnitude to the positive alteration Lat produced by the change of temperature, since the span does not alter. Hence

$$Lat = \frac{Ht}{E}\int_A^B y^2 \cdot dl\;;\; \text{or, } Ht = LEat \div \int_A^B \frac{y^2}{I} \cdot dl \qquad (2)$$

Knowing Ht, the bending moment $Ht\,y$ everywhere is known, and hence the temperature stresses can be found. It will be noted that the integral is one of those already evaluated in § 220. The line of thrust for Ht is evidently the line AB, which with the centre line of the arch forms the bending-moment diagram. The temperature stresses must be properly combined with those due to the loads on the arch.

Direction-fixed Arch.—In a direction-fixed arch, if as in most practical cases the arch be symmetrical about its centre, the effect of an increase in temperature will be to call into play a horizontal thrust Ht preventing an alteration in length of the span, and a fixing moment M_{1t} at each support preventing any change of direction there, Fig. 350.

As in Fig. 348, origin will be taken at the centre C. Suppose the bending moment there, due to temperature effects, to be M_{0t}. There will be no vertical force at C due to this cause. Then the bending moment
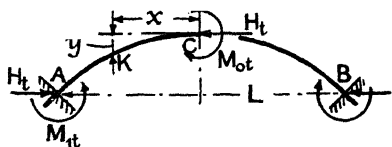
FIG. 350.

at $K(xy)$ will be $M = M_{0t} - H_t y$, and the resulting change in the length of span, § 222, will be

$$\int_A^B \frac{My}{EI} \cdot dl = 2 \int_0^{\frac{l}{2}} \frac{1}{EI}(M_{0t} - H_t y) \cdot dl.$$

The change in the length of span due to a rise $t°$ in temperature $= Lat$, hence the total change in span, which must be zero, is

$$2 \int_0^{\frac{l}{2}} \frac{1}{EI}(M_{0t} - H_t y)y \cdot dl + Lat = 0$$

whence

$$2M_{0t} \int_0^{\frac{l}{2}} \frac{y}{I} \cdot dl - 2H_t \int_0^{\frac{l}{2}} \frac{y^2}{I} \cdot dl + ELat = 0 \qquad . \qquad . \quad (3)$$

Further, since the ends of the arch are fixed in direction, the total change of slope from A to B must be zero ; hence, see eq. (6), § 222,

$$\int_A^B \frac{M}{EI} \cdot dl = \int_A^B \frac{1}{EI}(M_{0t} - H_t y) \cdot dl = 0$$

whence

$$2M_{0t} \int_0^{\frac{l}{2}} \frac{dl}{I} - 2H_t \int_0^{\frac{l}{2}} \frac{y}{I} \cdot dl = 0 \qquad . \qquad . \quad (4)$$

Solving eqs. (3) and (4) as simultaneous,

$$H_t = \cdot \frac{ELat \rfloor_0^{-\frac{w v}{I}}}{2\left[\int_0^{\frac{l}{2}} \frac{y^2}{I} \cdot dl \times \int_0^{\frac{l}{2}} \frac{dl}{I} - \left\{ \int_0^{\frac{l}{2}} \frac{y}{I} \cdot dl \right\}^2 \right]} \qquad (5)$$

$$M_{0t} = \frac{ELat \int_0^{\frac{l}{2}} \frac{y}{I} \cdot dl}{2\left[\int_0^{\frac{l}{2}} \frac{y^2}{I} \cdot dl \times \int_0^{\frac{l}{2}} \frac{dl}{I} - \left\{ \int_0^{\frac{l}{2}} \frac{y}{I} \cdot dl \right\}^2 \right]} \qquad (6)$$

and

$$M_{1t} = -H_t D + M_{0t} \qquad . \qquad . \qquad . \qquad . \qquad . \quad (7)$$

From these equations the stresses due to temperature can be found in the usual way, and must be properly combined with those due to the loads on the arch (see § 322).

TRAVELLING LOADS ON ARCHES

226. Influence Lines for Three-hinged Arches.—Let ACB, Fig. 351, be a three-hinged arch, over which a load $W =$ unity passes from left to right. Consider the conditions when W is at some point G between A

and C, and distant z from A. The line of application of the reaction R_2 will pass through B and C, and intersect the load line and the reaction R_1 in the point G. Resolve R_2 into its vertical and horizontal components V_2 and H. The component H will be the horizontal thrust of the arch when W is in the position shown. Taking moments about A, $V_2 = Wz/L$; taking moments about C, $HD = V_2L/2$, and $H = Wz/2D$; or, when $W =$ unity,

$$H = \frac{z}{2D} \qquad . \quad (1)$$

This will reach its maximum value when W is at C and $z = L/2$, max. $H = WL/4D$; or, when $W=$unity, max. $H = L/4D$. When W crosses to the right-hand half of the arch, by taking moments about C, $HD = V_1L/2$, where $V_1 = W(L-z)/L$; hence $H = W(L-z)/2D$, or when $W =$ unity,

$$H = \frac{L-z}{2D} \qquad . \quad (2)$$
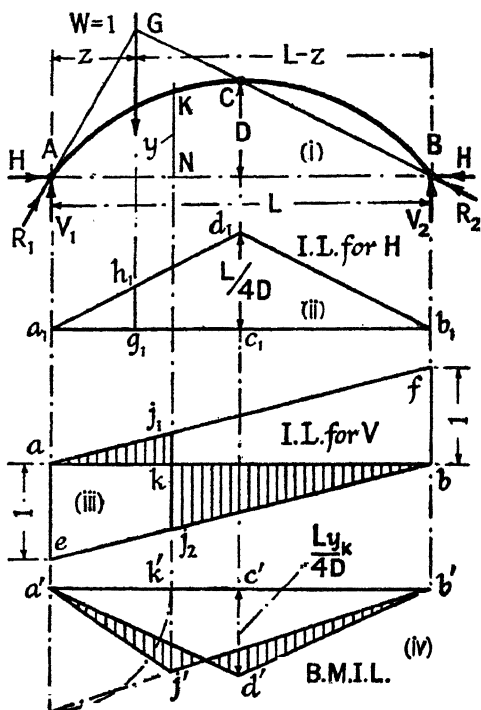
Fig. 351.

The influence line for H will be the double triangle $a_1d_1b_1$, (ii) Fig. 351 ; the ordinate g_1h_1 of which, under the load, gives the magnitude of H for a unit load at G. The straight line a_1d_1 is the graph of eq. (1) ; d_1b_1 is the graph of eq. (2). The maximum ordinate $c_1d_1 = L/4D$; and the ordinate g_1h_1 under the load $= z/2D$.

The influence lines aeb, afb, for the vertical reactions, (iii) Fig. 351, are identical with those for a simple beam, § 32, and aj_1j_2b is the influence line

Fig. 352.

for the *vertical* shear V, i.e. for the vertical component of the thrust at K·
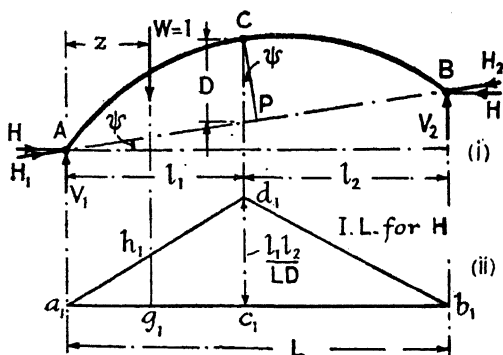
For an unsymmetrical arch carrying a vertical load system, Fig. 352,

if H_1 and H_2, V_1 and V_2 be the components of the end reactions, $H = H_1 \cos \psi = H_2 \cos \psi$. The magnitudes of V_1 and V_2 are the same as in the previous case. Taking moments about C,

$$V_2 l_2 = H_2 \times CP = H_1 D \cos \psi = HD.$$

But $V_2 = Wz/L$, hence,

$$H = \frac{V_2 l_2}{D} \cdot \frac{W l_2 z}{LD} ; \text{ or if } W \quad 1, H = \frac{l_2 z}{LD} \qquad (3)$$

max. H occurs when the load is at C, and $z = l_1$; max. $H = l_1 l_2 / LD$. The influence line for H is the double triangle $a_1 d_1 b_1$, (ii) Fig. 352, of which the maximum ordinate is $l_1 l_2 / LD$.

The influence line for the bending moment at any section K of the arch in Fig. 351 can be set out as follows : From eq. (2), § 216,

$$M = M' + Hy \qquad . \qquad . \qquad (4)$$

where M is the bending moment at K ; M' is the negative bending moment which would exist at a similarly situated section of a beam of span L, supported at the ends and carrying a similarly placed unit load ; y is the ordinate of the centre line of the arch at the section K. Draw an influence line $a'j'b'$, (iv) Fig. 351, for a unit load passing over the similarly situated beam, § 27, and on the same base line plot an influence line for Hy_K. The values for H are obtained from (ii) ; y_K is the ordinate KN at the point K. The maximum ordinate $c'd' = c_1 d_1 \times KN$. Then, from eq. (4), the difference in the ordinates of the two influence lines in (iv) forms the influence line for M, the bending moment at K.

This applies equally to the unsymmetrical arch of Fig. 352.

Stresses on a Cross-section.—Having set out the bending-moment influence line, (iv) Fig. 351, the bending moment at K can be found, for any position of the moving load, from the ordinates or area of this diagram, under the moving load, in the usual way. The stress f_b due to bending can therefore be computed. To this must be added the direct stress due to the thrust. The magnitude of the horizontal thrust for the same position of the moving load can be found from the ordinates or area under that load in (ii) ; and similarly, the magnitude of the vertical component V of the thrust at K can be found from (iii). These two forces can be compounded to find F, the total thrust on the section, (ii) Fig. 338, which in turn can be resolved into F_a and S, the normal and tangential components of the force on the section * [see eqs. (2) and (3), § 229]. The direct stress $f_a = F_a/a$, which combined with f_b gives the total stress on the cross-section (see the worked example below). This operation must be repeated for a number of positions of the moving load, in order to find the maximum stress which may occur on any cross-section.

The process of finding the stresses f_a and f_b separately, and then

---

* Influence lines for F_a and S can be constructed by the methods given in § 229, Fig. 359.

combining them, can be avoided by making use of the properties of the core, § 97, Vol. I. The stress anywhere on a cross-section is

$$f = f_a + f_b = \frac{F_a}{a} + \frac{Mv}{I} = \frac{F_a}{a} + \frac{F_a e v}{I} = \frac{F_a v}{I} \left\{ \frac{\kappa^2}{v} + e \right.$$

$$= \frac{F_a}{Z} (\omega + e) \text{ at the extreme fibres.}$$

F_a is the normal component of the thrust, and e is the distance of its point of application from the centroid, (i) Fig. 353 ; a is the area, and $Z = I/v$ is the modulus of the cross-section ; $\omega = \kappa^2/v = I/av = Z/a$ is the radius of the core. At the top of the cross-section (extrados), $v = v_1$, $Z = Z_1$, $\omega = \omega_1$; call the stress f_{max}. At the bottom (intrados), $v = -v_2$, $Z = -Z_2$, $\omega = -\omega_2$; call the stress f_{min}. Then,

$$f_{max.} = \frac{F_a}{Z_1}(\omega_1 + e) \, ; \; f_{min.} = \frac{F_a}{Z_2}(-\omega_2 + e) \quad (5)$$

In this equation F_a, being a compressive force, is to be given a negative sign ; e is positive when it falls above the centre line, and negative when it falls below. A negative value for the stress denotes compression.

Set out the radius of the core on each side of the centre line as shown in (i) Fig. 353 ; ω_1 is set out below the centroid and ω_2 above it (cf. Fig. 162, Vol. I). Then $F_a(e + \omega_1)$ and $F_a(e - \omega_2)$ in eq. (5) are the moments of F_a about the edges of the core. If, therefore, moments be taken about K_2 for the extrados stress and about K_1 for the intrados stress (instead of about K as heretofore), the total combined stresses $f_{max.}$ and $f_{min.}$ are obtained directly, for $BK_2 = (e + \omega_1)$ and $BK_1 = (e - \omega_2)$.

FIG. 353.

A separate bending moment influence line is required for each of the two stresses. For the extrados stress, $y = KN$ in eq. (4) (from which the bending moment influence line is set out) is replaced by K_2N_2. The vertical $k'j'$ of (iv) Fig. 351 will fall in line with K_2N_2 [see the full lines in (ii) Fig. 353], and the ordinate $c'd'$ of (iv) Fig. 351 will become $c'd' = c_1d_1 \times K_2N_2$; otherwise the construction is exactly similar to that used in (iv) Fig. 351. For the intrados stress, KN is replaced by K_1N_1 ; $k'j'$ falls in line with K_1N_1 [see the broken lines in (ii) Fig. 353] ; and $c'd' = c_1d_1 \times K_1N_1$. Then $f_{max.} = M_{K2}/Z_2$, and $f_{min.} = M_{K1}/Z_1$.

In a masonry arch of rectangular cross-section the radii of the core are $D/6$, and the points K_1 and K_2 lie on the boundary of the middle third of the arch.
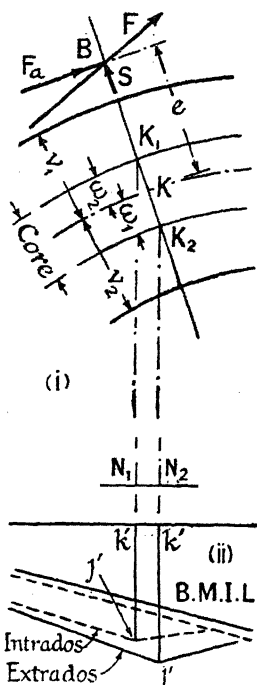
By this device, the maximum extrados and intrados stresses can at once be determined from the influence lines, see p. 506.

Worked Example.—Suppose (i) Fig. 354 to represent a three-hinged arch of 40 ft. span, 10 ft. rise, carrying a uniform load of 1 ton per foot which covers the left-hand half of the span. Assuming that the load is transmitted directly to the arch, find by means of influence lines the maximum and minimum stresses at the section K, distant 13 ft. measured horizontally from A.

The horizontal thrust of the arch will be given by the area under the load of (ii) Fig. 351, i.e. by the area $d_1 a_1 c_1$,

$$c_1 d_1 = \frac{L}{4D} - \frac{40}{4 \times 10} \quad 1,$$

therefore the area $d_1 a_1 c_1 = \frac{1}{2} \times 20 \times 1 = 10$, and $H = 10 \times 1$ ton/ft. $= 10$ tons. From (iii) Fig. 351, since $ae = bf = 1$, and V_1 and V_2 are given by the areas under the load of the triangles aeb and afb respectively,

$$V_1 = \tfrac{3}{4} \times 20 \times 1 \text{ ton/ft.} = 15 \text{ tons};$$
$$V_2 = \tfrac{1}{4} \times 20 \times 1 \text{ ton/ft.} = 5 \text{ tons.}$$

The vertical component of the thrust at K is given by the area under the load of the figure $a j_1 \hat{f}_2 b$, and is,

$$V = (\tfrac{1}{2} \times 13 \times 0 \cdot 325 - \tfrac{1}{2} \times 7 \times 0 \cdot 675) \times 1 \text{ ton/ft.} = -2 \text{ tons,}$$

and is therefore an upward force. The graphical determination of the forces on the cross-section is given in (ii) Fig. 354. The thrust at K, which is the resultant of
$H = 10$ tons and $V = 2$
tons, is $F = 10 \cdot 20$ tons;
resolving this normally
and tangentially to the
section at K, the normal
component $F_a = 10 \cdot 17$
tons, the tangential
component or shearing
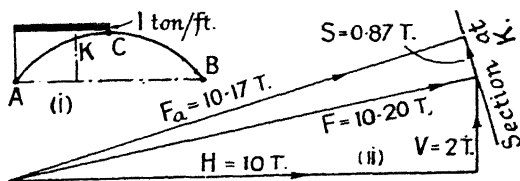
FIG. 354.

force on the cross-section is $S = 0 \cdot 87$ tons. The bending moment at K is given by the area under the load of (iv) Fig. 351. The negative area under the load of the triangle $a'j'b'$ represents $- 110 \cdot 5$ ft.^{2} $\times$ 1 ton/ft. $= - 110 \cdot 5$ ft.-tons ; $(k'j' = 8 \cdot 78$ ft.). The ordinate $c_1 d_1$ of (ii) $= 1$ (see above), and $KN = 9$ ft. ; therefore $c'd' = 9$ ft., and the area under the load of the triangle $a'd'b'$ represents $+ 90 \cdot 0$ ft.^{2} $\times$ 1 ton—ft. $= + 90$ ft.-tons. Hence the bending moment at K is $M_{\bar{K}} = - 110 \cdot 5 + 90 \cdot 0 = - 20 \cdot 5$ ft.-tons, or $- 246$ in.-tons.

The area of the cross-section is $21 \cdot 2$ sq. in. ; the relevant moment of inertia is 950 in.^{4}, and the depth of the section is 20 in. ; the section is symmetrical, hence $Z = 950 \div 10 = \pm 95$ in.^{3}

The direct stress on the cross-section is

$$\frac{F_a}{a} = - \frac{10 \cdot 17}{21 \cdot 2} = - 0 \cdot 48 \text{ tons/sq. in.}$$

the negative sign denoting compression.

The maximum bending stress is

$$\frac{M_K}{Z} = \pm \frac{246}{95} = \pm 2 \cdot 59 \text{ tons/sq. in.}$$

Hence the maximum stress is $- 0 \cdot 48 - 2 \cdot 59 = - 3 \cdot 07$ tons/sq. in.; and the minimum stress is $- 0 \cdot 48 + 2 \cdot 59 = + 2 \cdot 11$ tons/sq. in.; the $+$ sign denoting tension.

These stresses could have been found by means of the properties of the core. The radii of the core $\omega_1 = - \omega_2 = Z/a = 95 \div 21 \cdot 2 = 4 \cdot 48$ inches. Since $M_K = Fa \times e$; $e = M_K/Fa = - 246 \div - 10 \cdot 17 = + 24 \cdot 18$ inches. Then, from eq. (5),

$$f_{max.} = \frac{Fa}{Z_1} (\omega_1 + e) \quad \frac{10 \cdot 17}{95} \{4 \cdot 48 + 24 \cdot 18\} = - 3 \cdot 07 \text{ tons/sq. in.}$$

$$f_{min.} = \frac{Fa}{Z_2} (\omega_2 + e) = + \frac{10 \cdot 17}{95} \{- 4 \cdot 48 + 24 \cdot 18\} = + 2 \cdot 11 \text{ tons/sq. in.}$$

Alternatively, bending moment influence lines could be set out for K_2 and K_1 as before explained (see Fig. 353). From a full-size set-out, KK_2 measured horizontally is $0 \cdot 105$ ft., and AK_2 is $13 \cdot 105$ ft.; $K_2N_2 = 8 \cdot 642$; $k'j' = 8 \cdot 812$ ft.; $c'd' = 8 \cdot 642$ ft.; the area under the load represents $- 110 \cdot 71 + 86 \cdot 42 = - 24 \cdot 29$ ft.-tons, and the maximum stress at the extrados is $- 24 \cdot 29 \times 12/95 = - 3 \cdot 07$ tons/sq. in. Similarly, for the intrados stress, AK_1 measured horizontally is $12 \cdot 895$ ft.; $K_1N_1 = 9 \cdot 358$ ft.; $k'j' = 8 \cdot 738$ ft.; $c'd' = 9 \cdot 358$ ft.; the area under the load represents $- 110 \cdot 29 + 93 \cdot 58 = - 16 \cdot 71$ ft.-tons, and the minimum stress is $- 16 \cdot 71 \times 12/ (- 95) = + 2 \cdot 11$ tons/sq. in.

227. Influence Lines for Three-hinged Spandrel-braced Arch.—Let ACB, (i) Fig. 355, be a spandrel-braced arch hinged at A, B, and C, and
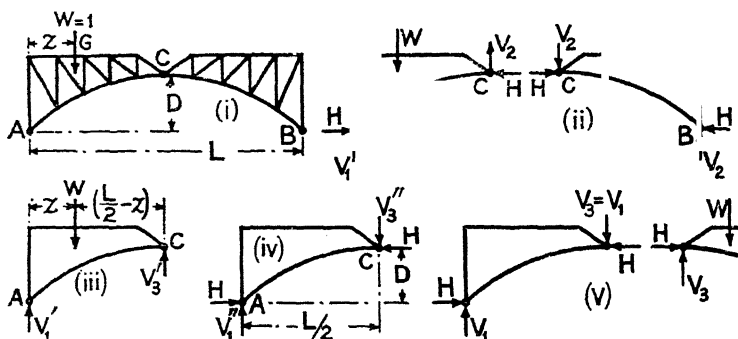
FIG. 355.

suppose that a unit load W passes over it from left to right. When the load is at G, distant z from A, the vertical reactions will be $V_1 = W(L-z)/L$, $V_2 = Wz/L$, and the horizontal thrust $H = Wz/2D$ (see § 226). The external forces acting on the two halves of the arch will then be as shown at (ii). It is evident that each half is in equilibrium. The forces acting

on the left-hand half can be resolved into two groups as shown at (iii) and (iv) Fig. 355. Considering the load W by itself, (iii), it will produce vertical reactions at A and C of $V_1' = \dfrac{2W}{L}\left\{\dfrac{L}{2} - z\right\}$ and $V_2' = \dfrac{2W}{L}z$ respectively. Considering the two horizontal thrusts HH by themselves, (iv), it is evident that, for equilibrium, vertical reactions V_1'' and $- V_3''$ must be called into play at A and C, such that $H \times D = V_1'' \times L/2$, and that

$$V_1'' = - V_3'' = \frac{2HD}{L} = \frac{2D}{L} \cdot \frac{Wz}{2D} = \frac{Wz}{L}$$

If (iii) be superposed on (iv), it will be seen that the state of affairs shown at the left-hand side of (ii) will be obtained, for

$$V_1' + V_2'' = \frac{2W}{L}\left\{\frac{L}{2} - z\right\} + \frac{Wz}{L} = \frac{W}{L}(L - z) = V_1$$

$$V_3' - V_3'' = \frac{2W}{L}z - \frac{Wz}{L} = \frac{Wz}{L} = V_2$$

If then the influence line for any bar K_1Q_2, (i) Fig. 356, be found for both the load conditions shown at (iii) and at (iv) Fig. 355, and the two be superposed, the influence line for the conditions shown at (ii) Fig. 355 will be obtained. The influence line for load condition (iii) Fig. 355 is evidently that for a braced frame supported at each end, and is found by the methods of § 35. It is shown in (ii) Fig. 356 and is obtained by finding the intersection point I and setting up $in = r(r + L/2)/(L/2)r_3$. The influence line for load condition (iv) Fig. 355 will be a triangle aeb; for, taking moments about I, (i) Fig. 356, if F_3'' be the force in K_1Q_2, for the conditions shown in (iv) Fig. 355,

$$F_3''r_3 = Hd - V_3''r = \frac{Wz}{2D}d - \frac{Wz}{L}r$$

or, if W = unity,

$$\frac{z}{r_3}\left\{\frac{d}{2D} - \frac{r}{L}\right\} \tag{1}$$

This is the equation to the straight line ae plotted as shown, for it will be observed that for the particular load position, the force in K_1Q_2 due to load condition (iv), Fig. 355, is compressive, and adds to that due to load condition (iii), also compressive.

When W passes on to the right-hand half of the arch, the forces on the left-hand side are as shown in (v) Fig. 355. V_1 is still $W(L - z)/L$, and $V_1 \times L/2 = H \times D$, so that $H = V_1L/2D = W(L - z)/2D$, and $V_3 = V_1$. Taking moments about I as before,

$$F_3r_3 = Hd - V_3r = \frac{W(L - z)}{2D}d - \frac{W(L - z)}{L}r$$

or, if W = unity,

$$F_3 = \frac{L - z}{r_3}\left\{\frac{d}{2D} - \frac{r}{L}\right\} \tag{2}$$

the same equation as (1), with $(L - z)$ substituted for z. This is the equation to the straight line eb. The complete influence line is shown in (ii) Fig. 356 ; aeb is the new base line.

The influence lines for the bars K_1K_2, Q_1Q_2 are found in a similar way. The influence line for F_1, the force in the bar K_1K_2 for the load condition (iii) Fig. 355, found by the methods of § 35, is the triangle $a'j_2'c'$, (iii)
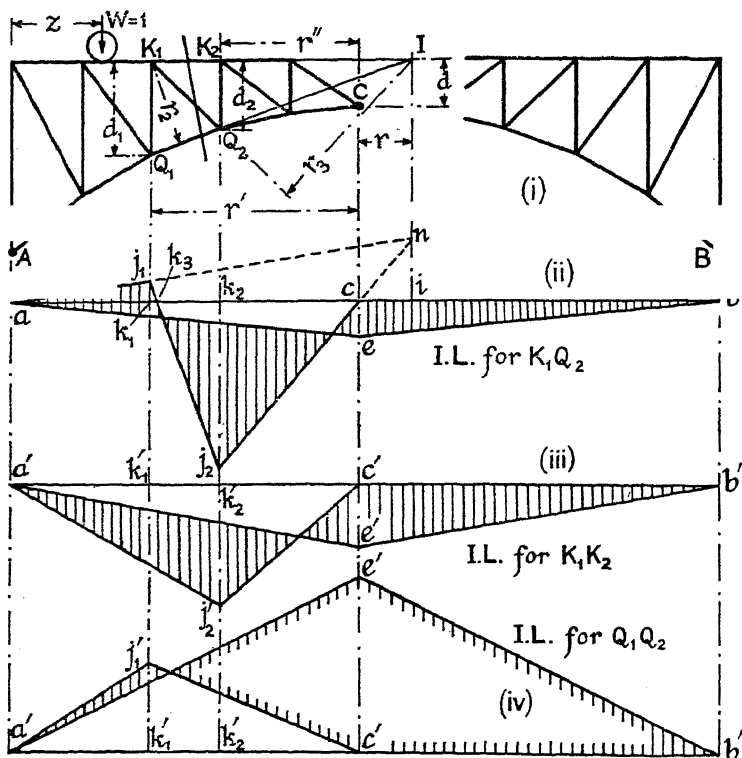
FIG. 356.

Fig. 356, the intersection point I coinciding with Q_2. For the load condition (iv) Fig. 355, taking moments about Q_2,

$$F_1'' \times d_2 = H(d_2 - d) - V_3''r'' = \frac{Wz}{2D}(d_2 - d) - \frac{Wz}{L}r''$$

or, when $W = $ unity,

$$F_1'' = \frac{z}{d_2}\left\{\frac{d_2 - d}{2D}\right. \qquad . \quad (3)$$

This is the equation to the straight line $a'e'$; the complete influence line is shown at (iii) Fig. 356.

Similarly, for the force F_2 in bar Q_1Q_2, the influence line for the load

condition (iii) Fig. 355 is the triangle $a'j_1'c'$, (iv) Fig. 356. For the load condition (iv), taking moments about K_1, if W = unity,

$$F_2''r_2 = Hd + V_3''r' \; ; \text{ and } F_2'' = \frac{\kappa}{r_2}\left\{\frac{d}{2D} + \frac{r'}{L}\right\} \qquad (4)$$

This is the equation to the straight line $a'e'$ in (iv) Fig. 356, which shows the complete influence line. The vertical scale of (iii) and (iv) is one-half that of (ii).

228. Unit Panel-Point Load Method.—Another method of treating the problem of travelling loads on a spandrel-braced arch is to place a unit load at each of the panel points of the top chord in turn, and by drawing stress diagrams, or otherwise, to find the forces in all the members of the arch due to each of these unit loads. The forces thus obtained are tabulated, and the actual forces in the bars are found from the real loads at the panel points by multiplication.

The forces due to the dead load are first obtained, and then the forces for a number of different positions of the travelling load. These are then combined to find the maximum and minimum forces in each of the bars.

229. Influence Lines for Two-hinged Arches.—Owing to its statically indeterminate nature, the construction of influence lines for the two-hinged arch is more complicated than in the case of a three-hinged arch, but where the value of H can be expressed in terms of a single variable the construction is simple.

Two-hinged Parabolic Arch.—It was proved in § 220, eq. (13), that the value of H for a two-hinged parabolic arch in which $I = I_0 \sec \theta$ is

$$H = \frac{5}{8L^3D}l_1(L - l_1)(L^2 + Ll_1 - l_1^2)$$

if W = unity, and l_1 is its horizontal distance from the left-hand abutment. If, for different values of l_1, a curve be plotted, (ii) Fig. 357, in which the ordinate under any load position gives the value of H, this curve will be the influence line for the horizontal thrust of the arch.

From eq. (2), § 216, the bending moment at any section K of the arch is

$$M = M' + Hy$$

where M' is the negative bending moment which would exist at a similarly placed section of a similarly loaded beam, of span L, supported at its ends. Draw

FIG. 357.

an influence line $a'j'b'$, (iii) Fig. 357, for a unit load passing over the beam, § 27, and on the same base line plot an influence line for
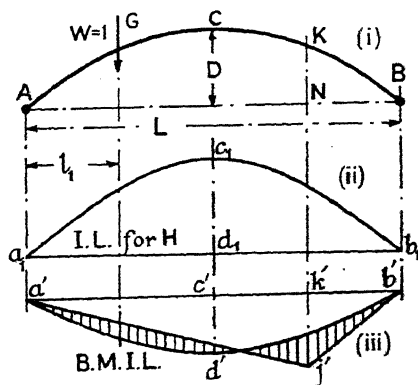
Hy_K. The values for H are got from (ii), and y_K is the ordinate at the point $K = KN$. Then the difference in the ordinates of the two influence lines in (iii) gives the influence line for M, the bending moment at K (cf. Fig. 351).

The General Case.—A not very laborious solution of the general case, in which the arch may have any shape and I vary in any way whatsoever, is to divide the centre line into segments for which $\delta l/I$ is constant, by the construction given in Fig. 343. Place a unit load at the end of each division in turn, and find the value of H for each load position from eq. (9), § 220. The same values of y hold throughout this computation, and the integral in the de-
nominator is the same for all load positions. The influence line for H can then be plotted as in (ii) Fig. 357, and the influence line for the bending moment follows as in (iii) Fig. 357.

FIG. 358.

Symmetrical Arches.—
When the arch is symmetrical the work can be much reduced by the following device : Divide each half of the arch into the same number of segments. Place the load W = unity at the end of a segment, for example at 3, (i) Fig. 358, and draw the M′ diagram $a'g'b'$, (ii), as for a beam. If the centre line of the arch is divided into equal segments, the magnitude of H from eq. (6), § 220, is

$$H = \Sigma_A^B \frac{-M'y}{I} \div \Sigma_A^B \frac{y^2}{I}$$

Consider the product $-M'y$ for the segments 2.3, 2.3 on opposite sides of the centre line. On the left, $-M' = \alpha\beta$; on the right, $-M' = \epsilon\zeta$; y is the same for each segment. For the two segments, $\Sigma - M'y = (\alpha\beta + \epsilon\zeta)y$. Make $\beta\gamma = \epsilon\zeta$; then $\Sigma - M'y = \alpha\gamma \times y$. Now it will be seen that $\alpha\gamma = a'a = x$; therefore for these two segments $\Sigma - M'y = xy$. This applies from A to G. Treating segments 3.4, 3.4 in a similar way, it will be found that $a_1\gamma_1 = z$, and for these two segments $\Sigma - M'y = zy$. This applies to all segments from G to C. The expression for H can therefore be written

$$H = \frac{\Sigma_A^G \frac{xy}{I} + z\Sigma_G^C \frac{y}{I}}{2\Sigma_A^C \frac{y^2}{I}} \qquad . \quad (1)$$
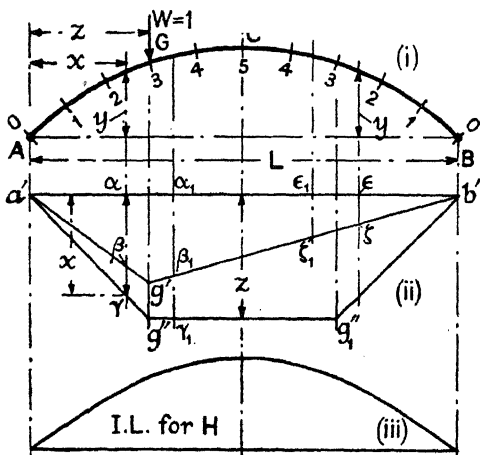
z is a constant for the particular load position. The summations for two load positions 3 and 5 of a particular arch are as follows; the other positions can be similarly treated.

Two-HINGED SYMMETRICAL ARCH. Span 100 ft. Rise 20 ft. Ratio 5 : 1.

								Load Point 3 $z = 28 \cdot 27$.		Load Point 5 $z = 50$.	
Ord.	δl	x	y	I	$\frac{y}{I}$	$\frac{y^2}{I}$	$\frac{xy}{I}$	$\frac{xy}{I}$	$\frac{y}{I}$	$\frac{xy}{I}$	$\frac{y}{I}$
0		4·14	3·65		3·65	13·32	15·11	15·11		15·11	
1		13·18	9·95		9·95	99·00	131·14	131·14		131·14	
2		23·07	14·81		14·81	219·33	341·67	341·67		341·67	
3		33·59	18·12		18·12	328·33	608·65		18·12	608·65	
4		44·49	19·79		19·79	391·64	880·46		19·79	880·46	
5											

Equal Segments. I = const. taken as unity.

$$\Sigma = \frac{1051 \cdot 62}{2}$$

$$\text{Divisor} \quad . \quad 2103 \cdot 24$$

487·92   37·91   1977·03   0

For load point 3, $\quad H = \dfrac{487 \cdot 92 + 28 \cdot 27 \times 37 \cdot 91}{2103 \cdot 24} = 0 \cdot 742$

For load point 5, $\quad H = \dfrac{1977 \cdot 03 + 50 \times 0}{2103 \cdot 24} = 0 \cdot 940$

See eq. (1), § 229.

The method is not dependent on the way in which the half centre line is divided up, but the appropriate expression for H must be used.

Knowing the value of H for each load position, the influence line can be set out as in Fig. 358.

Influence Lines for the Normal Component of the Thrust and for the Shearing Force.—Having drawn the influence lines for H the horizontal thrust, and V the vertical shear (see for example (iii) Fig. 351), the influence lines for F_a the normal component of the thrust, and for S the shearing force, on a right cross-section of the arch can be found as follows : Consider the cross-section at K, (i) Fig. 359. The normal component of the thrust at K is the sum of the components of H and V acting perpendicularly to the cross-section at K, which from (ii) and (iii) Fig. 359 is

$$F_a = H \cos \theta + V \sin \theta \quad . \quad . \quad . \quad . \quad (2)$$

θ is the inclination of the centre line of the arch to the horizontal at the point K.

The shearing force on the cross-section at K is the sum of the components of H and V acting tangentially to the said cross-section, which from (ii) and (iii) Fig. 359 is

$$S = V \cos \theta - H \sin \theta \quad . \quad (3)$$

The influence line for F_a is derived from the influence lines for H and V, (iv) and (v) Fig. 359, by multiplying the ordinates H by $\cos \theta$ and the ordinates V by $\sin \theta$ and adding them. The V $\sin \theta$ diagram is conveniently set out by means of the graphical device indicated. The shaded area (vi) is the complete influence line.

Similarly, the influence line for S is obtained by multiplying the ordinates V by $\cos \theta$ and the ordinates H by $\sin \theta$ and subtracting them. The shaded area in (vii) is the complete influence line.

These constructions are equally applicable to a three-hinged arch, Fig. 351.

230. Reaction Loci.—Suppose ACB, (i) Fig. 360, to be a two-hinged arch loaded with a unit load at G. Then if R_1 and R_2 be the reactions for this load condition, they will intersect at the point G on the load line. If now another position for W be taken, a fresh position for G will be
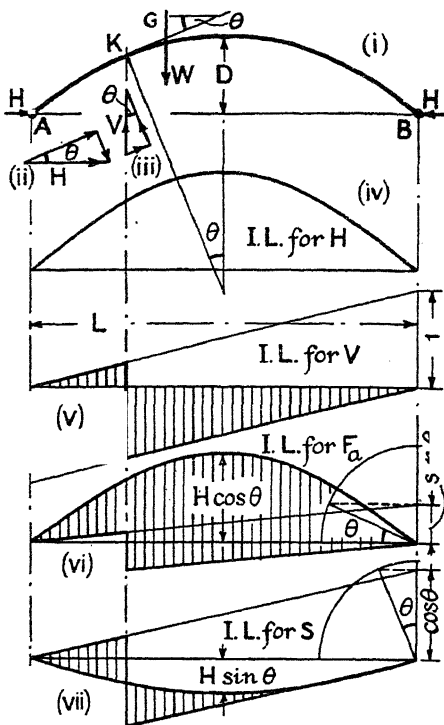
Fig. 359.
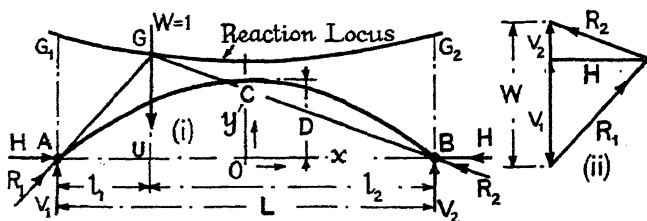
Fig. 360.

obtained. In this way a locus G_1GG_2 may be drawn, which will give the directions of the reactions at once for any position of the unit load. The magnitudes of R_1, R_2, V_1, V_2, and H can then be obtained from a polygon of external forces, (ii). If the load W be of magnitude

other than unity, the corresponding magnitudes of the reactions can be obtained by simple multiplication. If there be more than one load on the arch, the reactions for each, separately considered, must be compounded to find the total reactions.

In certain cases the equation to the reaction locus can be found, and the curve plotted from its equation. Suppose ACB, (i) Fig. 360, to be a parabolic arch, span L, rise D, in which $I = I_0 \sec \theta$. Then from (i) and (ii) Fig. 360, by similar triangles, $\dfrac{GU}{l_1} = \dfrac{V_1}{H}$. But $V_1 = \dfrac{W l_2}{L}$ l when W is unity ; and the magnitude of H is given by eq. (13), § 220, hence

$$GU = \frac{V_1 l_1}{H} = \frac{l_1 l_2}{HL} = \frac{l_1(L - l_1)}{\cdot} \times \frac{8L^3D}{5l_1(L - l_1)(L^2 + Ll_1 - l_1^2)}$$

$$\cdot \frac{8L^2D}{5(L^2 + Ll_1 - l_1^2)} \tag{1}$$

from which the locus can be plotted.

The form of the reaction locus depends on the shape and structure of the arch. For the Niagara Falls spandrel-braced arch, Messrs. Johnson, Bryan and Turneaure * found for the equation to the locus

$$y' = \frac{2 \cdot 5(D - d)x^2}{L^2} + D + 2 \cdot 2d \qquad . \tag{2}$$

Origin is taken at the centre of the line AB ; y' is the ordinate to the curve. If this equation be applied to other spandrel-braced arches, it is stated that the error will not exceed 5 %.

Freeman † gives for the equation to the locus for a spandrel-braced arch an expression equivalent to

$$y' = (D + d)\left\{ 1 \cdot 3 - 0 \cdot 2 \sin \frac{\pi}{2}\left(1 - \frac{4x}{L}\right.\right. \qquad . \tag{3}$$

This equation fits the locus for the Victoria Falls arch with some degree of accuracy.

The influence line for H can be constructed by plotting values for a number of positions of the moving load. From this, and the influence line for V, the influence lines for M, F_a, and S can be derived, § 229.

231. Influence Lines for Direction-fixed Arches.—These may be treated by the method of Müller-Breslau [15] (Bd. II, Ab. 1, p. 304). A very
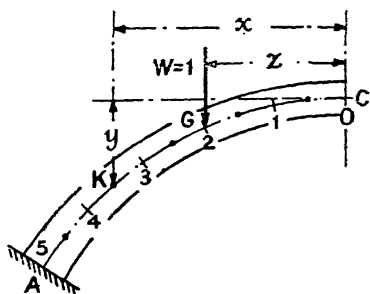
FIG. 361.

* ' The Theory and Practice of Modern Framed Structures,' New York, 1893.

† Proc. Inst. C.E., vol. clxvii, 1906-7, p. 352.

complete exposition will be found in Molitor * (chap. xv, p. 298), to which reference may be made. When the arch is symmetrical, the analysis of § 222, p. 495, affords a simple solution. Divide the centre line of the half arch into a number of equal segments, Fig. 361, and apply a load $W = 1$ at the end of a segment, for example at 2. Then the term $W \Sigma_G^\Delta \dfrac{(x-z)y}{I}$, which appears in eqs. (21) and (23), § 222, may be broken up into $\Sigma_G^\Delta \dfrac{xy}{I} - z \Sigma_G^\Delta \dfrac{y}{I}$; for $W =$ unity, and z is a constant for the particular load position. x and y are the ordinates at the centre of each segment. Similarly, the term $\Sigma_G^\Delta \dfrac{x-z}{I}$ becomes $\Sigma_G^\Delta \dfrac{x}{I} - z \Sigma_G^\Delta \dfrac{1}{I}$; and $\Sigma_G^\Delta \dfrac{(x-z)x}{I}$ becomes $\Sigma_G^\Delta \dfrac{x^2}{I} - z \Sigma_G^\Delta \dfrac{x}{I}$.

The tabular calculation to be adopted is the following :

Ordin-ate.	δl	x	y	I	$\dfrac{1}{I}$	$\dfrac{x}{I}$	$\dfrac{y}{I}$	$\dfrac{x^2}{I}$	$\dfrac{y^2}{I}$	$\dfrac{xy}{I}$	$\dfrac{1}{I}$	$\dfrac{x}{I}$	$\dfrac{y}{I}$	$\dfrac{x^2}{I}$	$\dfrac{xy}{I}$
											Load Point 2, $z =$ * *				
0	* *	* *	* *	* *	* *	* *	* *	* *	* *	* *					
1	* *	* *	* *	* *	* *	* *	* *	* *	* *	* *					
2	* *	* *	* *	* *	* *	* *	* *	* *	* *	* *	* *	* *	* *	* *	* *
3	* *	* *	* *	* *	* *	* *	* *	* *	* *	* *	* *	* *	* *	* *	* *
4	* *	* *	* *	* *	* *	* *	* *	* *	* *	* *	* *	* *	* *	* *	* *
5															
$\Sigma =$	A_1	A_2	A_3	A_4	A_5	A_6					B_1	B_2	B_3	B_4	B_6

Then, from eqs. (21), (22) and (23), § 222,

$$H = \frac{(B_6 - zB_3)A_1 - (B_2 - zB_1)A_3}{2[A_5 A_1 - A_3^2]} ; \quad V_0 = \frac{B_4 - zB_2}{2A_4} ;$$

$$M_0 = \frac{(B_6 - zB_3)A_3 - (B_2 - zB_1)A_5}{2[A_5 A_1 - A_3^2]}$$

The third section of the Table is only filled up below the load point indicated. The figures in this section are merely quoted from the second section. The load $W = 1$ is placed at the end of each segment in turn, and the values of H, V_0, and M_0 determined. The denominator is always the same. From these values the influence lines are plotted. For the

* Ref. No. 16, Chapter V, Bib.

complete working out of an arch direction-fixed at the ends, see § 322, where the shortening of the arch axis due to direct thrust is also taken into account.

BIBLIOGRAPHY

Early Memoirs on Arches

1. LAMÉ AND CLAPEYRON. *Jour. d. Voies d. Communication*, 1826; GERSTNER, *Handbuch der Mechanik*, 1831; MOSELEY, *Phil. Mag.*, 1833; PONCELET, *Mém. d. l'Officier du Génie*, 1835.

Theory of Arches

2. BRESSE. Recherches analytiques sur la flexion et la résistance des pièces courbes. Paris, 1854.
3. FRÄNKEL. Berechnung eiserner Bogenbrücken. *Der Civilingenieur*, 1867, p. 75.
4. WINKLER. Ueber den Einfluss der Temperatur bei Bogenbrücken. *Der Civilingenieur*, 1867, p. 95; *Mitt. d. Arch.- u. Ing. Ver. f. Böhmen*, 1867, p. 14.
5. —— Vortrag über die Berechnung von Bogenbrücken. *Mitt. d. Arch.- u. Ing. Ver. f. Böhmen*, 1868; 1869, p. 1.
6. —— Beitrag zur Theorie der elastischen Bogenträger. *Zeit. d. Arch.- u. Ing. Ver. z. Hannover*, 1879, p. 199. (Influence Lines for Fixed Arches.)
7. MOHR. Beitrag zur Theorie der elastischen Bogenträger. *Zeit. d. Arch.- u. Ing. Ver. z. Hannover*, 1870, p. 389.
8. —— Beitrag zur Theorie der Bogenfachwerksträger. *Ibid.*, 1874, p. 223; 1874, p. 509; 1875, p. 17.
9. —— Beitrag zur Theorie des Bogenfachwerks. *Ibid.*, 1881, p. 243.
10. WEYRAUCH. Theorie der elastischen Bogenträger. *Zeit. f. Baukunde*, 1878, pp. 31, 367, 549.
11. —— *Elastische Bogenträger*. Munich, 1896.
12. EDDY. *Researches in Graphical Statics*. New York, 1877; also *Amer. Jour. of Math.*, vol. i, 1878.
13. MÜLLER-BRESLAU. *Theorie und Berechnung der eisernen Bogenbrücken*. Berlin, 1880.
14. —— Vereinfachung der Theorie der statisch unbestimmten Bogenträger. *Zeit. d. Arch.- u. Ing. Ver. z. Hannover*, 1884, p. 575.
15. —— *Die graphische Statik der Baukonstruktionen*. Bd. I, Leipzig, 5th ed., 1912; Bd. II, Ab. 1, 5th ed., Stuttgart, 1922.
16. ENGESSER. *Theorie und Berechnung der Bogenfachwerkträger ohne Scheitelgelenk*. Berlin, 1880.
17. AM ENDE. The Theory of Arches. *Engg.* June 3, 1881, p. 557 et seq.
18. RITTER. *Der elastische Bogen, berechnet mit Hilfe der graphischen Statik*. Zurich, 1886.
19. MELAN. Theorie der eisernen Bogenbrücken und Hängebrücken. *Handbuch der Ingenieurwissenschaften*, Bd. II, Ab. iv, 1888; see translation of 3rd ed., Bd. II, Ab. v, 1906, by STEINMAN. *Theory of Arches and Suspension Bridges*. Chicago, 1913; extensive bibliography, 1850–1904.
20. —— Ueber den Einfluss der Wärme auf elastische Systeme. *Wochenschr. d. öst. Ing.- u. Arch.-Ver.*, 1883, p. 183.
21. GREENE. *Trusses and Arches Analyzed and Discussed by Graphical Methods*, Pt. iii. New York, 1888.
22. MARTIN. Arched Ribs and Voussior Arches. *Proc. Inst. C.E.*, vol. xciii, p. 462.

23. YOUNG. Rankine's Treatment of the Elastic Arch. *Proc. Inst. C.E.*, vol. cxxxi, 1897–8, p. 323.

24. FREEMAN. The Design of a Two-hinged Spandrel-Braced Steel Arch. *Proc. Inst. C.E.*, vol. clxvii, 1906–7, p. 343.

25. HUDSON. The Computations in Open-Webbed Arches without Hinges. *Proc. Amer. Soc. C.E.*, vol. xxxv, 1909.

26. CHILDS. On the Theory of Arched Ribs. *Proc. Inst. C.E.*, vol. cxci, 1912–13, p. 286.

27. MASON. A Method of Finding the Forces in Framed Ribs with Fixed Ends. *Proc. Inst. C.E.*, vol. cxciii, 1912–13, p. 283.

28. LEA. Influence Diagrams for an Arch-Rib Hinged at the Ends Only. *Proc. Inst. C.E.*, vol. cxcix, 1914–15, p. 347.

29. MAGNEL. Design of Flat Arches with Fixed Ends. *Engg.* Apl. 27, 1917, p. 391 ; Influence Lines for Arches, *Engg.* Dec. 26, 1919, p. 843.

30. McCULLOUGH AND THAYER. *Elastic Arch Bridges.* New York, 1931.

Notable Arched Bridges

31. BUCK. The Niagara Railway Arch. *Trans. Amer. Soc. C.E.*, vol. xl, 1898, p. 125 ; *Proc. Inst. C.E.*, vol. cxliv, 1900–1, p. 69.

32. HOBSON. The Victoria Falls Bridge. *Proc. Inst. C.E.*, vol. clxx, 1906–7, p. 1.

33. AMMANN. The Hell Gate Arch Bridge. *Trans. Amer. Soc. C.E.*, vol. lxxxii, 1918, p. 852.

34. FREEMAN. Sydney Harbour Bridge. *Proc. Inst. C.E.*, vol. 238, 1933–4, p. 153 et seq.

QUESTIONS ON CHAPTER XIII

1. An arched rib is circular, 80 ft. span, rise 16 ft., hinged at the centre and at the springings, and is loaded with a concentrated load of 8 tons at a point 15 ft. to the left of the centre measured horizontally. Find (1) the horizontal thrust, (2) the reaction at each springing, and the angle each reaction makes with the horizontal, (3) the bending moment under the 8-ton load. (U.L.)

Ans. $H = 6\frac{1}{4}$ tons ; $R_1 = 8\cdot33$; $\theta_1 = 41° 21'$; $R_2 = 6\cdot73$; $\theta_2 = 21° 48'$; $- 40\cdot75$ ft.-tons.

2. A circular arched rib, span 50 ft., rise 10 ft., is hinged at the crown and at the springings. It carries a load of 6 tons placed 12 ft. from the left hinge, and one of 10 tons placed 30 ft. from the left hinge, the distances being measured horizontally. Draw a diagram of bending moment for the arched rib, and state the value of the maximum bending moment. Find the reactions at the hinges. (U.L.)

Ans. Max. $M = - 17\cdot42$ ft.-tons ; $R_1 = 16\cdot07$; $R_2 = 15\cdot50$; R (centre pin) $= 13\cdot84$; $H = 13\cdot6$ tons.

3. A circular 3-hinged arch, span 100 ft., rise 20 ft., carries vertical loads of 5, 8, 7 and 6 tons acting 20, 40, 70, and 90 ft. respectively from the left-hand hinge, the distances being measured horizontally. Draw a line of thrust for the given load system passing through the three hinges, and hence determine the horizontal thrust of the arch. (I.C.E.)

Ans. $H = 17\cdot25$ tons.

4. A circular arched rib is hinged at the crown and springings and carries the loads shown in (i) Fig. 362. Find the reactions at the hinges, and draw the line of thrust. (U.L.)

Ans. See § 219, $V_A = 2\cdot45$; $H_A = 2\cdot25$; $V_B = 1\cdot67$; $H_B = 0\cdot91$; $V_C = 0\cdot33$; $H_C = 4\cdot37$ tons.

5. A parabolic arch rib, span 64 ft., rise 12·8 ft., is hinged at the ends. It is loaded with two weights of 2 tons each, concentrated at points 8 ft. and 16 ft. from the centre, measured horizontally, on the left half of the span. Determine (1) the reactions, (2) the horizontal thrust, (3) the bending moments under each load, (4) the maximum positive bending moment, and (5) the axial thrusts at each load. Take $I = I_0 \sec \theta$. (U.L.)

Ans. $V_1 = 2\frac{3}{4}$; $V_2 = 1\frac{1}{4}$; $H = 3 \cdot 2$ tons; B.M. $= 13 \cdot 28$; $11 \cdot 6$; max. $= + 10 \cdot 73$ ft.-tons; axial thrusts $= 3 \cdot 25$; $2 \cdot 9$ tons.

6. The two abutments of a semicircular arch of radius R, moment of inertia I, sectional area a_1, are connected by pin joints to a horizontal tie whose sectional area is a_2. The structure rests without constraint with its ends on two walls, and a load W is suspended from the crown of the arch. Find expressions for the stress and strain in the horizontal tension member. Neglect the shear stresses, assume the wall reactions vertical, and take E to be the same in both arch and tie. (U.L.)

Ans. See § 79, Fig. 117.

7. The span of a circular arched rib of constant cross section, hinged at the springings, is 100 ft. and the rise is 12 ft. The cross section of the rib is symmetrical and 2 ft. 6 in. deep. Find the maximum change in the bending stress due to a change in temperature of 50° F. Take $a = 0 \cdot 0000062$, and $E = 13,000$ tons/sq. in.

Ans. $f = LEatDv_1 / \int y^2 dl = 0 \cdot 72$ tons/sq. in.
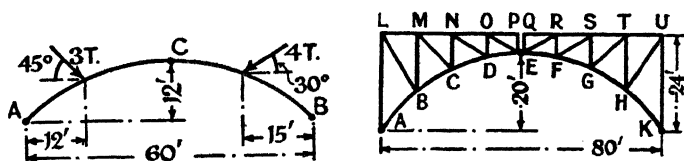
FIG. 362.

8. A parabolic arch with fixed ends has a span of 140 ft. and a rise of 30 ft. A vertical load of 5 tons rests on the arch at a distance 30 ft. to the left of the centre of the span, measured horizontally. Determine (1) the resultant reactions at the springings, (2) the bending moments at the springings, (3) the bending moment in the arch at the point of application of the load. Take I as constant. (U.L.)

Ans. Use methods of § 222.

9. A three-hinged segmental arch has a span of 150 ft. and a rise of 12 ft. Two loads each of 8 tons roll over the arch at a distance apart of 10 ft. Find (1) the thrust H, and (2) the bending moment at 40 ft. from one support, when the leading load is vertically above this section. (U.L.)

Ans. $H = 23\frac{1}{4}$ tons; B.M. $= 190 \cdot 4$ ft.-tons.

10. A metal arch, 80 ft. span, 16 ft. rise, is hinged at the centre and at both ends. The centre line of the arch is segmental. A load of 20 tons rolls over the arch. Find the maximum bending moment on the arch and the reactions at the three hinges when the load is in the position which produces the maximum bending moment. (U.L.)

Ans. Max. M $= 148 \cdot 4$ ft.-tons, under load $16 \cdot 8$ ft. from A. $V_1 = 15 \cdot 8$; $V_2 = 4 \cdot 2$; $V_3 = 4 \cdot 2$; $H = 10 \cdot 5$; $R_1 = 19 \cdot 0$; $R_2 = 11 \cdot 3$; $R_3 = 11 \cdot 3$ tons.

11. (ii) Fig. 362 shows a three-hinged spandrel-braced arch, 80 ft. span, 20 ft. rise, depth at springings 24 ft., lower chord parabolic. Each bay is 10 ft. long. The live load is 2 tons per ft. run and is longer than the span, the dead

load is 1 ton per ft. run. Show how to find the maximum and minimum forces in each member and determine the forces in MN, MC, MB and BC. (U.L. modified.)

Ans. Forces : MN $= 0 \pm 13 \cdot 4$; MC $= 0 \pm 4 \cdot 8$; MB $= - 5 - 10$ $- 3 \cdot 2$; $- 5 + 3 \cdot 2$; BC $= - 23 \cdot 7 - 48 \cdot 8$; $- 23 \cdot 7 + 1 \cdot 5$ tons (per girder).
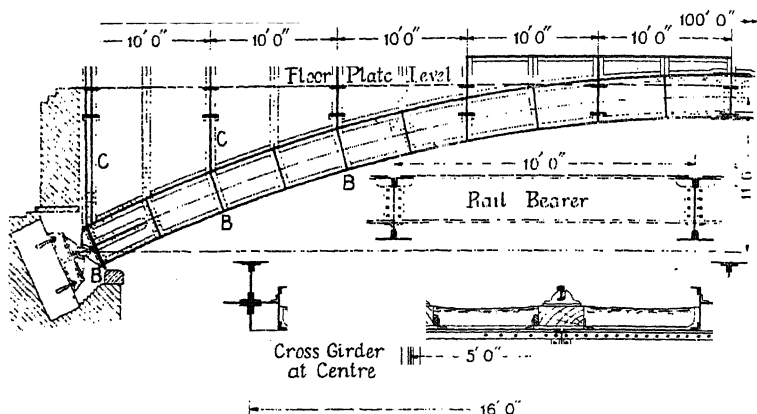
FIG. 363.

12. Design for a two-hinged, mild steel, single track, arched railway bridge. Span 100 ft., rise 11 ft. 6 in., Fig. 363. To carry a 20-unit Ministry of Transport Loading, § 22 ; equivalent live load $= 2 \cdot 6$ tons/ft., maximum axle load $= 25$ tons. Use the stresses and impact formula given in § 196 ; i for the arched ribs $= 0 \cdot 45$. Wind pressure $= 38 \cdot 5$ lb./sq. ft. on the empty bridge ; 30 lb./sq. ft. on the loaded bridge and train. Temperature variation $\pm 30°$ F. Dead load on each arched rib may be taken as $0 \cdot 75$ ton/ft. as a first approximation. Design the floor system by the methods of § 196 and the ribs by the methods of § 229 (symmetrical arches). A segmental arch is suggested.

CHAPTER XIV

SUSPENSION CHAINS AND BRIDGES

232. The Catenary.—The curve in which a uniform flexible chain (supposed inextensible) hangs, when loaded merely with its own weight, is called a *catenary*. The properties of this curve are frequently required in engineering problems. Let ACB, (i) Fig. 364, represent a uniform hanging chain of weight w per unit of length, supported at any two points A and B. P is any point on the curve, of which the co-ordinates are x and y. Consider the portion CP of the curve, length s. There are three forces acting on it, a horizontal tension H at C; a tension T at P, tangent to the curve; and ws the weight of the chain between C and P. These three forces are in equilibrium and
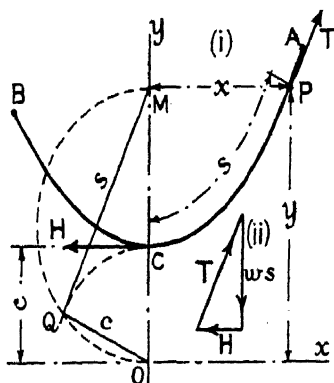
FIG. 364.

may be represented by a triangle as shown in (ii). Since T is tangent to the curve at P, the slope of the chain there will be $\dfrac{dy}{dx} = \dfrac{ws}{H} = \dfrac{s}{c}$, where $H = wc$. Make $OC = c$, and take origin at O.

Now $(ds)^2 = (dy)^2 + (dx)^2$, and $\dfrac{ds}{dy} = \sqrt{1 + \left(\dfrac{dx}{dy}\right)^2} = \sqrt{1 + \dfrac{c^2}{s^2}}$.

Hence $\dfrac{dy}{ds} = \dfrac{s}{\sqrt{s^2 + c^2}}$; or, $y = \sqrt{s^2 + c^2}$, for $s = 0$ when $y = c$; from which,

$$: y^2 - c^2 \qquad (1)$$

and $\dfrac{dy}{dx} = \dfrac{s}{} = \dfrac{\sqrt{y^2 - c^2}}{} \cdot$ or, $\dfrac{dx}{dy} =$

By integration, $\dfrac{x}{c} = \log\{y + \sqrt{y^2 - c^2}\} + C_1$.

When $x = 0$, $y = c$; hence $C_1 = -\log c$, and

$$\dfrac{x}{c} = \log \dfrac{y + \sqrt{y^2 - }}{} \qquad \log \dfrac{y + s}{c}\ ;\ \text{or}, y + \qquad : y + s :: ce^{\frac{x}{c}} \ . \ (2)$$

whence, $1 - c^2 = s^2 = \{ce^{\frac{x}{c}} - y\}^2$,

from which, $y = \dfrac{c}{2}\left\{e^{\frac{x}{c}} + e^{-\frac{x}{c}}\right\} = c\cosh\dfrac{x}{c}$.   .   . (3)

which is the equation to the catenary. Differentiate, $\dfrac{dy}{dx} = \sinh\dfrac{x}{c}$;

and, $s = c\,\dfrac{dy}{dx} = c\sinh\dfrac{x}{c}$.   .   .   . (4)

The length s can be determined by the simple construction shown in Fig. 364. In the triangle MOQ, OM $= y$, OQ $= c$. Hence

$$QM^2 = OM^2 - OQ^2 = y^2 - c^2,$$

or from eq. (1), QM $= s$. QM is parallel to the tangent at P. From the triangle of forces (ii), $T^2 = (ws)^2 + H^2 = (ws)^2 + (wc)^2 = w^2(s^2 + c^2) = w^2y^2$ [eq. (1)]. Hence $T = wy$. That is to say, the tension in the chain at any point is equal to the ordinate of the curve at that point multiplied by the weight per unit of length of the chain; and the difference between the tensions at any two points is equal to the difference between the ordinates multiplied by the weight per unit of length of the chain. It will be observed that H is the horizontal component of T for any position of the point P. In other words, the horizontal component of the force in the chain is constant.

Problem.—Given the length l of a chain, supported at any two points A and B, to find the shape of the curve if H, the horizontal component of the tension in the chain, be known. Suppose C, Fig. 365, to be the

FIG. 365.

vertex of the curve. Take origin at O, such that $OC = c = H/w$, where w is the weight of the chain per unit of length. Let the co-ordinates of A and B be x_1y_1 and x_2y_2 respectively. Then the equation to the curve is $y = c\cosh x/c$, and since both A and B lie on the curve, $y_1 = c\cosh\dfrac{x_1}{c}$;

$y_2 = c\cosh\dfrac{x_2}{c}$; and

$$y_1 - y_2 = c\left\{\cosh\frac{x_1}{c} - \cosh\frac{x_2}{c}\right\} = 2c\sinh\frac{x_1 - x_2}{2c}\sinh\frac{x_1 + x_2}{2c}$$

Further, since $s = c\sinh\dfrac{x}{c}$, $s_1 = c\sinh\dfrac{x_1}{c}$; $s_2 = c\sinh\dfrac{x_2}{c}$; and

$$(s_1 - s_2) = c\left\{\sinh\frac{x_1}{c} - \sinh\frac{x_2}{c}\right\} = 2c\sinh\frac{x_1 - x_2}{2c}\cosh\frac{x_1 + x_2}{2c}$$
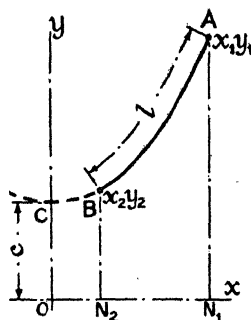
Then $\dfrac{y_1 - y_2}{s_1 - s_2} = \dfrac{y_1 - }{l}$ $= \tanh\dfrac{x_1 + x_2}{2c}$ (5)

which may be written

$$\cosh^2 \frac{x_1 + x_2}{2c} \cdot l^2 - (y_1 - y_2)^2 \qquad \text{. (6)}$$

Again, $\qquad (s_1 - s_2)^2 = 4c^2 \sinh^2 \frac{x_1 - x_2}{2c} \cosh^2 \frac{x_1 + x_2}{2c}$

$$(y_1 - y_2)^2 = 4c^2 \sinh^2 \frac{x_1 - x_2}{2c} \sinh^2 \frac{x_1 + x_2}{2c}$$

and

$$(s_1 - s_2)^2 - (y_1 - y_2)^2 = 4c^2 \sinh^2 \frac{x_1 - x_2}{2c} \left\{ \cosh^2 \frac{x_1 + x_2}{2c} - \sinh^2 \frac{x_1 + x_2}{2c} \right\}$$

$$2c^2 \left\{ 2 \sinh^2 \frac{x_1 - x_2}{2c} + 1 - 1 \right\} = 2c^2 \left\{ \cosh \frac{x_1 - x_2}{c} - 1 \right\}$$

Therefore,

$$\cosh \frac{x_1 - x_2}{c} = \frac{(s_1 - s_2)^2 - (y_1 - y_2)^2}{2c^2} + 1 = \frac{l^2 - (y_1 - y_2)^2}{2c^2} + 1 \text{ . (7)}$$

Knowing l, c, and $(y_1 - y_2)$, the value of $(x_1 - x_2)$ can be obtained from eq. (7) ; $(x_1 + x_2)$ can be found from eq. (5) or (6), hence x_1 and x_2 are known and therefore the shape of the chain is determined, and hence the tension T everywhere.

Example.—The horizontal force on a floating structure moored by a chain is $3 \cdot 6$ tons. The length of the chain is 150 ft., and the vertical distance between the anchor and the point of suspension on the structure is 30 ft. If the chain weighs in water $0 \cdot 0145$ tons per ft., find the horizontal distance between the anchor and the point of suspension. If, due to wind pressure, the horizontal force increase to 36 tons, find the increase in this horizontal distance.

When the horizontal force is $3 \cdot 6$ tons, $c = \dfrac{H}{w} = \dfrac{3 \cdot 6}{0 \cdot 0145} = 248 \cdot 2$ ft.

If the values of x_1 and x_2 be determined from eqs. (6) and (7), it will be found that x_2 is negative. This implies that the chain will not be lifted entirely off the bottom, and that the vertex of the curve will lie on the ground line. If, then, x_1 and y_1 be the co-ordinates of the point of suspension (a point on the curve), $y_1 = 248 \cdot 2 + 30 = 278 \cdot 2$ ft., and from eq. (3),

$$y_1 = c \cosh \frac{x_1}{c}, \text{ or, } \cosh \frac{x_1}{c} = \frac{y_1}{c} = \frac{278 \cdot 2}{248 \cdot 2} = 1 \cdot 120.$$

From a table of hyperbolic cosines, $x_1/c = 0 \cdot 4853$, or $x_1 = 0 \cdot 4853 \times 248 \cdot 2$ = $120 \cdot 5$ ft. The length of the curve from the vertex to the point of suspension is $s_1 = \sqrt{y_1^2 - c^2}$ [see eq. (1)], and

$$s_1 = \sqrt{278 \cdot 2^2 - 248 \cdot 2^2} = 125 \cdot 7 \text{ ft.}$$

The total length of the chain is 150 ft., so that $150 - 125 \cdot 7 \quad 24 \cdot 3$ ft.

of chain will lie on the ground, and the horizontal distance between the anchor and the point of suspension will be

$$24 \cdot 3 + x_1 = 24 \cdot 3 + 120 \cdot 5 = 144 \cdot 8 \text{ ft.}$$

When, due to wind pressure, the horizontal force increases to 36 tons, $c = \dfrac{H}{w} = \dfrac{36}{0 \cdot 0145} = 2482$ ft. The chain will now be lifted right off the bottom; $(y_1 - y_2) = 30$ ft., and $l = 150$ ft. From eq. (7),

$$\cosh \frac{x_1 - x_2}{c} = \frac{l^2 - (y_1 - y_2)^2}{2c^2} + 1 = \frac{150^2 - 30^2}{2 \times 2482^2} + 1 = 1 \cdot 00175 ;$$

$$\frac{x_1 - x_2}{c} : 0 \cdot 0593 ; \quad (x_1 - x_2) = 0 \cdot 0593 \times 2482 = 147 \cdot 2 \text{ ft.}$$

This is the new horizontal distance between the anchor and the point of suspension. The increase in this distance is, therefore, $147 \cdot 2 - 144 \cdot 8 = 2 \cdot 4$ ft. To determine the shape of the curve, $(x_1 + x_2)$ must be found from eq. (6),

$$\cosh^2 \frac{x_1 + x_2}{2c} = \frac{l^2}{l^2 - (y_1 - y_2)^2} = \frac{150^2}{150^2 - 30^2} :$$

from which,

$$\overline{\quad 2c \quad} - \cdots \cdots , \quad \overline{\quad 2c \quad} - 0 \cdot 205 ;$$

$$(x_1 + x_2) = 2 \times 2482 \times 0 \cdot 205 = 1017 \cdot 6 \text{ ft.}$$

; follows that $x_1 = 582 \cdot 4$ ft., and $x_2 = 435 \cdot 2$ ft. The vertex of the curve is now known, values of y can be determined, and the tension everywhere can be calculated from the equation $T = wy$.

233. Uniformly Distributed Load—The Parabola.—If, as in a suspension bridge, the chain support a roadway carrying a uniformly distributed load
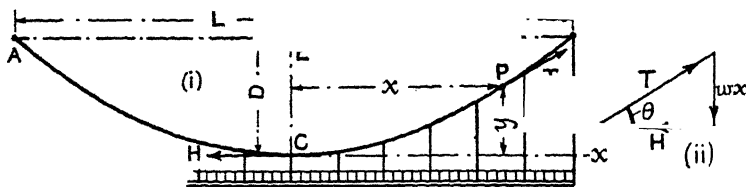
FIG. 366.

w per unit of length, such that the weight of the chain is negligible relative thereto, the curve assumed by the chain will be a parabola. As before, let P, (i) Fig. 366, be any point on the chain, and C the vertex of the curve. Take origin at C, and consider the equilibrium of the portion CP of the chain. The three forces acting on this portion are : H, the horizontal tension in the chain at C ; T, the tension at P, which will act tangentially to the chain at P ; and wx, the load on that portion of the roadway which subtends CP. These three forces will be in equilibrium and can be

represented by the triangle of forces shown in (ii). If, then, x and y be the co-ordinates of P, the slope of the chain at P will be

$$\frac{dy}{dx} = \tan\theta = \frac{wx}{H} \; ; \text{ whence, by integration, } y = \frac{wx^2}{2H} \qquad (1)$$

No constant need be added, for $y = 0$ when $x = 0$. This is the equation to a parabola, with its vertex at C. If the two points of support A and B be at the same level, and AB $= L$, CE $= D$; then $y = D$ when $x = L/2$. Hence, from eq. (1),

$$D = \frac{wL^2}{8H} \; ; \text{ or, } H = \frac{wL^2}{8D} \qquad . \qquad . \qquad (2)$$

T, the tension at any point P, is given by

$$T = \sqrt{H^2 + (wx)^2} \qquad (3)$$

At A or B, where $x = \frac{L}{2}$,

$$\frac{wL}{2}\sqrt{1 + \frac{L^2}{16D^2}} \qquad (4)$$

This is the maximum tension in the chain.

234. The Link Polygon.—The shape of a chain carrying a number of separate vertical loads is obtained by drawing the funicular or link polygon for the system by the ordinary graphical construction, as shown in Fig. 367. In the force polygon, the triangle Oef is the triangle of forces for the point J_2. Since ef represents the force W_2, Oe represents the tension

FIG. 367.

in the link J_1J_2, and fO the tension in the link J_2J_3. Thus the tension in every link is given by the force polygon. The horizontal line Oh represents H, the horizontal component of the force in any one of the links, which component is the same from one end of the chain to the other. The reactions at the points A and B are equal in magnitude, but opposite in direction, to the tensions in the links AJ$_1$ and BJ$_3$ respectively.

If the points AB be joined, the ordinate JN of the funicular polygon represents the moment M of all the external forces to one side of J, and is such that

$$M = JN \times Oh = y \times H \; ; \text{ hence, } H = M/y \qquad . \qquad . \qquad (1)$$

In the case of a uniformly distributed load w per unit of length, the value of M at the centre of the span L is $wL^2/8$; the ordinate y at the centre of the span becomes the dip D. Hence, $H = wL^2/8D$, the result obtained in eq. (2), § 233.

235. Suspension Bridges.—The suspension bridge in its most elementary form is shown at (i) Fig. 368. The roadway AB, spanning from
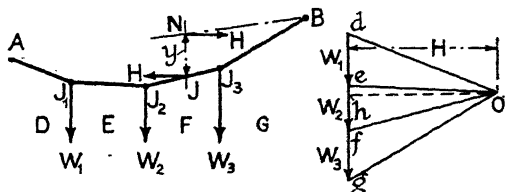
support to support, is hung by vertical suspenders from a suspension chain PQCUV. This chain is carried by vertical towers AQ and BU, over which it passes, and is anchored at P and V. The portions QP and UV are called the back stays. In order to relieve the towers of the bending moment which would otherwise come upon them, a saddle is provided at the top of each tower, over which the chain passes. This permits a small to-and-fro movement, so that, except for the effects of friction, the reaction at the top of the tower is always vertical.

Such an arrangement evidently makes an economical bridge, especially for large spans, for all the main members are in tension ; but although such a structure would safely carry a uniformly distributed load, it is very unsuitable for heavy moving loads. It has been seen that, for a given arrangement of loads, the shape of the chain is represented by the corresponding funicular polygon. It follows that the shape of the chain
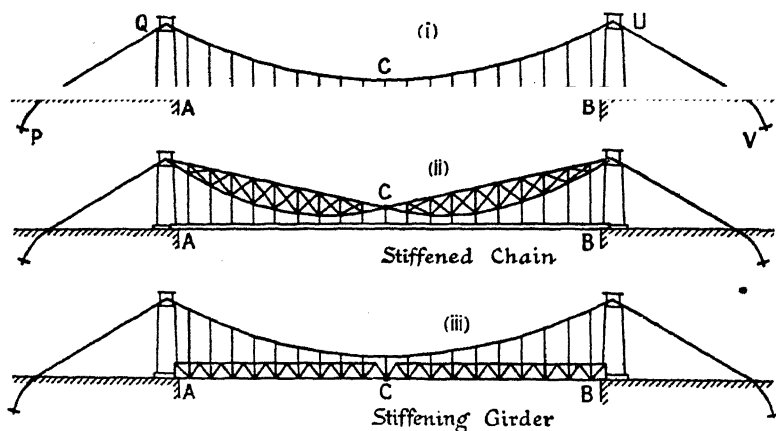
FIG. 368.

is different for each different arrangement of loading. The passage of a moving load across the bridge would therefore produce continuous alteration to the shape of the chain, whence would result large deformations and oscillations in the roadway. Only when the moving load is relatively very small in comparison with the proper weight of the roadway could a simple suspension bridge be used with safety. To overcome this difficulty, the bridge must be so stiffened that it will retain its *shape* under all load conditions ; all deformation, except that due to the elasticity of the material, must be prevented.

Two methods are adopted to give this rigidity : a *stiffened chain* may be used, (ii) Fig. 368, or else a *stiffened roadway*, (iii) Fig. 368.

In the first method the flexible chain is replaced by a stiff frame, which may be formed of two parabolic members braced together to form a truss, or the top members may be straight, (ii) Fig. 368. A hinge is provided at the centre of the span. The whole construction may be

regarded as an inverted 3-hinged arch and designed in a similar way, Chapter XIII. It is statically determinate. The stresses are due to the combination of tension with bending, instead of thrust with bending, as in the arch. The influence lines for the stiff frames will be exactly similar to those for a corresponding 3-hinged arch. The floor is supported by vertical suspension rods, as in the simple suspension bridge. The Tower Bridge, London, is a well-known instance of this method of construction.

Alternatively, the floor may be stiffened by girders, as shown in (iii). The function of these stiffening girders is so to distribute the load that the chain will retain its shape, and by their rigidity to prevent deformation of the floor. The stiffening girder may be in one span from A to B, supported at these points, or it may be, in addition, hinged at the centre. The supports at A and B must be able to prevent the girder from rising. The advantage of the centre hinge is that it relieves the stiffening girder of temperature stresses, which, in a span without a central hinge, may be considerable. It is, however, easier to carry the wind pressure on the bridge without the central hinge, and despite temperature stresses the stiffening girder without the central hinge is considered to be the lighter construction and is the common practice.

236. Stresses in the Stiffening Girder.—(i) Fig. 369 represents a suspension bridge in which the floor is stiffened by a girder AB. Suppose
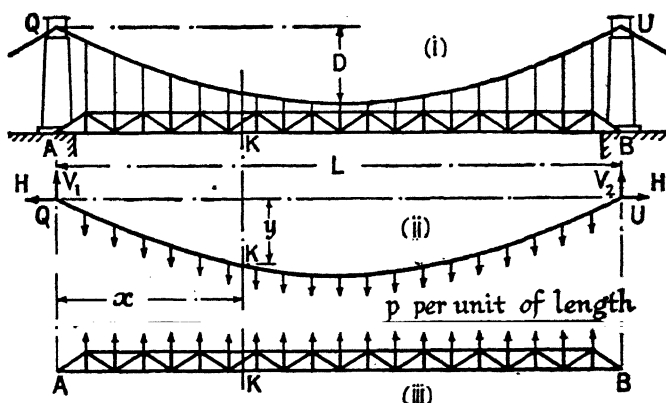
FIG. 369.

that the vertical force in the suspension rods due to the loads on the floor be p per unit of length. The suspension rods are assumed to be sufficiently close together for these forces to be regarded as a distributed load. Then the forces acting on the chain will be as shown in (ii) Fig. 369, and those acting on the stiffening girder will be as shown in (iii).

From the theory of the funicular polygon, the curve which represents the shape of the chain under the action of the vertical supporting forces p will also represent the bending-moment diagram for the stiffening girder

due to these same supporting forces, and the relevant reactions at A and B (cf. § 234). Hence, if y be the ordinate of the curve at some point K distant x from A, and H be the horizontal tension in the chain, (ii), Hy will be the bending moment in the stiffening girder at K due to the forces p. Let the bending moment at K due to the actual loads on the bridge, separately considered, be M′.* This bending moment is found in the ordinary way on the assumption that the stiffening girder is a simple beam supported at A and B. Then M, the total bending moment in the stiffening girder at K, is

$$M = M' + Hy \quad . \quad . \quad . \quad . \quad . \quad (1)$$

the same equation as that which gives the bending moment at any section of an arch, eq. (2), § 216. In eq. (1), bending moments tending to make the girder convex upward are considered as positive, and M′ for the downward acting loads is negative.

The shearing force S at any section K is dM/dx, § 34, Vol. I. Hence,

$$S = \frac{dM}{dx} = \frac{dM'}{dx} + H\frac{dy}{dx} = S' + H\frac{dy}{dx} \quad . \quad . \quad . \quad (2)$$

where $dM'/dx = S'$ is the shearing force on the stiffening girder at K due to the actual loads on the bridge, and calculated as in the case of an ordinary beam supported at A and B ; dy/dx is the slope of the chain at K. If w denote the *total* load per unit of length on the stiffening girder,

$$w = \frac{dS}{dx} = \frac{d^2M}{dx^2} = \frac{d^2M'}{dx^2} + H\frac{d^2y}{dx^2} = \frac{dS'}{dx} + H\frac{d^2y}{dx^2} = w' + H\frac{d^2y}{dx^2} \quad . \quad (3)$$

where w' denotes the actual loads on the bridge per unit of length. But the total load per unit of length on the stiffening girder is $p + w'$. Hence

$$p + w' = w' + H\frac{d^2y}{dx^2} ; \text{ and } p = H\frac{d^2y}{dx^2} \quad . \quad . \quad (4)$$

The bending moment on the stiffening girder will be a maximum when $dM/dx = 0$; or, from eq. (2), when

$$H\frac{dy}{dx} = -S' ; \text{ and } \frac{dy}{dx} = -\frac{S'}{H} \quad . \quad . \quad . \quad (5)$$

Parabolic Chain.—Suppose that the vertical suspension rods are numerous, and that their length has been so adjusted that the shape of the chain is parabolic ; let it also be assumed that the stiffening girder is so rigid that the chain retains this shape in all conditions of loading. As shown in (i) Fig. 369, and as is usual in practice, suppose that bridge and chain are symmetrical about their mid-point ; take origin at Q and let QU be the axis of x. Then the equation to the curve is $y = cx(L - x)$,

---

* For convenience, throughout this chapter, the bridge is conceived as though supported by a single chain. The area of, and forces acting on, this ideal chain must be properly proportioned between the actual number of chains, however many there be.

where c is a constant. If the dip at the centre of the chain be D, $y = $ D when $x = $ L/2, and $c = $ 4D/L^2; hence

$$y = \frac{4D}{L^2} x(L - x) \qquad . \qquad . \qquad . \qquad . \qquad . \qquad (6)$$

$$\frac{dy}{dx} = \frac{4D}{L^2}(L - 2x) \ ; \ \frac{d^2y}{dx^2} = -\frac{8D}{L^2} \qquad . \qquad . \qquad . \qquad (7)$$

Therefore, from eq. (4),

$$p = -\frac{8HD}{L^2} \qquad . \qquad . \qquad . \qquad . \qquad . \qquad . \qquad (8)$$

and since H must be constant from end to end of the chain, p must be a uniform load acting upward.

Uniform Load covering the Span.—If the actual load w' on the bridge be uniform and cover the span, $p = - w'$; hence, $p + w'$ is zero everywhere, and M, the bending moment on the stiffening girder, is zero everywhere ; whence, from eq. (1), H$y = - $M'. M' is the bending moment on the stiffening girder supposing it simply supported at the ends. At the centre of the span, M' $= - w'$L^2/8, and $y = $ D,

$$HD = \frac{w'L^2}{8}, \text{ and } H = \frac{w'L^2}{8D} \qquad . \qquad . \qquad . \qquad (9)$$

as found in eq. (2), § 233. This equation gives the horizontal tension in the chain due to the weight of the stiffening girder and floor, or for any other uniform load entirely covering the span. It will be observed that the construction of the stiffening girder, whether hinged at the centre or not, does not affect this value.

237. Stiffening Girder with Parallel Flanges and a Central Hinge : Parabolic Chain.—If the stiffening girder be hinged at its mid-point C, as shown in (i) Fig. 370, the bending moment at C must be zero ; y at the centre $= $ D, and from eq. (1), § 236,

$$H = -\frac{M_C'}{D} \ ; \text{ hence, } M = M' - \frac{M_C'}{D} y \ . \qquad . \qquad . \qquad (1)$$

The values of S and w follow from eqs. (2) and (3), § 236.

Single Concentrated Load on the Bridge.—Suppose the bridge to carry a single concentrated load W, distant z from A. Then, considering the whole span as a single beam supported at A and B, $R_2' = \dfrac{Wz}{L}$;

$$M_C' = - R_2' \times \frac{L}{2} = - \frac{Wz}{L} \times \frac{L}{2} = - \frac{Wz}{2} \ ; \text{ and from eq. (1),}$$

$$H = -\frac{M_C'}{D} = \frac{Wz}{2D} \qquad . \qquad . \qquad . \qquad . \qquad (2)$$

From eq. (8), § 236,

$$p = -\frac{8HD}{L^2} = -\frac{8D}{L^2} \cdot \frac{Wz}{2D} = -\frac{4Wz}{L^2} \qquad . \qquad . \qquad (3)$$

the minus sign indicates an upward force.

The arrangement of forces on the stiffening girder is shown in (ii) Fig. 370, and the above values can be obtained from first principles as
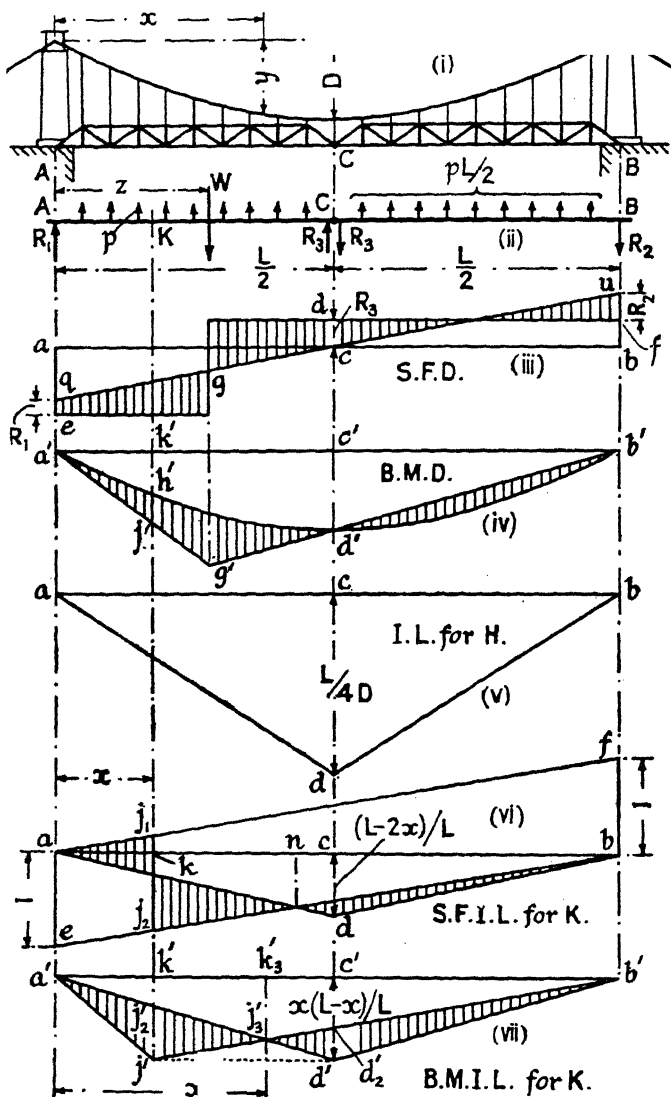
FIG. 370.

follows : the total load on the half-span CB is $pL/2$, each of the downward reactions is $R_2 = R_3 = pL/4$. Considering the half-span AC, and taking moments about A,

$$R_3 \frac{L}{2} + \frac{pL}{2} \cdot \frac{L}{4} - Wz = 0, \text{ where } R_3 = \frac{pL}{4}$$

hence,

$$p = \frac{4Wz}{L^2} \; ; \; R_2 \; : \; R_3 = \frac{Wz}{L} \; ; \; R_1 = W - R_3 - \frac{pL}{2} = W \left(1 - \frac{3z}{L} \right) \quad (4)$$

From eq. (8), § 236, for a parabolic chain,

$$H = \frac{pL^2}{8D} = \frac{4Wz}{L^2} \times \frac{L^2}{8D} = \frac{Wz}{2D}$$

The shearing-force diagram is shown in (iii) Fig. 370. From eq. (2), § 236, the shearing force $S = S' + H\dfrac{dy}{dx}$ where $H = \dfrac{Wz}{2D}$, and from eq. (7),

§ 236, $\dfrac{dy}{dx} = \dfrac{4D}{L^2} (L - 2x)$. Hence,

$$S = S' + \frac{Wz}{2D} \cdot \frac{4D}{L^2} (L - 2x) = S' + \frac{2Wz}{L^2} (L - 2x) \quad (5)$$

In (iii), $aegfb$ is the S' diagram drawn as if the girder were a simple beam supported at A and B, and qgu is the graph of $2Wz(L - 2x)/L^2$. The difference between the ordinates of the two diagrams, shaded in the figure, represents the shearing-force diagram, qu is the base line. The values of R_1, R_2, and R_3 are indicated, and it will be noted that $R_2 = R_3$ in magnitude, which suggests a simple way of setting out the diagram. It will also be noticed that the shearing force changes sign where the bending moment is a maximum. The double triangle $aqcub$ is evidently the shearing-force diagram for the uniformly distributed upward load p.

The bending-moment diagram is shown in (iv). The parabola $a'd'b'$ is the bending-moment diagram for the uniform load p; the ordinate $c'd' = \dfrac{pL^2}{\,} \dfrac{4Wz}{L^2} \times \dfrac{L^2}{8} = \dfrac{Wz}{2} = HD$: $\dfrac{R_2 L}{2}$. The triangle $a'g'b'$ is the negative bending-moment diagram for the load W. The line $g'b'$ must pass through d', for the bending moment at the pin is zero. The shaded area is the complete bending-moment diagram. At any section K, $k'j' = M'$; $k'h' = Hy$; $h'j' = M$; and $M = M' + Hy$.

Influence Lines.—From eq. (2), $H = Wz/2D$; if $W = $ unity, $H = z/2D$. This is the equation to the influence line for H between A and C. The complete influence line is the triangle adb, (v) Fig. 370. The maximum ordinate occurs at the centre of the span where $z = L/2$, and is $H = L/4D$ (cf. § 226).

From eq. (2), § 236, $S = S' + H (dy/dx)$. For the point K, let $dy/dx = \sigma_K$. Then

$$S_K = S_K' + H\sigma_K.$$

From eq. (7), § 236, $\sigma_K = \dfrac{dy}{dx} = \dfrac{4D}{L^2} (L - 2x)$. The influence line for S_K', the shearing force at K for the stiffening girder considered as a simple beam supported by A and B, is the figure aj_1j_2b, (vi) Fig. 370, where $ae = bf$

2 M

= unity.   The influence line for $H\sigma_K$ is the triangle adb, obtained by multiplying the ordinates of (v) by σ_K.   The maximum ordinate of (vi) is

$$cd = H_{max.} \times \sigma_K = \frac{L}{4D} \times \frac{4D}{L^2} (L - 2x) = (L - 2x)/L.$$

The shaded area in (vi), representing the difference between the ordinates of the two diagrams, is the complete shearing force influence line, of which adb is the base line.   When $x < L/4$, d falls outside be; when $L/4 < x < L/2$, d falls inside be; when $x > L/2$, cd is plotted upward from ab.

From eq. (1), § 236, $M = M' + Hy$; for the point K,

$$M_K = M_K' + Hy_K.$$

From eq. (6), § 236, $y_K = \frac{4D}{L^2} x(L - x)$.   The influence line for M_K' is the triangle $a'j'b'$, (vii) Fig. 370, where $k'j' = x(L - x)/L$ (see § 27).   The influence line for Hy_K is the triangle $a'd'b'$, obtained by multiplying the ordinates of (v) by y_K.   The maximum ordinate of (vii) is

$$c'd' = H_{max.} \times y_K = \frac{Ly_K}{4D} = \frac{L}{4D} \cdot \frac{4D}{L^2} x(L - x) = \frac{x(L - x)}{L}.$$

Therefore $c'd' = k'j'$, a useful relation in setting out the diagram.

Maximum Values for a Single Concentrated Load.—For a single concentrated load W, the maximum values of the shearing force are obtained
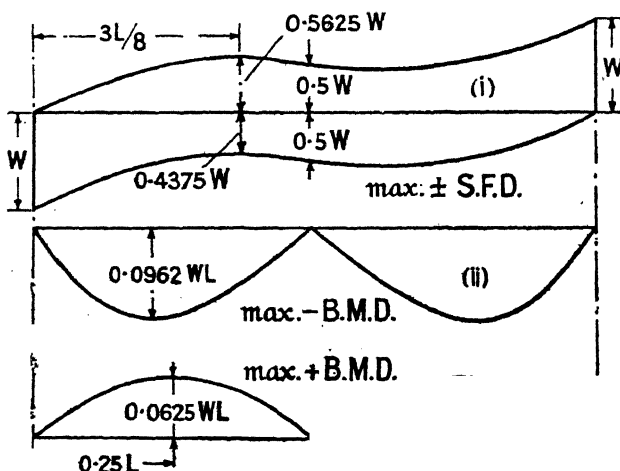
FIG. 371.

at once from the shear influence line (vi).   At the ends of the span the maximum shearing forces are $\mp$ W; at C, the centre of the span, the maximum shearing forces are $\pm$ W/2.   The maximum shearing-force diagram is shown in (i) Fig. 371; it is set out graphically from the influence line.

Since in (vii) Fig. 370, $k'j' = c'd'$, it is evident that the maximum negative bending moment at K always occurs when W is at K ; and the maximum positive bending moment at K occurs when W is at C. From the geometry of the figure, since $k'j' = c'd'$, the maximum negative bending moment at K is

$$W \times j_2'j' = W \cdot c'd' \left\{ \left(\frac{x}{L/2} \right) - \right\} \quad - - - \quad \frac{Wx(L - x)(L - 2x)}{L^2} \quad (6)$$

and the maximum positive bending moment at K is

$$W \times d'd_2' \doteq W \quad k'j' \left\{ 1 - \frac{x}{2}/(L - x) \right. = + \frac{Wx(L - 2x)}{2L} \quad (7)$$

Eqs. (6) and (7) apply only from A to C ; but the maximum bending-moment diagrams are symmetrical about C, and are set out from these equations in (ii) and (iii) Fig. 371. To find the maximum negative bending moment anywhere on the girder, differentiate eq. (6) with respect to x and equate to zero, $L^2 - 6Lx + 6x^2 = 0$; $x = 0 \cdot 211L$. Putting this value in eq. (6), the maximum negative bending moment is $0 \cdot 0962WL$.

To find the maximum positive bending moment anywhere on the girder, differentiate eq. (7) with respect to x and equate to zero, $L - 4x = 0$; $x = 0 \cdot 25L$, and max. $+ M = WL/16$.

Maximum Values for a Uniformly Distributed Load Longer than the Span.—The maximum $+$ and $-$ shearing-force diagrams for a uniform
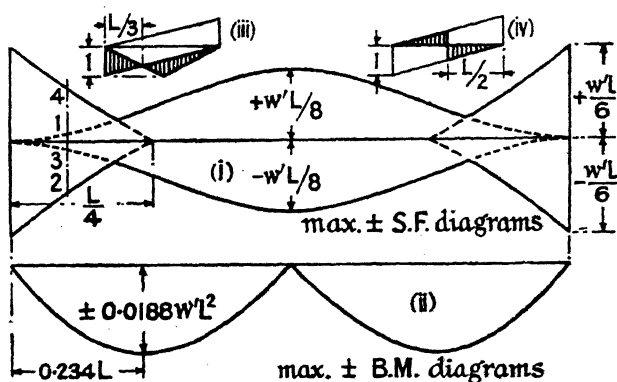
FIG. 372.

load w' per unit of length, longer than the span, crossing the bridge from A to B, can be obtained from the areas of the shearing-force influence line, (vi) Fig. 370. The curves are set out in (i) Fig. 372. While $x < L/4$ there are four possible maxima : (1) positive, when the front of the load covers ak, (vi) Fig. 370 ; (2) negative, when the front of the load covers an ; (3) negative, when the back of the load covers kb ; (4) positive, when the back of the load covers nb. When $L/4 < x < 3L/4$. Nos. 2 and 4 disappear. The curves in (i) Fig. 372 are numbered to

suit. The maximum + and − shearing forces occur at the ends and at the centre ; the influence lines for these cases are shown in (iii) and (iv) Fig. 372. From the shaded areas the values are,

$$\text{At the ends} \quad \pm \text{max. S.F.} = w' \times \frac{1}{2} \times 1 \times \frac{L}{3} = \frac{w'L}{6}$$

$$\text{At the middle} \quad \pm \text{max. S.F.} = w' \times \frac{1}{2} \times \frac{1}{2} \times \frac{L}{2} = \frac{w'L}{8}$$

The maximum negative bending moment at K occurs when the load covers the length $a'k_3' = x_3$, (vii) Fig. 370, and the maximum positive bending moment at K occurs when the load covers the length $k_3'b' = L - x_3$. Since the ordinates $k'j'$ and $c'd'$ are equal, the areas of the triangles $a'j'b'$ and $a'd'b'$ are equal. Subtract the area of the triangle $a'j_3'b'$, and the areas $a'j'j_3'$ and $b'd'j_3'$ are equal, that is to say, the maximum negative and maximum positive bending moments at K are equal in magnitude. From the geometry of the figure,

$$\frac{c'd'}{k_3'j_3'} = \frac{\_\!\_/2}{x_3} = \frac{k'j'}{k_3'j_3'} = \frac{L - x}{L - x_3} ; \quad x_3(L - x) = \frac{L}{2}(L - x_3)$$

and $x_3 = L^2/(3L - 2x)$. Hence the equal negative and positive areas of the influence line under the load are

$$j_2'j' \times \frac{x_3}{2} = \frac{x(L - x)(L - 2x)}{L^2} \times \frac{L^2}{2(3L - 2x)}$$

and the maximum positive and negative bending moments at K, due to the uniform load w', are

$$\text{max.} \pm M_K = \frac{w'x(L - x)(L - 2x)}{2(3L - 2x)} \quad . \quad . \quad (8)$$

This equation only applies from A to C, but the maximum bending-moment diagrams are symmetrical about C. They are plotted from this equation in (ii) Fig. 372. To find the maximum bending moments at any position on the girder, differentiate eq. (8) with respect to x and equate to zero

$$3L^3 - 18L^2x + 24Lx^2 - 8x^3 = 0$$

whence $x = 0 \cdot 234L$ and max. $\pm M = 0 \cdot 0188\ w'L^2$.

238. Stiffening Girder with Parallel Flanges. No Central Hinge : Parabolic Chain.—In Fig. 373 the stiffening girder is anchored to its supports A and B and has no hinge at the centre. This arrangement is statically indeterminate, for it is evident that, were they sufficiently strong, either the chain alone, or the stiffening girder alone, could support the floor from abutment to abutment.

As an approximate method of finding the stresses in the chain and girder, it is sometimes assumed that the girder is sufficiently rigid to spread any load on the bridge uniformly over the span, and that the chain therefore carries the whole load. The reactions R_1 and R_2 must then be equal and opposite. It may be shown as follows that this assumption

is untenable. If W be the total load on the bridge, and the stiffening girder be sufficiently rigid to spread it uniformly over the span,

$$p = \frac{W}{L} \; ; \text{ and, from eq. (8), § 236, } H = \frac{pL^2}{8D} = \frac{WL}{8D}.$$
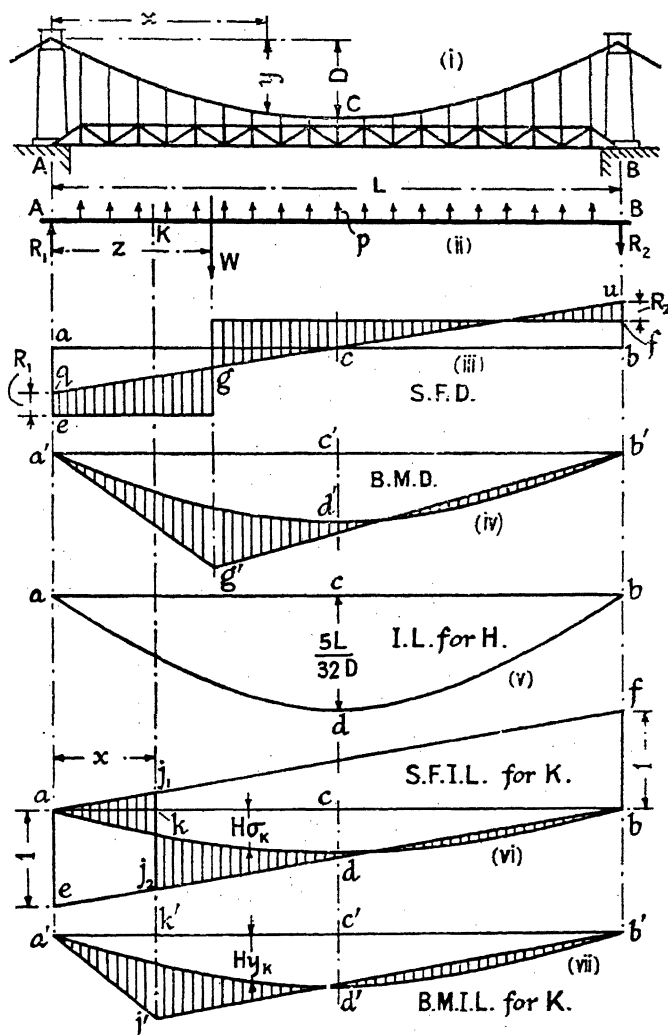
FIG. 373.

It follows that H is constant for any load system of magnitude W. Suppose W to be a single concentrated load just entering the bridge. From eq. (1), § 236, the bending moment anywhere, and therefore at the end of the span, is $M = M' + Hy$. But whether the stiffening girder is regarded as a beam simply supported at its ends, or whether it is supported by the chain, the bending moment at the ends of the span for a load W

just entering the bridge must be zero ; that is to say, for the end cross-sections, both M' and M are zero. Hence Hy is zero, and consequently H is zero, not WL/8D, as according to the above assumption it should be.

It is necessary to take into account the relative stiffness of the different parts of the bridge in order to find H ; strain energy considerations (Chapter V) may be used to solve the problem. A number of studies have been made of this question (see Refs. Nos. 20 to 29, Bibliography) ; the following treatment, based on § 89, is approximate.

The structure may be regarded as a redundant frame built up of bars forming (i) the chain, (ii) the vertical suspension rods, and (iii) the stiffening girder. It is clearly redundant, but there is only one redundant bar, for if the lowest link of the chain be removed, neither the chain nor the suspension rods could carry any load. Remove this link, and find the forces F_W in the remaining bars due to the actual loads. Then remove the applied loads, replace the redundant link by unit loads, and find the forces F' in all the bars due to the unit loads ; the force F' in the redundant member will be unity. Then from eq. (1), § 89,

$$X = F_r = H = - \frac{\Sigma F_W F' \lambda}{\Sigma (F')^2 \lambda}$$

for in this case the force F_r in the redundant link is H. It is convenient to treat the three components of the structure separately. Let T denote the tensions in the links, P the tensions in the suspension rods, and F the forces in the bars of the stiffening girder. T_W is the force in a link due to the actual loads ; T' that due to the unit loads ; and so on. Then

$$H = - \frac{\Sigma T_W T' \lambda + \Sigma P_W P' \lambda + \Sigma F_W F' \lambda}{\Sigma (T')^2 \lambda + \Sigma (P')^2 \lambda + \Sigma (F')^2 \lambda}.$$

Since there can be no forces in the chain links or in the suspension rods, due to the actual loads, when the lowest link of the chain has been removed, it follows that T_W and P_W are all zero, hence

$$H = - \frac{\Sigma F_W F' \lambda}{\Sigma (T')^2 \lambda + \Sigma (P')^2 \lambda + \Sigma (F')^2 \lambda} \qquad . \qquad . \qquad (1)$$

an equation giving H in terms of forces which can be found from the shape and dimensions of the parts of the bridge.

In the present instance, let it be assumed that the shape of the chain is parabolic, and that the areas of the links are so proportioned that the stress f in the links is constant from end to end of the chain. Let the area of the lowest link be a_0 ; then H, the tension in that link, is $a_0 f$, and $f = H/a_0$. Consider any link of length l, and area a ; let the tension in it be T. Then

$$a = \frac{T}{f}, \text{ and } \lambda = \frac{l}{a} = \frac{l}{T} \cdot f = \frac{lH}{Ta_0} ;$$

if H be put equal to unity, T = T' and $\lambda = l/T'a_0$. Further, from Fig. 374, $\frac{T}{H} = \frac{l}{x}$; $T = H \frac{l}{x} = H \sec \theta$; and when H = unity, T = T' = $\sec \theta$.

Then

$$(T')^2\lambda = \frac{(T')^2 l}{T' a_n} = \frac{l \sec \theta}{a_n} = \frac{x \sec^2 \theta}{a_n}$$

for $l = x \sec \theta$, and

$$\Sigma (T')^2\lambda = \frac{1}{a_0} \Sigma x \sec^2 \theta = \frac{1}{a_0} \Sigma x(1 + \tan^2 \theta)$$

Conceiving the chain as a continuous parabolic curve, and letting x get smaller and smaller without limit,

$$(T')^2\lambda = \frac{1}{a_0} \int (1 + \tan^2 \theta) dx$$

Taking origin for the present purpose at C, (i) Fig. 373, the equation to the curve is $y = \dfrac{4D}{L^2} x^2$; $\tan \theta = \dfrac{dy}{dx} = \dfrac{8Dx}{L^2}$; and, including both halves of the curve,

$$\Sigma (T')^2\lambda = \frac{2}{a_0} \int^{L/2} \left\{ 1 + \frac{64D^2 x^2}{L^4} \right\} dx = \frac{1}{a_0}\left[L + \frac{16D^2}{3L} \right] \qquad . \quad (2)$$

The internal work stored in the suspension rods will be small relatively to that stored in the chain and the stiffening girder, and therefore the summation $\Sigma (P')^2\lambda$ will be neglected in what follows. If the dimensions of the rods were known, it could easily be taken into account.

Consider next the stresses in the stiffening girder. Let D_1 denote the depth of this girder, and suppose that the area of all the members of both flanges be a_1. If, at any section $Q_1 K_1$, Fig. 374, the bending moment be M, the force in a flange member such as $Q_1 Q_2$ will be $F = M/D_1$. If the length of the member be l_1, the value of λ is l_1/a_1.

From eq. (1), § 236, the bending moment in the stiffening girder is

$$M = M' + Hy.$$

FIG. 374.

Assuming (see above) that all the applied loads have been removed from the bridge, the bending moment M', due to them, must be zero. If also the force in the lowest link of the chain be made unity (H = 1), then M = y, and in these conditions F = F'. Assuming parabolic initial curvature, and taking origin at one end of the span, $y = \dfrac{4D}{L^2} x(L - x)$ [see eq. (6), § 236]. Then

$$F' = \frac{M}{D_1} = \frac{y}{D_1} = \frac{4D}{L^2 D_1} x(L - x) \qquad (3)$$

and

$$\Sigma (F')^2\lambda = \Sigma \frac{16D^2}{L^4 D_1^2} x^2(L - x)^2 \frac{l_1}{a_1}$$
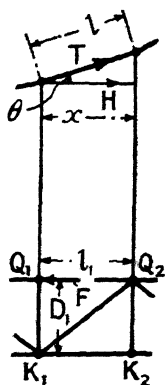
Regarding the flanges as continuous members from end to end of the span ; letting l_1 get smaller and smaller without limit until it becomes dx ; for both the flanges

$$\Sigma \, (F')^2\lambda = \frac{32D^2}{L^4D_1{}^2a_1} \int_0^L (x^2)(L-x)^2 dx = \frac{16LD^2}{15D_1{}^2a_1}. \qquad (4)$$

Suppose that the applied load on the bridge is a single load W distant z from A, Fig. 375. Then the bending moment under the load is $- Wz(L-z)/L$; and at any section distant x from A, if $x < z$, the bending moment is $- W(L-z)x/L$, or if $x > z$, is $- Wz(L-x)/L$. The forces F_W in the flanges of the stiffening girder, for these two cases, are
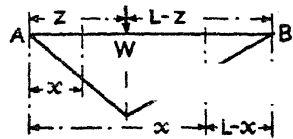
FIG. 375.

$$F_W = \frac{M}{D_1} = - \frac{W}{D_1}(L-z)\frac{x}{L} \; ; \; F_W = - \frac{W}{D_1} z \frac{(L-x)}{L}.$$

The summation $\Sigma F_W F'\lambda$ must be split into two parts to correspond with these two values. Inserting the values of F_W, F' (eq. 3), and λ, and treating the two flanges as continuous members as before,

$$\Sigma F_W F'\lambda = 2\int_0^z \left\{ - \frac{W}{D_1}(L-z)\frac{x}{L} \right\} \left\{ \frac{4D}{L^2D_1} x(L-x) \right\} \frac{dx}{a_1}$$

$$+ 2\int_z^L \left\{ - \frac{W}{D_1} z \frac{L-x}{L} \right\} \left\{ \frac{4D}{L^2D_1} x(L-x) \right\} \frac{dx}{a_1}$$

$$\frac{WD}{D_1{}^2a_1}\left[(L-z)\int_0^z x^2(L-x)dx + z\int_z^L x(L-x)^2 dx \right]$$

$$\frac{}{3L^2D_1{}^2a_1} \cdot z(L^3 - 2Lz^2 + z^3) \qquad (5)$$

From eq. (1),

$$H = - \frac{\Sigma F_W F'\lambda}{\Sigma (T')^2\lambda + \Sigma (P')^2\lambda + \Sigma (F')^2\lambda}$$

Putting in the ascertained values, eqs. (5), (2), and (4),

$$H = - \frac{- \dfrac{2WD}{3L^2D_1{}^2a_1} \cdot z(L^3 - 2Lz^2 + z^3)}{\dfrac{1}{a_0}\left[L + \dfrac{16D^2}{3L} \right] + \dfrac{16LD^2}{15D_1{}^2a_1}} \qquad (5a)$$

which simplifies to

$$H = z(L-z)(L^2 - Lz - z^2)\chi W \quad . \qquad (6)$$

where

$$\chi = \frac{D}{L} \cdot \frac{10}{\dfrac{5D_1{}^2a_1}{}[3L^2 + 16D^2] + 16L^2D^2}$$

$$\frac{D}{L} \cdot \frac{}{\dfrac{5I_1}{a_0}[3L^2 \quad 16D^2] + 8L^2D^2} \qquad (7)$$

if $I_1 = D_1{}^2 a_1/2$ is the moment of inertia of the stiffening girder. In finding these formulae, the deformation of the suspension rods, that of the web bracing of the stiffening girder, and any deflection in the chain, have been neglected. The equations can only be applied when I_1 and a_0 are known. An approximation which may be used for the purpose of preliminary design can be obtained as follows : Eq. (7) may be written

$$\chi = \frac{10D}{L^3} \cdot \frac{1}{\dfrac{5D_1{}^2 a_1}{a_0}\left[3 + 16\dfrac{D^2}{L^2}\right] + 16D^2}$$

In practical cases the value of D/L will be about $\frac{1}{10}$ or slightly greater, and the equation may be written

$$\chi = \frac{5D}{8L^3} \cdot \frac{1}{\dfrac{D_1{}^2 a_1}{a_0} + D^2} = \frac{5D}{8L^3} \cdot \frac{1}{\dfrac{2I_1}{a_0} + D^2}$$

If the girder were infinitely stiff, $I_1 = \infty$, and $\chi = 0$; if the girder were perfectly flexible, $I_1 = 0$, and $\chi = 5/(8L^3D)$. In practical cases its value will not differ much from $1/(2L^3D)$, and eq. (6) becomes

$$H = \frac{W}{2L^3D} z(L - z)(L^2 + Lz - z^2) \tag{8}$$

This curve has been plotted accurately in (v) Fig. 373, for $W = 1$. It will be found to differ very slightly from the parabola

$$H = \frac{5W}{8LD} z(L - z) \tag{9}$$

which equation can be used for the preliminary design.

The value $H = \frac{1}{8}WL/D$, based on the assumption, p. 533, that the stiffening girder spreads the load uniformly over the span, is likely to be most nearly correct when W is at the centre of the span, $z = L/2$, in which case, from eq. (8) or (9), $H = \frac{5}{32}WL/D$, a not very different value, but showing that the stiffening girder is more flexible than the said assumption implies.

The shearing-force diagram for a single concentrated load W, distant z from A, is shown in (iii) Fig. 373, set out from eq. (2), § 236 [see also eq. (7), § 236],

$$S = S' + H\frac{dy}{dx} = S' + H \cdot \frac{4D}{L^2}(L - 2x).$$

The value of H for the given load position is obtained from either eq. (8) or eq. (9). The diagram, (iii) Fig. 373, is similar to (iii) Fig. 370 ; $aq = bu = 4HD/L.$

The bending-moment diagram for the same load position is shown in (iv) Fig. 373, set out from eq. (1), § 236 [see also eq. (6), § 236].

$$M = M' + Hy = M' + H \cdot \frac{4D}{L^2}x(L - x).$$

The value of H is obtained from eq. (8) or eq. (9) as before. The diagram is similar to (iv) Fig. 370 ; $c'd'$ the central ordinate of the parabola $a'd'b' = HD$.

Influence Lines.—These are similar to (v), (vi), and (vii), Fig. 370, *q.v.*, and are set out in similar fashion, except that the influence line for H approximates to a parabola instead of being a triangle.

From eq. (8), if W = unity,

$$H = \frac{1}{2L^3D}z(L - z)(L^2 + Lz - z^2).$$

This is the equation to the influence line for H, and is set out in (v) Fig. 373. The maximum ordinate, at the centre of the span, is $5L/32D$. Alternatively, the curve can be set out from eq. (9), if W in that equation be put equal to unity.

From eq. (2), § 236, for the point K,

$$S_K = S_K' + H\frac{dy}{dx} = S_K' + H\sigma_K$$

from which the shearing force influence line for K, (vi), is obtained. The curve adb is obtained by multiplying the ordinates of (v) by

$$\sigma_K = 4D(L - 2x)/L^2.$$

From eq. (1), § 236, for the point K, $M_K = M_K' + Hy_K$, from which the bending moment influence line for K, (vii), can be set out. The curve $a'd'b'$ is obtained by multiplying the ordinates of (v) by

$$y_K = 4Dx(L - x)/L^2.$$

The maximum shearing-force and bending-moment diagrams can be obtained from the influence lines as were those in Figs. 371 and 372.

Temperature Stresses.—The effect of changes in temperature in altering the length of the chain and suspension rods of the bridge may be found by use of eq. (4), § 93,

$$X_t = -\frac{\Sigma F'atl}{\Sigma(F')^2l/Ea} = -E\frac{\Sigma F'atl}{\Sigma(F')^2\lambda}$$

In this equation l is the length of a member, t the alteration of temperature in degrees, and α the coefficient of expansion per degree. Treating the three component parts of the structure separately as before, and using the symbols T, P, and F for the chain links, suspension rods, and bars of the stiffening girder, respectively, the above equation becomes

$$X_t = -E\frac{\Sigma T'atl + \Sigma P'atl}{\Sigma(T')^2\lambda + \Sigma(P')^2\lambda + \Sigma(F')^2\lambda} = H_t \quad . \quad . \ (10)$$

cf. eq. (1), where the symbols are defined. H_t is the increase in the horizontal tension due to a rise in temperature t. Ignoring as before the effect of the suspension rods, the equation becomes

$$H_t = -E\frac{at\Sigma T'l}{\Sigma(T')^2\lambda + \Sigma(F')^2\lambda}$$

But (see above), when $H = 1$, $T' = \sec\theta$, and $T'l = l\sec\theta = x\sec^2\theta$ (Fig. 374). Hence, $\Sigma\,T'l = (L + 16\,D^2/3L)$ [c.f. eq. (2)]. The denominator has previously evaluated [see eq. (5a)], therefore

$$H_t = -\ \dfrac{Eat\ (L + 16D^2/3L)}{\dfrac{1}{a_0}\left[L + \dfrac{16D^2}{3L}\right] + \dfrac{16LD^2}{15D_1{}^2a_1}}$$

$$\dfrac{Eat\ (L + 16D^2/3L)}{\dfrac{1}{a_0}\left[L + \dfrac{16D^2}{3L}\right] + \dfrac{8LD^2}{15I_1}} \qquad . \quad (11)$$

where, as before, $I_1 = D_1{}^2a_1/2$ is the moment of inertia of the stiffening girder.

At any point in the stiffening girder, the bending moment induced by this change in H will be

$$M = H_t y = \frac{4D}{L^2}H_t\,x(L - x) \qquad . \qquad . \qquad . \ (12)$$

See eq. (6), § 236.

CONTINUOUS GIRDER AND CANTILEVER BRIDGES

239. **Continuous Girder Bridges.**—It follows from the theory of continuous beams, Chapter VI, Vol. I, that in a large bridge of more
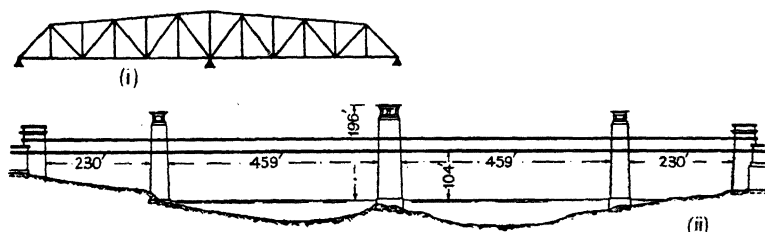
FIG. 376.

than one span, the bending moment everywhere, and consequently the weight and cost of the bridge, can be considerably reduced by making the girders continuous over the piers, (i) Fig. 376.

Although one of the earliest long-span bridges, the Britannia Bridge [31] over the Menai Straits, (ii), was a successful example of this type, continuous girder bridges have not been very generally employed for the following reasons :

One of the conditions assumed in the usual theory is that all the supports are at the same level, and that they remain level when the load is applied. This is a difficult condition to ensure in practice. Even if the piers of a bridge are made level when first constructed, they are liable to slight settlement, unless they can be carried down to solid rock. If they are constructed of metal, they will expand with differences of

temperature. Such variations may materially alter the bending moments and stress distribution in a continuous girder bridge, especially if the spans are short and the girders are deep and stiff. In very long spans the effect may not be so serious.

A second objection to the use of continuous girders in large bridges is that the complete girder is usually too large to erect in one piece. It is possible in some cases to roll the girder out, but this involves special stiffening to resist the exceptional stresses set up. As a rule, each span must be lifted into place separately, and connected to its neighbours afterwards. Now the connections, whatever form they may take, will in their normal condition be in a state of strain, and even if that state be due to the weight proper of the girder alone, it is necessary to ensure that the strain is of the correct amount, otherwise the entire distribution of stress in the girder will be altered. This is not easy to do, with the result that unknown initial stresses may exist in the girders.

These uncertainties are inevitable in continuous girder bridges, and have led many bridge engineers to prefer separate spans.

240. Cantilever Bridges.—Many of the advantages of a continuous girder bridge, without the countervailing disadvantages, may be obtained
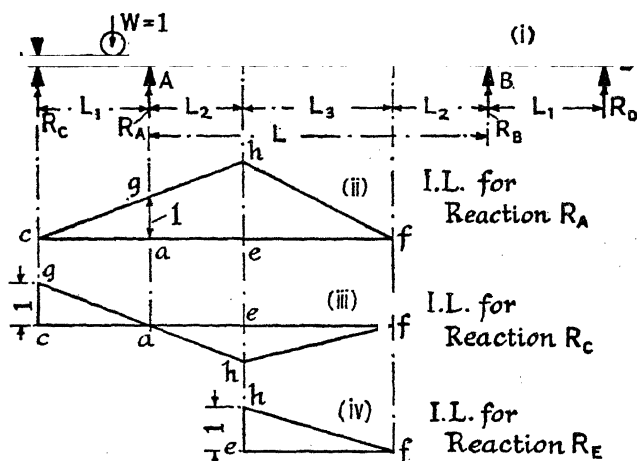
FIG. 377.

by adopting the type known as the *cantilever bridge*. In a continuous girder bridge, the position of the points of no bending moment are different for each different load condition. In a cantilever bridge, these points are fixed by making an actual joint in the girder. (i) Fig. 377 shows an example. This bridge consists of two cantilevers AC, AE, built out from each pier, and carrying a suspended span EF. The ends C and D are anchored down to prevent them from lifting due to the weight of the suspended span and the loads on it ; E and F are the joints. The stresses in such a bridge are statically determinate.

The Forth Bridge, Fig. 77, is a well-known example of this type, which is a common one for large bridges. Fig. 378 and Fig. 379 show other examples of cantilever bridges. The cantilever construction is very suitable for building out from the piers.

241. **Influence Lines for Cantilever Bridges.**—*Note :* When considering the effects produced by a unit load passing over a cantilever bridge or similar structure, it is well to regard the structure as weightless, and to rid one's mind of previous conceptions as to the effect of the suspended span, methods of anchorage, the sense of the end reactions, etc., concentrating the attention on the effects produced by the single moving load.

Reaction Influence Lines.—Let (i) Fig. 377 represent a cantilever bridge with two cantilever spans CE, DF, and a central suspended span EF. For the purpose of finding the reaction influence lines, it is unnecessary to consider the bracing. Let R_A be the reaction at the pier A. The influence line for this reaction is shown at (ii). When the unit load W enters the bridge at C, the reaction at A will be zero. As W advances, R_A will increase, until, when the load is at A, $R_A = W = 1$. When W passes A, R_A will continue to increase at the same rate as before until W reaches the suspension point E, when $R_A = W(L_1 + L_2)/L_1$. As the load W travels along the suspended span, R_A will steadily diminish, and when W enters the right-hand cantilever arm, R_A becomes zero. The influence line for R_A is therefore a triangle $cghf$, (ii), the ordinate ag = unity, and $eh = (L_1 + L_2)/L_1$.

The reaction influence line for R_C is shown at (iii). When W is at C, the reaction $R_C = W = 1$ (forget the weight of the bridge and think of the arm CA as a span supported at C and A). As W advances, R_C will diminish, until when W arrives at A, $R_C = 0$. When W passes A, the reaction at C will become negative, i.e. it will act downwards, and will go on increasing in magnitude until, when W reaches E, $R_C = WL_2/L_1$. As W passes along the suspended span, R_C will gradually diminish, becoming zero when W enters the right-hand cantilever. This is shown in (iii), where $cg = 1$ and $eh = L_2/L_1$.

The influence line for the reaction at E from the suspended span is the same as that for any other span supported at the ends. It is shown at (iv) (cf. Fig. 59).

Influence Lines for Anchor Arm.—Let Fig. 378 represent a conventional cantilever bridge ; AC is the anchor arm. If the bridge be regarded as a weightless structure, it will be evident that while the load is between C and A the anchor arm will act as a lattice girder supported at A and C. The influence lines are then as given in § 35, Fig. 64. Taking $K_1K_2Q_2Q_1$ as a typical panel, the influence line for the diagonal K_1Q_2 is cj_1j_2a, (ii) Fig. 378, where $cg = r/r_3$ (compare § 35).

When the load passes A, the reaction R_C becomes negative and increases until W passes E, when it begins to diminish and ultimately becomes zero when W passes F, (iii) Fig. 377. But after the load has passed Q_2K_2, the only force to the left of the panel K_1Q_2 is R_C. Hence the force in K_1Q_2 will depend solely on the magnitude of R_C, and will

increase and decrease in direct proportion thereto. Therefore, to complete the influence line, produce ga to h and join hf; the complete influence line for K_1Q_2 is cj_1j_2ahf.

It will be evident that the force in Q_2K_2 bears a constant ratio to the force in K_1Q_2; and can be found by multiplying the force in K_1Q_2 by
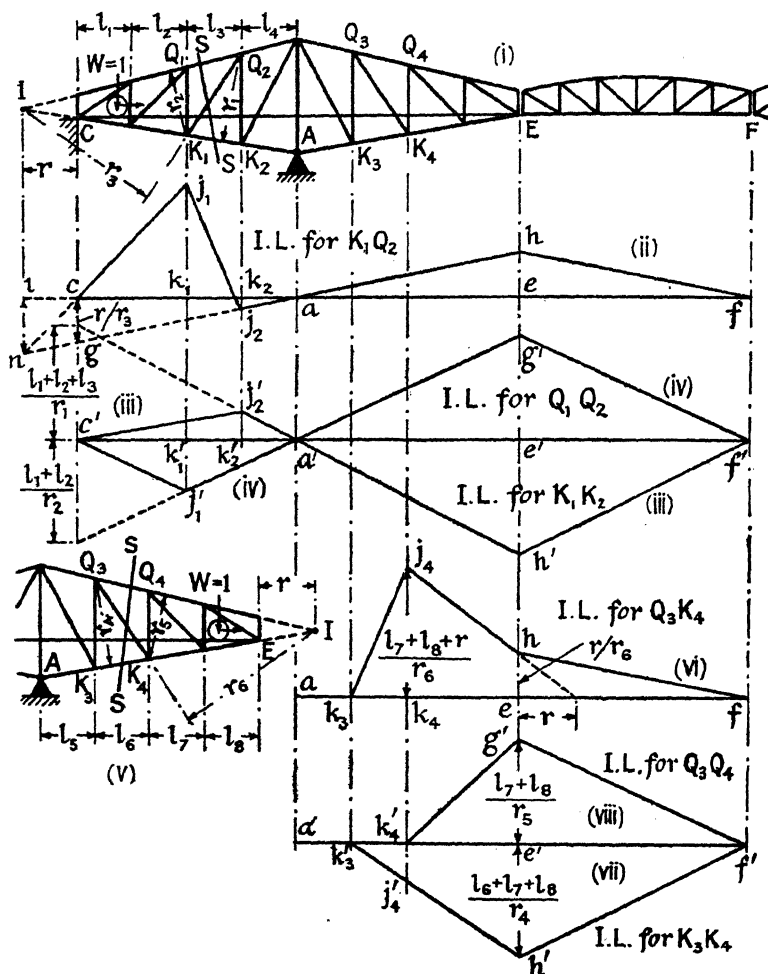
FIG. 378.

$r_3/(r + l_1 + l_2 + l_3)$. Allowance must be made when necessary for the incidence of the load from the cross girders on to the verticals.

Considering next the bottom flange K_1K_2, the other two bars cut by the section SS meet in Q_2. While the load is between A and C, the influence line $c'j_2'a'$ for this bar is similar to that for K_1K_2, (iv) Fig. 64, and is shown in (iii) Fig. 378; the end ordinate is $(l_1 + l_2 + l_3)/r_1$. After

the load has passed A, the same arguments apply to K_1K_2 as to K_1Q_2, and the influence line can be completed by producing $j_2'a'$ to h' and joining h' to f'.

The influence line $c'j_1'a'$, (iv), for Q_1Q_2, while the load is between A and C, will be similar to (vii) Fig. 64. As before, it can be completed for load positions between A and F by producing $j_1'a'$ to g' and joining g' to f'. (iii) and (iv) are plotted on the same base line $c'f'$.

Influence Lines for Cantilever Arm.—While the load is between A and C, there will be no stress in the cantilever arm AE. When the load passes A, this arm will be in the condition of a projecting cantilever with a load advancing towards its free end [(v) Fig. 378]. Consider the typical panel $Q_3K_3K_4Q_4$, and cut it by a section SS. There will be no stress in Q_3K_4 until W passes Q_3K_3, after which the force F_6 in that member will steadily increase as shown by k_3j_4 in the influence line (vi), until the point Q_4K_4 is reached. At this point, taking moments about I,

$$F_6r_6 = W(l_7 + l_8 + r), \text{ and } F_6 = (l_7 + l_8 + r)/r_6, \text{ since } W = \text{unity.}$$

Therefore the ordinate $k_4j_4 = (l_7 + l_8 + r)/r_6$. As W advances, the force in Q_3K_4 will decrease, until, when W reaches E, $F_6r_6 = Wr$; and $eh = r/r_6$. As the load travels along the suspended span, R_E, and therefore the force in Q_3K_4, will steadily decrease; this is shown by hf.

Consider next the bottom flange member K_3K_4. There will be no force in this bar until W passes Q_3K_3, after which F_4, the force in it, will continuously increase until W reaches Q_4K_4, when, taking moments about Q_3, $F_4r_4 = Wl_6$; hence the ordinate $k_4'j_4'$ of the influence line (vii) is equal to l_6/r_4. The stress in K_3K_4 will continue to increase until W reaches E, when $F_4r_4 = W(l_6 + l_7 + l_8)$; and $e'h' = (l_6 + l_7 + l_8)/r_4$. As W travels along the span EF, the force in K_3K_4 will continually diminish as shown by the line $h'f'$; (vii) is the complete influence line.

There will be no force in the upper flange member Q_3Q_4 until W passes Q_4K_4, after which the force F_5 in it will increase until E is reached. Taking moments about K_4,

$$F_5r_5 = W(l_7 + l_8); \text{ and } e'g' = (l_7 + l_8)/r_5.$$

The force in Q_3Q_4 will steadily diminish as W travels along EF. The complete influence line is shown at (viii).

With the influence lines plotted as shown in Fig. 378, an ordinate above the base line implies a tension in the member, and an ordinate below the base line implies a compression. The influence lines for the right-hand cantilever spans are exactly similar to those of Fig. 378, but of the opposite hand. For clearness, (ii) and (vi) of Fig. 378 have been plotted to double the vertical scale of the other influence lines in that figure.

The whole series of influence lines can best be set out by assuming the cantilever span fixed in space at A and loaded with a unit load at C. The forces in the members of the arm AC, due to this load, will give the ordinates of the influence lines on the vertical through C (see § 35).

Similarly, the forces in the members of the arm AE, due to a unit load at E, will give the ordinates on the vertical through E of the influence lines for the arm AE.

LONG-SPAN BRIDGES

242. Types.—The following types of bridge are used for long spans : *Cantilever Bridges.*—This type is illustrated and discussed in § 240 *et seq.* The Forth Bridge,[35] Fig. 77, and the Quebec Bridge [38] over the St. Lawrence, Fig. 379, are two well-known examples. The K bracing in the cantilever webs of the latter should be noticed.

FIG. 379.—Quebec Bridge.

Continuous Girder Bridges.—Continuous girder bridges are sometimes used for long spans. The Ohio River Bridge at Sciotville,[40] Fig. 380, is an example.
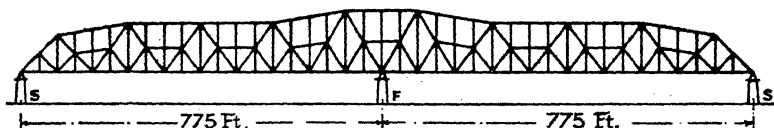
FIG. 380.*—Ohio Bridge, Sciotville.

Arches.—The two-hinged braced arch is frequently adopted for long spans. A typical example is the Hell Gate Bridge, New York (see § 94 and Fig. 130). The Sydney Harbour Bridge, Fig. 381, is of this
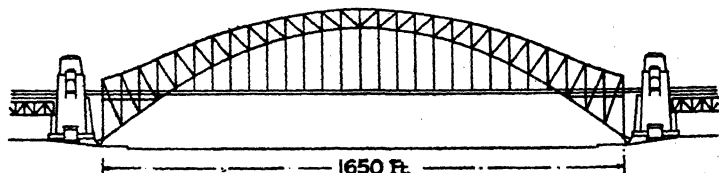
FIG. 381.—Sydney Harbour Bridge.

type. Tied arches, Fig. 127, are occasionally used ; the bridge over the Rhine at Mainz is an example. Two-hinged spandrel-braced arches are

* F = fixed bearing ; S = sliding bearing.

suitable for spanning deep gorges. The Victoria Falls and Niagara Arches are well-known examples.

Cantilever Arch.—Except for large masonry arches, the arch with fixed ends is not usually employed for long spans.* A type, Fig. 382, in

FIG. 382.

which anchor arms are built out cantilever fashion from the arch and supply the fixing moments at the main abutments, is termed a cantilever arch.

Suspension Bridges.—The three-span stiffened suspension bridge is one of the best types for very long spans, and a number of notable examples have been constructed, particularly in America, which include the Delaware River Bridge,[41] Fig. 383 ; the George Washington Bridge,[42] main span 3,500 ft. ; and the Golden Gate Bridge,[43] main span 4,200 ft.
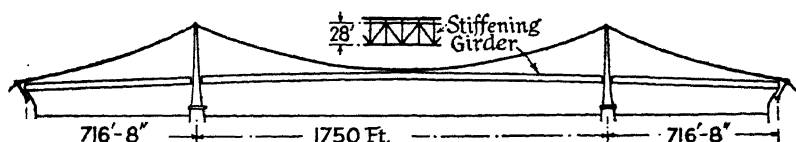
FIG. 383.—Delaware River Bridge.

In Fig. 384, which represents a bridge over the Rhine at Cologne,[39] the stiffening girder is continuous over the three spans and the chain
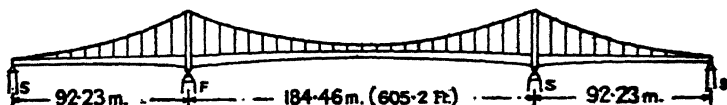
FIG. 384.—Rhine Bridge, Cologne.

is attached to the shore end of the anchor arms. Such a bridge is termed *self-anchored* ; the cost of the abutments is much reduced. It does not appear to be a very economical type for spans of great length, as the stiffening girder has to resist the horizontal tension in the chain.

For the elementary theory of suspension bridges, see § 235 *et seq.* For the more exact treatments used in long-span bridges, see the Bibliography of this chapter, Refs. Nos. 20–29. The commonly adopted ratio of dip to span ranges from $\frac{1}{10}$ to $\frac{1}{8}$.

---

* A steel arch of 800 ft. span, with direction-fixed ends, has recently been constructed in New York. *Eng. News.-Rcd.* vol. 117, p. 232.

Combined Arch and Chain Bridges.—Fig. 385 shows a form of bridge suggested by Professor Krivoshein,[18] in which a cantilever arch is combined with suspension chains. It is a self-anchored type, and appears to show considerable economy over either a plain 3-span suspension type, or the self-anchored suspension bridge. Over the main span, the horizontal tension in the chain is balanced by the horizontal thrust of the

-600Ft.····   — — 1800 Ft. ——   S   600Ft.—
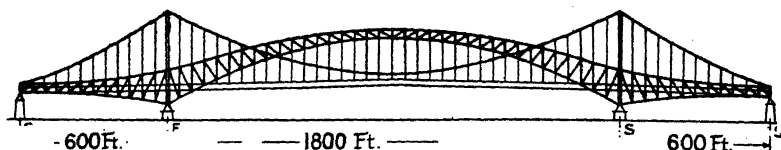
FIG. 385.

arch, and the roadway girder is relieved of this stress. The type may be regarded, therefore, as a development of the Saltash type, (ii) Fig. 280.

243. Choice of Type.—As to which type of long-span bridge is most economical depends very largely on the situation, and particularly on the foundation possibilities. For example, if rock abutments are available, anchorage is easy, and the self-anchored types of suspension bridges and their variants have no great advantage over the plain types. A deep gorge may suggest a spandrel-braced arch, Fig. 340, the sides of the gorge forming natural abutments for the arch. In situations where it is impossible to obtain suitable abutments for an arch, a tied arch might be used (cf. Fig. 127), but if the tie obstruct the waterway, this form is precluded, and another must be adopted. Again, foundations for piers may be possible only at particular points on the line of the bridge, a circumstance which will determine the number and length of the spans. Such local considerations will usually outweigh the intrinsic merits of any one type. For a discussion of this question, see a paper by Waddell before the Western Society of Engineers.*

With the exception of simple cantilever bridges, most types of long-span bridges are statically indeterminate, and strain-energy methods must be employed to determine the stresses (see for example § 94 and § 238). The magnitude of these structures is far too great to permit simplifying assumptions to be made.

VIADUCTS

244. Viaducts.—The term *viaduct* is commonly used to designate a structure carrying a railway or roadway across a valley, and consisting of a number of contiguous, moderately short spans, supported on a series of piers. The piers may be of steel (§ 246), masonry, brickwork, or timber. They are usually tall ; for heights less than 50–60 feet it is often more

* *Jour.*, vol. xxxii, October 1927, p. 313.

economical to construct an embankment. The spans between the piers may be bridged by steel girders, or by masonry or brick arches. A series of arches of the type shown in Fig. 500 would be called a brick viaduct. Timber trusses on timber trestles were formerly common in America. Viaducts, both piers and spans, are frequently constructed of reinforced-concrete.

The spans in such structures may range from 30 to 60 feet, but site considerations, suitability of foundations, and other local conditions are the determining factors.

BIBLIOGRAPHY

Tensions in Wires and Cables

1. MINCHEN. Catenary Problems. *Engg.*, Feb. 7, 1896, p. 173.
2. WOODHOUSE. Testing the Elasticity of Wires. *Jour. I.E.E.*, vol. 44, 1910, p. 817.
3. SWIFT. The Elasticity of Wires and Cables. *Engg.*, Apl. 30, 1926, p. 547.
4. WATSON. Sags and Tensions in Overhead Wires with Supports at Different Levels. *The Engr.*, June 13, 1930, p. 651.
5. WALMSLEY. Length, Tension, and Sag of Stay-Ropes. *Select. Eng. Pap. I.C.E.*, No. 19, 1924.

Suspension Bridges

6. RANKINE. *Applied Mechanics*. 2nd ed., p. 375; also *Civil Eng. and Arch. Jour.*, Nov. and Dec. 1860.
7. AIRY. Suspension Bridge with Stiffened Roadway. *Proc. Inst. C.E.*, vol. xxvi, 1867, p. 258.
8. FIDLER. Suspension Bridges and Arches. *Engg.*, Apl. 30, 1875, p. 372; Nov. 5, 1875, p. 351; Mar. 25, 1881, p. 297; also CHASE, *The Engr.*, May 7, 1909, p. 469.
9. MÜLLER-BRESLAU. Theorie der durch einen Balkenversteiften Ketter. *Zeit. d. Arch.- u. Ing. Ver. z. Hannover*, 1881, p. 57; 1883, p. 347.
10. LÉVY. Calcul des ponts suspendus rigides. *Ann. d. Ponts et Chaussées*, t. xii, 2ᵉ sem., 1886, p. 179.
11. MELAN. See Ref. No. 19, Chap. XIII, Bib.
12. GODARD. Recherches sur le calcul de la résistance des tabliers des ponts suspendus. *Ann. d. Ponts et Chaussées.* 7ᵉ serie, t. viii, 1894, p. 105; see t. ix, 1895, p. 456.
13. AM ENDE. Suspension Bridges with Stiffening Girders. *Proc. Inst. C.E.*, vol. cxxxvii, 1898–9, p. 306.
14. BOHNY. *Theorie und Konstruktion versteifter Hängebrücken*. Leipzig, 1905.
15. STEINMAN. *A Practical Treatise on Suspension Bridges*. New York, 2nd ed., 1929.
16. WADDELL. Comparative Economics of Wire-Cables and High-Alloy Steel Eye-Bar Cables. *Proc. Eng. Soc. West. Penn.*, vol. xxxvi, 1920–1, p. 418.
17. WADDELL. Quantities and Costs of Flooring for Long-Span Suspension Bridges. *Proc. Amer. Soc. C.E.*, Nov. 1926, p. 1761; see also *Engg.*, Dec. 31, 1926, p. 827.

18. KRIVOSHEIN. Combined Suspension and Arch Bridge. See p. 247, Ref. No. 28, Chap. V, Bib.; also MELAN, *Der Bauingenieur*, 1929, p. 262.
19. BLEICH. *Die Berechnung verankerter Hängebrücken.* Vienna, 1935.

The Stiffening Girder : More Exact Theories

20. MELAN. Ref. No. 19, Chap. XIII, Bib. ; see p. 76 in Steinman's translation, 1913. AM ENDE, Ref. No. 13, above.
21. MÜLLER-BRESLAU. *Die Graphische Statik der Baukonstruktionen*, Bd. II, Abt i, Stuttgart, 5th ed., 1925, p. 274.
22. MOISSEIFF. See the *Final Report of the Board of Engineers to Delaware River Bridge Joint Commission*, 1926 ; also *Jour. Frank. Inst.*, Oct. 1925, p. 436.
23. MARTIN. The Theory of the Stiffened Suspension Bridge. *Engg.*, Apl. 29, 1927, p. 506 ; Jan. 6, 1928, p. 1 (variable I).
24. PIGEAUD. Nouvelles recherches sur le calcul des ponts suspendus et de leur poutres de rigidité. *Le Génie Civil*, t. xci, 1927, p. 6 ; also t. lxxxiv, 1924, p. 345.
25. TIMOSHENKO. The Stiffness of Suspension Bridges. *Proc. Amer. Soc. C.E.*, May 1928, p. 1464.
26. PRIESTER. Application of Trigonometric Series to Cable Stress Analysis in Suspension Bridges. *Eng. Res. Bull.* No. 12, Univ. Michigan, 1929.
27. FRITSCHE. Zur genauen Theorie der Hängebrücken. *Die Bautechnik*, Heft 40, 1929.
28. KRIVOSHEIN. La théorie exacte des ponts suspendus à trois travées. II. *Int. Tagung für Brück.- u. Hochbau.* Wien, 1930 ; see also Ref. No. 28, Chap. V, Bib., App. iii, p. 278.
29. BLEICH. Ref. No. 19 ; DANA AND RAPP, Ref. No. 42 ; STEINMAN, *Proc. Amer. Soc. C.E.*, vol. 60, 1934, p. 323 ; MOISSEIFF AND LEINHARD (Action of Lateral Forces), *Trans. Amer. Soc. C.E.*, vol. 98, 1933, p. 1080.

Long Span Bridges

30. BAKER. *Long Span Railway Bridges.* London, 1867.
31. HOOL AND KINNE. *Movable and Long Span Bridges.* New York, 1923.
32. WADDELL. Economic Proportions and Weights of Modern Highway Cantilever Bridges. *Proc. Amer. Soc. C.E.*, Jan. 1932, p. 137.
33. KRIVOSHEIN. See Ref. No. 28, Chap. V, Bib.

Notable Long-Span Bridges

34. CLARK. *The Britannia and Conway Tubular Bridges.* London, 1850.
35. BAKER. The Forth Bridge. *Rpt. Brit. Assoc.* Montreal, 1884 ; see *Engg.*, Aug. 29, 1884, p. 213. Also Ref. No. 5, Chap. III, Bib.
36. FRASER. Strengthening the Floor, etc., of the Forth Bridge. *Proc. Inst. C.E.*, vol. ccxv, 1922–3, p. 120.
37. CRUTTWELL. The Tower Bridge. Foundations : *Proc. Inst. C.E.*, vol. cxiii, 1892–3, p. 117 ; Superstructure : vol. cxxvii, 1896–7, p. 35.
38. MODJESKI. Design of Large Bridges with Special Reference to the Quebec Bridge. *Jour. Frank. Inst.*, Sept. 1913, p. 239 ; see also *Engg.*, Sept. 18, 1914, p. 349.
39. DIETZ. Die zweite feste Strassenbrücke über den Rhein in Köln. *Zeit. Ver. deu. Ing.*, Aug. 7, 1920, p. 613.
40. LINDENTHAL. The Continuous Girder Truss Bridge over the Ohio River at Sciotsville, Ohio. *Trans. Amer. Soc. C.E.*, vol. lxxxv, 1922, p. 1910 ; see *Engg.*, Jan. 25, 1918, p. 81.

41. DELAWARE RIVER SUSPENSION BRIDGE. *Jour. Frank. Inst.*, Oct. 1925, pp. 417, 436 ; June 1926, pp. 691, 712, 735 ; *Engg.*, Oct. 26, 1928 p. 511.

42. GEORGE WASHINGTON BRIDGE (HUDSON RIVER) (Main Span 3,500 ft.). *Trans. Amer. Soc. C.E.*, vol. 97, 1933 ; AMMANN, *General Conception and Development of Design* ; DANA, ANDERSON AND RAPP, *Design of Superstructure*, and other papers.

43. GOLDEN GATE BRIDGE (Span 4,200 ft.). *The Engr.*, July 24, 1936, p. 78 ; SAN FRANCISCO-OAKLAND BAY BRIDGE (Main Span 2,310 ft.). *Mech. Eng.*, New York, vol. 58, p. 7 ; *Engg.*, Mar. 29, 1935, p. 329.

For Large Arched Bridges, see Ref. Nos. 31–34, Chap. XIII, Bib.

QUESTIONS ON CHAPTER XIV

1. A 2-in. wire rope, 4 lb. per fathom, is 200 ft. long and is suspended at two points at the same level 150 ft. apart. Find the deflection at the centre and the maximum and minimum tensions in the rope.
   Ans. 58·86 ft. ; 76·25 lb. ; 37·0 lb.

2. What would the maximum tension in the rope of Q. No. 1 have to be to reduce the dip to 2 ft., and what would then be the length of the rope between the points of support ?
   Ans. 939·2 lb. ; 150·08 ft.

3. Prove that for a chain suspended from two points·at the same level, when the ratio of L/D is small, the total length of the catenary is given approximately by the expression $l = L + 8D^2/3L$. Show that this is also true when the curve is a parabola.

4. Using the formula of Q. No. 3, find the length of a suspension chain 500 ft. span and dip 25 ft. What would be the increase in length for a rise in temperature of 40° F. if $a = 0·000006$, and what would be the increased dip ?
   Ans. 503·33 ft. ; 503·45 ft. ; 25·45 ft.

5. Find an expression for the tension at any section of a suspension chain hanging in a parabolic curve and carrying a uniformly distributed load. Calculate the maximum and minimum tensions in the chains of a suspension bridge, 300 ft. span and 30 ft. dip, when the total load is 1¼ tons/ft. run. (U.L.)
   Ans. 302·9 ; 281·3 tons, if two chains.

6. A suspension bridge, span 500 ft., dip 50 ft., carries a uniformly distributed load of 1¼ tons per ft. of span. The anchor chains have an inclination of 45° and may be assumed to be straight. The suspension and anchor chains are attached to saddles free to move horizontally on the piers. Determine : (a) the maximum and minimum tensions in the suspension chains ; (b) the thrust on the piers ; (c) the tension in the anchor chains. (U.L.)
   Ans. (a) 468·8, 504·9 ; (b) 656·3 ; (c) 662·8 tons, if two chains.

7. Why is it necessary to stiffen suspension bridges ? A uniformly distributed load w per ft. run covers half the length of a suspension bridge stiffened by girders hinged at the centre and freely supported at the ends. Draw a curve showing the bending moment at each point of the span, and find the position and magnitude of the maximum positive and negative bending moments. State clearly the assumptions made in arriving at the results. (U.L.)
   Ans. $\pm wL^2/64$; centre each half span.

8. Assuming that the chain of a stiffened suspension bridge of span L hangs in a parabolic curve, and that the stiffening girders are hinged at both ends and at the centre, find the positions of a rolling load W which will produce the maximum positive and negative bending moments in the stiffening girder, and the magnitude of these moments. (U.L.)

Ans. See (ii) and (iii) Fig. 371.

9. In a suspension bridge with stiffening girders not hinged at the centre, the span is 500 ft., dip 70 ft., area of lowest link of each chain 50 sq. in., moment of inertia of each stiffening girder $1 \cdot 7 \times 10^6$ in.^{4}. Assuming that the shape of the chain is parabolic, find the increase in the horizontal tension in the chain per 10° F. fall in temperature. Take $a = 0 \cdot 000006$.

Ans. $3 \cdot 54$ tons.

10. If in Q. No. 9 the stiffening girder be 20 ft. deep, find the bending stress per square inch at the centre of the girder resulting from the 10° change in temperature.

Ans. $0 \cdot 21$ ton/sq. in.

CHAPTER XV

MISCELLANEOUS STRUCTURES

245. Trussed Beams.—In Chapter I the trussed beam was treated as a pin-jointed frame. As ordinarily constructed, the beam proper AB, (i) Fig. 386, is continuous, and will not behave as a member hinged at C. If the continuity at C be taken into account the frame becomes statically indeterminate, and must be treated by the methods of § 91, Chapter V.

Suppose that a single load W be applied at the point D distant z from A $(z < L/2)$. Treat bar No. 2 as the redundant member, remove it from the frame and find the forces due to W in the rest of the bars. In these circumstances there can be no forces in bars No. 3, but the load will produce a bending moment in the beam, bar No. 1, of which the maximum value is $- Wz (L - z)/L$ at D; $a'f'b'$ is the bending-moment diagram. Next, remove W from the beam and apply loads of unit magnitude in place of bar No. 2. Assume that the force in bar No. 2 is compressive, so that the unit load will act upward at C and downward at E. The unit load at C will produce a + bending moment everywhere in AB of which the maximum value at C is $L/4$; $a'e'b'$ in (iii) is the bending-moment diagram. The unit load at E will produce forces of $l_3/2l_2$ in bars No. 3, and a longitudinal force of $L/4l_2$ in the beam, bar No. 1. Since both beams, and ties and struts occur in this frame, eq. (12), § 91, must be applied. To simplify the analysis, since the effect of the shearing force in the beam will be small, the S terms may be neglected; further, the cross-section of the beam will be assumed constant, and since the longitudinal force therein will be the same from end to end, so far as this force is concerned the beam may be regarded as one of the bars
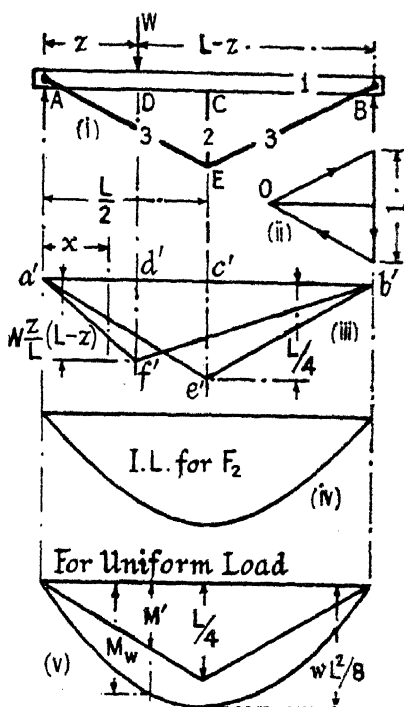
FIG. 386.

of the frame, and included in the F terms, when the N terms disappear. Eq. (12), § 91, then becomes

$$X = F_2 = -\frac{\sum \dfrac{F_W F' l}{Ea} + \displaystyle\int_0^l \dfrac{M_W M'}{EI} \cdot dl}{\sum \dfrac{(F')^2 l}{Ea} + \displaystyle\int_0^l \dfrac{(M')^2}{EI} \, dl} \qquad . \qquad . \qquad . \quad (1)$$

Dealing first with the bending moment, the value of M_W everywhere is given by the bending-moment diagram $a'f'b'$, (iii) Fig. 386. At any section distant x from A

$$\text{if } x < z, \qquad M_W = -\frac{W(L-z)}{L}\, x$$

$$\text{if } x > z, \qquad M_W = -\frac{Wz}{L}(L-x).$$

The values of M' are given by the bending-moment diagram $a'e'b'$, (iii) Fig. 386. At any section distant x from A,

$$\text{if } x < z, \qquad M' = + x/2$$
$$\text{if } x > z, \qquad M' = + (L-x)/2.$$

The integral $\dfrac{1}{EI}\displaystyle\int_0^l M_W M' \cdot dl$ must be split into three parts corresponding to the lengths $a'd'$, $d'c'$, and $c'b'$, (iii), of the beam AB,

$$\frac{1}{EI}\int_0^l M_W M'\, dl = \frac{1}{E_1 I_1}\int_0^z -\frac{W(L-z)}{L}\, x \cdot \frac{x}{2} \cdot dx$$

$$+ \frac{1}{E_1 I_1}\int_z^{L/2} -\frac{Wz}{L}(L-x)\frac{x}{2} \cdot dx$$

$$+ \frac{1}{E_1 I_1}\int_{L/2}^{L} -\frac{Wz}{L}(L-x)\frac{L-x}{2} \cdot dx$$

$$= -\frac{W}{48 E_1 I_1} \cdot z(3L^2 - 4z^2)$$

where E_1 and I_1 have reference to the beam.

Since the strut, bar No. 2, occurs in the middle of the span, the integral $\dfrac{1}{EI}\displaystyle\int_0^l (M')^2 dl$ for the two halves of the beam may be written

$$\frac{1}{EI}\int_0^l (M')^2\, dl = \frac{2}{E_1 I_1}\int_0^{L/2}\left(\frac{x}{2}\right)^2 dx = \frac{L^3}{48 E_1 I_1}.$$

Considering next the forces in the bars of the frame, as was seen above there are no forces in the bars due to W when bar No. 2 is removed. Hence $F_W = 0$ in all cases, and the first summation in the numerator disappears.

For the beam, bar No. 1, $F' = L/4l_2$ (see above), and

$$\frac{1}{E}(F')^2\frac{l}{a} = \frac{1}{E_1}\left\{\frac{L}{4l_2}\right\}^2\frac{L}{a_1} = \frac{L^3}{16 l_2{}^2 E_1 a_1}.$$

For bar No. 2, $F' = 1$, and

$$\frac{1}{E} (F')^2 \frac{l}{a} = \frac{1}{E_2} (1)^2 \frac{l_2}{a_2} = \frac{l_2}{E_2 a_2}.$$

For the two bars No. 3, F' $l_3/2l_2$, and

$$\frac{1}{E} (F')^2 \frac{l}{a} = \frac{2}{E_-} \left\{ \frac{l_3}{2l_2} \right\}^2 \frac{l_3}{a_3} = \frac{l_3{}^3}{2l_2{}^2 E_3 a_3}$$

Then

$$\frac{\dfrac{W}{48E_1 I_1} \cdot z(3L^2 - 4z^2)}{\dfrac{L^3}{16l_2{}^2 E_1 a_1} + \dfrac{l_3}{E_2 a_2} + \dfrac{l_3}{2l_2{}^2 E_3 a_3} + \dfrac{L^3}{48E_1 I_1}} \qquad (2)$$

Knowing F_2, the bending moment everywhere on the beam can be found, and also the forces in the bars. The equation is only valid for values of $z < L/2$. Let

$$48E_1 I_1 \left[\frac{1}{\dfrac{L^3}{16l_2{}^2 E_1 a_1} + \dfrac{l_3}{E_2 a_2} + \dfrac{l_3{}^3}{2l_2{}^2 E_3 a_3} + \dfrac{L^3}{48E_1 I_1}} \right] = \chi \qquad (3)$$

where χ is a constant for the frame, and can be calculated when its dimensions are known, then

$$F_2 = W\chi z(3L^2 - 4z^2) \qquad . \qquad . \qquad . \qquad . \qquad (4)$$

If W be put equal to unity, this equation will be the equation to the influence line for F_2 from $z = 0$ to $z = L/2$. The curve is symmetrical about the centre of the beam, and is plotted in (iv) Fig. 386. From this curve the value of F_2 for any load arrangement can at once be found, and hence the stresses everywhere in the truss determined.

Alternatively, certain load conditions can be treated from first principles without using an influence line. Thus, for a uniform load completely covering the span, the M_W bending-moment diagram is a parabola, (v) Fig. 386, $M_W = - wx (L - x)/2$; max. ordinate $- wL^2/8$, and the integral, eq. (1),

$$\frac{1}{EI} \int_0^l M_W M' \cdot dl = - \frac{2}{E_1 I_1} \int_0^{L/2} \frac{w}{2} \cdot x (L - x) \frac{x}{2} \cdot dx = - \frac{5wL^4}{384E_1 I_1}$$

The denominator will be the same for all cases, hence,

$$F_2 : \frac{\dfrac{5wL^4}{384E_1 I_1}}{\dfrac{L^3}{16l_2{}^2 E_1 a_1} + \dfrac{l_3}{E_2 a_2} + \dfrac{l_3}{2l_2{}^2 E_3 a_3} + \dfrac{L^3}{48E_1 I_1}} \qquad \qquad 5wL^4 \qquad (5)$$

$$= w \text{ [total area of the influence line (iv)].}$$

It is to be observed that the numerator in the equations for F_2 is the central deflection of the member AB considered as a plain beam carrying the applied load.

246. Braced Piers.—(i) Fig. 387 represents a braced pier supporting a deck bridge. The maximum stresses in the pier will occur when the bridge is carrying a train, and is subjected at the same time to wind pressure.* The total vertical load W on the pier can be found from the weight of the bridge superstructure plus that of the train. It must include the effect of impact, §§ 61 and 63. The resultant wind pressure
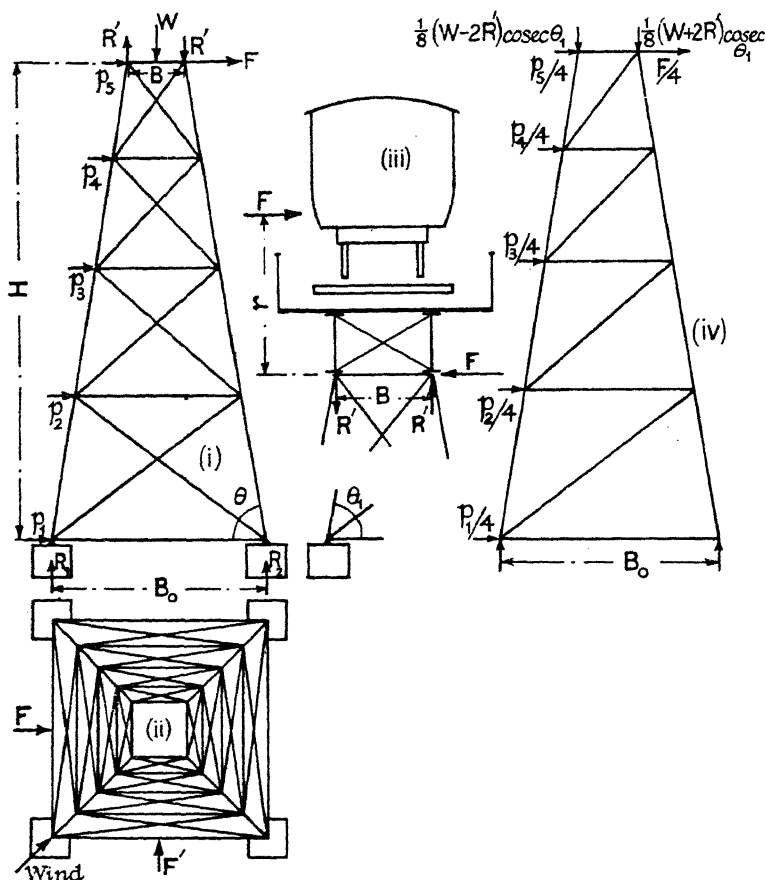
FIG. 387.

on the pier from the bridge and train can be found from the principles of § 52 (cf. Fig. 87). Let it be represented by a force F acting at a distance r above the top of the pier. Then, as will be seen from (iii), there will be two vertical reactions R' acting on the top of the pier due to this wind pressure, one acting upwards, the other downwards, of magnitude

$$R' = Fr \div B$$

* According to the British Standard Specification No. 153, 1933, the alternative cases of the empty structure subjected to a 50 lb. wind pressure or the loaded structure subjected to a 30 lb. wind pressure must be considered (see § 52).

and a horizontal reaction equal to F. The total downward forces acting at the four corners of the pier will be, therefore,

$$\frac{W}{4} \pm \frac{R'}{2} = \frac{W}{4} \pm \frac{Fr}{2B}.$$

In addition, the forces $p_1 \ldots p_5$ acting on the pier due to the wind pressure on the frame itself must be taken into account, and if the pier be very tall and heavy, the stresses due to its own weight must also be allowed for. If the viaduct be curved in plan, the centrifugal force due to the train passing round the curve, § 193, must be combined with the lateral wind pressure.

Since the wind may blow from any direction, it is usual to cross-brace the pier as shown ; to find the forces in the different bars it is then necessary to divide the frames into their two components, halving all the loads on the frame, and find the forces in each component, combining them afterwards as explained in § 7. One of the component frames is shown in (iv), with the forces acting on it. If the batter on the pier is considerable, it will be necessary to develop the true shape of the component frame as in (iv), and to resolve the vertical load in the plane of the frame.

To find the forces in the bracing on the sides of the pier parallel to the track, the wind pressure F' on the end of the train (or trains), girders, and the pier, must be found ; these must be combined with any loads due to acceleration or braking, § 193. Since the wind may blow diagonally, when (see Fig. 82) its intensity on planes at 45° will be, practically speaking, equal to its normal intensity, the forces in the four main corner members due to wind pressure will be the combination of both lateral and longitudinal wind loads, which must be properly combined (cf. § 48 : *Tall Masts*).

On these assumptions, a wind pressure of 30 lb./sq. ft. should be allowed for in exposed positions, but the permissible working stresses in the material for all combinations of loading may be raised by 25 %.

FIG. 388.

The reactions $R_1 \ldots R_4$ on the concrete foundations can be found from the two sets of forces, lateral plus longitudinal, taking into account
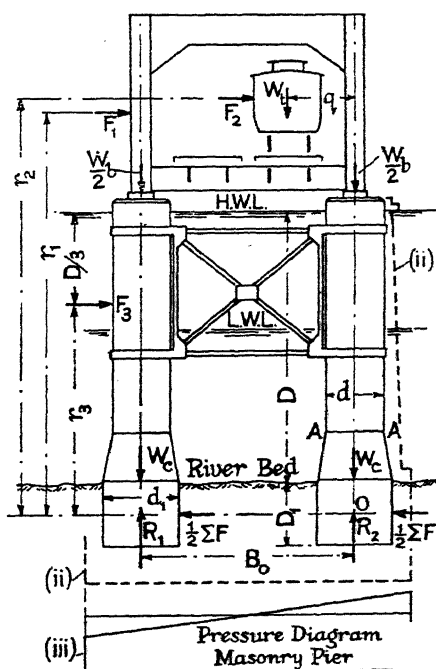
for this purpose the weight of the pier itself and also that of the concrete footings.

The factor of safety against overturning should be at least $1\cdot5$, whether for the loaded or empty bridge. The methods of § 52 may be followed. Messrs. Arrol's suggest (Bridge and Structural Engineers' Handbook) that the width of the base should be $B_0 = B + H/3$ transversely, and $B_0' = B + H/6$ longitudinally.

247. Cylinder Bridge Piers.—Fig. 388 shows a common type of bridge pier, consisting of two cylinders sunk into the river bed, and braced together at the top. It is necessary to provide a factor of safety of at least $1\frac{1}{2}$ against overturning, and to ensure that the allowable pressure on the river bed is not exceeded.

If F_1 = the wind pressure on the bridge, tons,
$\quad F_2$ = that on the train, tons,
$\quad F_3$ = $2Ddv^2/3090$ tons = the resistance to the river current of v ft./sec,
$\quad W_b$ = the weight of the bridge coming on the pier, tons,
$\quad W_t$ = the weight of one train coming on the pier, tons,
$\quad W_c$ = the inclusive weight of one cylinder, tons,

then, taking moments about O, the dimensions being in feet,

The overturning moment $M_0 = F_1r_1 + F_2r_2 + F_3r_3$.
The righting moment $\quad M_R = (Wb/2 + Wc - P + p)B_0 + W_tq$.
Factor of Safety $\quad\quad = M_R \div M_0 \gtrless 1\frac{1}{2}$.

W_t = the weight of one empty train standing over the leeward pier, Fig. 388; $P = \frac{\pi}{4}d_1^2(D + D_1)/35$ is the upward water pressure on the bottom of the cylinder (in all but impervious foundations);

$p = \frac{\pi}{4}(d_1^2 - d^2)D/35$ is the downward water pressure on the conical part of the cylinder; when D_1 is great, take O from 5 to 10 ft. down, depending on the lateral resistance of the river bed.

The maximum value of R_2 will occur when two heavy trains are crossing the bridge :

$R_2 = Wb/2 + W_t(1 + i) + Wc - P + p + (F_1r_1 + F_2r_2 + F_3r_3)/B_0$.

i = the impact factor, $P = 0$ in impervious soils. The bearing pressure $R_2 \div \frac{\pi}{4}d_1^2$ must not exceed that allowable on the river bed.* The pressure on the concrete in the cylinder at section AA should be similarly investigated.

Skin Friction.—When D_1 is great, skin friction * between the cylinders and the river bed may be an important factor; it is frequently neglected.

In the case of masonry piers, indicated in (ii) Fig. 388, the resultant pressure on the foundation should fall within the middle third.

248. Wall Crane.—A common type of wall crane is shown in (i) Fig. 389. It consists of a beam AB along which the load travels. The beam is rigidly connected to a vertical post DG at A, and its outer end

---

* For permissible values see Newman, *Cylinder Bridge Piers*, or Arrol's *Handbook*.

is supported by a tie bar BC. The crane turns in bearings at G and D. The structure is statically indeterminate, and the forces in the members must be found from strain-energy considerations. The method of § 91 will be used.

Remove the tie bar BC, leaving the structure DAB (ii) as the principal system. The lengths, areas, and moments of inertia of the bars are
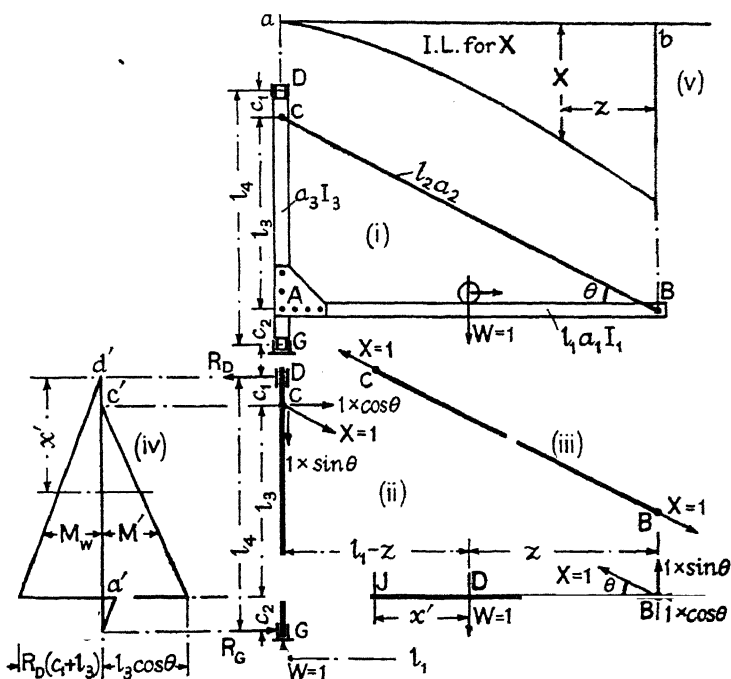
Fig. 389.

indicated on the figure. Considering first the beam AB, the bending moment at any section J due to a unit load W is

$$M_W = + Wx' = + x', \text{ since } W = 1.$$

Replace the forces in the tie bar by unit forces $X = 1$, acting at B and C along the direction of the tie bar as shown in (ii). The vertical and horizontal components of the unit force at B will be $1 \times \sin\theta$ and $1 \times \cos\theta$ as indicated, hence the bending moment at J due to X is

$$M' = -(1 \times \sin\theta)(z + x') = -(z + x')\sin\theta$$

and for the beam AB, between the limits $x' = 0$ and $x' = l_1 - z$, that is from D to A, the integral

$$\frac{1}{EI_1}\int M_W M' . dl = \frac{1}{EI_1}\int_0^{l_1-z} - x'(z + x')\sin\theta . dx'$$

$$- \frac{1}{EI_1}(\sin\theta)\int_0^{l_1-z}\{x'z + (x')^2\}dx' = -\frac{(2l_1 + z)(l_1 - z)^2}{6EI_1}\sin\theta \quad (1)$$

M_W between B and D is zero, and therefore $M_W M'$ is zero.

At any point distant x from B, the bending moment due to $X = 1$ is $M' = - (1 \times \sin\theta)x = - x\sin\theta$, and for the whole length,

$$\frac{1}{EI_1}\int (M')^2\, dl = \frac{1}{EI_1}\sin^2\theta\int_0^{l_1} x^2.\, dx = \frac{l_1^3}{3EI_1}\sin^2\theta \quad . \qquad . \quad (2)$$

The load W produces no longitudinal force in AB; that due to 1 is $1 \times \cos\theta$. Hence

$$F_W F'l/Ea = 0\,; \quad (F')^2l/Ea = l_1(\cos^2\theta)/Ea_1 \qquad\qquad (3)$$

The effect of the shearing force in AB will be neglected.

Considering next the vertical post DG, the forces and moments are as shown in (ii) and (iv) Fig. 389. At any section distant x' from D,

$$M_W : R_D x' = \frac{l_1 - z}{l_1}x', \text{ since } R_D = W(l_1 - z)/l_1, \text{ and } W = 1\,;$$

and at the same section, $M' = - (1 \times \cos\theta)(x' - c_1)$. Hence, for the vertical post, the integral

$$\frac{1}{EI_3}\int M_W M'.\, dl \quad - \frac{1}{EI_3}\int_{c_1}^{c_1+l_3}\frac{l_1 - z}{l_4}x'(x' - c_1)\cos\theta.\, dx'$$

$$= - \frac{1}{EI_3}\cdot\frac{l_1 - z}{l_4}\cos\theta\int_{c_1}^{c_1+l_3}x'(x' - c_1)dx'$$

$$- - \frac{1}{6EI_3}\cdot\frac{l_1 - z}{l_4}(2l_3 + 3c_1)l_3^2\cos\theta \qquad\qquad (4)$$

M' is zero between D and C, and also between A and G. For the vertical post, the integral

$$\frac{1}{EI_3}\int (M')^2 dl = \frac{1}{EI_3}\int_{c_1}^{c_1+l_3}\cos^2\theta(x' - c_1)^2 dx = \frac{\cos^2\theta}{EI_3}\cdot\frac{l_3^3}{3} \qquad . \quad (5)$$

The load produces no longitudinal force in DA; that due to $X = 1$ is $1 \times \sin\theta$. Hence,

$$F_W F'l/Ea = 0\,; \quad (F')^2l/Ea = l_3(\sin^2\theta)/Ea_3 \qquad . \qquad . \quad (6)$$

For the bar BC, considered separately, (iii), $F_W = 0$, $F' = X = 1$. Hence

$$(F')^2l/Ea = \frac{l_2}{Ea_2} \qquad . \qquad . \qquad . \qquad . \quad (7)$$

Then from eq. (12), § 91,

$$X = - \frac{\dfrac{F_W F'l}{Ea} + \displaystyle\int_0^l\frac{M_W M'}{EI}\cdot dl}{\dfrac{(F')^2l}{Ea} + \displaystyle\int_0^l\frac{(M')^2}{EI}dl}$$

Inserting the values in the numerator from eqs. (1) and (4), and in the denominator from eqs. (2), (3), (5), (6), and (7), and rearranging,

$$X = \cdot\frac{\dfrac{(2l_1 + z)(l_1 - z)^2}{6EI_1}\sin\theta + \dfrac{1}{6EI_3}\cdot\dfrac{l_1 - z}{l_4}(2l_3 + 3c_1)l_3^2\cos\theta}{\dfrac{l_1^3}{3EI_1}\sin^2\theta + \dfrac{l_3^3}{3EI_3}\cos^2\theta + \dfrac{l_1\cos^2\theta}{Ea_1} + \dfrac{l_3\sin^2\theta}{Ea_3} + \dfrac{l_2}{Ea_2}}. \quad (8)$$

But $\sin \theta = l_3/l_2$, and $\cos \theta = l_1/l_2$; if all the members are made of the same material, $E = \text{const.}$, and

$$X = \frac{l_2 l_3 \left\{ (2l_1 + z)(l_1 - z)^2 I_3 + \dfrac{l_1 - z}{l_4}(2l_3 + 3c_1)I_1 l_1 l_3 \right\}}{2l_1{}^2 l_3{}^2 \{I_1 l_3 + I_3 l_1\} + 6 I_1 I_3 \left| \dfrac{l_1{}^3}{a_1} + \dfrac{l_2{}^3}{a_2} + \dfrac{l_3{}^3}{a_3} \right|} \qquad (9)$$

If the crane is built into a rigid wall, the terms in eq. (8) with a_3 or I_3 in the denominator will disappear, and if E be constant,

$$X = \frac{(2l_1 + z)(l_1 - z)^2 l_2 l_3}{6 I_1 \left| \dfrac{l_1{}^3 l_3{}^2}{3 I_1} + \dfrac{l_1{}^3}{a_1} + \dfrac{l_2{}^3}{a_2} \right|} \qquad (10)$$

Knowing X, the force in the tie bar, the forces and moments in all the bars of the frame can easily be found. If W have a value other than unity, the force in the tie bar $= WX$. Let

$$\frac{l_2 l_3}{2l_1{}^2 l_3{}^2 \{I_1 l_3 + I_3 l_1\} + 6 I_1 I_3 \left| \dfrac{l_1{}^3}{a_1} + \dfrac{l_2{}^3}{a_2} + \dfrac{l_3{}^3}{a_3} \right|} = \chi$$

where χ is a constant for the particular frame. Then

$$X = \chi \left\{ (2l_1 + z)(l_1 - z)^2 I_3 + \frac{l \cdot z}{l_4}(2l_3 + 3c_1)I_1 l_1 l_3 \right\} \qquad (11)$$

This equation will give the value of X for a load $W = 1$ at any position distant z from B. In other words, it is the equation to the influence line for X, and from it the value of X for any load condition on AB can at once be found. This influence line has been plotted in (v) for the frame shown in Fig. 389 and particular values of the constants. The ordinate of the curve under the load gives the magnitude of the tension in the tie bar, which increases rapidly as W rolls out towards B.

248a. The Wichert Truss.—The continuous girder is an economical type, but has the disadvantage that it may be subjected to severe addi-tional stress due to pier settle-ment and/or changes in tem-perature, § 239 ; and since it is statically indeterminate, the computations are somewhat involved. It is claimed that
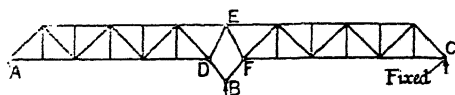
Fig. 389A.

the *Wichert Truss*, Fig. 389A, presents all the advantages of the con-tinuous girder without these disadvantages. The truss is supported at A and C in the usual way, but at B the middle support takes the form of a pin-connected quadrilateral $BDEF$. A simple model will best ex-plain its action. Such a truss is statically determinate, and the influence lines are straight lines. It is stated that there is a saving in material, both in the trusses and at the piers, and that the time of erection is reduced. The principle can be applied to arched structures

and other types. For further exposition, see a book by Dr. Steinman [15] where the subject is fully discussed.

249. Vierendeel Girders.—In 1896 Vierendeel[7] suggested a method of constructing open-web girders in which the diagonals are omitted. The girder consists of top and bottom flanges connected by verticals, the junctions are stiff joints; a typical example is shown in Fig. 390. A number of bridges have been built on this system with success and, it is claimed, considerable economy. It appears to be a very suitable type for open-web girders of welded construction or of reinforced concrete.

Vierendeel girders are statically indeterminate. The stresses in them may be determined by a consideration of the elastic displacements, or by strain-energy methods. If there be many panels, an exact treatment is laborious : the following method may be used as a first approximation. Consider the distortion of any one panel of the girder shown in (i) Fig. 391. There will be points of inflexion J and K in the verticals, which will be
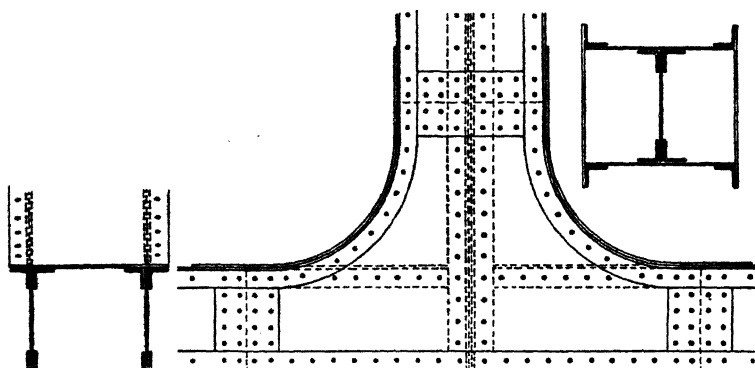
FIG. 390.

assumed to occur at the mid-height of these members. The upper and lower halves of the girder have been separated for clearness at the points of inflexion, where horizontal and vertical forces H and V will act. The portion of the girder to the left of AC being removed, its effects on the panel CB will be represented by a horizontal force F_1, a vertical shearing force S_1'', and a moment $M_{2\cdot1}''$ in the flange at A, and similarly by F_1, S_1' and $M_{2\cdot1}'$ at C. The configuration of the points B and G, and the slope of the flanges at these points, will be determined by the distortion of that part of the girder to the left of BG, and for present purposes the flanges at B and G may be regarded as fixed in position and direction. The method of attack is to calculate the horizontal distance l between J and K, first by considering the lower half, and secondly the upper half, of the panel. Equating these two values, a relation between H_2 and H_3 is obtained, which, successively applied to each panel, enables the value of H for every vertical to be found. Knowing these values, the stresses in all the members follow from statical considerations. The longitudinal strains in all the members will be neglected.

From the geometry of the lower portion of the panel,

$$l = A_0B_0 = A_0A + l'' - BB_0, \text{ where } AB = l''.$$

BK may be regarded as a vertical cantilever loaded with a horizontal force H_3 at K. Therefore

$$BB_0 = \frac{H_3}{3EI_3}\left(\frac{D_3}{2}\right)^3 = \frac{H_3D_3{}^3}{24EI_3}.$$

The displacement A_0A is composed of two parts, $H_2D_2{}^3/24EI_2$ due to the deflection of AJ, plus that due to the bending of AB magnified by
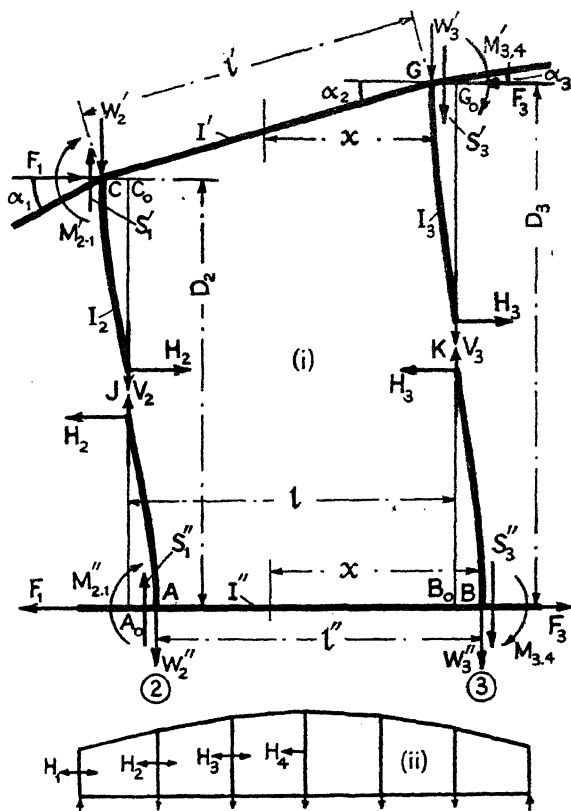
FIG. 391.

the arm AJ. The vertical force acting at A is $(S_1'' - W_2'' + V_2)$. Hence at any point distant x from B, the downward bending moment is

$$M = H_2D_2/2 - M_{2 \cdot 1}'' - (S_1'' - W_2'' + V_2)(l'' - x).$$

The change of slope at A produced by this moment is $\dfrac{1}{EI''}\displaystyle\int_0^{l''} M \, . \, dx,$ where

$$\int_0^{l''} M \, . \, dx = (H_2D_2/2 - M_{2 \cdot 1}'')l'' - (S_1'' - W_2'' + V_2)(l'')^2/2.$$

2 O

Hence

$$A_0A = \frac{H_2D_2{}^3}{24EI_2} + \frac{1}{EI''}\int_(^l M \cdot dx \times JA$$

$$\frac{H_2D_2{}^3}{24EI_2} + \frac{D_2}{2EI''}\left[\left\{\frac{H_2D_2}{2} - M_{2\cdot1}''\right\}l'' - (S_1'' - W_2'' + V_2)\frac{(l'')^2}{2}\right]$$

and

$$l = l'' + \frac{H_2D_2{}^2}{24E\chi_2} + \frac{H_2D_2{}^2}{4E\chi''} - \frac{M_{2\cdot1}''D_2}{2E\chi''} - (S_1'' - W_2'' + V_2)\frac{D_2l''}{4E\chi''} - \frac{H_3D_3{}^2}{24E\chi_3}$$

where $\chi_2 = I_2/D_2$; $\chi_3 = I_3/D_3$; and $\chi'' = I''/l''$.

Treating the upper flange in a similar way, $l =$ horizontal projection of $CG + GG_0 - CC_0$, where the horizontal projection of $CG = l''$. As before, $GG_0 = H_3D_3{}^3/24EI_3$. The displacement CC_0 is composed of two parts, $H_2D_2{}^3/24EI_2$, due to the deflection of CJ, plus the magnified effect of the bending of CG. The vertical force acting at C is $(S_1' - W_2' - V_2)$. The vertical force S_1' is the sum of the vertical components of the normal shearing force and of the longitudinal force in the upper flange at C, and F_1 is the algebraic sum of the horizontal components of these two forces. At any point distant x measured horizontally from G, the downward bending moment is

$$M = H_2\{D_2/2 + (l'' - x)\tan\alpha_2\} + F_1(l'' - x)\tan\alpha_2$$
$$- M_{2\cdot1}' - (S_1' - W_2' - V_2)(l''-x)$$

The change of slope at C produced by this bending moment is $\dfrac{1}{EI'}\displaystyle\int_G^0 M \cdot ds$,

where $CG = l' = l'' \sec\alpha_2$, and δs is an element of this length. Then

$$M = H_2\{D_2/2 + (l' - s)\sin\alpha_2\} + F_1(l' - s)\sin\alpha_2$$
$$- M_{2\cdot1}' - (S_1' - W_2' - V_2)(l' - s)\cos\alpha_2$$

and

$$\int^{l'} M \cdot ds = H_2\left\{\frac{D_2l'}{2} + \frac{(l')^2\sin\alpha_2}{2}\right\} + F_1\frac{(l')^2\sin\alpha_2}{2} - M_{2\cdot1}'l$$
$$- (S_1' - W_2' - V_2)\frac{(l')^2\cos\alpha_2}{2}$$

Hence, putting $l'' \sec\alpha_2$ for l',

$$CC_0 = \frac{H_2D_2{}^3}{24EI_2} + \frac{1}{EI'}\int_0^{l'} M \cdot ds \times CJ$$

$$\frac{H_2D_2{}^3}{24EI_2} + \frac{D_2}{2EI'}\left[H_2\left\{\frac{D_2l''\sec\alpha_2}{2} + \frac{(l'')^2\tan\alpha_2\sec\alpha_2}{2}\right.\right.$$
$$+ \frac{F_1(l'')^2\tan\alpha_2\sec\alpha_2}{2} - M_{2\cdot1}l''\sec\alpha_2 - (S_1' - W_2' - V_2)\frac{(l'')^2\sec\alpha_2}{2}\right]$$

and

$$l = l'' + \frac{H_3D_3{}^2}{24E\chi_3} - \frac{H_2D_2{}^2}{24E\chi_2} - \frac{H_2D_2}{4E\chi'}(D_2 + l''\tan\alpha_2) - \frac{F_1D_2}{4E\chi'}(l''\tan\alpha_2)$$
$$+ \frac{M_{2\cdot1}D_2}{2E\chi'} + (S_1' - W_2' - V_2)\frac{D_2l''}{4E\chi'} \qquad . \qquad (2)$$

where $\chi' = I'/l' = I'/l'' \sec a_2$; and $l'' \tan a_2 = D_3 - D_2$. Equating the two values of l from eqs. (1) and (2), and simplifying,

$$\frac{H_3 D_3{}^2}{\chi_3} - \frac{H_2 D_2{}^2}{\chi_2} = H_2 D \cdot \left\{\frac{3D_3}{\chi'} + \frac{3D_2}{\chi''}\right\} + \frac{3F_1}{\chi'}(D_3 - D_2)D_2$$

$$- 6D_2\left\{\frac{M_{2 \cdot 1}{}'}{\chi'} + \frac{M_{2 \cdot 1}{}''}{\chi''}\right\} - (S_1{}' - W_2{}' - V_2)\frac{3l''D_2}{\chi'}$$

$$- (S_1{}'' - W_2{}'' + V_2)\frac{3l''D_2}{\chi''} \quad (3)$$

In most practical cases χ' and χ'' will not differ greatly in the same panel. Let $\chi' = \chi'' = \chi$; the value of χ may be taken as a mean between those of χ' and χ''. Then

$$\frac{H_3 D_3{}^2}{\chi_3} - \frac{H_2 D_2{}^2}{\chi_2} = \frac{3D_2}{\chi^2}[H_2(D_3 + D_2) + F_1(D_3 - D_2)$$

$$- 2(M_{2 \cdot 1}{}' + M_{2 \cdot 1}{}'') - l''(S_1{}' - W_2{}' + S_1{}'' - W_2{}'')] \quad (4)$$

Let M_2 be the external bending moment at AC due to the applied forces and reactions. Then, taking moments about A,

$$M_2 = F_1 D_2 + M_{2 \cdot 1}{}' + M_{2 \cdot 1}{}'', \text{ and } M_{2 \cdot 1}{}' + M_{2 \cdot 1}{}'' = M_2 - F_1 D_2.$$

If S_2 be the external shearing force in the panel CB,

$$S_2 = S_1{}' - W_2{}' + S_1{}'' - W_2{}''.$$

Inserting these values in eq. (4),

$$\frac{H_3 D_3{}^2}{\chi_3} - \frac{H_2 D_2{}^2}{\chi_2} = \frac{3D_2}{\chi^2}[H_2(D_3 + D_2) + F_1(D_3 + D_2) - (2M_2 + S_2 l'')]$$

$$\frac{3\Sigma_1^2 H}{\chi}(D_3 + D_2)D_2 - \frac{6D_2}{\chi}M_{2\frac{1}{2}} \quad (5)$$

for $H_2 + F_1 = F_2 = \Sigma_1^2 H$, i.e. the sum of all the horizontal forces H up to and including H_2; since $F_1 = H_1$; $F_2 = H_1 + H_2$, and so on (see Fig. 391). Also $M_2 + S_2 l''/2 = M_{2\frac{1}{2}}$ is the external bending moment at the centre of the panel CB. If AC be the rth vertical of the girder, and BG the $(r + 1)$th, eq. (5) may be written

$$\frac{H_{r+1} D_{r+1}{}^2}{\chi_{r+1}} - \frac{H_r D_r{}^2}{\chi_r} = \frac{3(D_{r+1} + D_r)D_r}{\chi}\Sigma_1^r H - \frac{6D_r}{\chi}M_{r+\frac{1}{2}} \quad . \quad (6)$$

$$\frac{H_{r+1} D_{r+1}{}^-}{I_{r+\frac{1}{2}}} - \frac{H_r D_r{}^3}{I_r} = \frac{3l''}{I}(D_{r+1} + D_r)D_r\Sigma_1^r H - \frac{6l''}{I}D_r M_{r+\frac{1}{2}} \quad . \quad (7)^*$$

where I/l'' is the mean of I'/l' and I'/l'' for the panel in question. If the

---

* Vierendeel's formula for girders of this type is

$$H_{r+1} D_{r+1}{}^3 = H_r D_r{}^3 (3D_{r+1} - D_r)/2 + l''\{3D_{r+1} D_r + (D_{r+1} - D_r)^2\}\Sigma_1^r H$$

$$- 3l'' (D_{r+1} + D_r) M_r + {}_1/2 + S_r (l'')^2 (D_{r+1} + 2D_r)/2$$

obtained by assuming that the upper flange is hinged to the top of all the verticals and that I is constant.

girder is parallel, $D_{r+1} = D_r = D$; and $I_{r+1} = I_r = I$; this equation reduces to Vierendeel's formula,

$$H_{r+1} - H_r = \frac{6l''}{D}\Sigma_1^r H - \frac{6l''}{D^2}M_{r+\frac{1}{2}} \qquad . \qquad . \qquad . \quad (8)$$

Eq. (7) is of the form $aH_{r+1} - bH_r = c\Sigma_1^r H - d$, where a, b, c, and d can be found directly from the dimensions and loading of the girder. Consider a symmetrical girder of six panels symmetrically loaded, (ii) Fig. 391; find a, b, c and d for each panel in turn, and apply eq. (7) to each. Starting with the end post, $H = H_1$,

$$a_{1\cdot2}H_2 - b_{1\cdot2}H_1 = c_{1\cdot2}H_1 - d_{1\cdot2}$$
$$a_{2\cdot3}H_3 - b_{2\cdot3}H_2 = c_{2\cdot3}(H_1 + H_2) - d_{2\cdot3}$$
$$a_{3\cdot4}H_4 - b_{3\cdot4}H_3 = c_{3\cdot4}(H_1 + H_2 + H_3) - d_{3\cdot4};$$

$H_4 = 0$, since the conditions are symmetrical. Solving these equations, $H_1 \ldots H_4$ are known. It is necessary to work accurately.

From (i) Fig. 392 and (i) Fig. 391,

$$M_{3\cdot2}'' = M_{2\cdot1}'' + (S_1'' - W_2'' + V_2)l'' - H_2D_2/2 \qquad . \qquad . \qquad . \quad (9)$$

$$M_{3\cdot2}' = M_{2\cdot1}' + (S_1' - W_2' - V_2)l'' - H_2\{D_2/2 + (D_3 - D_2)\} - F_1(D_3 - D_2)$$
$$= M_{2\cdot1}' + (S_1' - W_2' - V_2)l'' - H_2D_2/2 - F_2(D_3 - D_2) \qquad . \quad (10)$$

Suppose that $M_{3\cdot2}' = k \cdot M_{3\cdot2}''$. Then

$$V_2 = \frac{M_{2\cdot1}' - kM_{2\cdot1}''}{(1+k)l''} + \frac{(S_1' - W_2') - k(S_1'' - W_2'')}{1+k} - \frac{F_2(D_3 - D_2)}{(1+k)l''}$$
$$- \frac{H_2D_2}{2}\frac{(1-k)}{(1+k)l''} \qquad . \quad (11)$$

and

$$V_r = \frac{M_{r,r-1}' - kM_{r,r-1}''}{(1+k)l''} + \frac{(S_{r-1}' - W_r') - k(S_{r-1}'' - W_r'')}{1+k}$$
$$- \frac{(D_{r+1} - D_r)}{(1+k)l''}\Sigma_1^r H - \frac{H_rD_r}{2}. \qquad (12)$$

k and l'' are to be given the correct values for the panel under consideration. The value of k might be obtained from the condition that the vertical deflection of J must be the same whether the top or bottom half of the girder be considered, but the expression is complicated. If, with Vierendeel, it be assumed that $M' : M'' :: I'/l' : I''/l''$, which is only approximately true, since the ratio M'/M'' is not constant across the panel,

$$k = \frac{I'l''}{I''l'} \qquad (13)$$

which may be used in default of a more exact value. If the girder is parallel, and $I' = I''$ everywhere, $k = 1$ and eq. (12) becomes

$$V_r = \frac{- W_r' + W_r''}{} \qquad (14)$$

a negative sign indicates that V_r acts in the opposite direction to that shown in Fig. 392.

Having obtained the values of H, in order to find the moments and

forces everywhere, start at one end of the girder. For the first panel, $M_{1\cdot2}'' = - H_1D_1/2$; $M_{1\cdot2}' = - H_1D_1/2$; Fig. 392. $M_{2\cdot1}'' = (R - V_1)l''$ $- H_1D_1/2$; $M_{2\cdot1}' = (V_1 - W_1')l'' - H_1(D_2 - D_1 + D_1/2)$; $M_{2\cdot1}'$ $k_1 \cdot M_{2\cdot1}''$, where $k_1 = I_1'l''/I_1''l'$; hence V_1 can be found and the bending moments. Knowing $M_{2\cdot1}'$ and $M_{2\cdot1}''$, V_2 can be found from eq. (12), or by taking moments as in the case of V_1. $M_{2\cdot3}'' = M_{2\cdot1}'' - H_2D_2/2$; $M_{2\cdot3}' = M_{2\cdot1}' - H_2D_2/2$. For $M_{3\cdot2}$, see eqs. (9) and (10). $F_1 = H_1$:
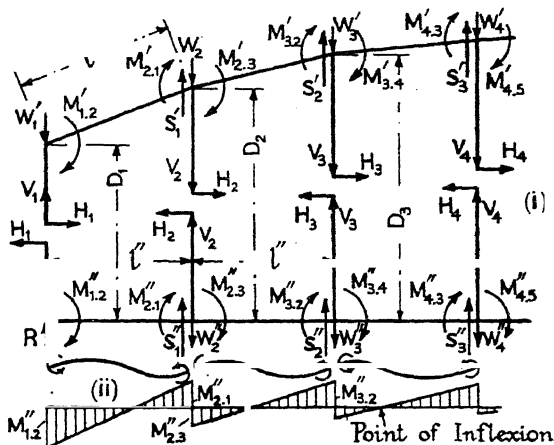
FIG. 392.

$F_2 = H_1 + H_2$; and so on. Note that the end bending moments acting on the flange members are reversed in sign to those shown in (i) Fig. 392 ; see (ii).

250. Rigid-frame Bridges.—This type of bridge, suitable for short spans, has been developed in America by Mr. A. G. Hayden,[14] in collaboration with Mr. G. D. Clarke, the latter being responsible for the architectural treatment. It consists of a very flat arch made continuous with its abutment walls, Fig. 393, so that the combination forms a stiff portal. Such bridges have advantages from an aesthetic point of view, there is considerable saving in the cost of the abutments, and owing to the flatness of the arch the approach gradients are reduced. For spans of from 35 to 80 feet in reinforced-concrete, and from 80 to 120 feet in steel, the rigid-frame bridge is claimed to be more economical than the ordinary types of reinforced-concrete or steel bridges.

Fig. 393 shows a typical example of about 50-ft. span. The dead loads on the structure consist of its own weight and the horizontal earth pressure on the abutment walls. The feet may be hinged or fixed in direction, and the stresses are calculated as for a two-hinged or fixed-ended arch, §§ 220 and 222. To find the stresses due to the live load, influence lines should be constructed for a unit load moving over the bridge. Types are shown in Fig. 393 : (ii) is the influence line for the horizontal thrust H, (iii) gives the bending moment influence lines for the points Nos. 2, 5, and 9, obtained on the assumption that the ends

are hinged.　The method of § 229 (*General Case*) might be used to find these.　It is necessary to investigate the effect of variations in temperature and movement of the abutments in such structures.

Detailed calculations for rigid-frame bridges of the above type, for similar bridges with direction-fixed ends, and also for skew spans, are
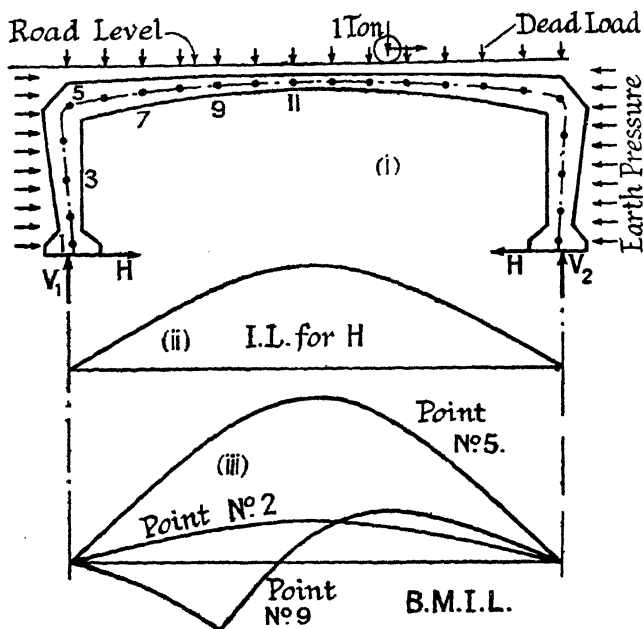
FIG. 393.

given in Hayden's book,[14] to which reference should be made for further information.

251. Incomplete Frames.—A frame composed of just sufficient bars to divide it into triangles, § 3, is statically determinate and is called a *perfect frame*.　Frames which contain less than this number of bars are called *incomplete or imperfect frames*.　Such frames depend for their strength and stability on the rigidity of their parts and joints, and the stresses in them cannot be determined from statical considerations. The common bicycle frame is an incomplete frame which depends on the stiffness of its bars and joints for stability.　Vierendeel girders, § 249, are incomplete frames of the same type, as are stiff portals, § 106.　In the roof trusses of Fig. 394, the stability of the structure depends on the stiffness of the tie beam and its capacity to carry bending moments. Many other incomplete frames are employed in practice with success. Such frames are incomplete or imperfect only in the statical sense, and may be well fitted for their functions.　No methods, generally applicable, can be given for the purpose of determining the stresses in incomplete frames ; each type requires particular treatment.

BIBLIOGRAPHY

Tanks, Silos, etc.

1. ROBERTS. On the Pressure of Wheat Stored in Elongated Cells or Bins. *Engg.*, Oct. 27, 1882, p. 399 ; also AIRY, *Proc. Inst. C.E.*, vol. cxxxi, 1897–8, p. 347 ; vol. cxxxvi, 1898–9, p. 336.
2. JANSSEN. Versuche über Getreidedruck in Silozellen. *Zeit. Ver. deu. Ing.*, Aug. 31, 1895, p. 1046 ; also PRANTE, Sept. 26, 1896, p. 1122 ; PLEISSNER, June 23, 1906, p. 976 ; and KÖNEN, Zent. d. Bauverwaltung, 1896, p. 446.
3. HAMMOND SMITH. A Laboratory Method of Determining Pressures on Walls and Bins. *Proc. Amer. Soc. Test. Mat.*, 1915, Pt. II, p. 382.
4. BECK. *Tank Construction.* Manchester, 1921.
5. FORCHHEIMER. *Die Berechnung ebener und gekrümmter Behälterböden.* Berlin, 3rd ed., 1931.
6. KOTTENMEIER. *Der Stahlhälterbau.* Berlin, 1931.

See also CAIN, Ref. No. 15, and KETCHUM, Ref. No. 17, Chap. XVIII, and GRAY, Ref. No. 60, Chap. XVII.

Vierendeel Girders

7. VIERENDEEL. *Cours de stabilité des constructions*, tome viii, *Calcul des Poutres Vierendeel.* Louvain, 1912 ; and *Rev. Univ. Min. Mét.*, 8ᵉ serie, t. 3, p. 129, 1930 ; also THOMAS, 7ᵉ serie, t. 4, p. 209, 1924.
8. MECKLENBECK UND EHRLICH. Knotenpunkte von Vierendeelträgern und verwandte Gebilde. *Eisenbau*, 1913, pp. 19 and 67 ; also 1914, p. 142 (exps. on panel-point construction).
9. KRISO. *Statik der Vierendeelträger.* Berlin, 1922.
10. IHLENBURG. Die Berechnung des Vierendeelträgers nach der Deformationsmethode. *Der Bauingenieur*, 1933, p. 385.
11. BATEMAN. The Open-Frame Girder. *Jour. Inst. C.E.*, Nov. 1935, p. 67.
12. YOUNG. Analysis of Vierendeel Trusses. *Proc. Amer. Soc. C.E.*, Aug. 1936, p. 833.

Miscellaneous Framework

13. STURZENEGGER. *Maste und Türme in Stahl.* Berlin, 1929.
14. HAYDEN. *The Rigid Frame Bridge.* New York, 1931.
15. STEINMAN. *The Wichert Truss.* New York, 1932.

QUESTIONS ON CHAPTER XV

1. In Fig. 386, AB is a 15 × 15 in. timber beam and the span L = 40 ft. Bars Nos. 2 and 3 are of mild steel, $l_2 = 5$ ft.; $a_2 = 4 \cdot 2$ sq. in. ; $a_3 = 1 \cdot 77$ sq. in. E timber = 540 tons/sq. in.; E steel = 13,000 tons/sq. in. Draw the I.L. for F_2 ; find F_2 for a load of 5 tons placed 12 ft. from A. Find also the stresses in all the members.

Ans. $\chi = 1/(122 \cdot 43 \times 10^6)$; $F_2 = 3 \cdot 58$, $F_1 = 7 \cdot 16$, $F_3 = 7 \cdot 38$ tons ; $f_1 = 980 + 71 = 1051$ lb./sq. in. in the beam ; $f_2 = 0 \cdot 85$, $f_3 = 4 \cdot 17$ tons/sq. in.

2. Using the value of F_2 from eq. (4), § 245, obtain expressions for the bending moment M_D under the load W distant $z = nL$ from A, Fig. 386, and for M_C at the centre of the beam.

Ans. $M_D = - WLn\{1 - (\tfrac{3}{2}L^3\chi + 1)n + 2L^3\chi n^3\}$; $M_C = \tfrac{1}{4}WLn\{(3L^3\chi - 2) - 4L^3\chi n^2\}$. Hence show by differentiation that the position of W for

maximum values of M_D and M_C is given respectively by the expressions:
$1 - (3L^2\chi + 2)n + 8n^3 = 0$; $3L^3\chi(1 - 4n^2) = 2$.

3. A 12×12-in. beam of timber is 24 ft. span. It is trussed by a cast-iron strut at the centre supported by two mild steel tie rods $1\frac{1}{4}$ in. diam. passing from the bottom of the strut to the ends of the beam. The strut is 3 ft. long, and its cross section is $2 \cdot 5$ sq. in. Find the stresses in the strut and tie rods when the beam carries a uniformly distributed load of 20,000 lb. E timber $= 1,500,000$; E cast iron $= 15,000,000$; E mild steel $= 30,000,000$ lb./sq. in. (U.L.)

Ans. $\chi = 1/(28 \cdot 92 \times 10^6)$; $F_2 = 10,325$, $F_3 = 21,280$ lb.; $f_2 = 4130$, $f_3 = 17,310$ lb./sq. in.

4. Using the theory of § 248, design a swinging wall crane to carry a load of 5 tons, maximum radius 10 ft. The horizontal reactions are not to exceed 8 tons.

5. In the frame shown at (5) Fig. 394, assume that the points of inflexion
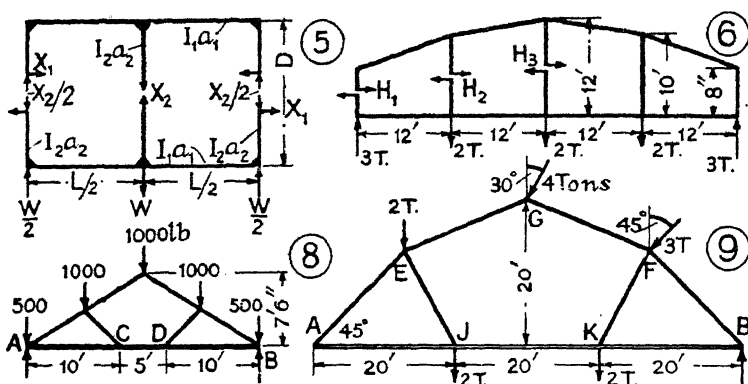
FIG. 394.

occur at the mid-points of the verticals, and using a strain-energy method, find the unknown forces X_1 and X_2.

Ans. $X_1 = WDL^2 \div 8\left\{D^2L + \dfrac{4I_1L}{a_1} + \dfrac{I_1D^3}{3I_2}\right\}$; $X_2 = W \div \left\{2 + \dfrac{72I_1D}{a_2L^3}\right\}$.

6. In the Vierendeel girder shown in (6) Fig. 394, if the I of all the members be the same, find all the H values.

Ans. $H_1 = 5 \cdot 110$; $H_2 = 3 \cdot 212$; $H_3 = 0$ tons.

7. If in the girder of Q. No. 6, the flanges were parallel, and the depth of the girder 12 ft., find by Vierendeel's formula, eq. (8), § 249, all the H values.

Ans. $H_1 = 3 \cdot 164$; $H_2 = 4 \cdot 146$; $H_3 = 0$ tons.

8. In Fig. 394, (8) represents diagrammatically a timber roof truss, supported at A and B and loaded as indicated. AB is a timber beam 11×5 in. in cross section. Find the maximum stress per square inch in the part CD of this tie beam. (I.C.E.)

Ans. 771 lb./sq. in.

9. Draw the shearing-force and bending-moment diagrams for the tie beam AB of the roof truss shown in (9) Fig. 394, for the loading indicated. $AE = EG = GF = FB$. The reaction at B is vertical. (U.L.)

Ans. Shearing forces : $S_A = 2 \cdot 01$, $S_B = 2 \cdot 77$ tons ; bending moments : $M_J = 40 \cdot 2$, $M_K = 55 \cdot 4$ ft. tons.

CHAPTER XVI

THE BUILDING MATERIALS

TIMBER

252. Classification.—The timber used for constructional purposes is obtained from the class of trees called by botanists *exogens*, i.e. trees in which growth takes place by the annual addition of an external layer or ring of cellular tissue and woody fibre. It may be subdivided into hard woods and soft woods. The hard woods come from the broad-leaved deciduous trees. The chief varieties are: oak, elm, beech, greenheart, walnut, mahogany, maple, and teak. Bass, though obtained from a broad-leaved tree, is classed as a soft wood. The soft woods are obtained from the coniferous or needle-leaved trees; these include the pines and firs. The chief varieties are: *Pinus sylvestris*, commonly known as northern pine, Scotch fir, red or yellow fir or deal; *Pinus resinosa*, known as red pine or American deal; *Pinus strobus*, white or yellow pine, the American long-leaved pine; Kauri pine; and pitch pine (*Pinus rigida*); *Picea excelsa*, known as Norway spruce, spruce fir, or white deal; Douglas spruce or fir; *Abies pectinata*, silver fir; and larch.

253. Structure.—As shown by a transverse section, the stem of an exogenous tree is made up of the following parts: (i) the *medulla* or *pith*, (ii) the *medullary sheath* and *rays*, (iii) the *annual rings*, and (iv) the *bark*. The pith, which occurs at the centre of the tree, is composed entirely of cellular tissue. It is enclosed by a thin membrane called the medullary sheath, from which radiate the medullary rays, thin layers of a muriform cellular tissue. The annual rings are deposited immediately outside the medullary sheath, in the form of concentric layers of cellular tissue and woody fibre. In temperate climates one ring is added each year. It consists of two parts: a soft inner portion composed of cellular tissue, light in colour, formed early in the year, called *spring wood*; and an outer portion, darker and harder, composed of woody fibre, formed late in the summer, and termed *autumn wood*. The annual rings nearer the centre of the tree are harder and closer in grain than those near the circumference, and are called the *heartwood* or *duramen*. This is the part of the tree used for constructional purposes. The softer rings near the circumference are called *sapwood* or *alburnum*. They are lighter in colour and more open in grain. Sapwood should not be used for constructional work,

as it is immature timber, not properly hardened, and readily decomposes. The bark is the familiar external covering of the tree.

254. Felling and Seasoning.—The tree should be felled on reaching maturity, for the strongest and most durable timber is obtained from trees in their prime. The proportion of heartwood is then at its maximum and the heartwood has not commenced to decay. Oak trees reach maturity in about 100 years; elm, ash, and larch in from 50 to 100 years; firs and pines in from 70 to 100 years. The best time for felling is at midwinter, when the sap has ceased to flow and the contained moisture is at its minimum. Immediately after felling the trunk should be stripped of its bark to allow the moisture to evaporate, and as soon afterwards as possible it should be sawn into scantlings, otherwise large shakes and splits will occur due to shrinkage.

Before the timber can be used for constructional work it must be seasoned, i.e. the moisture and unhardened sap must be dried out. The natural and best method of seasoning is to stack the timber carefully in open sheds, with distance pieces between each scantling, so that the air can circulate freely all round. This produces the strongest and most durable timber, but it requires a considerable time to accomplish, particularly if the timber be large. To hasten the process, the timber may be dried by warmed air in chambers or kilns. The timber is stacked in the drying chamber in the manner described above, and is exposed to currents of warmed air from a fan. The temperature and humidity of this air are so controlled that the rate of evaporation from the timber does not exceed a certain figure which experience has shown will not lead to deterioration of the material. In modifications of the method the timber is moved slowly through a long tunnel, in which the temperature of the circulating air gradually increases as the timber passes along, so that the required rate of evaporation is maintained. It is claimed that this method of seasoning produces timber equal in quality to that obtained by natural seasoning.

Another method, called water seasoning, is completely to submerge the green timber in running water for about fourteen days, with the butt end up-stream. The water enters the pores of the wood, dilutes and drives out the sap. The timber is then dried in a shed as before, but the time taken is much reduced.

255. Defects in Timber.—The more important defects to be looked for in timber are : *Cup Shakes,* or splitting due to the separation of one annual ring from the next. *Star Shakes,* which are splits radiating from the centre of the tree towards the circumference. *Heart Shakes,* or splits through the heartwood, usually found in old trees. *Foxiness* is a dull reddish stain, and *Doatiness* is a speckled stain, both indicating incipient decay. *Waney Edges* are edges formed by the natural curvature of the circumference. The inference is that the timber contains a large proportion of sapwood.

256. Characteristics of Good Timber.—The timber should be free from defects, firm and clean in appearance, and when struck should

emit a clear ringing sound. The cellular tissue should be hard and compact, the annular rings narrow, and the proportion of sapwood not unduly large. If the tree has been felled too young, the proportion of sapwood is large and the heartwood is softer than in a mature tree. If the tree is very old, the heartwood is brittle, and often decayed. The width of the rings indicates the rate of growth of the tree. Wide rings indicate rapid growth, narrow rings slow growth. The rings near the centre are usually wider than those at the circumference, but the width and arrangement of the rings commonly varies in trees of the same variety, and in different parts of the same tree. Timber in which the rings are wide, indicating too rapid growth, is usually soft and weak (see Fig. 402).

257. Strength of Timber.—The strength and other mechanical properties of timber are found to depend on (see § 271) :

Its density.
The rate of growth (rings per inch).
Percentage of autumn wood.
Moisture content.
Number and arrangement of the knots (see § 262).
Position in the tree.
Size of the specimen (see § 262).
Defects in the timber (see § 255).

Before considering the results of tests, the methods of determining the density, rings per inch, percentage of autumn wood, and moisture content, will be briefly described.

258. Density or Specific Gravity.—A block of the timber is cut to a definite size and weighed. The specific gravity is obtained by dividing the weight in grammes by the volume in cubic centimetres. The specific gravity thus obtained will evidently depend on the percentage of moisture which the specimen contains. A second determination is therefore made, after the block has been dried in an oven at 100° C. until it ceases to lose weight. It is again measured and weighed, and the specific gravity found as before. This is the specific gravity oven-dry, and it is used for purposes of comparison.

Not only is the density affected by the moisture content, but it also depends on the width of the annual rings, the percentage of autumn wood, and on the part of the tree from which the specimen was taken.

259. Rings per Inch.—The width of the annual rings is determined by drawing a radial line one inch long on the end section and counting the number of rings which cross the line. The result is stated as so many rings per inch. When the number and arrangement of the rings varies over the cross-section, a number of counts are made at different places, and an average taken.

260. Percentage of Autumn Wood.—This is determined by estimating the ratio of the added areas of dark woody fibres to the total area of cross-section.

261. Moisture Content.—The percentage of moisture in a specimen is obtained by weighing a small slice, or borings from the specimen, before and after drying. The ratio of the loss of weight to the dried weight is called the percentage of moisture. The borings should be taken from as near to the point of fracture as possible. They are dried in an oven with a free circulation of air at 100° C. until they cease to lose weight. If w_1 and w_2 be the weights before and after drying, the percentage of moisture is $100(w_1 - w_2)/w_2$. In large specimens, a determination may be made at a number of points, and an average taken.

To obtain test results which are strictly comparable, certain experimenters have proposed the adoption of a *standard percentage of moisture*. Timber which has been thoroughly dried in a kiln is found, on exposure to the atmosphere, to absorb about 12 to 15 % of moisture. Bauschinger adopted the latter figure as a standard percentage of moisture, and it is commonly accepted. In America it is more usual to take 12 % as the standard percentage.

Before testing, the specimens are dried in a kiln, until the desired moisture content is obtained.

262. Effect of Size of Test-Piece. Knots.—The size of the test-piece has considerable effect on the strength of timber as determined in the testing machine. A large specimen is far from being homogeneous and nearly always contains knots, shakes, and other defects. A small specimen is usually free from such defects, and the percentage of moisture is much more uniform. For these reasons the strength of small specimens is nearly always greater than that of large specimens. The effect of size on the bending and compressive strength of timber is plainly evident in Fig. 401.

Knots.—From compressive tests parallel to the grain, the relative strength of large specimens is of the following order (Bull. No. 108, U.S. Forest Service) :

No knots		100
Sound knots ½ inch diameter or less	. . .	95
„ „ ½ to 1½ inches diameter	. . .	90
„ „ over 1½ inches diameter	. . .	80

263. Tests on Timber.—The more usual tests are : tensile, compressive, shear, bending, and cleavage or splitting tests. Notched bar and hardness tests are sometimes made.

264. Tensile Tests.—The tensile test is similar in character to that used for metals, except that the ends of the specimen have to be greatly enlarged, or the specimen will fail by shearing or crushing in the grips. A common form of test-piece is shown in Fig. 395.
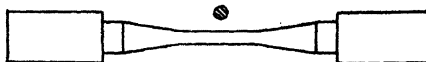
Fig. 395.

The results of some tension tests on timber specimens will be found in the Table on p. 577.

265. Compression Tests.—Compression tests may be made along or across the grain. For tests along the grain the specimens are usually short prisms about $2 \times 2 \times 4$ inches in size. Failure usually takes place either by collapse of the walls of the cells of which the internal structure is composed, or by local kinking of the fibres which frequently commences at a knot, Fig. 396. On the tangential surface of the specimen the line of fracture is usually inclined, on the radial surface it may remain normal to the fibres. The compression is accompanied by longitudinal shearing along the fibres, and splitting often occurs. It is found that the fibres split rather than separate.
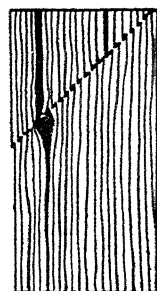
Fig. 396.

In tests where the pressure is applied across the grain, failure occurs due to splitting along the fibres. The propagation of cracks may easily be observed, first dividing two annual rings for a short distance, then crossing the ring, again following the contour of the next ring for a short distance, then again crossing that ring, and so on until the specimen is completely disintegrated.

For results of compression tests see the Table, p. 577.

266. Shear Tests.—The most satisfactory shear test on timber (across the grain) is by the Izod method, Fig. 284, Vol. I. Here the specimen is in double shear. Some results are given in the Table, p. 577.

Tests are sometimes made on wooden pins in double shear; in other tests the specimen is placed in single shear along the grain.
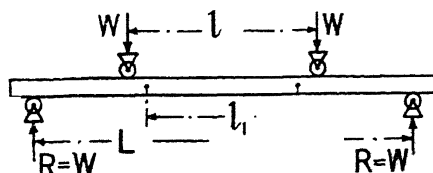
Fig. 397.

267. Bending Tests.—This is one of the simplest and commonest tests for timber. Four-point loading is usually adopted, Fig. 397. The specimens are of rectangular cross-section, and may be of large dimensions, i.e. of a size used in practice. Failure may occur in tension or compression (cross-breaking), or by longitudinal shear. In short specimens the latter is a very common mode of failure, owing to the weakness of timber

Cross Break in Tension

Primary failure, Longitudinal Shear

Final Cross Break in Tension

Fig. 398.

in resisting such shear. Some typical fractures for a central load are sketched in Fig. 398.
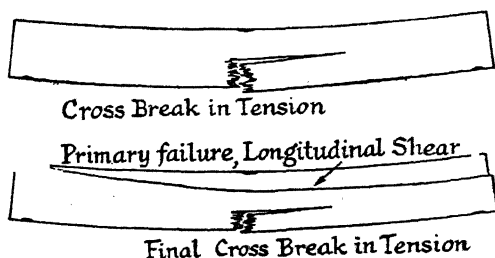
From the breaking load, a *modulus of rupture* μ is calculated, which

figure would be the stress in the material were it elastic up to the breaking point. This modulus may be regarded as an indication of the relative strength of the specimen in bending. For a rectangular specimen B × D, loaded as shown in Fig. 397, if W be the magnitude of each load at the failure point,

$$M = \frac{W(L - l)}{2} = \mu Z = \mu \times \frac{1}{6}BD^2.$$

Hence $$\mu = \frac{3W(L - l)}{BD^2}.$$

Values of μ for the commonly occurring timbers are given in the Table, p. 577.

268. Elastic Constants for Timber.—Observations with an extensometer in tension experiments, and with a compressometer in compression experiments, are made on timber specimens in order to determine the proportional limit and the modulus of elasticity. The resulting load-extension or load-contraction diagrams are of the same type as those obtained for metals, (i) Fig. 399. Up to the proportional limit the points lie on a straight line, the departure from this straight line determines the proportional limit, which is clearly defined in most timbers. The modulus of elasticity can be obtained from the slope of the straight line.

The bending test is also a convenient method of determining the modulus of elasticity of timber. If the load be plotted
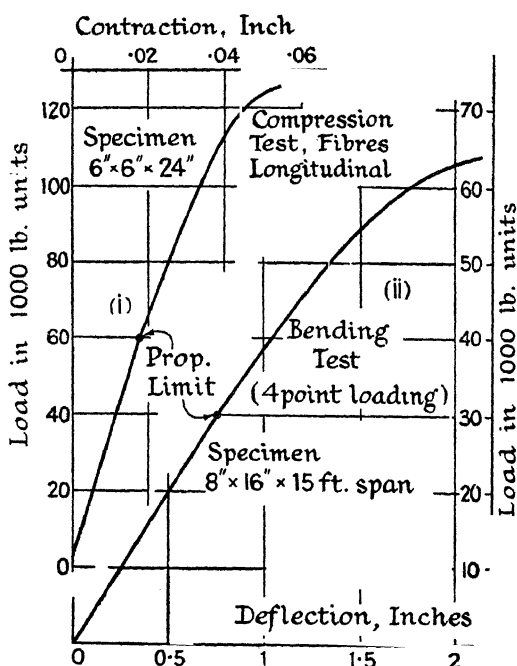
FIG. 399.—(U.S. Forest Service, Bull. No. 108.)

against accurately observed deflections, say at the middle of the beam, a diagram of the type shown in (ii) Fig. 399 will be obtained. As in the tension test, the points lie on a straight line up to the proportional limit. For accurate work it is best to measure the deflection in a central length l_1 shorter than l, Fig. 397. Over the length l_1 the bending moment is constant and the shearing force zero. A suitably arranged deflectometer should be arranged to ensure accurate readings. If y be the central deflection in

the length l_1 shortly before the proportional limit is reached, and W be the magnitude of each load when this deflection is produced,

$$E \quad \frac{6W(L - l)l_1^2}{8BD^3y}.$$

269. Special Tests.—A *splitting* or *cleavage test* has been introduced by the Department of Agriculture, U.S.A., the nature of which is indicated in Fig. 400.

Notched bar tests, § 256, Vol. I, are sometimes made. The specimen is fixed in a vice of the Izod type, and protected with a cap where it is hit by the striker. The notch is of the Charpy type. *Ball indentation tests* are made to determine the relative hardness of different kinds of timber. Another frequently made test is the determination of the *resistance to withdrawal of nails and screws*. *Wear*, or *resistance to abrasion*, tests for wood blocks are also made.

270. Time Effects.—It is found that the rate of loading considerably affects the strength of timber, particularly if the timber be green. Standard rates of increasing the strain in timber are therefore specified.

FIG. 400.

From some experiments by Thurston and J. B. Johnson * it would appear that 50 to 60 per cent. of the short time breaking load, as determined in an ordinary test, is sufficient to bring about failure of the specimen if applied for a sufficiently long period.

271. The Influence of the Physical Condition of Timber on its Mechanical Properties.—The factors which influence the strength and other mechanical properties of timber are enumerated in § 257. The following is a brief summary of their effects, drawn largely from the work of the U.S. Forest Service.

Density.—In sound timber with a given moisture content, the strength and stiffness of the timber increase as its density increases. This will be evident from Fig. 401,

* See Johnson's *Materials of Construction*, 6th Ed., p. 208.
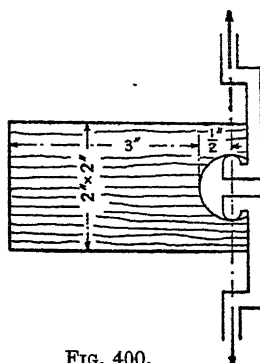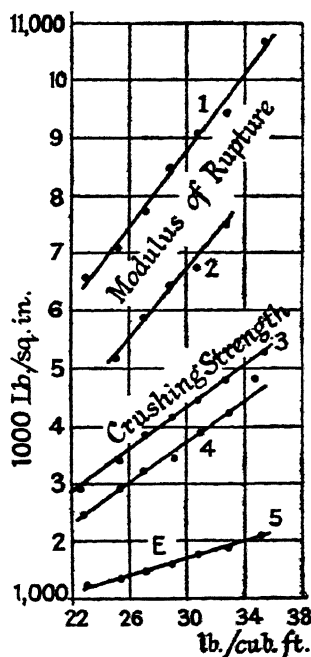
FIG. 401.
(Bull. No. 88, U.S. Forest Service.)
Curve 1. Small Beams, 2″ × 2″ × 24″.
  „ 2. Large Beams, 8″ × 16″ × 186″.
  „ 3. Small Specimens, 2″ × 2″ × 10″.
  „ 4. Large Specimens, 6″ × 6″ × 18″.
  „ 5. Large and Small Beams.

plotted on a base line representing the dry weight of the timber. In the compression tests the load direction was parallel to the grain. The size of the specimen does not much affect the value of E. The averages of many experiments (Bull. No. 676, U.S. Dept. Agric.) on small sound specimens of a large variety of timbers may be represented by the formula

$$\phi = C\rho^n$$

where ϕ denotes the mechanical property under consideration; ρ is the specific gravity of the timber, based on the volume of the test-piece and the oven-dry weight of the timber; C and n are constants with the following values:

ϕ	Unit.	Green.		Air dry.	
		C	n	C	n
Modulus of Rupture . .	lb./sq. in. .	18,500	1·25	26,200	1·25
Ditto, average 113 varieties .	lb./sq. in. .	19,140	1·27	25,530	1·20
Modulus of Elasticity .	1000 lb./sq. in.	2,500	1·0	3,000	1·0
Work to maximum Load .	in. lb./in.^{3} .	42·7	2·0	38·9	2·0
Compressive Strength:					
Parallel to grain . .	lb./sq. in. .	6.900	1·0	12,000	1·0
Normal to grain . .	lb./sq. in. .	2,900	2·25	5,200	2·25
Shear Strength (tangential) .	lb./sq. in. .	2,750	1·33	4,000	1·33
Tension across Grain . .	lb./sq. in. .	1,950	2·0	2,100	2·0

Rate of Growth : Rings per Inch.—Fig. 402 shows the relation between the strength of three varieties of timber and the rings per inch. Wide
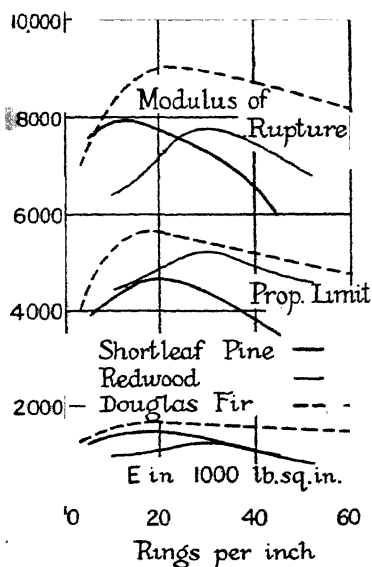
FIG. 402.
(Bull. No. 108, U.S. Forest Service.)
Units : lb./sq.in.
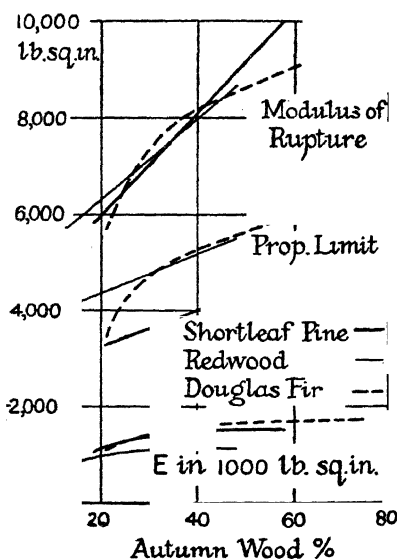
FIG. 403.
(Bull. No. 108, U.S. Forest Service.)

RESULTS OF TESTS ON TIMBER.

Small Clear Pieces in a Green Condition.　Bull. No. 556 U.S. Dept. of Agriculture.

| | Variety. | Rings per inch. | Autumn Wood, %. | Moisture Content, %. | Specific Gravity, Oven-Dry. | Weight Green, lb./cub. ft. | Shrinkage,* from green to oven-dry. | | | Bending. | | | | | Compression parallel to grain. | | Comp. perp. to grain. Prop. Limit. | Shear parallel to grain. Ult. Str. | Tension perp. to grain. Ult. Str. | Ball Hardness.‡ | |
							In Volume.	Radial.	Tangential.	Prop. Limit.	Mod. of Rupture.	E.	† Work to P.L.	Max. Load.	P.L.	Crush. Str.				On end (lb.).	On side (lb.).
1	Ash, white	16	50	43	0·60	46	12·6	4·2	6·5	4·90	9·10	1350	1·03	13·4	3·23	3·80	0·80	1·26	0·62	1000	900
2	Beech	19	30	62	0·66	55	16·2	4·8	10·6	4·50	8·20	1240	0·99	12·5	2·55	3·28	0·61	1·21	0·76	950	820
3	Birch, yellow	19	26	68	0·66	58	16·0	7·4	9·0	4·60	8·60	1540	0·80	16·6	2·76	3·46	0·45	1·11	0·48	820	740
4	Chestnut	10	48	122	0·46	55	11·6	3·4	6·7	3·10	5·60	930	0·59	7·0	2·04	2·47	0·38	0·80	0·43	530	420
5	Elm, white	18	31	88	0·54	52	14·4	4·2	9·5	3·60	6·90	1030	0·83	11·0	2·29	2·88	0·39	0·92	0·56	610	550
6	Gum, red	16	..	81	0·53	50	15·0	5·3	9·9	3·70	6·80	1150	0·81	9·4	2·36	2·84	0·46	1·07	0·51	630	520
7	Oak, white	17	60	62	0·71	62	15·8	5·3	9·0	4·70	8·30	1250	1·08	11·5	2·99	3·56	0·83	1·25	0·77	1120	1060
8	Poplar, yellow	14		64	0·42	38	11·4	4·1	6·9	3·20	5·60	1210	0·48	5·6	2·00	2·55	0·31	0·79	0·46	420	340
9	Sycamore	16	77	83	0·54	52	14·2	5·1	7·6	3·30	6·50	1060	0·60	7·5	2·39	2·92	0·45	1·00	0·63	700	610
10	Douglas Fir	22	27	38	0·44	34	10·6	3·6	6·2	3·60	6·40	1180	0·65	6·8	2·52	3·00	0·44	0·88	0·35	450	400
11	Fir, white	22	30	156	0·39	56	10·2	3·4	7·0	3·90	6·00	1130	0·77	5·2	2·61	2·80	0·44	0·73	0·26	380	330
12	Larch	32	37	58	0·59	48	13·2	4·2	8·1	4·60	7·50	1350	1·01	7·1	3·25	3·80	0·56	0·92	0·23	470	450
13	Pine, long leaf	18	39	47	0·64	50	12·3	5·3	7·5	5·40	8·70	1630	1·00	8·0	3·84	4·39	0·60	1·07	0·29	550	590
14	Pine, Norway	22	41	54	0·51	42	11·5	4·6	7·2	3·70	6·40	1380	0·59	6·0	2·47	3·08	0·36	0·78	0·19	360	340
15	Pine, pitch	12	30	85	0·54	54	11·7	4·8	7·4	3·70	6·70	1120	0·75	8·5	2·10	3·04	0·51	0·95	0·35	400	480
16	Pine, short leaf	12	40	64	0·58	50	12·6	5·1	8·2	4·50	8·00	1450	0·79	8·7	3·65	3·81	0·48	0·89	0·33	490	560
17	Pine, yellow	20	22	95	0·42	46	11·0	3·9	6·4	3·10	5·20	1010	0·54	5·1	2·08	2·46	0·34	0·68	0·28	310	320
18	Spruce, red	17	27	43	0·41	34	11·8	3·8	7·8	3·40	5·70	1180	0·56	6·1	2·36	2·74	0·35	0·77	0·22	420	350
19	Spruce, white	14	27	46	0·43	33	14·8	3·7	7·3	3·30	5·40	980	0·60	5·7	2·28	2·38	0·27	0·67	0·20	300	280

Units : Stresses in 1000 lb./sq. in.

* Per cent. of dimensions when green.　† In.-lb. per cub. in.　‡ Load required to embed a 0·444-inch ball one-half its diameter.

rings, indicating too rapid growth, signify weak timber ; a medium rate of growth produces the strongest timber.

Percentage of Autumn Wood.— It will be evident from Fig. 403 that the larger the percentage of autumn wood the stronger the timber.

*Moisture Content.—*The drier the timber the greater its strength, provided that the moisture content does not exceed the saturation point, Fig. 404. This figure shows the variation in the modulus of rupture with the moisture per cent., based on the dry weight, for specimens of small cross-section; similar variations are observed in the compressive strength and modulus of elasticity. Large members dry so slowly in air that increase in strength on this account should not be expected.

*Position in Tree.—*The density, and therefore the strength, of the timber is greatest in the butt of the tree, and between the medullary sheath and the middle annual ring.

FIG. 404.
(Bull. No. 70, U.S. Forest Service.)

*Working Stresses,—*The 1935 A.R.E.A. Specification for Steel Railway Bridges recommends the following extreme fibre stresses for structural timber in bending :

				lb./sq.in.
Yellow pine, dense structural grade	.	.	.	1,500
Douglas pine, close grain, structural grade	.	.	.	1,400
White oak	.	.	.	1,200
White pine, Norway pine, or *Spruce*	.	.	.	800

STONE

272. Natural Stones.—The three kinds of stone commonly employed in engineering work are (i) granites, (ii) sandstones, (iii) limestones, including the dolomites or magnesian limestones. The *granites* are igneous rocks, formed by volcanic action, composed of crystals of quartz, amorphous felspar, and mica grains, fused together. The *sandstones* are aqueous rocks composed of grains of sand (chiefly quartz) cemented together by silica, carbonate of lime, or other material. The strength and durability of the stone depend chiefly on the nature of this cement. The most durable stones are those composed of grains of silica (quartz) cemented together by siliceous material. The *limestones* are aqueous rocks composed principally of carbonate of lime. They consist either of

crystallised grains of carbonate of lime cemented together by the same material ; or, in the *oolite* stones, of rounded grains of calcareous matter similarly cemented, often formed about a nucleus of a small shell, so that the structure of the stone resembles that of a fish roe. The *dolomites* or magnesian limestones contain about equal proportions of carbonate of lime and carbonate of magnesia. When these carbonates are in crystalline form, the stone is very hard and durable.

For names and descriptions of the varieties of building stones commonly used in this country, see § 350.

273. Tests.—The tests to which stones are subjected are : (i) the crushing test, (ii) density determination, (iii) tests for absorption, (iv) the acid test, and (v) microscopic examination. Bending tests, and a determination of the elastic constants are sometimes made. For certain purposes, abrasion tests to determine the resistance to wear are necessary.

274. Crushing Tests.—The usual test-piece is a cube of 4 inch sides. In America, a cylindrical specimen 6 inches in diameter and 12 inches high is preferred. The test is carried out in a similar manner to the compression test for metals, § 226, Vol. I, but in brittle materials like stone, the greatest care must be taken that the ends are flat and parallel, and that the load is axially applied, otherwise a marked reduction in the apparent strength of the specimen will result.

The most satisfactory way of treating the ends of a stone specimen is to dress them as nearly flat and parallel as possible, and then coat them with thin layers of plaster of Paris. These surfaces are rubbed down true and flat, so that the ends are perfectly parallel. The ends, thus prepared, are placed in direct contact with the pressure plates of the testing machine. It is a mistake to interpose a soft substance such as sheet lead, or thin layers of wood, with the idea of securing a more uniform pressure distribution. The heavy compressive load causes lateral flow in the soft layers, with the result that the lateral tensions which accompany the longitudinal contraction cause the stone specimen to split along planes parallel to the direction of the load, and a reduction in the apparent strength of from 36 to 55 per cent. (Hudson Beare [25]) is the result. If the lateral expansion be prevented by friction between the pressure plates and the specimen, failure takes place by shearing. Föppl * showed that by greasing the ends of the specimen, in order to reduce the friction, a reduction in strength occurs of the order of 50 per cent. or more.

FIG. 405.

The normal fracture is of the double cone type, Fig. 405, commonly observed in brittle materials under compression. The base angle of the cone is about 60°, so that, in order to obtain a complete double cone, the specimen should be at least two diameters high, as is the American practice. It is found that for values less than two, the strength varies
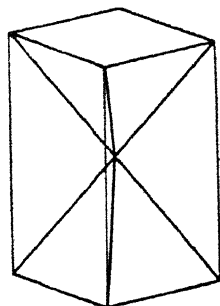
* Proc. Int. Assoc. Test. Mat., 6th Cong. 1912, Paper XXVIII7.

with the ratio of height to diameter, but in geometrically similar test-pieces such as cubes, the crushing strength per square foot for a given material is constant.

According to the tests made by Professor Sir Thomas Hudson Beare [25] on $2\frac{1}{4}$ inch cubes, the mean crushing strengths of the different classes of stones are as follows : granites 1112·2 ; sandstones 489·8 ; dolomites 500·5 ; oolitic limestones 141·3, all in tons/sq. ft. Some more detailed results are given in the Table, § 350.

In masonry structures the blocks should be so arranged that the pressure is applied perpendicularly to the planes of stratification (see § 351). This condition should also be complied with when testing stratified stones. Tests on a Yorkshire sandstone [25] with the pressure first perpendicular to, and second parallel to, the planes of stratification, gave in the first case a crushing strength of 996·8 tons/sq. ft., and in the second case 1035·0 tons/sq. ft. The load-contraction diagrams are shown in Fig. 406.

275. Elastic Constants.—Typical load-contraction diagrams for a Yorkshire sandstone (Lightcliffe, Bed No. 4) in compression are given in Fig. 406. These were obtained by means of a special extensometer [25] which gave the contraction in a length of $1\frac{1}{2}$ inches. Tests on stones of all classes generally show, on first loading, considerable permanent set. On second loading the stones become much more nearly elastic. Hudson Beare's mean figures for the modulus of elasticity on second loading are : granites 522,100 ; sandstones 132,280 ; dolomites 321,000 ; oolitic limestones 150,750 ; all in tons/sq. ft. The modulus as here given is the ratio of increase in stress to increase in strain for a specified range of stress.

Fig. 406 is of further interest in that curves A and B were obtained from tests in which the pressure was perpendicular to the planes of stratification, and curves C and D from tests in which the pressure was parallel to those planes. In the first case the modulus of elasticity on second loading was 127,800, and in the second case 241,400 tons/sq. ft.

FIG. 406.

A. Pressure perpendicular to bedding planes, 1st Test.
B. Pressure perpendicular to bedding planes, 2nd Test.
C. Pressure parallel to bedding planes, 1st Test.
D. Pressure parallel to bedding planes, 2nd Test.

276. Density.—To evaporate the contained water, the sample is first dried by heating in a kiln to 100° C. until it ceases to lose weight. When cool, it is given a thin coating of paraffin wax to exclude moisture. The specific gravity is then determined by weighing in air and water in the usual way. The weight per cube foot is 62·4 × specific gravity.

277. Absorption.—To determine the amount of water which the stone will absorb, a specimen is first heated to 100° C. until it is thoroughly dry, and then weighed in air. It is next immersed in water and left to soak for three or four days. After removal from the water, it is wiped dry and at once re-weighed. The increase in weight × 100, divided by the weight in air, gives the percentage absorption. This figure may be regarded as an indication of the weathering power of the stone, for the more absorbent it is, the more likely are rain and moisture, which contain destructive acids, to penetrate; and the greater the likelihood of consequent injury through frost. Hudson Beare's average figures are : granites 0·27 % ; sandstones 4·68 % ; dolomites 5·43 % ; oolitic limestones 8·96 % ; see also the Table, § 350.

278. Acid Test.—A specimen of the stone is immersed in a weak solution (about 1 %) of hydrochloric and sulphuric acids for several days. The solution should be agitated at intervals. When removed from the acid, the edges of the specimen should still be sharp and the surface grains intact. Loose grains on the surface imply poor weathering qualities.

Effervescence from sandstone, when treated with acid, indicates the presence of lime, which in certain stones forms the cementing material. Such stones will not weather well, particularly in towns.

279. Microscopic Tests.—Valuable information as to the strength and durability of stones can be obtained from a microscopic examination. The microscope will reveal the mineral composition and its arrangement, the nature of the cementing material, the texture and bonding of the particles, and whether the stone contains injurious matter or partly decomposed minerals. From these observations much may be inferred as to the suitability of the stone for a given purpose.

Thus, in the granites, a compact non-porous texture, with tightly interlocked crystals, a fine uniform grain, and with the mica and felspar in an undecomposed condition, imply a very strong durable stone. In the sandstones and limestones also, a fine grain of uniform size is indicative of strength, whereas in the weaker stones the grain is non-uniform or coarse. Much depends on the nature of the cementing material, and on the shape, arrangement, and bonding of the grains. The cement adheres better to sharp angular grains than to rounded ones. When the grains are loosely compacted, and cemented at the points of contact only, a weak stone is the result. In a strong stone the whole of the pore spaces are filled with cement. When the grains hardly touch, but are bound together by a matrix of cement, the latter determines the strength of the stone. Decomposed minerals, such as felspar, are sources of weakness. The size and shape of the pores, and the mode of connection one to another, have considerable effect on the durability of the stone.

If, therefore, the microscope reveals a fine grain, closely interlocking angular particles, with the interstices filled with cement, the inference is that the stone is hard and durable. If the grains are coarse and

rounded, hardly touching, with little or no cement in the pore spaces, it implies that the stone is weak and not likely to weather well.

For a microscopic analysis on the above principles of a number of commonly employed building stones, reference should be made to a paper by Morton [32] read before the British Association at Oxford, 1926.

280. **Effect of Physical Condition.**—A number of experiments have been made on stones subjected to atmospheric influences, effect of frost, soaking in water, alternations in temperature, the action of slightly acid rain water, etc., with the object of ascertaining how the strength of the stone is affected by its physical condition. Thus Baldwin-Wiseman and Griffiths [27] showed that the strength of stone is much reduced if it be previously soaked in water, or subjected to high temperatures for longer or shorter intervals, and cooled at different rates. For further information on this subject see Hirchwald.[30]

Baldwin-Wiseman and Griffiths also determined the thermal and electrical properties of various stones.

281. **Brickwork.**—For the results of tests on bricks and brickwork, see § 369.

CEMENT

282. **Cements.**—The cements commonly used for constructional work are : (i) lime, including hydrated lime ; (ii) hydraulic cements, of which the most important are Portland cement and aluminous cement.

283. **Lime Cements.**—Lime is obtained by burning chalk or limestone in a kiln at about 500° C. At this temperature the CO_2 is driven off from the calcium carbonate, leaving CaO, quicklime. This, when mixed with sand and slaked with water, forms the mortar commonly used in building construction. Setting occurs owing to the lime drying, but the outer surface of the mortar hardens later, by the lime absorbing CO_2 from the atmosphere. Setting is accompanied by considerable increase in volume. Hydrated lime is made by adding a *definite* proportion of water to quicklime. The process of slaking is thus kept under control, and a superior mortar can be obtained. After screening, the slaked lime is finely ground.

284. **Hydraulic Cements.**—Lime cements are non-hydraulic, they will not withstand the action of water. By mixing material containing silica in an active condition, and water with the lime, a *hydraulic cement* is obtained, i.e. one which will set and harden under water. The siliceous materials formerly employed were usually of volcanic origin, such as pumice or turfa ; in modern cements of this type, granulated blast-furnace slag is used. This is mixed with the slaked lime, and the mixture is finely ground. The product, *slag cement*, sets slowly, but ultimately reaches a strength approximating to Portland cement.

In cements of the Portland type, definite chemical combination of the lime and silica is brought about by calcination, followed by grinding. *Hydraulic lime* and *Roman cement*, obtained by burning limestones containing a percentage of clay, are natural cements of this type.

285. Portland Cement.—Portland cement is manufactured by intimately mixing together definite proportions of carbonate of lime and silicate of alumina, burning the mixture at a high temperature, and grinding the resulting clinker to a very fine powder—the Portland cement of commerce. The materials commonly used for the carbonate of lime are chalk and limestone ; and for the silicate of alumina are clay, Medway mud, or shale, depending on local circumstances ; the important point is to provide the correct proportions of lime, silica, and alumina. To ensure intimate mixing, the raw materials are ground to powder. When hard limestones and clay are used, they may be ground in a dry state ; but the greater part of present-day Portland cement is made by the 'wet' process. In this, the materials used are either chalk and clay, or chalk and Medway mud. These are ground together with water to form a *slurry*. This slurry is fed or sprayed into the top end of a rotary kiln, which is a long, slightly inclined cylinder with a refractory lining. Some modern kilns are 250 feet long, 11 feet in diameter, and have a capacity of 15 tons per hour. A powerful jet of flame is driven up the kiln from the lower end by injecting finely powdered coal through a nozzle by means of an air blast. At the top end of the kiln, where the temperature is lowest, the slurry is dried. As the kiln rotates, the dried slurry slowly descends, its temperature gradually rising, CO_2 is driven off from the carbonate of lime, and the latter begins to react chemically on the silicate of alumina. When the region of the flame is reached, the temperature is raised to a white heat, 1500° C., chemical combination between the lime and silicate is completed, and the product leaves the kiln in the form of small particles of clinker. These particles are cooled by a current of air. The air, thus heated, is used in the burner to heat the kiln, the process thus being made regenerative. The cooled clinker is a dark hard substance ; the cement is obtained by grinding this in a special mill to a very fine powder. Nothing may be added after burning but a small quantity (1 to 2 %) of calcium sulphate (gypsum), and about the same quantity of water. The calcium sulphate is added to produce a slower setting cement.

The product thus obtained is a slow setting hydraulic cement, which hardens with very little change in volume. Its hydraulic properties are due to the presence of silicate of alumina. Properly treated, it exhibits considerable tensile strength as a cement, and the concrete made by its means is a most valuable material of construction, of great strength and permanency. The relative slowness in setting of the cement gives sufficient time for the concrete to be properly mixed and placed in position.

In this country the quality of the cement is governed by the British Standard Specification No. 12—1931, which contains regulations to which the cement must conform. Its properties depend on certain characteristics, chiefly on chemical composition and fineness in grinding. Tests are specified to ensure the suitability of the cement in these respects, and others to determine the strength, the time of setting, and the soundness.

Chemical Composition.—The composition of a typical Portland cement is as follows :

	Per cent.
Silica (SiO₂)	22·0
Insoluble residue	1·0
Alumina (Al₂O₃)	8·0
Ferric oxide (Fe₂O₃)	2·5
Lime (CaO)	62·5
Magnesia (MgO)	1·0
Sulphuric anhydride (SO₃)	1·5
Carbonic anhydride (CO₂)	0·5
Water (H₂O)	0·5
Alkalis and loss	0·5
	100·0

Certain limiting proportions are laid down by the standard specifications.

286. Mechanical Tests on Cements.—These usually include (i) Fineness ; (ii) Tensile strength (cement and sand) ; (iii) Setting time ; (iv) Soundness. For full particulars of the standard tests, the British Standard for Portland Cement should be consulted.

Sampling.—In order to obtain a representative sample of a bulk of cement, equal portions should be taken from twelve different bags and thoroughly mixed together. The sample thus obtained should weigh 10 lb., sufficient to carry out all the tests twice over ; it should be stored in air-tight tins.

287. Fineness Tests.—The fineness of the cement is determined by the amount of residue left on standard sieves of specified dimensions, after being continuously sifted for a definite period. The dimensions of the standard sieves are : (1) meshes per inch 170 × 170, diameter of wires 0·0024 inch ; (2) meshes per inch 72 × 72, diameter of wires 0·0056 inch. The sieves are arranged in a nest, with the coarse sieve on top and a container below. 100 grammes of cement are placed in the top sieve, and the whole is continuously sifted for 15 minutes. The residue on the coarse sieve should not exceed 1 %, and that on the fine sieve should not exceed 10% of the original weight. The residue on the fine sieve is obtained by adding the two residues together.

The strength of concrete increases with the fineness of the cement from which it is made. Fine grinding also shortens the time of hardening of the cement. *Note :* Distinguish between *setting* and *hardening* ; see § 289.

288. Tensile Strength.—Although in practice cement should not be subjected to tensile stress, tension tests form a quick and convenient way of obtaining an indication of the strength of the cement. Such tests are sometimes made on neat cement, but tests on a mixture of cement and sand discriminate better between a coarsely and a finely ground cement.

Normal Consistency.—In order to arrive at the amount of water necessary for gauging the cement and sand, it is first necessary to determine the amount of water required to make a cement paste of normal consistency. For this purpose the Vicat apparatus shown in Fig. 409 is

used. The cement is mixed with a measured amount of water, the mould is completely filled with this paste and smoothed off at the top. The needle in the Vicat apparatus is replaced by a cylindrical plunger, 10 mm. in diameter, with a flat end. This is gently lowered on to the surface of the paste and allowed to sink in. According to the Specification of the American Society of Testing Materials, who originated the test, the paste is of normal consistency when the plunger penetrates 10 mm. below the surface in a ½ minute. According to the British Standard, the plunger should penetrate from 33 to 35 mm., but only 0·78 of the water required for such a paste is to be used in a paste of normal consistency. The amount of water is expressed as a percentage by weight of the dry cement. A series of trials are carried out to determine the correct percentage.

Tests on Cement and Sand.—For the tests on mixtures of cement and sand, the standard sand used is obtained from Leighton Buzzard and is what is known as the white variety. It is thoroughly washed and dried, and graded so as to pass through a standard sieve of 18 × 18 meshes per inch, diameter of wire 0·022 inch, and be retained on a standard sieve of 25 × 25 meshes per inch, diameter of wire 0·0164 inch.

Fig. 407.

The mixture used is 1 of cement to 3 of sand by weight, and the British Standard percentage of water is ¼P + 2·50, where P is the percentage required to produce a paste of normal consistency. The cement, thus gauged, is moulded into briquettes of the shape shown in (i) Fig. 407.

The moulds, Fig. 408, may be single or multiple ; they are made in two halves so that the briquette can be easily removed. These moulds are placed on a
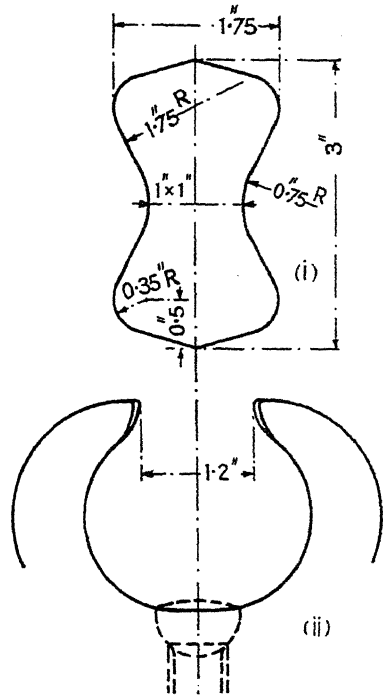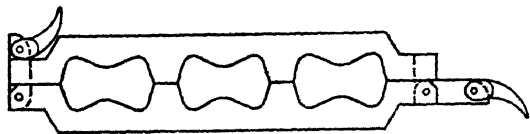
Fig. 408.

non-porous plate, slate or glass, and filled with the mixture. After filling, a small heap of the mixture is placed on top and beaten down with the flat of the standard spatula, which has a lenticular blade 2·88 in. long and 1·81 in. broad. The mould is then turned over and another small heap is similarly beaten down from the other side, until water

appears on the surface, when the briquette is finished off smoothly with a trowel, level with the top of the mould. The temperature of the room and of the water should be maintained within a range of 58° to 64° F. The briquettes, thus prepared, are kept in a damp atmosphere for 24 hours after gauging (preferably in a box lined with cloth or felt which is kept wet), when they are removed from the moulds and immediately immersed in clean fresh water, also at a temperature of from 58° to 64° F., which should be changed every 7 days. They are left immersed until required for the test ; when removed from the water they should be tested at once without being allowed to dry.

The tensile test is carried out in a small lever testing machine arranged for the purpose. The load is applied either by rolling a weight along the beam, or by running water or lead shot into a tank. The rate of loading has considerable effect on the apparent strength of the specimen, and it is important that the load be applied at the standard rate of 500 lb. per minute, and without shock. The form of the shackle is shown in (ii) Fig. 407. Care must be taken correctly to centre the specimen, or a reduction in the breaking load will be the result. The British Standard requires that the average strength of 6 briquettes, tested 72 hours after gauging, shall not be less than 300 lb./sq. in.; and that of 6 more, tested after seven days, shall show an increase and be not less than 375 lb./sq. in.

289. Setting Time.—The setting and hardening of Portland cement may be divided into three stages. Some 30 minutes after the water has been added to the cement, the mixture ceases to be plastic. This is due to chemical action between the water and the cement, and is called the *initial set*. The process continues, and after a lapse of about 10 hours the mixture reaches a condition called *final set*. It is by no means completely hard, and the third stage during which it attains its permanent form is called *hardening*.

To determine the initial time of setting, an apparatus called a *Vicat Needle* is employed, Fig. 409. A circular mould, 80 mm. diameter and 40 mm. high, resting on a non-porous plate, is completely filled with neat cement paste of normal consistency. The needle is a bar 1 mm. square with a flat end. It is mounted in a frame, so that it can slide vertically up and down, and the depth of penetration is read off on a scale. It is loaded with a weight of 300 grammes. The *initial setting time* is defined as the period elapsing between the time when the water
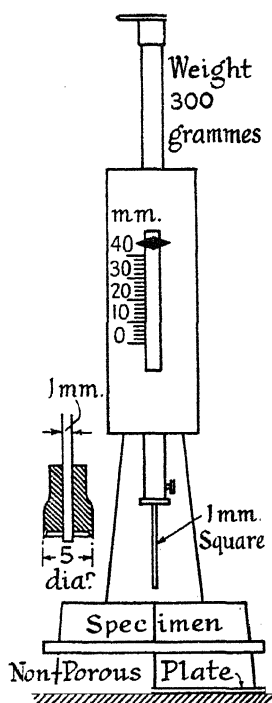
FIG. 409.

was added to the cement, and the time at which the needle ceases completely to pierce the cement in the mould. In making the experiment, the flat end of the needle is gently lowered until it touches the surface of the cement. It is then quickly released and allowed to sink into the cement. The process is repeated until the needle fails completely to pierce the specimen.

The *final setting time* is determined by means of the same apparatus, but a circular cutting edge, 5 mm. diameter, Fig. 409, is attached to the square rod in such a manner that the latter projects 0·5 mm. When, on gently applying the needle to the specimen, the square projection still makes an impression, but the circular cutting edge fails to do so, final set is deemed to have taken place.

For a *normal-setting cement* the initial time of setting should not be less than 30 minutes, and the final setting time not more than 10 hours. For a *quick-setting cement* these periods may be respectively 5 minutes and 30 minutes.

The latter is only used where rapid work is imperative. The slow setting time is a most valuable property of normal Portland cement, for it enables the mixing and putting in place of the concrete to be accomplished before initial set takes place. When once initial set has occurred the concrete must not be disturbed until it has hardened, otherwise serious diminution in its strength will be the result.

In making tests for the times of setting it is important that the standard conditions, percentage of water, temperature of room and of water, be complied with, otherwise these times will be affected. The tests should be conducted in a moist atmosphere.

290. Test for Soundness.— A sound cement is one which does not crack, swell, blow, or otherwise disintegrate during setting and hardening. The test of soundness is that the volume remains constant. To ascertain this the *Le Chatelier* test is used. The apparatus is shown in Fig. 410. A cylindrical brass mould, 30 mm. diameter and 30 mm. long, is slit
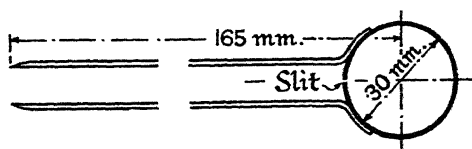
FIG. 410.

longitudinally. Attached, one to each side of the slit, are two pointers 165 mm. long, to the centre of the mould. The ends of these pointers are temporarily fastened together, and the mould is placed on a glass plate and filled with cement paste of normal consistency as in the previous tests. The top is then covered with a second glass plate held down by a weight, and the whole is immersed in water at a temperature of 58° to 64° F. for 24 hours. At the end of this period the fastening between the pointers is removed, and the distance apart of the ends of the pointers accurately measured. The mould is then placed in cold water, which is brought to the boiling point in 25 to 30 minutes and kept boiling for three hours. The reason for boiling the cement is to expedite the test, which

would otherwise have to be continued during the whole normal period of hardening of the cement. At the end of the three hours the mould is removed from the water, allowed to cool, and the distance apart of the ends of the pointers again measured. The difference between the two measurements is an indication of the expansion of the cement and should not exceed 10 mm. If the cement fail to pass this test, the expansion must not exceed 5 mm. in a further test after the cement has been aerated for seven days.

291. Rapid-hardening Cements.—Rapid-hardening cements are so called because mortars and concrete made with them harden and attain their strength far more rapidly than when made with ordinary Portland cement. A rapid-hardening cement must be distinguished from a quick-setting cement, § 289. Notwithstanding its rapid-hardening qualities it is not quick-setting, but gives ample time for mixing and placing in position before initial set takes place. There are two types : rapid-hardening Portland, and aluminous cement.

Rapid-hardening Portland Cement.—This is made from the same materials and by similar processes as ordinary Portland cement. The chemical composition of the finished product is slightly different, in that it has a greater proportion of lime, CaO. The calcination is more prolonged, resulting in a harder clinker. This has to be more finely ground, so that the residue on a 170 × 170 sieve is only from 1 to 2 %. The tensile strength of a 1 cement : 3 sand mixture of this cement, at the end of seven days, can be guaranteed at 600 lb./sq. in. At the end of six months the average strength of this mixture will reach 720 lb./sq. in. in tension, and 7,300 lb./sq. in. in compression. These figures may be considerably exceeded. The initial setting time ranges from 90 to 110 minutes, and the final setting time from $2\frac{1}{2}$ to 3 hours. In the Le Chatelier test for soundness, the expansion usually does not exceed 2 mm. The neat cement is gauged with from 20 to 25 % of water, and the 1 : 3 mixture with from $7\frac{1}{2}$ to 9 %, depending on the make of cement.

Aluminous Cement.—This is manufactured by fusing together in a blast furnace lumps of bauxite (an indurated clay with a very high alumina content) with lime or calcium carbonate in definite proportions. The molten material is cast into pigs, cooled, broken up, and finely ground to make the cement. An analysis of the finished product may contain [44]

	Per cent.
Silica (SiO_2)	5·95
Alumina (Al_2O_3)	38·95
Ferric oxide (Fe_2O_3)	9·86
Ferrous oxide (FeO)	6·25
Titanium dioxide (TiO_2)	2·00
Lime (CaO)	36·25

Considerable variations in the chemical content are possible without affecting the qualities of the cement, but the percentage of Al_2O_3 to that of CaO should not be less than 0·85 nor greater than 1·3.

The cement is almost black in colour, and concrete made with it is darker than ordinary concrete. It is not necessary to grind it so finely

as is the case with a rapid-hardening Portland cement, and the residue left on a 170×170 sieve is about 8 %. The tensile strength of a 1 : 3 mixture, gauged with 8 % of water, should exceed 450 lb./sq. in. in 24 hours, and should reach 600 lb./sq. in. in seven days. This attains, therefore, a greater strength in 24 hours than does ordinary Portland cement mortar in three months, but its strength does not increase with age at the same rate as the latter. The minimum crushing strength of 3-inch cubes of 1 : 3 mixture, tested 24 hours after gauging, is 5,000 lb./sq. in. The initial setting time ranges from $1\frac{1}{2}$ to $4\frac{1}{2}$ hours, and the final setting time from $2\frac{1}{2}$ to $5\frac{1}{2}$ hours. The expansion in the Le Chatelier test is less than 1 mm.

The following Table gives some comparative figures regarding the strength in lb./sq. in. of 1 : 3 mortars made with the three cements :

Tensile Strength. 1 *cement* : 3 *sand*

	24 hours.	7 days.
Ordinary Portland cement	100	400
Rapid-hardening Portland cement	420	650
Aluminous cement	525	640

Compressive Strength. 1 *cement* : 3 *sand*

	24 hours.	7 days.
Ordinary Portland cement	800	5,000
Rapid-hardening Portland cement	3,500	9,000
Aluminous cement	7,000	10,000

It will be observed that not only do the rapid-hardening cements attain their full strength much earlier, but they are intrinsically stronger than the ordinary Portland cement. They are, however, more expensive per ton ; but in making an estimate of relative cost, the saving in time, and re-use of shuttering, which can be struck much earlier in the case of the rapid-hardening cements, must be taken into account. Rapid-hardening cements, particularly aluminous cements, give out much heat during hardening, which enables work to be carried on during frosty weather. Aluminous cement also possesses the advantage that it will resist the action of sea-water and water containing sulphates, which attack Portland cement.

CONCRETE

292. The Material.—Concrete is made by mixing together definite proportions of cement, sand or fine aggregate, and a hard coarse aggregate, and adding water. The cement and sand form a mortar which cements the whole mass together, thus forming an artificial stone possessing considerable crushing resistance, which can be moulded, before it sets, into required shapes.

The materials of which it is made vary widely. To form the mortar, or *matrix* as it is termed, Portland or other cements may be used ; or, for certain classes of work, hydraulic lime. The coarse aggregate may be a hard broken stone, or gravel, when a superior concrete is required ; for less important work broken bricks, hard clinker, or coke breeze may be employed. Concrete made with the latter aggregates will not resist fire.

The two most important kinds of concrete used in ordinary engineering work are : (i) the concrete used in mass constructions, in which the proportion of cement to sand plus aggregate ranges from about 1 : 3 to 1 : 12, a common proportion for ordinary foundation work being 1 : 6. The aggregate is usually limited in size to that which will pass a 2-inch square mesh ; (ii) the concrete used for reinforced-concrete structures, in which for ordinary work a 1 : 2 : 4 mixture is commonly adopted (1 cement, 2 sand, 4 coarse aggregate). The coarse aggregate is limited in size to that which will pass a $\frac{3}{4}$-inch square mesh.

A 1 : 6 concrete must be distinguished from a 1 : 2 : 4 concrete. The proportions are determined by volume, not by weight, and if 2 volumes of sand be mixed with 4 volumes of coarse aggregate, the mixture will only occupy about $4\frac{1}{2}$ volumes, not 6 volumes, for the sand fills the interstices in the aggregate.

The compressive strength of concrete appears to depend on : (a) the nature of its constituents, (b) the proportions, (c) the grading, (d) the water ratio, (e) the manipulation. It will be convenient to consider these factors separately.

293. The Cements.—The relative tensile strengths of ordinary Portland cement, rapid-hardening Portland cement, and aluminous cement have been discussed in § 291. Some figures showing the relative compressive strength of concrete made with these cements are given in § 301. Roughly speaking, at the end of three months, concretes of normal proportions, made with either of the rapid-hardening cements, are at least 25 % stronger than similar concrete made with ordinary Portland cement.

294. The Aggregates.—The fine aggregate should consist of hard clean particles, free from organic matter. A sharp sand, or hard stone screenings, forms a suitable material. The particles should pass a $\frac{3}{16}$-inch mesh.

The coarse aggregate should also be hard and clean, free from clay or organic matter. Hard broken stone—granite, sandstone or limestone ; flint gravel from a pit when free from clay ; shingle from the seashore or a river bed, spoken of as ballast ; all form suitable materials for a strong concrete. Some difference of opinion exists as to whether the rough angular pieces of broken stone make a stronger concrete than the smoother and rounder stones found in the ballast. There appears to be less tendency for the stones to separate out and to form ' pockets ' in the case of the ballast concrete, i.e. the rounded stones pack better and the concrete is more likely to be sound throughout ; but if properly graded and mixed, broken stone concrete has a slightly greater crushing strength.

295. Best Proportions.—Theoretically, it would appear that the minimum amount of fine aggregate is that which would just fill the interstices or *voids* in the coarse aggregate, and the minimum amount of cement is that which is just sufficient to fill the interstices in the fine aggregate, plus the amount required to give all the particles a coating of cement. To determine the percentage of voids, a known volume is filled with the aggregate. Water is added until it just covers the aggregate. The

volume of this water is the volume of the voids. To make a workable concrete, the volume of the fine aggregate must exceed that of the voids in the coarse aggregate by about 5 to 10 % ; and similarly, the volume of the cement must exceed that of the voids in the fine aggregate by about 10 %. The volume of cement necessary decreases with increase in size of the coarse aggregate.

Such a method of determining the proportions of the mixture does not of necessity make the strongest concrete ; much depends on grading the size of the aggregates.

296. Grading.—Professor Duff Abrams [47] has introduced a method of proportioning aggregates based on a *fineness modulus*, by means of which

Sieve. Size.*	Size of Opening. inch.	Medium Sand. ' B.'	Pebbles. ' E.'	Concrete Aggregate ' G ' 25% ' B ' + 75% ' E.'
100	0·0058	91	100	98
50	0·0116	70	100	92
30	0·0232	46	100	86
16	0·0464	24	100	81
8	0·093	10	100	78
4	0·185	0	95	71
⅜ in.	0·375	—	66	49
¾ in.	0·75	—	25	19
1¼ in.	1·50	—	0	0
Fineness Modulus		2·41	6·86	5·74

* Tyler Series.

the gradation of particles producing the strongest, or the most economical concrete for a particular purpose, can be determined. The method can be applied either to the fine or coarse aggregate, or to the combination. The manner in which the fineness modulus is determined will be evident from the Table above which gives some of Professor Abrams' results.

A series of sieves are used, each of which has a width of opening double that of its predecessor. A weighed sample of the aggregate is sifted through each in turn, and the weight of the residue, expressed as a percentage of the weight of the sample, is entered in the Table. The addition of all these percentages divided by 100, gives the fineness modulus.
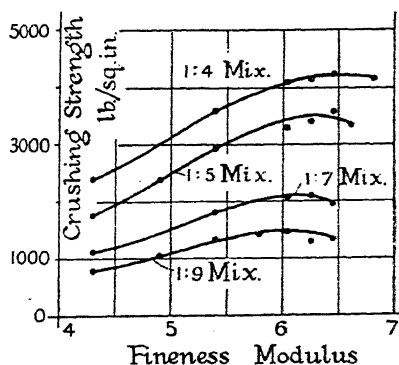
Fig. 411. (Abrams.)

All aggregates graded 0–1¼ in.

Abrams showed that for a given *mix*, i.e. ratio of cement to total aggregate by volume, the compressive strength is the same for all gradings having the same fineness modulus, irrespective of how the size of the particles may vary. Further (see Fig. 411), that for a given mix and different fineness moduli, there is a particular modulus for which the compressive strength is a maximum. Fig. 412 shows the maximum permissible fineness moduli for different mixes and different aggregate ranges. Curve A may be taken as applying to mass concrete, Curve B to reinforced-concrete, Curves C and D apply to mortars. Fig. 412 has reference to sand and pebble aggregates. For crushed stone or slag as coarse aggregate, reduce the fineness moduli by 0·25 ; also, if stone screenings be used for the fine aggregate, reduce the values by 0·25. Sand or screenings used for the fine aggregate must not have a higher fineness modulus than that permitted for mortars of the same mix.

Having found the fineness modulus m_1 for the fine aggregate available, and that for the coarse aggregate, m_2, as in the Table, p. 591, and decided on the requisite modulus m for the combined aggregate, having regard to the strength required and the mix, Figs. 411 and 412, the necessary proportion of fine to combined aggregate can be found from the formula

$$\frac{\text{vol. of fine aggregate}}{\text{vol. of combined aggregate}} \quad \frac{m_2 - m}{m_2 - m_1}$$

Thus, in the Table on p. 591, to obtain a combined aggregate ' G ' ($m = 5\cdot74$) from the sand ' B ' ($m_1 = 2\cdot41$), and the coarse aggregate ' E ' ($m_2 = 6\cdot86$), the ratio in question must be

$$\frac{6\cdot86 - 5\cdot74}{6\cdot86 - 2\cdot41} = \frac{1\cdot12}{4\cdot45} = \frac{1}{4}$$

and 25 % ' B ' by volume plus 75 % ' E ' must be used.

297. Water Ratio Theory.—Exhaustive experiments by Abrams [47] have shown that, for given materials and conditions, the strength of the concrete is determined by the ratio of the volume of the mixing water to the volume of the cement, called the *water ratio* or *water-cement ratio*, provided that a workable mixture is obtained, irrespective of the volumes of the other materials so long as they are suitable and clean. A certain quantity of water is required to hydrate the cement. This quantity
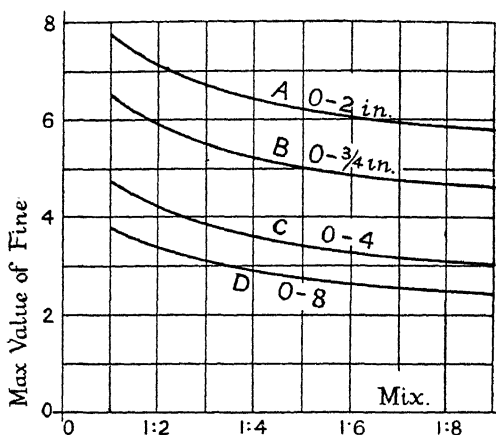
produces the maximum adhesive power, more water reduces the adhesive power and weakens the concrete, hence the water ratio should be a minimum, Fig. 413. A dry mix, more cement, coarser aggregate, all
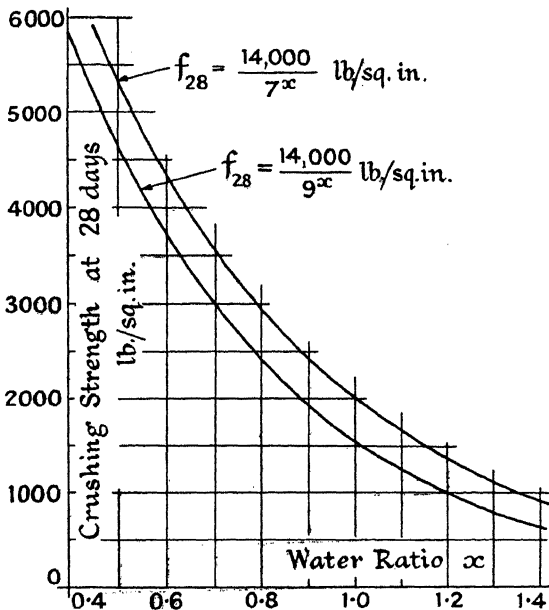
FIG. 413.

imply a smaller water ratio and increase in the strength of the concrete. For normal concrete, made with American Portland cement (1918), under average conditions, the compressive strength of $12'' \times 6''$ cylindrical specimens at 28 days was represented by the formula

$$f_{28} = \frac{14,000}{7^x} \text{ lb./sq. in.} \quad (1)$$

where x is the water ratio. When the operations are not under rigid control, the denominator should be changed to 9^x, Fig. 413.

It will be evident that, subject to complete hydration and the production of a workable mixture, the less water used the better. As a practical means of determining the minimum amount of water necessary to produce a workable mixture, the *slump test* has been devised. The apparatus consists of a hollow cone of the dimensions shown in Fig. 414. This is placed on a non-absorbent surface and filled with the concrete in 3-inch layers, each of which is rodded 25 times with a pointed $\frac{5}{8}$-inch rod, and
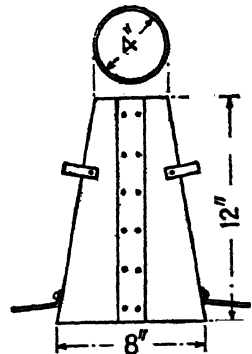
FIG. 414.

2 Q

finally struck off level with the top. Three minutes later the cone is lifted vertically and the moulded concrete is allowed to subside until quiescent. The height of the specimen is then measured ; the amount by which it is less than 12 inches is called the *slump*. A slump of $\frac{1}{2}$ to 1 inch indicates that the minimum quantity of water has just been exceeded. Increased slumps are necessary to ensure workability. In mass concrete the slump should not exceed 2 inches ; in reinforced-concrete work it should not exceed 3 inches in heavy sections, nor 6 inches in thin confined sections.

Typical graphs showing the relationship between the different factors under discussion are plotted in Fig. 415. These correspond to the lower
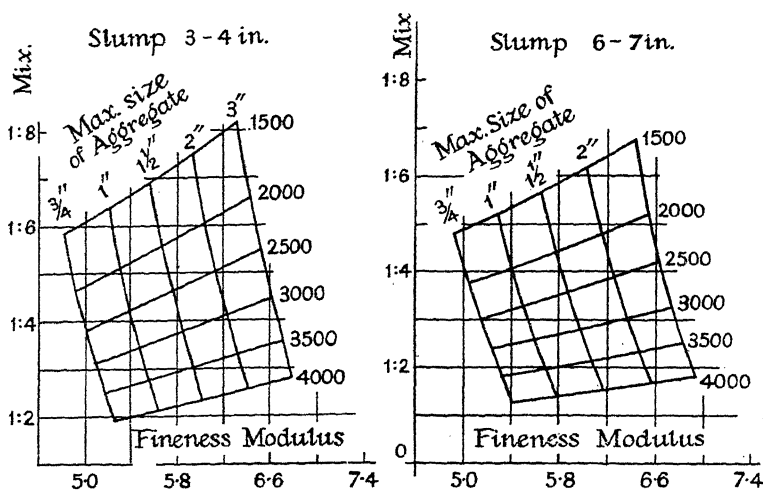
FIG. 415 (Abrams).

curve in Fig. 398; they give the necessary mix for a required strength and slump.*

If eq. (1) be written in the form $f = A/B^x$

$$\log f_{28} = \log A - x \log B \quad . \qquad . \qquad . \qquad . \qquad (2)$$

Plotting the values of f_{28} to a logarithmic scale, the curves become straight lines, Fig. 416, all of which pass through the point A = 14,000 lb./sq. in., which represents the theoretical value of f_{28} when $x = 0$. B, which depends on the quality of the cement, is indicated by the slope of the lines, and by suitably choosing B, the diagram will give the strength of the concrete at any time up to say 3 months. Abrams'† values for B are given in the Table, p. 595.

* For corresponding experiments on British Portland and rapid-hardening Portland cements, and the application of these theories to practice, see Wynn and Andrews.[53] Professor Abrams' theory does not apply to aluminous cement, for which a small excess of water is not disadvantageous.

† See Abrams in the discussion on ' Some Long-time Tests of Concrete,' M. O. Withey, *Jour. Amer. Conc. Inst.*, 1931.

VALUES OF B.

	8 hrs.	1 day.	3 days.	7 days.	28 days.	3 months.
High Early Strength P.C. Concrete .	58·4	9·5	5·9	4·7	3·7	3·4
Ordinary P.C. Concrete	—	27·7	11·0	7·5	4·9	3·9

These values have reference to modern American Portland cement concretes.
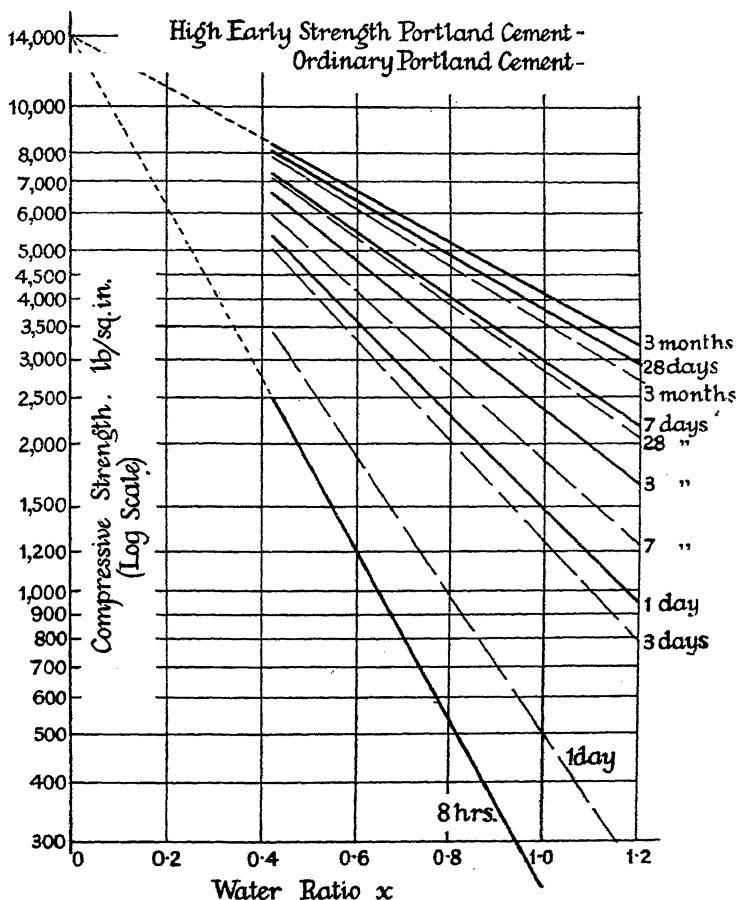
FIG. 416 (Abrams).

In determining the water ratio, any water absorbed by the aggregate should be deducted from the total quantity.

Later experiment has shown that the compressive strength for a given water ratio decreases with fall in temperature.

The correct water ratio for a particular purpose is not the same for

all cements or for all aggregates. Experiments with the availabl₁ materials are necessary.

298. Manipulation.—Given the proper proportions of materials an₍ water, the strength of the concrete will depend very largely on th₁ workmanship. Careful measurement of the constituents is necessary They must be thoroughly mixed so as to produce a homogeneous mass For small quantities hand mixing is possible, for large quantities machin₁ mixing is universal. The concrete must be carefully deposited in plac₁ in relatively thin layers before it commences to set ; it should be carefull₃ rodded or tamped to consolidate it. Experiments on 12 × 6 incl cylindrical specimens have shown that 20 to 30 strokes with a ⅝-inch roc pushed into the concrete, or a similar number of blows with a 2-lb tamper, will increase its compressive strength from 2,200 to 2,800 lb./sq in. Very dense strong concrete can be made by vibrating the forms b₃ means of a pneumatic hammer. The work of concreting should be carried on continuously. When it is necessary to bond new work on tc old, the surface of the latter should be carefully cleaned and roughened thoroughly wetted, and coated with 1 : 1 cement mortar. Portland cement concrete should not be deposited during freezing weather.

It may be pointed out that compressive tests on concrete, made undeɪ practical working conditions, show that a reduction in strength of the order of 20 %, compared with that made in a laboratory, is not uncom- mon * (cf. Fig. 413).

299. Curing.—To obtain a strong durable concrete it is necessary to keep the freshly deposited material moist and at a suitable temperature for at least 7 days, to permit it to harden. A low temperature during curing reduces the strength.

300. Tests on Concrete.—The commonest test on concrete is the crushing test. Shearing, tensile, and bending tests are sometimes made, and a determination of the elastic constants is of importance in con- nection with reinforced-concrete.

301. Crushing Tests.—The test-piece usually employed in this country is a cube with from 6 to 10 inch sides. In America, for aggregates which will pass a 2-inch mesh, a cylindrical test-piece 6 inches diameter and 12 inches long is preferred, for the reasons discussed in § 274. The crushing strength for a 6-inch cube will be from 15 to 20 % greater than for a 6 × 12 inch cylinder. The test is made in a similar manner to that used for stone specimens, § 274, and the fracture is of the same type. Some values for the crushing strength (laboratory tests) of a 1 : 2 : 4 concrete, made (a) with ordinary Portland cement, (b) with rapid-hardening Portland cement, and (c) with aluminous cement, are as follows :

	24 hours.	7 days.	28 days.
Ordinary Portland Cement, 6 % water	—	2,860	4,440
Rapid-hardening Portland Cement, 6 % water	1,750	5,360	6,810
Aluminous Cement, 7 % water	6,200	8,100	8,800

All in lb./sq. in.

* See for example *Proc. Amer. Soc. C.E.*, January 1925.

The aggregate used was ballast. The strength of concrete on a job may fall well below these figures.

In making a test cube, the mould, which should be of metal with plane parallel ends, is placed on a glass plate and the concrete is deposited in 2-inch layers, each layer being rodded 25 times with a pointed ½-inch rod. The top should be struck off level, and after two hours, made perfectly flat and level by means of a thin layer of neat cement mortar. After 24 hours the cubes should be removed from the moulds and placed in water at from 58° to 64° F., or buried in damp sand, until required for the test. In practical work, the concrete for a test cube should be taken from a form immediately after depositing, or from the mix immediately before depositing.

Fig. 417 shows the variation in crushing strength with age in laboratory specimens with different kinds of cement.
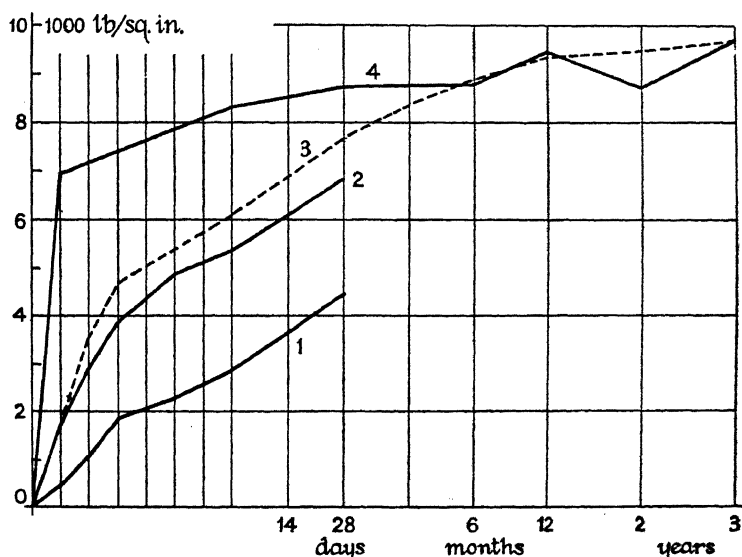
FIG. 417.

1. Ordinary Portland Cement Concrete. Mix 1 : 2 : 4, 6 % water, 6 in. cubes.
2. Rapid-hardening Portland Cement Concrete. Mix 1 : 2 : 4, 6 % water, 6 in. cubes.
3. Early tests on Ciment Fondu (Ponts et Chaussées Lab., Paris, 1916). Mix 400 kg. cement, 300 litres sand, 900 litres gravel, 7·9 % water, 200 mm. cubes, stored in air.
4. High Aluminous Cement Concrete. Mix 1 : 2 : 4, 6 in. cubes.

302. Elastic Constants.—Fig. 418 (Davis and Troxell[68]) represents a typical compressive stress-strain diagram for a concrete specimen at the age of three months, and also the corresponding lateral expansion diagram. The specimen was a 6-inch cylinder, 12 inches high, capped

with neat cement, and bedded on a thin layer of plaster of Paris. The concrete was graded to approach maximum density. The secant modulus E was found to increase with the age of the specimen, rapidly at first and then slower, but decreased as the stress increased. The value of E was higher for richer mixes and denser aggregates. There was no direct relationship between E and the compressive stress which could be generally applied; but with constant conditions, the higher the ultimate strength, the greater the secant modulus at a given stress. At 800 lb./sq. in. the values obtained for this modulus were :

FIG. 418.

	1 : 3½ mix.	1 : 4½ mix (by weight).
At 200 days	4,400,000	4,800,000
1000 days	5,200,000	5,100,000 lb./sq. in.
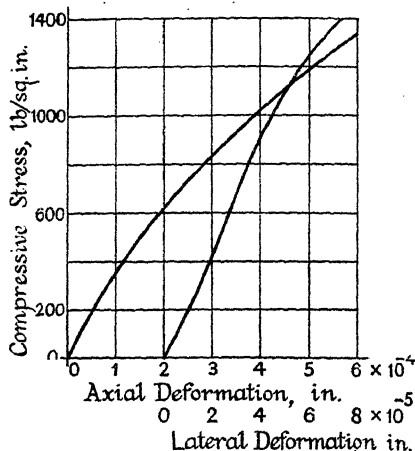
Defining Poisson's ratio as the ratio of unit lateral extension to unit axial contraction immediately on application of the load, the values obtained at a stress of 800 lb./sq. in. were :

1 month.	6 months.	1 year and beyond.
0·15 to 0·17	0·19	0·20

Poisson's ratio increases with age at a gradually decreasing rate. It does not vary materially with the richness of the mix, or kind of aggregate.

From experiments on 6 × 12 inch cylindrical specimens at 28 days, of sand and pebble concrete proportioned by sieve analysis, for a variety of mixes ranging from 1 : 7 to 1 : 3, Stanton Walker [64] gives for the average value of the secant modulus at 25 % of the ultimate strength :

Compressive Strength at 28 days.	Modulus.
1,000	$2 \cdot 38 \times 10^6$
1,500	2·79
2,000	3·21
3,000	3·87
4,000	4·36
5,000	4·86

As average values, he suggests for the initial tangent modulus $E = 33,000 \, (f_{28})^{\frac{1}{2}}$; and at 25% of the compressive strength $E = 66,000 \, (f_{28})^{\frac{1}{2}}$.

Professor Lea [66] suggests the formula $E = 1 \cdot 8 + 7 \cdot 5(1 - x)$ million lb./sq. in. as a mean value for E at 5–600 lb./sq. in. ; x is the water-cement ratio. The value of E was found to depend more upon this ratio than on the mix or materials.

303. Shrinkage.—As in the case of many other substances, the volume and length of a concrete specimen increase when it absorbs moisture and diminish as the moisture dries out. Such changes take place for at least 20 years. From the moment of setting, a concrete structure drying in air will shrink, at first rapidly, and then more and more slowly. Such shrinking may, in certain circumstances, produce cracking and severe internal stresses in the structure. Similar shrinkage phenomena take place in neat cement and mortar specimens, and in the aggregate. The magnitude of the volumetric changes depends on the materials, the mix, the manipulation, and apparently on any influence which affects the porosity of the concrete. It also depends on the size and shape of the specimen, and whether or not it is reinforced. It is greater in rich mixes than in lean ones, and less when the aggregate is of quartz or granite than when it is of gravel or sandstone. For $3'' \times 3'' \times 40''$ specimens of a $1 . 2 : 3$ mix, water-cement ratio $0 \cdot 9$, fineness modulus $5 \cdot 58$, R. E. Davis [78] gives the following figures for the percentage change in volume in three months :

Aggregate.	Contraction in Air.	Expansion in Water.
Gravel . . .	0·079	0·0074
Sandstone . .	0·075	0·0055
Limestone . .	0·039	0·0050
Granite . . .	0·037	0·0131
Quartz . . .	0·036	0·0094

The effect of reinforcement is to reduce the shrinkage. According to Matsumoto [76] the shrinkage stress in the steel of a reinforced-concrete specimen may reach the working stress if the percentage of steel is less than $1 \cdot 5$; and the ultimate strength of a $1 : 2 : 4$ concrete may be exceeded if the percentage of steel is greater than $1 \cdot 5$.

304. Plastic Flow or Creep.—As will be seen from Fig. 418, the elasticity of concrete is imperfect, and *plastic flow* or *creep* takes place under sustained loads (cf. Fig. 274, Vol. I). As in mild steel also, partial recovery takes place on removal of the load, Fig. 304, Vol. I. The rate of creep depends on the mix, the materials, the age, the magnitude of the stress, and the reinforcement if any ; it decreases with time, but continues for at least 2 years. The rate of creep is greater the leaner the mix, and is less the higher the fineness modulus of the aggregate, i.e. for the denser concretes. For a $1 : 7$ mix, fineness modulus $3 \cdot 62$, the total creep per 100 ft. in 5 months exceeded $\frac{1}{2}$ inch, but for a $1 : 4$ mix it approximated to $\frac{1}{8}$ inch. The rate of creep increases with the water-cement ratio. It is least for aggregates of granite and quartz, and greatest for gravel and sandstone. At 800 lb./sq. in., the total creep per 100 feet in 2 years ranged from $\frac{1}{2}$ inch in limestone concrete to $1\frac{1}{2}$ inches in metamorphic sandstone. It is greater for concrete stored in air than in water. Longitudinal reinforcement~~ considers reduces~~ reduces both shrinkage and creep in

specimens stored in air; but the combined effect of shrinkage and creep, in a column supporting a long sustained load, is to transfer the stress from the concrete to the steel until the yield point of the steel is reached. The effects of shrinkage and creep in producing shrinkage stresses are opposed to one another, and the stress developed depends on the relative rates of shrinkage and creep; see Refs. Nos. 79 and 80, Bib.

305. Temperature Effects.—The coefficient of linear expansion for Portland cement concrete is usually taken as $\alpha = 0\cdot0000055$ per degree Fahrenheit. It varies [77] with the aggregate used, averaging about $0\cdot0000065$ for sandstone; $0\cdot0000060$ for gravel; and $0\cdot0000038$ for limestone concrete; increasing with the richness of the mix, but is slightly less for wet than for dry mixes. The average value for concrete made with high aluminous cement is about $0\cdot0000052$; the variation with mix and range of temperature is not large.

BIBLIOGRAPHY

Timber

1. BAUSCHINGER. Versuche über die Festigkeit von Bauhölzen. *Deu. Industrie Zeit.*, Oct. 29, 1879, p. 445; see also *Mitt. a.d. Mech.-Tech. Lab.*, München, 1883, 1887.
2. WATERTOWN ARSENAL. Reports of the Tests of Metals. (Many Tests.)
3. WARREN. *The Strength and Elasticity of Australian Timbers*, Sydney, 1892; *N.S. Wales Hardwood Timbers*, Sydney, 1911; *Timber Physics*, Sydney, 1915.
4. U.S. FOREST PRODUCTS LAB. *Bulletins* : No. 10, Physical Properties; Nos. 70, 80, 88, 108, 112, and *Circ.* Nos. 15, 213, Mechanical Properties; *Bull.* Nos. 78, 107, 118, 126, Preservation of Timber.
5. RECORD. *Identification of the Timbers of Temperate North America.* New York, 1934.
6. WEISS. *The Preservation of Structural Timber.* New York, 2nd ed., 1916.
7. HORNE. Strength and other Properties of Scots Pine. *Proc. Inst. C.E.*, vol. ccix, 1919–20, p. 375; also *Engg.*, Sept. 9, 1921, p. 387.
8. ROBINSON. The Microscopical Features of Mechanical Strains in Timber. *Phil. Trans. Roy. Soc.* B, vol. 210, 1920, p. 49.
9. JOHNSON. *Materials of Construction*, New York, 6th ed., 1925, chaps. iv, v and vi.
10. GARRATT. The Mechanical Properties of Wood. New York, 1931.
11. BRITISH FORESTS PRODUCTS RESEARCH. Spec. Rpt. No. 1, *Air Seasoning and Conditioning*, see *Engg.*, cxxiv, p. 774; Nos. 2 and 3, *Kilns*, *Engg.*, cxxv, p. 348; *Laboratory*, *Engg.*, cxxviii, p. 487; *Timber Mechanics*, *ibid.*, p. 601; *Tests Home Grown Timbers*, see Bull. Nos. 3, 7, 10 and 12, and *Engg.*, cxxxix, p. 667; *Tests Scots Pine*, Bull. No. 15.

Timber Columns

12. BAUSCHINGER. Ref. No. 1.
13. BURR. *The Elasticity and Resistance of Materials.* New York, 1883 (Shaler Smith's exps.).
14. WATERTOWN ARSENAL. *Reports of the Tests of Metals,* 1883, 1896–7–8, 1901–5–8 (Year of Publication).
15. LANZA. *Applied Mechanics.* New York, 1st ed., 1885, p. 651.

16. TETMAJER. *Die Gesetze der Knickung*, etc. Zürich, 1896; repub. Leipzig, 1903.
17. OSTENFELD. Eccentrically Loaded Columns. *Ingeniorvidenskabelige Skrifter*. Copenhagen, No. 19, 1929; No. 26, 1931.

Timber Construction

18. LANG. *Das Holz als Baustoff*. Berlin, 1915.
19. JACOBY. Structural Details, or Elements of Design in Heavy Framing. New York, 1921.
20. BERKENBLIT. Behaviour of Timber Structural Framework under Stress. *Eng. News.-Rcd.*, June 6, 1929, p. 898.
21. SCHAECHTERLE. Holz als Baukonstruktionsmittel. *Zeit. Ver. deu. Ing.*, Dec. 14, 1929, p. 1771.
22. For TIMBER JOINTS see GRAF, *Der Bauingenieur*, 1922, pp. 100, 141; LEWE, *Der Eisenbau*, 1922, p. 129; STAMER, *Zeit. Ver. deu. Ing.*, Apl. 27, 1929, p. 584.
23. JACOBY AND DAVIS. *Timber Design and Construction*. New York, 1930.

Stone

24. BAUSCHINGER. Untersuchungen über die Elasticität der wichtigsten natürlichen Bausteine in Bayern. *Mitt. a.d. Mech.-Tech. Lab. München*, Heft X, 1884.
25. HUDSON BEARE. Building-Stones of Great Britain, their Crushing-Strength and other Properties. *Proc. Inst. C.E.*, vol. cvii, 1891-2, p. 341.
26. WATERTOWN ARSENAL. Reports of the Tests of Metals, 1895, 1896 et seq. (Year of Publication).
27. BALDWIN-WISEMAN AND GRIFFITH. The Physical Properties of Building-Material. *Proc. Inst. C.E.*, vol. clxxix, 1909-10, p. 290.
28. HOWE. *Geology of Building Stones*. London, 1910 (Chap. on Testing).
29. —— *Stones and Quarries*. London, 1920.
30. HIRSCHWALD. *Handbuch der bautechnischen Gesteinsprüfung*. Berlin 1912.
31. JOHNSON. Ref. No. 9, chap. vii.
32. MORTON. The Composition and Texture of Sandstones and Limestones in Relation to Strength and Durability. *Rpt. Brit. Assoc.* 1926; see *Engg.*, Sept. 24, 1926, p. 401.
33. RIES AND WATSON. *Engineering Geology*. New York, 4th ed., 1931 (Chap. on Building Stones).
34. GILCHRIST AND EVANS. Elasticity and Hysteresis of Rocks and Artificial Stones. *Engg.*, Oct. 28, 1932, p. 519.
35. SCHAFFER. The Weathering of Natural Building Stones. *Spec. Rpt.* No. 18, *Building Res. Stn.*, 1932; see *Engg.*, Dec. 30, 1932, p. 761.

For Bricks and Brickwork see Chap. XIX.

Cements

36. BUTLER. *Portland Cement, Its Manufacture, Testing and Use*. London, 1913.
37. BLOUNT. *Cement*. London, 1920.
38. SEARLE. *Cement, Concrete and Bricks*. London, 2nd ed., 1926.
39. ECKEL. *Cements, Limes and Plasters*. New York, 1928.
40. LEA AND DESCH. *Chemistry of Cement and Concrete*. London, 1935.
41. INST. STRUCTURAL ENGS. Report of Committee on Aluminous, Rapid-hardening Portland, and other Cements. June 1926.
42. —— Proposed Specifications: R. H. Portland. *The Struct. Engr.* No. 11, 1928; High Aluminous, Oct. 1930.

43. HIGH ALUMINOUS CEMENTS. *Engg.*, Nov. 16, 1923, p. 631 (Ponts et Chaussées exps.).
44. LAFARGE Co. *The Characteristics of Ciment Fondu.* London, 1932.
45. DAVIS. *Portland Cement.* London, 1934.
46. B.S.I. British Standard Specification for Portland Cement No. 12, 1931.

Concrete

47. ABRAMS. Design of Concrete Mixtures. Bull. No. 1, *Struc. Mat. Res. Lab., Lewis Inst., Chicago,* 1918 (revised 1925) ; *Eng. News.-Rcd.,* May 2, 1918, p. 873 ; *Proc. Amer. Conc. Inst.,* 1931, p. 1330.
48. TALBOT AND RICHART. The Strength of Concrete, its Relation to the Cement, Aggregates, and Water. *Univ. Illinois Eng. Exp. Stn.* Bull. No. 137, 1923 ; see also *Proc. Amer. Soc. Test. Mat.,* vol. xxi, 1921, p. 940.
49. DAVEY. The Consistence of Cement Pastes, Mortars, and Concrete. Tech. Pap. No. 5, *Building Res. Stn.,* 1926.
50. HATT. Researches in Concrete. *Perdue Univ. Eng. Exp. Stn.* Bull. No. 24, 1925 (Review of Concrete Research, with extensive Bib.).
51. TAYLOR, THOMPSON AND SMULSKI. *Concrete, Plain and Reinforced.* New York, 4th ed., 1925.
52. LORD. Notes on Concrete—Wacker Drive, Chicago. *Proc. Amer. Conc. Inst.,* 1927.
53. WYNN AND ANDREWS. Modern Methods of Concrete Making. London, 2nd ed., 1928.
54. GOLDBECK. Workability. *Proc. Amer. Conc. Inst.,* 1928.
55. BAUER. *Plain Concrete.* New York, 1928.
56. MCMILLAN. *Basic Principles of Concrete Making.* New York, 1929.
57. SUENSON. Strength and Density of Concrete as Affected by the Water-Cement Ratio. *Eng. Ab. I.C.E.,* 1929, No. 40 : 28.
58. GONNERMAN. A Study of Methods of Curing Concrete. *Proc. Amer. Conc. Inst.,* vol. xxvi, 1930, p. 358.
59. WALKER. Effect of Characteristics of Coarse Aggregate on the Quality of Concrete. Bull. No. 5, *Nat. Sand and Gravel Assoc. Inc. U.S.A.* ; see also Rpt. of Committee E. 5, *Proc. Amer. Conc. Inst.,* 1927.
60. SYMPOSIUM ON MINERAL AGGREGATES. *Amer. Soc. Test. Mat.* 1929 ; see *Engg.,* Dec. 19, 1930, p. 764.
61. SINGLETON GREEN. *Concrete Engineering* : vol. i, *Practical Concrete,* London, 1933 ; vol. ii, *Properties of Concrete,* London, 1935.

Elastic Constants and Properties of Concrete

62. BACH. For summary of early researches (1895 et seq.) see *Elastizität und Festigkeit,* § 9 ; also Versuche über die Elastizität und Druck-festigkeit von Körpern aus Zement, Zementmörtel, und Beton. *Zeit. Ver. deu. Ing.,* Nov. 28, 1926, p. 1382.
63. TALBOT. Tests of Reinforced-Concrete Beams. *Univ. Illinois Eng. Exp. Stn.* Bull. No. 14, 1907.
64. WALKER. Modulus of Elasticity of Concrete. *Proc. Amer. Soc. Test. Mat.* 1919, Pt. II, p. 510.
65. LEA. The Modulus of Elasticity of Concrete. *Proc. Conc. Inst.,* Apl. 1921.
66. —— Fundamental Assumptions in R.-C. Design. *Select. Eng. Paper I.C.E.* No. 164, 1934.
67. HATT AND MILLS. Physical and Mechanical Properties of Portland Cements and Concretes. *Perdue Univ. Eng. Exp. Stn.* Bull. No. 34, 1928.
68. DAVIS AND TROXELL. Modulus of Elasticity and Poisson's Ratio for Concrete, etc. *Proc. Amer. Soc. Test. Mat.* 1929, Pt. II, p. 678.

69. JOHNSON. Concrete in Tension. *Public Roads*, Feb. 1929.
70. NOBLE. The Effect of Aggregate and other Variables on the Elastic Properties of Concrete. *Kansas St. Coll. Eng. Exp. Stn.* Bull. No. 29, 1932.
71. GILCHRIST, EVANS AND WHITAKER. Stress-Strain Relations in Concrete. Paper No. 4852, *Inst. C.E.*, 1932.
72. SHEAR AND TORSIONAL STRENGTH. MÖRSCH, *Eisenbetonbau*, 3rd ed., 1908, chap. iii ; TALBOT, Bull. No. 8, *Univ. Illinois Eng. Exp. Stn.*, 1906.
73. FATIGUE. VAN ORNUM, *Trans. Amer. Soc. C.E.*, vol. li, 1903, p. 443 ; vol. lviii, 1907, p. 294 ; also 1924, p. 1196 ; CLEMMER, *Proc. Amer. Soc. Test. Mat.* 1922, Pt. II, p. 408.
74. FIELD BENDING TESTS. CLEMMER AND BURGGRAF, ALSO WEIPKING, *Proc. Amer. Conc. Inst.*, vol. xxiv, 1928 ; REAGEL AND WILLIS, *Public Roads*, Apl. 1931 ; KELLERMANN, *Public Roads*, Jan. 1933.

Shrinkage, Creep and Plastic Flow

75. SHRINKAGE. *Proc. Amer. Conc. Inst.* : GOLDBERG AND SMITH, 1916, p. 324 ; LORD, 1917, p. 45 ; HOLLISTER, 1919, p. 127 ; LAGAARD, 1921, p. 172.
76. MATSUMOTO. Study of the Effect of Moisture Content upon Expansion and Contraction of Plain and Reinforced Concrete. *Univ. Illinois, Eng. Exp. Stn.* Bull. No. 126, 1921.
77. DAVIS AND TROXELL. Volume Changes in Portland Cement Mortars and Concretes. *Proc. Amer. Conc. Inst.*, vol. xxv, 1929.
78. DAVIS, R. E. A Summary of the Results of Investigations having to do with Volumetric Changes in Cements, Mortars, and Concretes, due to causes other than Stress. *Proc. Amer. Conc. Inst.*, vol. xxvi, 1930, p. 407.
79. GLANVILLE. Shrinkage Stresses, Tech. Paper No. 11, 1930 ; Creep or Flow of Concrete under Load, Tech. Paper No. 12, 1930. *Building Res. Stn.*
80. DAVIS, R. E. AND H. E. Flow of Concrete under the Action of Sustained Loads. *Proc. Amer. Conc. Inst.*, vol. xxvii, 1931, pp. 677, 761.
81. SHANK. The Mechanics of Plastic Flow of Concrete. *Proc. Amer. Conc. Inst.*, vol. xxxii, 1935, p. 149.
82. REPORT OF COMMITTEE on the Effect of Plastic Flow and Volume Changes on Design. *Proc. Amer. Conc. Inst.*, vol. xxxiii, 1936, p. 123.

CHAPTER XVII

REINFORCED-CONCRETE

306. The Material.—The resistance to tension and to shear of ordinary plain concrete is small, hence the material cannot be employed in situations where these stresses are of considerable magnitude. , By embedding steel bars in the concrete, so arranged that they carry the tensile and shear stresses which the concrete by itself is unable to resist, a very valuable constructional material is obtained, with a wide field of application. This is called *reinforced-concrete*. Three circumstances render such a combination useful for practical work : (i) the concrete contracts slightly while setting in air, and tends to grip the steel, causing the two to adhere ; the concrete is able, therefore, to transmit to the steel those stresses which it cannot carry ; (ii) the linear coefficient of expansion by heat of concrete and steel are very nearly equal, hence no serious stresses due to variations in temperature occur ; (iii) the coating of cement protects the steel and tends to preserve it from corrosion.

307. Advantages and Disadvantages of Reinforced-Concrete.—The advantages are :

> The materials are easily obtained. It is easy to make. It is very durable. The cost of maintenance is practically nil. No painting is required. It is impermeable to moisture, but special precautions are necessary to resist a head of water.
> Its monolithic character gives great rigidity.
> Its fire-resisting properties are good, and it is a poor conductor of heat.

Some of the disadvantages are :

> Its own weight is a considerable percentage of the load to be carried and must always be taken into account in design. Reinforced-concrete construction is heavier than steel construction (but lighter than mass construction in stone or plain concrete).
> A considerable quantity of timber is required for the forms and false-work necessary during erection.

308. Materials and Manufacture.—The concrete used for reinforced work should be of a high quality, carefully prepared from clean and good materials. Ordinary Portland or a rapid-hardening cement may be used. The coarse aggregate should pass a $\frac{3}{4}$-inch mesh and be retained on a $\frac{3}{16}$-inch mesh. The fine aggregate should pass a $\frac{3}{16}$-inch mesh. The aggregate should be well graded, hard and non-porous, and for preference,

proportioned by the methods described in § 296. It is common practice for ordinary work, however, to use a 1 : 2 : 4 mix (1 of cement, 2 of sand, and 4 of coarse aggregate, by volume). The mixing is done in a concrete-mixer. A moderately wet mix is necessary for reinforced-concrete work in order to get the concrete between the reinforcement and into the small spaces to be filled. A slump, § 297, of 5 to 6 inches is permitted. The concrete must be deposited and well 'rodded' in position before setting commences, otherwise the quality of the concrete will be adversely affected. Test cubes should be made at intervals to check the strength of the concrete. At joints between old and new work, the old work should be cleaned, roughened, thoroughly wetted, and coated with 1 : 1 cement mortar before the new concrete is deposited.

Forms.—The forms or moulds are made of timber (sometimes of metal) of a size and shape suitable for the finished work. They must be of sufficient strength and rigidity to support the wet material and allow it to be properly tamped, and so constructed that they may be easily removed when the concrete has hardened. A typical arrangement of formwork for a slab and beam floor is shown in Fig. 419. The interior of the forms must be oiled or soaped to prevent the concrete adhering to the wood. Care must be taken that the reinforcement is not pushed out of position while the concrete is being placed. Small

FIG. 419.

blocks of concrete called bar spacers are employed to hold the bars in place and at the correct distance above the forms.
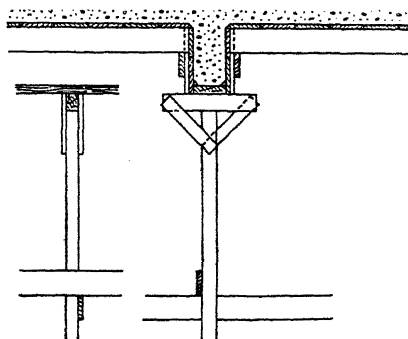
The Reinforcement.—Round bars of mild steel, of the ordinary quality used in structural work and complying with the British Standard Specification, are commonly used for reinforcement; but hard-drawn steel wire and high yield-point steels are also employed. The main longitudinal members in tension should not be less than $\frac{3}{8}$ inch diameter, and the main longitudinals in columns should not be less than $\frac{1}{2}$ inch diameter. No bar should exceed 2 inches in diameter. All bars should be carefully cleaned of rust, loose scale, oil, etc., before being used. Unless otherwise effectively secured (see *Anchorage*, § 317), the ends of all tension and shear members should be provided with a hooked end, (i) Fig. 420. If a bar be hooked tightly over a main reinforcing bar running transversely to it, (ii), it may be regarded as securely anchored. An alternative method of anchoring the end is shown at (iii) Fig. 420. Square bars and special shapes for reinforcement have been extensively employed. These include various patterns of bars with notches and

projections intended to increase the bond between the concrete and the steel. Such material is usually strain-hardened during the process of notching. Wire meshes are largely used for floor slabs, reinforced-concrete roads, and in other positions where it is convenient to introduce the reinforcement in sheets instead of single bars.

Cover and Arrangement of Bars.—The *cover* is the thickness of concrete outside the reinforcement, (iv) Fig. 420. In interior beams and columns this should not be less than 1 inch, and not less than the diameter of the longitudinal bar covered. In slabs and walls, not less than ½ inch anywhere, and not less than the diameter of bar covered. The end cover outside a hook, (i) Fig. 420, should not be less than 2 inches, nor less than twice the diameter of the bar. The space between two bars should not be less than 1 inch (size of coarse aggregate plus ¼ inch), nor less than

FIG. 420.

the diameter of the bars, and the minimum space between two tiers of bars should be ½ inch. These minimum spaces may be increased with advantage. Splices in mild steel tensile reinforcement should be overlapped a distance $l = \dfrac{\phi}{4} f_t/f_s'$, where ϕ is the diameter of the bar, f_t the tensile stress therein, and f_s' the permitted bond stress.

309. Working Stresses.—It is now becoming customary to divide concrete into grades, depending on the degree of control exercised on the works. In the *ordinary grade*, no rigid control or field tests are called for. In *high grade* concrete, effective field control, field tests for strength, and daily slump tests are required. In special cases where, in addition, the water content is rigidly controlled, and the aggregate is graded, certain specifications propose to base the working stresses on the strength obtained in the preliminary tests, subject to specified limitations.

The permitted working stresses in each grade are usually based on the minimum compressive strengths, expected or ascertained, at 28 days.

ORDINARY GRADE. Expected ultimate strength at 28 days in field tests :

1915 *L.C.C. Rules.* $f = 2,800 - 200V$ lb./sq. in., where V is the added volume of the aggregates, measured separately, per volume of cement.

1934 *Proposed British Code of Practice.* $f = 3,600 - 225V$ lb./sq. in. approx.

The Table on p. 608 gives the allowed working stresses in ordinary grade 1 : 2 : 4 concrete according to different authorities.

HIGH GRADE. Ultimate strength at 28 days, in field tests : 1934 *Proposed British Code of Practice*. $f = 4,650 - 300V$ lb./sq. in. approx.

The following rules are laid down by the *Ministry of Transport* (1931) for road bridges :

Mix. lb. : cu. ft. : cu. ft.	Working Stress f_c lb./sq. in.	Modular Ratio. m	Crushing Strength of 6 in. cubes.	
			Normal Test.* lb./sq. in.	Additional Test.† lb./sq. in.
A : 2 : 4	5A + 300	—	15A + 900	10A + 600
90 : 2 : 4	750	15	2,250	1,500
120 : 2 : 4	900	15	2,700	1,800
150 : 2 : 4	1,050	12	3,150	2,100
180 : 2 : 4	1,200	10	3,600	2,400

* At 28 days, ordinary Portland cement ; at 7 days, rapid-hardening Portland cement.

† At 7 days, ordinary Portland cement ; at 3 days, rapid-hardening Portland cement (if required).

The cement must comply with the current B.S.I. specification for Portland cement. Concrete taken from the mixer or from between the forms must consistently show the specified crushing strength. The cement must be weighed and not measured by volume ; 90 lb. of cement = 1 cub. ft.

Modular Ratio.—L.C.C. (1915), $m = 9,000 \div$ safe f_c ; U.S.A. (1936), $m = 30,000 \div$ ult. str. at 28 days ; 1934 Code of Practice, $m = 40,000 \div$ ult. str. at 28 days ; assumed value to take account of creep.

310. **Experiments on Reinforced-Concrete.** — Space considerations prevent a detailed account of the experimental work done on reinforced-concrete. Summaries will be found in Taylor, Thompson, and Smulski,[8] and in Mörsch.[1]

311. **Stresses due to Bending.**—The simple theory given in § 38, Vol. I, for the stresses in a beam will not apply to a beam of reinforced-concrete, composed as it is of two materials with different moduli of elasticity. The usual theory for such beams is as follows : It is assumed (*a*) that plane and normal sections of the beam remain plane and normal after bending, (*b*) that the resistance of the concrete to tension is zero, (*c*) that the compressive stress in the concrete is proportional to the strain, i.e. that E_c, the modulus of elasticity of concrete, is constant over the range of working stress, and (*d*) that the grip or adhesion between the concrete and the reinforcement, supplemented by the anchorage of the bars, is sufficient to make the two materials act together in resisting the straining forces. It is probable that none of these assumptions is, strictly speaking, accurate, but the successful design of reinforced-concrete structures proves that no serious error results from them.

1 : 2 : 4 Ordinary Grade Concrete

Unit : lb./sq. in.

	L.C.C. (1915).		U.S.A.* (1936).		Code of Practice (1934).	
	Stress	%‡	Stress	%‡	Stress	%‡
Ultimate Crushing Strength.						
Preliminary Test at 28 days					3,375	150
Field Test at 28 days	1,600 / 2,400†	... / 100	2,000§	100	2,250	100
Permissible Working Stresses.						
In Beams:						
Compression in extreme fibres	600	25	800	40	750	33⅓
Shear, without web reinforcement	60	2½	40	(a) 2	75	3⅓
Shear, with web reinforcement	(200)	(8⅓)	120	(b) 6	(300)	(13⅓)
Bond or Adhesion, plain bars	60	2½	80	4	100‖	
Ditto, Bars hooked each end	100					
Ditto, Deformed bars	...		100			
Modular Ratio		15		15		18
In Short Columns with lateral reinforcement.						
Direct Compression	600	25	308	15·4	600	
Hooped Columns			440	(c) 22		
					See Regulations, and § 321.	

* Proposed Regulations, Amer. Conc. Inst. *Proc.* vol. 32, p. 407.
† At 4 months.
‡ The same percentages can be used for other mixes and for high-grade concrete.
‖ Shear stress + 25 lb.
§ Strength of concrete with specified water content ; mix not specified.
(a) = ordinary anchorage ; if special anchorage take 3 %.
(b) =   „   „   „   „   „   12 %.
Special anchorage = every longitudinal bar with standard hook, or made continuous with reinforcement for reversed bending.
(c) On gross area.

(i) Fig. 421 represents the cross-section of a reinforced-concrete beam of breadth b and effective depth d. The effective depth is the distance from AB, the outer edge of the beam in compression, to the centre of area of the tensile reinforcement, represented in the figure by the three round bars.

If NN be the neutral axis, that portion of the cross-section above NN is in compression, the portion below is in tension, but any tensile stress in the concrete below NN is neglected (Assumption b). The beam, in effect, is assumed to consist of the rectangular area ABNN in compression, and the bars forming the reinforcement in tension.

FIG. 421.

If plane normal sections remain plane and normal after bending, it

follows, exactly as in the ordinary beam, § 38, Vol. I, that the strain at any point on the cross-section varies directly as the distance of that point from the neutral axis. The strain diagram will therefore be the double triangle shown at (ii) Fig. 421, and eq. (1), § 38, Vol. I, $\dfrac{f}{v} = \dfrac{E}{R}$, will hold for the reinforced-concrete beam ; f is the stress at any point distant v from the neutral axis, E the modulus of elasticity, and R the radius of curvature. It follows that the stress in the concrete on the compressive side of the beam will vary from zero at the neutral axis to a maximum f_c at the edge AB, (iii) Fig. 421. If $f = f_c$, where $v = v_c$, $\dfrac{f_c}{v_c} = \dfrac{E_c}{R}$ E_c is the modulus of elasticity of the concrete in compression. Eq. (1), quoted above, will likewise apply to the tensile reinforcement, and if f_t be the stress therein and v_t its distance from the neutral axis, $\dfrac{f_t}{v_t} = \dfrac{E_t}{R}$, where E_t is the modulus of elasticity of the tensile reinforcement ; v_t is measured from the neutral axis to the centre of area of the tensile reinforcement, and the small variation in the stress in the reinforcement is neglected. The equations for f_c and f_t may be written thus :

$$\frac{1}{R} = \frac{f_c}{E_c v_c} = \frac{f_t}{E_t v_t} \qquad . \qquad . \qquad . \qquad . \quad (1)$$

The variation in stress over the cross-section is shown at (iii) Fig. 421.

Since the stresses on a cross-section are produced by a bending moment, and no longitudinal force exists, it follows that the sum of all the forces on a cross-section must be zero, exactly as in the case of the ordinary beam. That is to say, the total compressive force F_c on the cross-section is equal in magnitude to the total tensile force F_t on the cross-section. Now the compressive force on an elementary strip of width δv distant v from the neutral axis, (i) Fig. 421, is $fb . \delta v$. Hence the total compressive force on the cross-section is $F_c = \displaystyle\int_0^{v_c} fb . dv$. But $\dfrac{f}{v} = \dfrac{E_c}{R} = \dfrac{f_c}{v_c}$; therefore,

$$F_c = b \frac{f_c}{v_c} \int_0^{v_c} v . dv = \frac{b f_c v_c}{2}.$$

The total tensile force on the cross-section is $F_t = a_t f_t$, where a_t is the area of the tensile reinforcement. But since $F_c = F_t$,

$$\frac{b f_c v_c}{2} = a_t f_t, \text{ and } v_c = \frac{f_t}{f_c} . \frac{2a_t}{b} \qquad (2)$$

From eq. (1), $\dfrac{f_t}{f_c} = \dfrac{E_t v_t}{E_c v_c} = m \dfrac{v_t}{v_c}$, where $m = \dfrac{E_t}{E_c}$ is the *modular ratio*. Also $v_c + v_t = d$, from which $\dfrac{v_t}{v_c} = \dfrac{d - v_c}{v_c}$ and $\dfrac{f_t}{f_c} = m\dfrac{d - v_c}{v_c}$. Substituting in eq. (2),

$$2m a_t (d - v_c), \text{ and } v_c = \frac{m a_t}{b} \left\{ \sqrt{1 + \frac{2bd}{m a_t}} - 1 \right\} \qquad (3)$$

an equation which determines the position of the neutral axis.

The moment of resistance can be obtained by taking moments about the neutral axis. The moment about NN of the force on the elementary strip $b \cdot \delta v$ is $fbv \cdot \delta v$. Hence the total moment of the compressive forces on the cross-section is $\int_0^{v_c} fbv \cdot dv = \dfrac{bfc}{v_c}\int_0^{v_c} v^2 \cdot dv = \dfrac{bf_c v_c^2}{3}$; for $\dfrac{f}{v} = \dfrac{f_c}{v_c}$.

The moment about the neutral axis of the tensile force in the reinforcement is $a_t f_t v_t$. The moment of resistance, which is equal to the bending moment M on the cross-section, is the sum of these two moments. Hence,

$M = \dfrac{bf_c v_c^2}{3} + a_t f_t v_t$. But from eq. (2), $a_t f_t = bf_c v_c / 2$, and $v_t = d - v_c$.

Therefore, $\quad M = \dfrac{bf_c v_c^2}{3} + \dfrac{bf_c v_c}{2}(d - v_c) = \dfrac{bv_c}{2}f_c\left\{d - \dfrac{v_c}{3}\right\}$ . . (4)

where $\left(d - \dfrac{v_c}{3}\right) = V$ is called the arm of the moment of resistance of the cross-section, see Fig. 428. Eq. (4) can also be written

$$M = \frac{a_t f_t}{3}\{2d + v_t\} = a_t f_t\left\{d - \frac{v_c}{3}\right\} \qquad . \qquad . \qquad . \qquad (5)$$

Let the ratio $f_t/f_c = k$. Then, from eq. (1),

$$\frac{f_t}{f_c} = \frac{E_t v_t}{E_c v_c} = m\frac{v_t}{v_c} = k \text{ ; and } \frac{v_t}{v_c} = \frac{k}{m} \qquad . \qquad . \qquad . \qquad (6)$$

But $v_c + v_t = d$; hence

$$v_c = \frac{m}{m + k}d, \text{ and } v_t = \frac{k}{m + k}d \qquad . \qquad . \qquad . \qquad (7)$$

From eq. (2), $\quad a_t = \dfrac{bf_c v_c}{2f_t} = \dfrac{b}{2}\cdot\dfrac{1}{k}\cdot\dfrac{md}{m + k} = \dfrac{bd}{2}\dfrac{m}{k\,(m + k)}$ . . (8)

and from eq. (4),

$$M = \frac{bv_c}{2}f_c\left\{d - \frac{v_c}{3}\right\} = \frac{bf_c}{6}\frac{md}{m + k}\left\{3d - \frac{md}{m + k}\right\} = \frac{1}{6}bd^2 f_c \frac{(2m + 3k)m}{(m + k)^2} \quad (9)$$

Eq. (9) is of the same form as the moment of resistance equation for an ordinary rectangular beam, except that the stress f_c is multiplied by a coefficient depending on the relative properties of the steel and concrete. For a given bending moment, and given values of f_c, m, and k, the value of bd^2 can be obtained from it. A suitable section can then be chosen. The value of d should not be less than $\frac{1}{20}$th the span, nor should b be less than $\frac{1}{20}$th the span, unless adequate stiffening against lateral bending be provided. Knowing b and d, the necessary area of tensile reinforcement is obtained from eq. (8).

Theoretically, other things being equal, f_c and f_t should reach their maximum allowable values at the same time. Thus, for a $1:2:4$ Portland cement concrete, and ordinary mild steel reinforcement, if $m = 15$, $f_c = 750$ lb./sq. in., and $f_t = 18{,}000$ lb./sq. in., the value of k is $18{,}000 \div 750 = 24$. Inserting these values for m and k in eqs. (7), (8), and (9),

$$v_c = 0\cdot38d \; ; \; a_t = 0\cdot00801bd \; ; \text{ and } M = 125\cdot7bd^2 \text{ in.-lb.} \qquad (10)$$

If the same values for the stresses and for k be used, but m be taken as 18,

$$v_c = 3d/7 = 0\cdot43d \; ; \; a_t = bd/112 = 0\cdot00893\,bd \; ;$$

and $\quad M = 137\cdot7bd^2$ in.-lb. $\qquad$. $\qquad$. $\qquad$. $\qquad$. $\qquad$. (10a)

Corresponding figures for other stresses and values of m are easily obtained.

· The area of tensile steel reinforcement is usually expressed as a percentage of the area bd, thus,

$$\text{percentage of steel} = \rho = \frac{100a_t}{bd} \qquad . \qquad . \qquad . \qquad . \qquad . \quad (11)$$

From eq. (3),

$$a_t = \frac{bv_c}{2}\cdot\frac{f_c}{f_t} = \frac{bv_c^2}{2m(d-v_c)} \cdot \qquad . \qquad . \qquad . \quad (12)$$

and the percentage of steel

$$\rho = \frac{50v_c^2}{md(d-v_c)} \qquad . \qquad . \qquad . \qquad . \quad (13)$$

which may be written

$$v_c = \frac{\rho md}{100}\left\{ \sqrt{\frac{200}{\rho m}+1} - 1 \right\} \qquad . \qquad . \qquad . \quad (14)$$

In sections where f_t and f_c reach their maximum allowable values simultaneously, the value of a_t is given by eq. (8), and the percentage of steel is

$$\rho = \frac{100a_t}{bd} = \frac{100m}{2k(m+k)} \qquad . \qquad . \qquad . \quad (15)$$

For a $1:2:4$ Portland cement concrete, $m = 15$, $k = 24$, $\rho = 0\cdot801\,\%$, or if $m = 18$, $k = 24$, $\rho = 0\cdot893\,\%$.

312. Use of Graphs and Tables.—The application of the above formulae is greatly facilitated by the use of graphs and tables. Such aids to calculation are to be found in all the standard books on the subject. Some useful curves for rectangular beams and slabs, with single reinforcement, are given in Fig. 422. From eq. (14), § 311,

$$\frac{v_c}{d} = \frac{\rho m}{100}\left\{ \sqrt{\frac{200}{\rho m}+1} - 1 \right\} \qquad . \qquad . \qquad . \quad (1)$$

whence it will be seen that v_c/d is a function of m and of ρ, the percentage reinforcement, and can be plotted on a base line representing ρ ; see (i) Fig. 422. From eqs. (5) and (4), § 311,

$$M = a_t f_t\left\{ d - \frac{v_c}{3} \right\} \qquad\qquad M = \frac{bv_c}{2}f_c\left\{ d - \frac{v_c}{3} \right\}$$

$$= \rho\frac{bd^2}{100}f_t\left\{ 1 - \frac{v_c}{3d} \right\} \qquad\qquad = \frac{bd^2}{2}\cdot\frac{v_c}{d}\cdot f_c\left\{ 1 - \frac{v_c}{3d} \right\}$$

whence,

$$\frac{M}{bd^2} = \frac{\rho}{100}f_t\left\{ 1 - \frac{v_c}{3d} \right\} \qquad\qquad \frac{M}{bd^2} = \frac{1}{2}\frac{v_c}{d}\cdot f_c\left\{ 1 - \frac{v_c}{3d} \right\} \quad . \quad (2)$$

v_c/d has been shown to be a function of ρ and m, so that M/bd^2 is also a function of ρ and m, and may be plotted on the same base line, using
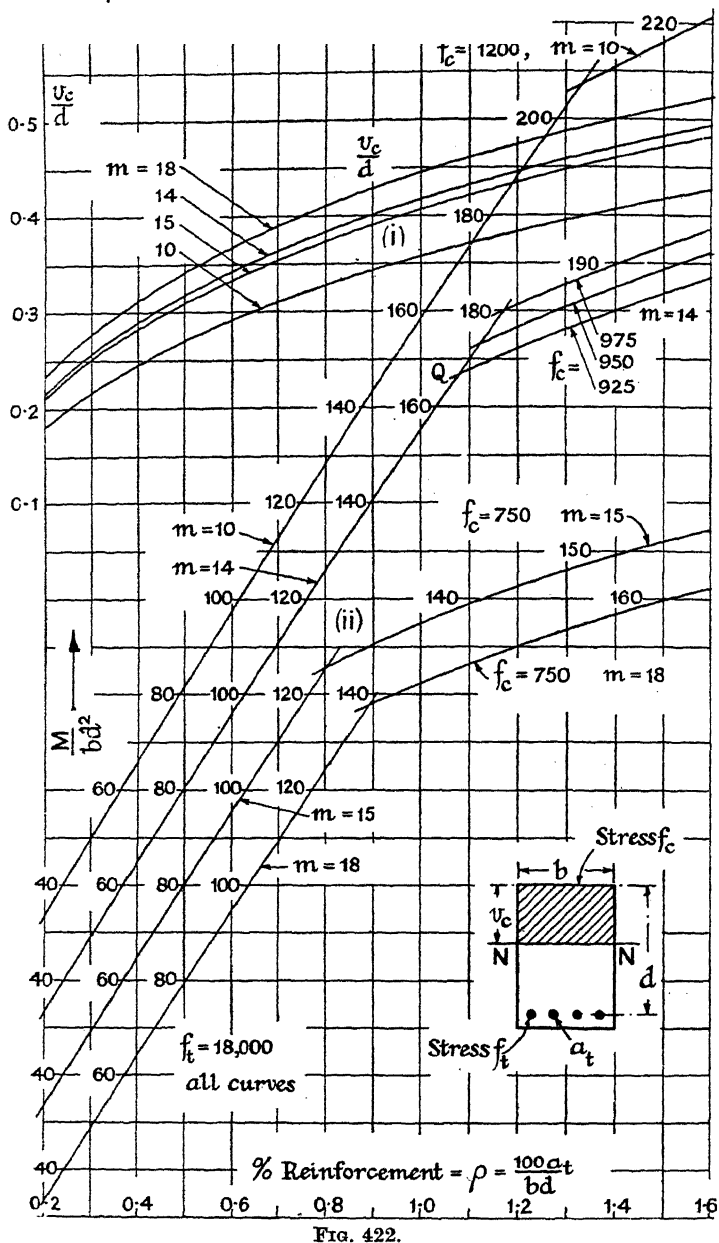
FIG. 422.

the values of v_c/d just found, (ii) Fig. 422. In these curves, $f_t = 18,000$ lb./sq. in. and f_c ranges from 750 to 1,200 lb./sq. in. as indicated. At points

such as Q, *both* steel and concrete will work at the specified maximum stresses ; for lower values of ρ the concrete will be understressed ; for higher values of ρ the steel will be understressed. For given values of M, b, and d, M/bd^2 can be found, and ρ and v_c read from the curves. From eq. (11), § 311, $a_t = \rho bd/100$. Applications will be found in the worked examples.

313. Tee Beams.—In most reinforced-concrete floors the floor beams are moulded in one with the slabs forming the floor proper, Fig. 423, the whole forming a monolithic construction. In these circumstances it is evident that part of the slab will be compressed when the floor beam bends, and in consequence, will act as part of the floor beam. For the purposes of calculation, therefore, the shape of the floor beam should be taken as that shown hatched in (i) Fig. 423. Such a beam is called a *tee beam*, from its outline. It is not possible to determine exactly how
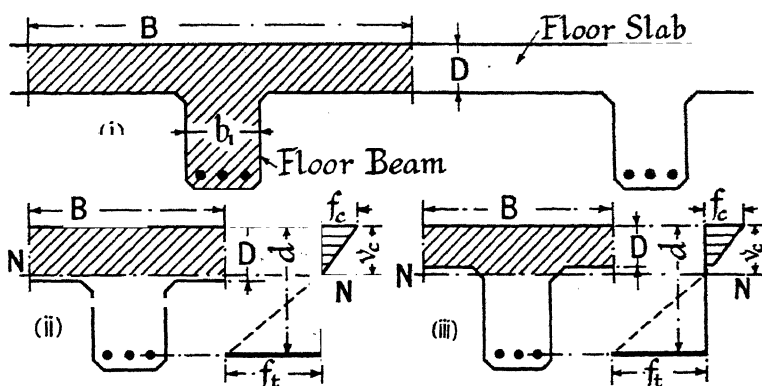
FIG. 423.

much of the sectional area of the floor slab should be counted in as forming part of the floor beam, but certain empirical rules have been laid down which give reasonable results in practice. For example, the breadth B of the flange or table of the tee should be taken as not more than (a) one-third of the effective span of the tee beam, (b) the distance between the centres of the ribs of the tee beams, or (c) twelve times the thickness D plus b_1 the breadth of the rib, whichever be the least.

When finding the moment of resistance of a tee beam, two cases occur : In the first, the neutral axis NN falls above the bottom of the slab, as shown at (ii) Fig. 423. The concrete below the neutral axis is in tension and is neglected in the analysis. Hence the fact that the beam is shaped as shown at (ii) makes no difference to its moment of resistance, and the formulae found in § 311 for plain beams are applicable, except that B, the width of the table, should be substituted for b. In the second case the neutral axis falls below the bottom of the slab, as shown at (iii), and the expressions for the plain beam no longer apply, for now the compression area is affected, being no longer rectangular. The exact expression

for the moment of resistance of the compression area shown in (iii) is complicated. To obtain an expression suitable for use in practice, therefore, it is usual to neglect the small area between the bottom of the slab and the neutral axis, and to assume that the compression area is the rectangle B × D. The stress on the area neglected is small, and its moment about the neutral axis trifling ; the error introduced is negligible.

In (iii), as in the plain beam, the position of the neutral axis is determined by the condition that the total longitudinal force on the cross-section is zero. The expression for F_c, the total compressive force on the cross-section, is identical with that given in § 311 except that the lower limit is $(v_c - D)$ instead of zero. Hence

$$F_c = \int_{v_c - D}^{v_e} f B \cdot dv = B \frac{f_c}{v_c} \int_{v_c - D}^{v_c} v \cdot dv = \frac{Bf_c}{2v_c}(2v_cD - D^2) = BD\left(v_c - \frac{D}{2}\right)\frac{f_c}{v_c}.$$

The tensile force $F_t = a_t f_t$ as before. Hence, if $F_c = F_t$,

$$BD\left(v_c - \frac{D}{2}\right)\frac{f_c}{v_c} = a_t f_t \qquad . \qquad . \qquad . \quad (1)$$

As in § 311,

$$\frac{f_t}{f_c} = m\frac{v_t}{v_c} : \quad \frac{d - v_c}{v_c}$$

and

$$\frac{BD}{v_c}\left(v_c - \frac{D}{2}\right) \quad a_t\, m\frac{d - v_c}{v_c},$$

from which

$$v_c \quad \frac{2ma_td + BD^2}{2(ma_t + BD)} \qquad . \qquad . \qquad (2)$$

which determines the position of the neutral axis.

The moment of resistance is obtained by taking moments about the neutral axis. The moment of the compressive forces about NN is

$$\int_{v_c - D}^{v_e} fbv \cdot dv = \frac{Bf_c}{v_c} \int_{v_e - D}^{v_c} v^2 \cdot dv = \frac{Bf_c}{3v_c}\{v_c^3 \quad (v_c - D)^3\}$$

$$- \frac{BDf_c}{3v_c}\{3v_c^2 - 3v_cD + D^2\}; \text{ for } \frac{f}{v} = \frac{f_c}{v_c}.$$

The moment of the tensile force in the reinforcement is $a_t f_t v_t$. Hence the moment of resistance, which is equal to the bending moment on the cross-section, is

$$M = \frac{BDf_c}{3v_c}\{3v_c^2 - 3v_cD + D^2\} + a_t f_t v_t . \qquad . \qquad .. \quad (3)$$

But, from eq. (1), $a_t f_t = BD\left(v_c - \frac{D}{2}\right)\frac{f_c}{v_c}$, and $v_t = d - v_c$. Hence,

$$M \quad \frac{BDf_c}{3v_c}\{3v_c^2 - 3v_cD + D^2\} + BD\left(v_c - \frac{D}{2}\right)\frac{f_c}{v_c}(d - v_c)$$

$$= \frac{BD}{6} \cdot \frac{f_c}{v_c}\{6v_cd - 3v_cD - 3Dd + 2D^2\}$$

$$= \frac{BD}{6} \cdot \frac{f_c}{v_c}\{3d(2v_c - D) - D(3v_c - 2D)\} \qquad (4)$$

If, from eq. (1), $\dfrac{1}{\left(v_c - \dfrac{D}{2}\right)}$ be substituted for $\dfrac{BDf_c}{3v_c}$ in eq. (3), this

reduces to

$$M = a_t f_t \left\{ d - \frac{D}{3} \frac{3v_c - 2D}{2v_c - D} \right\} \qquad \qquad . \quad (5)$$

If $m = E_t/E_c$; and $k = f_t/f_c$ as before, eq. (1) reduces to

$$a_t = \frac{BD}{k} \left\{ 1 - \frac{D}{d} \frac{m + k}{2m} \right\} \qquad \qquad . \quad (6)$$

and eq. (4) to

$$M = \frac{BD}{6} f_c \left\{ 6(d - D) - 3\frac{k}{m}D + 2\frac{D^2}{d} \frac{m + k}{m} \right\} \qquad . \quad (7)$$

For the values of k when the stresses in concrete and steel both reach their maximum value at the same time, see § 311.

The above expressions are awkward to apply without the aid of graphs, and it is often assumed, as a first approximation, that F_c acts at the centre of area of the area BD, and F_t at the centre of area of the reinforcement. The arm of the couple resisting the bending moment is then

$$V = \left(d - \frac{D}{2} \right) \text{ and }$$

$$M = a_t f_t \left(d - \frac{D}{2} \right) \qquad \qquad (8)$$

From this equation the area a_t for a given depth d is at once determined. Knowing d and a_t, the value of v_c should be found from eq. (2), and hence the value of f_c checked from eq. (3). Better still, the values of f_c and f_t can be obtained by the methods of § 315 (see p. 634).

314. Beams with Double Reinforcement.—When it is desired to reduce the depth of a reinforced-concrete beam to a minimum, reinforcement is introduced on the compression side, as shown at (i) Fig. 424. To balance the resulting increase in compressive resistance, a larger area of tensile reinforcement is provided, and for a given bending moment a shallower beam can be used. This is not usually an economical proceeding, for

FIG. 424.

the steel in compression works under disadvantageous conditions.
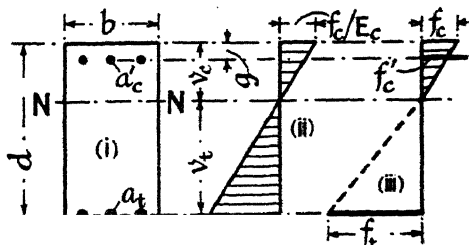
The method of finding the moment of resistance of the beam is similar to that of § 311, but the resistance of the steel in compression must be taken into account. Let a_c' be the area of this steel, and f_c' the stress therein. Then $f_c' = E \times$ strain in the elementary strip of which a_c'

forms a part. The strain at the top edge of the beam is f_c/E_c ; at a distance g below it is $\dfrac{f_c}{E_c}\dfrac{v_c - g}{v_c}$. This is the strain in both steel and concrete ; for steel, $E = E_t$; and $f_c' = E_t \cdot \dfrac{f_c}{E_c}\dfrac{v_c - g}{v_c} = mf_c\dfrac{v_c - g}{v_c}$, where $m = E_t/E_c$. The total force in the compressive steel is, therefore, $a_c'f_c' = ma_c'f_c\dfrac{v_c - g}{v_c}$. A correction is necessary in that the steel displaces an equal area of concrete in which the stress is $f_c(v_c - g)/v_c$ and the force is $a_c'f_c(v_c - g)/v_c$. Hence the net increase in compressive force due to the compressive steel is $(m - 1)a_c'f_c(v_c - g)/v_c$. The compressive force on the area bv_c of concrete in compression is $bv_cf_c/2$ (see § 311), and the total compressive force on the cross-section is $F_c = \dfrac{bf_cv_c}{2} + (m - 1)a_c'f_c\dfrac{v_c - g}{v_c}$. The tensile force on the cross-section is $F_t = a_tf_t$, and since $F_c = F_t$,

$$\frac{bf_cv_c}{2} + (m - 1)a_c'f_c\frac{v_c - g}{v_c} = a_tf_t \tag{1}$$

From eq. (1), § 311, $\dfrac{f_t}{f_c} = m\dfrac{v_t}{v_c} = m\dfrac{d}{v_c}\cdot\dfrac{v_c}{v_c}$ whence

$$v_c^2 = \frac{2ma_t}{b}(d - v_c) - \frac{2(m - 1)a_c'}{b}(v_c - g) \tag{2}$$

The moment of resistance can be obtained by taking moments about the neutral axis. The moment of the forces on the compressive side of the section is

$$\frac{bf_cv_c}{2} \times \frac{2v_c}{3} + (m - 1)a_c'f_c\frac{v_c -}{v_c} \times (v_c - g)$$

and on the tension side is $a_tf_tv_t$. Hence the moment of resistance is

$$M \quad \frac{bf_cv_c^2}{3} + (m - 1)a_c'f_c\frac{(v_c - g)^2}{v_c} + a_tf_tv_t.$$

Inserting the value of a_tf_t from eq. (1), and putting $v_t = d - v_c$,

$$M = \left[\frac{bv_c}{2}\left\{d - \frac{v_c}{3}\right\} + (m - 1)a_c'\frac{v_c - g}{v_c}(d - g)\right]f_c \tag{3}$$

Knowing the dimensions of the beam and the size of the reinforcement, v_c can be obtained from eq. (2), and, for a given value of f_c, M from eq. (3) ; the corresponding value of f_t is $f_t = mf_cv_t/v_c$, eq. (1), § 311. The reverse operation, given the bending moment to find the dimensions of the beam, in the absence of graphs, is tedious. In cases where v_c is not very different from $3g$, simplification without great error can be effected by assuming that the force on the compressive reinforcement acts at the centre of pressure of the compressive side of the beam, i.e. that $g = v_c/3$. The

arm of the couple resisting the bending moment will then be $V = d - v_c/3$, as in a singly reinforced beam. If then a singly reinforced beam of the required depth and width be taken, in which f_c and f_t both attain their maximum values, p. 610, and a compressive reinforcement a_c' be inserted, and also the area of the tensile reinforcement be increased so that the neutral axis is not moved, v_c will be the same in the two cases and the ratio $k = f_t/f_c$ will be unaltered. From § 311 the safe bending moment M_1 on the singly reinforced beam can be calculated; if the doubly reinforced beam has to carry a bending moment M, the difference $(M - M_1)$ must be carried by the extra reinforcement. The arm of the couple $(d - v_c/3)$ is known from the singly reinforced section, hence the force to be carried by the compressive reinforcement is

$$\frac{M - M_1}{d - v_c/3} - a_c'f_c' - (m - 1)a_c'f_c\frac{v_c - g}{v_c} = \frac{2}{3}(m - 1)a_c'f_c$$

(see above), from which a_c' is found. The required increase a_t' in the area of the tension steel is given by $\dfrac{M - M_1}{d - v_c/3} = a_t'f_t$; this area a_t', added to the tension area of the singly reinforced beam, gives the area a_t of the doubly reinforced member.

Example.—A $12'' \times 6''$, $d = 10 \cdot 6$ in., $1 : 2 : 4$ mix, P.C. r.-c. beam, $m = 18$, doubly reinforced, has to carry a bending moment of $140{,}000$ in.-lb. Find the necessary areas of tensile and compressive steel. From eq. (10a), § 311, for a singly reinforced beam of these dimensions, $M_1 = 137 \cdot 7bd^2 = 137 \cdot 7 \times 6 \times 10 \cdot 6^2 = 92{,}850$ in.-lb.; $v_c = 3d/7 = 3 \times 10 \cdot 6/7 = 4 \cdot 54$; $d - v_c/3 = 10 \cdot 6 - 1 \cdot 51 = 9 \cdot 09$; $a_t = bd/112 = 10 \cdot 6 \times 6/112 = 0 \cdot 568$. $M - M_1 = 140{,}000 - 92{,}850 = 47{,}150$; $a_c' \dfrac{47{,}150 \times 3}{9 \cdot 09 \times 2 \times 17 \times 750} = 0 \cdot 61$; and $a_t \dfrac{47{,}150}{9 \cdot 09 \times 18{,}000} + 0 \cdot 568 \quad 0 \cdot 86$ sq. in.

All the necessary details of the cross-section are thus determined. The actual stresses in the materials should then be checked by the methods of § 315, with the compressive reinforcements in their proper place.

An exactly similar procedure can be adopted in the case of tee beams with double reinforcement, but as in § 313, when the neutral axis falls below the slab, the arm V may be taken as $\left(d - \dfrac{D}{2}\right)$ instead of $\left(d - \dfrac{v_c}{3}\right)$, as a first approximation.

315. Moment of Inertia and Section Modulus of Reinforced-Concrete Beam.—As shown in § 40, Vol. I, the moment of resistance of the forces on a cross-section of a beam is the integral of the expression $\dfrac{E}{R}bv^2 \cdot \delta v$ summed from top to bottom of the beam, i.e. it is equal to the integral $\displaystyle\int_{-v_2}^{v_1} \frac{E}{R}bv^2 \cdot dv$. When E is constant, this reduces to $EI/R = M$, the well-known

formula. If E be not constant, the integral becomes $M = \dfrac{1}{R}\displaystyle\int_{-v_2}^{v_1} Ebv^2 \cdot dv$.
In a reinforced-concrete beam, let $E = mE_c$, where m is a coefficient depending on the material; $m = 1$ for concrete, and $m = E_t/E_c$ for the tensile reinforcement. Then $M = \dfrac{1}{R}\displaystyle\int_{v_t}^{v_c} mE_cbv^2 \cdot dv = \dfrac{E_c}{R}\displaystyle\int_{v_t}^{v_c} mbv^2 \cdot dv$, the limits v_c and v_t, which replace v_1 and v_2, signifying that the integration is carried over the whole cross-section. Let $\displaystyle\int_{v_t}^{v_c} mbv^2 \cdot dv = I_c$. Then the equation becomes

$$\frac{M}{I_c} = \frac{E_c}{R} = \frac{f_c}{v_c} \quad . \qquad . \qquad . \qquad . \qquad . \quad (1)$$

for from eq. (1), § 311, $\dfrac{1}{R} = \dfrac{f_c}{E_c v_c}$. Now eq. (1) above is identical in form with eq. (1) of § 40, Vol. I. It follows that I_c can be regarded as the equivalent in a reinforced-concrete beam of the moment of inertia I in an ordinary beam, and may therefore be termed the moment of inertia of the reinforced-concrete beam. Also, from eq. (1),

$$f_c = \frac{M}{I_c} v_c \quad . \qquad . \qquad . \qquad . \qquad . \quad (2)$$

analogous to eq. (2) of § 40, Vol. I; and if $I_c/v_c = Z_c$, Z_c is the section modulus of the beam on the concrete side, and

$$M = f_c Z_c \quad . \qquad . \qquad . \qquad . \qquad . \quad (3)$$

In a layer of concrete distant v from the neutral axis, the stress would be $f_c = Mv/I_c$. The stress in a similarly situated steel bar would be m times this, where $m = E_t/E_c$. Hence the stress in a steel bar distant v from the neutral axis is $f = Mmv/I_c$. This applies to steel in tension or in compression. For the tensile reinforcement, $f = f_t$ and $v = v_t$; hence,

$$f_t = \frac{M}{I_c} mv_t \quad . \qquad . \qquad . \qquad . \qquad . \quad (4)$$

or, if $Z_t = \dfrac{I_c}{mv_t}$, $\qquad\qquad M = f_t Z_t \quad . \qquad . \qquad . \qquad . \qquad . \quad (5)$

If, as in Fig. 435, there be two (or more) layers of tensile steel, v_t and f_t in eqs. (4) and (5) have reference to the lower layer. In such cases the total tensile force on the cross-section $F_t = \Sigma\, a_t f_t$, in which expression the appropriate values of a_t and f_t for each layer must be inserted. Then since $M = F_t V$, the arm

$$V = M/\Sigma\, a_t f_t = I_c/m\Sigma\, a_t v_t \quad . \qquad . \qquad . \qquad . \quad (6)$$

For the compressive reinforcement, $v = v_c - g$, Fig. 424, and $f = f_c'$. Hence

$$f_c' = Mm(v_c - g)/I_c \quad . \qquad . \qquad . \qquad . \quad (7)$$

where g is the distance of the compressive reinforcement from the top of the beam.

Now just as I in an ordinary beam can be determined by a tabular method of calculation, § 48, Vol. I ; by the same method of tabular calculation I_c can be determined, except that each area in the calculation for I_c must be multiplied by the appropriate value of m, for the integral for I_c includes the factor m, which the integral for I does not. The process is exactly similar to that for an unsymmetrical section, Vol. I, p. 82, and need not be further elaborated. A typical calculation for the section given in Fig. 424 is set forth below. For convenience, moments are taken about the top of the beam. The value of m for concrete is 1 ; that for steel in tension is E_t/E_c, taken in the Table as 15 ; that for steel in compression less the replaced concrete is $(E_t/E_c - 1) = 14$ in the Table (cf. § 314).

MOMENT OF INERTIA OF CROSS-SECTION WITH DOUBLE REINFORCEMENT. (i) FIG. 424.

Part.	a'	m	ma'	h'	$ma'h'$	$ma'(h')^2$	mI'
Concrete in compression . . .	bv_c	1	bv_c	$\dfrac{v_c}{2}$	$\dfrac{bv_c^2}{2}$	$\dfrac{bv_c^3}{4}$	$\dfrac{bv_c^3}{12}$
Steel in compression .	a_c'	14	$14a_c'$	g	$14a_c'g$	$14a_c'g^2$	
Steel in tension .	a_t	15	$15a_t$	d	$15a_td$	$15a_td^2$	
			$\Sigma\, ma'$		$\Sigma\, ma'h'$	$\Sigma\, ma'(h')^2$	$\Sigma\, mI'$

$$v_c = \frac{\Sigma\, ma'h'}{\Sigma\, ma'} \qquad I_c = \Sigma\, ma'(h')^2 + \Sigma\, m'I - \frac{(\Sigma ma'h')^2}{\Sigma\, ma'}$$

$$v_t = (d - v_c) \qquad Z_c = \frac{I_c}{v_c} \quad \text{and} \quad Z_t = \frac{I_c}{mv_t}$$

The arm V $\dfrac{M}{ma_tv_t}$; since, from eq. (5),

$$f_t = \frac{M}{Z_t} = \frac{M}{I_c} mv_t.$$

The determination of v_c involves the solution of a quadratic equation,

$$v_c(\Sigma\, ma') = \Sigma\, ma'h' \ . \qquad . \qquad . \quad (8)$$

Unless suitable graphs are available, the above is one of the quickest methods of finding the stresses in any r.-c. beam, excepting a plain rectangular section with single reinforcement.

FIG. 425.

Worked Example.—To find the safe bending moment on the section dimensioned in Fig. 425 when $f_t = 18{,}000$, $f_c = 750$ lb./sq. in., and $m = 18$. Take moments about the top of the beam.
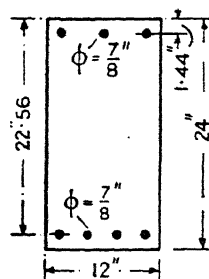
Part.	a'	m	ma'	h'	$ma'h'$	$ma'(h')^2$	mI'
Concrete in compression	$12v_c$	1	$12v_c$	$v_c/2$	$6v_c{}^2$	$3\,v_c{}^3$	$v_c{}^3$
Steel in compression	1·8	17	30·6	1·44	44·1	63·5	
Steel in tension	2·4	18	43·2	22·56	974·6	21,987·0	
			$73·8+12v_c$		$1018·7+6v_c{}^2$	$22,050·5+3v_c{}^3$	$v_c{}^3$

$$v_c = \frac{1018·7 + 6v_c{}^2}{73·8 + 12v_c} = 8·26 ; \quad v_t = 22·56 - 8·26 = 14·3.$$

$$I_c = 22,050·5 + 3v_c{}^3 + v_c{}^3 - \frac{(1018·7 + 6v_c{}^2)^2}{73·8 + 12v_c} = 12,510.$$

$$\frac{12,510}{8·26} = 1514 ; \ \text{Safe M} = 1514 \times 750 = 1,135,500 \text{ in.-lb.}$$

$$Z_t = \frac{12,510}{18 \times 14·3} : : 48·60 ; \ \text{Safe M} = 48·6 \times 18,000 = 874,800 \text{ in.-lb.}$$

The latter figure is the safe bending moment on the section.

The above example, although primarily intended to elucidate the method of calculation, serves also to illustrate the ineffectiveness of compressive steel as a means of increasing the moment of resistance, unless balanced by extra tensile steel. The section without the three top $\frac{7}{8}$-inch bars satisfies eq. (10a), § 311 : $a_t = bd/112 = 12 \times 22·56/112 = 2·42$ sq. in. ; and the safe bending moment is $137·7bd^2 = 841,400$ in.-lb., or only 4 % less than the section of Fig. 425.

To make this an economical section, a_t must be increased until $v_c = 3d/7 = 3 \times 22·34 \div 7 = 9·57$ [see eq. (10a), § 311 ; an increased cover will be necessary]. The required value of a_t can be found as follows. Take moments about the top of the beam.

Part.	a'	m	ma'	h'	$ma'h'$
Concrete in compression $= 12v_c$	114·8	1	114·8	4·79	549·9
Steel in compression	1·8	17	30·6	1·44	44·1
Steel in tension	a_t	18	$18a_t$	22·34	$402·1\,a_t$
			$145·4+$ $18\,a_t$		$594·0+$ $402·1a_t$

$$v_c = \frac{594·0 + 402·1a_t}{145·4 + 18a_t} = 9·57, \text{ whence } a_t = 3·47 \text{ sq. in.}$$

Four $1\frac{1}{16}$ bars will be required, and by the tabular method above, safe M $= 1,230,400$ in.-lb., a 46 % increase.

316. Combination of Direct Stress with Bending.—Many cases occur in practice, for example, columns and arched ribs, in which a reinforced-concrete member has to resist both direct stress and a bending moment. In the following consideration of these conditions, it will be assumed that bending takes place about one of the principal axes of the cross-section only (uniplanar bending). The general formulae for such combinations of stress are given in Chapter VIII, Vol. I (cf. § 354 of the present volume).

In reinforced-concrete construction it is necessary to distinguish between members in which the stress on the cross-section is wholly compressive, and those in which the stress is wholly or partly tensile.

Case I. Stress Wholly Compressive.—In Fig. 426, suppose that a normal force F act on the cross-section at a distance e from the centre
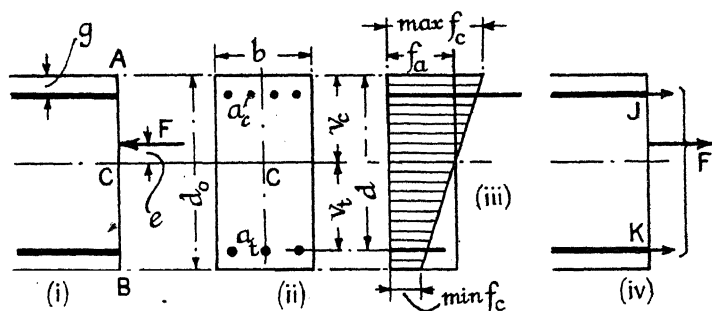
FIG. 426.

of resistance C. As in § 354, the effect will be equivalent to a direct compression F producing a uniform strain s_a all over the cross-section, plus a bending moment Fe. The corresponding diagram of stress in the concrete is shown at (iii) Fig. 426 : $f_a = E_c s_a$ is the stress due to the direct compression, and f_b the stress due to the bending moment. As in § 321, the equivalent area of cross-section, allowing for the different values of E, is $b d_0 + (m - 1)(a_c' + a_t)$,* where d_0 is the overall depth of the cross-section. The direct stress in the concrete is, therefore,

$$f_a = \frac{F}{b d_0 + (m - 1)(a_c' + a_t)} \qquad . \qquad . \qquad . \quad (1)$$

The maximum stresses in the concrete due to bending, § 315, at A and B respectively, are :

$$f_b = \frac{M v_c}{I_c} = \frac{F e v_c}{I_c} ; \quad f_b = \frac{M}{I_c}(d_0 - v_c) = \frac{F e}{I_c}(d_0 - v_c) \quad . \quad (2)$$

I_c and v_c are found exactly as in § 315, except that the whole area of the concrete is counted in; since both a_t and a_c' are in compression, use

---

* These symbols have been retained to correspond with those of § 314, but there is no tension anywhere ; the neutral axis lies outside the cross-section, and does not coincide with CC.

$(m-1)$ instead of m for both areas (see the worked example below). The maximum and minimum stresses in the concrete at A and B respectively are :

$$\text{max. } f_c = f_a + f_b = F \left\{ \frac{1}{\overline{bd_0} + (m-1)(a_c' + a_t)} + \frac{ev_c}{I_c} \right\} \tag{3}$$

$$\text{min. } f_c = f_a - f_b = F \left\{ \frac{1}{\overline{bd_0} + (m-1)(a_c' + a_t)} - \frac{e(d_0 - v_c)}{I_c} \right\} \tag{4}$$

The stresses in the steel are :

$$\text{In } a_c', \quad f = mF \left\{ \frac{1}{\overline{bd_0} + (m-1)(a_c' + a_t)} + \frac{e(v_c - g)}{I_c} \right\} \tag{5}$$

$$\text{In } a_t, \quad f = mF \left\{ \frac{1}{\overline{bd_0} + (m-1)(a_c' + a_t)} - \frac{ev_t}{I_c} \right\} \tag{6}$$

Worked Example.—In Fig. 426, $b = 12$, $d_0 = 24$, $g = 1\cdot44$, $d = 22\cdot56$, $a_c' = 2\cdot4$, $a_t = 1\cdot8$, and $m = 18$. If a force $F = 90$ tons be applied 10 inches below the top of the cross-section, find the stresses in the concrete and steel. Taking moments about the top of the section,

Part.	a'	m	ma'	h'	$ma'h'$	$ma'(h')^2$	mI'
Whole area of the concrete	288	1	288	12	3,456	41,472	13,824
Top Steel (a_c') . .	2·4	17	40·8	1·44	58·7	85	
Bottom Steel (a_t) . .	1·8	17	30·6	22·56	690·3	15,573	
			359·4		4,205·0	57,130	13,824

$$v_c = \frac{4,205\cdot0}{359\cdot4} = 11\cdot7; \ d_0 - v_c = 24 - 11\cdot7 = 12\cdot3; \ e = v_c - 10 = 11\cdot7 - 10$$
$$= 1\cdot7 \text{ in.}$$

$$I_c = 57,130 + 13,824 - \frac{(4,205\cdot0)^2}{359\cdot4} = 21,755.$$

Then, see eqs. (3), (4), (5), and (6),

$$\text{max. } f_c = f_a + f_b = \frac{90 \times 2,240}{359\cdot4} + \frac{90 \times 2,240 \times 1\cdot7 \times 11\cdot7}{21,755} = 746 ;$$

$$\text{min. } f_c = f_a - f_b = \frac{90 \times 2,240}{359\cdot4} - \frac{90 \times 2,240 \times 1\cdot7 \times 12\cdot3}{21,755} = 367.$$

$$\text{Stress in } a_c' = \frac{18 \times 90 \times 2,240}{359\cdot4} + \frac{18 \times 90 \times 2,240 \times 1\cdot7 \times 10\cdot26}{21,755} = 13,006.$$

$$\text{Stress in } a_t = \frac{18 \times 90 \times 2,240}{359\cdot4} - \frac{18 \times 90 \times 2,240 \times 1\cdot7 \times 10\cdot86}{12,755} = 7,017,$$

for $(v_c - g) = 11\cdot7 - 1\cdot44 = 10\cdot26$; and $v_t = 22\cdot56 - 11\cdot7 = 10\cdot86$. Units : lb. ; in. ; lb./sq. in.

Validity Limit.—In the limiting case, before tension appears on the cross-section, min. f_c from eq. (4) becomes zero, when

$$e = \frac{I_c}{(d_0 - v_c)\{bd_0 + (m - 1)\,(ac' + a_t)\}} = \frac{I_c}{(d_0 - v_c)\,\Sigma(ma')} \quad \text{[from table] (7)}$$

$$\frac{bd_0{}^3 - 3bd_0\,v_c\,(d_0 - v_c) + (m - 1)\{ac'(v_c - g)^2 + a_tv_t{}^2\}}{3(d_0 - v_c)\{bd_0 + (m - 1)(ac' + a_t)\}} \tag{8}$$

for $\quad I_c = bd_0{}^3/3 - bd_0v_c\,(d_0 - v_c) + (m - 1)\{ac'\,(v_c - g)^2 + a_tv_t{}^2\}$ (9)

Case II. Stress wholly Tensile.—When F is tensile, and falls between the reinforcements, (iv) Fig. 426, the stress on the section is entirely tensile. In this case the concrete is neglected altogether, and the distribution of stress in the reinforcement is determined by taking moments about J or K.

Case III. When both Tension and Compression occur.—In cases where e exceeds the value given by eq. (7), both tension and compression will
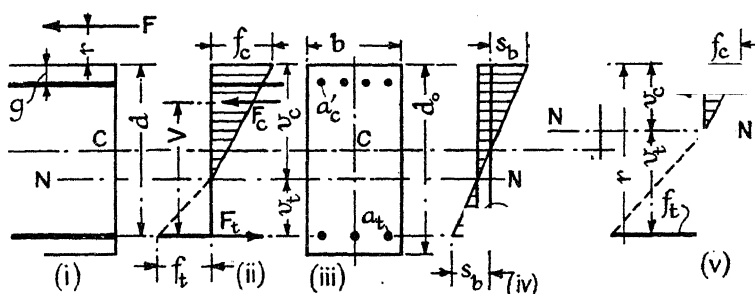
FIG. 427.

occur, and the above formulae no longer apply. In (i) Fig. 427, let F be a compressive force acting on the cross-section at a distance r from the top compressive edge. If r be sufficiently great, s_b, the strain due to bending, will exceed s_a, the strain due to direct compression, (iv), the neutral axis NN will fall within the cross-section, and the lower edge of the member will be in tension. The distribution of stress on the cross-section will be as shown in (ii). If F_c be the total compressive force on the cross-section,

$$F_c = \frac{bv_cf_t}{2} + ac'f_c' = \frac{bv_cf_c}{2} + (m - 1)\,ac'f_c\,\frac{v_c - g}{v_c} \tag{10}$$

and the total tensile force on the cross-section will be $F_t = a_tf_t$ (cf. § 314). For equilibrium, the difference between F_c and F_t must equal F, $F_c - F_t$ = F ; and the moment of F_c plus that of F_t must equal the moment of F about any point. Take moments about the line of action of F_t, then $F_cV = F(d + r)$.

From the first relation,

$$F = F_c - F_t = \frac{bv_cf_c}{2} + (m-1)\,a_c'f_c\,\frac{v_c-g}{v_c}\ \cdot a_tf_t$$

$$= \frac{bv_cf_c}{2} + (m-1)a_c'f_c\frac{v_c-!}{v_c}\ - ma_tf_c\frac{d-v_c}{v_c} \tag{11}$$

for $a_tf_t = ma_t f_c(d-v_c)/v_c$ (cf. § 314).

From the second relation, using eq. (11),

$$F(d \div r) = \left\{\frac{bv_cf_c}{2} + (m\quad 1)\,a_c'f_c\,\frac{v_c-g}{v_c}\ - ma_tf_c\,\frac{d-v_c}{v_c}\right\}(d+r)$$

$$= F_cV = \frac{bv_cf_c}{2}\left\{d - \frac{v_c}{2}\right\} + (m-1)\,a_c'f_c\,\frac{v_c-g}{v_c}\,(d-g)$$

whence,

$$\frac{bv_c^2}{6}\,(v_c + 3r) = ma_t\,(d+r)\,(d-v_c) - (m-1)\,a_c'\,(g+r)\,(v_c-g) \tag{12}$$

To obtain v_c, plot graphs of the expressions on each side of the equation on a v_c base line, using a series of values for v_c. The intersection of the two curves gives the required value for v_c. Knowing v_c, the stress f_c is obtained from eq. (11), and F_c from eq. (10). Since

$$F_t = a_tf_t = ma_tf_c\,(d-v_c)/v_c\,; \qquad f_t = mf_c\,(d-v_c)/v_c \qquad . \tag{13}$$

Note that when F acts below the top of the section, r is to be given a minus sign. If the section be only singly reinforced, the same equations hold, but a_c' is to be put equal to zero.

It will be found by trial that when F is a tensile force, (v) Fig. 427, the same formulae apply, but r, which still denotes the distance of F from the compressive edge of the member, must be given a minus sign.

Worked Example.—If $b = 12$, $d = 22\cdot56$, $g = 1\cdot44$, $a_c' = 2\cdot4$, and $a_t = 1\cdot8$, find the stresses if F = 70,000 lb. (comp.), $r = -6$ in., and $m = 18$. Substituting in eq.(12),

$v_c^2\,(v_c - 18)$
$\quad = 5,918\cdot2 - 175\cdot25\,v_c$,
and $v_c = 22\cdot15$; whence from
eq. (11),
F = $95\cdot36, f_c = 70,000$ lb., and
$f_c = 734$ lb./sq. in. From eq.
(13), $f_t = 0\cdot333f_c = 245$ lb./
sq. in.

FIG. 428.

317. Shear Stress.—In a plain rectangular reinforced-concrete beam with single reinforcement, (i) Fig. 428, let M denote the bending moment at any section distant x from some origin. From eq. (5), § 311, M = $a_tf_t(d - v_c/3)$, and therefore the shearing force on the cross-section is

$$S = \frac{dM}{dx} = \frac{d}{dx}\left[a_tf_t\left\{d - \frac{v_c}{3}\right\}\right]$$
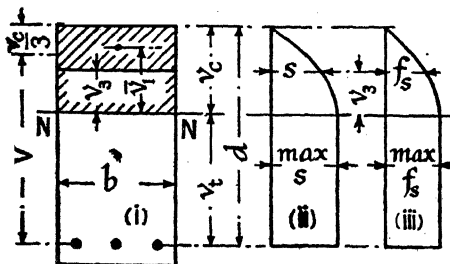
whence

$$\frac{d}{dx}(a_t f_t) = \frac{S}{d - v_c/3} \cdot \frac{S}{V} \qquad (1)$$

for $\frac{u}{dx}(a_t f_t)$ is the rate of increase in the force in the tensile reinforcement with respect to x; that is to say, it is s, the shear per unit of length of § 81, Vol. I. From eq. (1), s is equal to the total shearing force divided by the arm $V = (d - v_c/3)$. If b be the breadth of the beam in the neighbourhood of the tensile reinforcement, the shear stress in the concrete there is

$$f_s = \frac{s}{b} = \frac{S}{d - \dfrac{v_c}{3}} \cdot \frac{S}{bV} \qquad (2)$$

Bond Stress.—In a reinforced-concrete beam, if Σq be the total perimeter of the tensile reinforcement, and f_s' the shear stress or adhesion per unit of area between the concrete and the steel, then $(\Sigma q \times 1 \times f_s')$ is the increase in the force in the tensile reinforcement per unit of length $= s$. Then

$$s = (\Sigma q) f_s'; \text{ and } f_s' = \frac{s}{\Sigma q} = \frac{S}{\left(d - \dfrac{v_c}{3}\right)\Sigma q} = \frac{S}{V\Sigma q} \qquad . \quad (3)$$

and the value of f_s', thus calculated, must not exceed the safe *bond stress* given in § 309. Should the reinforcement bars not be all of the same diameter, it is necessary to consider the adhesion of the largest bars individually. From eq. (3), the necessary perimeter of the tensile reinforcement is

$$\Sigma q = \frac{S}{f_s'\left(d - \dfrac{v_c}{3}\right)} = \frac{S}{Vf_s'} \qquad . \qquad . \qquad . \quad (4)$$

Anchorage.—If f_t be the stress in a bar of diameter ϕ, the force in the bar is $\frac{\pi}{4}\phi^2 f_t$. The perimetrical area of a length l is $\pi\phi l$; if f_s' be the safe bond stress, the length l necessary to form an effective anchor is

$$l = \frac{\pi}{4}\phi^2 f_t \div \pi\phi f_s' = \frac{\phi}{4} f_t / f_s';$$

and such a length of straight bar may, in suitable cases, replace a hook.

Distribution of Shear Stress.—On the compression side, the reinforced-concrete beam is in exactly the same condition as a rectangular beam of any other material, the compressive stress varying from zero at the neutral axis to a maximum at the extreme fibres. The distribution of shear stress over this part of the cross-section is found exactly as in § 81, Vol. I, and the equations there given will apply. Thus eqs. (4) and (5) of that article will give s, the shear per unit of length, and f_s, the shear stress,

respectively, at a point distant v_3 from the neutral axis, (i) Fig. 428. For the reinforced-concrete beam these equations become

$$s = S \frac{a_1 \bar{v}_1}{I_c} = S \frac{(v_c^2 - v_3^2)b}{2I_c} \qquad . \qquad . \qquad . \quad (5)$$

$$f_s = \frac{S}{b} \frac{a_1 \bar{v}_1}{I_c} = S \frac{(v_c^2 - v_3^2)}{2I_c} . \qquad . \qquad . \qquad . \quad (6)$$

As in the case of the beam of ordinary material, Fig. 138, Vol. I, each of these equations represents a parabola as shown at (ii) and (iii) Fig. 428, the maximum ordinates occurring at the neutral axis, where $v_3 = 0$; the maximum values are

$$\text{max. } s = S \frac{b v_c^2}{2I_c} = \frac{S}{d - \dfrac{v_c}{3}} = \frac{S}{V} \qquad . \qquad . \qquad . \quad (7)$$

$$\text{max. } f_s = S \frac{v_c^2}{2I_c} = \frac{S}{b \left(d - \dfrac{v_c}{3} \right)} = \frac{S}{bV} . \qquad . \qquad . \quad (8)$$

for, from eq. (2), § 315, and eq. (4), § 311,

$$I_c = \frac{M v_c}{f_c} = \frac{b v_c^2}{2} \left(d - \frac{v_c}{3} \right).$$

These values are the same as those given by eqs. (1) and (2), and it will be evident that since the concrete is assumed unable to resist tension, the shear stress on the tension side will be the same for all values of v, as shown in (ii) and (iii) Fig. 428. These figures represent, therefore, the distribution of vertical or horizontal shear over the whole cross-section.

From eq. (7), § 311, $v_c = \dfrac{m}{m + k}d$, and the arm

$$V = \left(d - \frac{v_c}{3} \right) = d \left\{ 1 - \frac{m}{3(m + k)} \right\} = d \left\{ \frac{2m + 3k}{3 (m + k)} \right\}$$

Hence, from eqs. (1), (2), and (4),

$$s = \frac{S}{d} \left\{ \frac{3(m + k)}{2m + 3k} \right\} ; f_s = \frac{S}{bd} \left\{ \frac{3(m + k)}{2m + 3k} \right\} ;$$

and

$$\Sigma q = \frac{S}{d \times f_s} \left\{ \frac{3(m + k)}{2m + 3k} \right\} \qquad . \qquad . \qquad . \quad (9)$$

For a beam of $1 : 2 : 4$ Portland cement concrete (see § 311), if $m = 18$ and $k = 24$,

$$s = \frac{7S}{6d} ; f_s = \frac{7S}{6bd} ; \text{ and } \Sigma q = \frac{7S}{6df_s} , \qquad . \qquad . \quad (10)$$

the arm $V = 6d/7 = 0 \cdot 857d$.

Eqs. (1), (2), and (4) hold for either rectangular or tee beams, but for tee beams in which the neutral axis falls below the bottom of the slab, $d - D/2$ may, as an approximation, be substituted for $(d - v_c/3)$ as the

value of the arm V. Also, b is to be replaced by b_1, the breadth of the rib. It is always necessary to ascertain that the shear stress in the rib does not exceed the allowable stress in the concrete.

More general expressions, applying to any type of beam, can be deduced from eq. (5), § 315 : $f_t = \dfrac{M}{Z_t} = \dfrac{M}{I_c} m v_t$. For a single layer of tensile steel, $a_t f_t = \dfrac{M}{I_c} m a_t v_t$, and

$$\frac{d}{dx}(a_t f_t) = \frac{dM}{dx} \cdot \frac{m a_t v_t}{I_c} = \frac{S}{I_c} m a_t v_t = s \qquad . \qquad (11)$$

an equation analogous to eq. (4), § 81, Vol. I. It follows that, in the neighbourhood of the tensile reinforcement,

$$f_s = \frac{S}{b I_c} m a_t v_t \qquad . \qquad . \qquad . \qquad . \qquad (12)$$

and the requisite perimeter of the tensile reinforcement is

$$\Sigma\, q = \frac{S}{f_s' I_c} m a_t v_t \qquad . \qquad . \qquad . \qquad . \qquad (13)$$

When there are two (or more) layers of tensile steel (cf. Fig. 435), if a_t and v_t in eqs. (11), (12), and (13) have reference to the lower layer, these equations give the values of s, f_s, and $\Sigma\, q$ at or for that layer. Eqs. (11) and (13) will give s and $\Sigma\, q$ for the upper layer if a_t and v_t have reference to the upper layer. To find max. s and max. f_s, Fig. 428, eqs. (11) and (12) must be written

$$\text{max. } s = \frac{S}{I_c} m\, \Sigma\, a_t v_t; \quad \text{max. } f_s = \frac{S}{b I_c} m\, \Sigma\, a_t v_t \qquad . \quad (14), (15)$$

in which expressions the appropriate values of a_t and v_t for each layer must be inserted.

It is proper to remark that the above theory presumes that the stresses in a reinforced-concrete beam are developed in a similar way to those in an ordinary solid beam. When bars are bent up to carry part of the shearing force, § 318, and so-called 'truss action' takes place, the conditions approximate rather to those in a lattice girder.

318. Shear Reinforcement.—If the shear stress f_s exceed the permissible value for the concrete employed, it is necessary to introduce reinforcement to carry the shear. This takes the form of diagonal and/or vertical bars arranged as shown in Fig. 429. These bars are the equivalents of the tension members of the web of a lattice girder, the concrete itself acting as the compression members. There is little doubt that the state of affairs existing in the web is roughly as represented in Fig. 429, where the probable lines of diagonal compressive stress in the concrete are indicated by the thin parallel lines. It is customary to turn up the tensile reinforcement bars, when the reduction in bending moment towards the ends of the beam will permit, to form the diagonal shear members, (i) and (iii) Fig. 429. The vertical members shown at (ii)

and (iv) are called *stirrups*; they are introduced especially to resist the shear. Stirrups are generally made of round bar, usually smaller in diameter than the tensile reinforcement, but not less than $\frac{1}{4}$ inch. Typical shapes are shown at (v) to (viii) Fig. 429.

If the shear reinforcement is to develop anything like the permissible
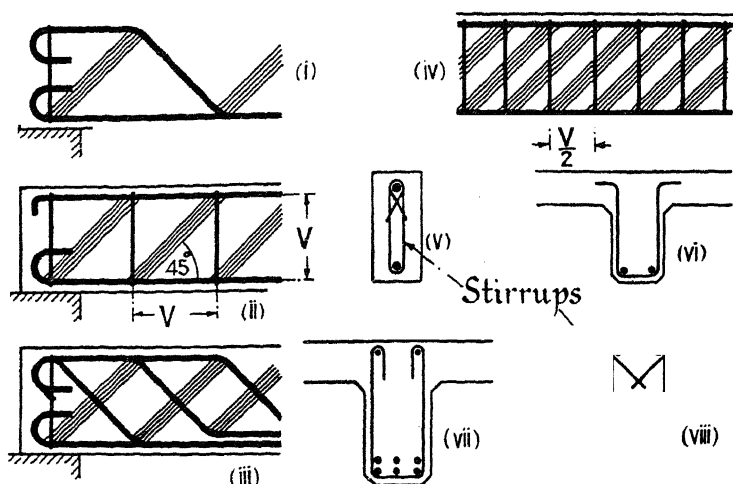
FIG. 429.

tensile stress for the steel, the resulting tensile strain in the concrete will exceed that which the concrete can safely carry, and it will crack. Its resistance to shear proper will then be small, and it is customary to neglect it altogether, sufficient reinforcement being provided to carry the total shearing force; but in no case should the value of f_s, found
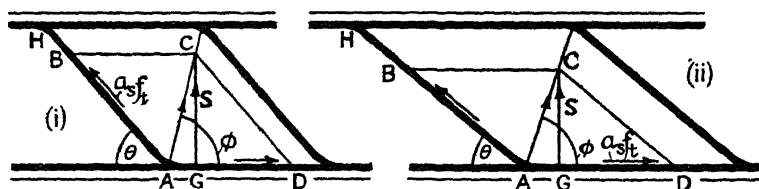
FIG. 430.

from eq. (2), § 317, exceed four times the permissible shear stress in the concrete.

Safe Shearing Force.—The vertical shearing force which a system of diagonals, (i) Fig. 429, will safely carry can be determined from the parallelogram of forces in Fig. 430. AB represents the force in the diagonal, AD the force in the horizontal branch, the resultant AC is the diagonal compression in the concrete. Then $GC = AC \sin \phi$ represents the vertical shearing force which the system will carry. Let a_s be the

sum of the areas of the diagonal bars AH, and f_t the safe tensile stress therein. Then $a_s f_t$ is the maximum safe value of either of the forces AB or AD. Two cases may be distinguished. In (i) Fig. 430, AB > AD, and $\phi > (90 - \theta/2)$. Then $AB = a_s f_t$, and if S be the safe vertical shearing force,

$$S = a_s f_t \sin \theta \qquad . \qquad . \qquad . \qquad . \qquad . \qquad . \qquad (1)$$

In (ii) Fig. 429, AD > AB, $\phi < (90 - \theta/2)$. Then $AD = a_s f_t$, and

$$S = a_s f_t \sin \theta \sin \phi / \sin (\theta + \phi) \qquad . \qquad . \qquad . \qquad (2)$$

It is simpler to draw the parallelogram.

In cases like (iii) Fig. 429, the vertical shearing force which each system will safely carry should be separately determined, and then added together.

In (ii) Fig. 429, the vertical shearing force is equal to the vertical component of the diagonal force in the concrete, which component is equal to the tension in a stirrup. Hence, if a_s be the area of a stirrup, and f_t the tensile stress in it, the shearing force S is

$$S = a_s f_t \qquad . \qquad . \qquad . \qquad . \qquad . \qquad (3)$$

The stirrups are here spaced V = the arm of the resistance moment apart, and the diagonal force in the concrete is assumed to be inclined at 45°. If an intermediate stirrup be introduced between each existing stirrup, as shown at (iv) Fig. 429, this is equivalent to superposing a second web system on the first, and the double web system will carry a shearing force S of twice the magnitude of the single system ; $S = 2a_s f_t$. If now n intermediate stirrups be introduced, spaced at a distance $\cdot p = V/(n + 1)$ apart, the total shearing force which the system will carry will be $S = (n + 1) a_s f_t$. But $(n + 1) = V/p$, hence

$$\frac{V}{p} a_s f_t \; ; \; \text{or,} \; a_s f_t = \frac{S}{V} p = \qquad . \qquad (4)$$

This formula may be written in a different way. Suppose that at two sections of the beam, p apart, the respective bending moments are M_1 and M_2, and that the corresponding stresses in the tensile reinforcement are f_1 and f_2. Then

$$\frac{M_2}{V} - \frac{M_1}{V} = a_t f_2 - a_t f_1 \; : \; sp = S,$$

for $(a_t f_2 - a_t f_1)$ is the increase in the tensile force in a length p. Hence, from eq. (3),

$$a_s f_t = \frac{M_2 - M_1}{V} \qquad . \qquad . \qquad . \qquad . \qquad (5)$$

From either eq. (4) or (5) the pitch and area of the stirrups can be found (see the worked example, § 319).

If both stirrups and diagonal bars be provided, Fig. 435, the safe shearing force which the combination will carry is the addition of the safe shearing force on each system.

When the beam is continuous over a support, the reinforcement will be arranged after the manner shown in Fig. 431, the shearing force being carried by diagonal bars and vertical stirrups as before. The diagonal bars are carried over the supports to act as the tensile reinforcement at the top of the beam, in order to withstand the reversed bending moment at the supports. Such beams are often provided with a haunch as shown in Fig. 431. Owing to its inclination, the compressive force in the haunch helps to resist the shearing action at the ends of the beam. If F_c be the compressive force in the haunch, its vertical component will be $F_c \sin \theta$, which is the shearing force carried by the haunch. The inclination θ should not exceed $30°$.

In designing shear reinforcement the following points should be noted. This reinforcement should extend from the tensile reinforcement at least to the centre of pressure of the concrete in compression. Stirrups should be passed round the tensile reinforcement and hooked over longitudinal bars provided for the purpose in the compression area, (vii) Fig. 429, or
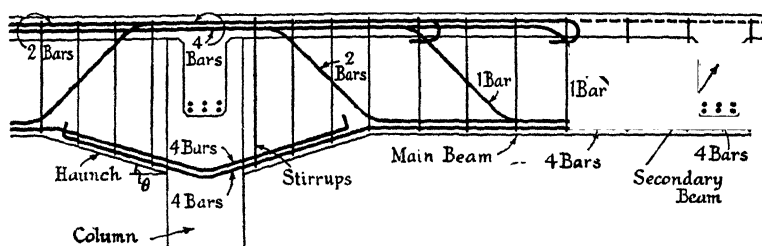
FIG. 431.

else passed round both the tensile and compressive reinforcement as shown in (viii) Fig. 429. This serves the additional purpose of preventing the compressive reinforcement from buckling. The ends of diagonal reinforcement should be hooked, (i) and (iii) Fig. 429, unless it is carried over a support as shown in Fig. 431, or otherwise provided with an effective anchorage. To obviate too great a compressive stress on the concrete at the bend, the radius of a bar where it is turned up to form the diagonal should not be too sharp, say from 4ϕ to 6ϕ. The distance centre to centre of the stirrups should not exceed the arm of the resistance moment. They must of course be placed closer together if required to carry the shearing force. If in a slab or beam the concrete alone will carry the shearing force, the tensile reinforcement should be carried to the ends of the beam and, for preference, one-half the bars should be bent up in the form of shear resistance.

319. Design for a Slab and Beam Floor.—As a simple example of reinforced-concrete design, the calculations for a warehouse floor to carry 200 lb./sq. ft. will be outlined. The arrangement proposed is shown in Fig. 433. Beams, spaced 10 ft. centres, and resting on 18-in. brick walls, support the floor slabs ; the slab reinforcement runs at right angles

to the beams. A granolithic finish, 1 inch thick, applied after the slabs have hardened, is to be provided. A 1 : 2 : 4 Portland cement concrete will be used, and the normal working stresses of § 309 adopted.

Design of the Floor Slabs.—The weight per square foot carried by the floor slabs is estimated to be :

Applied load	200
5 in. reinforced-concrete at 144 lb./cub. ft.	60 (assumed)
1 in. granolithic finish, at 12 lb./sq. ft.	12
Total	272 lb./sq. ft.

A strip of the floor slab, 1 ft. wide, may be regarded as a continuous beam resting on the walls at the extreme ends of the building and continuous over the floor beams. According to the conventional rules, for the intermediate spans the slab must be designed to carry a bending moment of WL/12 at both ends and middle of the span, which moment·
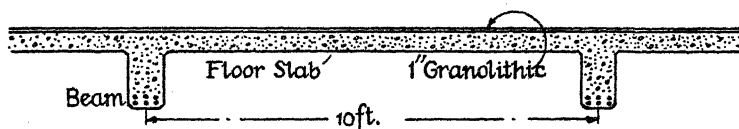
FIG. 433.

must be increased to WL/10 for the end spans, since the end span is merely supported at the extreme end. Dealing with an intermediate span, L = 10 ft.,

$$W = 1 \times 10 \times 272 = 2720 \text{ lb.}$$
$$WL/12 = (2720 \times 10 \times 12) \div 12 = 27200 \text{ in.-lb.}$$

If $f_c = 750$; $f_t = 18{,}000$ lb./sq. in. ; and $m = 18$; from eq. (10a), § 311, since $b = 12$ in.,

$$M = WL/12 = 137 \cdot 7bd^2 = 27{,}200$$
$$d^2 = 27{,}200 \div (137 \cdot 7 \times 12), \text{ and } d = 4 \cdot 1 \text{ in.}$$

Assuming an overall depth of slab of 5 in., ½ in. diameter bars, and ½ in. cover (see § 308), the effective depth will be 4¼ in., or slightly deeper than is required. $\dfrac{M}{bd^2} = \dfrac{27{,}200}{12 \times 4 \cdot 25^2} = 125 \cdot 5$; and from Fig. 422, $\rho = 0 \cdot 812$ and $v_c = 0 \cdot 414d = 1 \cdot 76$ in. ; whence, from eq. (11), § 311,

$$a_t = \frac{\rho b d}{100} = \frac{0 \cdot 812 \times 12 \times 4 \cdot 25}{100} = 0 \cdot 42 \text{ sq. in. per ft.}$$

It will be found that ½ in. diameter bars, spaced 5½ in. centres, will give this area. These will be arranged as shown in Fig. 434. To carry the reversed bending moment at the ends of the span, the same number of bars will be required as at the centre. This is accomplished by bending up every alternate bar of the adjacent spans. These bars are carried over the supports and about one-quarter the way along the adjacent span as shown. In addition, transverse bars, ⅜ in. diameter,

spaced about $4d = 17$ in. apart, should be provided in the positions indicated, to help distribute the load and prevent cracks.

From eq. (2), § 317, the maximum shear stress in the concrete at the ends of the span is $f_s = S \Big/ b \left(d - \dfrac{t_c}{3}\right)$. Taking $S = W/2 = 1360$ lb.,

$$f_s = \frac{1360}{12(4 \cdot 25 - 1 \cdot 76/3)} = 31 \text{ lb./sq. in.},$$

which is well within the allowed shear stress of 75 lb./sq. in. No reinforcement against shear, therefore, is necessary.

To carry the increased bending moment $WL/10$ in the end spans, the slab must be made thicker, or the pitch of the reinforcement may be reduced.
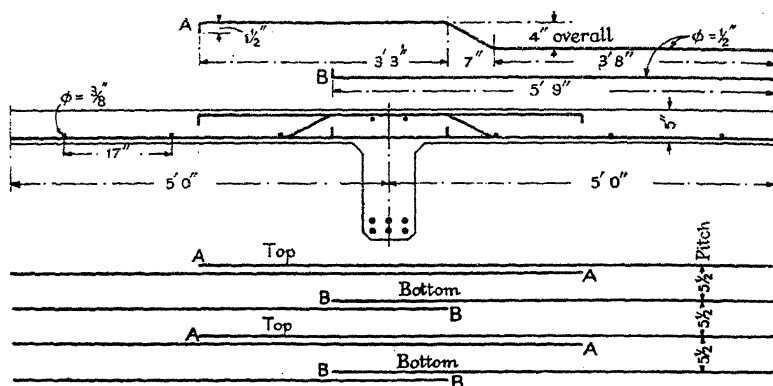
FIG. 434.

Design of the Floor Beams.—Assuming that the weight of the ribs of these beams is 120 lb./ft., the total load per ft. on a beam (at 10 ft. spacing) is

$$10 \times 1 \times 272 + 120 = 2840 \text{ lb.}$$

The clear width between the walls is 16 ft., hence the load on the beam is $16 \times 2840 = 45,440$ lb., and the maximum shearing force is 22,720 lb. Assuming that the beams are carried $13\frac{1}{2}$ in. into the brick wall at each end, the actual span is $12 \times 16 + 13\frac{1}{2} = 205\frac{1}{2}$ in. The bending moment at the centre of the span is

$$\frac{45,440 \times 205\frac{1}{2}}{} \quad \frac{45,440 \times 16 \times 12}{} \quad 1,243,920 \text{ in.-lb.}$$

The shearing-force and bending-moment diagrams are shown in Fig. 435. From the rules given in § 313, the width of slab which may be counted in as forming part of this T beam is

$$12D + b_1 = 60 + 8 = 68 \text{ in.}$$

Using eq. (10a), § 311, as a first approximation, $M = 137 \cdot 7bd^2 = 1,243,920$,

where $b = 68$, hence $d = 11 \cdot 6$ in.; also $a_t = bd/112 = 7 \cdot 04$ sq. in. Eight $1\frac{1}{16}$ bars would be required. Although this is a possible section, a much more practical design will be obtained by increasing the depth.
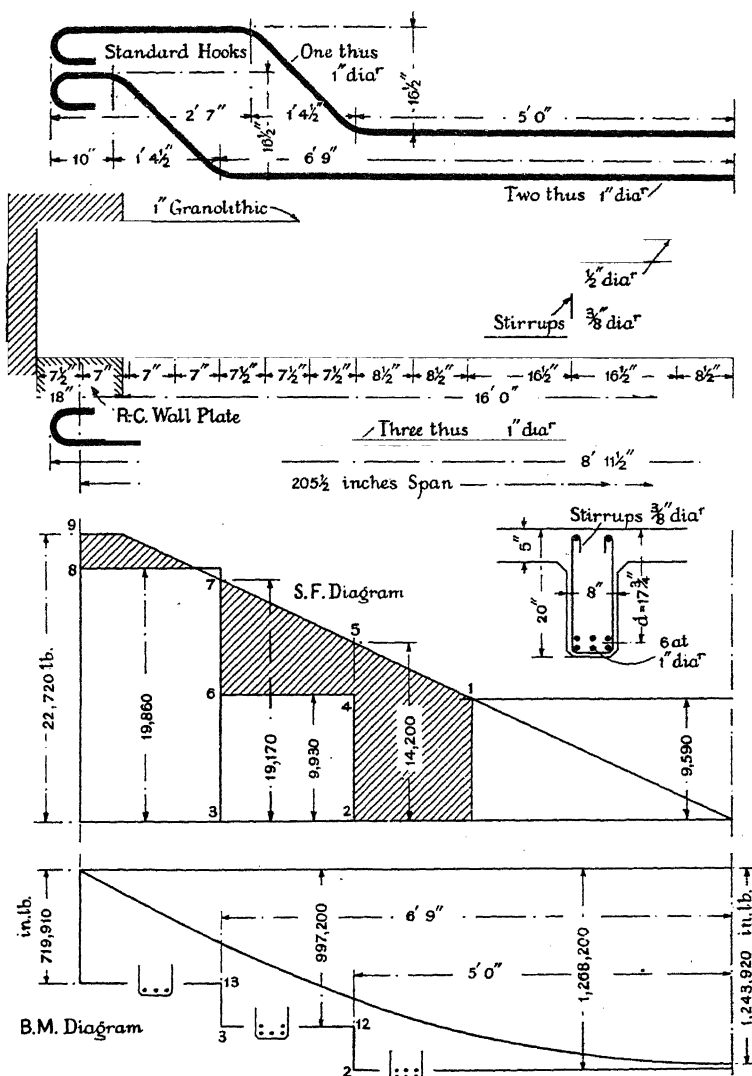
FIG. 435.

Try $V = 16$ inches. Then $a_t = \dfrac{1,243,920}{16 \times 18,000} = 4 \cdot 4$ sq. n. Either 8 bars $\frac{7}{8}$ in. diameter, or 6 bars 1 in. diameter, would be suitable. Choosing the latter alternative, try the section shown in Fig. 435. From eq. (2),

§ 317, the shear stress in the rib of the beam is $f_s = S/b_1 V$, which must in no circumstances exceed $4 \times 75 = 300$ lb./sq. in. Hence b_1, the width of the rib, must be at least

$$b_1 : \frac{22,720}{16 \times 300} = 4 \cdot 8 \text{ in.}$$

From eq. (4), § 317, if f_s' be limited to 2×100 lb./sq. in.,

$$\Sigma q : \frac{S}{V f_s'} = \frac{22,720}{16 \times 2 \times 100} = 7 \cdot 1 \text{ in.}$$

If the three bottom bars are carried to the ends of the beam, their perimeter is $9 \cdot 42$ in., so that the proposed section is quite suitable in these two respects. A breadth of 8 in. is sufficient to contain the bars and give the prescribed clearances.

The moment of resistance of the cross-section is calculated as follows : Since the neutral axis falls below the slab, the whole depth D will be counted in as forming the compression area. Take moments about the top of the beam.

Part.	a'	m	ma'	h'	mah'	$ma'(h')^2$	mI'
Concrete in compression, 68 × 5	340	1	340·0	$2\frac{1}{2}$	850·0	2,125·0	708·4
Steel in tension (upper)	2·34	18	42·1	17	715·7	12,166·9	—
Steel in tension (lower)	2·34	18	42·1	$18\frac{1}{2}$	778·8	14,407·8	—
			424·2		2,344·5	28,699·7	708·4

$$v_c = \frac{2344 \cdot 5}{424 \cdot 2} = 5 \cdot 53 \qquad\qquad v_t = 18 \cdot 5 - 5 \cdot 53 = 12 \cdot 97$$

$$I_c = 28,699 \cdot 7 + 708 \cdot 4 - (2344 \cdot 5^2 \div 424 \cdot 2) = 16,450$$

$$Z_t = \frac{16,450}{18 \times 12 \cdot 97} = 70 \cdot 46 ; \text{ Safe M} : = f_t Z_t = 18,000 \times 70 \cdot 46 = 1,268,200 \text{ in.-lb.,}$$

which is sufficient. After turning up one of the upper layer of bars, safe M = 997,200 in.-lb., and when all three bars of the upper layer are turned up, safe M = 719,910 in.-lb. ; $v_c = 4 \cdot 21$, and V = $17 \cdot 1$ in., which is satisfactory. Lines representing these moments are plotted on the bending-moment diagram, Fig. 435, and determine the positions of the turning-up points.

From eq. (15), § 317, if the maximum shearing stress in the concrete be limited to 75 lb./sq. in., the safe shearing force near the centre of the beam, without shear reinforcement, is

$$S = \frac{b_1 I_c f_s}{m \Sigma a_t v_t} = \frac{8 \times 16,450 \times 75}{18 (2 \cdot 34 \times 12 \cdot 97 + 2 \cdot 34 \times 11 \cdot 47)} = 9590 \text{ lb.}$$

The approximate value of V for the central cross-section is (mean $d - v_C/3$) $= 17 \cdot 75 - 5 \cdot 53/3 = 15 \cdot 91$ in. Hence, from eq. (2), § 297,

$$S = b_1 V f_s = 8 \times 15 \cdot 91 \times 75 = 9550 \text{ lb.,}$$

which checks the above figure.

The horizontal line representing this shearing force cuts the S.F. diagram at the point 1, which is 3 ft. 5 in. from the centre. Over the middle 6 ft. 10 in. of the beam, therefore, the stirrups can be spaced at their maximum pitch $= V$, say about 16 in. apart. One bar of the top layer of reinforcement can be bent up at 45° at the point 2, which is 5 ft. from the centre, and the other two bars at the point 3, which is 6 ft. 9 in. from the centre. It will be seen from the B.M. diagram that points 12 and 13 are well outside the curve; and, from the elevation, that the arrangement forms a suitable truss. Applying the test of Fig. 430, it will be found that it is safe to stress the turned-up bars to 18,000 lb./sq. in. Hence from eq. (1), § 318, the shearing force one bar will carry (area of bar $0 \cdot 78$ sq. in., $\theta = 45°$) is

$$S = a_s f_t \sin \theta = 0 \cdot 78 \times 18,000 \times 0 \cdot 707 = 9930 \text{ lb.,}$$

represented in the S.F. diagram by the area 2.6; and, where two bars turn up, twice this value, represented by the area 3.8. The shearing force which must be carried by the stirrups is indicated by the shaded area. From eq. (4), § 318, $\frac{3}{8}$ in. diameter stirrups with two verticals (area $2 \times 0 \cdot 11$ sq. in.), p inches apart, will carry a shearing force of

$$S = \frac{V}{p} a_s f_t = \frac{15 \cdot 91}{p} \times 0 \cdot 22 \times 18,000 = \frac{63,010}{p} \text{ lb.}$$

A convenient arrangement of stirrups is shown in Fig. 435. At $8\frac{1}{2}$ in. pitch a two-branch stirrup will carry a shearing force of $63,010 \div 8\frac{1}{2} = 7,413$ lb., so that if the stirrup at 2.5 is assumed to carry the whole shearing force of 14,200 lb., a double (four-branch) stirrup must be used. At $7\frac{1}{2}$ in. pitch a two-branch stirrup will carry 8,400 lb., and a four-branch stirrup will also be necessary at 6.7.

320. **Design for a R.-C. Retaining Wall.**—The wall is to support a bank of earth sloping upward with a gradient of 1 : 2 from the top of the wall, which is 25 feet above ground level. The earth weighs 100 lb./cub. ft., and its natural slope is 35°. The soil on which the foundations rest is capable of carrying a pressure of 2 tons/sq. ft. A 1 : 2 : 4 Portland cement concrete will be used, and the following working stresses adopted: $f_c = 750$ lb./sq. in.; $f_t = 18,000$ lb./sq. in.

1. *Proportions.*—The foundations will be carried down 4 ft. below the ground level on account of frost, so that the total height of the wall will be $25 + 4 = 29$ ft. For a wall of this height a counterfort design will be the most economical. The width of the base will be taken as $0 \cdot 6$ of the height of the wall, $29 \times 0 \cdot 6 = 17$ ft., and the vertical face will be set back $0 \cdot 3$ of the width of the base, $0 \cdot 3 \times 17 = 5$ ft. These are normal proportions for such a wall. The proposed outline will then be as shown in Fig. 436.
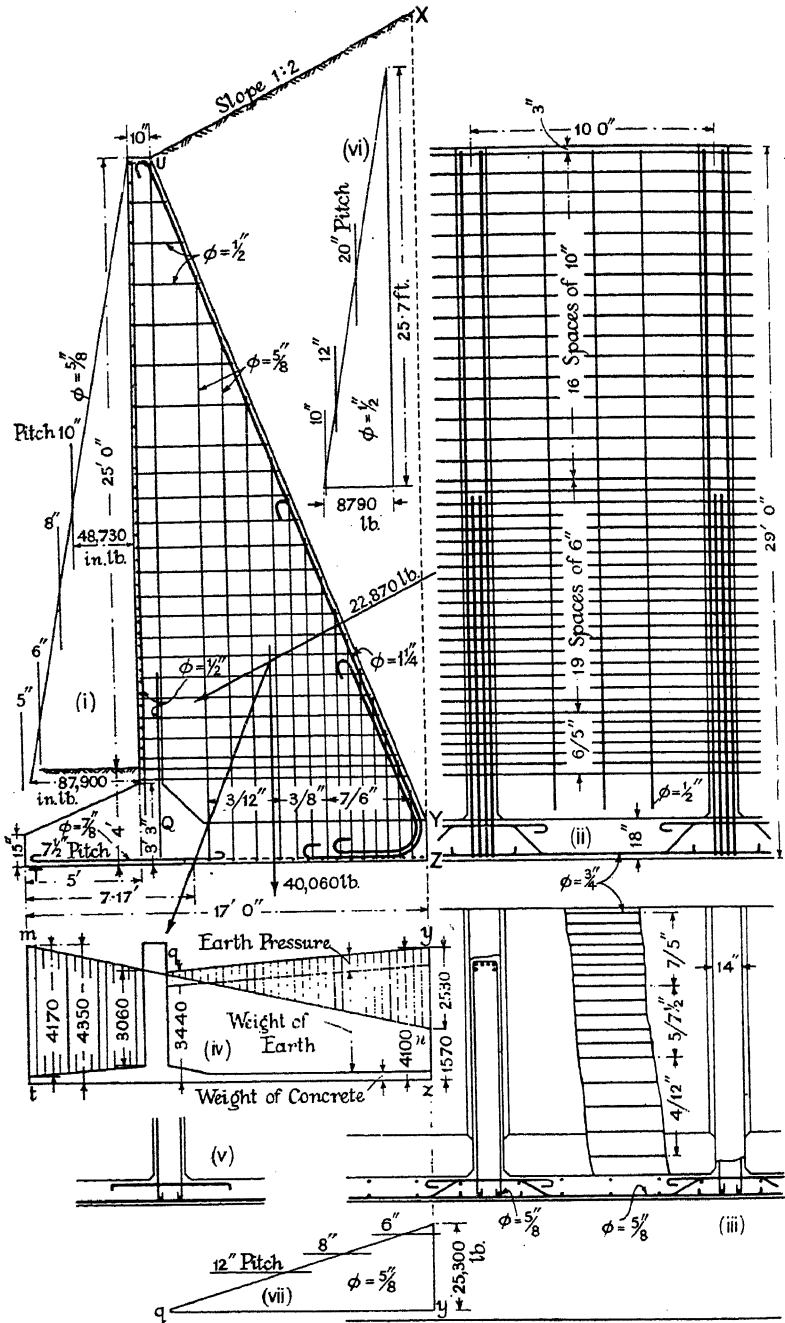
FIG. 436.

2. *Earth Pressure.*—The pressure on the back of the wall will be found from the Rankine theory given in § 325. In this example, $\tan \alpha = 1/2$; $\alpha = 26° 34'$; $\phi = 35°$; and from eq. (3), § 325, or from the construction given in Fig. 447, $\dfrac{p'}{p} = 0 \cdot 427$, and $p' = 0 \cdot 427 wh \cos \alpha = 0 \cdot 427 \times 100 \times 0 \cdot 894h = 38 \cdot 2h$ lb./sq. ft., where h is the depth below the surface.

This is the pressure parallel to the sloping upper surface. The corresponding pressure normal to the back of the wall is

$$p' \cos \alpha = 38 \cdot 2 \times 0 \cdot 894h = 34 \cdot 2h \text{ lb./sq. ft.}$$

3. *Vertical Wall.*—Suppose the counterforts to be placed L ft. centre to centre, and consider a strip of the vertical wall as a beam spanning from counterfort to counterfort. If the strip be 1 ft. wide and h ft. below the top of the wall, the load on it will be

$$W = L \times 1 \times 34 \cdot 2h = 34 \cdot 2Lh \text{ lb.}$$

Since the strip is continuous over many spans, it may be regarded as a continuous beam, when the maximum bending moment anywhere will be WL/12. For end bays, or where, due to expansion joints or otherwise, the continuity is lost, the maximum bending moment must be taken as WL/10, or else properly determined. For the normal bays,

$$M = \frac{WL}{12} = \frac{34 \cdot 2Lh \times 12L}{12} = 34 \cdot 2L^2h \text{ in.-lb.}$$

Suppose that at a point just above the toe, where $h = 25 \cdot 7$ ft., both steel and concrete work at their maximum permitted stresses. Then, for single reinforcement, from eq. (10a), § 311, if $m = 18$, $M = 137 \cdot 7bd^2$, where in this case $b = 12$ inches. Hence,

$$34 \cdot 2L^2 \times 25 \cdot 7 = 137 \cdot 7 \times 12 \times d^2 ; \text{ and } L = 1 \cdot 37d.$$

For a wall of the dimensions under consideration, the spacing of the counterforts would range from 8 to 10 ft., and the total thickness of the wall would normally not be less than 10 in. When an ordinary 1 : 2 : 4 concrete is used, it is customary in structures like retaining walls, which are continuously exposed to wet, to allow a thicker cover for the reinforcement than is usual in buildings; say $1\frac{1}{2}$ to 2 in. in a case like the present. For a wall 10 in. thick, therefore, d might be taken as 8 in., when $L = 8 \times 1 \cdot 37 = 10 \cdot 9$ ft. Alternatively, if $L = 10$ ft., $d = 7 \cdot 3$ in., not a very different value. As a practical compromise, a thickness of 10 in., with a spacing of counterforts of 10 ft., will be adopted ; the wall will be kept of uniform thickness top to bottom, i.e. not less than 10 in., but the steel bars will be spaced out towards the top, as the load and bending moment fall off. Assume $\frac{5}{8}$ in. diameter as the size of the reinforcement, area $0 \cdot 307$ sq. in., and let p be the required pitch of the bars at any point y ft. from the top. Then the area of the steel per 12 in. of depth is $0 \cdot 307 \times 12 \div p = 3 \cdot 684/p$. Allowing $1\frac{1}{2}$ in. of cover for the $\frac{5}{8}$ in. bars, the value of d will be $(10 - 1\frac{1}{2} - \frac{5}{16}) = 8 \cdot 18$ in. ; $bd = 12 \times 8 \cdot 18$, and the percentage reinforcement will be

$$\rho = (100 \times 3 \cdot 684) \div (12 \times 8 \cdot 18 \times p) = 3 \cdot 753/p,$$

or if	p	5	6	8	10
	ρ	0·751	0·626	0·469	0·375
	$\dfrac{M}{bd^2}$	117·2	98·5	75·1	60·7
	M	94,120	79,090	60,300	48,730

The third line in this Table is obtained from Fig. 422, using the value of ρ in the second line, or may be calculated from eqs. (1) and (2), § 312. The value of M in the fourth line follows from the known values of b, d, and f_t : $b = 12$; $d = 8·18$; $f_t = 18,000$ lb./sq. in. The proper arrangement of bars may be determined graphically, (i) Fig. 436. The bending moment M $= 34·2$ L$^2h = 3,420h$ in.-lb. ; this is represented by a triangle, the ordinate of which at $h = 25·7$ ft. is 87,900 in.-lb. If the safe bending moment for each different pitch of bars, from the Table above, be plotted on this diagram, the necessary extent of each pitch is evident, and the bars can be arranged accordingly. Since the pressure is on the back of the wall, the face of the wall will be in tension near the centre of the span, and in compression opposite the counterforts. The bars should therefore be bent as shown in (iii) Fig. 436. To obviate bending the bars, the main reinforcement is sometimes run right through at the face of the wall, and a second set of longitudinal bars is provided at the counterforts to carry the tensile stress there, (v) Fig. 436.

The counterforts will be made 14 in. wide (see below). Hence the maximum shearing force on a vertical strip of wall, 1 ft. wide, just above the toe, is

$$\tfrac{1}{2} \times 34·2 \ (\text{L} - 1·16)h = \tfrac{1}{2} \times 34·2(10 - 1·16)25·7 = 3890 \ \text{lb.}$$

The allowable shear stress on a 1 : 2 : 4 concrete is 75 lb./sq. in., and the actual shear stress given by eq. (2), § 317, is

$$f_s = \frac{\text{S}}{b(d - v_c/3)} = \frac{3890}{12(8·18 - 0·134 \times 8·18)} = 45·8 \ \text{lb./sq. in.}$$

for, from Fig. 422, when $\rho = 0·751$, $v_c = 0·402d$. No shear reinforcement, therefore, is required, for the stress gets smaller higher up the wall. Had the allowable shear stress been exceeded, it would have been more economical to thicken the wall than to introduce stirrups. The thickness could then have been reduced higher up the wall as the stress falls off.

4. *Pressure on the Base.*—In order to design the base of the wall, and the counterforts, it is first necessary to estimate the pressure on the bottom and top of the base. The weight and centre of gravity of the wall proper, per foot of length, is calculated as follows, moments being taken about the front of the toe T.

	Cub. ft.	Leverage.	Moment.
Toe	11·25	2·87	32·3
Vertical Wall . . .	24·17	5·42	131·0
Base Slab and Fillet . .	18·28	11·0	201·1
One-tenth of the Counterfort	17·91	9·56	171·2
	71·61	(7·48)	535·6

Weight $= 71·61 \times 144$ 10,310 lb.

C. of G. $= \dfrac{535·6}{71·61} = 7·48$ ft. from the front of the toe T.

The weight of the superincumbent earth, UY, (i) Fig. 436, on the base is 29,750 lb. ; its C. of G. lies $11 \cdot 61$ ft. from the front of the toe T. The total earth pressure on the surface XZ, (i) Fig. 436 [cf. eq. (2), § 327], is

$$\mathrm{P}' = \int_0^{\mathrm{H}} p' \cdot dh = 38 \cdot 2 \int_0^{\mathrm{H}} h \cdot dh = \frac{38 \cdot 2}{2} \times (34 \cdot 6)^2 = 22{,}870 \text{ lb.,}$$

since $p' = 38 \cdot 2h$ lb./sq. ft., and $\mathrm{H} = 34 \cdot 6$ ft. The horizontal component of $\mathrm{P}' = \mathrm{P}' \cos 26° 34' = 20{,}460$ lb. The vertical component of $\mathrm{P}' = \mathrm{P}'$ $\sin 26° 34' = 10{,}230$ lb. The horizontal component acts $34 \cdot 6 \div 3$ $= 11 \cdot 53$ ft. up from Z ; the vertical component acts through Z. Taking moments about T,

	lb.	ft.	ft.-lb.
Wall	10,310	7·48	77,120
Earth	29,750	11·61	345,400
	40,060	10·54	422,520
Vertical Component of Earth Pressure	10,230	17·0	173,910
	50,290		596,430

Less moment of horizontal component of earth pressure, $20{,}460 \times 11 \cdot 53$ . . . $235{,}900$

Total moment about T . . $= 360{,}530$

The resultant cuts the base line at $\dfrac{360{,}530}{50{,}290}$ $7 \cdot 17$ ft. from T.

This point lies well within the middle third of the base. The graphical confirmation of this calculation is given in (i) Fig. 436.

'Factor of Safety' against overturning $= \dfrac{596{,}430}{235{,}900} - 2 \cdot 53$.

Eccentricity $= e = \dfrac{17}{2} - 7 \cdot 17 = 1 \cdot 33$ ft.

From eqs. (3) and (4), § 354, the maximum and minimum pressures on the underside of the base (max. allowable $= 2$ tons/sq. ft.) are

$$p = \frac{\mathrm{W}}{a}\left\{1 \pm \frac{6e}{\mathrm{D}}\right\} = \frac{50{,}290}{17 \times 1}\left\{1 \pm \frac{6 \times 1 \cdot 33}{17}\right.$$

$p_{\max.} = 4350$ lb./sq. ft. ; $p_{\min.} = 1570$ lb./sq. ft.

The variation in pressure is shown by the figure *tmnz*, (iv) Fig. 436.

The pressure acting downward on the base slab is made up of three parts : (i) its own weight ; (ii) the weight of the superincumbent earth ; (iii) the vertical component of the pressure p' acting on the top of the slab. The slab is 18 in. thick, hence its own weight is $18 \times 144 \div 12 = 220$ lb./sq. ft. The depth of the earth at Q is $27 \cdot 5$ ft., it weighs 100 lb./cub. ft., hence the pressure on the slab is 2750 lb./sq. ft. At Y the depth is $33 \cdot 1$ ft., hence the pressure is 3310 lb./sq. ft. The vertical component of the pressure p' is $38 \cdot 2h(\sin 26° 34')$. At Q, $h = 27 \cdot 5$ ft. and the vertical component $= 470$ lb./sq. ft. ; at Y, $h = 33 \cdot 1$ ft. and the vertical component $= 570$ lb./sq. ft. These pressures are also plotted in (iv)

Fig. 436 ; their sum at Q is $220 + 2750 + 470 = 3440$ lb./sq. ft. ; and at Y is $220 + 3310 + 570 = 4100$ lb./sq. ft. The difference between the upward and downward pressure on the base slab is represented by the shaded figure in (iv), and reaches a maximum of 2530 lb./sq. ft. at Y. The slab must be designed to carry this load.

5. *Base Slab.*—The thickness of this slab has been assumed to be 18 in. ; the shear stress in the concrete will usually be the determining factor. Considering a strip 1 ft. wide at the edge Y of the slab, where the load is 2530 lb./sq. ft., the maximum shearing force on the strip is

$$\tfrac{1}{2} \times 2530(10 - 1\cdot16) = 11,180 \text{ lb.}$$

Assuming that $v_c = 0\cdot43d$, and that the lever arm $V = 0\cdot86d$; from eq. (2), § 317, if the shear stress is not to exceed 75 lb./sq. in.,

$$d = \frac{11,180}{12 \times 0\cdot86 \times 75} = 14\cdot5 \text{ in.}$$

An overall depth of 18 in. as assumed will be ample.

The total load on the above strip, considering it as a continuous beam of 10 ft. span, is $10 \times 1 \times 2530 = 25,300$ lb. ; and the maximum bending moment, $WL/12$, is

$$M = \frac{25,300 \times 10 \times 12}{12} = 253,000 \text{ in.-lb.}$$

whence, $\dfrac{M}{bd^2} \quad \dfrac{253,000}{12 \times (16\cdot0)^2} = 82\cdot4$

for d may be taken as $16\cdot0$ in. From Fig. 422, $\rho = 0\cdot522$ % ; whence

$$a_t = \frac{\rho bd}{100} = \frac{0\cdot522 \times 12 \times 16\cdot0}{100} = 1\cdot01 \text{ sq. in. per foot.}$$

Bars $\tfrac{3}{4}$ in. diameter (area 0·442 sq. in.) at 5 in. pitch will provide this area ; as shown in Fig. 436, this pitch may be increased to 12 in. as the pressure falls off towards Q. A diagram similar to that for the vertical wall (i) will serve to fix the proper spacing. As the bottom of the slab near the centre of the span will be in tension, and opposite the counterforts will be in compression, the bars should be bent as shown in (ii) Fig. 436. Alternatively, a second set of reinforcement might be provided at the counterforts, as indicated in (v) Fig. 436.

6. *Counterforts.*—These may be regarded as cantilevers projecting 27·5 feet above the base slab, and supporting an area $10 \times 27\cdot5$ sq. ft. of vertical wall against the horizontal component of the earth pressure, viz. $p' \cos a = 34\cdot2h$ lb./sq. ft. The total horizontal pressure on this area is $P' \cos a = \tfrac{1}{2}p'H^2 \cos a = \tfrac{1}{2} \times 34\cdot2 \times 27\cdot5^2 \times 10 = 129,320$ lb. This force acts at a point 9·17 ft. ($\tfrac{1}{3}$ the way up) above the base plate. The moment it produces is resisted by a tee beam, shown in (iii) Fig. 436. The arm of the resistance moment at the base, measured at right angles to the reinforcement [see (i) Fig. 416], is approximately 10·4 ft. Hence

the force in the tensile reinforcement is $F = (129{,}320 \times 9 \cdot 17) \div 10 \cdot 4$ lb., and at 18,000 lb./sq. in. the area required is

$$at \quad \frac{129{,}320 \times 9 \cdot 17}{10 \cdot 4 \times 18{,}000} = 6 \cdot 34 \text{ sq. in.}$$

Six $1\frac{1}{4}$-in. diameter bars, giving an area of $7 \cdot 32$ sq. in., will be required, arranged in two layers, 4 in the outer and 2 in the inner layer. The points to which the bars must extend can be determined from the bending-moment diagram, (i) Fig. 437, a cubic parabola, maximum ordinate $129{,}320 \times 9 \cdot 17 = 1{,}185{,}860$ ft./lb. If $F_V = F \cos \chi$, (ii) Fig. 437, be the vertical component of the force in the tensile reinforcement, the bending moment at any horizontal section is $F_V h$, where h is the horizontal arm of the resistance moment (cf. § 180). Plot a diagram showing $F_V = M/h$ at every cross-section, (i) Fig. 437, maximum ordinate $= 1{,}185{,}860 \div 11 \cdot 3 = 104{,}940$ lb.; the value of F_V per $1\frac{1}{4}$ in. bar is $F_V = a_t f_t \cos \chi = 1 \cdot 22 \times 18{,}000 \times 0 \cdot 926 = 20{,}330$ lb. If a series of lines be plotted from the base line of (i), representing the value of 2, 4, and 6 bars, the necessary length of the bars is at once determined. Strictly speaking, the counterfort is equally a cantilever projecting from the vertical wall and supporting the base slab, and the lower portion of the counterfort reinforcement should be designed from this point of view, but it is customary to anchor all the reinforcement in the base slab, as indicated in (i) Fig. 436.
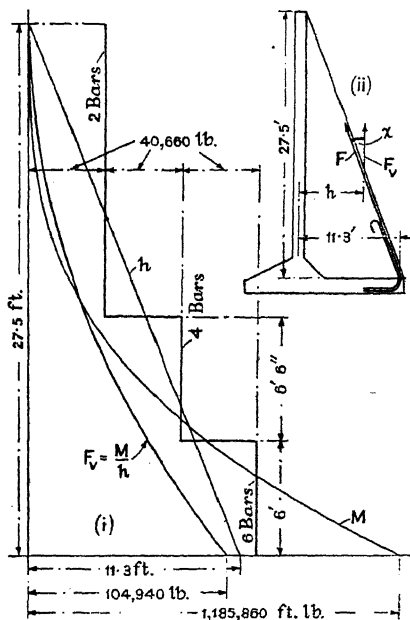
FIG. 437.

It has been assumed in the above calculation that the compressive stress in the concrete is within the permitted limits. At a point $25 \cdot 7$ ft. from the top of the wall, the value of F_V from the diagram is 91,650 lb. To this must be added the vertical component of the pressure acting on the face of the wall, which is

$$P' \sin \alpha = \tfrac{1}{2} \times 38 \cdot 2 \times 25 \cdot 7^2 \times 10 \times 0 \cdot 447 = 56{,}390 \text{ lb.}$$

Hence the total vertical compressive force on the compression flange of the counterfort is $91{,}650 + 56{,}390 = 148{,}040$ lb. Counting in the whole 10 ft., the area carrying this force is 120×10 sq. in. and the compressive stress in the concrete is only $f_c = \dfrac{148{,}040}{120 \times 10} = 124$ lb./sq. in.

The maximum shear stress in the counterfort rib can be found thus : At 25·7 ft. below the top, the total shearing force on the rib is

$$P' \cos a = \tfrac{1}{2} \times 38 \cdot 2 \times 25 \cdot 7^2 \times 10 \times 0 \cdot 894 = 112,780 \text{ lb.}$$

Subtract the component perpendicular to the wall of the force in the tension flange, which is

$$F \sin \chi = F_V \tan \chi = 91,650 \times 0 \cdot 406 = 37,210 \text{ lb.,}$$

and the shearing force to be resisted by the web is $112,780 - 37,210 = 75,570$ lb. From eq. (2), § 317, the maximum shear stress is

$$f_s = \frac{S}{b_1(d - D/2)} = \frac{S}{b_1 V} \quad \frac{75,570}{14 \times 126 \cdot 7} = 43 \text{ lb./sq. in.}$$

No stiffening for shear proper is therefore necessary, but ties must be provided to carry the tensile stress between the wall and the rib, and that between the rib and the base slab. These ties will be carried right round the main tensile reinforcement in the rib, and anchored round bars in the slabs. The load per foot of height, tending to part the vertical wall from the rib, is $34 \cdot 2 \times h \times 10 \times 1 = 342h$ lb./ft. The diagram showing the variation in this load will be a triangle, (vi) Fig. 436, maximum ordinate $= 8790$ lb. The safe tensile load on a two-branch stirrup, $\tfrac{1}{2}$ inch in diameter, is $2 \times 0 \cdot 196 \times 18,000 = 7060$ lb. If these be spaced p inches apart, the safe load per foot of height is $7060 \times 12/p$ lb. If lines corresponding to different values of p be plotted, the necessary pitch of stirrups is easily determined. A similar diagram will determine the pitch of the vertical stirrups, (vii) Fig. 436. The load ranges from 0 at q to 2530 lb./sq. ft. at y, (iv) Fig. 436.

7. *Toe.*—The toe forms a cantilever projecting 5 ft. from the vertical wall and loaded with an upward pressure ranging from 4170 lb./sq. ft. at T to 3060 lb./sq. ft. at the face of the wall, (iv) Fig. 436. The load per foot of length of the cantilever is 18,080 lb. ; it acts at 31·5 in. from the face of the wall. Hence $M = 569,600$ in.-lb. ; $b = 12$ in. ; $d = 37$ in. ; and $M/bd^2 = 34 \cdot 7$; $\rho = 0 \cdot 21$ % ; $a_t = \rho bd/100 = 0 \cdot 94$ sq. in. per foot. $\tfrac{7}{8}$-in. bars spaced at $7\tfrac{1}{2}$ in. pitch will provide the necessary area. The shear stress in the toe is small.

321. Reinforced-Concrete Columns.—If a short reinforced-concrete column of length L, such as is shown in Fig. 438, be compressed by a load W, and δL be the contraction in length, the strain everywhere is $\delta L/L$. Hence the compressive stress in the concrete is $E_c \times \text{strain} = E_c \cdot \delta L/L = f_c$. The strain in the longitudinal reinforcement is also $\delta L/L$, and the compressive stress therein is $E_t \cdot \delta L/L = f_c''$. Let A be the area of the column, and a_c the total area of the longitudinal reinforcement. Then the area of the concrete is $(A - a_c)$, and the load which it carries is
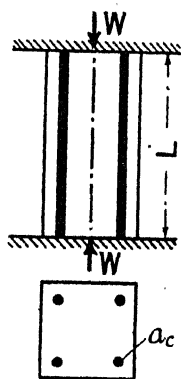
FIG. 438.

$(A - a_c)f_c$; that carried by the steel is $a_c f_c''$. The total load carried by the column is, therefore,

$$(A - a_c)f_c + a_c f_c'' = (A - a_c)\frac{E_c}{T} \cdot \delta L + a_c \frac{E_t}{T} \cdot \delta L = W.$$

Putting $E_t = mE_c$, this reduces to

$$W = \{A - a_c + ma_c\}\frac{E_c}{L} \cdot \delta L = \{A + (m - 1)a_c\}f_c \qquad (1)$$

for $\frac{E_c}{L} \cdot \delta L = f_c$. It follows that

$$\delta L = \frac{f_c L}{E_c} = \frac{WL}{E_c\{A + (m - 1)a_c\}} = \frac{f_c'' L}{E_t} \qquad (2)$$

and

$$f_c'' = mf_c \qquad . \qquad . \qquad . \qquad (3)$$

Such an elementary member as is discussed above would not be suitable for practical columns, in which the longitudinal bars are of considerable length compared with their diameter, and it is necessary to tie them together with lateral binding to prevent buckling. Further, questions of creep and shrinkage, §§ 303 and 304, come into consideration.

For the safe load on axially loaded columns $(qL/D < 15)$ with lateral ties, Fig. 440, the L.C.C. Code of Practice lays down certain rules which may be expressed by the following formulae :

$$W = 0 \cdot 8f_c(A - a_c) + \tfrac{3}{4}a_c f_t \qquad . \qquad . \qquad (4)$$

where W denotes the safe axial load, f_c and f_t the permitted stresses in bending (see § 309), A the area of the column proper, and a_c the total area of the longitudinal steel.

When the lateral reinforcement takes the form of a continuous helix, Fig. 439, this lateral reinforcement, if of suitable dimensions, tends to prevent the concrete which it encloses from expanding laterally,

FIG. 439.

and, in consequence, the concrete 'core' will safely carry higher stress. The safe axial load is given by the formula

$$W = 0 \cdot 8A_c f_c + \tfrac{3}{2}(a_c/2 + \psi)f_t \qquad . \qquad . \qquad (5)$$

where A_c denotes the area of the core, and ψ the volume of the helix in cubic inches per inch of length of the column. The larger of the values given by eqs. (4) and (5) is to be taken as the safe axial load, which nevertheless is not to exceed $\tfrac{3}{2}(A - a_c)f_c$.

If the length of the column is such that $qL/D > 12$, or $qL/\kappa > 50$, the above values are to be multiplied by a reduction factor χ given by

$$\chi = \tfrac{3}{2} - L/30D = \tfrac{3}{2} - \tfrac{1}{100}L/\kappa \qquad . \qquad . \qquad (6)$$
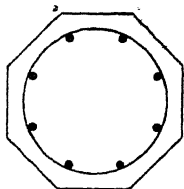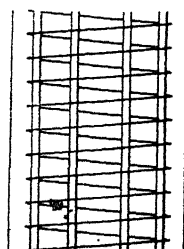
In a column with helical reinforcement, the value of D or κ is to be found from the dimensions of the core.

The above formula may be used for all internal columns supporting an approximately symmetrical arrangement of beams. Where, as in the case of an external column supporting the end of a beam, the column is subjected to a bending moment, it must be designed to resist both the bending moment and the longitudinal load.

The following practical rules regarding the reinforcement of such columns should be observed. The longitudinal bars should not be less than $\frac{1}{2}$ inch diameter, nor greater than 2 inches. There should not be less than four longitudinals in a square, nor six in a column with helical reinforcement. The total area of longitudinal reinforcement should be at least $0\cdot8$ % of the area A, and not more than 8 %. At joints (see Fig. 440), the longitudinals should overlap a distance $l = \frac{1}{4}\phi f_c''/f_s'$, max. $= 24\phi$, where ϕ is the diameter of the bar, f_c'' the compressive stress therein, and f_s' the permitted bond stress. The diameter of any lateral binding should not be less than $\frac{3}{16}$ inch. The pitch of the lateral ties should not exceed the least lateral dimension D, or 12 times the diameter of any longitudinal bar. It should not be greater than 12 inches or less than 6 inches. The pitch of the helix, Fig. 439, should not exceed 3 inches or one-sixth the diameter of the core; it should not be less than 1 inch, or three times its own diameter. The volume of the lateral binding should not be less than $0\cdot4$ % of the gross volume of the column.

Fig. 440 shows a typical reinforced-concrete column as used in the interior of a building, with its footing. The method of attaching the column to the latter by means of splice bars should be observed, and the method of changing section at a floor. The inclined part of the vertical bars should be kept within the region of the floor beams. The arrangement of the lateral binding in an eight-bar column should also be noted.

FIG. 440.

322. Design for a Reinforced-Concrete Arch with Direction-fixed Ends.—1. *Particulars.*—Span 100 feet, width of roadway 20 feet, two 5 feet
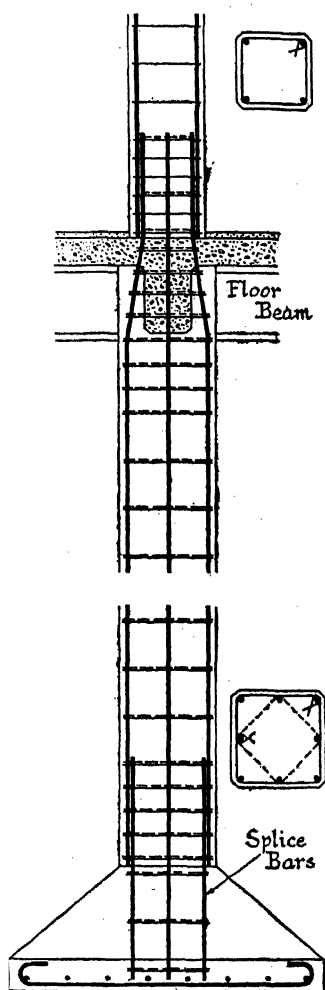
sidewalks. To carry the standard M.T. loading,* see § 23. Foundations in compact gravel, safe bearing pressure = 4 tons/sq. ft. Some regard to appearance is desirable.

2. *Dimensions of Arch.*—The proposed construction is shown in (i) Fig. 441. For a 100-ft. span, an open-spandrel arch will be used, with columns 10 ft. apart. These will be carried by two arched ribs with a ratio rise to span of 1 : 5.

3. *Materials and Stresses.*—To make as light a design as possible, a 180 lb. : 2 : 4 cub. ft. concrete will be used for the arch ribs and roadway, $f_c = 1200$ lb./sq. in. Ordinary B.S. mild steel round bars will be used for the reinforcement, $f_t = 18,000$ lb./sq. in.† ; $m = 10$. For the abutments proper, a 1 : 6 mass concrete will be employed ; and a 90 lb. : 2 : 4 concrete for the abutment walls.

4. *Design of Roadway Slabs.*—As shown in (iii) Fig. 441, the roadway will consist of a continuous slab supported by transverse girders 10 ft. pitch, which are carried by the columns. A 2-in. asphalt wearing surface will be provided. Assume a thickness for the slab of $7\frac{1}{2}$ in. The weight per sq. ft. of the roadway is : 2 in. asphalt = 20 lb. + $7\frac{1}{2}$ in. concrete = 90 lb., total 110 lb. If 6-inch fillets are provided, the span may be taken as the distance between the ribs, viz. $10 - 1 \cdot 17 = 8 \cdot 83$ ft. The slab is continuous over many spans, so that the maximum dead load bending moment per foot of width $= wL^2/12 = 110 \times 8 \cdot 83^2 \div 12 \doteqdot 715$ ft.-lb. From the M.T. curve, Fig. 50, for a loaded span of $8 \cdot 83$ ft., the prescribed live load is 335 lb./sq. ft., plus a knife-edge load of 2700 lb./ft. placed in the worst position, in this case transversely at the centre of the span. These values include impact. The live load bending moment at the centre of the span, per foot of width, is, therefore,

$$wL^2/8 = 335 \times 8 \cdot 83^2 \div 8 = 3265$$
$$WL/4 = 2700 \times 8 \cdot 83 \div 4 = 5961$$
$$\overline{ 9226 \text{ ft.-lb.}}$$

To allow for continuity, an empirical coefficient of $0 \cdot 8$ will be taken. The same reinforcement will be used top and bottom of the slab, and both sets of bars will be carried right through to allow for the altering position of the moving load. The maximum bending moment anywhere will then be $715 + 0 \cdot 8 \times 9226 = 8096$ ft.-lb. per ft. of width. By the methods of § 319 it may be shown that a $7\frac{1}{2}$-in. slab, $d = 6 \cdot 37$ in., $\rho = 1 \cdot 28$ %, $f_c = 1200$, $f_t = 18,000$ lb./sq. in., $m = 10$, $\frac{3}{4}$-in. bars at 5-in. pitch, will safely carry this bending moment. The effect of the reinforcement on the compression side of the slab has been neglected. The shear stress is small and no shear reinforcement is required.

From Fig. 50, for a span of $8 \cdot 83$ ft., distribution steel, running transversely, equal to 57 % of the main reinforcement is to be introduced. If $\frac{3}{4}$-in. bars are used, the spacing should be 5 in. $\div 0 \cdot 57 = 8 \cdot 8$ in. An $8\frac{1}{2}$-in. pitch, as indicated in (iii) Fig. 441, will be convenient.

---

* For Ministry of Transport practice, refer to *Reinforced Concrete Bridge Design,* Chettoe and Adams, London, 1933.

† $f_t = 16,000$ lb./sq. in. (Ministry of Transport Regulations).
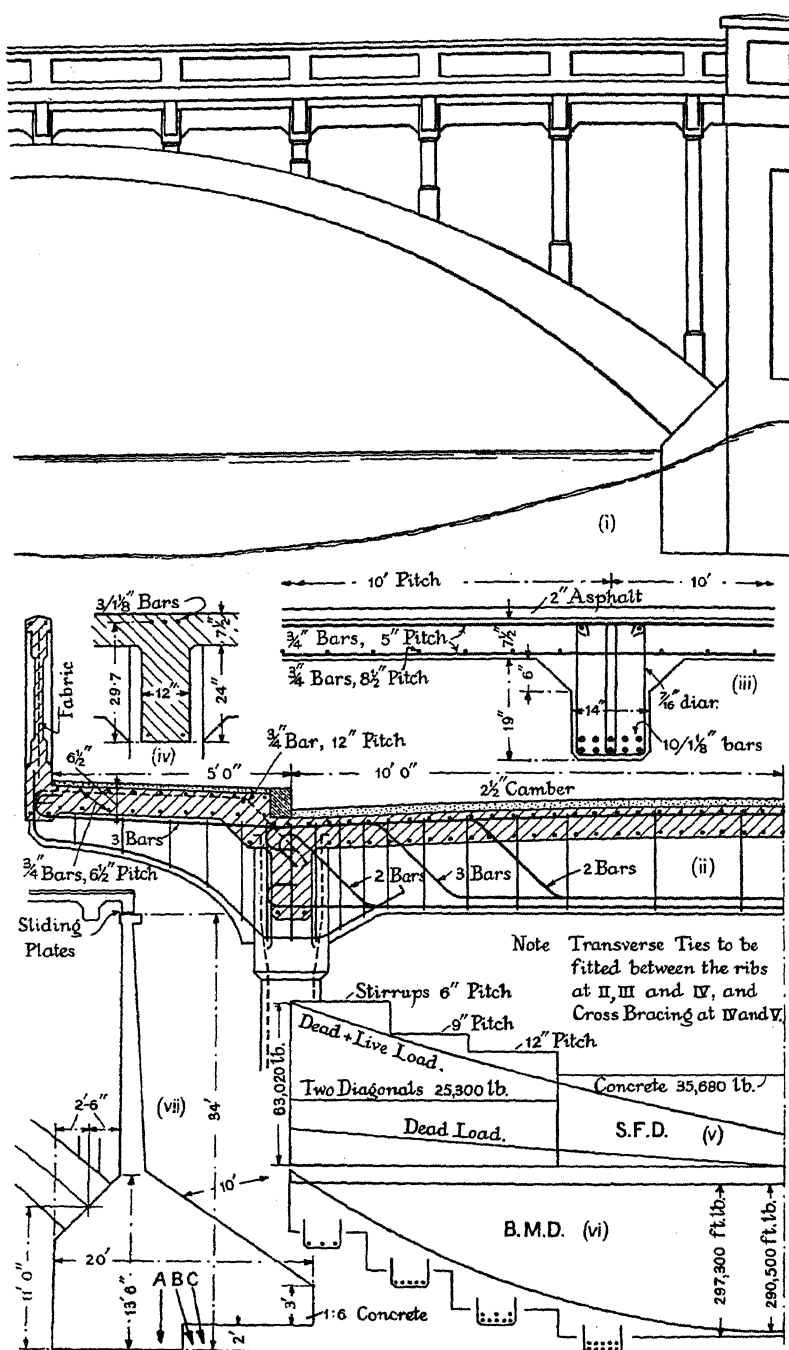
FIG. 441.

In the end panels of the roadway, and at transverse beam V, no reduction in bending moment on account of continuity is permissible. The 5-in. spacing of the main reinforcement must be reduced to suit.

5. *Design of Sidewalk Slabs.*—The sidewalks are supported on brackets in line with the transverse beams, and the span of the floor slabs will be 8·83 ft. They must carry a load of 100 lb./sq. ft., but provision is to be made for a vehicle mounting the pavement. It will therefore be assumed that the sidewalk slab carries a bending moment equal to $\frac{2}{3}$ of the live load bending moment on the road slab; i.e. it will carry the same loading, but at 50 % increased stresses. A $6\frac{1}{2}$-in. slab will be found suitable, with a 1-in. asphalt wearing surface. Weight of floor $(10 + 78)$ lb./sq. ft.; max. bending moment 5492 ft.-lb.; $d = 5 \cdot 37$ in.; $\rho = 1 \cdot 22$; $\frac{3}{4}$-in. bars at $6\frac{1}{2}$-in. pitch will be required. The shear stress is small.

6. *Transverse Beams.*—The cross-section is shown in (iii) Fig. 441. Span 20 ft. The allowable width of slab to be counted in is $\frac{1}{4}$ × span * = 5 ft.; weight of beam per foot of width: slab, $10 \times 1 \times 110 = 1100$ lb.; rib, 19×14 in. $= 266$ lb.; fillets, 6×6 in. $= 36$ lb.; total, 1402 lb. Uniformly distributed live load on span of 20 ft. $= 220$ lb./sq. ft., Fig. 50, i.e. $1 \times 10 \times 220 = 2200$ lb./ft.; knife-edge load, end to end of beam, 2700 lb./ft. Total load per foot $= 1402 + 2200 + 2700 = 6302$ lb. Bending moment at centre $= wL^2/8 = 6302 \times 20^2 \div 8 = 315{,}100$ ft.-lb. This will be reduced by the weight of the overhanging footpath, 5430 lb. at $2 \cdot 5$ ft., and parapet wall 2100 lb. at $5 \cdot 25$ ft., $= 24{,}600$ ft.-lb., so that the maximum bending moment on the transverse beam is 290,500 ft.-lb. The calculation for the moments of inertia and resistance of the central cross-section, (iii), is as follows (see § 315).

Moments about top of slab. Inch units.

Part.	a'		$ma'h'$		$ma'(h')^2$	mI'
Slab, 60 × $7\frac{1}{2}$	450	1	450	3·75	1687	6,326	2110
5/$1\frac{1}{4}$ bars	4·97	10	49·7	22·56	1121	25,294	
5/$1\frac{1}{4}$ bars	4·97	10	49·7	24·68	1227	30,272	
		549·4		4035	61,892	2110

$$v_c = \frac{4035}{549 \cdot 4} = 7 \cdot 34 \qquad \frac{4035^2}{549 \cdot 4} = 29{,}635$$

$$v_t = 24 \cdot 68 - 7 \cdot 34 = 17 \cdot 34 \qquad I_c \quad 32{,}257 + 2110$$

$$Z_c = \frac{34{,}367}{7 \cdot 34} = 4682; \; Z_t = \frac{34{,}367}{10 \times 17 \cdot 34} \quad 198 \cdot 2; \qquad 34{,}367$$

$$\frac{290{,}500 \times 12}{4682} = 745 \text{ lb./sq. in.}; \; f_t = \frac{290{,}500 \times 12}{198 \cdot 2} = 17{,}590 \text{ lb./sq. in.}$$

The design of the beam is similar to that of Fig. 435, but the safe shear stress $= 120$, and the safe bond stress $= 145$ lb./sq. in. The bending-moment and shearing-force diagrams are given in Fig. 441.

* $\frac{1}{4}$ of span; pitch; or 12 × slab thickness, whichever be the least.

In setting out the latter, it should be noticed that since the live load (2200 + 2700) lb./ft. may be applied anywhere on the beam, it is equivalent to a uniform load, longer than the span, crossing the beam transversely (see § 18), and the shape of the shearing-force diagram is as shown. The maximum shearing force is 63,020 lb. ; $V = 21 \cdot 2$; breadth of rib, $b_1 = 14$ in. ; from eq. (2), § 317, the maximum shear stress is

$$f_s = \frac{S}{b_1 V} = \frac{63,020}{14 \times 21 \cdot 2} = 213 \text{ lb./sq. in.,}$$

or less than twice the safe shear stress on plain concrete. The width 14 in. is therefore permissible. The turn-up of the bars is indicated in Fig. 441.

7. *Cantilever Brackets.*—The cross-section through the cantilever brackets is shown in (iv) Fig. 441. The bending-moment acting thereon is 24,600 ft.-lb. due to the dead load (see above), plus that due to $\frac{2}{3}$ the live load on the transverse beam ($\frac{2}{3} \times 4900 = 3270$ lb./ft.), i.e. a bending moment of $5 \times 3270 \times 2\frac{1}{2} = 40,880$ ft.-lb. ; a total bending moment of 65,480 ft.-lb. The stress in the concrete is 501 lb./sq. in., and in the steel is 9990 lb./sq. in. This stress has been kept low to avoid cracking in the sidewalk slab above the bracket. The shear stress is 76 lb./sq. in.

8. *Vertical Columns.*—These will be made 15 in. square with four 1-in. longitudinal bars ; equivalent area $= 15 \times 15 + 4 \times 9 \times 0 \cdot 785$ $= 253$ sq. in. Taking the sidewalks for this purpose as loaded with 100 lb./sq. ft., the maximum load on a column is :

Vertical shear from transverse beam	= 63,160 lb.
Dead load from sidewalk	= 7,530 lb.
Longitudinal beam top of column	1,550 lb.
Live load on sidewalk, $10 \times 5 \times 100$	5,000 lb.
	77,240 lb.

so that the direct stress is only $77,240 \div 253 = 307$ lb./sq. in. The ratio L/D for column IV is $14 \div 1 \cdot 25 = 11 \cdot 2$. These columns will be subjected to secondary bending moments in both directions due to frame distortion, wind pressure, etc., and the direct stress should not exceed 50 % of that allowable (960 lb./sq. in.). Columns IV and V are cross-braced transversely to give lateral stiffness.

9. *The Arched Ribs.*—As stated above, the roadway will be carried by two arched ribs, ratio rise/span $= 1 : 5$, so that the rise of the arch will be 20 ft. According to Williams' proportions, § 357, with a $1 : 1 : 2$ concrete, $f_c = 1100$ lb./sq. in., the most economical depth at the crown would be $2 \cdot 5\left\{ \dfrac{100}{200} + 1 \right\} = 3 \cdot 75$ ft. ; the total area of cross-section necessary would be $\dfrac{100}{200} \times 25 * = 12 \cdot 5$ sq. ft. ; and the depth at the springings $2 \times 3 \cdot 75 = 7 \cdot 5$ ft.. Such proportions, though economical, would make the arch look very thick and heavy, and the ribs would be only $1 \cdot 67$ ft. wide, which is undesirably narrow in proportion. Chiefly for the sake of appearance, a rib $2 \cdot 5$ ft. deep at the crown and 5 ft. wide

* Equivalent width, taking reduced load on sidewalks into account.

at the springings, will be tried. This is $33\frac{1}{3}$ % shallower, and from § 357 a $33\frac{1}{3} \times 1\cdot25 = 42$ % increase in area must be provided, i.e. a total area
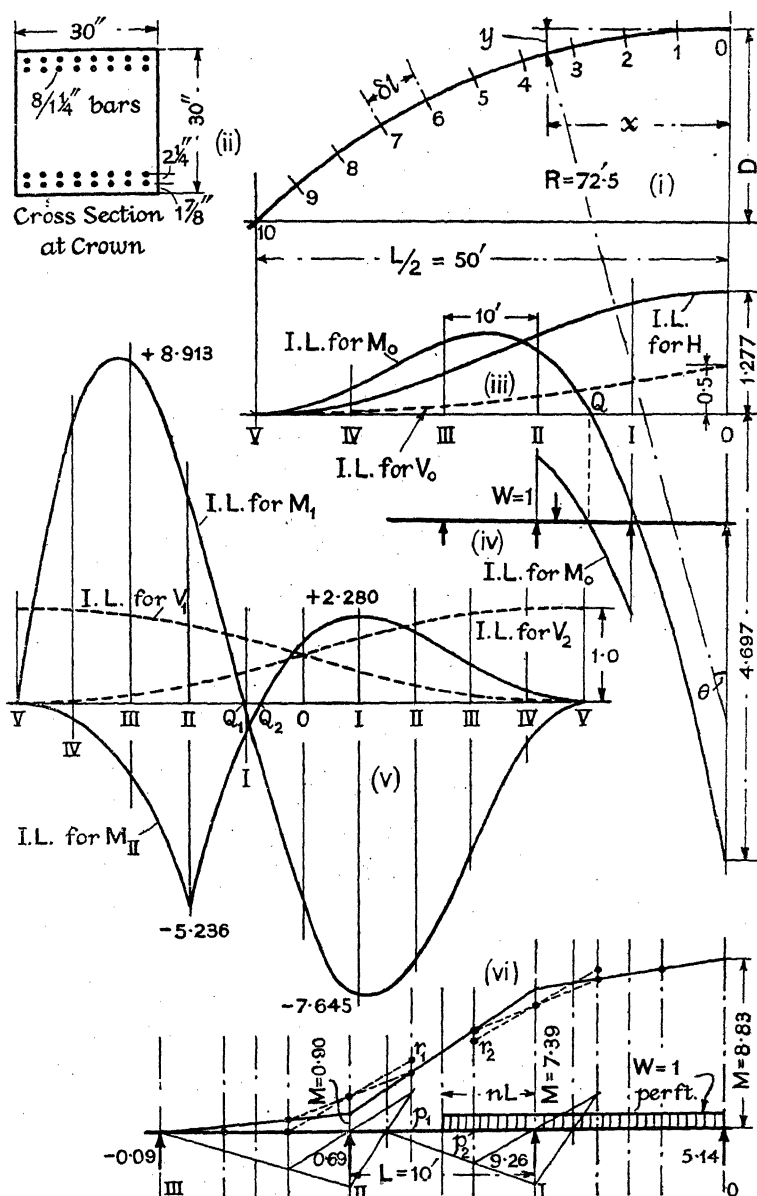
FIG. 442.

of $12\cdot5 \times 1\cdot42 = 17\cdot7$ sq. ft. With the assumed 1 % of reinforcement and $(m - 1) = 9$, the equivalent area of concrete $= 17\cdot7 \times 144 \times 1\cdot09$

= 2778 sq. in., or 1389 sq. in. per rib. Since the permissible stress is increased from 1100 to 1200 lb./sq. in., this area may be reduced to 1273 sq. in. A convenient section will be as shown at (ii) Fig. 442, for which the equivalent concrete area is $30 \times 30 + 32 \times 1 \cdot 227 \times 9$ = 1253 sq. in. This will be tried.

10. *Calculation of δl, x, and y.*—Divide the half centre line into ten equal parts, (i) Fig. 442. The ribs will be made segmental, and the radius of the centre line is $R = L^2/8D + D/2$; $L = 100$; $D = 20$; and $R = 72 \cdot 5$ ft. The angle subtended at the centre by the half arch $= 43° 36 \cdot 17'$; the half length of the centre line $l/2 = 55 \cdot 17$ ft.; and $\delta l = 5 \cdot 517$ ft. Further, $x = R \sin \theta$ and $y = R(1 - \cos \theta)$, whence the value of x and y at the centre point and end of each segment can be calculated. The values for the centre points are entered on Table I; those for the end points are required later for the values of z, Table II. Work in feet.

11. *Depth of Rib.*—The depth of the rib is $2 \cdot 5$ ft. at the crown and 5 ft. at the springings. It will be assumed to increase proportionately to the cube of the distance from the crown, measured along the arc. Hence, if d_0 be the depth of the rib, at the centre of the nth segment from the crown $d_0 = 2 \cdot 5 + (2n - 1)^3/3200$ ft. Calculate the value of d_0 at the centre of each segment ($n = 1 \ldots 10$).

Half Arch: Feet Units.   TABLE I.

Ordinate	δl	x	y	I	a	$\dfrac{1}{I}$	$\dfrac{x}{I}$	$\dfrac{y}{I}$	$\dfrac{x^2}{I}$	$\dfrac{y^2}{I}$	$\dfrac{xy}{I}$	$\dfrac{1}{a}$
0												
1		2·76	0·05	5·73	8·70	0·175	0·482	0·009	1·33	0·00	0·02	0·115
2		8·26	0·47	5·75	8·71	0·174	1·436	0·082	11·87	0·04	0·67	0·115
3		13·71	1·31	5·98	8·80	0·167	2·293	0·219	31·43	0·29	3·00	0·114
4		19·08	2·56	6·43	8·97	0·156	2·967	0·398	56·62	1·02	7·60	0·111
5		24·37	4·21	7·29	9·27	0·137	3·343	0·578	81·47	2·43	14·07	0·108
6		29·47	6·26	8·76	9·74	0·114	3·364	0·715	99·14	4·47	21·06	0·103
7		34·42	8·69	11·19	10·42	0·089	3·076	0·777	105·87	6·75	26·73	0·096
8		39·17	11·49	15·10	11·34	0·066	2·594	0·761	101·61	8·74	29·81	0·088
9		43·70	14·65	21·37	12·54	0·047	2·045	0·686	89·36	10·04	29·96	0·080
10		47·97	18·14	31·39	14·06	0·032	1·528	0·578	73·31	10·48	27·72	0·071

(Left margin, spanning rows: $\delta l = 5 \cdot 517$; 10 equal segments: $\delta l = 5 \cdot 517$.)

Totals .

$\dfrac{1}{I}$	$\dfrac{x}{I}$	$\dfrac{y}{I}$	$\dfrac{x^2}{I}$	$\dfrac{y^2}{I}$	$\dfrac{xy}{I}$	$\dfrac{1}{a}$
1·157	23·128	4·803	652·01	44·26	160·64	1·001
$= A_1$	$= A_2$	$= A_3$	$= A_4$	$= A_5$	$= A_6$	$= A_7$

$$A_5' = A_5 + A_7 = 44 \cdot 26 + 1 \cdot 00 = 45 \cdot 26$$

12. *Calculation of* I *and* a.—The equivalent I of the cross-section is given by the expression $I = \frac{1}{12}Bd_0{}^3 + \Sigma\,(m - 1)ar^2$, where B, its breadth, $= 2 \cdot 5$ ft. ; d_0 is its depth in ft. ; $m = 10$; $(m - 1)a$ for sixteen $1\frac{1}{4}$-in. bars $= 9 \times 16 \times 1 \cdot 227/144 = 1 \cdot 227$ sq. ft. ; $r = (d_0/2 - 0 \cdot 16)$, and $(d_0/2 - 0 \cdot 34)$ ft., for the outer and inner layers respectively. Hence,

$$I = \tfrac{1}{12} \times 2 \cdot 5 \times d_0{}^3 + 1 \cdot 227\{(d_0/2 - 0 \cdot 34)^2 + (d_0/2 - 0 \cdot 16)^2\}$$
$$= 5d_0{}^3/24 - 0 \cdot 613(d_0{}^2 - d_0 + 0 \cdot 282),$$

from which the value of I at the centre of every segment can be obtained. These values are entered on Table I. The equivalent area of cross-section is $2\frac{1}{2}d_0 + 2 \cdot 454$ sq. ft., from which the areas at the centre points of the segments can be calculated. These are also entered in the Table.

13. *Table I. Calculation of* A_1 *to* A_7.—Table I can now be completed as indicated. The addition of the columns gives $A_1 \ldots A_7$. As it is intended to take into account the effect of the direct compression, columns a and $1/a$ are included. Great accuracy is necessary in the computation.

14. *Table II. Calculation of* B_1 *to* B_6.—In order to find the values of $B_1 \ldots B_6$, it is unnecessary to write out supplementary tables for each load point as has been done for demonstration purposes on p. 514

TABLE II. (Figures from Table I.)

Load Point.	B_1 $\dfrac{1}{I}$	B_2 $\dfrac{x}{I}$	B_3 $\dfrac{y}{I}$	B_4 $\dfrac{x^2}{I}$	B_6 $\dfrac{xy}{I}$
9 ($z = 45 \cdot 86$)	0·032 0·047	1·528 2·045	0·578 0·686	73·31 89·36	27·72 29·96
8 ($z = 41 \cdot 46$)	0·079 0·066	3·573 2·594	1·264 0·761	162·67 101·61	57·68 29·81
7 ($z = 36 \cdot 82$)	0·145 0·089	6·167 3·076	2·025 0·777	264·28 105·87	87·49 26·73
6 ($z = 31 \cdot 97$)	0·234 0·114	9·243 3·364	2·802 0·715	370·15 99·14	114·22 21·06
5 ($z = 26 \cdot 93$)	0·348 0·137	12·607 3·343	3·517 0·578	469·29 81·47	135·28 14·07
4 ($z = 21 \cdot 73$)	0·485 0·156	15·950 2·967	4·095 0·398	550·76 56·62	149·35 7·60
3 ($z = 16 \cdot 41$)	0·641 0·167	18·917 2·293	4·493 0·219	607·38 31·43	156·95 3·00
2 ($z = 10 \cdot 99$)	0·808 0·174	21·210 1·436	4·712 0·082	638·81 11·87	159·95 0·67
1 ($z = 5 \cdot 51$)	0·982 0·175	22·646 0·482	4·794 0 009	650·68 1·33	160·62 0·02
0 ($z = 0$)	1·157 $= A_1$	23·128 $= A_2$	4·803 $= A_3$	652·01 $= A_4$	160·64 $= A_6$

for load point 3. The totals $B_1 \ldots B_6$ can be at once obtained by the process of continued addition given in Table II. The required values for load point 9 are copied direct from the bottom line of Table I; the addition of the second line from the bottom gives the values for load point 8, and so on. The totals for load point 0 at the bottom of the table should check with $A_1 \ldots A_6$ in Table I. The values for z already found for each load point should be added.

15. *Equations for* H, V_0, *and* M_0. *Effect of Direct Thrust.*—If the effect of the direct thrust be neglected, the values of H, V_0, and M_0 are given by eqs. (21), (22), and (23) of § 222; for the purpose of constructing influence lines it is convenient to modify these equations as explained in § 231. If, as in § 223, the effect of direct thrust be taken into account, the term $\Sigma y^2/I$ in these equations is changed to $(\Sigma y^2/I + \Sigma 1/a)$, which is equivalent to replacing A_5 in the equations of § 231 by $(A_5 + A_7) = A_5'$ (see Table I), when the equations become

$$H = \frac{(B_6 - zB_3)A_1 - (B_2 - zB_1)A_3}{2[A_5'A_1 - A_3^2]} ; \quad V_0 = \frac{B_4 - zB_2}{2A_4} ;$$

$$M_0 = \frac{(B_6 - zB_3)A_3 - (B_2 - zB_1)A_5'}{2[A_5'A_1 - A_3^2]}$$

16. *Calculation of* H, M_0 *and* V_0.—The denominator in all cases ·for H and M_0 is

$$2[A_5'A_1 - A_3^2] = 2[45 \cdot 26 \times 1 \cdot 157 - 4 \cdot 803^2] = 58 \cdot 59.$$

Typical calculations for load point 4 are :

$$H = [(B_6 - zB_3)A_1 - (B_2 - zB_1)A_3] \div 58 \cdot 59$$
$$= [(149 \cdot 35 - 21 \cdot 73 \times 4 \cdot 095) \times 1 \cdot 157$$
$$\qquad - (15 \cdot 95 - 21 \cdot 73 \times 0 \cdot 485) \times 4 \cdot 803] \div 58 \cdot 59$$
$$= 0 \cdot 749.$$
$$M_0 = [(B_6 - zB_3)A_3 - (B_2 - zB_1)A_5'] \div 58 \cdot 59$$
$$= [(149 \cdot 35 - 21 \cdot 73 \times 4 \cdot 095) \times 4 \cdot 803$$
$$\qquad - (15 \cdot 95 - 21 \cdot 73 \times 0 \cdot 485) \times 45 \cdot 26] \div 58 \cdot 59$$
$$= 0 \cdot 768.$$

Note that the expressions enclosed in the ( ) brackets are the same for H and M_0.

$$V_0 = (B_4 - zB_2) \div 2A_4 = (550 \cdot 76 - 21 \cdot 73 \times 15 \cdot 95) \div 1304 = 0 \cdot 157.$$

The values for the half-arch are as follows :

Load Point.	10	9	8	7	6	5	4	3	2	1	0
H	0	0·019	0·080	0·187	0·342	0·536	0·749	0·955	1·125	1·237	1·277
M_0	0	+0·053	+0·202	+0·420	+0·659	+0·827	+0·768	+0·335	−0·657	−2·312	−4·697
V_0	0	0·002	0·011	0·029	0·057	0·100	0·157	0·228	0·311	0·403	0·500

17. *Construction of Influence Lines.*—Plot the above values under the appropriate load point on an x base line, (iii) Fig. 442, to a large scale. These curves are the required influence lines for H, M_0 and V_0. Measure accurately the ordinates at the points where the vertical columns occur, which are spaced 10 ft. apart. These ordinates are given in the top three lines of Table III.

18. *Influence Lines for* M_1, M_{II}, V_1 *and* V_2.—Using the values thus obtained, the bending moment at any point on the arch can be found. It is convenient to draw the influence line for M_1, the bending moment at the left springing, and for an intermediate load point, say at Column II. From Fig. 348, the bending moments at A and at B are

$$M_1 = W(L/2 - z) - HD - V_0L/2 + M_0 = (50 - z) - 20H - 50V_0 + M_0$$
$$M_2 = - HD + V_0L/2 + M_0 = - 20H + 50V_0 + M_0.$$

Place the load $W = 1$ successively at each column (0 . . . V), and find the values of M_1 and M_2; plot them under the respective load points, the values of M_1 to the left of the centre, those of M_2 to the right, as shown in (v) Fig. 442. The resulting diagram is the influence line for M_1; for the value of M_1 for a load point to the right is equal to that of M_2 for a symmetrically placed load point to the left.

Example.—Load at Col. III, $z = 30$, $H = 0 \cdot 414$ (see Table III), $M_0 = + 0 \cdot 743$, $V_0 = 0 \cdot 071$;

$$M_1 = (50 - 30) - 20 \times 0 \cdot 414 - 50 \times 0 \cdot 071 + 0 \cdot 743 = + 8 \cdot 913$$
$$M_2 = - 20 \times 0 \cdot 414 + 50 \times 0 \cdot 071 + 0 \cdot 743 = - 3 \cdot 987 = M_1, \text{Col. III, right.}$$

The values for M_1 for the complete arch are given in Table III.

The co-ordinates of the centre line at Col. II (left) are $x = 20, y = 2 \cdot 88$, and the bending moment there, Fig. 348, is

$$M_{II} = - Hy - V_0x + M_0 = - 2 \cdot 88H - 20V_0 + M_0.$$

When W crosses to the right-hand side of the arch, V_0 becomes negative as indicated in Table III. This equation holds for all load points except when W is between II and the centre, when

$$M_{II} = - 2 \cdot 88H - 20V_0 + M_0 + W(x - z).$$

Placing W successively at the top of each column, the value of M_{II} can be calculated from the above formulae, using the values of H, M_0, and V_0 from Table III. The results are entered in line 5 of that table and the influence line is plotted in (v) Fig. 442.

Examples :

Load Point IV (left) :

$$M_{II} = - 2 \cdot 88 \times 0 \cdot 108 - 20 \times 0 \cdot 016 + 0 \cdot 263 = - 0 \cdot 368.$$

Load Point I (left) :

$$[(x - z) = 10]$$
$$M_{II} = 1 \times 10 - 2 \cdot 88 \times 1 \cdot 151 - 20 \times 0 \cdot 326 - 0 \cdot 925 = - 0 \cdot 760.$$

Load Point IV (right) :

$$M_{II} = - 2 \cdot 88 \times 0 \cdot 108 + 20 \times 0 \cdot 016 + 0 \cdot 263 = + 0 \cdot 272.$$

Whole Arch : Units : Feet : lb.   TABLI

Column No.		IV	III	II	
ORDINATES OF INFLUENCE LINES.					
For $H = h$	0	0.108	0.414	0.817	1.151
$M_0 = m_0$	0	+ 0.263	+ 0.743	0.677	−0.925
	0	+ 0.016	+ 0.071	0.178	+0.326
$M'_1 = \tilde{m}_1$	0	+ 7.303	+ 8.913	5.437	−0.245
$M_{II} = m_{II}$	0	− 0.368	− 1.869	5.236	−0.760
$V_1 = v_1$	1.00	0.984	0.929	0.822	0.674
$V_2 = v_2$	0	0.016	0.071	0.178	0.326
DEAD LOAD EFFECTS.					
Load W lb.	40,700	51,230	41,670	39,120	34,240
$H = \Sigma Wh$	0	5,530	17,250	31,960	39,410
$M_0 = \Sigma Wm_0$	0	+ 13,470	+ 30,960	+ 26,480	−31,670
$M_1 = \Sigma Wm_1$	0	+374,130	+371,410	+212,700	− 8,390

LIVE LOAD EFFECTS.   Distributed Load 2700 lb./ft.   Knife Edge Load 27,000 lb.

		IV	III	II	
Q (left) to Q (right) loaded.					
Reactions r			− 0.09	0.69	9.26
$H = 2700\,\Sigma rh +$ K.E. $\times 1.277$			− 100	1,520	28,780
$M_0 = 2700\,\Sigma rm_0 +$ K.E. $\times (-4.697)$			− 180	+ 1260	−23,130
V to I (left) loaded.					
Reactions r	3.93	11.40	9.45	10.80	4.82
$H = 2700\,\Sigma rh +$ K.E. $\times 0.414$	0	3,320	10,560 / 11,180	23,820	14,980
$M_1 = 2700\,\Sigma rm_1 +$ K.E. $\times 8.913$	0	+224,790	+227,420 / +240,650	+158,540	−3,190
$V_1 = 2700\,\Sigma rv_1 +$ K.E. $\times 0.929$	10,610	30,290	23,700 / 25,080	23,970	8,770
I (left) to V (right) loaded.					
Reactions r				− 0.41	+ 4.87
$H = 2700\,\Sigma rh +$ K.E. $\times 1.151$				− 900	15,130
$M_1 = 2700\,\Sigma rm_1 +$ K.E. $\times (-7.645)$				− 6,020	−3,220
$V_1 = 2700\,\Sigma rv_1 +$ K.E. $\times 0.326$				− 910	8,860
V (left) to Q₂ loaded.					
Reactions r	3.93	11.38	9.52	10.58	7.31
$H = 2700\,\Sigma rh +$ K.E. $\times 0.817$	0	3,320	10,640	23,340 / 22,060	22,720
$M_{II} = 2700\,\Sigma rm_{II} +$ K.E. $\times (-5.236)$	0	·11,310	48,040	−149,570 / −141,370	−15,000
$V_0 = 2700\,\Sigma rv_0 +$ K.E. $\times 0.178$	0	490	1,830	5,090 / 4,810	6,430
Q₂ to V (right) loaded.					
Reactions r				− 0.28	2.47
$H = 2700\,\Sigma rh +$ K.E. $\times 1.151$				− 620	7,680
$M_{II} = 2700\,\Sigma rm_{II} +$ K.E. $\times 2.28$				+ 3,960	· 5,070
$V_1 = 2700\,\Sigma rv_1 +$ K.E. $\times 0.326$				− 620	4,500

III. (See Fig. 442.)

0 (Crown)	II	III	IV			Totals.
1·277	1·151	0·817	0·414	0·108	0	
4·697	− 0·925	+ 0·677	+ 0·743	+0·263	0	
0·500	− 0·326*	− 0·178	− 0·071	−0·016	0	
5·237	− 7·645	− 6·763	− 3·987	−1·097	0	
+ 1·625	+ 2·280	+ 1·884	+ 0·971	+0·272	0	
0·500	0·326	0·178	0·071	0·016	0	
0·500	0·674	0·822	0·929	0·984	1·00	
33,950	34,240	39,120	41,670	51,230	40,700	$W = 447,870$ lb.
43,350	39,410	31,960	17,250	5,530	0	$H = 231,650$ lb.
-159,460	- 31,670	+ 26,480	+ 30,960	+13,470	0	$M_0 = -80,980$ ft.-lb
-177,800	-261,760	−264,570	−166,140	−56,200	0	$M_1 = +23,380$ ft.-lb
10·28	9·26	0·69	− 0·09			
35,440 } 34,880 }	28,780	1,520	− 100			$H = 130,320$ lb.
-130,370 } -126,820 }	− 23,130	+ 1,260	− 180			$M_4 = -301,290$ ft.-lb
− 0·40						
− 1,380						$H = 62,480$ lb.
+ 5,660						$M_1 = +853,870$ ft.-lb.
− 5,400						$V_1 = 117,020$ lb.
+ 10·70	+ 9·78	+ 10·15	+ 9·63	+ 11 34	+ 3·94	
36,890	30,390 } 31,080 }	22,390	10,760	3,310	0	$H = 149,050$ lb.
151,300	−201,870 } −206,420 }	−185,340	−103,670	−33,590	0	$M_1 = -891,430$ ft.-lb
14,440	8,610 8,800	4,880	1,850	490	0	$V_1 = 47,020$ lb.
− 0·22						
− 760						$H = 81,320$ lb.
− 970						$M_{II} = -366,260$ ft.-lb.
− 300						$V_0 = 18,350$ lb.
10·39	9·89	10·12	9·63	11·34	3·94	
35,820	30,740 } 31,080 }	22,320	10,760	3,310	0	$H = 141,090$ lb.
+ 45,590	+ 60,880 } + 61,560 }	51,480	25,250	8,330	0	$M_{II} = +251,980$ ft.-lb
14,030	8,710 } 8,800 }	4,860	1,850	490	0	$V_1 = 42,620$ lb.

* V_0 to the right acts downward.

From Fig. 348, $V_2 = V_0$; also $V_1 + V_2 = W = 1$. The values of V_1 and V_2 are, therefore, as given in Table III, and the influence lines as set out in (v) Fig. 442.

19. *Dead Load Effects.*—From the dimensions of the arch as determined, calculate the proportion of the weight thereof acting on one rib at each load point $0 \ldots V$. These are given in Table III, line 8. A typical case is appended:

<div style="text-align:center">COL. III.</div>

Rib proper	11,610
Half Transverse between ribs	3,680
Column	2,420
Half Transverse Beam	2,980
Longitudinal Beam	1,550
Half Roadway Slab	11,900
Bracket	1,030
Sidewalk Slab	4,400
Parapet Wall	2,100
Total	41,670 lb.

The values $H = \Sigma Wh = 231,650$ lb.; $M_0 = \Sigma Wm_0 = -80,980$ ft.-lb. are obtained by multiplying the loads W by the ordinates of the influence lines, Table III, and adding. The values of V_1 and V_2 are each $\frac{1}{4}$ the total weight of the arch $= 223,940$ lb. The moment at the springings $M_1 = M_2 = \Sigma Wm_1$ (Table III) $= +23,380$ ft.-lb.

20. *Live Load Effects.*—Any 'loaded length' which need be considered in the present design will be over 10 ft., and from Fig. 50 the prescribed uniformly distributed load is 220 lb./sq. ft. plus a knife-edge load in the position producing the greatest effect of 2700 lb./ft. In addition, the sidewalks will carry 100 lb./sq. ft. On one rib, therefore, the uniformly distributed load per foot of length will be $10 \times 1 \times 220 + 5 \times 1 \times 100 = 2700$ lb./ft., plus the knife-edge load of $10 \times 2700 = 27,000$ lb.

Of the efforts stressing the arched rib, by far the most important is the bending moment, and the bending-moment influence line will determine the load position producing the worst effects.

Crown.—The maximum live load bending moment at the crown will evidently occur when the live load covers the arch between the points QQ, (iii) Fig. 442, on each side of the centre, and is negative. Here the effect of the continuity of the slab floor becomes of importance, because any load between Cols. I and II produces a reaction on Col. II which lessens the bending moment at the crown. If a load $W = 1$ cross the span between I and II, and, treating the slab as continuous, an influence line be drawn for $-M_0$, using the values of m_0 from Table III, it takes the form shown in (iv) Fig. 442, the curve cutting the base line very close to Q, whence it appears that the continuity does not much affect the position of the load for maximum bending moment. For simplicity, it will be assumed that the load half covers span I to II, viz. the middle 30 ft. of the arch, and that the bending moment in the floor slab at III is zero. The reactions for a uniform load of 1 unit per ft. run, found by

means of characteristic points,* (vi) Fig. 442, are then as shown in the figure and tabulated in line 12, Table III. For a uniform load of 2700 lb./ft., and a knife-edge load of 27,000 lb. at the crown

$$H = 2700 \, \Sigma \, rh + 27{,}000 \times 1\cdot277 = 130{,}320 \text{ lb.}$$
$$M_0 = 2700 \, \Sigma \, rm_0 + 27{,}000 \times (\, - \, 4\cdot697) = \, - \, 301{,}290 \text{ ft.-lb.}$$

These values are calculated and tabulated in Table III. V_0 at the centre = zero.

Springings.—At the springing A the bending moment is M_1; two cases must be considered, (i) when the load extends from V (left) to Q_1, producing a + moment at A, (v) Fig. 442; and (ii) when the load extends from Q_1 to V (right), producing a − moment at A. By a process similar to that employed above, (iv) Fig. 442, it may be shown that when a unit load crosses span II to I (left), the influence line for M_1 cuts the base line close to Q_1, and again the effect of continuity is small. For practical purposes it may be assumed that the load for condition (i) extends from V to I (left), and that the bending moment at 0 is zero ; and for condition (ii) that the load extends from I (left) to V (right), and that the bending moment at II (left) is zero. The reactions for a load of 1 unit per ft. run, for these two cases, found by characteristic points, are given in lines 16 and 20 of Table III, and the values of H, M_1, and V_1 are calculated as before. The knife-edge load is placed above the maximum ordinate of the M_1 influence line.

Column II.—From Table III it will be seen that the maximum bending moment at II will occur when the load extends from V (left) to Q_2, (v) Fig. 442. Taken for practical purposes as extending $2\frac{1}{2}$ ft. from I (left) towards 0, and assuming that the bending moment at 0 is zero, the reactions found by characteristic points are as given in line 25 of Table III, and the value of M_{II} is calculated therefrom as before. The knife-edge load is assumed to occur at II (left).

21. *Temperature Effects.*—The bending moment and thrust due to change in temperature can be found from eqs. (5) and (6), § 225. Modified to suit a division of the centre line into finite equal segments, these equations become

$$H_t = \cfrac{ELat \, \Sigma_A^c \frac{1}{I}}{2\left[\, \Sigma_A^c \frac{y^2}{I} \times \Sigma_A^c \frac{1}{I} - \left\{ \Sigma_A^c \frac{y}{I} \right\}^2 \right] \delta l} = \frac{ELat \times A_1}{2[A_5 A_1 - A_3{}^2] \delta l}$$

$$M_0 t = \cfrac{ELat \, \Sigma_A^c \frac{y}{I}}{\left[\, \Sigma_A^c \frac{y^2}{I} \times \Sigma_A^c \frac{1}{I} - \left\{ \Sigma_A^c \frac{y}{I} \right\}^2 \right] \delta l} = \frac{ELat \times A_3}{2[A_5 A_1 - A_3{}^2] \delta l}$$

---

* The characteristic points for a uniform load partly covering a span, (vi) Fig. 442, are

$$p_1 r_1 = \frac{wL^2}{12} \, n^2 \, (2 - n^2) \, ; \quad p_2 r_2 = \frac{wL^2}{12} \, n^2 \, (2 - n)^2 \, ; \quad \text{and } R_1 = \frac{wL}{2} \, n^2 \, ; \quad R_2 = \frac{wL}{2} n \, (2 - n).$$

Note that when dividing through by δl, this factor still appears in the denominator. In this country it is considered sufficient to allow for a variation in temperature of $\pm 30°$ F., i.e. above and below the mean temperature. For the concrete to be used, take $E = 3,000,000$ lb./sq. in. and $\alpha = 0 \cdot 000006$; $\delta l = 5 \cdot 517$ ft. Then, for a rise of $30°$,

$$H_t = \frac{3,000,000 \times 144 \times 100 \times 0 \cdot 000006 \times 30 \times 1 \cdot 157}{2[44 \cdot 26 \times 1 \cdot 157 - 4 \cdot 803^2] \times 5 \cdot 517 = 56 \cdot 28} = 28,980 \text{ lb.}$$

$$M_0t = \frac{3,000,000 \times 144 \times 100 \times 0 \cdot 000006 \times 30 \times 4 \cdot 803}{56 \cdot 28} = 120,290 \text{ ft.-lb.}$$

$$M_1t = - H_tD + M_0t = - 28,980 \times 20 + 120,290 = - 459,310 \text{ ft.-lb.}$$

$$M_{II}t = - H_t y + M_0t = - 28,980 \times 2 \cdot 88 + 120,290 = + 36,830 \text{ ft.-lb.}$$

$$V_1 = V_2 = V_0 = 0.$$

22. *Shrinkage Effects.*—As concrete hardens, it contracts an amount ranging from $0 \cdot 03$ to $0 \cdot 05$ % of its length, depending on the conditions. This contraction takes place more rapidly at first, getting slower and slower. About one-half of the total contraction takes place within the first three months in the case of Portland cement concrete, and within the first week with aluminous cement. To mitigate the effects of shrinkage in the case of an arched rib, it is common to leave gaps in the ribs when concreting, usually at the springings or the crown, and to splice the reinforcement at these points, in order to leave the rib free to contract. At the end of a month the arch is finally keyed up and the spaces made solid with concrete.* In these circumstances, it is considered sufficient to allow for a $0 \cdot 01$% contraction in length,† which is, practically speaking, equivalent to a change in temperature of $- 15°$ F., the two contractions producing similar effects. In other words, the effect of shrinkage is to produce thrusts and moments of one-half the magnitude of those found in ¶ 21 for a $30°$ fall in temperature.

23. *Calculation of Stresses.*—It is now possible to calculate the stresses in the arch.

At the Crown.—Live load extends from Q to Q. The worst combination of effects will be : dead load + live load + $30°$ fall in temperature + shrinkage. The forces and moments are given in the top Table, p. 659.

Assuming in the first instance that the concrete does not crack, the stresses therein will be given by the expression $f_{max.} = H/a \pm Mv_c/I$. From ¶ 9, $a = 1253$ sq. in. ; from ¶ 12, $I = 5 \cdot 73$ ft.⁴ ; $v_c = 1 \cdot 25$ ft.

Then $f_{max.} = \dfrac{318,500}{1253} \pm \dfrac{562,710 \times 1 \cdot 25}{5 \cdot 73 \times 144} = \left.\begin{array}{l} 1107 \text{ comp.} \\ 599 \text{ tension} \end{array}\right\}$ lb./sq. in.

Under a tensile stress of 599 lb./sq. in. the concrete would certainly

---

* An alternative method of reducing the effects of shrinkage, proposed by Considère, is to introduce temporary hinges at the crown and springings. which are concreted up solid when the arch is complete. The arch thus carries the dead load as a 3-hinged arch, and the live load as a direction-fixed arch. For the design of these hinges, and the method of calculation, see *Reinforced Concrete Bridges,* W. L. Scott, 3rd ed., London, 1931.

† See *Reinforced Concrete Bridge Design,* Chettoe and Adams, London, 1933.

Stress due to	H (lb.)	M_0 (ft.-lb.)	V_0 (lb.)
Dead load (Table III) . . .	231,650	− 80,980	—
Live load (Table III) . . .	130,320	− 301,290	—
30° fall temp. (¶ 21) . . .	− 28,980	− 120,290	—
Shrinkage (¶ 22)	− 14,490	− 60,150	—
Total	318,500	− 562,710	—

crack, and the stresses must be determined by the methods of § 316, Case III. In eq. (12), § 316,

$$\frac{bv_c^2}{6}(v_c + 3r) = m_{at}(d + r)(d - v_c) - (m - 1)a_c'(g + r)(v_c - g)$$

$$r = e - d_0/2 = \frac{M_0}{H} - \frac{d_0}{2} = \left\{\frac{562,710}{318,500} - 1\cdot 25\right\} \times 12 = 6\cdot 2 \text{ in.}$$

$b = 30$; $m_{at} = 196\cdot 3$; $d = 27$; $(m - 1)a_c' = 176\cdot 7$; $g = 3$; whence $v_c^2(18\cdot 6 + v_c) = 36,168\cdot 0 - 1628\cdot 56\,v_c$; and (graphically) $v_c = 16\cdot 42$ in. From eqs. (11) and (13), § 316,

$$F = H = 318,500 = f_c\left\{\frac{30 \times 16\cdot 42}{2} + 176\cdot 7 \times \frac{13\cdot 42}{16\cdot 42} - 196\cdot 3 \times \frac{10\cdot 58}{16\cdot 42}\right\}$$

and $f_c = 1205$ lb./sq. in.; $f_t = \dfrac{10 \times 1205 \times 10\cdot 58}{16\cdot 42} = 7770$ lb./sq. in.

At the Springings. Condition (i), + *Moment.*—Live load extends from V to I (left). The worst combination of effects will be : dead load + live load + 30° fall in temperature + shrinkage.

Stress due to	H (lb.)	M_1 (ft.-lb.)	V_1 (lb.)
Dead load (Table III) . . .	231,650	+ 23,380	223,940
Live load (Table III) . . .	62,480	+ 853,870	117,020
30° fall temp. (¶ 21) . . .	− 28,980	+ 459,310	—
Shrinkage (¶ 22)	− 14,490	+ 229,660	—
Total	250,660	+ 1,566,220	340,960

Condition (ii), − *Moment.*—Live load extends from I (left) to V (right). The worst combination of effects will be : dead load + live load + 30° rise in temperature + shrinkage (see the top Table, p. 660.)

Of the two condition (i) produces the greater stresses. The normal force on the end cross-section is $F_a = H \cos \theta + V \sin \theta = 250,660 \times 52\cdot 5 \div 72\cdot 5 + 340,960 \times 50 \div 72\cdot 5 = 416,660$ lb.; for, from the geometry of the arch, $\cos \theta = 52\cdot 5 \div 72\cdot 5$; $\sin \theta = 50 \div 72\cdot 5$. The eccentricity $e = (1,566,220 \div 416,660) \times 12 = 45\cdot 1$ in.

Then in eq. (12), § 316, given above, $r = e - d_0/2 = 45\cdot 1 - 30 = 15\cdot 10$;

Stress due to	H (lb.)	M_1 (ft.-lb.)	V_1 (lb.)
Dead load (Table III) . . .	231,650	+ 23,380	223,940
Live load (Table III) . . .	149,050	− 891,430	47,020
30° rise temp. (¶ 21) . . .	28,980	− 459,310	—
Shrinkage (¶ 22)	− 14,490	+ 229,660	—
Total	395,190	− 1,097,700	270,960

$b = 30$; $mat = 196 \cdot 3$; $d = 57$; $(m - 1)ac' = 176 \cdot 7$; $g = 3$ in.,

whence, $5v_c{}^2(45 \cdot 30 + v_c) = 196 \cdot 3 \times 72 \cdot 1(57 - v_c) - 176 \cdot 7 \times 18 \cdot 1(v_c - 3)$

and (graphically) $v_c = 29 \cdot 02$ in. From eqs. (11) and (13), § 316,

$$F = F_a = 416,660 = f_c \left\{ 30 \times 29 \cdot 02 + 176 \cdot 7 \times \frac{26 \cdot 02}{29 \cdot 02} - 196 \cdot 3 \times \frac{27 \cdot 98}{29 \cdot 02} \right\}$$

and $f_c = 1031$ lb./sq. in.; $f_t = \dfrac{10 \times 1031 \times 27 \cdot 98}{29 \cdot 02} = 9940$ lb./sq. in.

At Col. II. Condition (i), − *Moment.*—Live load extends from V (left) to Q_2. The worst combination of effects will be : dead load + live load + 30° fall in temperature + shrinkage. The bending moment at II, $x = 20$, $y = 2 \cdot 88$ ft., due to the *dead load* is

$M_{II} = \Sigma W(x - z) - Hy - V_0 x + M_0$
$= (33,950 \div 2) \times 20 + 34,240 \times 10 - 231,650 \times 2 \cdot 88 - 80,980$
$= - 66,230$ ft.-lb. (See Fig. 442 and Table III ; $V_0 = 0$)
$V_{II} = (33,950 \div 2) + 34,240 + 39,120 - V_0 = 90,340$ lb.

The bending moment due to a *rise in temperature* of 30° (see ¶ 21) is
$M_{IIt} = - Hty + M_{0t} = - 28,980 \times 2 \cdot 88 + 120,290 = + 36,830$ ft.-lb. ;
that due to shrinkage is $- \frac{1}{2}M_{IIt} = - 18,420$ ft.-lb. From Table III,
for the *live load*, $H = 81,320$ lb. ; $M_{II} = - 366,260$ ft.-lb.

$V_{II} = \Sigma W$ (live) $\times r + $ K.E. load $- V_0$
$= (2700 \div 2) \times - 0 \cdot 22 + 2700 \times 7 \cdot 31 + 2700 \times 10 \cdot 58 + 27,000 - 18,350$
$= 56,660$ lb.

Stress due to	H (lb.)	M_{II} (ft.-lb.)	V_{II} (lb.)
Dead load	231,650	− 66,230	90,340
Live load	81,320	− 366,260	56,660
30° fall temp.	− 28,980	− 36,830	
Shrinkage	− 14,490	− 18,420	
Total	269,500	− 487,740	147,000

Condition (ii), + *Moment.*—Live load extends from Q_2 to V (right). The worst combination of effects will be : dead load + live load + 30° rise in temperature + shrinkage. The values have all been calculated.

Stress due to	H (lb.)	M_{II} (ft.-lb.)	V_{II} (lb.)
Dead load (above)	231,650	− 66,230	90,340
Live load (Table III) . . .	141,090	+ 251,980	42,620
30° rise temp. (above) . . .	28,980	+ 36,830	$(V_{II}=V_1)$
Shrinkage (above)	− 14,490	− 18,420	
Total	387,230	+ 204,160	132,960

Condition (i) produces the greater stresses. The normal force on the cross-section is $F_a = H \cos\theta + V \sin\theta = 269{,}500 + 69 \cdot 62 \div 72 \cdot 5 + 147{,}000 \times 20 \div 72 \cdot 5 = 299{,}350$ lb. ; for $\cos\theta = 69 \cdot 62 \div 72 \cdot 5$; $\sin\theta = 20 \div 72 \cdot 5$. The eccentricity $e = (487{,}740 \div 299{,}350) \times 12 = 19 \cdot 55$ in. At $x = 20$ ft., $d_0 = 31 \cdot 5$ in. ; $r = e - d_0/2 = 3 \cdot 8$; $b = 30$; $ma_t = 196 \cdot 3$; $d = 28 \cdot 5$; $(m-1) a_c' = 176 \cdot 7$; $g = 3$ in., whence, from eq. (12), § 316, $5v_c^2 (11 \cdot 4 + v_c) = 196 \cdot 3 \times 32 \cdot 3 (28 \cdot 5 - v_c) - 176 \cdot 7 \times 6 \cdot 8 (v_c - 3)$, from which (graphically) $v_c = 18 \cdot 06$ in. From eqs. (11) and (13), § 316,

$$F = F_a = 299{,}350 = f_c \; \frac{30 \times 18 \cdot 06}{2} + 176 \cdot 7 \frac{15 \cdot 06}{18 \cdot 06} - 196 \cdot 3 \times \frac{10 \cdot 44}{18 \cdot 06} \Big\}$$

and $\quad f_c = 1092$ lb./sq. in. ; $f_t = \dfrac{10 \times 1092 \times 10 \cdot 44}{18 \cdot 06} = 6313$ lb./sq. in.

At the crown, springings, and at an intermediate point II, therefore, the stresses in the arched rib are permissible in both concrete and steel. The cross-section proposed may be adopted.

24. *Foundations.*—The abutments and the lines of thrust are shown in (vii) Fig. 441.

A = Dead load + shrinkage.

B = Dead load + live load + 30° rise in temp. + shrinkage (arch fully covered).

C = Ditto, when − M_1 is a min. (see *At the Springings*, Condition (ii), ¶ 23). Maximum pressure on the ground = $2 \cdot 6$ tons/sq. ft.

BIBLIOGRAPHY

General Treatises

1. Mörsch. *Der Eisenbetonbau*, 3rd ed., 1908 ; trans. by Goodrich, *Concrete-Steel Construction*. New York, 1910.
2. R.I.B.A. Second Report of Committee on Reinforced-Concrete. London, 1911.
3. Faber and Bowie. *Reinforced-Concrete Design*. London, vol. i, *Theory*, 1912 ; vol. ii, *Practice*, 1924.
4. Turneaure and Maurer. *Principles of Reinforced-Concrete Construction*. New York, 4th ed., 1932.
5. Marsh and Dunn. *Manual of Reinforced-Concrete*, 4th ed., London, 1922.

6. HOOL AND KINNE. *Reinforced-Concrete and Masonry Structures*. New York, 1924.
7. MANNING. *Reinforced-Concrete Design*, 2nd ed., London, 1936.
8. TAYLOR, THOMPSON AND SMULSKI. *Concrete : Plain and Reinforced*. New York, vol. i, 4th ed., 1925.
9. AMERICAN JOINT COMMITTEE. Report of, see *Proc. Amer. Soc. C.E.*, Oct. 1924.
10. URQUHART AND O'ROURKE. *Design of Concrete Structures*. New York, 1935.
11. HOOL. *Reinforced-Concrete Construction*. New York, 1927, vol. i, Fundamental Principles.
12. SCOTT, E. A. *Arrol's Reinforced-Concrete Reference Book*. London, 1930.
13. WYNN. *Design and Construction of Formwork for Concrete Structures*. London, 2nd ed., 1930.

Reviews of Experimental Work

14. MÖRSCH. Ref. No. 1 ; TAYLOR, THOMPSON AND SMULSKI, Ref. No. 8.

Experiments on Beams and Slabs

15. BACH. Versuch mit Eisenbetonbalken. *Mitt. ü. Forschungsarbeiten, V.d.I.* Hefte 39, 45 to 47, 1907 ; 90 and 91, 1910 ; see also 72 to 74, 1909, and 95, 1910.
16. —— Zur Frage der Dehnungsfähigkeit des Betons mit und ohne Eiseneinlagen. *Zeit. Ver. deu. Ing.*, June 26, 1907, p. 1027.
17. TURNEAURE. Tests on Reinforced-Concrete Beams. *Proc. Amer. Soc. Test. Mat.*, 1904, p. 498.
18. TALBOT. Tests of Reinforced-Concrete Beams. *Univ. Illinois Eng. Exp. Stn.* Bull. No. 1, 1904 ; No. 4, 1906 ; No. 12, 1907 (T Beams) ; No. 14, 1907 ; No. 28, 1909.
19. TALBOT AND SLATER. Tests of R.-C. Flat Slab Structure. *Univ. Illinois, Eng. Exp. Stn.* Bull. No. 84, 1916 ; also No. 106, 1918.
20. GOLDBECK. The Influence of Total Width on the Effective Width of R.-C. Slabs Subjected to Central Concentrated Loading. *Proc. Amer. Conc. Inst.*, vol. xiii, 1917, p. 78.
21. GOLDBECK AND FAIRBANK. Tests of Large-Sized R.-C. Slab Subjected to Eccentric Concentrated Loads. *U.S.A. Jour. Agric. Res.*, vol. xi, No. 10, Dec. 1917.

Shear and Diagonal Tension in R.-C. Beams

22. MÖRSCH. *Der Eisenbetonbau.* See Ref. No. 1, chap. x (1906 exps.).
23. BACH. Versuch mit Eisenbetonbalken, Zweiter Teil. *Mitt. ü. Forschungsarbeiten V.d.I.*, Hefte 45–47, 1907.
24. BACH U. GRAF. Versuche mit Eisenbetonbalken zur Ermittlung der Widerstandsfähigkeit verschiedener Bewehrung gegen Schubkräfte. *Deu. Ausschuss für Eisenbeton.* Hefte 10, 12, 20, Berlin, 1911–12 ; also Hefte 48, 1921 ; 58, 1928 ; 67, 1931 ; 80, 1935.
25. TALBOT. Tests of R.-C. Beams (Resistance to Web Stresses). *Univ. Illinois Eng. Exp. Stn.* Bull. No. 29, 1909 ; also WITHEY, *Univ. Wisconsin*, Bull. Nos. 175 and 197, 1906–7.
26. FABER. Researches on R.-C. Beams. *Conc. and Const. Eng.*, 1916, p. 361.
27. —— *R.-C. Beams in Bending and Shear*. London, 1924.
28. SLATER, LORD, AND ZIPPRODT. Shear Tests on R.-C. Beams. *U.S. Bur. Stds.* Tech. Pap. No. 314, 1926 ; RICHART, *Univ. Illinois Eng. Exp. Stn.* Bull. No. 166, 1927 ; MYLREA, *Proc. Amer. Soc. C.E.*, Apl. 1929, p. 1089.
29. GILCHRIST. Experiments on Shearing Strength of R.-C. Beams. *Engg.*, Oct. 28, 1927, p. 563 ; also Sept. 17, 1915, p. 293.

30. EVANS AND TOMLINSON. Shear Stress Distribution in R.-C. Beams. *Engg.*, Feb. 8, 1935, p. 158 ; Sept. 11, 1936, p. 269.

Bond Resistance

31. BACH. Versuche über den Gleitwiderstand einbetonierte Eisen. *Mitt. ü. Forschungsarbeiten. V.d.I.* Heft 22, 1905 ; also *Zeits. Ver. deu. Ing.*, May 27, 1911, p. 859.
32. COMMISSION DE CIMENT ARMÉ. Expériences, rapports, etc., relatives à la emploi du béton armé. Paris, 1907.
33. TALBOT. Tests of Concrete. I, Shear ; II, Bond. *Univ. Illinois Eng. Exp. Stn.* Bull. No. 8, 1906 ; also WITHEY, *Univ. Wisconsin,* Bull. No. 321, 1909, p. 27.
34. ABRAMS. Tests of Bond between Concrete and Steel. *Univ. Illinois Eng. Exp. Stn.* Bull. No. 71, 1913 ; also Bull. No. 17, *Struc. Mat. Res. Lab. Lewis Inst. Chic.,* 1926, see *Engg.,* Feb. 26, 1926, p. 268.
35. GLANVILLE. Bond Resistance. Tech. Pap. No. 11, *Build. Res. Stn.,* 1930.
36. POSEN. Tests for Anchorages for Reinforcing Bars. Eng. Bull. No. 3, *Univ. Iowa,* 1933.

Reinforced-Concrete Columns

37. CONSIDÈRE. Hooped Columns, see *Le Genié Civil,* Nov. 1902, Dec. 1902, Jan. 1903 ; *Beton u. Eisen,* 1902, No. 5.
38. WATERTOWN ARSENAL. *Reports on the Tests of Metals,* 1905, p. 386 ; 1906, pp. 344, 377 ; 1907, p. 535 ; 1908, p. 242 ; (year of publication).
39. BACH. Druckversuche mit Eisenbetonkörpern. Berlin, 1905 ; see *Mitt. ü. Forschungsarbeiten V.d.I.,* Heft 29, 1905 ; *Zeit. Ver. deu. Ing.,* Dec. 13, 1913, p. 1969.
40. TALBOT. Tests of Concrete and Reinforced-Concrete Columns. *Univ. Illinois Eng. Exp. Stn.* Bull. No. 10, 1907 ; No. 20, 1908.
41. SPITZER. Versuche mit Eisenbetonsaulen. *Mitt. ü. Versuche v. Oest. Eisenbeton Ausschuss,* Heft iii, 1910 ; EMPERGER, Heft xi, 1927 ; Heft xii, 1931 ; see *Engg.,* Aug. 5, 1927, p. 188 ; Oct. 23, 1931, p. 515.
42. WITHEY. *Univ. Wisconsin.* Bull. No. 466, 1911 ; see Ref. No. 8 (Spiral Columns).
43. TALBOT AND LORD. Tests of Columns (Concrete Reinforcement for Steel Cols.). *Univ. Illinois Eng. Exp. Stn.* Bull. No. 56, 1912 ; TALBOT, Wall and Column Footings, Bull. No. 67, 1913.
44. RICHART AND BROWN. An Investigation of Reinforced-Concrete Columns. *Univ. Illinois Eng. Exp. Stn.* Bull. No. 267, 1934.

Flat Slab Tests

NICHOLS, *Trans. Amer. Soc. C.E.,* vol. lxxvii, 1914, p. 1670 ; HATT, *Proc. Amer. Conc. Inst.,* 1918, pp. 177, 206 ; WESTERGAARD AND SLATER, *Proc. Amer. Conc. Inst.,* 1921.

Torsion

45. BACH U. GRAF. Versuche über die Widerstandsfähigkeit von Beton und Eisenbeton gegen Verdrehung. *Deu. Ausschuss für Eisenbeton,* Heft 16. Berlin, 1912.
46. GRAF U. MÖRSCH. Verdrehungsversuche zur Klärung der Schubfestigkeit von Eisenbeton. Berlin, 1922.
47. YOUNG, SAGAR AND HUGHES. Torsional Strength of Rectangular Sections of Concrete, Plain and Reinforced. *Univ. of Toronto Eng. Res. Bull.* No. 3, 1922.
48. MIYAMOTO. Torsional Strength of Reinforced-Concrete. *Conc. Const. Eng.,* vol. 22, 1927.

49. TURNER AND DAVIES. Plain and Reinforced-Concrete in Torsion. *Select. Eng. Pap. I.C.E.*, No. 165, 1934.

R.-C. Bridges, Arches, and other Structures.

50. MELAN. *Plain and Reinforced-Concrete Arches* (trans. by Steinman). New York, 1917.
51. HOOL. *Reinforced-Concrete Construction.* New York, 1927–28. Vol. ii, *Retaining Walls and Buildings* ; vol. iii, *Bridges and Culverts.*
52. WILSON. Laboratory Tests on R.-C. Arched Ribs. *Univ. Illinois Eng. Exp. Stn.* Bull. No. 202, 1930.
53. —— Laboratory Tests on R.-C. Arches with Decks. *Univ. Illinois Eng. Exp. Stn.* Bull. No. 226, 1931.
54. SCOTT, W. L. *Reinforced-Concrete Bridges.* London, 3rd ed., 1931.
55. MANNING. Reinforced-Concrete Arch Design. 1933.
56. CHETTOE AND ADAMS. Reinforced-Concrete Bridge Design. London, 1933.
57. AMER. Soc. C.E. Final Report of Special Committee on Concrete and Reinforced-Concrete Arches. *Trans. Amer. Soc. C.E.*, vol. 100, 1935, p. 1427.
58. WILSON AND KLUGE. Laboratory Tests of Three-Span R.-C. Arch Bridges with Decks on Slender Piers. *Univ. Illinois Eng. Exp. Stn.* Bull. No. 270, 1935 ; also Bull. No. 269, 1934 ; see also *Trans. Amer. Soc. C.E.*, vol. 100, 1935, p. 424, Multi-Span R.-C. Arches.
59. EREMIN. Wind Stress on R.-C. Arch Bridges. *Proc. Amer. Soc. C.E.*, Dec. 1935.
60. GRAY. *Reinforced-Concrete Reservoirs and Tanks.* London, 1932.
61. —— *Reinforced-Concrete Water Towers, Bunkers, Silos, and Gantries.* London, 1933.

QUESTIONS ON CHAPTER XVII

1. In a rectangular cross-section reinforced-concrete beam, the reinforcement is on the tension side only, the percentage of steel area is $0 \cdot 8$, and the centres of the steel bars are 18 in. below the compression face of the beam. Find (1) the distance of the neutral plane below the compression face, (2) the tensile stress in the steel if the maximum compressive stress in the concrete is not to exceed 600 lb./sq. in. Take $E_s = 15 \ E_c$. (U.L. modified.)
Ans. $v_c = 6 \cdot 92$ in. ; 14,410 lb./sq. in.

2. A reinforced-concrete beam, having tensile reinforcement only, is 12 in. wide and 18 in. deep from the top to the centre of the reinforcement. Stresses of 600 lb./sq. in. push in the concrete, and 16,000 lb./sq. in. pull in the steel are to be attained simultaneously. Find the area of steel required, the position of the neutral axis, and the moment of resistance of the section ; $E_s = 15 \ E_c$. It is expected that this question will be worked from first principles. (U.L.)
Ans. $a_t = 1 \cdot 46$ sq. in. ; $v_c = 6 \cdot 48$ in. ; $M = 369,360$ in.-lb.

3. A concrete beam 15 ft. long × 12 in. broad × 15 in. deep is reinforced by four ¾-in. sq. steel bars, having their centres 2 in. from the bottom of the beam. Determine the uniform loading which may be applied without the stress in the concrete exceeding 600 lb./sq. in., and ascertain the resulting stress in the steel. Take the steel-concrete modular ratio as 15. (U.L.)
Ans. 722 lb./ft. ; 9,900 lb./sq. in.

4. In a reinforced-concrete T beam the thickness of the slab is 5 in., and a width of 60 in. may be counted in. The tensile reinforcement consists of four bars 1 in. diam., and the effective depth d of the beam is 22 in. The

neutral axis falls $0 \cdot 2$ in. below the bottom of the slab. Find the safe bending moment on the beam if the stress in the steel is not to exceed 16,000 lb./sq. in., or in the concrete 600 lb./sq. in. $m = E_s : E_c = 15$. (I.C.E.)

Ans. 1,018,770 in.-lb.

5. A reinforced-concrete T beam has the following dimensions : Compression flange, 5 ft. wide, 8 in. thick, web 15 in. wide. Overall depth 42 in. Top of compression flange to centre of reinforcement 40 in. It carries a bending moment of 580,000 ft.-lb. The reinforcement consists of 10 steel rods whose total area is 14 sq. in. Take $E_s/E_c = 15$ and find (a) the position of the neutral axis, and (b) the unit stresses in the steel and concrete. (U.L.)

Ans. Use method of § 315 ; $v_c = 14 \cdot 96$ in. ; $f_t = 13,620$ lb./sq. in. ; $f_c = 543$ lb./sq. in.

6. The cross-section of a doubly reinforced concrete beam is 15 in. wide and 30 in. effective depth. The area of the tension steel is $4 \cdot 5$ sq. in. and that of the compression steel is $2 \cdot 25$ sq. in. The latter is placed 3 in. from the top of the beam. Find the position of the neutral axis, and the tensile moment of resistance of the section, if the tensile stress in the steel is 16,000 lb./sq. in. Take $E_s/E_c = 15$. (U.L.)

Ans. $v_c = 11 \cdot 46$ in. ; 1,895,000 in.-lb.

7. Show by a diagram the distribution of shear stress over the cross-section in a singly reinforced concrete beam, the tension in the concrete being neglected. Find the maximum value, and explain carefully the effect of vertical and diagonal shear members or stirrups. (U.L.)

Ans. See §§ 317 and 318.

8. A reinforced-concrete beam 10 in. wide, and 22 in. deep has four 1-in. diameter bars placed with their centre lines 2 in. from the lower edge. The beam has a span of 16 ft. The compressive stress in the concrete is not to exceed 600 lb./sq. in. The modular ratio is 15. Determine : (1) the load per foot run the beam will carry, (2) the stress in the steel, (3) suitable reinforcements for resisting shear, (4) the maximum shear stress between the steel and the concrete. (U.L.)

Ans. 1,280 lb./ft. ; 9,370 lb./sq. in. ; turn two bars up at 45°, $\frac{5}{16}$-in. stirrups, 16-in. pitch ; max. $f'_s = 98$ lb./sq. in.

9. A reinforced-concrete T beam has to carry a uniformly distributed load of 1,500 lb. per ft. of span. The span is 20 ft. and the ends fixed ; it may be assumed that the bending moments at the ends and at the centre of the span are equal. There is tensile reinforcement only, and the bars are not to exceed $\frac{7}{8}$-in. diameter. The slab is 48 in. wide and 4 in. thick. The working stresses are 16,000 lb./sq. in. in the steel, and 600 lb./sq. in. compression in the concrete, and the modular ratio is 15. Design the mid-section of the beam. (U.L.)

Ans. $M = WL/16$; 14 in. overall ; $d = 12$ in. (min.) ; $b_1 = 8$ in. ; five $\frac{7}{8}$-in. bars.

10. Design a reinforced-concrete beam with double reinforcement to the following particulars : Section rectangular, 10 in. broad. Depth from top of beam to centre of tensile reinforcement 18 in. ; depth from top of beam to centre of compressive reinforcement 2 in. ; moment of resistance 500,000 in.-lb. Stresses of 600 and 16,000 lb./sq. in. for the concrete in compression and for the steel in tension respectively are not to be exceeded. Ratio of the elastic moduli 15. Find the area of the tensile steel and of the compressive steel, and the position of the neutral axis. State the intensity of stress on both steel reinforcements and on the concrete. (U.L.)

Ans. $a_t = 1 \cdot 98$; $a_c' = 2 \cdot 17$ in. ; use $5/\frac{3}{4}$-in. rods for both ; $v_c = 6 \cdot 73$ in. ; $f_t = 14,340$; $f_c = 571$; $f_c' = 6020$ lb./sq. in.

11. A reinforced-concrete column 6 ft. long is 8 in. square in section and is reinforced by four steel bars each 1 sq. in. in cross-section. The column

carries a load of 36 tons. Determine the amount of load taken by the concrete and steel respectively, and the shortening of the column. $E_s = 13,000$ tons/sq. in. ; $E_s/E_c = 15$. (U.L.)

Ans. Each 18 tons ; $\delta L = 0 \cdot 025$ inch.

12. Explain how the longitudinal and hoop reinforcement is allowed for in calculating the safe load on a reinforced-concrete column. Such a column, supposed short, is to carry an axial load of 50 tons. The working stress of plain concrete is to be taken as 500 lb./sq. in. and the nature and amount of the hooping reinforcement is such that the safe working stress will be increased 30 %. The longitudinal reinforcement is to be 4 % and $m = 15$. Find the diameter of the hooped core. (U.L.)

Ans. 12 inches.

CHAPTER XVIII

EARTH PRESSURE AND FOUNDATIONS

323. Stability of Earthwork.—Failure in an earthwork is due to part of the mass slipping or sliding relatively to the rest. This tendency to slide is resisted by the adhesion and friction of the particles of earth between themselves. In certain theories of earth pressure, the adhesion is neglected entirely, and it is assumed that the mass of earth is composed of particles which do not cohere, but are held in position by the friction one on another; that is, to assume that the mass is granular. While such a theory may represent with some degree of accuracy the condition of a mass of fine dry sand, it is evident that a stiff heavy clay, or well-rammed earth, would behave in a very different manner, § 331. When coherent earth is exposed to the weather, the action of the elements, air, rain, frost, and drought, tends to destroy any adhesion there may be between the particles, and it is then usual to place reliance on friction alone for stability. Stiff clay, not subject to the weather, may be otherwise treated, § 331 *et seq.*

324. Angle of Repose.—If a mass of earth be left to itself for a considerable time, with no lateral support, its sloping sides will be found to have weathered to a certain more or less definite angle. This angle is called the *angle of repose*. Assuming the particles of the mass to be without cohesion, this angle is evidently equal to ϕ, the angle of friction between the particles, of which the tangent μ is the coefficient of friction. If a sloping bank be constructed, making an angle with the horizontal greater than the angle of repose, the upper layers of particles will, in time, slide down, until the slope becomes equal to the friction angle. A slope less than the angle of repose should retain its formation permanently. The following Table gives average values for ϕ and μ for a number of materials, together with their weight per cubic foot.

Material.	Angle of Repose ϕ.	Coefficient of Friction μ.	Weight lb./cub. ft
Sand, fine, dry . .	30°	0·58	100
Sand, wet . .	25°	0·47	120
Gravel . . .	40°	0·84	110
Shingle . .	35°	0·70	110
Clay, dry . .	30°	0·58	110
Clay, very wet . .	15°	0·27	130
Earth, loamy, dry .	30°	0·58	90
Earth, loamy, wet .	15°	0·27	110

These values may vary considerably, depending on the material and its condition.

325. Stability of Loose Earth. Rankine's Theory.—Rankine considered a mass of loose earth of indefinite extent, having a plane top surface, and subjected to its own weight. He assumed that the earth is incompressible, homogeneous, and granular ; and that the particles of which it is composed are without cohesion, but are held in place by friction, one on another. Then it follows that, for stability, the direction of the pressure on any plane surface within the mass cannot make an angle with the normal to that surface greater than the angle of repose of the earth, otherwise slipping will result. If AC, Fig. 443, be any plane surface within the mass, OQ the normal thereto, PO the direction of the pressure on the plane, then the angle POQ $= \psi$ must be less than ϕ, the angle of repose. Granting Rankine's assumptions, the ellipse of stress theory, § 17, Vol. I, may be applied to the problem. Two cases arise.
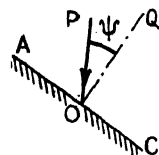
Fig. 443.

Case 1. *Horizontal Upper Surface.*—In the first instance, UU, the top surface of the mass, will be supposed horizontal. Let ABCD, (i) Fig. 444, be a small rectangular element of earth within the mass. Suppose that, due to the weight of the earth above it, there be a pressure p_1 on the plane AB, which pressure is balanced by an equal upward pressure on the plane CD. The element is supposed so small that its own weight may be neglected. Since it is assumed that the particles of which the element is composed have no cohesion, equal and opposite pressures $p_2 p_2$ must be applied to the vertical surfaces AD and BC, in
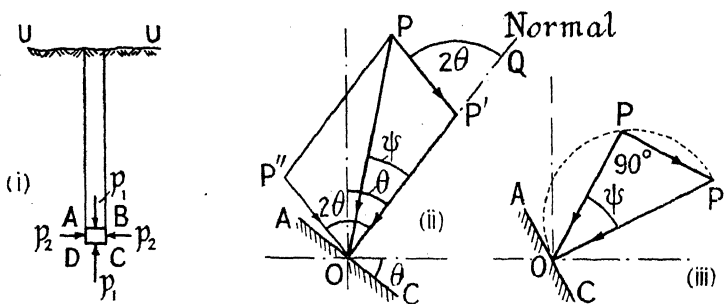
Fig. 444.

order to maintain the equilibrium. Then this element is in the same condition as that shown in Fig. 21, Vol. I, except that the direction of the stresses is reversed, and the theory there given can be used to discover the pressure on the interface AC. It is convenient to use Rankine's construction, Fig. 23, Vol. I. It is there shown that the two pressures p_1 and p_2 will produce a pressure $P'O = (p_1 + p_2)/2$ normal to the interface AC, (ii) Fig. 444, together with a pressure $P''O = (p_1 - p_2)/2$ in a direction making an angle $P'OP'' = 2\theta$ with the normal, where θ is the angle which the plane AOC makes with the horizontal. Then PO, making an angle ψ with the normal, represents the resultant intensity of

pressure on the interface AC. Now it is evident that, for given values of p_1 and p_2, the angle ψ will be different on different interfaces, but it will be a maximum when the angle OPP' is a right angle, (iii) Fig. 444, i.e. when

$$\sin \psi = \frac{\text{PP}'}{\text{P}'\text{O}} \cdot \frac{\text{P}''\text{O}}{\text{P}'\text{O}} = \frac{\dfrac{p_1 - p_2}{2}}{\dfrac{p_1 + p_2}{2}} = \frac{p_1 - p_2}{p_1 + p_2}$$

This gives the maximum angle which the resultant pressure on *any* interface can make with the normal to that interface, and by the principle enunciated above, this angle must not exceed ϕ, the angle of repose, or slipping will result. Hence,

$$\sin \psi \quad \frac{- p_2}{p_1 + p_2} \lessgtr \sin \phi$$

from which,

$$\frac{p_2}{p_1} \gtrless \frac{1 - \sin \phi}{1 + \sin \phi} . \qquad . \quad (1)$$

This equation determines the least value of p_2, the intensity of pressure on the planes AD and BC, which will maintain a pressure p_1 on the planes AB and CD at right angles thereto, if the angle of repose of the earth be ϕ.

The pressures p_1 and p_2 are ' principal stresses ' as defined in § 17, Vol. I. There is evidently a third principal stress, acting normally to the plane ABCD, equal in magnitude to p_2.

Case 2. Sloping Upper Surface.—Next suppose that the top surface of the mass makes an angle α with the horizontal, Fig. 445. In this case, Rankine assumed that the pressure p on the faces JK and ML of a rhombic element JKLM, of which the sides JK and ML are parallel to the upper surface of the mass, would be maintained by a pressure p' on the vertical faces JM and KL. It will be observed that each of these pressures is parallel to the face on which the other acts. Such pressures are called *conjugate pressures*, because they are represented in magnitude and direction by conjugate semi-diameters of the ellipse of stress. The ratio between these conjugate pressures, p and p', can be found by Rankine's construction. Let p_1 and p_2 be

FIG. 445.

the corresponding principal stresses (pressures). The direction of these is at present unknown; suppose, however, that in (i) Fig. 446, Oy and Ox be the directions of the greatest and least principal stresses, and OQ the normal to the plane JOK on which the pressure is p. Then if P'O $= (p_1 + p_2)/2$, and PP' $= (p_1 - p_2)/2$, PO represents the pressure p on the plane JOK. Further, since the pressure on the plane JK is parallel to the plane

KL, OQ_1 at right angles to PO will be the normal to the plane KOL. If, then, $P_1'O = (p_1 + p_2)/2$, and $P_1P_1' = (p_1 - p_2)/2$, by the same construction, P_1O will represent p', the pressure on the plane KL. But this pressure is parallel to the plane JK, therefore P_1O must coincide with the line JOK. Consider the two triangles $OP'P$ and $OP_1'P_1$. It is evident that since both the angles POQ_1 and QOP_1 are right angles, the angle POP' is equal
to the angle P_1OP_1'. But the angle POP' is the angle between the plane KL and the normal to the plane JK, i.e. it is the angle α which the sloping upper surface makes with the horizontal. Hence, the angle $POP' =$ the angle $P_1OP_1' = \alpha$. Further, the length $OP' = OP_1' = (p_1 + p_2)/2$, and $PP' = P_1P_1' = (p_1 - p_2)/2$. If, therefore, the two triangles $OP'P$ and $OP_1'P_1$ be superposed, (ii) Fig. 446 is obtained, in which
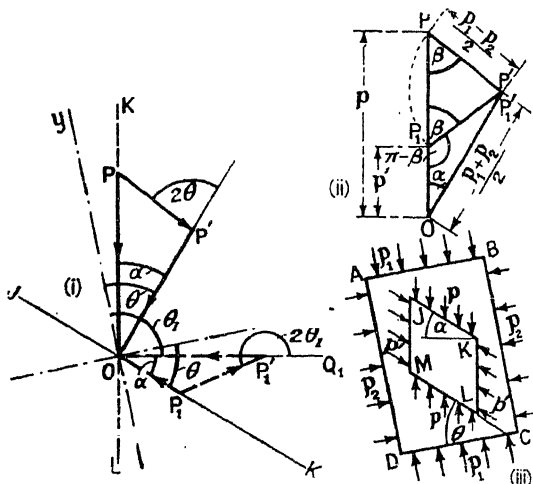
Fig. 446.

$OP = p$, $OP_1 = p'$, and the angle $POP' = \alpha$. From this figure the ratio of p' to p can be found. It is evidently an example of the ' ambiguous case ' in the solution of triangles theory. Let the angle $P'PP_1 = P_1'P_1P = \beta$; then the angle $OP_1P' = \pi - \beta$. Applying the well-known formula $a = b \cos C + c \cos B$ to the triangle OPP', $p = OP' \cos \alpha + PP' \cos \beta$; and for the triangle OP_1P_1', $p' = OP_1' \cos \alpha + P_1P_1' \cos (\pi - \beta) = OP_1' \cos \alpha - P_1P_1' \cos \beta$. Hence,

$$\frac{p'}{p} \quad \frac{\cos \alpha - \dfrac{PP'}{OP'} \cos \beta}{\cos \alpha + \dfrac{PP'}{OP'} \cos \beta} \tag{2}$$

Now $\dfrac{PP'}{OP'} = \dfrac{p_1 - p_2}{p_1 + p_2}$. But at the moment when slipping is about to occur, from eq. (1), $\dfrac{p_1 - p_2}{p_1 + p_2} = \sin \phi$, and, therefore, $\dfrac{PP'}{OP'} = \sin \phi$. Further, applying the formula $\dfrac{c}{b} = \dfrac{\sin C}{\sin B}$ to the triangle $OP'P$; $\dfrac{PP'}{OP'} = \dfrac{\sin \alpha}{\sin \beta}$.

Hence, $\dfrac{\sin \alpha}{\sin \beta} = \sin \phi$, from which, $\sin \beta = \sqrt{1 - \cos^2\beta} = \dfrac{\sin \alpha}{\sin \phi}$, and

$$\cos \beta = \frac{\sqrt{\sin^2 \phi - \sin^2 \alpha}}{\sin \phi} = \frac{\sqrt{\cos^2 \alpha - \cos^2 \phi}}{\sin \phi}.$$

or, since

$$\frac{PP'}{OP'} = \sin \phi, \quad \frac{PP'}{OP'} \cos \beta = \sqrt{\cos^2 \alpha - \cos^2 \phi}.$$

Inserting this value in eq. (2),

$$\frac{p'}{p} = \frac{\cos \alpha - \sqrt{\cos^2 \alpha - \cos^2 \phi}}{\cos \alpha + \sqrt{\cos^2 \alpha - \cos^2 \phi}} \tag{3}$$

For a given value of p, this equation gives the least value of p' which will prevent slipping. It will be noticed that, if $\alpha = 0$, this equation reduces to eq. (9), as it should. In this particular case, $p = p_1$ and $p' = p_2$ are the principal stresses. If $\alpha = \phi$, that is to say, if the slope of the upper surface is the greatest possible consistent with stability, $p' = p$. In this case, therefore, $OP_1 = OP$, (ii) Fig. 446, i.e. the two points P_1 and P coalesce, and the line OP_1P becomes tangent to the circle through P and P_1 struck with P' as centre. This leads to the construction shown in Fig. 447 for determining the ratio of p' to p, which is due to Rankine. With centre P', describe the semicircle XRPY, and draw OR a tangent thereto, making an angle ϕ with OY. Then if OP_1P be drawn, making an angle α with OY, $\dfrac{OP_1}{OP} = \dfrac{p'}{p}$. This figure is evidently a reproduction of (ii) Fig. 446, OR representing the limiting case when $\alpha = \phi$, and $OP_1 = OP = OR$.

FIG. 447.

The directions Ox and Oy of the principal stresses are given by Fig. 446. Their magnitudes can be obtained by the ellipse of stress theory, or graphically from Fig. 447.

$$p_1 = \frac{p(1 + \sin \phi)}{\cos \alpha + \sqrt{\cos^2 \alpha - \cos^2 \phi}} = OY \tag{4}$$

$$p_2 = \frac{p(1 - \sin \phi)}{\cos \alpha + \sqrt{\cos^2 \alpha - \cos^2 \phi}} = OX \tag{5}$$

The relation between p and p', p_1 and p_2, is shown at (iii) Fig. 446. As in Case 1 there is a third principal stress, acting perpendicularly to the plane ABCD, and equal in magnitude to p_2.

Knowing w, the weight per cubic foot of the earth, the magnitude of p for any depth h below the surface can be found. From Fig. 445, the weight of the prism of earth VJKV, supposed of unit length perpendicular to the paper, is $wh . JK . \cos \alpha$, where $JK . \cos \alpha$ is the area of a right cross-section. But this weight produces the pressure p on the area JK. Hence $p . JK = wh . JK . \cos \alpha$, and

$$p = wh \cos \alpha \qquad . \qquad . \qquad . \qquad . \qquad . \tag{6}$$

If in Fig. 447, PZ be drawn perpendicular to OP, OZ represents wh to the scale of the diagram.

If the upper surface of the mass of earth be horizontal, Case 1, $a = 0$ and

$$p = wh = p_1 \quad . \quad . \quad . \quad . \quad . \quad (7)$$

326. Earth Pressure on Vertical Retaining Wall without Surcharge. Friction neglected.—Suppose that the earth be held up by a retaining wall as shown in Fig. 448, its upper surface being horizontal, i.e. without surcharge. The lateral pressure of the earth will react against the vertical face EV of the wall, tending to overturn it. Consider the pressure on an elementary width δh, at a distance h below the upper surface of the earth, and of length unity perpendicular to the plane of the paper. The intensity of pressure on this element will be equal to p_2, the pressure on the plane BC of the element ABCD. But from eqs. (1) and (7), § 325,

$$p_2 = p_1 \frac{1 - \sin \phi}{1 + \sin \phi} = wh \frac{1 - \sin \phi}{1 + \sin \phi} \qquad (1)$$

where $p_1 = wh$ is the pressure on the plane AB. Hence the pressure on the element δh will be

$$p_2 . \delta h = \frac{1 - \sin \phi}{1 + \sin \phi} wh . \delta h,$$
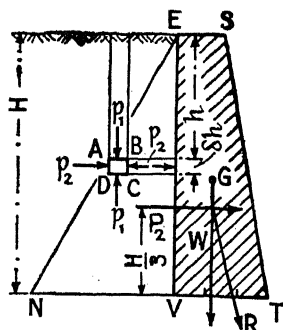
FIG. 448.

and the total pressure on the surface EV per unit of length of wall will be

$$P_2 = \int_0^H p_2 . dh = \frac{1 - \sin \phi}{1 + \sin \phi} w \int_0^H h . dh = \frac{wH^2}{2} . \frac{1 - \sin \phi}{1 + \sin \phi} \quad . \quad (2)$$

where H is the total height of the retaining wall. If H be measured in feet, and w in lb. per cub. ft., P_2 is in pounds. From eq. (1) it follows that p_2 varies as h, hence the diagram of pressure on the back of the wall is the triangle ENV, of which the maximum ordinate $NV = wH\dfrac{1 - \sin \phi}{1 + \sin \phi}$. It follows that the resultant P_2 acts at a distance $\frac{2}{3}H$ from the upper surface. P_2 is a horizontal force, and can be combined with W, the weight of the retaining wall per unit of length, which acts through G, the centre of gravity of the wall, to obtain the magnitude and direction of R, the resultant force on the base VT. Knowing the distribution of pressure ENV on EV, the back of the wall, the stability of the wall can be tested exactly as in the case of the masonry dam, § 363.

In that it neglects the friction on the back of the wall, the above theory leads to an over-estimate of the overturning effort (see § 329).

327. Earth Pressure on Vertical Retaining Wall with Surcharge.—When the surface of the earth slopes upward from the top of the retaining wall, as shown in Fig. 449, the formation is spoken of as a retaining wall *with surcharge*. To this, the formulae of § 325, Case 2, will apply. The lateral pressure p', acting parallel to the sloping upper surface,* will tend

* This is equivalent to assuming that the angle of friction on the back of the wall $\phi' = a$. In practice $\phi' = \phi$ (approximately), and this theory also over-estimates the overturning moment, except when $a = \phi$, when it agrees with the wedge theory, § 329.

to overturn the wall.   As before, consider an elementary width δh at a distance h below the upper surface of the earth, and of length unity perpendicular to the plane of the paper.   The intensity of pressure on this surface will be equal to p', the pressure on the plane KL of the element JKLM.   From eqs. (3) and (6), § 325,

$$p' = p\frac{\cos\alpha - \sqrt{\cos^2\alpha - \cos^2\phi}}{\cos\alpha + \sqrt{\cos^2\alpha - \cos^2\phi}} = wh\cos\alpha\ \frac{\cos\alpha - \sqrt{\cos^2\alpha - \cos^2\phi}}{\cos\alpha + \sqrt{\cos^2\alpha - \cos^2\phi}} \ . \ (1)$$

where $p = wh\cos\alpha$ is the pressure on the plane JK, and α is the angle of the surcharge.   Hence the pressure on the element δh will be $p' \cdot \delta h$, and the total pressure on the surface EV per unit of length of wall will be

$$P' = \int_0^H p' \cdot dh = \frac{\cos\alpha - \sqrt{\cos^2\alpha - \cos^2\phi}}{\cos\alpha + \sqrt{\cos^2\alpha - \cos^2\phi}}\ w \ \cos\alpha \Big\rvert_0 \ h \cdot dh$$

$$\frac{wH^2}{2}\cos\alpha\ \frac{\cos\alpha - \sqrt{\cos^2\alpha - \cos^2\phi}}{\cos\alpha + \sqrt{\cos^2\alpha - \cos^2\phi}} \quad\quad (2)$$
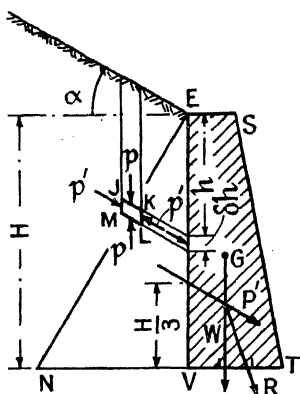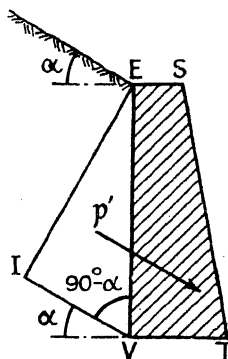
FIG. 449.   FIG. 450.

H is the total height of the retaining wall.   If H be measured in feet, and w in lb. per cub. ft., P' will be in pounds.   Since, from eq. (1), p' varies as h, the triangle ENV represents the distribution of pressure on the surface EV.   The maximum ordinate

$$NV = wH\cos\alpha\ \frac{\cos\alpha - \sqrt{\cos^2\alpha - \cos^2\phi}}{\cos\alpha + \sqrt{\cos^2\alpha - \cos^2\phi}} \quad\quad . \ (3)$$

The resultant pressure P' will act, therefore, at a distance $\frac{2}{3}$H from E, and in a direction parallel to the sloping upper surface.   The resultant force R on the base VT will be the resultant of P' and the weight W of the retaining wall per unit of length.   The stability of the wall at every horizontal cross-section can be tested exactly as in the case of a masonry dam, § 363, but it must be borne in mind that the pressure everywhere on

2 x

the surface EV is always parallel to the sloping upper surface of the earth.

Rankine has shown that the magnitude of the force P' is equal to the weight of a triangular mass of earth EVI, Fig. 450, such that VI, which is parallel to the sloping upper surface, is equal to $EV \cdot \dfrac{OP_1}{OP}$, where OP_1 and OP are obtained from Fig. 447. The area of the triangle EVI is $\frac{1}{2}EV \cdot VI \sin(90 - a) = \frac{1}{2}H \cdot H\dfrac{OP_1}{OP} \cos a = \frac{1}{2}H^2 \cos a \times$

$\dfrac{\cos a - \sqrt{\cos^2 a - }}{\cos a + \sqrt{\cos^2 a - \cos^2 \phi}}$. Therefore the weight of this triangular mass of unit thickness is

$$\tfrac{1}{2}wH^2 \cos a \; \frac{\cos a - \sqrt{\cos^2 a - \cos^2 \phi}}{\cos a + \sqrt{\cos^2 a - \cos^2 \phi}} = P' \;\; [\text{see eq. (2) }].$$

Thus, by the use of Fig. 447 and Fig. 450, the magnitude of P' is easily obtained. The construction holds equally well if the upper surface be horizontal, $a = 0$.

328. Earth Pressure on Retaining Walls. Special Cases.—If the back of the wall be stepped, as shown at (i) Fig. 451, P' is the pressure
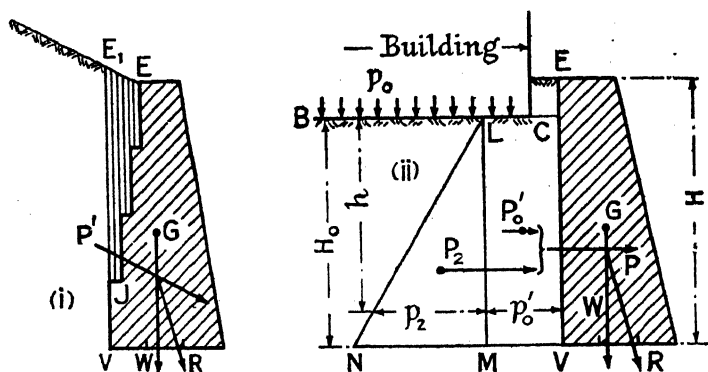
FIG. 451.

on the plane E_1V, and is determined by the methods of the preceding article. In this case, however, W is the weight of the retaining wall plus that of the portion of earth E_1EJ, and G is the common centre of gravity of these two weights. Otherwise the procedure is the same as before (see also Fig. 455).

If the wall has to resist the overturning thrust resulting from an external load, in addition to the pressure due to the weight of the earth, as for example the weight of a building built close up to the wall, (ii) Fig. 451, the force P will be the resultant of two components, one due to the weight of the building, the second due to the weight of the earth.

Suppose that p_0 be the uniform pressure produced on the surface BC by the weight of the building. Then p_0', the lateral pressure on any vertical plane necessary to resist this pressure, is, from eq. (1), § 325, $p_0' = p_0 \dfrac{1 - \sin \phi}{1 + \sin \phi}$. This lateral pressure p_0' will act on the back of the wall. It will be uniform from top to bottom and is represented by the rectangle CLMV. Its resultant per unit of length of wall is $P_0' = p_0'.CV = p_0'.H_0 = p_0 H_0 \dfrac{1 - \sin \phi}{1 + \sin \phi}$, and will act halfway between C and V. The lateral pressure on the plane CV due to the weight of the earth will vary from zero at C to a maximum at V, and is represented by the triangle LNM. Its resultant is given by eq. (2), § 326, $P_2 = \dfrac{w H_0^2}{2} \cdot \dfrac{\sin \phi}{1 + \sin \phi}$, which acts at a distance $\frac{1}{3}$CV above V. Both P_0' and P_2 are horizontal forces.

The total pressure P on the plane CV is the resultant of P_0' and P_2,

$$P = P_0' + P_2 = p_0 H_0 \frac{1 - \sin \phi}{1 + \sin \phi} + \frac{w H_0^2}{2} \frac{1 - \sin \phi}{1 + \sin \phi}$$

$$= \left(p_0 H_0 + \frac{w H_0^2}{2} \right) \left(\frac{1 - \sin \phi}{1 + \sin \phi} \right) \qquad . \quad (1)$$

It will act at the centre of pressure of these two forces, that is to say, at a distance $\dfrac{H_0}{3} \cdot \dfrac{w H_0 + 3 p_0}{w H_0 + 2 p_0}$ from V.

329. Earth Pressure on Retaining Walls. Other Formulae.—While Rankine's theory is probably substantially correct for a mass of material such as fine, dry, loose sand left to itself, § 335, it has been shown experimentally that the theory given in §§ 326–8 over-estimates the overturning effort on the back of a retaining wall, even in the case of dry pulverulent materials. The pressure p_2 given by eq. (1), § 326, is accurately the pressure across an ideal vertical plane through such material, but when subjected to such pressure, the retaining wall, not being rigid, moves forward slightly, the earth slips, or tends to slip, down the wall, and the resultant pressure then makes an angle with the normal to the wall equal to the angle of friction between the earth and the wall. This friction has not been taken into account in § 326. Poisson, Boussinesq, Weyrauch, Résal, Cain and others (see Bib.) have given analyses which include the effect of the friction on the back of the wall. Of these, that of Résal is perhaps the most satisfactory, but it is complicated, and the simpler *wedge theory* given below is sufficiently accurate for all practical purposes. Recent experiments by Professor Jenkin [36], with dry sand, confirm the accuracy of these analyses.

The Wedge Theory.—Fig. 452 is a sketch from a photograph of an experiment by Professor Takabeya [34] in which dry loose sand was arranged in coloured layers behind a model retaining wall about 50 cm. high ; the retaining wall was moved forward 2 cm., the sand slipped down

behind the wall, and a definite inclined plane of rupture was produced. The pressure on the wall from the wedge of sand, included between the wall and the plane of rupture, is the force tending to overturn the wall.
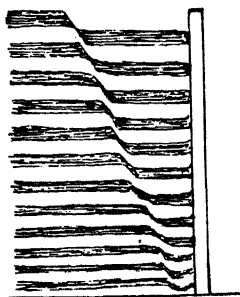
FIG. 452.
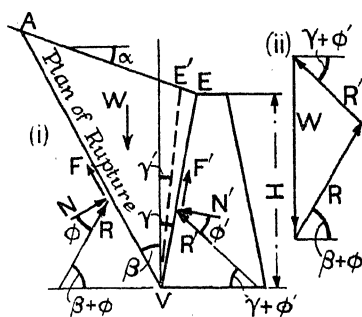
FIG. 453.

Fig. 453 represents a retaining wall with surcharge. Let

R' = the reaction between the wall and the wedge.
N' = its normal component.
F' = the frictional resistance on the back of the wall.
R = the reaction across the plane of rupture.
N = its normal component.
F = the frictional resistance along the plane of rupture.
F_H = the horizontal component of R' or R.
w = the weight of the earth filling per unit volume.
W = the weight of the wedge.
H = the height of the wall.
a = the angle of the surcharge.
β = the inclination of the plane of rupture to the vertical.
γ = the inclination of the back of the wall to the vertical. In Fig. 453, γ is positive; in Fig. 454, γ is negative.

$\tan \phi$ = the coefficient of friction along the plane of rupture.
$\tan \phi'$ = the coefficient of friction along the back of the wall.

Then, for any angle β, it may be shown that

$$R' = \frac{wH^2}{2 \cos^2 \gamma} \cos (a - \gamma) \frac{\sin (\beta + \gamma) \cos (\beta + \phi)}{\cos (\beta + a) \sin (\beta + \gamma + \phi + \phi')} \quad (1)$$

and $F_H = R' \cos (\gamma + \phi') = \frac{wH^2}{2 \cos^2 \gamma} \cos (a - \gamma) \times$

$$\cos (\gamma + \phi') \frac{\sin (\beta + \gamma) \cos (\beta + \phi)}{\cos (\beta + a) \sin (\beta + \gamma + \phi + \phi')} \quad (2)$$

The maximum value of R' and F_H will occur when

$$\frac{d}{d\beta} \frac{\sin (\beta + \gamma) \cos (\beta + \phi)}{\cos (\beta + a) \sin (\beta + \gamma + \phi + \phi')} = 0 \quad (3)$$

Also the value of ϕ' cannot exceed ϕ, or sliding would take place along a plane close up to and parallel with the wall, leaving a thin film of earth adhering thereto. The solution of these equations, even in the simplified cases, is rather unmanageable, and it is better to use the graphical construction given in § 330.

When the value of γ is positive and large, the earth may rupture along a second plane such as E'V, Fig. 453, making an angle γ' with the vertical, rather than slide down the back of the wall (cf. Jenkin [36]). Eqs. (1) and (2) hold for this case also, if γ' is written for γ, and ϕ' is replaced by ϕ. The solution for maximum thrust is given as in eq. (3) by putting $d/d\beta = 0$ and $d/d\gamma' = 0$, when

$$\beta = \tfrac{1}{2}(\pi/2 - \phi + \epsilon - \alpha) \text{ and } \gamma' = \tfrac{1}{2}(\pi/2 - \phi - \epsilon + \alpha) \quad . \quad (4)$$

where $\qquad\qquad \sin \epsilon = \sin \alpha/\sin \phi \quad . \quad . \quad . \quad . \quad (5)$

If then γ' be less than γ, from the given values of α and $\phi = \phi'$ (usually taken as the angle of repose of the earth), ϵ can be found from eq. (5), and β and γ' from eq. (4). Inserting the values of α and β, and the value γ' for γ, in eqs. (1) and (2), the maximum force R' (or F_H its horizontal component) which can be exerted against a rough wall is obtained. R' will make an angle $(\gamma' + \phi)$ with the *horizontal* (see Fig. 453). In this latter case, the wedge of earth E'VE must be counted in as forming part of the wall.

Experiment has shown that the point of application of R' is not of necessity $\tfrac{1}{3}$ the way up VE. Jenkin suggests : 0·4 when $\gamma = -10°$ to $+ 25°$; 0·45 when $\gamma > + 25°$; $\tfrac{1}{3}$ when $\gamma = -15°$ to $-30°$; but if $\alpha = \phi$ take 0·55 (see also Feld, § 335).

330. The Wedge Theory. Rebhann's Construction.—The following
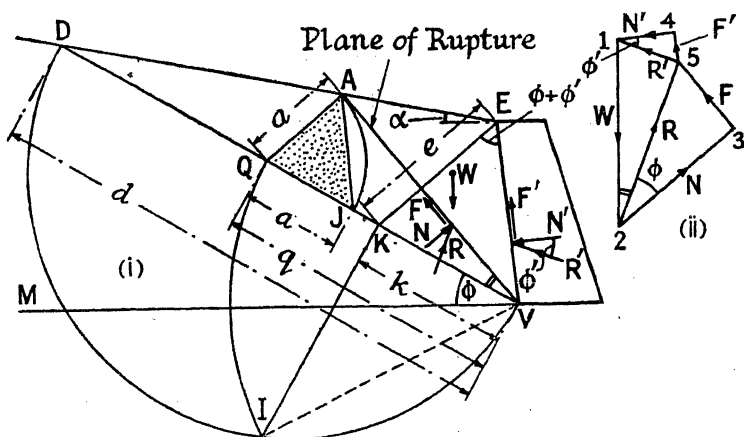
FIG. 454.

graphical construction * was proposed by Rebhann (1871) to determine the value of R' (for symbols see § 329).

In Fig. 454 AV is the plane of rupture. Consider the equilibrium of the wedge of earth AVE. The forces acting on it are its own weight W, the normal and tangential forces N and F on the plane AV, and the

* For several modifications, see Cormack, *Proc. Inst. C.E.*, vol. 234, 1931-32, p. 199.

normal and tangential forces N′ and F′ on the back of the wall EV, (i). Assuming as before that the earth depends on friction for stability, $F/N = \tan \phi$; $F'/N' = \tan \phi'$. These forces are represented in the force polygon, (ii). Draw a vertical 1,2 to represent W ; 2,3 perpendicular to AV to represent N ; 4,1 perpendicular to EV to represent N′ ; draw 2,5 making an angle ϕ with 2,3, and 5,1 making an angle ϕ' with 4,1. Then 2,5 represents the resultant pressure R on the plane AV, and 5,1 the resultant pressure R′ on the plane EV. The three forces 1,2 2,5 5,1 must be in equilibrium, and their relative magnitudes are represented by the sides of the triangle 1,2,5. It is required to find the position of AV which will make R′ a maximum. Draw DV making an angle ϕ with VM.

Since in (ii), 1,2 is perpendicular to VM ; 2,3 is perpendicular to AV ;

$$\angle \text{MVA} = \angle 1,2,3; \quad \angle \text{MVQ} = \angle 3,2,5 = \phi;$$

therefore, $\angle \text{QVA} = \angle 5,2,1.$

Draw AQ such that the $\angle \text{QAV} = \angle 1,5,2$, and EK parallel thereto. Then the triangles QAV and 1,5,2 are similar, and

$$\frac{W}{R'} = \frac{QV}{AQ}; \text{ or, } R' = W \cdot \frac{AQ}{QV} \quad . \quad . \quad . \quad . \quad (1)$$

But $W = \dfrac{w}{2}AE \quad EV \sin AEV = \left(\dfrac{w}{2}DE \cdot EV \sin AEV\right)\dfrac{QK}{DK},$

for the triangles DAQ and DEK are similar, and $\dfrac{AE}{QK} = \dfrac{DE}{DK}$. Now $\left(\dfrac{w}{2} DE \cdot EV \sin AEV\right)$ is the weight of the wedge DEV $= W_0$, and is constant for any particular case. Hence, from eq. (1),

$$R' = W_0 \frac{QK}{DK} \cdot \frac{AQ}{QV} = W_0 \frac{q-k}{d-k} \cdot \frac{a}{q}.$$

Further, $\dfrac{a}{e} = \dfrac{DQ}{DK} = \dfrac{d-q}{d-k}$; whence,

$$R' = W_0 \frac{q-k}{d-k} \cdot \frac{d-q}{d-k} \cdot \frac{e}{q} = W_0 \frac{e}{(d-k)^2} \frac{(q-k)(d-q)}{q}.$$

It may easily be shown that the angle KEV $= \phi + \phi'$, so that k and e are constant, and in the equation q is the only length which varies when different positions of the plane AV are examined. The equation may be written

$$R' = W_0 \frac{e}{(d-k)^2}\left\{ d + k - \left(q + \frac{dk}{q}\right)\right\}$$

This is a maximum when $(q + dk/q)$ is a minimum, i.e. when $q = \sqrt{dk}$, and q is a mean proportional between d and k. Draw a semicircle on DV as base, and erect KI perpendicular to DV ; then VI is the value of q which makes R′ a maximum, when

$$R' = W_0 \frac{e}{(d-k)^2}\{d + k - 2\sqrt{dk}\} \tag{2}$$

This value of R′ represents the resultant pressure on the back of the wall, and the corresponding position of the plane AV is the plane of rupture. Since the angle KEV $= \phi + \phi'$, the point K is readily determined, and hence the value of q which makes R′ a maximum is found from the construction given.

Since the triangles DAQ, VAQ have a common vertex A, and stand on the same base line DV, their areas will be proportional to the lengths of their bases, therefore $\dfrac{\Delta \text{ DAQ}}{\Delta \text{ VAQ}} = \dfrac{d-q}{q}$; and the

$$\Delta \text{ DAQ} + \Delta \text{ VAQ} \; : \Delta \text{ DVA} = \frac{d}{q} \; \Delta \text{ VAQ}.$$

For similar reasons, $\qquad \dfrac{\Delta \text{ DVA}}{\Delta \text{ EVA}} = \dfrac{\text{DA}}{\text{EA}} = \dfrac{\text{DQ}}{\text{QK}} = \dfrac{d-q}{q-k}$

Hence, $\qquad \Delta \text{ DVA} = \dfrac{d}{q} \cdot \Delta \text{ VAQ} = \dfrac{d-q}{q-k} \; \Delta \text{ EVA}$

and $\qquad \dfrac{\Delta \text{ VAQ}}{\Delta \text{ EVA}} = \dfrac{q\,(d-q)}{d\,(q-k)} = 1$; since $q^2 = dk$.

That is to say, the areas of the two triangles VAQ and EVA are equal, and the plane of rupture divides the figure AEVQ into two equal areas. Make QJ $=$ QA ; then since the triangles JAQ and VAQ have a common vertex A, and stand on the same base line VQ, their areas are proportional to the lengths of their bases,

$$\dfrac{\Delta \text{ JAQ}}{\Delta \text{ VAQ}} = \dfrac{\text{JQ}}{\text{VQ}} = \dfrac{a}{q} = \dfrac{\Delta \text{ JAQ}}{\Delta \text{ EVA}}$$

since the triangles VAQ and EVA are equal in area. From eq. (1), R′ : W $= a : q$, therefore,

$$\dfrac{\text{R}'}{\text{W}} = \dfrac{\Delta \text{ JAQ}}{\Delta \text{EVA}},$$

and as the area of the triangle EVA represents the weight W, so the area of the triangle JAQ represents the maximum value of R′, i.e. the resultant pressure on the back of the retaining wall.

$$\text{R}' = w\,(\Delta \text{ JAQ}) \text{ per unit of length} \qquad . \qquad . \qquad . \qquad (3)$$

Rebhann's construction can be applied to (ii) Fig. 451 if the upper surface of the earth be raised sufficiently to produce an earth pressure p_0 on BC.

Experiment has shown that the reaction R′ does not in all cases act ⅓ the way up VE, as might appear from the above theory. The experimental positions are given in §§ 329 and 335. R′ will make an angle ϕ' with the normal to the back of the wall; as before explained, ϕ' cannot exceed ϕ and is usually taken as equal thereto.

When the value of $+ \gamma$ exceeds γ', § 329, set up VE′ making an angle γ' with the vertical, Fig. 453, and proceed with the construction of Fig. 454 as if VE′ were the back of the wall, assuming the wedge E′VE to form part of the wall as explained in § 329.

Fig. 455 shows the position of R′, as determined experimentally by Jenkin, due to the pressure of dry sand acting on the back of stepped retaining walls ; its magnitude is given by $R' = CwH^2$. This information may be used in preference to the procedure of § 328.

331. Cohesion in Earth.—In all the preceding theories of earth pressure, the earth has been regarded as a granular mass depending for stability on friction between the particles, a condition to which dry sand approximates. If the sand be wet, there will be a certain amount of cohesion between the grains, still more if it be mixed with clay, and the angle of repose will be increased. In firm stiff clays the cohesion may be considerable. Moist earth, well punned, will stand for a time at quite a steep angle. To such material the theory for a granular mass will not apply. In them, the friction between the particles is augmented by the resistance to shearing of the material. Both friction and shearing forces are tangential forces, but whereas the former is proportional to the normal
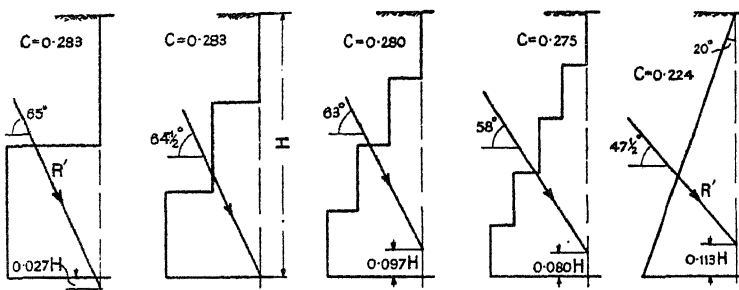
FIG. 455.

pressure between the particles, the latter is assumed to be independent thereof, so that the expression for p_t, the tangential resistance per sq. ft. opposing sliding, takes the form

$$p_t = \mu p_n + f_s \qquad (1)$$

where $\mu = \tan \phi$ is the coefficient of friction between the particles, p_n the normal pressure, and f_s the resistance of the material to shear ; an equation similar to that of the internal friction theory for materials in compression, § 228, Vol. I. It will be realised that this shearing resistance implies tensile and compressive stresses between the particles, in directions making angles of 45° with the direction of sliding, so that the effect is rightly spoken of as *cohesion*. A number of modifications to the theory of earth pressures have been given, introducing the effect of cohesion. The following is an approximate graphical treatment. It may be well to repeat that, in earth masses exposed to the weather, it would seldom be safe to rely on cohesion for stability.

332. Equilibrium due to Cohesion.—Let IEV, (i) Fig. 456, be a bank of earth standing at a greater angle than the angle of repose, so that it depends for stability on cohesion. Consider the equilibrium of the

triangle IEV. The weight of this, acting vertically downward, must be resisted by normal and tangential forces N and F_T respectively, acting on the plane IV. These three forces must be in equilibrium, and can be represented by the triangle of forces jel, (ii) Fig. 456. The tangential force F_T will be made up of the frictional resistance $F = N \tan \phi$ on the plane IV, plus F_s, the total shearing force on that plane. If ek be drawn in (ii), making an angle ϕ with el, the line lk will represent $F = N \tan \phi$, and kj will represent F_s. In (i), draw VD making an angle ϕ with VM ;
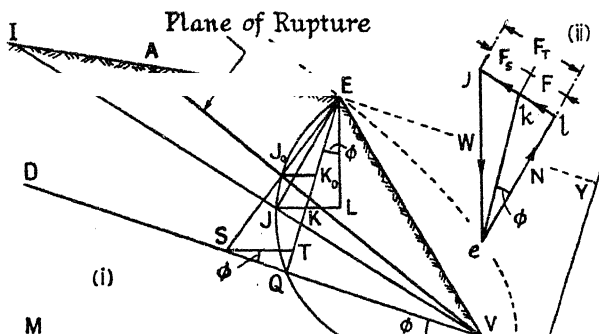
FIG. 456.

draw EJ at right angles to IV, and EQ at right angles to DV. Draw JL a horizontal line cutting EQ in K ; draw EL a vertical line.

The weight of the triangle of earth IEV, per unit of length, is

$$W = \frac{w}{2} IV . JE.$$

It will be evident that the figures EJKL and $ejkl$ are similar (they have been lettered to correspond), and

$$\frac{F_s}{W} = \frac{jk}{je} = \frac{JK}{JE}.$$

Therefore JK represents the force F_s to the same scale that JE represents the weight W ; hence,

$$F_s = W \frac{JK}{JE} = \frac{w}{2} IV . JE \frac{JK}{JE} = \frac{w}{2} IV . JK$$

and the average value of F_s on the plane IV, per square unit, is

$$f_s = \frac{F_s}{IV} = \frac{w}{2} . JK.$$

If w is in lb./cub. ft., JK must be measured in feet, and f_s will be in lb./sq. ft. Since the angle EJV is a right angle, the locus of the point J, for different planes similarly situated to IV, will be the semicircle EJQV on EV as diameter, and it is evident that the maximum value of JK will

be J_0K_0, where J_0 bisects the arc QE, hence the maximum value of f_s will occur on the plane AJ_0V. But from eq. (1), § 331, $f_s = p_t - \mu p_n$; that is to say, f_s is the tangential or shearing force on the plane after allowing for the effect of friction, and if it exceed the shearing strength of the earth the triangle will slide along AJ_0V, which is the plane of rupture. Since equal angles subtend equal arcs of a circle, whether at the centre or the circumference, and $EJ_0 = J_0Q$, it follows that the angles EVJ_0 and J_0VQ are equal, and AV bisects the angle EVD. Produce EJ_0 to S, draw ST parallel to J_0K_0. Then $EJ_0 = J_0S$, and $ST = 2J_0K_0$. Therefore,

$$\text{max.} f_s = \frac{w}{2} \cdot J_0K_0 = \frac{w}{4} \cdot ST.$$

Produce DV to O, make VO = SQ, draw OY at right angles to DO, and YE parallel thereto. Then YE = OQ = VS = VE. But if YE = VE, E lies on a parabola for which O is the origin, OY the directrix, and V the focus. This parabola is called the *parabola of cohesion*.

$$VO = SQ = ST \cos \phi = \frac{4}{w} (\text{max.} f_s) \cos \phi.$$

If the ultimate shearing resistance of the earth be substituted for max. f_s in the equation for VO, the resulting parabola will determine the maximum height of the point E consistent with stability, for this particular earth.

333. **Cohesive Earth. Ratio of Lateral to Direct Pressure.**—The ratio p_2/p_1, of lateral to direct pressure, in the case of coherent earth, can be found by a method similar to Rankine's construction, Fig. 447. In Fig. 457, as before, let $P'O = (p_1 + p_2)/2$, and $PP' = (p_1 - p_2)/2$; then PO $= p$ is the resultant pressure on the plane AOC, and $TO = p_n$ and $PT = p_t$ are the normal and tangential components of this pressure. From eq. (1), § 331, for coherent earth,

FIG. 457.

$$p_t = p_n \tan \phi + f_s \quad . \quad . \quad . \quad . \quad (1)$$

Draw OS making an angle ϕ (the friction angle) with OQ, and LM parallel thereto and distant f_s (measured along PT) from it. Then, in the particular case when LM is tangent to the circle at P,

$$p_t = PT = PS + ST = f_s + p_n \tan \phi,$$
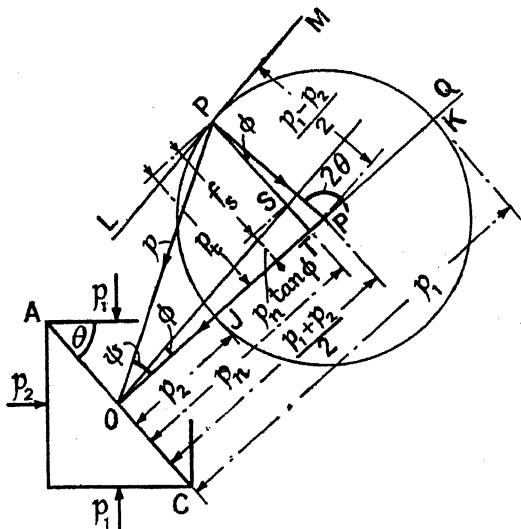
and the figure represents the pressure conditions for coherent earth. Further, PT is evidently the maximum ordinate of the semicircle which satisfies eq. (1). Therefore, for given values of p_1 and p_2, PT represents the maximum value of p_t; or conversely, for given values of p_1 and p_t, the value of p_2 will be a minimum. Now the angle P'PT $= \phi$; hence the angle PP'Q $= 90° + \phi$. But the angle PP'Q $= 2\theta$ (cf. Fig. 446), therefore $2\theta = 90° + \phi$, which determines the plane AC on which p_t is a maximum. From the figure,

$$p_n = \text{TO} = \text{P'O} - \text{P'T} = \frac{p_1 + p_2}{2} - \frac{p_1 - p_2}{2} \sin \phi$$

$$p_t = \text{PT} = \frac{p_1 - p_2}{2} \cos \phi = f_s + p_n \tan \phi.$$

These equations follow at once from eqs. (1) and (2), § 17, Vol. I, if 2θ be put equal to $90° + \phi$. Hence,

$$\frac{p_1 - p_2}{2} \cos \phi = f_s + \left\{ \frac{p_1 + p_2}{2} - \frac{p_1 - p_2}{2} \sin \phi \right\} \tan \phi$$

and

$$p_2 = \frac{p_1(1 - \sin \phi) - 2f_s \cos \phi}{1 + \sin \phi} \qquad . \quad (2)$$

Equivalent formulae have been given by Résal, Bell, and others. If $p_2 = 0$, $p_1 = (2f_s \cos \phi)/(1 - \sin \phi)$, and according to this theory, until p_1 reaches this value, equivalent to a depth,

$$h = \frac{2f_s \cos \phi}{w(1 - \sin \phi)} \qquad . \qquad . \qquad . \qquad (3)$$

there can be no pressure on the vertical back of a retaining wall. No very satisfactory theory for the pressure of cohesive earth on a retaining wall has yet been evolved.

334. Sliding.—The tendency of a structure such as a retaining wall, Fig. 436, or an arch foundation, Fig. 441, to slide, due to the lateral pressure on the structure, is opposed by (i) the blunt end resistance of the portion below the ground, (ii) the frictional resistance between the structure and the soil. The blunt end resistance is sometimes calculated from Rankine's formula, § 349, from which the lateral resistance at a depth h below the surface is $p = wh(1 + \sin \phi)/(1 - \sin \phi)$; hence the total blunt end resistance, if D be the depth below the surface, is $\text{R} = \frac{1}{2}w\text{D}^2(1 + \sin \phi)/(1 - \sin \phi)$, per foot of width.

The following figures have been given for the coefficient of friction, which varies very greatly with the moisture content of the soil.

Concrete on sand			$\mu = 0 \cdot 4$	Concrete on wet clay	.	$\mu = 0 \cdot 2$
gravel	.	.	$= 0 \cdot 6$	hard rock	.	$= 0 \cdot 6$
dry clay	.	.	$= 0 \cdot 5$	shale	. .	$= 0 \cdot 6$

335. Experiments on Earth Pressures.—Many experiments have been made to test the validity of the different theories of earth pressure. Most of these have been on a very small scale, boxes filled with sand, and the like. The vertical pressure at the base of a retaining wall 25 ft. high is of the order 1 to $1\frac{1}{2}$ tons per sq. ft., and it is more than doubtful

if the behaviour of earth in such small models really represents its behaviour in practice.

One of the early large-scale experiments was made by General Burgoyne,[6] who built the two retaining walls shown in Fig. 458. They were constructed of rough granite blocks laid dry, and the filling was loose earth (not rammed) weighing 142 lb./cub. ft. Its natural slope was $1\frac{1}{2} : 1$; the experiment was made during a wet winter. When the depth of earth filling behind each wall was 17 ft., it collapsed. Investigation shows that at the moment of collapse the line of thrust determined by means of Rankine's theory, § 326, passes right outside the base, whereas that found by the method of § 330 just falls within it.

Experimenting with sand under heavy pressure (his maximum pressure was equivalent to a depth of 1340 ft.), Wilson [9] found that the ratio p_2/p_1 for dry sand was constant and averaged $0 \cdot 32$, thus supporting Rankine's theory. Moisture in the sand produced cohesive forces between the particles, and the ratio fell to a minimum of $0 \cdot 20$ with about 9 % of water in the sand, rising again to $0 \cdot 32$ when the sand was saturated ($18\frac{1}{2}$ % of water). In wet sands the ratio increased as the pressure was increased.

The following is a summary of the results of some experiments made by Feld [24] on river sand : $w = 100$ lb./cub. ft., angle of repose 30° 15', angle of internal friction 28° 20'. The sand was filled in horizontal layers into a concrete bin, closed at one end by a vertical timber door,

FIG. 458.

6 ft. deep by 5 ft. wide. The door was free to move slightly ; the vertical component, and top and bottom horizontal components, of the thrust were measured separately.
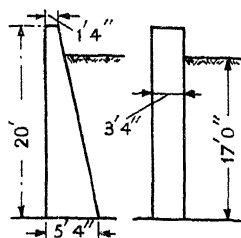
For a horizontal upper surface, the total horizontal pressure on the back of the door can well be represented by the expression $F_H = 0 \cdot 13 w H^2$ lb./ft. of width. When the depth of the filling was greater than 4 ft., the vertical pressure on the door was $F_V = 0 \cdot 084 w H^2$ lb./ft., so that the coefficient of friction was $0 \cdot 084 \div 0 \cdot 13 = 0 \cdot 65$, and $\phi' = 33°$. For depths up to 3 ft., $F_V = 0 \cdot 10 w H^2$, so that $\mu' = \tan \phi' = 0 \cdot 10 \div 0 \cdot 13 = 0 \cdot 77$, and $\phi' = 37\frac{1}{2}°$, which suggests that the coefficient of friction may vary with the pressure (see Fig. 459). The centre of pressure occurred from $0 \cdot 35H$ to $0 \cdot 40H$ up from the bottom of the door.

Moncrieff shows [31] that the experimental values for the horizontal thrust F_H are well represented by the wedge theory, i.e. $\phi = 28°$, $\phi' = 33°$, $\beta = \pi/4 - \phi/2$ (Poncelet's assumption).

For a wall with surcharge, Feld's values for the horizontal thrust are given with some accuracy by the formula $F_H = C_H w H^2$, where if the angle of the surcharge is α,

$\alpha =$		$-34°$	$-25°$	$-15°$	$-8°$	$0°$	$+8°$	$+15°$	$+25°$	$+34°$
$C_H =$		$0 \cdot 089$	$0 \cdot 089$	$0 \cdot 093$	$0 \cdot 102$	$0 \cdot 114$	$0 \cdot 131$	$0 \cdot 149$	$0 \cdot 180$	$0 \cdot 212$
$n =$		$\frac{1}{4}$	$\frac{1}{3}$	$\frac{1}{3}$	$\frac{1}{3}$	$0 \cdot 34$	$0 \cdot 35$	$0 \cdot 40$	$0 \cdot 40$	$0 \cdot 44$

The inclination of the resultant thrust R' to the normal to the back of the door was (for practical purposes) equal to the friction angle, and its point of application was nH up from the bottom.

Large-scale experiments made by Dr. Terzaghi [33] at the Massachusetts Institute of Technology on clean dry sand, % moisture $2 \cdot 6$ to $1 \cdot 5$, thoroughly tamped into place behind a retaining wall, showed that the total horizontal pressure on the wall may reach as much as 75 % of that due to the same sand considered as a fluid. On allowing the top of the wall to move forward $0 \cdot 1$ inch in $7 \cdot 12$ feet, the pressure fell to 10 % of the same fluid pressure. A movement of 1/1000th the height of the wall reduced the horizontal thrust to its minimum value. During this movement, a downward vertical pressure was developed on the back of the wall rising to about 75 % of the final horizontal pressure. With loosely filled sand, the horizontal pressure was about 40% of the corresponding fluid pressure, combined with a downward thrust of about 39 % of the horizontal pressure. With a forward movement of the top of the wall of $0 \cdot 1$ inch, the horizontal pressure fell to about 28 % of the fluid pressure, and the downward thrust rose to 50 % of the horizontal pressure. In all these cases the centre of pressure was about $\frac{1}{3}$rd the way up the wall, rising at times to $0 \cdot 4$. With sand saturated with water, the horizontal pressure was equal to the sum of that due to a depth of water equal to that of the filling, plus an earth pressure due to a filling having a weight equal to that of the sand less the weight of water displaced. The presence of the water had little effect on the values of ϕ and ϕ'. The pressure on the back of the wall due to coherent materials was very much less than that of the sand. The effect of drainage is discussed in the article cited.

FIG. 459.

A. Ottawa standard sand, loose, dry.
B. Till and abnormal till, compacted, saturated.
C. Ottawa standard sand, dense, dry.
D. Sand and gravel, compacted, saturated.

Internal friction experiments showed that μ, the coefficient of friction, was much greater for closely packed than for loose materials. As the pressure increased, μ decreased, and the difference in question lessened, Fig. 459.

Experiments with Cohesive Earth.—Experiments to determine the tangential resistance of cohesive earths have been made by Jacquinot and Frontard,[26] Bell,[18] Krey,[29] Gilboy,[64] and others. In Bell's experiments on the resistance to direct shear of clays, the apparatus was arranged as shown in (i) Fig. 460 ; and typical results are given in (ii). Whereas, in the case of sand, the value of p_t increased in direct proportion to p_n,

the resistance of clay is made up partly of a constant shear stress f_s, partly of a force increasing with the direct pressure p_n, thus confirming
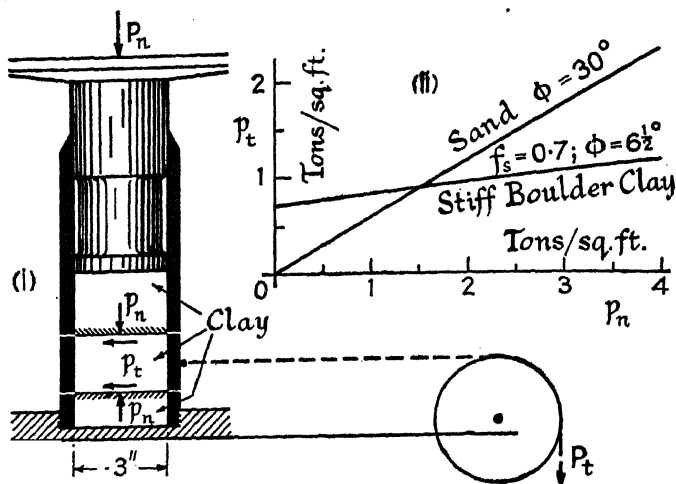
FIG. 460.

the form of the cohesion equation, eq. (1), § 333. Some average values from Mr. Bell's paper are given in the following Table :

	f_s tons/sq. ft.	ϕ°	D † inch.
Very soft puddle clay * .	0·2	0	1·3
Soft puddle clay . .	0·3	3	1·1
Moderately firm clay .	0·5	5	1·0
Stiff clay . . .	0·7	7	0·9
Very stiff boulder clay .	1·6	16	0·5

* Puddle clay = pure homogeneous plastic clay, free from sand or stones.
† D = diameter of impression made by 1⅝ inch steel ball dropping 1 foot on to specimen 1¾ inch thick.

In such determinations, time and moisture content are important factors. Some experiments by Cooling and Smith [39] well illustrate the latter point. The specimens were in the form of an annulus of clay under pure torsion, from which the shear strength was calculated. Some typical curves are plotted on a water-content base line in Fig. 461, from which it will be seen that the strength decreases rapidly as the water content increases. Further experiments, made on cylindrical specimens with conical ends [see (iii) Fig. 282, Vol. I] in pure compression,* showed that with the plastic clays the compressive strength was just twice the

* See also Jürgenson, ' The Shearing Resistance of Soils,' *Jour. Boston Soc. C.E.*, vol. xxi, 1934, p. 242.

shear strength, 'A,' Fig. 461, and the angle of the shear plane very nearly 45° (see § 14, Vol. I), showing that the tangential resistance was
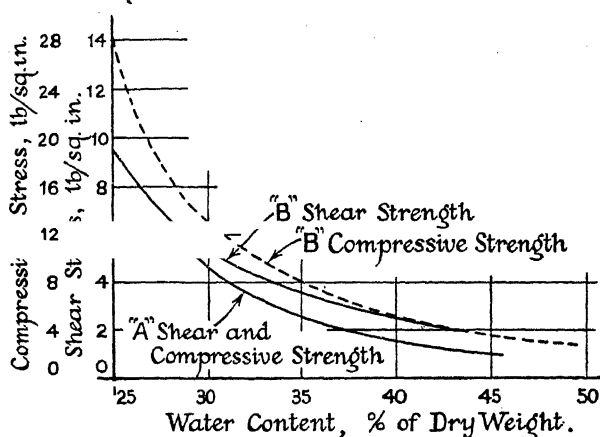
FIG. 461.

practically pure shear and the friction small. With sandy clays, ' B,' the compressive strength was more than twice the shear strength, suggesting that friction was playing a part.

	Coarse Sand. 2 to 0·2 mm.	Fine Sand. 0·2 to 0·02 mm.	Silt. 0·02 to 0·002 mm.	Clay. Less than 0·002 mm.
	Percentage of Dry Weight.			
A. Reading Clay . .	0	3·5	31·0	65·5
B. Silty Clay, Bagshot Beds	2·0	30·0	38·0	30·0

336. Soil Mechanics.—In recent years, due largely to the initiative of Professor Terzaghi, much research has been made into the constitution and physical properties of soils, with a view to predetermining their behaviour under foundation pressures. A number of special tests have been devised in order to investigate these properties, and research work is being carried out to correlate these tests with observations made on actual foundations.

The four characteristics on which the behaviour of soil depends are (i) *consolidation*, (ii) *permeability*, (iii) *compressive strength*, (iv) *shearing strength*. These in turn depend on (a) *its constituents*, (b) *its structure*, the arrangement of the particles and volume of the voids and their contents, (c) *the water content*.

Foundation pressure on soil produces two main effects, *consolidation*

and *lateral flow*, in different proportions and at different time rates, depending on the kind of soil. Consolidation or volume change depends largely on the voids. If these are filled with air, this change takes place rapidly; if filled with water, the rate of change will depend on the rate at which the water is squeezed out, i.e. on the permeability of the soil. In silts and coarse-grained muds, the process may take only a few years; in heavy clays, some hundreds of years. The larger the volume of voids, the greater the amount of consolidation under given conditions.

Accompanying the consolidation, and increasing the settlement, is the effect of lateral flow, which depends on the resistance to compression and shear ; cohesion in the soil is here the important consideration. In certain fine-grained silts and clays, when the water content is large, this is the chief cause of settlement. An important effect of cohesion is that, in soils where the shear strength is great, the settlement produced by given unit direct pressure increases in direct ratio to the diameter of the loaded area ; in cohesionless soils the size of the area has little effect. The ratio of the settlement for a surface foundation, to that for one at a depth d, varies as d/D, where D is the diameter of the loaded area; but the effect of the ratio d/D on the settlement is less the greater the cohesion. In cohesionless soils, a ratio $d/D = 1$ almost triples the bearing capacity, and reduces the ratio of the two settlements to one-third.[62]

Space considerations prevent a discussion of the methods of mechanical analysis used for soils, or of the different physical tests which have been devised. A number of methods of applying the test results to practical work have been tried, with some measure of success, but no procedure has yet been generally agreed.

FOUNDATIONS

337. Foundations.—The term *foundations* designates all the arrangements made at the base of a structure to transfer its weight to the ground on which it rests.

Two essential conditions for the stability of foundations are : first, that the pressure per sq. ft. between the structure and the soil on which it rests must not exceed the safe bearing pressure on the latter, or on the material of which the structure is composed ; secondly, the centre of pressure on any area forming part of the foundations must fall within the core of that area (§ 97, Vol. I), so that there may be no tendency to develop tension between the base of the structure and the soil. Where the base is rectangular in shape, as for example the base of a wall, this implies that the centre of pressure must everywhere lie within the middle third of the width. In soft ground, every care must be taken to avoid unequal settlement, by suitably proportioning the area of base to the load carried. In addition, the centre of area should lie well within the core, so that the pressure is as uniformly distributed as possible.

It is also desirable in foundations that the plane of the base should be as nearly as possible perpendicular to the direction of the pressure.

To prevent disintegration of the soil on which the foundations rest, due to the effects of frost and weather, it is necessary to sink the foundations below the surface of the earth some three or four feet in this country, and to greater depths still in countries subject to extremes of heat and cold. Efficient drainage is also necessary to carry off the surface water and to prevent the soil from becoming saturated.

338. Safe Bearing Pressures.—The following Table gives the safe bearing pressure on various kinds of soil. The figures must be taken as rough averages for the kind of soil indicated. In all important structures trial borings should be made, and the bearing pressure of the soil determined by experiment.

APPROXIMATE SAFE BEARING PRESSURES

		Tons/sq. ft.
Rock.	Hard—(Granite 40) . . .	25–30
	Ordinary	8–16
	Soft, or firm Shale. . . .	6–8
Gravel.	Hard and compact . . .	6–9
	Ordinary compact . . .	3–4
Chalk.	Hard white	4–6
	Soft	1–1¼
Clay.	Dry, hard and compact . .	4–6
	Ordinary, moderately dry . .	2
	Soft and moist	1
Sand.	Dry, laterally confined . . .	2–3
	Wet or loose	1
Earth.	Alluvial soil, firm	½–1

339. Types of Foundations.—Foundations may be divided roughly into two classes : those suitable for a hard unyielding stratum, hard rock, hard compact gravel, etc., and those suitable for a soft yielding soil or loose earth. In the former type, little more is necessary than the provision of suitable footings of sufficient bearing area. In the latter type, special construction is often required.

When a hard stratum overlies soft ground, it is better, if possible, not to penetrate through the hard material, but to provide sufficient area to reduce the bearing pressure to that permissible for the hard stratum, and to make the depth of the excavation as small as possible. When a soft stratum overlies a hard material, it is better to go through the soft material and make the foundation on the firm ground, unless the soft ground be too deep to permit this, when the foundation must be treated as one on yielding ground.

Rock Foundations.—When a foundation is carried down to the solid rock, it is only necessary to provide a flat surface perpendicular to the direction of the pressure, of sufficient area to carry the load. This area may be a plane surface, or in steps according to circumstances. The rock is cut and dressed level, loose and decayed portions being removed and holes and hollow places filled up with concrete. The crushing strength of the rock can be ascertained by experiment, and the bearing pressure should not exceed one-eighth of this.

Foundations on Firm Soil.—Foundations on firm compact gravel or

2 Y

hard clay are excavated to a depth of at least 3 ft. in the case of gravel, and 4 ft. in the case of clay, to exclude frost. The area is levelled, and may or may not be covered with concrete. Suitable footings must be provided to reduce the bearing pressure to that allowable. A well-arranged drainage system is necessary to prevent the soil becoming saturated with water and thus reducing or destroying its stability. Gravel makes a good foundation, but clay is often treacherous, especially if much subject to wet.

Foundations in Soft Soil.—The requisites for foundations in soft or loose earth are : sufficient bearing area—this usually involves special types of construction, § 340 *et seq.* ; a minimum depth of excavation below the surface, § 349 ; an adequate drainage system to prevent saturation of the soil. Care is necessary in foundations on a soft yielding material that the bearing areas be proportioned so as to obtain such a distribution of pressure on all parts of the foundation, that no unequal settlement will occur. If the kind of soil differ at different parts of the foundation, special consideration is necessary to prevent unequal settlement. Where the load on a structure is subject to variation, it is desirable to *proportion* the areas to suit the permanent load, but to provide sufficient area that the safe bearing pressure is never exceeded under any load conditions. It is perhaps wise to add that the weight of the foundation structure itself often forms a considerable addition to the load from the building itself.

340. Methods of Spreading the Load.—The more usual methods of increasing the bearing area in foundations are :

> Wide Footings, § 341.
> Concrete in Trenches or Rafts, § 342.
> Inverted Arches, § 343.
> Gillages, § 344.
> Piles, § 345.

341. Footings.—The area of base of a brick or masonry structure is very commonly increased by widening the lower portion of the walls in

Headers
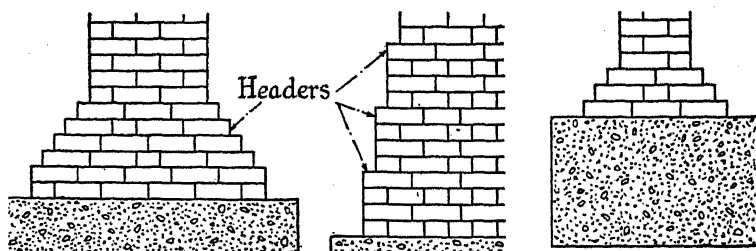
FIG. 462.

steps, Fig. 462. Such widened courses are called *footing* courses. The lowest course is usually made twice the width of the wall. No footing course should project more than $\frac{1}{4}$ the length of the bricks or stones of

which the wall is constructed. Each footing course may be from one to four bricks in thickness, the latter being suitable for heavy brick walls, piers, and abutments. The top layer of each course must consist entirely of headers. Footing courses for stone structures are sometimes made of brick, and *vice versa*.

342. Concrete in Trenches or Rafts.—Foundations for walls of buildings in soft soil are often supported on concrete in trenches, arranged to distribute the weight over a sufficient area. Such trenches are usually made about a foot wider than the lowest course of footings, and from 2 ft. or more in depth. Sometimes the whole area is covered with a layer of concrete, which should nowhere be less than 6 in. in thickness, and is made thicker under the footings. In the case of sand and other very soft material, the area carrying the load must be confined between sheet piles to prevent lateral spreading, Fig. 463. If the footings rest on a hard firm soil, such as a natural bed of gravel, concrete is not required. In less firm material, a bed of concrete from 8 to 12 in. wider than the footings and not less than 9 in. thick is used to spread the load.
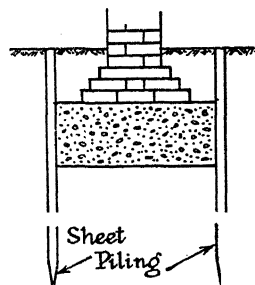
FIG. 463.

343. Inverted Arches.—In brick, masonry, or concrete structures, the necessary area for distributing the load may be obtained by the use of inverted arches, Fig. 464. This method is useful where openings occur in a wall. Such arches may be constructed of reinforced-concrete.
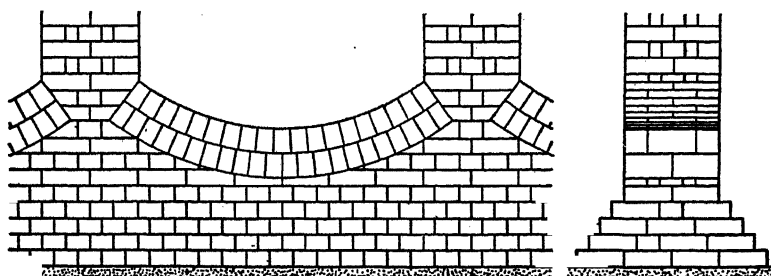
FIG. 464.

344. Grillages.—When it is necessary to spread the load over a considerable area in order to obtain a sufficiently low bearing pressure, a grillage is commonly adopted, Figs. 465 and 466. This consists of one or more tiers of **I** beams, arranged as shown in the figures so as to distribute the load. The spaces between these beams are filled in with concrete. Grillages are particularly useful in cases where a hard stratum covers a soft yielding material. The grillage spreads the load over a sufficient area of hard soil and prevents penetration. They are also

much used as the foundations for stanchions, Fig. 466, where a heavy load is concentrated on a limited area.

The type of grillage used for a wall foundation is shown in Fig. 465. The **I** beams are spaced at regular intervals, at right angles to the length of the wall, on a bed of concrete, which should not be less than 4 to 6 in. thick. The distance apart of the beams usually varies from 9 to 24 in. A space of not less than $4\frac{1}{2}$ or 5 in. should be arranged between each beam so that the concrete filling can be introduced and properly tamped. Such an arrangement is spoken of as a *single tier grillage*.

The dimensions of the **I** beams are found as follows : Let w be the weight per unit of length of the wall, including the load upon it ; and l the distance apart of the beams. Then the load on one beam is $W = wl$. This load W may be taken as uniformly distributed over the width L_1
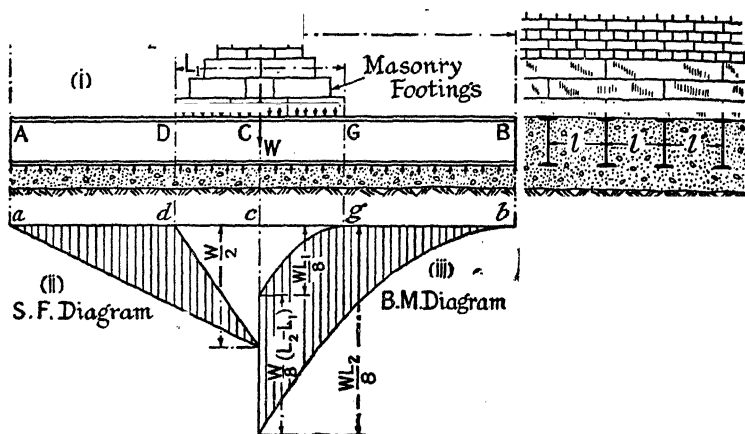
FIG. 465.

of the footings, (i) Fig. 465 ; it is the function of the **I** beam to spread it over an area of width L_2, the length of the **I** beam. There will be, therefore, an upward reaction on the **I** beam equal to W, which is assumed to be uniformly distributed over the length L_2. If p be the bearing pressure on the soil immediately beneath the **I** beams, $W = plL_2$, where lL_2 is the area over which one **I** beam distributes its load ; p must not exceed the safe bearing pressure on the soil. Since $W = wl$, $L_2 = w/p$. The shearing-force and bending-moment diagrams for the load on the **I** beam are shown at (ii) and (iii) Fig. 465. It is evident that the shearing force is a maximum at D, the edge of the footings, and is equal to

$$\text{max. } S = \frac{W}{2}\left\{\frac{L_2 - L_1}{L_2}\right\} \tag{1}$$

Further, that since the shearing force changes sign at C, the centre of the beam, the bending moment will be a maximum there. The upward bending moment at the centre, due to the underneath reaction, is $WL_2/8$;

and the bending moment there due to the downward load is $WL_1/8$. Therefore the actual bending moment at the centre is the difference,

$$M = \frac{W}{8}(L_2 \cdot L_1) \tag{2}$$

The two curves bounding the bending-moment diagram are each parabolas. If Z be the section modulus of the beam, and f the safe stress in it,

$$Z = \frac{W}{8f}(L_2 - L_1) = \frac{wl}{8f}(L_2 - L_1) \tag{3}$$

As will be seen from the following numerical example, however, unless the pitch l be otherwise fixed, it is often more convenient to determine the bending moment per foot run, rather than per beam, and to arrange the pitch to suit the Z of a convenient standard $\mathbf{I}$ beam.

Example.—The load on a 27-in. brick wall, including its own weight and that of the footings, is $19 \cdot 4$ tons per lineal foot ; and the width of the lower course of masonry footings is 54 in. If the safe bearing pressure on the soil be $1\frac{1}{2}$ tons per sq. ft., find the necessary pitch and dimensions of the $\mathbf{I}$ beams forming the grillage under the wall.

Assume that the concrete containing the $\mathbf{I}$ beams is 18 in. thick, and that, with the beams, it weighs 150 lb. per cub. ft. Then the spread weight of the grillage is $1\frac{1}{2} \times 150 = 225$ lb. per sq. ft. $= 0 \cdot 1$ ton per sq. ft., and the net safe bearing pressure on the soil is $1 \cdot 5 - 0 \cdot 1 = 1 \cdot 4$ tons per sq. ft. The safe load per foot run on the grillage is, therefore, $L_2 \times 1 \times 1 \cdot 4$ tons. This must equal $19 \cdot 4$ tons, the weight of the wall per foot. Hence $L_2 = 19 \cdot 4 \div 1 \cdot 4 = 13 \cdot 9$ ft., say 168 in. The bending moment at the centre of the beams, per foot run, is

$$M = \frac{W}{8} (L_2 - L_1) = \frac{19 \cdot 4}{8} (168 - 54) = 277 \text{ in.-tons ;}$$

since $W = 19 \cdot 4$ tons ; $L_2 = 168$ in. ; and $L_1 = 54$ in. The necessary Z per foot run, if f is not to exceed 8 tons/sq. in., is $277 \div 8 = 34 \cdot 7$ in.³ To obviate undue deflection, it is undesirable that the depth of the beams should be less than $\frac{1}{20}$ their length ; i.e. the beam should not be less than $168 \div 20 = 8 \cdot 4$ in. deep. A $10 \times 6 \times 40$ lb./ft., N.B.S.H.B. No. 6 ; $Z = 40 \cdot 9$ in.³ ; would require to be spaced not more than $40 \cdot 9 \div 34 \cdot 7 = 1 \cdot 18$ ft. apart. A $14 \times 5\frac{1}{2} \times 40$ lb./ft., N.B.S.B., No. 12 ; $Z = 53 \cdot 8$ in.³ ; would require to be spaced not more than $53 \cdot 8 \div 34 \cdot 7 = 1 \cdot 55$ ft. apart; say in round figures, 18 in. apart. The latter is the lighter and better solution. With a spacing $l = 18$ in., the load per beam is $W = wl = 19 \cdot 4 \times 1\frac{1}{2} = 29 \cdot 1$ tons. The maximum shearing force, from eq. (1), is

$$S = \frac{W}{2} \left\{ \frac{L_2 - L_1}{L_2} \right\} = \frac{29 \cdot 1}{2} \left\{ \frac{168 - 54}{168} \right\} = 9 \cdot 9 \text{ tons.}$$

The depth of the web of the beam is approximately $12 \cdot 4$ in., its thickness is $0 \cdot 37$ in. Hence the shearing force per sq. in. is $9 \cdot 9 \div (12 \cdot 4 \times 0 \cdot 37) = 2 \cdot 2$ tons per sq. in., a safe figure.

The type of grillage used as the foundation for a column is shown in Fig. 466. In this particular case there are three tiers of **I** beams. The beams in each tier should be connected together by bolts passing through the webs of the beams, with cast-iron separators or gas-pipe distance pieces between the webs ; and the flanges of each tier should be securely bolted to the flanges of the tier next above or below it. The method of calculation will be evident from the following example.

It is required to design a grillage for the base of a column formed of a compound section composed of two 10 × 8 in. B.S. beams with a 18 × ½ in. flange plate back and front, Fig. 466. The load on the column is 260 tons, and the safe load on the soil is 2 tons/sq. ft. Assume in the first instance that the weight of the grillage proper is 4 tons, and that of the concrete surrounding it 25 tons. The total weight to be spread is there-
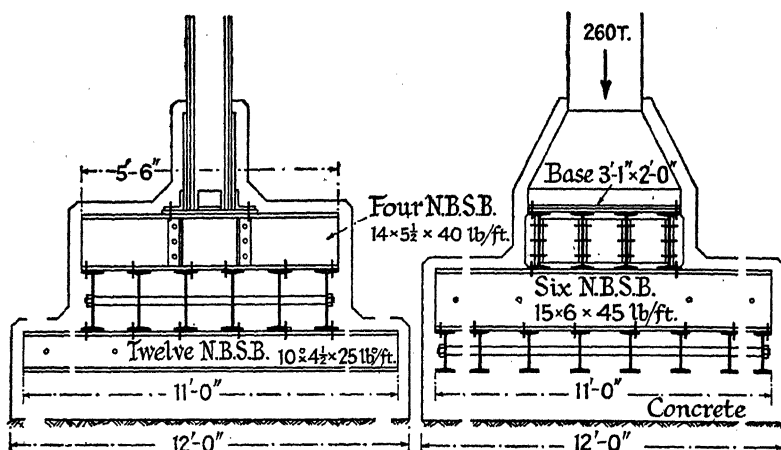
FIG. 466.

fore $260 + 4 + 25 = 289$ tons. To limit the pressure to 2 tons/sq. ft., an area of 144 sq. ft., say 12 × 12 ft., is required ; and allowing 6 in. of concrete outside the ends of the beams, the length of the beams of the lowest tier will be 11 ft. 0 in.

In a direction perpendicular to the flanges of the column, it will be convenient to spread the load over a width of column base of not more than 2 ft. If the top tier of beams be 5 ft. 6 in. long, it follows from eq. (2) that the maximum bending moment on these beams will be

$$\frac{W}{8}(L_2 - L_1) = \frac{260}{8}(66 - 24) = 1365 \text{ in.-tons,}$$

and at 8 * tons/sq. in. the total Z required will be 171 in.³ If four beams are used, the Z of each must be 42·8 in.³ A 13 × 5 × 35 lb./ft. N.B.S.B.,

---

* The L.C.C. Regulations of 1932 permit the normal stresses in the beams to be increased by 50 per cent. in grillages of the type shown in Fig. 466, if 1 : 6 concrete be used, with a minimum cover of 3".

$Z = 43 \cdot 6$, would carry the bending moment. The total load per beam is $260 \div 4 = 65$ tons ; and from eq. (1), the maximum shearing force is

$$\frac{W}{2} \left\{ \frac{L_2 - L_1}{L_2} \right\} = \frac{65}{2} \left\{ \frac{66 - 24}{66} \right\} = 20 \cdot 7 \text{ tons.}$$

The web area of the 13×5 is $11 \cdot 5 \times 0 \cdot 35$ sq. in., approximately, and the shear stress is $20 \cdot 7 \div 4 \cdot 0 = 5 \cdot 2$ tons/sq. in. Without taking into account buckling of the web, this exceeds the permissible limit, 5 tons/sq. in., and the next size, $14 \times 5\frac{1}{2} \times 40$ lb./ft., $Z = 53 \cdot 8$, will be chosen. The web area of this is $12 \cdot 4 \times 0 \cdot 37 = 4 \cdot 6$ sq. in., and the shear stress is $20 \cdot 7 \div 4 \cdot 6 = 4 \cdot 5$ tons/sq. in. Tested by eq. (1), § 174, the resistance to buckling is not quite sufficient just at the point of maximum shear, and channel stiffeners will be introduced as shown in Fig. 466. These will halve the length of the 45° elementary web columns (see Fig. 263), tie the upper tier beams together, and help to support the webs against the direct crush from the column load. If the channels are 10 in. wide, the base of the column perpendicular to the upper tier of beams must be 37 in. wide.

For the middle tier of beams, therefore, $L_2 = 132$ in., $L_1 = 37$ in. ; the maximum bending moment, eq. (2), is $\dfrac{260}{8} (132 - 37) = 3088$ in.-tons ; and the total Z required is $3088 \div 8 = 386$ in.[3] The length of the top tier being 5 ft. 6 in., it is possible to get six beams in the middle tier with 5 in. between them. The Z of each must therefore be $386 \div 6 = 64 \cdot 4$ in.[3] A N.B.S.B. $15 \times 6 \times 45$ lb., $Z = 65 \cdot 6$, will serve. The load per beam is $260 \div 6 = 43 \cdot 4$ tons, and the maximum shearing force, from eq. (1), is $\dfrac{43 \cdot 4}{2} \left\{ \dfrac{132 - 37}{132} \right\} = 15 \cdot 6$ tons. The web area is approximately $13 \cdot 3 \times 0 \cdot 38 = 5$ sq. in., and the shear stress is $15 \cdot 6 \div 5 \cdot 0 = 3 \cdot 1$ tons/sq. in.

In the lowest tier, $L_2 = 132$ in., $L_1 = 66$ in., the maximum bending moment is $\dfrac{260}{8} (132 - 66) = 2145$ in.-tons, and the total Z required is $2145 \div 8 = 269$ in.[3] In a width of 11 ft., fourteen beams can be placed with approximately 5 in. between them. The Z of each must be $269 \div 14 = 19 \cdot 2$ in.[3] The nearest N.B.S.B. is a $10 \times 4\frac{1}{2} \times 25$ lb./ft., $Z = 24 \cdot 4$ in.[3] ; if this be adopted, only $269 \div 24 \cdot 4 =$ say twelve beams (eleven would practically do) are required. The load per beam is $260 \div 12 = 21 \cdot 7$ tons, and the maximum shearing force is

$$\frac{21 \cdot 7}{2} \left\{ \frac{132 - 66}{132} \right\} = 5 \cdot 5 \text{ tons.}$$

The web area is approximately $8 \cdot 6 \times 0 \cdot 30 = 2 \cdot 6$ sq. in., and the shear stress is $2 \cdot 1$ tons/sq. in.

The grillage will rest on a bed of concrete, say 1 ft. thick, and will be arranged as indicated in Fig. 466. The lower tiers of beams will be tied together by bolts with gas-pipe distance pieces. It is essential in designing

grillages to leave sufficient space between the beams so that the concrete can be inserted and properly rammed.

345. Pile Foundations.—When foundations have to be constructed in soft ground of considerable depth, piles are frequently used, Fig. 467. If the soft ground overlies a stratum of firm hard material, at a distance not much exceeding 15 ft. below the surface, it is often considered better to carry the foundations themselves down to the firm ground ; or the weight of the superstructure may be supported on piers of brickwork or other suitable material carried down to the firm ground. If the depth of the soft ground ranges from 15 to 30 ft., piles may be driven down to the hard ground, in positions suitable for carrying the weight of the build-ing. If the depth of soft ground exceeds about 30 ft., reliance must be placed on the friction between the sides of the piles and the earth to support the load.

Piles may be made of timber or reinforced-concrete. Timber piles are square baulks of timber (common sizes 12 × 12 to 16 × 16 in.), the lower end is pointed and, except in very soft ground, is protected by an iron shoe, (i) Fig. 468. The upper end is hooped to prevent splitting while the pile is being driven into the ground. Sawn pitch-pine baulks can be obtained up to 40 ft. long ; Oregon pine up to 60 ft. long. Karri and jarrah wood piles are used to re-sist the attacks of wood-boring worms in tidal waters. The kind of timber used depends largely on what can be procured in the locality. Rein-forced-concrete piles, (ii) Fig. 468, are commonly made 12 to 24 in. square or octagonal, and are reinforced by longitudinal rods with suitable lateral binding. They are proof against the sources of decay to which timber piles are subject.

FIG. 467.

In designing pile foundations, care should be taken that the point of application of the load coincides as nearly as possible with the centre of resistance of the group of piles, so that all the piles are equally loaded, thus ensuring that the settlement is fairly uniform all over the foundation. In ordinary cases, piles should not be placed closer than 3 ft. centre to centre, or 4 ft. for large piles. Maximum spacing about 7 ft. 6 in.

Piles are driven by means of drop hammers falling by gravity, or by single- or double-acting steam hammers. The weight and fall of the
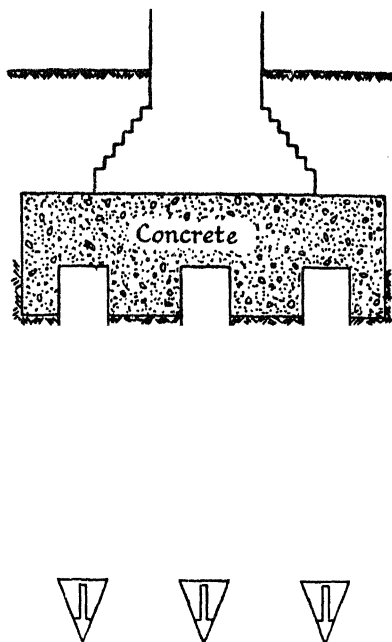
hammer depend on the size and type of the pile, and is usually specified. To drive timber piles, a light hammer with a long drop is used ; a 1-ton hammer falling 6 ft. may be regarded as typical. For reinforced-concrete piles, a heavy hammer with a short drop is used. For a 14-in. pile a 3-ton hammer falling 2 ft. 0 in. may be regarded as typical.* When driving a reinforced-concrete pile, a timber dolly is fitted, (iii) Fig. 468, with a rope or other mat between it and the head of the pile. This prevents disintegration of the concrete due to the blow. After driving, the heads of piles are cut off to the required length and embedded in a concrete slab on which the footings rest, Fig. 467.

Concrete piles formed *in situ* are frequently employed. A steel tube with a loose point is driven into the ground. Concrete is poured into the tube and tamped down while the tube is slowly withdrawn ; the concrete spreads and fills the hole, Fig. 469. Where necessary, reinforcement is introduced before filling in the concrete.

346. Supporting Power of Piles.—The supporting power of a pile is made up of two parts : (i) the frictional resistance of the sides of the pile against the earth, (ii) the blunt end or toe resistance. The magnitude of these resistances depends largely on the type of soil into which the pile is driven. From this point of view, Terzaghi [62] divides soils into two classes : (*a*) soils, such as sand and gravel, easily permeable by water ; (*b*) soils, such as fine-grained silts and fine clays, almost impervious to water. In soils of type (*a*) the resistance while the pile is being driven does not differ much from the resistance when the pile is at rest, and a fair estimate of its magnitude may be obtained from a pile formula (see
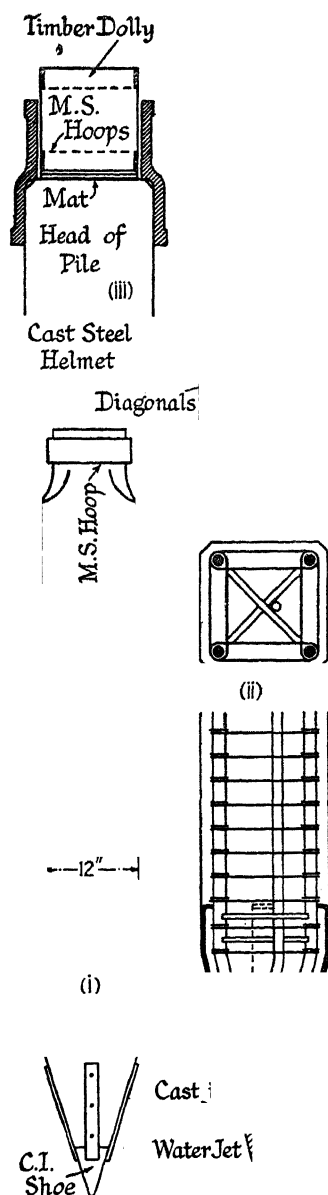
Fig. 468.

* The suggestions of the Joint Sub-Committee on Pile-Driving, *Jour. Inst. C.E.*, No. 6, April 1936, p. 587, may be consulted regarding the most appropriate driving conditions.

below) based on the penetration per blow. In soils of type (*b*), the water contained in the voids in the material below the toe is unable to escape during the blow, and offers a high resistance to penetration. Subsequent blows loosen the pile, which allows the water to escape up its sides, where it acts as a lubricant. Thus, during motion, the toe resistance is large and the friction small, whilst under static loading the friction may be considerable and the toe resistance small. Pile formulae based on penetration per blow will not apply in such cases ; an experimental pile should be driven and loaded to find its supporting power. To discriminate between the two types of soil, a test pile may be driven, and the penetration per blow measured before and after a period of not less than 24 hours' rest. If the two penetrations are equal, a pile formula may be used to determine the supporting power.

Pile Formulae.—The energy given out by the falling hammer is expended partly in overcoming the resistance to penetration of the ground, and partly in losses during driving. In driving a timber pile through soft ground, the losses may amount to 25 % of the total energy. In driving a heavy reinforced-concrete pile through firm ground, they may amount to 75 % or more. They include (i) the energy consumed in temporarily compressing the pile and the earth ; (ii) the energy absorbed in overcoming the inertia of the pile ; (iii) incidental losses in the pile-driving mechanism. By equating the energy of penetration plus the lost energy to the total energy of the falling hammer, a formula for the supporting power of the pile can be obtained. Many such pile formulae have been devised. Let
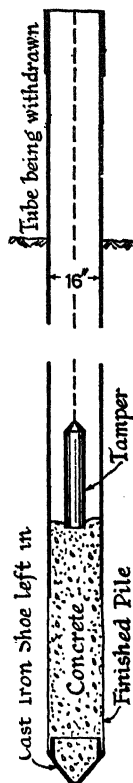
FIG. 469.

R = the supporting power of the pile under a static load in tons.
R′ = the resistance to penetration under impact in tons.
W_p = the inclusive weight of the pile including shoe, helmet, etc., tons.
l = the length of the pile in inches.
a = the area of the pile in sq. in.
W = the inclusive weight of the falling hammer in tons.
h and H = the height of the fall in inches and feet respectively.
s = the penetration of the blow or 'set' in inches.

Then Terzaghi.[62] gives as a general formula for the resistance to penetration of piles

$$R' \quad \frac{Ea}{l}\left[- s \pm \sqrt{s^2 + \frac{2Wh}{E}\left\{\frac{W + m^2W_p}{W + W_p}\right\}\frac{l}{a}} \right] \tag{1}$$

where *m* is a coefficient of restitution which ranges from 0 to 1 ; *m* = 0 for non-elastic impact ; *m* = 1 for perfectly elastic impact. For soils of type (*a*), see above, R = R′.

Retenbacher's Formula.—If $m = 0$ in eq. (1),

$$R \frac{W^2 h}{(W + W_p)(Rl/2Ea + s)} \tag{2}$$

Dutch Rule.—If in eq. (2), $Rl/2Ea$ is put $= 0$,

$$R = \frac{W^2 h}{(W + W_p)s} - \frac{12W^2 H}{(W + W_p)s} \qquad \tag{3}$$

a commonly used rule for reinforced-concrete piles; s is the average penetration per blow for the last six blows in inches. The factor of safety for dead loads is from 4 to 6 for concrete piles, and 6 to 8 for timber piles.

Wellington or Engineering-News Formula.—If $m = 1$, and $Rl/2Ea = c$, a constant

$$R = \frac{Wh}{s + c} \quad \frac{12WH}{s + c} \tag{4}$$

$c = 1$ for a drop hammer; $c = 0 \cdot 1$ for a steam hammer *; s is the average penetration per blow for the last 10 blows in inches. A factor of safety for dead loads of 6 is adopted.

Eqs. (3) and (4) are most applicable in the case of light driving where s exceeds $0 \cdot 2$ in.

Hiley Formula.—This formula takes into direct account the actual conditions which obtain during the pile driving, and is to be preferred on that account.

$$R_2 = R' + W + W_p = \frac{\eta W h e}{s + C/2} + W + W_p \qquad \tag{5}$$

where

$R_2 = $ the ultimate resistance of the ground in tons.

$\eta = $ the efficiency of the blow
  $= (1 + re^2)/(1 + r)$ when $1/e > r$; $\qquad r = W_p/W$
  $= r(1 + e)^2/(1 + r)^2$ when $1/e < r$.

  For steel ram of d.a. hammer on steel anvil.
$e = 0 \cdot 5$ for steel piles; $= 0 \cdot 4$ for timber piles.

  For c.i. ram of s.a. hammer, or drop hammer.
$e = 0 \cdot 4$ for r.c. piles without helmet.
  $= 0 \cdot 32$ for steel plate cover of wood cap on steel tubes.
  $= 0 \cdot 25$ for wood cap of helmet in good condition, driving r.c. pile; or directly on head of timber pile.
For a wood cap or head of timber pile in deteriorated condition, or for excess packing, $e = 0$.

$h_e = $ the equivalent free fall of the hammer in inches.
  $= 0 \cdot 9h$ for single-acting steam hammer.
  $= 0 \cdot 8h$ for winch-operated drop hammer; if released by triggers $h_e = h$.
  $= h(W + pA)/W$ for double-acting steam hammers; where $A = $ piston area, sq. in.; $p = $ mean pressure, lb./sq. in. $= 80$ per cent. of boiler pressure.
  $= h(pA - W)/W$ for pile extraction (hitting upwards).
  Inclined driving, $\theta°$ to the vertical, $\mu = 0 \cdot 1$.
  $= 0 \cdot 9h(\cos \theta - 0 \cdot 1 \sin \theta)$ for single-acting steam hammer.
  $= 0 \cdot 8h(\cos \theta - 0 \cdot 1 \sin \theta)$ for drop hammer.

$C = $ temporary elastic compression of cap, pile, and ground $= C_c + C_p + C_q$ inches.

* See a letter in *The Engineer*, December 3, 1926, p. 605.

Type of Driving $P = R_2/a$ lb./sq. in.	Easy. 500	Medium. 1000	Hard. 1500	Very Hard. 2000
C_c = Temporary Compression Allowance for Pile Head and Cap.				
Head of Timber Pile .	0·05	0·10	0·15	0·20
Short Dolly in Helmet .	0·05	0·10	0·15	0·20
3 to 4 in. Packing on Head of r.c. Pile . . .	0·07	0·15	0·22	0·30
1 to 1½ in. Mat Pad only on Head of r.c. Pile . .	0·03	0·05	0·075	0·10
Steel Cap for 16 in. Vibro Piling Tube . . .	0·04	0·08	0·12	0·16
C_p = Temporary Compression Values per 10 ft. Length of Piles.				
Timber Pile . . .	0·04	0·08	0·12	0·16
R.C. Pile . . .	0·03	0·06	0·09	0·12
Vibro Steel Piling Tube .	0·014	0·028	0·042	0·056
C_q = Temporary Compression of Ground (average cases). Penetrable Ground.				
For straight-sided Piles, 12–18 in. sides . .	0 to 0·10	0·10 to 0·20	0·10 to 0·30	0·05 to 0·20

For dead loads a factor of 3 to 4 is used.

Test loads of 50 % in excess of the working load should produce no settlement.

Example.—14 × 14 in. reinforced-concrete pile, 40 ft. long, with helmet and short dolly but no mat, weight of pile and helmet, etc., $W_p = 4$ tons. Driven by s.a. steam hammer, $W = 2$ tons; fall $h = 46$ in. Medium driving. Set for 10 blows = 1 in. Find the safe load on the pile if the factor of safety = 4.

$r = W_p/W = 2$; $e = 0·25$; $1/e = 4$; $1/e$ is $> r$;

$\eta = (1 + re^2)/(1 + r) = 0·38$; $h_e = 0·9 \times 46 = 41·4$ in. ;

$C = C_c + C_p + C_q = 0·10 + 4 \times 0·06 + 0·10 = 0·44$; $s = 0·10$.

From eq. (5),

$$R_2 = \frac{0·38 \times 2 \times 41·4}{0·10 + 0·22} + 2 + 4 = 104 \text{ tons ; safe load} = 26 \text{ tons.}$$

Piles Cast in situ.—For piles cast *in situ*, or where a penetration formula is inapplicable, the supporting power can be estimated from the formula

$$\text{safe R} \quad Af + \frac{ap_1}{144} = Af \cdot \frac{awD}{144} \left\{ \frac{1 + \sin \phi}{1 - \sin \phi} \right\}^2 \text{ lb.}$$

A = the surface area, sq. ft. ; f the frictional resistance, lb./sq. ft. ; a the area of cross-section, sq. in. ; p_1 = the toe resistance lb./sq. ft. [see eq. (1) § 349] ; D the depth of the toe below the surface (ft.) ; w the weight of the earth lb./cub. ft. ; ϕ the friction angle of the earth ; p_1 should not exceed four times the safe bearing pressure on the soil given in § 338. For mud and soft silt $f = 100$–150 ; soft wet clay or earth, $f = 150$–180 ; compact dry clay, $f = 300$–400 ; sand and gravel, $f = 500$–600 lb./sq. ft.

347. Sheet Piling.—Another method of constructing foundations in soft ground is to drive two parallel lines of sheet piles, Fig. 463, thus forming a trench in which the material is prevented from spreading laterally. Well-rammed sand, thus confined, makes a satisfactory foundation. Sheet piles may be made of tongued and grooved timber, (i) Fig. 470, or rolled steel sections, (ii), may be used. These interlock each with the next and so form a continuous surface. Sheet piling is often employed to exclude water from foundations or other excavations.
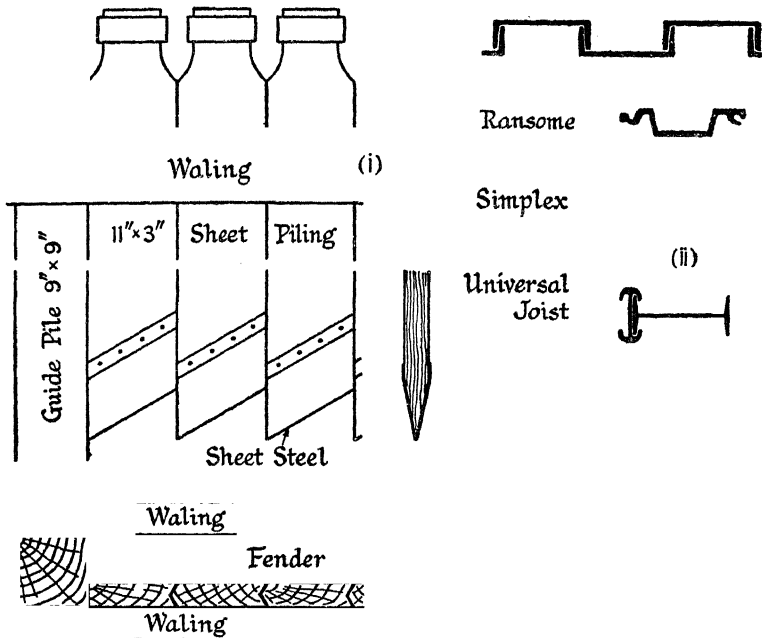
FIG. 470.

348. Cylinder and Caisson Foundations.—The safe load on bridge piers, either cylinders or caissons, is usually determined by the safe bearing pressure on the soil on which they rest. The friction between the soil and the cylinder or caisson, and the displacement or buoyancy of the same, is as a rule neglected when calculating the load which the pier will support. Such foundations are carried down to a firm compact strata well below the disintegrating influences of weather and water (see § 247).

349. Depth of Earth Foundations in Soft or Loose Soil.—The relation proved in eq. (1), § 325, leads to a simple method of determining the minimum depth of a foundation below the surface in loose earth. Suppose that due to the weight of a building there be a pressure p_1 on the area AB of its foundation, Fig. 471. To sustain this direct pressure

p_1 on the earth below the foundation, a lateral pressure p_2 is necessary, as shown at (i), the ratio of p_2 to p_1 being given by eq. (1), § 325,

$$p_2 = p_1 \frac{1 - \sin \phi}{1 + \sin \phi}.$$

But the lateral pressure p_2 must in its turn be sustained by a third pressure p_3 at right angles to p_2, as shown at (ii), which is an enlarged view of an element C in the neighbourhood of the point A. From the same equation, therefore,

$$p_3 = p_2 \frac{1 - \sin \phi}{1 + \sin \phi};$$

or, $p_3 = p_1 \left\{ \dfrac{1 - \sin \phi}{1 + \sin \phi} \right\}^2$

Now the pressure p_3 must be produced by the weight of a column of earth D in length, where D is the depth of the foundation below the surface. Hence, $p_3 = w\mathrm{D}$, where w is the weight of a cubic foot of earth, and

FIG. 471.

$$p_3 = w\mathrm{D} = p_1 \left\{ \frac{1 - \sin \phi}{1 + \sin \phi} \right\}^2 ; \quad \text{or, D} \quad \frac{p_1}{w} \left\{ \frac{1 - \sin \phi}{1 + \sin \phi} \right\}^2 \tag{1}$$

This equation determines the theoretical minimum depth of the foundation below the surface.
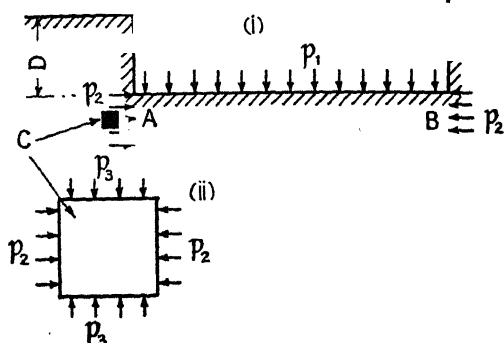
BIBLIOGRAPHY

Earth Pressure

1. COULOMB. *Mém. de Math. et Phys. Acad. Roy. des Sci. Paris,* Année 1773.
2. PONCELET. *Mémoire sur la stabilité des Revêtements,* 1845.
3. RANKINE. On the Stability of Loose Earth. *Phil. Trans. Roy. Soc.,* vol. cxlvii, 1857, p. 9.
4. SCHEFFLER. *Traité de la stabilité des constructions.* Paris, 1864 (takes cohesion into account).
5. BOUSSINESQ. Essai theorique sur l'équilibre dans massifs pulvérulents, etc. *Trans. Roy. Soc. de Belgique,* 1874 ; see in discussion Ref. No. 6.
6. BAKER. The Actual Lateral Pressure of Earthwork. *Proc. Inst. C.E.,* vol. lxv, 1881, p. 140.
7. DARWIN. On the Horizontal Thrust of a Mass of Sand. *Proc. Inst. C.E.,* vol. lxxi, 1882, p. 350.
8. LEYGUE. Nouvelle recherche sur la poussée des terres. *Ann. d. Ponts et Chaussées,* 1885, t. ii, p. 788.

9. WILSON. Some Experiments on Conjugate Pressures in Fine Sand and their Variation with the Presence of Water. *Proc. Inst. C.E.*, vol. cxlix, 1901–2, p. 208.

10. RÉSAL. *Poussée des terres.* Paris, t. i, 1903 ; t. ii, 1910. *Théorie des terres cohérentes.*

11. GOODRICH. Lateral Earth Pressures and Related Phenomena. *Trans. Amer. Soc. C.E.*, vol. liii, 1904, p. 270.

12. MEEM. Pressure, Resistance, and Stability of Earth. *Trans. Amer. Soc. C.E.*, vol. lxx, 1910, p. 352.

13. CAIN. Experiments on Retaining Walls and Pressures on Tunnels. *Trans. Amer. Soc. C.E.*, vol. lxxii, 1911, p. 403.

14. —— Cohesion in Earth. *Trans. Amer. Soc. C.E.*, vol. lxxx, 1916, p. 1315.

15. —— *Earth Pressure, Retaining Walls, and Bins.* New York, 1916.

16. HOWE. *Retaining Walls for Earth.* New York, 1913.

17. KETCHUM. *Walls, Bins, and Grain Elevators.* New York, 3rd ed., 1919.

18. BELL. The Lateral Pressure and Resistance of Clay, and the Supporting Power of Clay Foundations. *Proc. Inst. C.E.*, vol. cxcix, 1914–15, p. 233.

19. CROSTHWAITE. Experiments on Earth-Pressures. *Proc. Inst. C.E.*, vol. cciii, 1916–17, p. 124.

20. —— Experiments on the Horizontal Pressure of Sand. *Proc. Inst. C.E.*, vol. ccix, 1919–20, p. 252.

21. ACKERMANN. The Physical Properties of Clay. *Trans. Soc. Eng.*, 1919–23 (5 papers).

22. FULTON. Overturning Moments on Retaining Walls. *Proc. Inst. C.E.*, vol. ccix, 1919–20, p. 284.

23. HUMMEL AND FINNAN. The Distribution of Pressure on Surfaces Supporting a Mass of Granular Material. *Proc. Inst. C.E.*, vol. ccxii, 1920–21, p. 369.

24. FELD. Determination of Lateral Earth Pressures, etc. *Trans. Amer. Soc. C.E.*, vol. 86, 1923, p. 1448.

25. CAROTHERS. Stresses due to a Loaded Surface when Earth is Treated as an Elastic Solid. *Engg.*, July 14, 1924, p. 1.

26. AUBRY. *Cours de murs de soutènement,* Paris, 1925 ; (JACQUINOT ET FRONTARD, Cohesion in Clay).

27. HAWKEN. Stress in Cohesive Material and Earth Pressure. *Trans. Inst. Eng. Aust.*, 1925, p. 39 ; 1928, p. 147.

28. —— The General Equation of Stress in Frictional-Cohesive Material. *Jour. Inst. Eng. Aust.*, vol. ii, No. 7, 1930.

29. KREY. *Erddruck, Erdwiederstand und Tragfähigkeit des Baugrundes.* Berlin, 3rd ed., 1926.

30. STROYER. Earth-Pressure on Flexible Walls. *Proc. Inst. C.E.*, vol. 226, 1927–28, p. 116 ; *Jour. Inst. C.E.*, Nov. 1935, p. 94.

31. MONCRIEFF. Some Earth-Pressure Theories in Relation to Engineering Practice. *The Struct. Engr.*, vol. vi, 1928, p. 59.

32. VIVIAN. A Theory of Earth Pressures. *Select. Eng. Pap. I.C.E.*, No. 58, 1928.

33. TERZAGHI. Large Scale Retaining-Wall Tests. *Eng. News-Rcd.*, vol. 112, 1934, p. 136 *et seq.* ; also *Engg.*, May 30, 1930, p. 689.

34. TAKABEYA. Experimental Investigation on the Internal Granular Movements of Sand. *Mem. Fac. Eng. Hokkaido Imp. Univ.*, vol. 2, 1931, p. 167 ; see *Engg.*, Feb. 5, 1932, p. 148 ; May 13, 1932, p. 561.

35. RICE-OXLEY. A Generalized Mathematical Determination of Earth Pressure from the Wedge Theory. *Select Eng. Pap. I.C.E.*, No. 90, 1930.

36. JENKIN. The Pressure on Retaining Walls. *Proc. Inst. C.E.*, vol. 234, 1931–32, p. 103 ; also *Proc. Roy. Soc. A*, vol. 131, 1931, p. 53.

37. RAVENOR. The Laws of a Mass of Clay under Pressure. *Engg.*, May 24, 1935, p. 558 ; Dec. 13, 1935, p. 642.
38. INST. STRUC. ENGRS. Report on Gravity Retaining Walls and Concrete Walls, 1935.
39. COOLING AND SMITH. The Shearing Resistance of Soils. *Jour. Inst. C.E.*, June 1936, p. 333.

Foundations

40. NEWMAN. *Notes on Cylinder Bridge Piers and the Well System of Foundations.* London, 1893.
41. CORTHELL. *Allowable Pressures on Deep Foundations.* New York, 1916 ; also *Proc. Inst. C.E.*, vol. clxv, 1905–6, p. 249.
42. BURNSIDE. *Bridge Foundations.* London, 1916.
43. FOWLER. *Engineering and Bridge Foundations.* New York, 4th ed., 1923.
44. HOOL AND KINNE. *Foundations, Abutments, and Footings.* New York, 1923.
45. JACOBY AND DAVIS. *Foundations of Bridges and Buildings.* New York, 2nd ed., 1925.
46. KÖGEL. Druckverteilung im Baugrunde. *Die Bautechnic,* 1927, Hefte 29 and 30 ; 1928, Hefte 15 and 17 ; 1929, Hefte 18 and 52.
47. —— Ueber Baugrunde-Probebelastungen. *Die Bautechnic,* 1931, Heft 24.
48. SIMPSON. *Foundations.* (The Examination and Testing of the Ground, etc.) London, 1928.
49. WILLIAMS. *Design of Masonry Structures and Foundations.* New York, 2nd ed., 1930 ; also *Civil Engineering Handbook,* New York, 1934, p. 632.
50. FRÖHLICH. *Druckverteilung im Baugrunde.* Vienna, 1934.
51. CUMMINGS. Distribution of Stresses under a Foundation. *Proc. Amer. Soc. C.E.*, Aug. 1935.

Piles

52. RANKINE. See *A Manual of Civil Engineering,* 14th ed., p. 603.
53. SANDERS. Rule for Calculating the Weight that can be Safely Trusted upon a Pile. *Jour. Frank. Inst.*, vol. lii, 1851, p. 304.
54. WELLINGTON FORMULA. *Eng. News,* vol. xx, 1888, p. 59 ; Feb. 24, 1921, p. 344.
55. HILEY. A Rational Pile-driving Formula and its Application in Piling Practice Explained. *Engg.*, May 29, 1925, p. 657 ; see also June 2, 1922, p. 673 ; *Trans. Soc. Eng.*, 1923, p. 125 ; *The Struct. Engr.,* vol. viii, 1930, pp. 246, 278.
56. BENNETT. Pile-Driving and the Supporting-Capacity of Piles. *Select. Eng. Paper I.C.E.,* No. 111, 1931 ; see also *Engg.,* Jan. 29, 1932, p. 139.
57. DEAN. *Piles and Pile Driving.* London, 1935.
58. ALLIN. *The Resistance of Piles to Penetration.* London, 1935.
59. GLANVILLE, GRIME AND DAVIES. The Behaviour of Reinforced-Concrete Piles during Driving. *Jour. Inst. C.E.*, Dec. 1935, p. 150 ; Apl. 1936, p. 587 ; Practical Suggestions.

Soil Mechanics

60. TERZAGHI. Principles of Soil Mechanics. *Eng. News-Rcd.*, Nov. 5, 1925, p. 742 et seq.
61. —— *Erdbaumechanik.* Leipzig, 1925.
62. —— The Science of Foundations, Its Present and Future. *Trans. Amer. Soc. C.E.*, vol. xciii, 1929, p. 270.
63. HOUSEL. A Practical Method for the Selection of Foundations based on Fundamental Research in Soil Mechanics. *Eng. Res. Bull. No. 13, Univ. of Michigan,* Oct. 1929 ; see *Engg.,* May 16, 1930, p. 639 ; also *Eng. News-Rcd.*, vol. 110, p. 244.

64. GILBOY. Soil Mechanics Research. *Trans. Amer. Soc. C.E.*, vol. xcviii, 1933, p. 218.

65. AMER. Soc. C.E. *Committee on Earths and Foundations*. Progress Rpt. *Proc.*, vol. 59, 1933, p. 777.

66. LOOS. *Praktische Anwendung der Baugrunduntersuchungen*. Berlin, 1935.

67. TERZAGHI U. FRÖHLICH. *Theorie der Setzung von Tonschichten, etc.* Leipzig, 1936.

QUESTIONS ON CHAPTER XVIII

1. Find by Rankine's rule the total pressure of the earth on the vertical back of a retaining wall 20 ft. high if the upper surface of the earth is horizontal and level with the top of the wall. Angle of repose of the earth $= 30°$, weight of earth per cubic ft. $= 100$ lb.

Ans. 6667 lb.

2. Using Rebhann's construction, Fig. 454, find the vertical and horizontal components of the pressure on the back of the wall in Q. No. 1 if $\phi' = \phi$.

Ans. Hor. $= 5152$ lb. ; vert. $= 2975$ lb.

3. The vertical sides of a trench 8 ft. deep are supported by piling. Find the total load and overturning moment on the piling per foot run due to earth having a weight of 120 lb./cub. ft., and an angle of repose of 30°. The upper surface of the earth is horizontal. (U.L.)

Ans. 1280 lb. ; 3413 ft.-lb. by Rankine's rule ; 1141 lb. ; 3165 ft.-lb. by Rebhann's construction if $\phi' = \phi$.

4. A retaining wall is 30 ft. high and supports earth whose angle of repose is 35° which is heaped above the top of the wall at an angle of 25°. Find the total pressure per lineal foot against the vertical back of the wall. Draw the ellipse of stress for a point at the back of the wall 15 ft. below the surface. Weight of earth 110 lb./cub. ft. (U.L.)

Ans. 19,270 lb. ; acting parallel to the upper surface.

5. The vertical back of a retaining wall is 30 ft. high. The wall supports a bank of dry, loose earth, sloping upward from the top of the wall at an angle of 20° to the horizontal. The angle of repose of the earth is 35°. Draw a simple diagram, based on Rankine's theory of earth pressure, which gives the ratio of the conjugate pressures in such a mass of earth. Hence determine the pressure per foot run on the back of the retaining wall, and indicate where the resultant of this pressure acts, and its direction. Take the weight of earth as 90 lb./cub. ft. (I.C.E.)

Ans. 13,010 lb. ; 10 ft. up ; parallel to upper surface.

6. Find the total pressure on the back of the wall in Q. No. 5 by the wedge theory, if $\phi' = \phi$.

Ans. 13,590 lb. making an angle 35° to the horizontal, and acting $0·4H = 12$ ft. up.

7. Using the data given in § 335, for the retaining walls shown in Fig. 458, find the position of the line of thrust at the base level, (i) by Rankine's theory, § 326 ; (ii) by the wedge theory, § 330.

8. A foundation rests on earth having a weight of 120 lb./cub. ft. and an angle of repose of 30°. Find the minimum depth at which the base must be placed to prevent the earth heaving up, if the load is 5000 lb./sq. ft. (U.L.)

Ans. 4·63 ft.

9. A column carrying a load of 250 tons rests on a base 4 ft. square. The base is carried by a grillage having 6 I beams in the upper grill, and

2 z.

15 in the lower grill. Assuming that the load is distributed equally to each beam in each grill, that the pressure on the ground is 1¼ tons/sq. ft., and the stress in the beams 8 tons/sq. in., find suitable dimensions for the beams, and sketch the arrangement. (U.L.)

10. A circular brick chimney, 120 ft. high above the ground level, 7 ft. external diameter at the top, and 15 ft. external diameter at the ground level, stands on a concrete base 24 ft. square. The total weight of the chimney including lining and footings is 550 tons, that of the concrete base is 290 tons, and that of the superincumbent earth resting on the footings and concrete is 90 tons. The bottom of the concrete base is 15 ft. below ground level. The mean horizontal wind pressure is 30 lb./sq. ft., and the coefficient, allowing for the fact that the cross section is circular, is 0·52. Assume that the chimney tapers uniformly from top to ground level, and find the maximum and minimum pressures between the concrete base and the soil on which it rests. (I.C.E.)

Ans. 1·89 ; 1·35 tons/sq. ft.

11. A 12 × 12 in. timber pile, 30 ft. long, weighing 0·6 ton, is driven through soft ground by a 1-ton monkey dropping freely through 6 ft. (easy driving) to a set of ½ in. per blow. Find the ultimate resistance to penetration.

Ans. 48 tons (Wellington formula) ; 90 tons (Dutch rule) ; 78 tons (Hiley formula).

12. A 14 × 14 r.c. pile, 50 ft. long, weighing with helmet 5 tons, is driven by a s.a. steam hammer W = 3 tons, drop 2 ft., to a set of ¼ in. in 10 blows. A short timber dolly with 3-in. mat are employed. Assuming medium driving, find by the Hiley formula the safe supporting power of a pile, given a factor of safety of 3.

Ans. 28 tons.

CHAPTER XIX

MASONRY, BRICKWORK, AND MASS CONCRETE CONSTRUCTION

350. Stone used in Masonry Structures.—The stone employed for engineering work must possess considerable crushing resistance, be very durable when exposed to weather, and not be of an absorbent nature. The resistance to crushing and to absorption can be determined by experiment, §§ 274 and 277 ; the durability can best be judged from the results of years of experience of the behaviour of the stone in actual structures. The presence of certain undesirable constituents, however, is indicated by chemical and microscopic tests.

The three kinds of stone usually used are (1) granites, (2) sandstones, (3) limestones. The *granites* are hard stones, very durable, difficult to work, but capable of a fine finish. They are employed where much wear is to be expected, or where great accuracy in dimensions is necessary. Granite is used for the copings of dock walls, the bedstones for heavy girders, the sills of graving docks, and like positions, also when a good appearance is required. The best quality of stone comes from Aberdeen and Cornwall, large quantities are shipped from Norway Of the *sandstones*, the grits are the best for heavy engineering work. They are hard, coarse grained, and very durable, and much used for ashlar work. The following are the best-known varieties : *Craigleith* stone, a fine-grained stone containing 98 % of silica, very hard and durable. *Bramley Fall*, the name used to denote the coarse millstone grits of Yorkshire, hard and very durable. *Corsehill*, a hard red sandstone from Dumfries, which weathers well ; and *Darley Dale*, a hard compact grit from Derbyshire. The *limestones* are durable stones, softer than the sandstones and more porous. The commoner varieties are : *Portland* stone from Dorset, of which the best beds are the *Whitbed* and *True Roach*, both of which weather well. *Bath* stone, which is soft and easily worked, but must be laid on its natural bed if it is to endure. *Box Ground* is the best weathering stone of the Bath oolites. The best known Dolomites or magnesian limestones are the *Mansfield* stones and *Bolsover Moor* stone from Derbyshire.

In addition to the above there are, in many localities, other useful building stones. These vary greatly as regards strength, durability and porosity. Careful inquiry should therefore be made, before use, as to their suitability for the work in hand. Questions of relative cost, quantity available, and appearance, must also be taken into account.

MATERIALS AND STRUCTURES

PROPERTIES OF STONE.

[HUDSON BEARE (Ref. No. 25, Chapter XVI, Bib.)].

Kind of Stone.	Weight. lb./cub. ft.	Ultimate Crushing Strength. tons/sq. ft.	Absorption per cent. of Dry Weight of Stone.
Granites.			
Aberdeen, red	158–163	1210–1320	0·29–0·42
,, grey	158–172	850–1360	0·09–0·55
Cornwall, grey	162–165	956–1060	0·12
Sandstones.			
Bramley Fall, coarse white	132·2	240	3·70
Corsehill, red	130·4	440	7·94
Craigleith, grey-white	138·6	860	3·61
Grinshill, grey-white	122·5	210	7·80
Limestones.			
Portland, Whitbed *	132·2	205	7·51
Bath, Box Ground *	127·9	98	7·49–8·10
,, Corsham Down *	129·0	95	11·1
Crystalline limestone (Banchory)	174·7	950	
Dolomites.			
White Mansfield †	140·1	460	5·01
Red Mansfield	143·2	590	4·58
Mansfield Woodhouse ‡	145·4	580	4·62

* Oolitic. † Siliceous dolomite. ‡ Crystalline, yellow ; true dolomite.
A factor of safety of at least 10 should be used (see § 356).

351. Quarrying and Working Stone.—The stone is obtained from its quarry bed by blasting, or by splitting out by means of iron wedges. The large blocks thus procured are again split and sawn to approximately the required size. Stones like granite, which are granular in structure, split equally well along any plane. The aqueous stones split more easily along the planes of stratification, spoken of as the planes of cleavage. The particles of which these stones are composed were deposited in successive layers at the bottom of the sea or a lake, and afterwards consolidated into stone by pressure. They are, in consequence, built up in layers running parallel to the *natural bed* or plane on which they were deposited ; but owing to subsequent upheavals, this plane may not appear at the quarry in its original position. It is most important that the blocks for a masonry structure should be so cut and marked at the quarry that, when in position, the planes of stratification shall be as nearly as possible perpendicular to the direction of the pressure, and that only the edges of the layers should be exposed to the weather. Stones otherwise arranged disintegrate under atmospheric influences much more rapidly, for the layers tend to flake off successively when exposed to frost.

Dressing.—After the stone has been reduced to approximately the

required size, the top and bottom surfaces, called the top and bottom beds, should be worked true and flat right across. A smooth finish is not necessary, but hollow bedding, i.e. making the stones bed true round the edges only, should not be allowed. In addition, the vertical joints should be worked square and true for at least 4 to 6 in. from the face, depending on the size of the stone. The face, or exposed surface, is dressed in various ways, depending on the purpose for which the stone is intended. In the case of granite, the face may be left as it comes from the quarry after being split, the larger protuberances having been knocked off with a scabbling hammer. Blocks treated in this manner are called *quarry-* or *rock-faced* or *hammer-dressed*. The surface thus produced is necessarily irregular, and in order that a close joint may be made it is usual to cut a smooth surface with the axe all round the edge of the face. Such edges are said to be *drafted*. If the face is to be flat, it must be worked all over as are the top and bottom beds. It may be dressed with a pick (a hammer with a sharp point), *picked* or *close picked* ; or worked with the axe (a sharp-edged hammer producing a series of shallow indentations all over the surface), *single-axed* ; or the patent axe may be used in which there are a number of parallel blades, thus producing finer work, *patent-axed* ; depending on the degree of finish required. Granite may also be polished.

In the case of sandstones and limestones, the blocks, after being split and sawn, are worked with a hammer or mallet and chisels of various types, instead of being axed. The top and bottom beds and the vertical joints are dressed in the manner previously described. If the face has a drafted margin, the centre part may be left rough as when quarried, *rock-faced* ; or roughly dressed with a spalling hammer as in the case of granite. When a more ornamental treatment is desired, the centre part may be worked into ridges and depressions, a type of work known as *rusticated* or *vermiculated*. If the face is to be flat, the whole surface is worked over with a broad chisel. Such surfaces are spoken of as *tooled*, and the tooling may be fine or coarse, and of several different types as may be required. The face may be rubbed smooth, but most free-stones are too soft to take a polish. The softer varieties of stone may be finished with a *drag* or toothed comb, which produces a smooth face without tool marks.

Mouldings may be worked on stones, either by hand to template, or by machine. In the harder stones, owing to the difficulty of working, they should be of simple outline.

Having been worked to shape, the stones are allowed to season in the open air. When freshly quarried, the stone contains a quantity of mois-ture called *quarry sap*. This moisture renders the stone softer and easier to work. It should therefore be worked immediately after quarrying, and the sap dried out before the stone is built into place. The hardness of the stone is increased thereby, and the danger of disintegration by frost diminished. Working the stone at the quarry has the additional advantage that the cost of carriage to the site is reduced.

352. Types of Masonry Work.—The following are the types of masonry work commonly used in engineering work : *Block-in-Course* ; *Squared Coursed Rubble* ; *Ashlar* ; and *Rubble Concrete*.

Block-in-Course. — This is the type of construction used for harbour walls, embankments, and similar heavy work. A typical example is shown in Fig. 472. The stones are usually rock faced, squared, brought to good joints, and set in cement mortar (1 of cement to 3 of sand), or in hydraulic lime cement (1 of lime to 2 of sand). The blocks are built in courses, the height of which usually ranges from about 9 to 14 in., and should not exceed 24 to 30 in. in the largest class of work. All the stones of any one course are of the same height, but the height of all the courses need not necessarily be the same, they may diminish regularly from the bottom to the top. The arrangement of headers and stretchers and the method of bonding will be clear from Fig. 472. It is usual to specify minimum dimensions for the stones to be employed. No stone should be less in width than $1\frac{1}{2}$ times its thickness. The length of the headers and stretchers should be at least $2\frac{1}{2}$ times their thickness. In the smallest class of work no stone should have a bed area of less than 2 sq. ft., nor less than 15 sq. ft. in the largest. There should be one header for every two stretchers. The lap should not be less than the height of the course. The joints should not exceed from $\frac{1}{4}$ to $\frac{1}{2}$ in. in thickness. The interior stones, called *hearting* or *packing stones*, should be of the same height as the face stones, and of approximately the same size. They should be arranged to give the best possible bond and to break joint as far as is possible.

Course X

Course Y

FIG. 472.

Course

FIG. 473.

Squared Coursed Rubble.—This type of masonry, Fig. 473, is used for walls and other less massive constructions than block-in-course. The
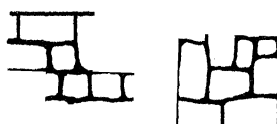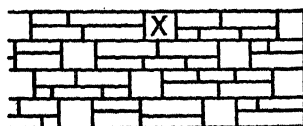
stones are squared, and built in courses of the same height, usually ranging from 8 to 14 in., but the individual stones need not be of the same height as the course. All the headers or bonding stones should be equal in height to the course, and there should be one header to three or four stretchers, which header should be at least 2 ft. long. No stone should be less than 4 in. in thickness, and there should be not more than two stones per course.

There are other types of rubble masonry, coursed and uncoursed, of various degrees of finish. These are chiefly used for the less important work, boundary walls, etc.

Ashlar.—In ashlar work the stones are of large size, carefully worked all round to exact dimensions, and set with joints usually not exceeding ⅛ to ¼ in. in thickness. It is the highest class of masonry work and is used where accurate shape and finish are necessary. It is commonly employed for dock sills, facing dock walls, quoins (exterior corners of walls), string courses, copings, parapets, arches, and wherever accurate workmanship and good appearance are required. An occasional course of ashlar is often introduced in rubble stone work to bring the whole true and level. In ashlar work the courses are usually not less than 12 in. in height, and all courses are of the same height. The sizes of the stones and arrangements of bonding may be similar to those
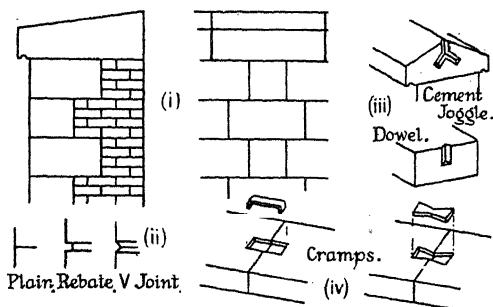
FIG. 474.

for block-in-course given above, but a very usual form of face bond for ashlar is similar to Flemish bond in brickwork. Often ashlar is used for the facing only of a wall, the backing being of rubble or brickwork, (i) Fig. 474. In this case the minimum thickness of facing should be 6 in. Fig. 474 shows some typical ashlar work. The joints may be plain, rebated, or V joints, (ii). The rebate may be formed half on each adjoining stone, or entirely on one stone, when it should be arranged to come at the top of the stone. (iii) and (iv) show some methods of dowelling and cramping where, as in coping stones, some connection between the blocks is desirable. A 1 to 1 cement is used for the joggles, and to bed in the cramps. The latter are made of copper, or wrought iron heavily galvanised to prevent rusting, which tends to split the stone.

Rubble Concrete.—This is a class of construction used for the hearting of large mass concrete structures such as masonry dams. Large blocks of stone, roughly squared, and weighing up to 8 tons, called *plums*, or *displacers*, are placed in the concrete, Fig. 475, and arranged roughly in courses, so that they break joint both horizontally and vertically. Some

of the stones are made to bond transversely as well as longitudinally; in fact, the construction may be regarded as a rough rubble wall on a very large scale. The stones should be placed as close together as is practicable, in order to increase the weight of the mass and to save concrete, but with not less than 6 in. of space between the stones, so that the concrete may be properly rammed. Care must be taken that all voids are filled with concrete, and it is not unusual to work the plums backward and forward

Rock Foundation

FIG. 475.

when in place to ensure proper bedding, an operation known as ' waggling.'
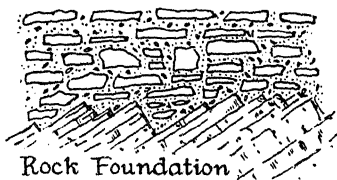
353. Masonry Structures. Conditions of Stability.—The conditions of stability for a masonry structure are :

(1) The blocks or voussoirs must not overturn at a joint. This condition implies that the line of action of the thrust at the joint, called the *line of thrust* or *line of resistance*, Fig. 476, must not fall outside the joint.
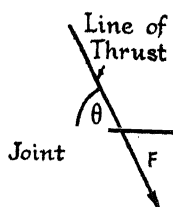
(2) The maximum compressive and tensile stresses must not exceed the permissible intensity for the materials. The permissible compressive stress depends on the kind of stone and cementing material used (see Table, § 356). The tensile

FIG. 476.

strength of mortar is small, and it is common to specify that no tensile stress shall exist in the structure, particularly if it be exposed to water pressure. As will be shown in § 354, this implies that the line of thrust must lie within a certain distance from the centre of area of the cross-section. In this case the second condition of stability includes the first.

(3) The blocks must not slide one on the other. This implies that the tangential component of the thrust, $F \cos \theta$, must not exceed the frictional or shearing resistance to sliding.

It is evident that an examination of the stability of a masonry structure involves a determination of the line of thrust.

354. Stresses in Masonry Structures.— Let AB, Fig. 477, be any normal cross-section of a masonry structure, and C the centre of area of that section. Let F be the resultant pressure acting across the section,

FIG. 477.

and Q its point of application. Then $N = F \sin \theta$ is the component normal to the section, and $S = F \cos \theta$ the tangential component, where θ is the angle which F makes with AB. Apply two equal and opposite
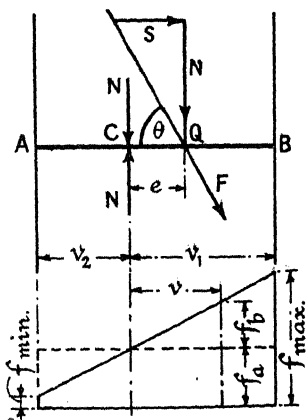
forces NN at the centre of area.C, as shown in the figure. These will not alter the equilibrium of the conditions. The force N at C, above the line AB, will produce a uniform compressive stress all over the cross-section of intensity $f_a = \dfrac{N}{a} = \dfrac{F}{a} \sin \theta$, where a is the area of the section. The other two forces NN, acting at C and Q, will form a couple of magnitude Ne, which is the bending moment M on the section. If I be the moment of inertia of the cross-section, and v the distance of any point on the section from the principal axis through C, the stress at the point, due to bending, is

$$f_b = \frac{Mv}{I} = \frac{Nev}{I} = \frac{Fev}{I} \sin \theta.$$

The total stress at the point is, therefore,

$$f = f_a + f_b = \frac{F}{a} \sin \theta + \frac{Fev}{I} \sin \theta = \frac{F}{a}\left\{1 + \frac{ev}{\kappa^2}\right\} \sin \theta.$$

The maximum value of f, which occurs where $v = + v_1$, is the maximum compressive stress on the cross-section,

$$f_{\text{max.}} = \frac{F}{a}\left\{1 + \frac{ev_1}{\kappa^2}\right\} \sin \theta = \frac{N}{a}\left\{1 + \frac{ev_1}{} \right. \tag{1}$$

The minimum value of f occurs where $v = - v_2$, and is

$$f_{\text{min.}} = \frac{F}{a}\left\{1 - \frac{ev_2}{\kappa^2}\right\} \sin \theta = \frac{N}{a}\left\{1 - \frac{ev_2}{} \right\} \tag{2}$$

If this value be negative, it implies that the stress is tensile. These two equations give the maximum and minimum stresses on the cross-section for given values of F, e, and θ.

In a masonry structure the cross-section is usually rectangular. If the breadth of the rectangle be B and the depth D,

$$\kappa^2 = \frac{I}{a} = \frac{\frac{1}{12}BD^3}{BD} = \frac{D^2}{12}; \quad v_1 = v_2 = \frac{}{}$$

Inserting these values in eqs. (1) and (2),

$$f_{\text{max.}} = \frac{F}{a}\left\{1 + \frac{6e}{D}\right\} \sin \theta = \frac{N}{a}\left\{1 + \frac{6e}{D}\right\} \qquad . \tag{3}$$

$$f_{\text{min.}} = \frac{F}{a}\left\{1 - \frac{6e}{D}\right\} \sin \theta = \frac{N}{a}\left\{1 - \frac{6e}{D}\right\} \qquad . \tag{4}$$

In many masonry structures it is usual to specify that the stress on the cross-section shall never become tensile, that is to say, that $f_{\text{min.}}$ must never become negative. The limiting condition for this is evidently

$$f_{\text{min.}} = 0; \text{ or, } 1 - \frac{ev_2}{\kappa^2} = 0, \text{ whence } e = \frac{\kappa^2}{v_2} \tag{5}$$

If the cross-section be rectangular, $B \times D$,

$$e = \frac{\kappa^2}{v_2} = \frac{D^2}{12} \times \frac{2}{D} = \frac{D}{6}.$$

It follows that, if no tensile stress is to exist on the cross-section, the point of application of the thrust F must fall within the middle third of the depth D. This is known as the *middle third* rule. If the cross-section be circular, of diameter D, $\kappa^2 = D^2/16$, and $v_2 = D/2$; hence $e = \kappa^2/v_2 = D/8$, and the point of application of the load must lie within the middle fourth of the cross-section.

The *average* shear stress on the cross-section will be

$$\frac{S}{a} = \frac{F}{a} \cos \theta \qquad . \qquad . \qquad . \qquad . \qquad . \quad (6)$$

If the cross-section be rectangular, the maximum value of the shear stress will be $\frac{3}{2} \cdot \frac{F}{a} \cos \theta$ (see § 81, Vol. I).

355. Tensile Stresses in Masonry Structures.—In structures such as masonry dams it is essential that the line of thrust pass within the middle third of each cross-section, otherwise cracks will occur on the upstream face, which is in contact with the water, and the water will percolate into the interior.

Nevertheless, it is a matter of common observation that in masonry structures which have safely carried their load for many years, the joints tend to open, showing that some tension exists. On these grounds, in structures such as masonry arches, where no question of percolation arises, some Engineers consider it sufficiently safe if, under the worst combination of external loads, the line of thrust pass within the middle half of the cross-section. In this case, for a rectangular cross-section, if the line of thrust just fall within the middle half, $e = D/4$; hence, from eq. (4), § 354,

$$f_{min.} = \frac{F}{a} \left\{ 1 - \frac{6}{D} \times \frac{D}{4} \right\} \sin \theta = -\frac{1}{2} \frac{F}{a} \sin \theta = -\tfrac{1}{2} f_a.$$

There is therefore a tensile stress of intensity equal to one-half the mean normal stress f_a, acting on the joint. If the mortar has sufficient strength to resist this tension, the maximum compressive stress, from eq. (3), § 354, will be

$$f_{max.} = \frac{F}{a} \left\{ 1 + \frac{6}{D} \times \frac{D}{4} \right\} \sin \theta = 2\tfrac{1}{2} f_a,$$

or two and a half times the mean normal stress. Had the line of thrust just passed within the middle third, the maximum compressive stress would have been equal to $2f_a$. This increase in the maximum compressive stress may be quite as important as the existence of a tensile stress.

To what extent it is safe, in particular cases, to permit tensile stress in masonry structures is largely a matter of judgment and experience. In doubtful cases it is best to adopt the middle third rule.

If the mortar is incapable of resisting the tensile stress, the joint will

open, and the distribution of stress will be completely changed. The crack, once started, will continue to extend until the centre of action of the compressive stress on the cross-section falls in line with the normal component N of the thrust. Assuming, as before, a straight line distribution of stress, the state of affairs will then be as shown in Fig. 478. The width of joint remaining in contact will be JB = $3(D/2 - e)$, so that, if the section be rectangular, the area in contact will be
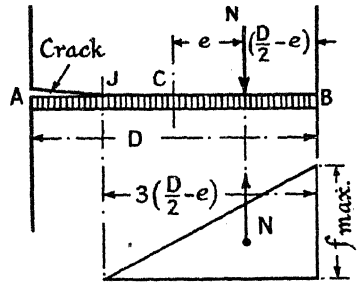
FIG. 478.

$$a \times \frac{JB}{AB} = w \cdot \frac{\left(\frac{D}{2} - e\right)}{D} = 3a \frac{D - 2e}{2D}$$

The resultant total stress must be equal to N, so that the mean stress

will be $\dfrac{-2e)}{2D}$ The maximum stress will be twice the mean,

hence

$$f\text{max.} = \frac{2N}{3a\dfrac{D - 2e}{2D}} = \frac{4ND}{3a(D - 2e)} = fa \frac{4D}{3(D - 2e)}.$$

If the line of thrust just fall within the middle half, $e = D/4$, and $f\text{max.} = 2\frac{2}{3}fa$, instead of $2\frac{1}{3}fa$ had the joint not opened.

356. **Working Stresses in Masonry.**—The compressive strength of masonry work is much less than that of the stone itself. It depends chiefly on the accuracy with which the stones are dressed, proper bonding, the thickness of the joints, and the strength of the mortar. Thin joints are stronger than thick ones, for the mortar tends to squeeze out under load. The following Table gives average figures.

SAFE COMPRESSIVE STRESSES IN MASONRY, TONS/SQ. FT.

	Minimum Crushing Strength.	* Ashlar, $\frac{1}{4}''$ Joints.	* Block in Course, $\frac{1}{2}''$ Joints.	* Square Coursed Rubble, 1″ Joints.	Uncoursed Rubble.
Granite . .	800	40	35	20	In 1 : 4 cement mortar 5
Siliceous Sandstone or Crystalline Limestone . .	400	30	30	15	In 1 : 2 lime mortar 3
Soft Sandstone or Limestone .	200	20	20	10	

* In 1 : 3 cement mortar.

In piers, if L/D exceed 5, these stresses should be reduced.

357. Masonry Arches.—Fig. 479 gives the terms used to denote the different parts of an arch.
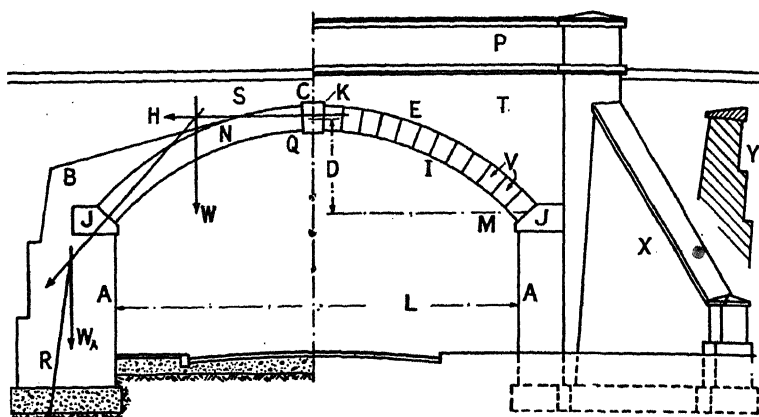
FIG. 479.

A. Abutment.	J. Springers.	Q. Soffit.
B. Backing.	K. Keystone.	S. Spandrel space.
C. Crown.	L. Span (clear).	T. Spandrel wall.
D. Rise.	M. Springing line.	V. Voussoirs.
E. Extrados.	N. Arch ring.	X. Wing wall.
I. Intrados.	P. Parapet.	Y. Section of wing wall.

This figure is representative of small arches whether constructed of masonry or of brick (see Fig. 500). The space between the roadway and the curve of the arch, called the *spandrel space*, is usually filled in. Directly on top of the arch ring is placed a concrete or masonry backing, which tapers up from the abutments tangent to the ring. Above this backing, the space is filled with dry earth filling up to the level of the roadway proper, Fig. 479. In larger arches, the weight of this filling would form an unnecessarily heavy load on the structure, and the filling is omitted. The roadway is then carried on *jack arches*, Fig. 480, spanning between a series of parallel longitudinal walls called *spandrel walls*, the outer two of which form the face of

FIG. 480.

the structure. Very large arches are constructed as shown in Fig. 481. The roadway is carried on a series of secondary arches running transversely to the main arch. The load from these is transmitted to the arch ring by a series of masonry piers. The spandrel space is quite open.
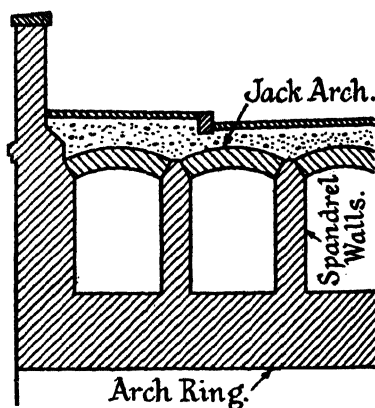
The arch ring rests at its ends on specially shaped stones called *springers*, J, Fig. 479, the upper surfaces of which are made approximately perpendicular to the line of thrust. These transmit the load to the abutments. The forces from the arch which act on the abutments are shown in Fig. 479. To find the total pressure on the foundations, these must be combined with the earth pressure acting on the back of the abutment wall. In arches of the type shown in Fig. 481, the ends of the arch ring may bear directly on the rock forming the sides of the valley, which is shaped to suit. Arches of this character, of which the ends are flat, and bear over a considerable area, are called *rigid arches*. In some cases, masonry arches have been constructed with hinges or quasi-hinges. These may take the form of a lead plate, about 1 in. thick and one-quarter the depth of the arch ring, inserted between the voussoirs at the crown and springings; or pin joints similar to those shown in Fig. 363 may be employed. They are attached to the end voussoirs by rag bolts. Similar joints have been used for concrete and reinforced-concrete
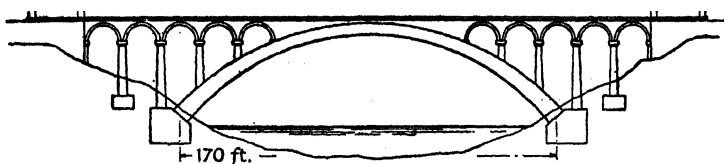
FIG. 481.

arches. The intention is to determine more accurately the line of thrust, and to relieve the arch of any temperature and shrinkage stresses.

Proportions of Masonry Arches.—When designing masonry structures it is necessary first of all to fix likely dimensions for the structure, based on successful designs, and then to test the stability of the proposal. For this purpose a number of rules have been given for the proportions of ordinary masonry arches. Let L = the span; R = the radius of curvature, and T = the thickness at the crown; D = the rise, and r = the ratio rise/span = D/L; all dimensions being in feet.

Molesworth gives, for railway arches, from 25–70 ft. span : $D = L/5$; $T = L/18$; width of abutments $L/5$ to $L/4$; width of piers $L/6$ to $L/7$.

Rankine gives : $T = \sqrt{0 \cdot 12R}$ for a single arch ; $T = \sqrt{0 \cdot 17R}$ for a series ; width of abutments $R/3$ to $R/5$ (at the springings).

Perronet's formula for circular or elliptic arches is : $T = L/30 + 1$.

Trautwine's rule for circular or elliptic arches of first-class cut stone is : $T = 0 \cdot 25 \sqrt{R + L/2} + 0 \cdot 2$; for second-class work, multiply by 9/8 ; for brick and rubble arches, multiply by 4/3. Width of abutments at springings = $R/5 + D/10 + 2$; at foundations, not less than two-thirds the height to springings.

The above formulae are intended to apply to small or medium span arches, designed for light loading.

Sir E. Owen Williams [10] has made a study of a series of 200 direction-

fixed arches up to 300 ft. span, designed to carry Ministry of Transport loading and impact, allowing for a temperature rise of 25° F. and fall of 20° F. in filled arches, and (on account of less protection from temperature changes) of 35° F. rise and 25° F. fall in open spandrel arches. It is assumed that the arch proper would be constructed in isolated blocks and keyed up after one month, thus eliminating shrinkage stresses. Arch shortening is taken into account, but the abutments are supposed rigid. The line of thrust is kept within the middle half, but in unreinforced arches the maximum tensile stress is limited to 100 lb./sq. in. The following practical rules are given :

Plain Masonry Arches.—*Filled Arches,* $T = L/50 + 1$; maximum compressive stress $f_c = 200 + (5 \cdot 85 \sqrt{L})/r$; *Open Spandrel Arches,* $T = L/50$; $f_c = 500 + L$ when $r = 0 \cdot 15$; $f_c = 400 + L/3$ when $r = 0 \cdot 30$; stresses in lb./sq. in. Thickness and area at springings twice that at crown.

PLAIN MASONRY ARCHES : LIMITS OF SPANS AND RISES FOR VARIOUS MATERIALS.

Material.	Max. f_c	Filled Arches.		Open-Spandrel.	
		$r = 0 \cdot 20$	$r = 0 \cdot 30$	$r = 0 \cdot 20$	$r = 0 \cdot 30$
	lb./sq. in.	feet.	feet.	feet.	feet.
Cut basalt or granite in cement mortar, or 1 : 1½ : 3 concrete	750	up to 200 at least	up to 200 at least	125 to 200 at least	125 to 200 at least
Cut basalt or granite in lime mortar	375	50	100		
Best quality bricks and rubble masonry in cement mortar, or 1 : 2 : 4 concrete	500	100	200		125 to 200 at least
Best quality stock bricks or stone, in lime mortar	250	50	50		
Common bricks in cement mortar, or 1 : 3 : 5 concrete	250	30	50		

NOTES.—It is inadvisable to use plain masonry arches for rises of less than $r = 0 \cdot 15$. With a stress of $f_c = 750$, and $r = 0 \cdot 15$, filled arches are possible from 100–200 ft. span, and open-spandrel arches from 150–200 ft. span. For rises of less than $0 \cdot 20$, the arch should be ribbed on the under side at the springings; f_c should not exceed 750 lb./sq. in. in unreinforced masonry.

Reinforced-Concrete Arches.—In all cases : 1 % reinforcement at crown ; thickness and area at springings, twice that at crown, ½ % reinforcement. The proportions are given in the Tables, p. 719.

Variation in Thickness.—The thickness of the above arches is assumed to vary from crown to springings as follows :

Section		0·0	0·5	1·5	2·5	3·5	4·5
Thickness		1·000	1·005	1·015	1·025	1·035	1·048
Section		5·5	6·5	7·5	8·5	9·5	10·0
Thickness		1·085	1·168	1·311	1·547	1·837	2·000

T IN FEET FOR R.-C. FILLED ARCHES UP TO 200 FT. SPAN.

r	Arched Slab full width of Bridge.		Arched Slab two-thirds width of Bridge.	
	Mix 1 : 1 : 2 ; $f_C = 1100$	Mix 1 : 1½ : 3 ; $f_C = 850$	Mix 1 : 1 : 2 ; $f_C = 1100$	Mix 1 : 1½ : 3 ; $f_C = 850$
0·1 0·15 and upward.	L/55 ; min. 12″ L/75 ; min. 9″	L/40 ; min. 15″ L/60 ; min. 9″	L/50 ; min. 12″ L/65 ; min. 9″	L/35 ; min. 15″ L/50 ; min. 9″

T IN FEET FOR R.-C. OPEN-SPANDREL ARCHES UP TO 300 FT. SPAN.

r	T for min. area (all concretes).	Mix 1 : 1 : 2 ; $f_C = 1100$.		Mix 1 : 1½ : 3 ; $f_C = 850$.	
		Min. crown area per foot of width of bridge, for depth T.	Add to min. area for every 10 per cent. reduction in T.	Min. crown area per foot of width of bridge, for depth T.	Add to min. area for every 10 per cent. reduction in T.
		sq. ft.	per cent.	sq. ft.	per cent.
0·10	1·6 (L/200+1)	L/75	nil.	L/60 *	nil
0·15	2·0 (L/200+1)	L/140	10	L/90	5
0·20	2·5 (L/200+1)	L/200	12·5	L/125	10
0·25	2·9 (L/200+1)	L/245	14	L/160	12·5
0·30	3·3 (L/200+1)	L/275	15	L/190	15

* Limited to 250 ft. span.

In small spans the thickness may be kept uniform. In larger filled arches it may be increased 50 % from crown to springings according to a linear law, but it is more economical (if possible) to increase the depth as the square of the distance from the crown, or even as the cube for still larger spans, § 322, and it may be necessary to make the depth at the springings twice that at the crown, particularly in arched ribs.

358. The Line of Thrust.—Experiment [6] has shown that large masonry arches approximate very closely in behaviour to elastic arches with direction-fixed ends, and the line of thrust may be determined as in § 222. In small arches, bearing in mind that the end conditions are very indeterminate, and that the load is transmitted to the arch ring through a mass of dry filling, Fig. 479, so that the incidence of the load is quite indefinite, an application of the theory for an elastic arch, § 222, hardly warrants the labour involved, particularly as experience has shown that if, for the given system of loads, a line of thrust can be drawn lying wholly within the middle third of the arch, or even within the middle half (see § 355), the arch will be perfectly stable in practice.

It is necessary to examine the arch in the following conditions :

(i) loaded with its own weight ;
(ii) when the moving load completely covers the arch ;
(iii) when the moving load half covers the arch.

The arch must be stable under each of these conditions. If the moving load be uniformly distributed, condition (ii) includes condition (i). It is not usual in such methods of treatment to attempt to determine the position of the moving load which produces the worst effect, but allowance should be made for impact where necessary.

Load Diagram.—The method of estimating the loads on a masonry or brick arch will be clear from Fig. 482. The data given has reference to the arch of Fig. 500. As-
sume that the structure is 1 ft. wide perpendicular to the paper. The span is divided up into a number of vertical strips, (i) Fig. 482. For each strip, the face area of the arch ring, concrete backing, earth filling, and road material, multiplied by their respective weights per cubic foot, will represent the weights of these materials carried by the arch. It is convenient, in order to find these weights, and the line of action of their resultant for each strip, to construct a *load diagram*, (ii), in which the heights of all the ordinates in (i) are multiplied by the weight per cubic foot of the respective materials, and the product is set up to some convenient scale. Thus, comparing any ordinate common to (i) and (ii),

FIG. 482.

the height $a_1'b_1'$ in (ii) is equal to the height a_1b_1 in (i), expressed in feet, multiplied by w_1, the weight of Thames ballast in lb./cub. ft. Similarly, $b_1'c_1'$ in (ii) is equal to b_1c_1 in (i), expressed in feet, multiplied by w_2, the weight of the dry filling in lb./cub. ft., and so on. The unit for all these heights is ft. $\times \dfrac{\text{lb.}}{\text{ft.}^3} = \text{lb./sq. ft.}$ When the arch carries a live load, the height $a_1'z_1'$ represents this live load in lb./sq. ft. of area of roadway.

The area $z_1'e_2'$ in (ii) represents the total load on the second strip,
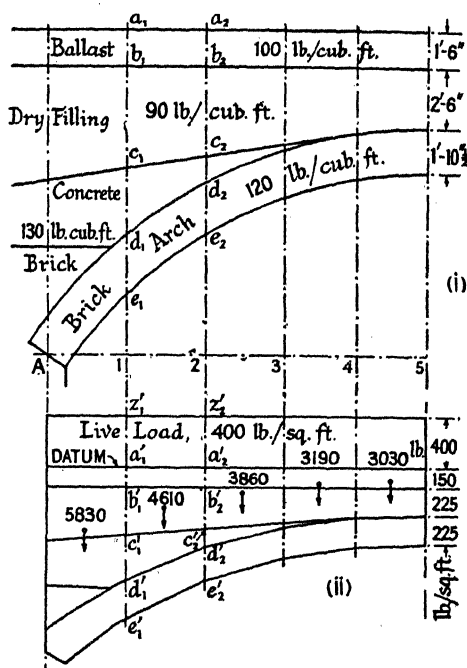
and the line of action of this load will pass through the centroid of this area. Suppose that in (ii) the horizontal scale be $1'' = a_1$ ft., and the vertical scale be $1'' = a_2$ lb./sq. ft. ; then, if the area $z_1'e_2'$ be a square inches, the total load represented by this area is $aa_1\dot{a}_2$ lb., since for the purpose of calculation the structure has been taken to be 1 foot wide. By finding the areas and centres of area of each strip of the load diagram (ii) in turn, the magnitude and position of all the loads on the arch are determined. All these loads are assumed to act vertically.

Fuller's Method.—Having found the loads on the arch, the graphical method of Professor Fuller may be used to find the line of thrust. Let ACB, (i) Fig. 483, represent the arch. For the given system of loads W_1, W_2, W_3, ... draw any line of thrust AED′QB passing through A and B (§ 217), the pole being O_1. From the highest point D′ of this line of thrust, draw any two lines D′A′ and D′B′ cutting the base line AB produced in A′ and B′ ; A′D′B′ is to be regarded as a line of thrust for the given loads, obtained by some curious kind of projection in which the funicular polygon takes the form of two intersecting straight lines. Evidently, if the point A becomes the point A′, and the point B becomes the point B′, the point E will become the point E′, and the point P the point P′, and so on. To obtain the middle third area in the new kind of projection, divide the base line AB into a number of parts 1, 2, 3, . . . Through the point 3, draw a vertical cutting FD′ in 3″, project horizontally across from 3″ to 3′ in the line A′D′, and draw a vertical through 3′. Then the vertical through 3″ in the old projection will be represented by the vertical through 3′ in the new. Project horizontally across from the points where 3,3″ cuts the middle third boundary lines of the arch to intersect the vertical through 3′. The intersection points so obtained lie on the middle third boundary lines in the new projection. By repeating this process for all the points 1, 2, 3, . . . the shaded area of (i) Fig. 483 will be obtained, which represents the middle third area in the new projection. If, now, a pair of straight lines $A_1D_1B_1$ can be drawn, meeting in D_1 on the vertical through D′, and lying entirely within the shaded area, it is possible to draw a line of thrust lying entirely within the middle third of the arch. If more than one solution is possible, the pair of straight lines lying nearest the centre line of the shaded area should be drawn. These will represent the most probable line of thrust. Draw A_1A_2, B_1B_2, horizontal lines ; join A_2B_2.

To draw a line of thrust corresponding to the straight lines $A_1D_1B_1$, draw Oh in the force polygon parallel to A_2B_2 (O_1h is parallel to AB). Make $H = H_1 \times \dfrac{D'G}{D_1G_1}$. A funicular polygon, drawn with the new pole O and passing through D_1, should lie wholly within the middle third. This is not shown in the figure.

If in such an arch it is possible to draw a line of thrust lying wholly within the middle third, or even (see § 355) within the middle half, of the arch ring, the arch may be regarded as stable. If, then, the safe compressive stress on the masonry be not exceeded, the arch will safely carry
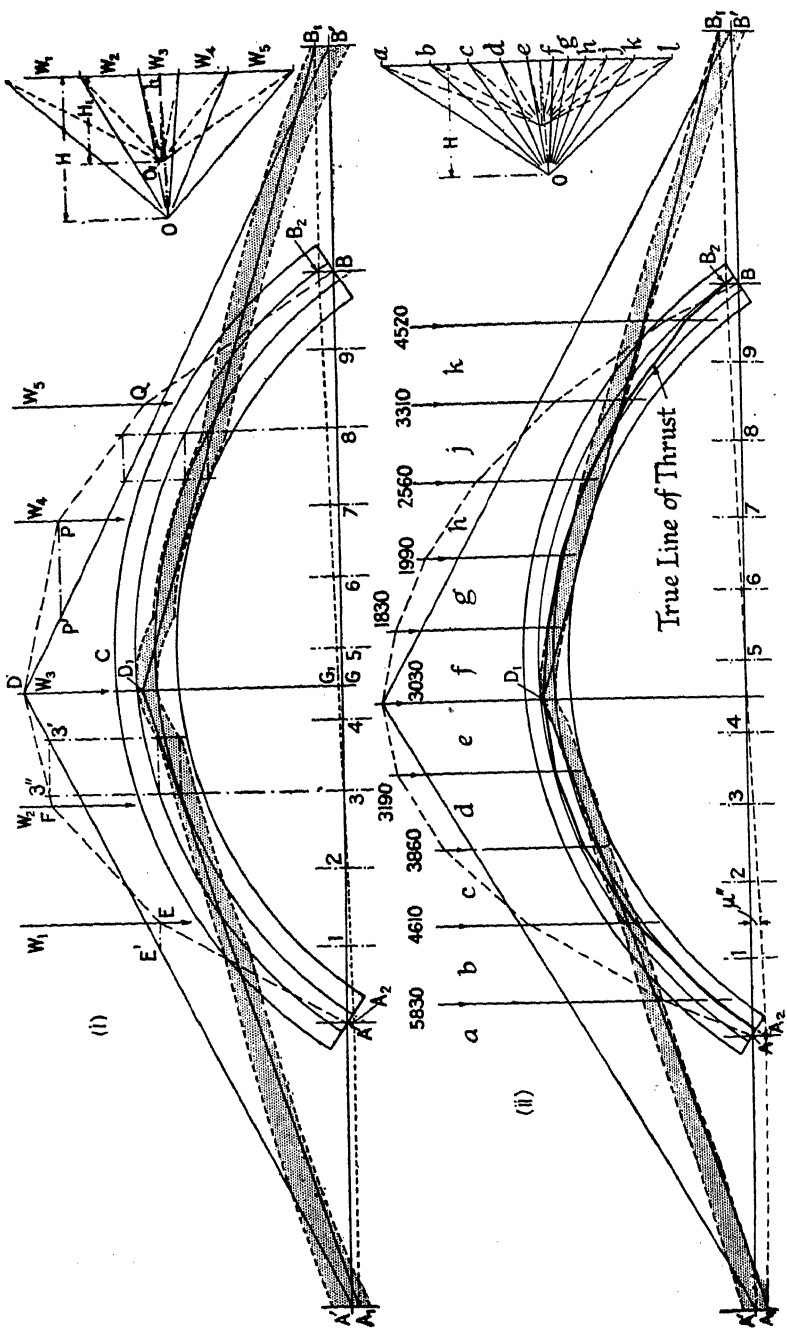
FIG. 483.

the given system of loads. If it be not·possible to draw such a line of thrust, or if the safe stress be exceeded, the thickness of the arch must be increased.

To demonstrate that the safe compressive stress has not been exceeded, the stresses in the material must be found by eq. (3), § 354. The thrust F at any section is represented to the force scale by the ray in the force polygon parallel to the line of thrust at the section. Its point of application is the point at which the line of thrust cuts the section, so that both F and e in the equation are known. From the dimensions of the arch, the maximum stress can be at once calculated.

(ii) Fig. 483 is an application of the method to the brick arch of Figs. 500 and 482. It is assumed that the left-hand half of the arch carries a live load of 400 lb./sq. ft. of area of roadway. The load diagram for the case is given in Fig. 482, which shows the loads carried by the left-hand half of the arch, and the positions of their lines of action. The loads on the right-hand half of the arch and their lines of action are found in a similar way, but there is no live load. The middle third area in Fuller's projection, (ii) Fig. 483, is obtained exactly as in (i) Fig. 483. It is just possible to draw two intersecting straight lines $A_1D_1B_1$ within this area, and it is therefore possible to draw a line of thrust lying within the middle third of the arch, as is shown in the figure. Under this ⸗ condition of loading, therefore, the arch is stable.

To complete the examination of this arch, lines of thrust for the cases in which the arch is unloaded, and when it is fully loaded, § 358, should be drawn.

The maximum stress in the material, under the conditions of (ii) Fig. 483, can be ascertained from eq. (3), § 354,

$$f_{\text{max.}} = \frac{F}{a}\left(1 + \frac{6e}{T}\right)\sin\theta = \frac{N}{a}\left(1 + \frac{6e}{T}\right) \qquad . \quad (1)$$

since the depth of the section is now T. The left-hand reaction, which is the greater of the two, is represented by the top outside ray of the force polygon, (ii) Fig. 483, and scales 23,700 lb. $= 10\cdot6$ tons. As will be seen from the figure, this force is, practically speaking, perpendicular to the end cross-section of the arch (i.e. $\theta = 90°$, and $N = F$), and it passes through the extreme corner of the middle third area. The arch is five bricks thick, hence its thickness $T = 22\frac{1}{4}$ inches ; $e = T/6$; and $a = (22\frac{1}{4} \div 12) \times 1 = 1\cdot85$ sq. ft. Hence, from eq. (1),

$$f_{\text{max.}} = \frac{10\cdot6}{1\cdot85}\left(1 + \frac{6T}{6T}\right) = \frac{2 \times 10\cdot6}{1\cdot85} = 11\cdot5 \text{ tons/sq. ft.}$$

This is the maximum stress anywhere in the arch. The normal thrust at the cross-section through D_1, near the crown of the arch, may be obtained by drawing a ray from the pole O in the force polygon normal to that cross-section. This ray scales 13,800 lb. $= 6\cdot2$ tons, which is the value of N. The distance e of the line of action of this force from the

centre of the cross-section scales $2\frac{3}{4}$ inches, $T = 22\frac{1}{4}$ inches, and $a = 1 \cdot 85$ sq. ft., as before. Hence, from eq. (1),

$$f_{max.} = \frac{6 \cdot 2}{1 \cdot 85} \left\{ 1 + \frac{6 \times 2 \cdot 75}{22 \cdot 25} \right\} = 5 \cdot 9 \text{ tons/sq. ft.}$$

To obtain the vertical components of the reactions, a horizontal line should be drawn through the pole O in the force polygon. This line will divide the load line into two parts, proportional in length to the vertical components of the two reactions. The length of this horizontal line, measured to the force scale, is the horizontal thrust H everywhere in the arch. The double triangle AA_2B_2B is the fixing moment diagram, and its ordinate μ'' at any section, measured to the length scale, multiplied by H measured to the force scale, gives the fixing moment at that section (see § 222).

359. Experiments on Arches.—In 1895 the Oest. Ing.- u. Arch.-Verein [6] published the results of some experiments on arches of masonry, brickwork, plain and reinforced-concrete, ranging in span from $1 \cdot 35$ to 23 metres. The largest arches of masonry and brickwork, set in Portland cement mortar, had a span of 23 m. ; rise $4 \cdot 6$ m. ; thickness at springings $1 \cdot 14$ m. ; at crown $0 \cdot 6$ m. The distortions of the arches under a load covering one-half the span were carefully measured as the load increased up to the failure point, and were found to agree well with deductions from the elastic theory, as did the positions where cracks occurred in the arches. The experiments may be held, therefore, to demonstrate that the elastic theory, § 222, may be safely applied to brick, stone, and concrete arches. This conclusion has been confirmed by the work of the Special Committee on Arches of the American Society of Civil Engineers.

360. Masonry Dams.—Masonry dams are high reservoir walls, built across a valley, for the purpose of impounding water, and thus converting the valley into a reservoir. Sections of typical masonry dams are shown in Fig. 484. Dams are constructed either of rubble concrete, often faced with rubble masonry, or they may be constructed entirely of rubble masonry. Concrete is used in many localities owing to the higher cost of masonry ; but in such dams, due to temperature stresses and shrinkage, cracks may occur, and the water penetrate into the interior, with in some cases a damaging effect on the concrete. Various remedies have been tried. ' Plums ' reduce the internal temperature rise, expansion joints are fitted at intervals, cooling pipes have been used. In some cases a special ' low-heat ' cement has been employed. A rich Portland cement concrete reinforced facing tends to prevent percolation.[39]

If the dam is straight in plan, so that the weight of the structure forms the real resistance to overturning due to water pressure, the dam is called a *gravity dam*. If the dam is curved in plan, and so constructed that it forms an arch resisting the water pressure, it is called an *arched dam*, § 366. The cross-section of an arched dam may be made much lighter than that of a gravity dam, Fig. 499, but the sides of the valley must form reliable abutments for the arch. The stresses set up in an arched dam

Squared Rubble Facing

Rubble Granite in 1:4 Cement Mortar

W.L.

Assuan Dam

Masonry in 1:2 Mortar

Vyrnwy Dam

W.L.

144'

Rubble Concrete

W.L.

10 0 50 100 Feet

Arch

W.L.

Ashlar Facing

Villar Dam.

W.L.

158'

Rubble Masonry.

151'

210'

Croton Dam

Re-filling

Rubble Masonry

185'
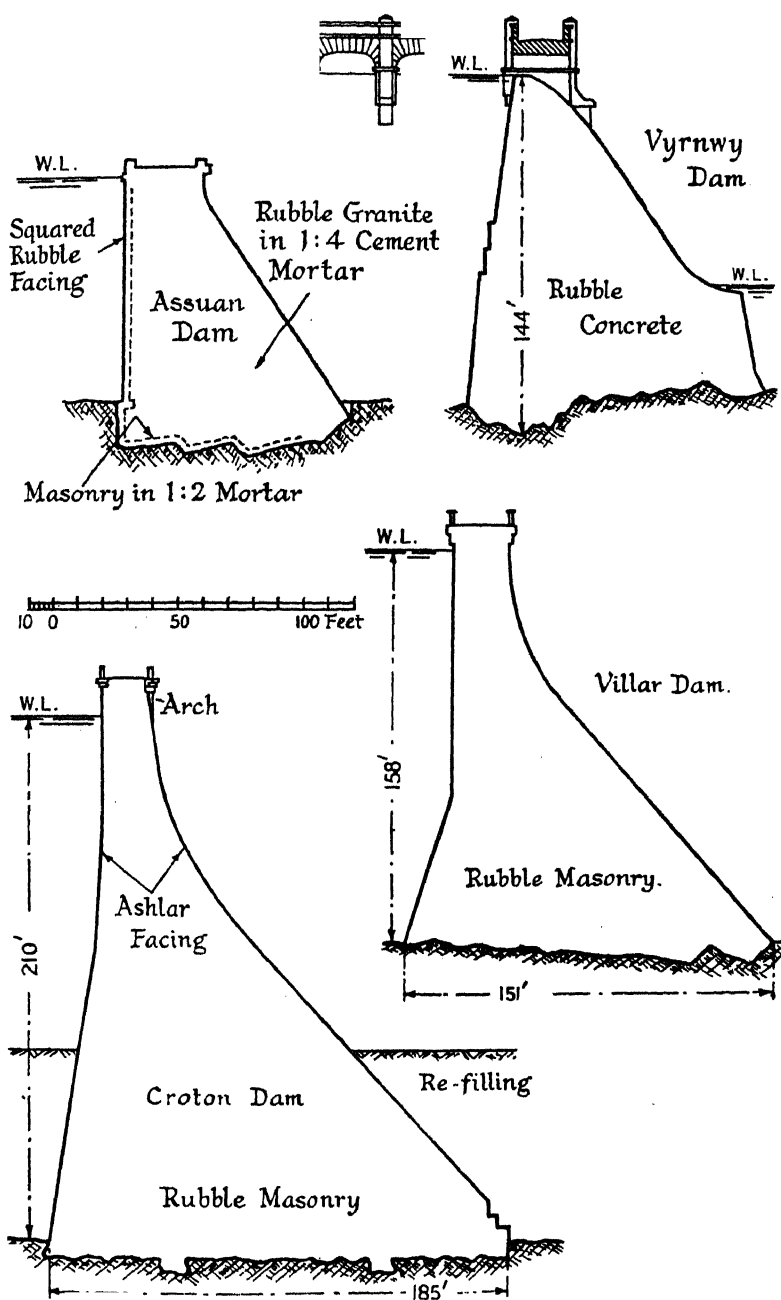
FIG. 484.

are less determinate than those in a gravity dam, and the effects of temperature and shrinkage are more important. A number of experimental investigations have been made to discover the exact behaviour of such structures when under load (see § 366). Some remarkable arched dams have been constructed in America and Australia, showing very considerable economy in material over the gravity type.

Constant Angle Dams.—Jorgensen [47] has pointed out that considerable economy is effected if the angle 2ϕ, Fig. 497, which the arch subtends at its centre, is kept constant and made equal to 133°, or for practical purposes, equal to 120°. As, owing to the shape of the valley, the dam will be wider at the top than at the bottom, this means decreasing the radius of curvature of the upstream face from top to bottom in proportion to the span. The dam is built as a series of arched rings with varying radii of curvature, the back of the dam being stepped to suit.

Multiple-arched Dams.—When suitable foundations exist, dams are sometimes made in the form of a series of arches supported on inter-
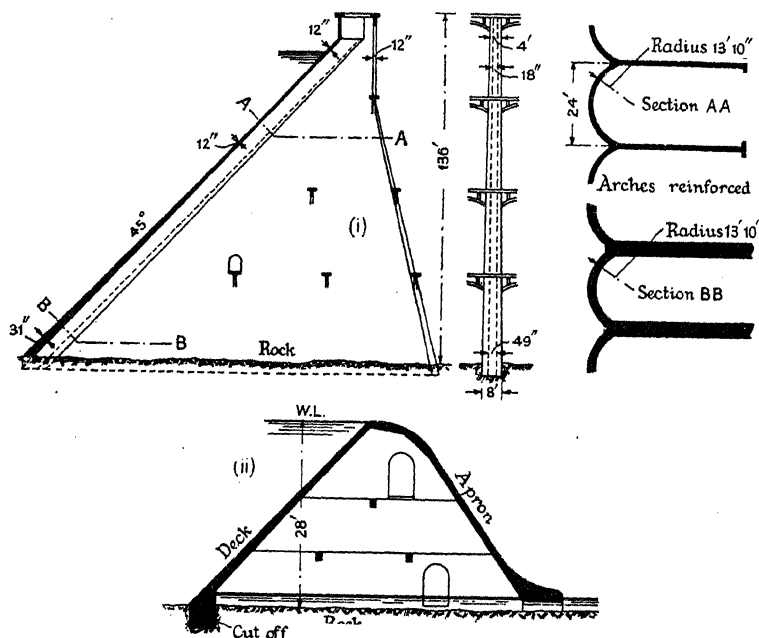
FIG. 485.

mediate buttresses, (i) Fig. 485. Such dams are called *multiple-arched dams.* The face of the dam may be vertical or inclined. A dam of this type would be constructed of concrete, and, although containing much less material than a gravity dam, is more expensive per cubic yard to build, owing to the necessity of form work during construction. Carried out in reinforced-concrete, the arches might be replaced by a series of flat slabs, usually inclined, (ii) Fig. 485, supported by the buttresses.

In another type of dam, the multiple arches are replaced by a series of egg-shaped domes, of which a horizontal section appears as a series of arches. This is called a *multiple-dome dam*.

When the water is required to flow over the top of a dam, or of part thereof, the top and back of the dam are curved, so as to permit a smooth flow for the water and to eliminate scouring at the toe as far as possible. Such a construction is called a *spillway* (see the Vyrnwy Dam, Fig. 484).

The foundations of masonry dams are carried down to the solid rock. This sometimes involves considerable excavation and removal of disintegrated rock. Having reached a good foundation, all rubbish and debris are cleared away, and any springs which may exist are stopped. The work of building then commences.

361. Stability of Gravity Dam.—The criteria for the stability of a masonry dam are : (i), that the compressive stress in the material on horizontal planes must nowhere exceed the allowed limit, which is usually about 8 to 10 tons/sq. ft. for ordinary rubble concrete or rubble masonry (in certain American dams this figure has been much exceeded *); and (ii), that the line of resistance of the dam, both when the reservoir is full and when it is empty, must lie within the middle third of every horizontal cross-section, Fig. 491. This stipulation is of importance in masonry dams, in order to avoid cracks in the upstream face, which would allow the water to penetrate the interior. Knowing the direction of the line of resistance, and the magnitude of the thrust, the maximum compressive stress in the material can be determined. These criteria are admittedly conventional, but suffice for the safety of the dam (see § 364).

362. Shape of Cross-Section. —The shape of the cross-section theoretically necessary for a gravity dam is a triangle, EVT, Fig. 486. Consider any horizontal section AB, (i), of this dam when the reservoir is empty. Let G be the centre of gravity, and W the weight of the portion EAB ; JK is the middle third of AB. Then, from the geometry of the figure, G lies in
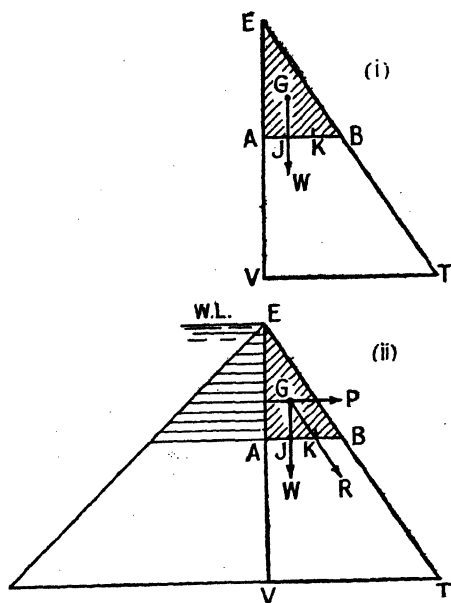
FIG. 486.

* In the Hetch-Hetchy Dam of 1 : 3 : 6 plum concrete, the stress when the reservoir was empty was 25 tons/sq. ft., and 16 tons/sq. ft. when full. In the Australian arched dams, a stress of 20 tons/sq. ft. was allowed on granite masonry, and 10 tons/sq. ft. on soft sandstone masonry.

the vertical through J. This is equally true for every other horizontal section, and it follows that, in a triangular dam, when the reservoir is empty, the line of resistance will always lie just within the middle third, and that the stress on the back ET will be zero. Next consider the section AB when the reservoir is full up to the level of the point E, (ii). Take the length of the dam as unity. Then the resultant water pressure on the area EA will be $P = \frac{1}{2}w\mathrm{EA}^2$, where w is the weight per cubic foot of the water. The weight of the triangle EAB is $W = \frac{1}{2}w_1\mathrm{EA}$. AB, where w_1 is the weight per cubic foot of the masonry. The force P will act through a point one-third of EA up from A, and the weight W will act through G and J as in (i). In this particular case, therefore, both forces will act through G. Suppose that R, the resultant of P and W, just passes through K ; JK as before is the middle third. Then GJK is the triangle of forces for the point G, and

$$\frac{P}{W} = \frac{JK}{GJ} = \frac{AB}{EA}.$$

Inserting the values of P and W,

$$\frac{P}{W} = \frac{AB}{EA} = \frac{\frac{1}{2}w\mathrm{EA}^2}{\frac{1}{2}w_1\mathrm{EA} . AB}$$

whence,

$$\frac{AB^2}{EA^2} = \frac{w}{w_1} ; \quad \text{or,} \quad \frac{AB}{EA} = \frac{VT}{EV} = \sqrt{\frac{w}{w_1}}.$$

But if R passes through K, the line of resistance when the reservoir is full lies just within the middle third at the section AB, and AB is any section. Therefore, if $VT = EV . \sqrt{w/w_1}$, the line of resistance will lie everywhere within the middle third, and a dam of these proportions would be stable provided that the material of which it is constructed has sufficient crushing resistance. Taking $w = 62\cdot4$ lb./cub. ft., and w_1 for rubble concrete at 160 lb./cub. ft. (S.G. $= w_1/w = 2\cdot57$), $VT = \frac{5}{8}EV$.

This theoretical section for the dam would not be suitable in practice. It would be undesirable to reduce the thickness of the masonry to an edge. The dam must be carried up a few feet above the highest water level, and for convenience it is usual to make a roadway over the top, Fig. 484. The top of the dam will therefore be shaped as shown in Fig. 487, and there will be an additional weight of masonry W', acting at G', the centre of area of the hatched portion at the top, to be taken into account. Considering the horizontal section AB when the reservoir is empty, it is evident that since the line of action of W' falls to the right of G, the resultant of W and W' will pass to the right of J, and will be well within the middle third. At this section the additional weight improves the conditions. At a section such as A_2B_2 the reverse is the case, for W_2, the weight of the triangular portion above UB_2, will act through J_2 as before, but the line of action of W' will pass to the left of J_2, and the

resultant of W_2 and W' will pass outside the middle third. To remedy this it is necessary to extend the face of the dam to V', and thus widen the middle third. At the section A_1B_1, where the line of action of W' cuts the boundary of the middle third of the triangular dam, W_1 and W' will fall in line. This is the limiting cross-section ; above it, W' improves the conditions ; below it, W' makes them worse. The additional width on the face of the dam must therefore extend at least as high as A_1B_1, or preferably a little higher. The distance VV' can be found by trial. The effect of W' on the conditions when the reservoir is full is evidently to improve them.
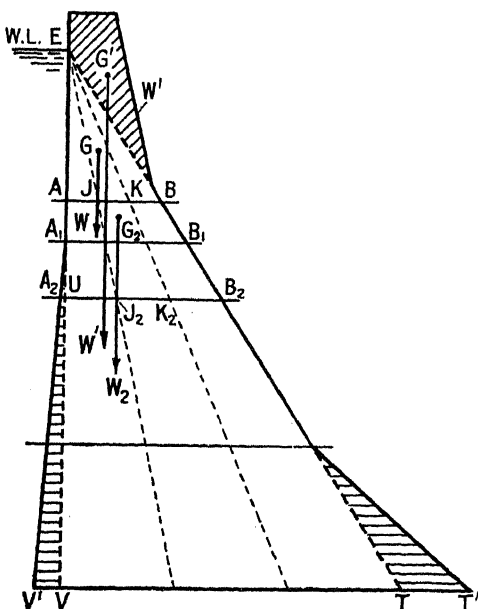
FIG. 487.

As the height of a dam such as is shown in Fig. 487 is increased, the maximum compressive stress on the base also increases, and at a certain height, above 100 to 120 ft., the maximum compressive stress will exceed the allowed limit. If it be desired to increase the height of the dam still further, it is necessary to add material to the toe of the dam as shown at TT' in Fig. 487.

Some of the earliest investigations regarding the correct shape for a masonry dam were made by Sazilly, Graeff, Delocre, and Bouvier (see Bibliography), who applied the trapezium law (i.e. the straight line distribution of stress, Fig. 477) to the problem. Molesworth has given formulae from which a cross-section can be set out which corresponds very closely with Bouvier's proposed cross-section. In Fig. 488, if ρ be the

FIG. 488.

specific gravity of the material of which the dam is composed, and f_c the permissible stress on any horizontal cross-section in tons per sq. ft.,
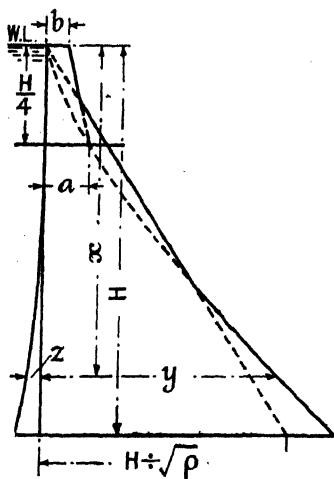
then
$$y = \sqrt{\frac{0.05\,x^3}{f_c + (0.03x)}}\;;\; z = \left(\frac{0.09x}{f_c}\right)^4$$

$b = 0.4a$; minimum value for y is $x/\sqrt{\rho}$. All dimensions are in feet.

This outline may be used as a first proposal for the shape of a dam.

In ordinary circumstances, the limiting pressure on horizontal sections ranges from 8 to 10 tons/sq. ft., depending on the class of masonry ; and the weight of the material ranges from 140 to 170 lb./cub. ft. ; $\rho = 2.24$ to 2.72.

363. Lines of Resistance.—Having decided on the outline of the dam, for example, Fig. 491,* the lines of resistance and the stresses on horizontal sections may be found as follows :

Reservoir Empty.—First suppose the reservoir to be empty. Divide the height of the dam into a number of parallel slices by horizontal planes 1.1, 2.2, 3.3, . . . (i) Fig. 489. Given w_1, the weight per cub. ft. of the masonry, find $W_1, W_2, W_3, \ldots$, the weight of each slice, on the assumption that the dam is of unit length perpendicular to the paper. Find also $G_1, G_2, G_3, \ldots$, the centres of gravity of each slice. The graphical method usually employed for this purpose is shown at (ii) Fig. 489. G lies on the line joining C_1 and C_2 at a distance up, measured vertically, of $d = \dfrac{c}{3} \cdot \dfrac{2a + b}{a + b}$ Then $W_1, W_2,$ $W_3, \ldots$ act at the points $G_1,$ $G_2, G_3, \ldots$ respectively. Consider section 1.1, (i) Fig. 489. The only

Fig. 489.

force acting on it is W_1, of which the line of action passes through G_1 and cuts 1.1 at Q_1. The thrust on the section 1.1 is therefore W_1, and its point of application is Q_1 ; Q_1 is a point on the line of thrust. Consider next the section 2.2. The force acting on it is the resultant of the two weights W_1 and W_2. Suppose the line of action of this resultant to cut the section 2.2 at Q_2. Then the thrust on section 2.2 is $(W_1 + W_2)$, its point of application is Q_2, and Q_2 is a point on the line of resistance. If x_1 and x_2 be the distances of G_1 and G_2 from the vertical through L, and x'' be the distance of Q_2 from the same line, then
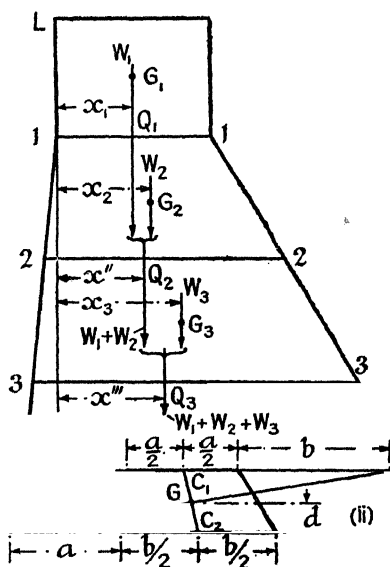
$$W_1 x_1 + W_2 x_2 = (W_1 + W_2)x'',\ \text{and}\ x'' = \frac{W_1 x_1 + W_2 x_2}{W_1 + W_2}.$$

* This outline is taken from the Periyar dam.[17]

In a similar way, the thrust on the plane 3.3 is $W_1 + W_2 + W_3$, and its point of application is Q_3 distant x''' from the vertical through L, where

$$x''' = \frac{W_1 x_1 + W_2 x_2 + W_3 x_3}{W_1 + W_2 + W_3}$$

Q_3 is a point on the line of thrust; and generally, for any other section, the distance from the same vertical of the point Q, which is the intersection of the line of resistance with that section, is

$$x^n = \frac{W_1 x_1 + W_2 x_2 + \ldots W_n x_n}{W_1 + W_2 + \ldots W_n} = \frac{\Sigma W x}{\Sigma W}$$

The line joining the points $Q_1, Q_2, \ldots$ is the line of resistance when the reservoir is empty.

Reservoir Full.—To draw the line of resistance when the reservoir is full, the forces $P_1, P_2, P_3, \ldots$ representing the water pressure on the
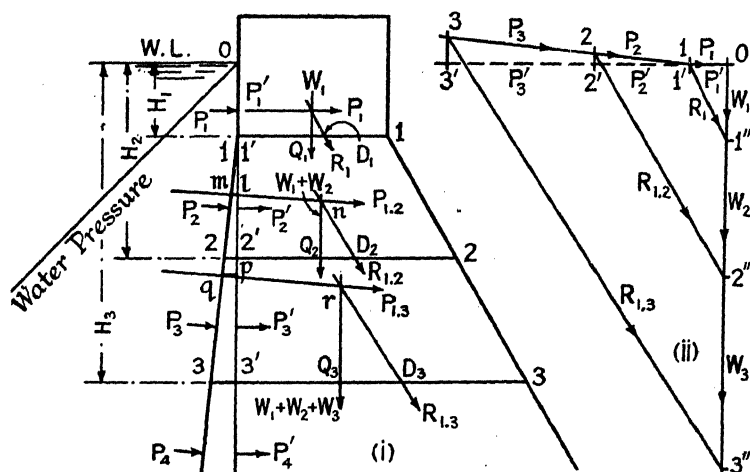
FIG. 490.

upstream face, must first be found. The magnitudes of these forces may be calculated from the mean depths of water on the face areas 0.1, 1.2, 2.3, ... (i) Fig. 490, but it is simpler to calculate their horizontal components $P_1', P_2', P_3', \ldots$, which may be determined by assuming the water to act on the vertical areas 0.1', 1'.2', 2'.3', ... Thus

$$P_1' = \frac{wH_1}{2} \times (\text{length } 0.1') \; ; \quad P_2' = \frac{w(H_1 + H_2)}{2} \times (\text{length } 1'.2') \; ;$$

$$P_3' = \frac{w(H_2 + H_3)}{2} \times (\text{length } 2'.3').$$

w denotes the weight per cub. ft. of the water; the dimensions are in feet. Set off these forces along the horizontal line 0, 1', 2', 3', ... (ii) Fig. 490, and draw the line 1, 2, 3, ... at right angles to the face of the dam. Then 0.1 represents the force P_1, 1.2 the force P_2, 2.3 the force

P_3, and so on. Along the vertical 0, 1″, 2″, 3″, ... set off $0.1″ = W_1$, $1″.2″ = W_2$, $2″.3″ = W_3$ ... These weights have already been calculated. Join 1.1″, 2.2″, 3.3″, ... as shown in the figure. Transfer the points Q_1, Q_2, Q_3, ... from (i) Fig. 489 to (i) Fig. 490.

On the top slice of the dam, two forces, W_1 and P_1, act. The resultant of these is represented by the diagonal 1.1″, (ii) Fig. 490. The line of action of W_1 is the vertical through Q_1, (i) Fig. 490 (see Fig. 489); the
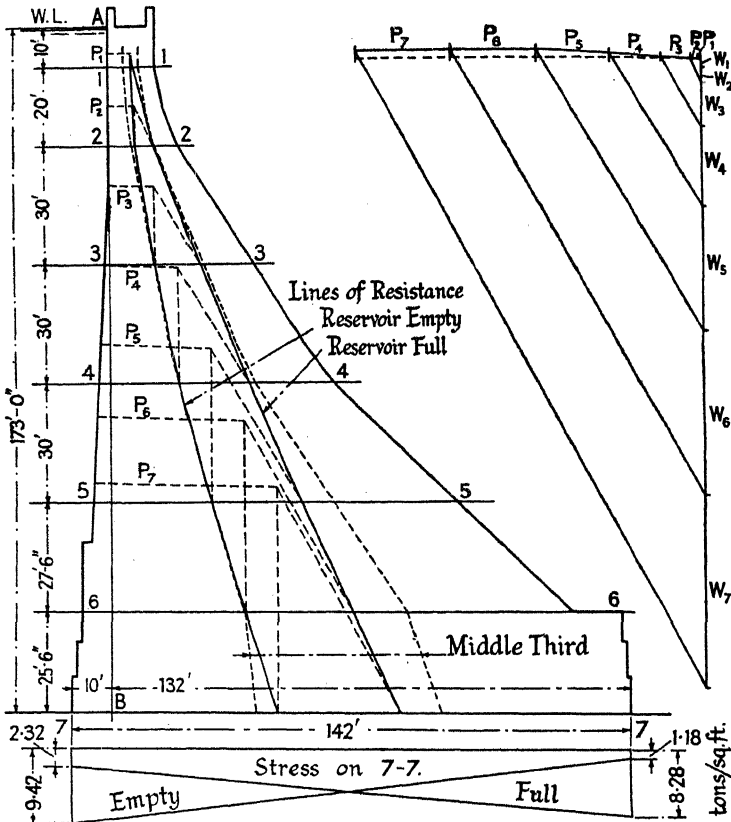
FIG. 491.

line of action of P_1 acts at a point two-thirds of 0.1 down from 0. The resultant R_1 will pass through the intersection of W_1 and P_1 and is parallel to 1.1″ in (ii). Since R_1 is the resultant of the only two forces which act above the section 1.1, R_1 is evidently the thrust on that section, and D_1, its point of application, is a point on the line of resistance. Above the section 2.2, four forces act : W_1 and W_2, the weights of the two top slices; P_1 and P_2 the water pressures on the areas 0.1 and 1.2. In (ii) Fig. 490, 0.2″ represents $(W_1 + W_2)$. A line joining 2.0 (not shown) represents $P_{1.2}$, the resultant of P_1 and P_2. The line 2.2″ represents $R_{1.2}$,

the resultant of all four forces. The line of application of $(W_1 + W_2)$ is the vertical through Q_2 already found (see Fig. 489). Since the batter on the upstream face of a masonry dam is very small, the force $P_{1.2}$ may be assumed to act at a point on the face two-thirds the way down from 0 to 2. Strictly speaking, its line of action should be obtained by taking moments of the forces P_1 and P_2 about 0, but this is an unnecessary refinement. Make $l.2' = \frac{1}{3}$ of $0.2'$, draw the horizontal lm; then m may be taken as the point of application of $P_{1.2}$ which will act parallel to the line 2.0 in (ii). Produce the line of action of $P_{1.2}$ to cut the vertical through Q_2 in n. Then $R_{1.2}$, drawn parallel to $2.2''$, will act through n. Since $R_{1.2}$ is the resultant of all the forces above the section 2.2, it is the thrust on that section, and D_2, its point of application, is a point on the line of resistance. Above the section 3.3, six forces act : $W_1 + W_2 + W_3$ acting along the vertical through Q_3 is the resultant of the three weights W_1, W_2, and W_3. The resultant $P_{1.3}$, represented by 0.3 (not shown) in (ii), is the resultant of the three water-pressure forces P_1, P_2, and P_3. This resultant may be taken as acting at a point on the face two-thirds the way down from 0 to 3. Make $p.3' = \frac{1}{3}$ of $0.3'$, draw the horizontal pq; then $P_{1.3}$ acts through q, is parallel to 3.0 in (ii), and intersects the vertical through Q_3 in r. $R_{1.3}$ in (ii) represents the resultant of all six forces. It acts through r in (i), and its point of application D_3 is a point on the line of resistance. A line drawn through D_1, D_2, D_3, . . . is the line of resistance for the dam when the reservoir is full. It is to be understood that Figs. 489 and 490 are much distorted to make the construction clearer.

The calculations for the Periyar dam are given in tabular form below. The weight of the material (concrete with rubble masonry facings) is taken at 145 lb./cub. ft. The lines of resistance are shown in Fig. 491. These lie within the middle third, showing that the dam is stable both when the reservoir is empty and when it is full.

RESERVOIR EMPTY.

Section	Weight of Slice = W.	ΣW	x	Wx	ΣWx	$x^n = \dfrac{\Sigma Wx}{\Sigma W}$
	Tons.	Tons.	Feet.	Ft.-tons.	Ft.-tons.	Feet.
0.0						
	$W_1 = 9\cdot1$		$6\cdot0$	$54\cdot6$		
1.1		$9\cdot1$			$54\cdot6$	$6\cdot0$
	$W_2 = 18\cdot8$		$7\cdot5$	$141\cdot0$		
2.2		$27\cdot9$			$195\cdot6$	$7\cdot0$
	$W_3 = 53\cdot9$		$14\cdot0$	$754\cdot6$		
3.3		$81\cdot8$			$950\cdot2$	$11\cdot6$
	$W_4 = 95\cdot0$		$22\cdot8$	$2{,}166$		
4.4		$176\cdot8$			$3{,}116$	$17\cdot6$
	$W_5 = 149\cdot2$		$35\cdot5$	$5{,}297$		
5.5		$326\cdot0$			$8{,}413$	$25\cdot8$
	$W_6 = 195\cdot6$		$48\cdot7$	$9{,}525$		
6.6		$521\cdot6$			$17{,}938$	$34\cdot4$
	$W_7 = 231\cdot0$		$61\cdot0$	$14{,}091$		
7.7		$752\cdot6$			$32{,}029$	$42\cdot6$

RESERVOIR FULL.

Section.	Height of Slice.	H	Water Pressure.	ΣP	Point of Application.*
	Feet.	Feet.	Tons.	Tons.	Feet.
0.0		0			
	10		$P_1' = 1·4$	1·4	166·3
1.1		10			
	20		$P_2' = 11·1$	12·5	153·0
2.2		30			
	30		$P_3' = 37·5$	50·0	133·0
3.3		60			
	30		$P_4' = 62·5$	112·5	113·0
4.4		90			
	30		$P_5' = 87·5$	200·0	93·0
5.5		120			
	27·5		$P_6' = 102·2$	302·2	74·7
6.6		147·5			
	25·5		$P_7' = 113·5$	415·7	57·7
7.7		173·0			

The stresses on horizontal planes can be determined from eqs. (3) and (4), § 354.

$$f_{\text{max.}} = \frac{N}{a}\left\{1 + \frac{6e}{D}\right\} ; \ f_{\text{min.}} = \frac{N}{a}\left\{1 - \frac{6e}{D}\right\}.$$

Considering section 7.7 at the base of the dam, when the reservoir is empty, the line of resistance intersects that section at a point 18·4 ft. to the left of the centre, i.e. $e = 18·4$. The weight of the dam on this section is 752·6 tons, which evidently is the value of N, the normal component of the thrust. The width of the dam at this section is $D = 142$ ft. ; hence, from the above equations,

$$f_{\text{max.}} = \frac{752·6}{142}\left\{1 + \frac{6 \times 18·4}{142}\right\} = 9·42 \text{ tons/sq. ft.}$$

$$f_{\text{min.}} = \frac{752·6}{142}\left\{1 \hspace{3cm} 1·18 \text{ tons/sq. ft.}\right.$$

The distribution of stress is shown at the bottom of Fig. 491.

When the reservoir is full, the line of resistance cuts section 7.7 at a point 13·3 ft. to the right of the centre. Hence $e = 13·3$ ft., the other factors remaining as before. The stresses are

$$f_{\text{max.}} = \frac{752·6}{142}\left\{1 + \frac{6 \times 13·3}{142}\right\} = 8·28 \text{ tons/sq. ft.}$$

$$f_{\text{min.}} = \frac{752·6}{142}\left\{1 - \frac{6 \times 13·3}{142}\right\} = 2·32 \text{ tons/sq. ft.}$$

This distribution of stress is shown in Fig. 491.

The stresses on other horizontal sections can be found in a similar way.

364. ·Experimental Determination of the Stresses.—The simple theory for the stresses in masonry dams, on which the methods of § 363 are based, is admittedly only approximate. That the distribution of normal stress follows a straight-line law is an assumption, and the effects of the shearing stresses are not taken into account. In 1904 Atcherley and Pearson published a memoir [27] on the stresses in dams in which the conventional methods of design were criticised, and in which it was suggested that the critical sections of a dam are not the horizontal sections, but the vertical sections near the outer toe, and that failure would occur due to tension on these sections. Further, it was suggested that the shear on the horizontal sections was an important consideration.

These conclusions led to a number of investigations, experimental and otherwise, of the stresses in dams. From experiments on a model dam made of gelatine, Sir Benjamin Baker inferred that the stresses at the base would be greatly influenced by the behaviour of the rock foundation on which the dam was built, and that the shear stress on the base was approximately uniformly distributed.

Ottley and Brightmore,[32] from a consideration of deformation measurements on a model dam of plasticine, confirm Baker's opinion that the shear stress on the base of the dam is approximately uniformly distributed; but conclude that on horizontal planes at higher levels, the intensity of shear stress varies very nearly uniformly from zero at the inner face to a maximum at the outer face. There is a gradual change from the one distribution to the other.
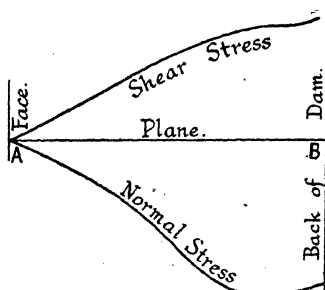
FIG. 492.

They also conclude that it is near the inner toe, not the outer, where tension in the dam and its rock foundation may be expected. Fig. 492 shows the distribution of normal and shearing stresses on a plane AB, sufficiently high above the base of the dam for the effect of the foundations to be negligible, as determined from the model dam, which was of triangular cross-section, the width at the base being equal to the height divided by the square root of the specific gravity of the material (see § 362). The distribution of stress on the base proper is different, because the mass of the rock foundation cannot deform (i.e. be displaced in a horizontal direction) to the same extent as would the dam proper, and this prevents the base of the dam from so deforming. As a result, tensions are set up on the vertical planes near the inner toe, both in the dam and in the rock, which tensions modify the distribution of shear stress, making it much more nearly uniform.

Wilson and Gore [33] experimented on model dams of india-rubber, loaded so as to reproduce the effects of gravity and the water pressure. The models represented dams resisting a head of water of 125 ft., designed according to the middle third rule. Two profiles were used; C, Fig. 493,

with sharp corners where it joins the foundations, and B, in which the

corners were well rounded. The strains in the rubber were ascertained, and from these the stresses were calculated. (i) Fig. 493 represents the distribution of vertical pressure on horizontal planes, thus found, in profile C; and (ii) the distribution of shear stress on the same planes. The foundation of the dam is supposed to be supported all round, as indicated by the shading.

Fig. 494 shows the ellipses of stress for the same conditions, indicating the directions of the major and minor principal stresses in the dam, and their relative magnitudes.

Some of the authors' conclusions are as follows : tensile stresses exist at the inner toe in all cases. In profile C these stresses act parallel to the faces of both foundation and dam, and are nearly of equal intensity (see the ellipses of stress in (ii) Fig. 494). These were the maximum tensile stresses in profile C. The stresses at the outer toe are compressive in all directions. In profile C these stresses act parallel to the faces of both dam and foundation, (iii) Fig. 494. They are nearly of equal intensity, and are the maximum compressive stresses in profile C. They considerably exceed the stresses assumed in the design. Rounding the corners, as in profile B, considerably reduces the stresses near the toes. Near the downstream
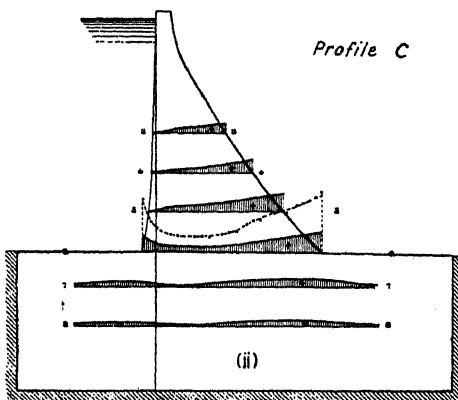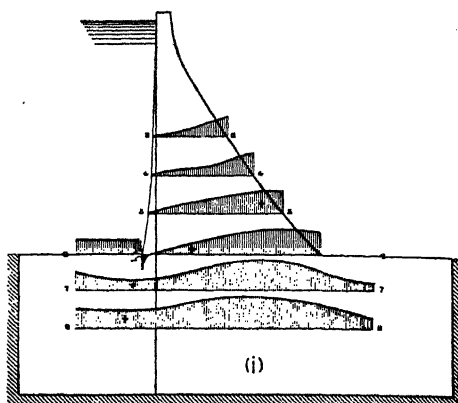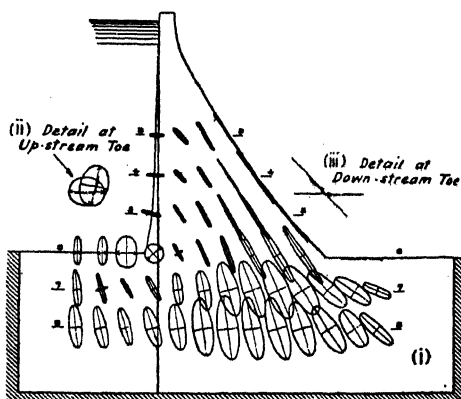
Profile C

FIG. 493.

FIG. 494.

face, (i) Fig. 494, the major axes of the ellipses of stress are tangential to the profile, showing that the maximum principal stresses near this face act on planes normal thereto. Near the upstream face, the major axes are normal to the profile, showing that the maximum principal stresses occur on planes parallel to this face. The maximum intensity of shear stress at each face occurs on planes at 45° to the face.

On sections above the base line 6.6 the distribution of vertical pressure on horizontal planes, (i) Fig. 493, while not unlike that found by the trapezium law (i.e. the ordinary straight line variation of stress), usually reaches a maximum near the line of resistance, and is lower towards the faces. This maximum never exceeds that calculated by the trapezium rule. Tension on the horizontal planes at the inner toe was observed in each case, and was of considerable magnitude in profile C. The maximum horizontal pressure on vertical planes occurs at the outer toe. Tension on these planes was observed at the inner toe. The distribution of shear stress on the upper horizontal sections is, roughly speaking, triangular, (ii) Fig. 493, but the junction of the dam with its foundation greatly affects the distribution of shear stress there.

Except near the foundations, the experiments do not indicate the existence of stresses which would imply weakness in dams of the usual type ; and it appears that the ordinary method of design may with safety be used to determine the strength and stability of such dams. This opinion is generally accepted, and provided that the lines of resistance lie within the middle third, and that the stresses on horizontal planes do not exceed the usually allowed limits, the dam may be regarded as safe, despite the possibility of tension near the inner toe, which in practice has not hitherto given cause for anxiety.

365. Uplift.—In all the preceding work it has been assumed that the dam is perfectly watertight. The necessity for avoiding cracks on the upstream face has been emphasised. If the dam be designed in the manner indicated, and properly constructed on an impervious foundation, no water should penetrate the interior. Even if, due to bad workmanship, a hole be left in the face of the dam, the stability of the dam will not be impaired so long as the tensile strength of the cement be not overcome. If the cement should crack, the water pressure,
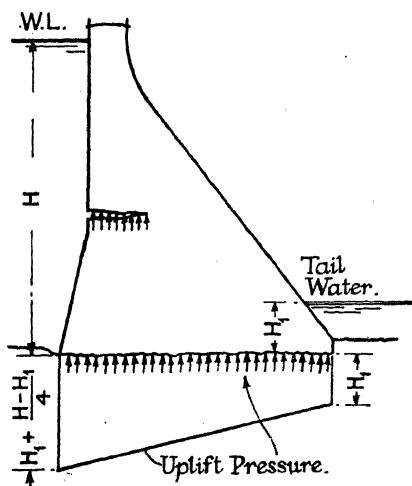
FIG. 495.

acting on the bottom of the portion above the crack, would help to overturn it, Fig. 495. A similar tendency will exist if the rock foundation

be not impervious to water, for then the water pressure, acting on the base of the dam, produces an overturning moment. This action is spoken of as *uplift*. With permeable foundations, it is usual to make allowance for uplift in the calculations. An assumption sometimes made is that the uplift pressure varies from full reservoir head at the inner toe to full tail-water head at the outer toe, but only acts on one-third the length of the base. From some uplift measurements made by the U.S. Bureau of Reclamation [43] it would appear that for the portion of the Wellwood dam founded on shale there was no uplift. For the portion founded on sandstone, the uplift pressure varied roughly as a straight line from full tail-water head at the outer toe, to full tail-water head plus onequarter the difference between the reservoir and tail-water heads at the inner toe, Fig. 495. Corresponding measurements at the American Falls dam showed a similar variation in head, but the uplift pressures were slightly higher. For a semi-graphical method of estimating uplift pressures, see Shulits.[45]
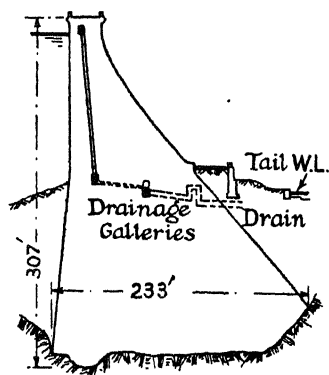
FIG. 496.

In certain large masonry dams, drains are provided inside the dam to relieve any interior pressure due to penetration of water, Fig. 496.

366. Arched Dams.—In an arched dam, § 360, the water pressure will be carried partly by arch action and partly by the cantilever action of the dam, Fig. 499. Except, perhaps, near the base of the dam, no great error is introduced by assuming that horizontal slices of the dam act as circular arches spanning between the sides of the valley, and subjected to radial water pressure, Fig. 497. Professor Cain[48] has given an analysis for such arches, the results of which are as follows: If p_1 be the water pressure lb./sq. ft., and R_1 the radius in ft. at the extrados; R the mean radius; T the uniform thickness in ft.; and N_0 the normal thrust at the crown in lb.; then, for a rectangular slice 1 ft. in depth,
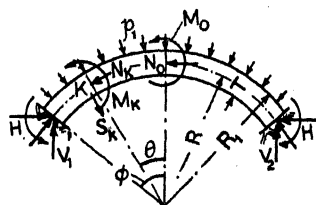
FIG. 497.

$$(p_1 R_1 - N_0) \frac{2\phi \sin \epsilon}{\chi} \cdot \frac{p_1 R_1 T^2}{12 R^3} \tag{1}$$

where

$$\chi = \left(1 + \frac{T^2}{12 R^2}\right) \phi \left(\phi + \frac{\sin 2\phi}{2}\right) - 2 \sin^2 \phi + 2 \cdot 88 \frac{T^2}{12 R^2} \phi \left(\phi - \frac{\sin 2\phi}{2}\right) \tag{2}$$

If M_K be the bending moment in ft./lb., and N_K = the normal thrust in lb. at any point K $(R . \theta)$, Fig. 497,

$$M_K = (p_1 R_1 - N_0) \left(\frac{\sin \phi}{\phi} - \cos \theta \right) R \quad . \tag{3}$$

$$N_1 \quad p_1 R_1 - (p_1 R_1 - N_0) \cos \theta \quad . \tag{4}$$

Extreme fibre stresses $= \dfrac{N}{T} \pm \dfrac{6M}{T^2}$ . . . . . (5)

For a temperature rise of $t° $ F. $(\alpha = 0 \cdot 0000055$ for concrete),

$$H_t = \frac{2 \sin \phi}{\chi} \cdot \frac{EI\alpha t}{R^2} \quad . \quad . \quad . \tag{6}$$

At crown, $\quad M_{0t} = + H_t \left(1 - \dfrac{\sin \phi}{\phi} \right)$;

at abutments, $M_{1t} = - H_t \left(\dfrac{\sin \phi}{\phi} - \cos \phi \right) R$ . . (7)

Extreme fibre stresses :

at crown, $\quad = H_t/T \pm 6M_{0t}/T^2$;

at abutments, $= H_t \cos \phi/T \pm 6M_{1t}/T^2$ . . (8)

As the dam is under water, shrinkage stresses are sometimes neglected.

Any exact method of design must of necessity take into account both arch and cantilever effects, and to gain some exact knowledge as to the
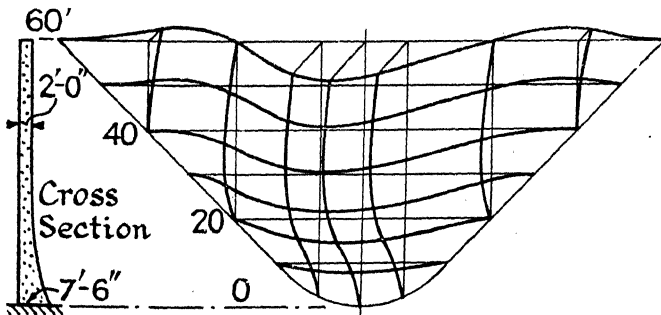
FIG. 498.

way in which such structures really react, and also as to the effects of temperature alterations, construction joints, and cracks, an experimental arch, radius 100 ft. and height 60 ft., was constructed at Stevenson Creek, California.[51] The cross-section was of the thin arch type, the radial thickness being 2 ft. from the crest to 30 ft. above the base, below which level there was a curved batter, the thickness increasing to 7 ft. 6 in. at the base. Fig. 498 shows the deflection curves under a head of 60 ft. on the developed vertical face, looking upstream. Maximum deflection = 0·388 in.

A method of analysis for arch dams, termed the *trial-load* method, has been developed by the Engineers of the U.S. Bureau of Reclamation, Denver, Colorado.[53] Starting from an assumed partition of load between the arches and cantilevers, the distribution is modified until the radial deflection of each system towards the centre of the arc is the same. Further adjustments are then made to take into account the shears and twists in the structure. From a series of such adjustments, a close approach to the true distribution of load can be obtained, giving deflections within about 3 % of the observed values.*

Fig. 499 shows the outline of the Pacoima arch dam, California, 372 ft. high (*Engineering*, January 18, 1929, p. 70), and the calculated
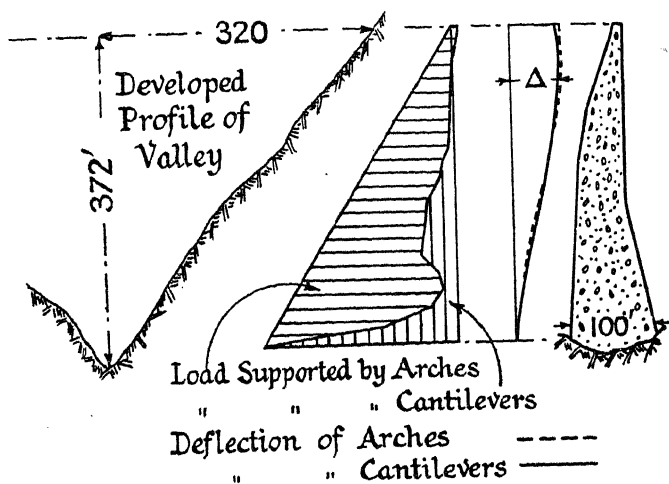
FIG. 499.

partition of load between the arches and cantilevers. The former carry most of the load. The deflection curves for arches and cantilevers show satisfactory agreement.

BRICKWORK

367. Bricks.—Ordinary bricks are made of clay of a suitable character. The clay is kneaded into a stiff paste, and then pressed into a mould. The brick, thus formed, is left to dry, and is afterwards burnt hard. The common types of bricks are *hand-made bricks*, *wire cuts*, and *pressed bricks*. Hand-made bricks are so called because the clay is pressed into the mould by hand ; they are formed with a *frog* or depression on one side. For wire cuts, the clay is kneaded in a pug mill, forced through a rectangular die, and cut up into bricks by means of a series of wires. They may be recognised by the absence of frogs. Pressed bricks are made from unburnt wire cuts. The soft brick is placed in a metal mould and then

* See *Arch Dam Investigation*, vol. ii, New York, 1935, for model tests in confirmation.

compressed. The overall sizes are thus slightly increased, and a frog is formed top and bottom of the brick. A superior brick is obtained by this process, having sharp edges and square faces. Such bricks are usually employed for facing ordinary brickwork.

A variety of makes of brick are employed in engineering work. The most common are *Staffordshire blues*, a hard, durable brick used for first-class work where great strength and resistance to wear is necessary. The outer skin is of a vitreous character, rendering the brick very impervious to moisture. *Red bricks* of good quality are used where appearance is required. *Stock bricks* (common bricks burnt in clamps) are used for interior work, and the heartings of masonry and brick constructions. Many special kinds of brick are used for particular purposes ; *glazed bricks, hollow bricks*, and *moulded bricks* where ornamental shapes are required.

The characteristics of good bricks are : strength and durability ; uniformity of shape, size and colour ; rectangular faces ; freedom from cracks and flaws ; sound and uniform texture when broken. Bricks should ring clearly when struck sharply together ; a dull sound indicates a soft or shaky brick. In an absorption test, § 277, a brick should not absorb more than 20 % of its own weight of water. In pressed bricks this value may be as low as 2 %.

368. Mortars.—The mortar used for brickwork in engineering structures should either be a cement mortar consisting of a 1 : 3 or 1 : 4 mixture (by volume) of Portland cement and sand ; or a lime mortar composed of one part by volume of lime and two parts by volume of sand. For good work in lime mortar, *blue lias* or other similar *grey stone* lime is employed. The sand should be clean and sharp. Cement mortar is used where strength is necessary ; for example, in arch rings. The crushing strength of a 1 : 3 Portland cement mortar may range from 1800 to 3800 lb./sq. in. ; and its tensile strength from 150 to 450 lb./sq. in. The crushing strength of a 1 : 2 lime mortar will be of the order of 100 lb./sq. in. ; its tensile strength is negligible.

369. Strength of Bricks and Brickwork.—The results of some experiments, taken from a *Report on Brickwork Tests* by a Committee of the R.I.B.A.[65], 1905, are as follows :

AVERAGE CRUSHING STRENGTH OF BRICKS (TONS/SQ. FT.).

Kind of Brick.	Cracked at	Crushed at
London Stocks, with frog	76·2	84·3
Burham Gaults	102·3	182·2
Leicester Red, no frog	248·1	382·1
Staffordshire Blue, wire cut, no frog	471·6	701·0
Fletton, machine pressed, with frog	—	220·8

Compressive tests on brickwork piers, 18 in. square and 6 ft. high, gave the following results. Two kinds of mortar were used : lime

mortar, one part grey stone lime, well slaked, two parts of washed river sand; cement mortar, one part Portland cement, four parts washed river sand.

STRENGTH OF BRICK PIERS (TONS/SQ. FT.).

Kind of Brick.	In lime mortar.		In cement mortar.	
	Commenced to fail.	Total Failure.	Commenced to fail.	Total Failure.
London Stocks	7·5–14·2	12·5– 18·6	9·0–27·4	17·0– 39·3
Burham Gaults	9·4–15·4	21·6– 31·1	18·7–37·2	30·0– 51·3
Leicester Red .	14·1–28·1	34·1– 45·4	23·1–62·3	50·4– 83·4
Staffordshire Blue	19·5–24·1	73·7–114·3	36·9–85·0	82·5–135·4
Fletton, pressed	24·1	30·7	43·9	56·2

The lower figure represents the strength with ordinary workmanship, the higher figure that when the workmanship was especially good.

To obtain the crushing strength of a brick, the frog is filled with a 1 : 3 cement mortar, and the brick is tested flat. The crushing strength thus obtained is very variable; differences of the order of 50 % of the mean value are common.

The crushing strength of brick piers and walls, uniformly loaded, is roughly dependent on the mean crushing strength of the bricks. Bragg [69] suggests the formula $f_P = cf_B$, where f_P is the mean crushing strength of the pier, and f_B that of an individual brick tested flat. For piers built with a 1 : 3 cement mortar, he gives the value $c = 0·27$. Beyer and Kreyfield,[69] for 12 × 12 in. piers built with a 1 : 3 Portland cement mortar, find that $c = 0·424$ for a height of 40 in. (nominal L/B, = 3·4), and $c = 0·38$ for a height of 84 in. (nominal L/B = 7). Glanville and Barnett,[73] for 18 × 18 in. brick piers, built with 1 : 3 Portland cement mortar, 8 ft. high (nominal L/B = 5·3), obtain the value $c = 0·33$. Bragg's value, $c = 0·27$, represents the lower limit of these experiments for values of $f_B < 10,000$ lb./sq. in. For higher values of f_B, due probably to the smaller relative strength of the mortar, $c = 0·2$ for the lower limit. This limit, for the whole range, may be represented by $f_P = f_B (45,000 - f_B)/155,000$ lb./sq. in. As in the case of the individual bricks, the crushing strength of brickwork is very variable, and differences of the order of 25 % are common.

The above values all have reference to first-class materials and workmanship. Stang, Parsons and McBurney [71] found that the strength of such brickwork was from 30 to 50 % greater than that of unsupervised commercial bricklaying (cf. the R.I.B.A. tests given above).

Increasing the strength of the mortar above 2000 lb./sq. in. does not much increase the strength of brickwork constructed of ordinary bricks, $f_B < 3000$. Brickwork in lime mortar is considerably weaker than that in cement mortar (cf. the R.I.B.A. tests).

The effect of the value of L/B on the strength of brickwork piers has been investigated at Watertown Arsenal,[64] by Kreuger [68] and others. The strength appears to fall rapidly from $L/B = 2$ to $L/B = 12$, and thenceforward at a much reduced rate up to about $L/B = 25$, the limit of the experiments.

The L.C.C. Code of Practice (1932) gives the following safe values for the pressure on brickwork, L/B not exceeding 6 :

Strength of Brick.*	Mortar.	Safe Pressure.
10,000 lb./sq. in.	1 : 3 cement	20 tons/sq. ft.
5,000	1 : 3 „	15
3,000	1 : 4 „	10
1,500	1 : 4 „	8
1,500	1 : 2 lime	4

* Tested after soaking until absorption is complete.

Glanville and Barnett [73] show from the lower limit of their tests that the above safe pressures imply a factor of safety of 5 for concentrically applied uniform loads ; reduced to $3\frac{1}{2}$ if the workmanship is poor.

If $L/B = 8$ use 80 % ; $L/B = 10$ use 60 % ; $L/B = 12$ use 40 % of the above safe pressures.

371. **Construction in Brickwork.**—The nominal size of burnt bricks is $8\frac{3}{4} \times 4\frac{1}{4} \times 2\frac{3}{4}$ in., so that with $\frac{1}{4}$-in. mortar joints they make up $9 \times 4\frac{1}{2} \times 3$ inches. With pressed bricks the joints are slightly thinner. There are, therefore, four courses per foot. Since all bricks are of a definite size, the dimensions of a brickwork structure must be made to correspond. Thus the thickness of a wall depends on the number of bricks in the width, and a wall is specified as a one-brick, two-brick, or three-brick wall, as the case may be. All vertical dimensions will be multiples of 3 inches, and longitudinal and lateral dimensions will be multiples of $4\frac{1}{2}$ inches.

The brick is made twice as long as it is wide to facilitate bonding. There are two common types of bond, English and Flemish. In *English bond*, as seen from the outside of the wall, each alternate course consists entirely of headers or stretchers. In *Flemish bond*, the alternate bricks in all courses are headers and stretchers. English bond is usually used for engineering work as it is considered to be somewhat stronger than Flemish, but the latter has the better appearance. The correct arrangement of each course, necessary to secure proper bonding, is illustrated in all books on Building Construction. In very thick walls, all the interior bricks are laid as headers ; it is then usual to lay the interior bricks of every sixth course diagonally, to improve the bonding. This is called a *raking* course.

372. **Typical Brickwork Structures.**—Brickwork is one of the commonest materials used in structural work, particularly in railway construction. Arches, viaducts, tunnel linings, sewers, retaining walls, bridge piers and abutments, foundations, buildings of all kinds, may all

be satisfactorily carried out in brickwork. Fig. 500 shows a typical brick arched viaduct; Fig. 501 a retaining wall constructed of brick.
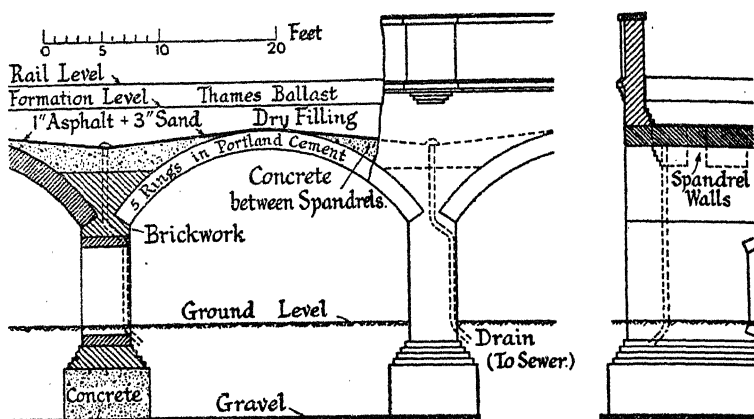
FIG. 500.

Foundations in brickwork are illustrated in Fig. 462. The method of constructing brick arches may be seen from Fig. 464. The arch is built up of superimposed rings one half-brick in thickness. The bricks are placed on edge, laid as stretchers parallel to the axis of the arch, and properly bonded. To tie the rings together, *lacing courses* are introduced. These consist of headers extending through two rings, thus forming a bond between them.

373. Calculations for Brick Structures.— The dimensions of many brickwork structures, particularly those of moderate size, are usually proportioned by empirical rules based on successful practice. In larger structures, calculations similar to those for masonry structures should be made. The criteria for stability are the same in both classes of construction, § 353. The line of thrust should be determined; it should lie within the middle third, since it is not desirable to permit tensile stresses of any magnitude in brickwork, particularly if set in lime mortar. The maximum stresses should also be ascertained. The procedure for the arch shown in Fig. 500 is given in Figs. 482 and 483. Fig. 482 is the load diagram for the arch. The line of thrust for the case in which a live load of 400 lb./sq. ft. of area of roadway covers the left-hand side of the arch
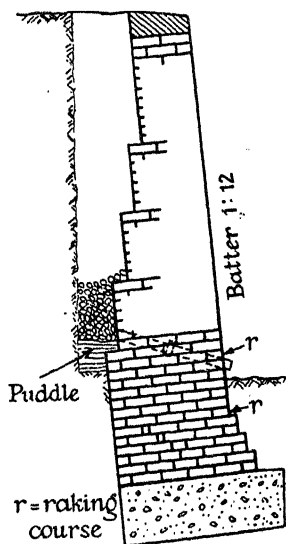
FIG. 501.

is determined in (ii) Fig. 483. This line of thrust lies wholly within the middle third of the arch. The stresses in the brickwork, both at the springings and at the crown, are determined in § 358. In each case they lie within allowable limits. To complete the investigation of the stability of the arch, the conditions when the load completely covers the arch should be similarly tested.

374. Mass Concrete.—Ordinary plain concrete is composed of materials easy to obtain ; it is simple to make, requiring no highly skilled labour ; it is easily moulded to any required shape, and when hardened is durable and not subject to corrosion. These properties have led to its extended use as a structural material, particularly in mass construction. Its resistance to tension and shear is small, and it should not be subjected to stresses of this nature of any considerable magnitude. Temperature and shrinkage stresses sometimes cause cracks and weakness, § 360.

Plain concrete is much used for foundations. A 1 : 6 mixture is
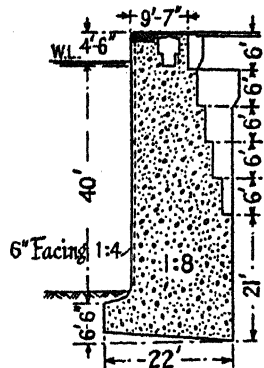
Fig. 502.
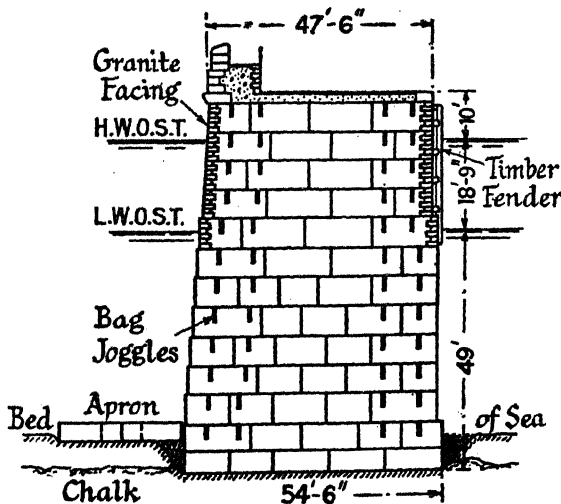
Fig. 503.

commonly employed. The concrete is laid in trenches and properly punned. The safe load on such concrete is :

1 : 6 mass concrete .	20 tons/sq. ft.
1 : 8 „ „ . .	15 „ „
1 : 12 „ „ .	5 „ „
1 : 2 : 4 concrete .	

Figs. 479 and 480 show two typical applications of plain concrete to mass constructions. Fig. 502 shows the cross-section of the quay wall used for the King George V Dock, London.* This wall was built of a 1 : 8 cement concrete faced with a 1 : 4 mixture, brought up together. Fig. 503 shows the cross-section of the breakwater for the Admiralty harbour at Dover.† In this instance the 1 : 6 concrete was pre-cast into blocks weighing from 25 to 41 tons ; which, after hardening, were lifted into place by a crane. The blocks were bonded, and further secured by joggles.

BIBLIOGRAPHY

General Treatises

1. BAKER. *A Treatise on Masonry Construction.* New York, 10th ed., 1919.
2. WILLIAMS. *The Design of Masonry Structures and Foundations.* New York, 2nd ed., 1930.
3. SPALDING, HYDE, AND ROBINSON. *Masonry Structures.* New York, 2nd ed., 1926.
4. HOOL AND KINNE. See Ref. No. 6, Chap. XVII.

Masonry Arches and Bridges

5. WINKLER. Lage der Stützlinie im Gewölbe. *Deu. Bauzeit,* 1879, p. 117 ; 1880, p. 58.
6. OEST. ING.-U. ARCH.-VER. *Gewölbe-Versuche ; Beilager ; Zeitschrift,* 1895 ; see *Engg.,* Feb. 21, 1896, p. 255.
7. TOLKMITT. *Leitfaden für das Entwerfen Gewölbter Brücken,* 1895 (formula for thickness at crown).
8. MOLITOR. See Ref. No. 16, Chap. V, Fixed Masonry Arches, p. 298.
9. ALEXANDER AND THOMSON. *The Scientific Design of Masonry Arches.* London, 1927 ; see also *Elem. App. Mech.,* chap. xiii.
10. WILLIAMS. The Philosophy of Masonry Arches. *Select. Eng. Pap.* I.C.E., No. 56, 1927.
11. AMER. SOC. C.E. See Ref. No. 57, Chap. XVII.

Masonry Dams

12. WEGMANN AND NOETZLI. *The Design and Construction of Dams.* New York, 8th ed., 1927.
13. SMITH, C. W. *Construction of Masonry Dams.* New York, 1915.
14. ZEIGLER. *Der Talsperrenbau.* Vol. ii, *Massiver Talsperren.* Berlin, 3rd ed., 1927.
15. KAMMÜLLER. *Die Theorie der Gewichtsstaumauern.* Berlin, 1929.
16. HANNA AND KENNEDY. *The Design of Dams.* New York.
17. NOTABLE DAMS :
    Furens Dam. *Ann. d. Ponts et Chaussées,* 1866, p. 184.
    Villar Dam. *Proc. Inst. C.E.,* vol. lxxi, 1882, p. 379.
    Vyrnwy Dam. *Proc. Inst. C.E.,* vol. cxxvi, 1895–6, p. 28.
    Periyar Dam. *Proc. Inst. C.E.,* vol. cxxviii, 1896–7, p. 140.
    Assuan Dam. *Proc. Inst. C.E.,* vol. clii, 1902–3, p. 87.
    Lake Cheeseman Dam. *Trans. Amer. Soc. C.E.,* vol. liii, 1904, p. 89.
    New Croton Dam. *The Engr.* Apl. 12, 1907, p. 364.
    Boulder Dam. *The Engr.,* Feb. 8, 1935, p. 154 ; *Engg.,* Jan. 1, 1936, p. 1.

* *Proc. Inst. C.E.,* vol. ccxvi, p. 374.   † *Ibid.,* vol. ccix, p. 37.

18. GRAEFF. Rapport sur la forme et de la mode de construction du barrage du Gouffre d'Enfer. *Ann. d. Ponts et Chaussées*, t. xii, 1866, p. 184 (Furens Dam).

19. DELOCRE. Mémoire sur la forme du profil à adopter pour les grands barrages en maçonnérie du reservoirs. *Ann. d. Ponts et Chaussées*, t. xii, 1866, p. 212.

20. RANKINE. Report on the Design and Construction of Masonry Dams. *The Engr.*, Jan. 5, 1872, p. 1.

21. —— Miscellaneous Scientific Papers. London, 1881.

22. BOUVIER. Calculs de résistance des grands barrages en maçonnérie. *Ann. d. Ponts et Chaussées*, Août, 1875, p. 173.

23. COVENTRY. The Design and Stability of Masonry Dams. *Proc. Inst. C.E.*, vol. lxxxv, 1885–6, p. 281.

24. KREUTER. On the Design of Masonry Dams. *Proc. Inst. C.E.*, vol. cxv, 1893–4, p. 63.

25. MOLESWORTH. Proposed Cross Section of Dams. *Proc. Inst. C.E.*, vol. cxv, 1893–4, p. 85.

26. LÉVY. Quelques considérations sur la construction des grands barrages. *Comptes Rendus*, cxxi, 1895, p. 288 ; cxxvii, 1898, p. 10 ; *Ann. d. Ponts et Chaussées*, 1894, pt. iv, p. 5.

27. ATCHERLEY AND PEARSON. On Some Disregarded Points in the Stability of Masonry Dams. *Draper's Co. Res. Mem.* London, 1904 ; see also *Engg.*, July 14, 1905, pp. 35, 171.

28. UNWIN. Note on the Theory of Unsymmetrical Masonry Dams. *Engg.*, Apl. 21, 1905, p. 513 ; May 12, 1905, p. 593 ; June 30, 1905, p. 825.

29. SMITH, B. A. Masonry Dams. *Engg.*, July 7, 1905, p. 10.

30. AM ENDE. Notes on Stresses in Masonry Dams. *Engg.*, Dec. 8, 1905, p. 751.

31. HILL. Stresses in Masonry Dams. *Proc. Inst. C.E.*, vol. clxxii, 1907–8, p. 134.

32. OTTLEY AND BRIGHTMORE. Experimental Investigation of the Stresses in Masonry Dams Subjected to Water Pressure. *Proc. Inst. C.E.*, vol. clxxii, 1907–8, p. 89.

33. WILSON AND GORE. Stresses in Dams : An Experimental Investigation by means of India-Rubber Models. *Proc. Inst. C.E.*, vol. clxxii, 1907–8, p. 107.

34. MOHR. Der Spannungszustand einer Staumaner. *Zeit. d. oest. Ing. u. Arch. Ver.*, 1908, p. 641 ; see also *Tech. Mechanik*.

35. CAIN. Stresses in Masonry Dams. *Trans. Amer. Soc. C.E.*, vol. lxiv, 1909, p. 208.

36. MERRIMAN. Effects of Temperature Changes in Masonry Dams. *Trans. Amer. Soc. C.E.*, 1908, vol. lxi, p. 413 ; also GOWEN, p. 399.

37. JAKOBSEN. Stresses in Gravity Dams by the Principle of Least Work. *Trans. Amer. Soc. C.E.*, vol. xcvi, 1932, p. 489.

38. BRAHTZ. The Stress Function and Photoelasticity applied to Dams. *Proc. Amer. Soc. C.E.*, Sept. 1935 ; SILVERMAN, *Proc.*, Nov. 1935, p. 1409.

39. HALCROW. The Design of Concrete Dams, etc. *Engg.*, June 1, 1934, p. 637 ; see also Sept. 6, 1935, p. 245 (Internal Temp. Effects).

Uplift

40. HILL. Fissures in Masonry Dams. *Proc. Inst. C.E.*, vol. cxxix, 1896–7, p. 350.

41. COLMAN. The Action of Water under Dams. *Trans. Amer. Soc. C.E.*, vol. lxxx, 1916, p. 421.

42. STODDARD. Intrusive Water in Masonry Dams. *Engg.*, Oct. 26, 1917, p. 430.

43. HINDS. Upward Pressure under Dams. *Proc. Amer. Soc. C.E.*, Mar. 1928, p. 690.
44. PARSONS. Hydrostatic Uplift in Pervious Soils. *Proc. Amer. Soc. C.E.*, Apl. 1928 ; also *Engg.*, Feb. 7, 1930, pp. 181, 235.
45. SHULITS. Flow Nets for Soil-Sepage Problems. *Engg.*, Aug. 17, 1934, p. 163 ; see also FORCHHEIMER, *Hydraulik*, 1930.

Arched Dams

46. WADE. Concrete and Masonry Dam-Construction in New South Wales. *Proc. Inst. C.E.*, vol. clxxviii, 1908–9, p. 1 ; also ccxvi, p. 302.
47. JORGENSEN. The Constant Angle Arch Dam. *Trans. Amer. Soc. C.E.*, vol. lxxviii, 1915, p. 685 ; *The Engr.*, Sept. 22, 1916 ; SUTHERLAND, *Engg.*, Apl. 10, 1936, p. 387.
48. CAIN. The Circular Arch under Normal Loads. *Trans. Amer. Soc. C.E.*, vol. lxxxv, 1922, p. 233.
49. NOETZLI. Improved Type of Multiple Arch Dam. *Trans. Amer. Soc. C.E.*, vol. lxxxvii, 1924, p. 342 ; Massive Buttress Type, *Engg.*, May 25, 1934, p. 590.
50. JAKOBSEN. Stresses in Thick Arches of Dams. *Trans. Amer. Soc. C.E.*, vol. xc, 1927, p. 475.
51. AMER. SOC. C.E. Rpt. of Committee on Arch Dam Investigation. *Proc.*, May 1928 ; see *Engg.*, Nov. 5, 1926, p. 562 ; Aug. 12, 1927, p. 191 ; July 6, 1928, p. 23 *et seq.*
52. —— Vol. ii, 1935 (Model tests) ; see *Engg.*, June 7, 1935, p. 591.
53. HOWELL AND JAQUITH. Analysis of Arch Dams by the Trial-Load Method. *Trans. Amer. Soc. C.E.*, vol. xciii, 1929, p. 1191 ; also SUTHERLAND, *Proc.*, Apl. 1928.
54. NOETZLI. The Coolidge Multiple-Dome Dam. *Engg.*, Feb. 14, 1930, p. 193.

Retaining Walls, Quay Walls, Graving Docks, etc.

See Bib., Chap. XVIII, for Earth Pressure on Retaining Walls.
55. COLEMAN. *Retaining Walls, Theory and Practice*. London, 1914.
56. HOWE. *Retaining Walls for Earth*. New York, 1914. PAASWELL. *Retaining Walls, their Design and Construction*. New York, 1920.
57. CUNNINGHAM. *Dock Engineering*. London, 1922.
58. —— *Harbour Engineering*. London, 3rd ed., 1928.
59. DU-PLAT TAYLOR. *Design, Construction, and Maintenance of Docks, Wharves and Piers*. London, 2nd ed., 1934.
60. GRANT. The Design of Piled Retaining Walls. *Engg.*, Sept. 4, 1932, p. 274.
61. WENTWORTH-SHIELDS. On the Stability of Deep-Water Quay-Walls. *Proc. Inst. C.E.*, vol. ccxiii, 1921–2, p. 135.
62. —— The Quay Walls of Southampton. *Rpt. Brit. Assoc.*, 1925 ; see *Engg.*, Sept. 4, 1925, p. 303.
63. YOUNG. The Design of a Dry Dock. *Trans. Inst. Jun. Eng.* ; see also SINCLAIR, *Engg.*, Mar. 9, 1917, p. 235.

Bricks and Brickwork

64. WATERTOWN ARSENAL. *Reports of the Tests of Metals*, 1884–5, 1905–6 (Year of Publication). Strength of Brick Piers.
65. ROYAL INSTITUTE OF BRITISH ARCHITECTS. *Report on Brickwork Tests*, 1905 ; see *Engg.*, June 15, 1906, p. 794.
66. POPPLEWELL. Strength of Brickwork Piers and Pillars of Portland Cement Concrete. *Proc. Inst. C.E.*, vol. clxi, 1904–5, p. 311.

67. TALBOT AND ABRAMS. Tests of Brick Columns, etc. *Univ. Illinois Eng. Exp. Stn.* Bull. No. 27, 1909 ; see also *Eng. Red.*, Mar. 22, 1913, p. 332 ; Apl. 10, 1915, p. 460.
68. KREUGER. Brickwork Tests and Formulas for Calculation. *Clayworker,* vol. 68, 1917, pp. 42, 168.
69. BRAGG. The Compressive Strength of Brick Piers. *U.S. Bur. Stnds.* Tech. Paper No. 111, 1918 ; see also BEYER AND KREFELD, *Engg.,* June 22, 1923, p. 780.
70. McBURNEY. The Effect of Strength of Brick on Compressive Strength of Brick Masonry. *Proc. Amer. Soc. Test. Mat.,* vol. xxviii, 1928, Pt. II, p. 605.
71. STANG, PARSONS AND McBURNEY. Compressive Strength of Clay Brick Walls. *U.S. Bur. Stnds. Jour. Res.,* vol. 3, 1929, p. 507.
72. THOMAS AND DAVEY. Strength Tests for Bricks. *The Struct. Engr.,* vol. vi, 1928, p. 297.
73. GLANVILLE AND BARNETT. Mechanical Properties of Bricks and Brickwork Masonry. *Build. Research Spl. Rept.,* No. 22, 1934.
74. PHILLIPS. Bond in Brickwork. *Proc. Inst. C.E.,* vol. clxxi, 1907–8, p. 330.
75. BOYD. Brick. *Proc. Amer. Soc. Test. Mat.,* vol. xxv, 1925, Pt. II, p. 315.
76. JAGGARD. *Brickwork and its Construction.* London, 1930.
77. SEARLE. *Modern Brickmaking.* London, 3rd ed., 1931.

Concrete Construction

78. HOOL AND PULVER. *Concrete Practice.* New York, 1926.
79. HATT AND VOSS. *Concrete Work.* New York, 1921.

QUESTIONS ON CHAPTER XIX

1. A solid masonry wall 14 in. thick and 12 ft. high above the ground is found to lean 2 in. out of vertical at the top. Find the greatest and least pressures on the horizontal section of the wall at the ground level, taking the weight of masonry as 140 lb./cub. ft., and assuming that the pressure varies uniformly across the section. (U.L.)

Ans. 16·7 ; 6·7 lb./sq. in.

2. The section of a brick pier is rectangular and hollow, the dimensions of the external and internal rectangles being 54 × 45 in., and 36 × 27 in. respectively. Find the maximum lateral distance from the centre of the point through which the line of action of the resultant thrust may pass, in order that there may be no tension in the section. (U.L.)

Ans. 10·7 in.

3. AB = 3 ft. is a joint between the voussoirs of a stone arch, which, for the purpose of calculation, can be taken as 1 ft. in thickness at right angles to the paper. The thrust across the joint is 10 tons, and its line of action cuts AB at a point 1 ft. 1 in. from B, and makes an angle of 8° with the normal to AB. Find the maximum compressive stress on the joint. (I.C.E.)

Ans. 6·05 tons./sq. ft.

4. A masonry pier is built up of cubical blocks of 8 ft. sides, the joints of which are perfectly bedded but no mortar is used. It supports a load of 100 tons at a distance of 2 ft. from one edge, and equidistant from the adjacent edges. Find the maximum compressive stress in the material, and the point at which the compressive stress becomes zero. What will be the

maximum compressive and tensile stresses in the material when the joints are perfectly cemented ? Neglect the weight of the masonry. (U.L.)

Ans. 4·17 tons/sq. ft. ; 2 ft. in ; 3·90 comp. ; 0·78 ten. tons/sq. ft.

5. At any cross-section in a masonry structure let e = the perpendicular distance of the point at which the line of thrust cuts the section from the principal axis about which bending occurs ; r = the radius of gyration of the section about that axis ; and y = the perpendicular distance of the extreme point on the contour of the section, where the stress is least, from the same axis. Prove that if no tensile stress is to exist on the cross-section :

$$e < \frac{r^2}{y}$$

Hence find the shape and size of the area within which the line of thrust must pass in the case of a cross-section of a circular brick chimney 15 ft. external diameter, and 3 ft. thick, if no tension is to exist in the brickwork. (I.C.E.)

Ans. A circle 5·1 ft. diam.

6. A mass concrete retaining wall with a vertical back, 30 ft. high, has to support a bank of earth without surcharge weighing 100 lb./sq. ft. The width of the wall at the top is 3 ft. and the weight of the concrete 140 lb./cub. ft. Using the 'wedge' theory, find the necessary width of the base if the resultant pressure is not to pass outside its middle third. Take the friction angle ϕ of the earth, and on the back of the wall ϕ', as 30°, and assume that the resultant pressure acts at a point 0·4 H up the back of the wall.

10½ ft.

Ordinates to Inner Face in Ft.: 1·3, 2·2, 3·6, 6·0, 8·73, 12·7

Depths in Ft.: 10, 20, 40, 80, 120, 160, 180

Ordinates to Outer Face: 17·4, 28·7, 47·3, 78·0, 113·5, 135·1

Base

Fig. 504.

7. Fig. 504 gives the section of a large dam for sustaining water pressure. The two curved faces are plotted from the vertical line. The weight of the masonry is 125 lb./cub. ft., and that of the water is 62·5 lb./cub. ft. Draw the lines of resistance with the reservoir empty and full, and report whether there is a tensile stress at any section, and whether the greatest compressive stress exceeds 6 tons/sq. ft. (U.L.)

8. A straight wall of rectangular section has water on one of its vertical faces and the water is level with the top of the wall. Show with diagrams how to obtain the principal stresses and the principal axes of stress at a point near the centre of the base of the wall. State what assumptions are involved in the method employed. (U.L.)

9. *Design for a Masonry Arch* carrying a public road (cf. Fig. 481), 150 ft. span, rise 35 ft., roadway 20 ft. wide, with two 5-ft. side walks, Fig. 480. Ministry of Transport loading § 23 ; proportions § 357 ; material, cut granite in 1 : 3 cement mortar, max. compressive stress 40 tons/sq. ft. ; rock foundations. Follow the methods of § 322.
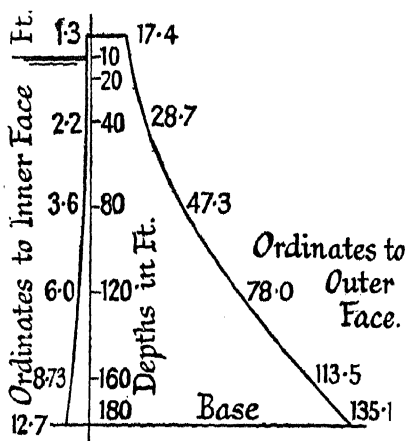
CHAPTER XX

EXPERIMENTAL DETERMINATION OF THE STRESSES IN STRUCTURES

375. **Experiments on Riveted Joints.**—Experiment has shown that the conventional assumptions regarding the behaviour of riveted joints by no means hold in practice. In the ordinary theory it is assumed that the load on the joint is carried by the shearing resistance of the rivets, that the load is shared equally between the rivets, and that the stress distribution throughout the joint is uniform. These assumptions may be approximately true near the point of failure, but are quite incorrect in the neighbourhood of the working load.

Frictional Resistance and Slip.—Fig. 505 represents the result of a tension experiment by Rudeloff [3] on a butt joint with double cover straps and 15 rivets on each side of the joint. Up to a load of about 70 tons, the joint approximates in behaviour to an elastic body, but at the point S *slipping* occurs, and the rate of extension suddenly increases. This happens when the growing load overcomes the frictional resistance of the joint, which frictional resistance is the consequence of the compression between the plates, resulting from the longitudinal tension in the rivets due to cooling after closing, and also to the pressure used to close the rivets. That the resistance under low loads is predominantly due to friction has been proved by making experiments on joints in which the holes are oval and larger than the rivets. Edwin Clark [*] found that a ⅞-in. iron rivet in a large oval hole, hand driven, carried 5·59 tons before slipping occurred, equivalent to a stress in the rivet of 9·3 tons/sq. in.

FIG. 505.

As the result of slip in a normal joint, more and more rivets begin to bear against the sides of their holes, and the resistance of the joint increases up to the point R, Fig. 505. Thenceforward the shearing resistance of the joint comes into play, and the total resistance rises rapidly.
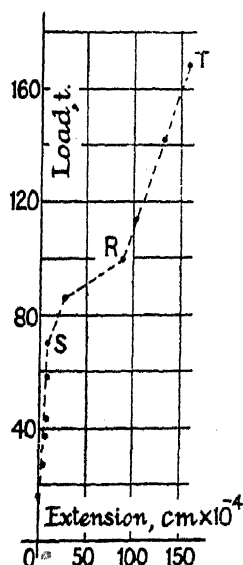
* The Britannia and Conway Tubular Bridges, 1850, vol. i, p. 393.

Many experiments have been made to determine the resistance to slip. With plates less than $\frac{3}{8}$ in. thick, of wrought iron or ordinary mild steel, the results obtained range from about 5 to 12 tons/sq. in. of rivet area, averaging from 7 to 8 tons/sq. in. The type of joint and method of closing the rivet do not appear much to affect this result. With thick plates, unless special precautions be taken, it is found difficult to ensure close contact between the plates, and the resistance to slip is lower, averaging, according to Montgomerie's experiments,[4] from 5 to 6 tons/sq. in. ; the variation in slip resistance is also much greater. With thick plates, hydraulic riveting, where great pressure is used to close the rivets, ensures better contact between the plates and gives higher slip resistance than does either hand or pneumatic riveting.

Partition of Load.—A second point established by experiment is that the load is not equally shared between the rivets in a joint. It is found that the extreme rivets in a line are more heavily loaded than the intermediate ones. Professor Batho[5] has determined experimentally the partition of load between the rivets in a butt joint with double cover straps in a flat bar, and has shown that the said distribution can be obtained theoretically from strain-energy considerations. Fig. 506 represents some of his results. For a joint, (i), with five rivets in line, in which the covers are one-half the thickness of the bar, each of the two end

FIG. 506.

rivets of the group carries about 40 % of the load, (ii) ; if the covers are equal in thickness to the bar, the extreme end rivet of the joint carries over 60 % of the load, (iii). Batho's theory indicates that when the number of rivets in line is five or more, the load on the extreme rivet is practically the same no matter how many rivets there be, the intermediate rivets carrying little of the load. This would suggest that it is uneconomical to put more than five rivets in line.
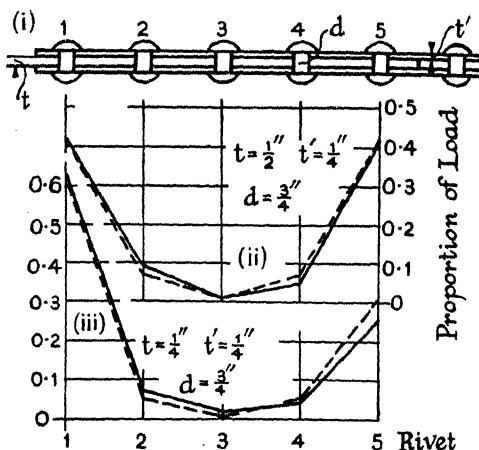
In explanation of these results, it is evident that if the rivets were perfectly rigid, the two end rivets would take all the load ; it is only by yielding slightly that they are able to pass some on to their neighbours. By finding the strain energy stored in the system, and using the principle of least work, Batho determines the load on each rivet in terms of a quantity K which depends on the action of the rivet and the proportions of the joint. He obtains values of K from the experiments. The dotted lines in Fig. 506 show the theoretical partition calculated in this manner,

and as will be seen, the method gives values which agree closely with the experimental observations indicated by the full lines. The results of similar experiments by Hertwig and Petermann [10] show general agreement with Batho's results. The distribution of load, thus determined, holds until the working load has been far exceeded; but with increasing load the overstrained end rivet begins to yield more and more, and the other rivets take up a larger share of the load. Unequal partition persists, however, at least up to the yield point of the joint.

Fitted bolts behave in a similar manner to rivets, but the distribution in load is affected by the amount of tension in the bolts occasioned by the tightening up. The behaviour of joints with black bolts (bolts which do not fit the holes) is also found to be generally similar to riveted joints up to the point at which slip occurs. A general redistribution of load between the bolts accompanies slip; when no more slip can take place, and the yield point of the joint is approached, the partition of the load is almost uniform. For experiments on joints with black bolts see Batho and Samawi.[11] They find that the average coefficient of friction between unpainted surfaces is $0 \cdot 35$, and point out that it is not possible, when working at a shear stress in the bolts of 4 tons/sq. in., to tighten up such bolts sufficiently to prevent slip.

Stress Distribution.—Measurements of the stress at different parts of riveted joints have been made, and as might be expected the distribution is by no means uniform.

D.E.V. Experiments.—A number of tests of riveted joints have been made by the Deutscher Eisenbau-Verband,[3] which tests have been supplemented by others made by Dörnen [6, 7]. These experiments confirm in general the conclusions set forth above; the following additions may be noted. In some experiments on flat bar specimens with double cover straps, fracture took place indifferently either by the bar tearing or by the rivets shearing when the ratio

$$\frac{\text{net area of the bar}}{\text{area of rivets in shear}} = \frac{a_t}{a_s} = 0 \cdot 74.$$

For riveted joints, also in double shear, Dörnen found that when $a_t/a_s = 0 \cdot 71$ the angle failed; when $a_t/a_s = 0 \cdot 85$ the rivets failed. Using hard steel rivets, so that failure by shear was obviated, he found that for equal strength in tension and bearing

$$\frac{\text{net area of the bar}}{\text{bearing area of the rivets}} = \frac{a_t}{a_b} = 3,$$

but in such circumstances the distance of the rivet from the edge of the bar should be at least $3\frac{1}{2}d$.

In the D.E.V. experiments, the load at which slip began was on an average 142 % in the case of toggle-joint riveting, and 54 % in the case of pneumatic riveting, greater than in the case of hand riveting. The ultimate strength of the joint was not influenced by the method of riveting. The resistance to slip was appreciably greater in riveted than in bolted

connections, but the ultimate strengths of the two kinds of joint were approximately the same. The arrangement of the rivets in a flat bar butt joint with double covers made no appreciable difference to the slip resistance of the joint, but the slip resistance is a very variable factor even with joints having the same arrangement of rivets. The load at which slip begins averages approximately 20 % of the shear strength of the joint. In a tie bar, the slip between the angles and the gusset at the extreme rivets was found to be nearly four times as great as at the two middle rivets.

Both in the D.E.V. and in Dörnen's[3, 6] experiments, it was found that, in an angle section tie bar with a supplementary cleat, (ii) Fig. 216, the slip between the tie bar and the gusset was much greater than between the tie bar and the cleat, showing that most of the load is transferred direct from tie bar to gusset. Dörnen found that when three rivets were used to connect both tie and supplementary cleat to the gusset plate, (ii) Fig. 216, the measured slip of the tie bar was about three times as great as that of the supplementary cleat. Lengthening the cleat and increasing the number of rivets connecting the cleat to the tie bar from three to five, (iia) Fig. 216, reduced the measured slip between the tie bar and cleat by about one-half.

Type of Joint.—Some tension experiments by Gayhart[9] on butt joints in $\frac{3}{4}$-in. plates, with double cover straps $\frac{1}{2}$ in. thick, are instructive. The rivets were 1 in. diameter in $1\frac{1}{16}$-in. holes, spaced $4\frac{1}{2}$ in. apart. Three classes of material were used for the plates : medium 60,000 lb. steel, high tensile 80,000 lb. steel, and a specially treated steel. Both medium and high tensile steel was used for the covers and rivets.

Seven types of joint were tested : (A) double riveted ; (B) treble riveted ; (C) quadruple riveted ; (D) treble riveted with the pitch doubled in the outer row ; (E) quadruple riveted similarly arranged ; (F) as (D), but with cover straps of unequal width ; (G) as (E), but with unequal straps. Great care was taken to ensure a tight joint and completely filled rivet holes. Comparing the ultimate strengths of the medium steel joints : type A was weakest but 12 % stronger than its theoretical worth, actual efficiency = 85 %. The respective efficiencies of the three treble-riveted joints were : B, 84 % ; D, 81 % ; F, 85 %. B was 10 % stronger than its theoretical worth ; D was 5 % weaker, which suggests that the omission of the alternate rivets in the outer row does not improve the joint (these joints were designed for plate failure). The results for the quadruple-riveted joints were practically identical, and the addition of the fourth row of rivets did not improve the joint. The two joints F and G with the unequal cover straps and omitted rivets had the highest efficiency.

The results for the high-tensile steel were similar. The joint B with three complete rows of rivets was slightly stronger than D with the omitted rivets. The strongest of all was the quadruple-riveted joint G with unequal covers and the omitted rivets.

Comparing the stresses (in lb./sq. in.) in the plates themselves when

slip first occurred : for the medium steel joints this was 6700 in joint A ; 9400 in joint B ; 8500 in D, and reached a maximum of 11,000 in E. The high-tensile steel showed up badly in this respect, the stresses at first slip being generally less than one-half those in the medium steel joints ; due, it is suggested, to less perfect plate contact. The stress in the special-treatment steel plates at first slip was 5200 lb./sq. in. with medium steel rivets, and 2400 lb./sq. in. with high-tensile steel rivets.

With medium steel rivets, at low intensities of plate stress, the outer row of rivets carried a larger portion of the total load than the others. At the design stress, in treble- and quadruple-riveted joints, the load is equalised between the rows. When alternate rivets were omitted in the outer rows, the distribution was not so uniform. In double-riveted joints, even at high stresses, the outer row carried two-thirds of the load. The distribution in the case of high-tensile steel rivets was not very different from the above.

376. Snap Head v. Countersunk Riveting.—The relative strength of riveted joints with snap head and countersunk rivets, respectively, has been investigated by Kommers.[12] The specimens were lap and butt joints in tension and bending. The average ultimate shear strength of the countersunk riveting was at least equal to that of the snap riveting, but the permanent slip (the residual elongation when the load was reduced to 1000 lb.) at working stresses was 3 to 6 times as great in joints with one countersunk head, and 5 to 8 times as great when both heads were countersunk, as in joints with snap heads. The corresponding elongations were from 1·7 to 2 and 2 to 4 times as great in the respective cases. In the bending tests, at working stresses, the deflection of the joints with countersunk rivets was from 10 to 80 % greater than in those with snap heads. The ultimate strength was about the same with each kind of head.

Kommers concludes, therefore, that for strength, either countersunk or snap-head riveting may be used. For rigidity, snap heads are preferable. For joints subjected to impact, where high capacity for absorbing energy is requisite, countersunk riveting should be employed.

377. Rivet Heads in Tension.—Young and Dunbar[14] made a number of tests on rivet heads subjected to pure tension, tension combined with flexure, and tension combined with shear. The rivets had cup (snap) heads. They found that in pure tension an increase in the grip length diminished the ultimate strength. As the diameter of the rivet increases, the ultimate tensile strength per square inch decreases. In general, machine-driven rivets gave higher resistances than did pneumatic percussion riveting. In many cases, no observable extension of the rivet occurred until a considerable load had been applied, showing that it is the initial tension in the rivet which carries the load, until the increasing applied tension exceeds the initial tension.

The combination of tension with flexure considerably reduced the tensile resistance of the rivets. Applying the load with an eccentricity of 1¼ in. from the centre line of the rivets produced a marked reduction

in the strength; but doubling the eccentricity did not lead to a proportional decrease in the resistance. With $1\frac{1}{8}$-in. eccentricity, machine-driven riveting was superior to pneumatic riveting, but when the eccentricity was increased to $2\frac{1}{4}$ in. there was little difference between the strength of the two kinds. The larger the rivet the less was its strength per square inch.

From the results of the tension combined with shear experiments, it would again appear that the average ultimate strength per square inch decreases as the diameter of the rivet increases. Increasing the grip length also diminishes the strength. Pneumatic riveting was inferior to machine-driven riveting when the shearing force S was one-half the tensile force T, but when S $=$ T there was little to choose between them. The following formulae are suggested to give the permissible tensile stress on rivet heads, based on a factor of safety of 4 on the ultimate strength:

For the combination of tension with flexure,

$$p_t = 21,000 - 8000d - 5500\sqrt{e}$$

where

$p_t =$ the permissible tensile stress on the rivet in lb./sq. in. on the area before driving.

$d\ =$ the diameter of the rivet before driving in inches.

$e\ =$ the eccentricity of loading in inches.

For the combination of tension and shear

$$p_t = 21,000 - 8000d - 6750\ (S/T)^2.$$

S is the total shearing force due to all causes in lb.
T is the total tensile force due to all causes in lb.

It is pointed out that this combination of loading was accompanied by incidental flexure of undetermined magnitude.

In the experiments, the diameter of the rivets ranged from $\frac{5}{8}$ to $\frac{7}{8}$ in., and the holes were punched $\frac{1}{16}$ in. larger than the rivet.

378. Stresses in Semi-stiff Frames.—Before a rational method of designing semi-stiff frames, such as a steel-framed building, becomes possible, some definite knowledge is required regarding the degree of rigidity which the commonly employed connections possess. A number of experiments have been made with this end in view; one of the earliest series was that made at the University of Illinois and reported in 1917.[16] Fig. 507 shows the types of specimens employed; the method of loading is indicated at A4. Assuming the joints to be perfectly rigid, certain changes of slope will take place under this loading; these can be calculated. The actual changes of slope at specific points on the specimen can be measured. The differences between the calculated and observed values are assumed to be due to slip and distortion at the joints. In this way an estimate of the rigidity of the joints is obtained. That distortion of the parts of a joint has considerable effect in reducing its rigidity may be · inferred from the manner of failure. Thus in A3 and A4 the cleats opened. In A5 the cleats opened and the rivets failed in tension; in A6 the cleats

opened. In A1 the column buckled, suggesting that distortion at the joint was not large, but in A2 (a joint similar to A1 but in which the gusset was attached by long cleats to one flange of the column) the gusset plate buckled.

Speaking generally, in types A1 and A2 the assumption of perfect
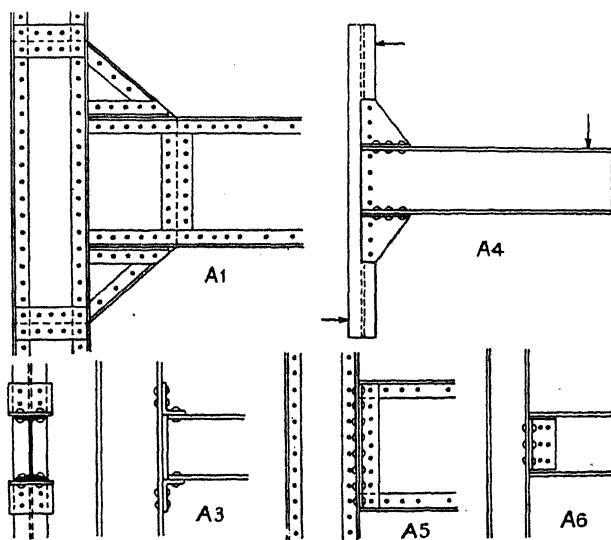
FIG. 507.

rigidity leads to no serious error. A3, A4, A5, and A6 must not be regarded as rigid joints, though A5 showed some indications of rigidity under low loads.

More recently, a number of experiments have been made by Berg,[18] Batho and Rowan,[19] Rathbun,[21] and others. A reference to Batho and Rowan's experiments will be found in § 378A. The test-piece used is of the form shown in Fig. 508, which represents one of Rathbun's specimens. This is supported beam fashion at each end, and loaded with a central load as indicated; alternatively, four-point loading may be employed to give pure bending at the connections. The angular change between the horizontal beam and the vertical column is observed, and plotted against the bending moment producing it (see Figs. 509 and 510A). In Rathbun's experiments, three types of connections were used : (i) plain web cleats ; (ii) flange cleats top and bottom of the beam, with or without web cleats ; (iii) split I connections, Fig. 508.
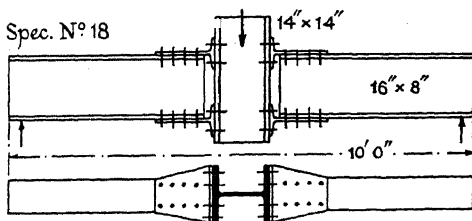
FIG. 508.

In types (i) and (ii) the column of Fig. 508 was replaced by a vertical plate.

The cleats in type (i) deformed badly under load, without much visible distress in the rivets or **I** beams. This type can be subjected to considerable angular deformation without seriously affecting the capacity to carry vertical loads. In type (ii) the chief deformation occurs in the flange cleat placed in tension, and in some cases in the rivets therein, not in the **I** beams. This suggests that the construction could be strengthened by thickening the flange cleats, which were ⅜ in. thick. The deformation in the working range of this type was much less than in type (i). In type (iii), constructed with a central vertical plate instead of an **I** column, the rivets failed in tension, or those in the horizontal beam sheared. The flanges in the beam showed distress long before failure. In
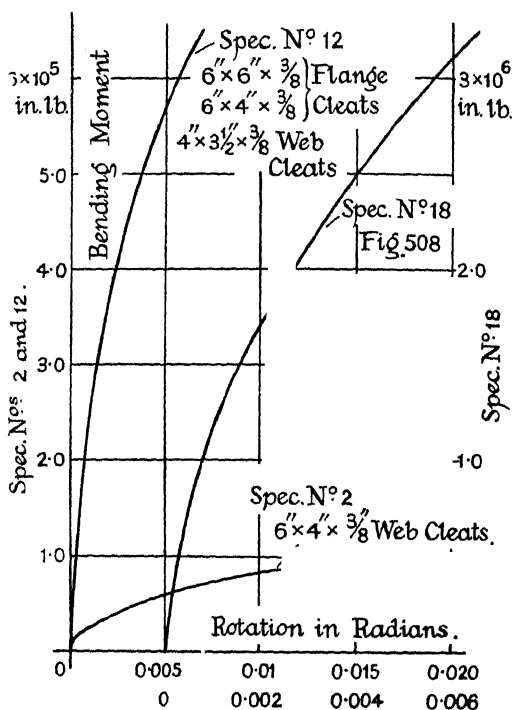
Fɪɢ. 509.

Exp. 18, Fig. 508, the column became distorted long before the connections passed the yield point. The stress was high in the central rivets and low in the outer ones. Type (iii) forms a relatively rigid connection.

In Fig. 509 the angular deformation is plotted against the bending moment. The connection for the 8-in. beams in Exp. No. 2 consisted of double 6 × 4 × ⅜-in. web cleats. For the 12-in. beams in Exp. No. 12 the flange cleats were 6 × 6 × ⅜ in. and 6 × 4 × ⅜ in. ; the web cleats were 4 × 3½ × ⅜ in. Specimen No. 18 is shown in Fig. 508.
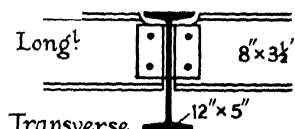
Fɪɢ. 510.

In some experiments by the D.E.V.[17] on cleated bolted connections between **I** beams, there were three longitudinal spans of 3·6 m. in line, which were freely supported at the extreme ends, the intermediate supports being transverse beams to which the longitudinals were attached by two-hole web cleats of the usual type, Fig. 510. The ends of the

transverse beams were freely supported. Each longitudinal span was loaded at the ⅓ points of the span, and the loads were increased in steps up to failure. The experimental conditions were made to correspond exactly with ordinary practical conditions. From the observed deflections, the fixing moments at the intermediate supports were calculated. The experiments proved that the beams were partially direction-fixed, and that under working loads the direction-fixing moments increase the carrying capacity of the longitudinal girders by at least 10 %. The tensile and shear stresses in the bolts remain within permissible limits, but attempts to find the tension in the bolts by direct measurement of the extensions proved abortive, due to the initial tightening-up tensions.

Owing to the equalisation in the partition of the load which takes place with bolts, and to the greater rigidity of riveted joints and consequent greater inequality in the load partition, the conclusion is reached that bolts are to be preferred to rivets.

378A. Report of the Steel Structures Research Committee.—The final Report (1936) of the Committee [22] contains the results of their investigations into the behaviour of steel-frame buildings under vertical loads, and proposed methods of design. This work is summarised in a paper by Professor Baker read before the Institution of Civil Engineers,[23] from which the following abstract has been made :—

The Committee find that, due to the semirigidity of the joints between the beams and stanchions, the bending moment on the beams is reduced, but that considerable bending moments are imposed on the stanchions. Excepting where, due to unsymmetrical conditions, sway takes place, S bending is the rule in the stanchions, the maximum bending

FIG. 510A.

moment occurring at their ends ; the ordinary column formulae, therefore, are inapplicable.

From observations on actual structures, and experiments in the testing machine (Batho and Rowan, 2nd Report), they find that, though far from rigid, the ordinary cleated connections will transmit a considerable bending moment. Measurement of the change of angle between beam
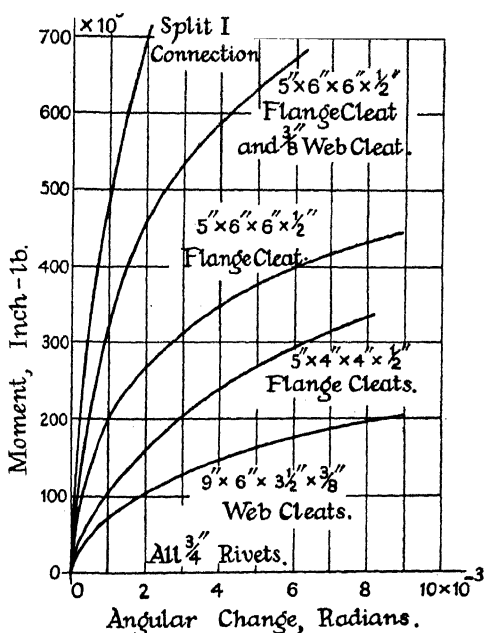
and stanchions shows that the deformation is not elastic (Fig. 510A). It is made up partly of deformation of the cleats, partly of elongation of the rivets, and partly of local deformation of the members connected. The yield point is exceeded in the cleats under relatively small moments, but in the structures themselves the probable angular change is sufficiently small not to be dangerous. On removal of the moment, permanent deformation is found to exist. The angular change for a given moment varies not only with the type of connection, but also with the workmanship, differences in the tension in bolts and rivets, and with abnormalities in the shape of the cleats. Bolted connections show more variation than riveted. The Committee propose lower limit curves for the purposes of design.

Calculations of the bending moments in a steel-frame building, made on the assumption that the joints are rigid, gave results which, though similar in character, differ considerably in magnitude from the experimental observations. Using the experimental curves for the semi-rigid connections, the Committee show that it is possible to interpret the observed bending moments with success.

They find that the filling in the floors and walls, and the encasement of the beams, connections, and stanchions, have much influence on the moments and stresses ; the most important effect being to eliminate sway due to want of symmetry. The addition of encasement diminishes the bending moment on the floor beams, but may increase the bending moments in the columns when the connections are light ; it may diminish them when the connections are rigid. Encased connections in the testing machine act almost as rigid joints until the concrete cracks ; afterwards the effect of the encasement is small.

The Committee propose to replace the usual conventional calculations for steel-frame buildings by a more rational process based on their observations. Considerable simplification, however, was found necessary to make the procedure manageable. For a detailed account of the experiments, and of the proposed method of design, the references cited should be consulted.

379. Stresses in Braced Frames.—A number of experimental studies have been made on the stresses in braced frames under specific load conditions. Generally speaking, these may be said to justify the usual elementary methods of finding the primary stresses in framework, even when the framework has stiff riveted joints ; but, in addition, these experiments demonstrate the existence of secondary bending moments of considerable magnitude resulting from the stiffness of the joints. If the stresses due to these secondary moments be taken into account, and properly combined with primary stresses, a close agreement between the theoretical and experimental stresses is obtained.

A notable experimental study of this character was made by Wyss [26] on the riveted girder shown in Fig. 513, the details of construction being similar to (i) Fig. 190. Some of the results of this research are discussed in ¶ 9, § 118. Wyss measured the deformations in the members and gussets

of his experimental girder, and from these measurements calculated the stresses everywhere. Making certain assumptions regarding the semi-stiffness of the gussets, he was able to interpret his measured values with considerable success. His memoir is worthy of careful study ; it must suffice here to mention one or two points of interest.
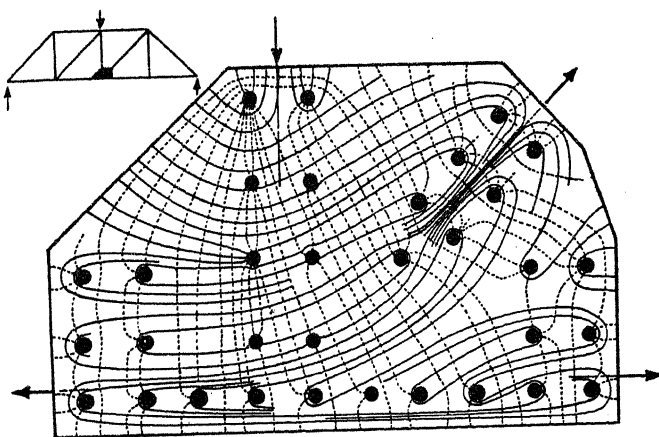
FIG. 511.

Fig. 511 represents the stress trajectories or lines of principal stresses in a typical gusset. From it, a conception may be obtained of the way in which the forces in the web members increase the forces in the flange, and the action of the gusset in this relation.
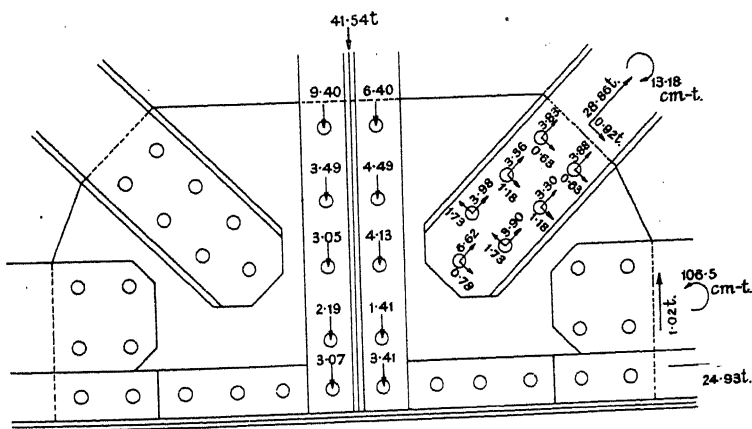
FIG. 512.

The measured loads on the rivets in the ends of typical web members are shown in Fig. 512. It will be seen that the force in the members is by no means equally distributed between the rivets ; the tendency for the load to concentrate on the end rivets will also be observed.

(ii) Fig. 513 shows the deflection curve, and (iii) the ascertained secondary bending moments. In view of its bearing on the column theory, the point of inflexion, indicating S-bending in all the members, should be noted. For diagrams of the distribution of stress in all parts of the girder, the original memoir must be consulted.
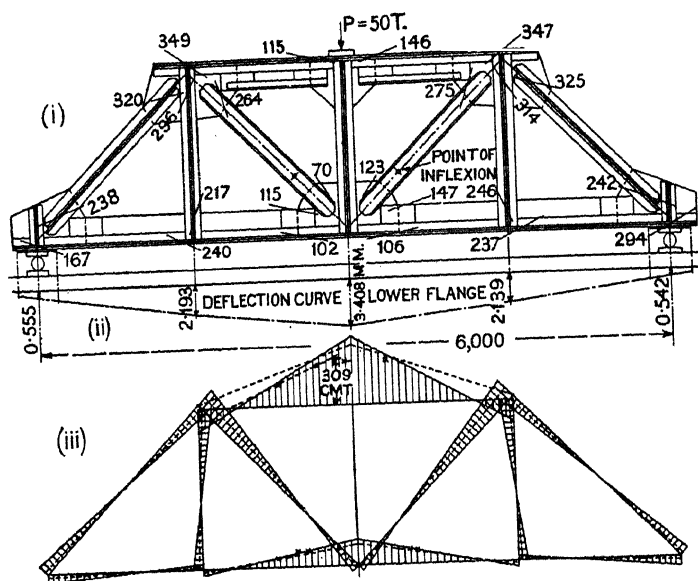
FIG. 513.

380. Model Analysis. Begg's Deformeter.—In statically indetermin-ate structures with many unknowns, the analysis becomes so involved that recourse is often made to experiments on models, in order to determine the stresses in the structure. The deformeter method devised by Professor Beggs [29] is convenient for this purpose. The stresses in any type of plane framework can thus be found, provided that all the forces act in the plane of the frame. The theory is based on the Maxwell-Betti theorems, § 84, and the statically indeterminate unknowns are found by measuring the relative displacements of points on a flat model of the structure. This model, which must be correctly proportioned as to area and/or moment of inertia of its parts, may be of thin celluloid, or of a good quality cardboard. To eliminate friction as far as possible, the model is supported on small steel balls resting on a sheet of glass ; a number of small weights are used to hold the model down and to prevent warping.*

Let Fig. 514 represent two bays of a stiff portal frame with direction-fixed feet. At each foot there will be a vertical reaction V, a horizontal force H, and a support moment M. There are thus nine statically

---

* For a number of desirable precautions in making the experiments, see Lobban, *Trans. Inst. Engrs. and Shipbuilders, Scotland*, vol. lxxvii, 1933–4, p. 169.

indeterminate unknowns. To find the magnitude of these when a load W, acting in any direction, is applied to the portal at any point D, the procedure is as follows : Give to the point A a definite vertical displacement $AA' = \Delta_{aa}$ without permitting the foot to rotate, measure the displacement Δ_{da} of the point D along the line of action of W. Then by Betti's theorem,

$$V \cdot \Delta_{aa} = W \cdot \Delta_{da} \; ; \; or, \; V = W \frac{\Delta_{da}}{\Delta_{aa}} \; . \qquad . \quad (1)$$

Similarly, to find H, give the point A a horizontal displacement Δ_{aa} without permitting it to rotate, and measure the displacement Δ_{da} of the point D along the line of action of W. Then as before,

$H \cdot \Delta_{aa} = W \cdot \Delta_{da} \; ; \; or,$

$$H = W \frac{\Delta_{da}}{\Delta_{aa}} \; . \qquad (2)$$

The horizontal thrust in two-hinged arches could be thus obtained. Thirdly, to find the moment M, give the foot A an angular movement Δ_{aa}/c, keeping the point fixed in position. Then if P be the force, acting at leverage c, necessary to produce this angular movement, and Δ_{da} be the corresponding displacement of D along the line of action of W,

$$P \cdot \Delta_{aa} = W \cdot \Delta_{da}.$$

Multiply each side of the equation by c. Then

FIG. 514.

$$Pc \cdot \Delta_{aa} = Wc \cdot \Delta_{da} \; ; \; and \; M = Pc = Wc \frac{\Delta_{da}}{\Delta_{aa}} \qquad (3)$$

In this manner the support moments in direction-fixed arches could be found.

From eqs. (1), (2), and (3), V, H, and M at A can be found, and similarly for the feet B and C. If the experiment be repeated for a number of different positions of W, and W be put equal to unity, influence lines for V, H, and M can be plotted, from which their magnitudes for any load condition can be ascertained. This merely entails measuring Δ_{da} at a number of points along the structure, having once set up a displacement Δ_{aa}.

The method used to produce the displacements is shown in Fig. 515. Attachments for the feet of the structure are provided of the form shown
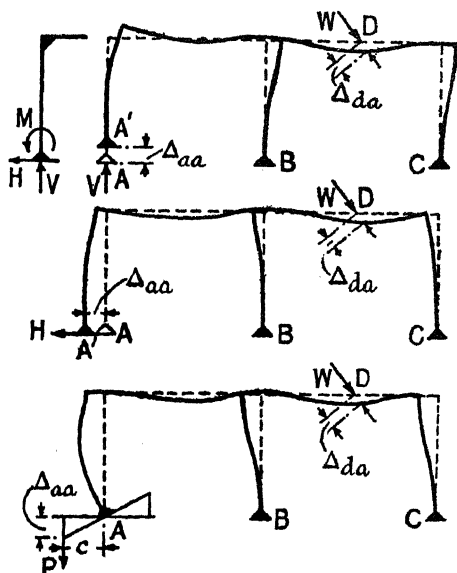
in (i) Fig. 515. These consist of two bars J and K kept together by springs. The top bar J is attached to the board on which the model is mounted, the feet of the structure are attached to K. The bars are held apart by plugs as indicated. To produce a vertical movement without rotation, the normal plugs at one of the feet are replaced by others of smaller diameter, (ii). Horizontal displacements are produced by inserting rectangular plugs, (iii), and angular movement by using two plugs of different diameters, (iv). The wedges are used to separate J and K for the purpose of inserting the plugs. Deflections to an accuracy of 1/40,000 inch can be thus produced. To measure the displacement of D, filar micrometer microscopes are employed.*
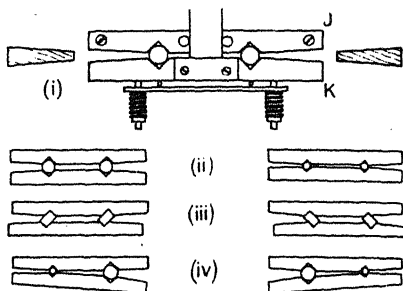
FIG. 515.

To find the force F_r in a redundant bar MN, Fig. 516, suppose it replaced by two equal and opposite forces F_r' and F_r'', each equal in magnitude to F_r. If F_r' alone be applied to the frame, it will produce at M a displacement Δ_{mm} along the line of action of F_r', and a displacement Δ_{dm} at D along the line of action of W. If F_r'' be applied alone, it will produce corresponding displacements at N of Δ_{nn}, and at D of Δ_{dn}. From the Maxwell-Betti theorems

$$F_r' \times \Delta_{mm} = W \times \Delta_{dm}$$

$$F_r'' \times \Delta_{nn} = W \times \Delta_{dn}$$

When the bar is in place, both F_r' and F_r'' will act together, and since each is equal to F_r,

$$F_r (\Delta_{mm} + \Delta_{nn}) = W(\Delta_{dm} + \Delta_{dn})$$

or $\quad F_r \times \Delta_{MN} = W \times \Delta_D$;

and $F_r = W \dfrac{\Delta_D}{\Delta_{MN}}$

where $\Delta_{MN} = (\Delta_{mm} + \Delta_{nn}) = $ the approach of M to N; and $\Delta_D = (\Delta_{dm} + \Delta_{dn}) = $ the total displacement of D.

FIG. 516.

To find F_r by means of the experimental apparatus, therefore, omit the redundant bar MN and cause M and N to approach by an amount Δ_{MN}. Measure Δ_D, the corresponding displacement of D along the line of action of W. Then, if W = unity,

$$F_r = \Delta_D / \Delta_{MN}.$$
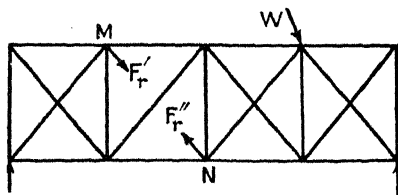
* Pippard and Sparkes show that, in simple cases, reasonably accurate results can be obtained from models cut from sheet xylonite, with displacements of such magnitude that they can be measured with a finely divided scale. *Jour. Inst. C.E.*, November 1936, p. 79.

F_r' acting at M will also give rise to a displacement Δ_{nm} at N, and F_r'' will produce a displacement Δ_{mn} at M. Since F_r' and F_r'' are equal, and act in opposite directions along the same line of action, $\Delta_{nm} = -\Delta_{mn}$, the sum of these displacements is zero, and they do not affect the value of Δ_{MN}.

Other Methods.—Professor Coker [30] uses flat nitro-cellulose models of structures, and by a combination of optical determinations with polarised light (see § 253, Vol. I), and lateral measurement of the change in thickness under load of the model, the direct stress, bending moment, and shear stress at any cross-section can be found.

A variation of the Beggs method due to El-Wahed, and termed by him the ' link-method,' may be mentioned.[31]

Satisfactory results have been obtained, both in this country [32] and in America, by constructing a suitably proportioned model structure, preferably of metal, and measuring the deflections and slopes produced under load by means of a micrometer microscope. From the observations thus obtained, the bending moments in the members of framed structures can be calculated directly from the slope-deflection equations, eqs. (25) and (26), § 105. An application of this method to 13 storeys of a building, by Large, Carpenter, and Morris, may be consulted (see Ref. No. 37, Bibliography, Chapter III).

BIBLIOGRAPHY

Experiments on Riveted Joints

See Bib., Chap. I, Vol. I, Refs. Nos. 1–9.

1. CLARK. *The Britannia and Conway Tubular Bridges*, London, 1850, vol. i, p. 389.
2. VAN DER KOLK. Experiments on the Frictional Resistance of Riveted Joints. *Proc. Inst. C.E.*, vol. cxxx, 1896–7, p. 332.
3. D.E.V. EXPERIMENTS. Zweiter Berichte über Festigkeitversuche mit Eisenkonstrucktionen. *Zeit. Ver. deu. Ing.*, July 26, 1909, p. 1019 ; see also *Der Eisenbau*, 1912, p. 229 ; and *Der Bauingenieur*, 1921, p. 450.
4. MONTGOMERIE. Experiments on Riveted Joints. *Trans. Inst. Eng. Ship. Scot.*, 1919–20, p. 284 ; also *Trans. I.N.A.*, vol. lxv, 1923, p. 179, and *Engg.*, June 8, 1923, p. 727.
5. BATHO. Partition of the Load in Riveted Joints. *Rpt. Brit. Assoc.*, 1920 ; see *Engg.*, Sept. 3, 1920, p. 314 ; *Jour. Frank. Inst.*, Nov. 1916, p. 553.
6. DÖRNEN. *Die bisherigen Anschlüsse steifer Fachwerkstäbe und ihre Verbesserung. Diss.* Berlin, 1924 ; see :—
7. SONNTAG. Grundsätzliche Fragen des Nietanschlusses von Fachwerk-stäben. *Glaser's Ann.*, Sept. 1, 1925, p. 94.
8. FINDEISEN. Versuche über die Beaspruchungen in den Laschen eines gestossenen Flacheisens bei Verwendung zylindrischer Bolzen. *Mitt. u. Forschungsarbeiten V.d.I.*, Heft 229, Berlin 1920 ; also *Rpt. 2nd Int. Cong. Bridge Struc. Eng.*, Vienna, 1929, p. 347 (Bearing Pressures), and GALLIK, ibid., p. 365.
9. GAYHART. Behaviour and Ultimate Strength of Riveted Joints under Load. *Trans. Soc. N.A. and Mar. E.* (Amer.), vol. 34, 1926, p. 55 ; see *Engg.*, Feb. 18, 1927, p. 209.

10. HERTWIG U. PETERMANN. Ueber die Verteilung einer Kraft auf die einzelnen Niete einer Neitreihe. *Bautechnic* 7 (*Der Stahlbau*, 2), p. 289; see *Eng. Ab. I.C.E.*, 1930, No. 43 : 91.

11. BATHO AND SAMAWI. Experimental and Theoretical Investigations on Riveted and Bolted Joints, etc. 1st *Rpt. Steel Struc. Res. Com.*, London, 1932, p. 113.

12. KOMMERS. Comparative Tests of Button Head and Countersunk Riveted Joints. *Univ. Wisconsin*, Bull. No. 5, vol. ix, 1925 ; see *The Engr.*, Dec. 11, 1925, p. 650.

13. SCHAECHTERLE. Fatigue Tests on Riveted Joints. *Bautechnic* 10 (*Der Stahlbau*, 5), p. 65 ; see *Eng. Ab. I.C.E.*, 1932, No. 52 : 73.

14. YOUNG AND DUNBAR. Permissible Stresses on Rivets in Tension. *Univ. Toronto Univ. Eng. Res. Bull.* No. 8, 1928, p. 389 ; also *Can. Eng.*, vol. lvi, 1929, p. 201.

15. HILL. Tests Indicate Strength of Tension-Rivet Connections. *Eng. News*, Apl. 12, 1917, p. 72.

Semi-Stiff Frames. Strength of Cleated Connections.

16. WILSON AND MOORE. Tests to Determine the Rigidity of Riveted Joints of Steel Structures. *Univ. Illinois Eng. Exp. Stn.*, Bull. No. 104, 1917 ; see *Engg.*, Dec. 6, 1918, p. 638.

17. REIN. Untersuchung einfacher Trägeranschlüsse. *Der Bauingenieur*, 1926, p. 214.

18. BERG. Wind-Bracing Connection Efficiency. *Proc. Amer. Soc. C.E.*, vol. 58, Jan. 1932, p. 3.

19. BATHO AND ROWAN. Investigations on Beam and Stanchion Connections. 2nd *Rpt. Steel Struc. Res. Com.* London, 1934, p. 61.

20. YOUNG AND JACKSON. The Relative Rigidity of Welded and Riveted Connections. *Can. Jour. of Research*, vol. 11, 1934, p. 62 ; see *Engg.*, Jan. 25, 1935, p. 101.

21. RATHBUN. Elastic Properties of Riveted Connections. *Proc. Amer. Soc. C.E.*, Jan. 1935, p. 3 ; see MOORE, *Proc.*, Nov. 1935, p. 1379.

22. STEEL STRUCTURES RESEARCH COMMITTEE, 1st Rpt., 1931, 2nd Rpt. 1934, Final Rpt. 1936 ; London.

23. BAKER. The Rational Design of Steel Building Frames. *Jour. Inst. C.E.*, June 1936, p. 127.

Tests on Braced Structures

24. RICKER. A Study of Roof Trusses. *Univ. Illinois Eng. Exp. Stn.*, Bull. No. 16, 1908.

25. LANDER, COOK AND PETAVEL. An Experimental Determination of the Stresses in a Roof Truss. *Proc. Inst. C.E.*, vol. clxxxix, 1911–12, p. 319 ; also PETERMANN, *Bautechnic* 10 (*Der Stahlbau*, 5), p. 33 ; see *Eng. Ab. I.C.E.*, 1932, No. 52 : 74.

26. WYSS. Beitrag zur Spannungsuntersuchungen an Knotenblechen eiserner Fachwerke. *Forschungsarbeiten V.d.I.*, Heft 262, 1923.

27. TUDSBERY AND GIBBS. An Account of an Examination of the Menai Suspension Bridge. *Proc. Inst. C.E.*, vol. ccxvii, 1923–4, p. 208.

For Impact Tests on Bridges, see Bib., Chap. IV.

For Secondary Stress Determinations, see Bib., Chap. VI.

Model Experiments

28. JOHANSEN. Research in Mechanical Engineering by Small Scale Apparatus. *Proc. I. Mech. E.*, Mar. 1929, p. 151.

29. BEGGS. The Use of Models in the Solution of Indeterminate Structures. *Jour. Frank. Inst.*, Mar. 1927, p. 375 ; *Proc. Amer. Conc. Inst.*, vol. xviii,

1922 ; see *Engg.*, July 13, 1928, p. 31 ; Sept. 6, 1929, p. 281 ; and Dec. 9, 1932, p. 671.

30. COKER. Some Experimental Methods and Apparatus for Determining the Stresses in Bridges and Framed Structures. *Proc. Inst. C.E.*, vol. 229, 1929–30, p. 33.

31. EL-WAHED. *Die Gelenkmethode.* Ein Verfahren zur Ermittlung statisch unbestimmter Grössen und deren Einflusslinien. Berlin, 1931 ; see *Engg.*, Mar. 11, 1932, p. 303.

32. BAKER. The Mechanical and Mathematical Stress Analysis of Steel Building Frames. *Select. Eng. Pap. I.C.E.*, No. 131, 1932.

33. LOBBAN. Mechanical Methods of Solution of Stresses in Frames. *Trans. Inst. Eng. and Shpbldrs., Scotland*, vol. lxxvii, 1933–4, p. 169.

34. WITMER AND BONNER. Tall Building Frames Studied by Means of Mechanical Models. *Proc. Amer. Soc. C.E.*, Jan. 1936, p. 3.

APPENDIX

PROPERTIES OF ROLLED STEEL SECTIONS

THE following Tables are reproduced with the kind permission of Messrs. Dorman, Long & Co., Ltd., Middlesbrough, from their *Handbook for Constructional Engineers*, and with the consent of the British Standards Institution.

DORMAN, LONG & CO. LIMITED.
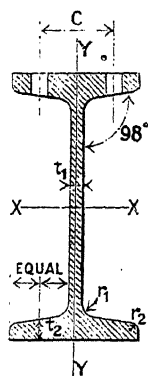
BEAMS.

DIMENSIONS.

Reference Mark	Size Inches	Weight per foot lbs.	Standard Thicknesses		Radii		Centres of Holes C Inches
			Web t_1	Flange t_2	Root r_1	Toe r_2	
B S B 140	24×7½	95	·57	1·011	·73	·36	4·5
,, 139	22×7	75	·50	·834	·69	·34	4·0
,, 138	20×7½	89	·60	1·010	·73	·36	4·5
,, 137	20×6½	65	·45	·820	·65	·32	3·75
,, 136	18×8	80	·50	·950	·77	·38	4·75
,, 135	18×7	75	·55	·928	·69	·34	4·0
,, 134	18×6	55	·42	·757	·61	·30	3·5
,, 133	16×8	75	·48	·938	·77	·38	4·75
,, 132	16×6	62	·55	·847	·61	·30	3·5
,, 131	16×6	50	·40	·726	·61	·30	3·5
,, 130	15×6	45	·38	·655	·61	·30	3·5
,, 129	15×5	42	·42	·647	·53	·26	2·75
,, 128	14×8	70	·46	·920	·77	·38	4·75
,, 127	14×6	57	·50	·873	·61	·30	3·5
,, 126	14×6	46	·40	·698	·61	·30	3·5
,, 125	13×5	35	·35	·604	·53	·26	2·75
,, 124	12×8	65	·43	·904	·77	·38	4·75
,, 123	12×6	54	·50	·883	·61	·30	3·5
,, 122	12×6	44	·40	·717	·61	·30	3·5
,, 121	12×5	32	·35	·550	·53	·26	2·75
,, 120	10×8	55	·40	·783	·77	·38	4·75
,, 119	10×6	40	·36	·709	·61	·30	3·5
,, 118	10×5	30	·36	.552	·53	·26	2·75
,, 117	10×4½	25	·30	·505	·49	·24	2·5
,, 116	9×7	50	·40	·825	·69	·34	4·0
,, 115	9×4	21	·30	·457	·45	·22	2·25
,, 114	8×6	35	·35	·648	·61	·30	3·5
,, 113	8×5	28	·35	·575	·53	·26	2·75
,, 112	8×4	18	·28	·398	·45	·22	2·25

DORMAN, LONG & CO. LIMITED.

BEAMS

DIMENSIONS AND PROPERTIES IN INCH UNITS.

Area Square Inches	Moments of Inertia		Radii of Gyration Inches		Section Moduli		Inches
	About X-X	About Y-Y	Abou X-X	Abou Y-Y	About X-X	About Y-Y	
27·94	2533 04	62·54	9·52	1·50	211·09	16·68	24 × 7½
22·06	1676·80	41·07	8·72	1·36	152·44	11·73	22 × 7
26·19	1672·85	62·54	7·99	1·55	167·29	16·68	20 × 7½
19·12	1226·17	32·56	8·01	1·31	122·62	10·02	20 × 6½
23·53	1292·07	69·43	7·41	1·72	143·56	17·36	18 × 8
22·09	1151·18	46 56	7·22	1·45	127·91	13·30	18 × 7
16·18	841·76	23·64	7·21	1·21	93·53	7·88	18 × 6
22·06	973 91	68·30	6·64	1·76	121·74	17·08	16 × 8
18·21	725·05	27·14	6·31	1·22	90·63	9·05	16 × 6
14·71	618.09	22·47	6·48	1·24	77·26	7·49	16 × 6
13·24	491·91	19·87	6·10	1·23	66·59	6·62	15 × 6
12·36	428·49	11·81	5·89	·98	57·13	4·72	15 × 5
20·59	705 58	66·67	5·85	1·80	100·80	16·67	14 × 8
16·78	533·34	27·94	5·64	1·29	76·19	9·31	14 × 6
13·59	442·57	21·45	5·71	1·26	63·22	7·15	14 × 6
10·30	283·51	10·82	5·25	1·03	43·62	4·33	13 × 5
19·12	487·77	65·18	5·05	1·85	81·30	16·30	12 × 8
15·89	375·77	28·28	4·86	1·33	62·63	9·43	12 × 6
13·00	316·76	22·12	4·94	1·30	52·79	7·37	12 × 6
9·45	221·07	9·69	4·84	1·01	36·84	3·88	12 × 5
16·18	288·69	54·74	4·22	1·84	57·74	13·69	10 × 8
11·77	204·80	21·76	4·17	1·36	40·96	7·25	10 × 6
8·85	146·23	9·73	4·06	1·05	29·25	3·89	10 × 5
7·35	122·34	6·49	4 08	·94	24·47	2·88	10 × 4½
14·71	208·13	40·17	3·76	1·65	46·25	11·48	9 × 7
6·18	81·13	4·15	3·62	·82	18·03	2·07	9 × 4
10·30	115·06	19·54	3·34	1·38	28·76	6·51	8 × 6
8·28	89·69	10·19	3·29	1·11	22·42	4·08	8 × 5
5·30	55·63	3·51	3·24	·81	13·91	1·75	8 × 4

DORMAN, LONG & CO. LIMITED.

BEAMS

DIMENSIONS AND PROPERTIES IN INCH UNITS.

Reference Mark	Size Inches	Weight per foot lbs.	Standard Thicknesses		Radii		Centres of Holes C Inches
			Web t_1	Flange t_2	Root r_1	Toe r_2	
BSB 111	7×4	16	·25	·387	·45	·22	2·25
„ 110	6×5	25	·41	·520	·53	·26	2·75
„ 109	6×4½	20	·37	·431	·49	·24	2·5
„ 108	6×3	12	·23	·377	·37	·18	1·5
„ 107	5×4½	20	·29	·513	·49	·24	2·5
„ 106	5×3	11	·22	·376	·37	·18	1·5
„ 105	4¾×1¾	6·5	·18	·325	·27	·13	..
„ 104	4×3	10	·24	·347	·37	·18	1·5
„ 103	4×1¾	5	·17	·239	·27	·13	..
„ 102	3×3	8·5	·20	·332	·37	·18	1·5
„ 101	3×1½	4	·16	·249	·25	·12	..

SPECIAL BEAMS

DIMENSIONS AND PROPERTIES IN INCH UNITS.

Reference Mark	Size Inches	Weight per foot lbs.	Standard Thicknesses		Radii		Centres of Holes C Inches
			Web t_1	Flange t_2	Root r_1	Toe r_2	
D L B 25A	15×5	39	·40	·590	·52	·26	2·75
D L B 20A	12×5	39	·44	·664	·54	·27	2·75

772

BEAMS

DIMENSIONS AND PROPERTIES IN INCH UNITS

Area Square Inches	Moments of Inertia		Radii of Gyration		Section Moduli		Size Inches
	About X-X	About Y-Y	About X-X	About Y-Y	About X-X	About Y-Y	
4·75	39·51	3·37	2·89	·84	11·29	1·69	7×4
7·37	43·69	9·10	2·44	1·11	14·56	3·64	6×5
5·89	34·71	5·40	2·43	·96	11·57	2·40	6×4½
3·53	20·99	1·46	2·44	·64	7·00	·97	6×3
5·88	25·03	6·59	2·06	1·06	10·01	2·93	5×4½
3·26	13·68	1·45	2·05	·67	5·47	·97	5×3
1·91	6·73	·26	1·88	·37	2·83	·30	4¾×1¾
2·94	7·79	1·33	1·63	·67	3·89	·88	4×3
1·47	3·66	·19	1·58	·36	1·83	·21	4×1¾
2·52	3·81	1·25	1·23	.70	2·54	·83	3×3
1·18	1·66	·13	1·19	·33	1·11	·17	3×1½

SPECIAL BEAMS

DIMENSIONS AND PROPERTIES IN INCH UNITS.

Area Square Inches	Moments of Inertia		Radii of Gyration		Section Moduli		Size Inches
	About X-X	About Y-Y	About X-X	About Y-Y	About X-X	About Y-Y	
11·48	395·2	10·23	5·87	·944	52·70	4·145	15×5
11·47	260·9	12·16	4·77	1·03	43·48	4·86	12×5

DORMAN, LONG & CO. LIMITED.

CHANNELS.

DIMENSIONS AND PROPERTIES IN INCH UNITS.

Reference Mark	Size Inches	Weight per foot lbs.	Standard Thicknesses		Radii		Dimension P
			Web t_1	Flange t_2	Root r_1	Toe r_2	
BSC 120A	17×4	51·28	·60*	·68	·60	·30	·91
,, 120	17×4	44·34	·48	·68	·60	·30	·92
,, 119A	15×4	42·49	·53*	·62	·60	·30	·94
,, 119	15×4	36·37	·41	·62	·60	·30	·97
,, 118A	13×4	38·92	·53*	·62	·60	·30	1·01
,, 118	13×4	33·18	·40	·62	·60	·30	1·04
,, 117A	12×4	36·63	·53*	·60	·60	·30	1·02
,, 117	12×4	31·33	·40	·60	·60	·30	1·06
,, 116A	12×3½	30·45	·48*	·50	·54	·27	·81
,, 116	12×3½	26·37	·38	·50	·54	·27	·83
,, 115A	11×3½	30·52	·48*	·58	·54	·27	·91
,, 115	11×3½	26·78	·38	·58	·54	·27	·93
,, 114A	10×3½	28·54	·48*	·56	·54	·27	·94
,, 114	10×3½	24·46	·36	·56	·54	·27	·97
,, 113A	10×3	21·33	·38*	·45	·48	·24	·73
,, 113	10×3	19·28	·32	·45	·48	·24	·74
,, 112B	9×3½	25·63	·45*	·54	·54	·27	·97
,, 112A	9×3½	23·49	·38*	·54	·54	·27	·99
,, 112	9×3½	22·27	·34	·54	·54	·27	1·00
,, 111A	9×3	19·91	·38*	·44	·48	·24	·76
,, 111	9×3	17·46	·30	·44	·48	·24	·78
,, 110A	8×3½	23·20	·43*	·52	·54	·27	1·01
,, 110	8×3½	20·21	·32	·52	.54	·27	1·05
,, 109A	8×3	18·68	·38*	·44	·48	·24	·81
″ 109	8×3	15·96	·28	·44	·48	·24	·83
,, 108A	7×3½	20·18	·38*	·50	·54	·27	1·07
,, 108	7×3½	18·28	·30	·50	·54	·27	1·09

*Thickness obtained by raising rolls.

DORMAN, LONG & CO. LIMITED.
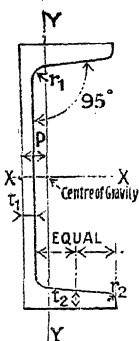
CHANNELS.

DIMENSIONS AND PROPERTIES IN INCH UNITS.

Area square inches	Moments of Inertia		Radii of Gyration Inches		Section Moduli		Size Inches
	About X-X	About Y-Y	About X-X	About Y-Y	Abou. X-X	About Y-Y	
15·08	569·31	16·96	6·14	1·06	66·98	5·28	17×4
13·04	520·18	15·26	6·32	1·08	61·20	4·96	17×4
12·50	382·85	14·97	5·54	1·09	51·05	4·71	15×4
10·70	349·10	13·34	5·71	1·12	46·55	4·40	15×4
11·45	270·66	14·51	4·86	1·13	41·64	4·64	13×4
9·76	246·86	12·76	5·03	1·14	37·98	4·31	13×4
10·77	218·81	13·80	4·51	1·13	36·47	4·44	12×4
9·21	200·09	12·12	4·66	1·15	33·35	4·12	12×4
8·96	174·13	7·96	4·41	·94	29·02	2·86	12×3½
7·76	159·73	7·15	4·54	·96	26·62	2·68	12×3½
8·98	152·96	8·86	4·13	·99	27·81	3·30	11×3½
7·88	141·87	7·93	4·24	1·00	25·80	3·09	11×3½
8·39	119·52	8·50	3·77	1·01	23·90	3·17	10×3½
7·19	109·52	7·42	3·90	1·02	21·90	2·93	10×3½
6·27	87·66	4·31	3·74	·83	17·53	1·85	10×3
5·67	82·66	3·98	3·82	·84	16·53	1·76	10×3
7·54	89·30	7·86	3·44	1·02	19·84	2.98	9×3½
6·91	85·05	7·26	3·51	1·03	18·90	2·85	9×3½
6·55	82·62	6·90	3·55	1·03	18·36	2·76	9×3½
5·86	67·38	4·18	3·39	·85	14·97	1·80	9×3
5·14	62·52	3·75	3·49	·86	13·89	1·69	9×3
6·82	65·27	7·30	3·09	1·03	16·32	2·81	8×3½
5·94	60·57	6·37	3·19	1·04	15·14	2·60	8×3½
5·49	50·99	4·11	3·05	·87	12·75	1·79	8×3
4·69	46·72	3·58	3·16	·87	11·68	1·65	8×3
5·94	45·12	6·48	2·76	1·05	12·89	2·58	7×3½
5·38	42·83	5·83	2·82	1·04	12·24	2·42	7×3½

CHANNELS.

DIMENSIONS AND PROPERTIES IN INCH UNITS.

Reference Mark	Size Inches	Weight per foot lbs.	Standard Thicknesses		Radii		Dimension
			Web t_1	Flange t_2	Root r_1	Toe r_2	P
BSC 107A	7×3	17·07	·38*	·42	·48	·24	·84
,, 107	7×3	14·22	·26	·42	·48	·24	·88
,, 106A	6×3½	18·52	·38*	·48	.54	·27	1·11
,, 106	6×3½	16·48	·28	·48	·54	·27	1·14
,, 105A	6×3	17·53	·43*	·48	·48	·24	·90
,, 105	6×3	16·51	·38	·48	·48	·24	·91
,, 104A	6×3	13·64	·31*	·38	·48	·24	·87
,, 104	6×3	12·41	·25	·38	·48	·24	·89
,, 103A	5×2½	11·24	·31*	·38	·42	·21	·76
,, 103	5×2½	10·22	·25	·38	·42	·21	·77
,, 102A	4×2	7·91	·30*	·31	·36	·18	·59
,, 102	4×2	7·09	·24	·31	·36	·18	·60
,, 101A	3×1½	5·11	·25*	·28	·30	·15	·48
,, 101	3×1½	4·60	·20	·28	·30	·15	·48

*Thickness obtained by raising the rolls.

SPECIAL CHANNELS.

DIMENSIONS AND PROPERTIES IN INCH UNITS.

Reference Mark	Size Inches	Weight per foot lbs.	Standard Thickness		Radii		Dimension
			Web t_1	Flange t_2	oot r_1	Toe r_2	P
SPECIAL	4½×1½	13·48	·63	·63	·44	·18	·481
SPECIAL	4×2½	10·66	·38	·38	·38	·22	·765

DORMAN, LONG & CO. LIMITED.

CHANNELS.

DIMENSIONS AND PROPERTIES IN INCH UNITS.

Area square inches	Moments of Inertia		Radii of Gyration Inches		Section Moduli		Size Inches
	About X-X	About Y-Y	About X-X	About Y-Y	About X-X	About Y-Y	
5·02	36·18	3·87	2·68	·88	10·34	1·70	7×3
4·18	32·75	3·26	2·80	·88	9·36	1·53	7×3
5·45	30·68	6·05	2·37	1·05	10·23	2·43	6×3½
4·85	28·88	5·29	2·44	1·05	9·63	2·25	6×3½
5·16	27·18	3·95	2·30	·88	9·06	1·84	6×3
4·86	26·28	3·70	2·33	·87	8·76	1·77	6×3
4·01	22·35	3·10	2·36	·88	7·45	1·42	6×3
3·65	21·27	2·83	2·41	·88	7·09	1·34	6×3
3·31	12·50	1·82	1·94	·74	5·00	1·01	5×2½
3·01	11·87	1·64	1·99	·74	4·75	·95	5×2½
2·33	5·38	·79	1·52	·58	2·69	·54	4×2
2·09	5·06	·70	1·56	·58	2·53	·50	4×2
1·50	1·94	·30	1·14	·44	1·29	·28	3×1½
1·35	1·82	·26	1·16	·44	1·22	·26	3×1½

SPECIAL CHANNELS.

DIMENSIONS AND PROPERTIES IN INCH UNITS.

Area square inches	Moments of Inertia		Radio of Gyration Inches		Section Moduli		Size Inches
	About X-X	About Y-Y	About X-X	About Y-Y	About X-X	About Y-Y	
3·964	9·043	·548	1·51	·372	4·019	·537	4½×1½
3·136	7·344	1·782	1·53	·754	3·672	1·027	4×2½

DORMAN, LONG & CO. LIMITED.

UNEQUAL ANGLES
DIMENSIONS AND PROPERTIES IN INCH UNITS.

Reference Mark	Size and Thickness	Area Square Inches	Weight per foot Lbs.	Radii Root	Radii Toe	Dimensions J	Dimensions P	Moments of Inertia About X-X	Moments of Inertia About Y-Y	Minimum Section Modulii About X-X	Minimum Section Modulii About Y-Y	Angles CC Degrees	Least Radius of Gyration
BSUA 123	9 × 4 × ½	6·25	21·25	·51	·36	3·27	·80	52·46	6·65	9·16	2·08	12½	·84
,, 123	,, ,, 9/16	7·00	23·79	·51	·36	3·30	·82	58·42	7·37	10·25	2·32	12	·84
,, 123	,, ,, ⅝	7·73	26·30	·51	·36	3·33	·85	64·23	8·06	11·33	2·56	12	·83
,, 123	,, ,, 11/16	8·47	28·78	·51	·36	3·36	·87	69·91	8·73	12·39	2·79	12	·83
,, 123	,, ,, ¾	9·19	31·24	·51	·36	3·38	·90	75·45	9·37	13·43	3·02	12	·83
,, 123	,, ,, 13/16	9·90	33·67	·51	·36	3·41	·92	80·86	9·99	14·46	3·25	12	·83
,, 123	,, ,, ⅞	10·61	36·07	·51	·36	3·43	·95	86·13	10·60	15·47	3·47	12	·83
BSUA 122	8 × 6 × ½	6·75	22·95	·54	·38	2·44	1·45	43·47	21·08	7·82	4·63	29	1·29
,, 122	,, ,, 9/16	7·56	25·70	·54	·38	2·47	1·47	48·43	23·44	8·75	5·18	29	1·29
,, 122	,, ,, ⅝	8·36	28·42	·54	·38	2·49	1·50	53·27	25·74	9·67	5·72	29	1·28
,, 122	,, ,, 11/16	9·15	31·12	·54	·38	2·52	1·52	57·99	27·97	10·58	6·25	29	1·28
,, 122	,, ,, ¾	9·94	33·79	·54	·38	2·54	1·55	62·60	30·14	11·47	6·77	29	1·28
,, 122	,, ,, 13/16	10·72	36·43	·54	·38	2·57	1·57	67·10	32·24	12·35	7·28	29	1·28
,, 122	,, ,, ⅞	11·48	39·05	·54	·38	2·59	1·60	71·49	34·29	13·22	7·79	28½	1·27
BSUA 121	8 × 4 × ½	5·75	19·55	·48	·34	2·83	·85	37·95	6·50	7·34	2·06	14½	·85
,, 121	,, ,, 9/16	6·43	21·87	·48	·34	2·86	·87	42·22	7·20	8·21	2·30	14½	·85
,, 121	,, ,, ⅝	7·11	24·17	·48	·34	2·88	·90	46·37	7·87	9·06	2·54	14½	·85
,, 121	,, ,, 11/16	7·78	26·44	·48	·34	2·91	·92	50·42	8·52	9·90	2·77	14½	·84
,, 121	,, ,, ¾	8·44	28·69	·48	·34	2·93	·94	54·36	9·14	10·73	2·99	14½	·84
BSUA 120	8 × 3½ × ⅜	4·17	14·19	·47	·33	2·89	·66	27·79	3·39	5·44	1·20	12	·73
,, 120	,, ,, 7/16	4·84	16·46	·47	·33	2·92	·69	32·08	3·89	6·31	1·39	12	·73
,, 120	,, ,, ½	5·50	18·70	·47	·33	2·95	·72	36·24	4·38	7·17	1·57	12	·73
,, 120	,, ,, 9/16	6·15	20·92	·47	·33	2·97	·74	40·30	4·84	8·02	1·75	12	·73
,, 120	,, ,, ⅝	6·80	23·11	·47	·33	3·00	·77	44·24	5·28	8·85	1·93	12	·72
BSUA 119	7 × 4 × ½	5·25	17·85	·45	·32	2·39	·90	26·26	6·33	5·70	2·04	18½	·86
,, 119	,, ,, 9/16	5·96	20·27	·45	·32	2·42	·93	29·17	7·00	6·37	2·28	18½	·86
,, 119	,, ,, ⅝	6·48	22·05	·45	·32	2·44	·95	32·00	7·64	7·02	2·51	18½	·86
,, 119	,, ,, 11/16	7·09	24·10	·45	·32	2·47	·98	34·75	8·26	7·67	2·73	18	·85
,, 119	,, ,, ¾	7·69	26·14	·45	·32	2·49	1·00	37·42	8·86	8·30	2·95	18	·85
BSUA 118	7 × 3½ × ⅜	3·80	12·91	·44	·31	2·44	·71	19·28	3·31	4·23	1·19	14½	·75
,, 118	,, ,, 7/16	4·40	14·97	·44	·31	2·47	·74	22·22	3·80	4·91	1·38	14½	·74
,, 118	,, ,, ½	5·00	17·00	·44	·31	2·50	·76	25·07	4·27	5·57	1·56	14½	·74
,, 118	,, ,, 9/16	5·59	19·01	·44	·31	2·53	·79	27·84	4·71	6·22	1·74	14½	·74
,, 118	,, ,, ⅝	6·17	20·99	·44	·31	2·55	·81	30·53	5·14	6·86	1·91	14½	·74
BSUA 117	6 × 4 × ⅜	3·61	12·28	·42	·29	1·91	·92	13·21	4·74	3·23	1·54	24	·87
,, 117	,, ,, 7/16	4·19	14·23	·42	·29	1·94	·95	15·21	5·44	3·75	1·78	24	·86
,, 117	,, ,, ½	4·75	16·16	·42	·29	1·97	·97	17·14	6·11	4·25	2·02	24	·86
,, 117	,, ,, 9/16	5·31	18·06	·42	·29	1·99	1·00	19·01	6·76	4·74	2·25	23½	·86
,, 117	,, ,, ⅝	5·86	19·93	·42	·29	2·02	1·02	20·82	7·37	5·23	2·48	23½	·86
,, 117	,, ,, 11/16	6·40	21·77	·42	·29	2·04	1·05	22·57	7·96	5·70	2·70	23½	·86
,, 117	,, ,, ¾	6·94	23·59	·42	·29	2·06	1·07	24·26	8·53	6·16	2·91	23½	·85

UNEQUAL ANGLES
DIMENSIONS AND PROPERTIES IN INCH UNITS.
(CONTINUED)

Reference Mark	Size and Thickness	Area Square Inches	Weight per foot Lbs.	Radii Root	Radii Toe	Dimensions J	Dimensions P	Moments of Inertia About X-X	Moments of Inertia About Y-Y	Minimum Section Moduli About X-X	Minimum Section Moduli About Y-Y	Angles α Degrees	Least Radius of Gyration
BSUA 116	6 ×3½ × 5/16	2·87	9·76	·41	·29	1·98	·75	10·65	2·72	2·65	·99	19	·76
,, 116	,, ,, 3/8	3·42	11·63	·41	·20	2·01	·77	12·62	3·21	3·16	1·18	19	·76
,, 116	,, ,, 7/16	3·96	13·48	·41	·29	2·04	·80	14·52	3·68	3·66	1·36	19	·75
,, 116	,, ,, 1/2	4·50	15·30	·41	·29	2·06	·82	16·36	4·13	4·15	1·54	19	·75
,, 116	,, ,, 9/16	5·03	17·09	·41	·29	2·09	·85	18·13	4·55	4·63	1·72	19	·75
,, 116	,, ,, 5/8	5·55	18·86	·41	·29	2·11	·87	19·85	4·96	5·11	1·89	18½	·75
BSUA 115	6 ×3 × 5/16	2·72	9·24	·39	·27	2·09	·61	10·13	1·74	2·59	·73	14½	·64
,, 115	,, ,, 3/8	3·24	11·00	·39	·27	2·12	·63	11·99	2·05	3·09	·87	14½	·64
,, 115	,, ,, 7/16	3·75	12·74	·39	·27	2·15	·66	13·78	2·34	3·58	1·00	14½	·64
,, 115	,, ,, 1/2	4·25	14·45	·39	·27	2·17	·68	15·51	2·62	4·05	1·13	14½	·63
,, 115	,, ,, 9/16	4·75	16·14	·39	·27	2·20	·71	17·18	2·88	4·52	1·26	14½	·63
,, 115	,, ,, 5/8	5·24	17·80	·39	·27	2·22	·73	18·80	3·14	4·98	1·38	14	·63
BSUA 114	5 ×4 × 3/8	3·24	11·00	·39	·27	1·51	1·01	7·97	4·53	2·28	1·52	32	·85
,, 114	,, ,, 7/16	3·75	12·74	·39	·27	1·53	1·04	9·15	5·19	2·64	1·75	32	·84
,, 114	,, ,, 1/2	4·25	14·45	·39	·27	1·56	1·06	10·29	5·83	2·99	1·98	32	·84
,, 114	,, ,, 9/16	4·75	16·14	·39	·27	1·58	1·09	11·39	6·44	3·33	2·21	32	·84
,, 114	,, ,, 5/8	5·24	17·80	·39	·27	1·61	1·11	12·44	7·02	3·67	2·43	32	·84
BSUA 113	5 ×3½ × 5/16	2·56	8·71	·38	·26	1·56	·82	6·46	2·62	1·88	·98	25½	·76
,, 113	,, ,, 3/8	3·05	10·37	·38	·26	1·59	·85	7·63	3·09	2·24	1·16	25½	·75
,, 113	,, ,, 7/16	3·53	12·00	·38	·26	1·62	·87	8·76	3·53	2·59	1·34	25½	·75
,, 113	,, ,, 1/2	4·00	13·61	·38	·26	1·64	·90	9·84	3·96	2·93	1·52	25½	·75
,, 113	,, ,, 9/16	4·47	15·19	·38	·26	1·66	·92	10·88	4·36	3·26	1·64	25	·75
,, 113	,, ,, 5/8	4·92	16·74	·38	·26	1·69	·94	11·89	4·74	3·59	1·86	25	·74
BSUA 112	5 ×3 × 5/16	2·40	8·17	·36	·25	1·66	·67	6·14	1·68	1·84	·72	20	·65
,, 112	,, ,, 3/8	2·86	9·73	·36	·25	1·68	·69	7·25	1·97	2·18	·85	20	·65
,, 112	,, ,, 7/16	3·31	11·25	·36	·25	1·71	·72	8·31	2·25	2·53	·99	20	·64
,, 112	,, ,, 1/2	3·75	12·75	·36	·25	1·73	·74	9·33	2·51	2·86	1·11	19½	·64
,, 112	,, ,, 9/16	4·18	14·23	·36	·25	1·76	·77	10·31	2·76	3·18	1·24	19½	·64
BSUA 111	4½ ×3 × 5/16	2·25	7·64	·35	·24	1·44	·70	4·59	1·64	1·50	·71	24	·65
,, 111	,, ,, 3/8	2·67	9·09	·35	·24	1·47	·73	5·41	1·92	1·79	·85	24	·64
,, 111	,, ,, 7/16	3·09	10·51	·35	·24	1·50	·75	6·19	2·19	2·06	·98	23½	·64
,, 111	,, ,, 1/2	3·50	11·91	·35	·24	1·52	·78	6·94	2·45	2·33	1·10	23½	·64
,, 111	,, ,, 9/16	3·90	13·27	·35	·24	1·55	·80	7·66	2·69	2·59	1·22	23½	·64
BSUA 110	4 ×3½ × 5/16	2·25	7·64	·35	·24	1·16	·92	3·47	2·47	1·22	·96	37	·72
,, 110	,, ,, 3/8	2·67	9·09	·35	·24	1·19	·94	4·09	2·91	1·45	1·37	37	·72
,, 110	,, ,, 7/16	3·09	10·51	·35	·24	1·21	·97	4·68	3·32	1·68	1·31	37	·72
,, 110	,, ,, 1/2	3·50	11·91	·35	·24	1·24	·99	5·24	3·72	1·90	1·48	37	·72
,, 110	,, ,, 9/16	3·90	13·27	·35	·24	1·26	1·01	5·77	4·09	2·11	1·65	37	·71
,, 110	,, ,, 5/8	4·30	14·61	·35	·24	1·29	1·04	6·28	4·45	2·31	1·81	36½	·71

DORMAN, LONG & CO. LIMITED.

UNEQUAL ANGLES.
DIMENSIONS AND PROPERTIES IN INCH UNITS.
(CONTINUED)

Reference Mark	Size and Thickness	Area Square Inches	Weight per foot Lbs.	Radii Root	Radii Toe	Dimensions J	Dimensions P	Moments of Inertia About X-X	Moments of Inertia About Y-Y	Minimum Section Moduli About X-X	Minimum Section Moduli About Y-Y	Angles CC Degrees	Least Radius of Gyration
BSUA 109	4 ×3 × 5/16	2·09	7·11	·33	·23	1·24	·75	3·30	1·59	1·20	·71	29	·64
" 109	" " 3/8	2·49	8·45	·33	·23	1·27	·77	3·89	1·87	1·42	·84	29	·64
" 109	" " 7/16	2·87	9·76	·33	·23	1·29	·80	4·44	2·13	1·64	·96	28½	·63
" 109	" " 1/2	3·25	11·05	·33	·23	1·32	·82	4·97	2·37	1·85	1·09	28½	·63
" 109	" " 9/16	3·62	12·31	·33	·23	1·34	·84	5·48	2·60	2·06	1·21	28½	·63
BSUA 108	4 ×2½ × 1/4	1·56	5·32	·32	·22	1·30	·56	2·54	·77	·94	·40	22	·54
" 108	" " 5/16	1·93	6·58	·32	·22	1·33	·59	3·11	·94	1·17	·49	22	·54
" 108	" " 3/8	2·30	7·81	·32	·22	1·36	·61	3·66	1·10	1·38	·58	21	·53
" 108	" " 7/16	2·65	9·02	·32	·22	1·38	·64	4·18	1·24	1·59	·67	21	·53
BSUA 107	3½ ×3 × 1/4	1·56	5·32	·32	·22	1·01	·77	1·86	1·26	·75	·56	36	·62
" 107	" " 5/16	1·93	6·58	·32	·22	1·04	·79	2·27	1·54	·92	·70	36	·62
" 107	" " 3/8	2·30	7·81	·32	·22	1·07	·82	2·67	1·80	1·10	·83	36	·62
" 107	" " 7/16	2·65	9·02	·32	·22	1·09	·84	3·04	2·05	1·26	·95	36	·62
" 107	" " 1/2	3·00	10·20	·32	·22	1·12	·87	3·40	2·28	1·43	1·07	35½	·61
" 107	" " 9/16	3·34	11·36	·32	·22	1·14	·89	3·74	2·51	1·58	1·19	35½	·61
BSUA 106	3½ ×2½ × 1/4	1·44	4·89	·30	·21	1·09	·60	1·75	·74	·73	·39	26½	·54
" 106	" " 5/16	1·78	6·04	·30	·21	1·12	·63	2·14	·91	·90	·48	26½	·53
" 106	" " 3/8	2·11	7·17	·30	·21	1·15	·65	2·51	1·06	1·07	·57	26	·53
" 106	" " 7/16	2·43	8·28	·30	·21	1·17	·68	2·86	1·20	1·23	·66	26	·53
BSUA 105	3 ×2½ × 1/4	1·31	4·47	·29	·20	·89	·65	1·14	·72	·54	·39	34½	·52
" 105	" " 5/16	1·62	5·51	·29	·20	·92	·67	1·39	·87	·67	·48	34½	·52
" 105	" " 3/8	1·92	6·54	·29	·20	·94	·70	1·62	1·02	·79	·56	34	·52
" 105	" " 7/16	2·22	7·53	·29	·20	·97	·72	1·84	1·15	·91	·65	34	·52
BSUA 104	3 ×2 × 3/16	·90	3·07	·27	·19	·95	·46	·81	·29	·40	·19	23½	·43
" 104	" " 1/4	1·19	4·04	·27	·19	·98	·48	1·06	·38	·52	·25	23½	·43
" 104	" " 5/16	1·46	4·98	·27	·19	1·00	·51	1·29	·45	·65	·30	23½	·43
" 104	" " 3/8	1·73	5·90	·27	·19	1·03	·53	1·50	·53	·76	·36	23	·42
" 104	" " 7/16	2·00	6·79	·27	·19	1·05	·56	1·71	·59	·88	·41	23	·42
BSUA 103	2½ ×2 × 3/16	·81	2·75	·26	·18	·75	·50	·49	·28	·28	·18	32	·42
" 103	" " 1/4	1·06	3·61	·26	·18	·77	·53	·63	·36	·37	·24	32	·42
" 103	" " 5/16	1·31	4·45	·26	·18	·80	·55	·77	·43	·45	·30	32	·42
" 103	" " 3/8	1·55	5·26	·26	·18	·82	·57	·89	·50	·53	·35	31½	·41
BSUA 102	2½ ×1½ × 3/16	·71	2·43	·24	·17	·83	·34	·45	·12	·27	·10	19½	·32
" 102	" " 1/4	·94	3·19	·24	·17	·86	·37	·58	·15	·35	·14	19½	·32
" 102	" " 5/16	1·15	3·92	·24	·17	·89	·39	·70	·18	·43	·17	19½	·32
BSUA 101	2 ×1½ × 3/16	·62	2·11	·23	·16	·63	·38	·24	·11	·17	·10	28½	·32
" 101	" " 1/4	·81	2·76	·23	·16	·65	·41	·31	·15	·23	·13	28½	·31
" 100	" " 5/16	1·00	3·39	·23	·16	·68	·43	·37	·17	·28	·16	28	·31

EQUAL ANGLES.

DIMENSIONS AND PROPERTIES IN INCH UNITS,
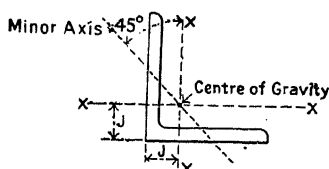
Reference Mark	Size and Thickness			Area Square Inches	Weight per foot Lbs.	Radii		Dimension J	Moment of Inertia About X-X	Minimum Section Modulus About X-X	Least Radius of Gyration
						Root	Toe				
BSEA 115	8	×8	×5/8	9·61	32·68	·60	·42	2·20	58·26	10·05	1·57
" 115	"	"	11/16	10·53	35·80	·60	·42	2·23	63·48	11·00	1·57
" 115	"	"	3/4	11·44	38·89	·60	·42	2·25	68·58	11·94	1·57
" 115	"	"	13/16	12·34	41·96	·60	·42	2·28	73·57	12·86	1·56
" 115	"	"	7/8	13·24	45·00	·60	·42	2·30	78·44	13·77	1·56
" 115	"	"	15/16	14·12	48·02	·60	·42	2·33	83·20	14·66	1·56
" 115	"	"	1	15·00	51·01	·60	·42	2·35	87·85	15·55	1·56
BSEA 114	7	×7	×1/2	6·75	22·95	·54	·38	1·91	31·42	6·17	1·38
" 114	"	"	9/16	7·56	25·70	·54	·38	1·93	34·98	6·90	1·37
" 114	"	"	5/8	8·36	28·42	·54	·38	1·96	38·45	7·63	1·37
" 114	"	"	11/16	9·15	31·12	·54	·38	1·98	41·83	8·34	1·37
" 114	"	"	3/4	9·94	33·79	·54	·38	2·01	45·12	9·04	1·37
" 114	"	"	13/16	10·72	36·43	·54	·38	2·03	48·33	9·73	1·36
" 114	"	"	7/8	11·48	39·05	·54	·38	2·06	51·45	10·41	1·36
" 114	"	"	15/16	12·25	41·64	·54	·38	2·08	54·50	11·07	1·36
" 114	"	"	1	13·00	44·20	·54	·38	2·10	57·46	11·73	1·36
BSEA 113	6	×6	×3/8	4·36	14·82	·48	·34	1·61	14·95	3·40	1·18
" 113	"	"	7/16	5·06	17·20	·48	·34	1·64	17·25	3·95	1·18
" 113	"	"	1/2	5·75	19·55	·48	·34	1·66	19·48	4·49	1·18
" 113	"	"	9/16	6·43	21·87	·48	·34	1·69	21·64	5·02	1·17
" 113	"	"	5/8	7·11	24·17	·48	·34	1·71	23·73	5·54	1·17
" 113	"	"	11/16	7·78	26·44	·48	·34	1·74	25·77	6·04	1·17
" 113	"	"	3/4	8·44	28·69	·48	·34	1·76	27·74	6·54	1·17
" 113	"	"	13/16	9·09	30·90	·48	·34	1·78	29·65	7·03	1·16
" 113	"	"	7/8	9·73	33·10	·48	·34	1·81	31·51	7·51	1·16
BSEA 112	5	×5	×3/8	3·61	12·28	·42	·29	1·37	8·53	2·35	·98
" 112	"	"	7/16	4·19	14·23	·42	·29	1·39	9·81	2·72	·98
" 112	"	"	1/2	4·75	16·16	·42	·29	1·42	11·04	3·08	·98
" 112	"	"	9/16	5·31	18·06	·42	·29	1·44	12·22	3·44	·97
" 112	"	"	5/8	5·86	19·93	·42	·29	1·47	13·37	3·78	·97
" 112	"	"	11/16	6·40	21·77	·42	·29	1·49	14·47	4·12	·97
" 112	"	"	3/4	6·94	23·59	·42	·29	1·51	15·54	4·46	·97

DORMAN, LONG & CO. LIMITED.

EQUAL ANGLES.

DIMENSIONS AND PROPERTIES IN INCH UNITS.

(CONTINUED)

Reference Mark	Size and Thickness	Area Square Inches	Weight per foot Lbs.	Radii Root	Radii Toe	Dimension J	Moment of Inertia About X-X	Minimum Section Modulus About X-X	Least Radius of Gyration
BSEA 111	4½ × 4½ × 5/16	2·72	9·24	·39	·27	1·22	5·21	1·59	·89
,, 111	,, ,, 3/8	3·24	11·00	·39	·27	1·24	6·15	1·89	·88
,, 111	,, ,, 7/16	3·75	12·74	·39	·27	1·27	7·05	2·18	·88
,, 111	,, ,, ½	4·25	14·45	·39	·27	1·29	7·92	2·47	·88
,, 111	,, ,, 9/16	4·75	16·14	·39	·27	1·32	8·76	2·75	·87
,, 111	,, ,, 5/8	5·24	17·80	·39	·27	1·34	9·56	3·03	·87
,, 111	,, ,, 11/16	5·72	19·44	·39	·27	1·37	10·34	3·30	·87
,, 111	,, ,, ¾	6·19	21·04	·39	·27	1·39	11·08	3·56	·87
BSEA 110	4 × 4 × 5/16	2·40	8·17	·36	·25	1·10	3·61	1·24	·78
,, 110	,, ,, 3/8	2·86	9·73	·36	·25	1·12	4·26	1·48	·78
,, 110	,, ,, 7/16	3·31	11·25	·36	·25	1·15	4·87	1·71	·78
,, 110	,, ,, ½	3·75	12·75	·36	·25	1·17	5·46	1·93	·78
,, 110	,, ,, 9/16	4·18	14·23	·36	·25	1·20	6·02	2·15	·77
,, 110	,, ,, 5/8	4·61	15·68	·36	·25	1·22	6·56	2·36	·77
,, 110	,, ,, 11/16	5·03	17·10	·36	·25	1·24	7·08	2·57	·77
,, 110	,, * ¾	5·44	18·49	·36	·25	1·26	7·57	2·77	·77
BSEA 109	3½ × 3½ × ¼	1·69	5·74	·33	·23	·95	1·94	·76	·69
,, 109	,, ,, 5/16	2·09	7·11	·33	·23	·97	2·38	·94	·68
,, 109	,, ,, 3/8	2·49	8·45	·33	·23	1·00	2·80	1·12	·68
,, 109	,, ,, 7/16	2·87	9·76	·33	·23	1·02	3·20	1·29	·68
,, 109	,, ,, ½	3·25	11·05	·33	·23	1·05	3·57	1·46	·68
,, 109	,, ,, 9/16	3·62	12·31	·33	·23	1·07	3·93	1·62	·68
,, 109	,, ,, 5/8	3·99	13·55	·33	·23	1·09	4·27	1·77	·68
BSEA 108	3 × 3 × ¼	1·44	4·89	·30	·21	·83	1·20	·55	·59
,, 108	,, ,, 5/16	1·78	6·04	·30	·21	·85	1·47	·68	·58
,, 108	,, ,, 3/8	2·11	7·17	·30	·21	·88	1·72	·81	·58
,, 108	,, ,, 7/16	2·43	8·28	·30	·21	·90	1·96	·93	·58
,, 108	,, ,, ½	2·75	9·35	·30	·21	·92	2·18	1·05	·58
,, 108	,, ,, 9/16	3·06	10·40	·30	·21	·95	2·39	1·16	·58

DORMAN, LONG & CO. LIMITED.

EQUAL ANGLES.

DIMENSIONS AND PROPERTIES IN INCH UNITS.
(CONTINUED)

Reference Mark	Size and Thickness	Area Square Inches	Weight per foot Lbs.	Radii Root	Radii Toe	Dimension J	Moment of Inertia About X-X	Minimum Section Modulus About X-X	Least Radius of Gyration
BSEA 107	2½ × 2½ × ¼	1·19	4·04	·27	·19	·70	·68	·38	·49
,, 107	,, ,, ⁵⁄₁₆	1·46	4·98	·27	·19	·73	·83	·47	·48
,, 107	,, ,, ³⁄₈	1·73	5·90	·27	·19	·75	·96	·55	·48
,, 107	,, ,, ⁷⁄₁₆	2·00	6·79	·27	·19	·78	1·09	·63	·48
,, 107	,, ,, ½	2·25	7·65	·27	·19	·80	1·21	·71	·48
BSEA 106	2¼ × 2¼ × ³⁄₁₆	·81	2·75	·26	·18	·62	·38	23	·44
,, 106	,, ,, ¼	1·06	3·61	·26	·18	·64	·49	·30	·44
,, 106	,, ,, ⁵⁄₁₆	1·31	4·45	·26	·18	·67	·59	·37	·43
,, 106	,, ,, ³⁄₈	1·55	5·26	·26	·18	·69	·69	·44	·43
BSEA 105	2 × 2 × ³⁄₁₆	·71	2·43	·24	·17	·56	·26	·18	·39
,, 105	,, ,, ¼	·94	3·19	·24	·17	·58	·34	·24	·39
,, 105	,, ,, ⁵⁄₁₆	1·15	3·92	·24	·17	·61	·40	·29	·38
,, 105	,, ,, ³⁄₈	1·36	4·62	·24	·17	·63	·47	·34	·38
BSEA 104	1¾ × 1¾ × ³⁄₁₆	·62	2·11	·23	·16	·49	·17	·14	·34
,, 104	,, ,, ¼	·81	2·76	·23	·16	·52	·22	·18	·34
,, 104	,, ,, ⁵⁄₁₆	1·00	3·39	·23	·16	·54	·26	·22	·34
BSEA 103	1½ × 1½ × ³⁄₁₆	·53	1·79	·21	·15	·43	·10	·10	·29
,, 103	,, ,, ¼	·69	2·34	·21	·15	·46	·13	·13	·29
,, 103	,, ,, ⁵⁄₁₆	·84	2·85	·21	·15	·48	·16	·16	·29
BSEA 102	1¼ × 1¼ × ⅛	·30	1·01	·20	·14	·34	·04	·05	·24
,, 102	,, ,, ³⁄₁₆	·43	1·47	·20	·14	·37	·06	·07	·24
,, 102	,, ,, ¼	·56	1·91	·20	·14	·40	·07	·09	·24
BSEA 101	1 × 1 × ⅛	·23	·80	·18	·13	·29	·02	·03	·19
,, 101	,, ,, ³⁄₁₆	·34	1·15	·18	·13	·31	·03	·04	·19
,, 101	,, ,, ¼	·44	1·49	·18	·13	·33	·04	·05	·19

INDEX

Numbers refer to pages. An asterisk indicates a footnote.